New Series

LANDOLT-BÖRNSTEIN

Numerical Data and Functional Relationships in Science and Technology

GROUP IV

VOLUME 11

Physical Chemistry

Ternary Alloy Systems

Phase Diagrams, Crystallographic and Thermodynamic Data

critically evaluated by MSIT®

SUBVOLUME D

Iron Systems

Part 2

Selected Systems from C-Cr-Fe to Co-Fe-S

Springer

Landolt-Börnstein
Numerical Data and Functional Relationships in Science and Technology
New Series / Editor in Chief: W. Martienssen

Group IV: Physical Chemistry
Volume 11

Ternary Alloy Systems

Phase Diagrams, Crystallographic and Thermodynamic Data

critically evaluated by MSIT®

Subvolume D
Iron Systems

Part 2
Selected Systems from C-Cr-Fe to Co-Fe-S

Editors
G. Effenberg and S. Ilyenko

Authors
Materials Science and International Team, MSIT®

Springer

MSI
The Materials Chemistry Knowledge Network

ISSN 1615-2018 (Physical Chemistry)

ISBN 978-3-540-74193-0 Springer Berlin Heidelberg New York

Library of Congress Cataloging in Publication Data
Zahlenwerte und Funktionen aus Naturwissenschaften und Technik, Neue Serie
Editor in Chief: W. Martienssen
Vol. IV/11D2: Editors: G. Effenberg, S. Ilyenko

At head of title: Landolt-Börnstein. Added t.p.: Numerical data and functional relationships in science and technology.
Tables chiefly in English.
Intended to supersede the Physikalisch-chemische Tabellen by H. Landolt and R. Börnstein of which the 6th ed. began publication in 1950 under title:
Zahlenwerte und Funktionen aus Physik, Chemie, Astronomie, Geophysik und Technik.
Vols. published after v. 1 of group I have imprint: Berlin, New York, Springer-Verlag
Includes bibliographies.
1. Physics--Tables. 2. Chemistry--Tables. 3. Engineering--Tables.
I. Börnstein, R. (Richard), 1852-1913. II. Landolt, H. (Hans), 1831-1910.
III. Physikalisch-chemische Tabellen. IV. Title: Numerical data and functional relationships in science and technology.
QC61.23 502'.12 62-53136

Springer is a part of Springer Science+Business Media
springeronline.com

Printed in Germany

Cover layout: Erich Kirchner, Heidelberg
Typesetting: Materials Science International Services GmbH, Stuttgart
Printing and Binding: AZ Druck, Kempten/Allgäu

SPIN: 1091 6063 63/3020 - 5 4 3 2 1 0 – Printed on acid-free paper

Editors: **Günter Effenberg**
Svitlana Ilyenko
Associate Editor: **Oleksandr Dovbenko**

MSI, Materials Science International Services GmbH
Postfach 800749, D-70507, Stuttgart, Germany
http://www.matport.com

Authors: Materials Science International Team, MSIT®

The present series of books results from collaborative evaluation programs performed by MSI and authored by MSIT®. In this program data and knowledge are contributed by many individuals and accumulated over almost twenty years, now. The content of this volume is a subset of the ongoing MSIT® Evaluation Programs. Authors of this volume are:

Nataliya Bochvar, Moscow, Russia

Anatoliy Bondar, Kyiv, Ukraine

Lesley Cornish, Randburg, South Africa

Simona Delsante, Genova, Italy

Tatyana Dobatkina, Moscow, Russia

Gautam Ghosh, Evanston, USA

Joachim Gröbner, Clausthal-Zellerfeld, Germany

K.C. Hari Kumar, Chennai, India

Volodymyr Ivanchenko, Kyiv, Ukraine

Kostyantyn Korniyenko, Kyiv, Ukraine

Artem Kozlov, Clausthal-Zellerfeld, Germany

Viktor Kuznetsov, Moscow, Russia

Nathalie Lebrun, Lille, France

Pierre Perrot, Lille, France

Tatiana Pryadko, Kyiv, Ukraine

Rainer Schmid-Fetzer, Clausthal-Zellerfeld, Germany

Elena Semenova, Kyiv, Ukraine

Elena Sheftel, Moscow, Russia

Nuri Solak, Stuttgart, Germany

Jean-Claude Tedenac, Montpellier, France

Vasyl Tomashik, Kyiv, Ukraine

Michail Turchanin, Kramatorsk, Ukraine

Tamara Velikanova, Kyiv, Ukraine

Tatyana Velikanova, Kyiv, Ukraine

Andy Watson, Leeds, U.K.

Institutions

The content of this volume is produced by MSI, Materials Science International Services GmbH and the international team of materials scientists, MSIT®. Contributions to this volume have been made from the following institutions:

The Baikov Institute of Metallurgy, Academy of Sciences, Moscow, Russia

Donbass State Mechanical Engineering Academy, Kramatorsk, Ukraine

I.M. Frantsevich Institute for Problems of Materials Science, National Academy of Sciences, Kyiv, Ukraine

Indian Institute of Technology Madras, Department of Metallurgical Engineering, Chennai, India

Institute for Semiconductor Physics, National Academy of Sciences, Kyiv, Ukraine

G.V. Kurdyumov Institute for Metal Physics, National Academy of Sciences, Kyiv, Ukraine

Max-Planck-Institut für Metallforschung, Institut für Werkstoffwissenschaft, Pulvermetallurgisches Laboratorium, Stuttgart, Germany

Moscow State University, Department of General Chemistry, Moscow, Russia

School of Chemical and Metallurgical Engineering, The University of the Witwatersrand, DST/NRF Centre of Excellence for Strong Material, South Afrika

Northwestern University, Department of Materials Science and Engineering, Evanston, USA

Technische Universität Clausthal, Metallurgisches Zentrum, Clausthal-Zellerfeld, Germany

Universite de Montpellier II, Laboratoire de Physico-chimie de la Matiere, Montpellier, France

Universita di Genova, Dipartimento di Chimica, Genova, Italy

Universite de Lille I, Laboratoire de Metallurgie Physique, Villeneuve d'ASCQ, France

University of Leeds, Department of Materials, School of Process, Environmental and Materials Engineering, Leeds, UK

Preface

The sub-series *Ternary Alloy Systems* of the *Landolt-Börnstein New Series* provides reliable and comprehensive descriptions of the materials constitution, based on critical intellectual evaluations of all data available at the time and it critically weights the different findings, also with respect to their compatibility with today's edge binary phase diagrams. Selected are ternary systems of importance to alloy development and systems which gained in the recent years otherwise scientific interest. In one ternary materials system, however, one may find alloys for various applications, depending on the chosen composition.

Reliable phase diagrams provide scientists and engineers with basic information of eminent importance for fundamental research and for the development and optimization of materials. So collections of such diagrams are extremely useful, if the data on which they are based have been subjected to critical evaluation, like in these volumes. Critical evaluation means: there where contradictory information is published data and conclusions are being analyzed, broken down to the firm facts and re-interpreted in the light of all present knowledge. Depending on the information available this can be a very difficult task to achieve. Critical evaluations establish descriptions of reliably known phase configurations and related data.

The evaluations are performed by MSIT®, Materials Science International Team, a group of scientists working together since 1984. Within this team skilled expertise is available for a broad range of methods, materials and applications. This joint competence is employed in the critical evaluation of the often conflicting literature data. Particularly helpful in this are targeted thermodynamic and atomistic calculations for individual equilibria, driving forces or complete phase diagram sections.

Conclusions on phase equilibria may be drawn from direct observations *e.g.* by microscope, from monitoring caloric or thermal effects or measuring properties such as electric resistivity, electro-magnetic or mechanical properties. Other examples of useful methods in materials chemistry are mass-spectrometry, thermo-gravimetry, measurement of electro-motive forces, X-ray and microprobe analyses. In each published case the applicability of the chosen method has to be validated, the way of actually performing the experiment or computer modeling has to be validated as well and the interpretation of the results with regard to the material's chemistry has to be verified. Therefore insight in materials constitution and phase reactions is gained from many distinctly different types of experiments, calculation and observations. Intellectual evaluations which interpret all data simultaneously reveal the chemistry of the materials system best.

An additional degree of complexity is introduced by the material itself, as the state of the material under test depends heavily on its history, in particular on the way of homogenization, thermal and mechanical treatments. All this is taken into account in an MSIT® expert evaluation.

To include binary data in the ternary evaluation is mandatory. Each of the three-dimensional ternary phase diagrams has edge binary systems as boundary planes; their data have to match the ternary data smoothly. At the same time each of the edge binary systems A-B is a boundary plane for many other ternary A-B-X systems. Therefore combining systematically binary and ternary evaluations increases confidence and reliability in both ternary and binary phase diagrams. This has started systematically for the first time here, by the MSIT® Evaluation Programs applied to the *Landolt-Börnstein New Series*. The degree of success, however, depends on both the nature of materials and scientists!

The multitude of correlated or inter-dependant data requires special care. Within MSIT® an evaluation routine has been established that proceeds knowledge driven and applies both, human based expertise and electronically formatted data and software tools. MSIT® internal discussions take place in almost all evaluation works and on many different specific questions the competence of a team is added to the work of individual authors. In some cases the authors of earlier published work contributed to the knowledge

base by making their original data records available for re-interpretation. All evaluation reports published here have undergone a thorough review process in which the reviewers had access to all the original data.

In publishing we have adopted a standard format that presents the reader with the data for each ternary system in a concise and consistent manner, as applied in the "MSIT® Workplace Phase Diagrams Online". The standard format and special features of the Landolt-Börnstein compendium are explained in the Introduction to the volume.

In spite of the skill and labor that have been put into this volume, it will not be faultless. All criticisms and suggestions that can help us to improve our work are very welcome. Please contact us via effenberg@msiwp.com. We hope that this volume will prove to be as useful for the materials scientist and engineer as the other volumes of *Landolt-Börnstein New Series* and the previous works of MSIT® have been. We hope that the *Landolt Börnstein Sub-series, Ternary Alloy Systems* will be well received by our colleagues in research and industry.

On behalf of the participating authors we want to thank all those who contributed their comments and insight during the evaluation process. In particular we thank the reviewers - Olga Fabrichnaya, Marina Bulanova, Yong Du and Lazar Rokhlin.

We all gratefully acknowledge the dedicated scientific desk editing by Oleksandra Berezhnytska, Oleksandr Rogovtsov and Oleksandra Zaikina.

Günter Effenberg, Svitlana Ilyenko and Oleksandr Dovbenko Stuttgart, April 2007

Foreword

Can you imagine a world without iron and steel? No? I can't either.

The story of mankind is intimately linked to the discovery and successful use of metals and their alloys. Amongst them iron and steel - we could define steel as 'a generally hard, strong, durable, malleable alloy of iron and carbon, usually containing between 0.2 and 1.5 percent carbon, often with other constituents such as manganese, chromium, nickel, molybdenum, copper, tungsten, cobalt, or silicon, depending on the desired alloy properties, and widely used as a structural material', have shaped our material world.

The story of iron takes us back to the period of the Hittite Empire around 1300 BC, when iron started to replace bronze as the chief metal used for weapons and tools. Until today the story remains uncompleted and the social and economic impact of the iron and steel industry is now beyond imagination. In the year 2005 1.13 billion tons of crude steel were produced. Compared to 2004 this is an increase of 6.8%. That same year the steel production in China increased from 280.5 to almost 350 million tons. Concerning stainless steel: according to the International Stainless Steel Forum (ISSF), the global production forecast for 2006 now stands at 27.8 million metric tons of stainless crude steel, up 14.3% compared to 2005.

An English poem from the 19th century tells us

> Gold is for the mistress
> Silver for the maid
> Copper for the craftsman
> Cunning at his trade
> Good said the baron
> Sitting in his hall
> But iron, cold iron
> Is master of them all

It is still actual and true.

The list of different steel grades and related applications is impressive and still growing: low carbon strip steels for automotive applications, low carbon structural steels, engineering steels, stainless steels, cast irons, and, more recently: dual phase steels, TRIP-steels, TWIP-steels, maraging steels, …

The list of applications seems endless: a wide range of properties from corrosion resistance to high tensile strength is covered. These properties depend on the percentage of carbon, the alloying elements, and increasingly on the thermo-mechanical treatments that aim at optimizing the microstructure.

Yet many potential improvements remain unexplored, also due to the increasing complexity of the new steel grades. For instance, a recently patent protected new die steel for hot deformation has the following composition specifications: C 0.46 – 0.58; Si 0.18 – 0.40; Mn 0.45 – 0.75, Cr 0.80 – 1.20; Ni 1.30 – 1.70; Mo 0.35 – 0.65; V 0.18 – 0.25; Al 0.01 – 0.04; Ti 0.002 – 0.04; B 0.001 – 0.003; Zr 0.02 – 0.04; Fe remaining.

Although many properties of steel are directly related to non-equilibrium states, it remains a fact that the equilibrium state creates the reference frame for all changes that might occur in any material - and consequently would effect its properties in use - that is actually not in its thermodynamic equilibrium state. This is what these volumes in the Landolt-Börnstein series stand for: they have collected the most reliable data on the possible phase equilibria in ternary iron based alloys. Therefore this first volume of data, as well as the other ones in a series of four to appear, is of immeasurable value for metallurgists and materials engineers that improve the properties of existing steels and develop new and more complex steel grades. It is about materials, it is about quality of life.

The well-recognized quality label of MSIT®, the Materials Science International Team, also applies to the present volume of the Landolt-Börnstein series. It should be available for every materials engineer, scientist and student.

Prof. Dr. ir. Patrick Wollants
Chairman - Department of Metallurgy and Materials Engineering
Katholieke Universiteit Leuven
Belgium

Contents

IV/11D2 Ternary Alloy Systems
Phase Diagrams, Crystallographic and Thermodynamic Data

Subvolume D Iron Systems

Part 2 Selected Systems from C-Cr-Fe to Co-Fe-S

Introduction

Ternary Systems

Introduction

Data Covered

The series focuses on light metal ternary systems and includes phase equilibria of importance for alloy development, processing or application, reporting on selected ternary systems of importance to industrial light alloy development and systems which gained otherwise scientific interest in the recent years.

General

The series provides consistent phase diagram descriptions for individual ternary systems. The representation of the equilibria of ternary systems as a function of temperature results in spacial diagrams whose sections and projections are generally published in the literature. Phase equilibria are described in terms of liquidus, solidus and solvus projections, isothermal and quasibinary sections; data on invariant equilibria are generally given in the form of tables.
The world literature is thoroughly and systematically searched back to the year 1900. Then, the published data are critically evaluated by experts in materials science and reviewed. Conflicting information is commented upon and errors and inconsistencies removed wherever possible. It considers those, and only those data, which are firmly established, comments on questionable findings and justifies re-interpretations made by the authors of the evaluation reports.
In general, the approach used to discuss the phase relationships is to consider changes in state and phase reactions which occur with decreasing temperature. This has influenced the terminology employed and is reflected in the tables and the reaction schemes presented.
The system reports present concise descriptions and hence do not repeat in the text facts which can clearly be read from the diagrams. For most purposes the use of the compendium is expected to be self-sufficient. However, a detailed bibliography of all cited references is given to enable original sources of information to be studied if required.

Structure of a System Report

The constitutional description of an alloy system consists of text and a table/diagram section which are separated by the bibliography referring to the original literature (see Fig. 1). The tables and diagrams carry the essential constitutional information and are commented on in the text if necessary.
Where published data allow, the following sections are provided in each report:

Introduction

The opening text reviews briefly the status of knowledge published on the system and outlines the experimental methods that have been applied. Furthermore, attention may be drawn to questions which are still open or to cases where conclusions from the evaluation work modified the published phase diagram.

Binary Systems

Where binary systems are accepted from standard compilations reference is made to these compilations. In other cases the accepted binary phase diagrams are reproduced for the convenience of the reader. The selection of the binary systems used as a basis for the evaluation of the ternary system was at the discretion of the assessor.

Solid Phases

The tabular listing of solid phases incorporates knowledge of the phases which is necessary or helpful for understanding the text and diagrams. Throughout a system report a unique phase name and abbreviation is allocated to each phase.

DOI: 10.1007/978-3-540-74196-1_1

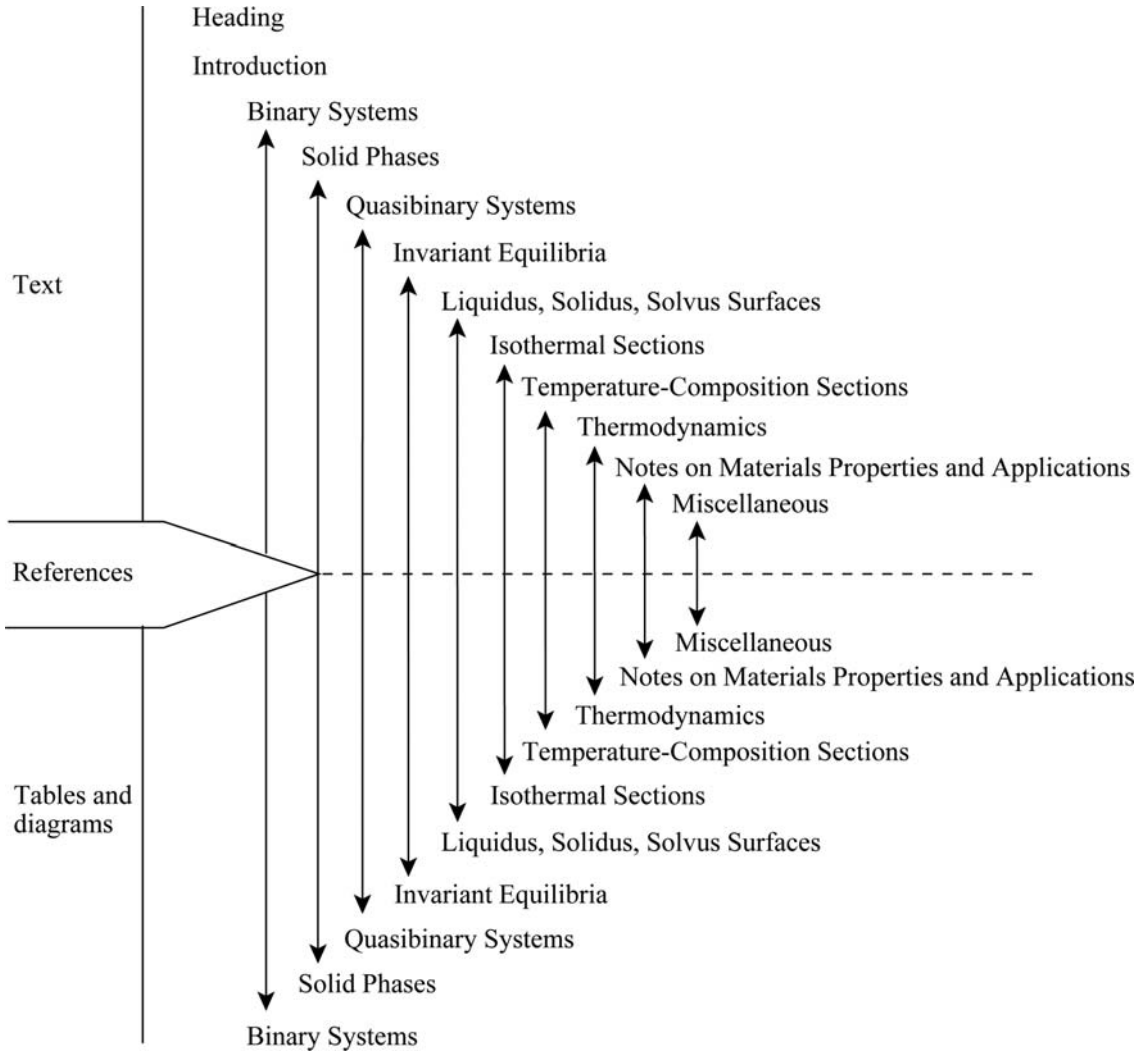

Fig. 1. Structure of a system report

Phases with the same formulae but different space lattices (e.g. allotropic transformation) are distinguished by:

- small letters (h), high temperature modification ($h_2 > h_1$)
  (r), room temperature modification
  (1), low temperature modification ($l_1 > l_2$)
- Greek letters, *e.g.*, ε, ε'
- Roman numerals, *e.g.*, (I) and (II) for different pressure modifications.

In the table "Solid Phases" ternary phases are denoted by * and different phases are separated by horizontal lines.

Quasibinary Systems

Quasibinary (pseudobinary) sections describe equilibria and can be read in the same way as binary diagrams. The notation used in quasibinary systems is the same as that of vertical sections, which are reported under "Temperature – Composition Sections".

DOI: 10.1007/978-3-540-74196-1_1

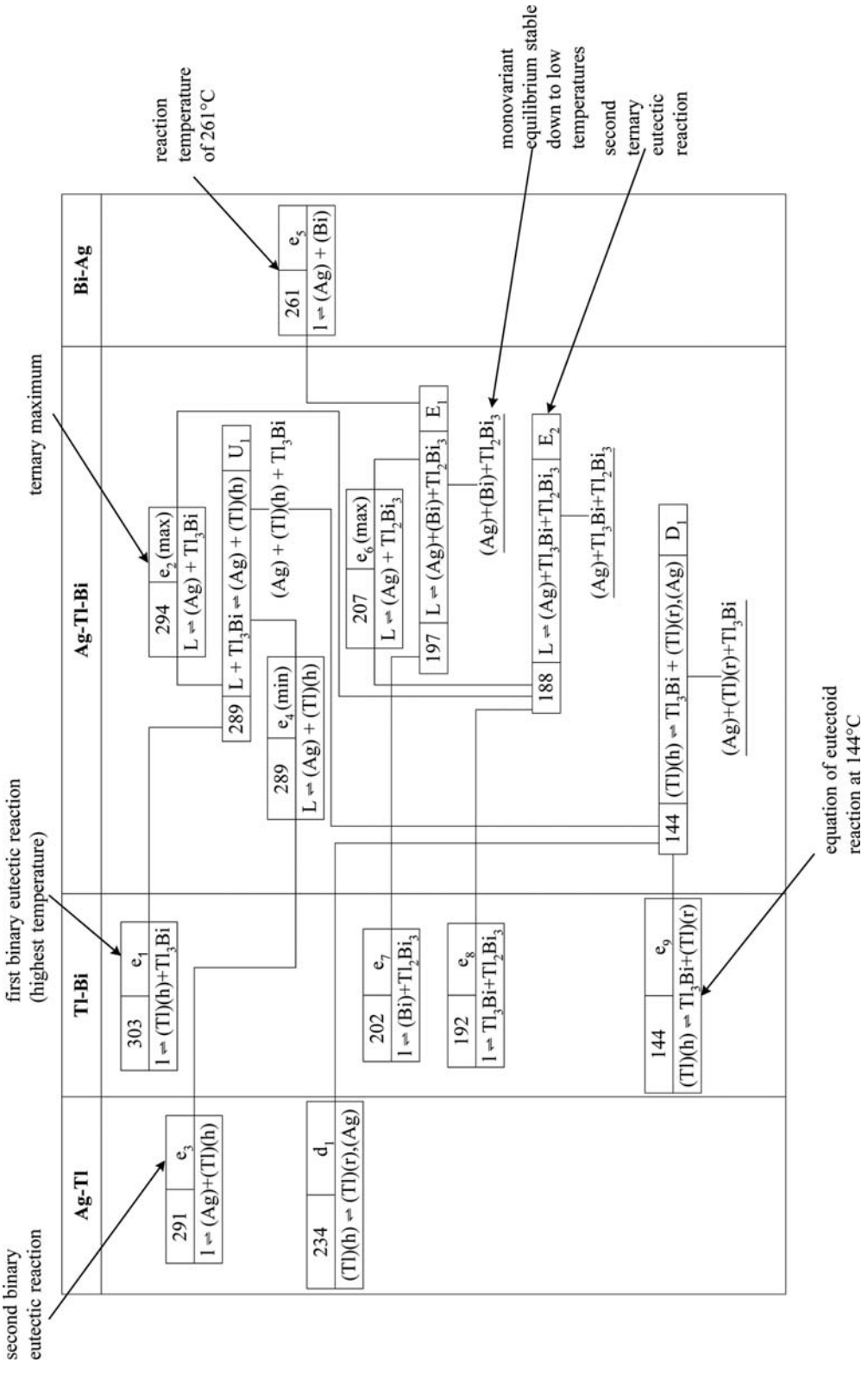

Fig. 2. Typical reaction scheme

DOI: 10.1007/978-3-540-74196-1_1

Invariant Equilibria

The invariant equilibria of a system are listed in the table "Invariant Equilibria" and, where possible, are described by a constitutional "Reaction Scheme" (Fig. 2).
The sequential numbering of invariant equilibria increases with decreasing temperature, one numbering for all binaries together and one for the ternary system.
Equilibria notations are used to indicate the reactions by which phases will be

- decomposed (e- and E-type reactions)
- formed (p- and P-type reactions)
- transformed (U-type reactions)

For transition reactions the letter U (Übergangsreaktion) is used in order to reserve the letter *T* to denote temperature. The letters d and D indicate degenerate equilibria which do not allow a distinction according to the above classes.

Liquidus, Solidus, Solvus Surfaces

The phase equilibria are commonly shown in triangular coordinates which allow a reading of the concentration of the constituents in at.%. In some cases mass% scaling is used for better data readability (see Figs. 3 and 4).
In the polythermal projection of the liquidus surface, monovariant liquidus grooves separate phase regions of primary crystallization and, where available, isothermal lines contour the liquidus surface (see Fig. 3).

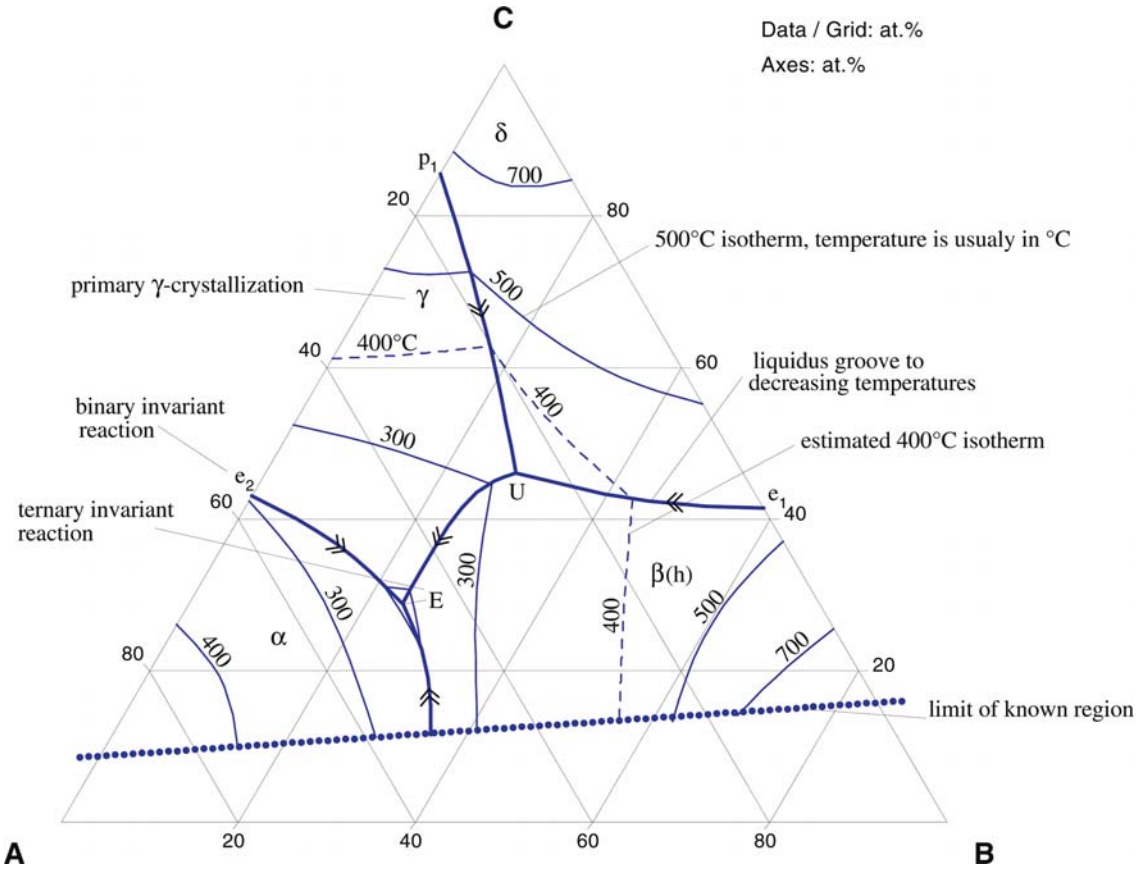

Fig. 3. Hypothetical liquidus surface showing notation employed

DOI: 10.1007/978-3-540-74196-1_1

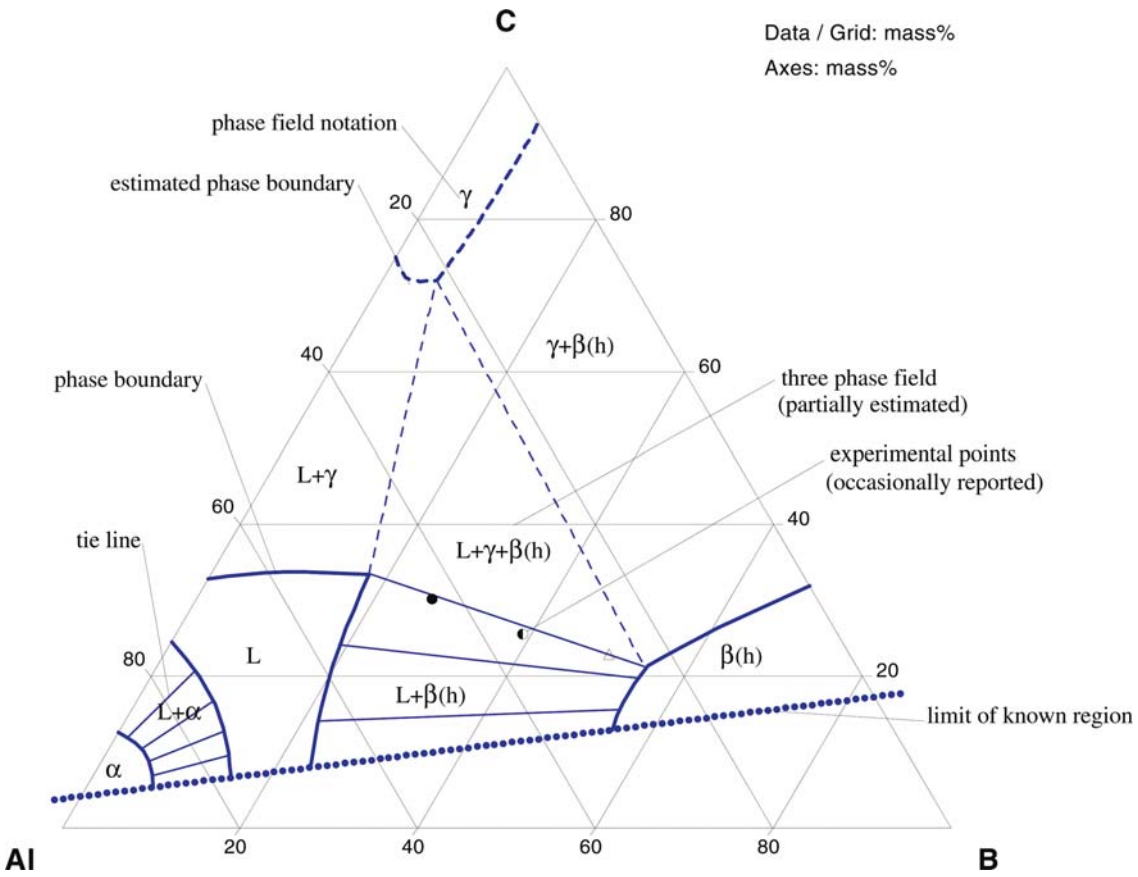

Fig. 4. Hypothetical isothermal section showing notation employed

Isothermal Sections

Phase equilibria at constant temperatures are plotted in the form of isothermal sections (see Fig. 4).

Temperature – Composition Sections

Non-quasibinary *T-x* sections (or vertical sections, isopleths, polythermal sections) show the phase fields where generally the tie lines are not in the same plane as the section. The notation employed for the latter (see Fig. 5) is the same as that used for binary and quasibinary phase diagrams.

Thermodynamics

Experimental ternary data are reported in some system reports and reference to thermodynamic modeling is made.

Notes on Materials Properties and Applications

Noteworthy physical and chemical materials properties and application areas are briefly reported if they were given in the original constitutional and phase diagram literature.

DOI: 10.1007/978-3-540-74196-1_1

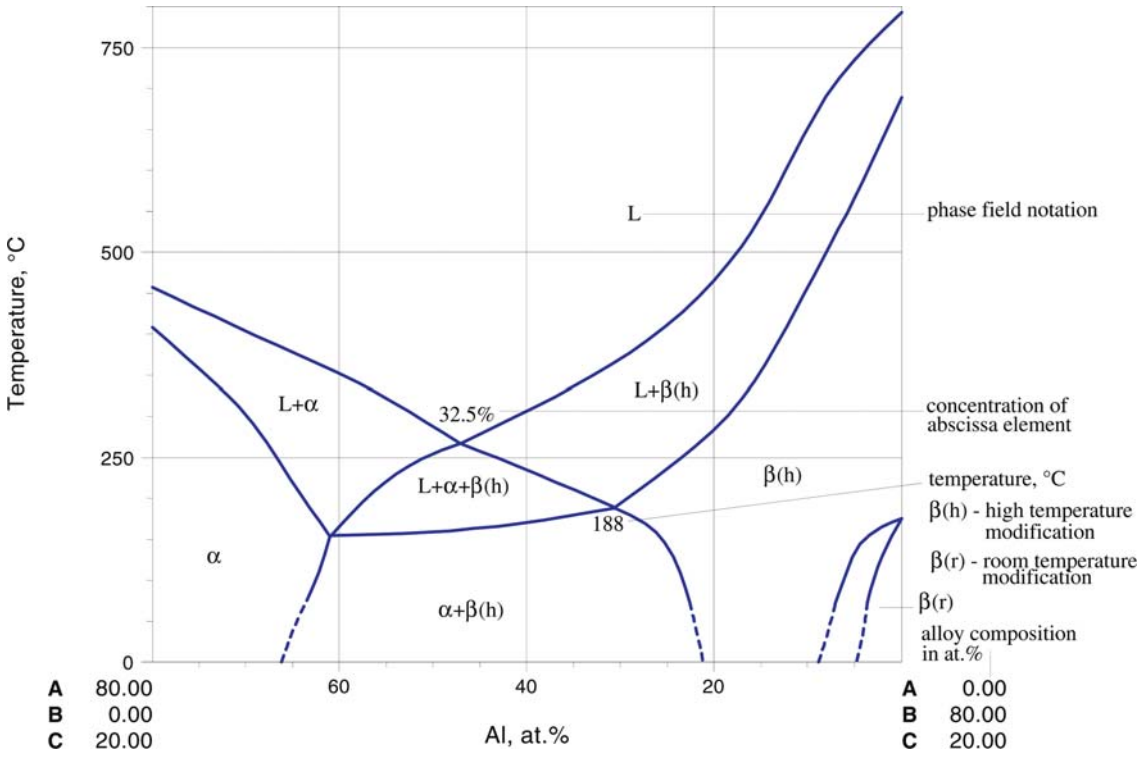

Fig. 5. Hypothetical vertical section showing notation employed

Miscellaneous

In this section noteworthy features are reported which are not described in preceding paragraphs. These include graphical data not covered by the general report format, such as lattice spacing – composition data, *p-T-x* diagrams, *etc.*

DOI: 10.1007/978-3-540-74196-1_1

References

The publications which form the bases of the assessments are listed in the following manner:
[1974Hay] Hayashi, M., Azakami, T., Kamed, M., "Effects of Third Elements on the Activity of Lead in Liquid Copper Base Alloys" (in Japanese), *Nippon Kogyo Kaishi*, **90**, 51–56 (1974) (Experimental, Thermodyn., 16)
This paper, for example, whose title is given in English, is actually written in Japanese. It was published in 1974 on pages 51–56, volume 90 of Nippon Kogyo Kaishi, the Journal of the Mining and Metallurgical Institute of Japan. It reports on experimental work that leads to thermodynamic data and it refers to 16 cross-references.
Additional conventions used in citing are:

to indicate the source of accepted phase diagrams

* to indicate key papers that significantly contributed to the understanding of the system.

Standard reference works given in the list "General References" are cited using their abbreviations and are not included in the reference list of each individual system.

General References

[C.A.] *Chemical Abstracts* - pathways to published research in the world's journal and patent literature - *http://www.cas.org/*

[Curr. Cont.] *Current Contents* - bibliographic multidisciplinary current awareness Web resource - *http://www.isinet.com/products/cap/ccc/*

[E] Elliott, R.P., *Constitution of Binary Alloys, First Supplement*, McGraw-Hill, New York (1965)

[G] Gmelin *Handbook of Inorganic Chemistry*, 8th ed., Springer-Verlag, Berlin

[H] Hansen, M., and Anderko, K., *Constitution of Binary Alloys*, McGraw-Hill, New York (1958)

[L-B] Landolt-Boernstein, *Numerical Data and Functional Relationships in Science and Technology (New Series). Group 3 (Crystal and Solid State Physics)*, Vol. 6, Eckerlin, P., Kandler, H., and Stegherr, A., *Structure Data of Elements and Intermetallic Phases* (1971); Vol. 7, Pies, W. and Weiss, A., *Crystal Structure of Inorganic Compounds*, Part c, Key Elements: N, P, As, Sb, Bi, C (1979); Group 4: *Macroscopic and Technical Properties of Matter*, Vol. 5, Predel, B., *Phase Equilibria, Crystallographic and Thermodynamic Data of Binary Alloys*, Subvol. a: Ac-Au ... Au-Zr (1991); Springer-Verlag, Berlin.

[Mas] Massalski, T.B. (Ed.), *Binary Alloy Phase Diagrams*, ASM, Metals Park, Ohio (1986)

[Mas2] Massalski, T.B. (Ed.), *Binary Alloy Phase Diagrams*, 2nd edition, ASM International, Metals Park, Ohio (1990)

[P] Pearson, W.B., *A Handbook of Lattice Spacings and Structures of Metals and Alloys*, Pergamon Press, New York, Vol. 1 (1958), Vol. 2 (1967)

[S] Shunk, F.A., *Constitution of Binary Alloys, Second Supplement*, McGraw-Hill, New York (1969)

[V-C] Villars, P. and Calvert, L.D., *Pearson's Handbook of Crystallographic Data for Intermetallic Phases*, ASM, Metals Park, Ohio (1985)

[V-C2] Villars, P. and Calvert, L.D., *Pearson's Handbook of Crystallographic Data for Intermetallic Phases*, 2nd edition, ASM, Metals Park, Ohio (1991)

DOI: 10.1007/978-3-540-74196-1_1

Index of alloy systems

Index of Ternary Iron Alloy Systems C-Cr-Fe to Co-Fe-S

DOI: 10.1007/978-3-540-74196-1_2

Carbon – Chromium – Iron

Anatoliy Bondar, Volodymyr Ivanchenko, Artem Kozlov, Jean-Claude Tedenac

Introduction

Owing to interest of the C-Cr-Fe alloys as a basis for irons and steels, the system has been under intense study for a period of about one hundred years. Investigations of the system with respect to phase relations, structures and thermodynamic are listed in Table 1. Crystal structures of the phases, the invariant reactions and studies of physical properties are listed in Table 2 to 4.

The first review of some commercial alloys of iron, chromium and carbon in the higher chromium range was already made in 1923 by [1923Mac]. The first reviews of phase equilibria in the C-Cr-Fe system were presented by [1936Mon, 1936Tof1, 1949Jae]. Some brief information on phase equilibria in this system may be found in [1972Jel, 1984Hol]. The first review of thermodynamic properties of Fe base systems including C-Cr-Fe system was presented by [1959Neu]. A projection of the metastable C-Cr-Fe phase diagram was constructed by [1976Gor] using their own data and information from the literature. Eutectic polyhedration of the C-Cr-Fe system has been performed by [1982Sil]. [1997Sil] refined the C-Fe diagram on the basis of the result of a thermodynamic analysis and generalization of data for the C-Fe and C-Cr-Fe systems. A general algorithm for the prediction of phase equilibria in multicomponent systems utilizing the thermodynamic properties of the phases involved has been proposed by [2000Ran]. The C-Cr-Fe system was used as an example to illustrate the approach in the case of ternary systems. Different semi-empirical equations for estimating the melting temperatures of low alloyed and stainless steels, including C-Cr-Fe, were analyzed by [2001Mie].

[1966Mes] reported an analysis of experimentally determined carbon activities in the C-Cr-Fe system as a means to check the self-consistency of the data from [1958Bun] related to the boundaries of the $\gamma + M_7C_3$ phase field at 1050°C. The partition coefficient of Cr between cementite and ferrite at 500-700°C was measured by [1976Ko]. The influence of temperature and alloying elements on the solubility of C in Fe rich ternary melts saturated with carbon was reviewed by [1969Sch].

Isoplethal sections at 5 and 20 at.% Cr have been calculated by [1995Par] using new computer software. The phase equilibria between liquid, austenite, ferrite and carbides were calculated using different models [1977Lun, 1977Wal, 1977Uhr1, 1977Uhr2, 1978Uhr, 1983Sil, 1987Sch, 1989Zhu1, 1989Zhu2, 1995Lee, 1999Nak]. Both thermochemical data and experimental information on the phase equilibria were used to evaluate the parameters needed for the description of the Gibbs energy of the individual phases. By using these values the phase equilibria were calculated and compared with experimental data. The most reliable thermodynamic assessments of the C-Cr-Fe system were performed by [1988And, 1991Hil, 1992Lee, 1995Lee, 1995Par]. Experimental studies of phase equilibria have been reviewed by [1984Riv, 1988Ray, 1994Rag, 2002Rag].

The technique of successive partial equilibria has been employed to predict the equilibrium precipitation of carbides in iron-based systems by [1996Ran]. The solidification path and solute redistribution between the solid and liquid phases have been modelled for the C-Cr-Fe alloys by [2002Him]. A thermodynamic analysis of phase transformations and reactions in the C-Cr-Fe alloys was carried out by [2005Als] with allowance made for all possible states in the temperature range of metal dusting in aggressive carboniferous media. The results were compared with data on the corrosion resistance of Cr steel pipes under oil refining conditions. The suitability of C-Cr-Fe alloys for semi-solid processing was investigated by [2005Bal] using a numerical simulation.

The trends in ternary carbide formation in Fe base systems have been briefly reviewed by [1967Gol, 1990Ere]. Aspects of the construction of diagrams of ternary systems formed by Cr and C with d-transition metals have been presented by [1996Bon, 1997Hil].

The reliability of cooling and heating data for use in the assessment of equilibrium and metastable states was discussed by [1993Zha] using the C-Cr-Fe alloys as an example. The effect of solute atoms on the chemical bonding of Fe_3C has been studied by [1997Miz] using first-principles molecular orbital calculations.

DOI: 10.1007/978-3-540-74196-1_3

MatCalc was applied by [2000Koz1] for the calculation of ortho-equilibrium (full equilibrium) and para-equilibrium (metastable) phase diagrams of Fe-C-2.8 mass% Cr. A new computer model for Scheil-Gulliver simulations taking into account back-diffusion of highly mobile alloying components has been applied by [2000Koz2] to the simulation of the segregation of Cr in the C-Cr-Fe alloys. The delineation of crystallization path in ternary C-Cr-Fe alloys has been presented by [2001Goe].

The $\gamma \rightleftharpoons \alpha$ transformation in low-carbon chromium steels at cooling rates ranging from 80 to 10^5 $K \cdot s^{-1}$ has been studied by [1973Mir, 1986Mir]. The nucleation, growth and morphology of carbides forming under decomposition of supersaturated austenite in near-eutectic white cast irons have been studied by [1992Pow, 1994Pow]. Morphology and thermodynamics of the bainitic transformation has been studied by [1991Eno]. The main features of phase transformations in chromium steels have been studied by [1996Jun, 1999Sht1, 1999Sht2, 1999Sht3, 1999Sht4]. They are as follows: the crystallography of pearlite with M_7C_3 carbide lamellae and the atomic structure at the ferrite/carbide interface [1999Sht1], the mechanism of austenite formation and the kinetics of cementite lamellae dissolution [1999Sht2], orientation relationships between ferrite, martensite and cementite [1999Sht3], morphology of ferrite precipitates within cementite and mechanism of their formation [1999Sht4]. The dissolution of cementite in austenite was studied experimentally by [1991Liu1, 1991Liu2]. The effect of alloying elements on precipitation in ferritic steels, including Fe-12.32 at.% Cr-0.693 at.% C has been modeled by [2003Yin]. The effect of carbon on the structure of austenitic and martensitic steels was discussed by [2003Gav]. In order to produce a simple mathematical relationship for the constitutive behavior of tempered martensitic steels, the tensile properties of model C-Cr-Fe alloys were measured by [2004Bon1, 2004Bon2]. Efforts were focused on the effect of the prior austenitic grain size on yield stress and strain hardening. The simulation of the kinetics of precipitation reactions in ferritic steels was performed by [2005Sch]. The influence of Cr on the Snoek peak of carbon in bcc iron was investigated by [2004Sai].

The simulation of diffusional reactions on the decomposition of cementite was investigated using the software package, DICTRA [1991Liu1, 2000Bor]. The effect of prior cold deformation on diffusion of carbon in chromium alloyed with iron was presented by [1968Mat]. [1969Bor, 1970Bor] investigated the effect of alloying with iron on the carbon diffusion in chromium. The carbon diffusivities in Cr-steels, both in austenite and ferrite, activity coefficients of carbon and carbon-chromium thermodynamic interaction parameters ε_C^{Cr} in austenitic and ferritic C-Cr-Fe solid solutions were estimated by [1995Mil]. The effective interdiffusion coefficients for the metallic elements in austenite and ferrite in the C-Cr-Fe system have been derived by [1995Pop, 1999Pop]. A review of the methods of determining the driving forces for diffusion of carbon and alloying elements, including Cr, upon phase transformations has been performed by [2001Sht]. Couple solute drag-effects in relation to ferrite formation in C-Cr-Fe steel have been studied by [2004Aar].

The thermodynamic analysis of martensite formation was performed in [2000Kun].

Influence of carbon on the viscosity of liquid C-Cr-Fe alloys has been studied by [1967Bau]. The wetting of Cr_3C_2 by liquid iron has been studied by [1966Yas].

[1985Vit, 1986Kli] studied sintering, structure and some mechanical properties of powdered alloys in the Cr_3C_2-Fe system. Laser surface alloying of Cr with electrolytic pure iron and carbon steels was carried out by [1983Mol] in order to produce high chromium ferritic steels. The morphology of ferrite was then investigated as a function of C and Cr contents of these alloys.

The carburization of Cr-alloyed steels has been studied by [1965Bun]. The decarburization of Fe-Cr alloys, containing about 0.1 mass% C and more, by hydrogen plasma was investigated by [1975Kan]. A thermodynamic estimation of the reduction behavior of Cr-Fe ore with carbon has been performed by [1998Hin]. The effect of intrinsic factors on primary and secondary arm spacing of dendrites of iron base solid solutions was investigated by [2003Kud]. An SEM study of the nucleation of M_7C_3 carbide during the eutectic solidification of high-chromium white irons has been presented by [2005Bed].

A study of the phase composition of two splat quenched alloys was presented by [1969Ruh]. [1983Ber] showed that metallic glass may be prepared by the rapid quenching of $Cr_{40}Fe_{41}C_{19}$.

DOI: 10.1007/978-3-540-74196-1_3

Binary Systems

The C-Fe phase diagram is accepted from the MSIT Binary Evaluation Program [2006MSIT]. For the Cr-Fe system, the phase diagram is taken from the assessment of [1987And], which is essentially the same as that given by [Mas2] and [1993Itk].
The C-Cr phase diagram is accepted as in [Mas2], which is based mainly on the review of [1990Ven]. This used the experimental data of [1969Rud] for the invariant reaction temperatures and the C solubility reported in [1977Pou, 1985Pou]. The invariant reaction temperatures were later confirmed by [1981Kno] using DTA analysis. Another version of the C-Cr phase diagram published in [1987Ere, 1996Bon] differs only by higher temperatures for the invariant reactions, which had also been confirmed by DTA studies [1985Koc, 1986Dan, 1989Gri]. They used alloys prepared from similar materials as used in the other work (electrolytically purified Cr of about 99.8-99.9 mass% Cr). Here, the version of [Mas2] is preferred due to the fact that the temperatures of [1969Rud, 1981Kno] were used in the available thermodynamic assessments of data on the C-Cr-Fe system.

Solid Phases

Crystallographic data of the binary and ternary phases are listed in Table 2. There are no ternary compounds in this system, apart from a metastable phase that was found by [1980Iwa] in alloys rapidly quenched from the liquid state. On the other hand, the binary phase Fe_3C is considered as metastable while in the ternary system the M_3C phase based on Fe_3C, is thermodynamically stable in the temperature range 658 to 1187°C [1988And] (658 to 1230°C after [1991Hil]), where it has the appearance of a ternary phase in the stable phase diagram (Figs. 1 to 4). As pointed in [1976Gor, 1984Riv, 1988Ray], the M_3C cementite phase is stabilized by approximately 1 mass% Cr. Its homogeneity range extends up to 17 mass% (14.5 at.%) Fe or $(Fe_{0.8}Cr_{0.2})_3C$ [1976Woo, 1974Ben]. The maximum Cr solubility in Fe_3C was found experimentally as 15.3 at.% or 18 mass% [1953Kuo1], 18.9 at.% or 22.2 mass% [1971Lei] and 20.4 at.% or 24.0 mass% at 700°C [1972Jel], 15.5 at.% or 18.5 mass% at 795°C [1970Jac], 12.8 at.% or 15 mass% [1928Wes] and 15 at.% or 17.6 mass% [1977Nis1] at 1000°C. Thermodynamic assessments resulted in a maximum Cr solubility of 13.1 at.% or 15.3 mass% [1988And] and 12.6 at.% or 14.8 mass% [1991Hil], which are somewhat lower than most of the experimental values.
Crystal structure and magnetic properties of solid solutions based on the Fe_3C binary compound were investigated by [1966Kud] and [1975Shi]. The temperature dependence of the lattice parameters and unit cell volume for cementite, pure and containing Cr, extracted from alloys annealed at 600 and 1000°C was investigated by [1979Kag]. At room temperature, the lattice parameters *vs* composition curves were shown to have a non-linear character. Materials containing less than 7 at.% Cr are ferromagnetic while those containing more than 7 and up to 20 at.% Cr are paramagnetic at room temperature. The lattice parameters of the ferromagnetic state are larger than those of the paramagnetic modification.
Investigations of the solubility of the third element in the carbides were carried out by [1928Wes, 1953Kuo1, 1965Glo, 1966Kud, 1967Las, 1970Jac, 1975Shi, 1979Kag, 2003Car1]. The maximum Fe solubility in $Cr_{23}C_6$ seems to be 34-34.5 at.% or 42.5-43 mass%, taking into account the data of [1976Woo, 1974Ben] and the assessment of [1988And].
Crystallographic investigations of the binary compound Cr_7C_3 and the solid solution based on this compound undertaken by [1965Glo, 1987Ber, 2003Nes, 2003Car1, 2003Car2] revealed a hexagonal symmetry, rather than the orthorhombic symmetry found by [1970Rou, 1985Kow]. The Fe solubility in Cr_7C_3 in equilibrium with $M_{23}C_6$ and the metallic phases was estimated to be 36.3 at.% or 49.0 mass% [1972Jel], 37.1 at.% or 50 mass% [1953Kuo2] and 37.7 at.% or 50.8 mass% [1971Lei] at 700°C, 46.7 at.% or 62.4 mass% at 795°C [1970Jac], 43.4 at.% or 58.1 mass% at 870°C [1976Woo], 41 at.% or 55 mass% [1928Wes] and 43 at.% or 57.6 mass% [1974Ben] at 1000°C. The maximum Fe solubility in Cr_7C_3 (in the equilibrium $M_7C_3 + M_{23}C_6 + (C)gr$) should be higher by 5 to 10 mass% or 4 to 8 at.% (as estimated in [1977Nis1, 1974Ben, 1988And, 2004Ten, 2005Ten]), which could reach the composition $(Cr_{0.2}Fe_{0.8})_3C_2$.
[1975Cos] investigated the solubility of carbon in two Cr-Fe alloys with 2.0 and 3.5 at.% Cr at 716°C (in the α phase). It was found that the solubility decreased with increasing Cr content. The solubility values are

DOI: 10.1007/978-3-540-74196-1_3

10.9 and 6.3 mass ppm, respectively, for alloys with 2.0 and 3.5 at.% Cr. At 1150°C, the maximum carbon solubility in the α phase, as found in [1974Ben], was about 0.1 mass% (at ~17 mass% Cr).
The homogeneity range of the γ phase was presented in [1991Hil] as a projection of boundary isotherms and solvus curves of monovariant reactions (Fig. 5). This work was the result of a thermodynamic assessment. As can be seen, the γ phase extends up to 2 mass% C (at 1150°C) and 19.5 mass% Cr (at 1300°C), whilst disappearing at 734°C.

Invariant Equilibria

The reaction scheme (Fig. 1, Table 3) is based on a compilation of experimental data given in [1984Riv, 1988Ray] for the high-temperature range including U_4 at 1160°C, and the thermodynamic assessment of 1991Hil] for the solid equilibria and E_1. The solid-state equilibria resulting from the thermodynamic assessment of [1991Hil] should be preferred to those of [1984Riv, 1988Ray], since [1991Hil] evaluated all available data on both phase equilibria and thermodynamics. It should be mentioned here that the actual solidification path of some alloys results in metastable equilibria, corresponding to Fig. 2, as noted below.

Liquidus, Solidus and Solvus Surfaces

The crystallization behavior of the system has been established by a number of workers [1923Aus, 1962Gri, 1970Jac, 1985Tho, 2001Goe, 2003Yam] (Fig. 2). These data (identification of primary phases, metallographic studies for as-cast alloys, melting points obtained by DTA or TA) indicate that there is a combined crystallization of the metallic α phase (Cr, αδFe) and the carbide M_7C_3 along with a monovariant eutectic reaction $L \rightleftharpoons \alpha + M_7C_3$ followed by $L \rightleftharpoons \gamma + M_7C_3$. The microstructure of an alloy showing both eutectics, $\alpha + M_7C_3$ and $\gamma + M_7C_3$, close to each other, was presented in [2001Goe]. However [1958Bun], by using metallography, dilatometry, XRD and chemical analysis to study annealed and quenched samples of 170 different alloy compositions, as well as extracted carbides, found evidence of the equilibrium $L + \gamma + M_{23}C_6$ in partially melted specimens. They presented their results in the form of isopleths, which showed $\gamma + M_{23}C_6$ the two phase field to be stable up to the solidus surface.
Thus, there is controversy over which monovariant phase equilibrium, $L + \alpha + M_7C_3$ or $L + \gamma + M_{23}C_6$, is stable on the liquidus surface. The former was found experimentally by [1962Gri, 1970Jac, 1985Tho, 2001Goe, 2003Yam] and calculated in the thermodynamic assessments by [1992Lee, 1995Lee, 1995Par, 2003Yam]. The latter was presented based on experiments of [1958Bun, 1972Jel], accepted in the reviews [1977Nis2, 1984Riv, 1986Sch, 1988Ray] (Fig. 3) and the thermodynamic assessments of [1988And, 1991Hil]. Thus, the equilibrium accepted in the thermodynamic assessments [1988And, 1991Hil, 1992Lee, 1995Lee, 1995Par] (which may be considered as interrelated as they originated from the same laboratory) changed from the latter to former equilibrium in subsequent work. As reported in [1992Lee], the liquidus surface close to the experimental data of [1985Tho] results from the reassessment of the ternary system and the binary C-Cr, mainly taking into consideration some data from the higher order system. Thermodynamically speaking, both variants are very close to each other and a small change in the thermodynamic parameters given by [1988And, 1991Hil], made in [1992Lee, 1995Lee, 1995Par], leads to the change in the phase equilibria. The temperature at which the $M_{23}C_6$ phase appears *via* the solid-state invariant reaction $\gamma + \alpha + M_7C_3 \rightleftharpoons M_{23}C_6$ was calculated to be 1070°C by [1995Par]. This is too low however, because [1988And] observed the three-phase equilibrium $\gamma + M_7C_3 + M_{23}C_6$ at 1200°C.
There is an explanation consistent with both versions of liquidus, but it implies rather unexpected properties of the phases in the ternary system. For the Fe rich $M_{23}C_6$ carbide, separation from the melt should be fully kinetically impeded (unlike the binary $Cr_{23}C_6$ carbide and the $Cr_{23}C_6$-based phase in a number of other ternary systems [1996Bon]). Thus, in the range of less than 60 mass% Cr, $M_{23}C_6$ never separates from the melt, neither as a primary nor as a eutectic phase. Even under the conditions of unidirectional solidification (the rate of solidification 10 to 150 mm/h), an alloy of a composition on the liquidus curve of the monovariant eutectic $L \rightleftharpoons \gamma + M_{23}C_6$ after [1958Bun, 1972Jel, 1984Riv, 1986Sch, 1988Ray, 1988And, 1991Hil], Fe - 30.8 Cr - 2.85 C (mass%) crystallized as $\gamma + M_7C_3$ [2003Lu]. This leads to the conclusion that Fig. 2 may be considered as a metastable liquidus surface projection and Fig. 3 the stable one.

DOI: 10.1007/978-3-540-74196-1_3

The alternative conclusion requires the rejection of all the data of [1958Bun] in the vicinity of the $\gamma + M_{23}C_6$ solidus temperatures, as well as those of [1972Jel], owing to doubts in the validity of their observation. Besides, one may assume that in the work of [1958Bun, 1972Jel], the Fe rich $M_{23}C_6$ carbide could have been formed during cooling after annealing, but such a high rate of $M_{23}C_6$ formation in the solid from unrelated phases has not been reported elsewhere. In both the study of a unidirectionally solidified Fe - 30.8 Cr - 2.85 C (mass%) alloy by [2003Lu] and in the study of an as-cast Fe - 30.0 Cr - 2.26 C (mass%) alloy by [2005Wie], trace amounts of $M_{23}C_6$ were detected as secondary phases as found by [2005Wie]. Earlier, the same authors [2004Wie] studied the rate of $M_{23}C_6$ formation at 900 to 1100°C in the latter alloy. It was found that after 2 h the fraction of $M_{23}C_6$ in the eutectic carbides was almost 99% after annealing at 1100°C, and about 75% and 33% after annealing at ~1000 and 900°C, respectively.

So, further investigations are needed to solve this problem. In the present evaluation the $L + \gamma + M_{23}C_6$ equilibrium is considered as stable, as suggested by [1958Bun, 1972Jel, 1984Riv, 1986Sch, 1988Ray, 1988And, 1991Hil]. Figure 3 presents the equilibrium liquidus surface. It was taken from [1984Riv, 1988Ray] with corrections relating to the monovariant reaction $L \rightleftharpoons \gamma + (C)gr$. To correct the invariant points e_2, e_3 and p_2 is impossible without destroying the system of monovariant liquidus lines and isotherms. For the alloy melting/solidification, another version (similar to the C-Fe system) should be applied, which is given in Fig. 2. It is based on the experimental results of [1985Tho] in the Fe rich range (up to 40 mass% Fe and 6 mass% C) and on the calculation of [1992Lee]. The recent experimental work of [2003Yam] is consistent with this version.

The liquidus surface projection of [1984Riv, 1988Ray] (Fig. 3) includes the isotherms of graphite saturation for the carbon-saturated melt as presented in [1962Gri] after extensive studies. More focused studies like those of [1956Oht] at 1545°C, Esin & Vatolin's work at 1460°C (cited in [1956Oht]), [1969Sch] at 1550°C and [1996Kob] at 1460°C are in agreement with the extensive work of [1962Gri]. Others are close to the results of [1962Gri] only at the Cr contents less than ~10 mass%, *e.g.* the results of [1970Had] at 1600°C and [2001Wan, 2002Wan] at 1450°C. The isotherms of [1956Oht] at 1445°C, of [1996Kob] at 1400 and 1500°C and of [1957San] at 1545°C are higher or lower by about 50°C and strongly bended. [2001Wan, 2002Wan] obtained a linear relationship expression of the carbon-saturated solubility in the C-Cr-Fe melt (the graphite liquidus) for the temperature interval from 1350 to 2000°C. This relationship was based on experimental data of [1970Had, 1996Kob, 1999Ma] and reads as follows: $x_C = 0.052 + 0.848 \cdot 10^{-4} T + 0.2544 x_{Cr}$ (where x_C is the carbon-saturated solubility in molar fraction, x_{Cr} is Cr molar fraction in liquid and T is temperature in K).

In Fig. 3 the primary surface of M_3C is also preferred from [1962Gri]. The surfaces of primary crystallization for $M_{23}C_6$ and M_7C_3 and for the metal phases α (αδ) and γ are presented after [1958Bun] and [1962Pep], the latter only at 70 mass% Cr. Later [1985Tho] confirmed the liquidus curve $L \rightleftharpoons \gamma + M_7C_3$ and the filed of primary crystallization for M_3C. For the Fe rich part up to 1.2 mass% C and 30 mass% Cr detailed liquidus isotherms are reported by [1984Kun].

Partition coefficients of Cr and C, k_{Cr} and k_C, in solid/liquid equilibria for alloys with 2 and 6 at.% Cr have been presented by [1989Bat]. More recent investigations of [2003Yam] obtained partition coefficients k_{Cr} and k_C for solid/liquid equilibria in the range of eutectics of the γ phase with M_7C_3 and M_3C, using EPMA on remelted ingots and calculations with the ThermoCalc package.

Figure 4, the projection of the solidus surface, corresponds with the liquidus surface in Fig. 3. Extensions of the phases in the solidus surface are mainly based on the thermodynamic assessment by [1988And] and experimental works on the solubility of Fe in chromium carbides and Cr in M_3C. The position of the γ phase and the Fe solubility in M_3C are taken from the thermodynamic assessment by [1991Hil] (Fig. 5).

Isothermal Sections

A number of isothermal sections presented in Figs. 6 to 12 display main peculiarities of the phase diagram. Data on composition of M_7C_3, $M_{23}C_6$ and M_3C in phase equilibria from 527°C up to melting are summarizes in Fig. 13.

Figure 6 shows at 1400 °C equilibria with an extensive liquid phase field, Fig. 7 at 1200°C, shows a narrow liquid field, shortly after the first appearance of the liquid phase. They were calculated by [1998Hin] using thermodynamic parameters of [1988And]. The 1200°C isothermal section of [1998Hin] contains the

DOI: 10.1007/978-3-540-74196-1_3

$\gamma + M_{23}C_6$ equilibrium in agreement with the experiments of [1988And], but in conflict with the computation of [1995Par] at 1200 and 1060°C and in disagreement with the isothermal sections of [1970Jac] at 1150 and 900°C.

The isothermal section at 1000°C is the most frequently reported one in literature, both from experimental data [1958Bun, 1964Bun, 1974Ben, 1977Nis1, 1977Nis2, 1994Sop] and from thermodynamic computation [1981Nis, 1988And, 1991Hil, 1992Lee, 1994Sop, 2004Bra, 2004Ten, 2005Ten]. The version presented in Fig. 8 is predominantly based on the data of [1974Ben].

The data of [1974Ben] are in good agreement with [1976Woo] at 870°C (Fig. 9). As seen in Fig. 13, it is impossible to choose any experimental data at 700°C being the most reliable ones. The 750 and 700°C isothermal sections are taken from [1979Sha1] and [1972Jel], respectively, although in the 700°C isothermal section of [1972Jel] the Cr solubility in cementite seems to be overestimated.

At this temperature the γ phase field is shaped like a binary carbide in the topology of the phase diagram. The 527°C isothermal section calculated by [1988And] is presented in Fig. 12. It demonstrates lower Fe solubility in $M_{23}C_6$ and M_7C_3, with the cementite phase being absent as shown in Figs. 1 and 5. At the same time, [1976Ko] gave data on the equilibrium ferrite + cementite ($\alpha + M_3C$) in the range of 500 to 700°C, and [1971Lei] presented equilibria of the cementite phase from 600 to 700°C. Thermodynamically the cementite phase M_3C should be considered as metastable at temperatures below its eutectoid decomposition $M_3C \rightleftharpoons \alpha + M_7C_3 + (C)gr$, 658°C [1988And] or 734°C [1991Hil]. The same phase equilibria and the absence of M_3C characterizes the 627°C isothermal section calculated by Ansara as cited in [1994Rag].

The dissertation of [2004Ten] and the subsequent publication [2005Ten] found after annealing at 800°C two three-phase alloys inside the M_7C_3+Cr_3C_2+(C)gr three-phase field. Their compositions were 9.6 C - 70.4 Cr - 20 Fe and 14.4 C - 65.6 Cr - 20 Fe (in mass%). Because these alloys are close to the M_7C_3 carbide, we have estimated from this the vertex at which the three-phase field meets the M_7C_3 carbide to be approximately $(Cr_{0.77}Fe_{0.23})_7C_3$.

Temperature – Composition Sections

Figures 14 to 21, a series of vertical sections by [1958Bun] reflect the C-Cr-Fe phase diagram quite well. Isothermal lines of the invariant equilibria $\gamma + M_{23}C_6 \rightleftharpoons \alpha + M_7C_3$ (U_5) and $\gamma + M_7C_3 \rightleftharpoons \alpha + M_3C$ (U_6) are remained as published in [1958Bun] at 795 and 760°C, respectively. Their temperatures and compositions can not be corrected to agree with the accepted reaction scheme (Fig. 1, Table 3). Such a correction would be in contradiction with experimental points of [1958Bun]. More experimental data are needed to achieve agreement with the reaction scheme and mutually consistent sets of isothermal and vertical sections. Corrections were made for the metastability of M_3C and its eutectoid decomposition at 658°C (E_3). The most interesting of the vertical sections were calculated in the course of thermodynamic computation by [1988And, 1992Lee] (the 13 mass% Cr isopleth) and by [2003Yin] (the 0.693 at.% C isopleth). Both are in good agreement with experimental data.

Thermodynamics

This chapter adds comments and details on experimental measurements which are summarized in Table 1. Thermodynamics of formation of $Cr_{23}C_6$ and mixed iron-chromium carbides $(Cr_{1-x}Fe_x)_{23}C_6$ were firstly investigated by [1965Ale]; these data were not further considered in this evaluation because of their internal inconsistencies. Later [1977Nis2, 1988Pil] experimentally examined stabilities of binary carbides and mixed M_3C, $M_{23}C_6$ and M_7C_3. Basing on thermodynamic analysis of phase equilibria [1989Leo1, 1989Leo2, 1991Leo] described the temperature dependencies of Gibbs energy of formation of the mixed carbides M_3C, $M_{23}C_6$, M_7C_3 and binary Cr_3C_2 by a regular solution model. The evaluations of the thermodynamic properties using the CALPHAD approach were also carried out by [1988And, 1991Gui, 1991Hil, 1992Lee, 1995Lee]. Recently, thermodynamic analysis of phase stabilities and transformations in the C-Cr-Fe system was performed by [2005Als] using the set of thermodynamic parameters of [1992Lee]. Based on estimates [2005Kun] developed thermodynamic parameters to describe the metastable martensite phase.

DOI: 10.1007/978-3-540-74196-1_3

The Cr contents in the cementite and α phase calculated by [1988And] at 700°C were close to earlier experimental data of [1976Ko], however the calculated Cr content in cementite was lower then experimentally measured by [1979Sha1] and [1972Jel]. The partition coefficient of Cr between the α phase and M_7C_3 at 700°C was higher than experimental measurements in [1972Jel]. To eliminate these discrepancies, [1991Hil] reassessed the thermodynamic parameters for M_7C_3 and $M_{23}C_6$. At 700°C, where M_7C_3 is in equilibrium with the α phase, the calculated and experimental solubilities of Cr in M_7C_3 are in good agreement, considered the discrepancy between the sets of data of [1972Jel] and [1985Wad]. The calculated solubility of $M_{23}C_6$ in the fcc γ phase with 25 mass% Cr *versus* temperature are virtually identical with the experimental results presented by [1981Nis]. A similar comparison between the γ phase and various carbides at 1000°C shows that the experimental data for M_7C_3 and cementite are well reproduced by the calculations. Later assessments by [1992Lee] used as a new description for the Cr carbides a mixture of data of [1987And] and [1990Kaj] giving twice as much weight to the data of [1987And].

The Gibbs energies of formation of the binary carbides, stable $Cr_{23}C_6$, Cr_7C_3, Cr_3C_2 and metastable Cr_3C, Fe_3C, $Fe_{23}C_6$, Fe_7C_3, were assessed by [1992Lee], as well as interaction parameters for all phases existing in the system. The Gibbs energies of formation of the ternary $(Cr_{1-y}Fe_y)_7C_3$ and $(Cr_{1-y}Fe_y)_{23}C_6$ from the binary carbides in the reactions are as follows (in J per one formula unit):

For the reaction:

$$(1-y)\cdot Cr_{23}C_6 + y\cdot Fe_{23}C_6 \rightleftharpoons (Cr_{1-y}Fe_y)_{23}C_6 \text{ and } (1-y)\cdot Cr_7C_3 + y\cdot Fe_7C_3 \rightleftharpoons (Cr_{1-y}Fe_y)_7C_3$$
$$\Delta G_f = 23\cdot G_{id.M} - y\cdot(1-y)\cdot(205342 - 141.6667\cdot T) \text{ and } \Delta G_f = 7\cdot G_{id.M} - y\cdot(1-y)\cdot(4520 + 10\cdot T).$$

For the cementite in the reaction

$$(1-y)\cdot Fe_3C + y\cdot Cr_3C \rightleftharpoons (Fe_{1-y}Cr_y)_3C$$
$$\Delta G_f = 3\cdot G_{id.M} + y\cdot(1-y)\cdot(25278 - 17.5\cdot T),$$

In here $G_{id.M}$ is the ideal Gibbs energy of metals mixing in their sublattices as $G_{id.M} = R\cdot T\cdot(y\cdot \ln y + (1-y)\cdot\ln(1-y))$.

For the C-Cr-Fe melts the enthalpy of formation was determined by means of isothermal calorimeter at 1627°C [1986Vit, 1987Vit, 1994Wit, 1995Wit] (Figs. 22 and 23). The enthalpies of mixing are continuously increasing from –44 to ~0 kJ·mol^{-1} passing from the Cr- and C-rich field to the Fe corner.

The activity coefficient of Cr in liquid alloys was measured by [1968Chi, 1970Had], and the values are in good agreement with those of [1956Oht, 1957San, 1962Gri, 1968Poi]. [1998Par] obtained the activity as a function of temperature: $\log a_{Cr} = 1.29 - 7.09\cdot x_C$ by measuring 23 samples. The activity interaction coefficients at constant concentration and temperatures between 1300 to 2000°C were presented by [2001Wan, 2002Wan] as follows:

$$\varepsilon_C^{Cr} = -0.467 - 4.426\cdot 10^4 / T + 0.099\cdot 10^4 / T^2;$$
$$\rho_C^{Cr} = 0.876 - 0.694\cdot 10^4 / T + 0.061\cdot 10^4 / T^2;$$
$$\rho_C^{C,Cr} = 1.407 + 0.571\cdot 10^4 / T;$$
$$\rho_{Cr}^{C} = -0.568 - 1.119\cdot 10^4 / T + 0.077\cdot 10^4 / T^2.$$

Interaction parameters $W_{XC} = (\partial(\mu_C)/\partial(X)_{x,\, x \rightleftharpoons 0}$ for the α and γ phases were presented by [1991Nis] as

$$W_{Cr,C}^{\alpha} = -344 + 0.185\cdot T, \text{ kJ}\cdot \text{mol}^{-1}. \text{ (670-1070°C)};$$
$$W_{Cr,C}^{\gamma} = -174 + 0.050\cdot T, \text{ kJ}\cdot \text{mol}^{-1}. \text{ (800-1400°C)};$$

which are consistent with the results of [1972Wad, 1971Gre].

[1956Oht] showed that Cr-Fe binary alloys follow Raoult's law but C-Cr-Fe alloys showed gradually negative deviation from Raoult's law when carbon was added. At 1540°C and Cr contents less than 30 at.% and at C contents less than 3 at.%, the interaction parameter was defined as $\varepsilon_C^{Cr} = (\partial(lnN_C)/\partial(N_{Cr}) = -1.40$. The effect of C at a given concentration on the activity coefficient of Cr, expressed in the interaction coefficient γ_{Cr}^{C}, is defined by the equation $\gamma_{Cr}^{C} = \gamma_{Cr} / \gamma'_{Cr}$, where γ'_{Cr} and γ_{Cr} are the activity coefficients of Cr in the Cr-Fe and C-Cr-Fe alloys, respectively. The activity coefficient and activity of Cr are expressed as

$$\log \gamma_{Cr}^{C} = -9\cdot N_{Cr}\cdot N_C / (1 - N_C)^2 = -5.5\cdot\log(1 + 0.8\cdot N_{Cr} / (1 - N_C));$$
$$a_{Cr} = N_{Cr}\cdot\exp(-2.3\cdot 9\cdot N_{Cr}\cdot N_C / (1 - N_C)^2).$$

DOI: 10.1007/978-3-540-74196-1_3

In the austenite phase the activity of C was experimentally studied by many teams: [1956Oht, 1959Neu, 1960Sch, 1963Bri, 1963Fle, 1964Pet, 1966Sch, 1968Chi, 1972Pre, 1972Wad, 1999Ma]. The results of the first six were reviewed by [1972Wad] who found good agreement as concerning the effect of Cr. Later by measuring C contents of two samples [1994Prz] gave new results showing, one more time, substantial agreement with the previous studies. The experimental data of [1977Nis1, 1977Nis2, 1971Gre, 1972Wad] on the C activity in the ternary austenite were described by [1977Uhr2] introducing the C activity and using pure graphite as standard state:

$$R\,T\cdot\ln a_C + \Delta^\circ G_C^{\gamma/(C)gr} = R\,T\cdot\ln(\gamma_C / (1 - \gamma_C)) + (42140 + 23.17\cdot T)_{\gamma C} + (-339200 + 187\cdot T)\gamma_M,\ J\cdot mol^{-1}.$$

In this equation $\gamma_i = x_i / (1 - x_i)$, where x_i is an atomic fraction. The equation is valid in the temperature range 1100-1312 K. [1960Sch] gives for the interaction coefficients for the γ phase:

$$\log \gamma_C^{Cr} = 3.8\cdot N_{Cr}^2 - 5.77\cdot N_{Cr} + 20\cdot N_{Cr}^2\cdot N_{C\text{-}Cr} - 29\cdot N_{Cr}\cdot N_{C\text{-}Cr},$$

where $N_{C\text{-}Cr}$ is the concentration of C in the γ phase in the ternary system. [2004Bra] calculated C isoactivity lines in austenite at 1000°C. The results are nearly identical with those of [1972Wad] and [1977Nis2]. In the latter work also the effect of carbide forming solutes on the activity of C in austenite was studied by [1971Gre]. The effect of temperature on the interaction parameter is given by the equation $\varepsilon_C^{Cr} = 9.88 - 18150/T$. Experimental data on the C activity were analyzed by [1977Uhr1]. Published data on the C solubility were used to determine its energy of interaction with Cr [1989Age]. A general semi-empirical expression for the activity coefficient of C in ternary C-Fe-X alloys, including the C-Cr-Fe system was presented by [1966Zup]. There they expressed thermodynamic properties of multicomponent systems and used as an example the C-Cr-Fe system to calculate the solubility of C in the Cr-Fe melts at 1550°C.
The effect of C on the activity of Cr in the austenite phase was studied by [1971Gre] in the range of 900-1125°C and compared with the effects that other addition elements have. The activities of Cr in the Fe rich alloys were investigated in [2004Ten, 2005Ten].
The activity of C in the ferrite has been studied by [1974Pet], where at 1 at.% Cr the activity coefficient was reported to be $\gamma_{Cr}^C = 0.50$.

Notes on Materials Properties and Applications

The C-Cr-Fe steels are used in many applications such as discs, gears, cutlery and turbine blades [2003Kat]. [2000Abe] showed, that under creep tests at 500°C additions of chromium lead to large strengthening effect induced by the co-segregation of chromium and carbon atoms on edge dislocations. This apparently results in a reduction of the dislocation climb velocity even in alloys containing very limited amount of alloying elements (0.023 at.% C, 0.11 at.% Cr). Carbide particles markedly retard the recovery of lath-martensitic structure during creep deformation, and this leads to a grate improvement of creep properties in low carbon steels. The addition of Mo or W to the low carbon steels does not give a large effect to retardation of recovery, but causes large solid solution strengthening [2000Iwa].
The C-Cr-Fe system is one of the base systems to develop heat-resistant martensitic steels (9Cr-0.1 mass% C) [2000Iwa]. The 7-9 Cr class of tempered martensitic steels are among the most promising candidate materials for structural application in fusion reactors. Despite their good thermophysical properties and good resistance against swelling under neutron irradiation, microstructural evolution takes place, which results in a degradation of their mechanical properties, collectively often addressed as “embrittlement” [2004Bon1, 2004Bon2, 2005Bon].
The C-Cr-Fe alloys are used to produce composite magneto-abrasive powders for finishing of polysurfaces [1983Pol].
High chromium white cast irons (WCIs) are ferrous based alloys containing 11-30 mass% Cr and 1.8-3.6 mass% C, with Mo, Mn, and sometimes Ni as additional alloying elements. The range of commercially important high Cr alloys contains from 15 to 26 mass% Cr. They are used in a variety of applications where stability against aggressive environments is a of importance. This applies to mining and mineral processing, cement production and to pulp and paper manufacturing industries. Superior abrasive wear resistance [1991Kan, 1997Dog, 1997Tab, 1999Mas], combined with relatively low production costs, makes these

DOI: 10.1007/978-3-540-74196-1_3

alloys particularly attractive for applications, where grinding, milling, and pumping equipment is used to process hard materials such as ore, coal, gravel, and cement. The alloys with a primarily austenitic matrix have a higher abrasion resistance than similar alloys with a pearlitic/bainitic matrix. Improvement in abrasion resistance is attributed to the ability of the austenite to transform to martensite at the wear surface during the abrasion process [1997Dog].

The alloys are often deposited by arc welding in which case the cooling rates can be sufficiently large (20-30 $K \cdot s^{-1}$) to freeze a non-equilibrium microstructure of M_7C_3 carbides in a matrix of metastable austenite. Because the austenite is retained from a very high temperature where its equilibrium chromium concentration can be as high as 16 mass%, it is resistant to corrosion. If the austenite subsequently transforms into an equilibrium mixture of ferrite and more M_7C_3 carbides, the much lower chromium concentration in the resulting ferrite is inadequate to support a continuous Cr_2O_3 film, so that the corrosion resistance of the matrix phase decreases [1990Ata].

With respect to the wear resistance and toughness [1999Per] pointed out some limitation in the use of Ni containing martensitic cast irons, compared to the advantages brought about by the use of high chromium WCIs of non-ledeburitic matrix. The effect of chromium on the anisotropy of Young's modulus and the thermoelastic coefficient of iron-cementite alloy castings were investigated by [1987Kag] at temperatures up to 500°C. An Elinvar property ("zero" thermal expansion) were observed in the Fe-4C-4 mass% Cr below the Curie temperature.

Investigations of the C-Cr-Fe materials properties are presented in Table 4.

Miscellaneous

High Cr WCIs can be described as *in-situ* composites with large, hard proeutectic and/or eutectic M_7C_3 carbides in a softer iron matrix (*i.e.*, austenite, martensite, ferrite, pearlite or bainite). The matrix structure that is observed more often in the as-cast high CWIs is austenite, but this can be changed after relatively simple heat treatments to one that is primarily or completely martensite. Dependent on the specific composition of the high Cr white iron, the carbides are typically of the M_7C_3 type, where M includes Fe, Cr, and other carbide forming elements. The M_7C_3 carbides grow as rods and blades with their long axes parallel to the heat flow direction in the mould [1984Kun, 1994Pow, 1996Tab]. In C-Cr-Fe alloys, lath martensite forms at high temperature, and below the lath formation temperature mainly $\{225\}_f$ plate martensite is formed. The bainite-like structures (BL) are formed under tempering at temperatures in the upper C curve in a T-T-T (time-temperature-transformation) diagram of 8 mass% Cr steels. When the Cr steel austenite with more than 0.36 mass% C is isothermally decomposed at temperatures between the austenite eutectoid decomposition and the formation of martensite (between Ae_1 and Ms points) two clearly separated C-curves appear in the T-T-T diagram. The upper C-curve arises from a eutectoid reaction, but a bainite reaction occurs in a lower C-curve. The BL shows fine lamellar structures covered by interphase precipitation products. The carbide particles precipitated in BL are not cementite but mainly $M_{23}C_6$ relating to ferrite with Kurdyumov-Sachs relationship. The growth direction of $M_{23}C_6$ is close to $<110>_{M23C6}//<111>_{(\alpha Fe)}$ which may correspond to <110>, in the parent phase. The transformation mechanism of BL is the same as that of a eutectoid decomposition. Therefore, in this case, BL is quite different from bainite where both diffusional and shear processes seem to occur [1996Jun].

At temperatures below 300°C the solid state transformation of martensite was studied by [2003Yam] who described the relation between Ms-temperatures (°C) and chromium and carbon contents as:

$$Ms = 383.11 - 207.42\ (\text{mass\% C}) - 20.65\ (\text{mass\% Cr}).$$

Using mishmetal to modify high-chromium white iron results in a refinement of the alloy structure and increases the wear resistance by 13.6% [1994Pee]. Adding Cu to the C-Cr-Fe melt decreases the decarburization reaction rate [2002Shi].

DOI: 10.1007/978-3-540-74196-1_3

Table 1. Investigations of the C-Cr-Fe Phase Relations, Structures and Thermodynamics

Reference	Method/Experimental Technique	Temperature/Composition/Phase Range Studied
[1907Goe]	DTA	up to 1535°C; 0 - 62 mass% Cr, 4 - 9.2 mass% C
[1911Arn]	Light microscopy, composition of the separated carbides as a function of Cr content	up to 1200°C; up to 12 mass% Cr and up to 1 mass% C
[1918Mur]	Light microscopy, magnetic analysis	cooling from 1200, 1100, and 1000°C; up to 28 mass% Cr and up to 1.6 mass% C, α and γ phases, martensite, double carbides
[1921Dae]	Light microscopy, TA	0.45 - 18.53 mass% Cr, 0.21 - 1.27 mass% C
[1921Rus]	Light microscopy, electrical resistance, DTA	up to 1200°C; up to 12 mass% Cr and 1 mass% C
[1923Aus]	Light microscopy, DTA	up to 50 mass% Cr and 7.1 mass% C
[1924Fis]	DTA	Fe - Cr - Cr_5C_2 - Fe_3C
[1926Mei]	DTA	Fe - 0.7 mass% C - (0 - 20) mass% Cr Fe - 2.5 mass% C - (0 - 20) mass% Cr
[1924Obe]	Light microscopy	1100°C; 0 - 14 mass% Cr and 0 - 1.6 mass% C
[1926Veg1] [1926Veg2]	Light microscopy, DTA	up to 1720°C; Fe - Cr - Cr_5C_2 - Fe_3C
[1927Sau]	Chemical analysis, magnetic analysis	$Fe_3C{\cdot}Cr_4C$; $Cr_{10}Fe_3C_6$
[1927Gro]	Light microscopy	0-18 mass% Cr and 0.15-0.35 mass% C
[1928Wes]	Light microscopy, X-ray analysis using powder method and dissolving of the iron matrix	alloys annealed at 1000°C and subsequently cooled at a rate of 0.5 to 1°C per min. 0 -77 mass% Cr and 0 - 11.1 mass% C
[1930Kri]	Light microscopy, DTA, hardness, magnetic properties	985 - 1370°C, 20 - 35 mass% Cr and 0.15 - 0.62 mass% C
[1930Mur] [1931Mur]	Light microscopy, magnetic analysis, dilatometry	up to 900°C; 9.5 - 22.08 mass% Cr and 0.03 - 1.09 mass% C
[1932Fri]	Light microscopy, TA	Cr_7C_3 - Fe_3C
[1932Sch]	Light microscopy, hardness	20 - 30 mass% Cr and 0.12 - 1.72 mass% C
[1933Wes]	X-ray analysis	$(Cr,Fe)_4C$ ($M_{23}C_6$)
[1934Luc]	DTA	up to 1700°C; 39.2 - 80 mass% Cr and 8.39 - 10.01 mass% C
[1935Aus]	Dilatometry, magnetic susceptibility	50 - 800°C, 3.25 - 10.58 mass% Cr and < 0.03 mass% C, α⇌γ transformation
[1935Tof]	Light microscopy, hardness	600 - 1500°C; 2 - 12.5 mass% Cr and 0.1 - 1.5 mass% C

(*continued*)

DOI: 10.1007/978-3-540-74196-1_3

Reference	Method/Experimental Technique	Temperature/Composition/Phase Range Studied
[1936Mur]	Magnetic analysis	900, 1100°C 0 - 27.8 mass% Cr and 0 - 1.55 mass% C
[1936Tof2] [1936Tof3]	Light microscopy, hardness, X-ray analysis, TA	15 - 69.1 mass% Cr and 0.08 - 1.86 mass% C
[1938And]	Fluidity tests, TA	1450 - 1580°C; 13.9 - 24.5 mass% Cr and 0.4 mass% C
[1940Mir]	Resistometry, X-ray analysis, magnetic properties of carbides extracted by dissolution of metallic matrix	0 - 20.4 mass% Cr and 0.46 - 1.54 mass% C
[1947Bla]	Resistometry, X-ray analysis	20 - 1200°C; 0 - 20.4 mass% Cr and 0.12 - 1.41 mass% C
[1948Gol]	X-ray analysis of bulk material and carbides extracted by dissolution of metallic matrix	1250, 1000, 800, and 590°C austenite, M_7C_3, martensite, ferrite, cementite, ternary carbide with the NaCl type structure
[1950Liv1, 1950Liv2]	X-ray analysis, electrical and mechanical properties	700°C, 600 - 400°C; 1.82 - 12.4 mass% Cr, 0.43 - 1.24 mass% C, $\alpha + M_3C$; $\alpha + M_3C + M_7C_3$; $\alpha + M_7C_3$; $\alpha + M_7C_3 + M_{23}C_6$
[1951Sho]	X-ray powder analysis of carbides extracted by dissolution of metallic matrix	815, and 595°C; 34.75 mass% Cr and 0.01 mass% C; 43.15 mass% Cr and 0.016 mass% C, $\alpha+\sigma$
[1951Zar]	Light microscopy, X-ray analysis, microhardness, Rockwell hardness, wear resistance	9 - 10 mass% Cr and 1.42 - 4.28 mass% C, as-cast condition, $\alpha + M_3C + M_7C_3$
[1952Edw]	Light microscopy, X-ray analysis	1250°C, up to 8 mass% Cr_3C_2
[1953Kuo1]	Light microscopy, X-ray powder analysis of carbides extracted by dissolution of metallic matrix	700°C, 0.48 - 24.2 mass% Cr; 0.22 - 1.02 mass% C, $\alpha + M_3C$; $\alpha + M_3C + M_7C_3$; $\alpha + M_7C_3$; $\alpha + M_7C_3 + M_{23}C_6$
[1953Kuo2]	X-ray diffraction, chemical analysis	400-750°C, 0.22-1.02 mass% C, 0.48-24.2 mass% Cr, M_3C, M_7C_3, $M_{23}C_6$
[1953Ric]	Study of the carbon solubility in Cr-Fe melts under conditions of Bouduard's equilibrium	1560-1760°C, 0.775-1.44 mass% C, 9.03-24.09 mass% Cr, liquid phase
[1956Oht]	Emf, electrode concentration cell	1540°C; 2.0 - 20 at.% Cr; 4.0 - 24 at.% C, liquid phase
[1957San]	Study of the carbon solubility in Fe-Cr melts under conditions of Bouduard's equilibrium in closed system with a slowest flow rate of CO	1460, 1545, and 1560°C; 0 - 24.5 at.% Cr, 0 - 6.46 at.% C, liquid phase

(*continued*)

DOI: 10.1007/978-3-540-74196-1_3

Reference	Method/Experimental Technique	Temperature/Composition/Phase Range Studied
[1958Bun]	Light microscopy, dilatometry, X-ray analysis, chemical analysis	Up to 1250°C; 0 - 38 mass% Cr, 0 - 4 mass% C, $\alpha + M_3C$; $\alpha + M_3C + M_7C_3$; $\alpha + M_7C_3$; $\alpha + M_7C_3 + M_{23}C_6$
[1959Fuw]	Equilibration of the melt with controlled mixtures of CO and CO_2	1560°C; 0 - 25 at.% Cr, 0 - 7 at.% C, liquid phase
[1960Pet]	Equilibration with controlled mixtures of CO and CO_2	800°C; 0.98 mass% Cr, 0.1 mass% C, α phase
[1960Sch]	Equilibration with controlled mixtures of CH_4 and H_2	950, 1000 and 1050°C; 0 - 10 at.% Cr
[1961Bae]	Light microscopy, thermomagnetic measurements	up to 1400°C; up to 31 mass% Cr and up to 0.2 mass% C, $\alpha \rightleftharpoons \gamma$ transformation
[1962Gri]	Light microscopy, saturation experiments in carbon crucible, thermal analysis during freezing, X-ray diffractometry	1900°C, up to 94 mass% Cr and 1.4 - 11.7 mass% C, liquidus surface;
[1962Pep]	Light microscopy, thermomagnetic measurements, DTA	up to 1700°C 69 - 74 mass% Cr, 0.88 - 10.6 mass% C, α, σ, M_7C_3, $M_{23}C_6$
[1963Bri]	Equilibration with controlled mixtures of CO and CO_2	1000°C; 0 - 4.35at.% Cr and 0.5 - 4.7 at.% C
[1963Fle]	Equilibration with controlled mixtures of CH_4/H_2	1000°C; 5.02 mass% Cr and 0.122 mass% C; 9.42 mass% Cr and 0.1 mass% C; γ phase
[1963Han]	Equilibrium CO pressure for the reaction between Cr_2O_3 and ferrochromium	1400, 1250, 1050°C; 46 - 88 mass% Cr, 0.4 - 4.85 mass% C, $\gamma + M_7C_3 + M_{23}C_6$
[1963Joh]	Laue method, X-ray diffractometry	quenched from 1228°C; 3.09 mass% Cr and 1.51 mass% C; austenite, martensite
[1963Kud]	X-ray diffraction	quenched with water from 1050°C, tempered with oil from 680°C, 0 - 19.2 at.% Cr and 26.1 - 27.4 at.% C; M_3C
[1964Bun]	Equilibration with controlled mixtures of CH_4/H_2	1000°C; up to 9 mass% Cr and up to 4 mass% C; $\gamma + M_3C$; $\gamma + M_7C_3 + M_3C$; $\gamma + M_7C_3$
[1964Pet]	Perfected radiometric method used for CH_4/H_2 mixture	900-980°C; 0.48 mass% Cr and 0.4 mass% C, austenite
[1965Ale]	Equilibration with controlled mixtures of CH_4/H_2, X-ray powder diffraction	900, 1200°C; $(Cr_{1-x}Fe_x)_{23}C_6$; x = 0.13, 0.34, 0.55

(*continued*)

DOI: 10.1007/978-3-540-74196-1_3

Reference	Method/Experimental Technique	Temperature/Composition/Phase Range Studied
[1965Glo]	X-ray diffractometry	synthesized at 1100°C; $(Cr_xFe_{7-x})C_3$; x = 1, 2, 3, 4, 4.95
[1966Gob]	Light microscopy, differential dilatometry	up to 1480°C; 0 - 20 mass% Cr and 0 - 2 mass% C; single phase γ domain
[1966Kud]	X-ray analysis	quenched with water from 1050°C, tempered with oil from 680°C; 1.3 - 19.2 at.% Cr and 27.9 - 27.4 at.% C, M_3C
[1966Sch]	Activity of C / vapor pressure for H_2/CH_4	1000°C, <9 mass% C, γ (austenite)
[1967Las]	X-ray analysis	$(Cr_{1-x}Fe_x)_7C_3$, $0 \le x \le 0.78$
[1968Chi]	Activity of C/ chemical analysis of C content	1000°C, <9 mass% C, γ (austenite)
[1968Sri]	Magnetically checking for carbide separation during quenching, TEM, electron diffraction	austenized at 1250°C and water quenched specimens were isothermally held at 285°C and finally quenched into cold water, 7.9 mass% Cr and 1.11 mass% C; 3.3 mass% Cr and 0.6 mass% C; Bainite transformation
[1970Had]	Activity measurements / chemical analysis	1600°C, < 0.25 at.% Cr, C-Cr-Fe liquid
[1970Jac]	DTA	Up to 1450°C, 5.78 - 65.71 mass% Cr and 0.56 - 8.42 mass% C, Liquidus surface
[1971Gre]	Equilibration with controlled mixtures of CH_4/H_2	900 - 1125°C; 4.35 - 14.3 mass% Cr, Solubility of carbon in austenite
[1971Kin]	A.R.L. electron microprobe	550 - 800°C, 2.99 mass% Cr and 0.13 mass% C, ferrite and bainaite
[1971Pog]	Light microscopy, X-ray analysis	1200 - 1350°C, 70 mass% Cr - 30 mass% Fe - C, Solubility of carbon in ferrochromium
[1971Swi]	Quantitative metallography method, dilatometry	680 - 800°C, 2.4 - 4.5 mass% Cr and 0.14 - 0.17 mass% C, austenite to ferrite transformation
[1971Vig]	DTA	up to 1450°C; 1 mass% Cr and 4.76 mass% C, Cementite, austenite, graphite

(*continued*)

DOI: 10.1007/978-3-540-74196-1_3

Reference	Method/Experimental Technique	Temperature/Composition/Phase Range Studied
[1972Foo]	Equilibrating C-Fe binary alloys with C-Cr-Fe ternary alloys in an isothermal closed chamber through transport in the gas phase	1550°C, 0.127-0.29 at.% C, 5.46-20.41 at.% Cr, Solubility of carbon in the liquid phase
[1972Gor]	Light microscopy	up to 1450°C; 5 - 20 mass% Cr and 4.5 - 6 mass% C, austenite, M_3C, M_7C_3
[1972Jel]	Light microscopy, chemical analysis of carbides extracted by dissolution of metallic matrix, Vickers hardness	700°C, 0.17-0.35 mass% C, 0.98-17.6 mass% Cr, $\alpha + M_{23}C_6$, $\alpha + M_{23}C_6 + M_7C_3$, $\alpha + M_7C_3 + M_3C$ 3-18.7 mass% C, 57.6-85 mass% Cr, $\alpha_1 + \sigma + M_{23}C_6$, $\sigma + M_{23}C_6$
[1972Wad]	Equilibration with controlled mixtures of CH_4/H_2	1201°C; 2.03 - 12 mass% Cr, $\gamma + M_7C_3$; $\gamma + M_{23}C_6$
[1973Gor1]	Light microscopy, X-ray microanalysis	1175-1475°C, 2, 4 mass% C, 20-75 mass% Cr, $\alpha + M_{23}C_6$, $\alpha + \gamma + M_{23}C_6$, $\alpha + M_7C_3$
[1973Gor2]	Light microscopy	1175-1475°C, 6.5, 7.0, 8.0, 9.0 mass% C, 0-25 mass% Cr
[1973Mir]	TA	High cooling rate from 1000°C 0.02 mass% C, 1.5 and 4.5 mass% Cr, austenite, ferrite, martensite, bainite
[1973Tar]	Light microscopy	5 mass% C, 14 mass% Cr , M_7C_3
[1974Ben]	Light microscopy, X-ray analysis, EMPA	900-1150°C , 0.3-6.0 at.% C, 0.28-57.6 at.% Cr; $\gamma + M_3C$, $\gamma + M_3C + M_7C_3$, $\gamma + M_7C_3$, $\gamma + M_7C_3 + M_{23}C_6$, $\gamma + M_{23}C_6$, $\alpha + \gamma + M_{23}C_6$, $\alpha + M_{23}C_6$
[1974Kun]	EMF	1700°C, 0.73-0.84 mass% C, 50-69 mass% Cr
[1974Pet]	Perfected radiometric method	800, 850, 890°C, Fe - 0.05, 0.1, 0.17, 0.35, 0.7 and 3.05 mass% Cr, α phase
[1974She]	Light microscopy	Quenched from 1150°C, 4.5-6 mass% C, 1-5 mass% Cr
[1975Cos]	Method for use of radioisotope solute to determine solid solubility	716°C, 1.02, 2.0 and 3.5 at.% Cr, <11 mass ppm C
[1975Shi]	High temperature diffractometry	Up to 427°C, $(Fe_{1-x}Cr_x)_3C$, $0 < x < 0.3$

(*continued*)

DOI: 10.1007/978-3-540-74196-1_3

Reference	Method/Experimental Technique	Temperature/Composition/Phase Range Studied
[1975Str]	EMPA	1000°C, 0.81-0.16 mass% C, 1.14-11.32 mass% Cr; $\gamma + M_3C$, $\gamma + M_3C + M_7C_3$, $\gamma + M_7C_3$, $\gamma + M_7C_3 + M_{23}C_6$, $\gamma + M_{23}C_6$, $\alpha + \gamma + M_{23}C_6$, $\alpha + M_{23}C_6$
[1976Cho]	Knudsen all-mass spectrometer combination	1630°C
[1976Kle]	Internal friction	Water-quenched from 670, 550, 390, 300 and 200°C, 0.012-0.021 mass% C, 0.5-2.4 mass% Cr, precipitation of M_3C
[1976She1]	Light microscopy, X-ray diffractometry	10 mass% C, 10-60 mass% Cr, M_7C_3, M_3C_2, M_3C
[1976She2]	Light microscopy	1000°C, 3 mass% C, 0-5 mass% Cr, M_3C
[1976Woo]	Light microscopy, X-ray diffractometry of the extracted residues, EMPA	Oil-quenched from 870°C, ~ 1 mass% C, 1.3-28.87 mass% Cr
[1977Nis1]	Light microscopy, EPMA, the ternary alloys were produced by carburizing the binary alloys with a sealed capsule technique	1000°C, 0.17-0.94 mass% C, 0-7.1 mass% Cr, $\gamma + M_3C$, $\gamma + M_3C + M_{23}C_6$, $\gamma + M_{23}C_6$
[1979Bee]	Light microscopy, TEM, high speed dilatometry, isothermal dilatometry	800-400°C, Fe-5 mass% Cr-0.2 mass% C, Fe-10 mass% Cr-0.2 mass% C, γ, $\alpha + \gamma + M_{23}C_6$, M_7C_3, martensite, bainite
[1979How]	TEM	isothermally transformed at 750-650°C, Fe-10.6 mass% Cr-0.22 mass% Fe, α, γ, $M_{23}C_6$
[1979Kag]	X-ray diffraction study of the electrolytically extracted carbides	quenched from 600, 700, 800, 900, 1000°C, Fe-4.1 mass% C-0.92 mass% Cr, Fe-3.91 mass% C-2.09 mass% Cr
[1979Sha1] [1979Sha2]	EMPA, automatic image analyzer, electron microscopy and EDAX of carbide extraction replicas, thermodynamic calculations	750, 770°C, 1-1.44 at.% C, 0.3-1.7 at.% Cr, $\alpha + \gamma$, $\gamma + M_3C$
[1980Bra]	Equilibration with controlled mixtures of CH_4/H_2	900, 1000 and 1100°C, up to 13 at.% Cr and 25 at.% C
[1980Iwa] [1981Ino]	TEM of alloys rapidly quenched from melts	up to 50 at.% Cr and 25 at.% C, γ, χ phase, ε phase
[1981Ogi]	Light microscopy, TA, EMPA	Up to 1525°C, Fe-1.56 mass% Cr-0.76 mass% C, Fe-1.56 mass% Cr-1.7 mass% C, $\gamma + L$

(*continued*)

DOI: 10.1007/978-3-540-74196-1_3

Reference	Method/Experimental Technique	Temperature/Composition/Phase Range Studied
[1982Hor]	Light microscopy, X-ray diffractometry	$Cr_{26}Fe_{60}C_{14}$, $Cr_{11}Fe_{69}C_{20}$, $Cr_{20}Fe_{60}C_{20}$, $Cr_{31}Fe_{49}C_{20}$. Phases formed during crystalline solidification and after annealing of glasses
[1982Kag]	Light microscopy and EPMA of the zone melted and rapid-cooled specimens	2.8-3.7 mass% C, 0.38-0.5 mass% Cr, Partition of Cr between γ and liquid
[1982Kun]	EMF	1600, 1650, 1700°C, 1.6 mass% C, 20-50 mass% Cr
[1982Yak]	X-ray diffractometry	1200°C, $(Cr_{23-x}Fe_x)C_6$, $7.4 \geq x \geq 1.7$
[1983Jan]	Saturation experiments in graphite crucible, wet chemical analyses	1450-1600°C
[1983Ume]	Light microscopy	austenized at 1150°C and quenched to 30°C, Fe - 1.44C - 3Cr mass%, Fe - 0.92C - 8Cr mass%; martensite
[1984Kun]	The liquid-solid equilibrium couples produced by directional solidification, DTA	up to 1540°C, 0-1.4 mass% C, 0-25 mass% Cr, (δFe) + L, γ + L, (δFe) + γ + L
[1984Pro]	X-ray diffractometry	Fe-1.05 mass% C-6,36 mass% Cr, Fe-1.36 mass% C-3.39 mass% Cr, Crystal structure of α-martensite
[1985Kow]	Electron diffractometry	Fe-4.5 mass% C-22 mass% Cr, M_7C_3
[1985Tho]	Light microscopy, DTA, SEM, X-ray diffractometry	Up to 1500°C, up to 6 mass% C and 40 mass% Cr; L, (δFe), γ, M_3C, $M_{23}C_6$, M_7C_3
[1985Wad]	Saturation with carbon using CH_4/H_2 mixtures, SEM with EDX, EPMA, TEM of extraction carbon replicas	712°C, up to 8.07 mass% Cr, α + M_3C, α + $M_{23}C_6$, α + M_7C_3
[1986Kli]	Light microscopy, dilatometry, EPMA, microhardness	up to 1200°C, sintering, 40, 50, 60, 70 mass% Fe + Cr_3C_2
[1986Mir]	TA, dilatometry, magnetometry, TEM	high rate cooling from 1080°C, 0.004-0.09 mass% C, 4.23-9.38 mass% Cr, austenite, ferrite, martensite, bainite
[1986Pea]	SEM, EDX, TEM	as cast and heat-treated as follows: 1 h at 800°C, furnace cool; 1 h at 1100°C, air cool; 1 h temper at 400°C, air cool; Fe - 2.44C - 30.6Cr - 0.71Si - 0.21Mn - 0.17Ni (mass%); γ - M_7C_3 - $M_{23}C_6$
[1986Sch]	DTA and saturation melts	up to 1440°C, up to 3 mass% C and 15 mass% Cr

(*continued*)

DOI: 10.1007/978-3-540-74196-1_3

Reference	Method/Experimental Technique	Temperature/Composition/Phase Range Studied
[1986Vit, 1987Vit]	Isothermal calorimetry	1700-1887°C, the whole range of existence of homogeneous liquid solutions, from Cr-Fe binary up to 37 at.% C
[1988Fra]	Quantimet image analyzer	unidirectionally solidified samples, 30 and 35 mass% Cr, 1.9-3.4 mass% C, $\alpha + M_7C_3$, $\gamma + M_7C_3$
[1988Mag]	DTA / DSC	up to 1155°C, Fe-4.26 mass% C-0.03 mass% Cr and Fe-3.99 mass% C-0.5 mass% Cr
[1988Pil]	Equilibration of a mixture Cr and $Cr_{23}C_6$ in liquid sodium, while continuously monitoring the carbon activity of sodium using an electrochemical carbon meter	612-694°C, $Cr_{23}C_6$
[1990Gol]	Light microscopy, replication and transmission electron microscopy	austenized at 1300°C and tempered at 700-525°C, quenched in iced brine; Pearlite and bainite reactions
[1990Pow]	Light microscopy, TA, SEM, Laue micro-focus back reflection	crystallization temperature, Fe - 3 mass% C - 20 mass% Cr, Fe - 4 mass% C - 20 mass% Cr; L, γ, M_7C_3
[1991Liu1]	SEM, TEM, EDS, X-ray diffractometry	910°C, Fe - 3.91 at.% C - 2.06 at.% Cr, $\gamma + M_3C$
[1991Liu2]	SEM, TEM	910°C, Fe - 3.91 at.% C - 2.06 at.% Cr, $\gamma + M_3C$, $\gamma + M_3C + M_7C_3$
[1991Mor]	Light microscopy, magnetometry	300-700°C, 1 mass% Cr; 0.37, 0.46, 0.61, 0.7 and 0.79 mass% C, bainite transformation
[1991Nis]	Diffusion couple experiments, chemical analyzes	0-1.04 mass% Cr and 20-180 mass ppm C, 700-1100°C
[1991Skr]	DSC, dilatometry, fractal analysis based on the results of light microscopy	Fe-0.64 mass% C-1.01 mass% Cr, martensite transformation
[1991Vod]	TEM	200°C, Fe-1.2 mass% C-1.12 mass% Cr, carbide precipitation during of martensite decomposition
[1992Pow]	SEM, EPMA	1000°C, Fe-29.3Cr-0.1Ni-2.5C-0.1Si-0.1Mn mass%, $\gamma + M_7C_3 + M_{23}C_6$
[1992Sop]	SEM+EDAX, TEM, electron diffraction	800°C, Fe-0.4 mass% C-20 mass% Cr, $\alpha + M_{23}C_6$

(*continued*)

DOI: 10.1007/978-3-540-74196-1_3

Reference	Method/Experimental Technique	Temperature/Composition/Phase Range Studied
[1993Kha]	X-ray diffraction	quenched from the melt on the water-cooled hearth, Fe - 37Cr - 13C at.%, $\alpha + M_{23}C_6$
[1993Sch]	Conversion electron Mössbauer spectroscopy (CEMS)	1200°C, Fe - 1.2 mass% C - 8 mass% Cr, austenite
[1994Kow]	Light microscopy, DTA, X-ray diffraction	Up to 1300°C, 2-3 mass% C, 35-55 mass% Cr, L, α, $M_{23}C_6$, M_7C_3
[1994Pow]	SEM, electron back scatter diffraction	as cast, Fe - 3C - 20Cr and Fe - 4C - 20Cr mass%, M_7C_3
[1994Prz]	Equilibration with controlled carburizing atmosphere: cracked methanol with propane-butane gas or with ethyl-acetate	900°C, up to 1.55 mass% Cr, austenite
[1994Sop]	SEM+EDAX, TEM, electron diffraction	795, 900, 1000°C, 0.01-0.86 mass% C, 15.1-30.1 mass% Cr, $\gamma/\alpha/M_{23}C_6$, $\gamma/M_7C_3/M_{23}C_6$, $\alpha/M_{23}C_6$
[1994Wit, 1995Wit]	Isothermal calorimetry	1700-1887°C, The whole range of existence of homogeneous liquid solutions, from Cr-Fe binary up to 37 at. % C
[1996Kob]	Chemical equilibrating technique between Fe-Cr-C_{satd} melt and Ag-Cr_2O_3 melt in equilibria with CO/CO_2 atmosphere	1200-1500°C, 2.23-10.7 mass% Cr and 5.0-7.01 mass% C, liquid
[1996Sop]	SEM+EDAX, TEM, electron diffraction, SEM, using carbon replicas technique	880, 1000°C, 0.14-0.92 mass% C, 15.1-26.9 mass% Cr, $\alpha + M_{23}C_6$; $\gamma + M_{23}C_6$
[1996Jun]	Light microscopy, SEM, TEM, electron diffraction	austenized at 1150°C and quenched, Kept isothermally at various temperatures between 250 and 800°C and finally quenched in water; 8.2 mass% Cr, 0.2 and 0.36 mass% C; α, γ, $M_{23}C_6$
[1997Akt]	Magnetic susceptibility measurements, TEM	Fe - 1.1C - 8.3 Cr mass%, Thermally and strain induced martensites
[1998Kay]	Replication and transmission electron microscopy, electron diffraction	up to 650°C, Fe - 0.43C - 3.63; Fe - 0.39C - 9.95Cr, mass%, $\gamma/M_7C_3/M_3C$
[1998Par]	Chemical equilibration technique, atomic absorption spectroscopy, LECO thermal analyzer	1650°C, up to 5.06 mass% C and up to 0.87 mass% Cr, liquid
[1999Ma]	Activity of C / chemical analysis of C content	1600°C, < 2 mass% C, liquid

(*continued*)

DOI: 10.1007/978-3-540-74196-1_3

Reference	Method/Experimental Technique	Temperature/Composition/Phase Range Studied
[1999Mas]	Light microscopy, dilatometry, X-ray analysis, EPMA	up to 1200°C, Fe - Cr_3C_2, $\alpha/\gamma/M_7C_3$
[1999Qia]	Light microscopy, SEM	980°C, Fe - 2.5C - 1.72Cr mass%, dissolution of eutectic $(Cr, Fe)_3C$
[1999Sht1]	TEM, electron diffraction	austenitized at 1250°C and tempered at 725°C, quenched in iced brine, Fe - 0.96C - 8.24Cr mass%, γ/M_7C_3
[1999Sht2]	TEM, electron diffraction	austenitized at 800-900°C, quenched in iced brine, Fe - 0.96C - 2.6Cr mass%, $\alpha/\gamma/M_7C_3/M_3C$
[1999Sht3]	TEM, electron diffraction	austenitized at 850-900°C, quenched in iced brine, Fe - 0.96C - 8.2Cr mass%, Fe - 0.2C - 8.2Cr mass%, $\alpha/\gamma/M_7C_3/M_{23}C_6$
[1999Sht4]	TEM, electron diffraction	austenitized at 800-950°C, Fe - 0.95C - 2.61Cr mass%, $\alpha/\gamma/M_3C$
[2000Oht]	TEM, EDX	400-950°C, Fe - 50Cr - 160 ppm C, M_7C_3, $M_{23}C_6$
[2001Mor]	DSC, dilatometry	up to 550°C, Fe - 0.98C - 1.39Cr mass%, retained austenite, martensite
[2001Ume]	X-ray diffraction, light microscopy, SEM, TEM, DSC	up to 1000°C, $(Cr_xFe_{1-x})_{75}C_{25}$, x = 0.1, 0.2, 0.3
[2002Wan]	Carbon saturated solubility	1450°C, 0 - 15.04 mass% Cr and 5.04-6.33 mass% C, liquid
[2003Car1]	TEM, electron diffraction	as cast, Fe - 2.72C - 26.6Cr mass%, M_7C_3
[2003Car2]	X-ray diffraction	as cast, Fe - 2.72C - 26.6Cr mass%, M_7C_3
[2003Kat]	Light microscopy, SEM, EDX, EPMA	as cast, austenized at 780°C and quenched in could water Fe - 0.92 mass% C - 1.64 mass% Cr, $\gamma + M_3C$
[2003Lin]	TEM, AFM	1200°C, water quenched, deep cooling with liquid nitrogen Fe - 1C - 8Cr mass%, martensite
[2003Lu]	X-ray diffraction, EPMA, FESEM	unidirectional crystallization, 2.65-3.51 mass% C, 27.1-30.8 mass% Cr, $\gamma/M_7C_3/M_{23}C_6$

(*continued*)

DOI: 10.1007/978-3-540-74196-1_3

Reference	Method/Experimental Technique	Temperature/Composition/Phase Range Studied
[2003Nes]	Laue micro-focus back reflection	M_7C_3
[2003Yam]	EPMA	1-4 mass% C, 1.5-25 mass% Cr liquid, primary crystals
[2004Ten, 2005Ten]	EMF measurements, X-ray diffraction, SEM	950°C, 0.7 - 14.4 mass% C, 16.4 - 77.2 mass% Cr, $\alpha + M_{23}C_6$, $\gamma + M_{23}C_6$, $M_{23}C_6 + M_7C_3$, $\gamma + M_7C_3$, $M_7C_3 + M_3C_2$, $M_7C_3 + C$
[2004Wie, 2005Wie]	Light microscopy, SEM, TEM	900-1100°C, Fe - 2.3C - 30Cr mass%, $\gamma/M_7C_3/M_{23}C_6$
[2005Kun]	Optical microscopy, SEM, XRD	Fe-11 mass% Cr- 0.1 mass% C, annealing at 600°C

Table 2. Crystallographic Data of Solid Phases

Phase/ Temperature Range [°C]	Pearson Symbol/ Space Group/ Prototype	Lattice Parameters [pm]	Comments/References
(C)gr < 3827	*hP*4 $P6_3/mmc$ C (graphite)	a = 246.12 c = 670.90	at 25°C [Mas2] sublimation point
α, Cr_xFe_{1-x}	*cI*2 $Im\bar{3}m$ W	a = 289.8 to 290.7	$0 \le x \le 1$, annealed at 800°C [V-C2]
α_{Cr}, (αCr) < 1863		a = 288.48	at 25°C [Mas2]
(δFe) 1538 - 1394		a = 293.15	at 1390°C [V-C2, Mas2]
α_{Fe}, (αFe) < 912		a = 286.65	at 20°C [Mas2]
γ, (γFe) 1394 - 912	*cF*4 $Fm\bar{3}m$ Cu	a = 364.77	1493-734°C in the ternary system at 920°C [V-C2]
$M_{23}C_6$, $(Cr_{1-x}Fe_x)_{23}C_6$	*cF*116 $Fm\bar{3}m$		$0 \le x < 0.44$
$Cr_{23}C_6$ < 1576	$Cr_{23}C_6$	a = 1065.0 α 0.2	[V-C2], [1972Bow]
		a = 1064.54 ± 0.06 a = 1061.99 ± 0.03 a = 1059.66 ± 0.02	x = 0.7 [1987Yak] x = 0.18 [1987Yak] x = 0.32 [1987Yak]
M_7C_3, $(Cr_{1-x}Fe_x)_7C_3$	*hP*80 *P*3*c*1		$0 \le x < 0.8$

(*continued*)

DOI: 10.1007/978-3-540-74196-1_3

Phase/ Temperature Range [°C]	Pearson Symbol/ Space Group/ Prototype	Lattice Parameters [pm]	Comments/References
Cr_7C_3	Cr_7C_3	a =1401	[V-C2], [1987Ber]
< 1727		c = 453	
		a = 1402.66	x = 0 [1965Glo]
		c = 453.16	
		a = 1400.64	x = 1/7 [1965Glo]
		c = 451.07	
		a = 1391.87	x = 3/7 [1965Glo]
		c = 450.62	
		a = 1383.36	x = 4.95/7 [1965Glo]
		c = 450.52	
Cr_3C_2	*oP*20	a = 553.29 ± 0.05	[V-C2], [1969Run]
< 811	*Pnma*	b = 282.90 ± 0.02	
	Cr_3C_2	c = 1147.19 ± 0.07	
M_3C, $(Fe_{1-x}Cr_x)_3C$	*oP*16		Stable in the range
	Pnma		0.02 < x < 0.2
Fe_3C	Fe_3C		and 1230 - 658°C
metastable		a = 509.0	[V-C2]
		b = 674.8	
		c = 452.3	
		a = 508.55	at 1.3 at.% Cr [1966Kud]
		b = 674.28	
		c = 452.30	
		a = 507.42	at 6.7 at.% Cr [1966Kud]
		b = 673.10	
		c = 451.70	
		a = 507.50	at 7.6 at.% Cr [1966Kud]
		b = 673.14	
		c = 451.80	
		a = 508.37	at 19.2 at.% Cr [1966Kud]
		b = 672.69	
		c = 452.21	
Fe_3C	*hP*8	a = 476.7	[V-C2]
metastable	$P6_322$	c = 435.4	
	Fe_3C		
σ, σCrFe	*tP*30	a = 879.66 ± 0.06	50.5 at.% Fe [V-C2]
830 - 512	$P4_2/mnm$	c = 455.82 ± 0.03	
	CrFe	a = 879.68 ± 0.05	51.8 at.% Fe [V-C2]
		c = 455.85 ± 0.03	
		a = 879.61 ± 0.04	52.2 at.% Fe [V-C2]
		c = 456.05 ± 0.03	
$Cr_{14}Fe_{29}C_7$	*cI*58	a = 895.0	[V-C2, 1980Iwa]
metastable	*I*43*m*		
	Mn		

DOI: 10.1007/978-3-540-74196-1_3

Table 3. Invariant Equilibria

Reaction	T [°C]	Type	Phase	Composition (at.%)		
				C	Cr	Fe
$L + Cr_3C_2 \rightleftharpoons M_7C_3 + (C)gr$	1585	U_1	L	34.7	45.3	20.1
			Cr_3C_2	~40	~60	~0
			M_7C_3	~30	55.5	14.5
			(C)gr	100	0	0
$L + \alpha \rightleftharpoons \gamma + M_{23}C_6$	1275	U_2	L	10.8	32.1	57.2
			α	1.3	26.1	72.6
			γ	4.2	23.1	72.7
			$M_{23}C_6$	20.7	48.6	30.7
$L + M_{23}C_6 \rightleftharpoons \gamma + M_7C_3$	1255	U_3	L	12.1	29.1	58.8
			$M_{23}C_6$	20.7	44.7	34.6
			γ	4.8	20.3	75.0
			M_7C_3	30.0	51.7	18.3
$L + M_7C_3 + (C)gr \rightleftharpoons M_3C$	1230	P	L	19.9	5.3	74.8
			M_7C_3	30.0	14.4	55.6
			(C)gr	100	0	0
			M_3C	25.0	7.2	67.8
$L + M_7C_3 \rightleftharpoons \gamma + M_3C$	1160	U_4	L	17.9	6.5	75.6
			M_7C_3	30.0	19.5	50.5
			γ	8.7	3.7	87.7
			M_3C	25.0	10.3	64.7
$L \rightleftharpoons \gamma + M_3C + (C)gr$	1149	E_1	L	~17.5	~1	81.5
			γ	9.2	1	89.8
			M_3C	25.0	1.5	73.5
			(C)gr	100	0	0
$\gamma + M_{23}C_6 \rightleftharpoons \alpha + M_7C_3$	855	U_5	γ	0.41	12.5	87.1
			$M_{23}C_6$	20.7	54.8	24.5
			α	0.095	13.9	86.0
			M_7C_3	30.0	62.3	7.7
$\alpha + \sigma + M_{23}C_6$	~830	d	No data			
$\gamma + M_7C_3 \rightleftharpoons \alpha + M_3C$	745	U_6	γ	2.7	1.3	96.0
			M_7C_3	30.0	37.4	32.6
			α	0.080	0.74	99.2
			M_3C	25.0	13.1	62.0
$\gamma \rightleftharpoons \alpha + M_3C + (C)gr$	734	E_2	γ	3.2	0.49	96.3
			α	0.085	0.25	99.7
			M_3C	25.0	4.9	70.2
			(C)gr	100	0	0
$M_3C \rightleftharpoons \alpha + M_7C_3 + (C)gr$	658	E_3	M_3C	25.0	11.3	63.8
			α	0.032	0.40	99.6
			M_7C_3	30.0	39.6	30.4
			(C)gr	100	0	0

(*continued*)

DOI: 10.1007/978-3-540-74196-1_3

Reaction	T [°C]	Type	Phase	Composition (at.%)		
				C	Cr	Fe
$M_7C_3 + (C)gr \rightleftharpoons \alpha + Cr_3C_2$	570	U_7	M_7C_3	30.0	46.9	23.1
			(C)gr	100	0	0
			α	0.0073	0.26	99.7
			Cr_3C_2	40	60	0
$\alpha_{Cr} + \alpha_{Fe} + \sigma + M_{23}C_6$	~512	D	No data			

Table 4. Investigations of the C-Cr-Fe Materials Properties

Reference	Method / Experimental Technique	Type of Property
[1911Arn]	Tensile tests	Tensile and yield strength, elongation, reduction area
[1930Mur] [1936Mur]	Magnetic analysis applying 160 Gauss of the magnetizing field at high temperatures	Magnetization-temperature curves
[1935Tof]	Hardness measurements	Hardness
[1938And]	Standard spiral mould	Fluidity
[1947Bla]	Temperature dependence of resistivity	Thermal coefficient of resistivity, specific resistance
[1951Zar]	Microhardness at 100 g loading	Microhardness
[1961Bae]	Temperature dependence of magnetic susceptibility	Curie temperature
[1966Yas]	Limiting wetting angle	Wetting of Cr_3C_2 by Fe
[1967Bau]	Rotary oscillation damping method	Effect of temperature on the kinematic viscosity of C-Cr-Fe alloys
[1972Jel]	Vickers hardness	Hardness
[1975Shi]	Temperature variation of lattice parameters	Thermal expansion of $(Cr,Fe)_3C$
[1980Pot]	Flexural strength, Brinell hardness	Mechanical properties of chromic cast iron
[1985Vit]	Ultimate tensile strength, Brinell hardness	Mechanical properties of sintered materials
[1986Kli]	Rockwell hardness, impact toughness, bending strength, microhardness	Mechanical properties of sintered materials
[1987Kag]	Young's modulus and thermoelastic coefficient	Young's moduli of cementite and perlite as function of carbon and chromium concentration
[1988Fra]	Tensile tests	Tensile strength

(*continued*)

DOI: 10.1007/978-3-540-74196-1_3

Reference	Method / Experimental Technique	Type of Property
[1997Akt]	A computerized ac susceptometer with a closed cycle refrigerator between 25 and –263°C	Magnetic susceptibility
[1997Dog]	High-stress abrasive wear test	Wear resistance
[1997Tab]	Vickers hardness, microhardness, pin-on-table abrasion test	Wear resistance, microhardness
[1999Mas]	Abrasive wear resistance test by subjecting specimens to friction against a layer of an aqueous suspension of white electrocorund	Wear resistance
[2000Abe]	Creep test at 500 and 700°C	Creep strength
[2000Iwa]	Vickers hardness, creep test at 600°C, 138 MPa	Creep strength
[2001Ume]	High temperature XRD, DSC, a flexural vibration method, microhardness tests	Coefficient of thermal expansion, specific heat, microhardness, Young's modulus
[2003Lu]	Tensile tests	Tensile strength of UDS eutectic composites as a function of the solidification rate
[2004Bon1]	Tensile tests	The effect of prior austenite grain size on the Yield stress and on the strain hardening
[2004Bon2]	Tensile tests	Post-yield behaviour, strain hardening
[2005Bon]	Tensile tests	Strain hardening of tempered martensitic alloys

DOI: 10.1007/978-3-540-74196-1_3

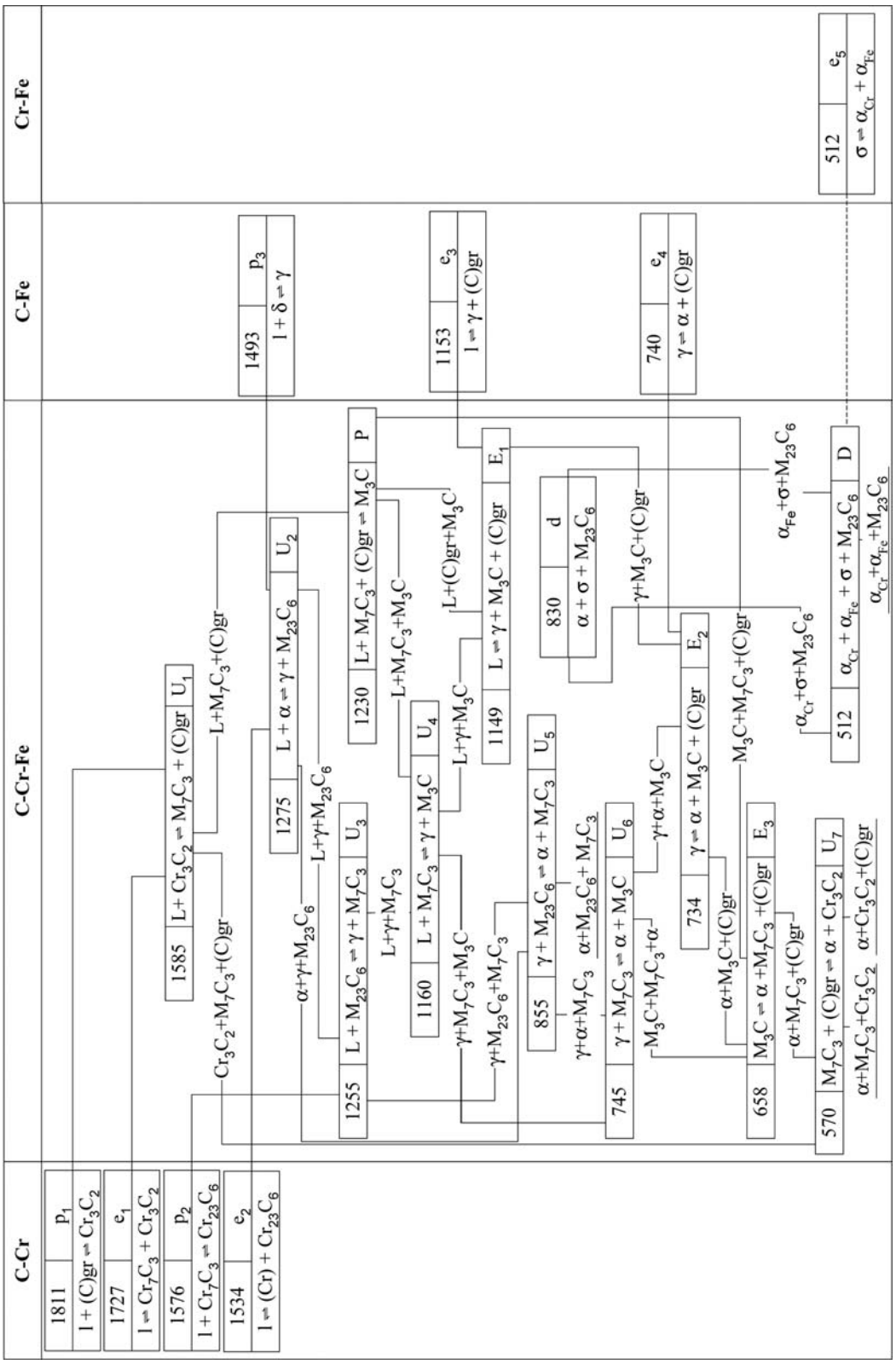

Fig. 1. C-Cr-Fe. Reaction scheme

DOI: 10.1007/978-3-540-74196-1_3

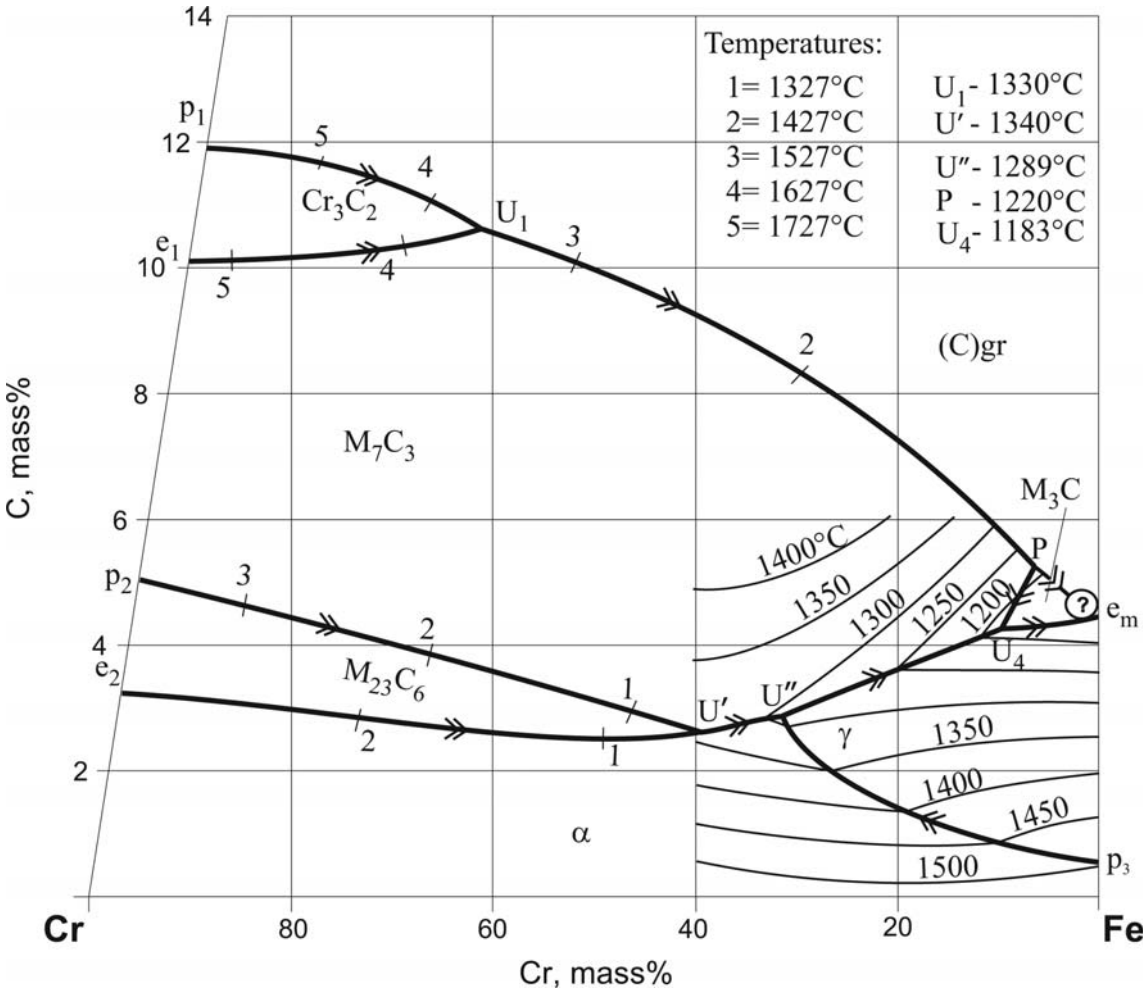

Fig. 2. C-Cr-Fe. Metastable liquidus surface projection

DOI: 10.1007/978-3-540-74196-1_3

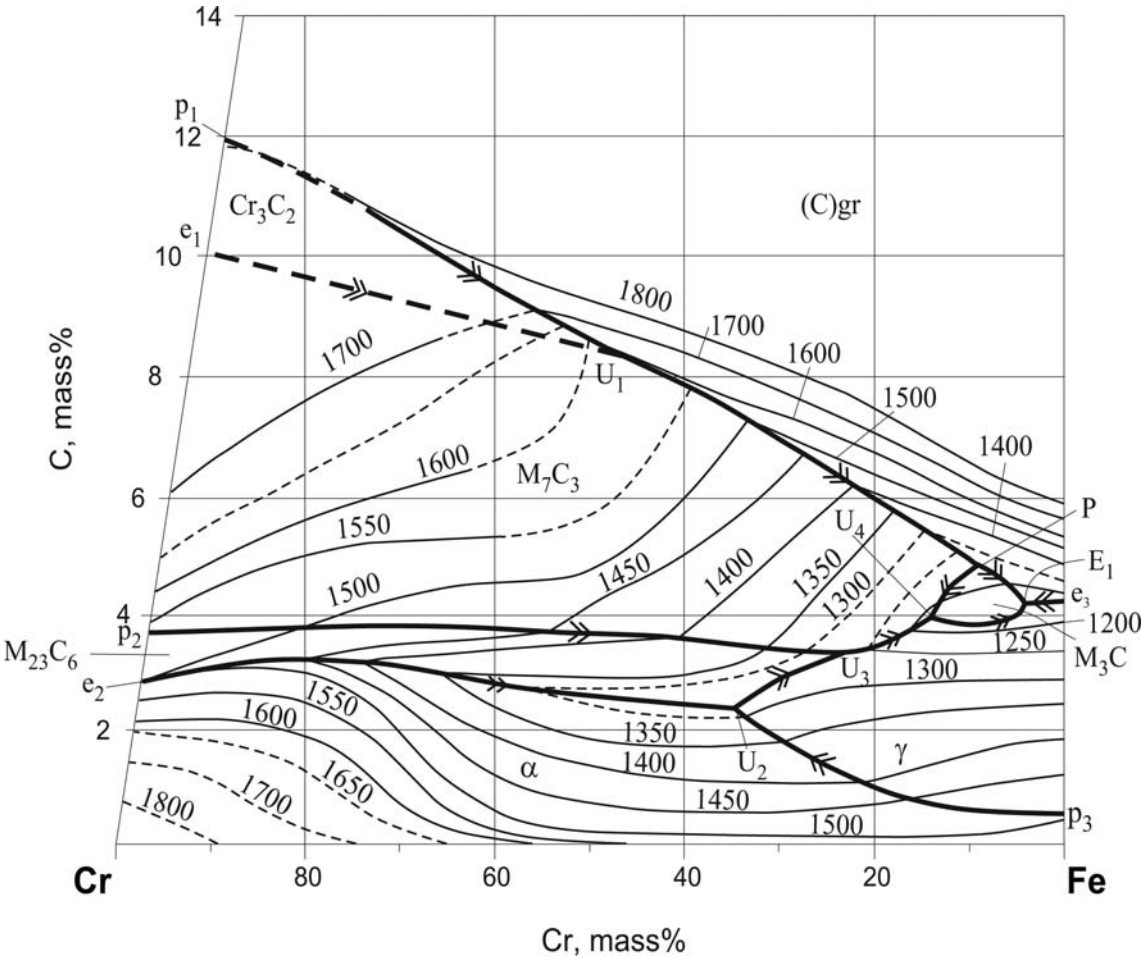

Fig. 3. C-Cr-Fe. Liquidus surface projection

DOI: 10.1007/978-3-540-74196-1_3

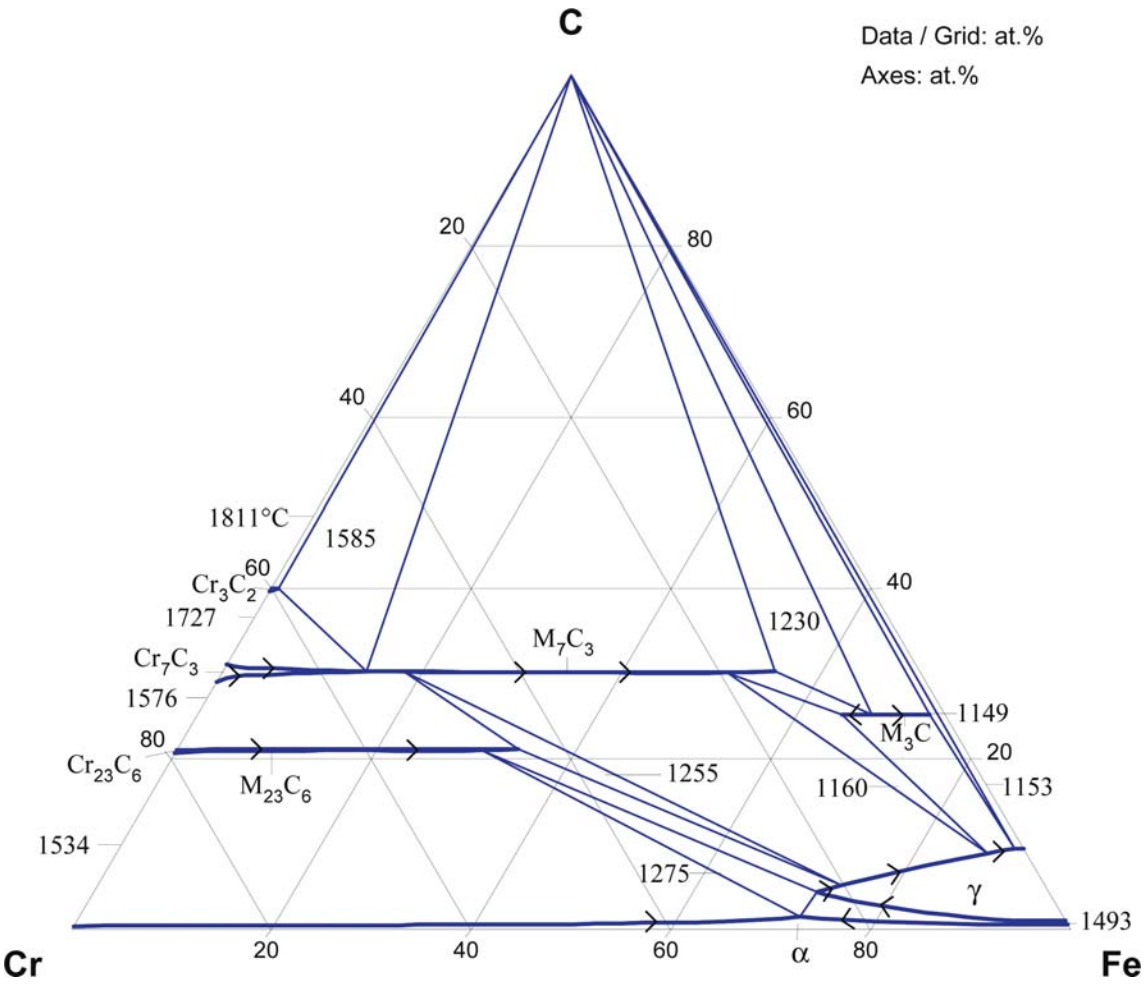

Fig. 4. C-Cr-Fe. Solidus surface projection

DOI: 10.1007/978-3-540-74196-1_3

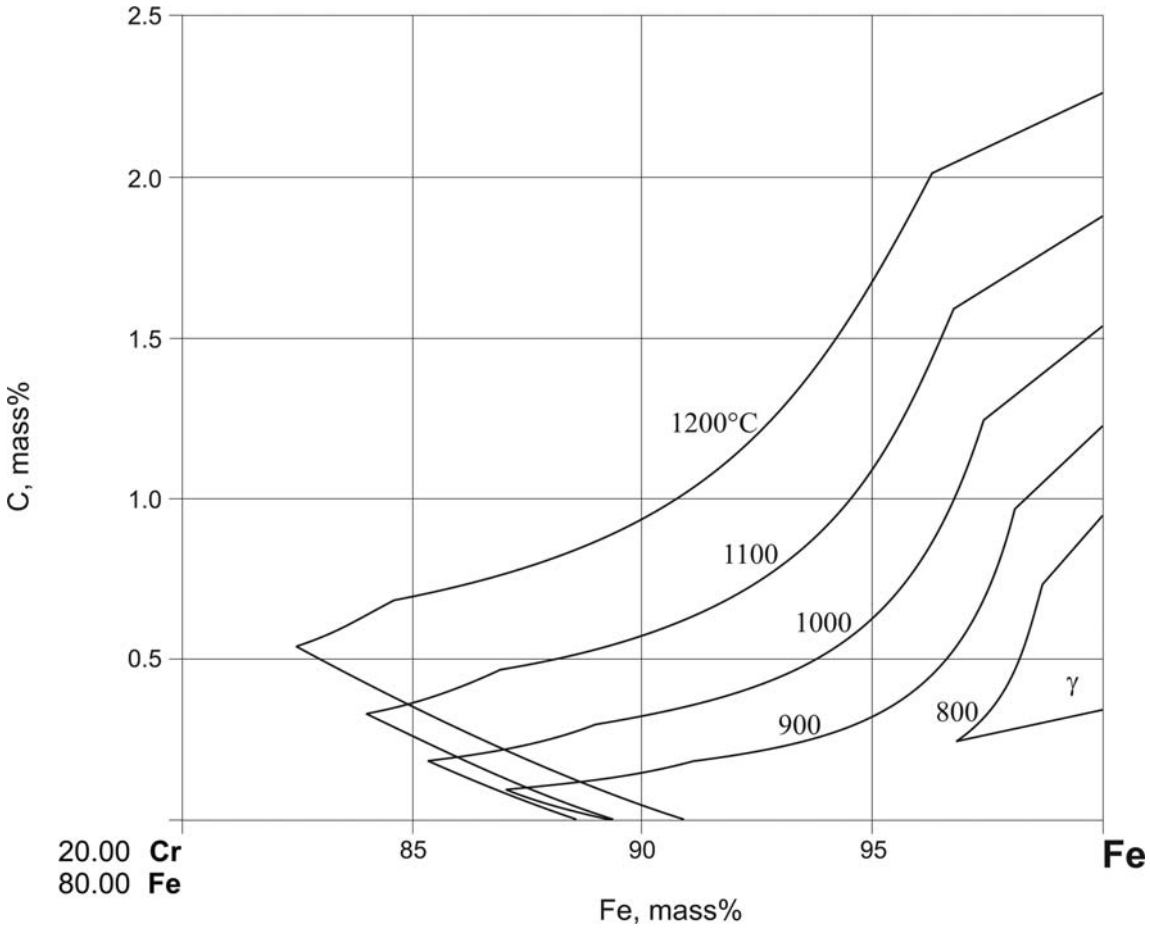

Fig. 5a. C-Cr-Fe. Extension of the homogeneity range of the fcc γ phase at different temperatures

DOI: 10.1007/978-3-540-74196-1_3

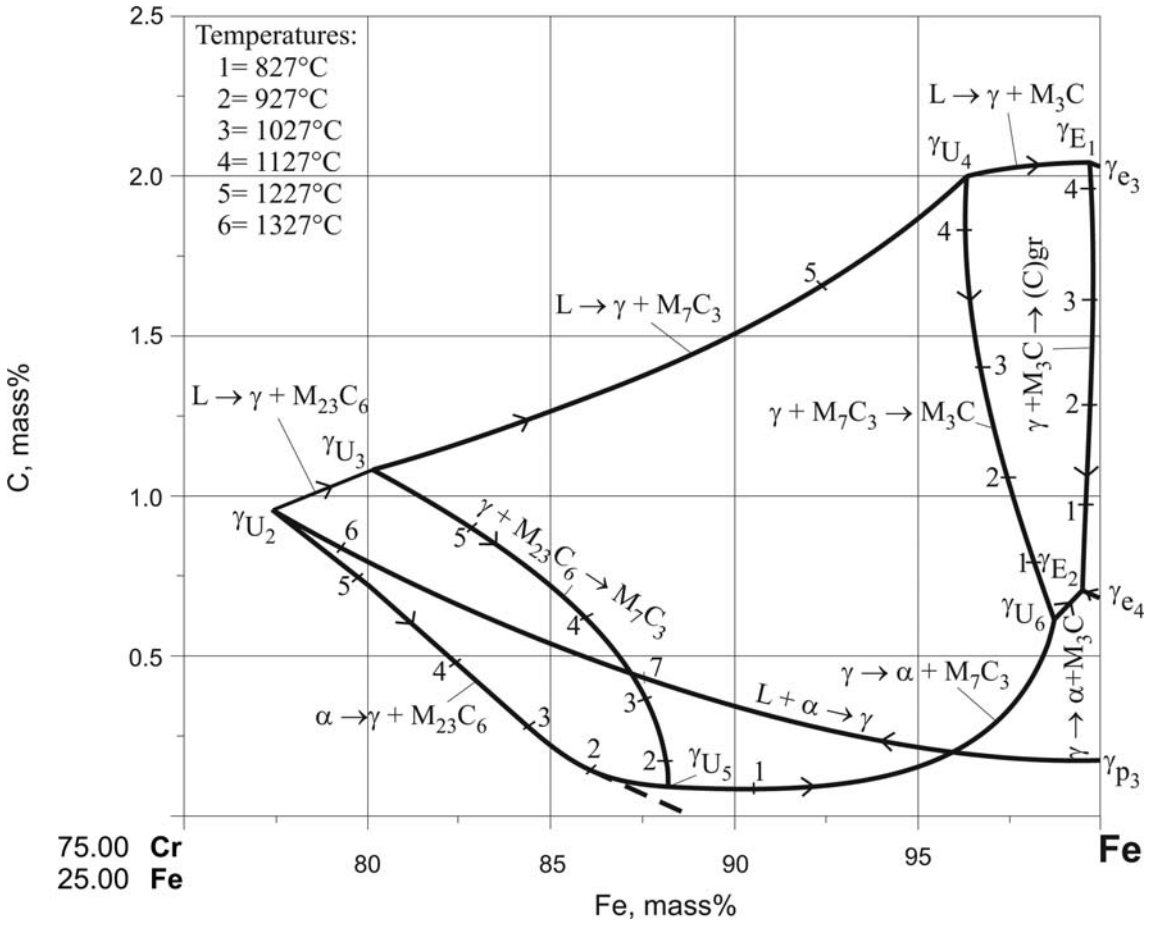

Fig. 5b. C-Cr-Fe. Solvus surface projection for the fcc γ phase

DOI: 10.1007/978-3-540-74196-1_3

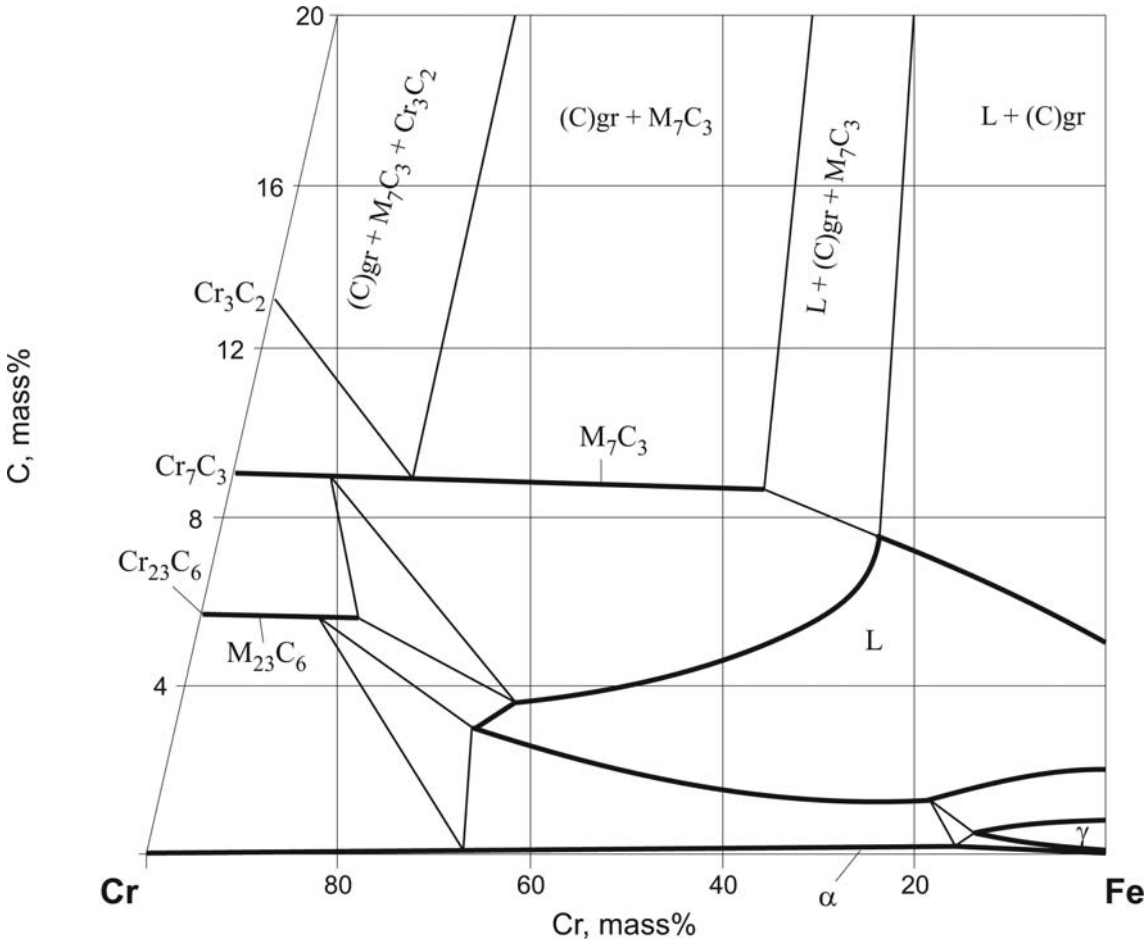

Fig. 6. C-Cr-Fe. Isothermal section at 1400°C

DOI: 10.1007/978-3-540-74196-1_3

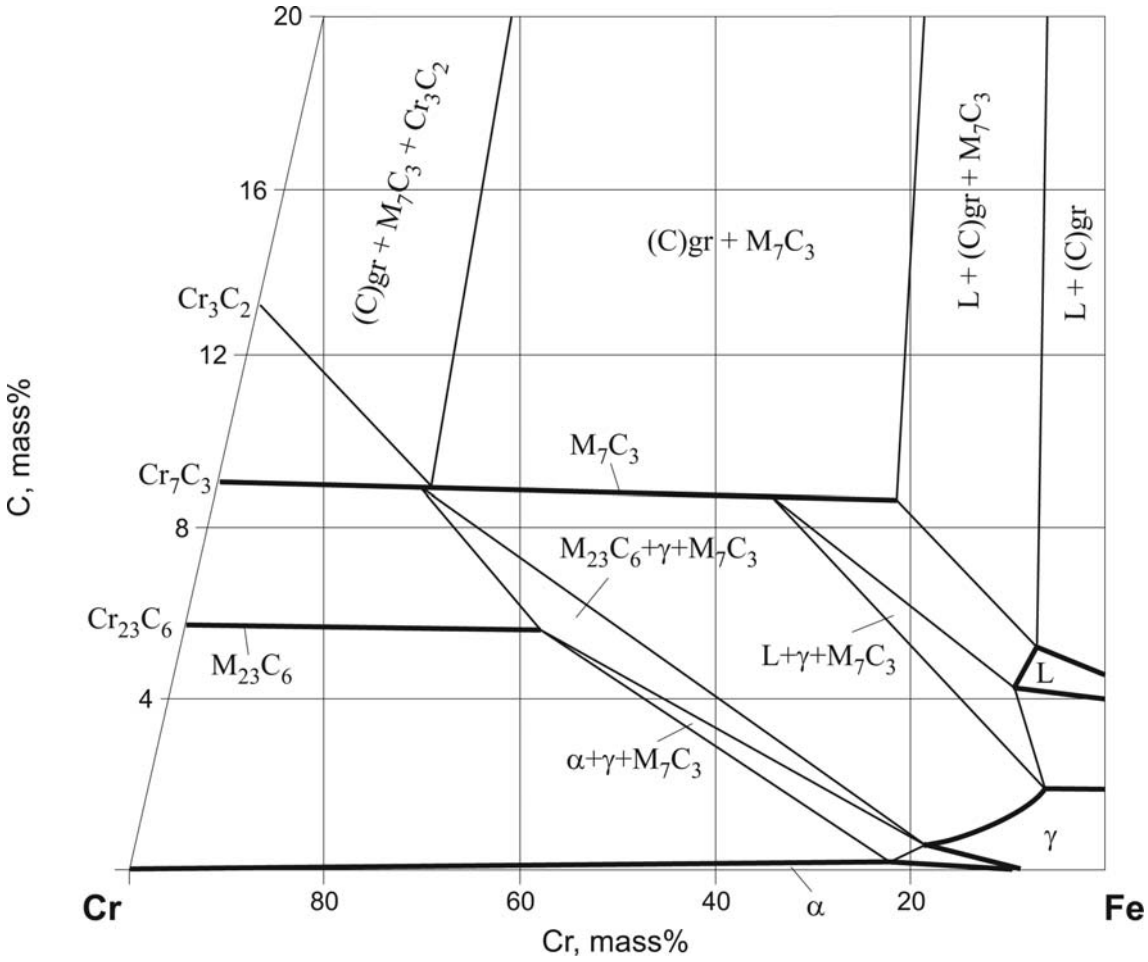

Fig. 7. C-Cr-Fe. Isothermal section at 1200°C

DOI: 10.1007/978-3-540-74196-1_3

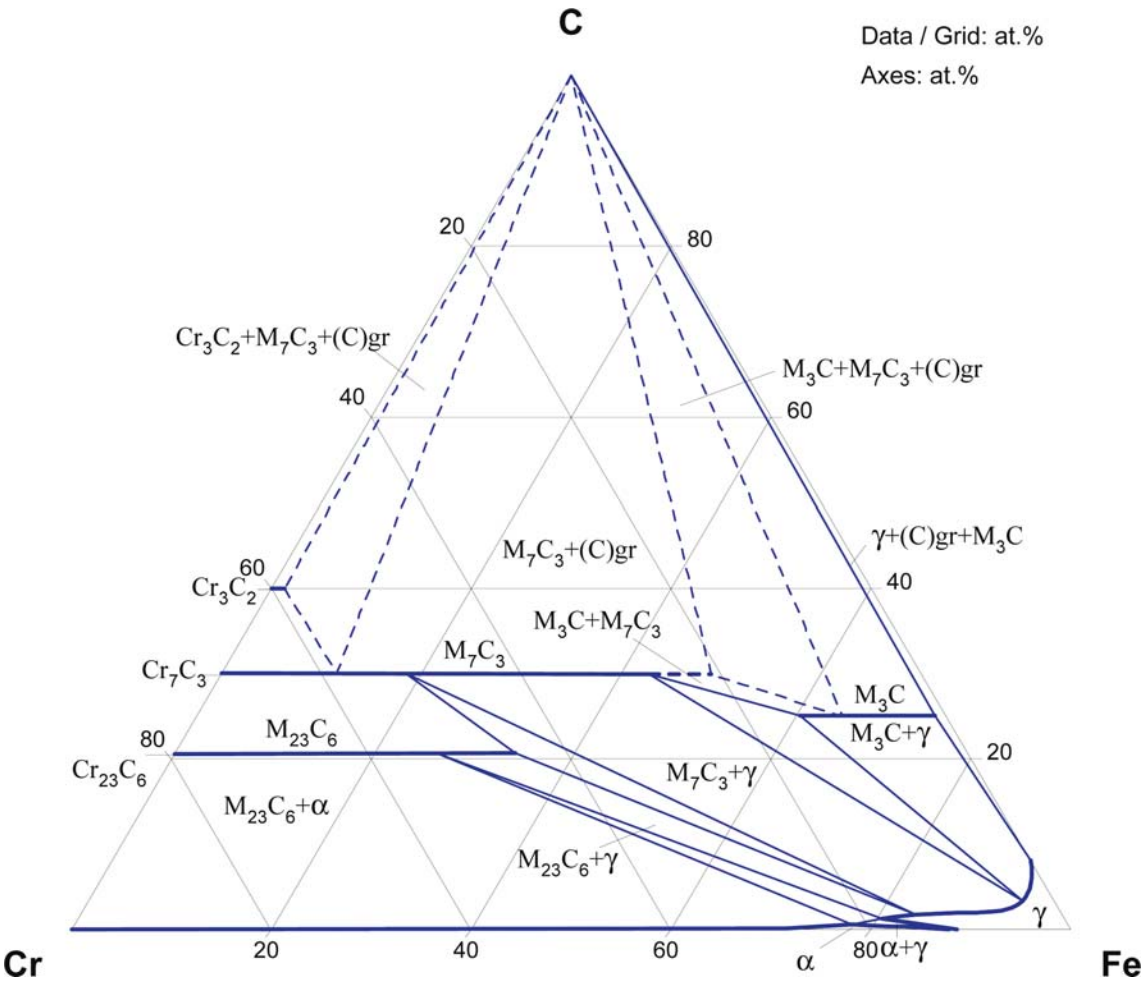

Fig. 8a. C-Cr-Fe. Isothermal section at 1000°C

DOI: 10.1007/978-3-540-74196-1_3

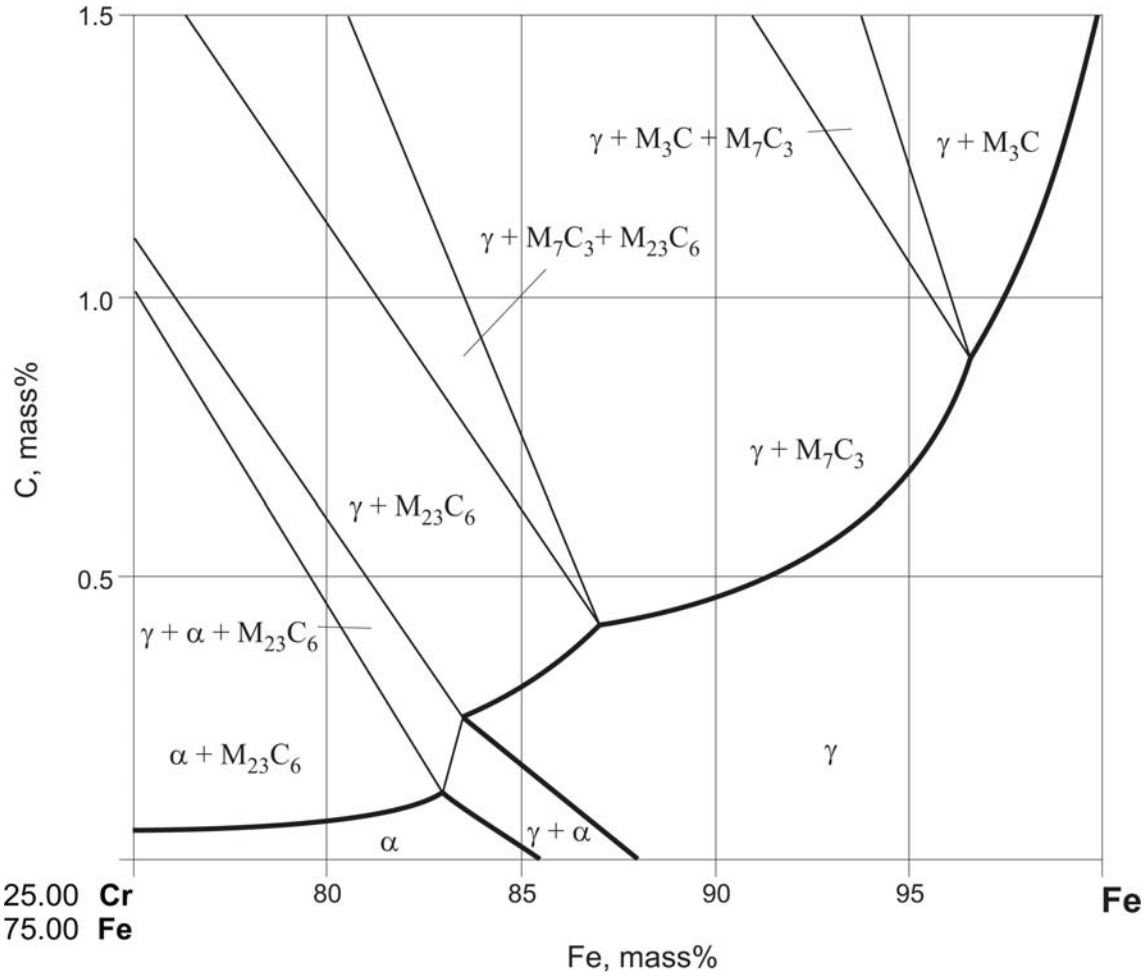

Fig. 8b. C-Cr-Fe. Isothermal section at 1000°C, Fe corner

DOI: 10.1007/978-3-540-74196-1_3

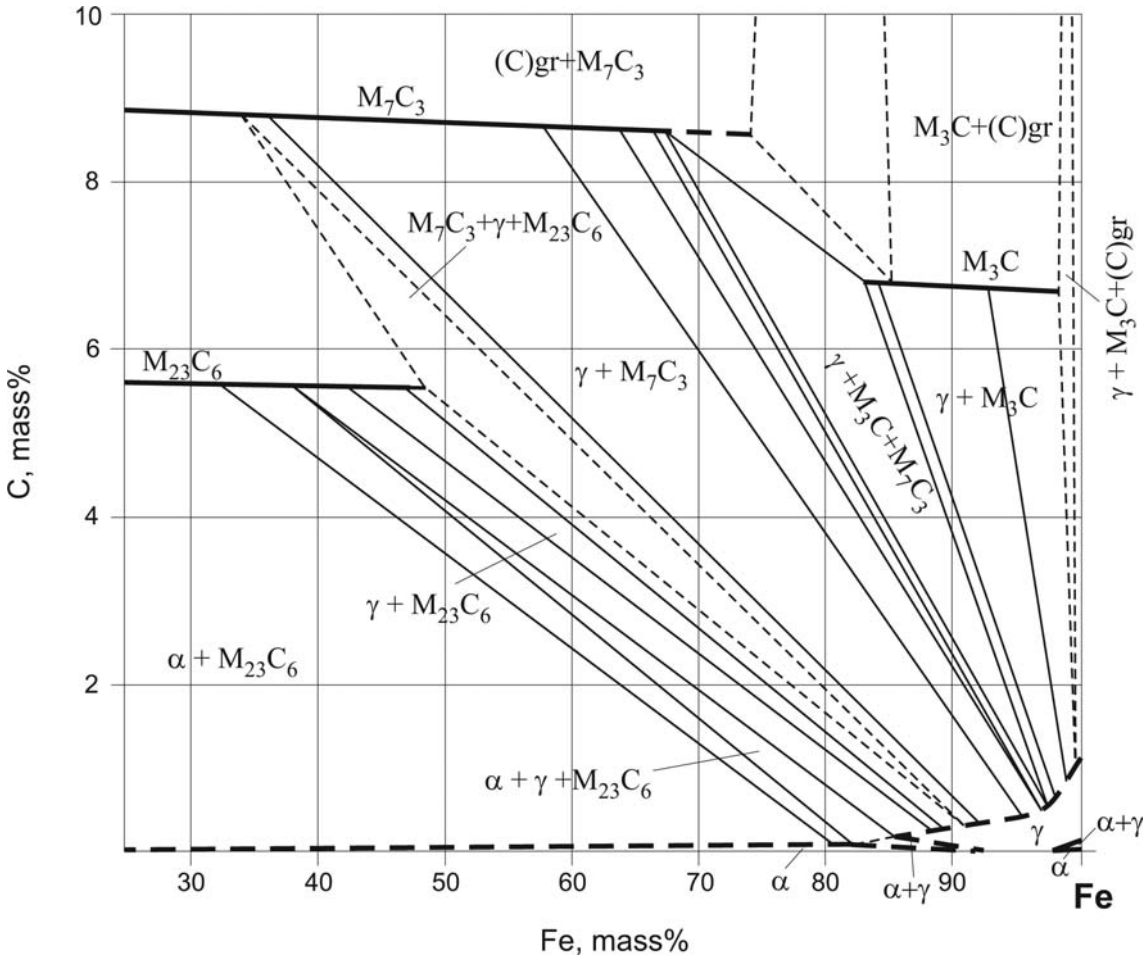

Fig. 9a. C-Cr-Fe. Isothermal section at 870°C

DOI: 10.1007/978-3-540-74196-1_3

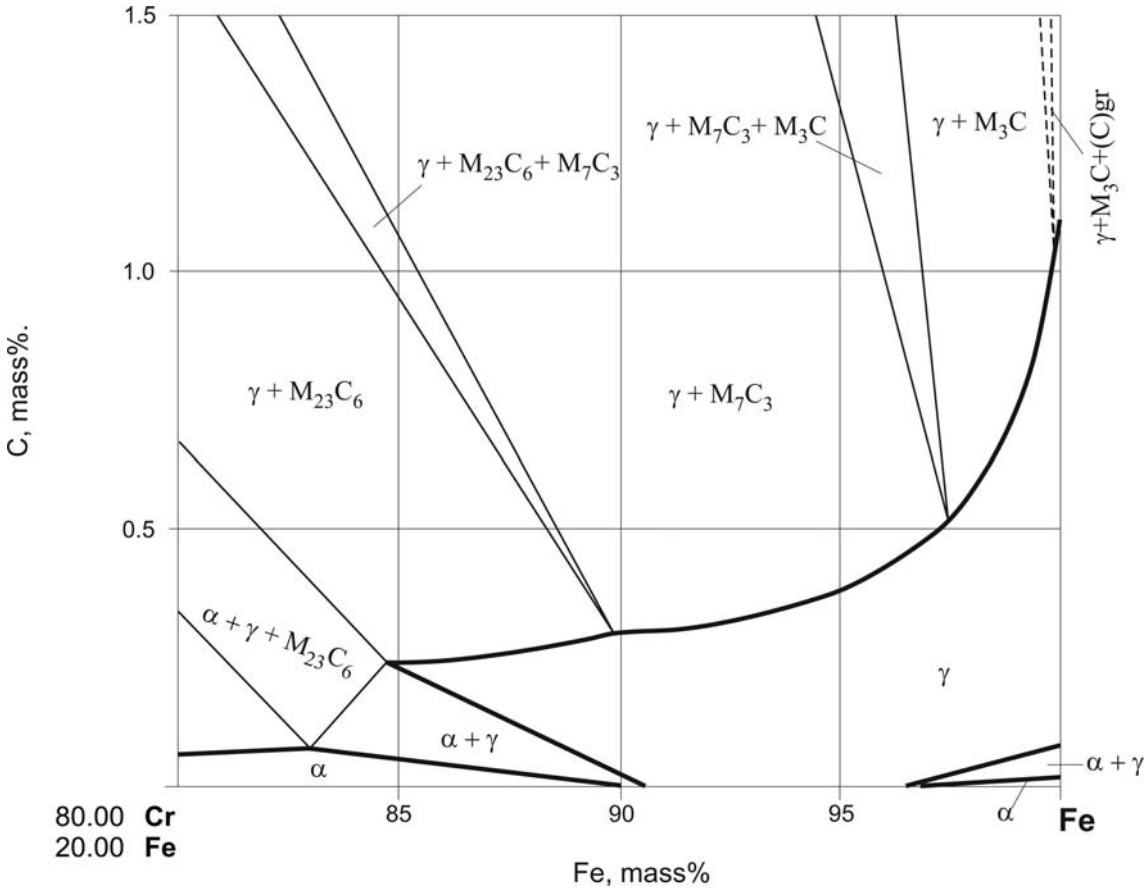

Fig. 9b. C-Cr-Fe. Isothermal section at 870°C, Fe corner

DOI: 10.1007/978-3-540-74196-1_3

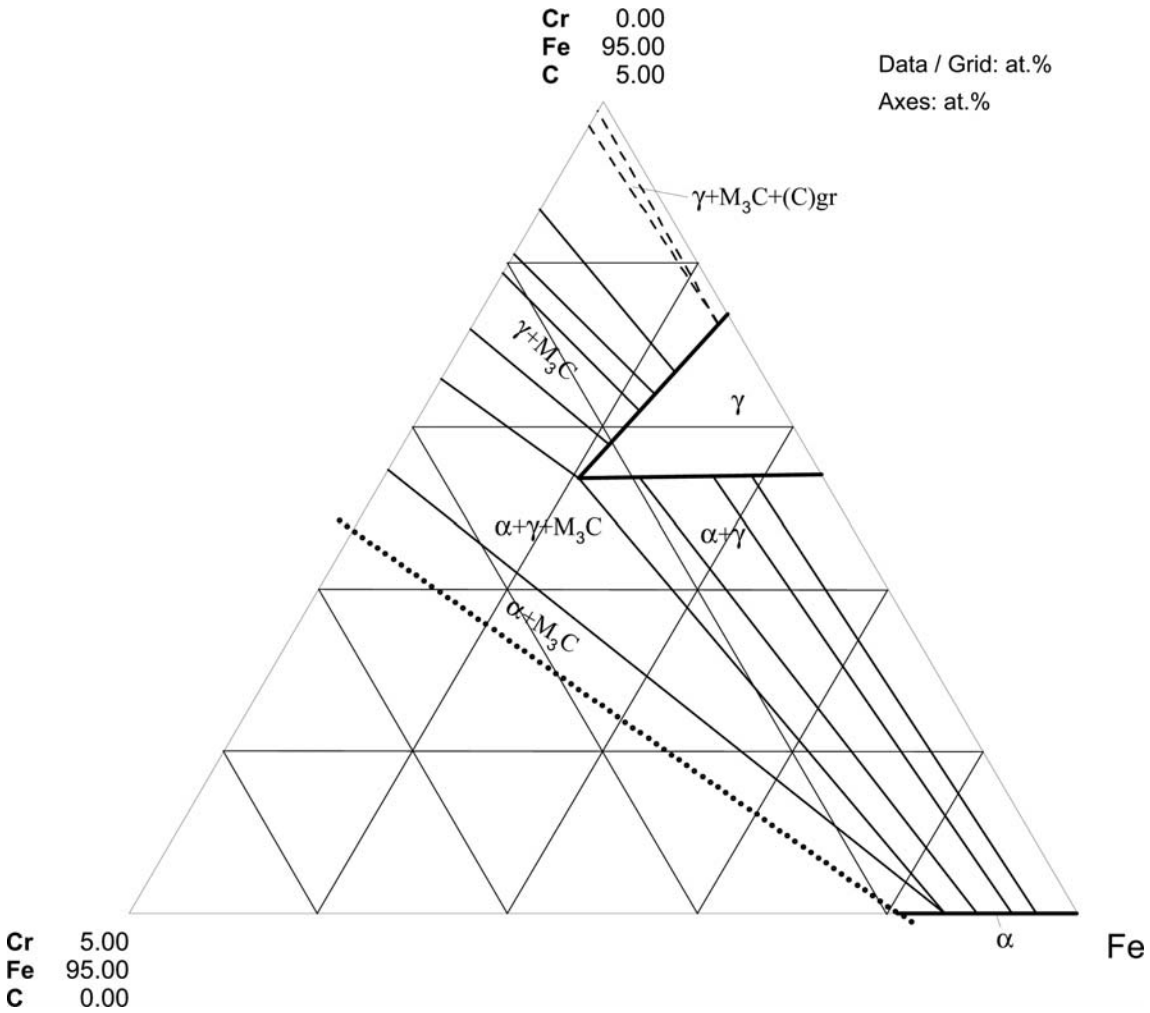

Fig. 10. C-Cr-Fe. Partial isothermal section at 750°C, equilibria of γ phase

DOI: 10.1007/978-3-540-74196-1_3

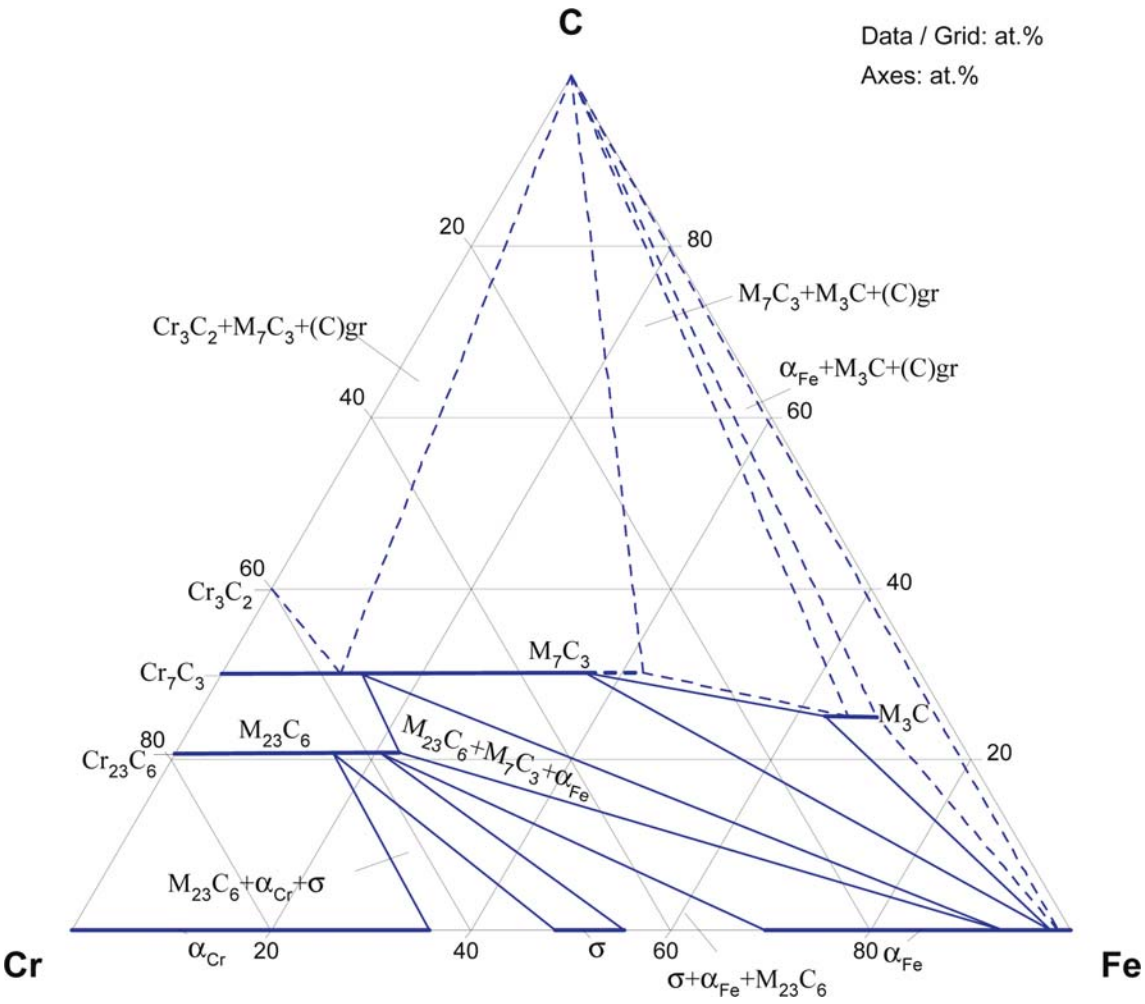

Fig. 11. C-Cr-Fe. Isothermal section at 700°C

DOI: 10.1007/978-3-540-74196-1_3

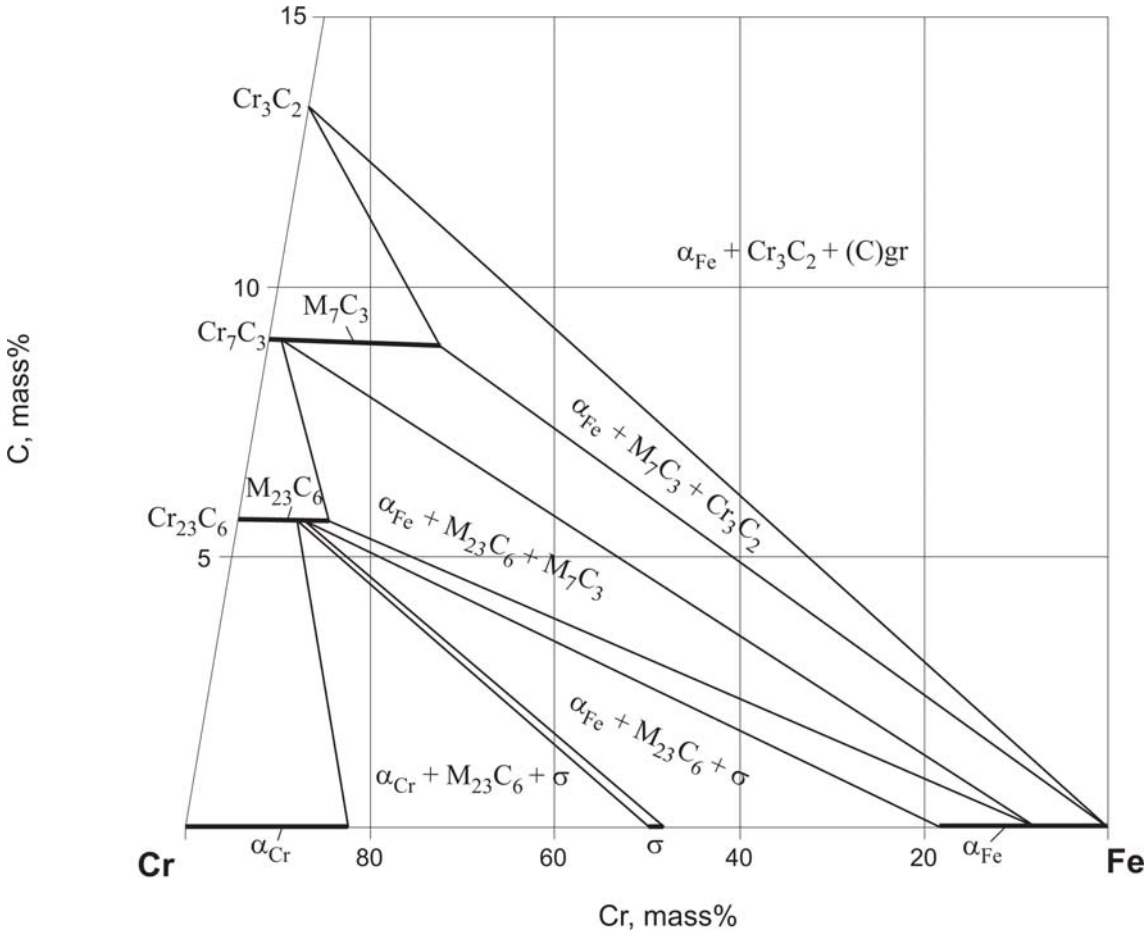

Fig. 12. C-Cr-Fe. Isothermal section at 527°C

DOI: 10.1007/978-3-540-74196-1_3

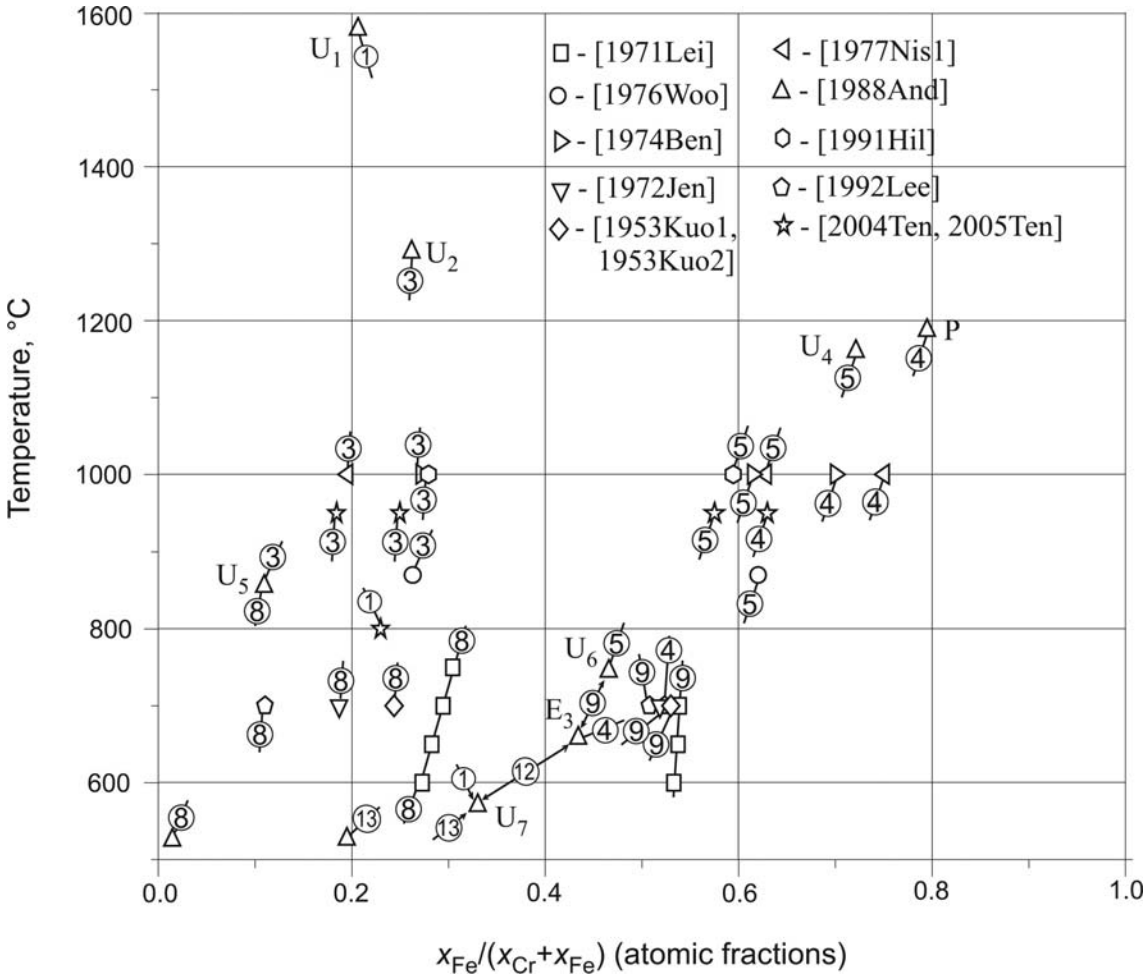

Fig. 13a. C-Cr-Fe. Composition of M_7C_3 carbide in equilibria
$Cr_3C_2+M_7C_3+(C)gr$ (1), $\alpha+\gamma+M_{23}C_6$ (2), $\gamma+M_{23}C_6+M_7C_3$ (3), $M_3C+M_7C_3+(C)gr$ (4), $\gamma+M_7C_3+M_3C$ (5), $\gamma+M_3C+(C)gr$ (6), $\alpha+\gamma+M_7C_3$ (7), $\alpha+M_{23}C_6+M_7C_3$ (8), $\alpha+M_3C+M_7C_3$ (9), $\alpha+\gamma+M_3C$ (10), $\alpha+M_3C+(C)gr$ (11), $\alpha+M_7C_3+(C)gr$ (12), $\alpha+M_7C_3+Cr_3C_2$ (13)

DOI: 10.1007/978-3-540-74196-1_3

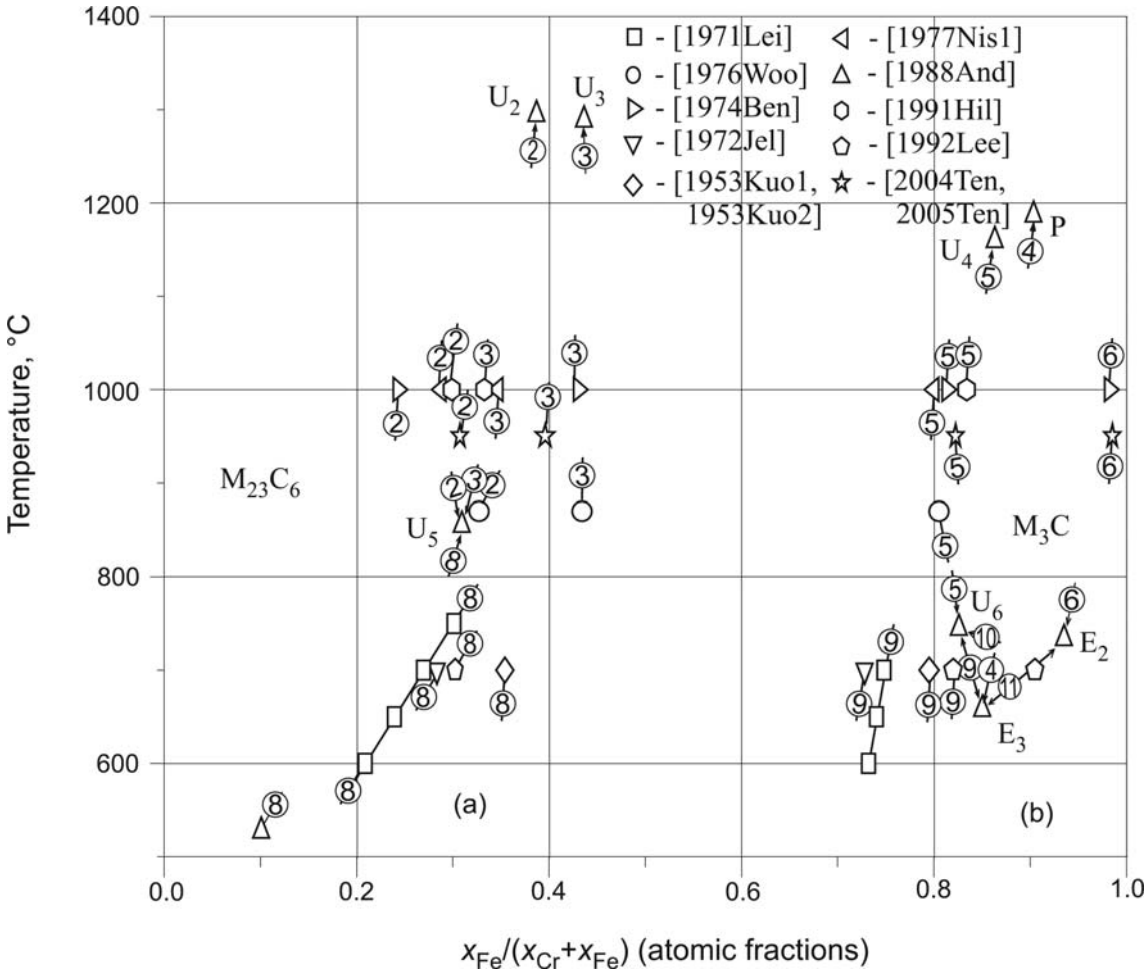

Fig. 13b. C-Cr-Fe. Composition of $M_{23}C_6$ (a) and M_3C (b) carbides in the equilibria Cr_3C_2+M_7C_3+(C)gr (1), α+γ+$M_{23}C_6$ (2), γ+$M_{23}C_6$+M_7C_3 (3), M_3C+M_7C_3+(C)gr (4), γ+M_7C_3+M_3C (5), γ+M_3C+(C)gr (6), α+γ+M_7C_3 (7), α+$M_{23}C_6$+M_7C_3 (8), α+M_3C+M_7C_3 (9), α+γ+M_3C (10), α+M_3C+(C)gr (11), α+M_7C_3+(C)gr (12), α+M_7C_3+Cr_3C_2 (13)

DOI: 10.1007/978-3-540-74196-1_3

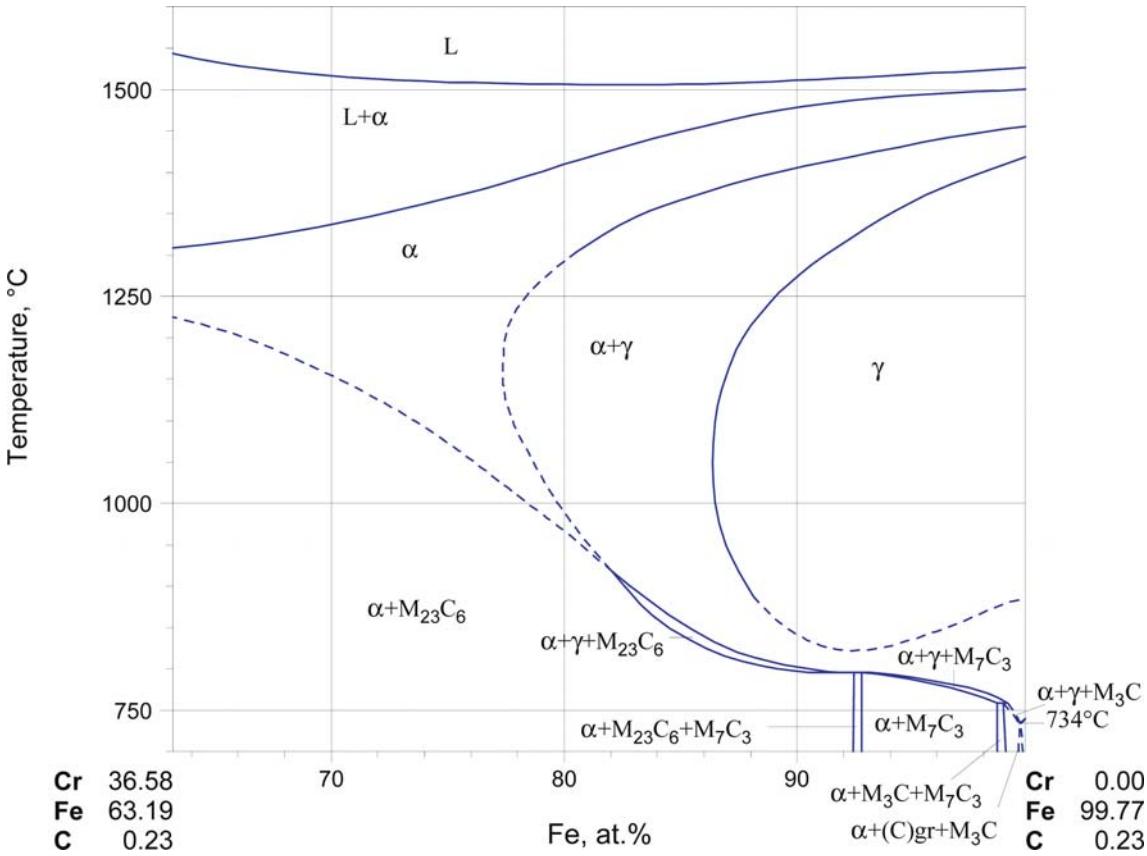

Fig. 14. C-Cr-Fe. Vertical section at 0.05 mass% C, plotted in at.%

DOI: 10.1007/978-3-540-74196-1_3

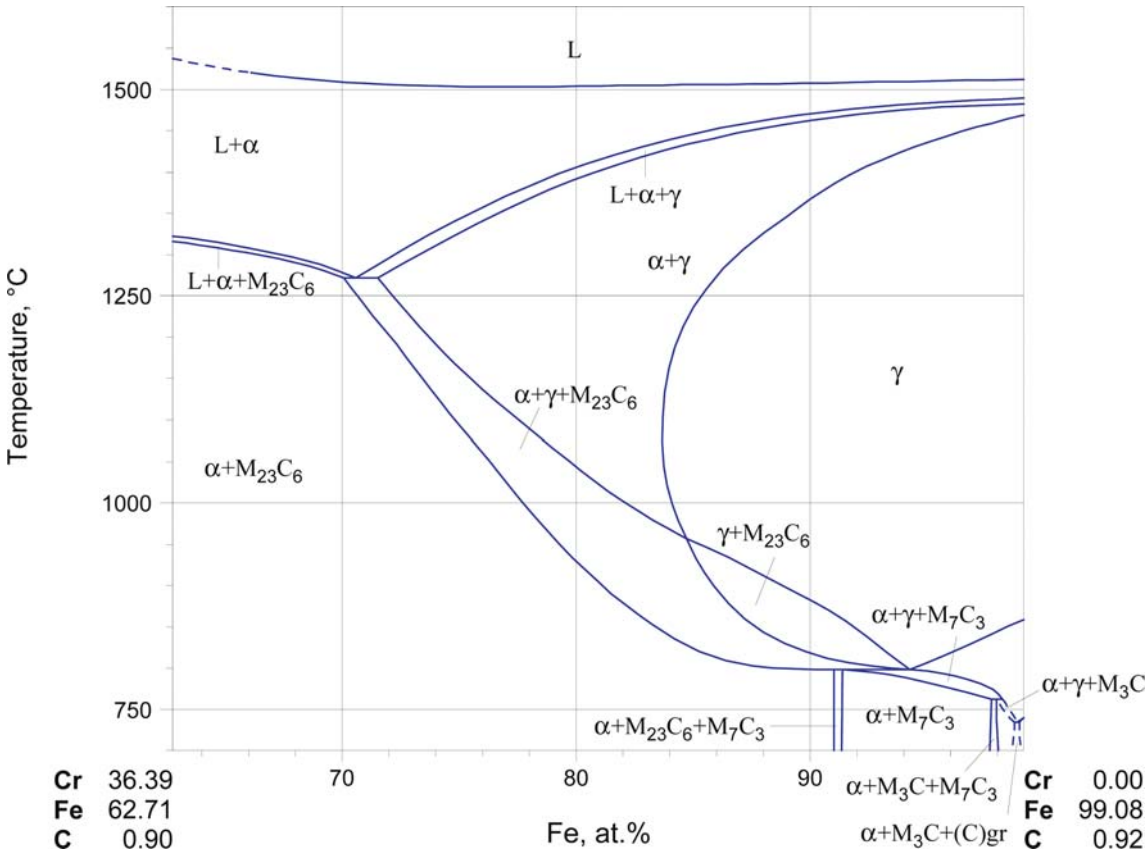

Fig. 15. C-Cr-Fe. Vertical section at 0.2 mass% C, plotted in at.%

DOI: 10.1007/978-3-540-74196-1_3

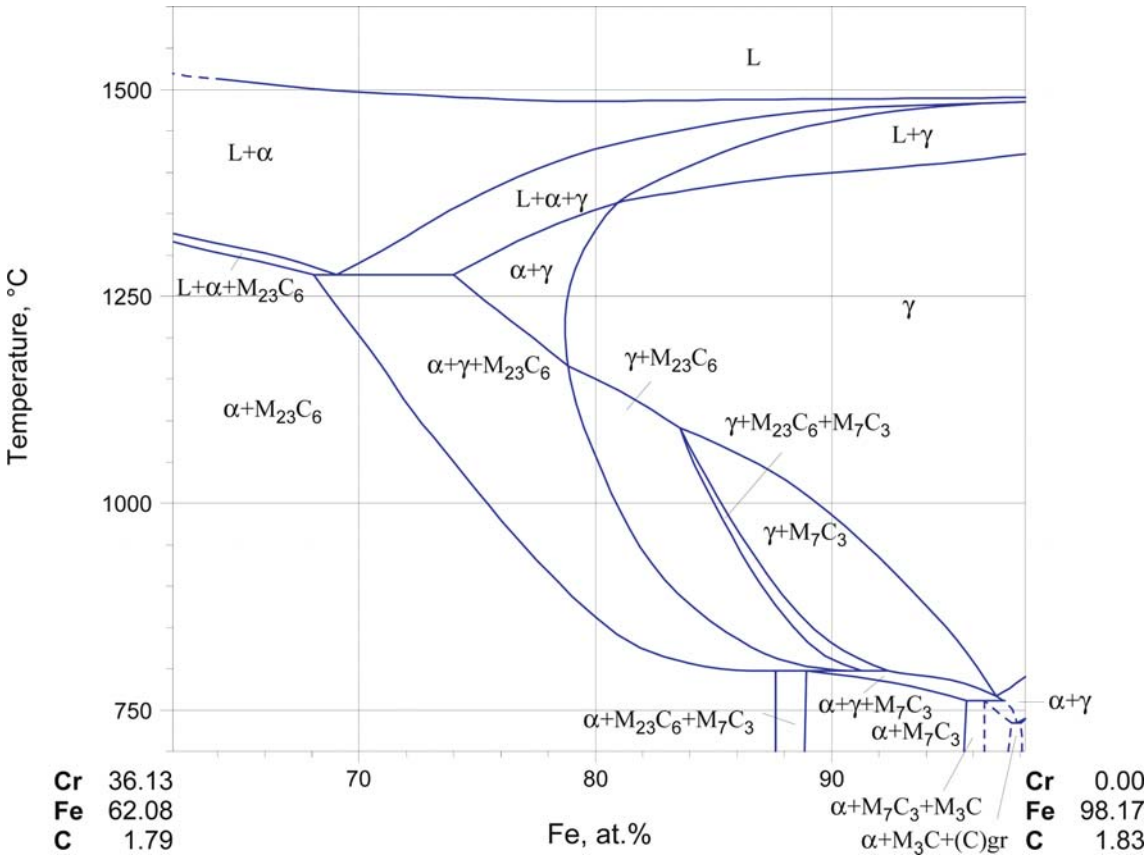

Fig. 16. C-Cr-Fe. Vertical section at 0.4 mass% C, plotted in at.%

DOI: 10.1007/978-3-540-74196-1_3

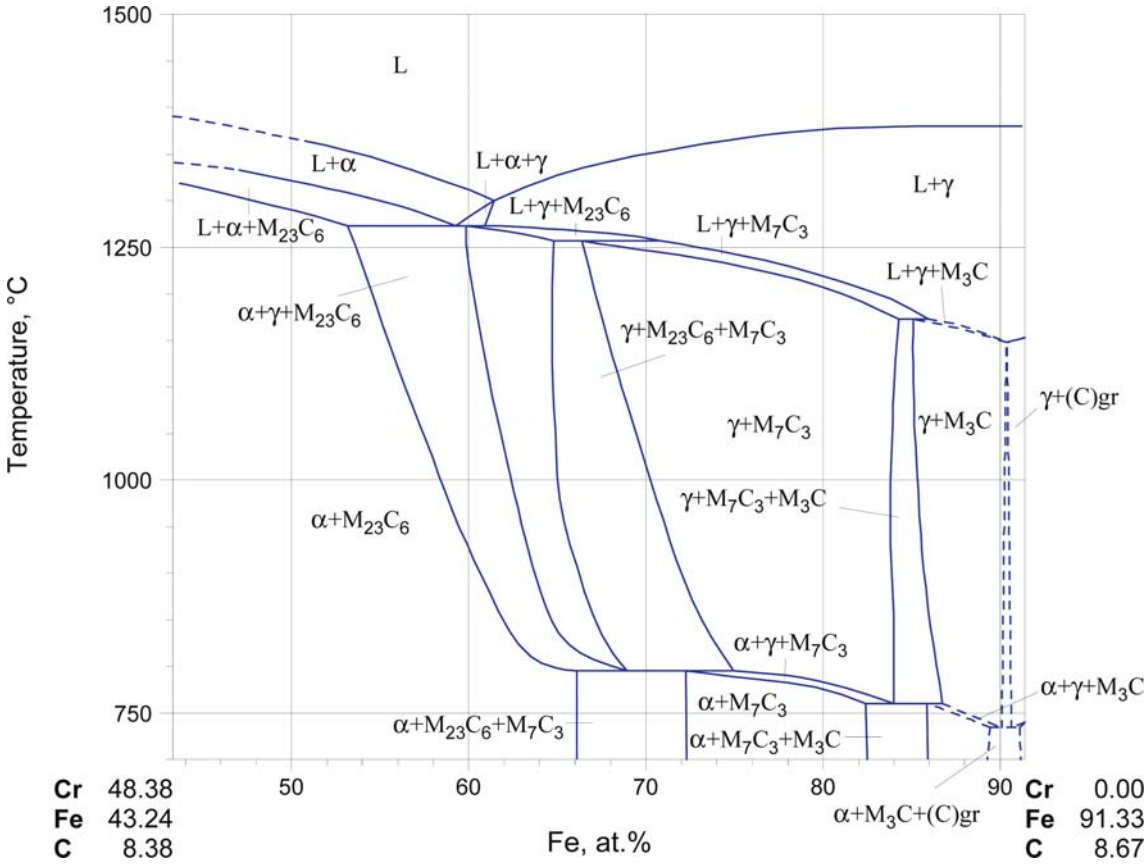

Fig. 17. C-Cr-Fe. Vertical section at 2 mass% C, plotted in at.%

DOI: 10.1007/978-3-540-74196-1_3

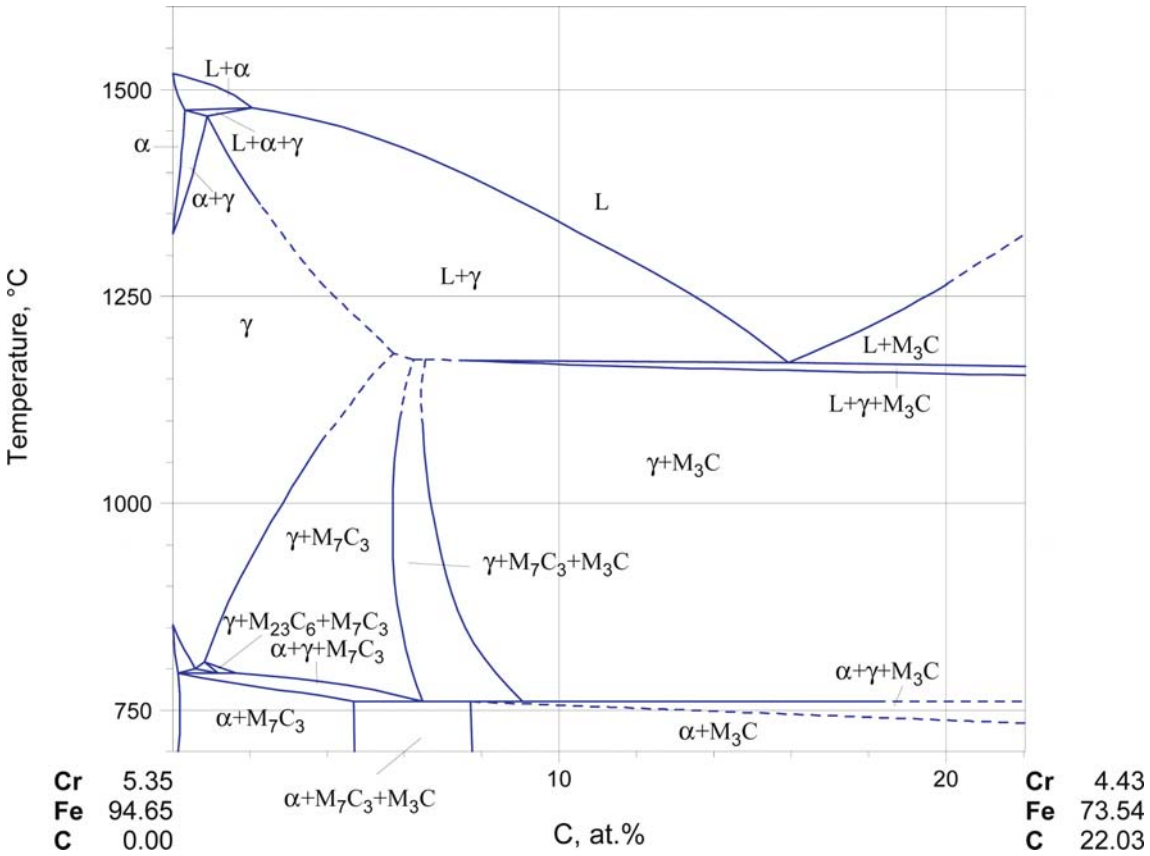

Fig. 18. C-Cr-Fe. Vertical section at 5 mass% Cr, plotted in at.%

DOI: 10.1007/978-3-540-74196-1_3

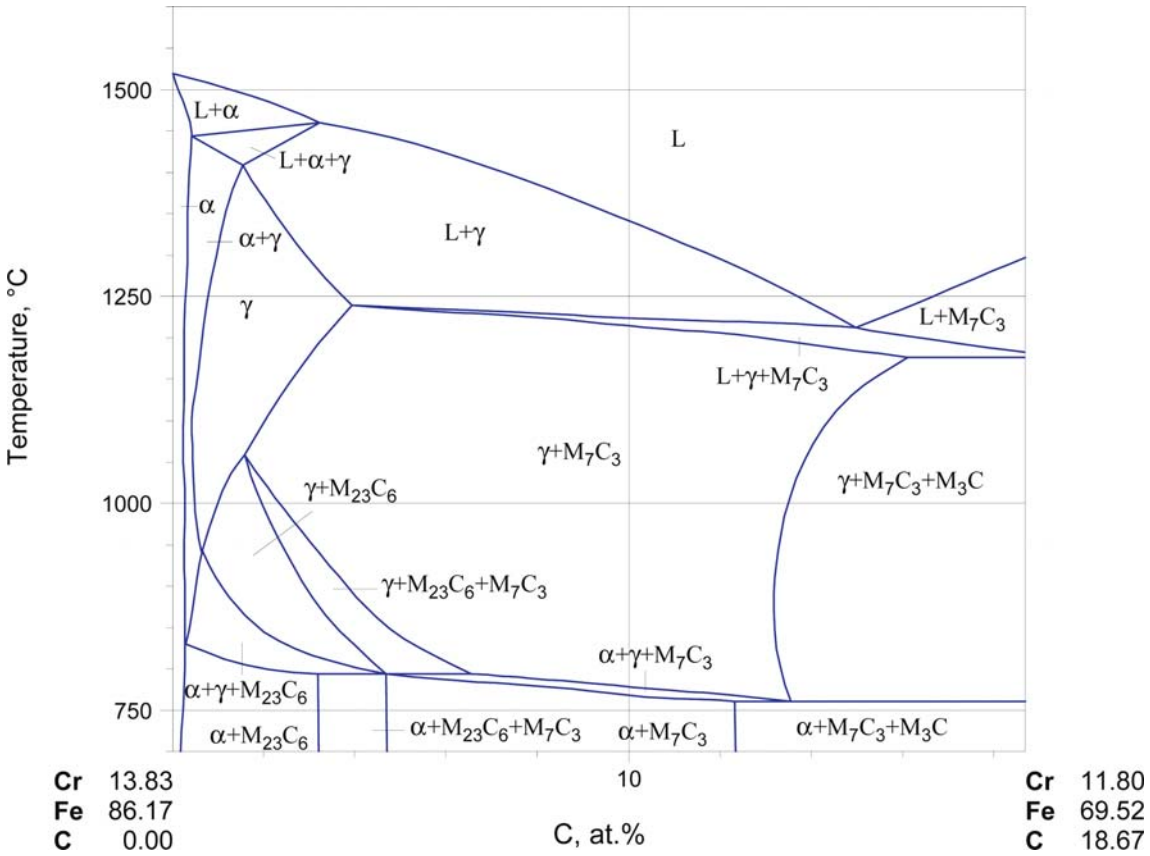

Fig. 19. C-Cr-Fe. Vertical section at 13 mass% Cr, plotted in at.%

DOI: 10.1007/978-3-540-74196-1_3

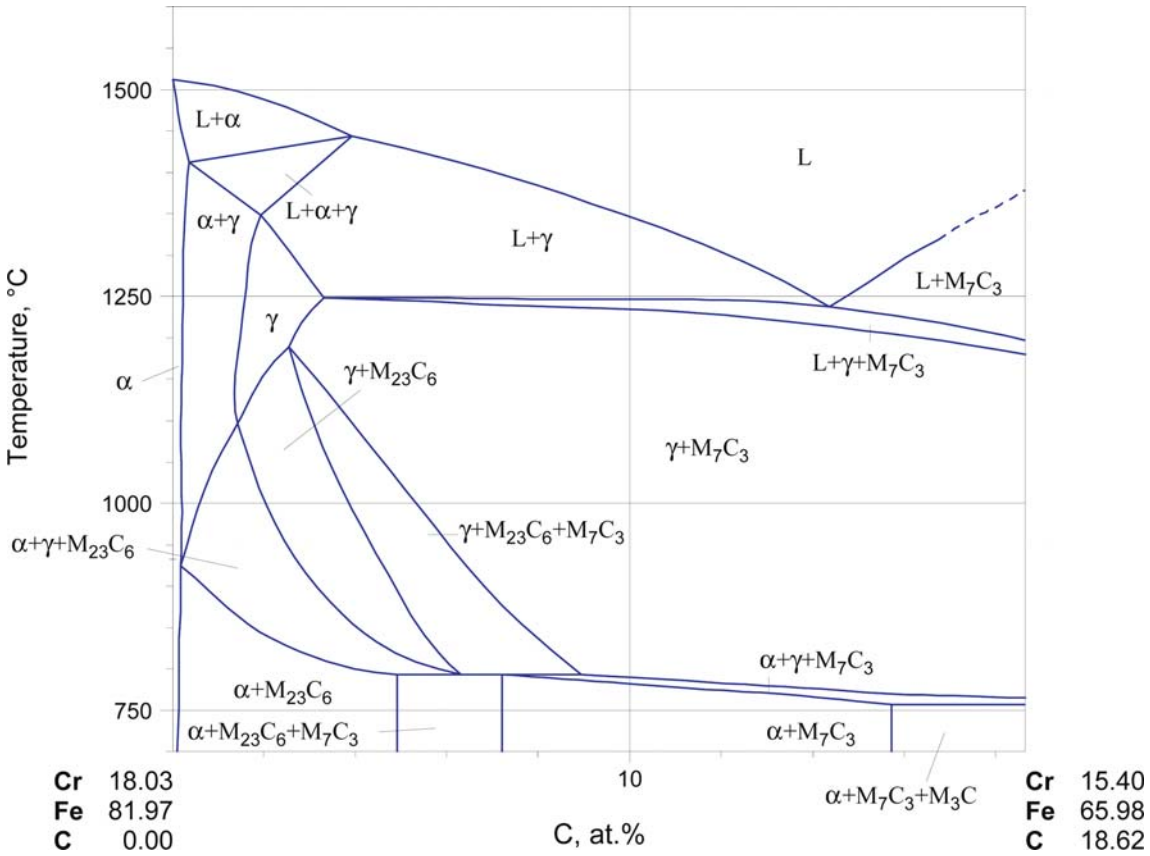

Fig. 20. C-Cr-Fe. Vertical section at 17 mass% Cr, plotted in at.%

DOI: 10.1007/978-3-540-74196-1_3

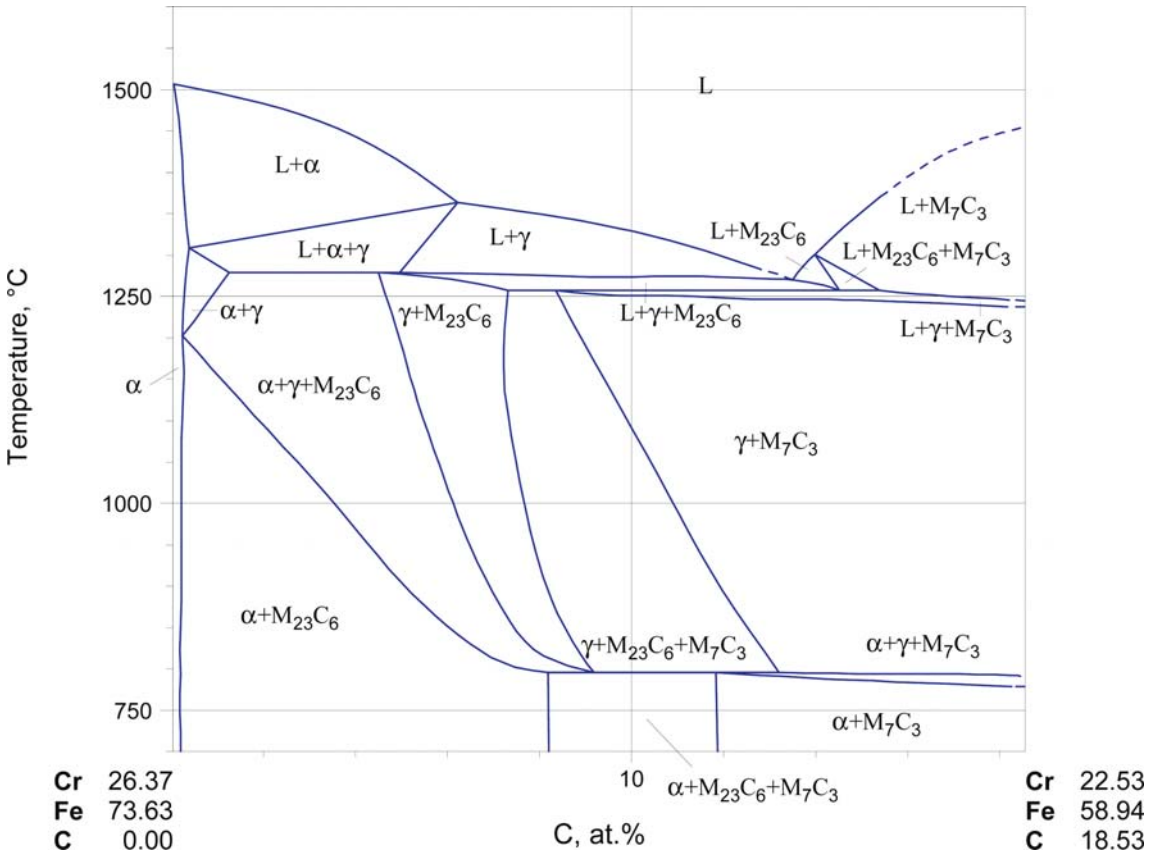

Fig. 21. C-Cr-Fe. Vertical section at 25 mass% Cr, plotted in at.%

DOI: 10.1007/978-3-540-74196-1_3

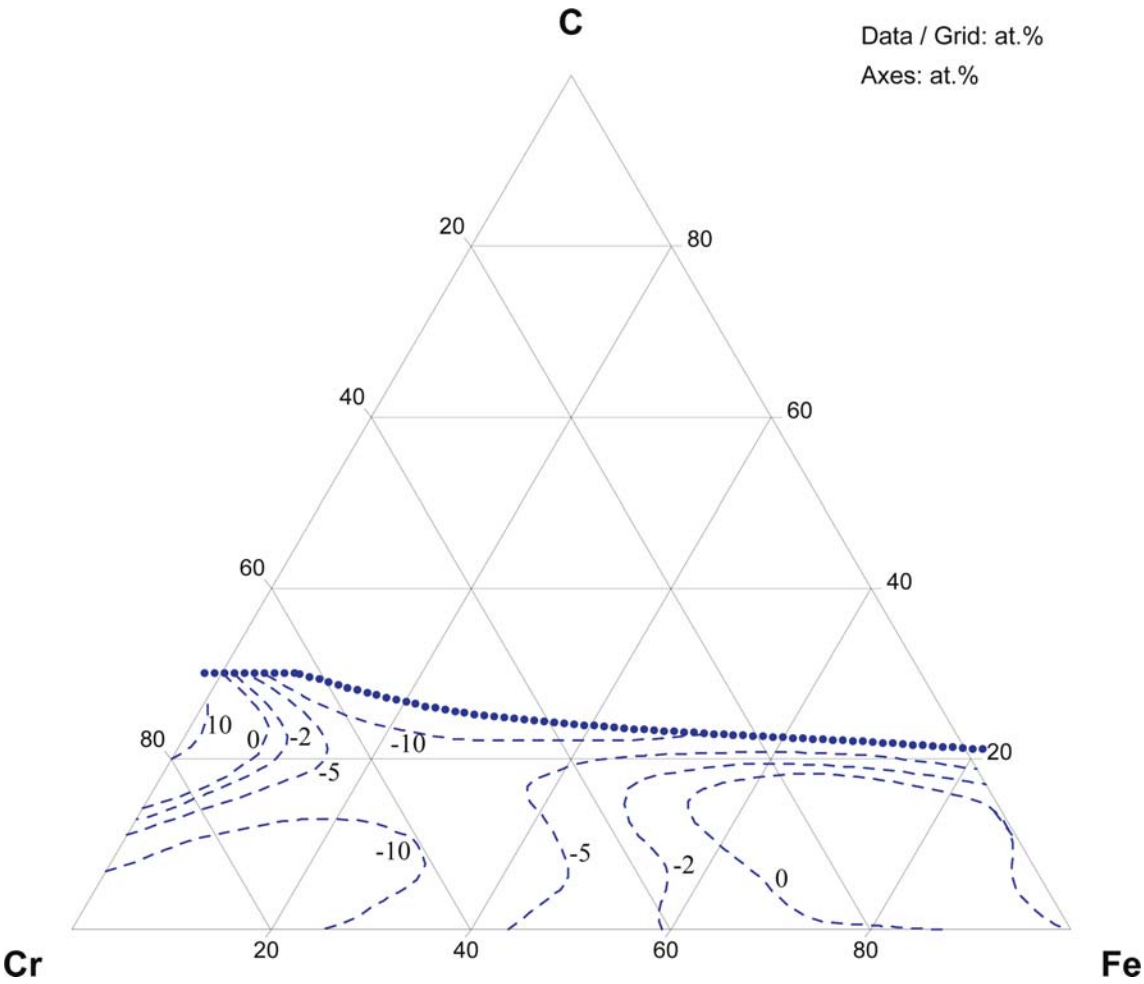

Fig. 22a. C-Cr-Fe. Partial enthalpy (kJ·mol^{-1}) of mixing for ternary C-Cr-Fe melts at 1627°C: iron

DOI: 10.1007/978-3-540-74196-1_3

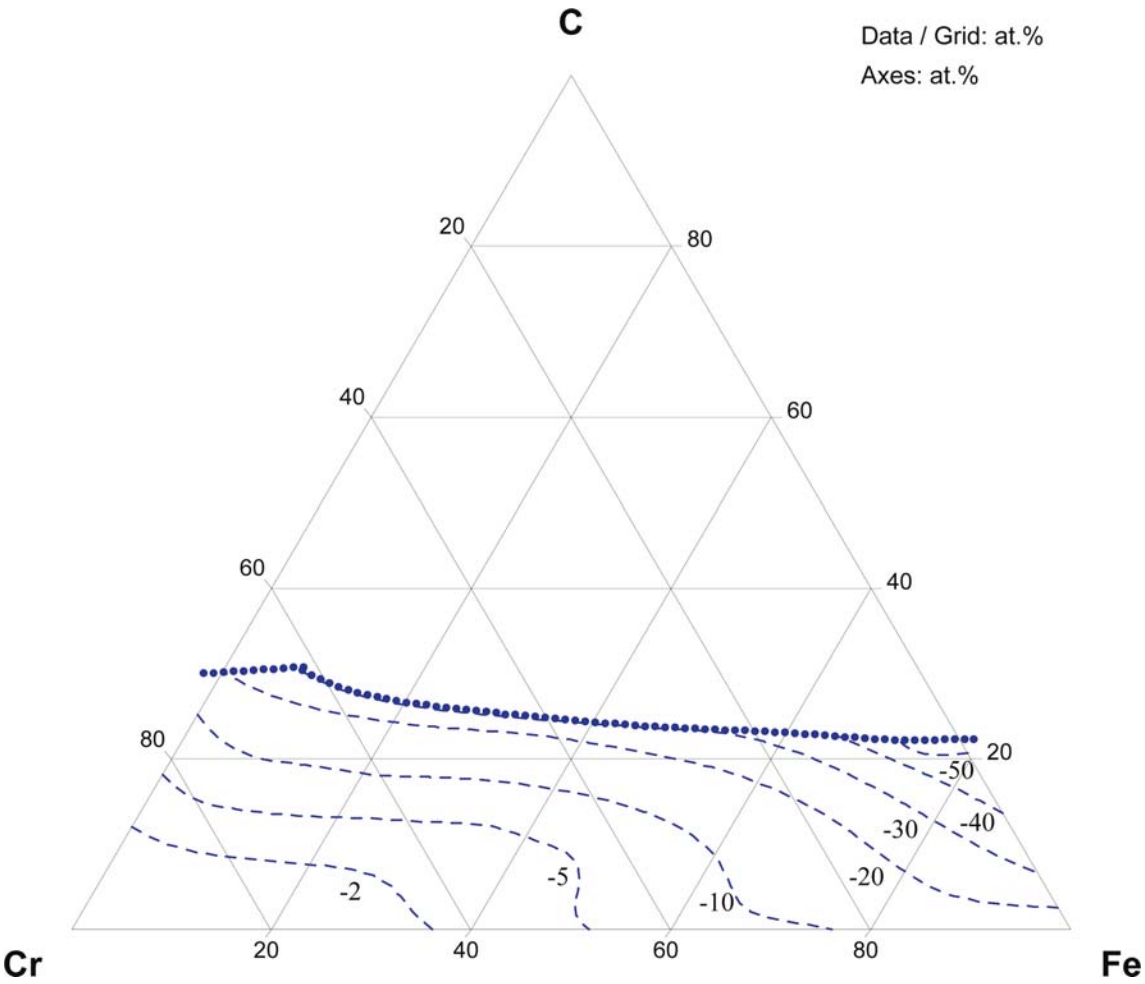

Fig. 22b. C-Cr-Fe. Partial enthalpy ($kJ \cdot mol^{-1}$) of mixing for ternary C-Cr-Fe melts at 1627°C: chromium

DOI: 10.1007/978-3-540-74196-1_3

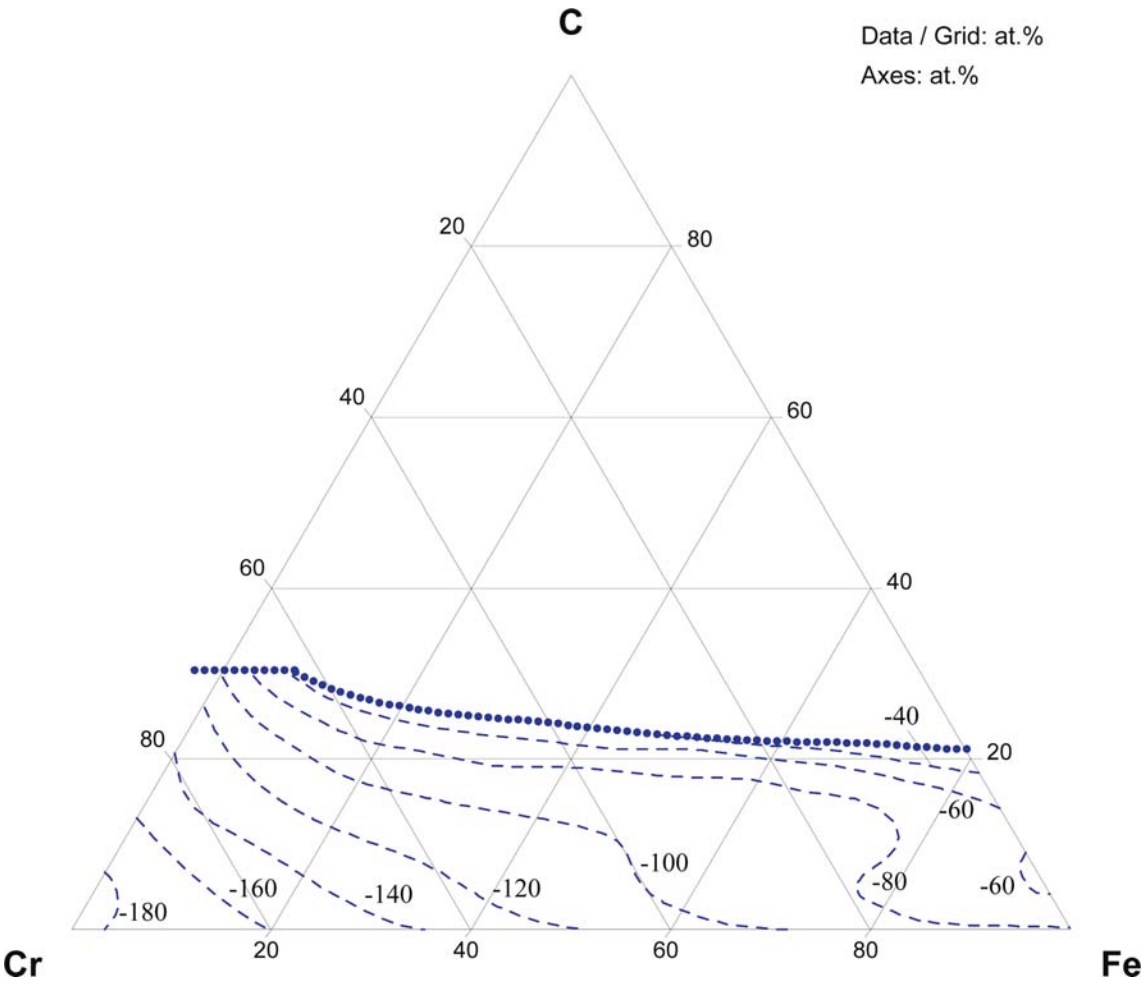

Fig. 22c. C-Cr-Fe. Partial enthalpy (kJ·mol^{-1}) of mixing for ternary C-Cr-Fe melts at 1627°C: undercooled liquid carbon

DOI: 10.1007/978-3-540-74196-1_3

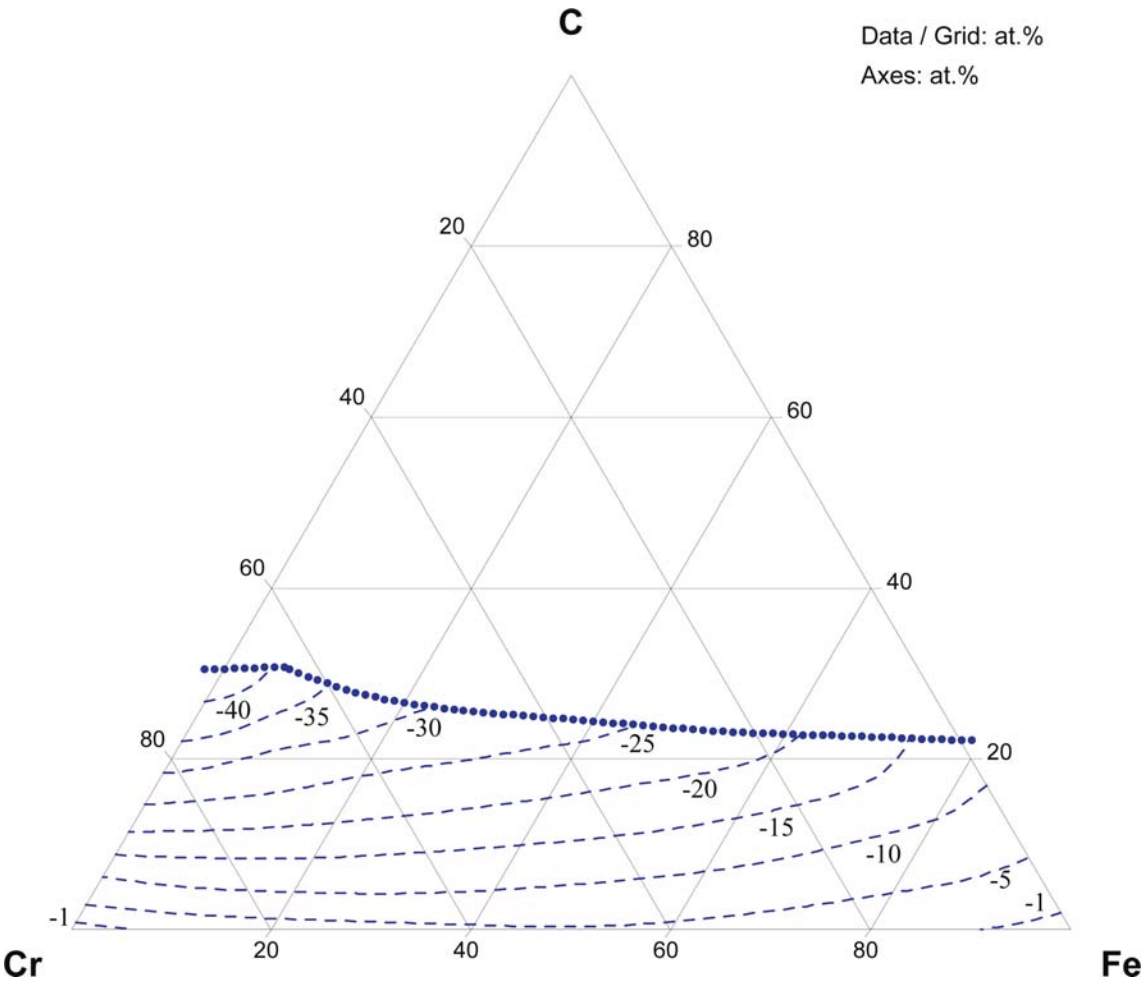

Fig. 23a. C-Cr-Fe. Integral excess enthalpy ($kJ \cdot mol^{-1}$) of formation of ternary C-Cr-Fe melts at 1627°C (reference state: liquid Cr, liquid Fe and undercooled liquid carbon)

DOI: 10.1007/978-3-540-74196-1_3

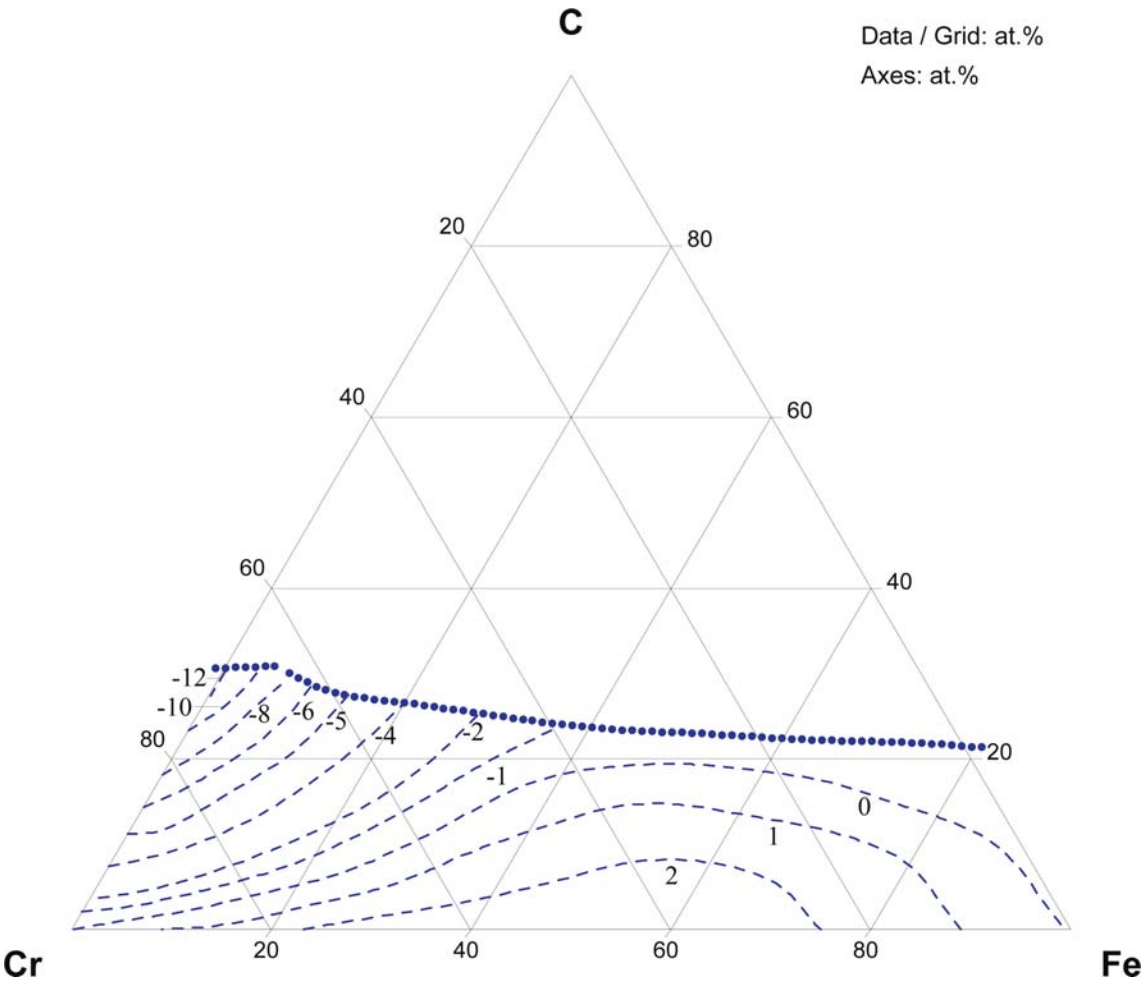

Fig. 23b. C-Cr-Fe. Integral entropy ($J \cdot mol^{-1} \cdot K^{-1}$) of formation of ternary C-Cr-Fe melts at 1627°C (reference state: liquid Cr, liquid Fe and undercooled liquid carbon)

DOI: 10.1007/978-3-540-74196-1_3

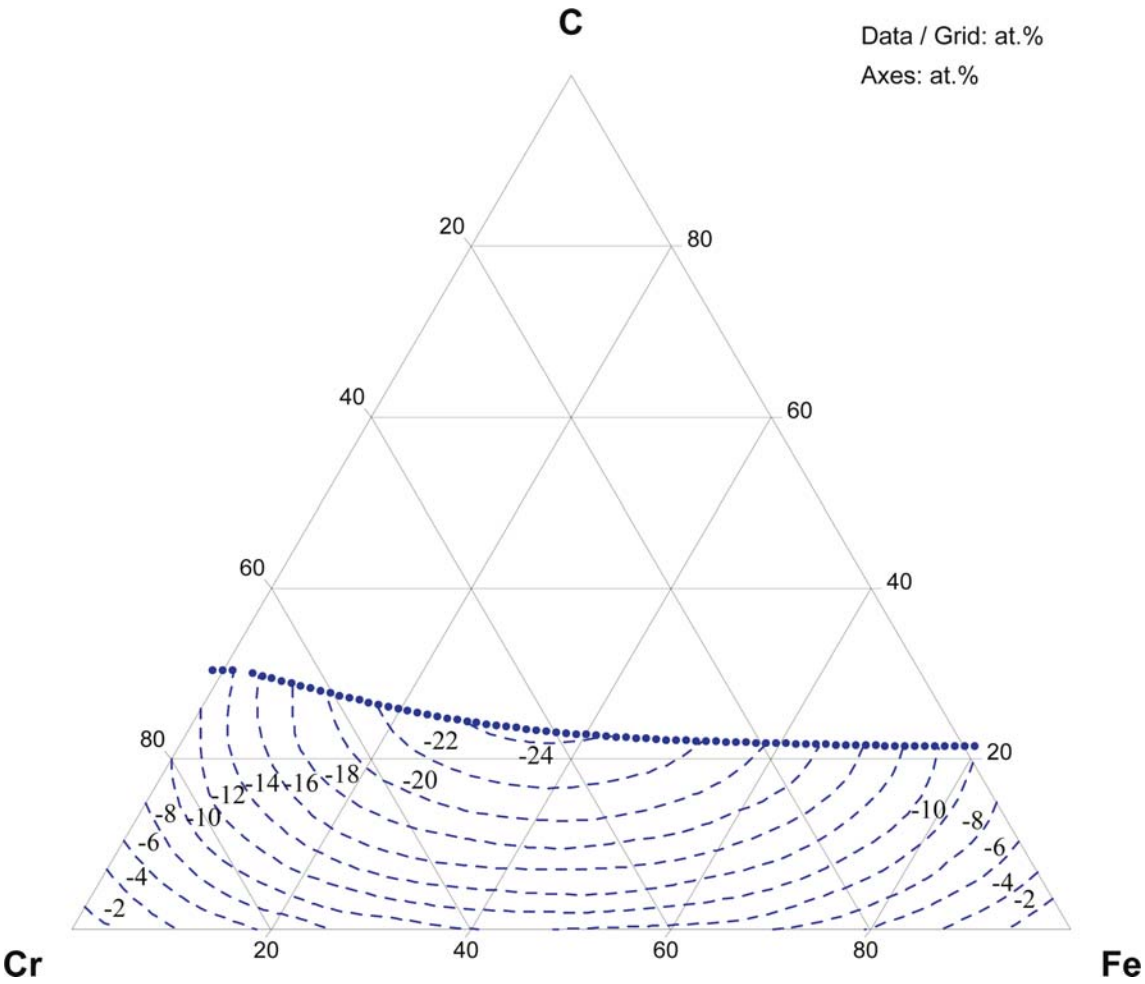

Fig. 23c. C-Cr-Fe. Integral excess Gibbs energy ($kJ \cdot mol^{-1}$) of formation of ternary C-Cr-Fe melts at 1627°C (reference state: liquid Cr, liquid Fe and undercooled liquid carbon)

DOI: 10.1007/978-3-540-74196-1_3

References

[1907Goe] Goerens, P., Stadeler, A. "Influence of Chromium on the on the Carbon Solubility in Iron and Carbides Forming" (in German), *Metallurgie*, **4**(1), 18–24 (1907) (Morphology, Phase Relations, Experimental, 5)

[1911Arn] Arnold, J.O., Read, A.A., "The Chemical and Mechanical Relations of Iron, Chromium and Carbon", *J. Iron Steel Inst.*, **83**, 249–268 (1911) (Morphology, Mechan. Prop., Experimental, 14)

[1918Mur] Murakami, T., "Ternary Alloys of Iron, Carbon and Chromium", *Sci. Rep. Tohoku Imp. Univ.*, **7**, 266–276 (1918) (Morphology, Phase Relations, Phase Diagram, Experimental, 9)

[1921Dae] Daeves, K., "The Solubility Limit of Carbon Under Quenching. 1. The Cromium-Iron-Carbon System" (in German), *Z. Anorg. Chem.*, **118**, 55–66 (1921) (Morphology, Phase Relations, Phase Diagram, Experimental, 24)

[1921Rus] Russell, T.F., "On the Constitution of Chromium Steels", *J. Iron Steel Inst.*, **104**(2), 247–295 (1921) (Morphology, Phase Diagram, Experimental, Electr. Prop., 10)

[1923Aus] Austin, C.R., "Alloys in the Ternary System Iron-Chromium-Carbon", *J. Iron Steel Inst., London*, **108**(2), 235–262 (1923) (Morphology, Phase Relations, Experimental, 11)

[1923Mac] MacQuigg, C.E., "Some Commercial Alloys of Iron, Chromium, and Carbon in the Higher Chromium Ranges", *Trans. Amer. Inst. Min. Met. Eng.*, **69**, 831–847 (1923) (Morphology, Phase Relations, Electr. Prop., Mechan. Prop., 10)

[1924Fis] Fischbeck, K., "The Iron-Chromium-Carbon Ternary System" (in German), *Stahl Eisen*, **44**(25), 715–719 (1924) (Phase Diagram, Review, 11)

[1924Obe] Oberhoffer, P., Daeves, K., Rapatz, F., "Carbon Solubility Limit Cheking in Chromium and Tungsten Steels" (in German), *Stahl Eisen*, **44**(16), 432 (1924) (Morphology, Phase Relations, Experimental, 20)

[1926Mei] Meierling, T., Denecke, W., "About the Ternary System Iron-Chromium-Carbon" (in German), *Z. Anorg. Chem.*, **151**, 113–120 (1926) (Phase Diagram, Experimental, 11)

[1926Veg1] Vegesack, A.V., "The Iron-Chromium-Carbon Ternary System" (in German), *Z. Anorg. Chem.*, **154**, 42–50 (1926) (Morphology, Phase Relations, Phase Diagram, Experimental, 26)

[1926Veg2] Vegesack, A.V., "Heterogeneous Liquidus-Solidus Equilibria in the Iron-Chromium-Carbon Ternary System" (in German), *Z. Anorg. Chem.*, **154**, 30–42 (1926) (Phase Relations, Phase Diagram, Experimental, 13)

[1927Gro] Grossmann, M.A., "Nature of the Chromium-Iron-Carbon Diagram", *Trans. Amer. Inst. Min. Met. Eng.*, **75**, 214–233 (1927) (Phase Diagram, Phase Relations, Experimental, 11)

[1927Sau] Sauerwald, F., Neudecker, H., Rudolph, J., "Ternary Systems with Iron and Carbon. I. "$Fe_3C{\cdot}Cr_4C$", $Cr_{10}C_6Fe_3$ Phases, "Physical Analysis of Extracts" (in German), *Z. Anorg. Chem.*, **161**, 316–320 (1927) (Phase Relations, Experimental, Magn. Prop., 9)

[1928Wes] Westgren, A., Phragmen, G., Negresco, Tr., "On the Structure of the Iron-Chromium-Carbon System", *J. Iron Steel Inst.*, **117**, 383–401 (1928) (Crys. Structure, Morphology, Phase Relations, Phase Diagram, Experimental, 22)

[1930Kri] Krivobok, V.N., Grossmann, M.A., "A Study of the Iron-Chromium-Carbon Constitutional Diagram", *Trans. Amer. Soc. Steel Treat.*, **18**, 760–807 (1930) (Crys. Structure, Morphology, Phase Diagram, Phase Relations, Experimental, 6)

[1930Mur] Murakami, T., Oka, K., Nishigori, S., "The Transformation and the Constitution of High Chromium Steels", *Tech. Rep. Tohoku Imp. Univ.*, **9**(3), 405–445 (1930) (Morphology, Phase Diagram, Phase Relations, Magn. Prop., 2)

[1931Mur] Murakami, T., Oka, K., Nishigori, S., "The Constitution of High-Chromium Steels" (in German), *Stahl Eisen*, **51**(40), 1234–1235 (1931) (Phase Diagram, Phase Relations, Experimental, 5)

[1932Fri] Friedmann, K., Sauerwald, F., "Investigation of the C-Cr-Fe Ternary System" (in German), *Z. Anorg. Chem.*, **203**, 72–74 (1932) (Morphology, Phase Relations, Experimental, 6)

DOI: 10.1007/978-3-540-74196-1_3

[1932Sch] Schmidt, M., Jungwirth, O., "A Contribution to Study of High Heat-Resistant Chromium Steel"(in German), *Arch. Eisenhuettenwes.*, **5**(8), 419–426 (1932) (Morphology, Phase Relations, Mechan. Prop., Experimental, 5)

[1933Wes] Westgren, A., "Complex Chromium and Iron Carbides", *Nature*, London, **132**, 480 (1933) (Crys. Structure, Experimental, 3)

[1934Luc] Lucas, O., Wentrup, H., "Emission of Carbon in the Fe-Cr-Si Alloys" (in German), *Z. Anorg. Allg. Chem.*, **220**, 329–333 (1934) (Phase Relations, Experimental, 2)

[1935Aus] Austin, J.B., Pierce, R.H.H., "Linear Thermal Expansion and Transformation Phenomena of Some Low-Carbon Iron-Chromium Alloys", *Trans. Amer. Inst. Min. Met. Eng.*, **116**, 289–308 (1935) (Phase Relations, Experimental, Magn. Prop., 18)

[1935Tof] Tofaute, W., Sponheuer, A., Bennek, H., "Transformation and Hardness of Steel with 1% 12% Cr" (in German), *Arch. Eisenhuettenwes.*, **8**(11), 499–506 (1935) (Phase Relations, Phase Diagram, Experimental, Mechan. Prop., 15)

[1936Mon] Monypenny, J.H.G., "Alloys of Iron, Carbon, and Chromin", *Iron Steel Inst., Special Rep.*, **14**, 39–61 (1936) (Phase Diagram, Review, 59)

[1936Mur] Murakami, T., Kishimoto, H., "On the Change of Transformation Points of Chromium Steels due to Cooling Gonditions", *Sci. Rep. Tohoku Imp. Univ.*, **25**, 726–744 (1936) (Crys. Structure, Morphology, Phase Relations, Experimental, Magn. Prop., 4)

[1936Tof1] Tofaute, W., Kuettner, C., Buettinghaus, A., "Iron-Chromium-Carbon Alloys", *Metallurgist*, **10**, 152–155 (1936) (Crys. Structure, Phase Diagram, Phase Relations, Abstract, 2)

[1936Tof2] Tofaute, W., Kuettner, C., Buettinghaus, A., "The Iron-Chromium-Chromium Carbide Cr_7C_3-Cementite System" (in German), *Arch. Eisenhuettenwes.*, **9**(12), 607–617 (1936) (Crys. Structure, Morphology, Phase Diagram, Phase Relations, Experimental, 19)

[1936Tof3] Tofaute, W., Kuettner, C., Buettinghaus, A., "The Iron-Chromium-Chromium Carbide Cr_7C_3-Cementite System"(in German), *Techn. Mitt. Krupp*, **4**(6), 181–194 (1936) (Crys. Structure, Morphology, Phase Diagram, Phase Relations, Experimental, 19)

[1938And] Andrew, J.H., Bottomley, G.T., Maddocks, W.R., Percival, R.T., "The Fluidity of Iron-Carbon and other Iron Alloys", *Iron Steel Inst., 3th Rep. Steel Castings Research Committee,* Publ. Offices Iron Steel Inst. 4, Grosvenor Gardens, London, S.W.1, 1938, (23), 5–32 (1938) (Phys. Prop., Experimental, 9)

[1940Mir] Mirkin, I.L., Blanter, M.E., "Equilibrium Condition of Fe-Cr-C Alloys" (in Russian), *Metallurgia*, **8**, 3–8 (1940) (Crys. Structure, Phase Relations, Phase Diagram, Electr. Prop., Magn. Prop. Experimental, 12)

[1947Bla] Blanter, M.E., "Electric Resistance of Fe-Cr-C Alloy at High Temperatures" (in Russian), *J. Tech. Phys.*, **17**(5), 549–556 (1947) (Crys. Structure, Phase Relations, Electr. Prop., Experimental, 16)

[1948Gol] Goldschmidt, H.J., "A New Carbide in Chromium Steels", *Nature*, **162**, 855–856 (1948) (Crys. Structure, Phase Relations, Experimental, 2)

[1949Jae] Jaenecke, E., "C-Fe-Cr" (in German), *Kurzgefasstes Handbuch aller Legierungen*, Winter Verlag Heidelberg, 692–696 (1949) (Phase Diagram, Review, 10)

[1950Liv1] Livshits, B.G., Popov, K.V., "Carbide Phases in the Chromium-Steels" (in Russian), *Production and Treatment of Steel.*, Sbornik Moskov. Inst. Stali, **29**, 303–331 (1950) (Phase Relations, Electr. Prop., Mechan. Prop., Experimental, 10)

[1950Liv2] Livshits, B.G., Popov, K.V., "Refinement of the Fe-Cr-C Phase Diagram" (in Russian), *Dokl. Akad. Nauk SSSR*, **70**(4), 633–635 (1950) (Crys. Structure, Phase Diagram, Experimental, 5)

[1951Sho] Shortsleeve, F.J., Nicholson, M.E., "Transformations in Ferritic Chromium Steels Between 1100 and 1500°F (595 and 815°C)", *Trans. Amer. Soc. Metals*, **43**, 142–160 (1951) (Crys. Structure, Phase Relations, Experimental, Kinetics, 5)

[1951Zar] Zarubin, N.M., Ivanov, E.A., Rozenfeld, S.E., "A Study of the Iron Base Alloys with High Content of Carbon and Chromium" (in Russian), *Liteynoe Proizvodstvo*, **10**, 26–28 (1951) (Morphology, Phase Relations, Mechan. Prop., 0)

DOI: 10.1007/978-3-540-74196-1_3

[1952Edw] Edwards, R., Raine, T., "The Solid Solubilities of Some Stable Carbides in Cobalt, Nickel and Iron at 1250°C", *Pulvermetallurgie, 1. Plansee Seminar, De Re Metallica,* 22–26 Juni, 1952, Reutte/Tirol, Benesovsky, F. (Ed.), Springer-Verlag, Wien, (1), 232–242 (1952) (Crys. Structure, Phase Relations, Experimental, 5)

[1953Kuo1] Kuo, K., "Carbides in Chromium, Molybdenum, and Tungsten Steels", *J. Iron Steel Inst.*, **173**, 363–375 (1953) (Crys. Structure, Phase Diagram, Phase Relations, Experimental, 45)

[1953Kuo2] Kuo, K., "X-Ray and Chemical Analysis of Carbides in Chromium Steel", *Jernkontorets Ann.*, **137**(5), 149–156 (1953) (Crys. Structure, Phase Relations, Experimental, 21)

[1953Ric] Richardson, F.D., Dennis, W.E., "Effect of Chromium on the Thermodynamic Activity of Carbon in Liquid Iron", *J. Iron Steel Inst., London*, **175**(3), 257–263 (1953) (Thermodyn., Experimental, 10)

[1956Oht] Ohtani, M., "On the Activities of Cr and C in Molten Fe-C-Cr Allloys", *Sci. Rep. Res. Inst. Tohoku Univ. A*, **8**, 337–351 (1956) (Thermodyn., Experimental, 27)

[1957San] Sanbongi, K., Ohtani, M., Toita, K., "On the Effect of Alloying Elements on the Solubility of Carbon in Molten Iron", *Sci. Rep. Res. Inst. Tohoku Univ. A*, **9**, 147–158 (1957) (Phase Relations, Thermodyn., Experimental, 20)

[1958Bun] Bungardt, K., Kunze, E., Horn, E., "A Study of the Iron-Chromium-Carbon System" (in German), *Arch. Eisenhuettenwes.*, **29**(3), 193–203 (1958) (Crys. Structure, Phase Diagram, Phase Relations, Experimental, 17)

[1959Fuw] Fuwa, T., Chipman, J., "Activity of Carbon in Liquid Iron alloys", *Trans. Metall. Soc. AIME*, **215**, 708–716 (1959) (Phase Relations, Thermodyn., Experimental, 22)

[1959Neu] Neumann, F., Schenck, H., Patterson, W., "Iron-Carbon Alloys in Thermodynamic Consideration" (in German), *Giesserei Tech.-Wiss. Beih.*, **23**, 1217–1246 (1959) (Phase Diagram, Phase Relations, Thermodyn., Theory, 72)

[1960Pet] Petrova, E.F., Lapshina, M.I., Shvartsman, L.A., "Influence of the Alloying Elements on the Thermodynamic Activity and Carbon Solubility in α-Iron" (in Russian), *Metalloved. Term. Obrab. Met.*, (4), 22–25 (1960) (Phase Relations, Thermodyn., Experimental, 2)

[1960Sch] Schenck, H., Kaiser, H., "Study of Carbon Activity in Solid Binary and Ternary Fe-Cr-C Alloys" (in German), *Arch. Eisenhuettenwes.*, **31**(4), 227–235 (1960) (Thermodyn., Experimental, 39)

[1961Bae] Baerlecken, E., Fischer, W.A., Lorenz, K., "Study of Impact Toughness and Resistance to Intercrystallite Corrosion for Alloyed Iron-Chromium Containing to 30 % Cr" (in German), *Stahl Eisen*, **81**(12), 768–778 (1961) (Crystal Structure, Morphology, Phase Diagram, Phase Relations, Experimental, Magn. Prop., 46)

[1962Gri] Griffing, N.R., Forgeng, W.D., Healy, G.W., "C-Cr-Fe Liquidus Surface", *Trans. AIME*, **224**, 148–159 (1962) (Crys. Structure, Morphology, Phase Diagram, Phase Relations, Experimental, 14)

[1962Pep] Pepperhoff, W., Buehler, H.-E., Dautzenberg, N., "About Constitution of the Cromium-Iron-Carbon System in the Domain of Technical Ferrochromium" (in German), *Arch. Eisenhuettenwes.*, **33**(9), 611–616 (1962) (Morphology, Phase Diagram, Phase Relations, Experimental, 9)

[1963Bri] Brigham, R.J., Kirkaldy, J.S., "The Interaction Parameter for Solutions of Carbon and Chromium in Austenite at 1000°C", *Trans. AIME*, **227**, 538–539 (1963) (Thermodyn., Experimental, 5)

[1963Fle] Flender, H., Wever, H., "Activity of Carbon in the Iron-Vanadium-Carbon and Iron-Chromium-Carbon Systems" (in German), *Arch. Eisenhuettenwes.*, **34**(10), 727–723 (1963) (Thermodyn., Experimental, 23)

[1963Han] Hancock, H.A., Pidgeon, L.M., "Equilibria Controlling the Decarburization of Solid Ferrochromium by Chromium Oxide", *Trans. AIME*, **227**, 608–614 (1963) (Thermodyn., Experimental, 13)

DOI: 10.1007/978-3-540-74196-1_3

[1963Joh] Johnson, K.A., Wayman, C.M., "The Crystallography of the Austenite-Martensite Transformation in an Fe-Cr-C Alloy", *Acta Crystallogr.*, **16**(6), 480–485 (1963) (Crys. Structure, Experimental, Theory, 16)

[1963Kud] Kudielka, H., Moeller, H., "Distribution of Cr in $(Fe,Cr)_3C$" (in German), *Z. Kristallogr.*, **118**, 213–222 (1963) (Crys. Structure, Experimental, 11)

[1964Bun] Bungardt, K., Preisendanz, H., Lehnert, G., "Effect of Chromium on Carbon Activity in the System Iron-Chromium-Carbon at 1000°C" (in German), *Arch. Eisenhuettenwes.*, **35**(10), 999–1007 (1964) (Phase Relations, Thermodyn., Experimental, 24)

[1964Pet] Petrova, E.F., Shvartsman, L.A., "Carbon-14 Determination of the Thermodynamic Activity of Carbon in Iron Alloyed with Chromium", *Russ. J. Phys. Chem. (Engl. Transl.)*, **38**(3), 410–412 (1964) (Thermodyn., Experimental, 4)

[1965Ale] Alekseev, V.I., Shvartsman, L.A., "Investigation of the Thermodyn. of Formation of Mixed Iron-Chromium Carbides of the Type $(Fe_xCr_y)_{23}C_6$", *Russ. Metall. (Engl. Transl.)*, **1**, 117–124 (1965) (Crys. Structure, Thermodyn., Experimental, 0)

[1965Bun] Bungardt, K., Preisendanz, H., Mersmann, T., "Carburization of Plain Carbon and Chrome-Alloy Steels in Hydrogen-Benzene Vapour Mixtures" (in German), *Arch. Eisenhuettenwes.*, **36**(10), 709–724 (1965) (Interface Phenomena, Kinetics, Experimental, 60)

[1965Glo] Glowacki, Z., Baer, J., Senczyk, D., "Synthesis and some Properties of the M_7C_3 Type Chromium-Iron Carbides" (in Polish), *Hutnik*, **32**(11), 399–404 (1965) (Crys. Structure, Experimental, 13)

[1966Gob] Gobin, F., Bouchy, C., "Establishment of Structure Diagrams for Steel With Chromium and Tungsten on Basis of Spatial Extension of Austenite Region in Ternary Alloys Iron - (Chromium or Tunsten)-Carbon" (in French), *Mem. Sci. Rev. Metall.*, **63**(1), 75–80 (1966) (Morphology, Phase Relations, Thermodyn., Experimental, 3)

[1966Kud] Kudielka, H., "The Anomalous Change in Volume of the Mixed Crystal Series $(Fe,Cr)_3C$ and its Particular Thermochemical and Magnetic Properties" (in German), *Arch. Eisenhuettenwes.*, **37**(9), 759–766 (1966) (Crys. Structure, Thermodyn., Experimental, 83)

[1966Mes] Messulam, L., Appleton, A.S., "The Relation of Carbon Activity Data for Fe-Cr-C Alloys to the Boundaries of the γ + $(Fe, Cr)_7C_3$ Phase Field at 1050°C", *Trans. AIME*, **236**, 222–224 (1966) (Phase Diagram, Phase Relations, Thermodyn., Review, 6)

[1966Sch] Schenk, H., Steinmetz, E., Gohlke, R., "Contribution to the Study of the Chemical Activity of the Elements P, S, Si, Cu and Cr in Molten Iron Solutions Saturated with Carbon" (in German), *Arch. Eisenhuettenwes.*, **37**(12), 919–924 (1966) (Thermodyn., Calculation, 30)

[1966Yas] Yasinskaya, G.A., "Wetting of the Refractory Carbides, Borides and Nitrides by Molten Metals" (in Russian), *Poroshk. Metall. (Kiev)*, **43**(7), 53–55 (1966) (Interface Phenomena, Experimental, 5)

[1966Zup] Zupp, R.R., Stevenson, D.A., "The Influence of Vanadium on the Activity of Carbon in the Fe-C-V System at 1000°C; Correlation of the Influence of Substitutional Solutes on the Activity Coefficient of Carbon in Iron base Systems", *Trans. AIME*, **236**, 1316–1323 (1966) (Thermodyn., Theory, 35)

[1967Bau] Baum, B.A., Gel'd, P.V., Kocherov, P.V., "Influence of Carbon on the Viscosity of Liquid Fe-Cr-C Alloys", *Russ. Metall. (Engl. Transl.)*, (5), 27–31 (1967) (Phys. Prop., Experimental, 15)

[1967Gol] Goldschmidt, H.J., "Carbides", *Interstitial Alloys, Butterworths, London*, 88–213 (1967) (Crys. Structure, Phase Relations, Review, 461)

[1967Las] Lassus, M., Riviere, R., Monnier, G., "Behaviour of Lattice Parameters of $(Cr, Fe)_7C_3$ Solid Solutions"(in French), *Compt. Rend. Acad. Sci. Paris, Ser. C*, **264**, 1057–1060 (1967) (Crys. Structure, Phase Relations, Experimental, 10)

[1968Chi] Chipman, J., Brush, E.F., "The Activity of Carbon in Alloyed Austentite at 1000°C", *Trans. AIME*, **242**, 35–41 (1968) (Thermodyn., Review, 21)

DOI: 10.1007/978-3-540-74196-1_3

[1968Mat] Matosyan, M.A., Golikov, V.M., "Effect of Prior Cold Plastic Deformation on Diffusion of Carbon in Alloys with Iron Base", *Phys. Met. Metall.*, **25**(2), 187–190 (1968) (Kinetics, Transport Phenomena, Experimental, 6)

[1968Poi] Poirier, D.R., "Activity of Carbon in Liquid Iron-Carbon-Chromium Solutions", *Trans. AIME*, **242**(2), 349–350 (1968) (Thermodyn., Review, 9)

[1968Sri] Srinivasan, G.R., Wayman, C.M., "Transmission Electron Microscope Study of the Bainite Transformation in Iron-Chromium Carbon Alloys", *Acta Metall.*, **16**(5), 609–620 (1968) (Crys. Structure, Morphology, Phase Relations, Experimental, 22)

[1969Bor] Borisov, E.V., Gruzin, P.L., Zemskii, S.V., "C and Mo in Cr, Cr-Fe, and Cr-Ta Alloys, Impurity Tracer Diffusion", *Diff. Data*, **3**, 266 (1969) (Kinetics, Transport Phenomena, Abstract, 0)

[1969Rud] Rudy, E., "Ternary Phase Equilibria in Transition Metal-Boron-Carbon-Silicon Systems. Part V. Compendium of Phase Diagram Data", Tech. Rep. AFML-TR-65-2, Part V, Air Force Materials Laboratory, Wright-Patterson AFB, OH, 1969 (Phase Diagram, Experimental, 1)

[1969Ruh] Ruhl, R.C., Cohen, M., "Splat Quenching of Iron-Carbon Alloys", *Trans. AIME*, **245**, 241–251 (1969) (Crys. Structure, Experimental, Phase Relations, 50)

[1969Run] Rundqist, S., Runnsjo, G., "Crystal Structure Refinement of Cr_3C_2", *Acta Chem. Scand.*, **23**, 1191–1199 (1969) (Crys. Structure, Experimental)

[1969Sch] Schuermann, E., Kramer, D., "Investigations on the Influnce of Temperature and on the Equivalent Effect of the Alloy Elements on the Solubility of Carbon in Iron-Rich Carbon-saturated Ternary and Multi-component Meltings" (in German), *Giessereiforschung*, **21**(1), 29–42 (1969) (Theory, Thermodyn., 35)

[1970Bor] Borisov, E.V., Gruzin, P.L., Zemskii, S.V., "Diffusion During the High-Temperature Service of Protective Coatings on Molybdenum", *Prot. Coat. Met.*, (2), 76–80 (1970), translated from *Zascitnye Pokrytija Metall.*, 2, 104, (1969) (Experimental, Kinetics, Transport Phenomena, 13)

[1970Had] Hadrys, H.G., Frohberg, M.G., Elliott, J.F., Lupis, C.H.P., "Activities in the Liquid Fe-Cr-C (sat), Fe-P-C(sat), and Fe-Cr-P System at 1600°C", *Metall. Trans.*, **1**, 1867–1874 (1970) (Thermodyn., Theory, 23)

[1970Jac] Jackson, R.S., "The Austenite Liquidus Surface and Constitutional Diagram for the Fe-Cr-C Metastable System", *J. Iron Steel Inst., London*, **208**(2), 163–167 (1970) (Phase Relations, Phase Diagram, Experimental, 36)

[1970Rou] Rouault, M.A., Herpin, P., Fruchart, M.R., "Crystallographic Investigation of Carbides Cr_7C_3 and Mn_7C_3", (in French), *Ann. Chemie*, **5**, 461–470 (1970) (Crys. Structure, Experimental, 29)

[1971Gre] Greenbank, J.C., "Carbon Solute Interactions in Fe-Cr-C, Fe-Mo-C and Fe-W-C Alloys", *J. Iron Steel Inst., London*, **209**, 986–990 (1971) (Phase Relations, Thermodyn., Experimental, 16)

[1971Kin] Kinsman, K.R., Eichen, E., Aaronson, H.I., "Electron Microprobe Study of the Carbon Content of Ferrite and Bainite in Fe-C-Mo and Fe-C-Cr Alloys", *Metall. Trans.*, **2**(1), 346–348 (1971) (Morphology, Phase Relations, Experimental, 26)

[1971Lei] Leiber, F., Koch, W., Schuermann, E., "Contribution to Study of Exchange Reactions and of Their Equilibria in Ferritic Steel. 2. Progression of the Exchange Reactions and Adjustment of the Equilibria of Fe-Cr-C-Alloys in the Temperature Range of the Pearlitic Stage" (in German), *Arch. Eisenhuettenwes.*, **42**(2), 106–110 (1971) (Phase Diagram, Phase Relations, Thermodyn., Experimental, 11)

[1971Pog] Pogorely, V.I., Chupakhin, Yu.M., "A Study of the Temperature Dependence of Carbon Solubility in Solid Ferrochromium" (in Russian), *Met. i. Koksokhim, Resp. Mezhved. Nauchno. Tekhn. Sbornik.*, **26**, 61–64 (1971) (Morphology, Phase Relations, Experimental, Kinetics, 6)

[1971Swi] Swinden, D.J., Woodhead, J.H., "Kinetics of the Nucleation and Growth of Proeutectoid Ferrite in Some Iron-Carbon-Chromium Alloys", *J. Iron Steel Inst., London*, **209**, 883–899 (1971) (Morphology, Phase Relations, Experimental, Kinetics, 40)

DOI: 10.1007/978-3-540-74196-1_3

[1971Vig] Vigneron, B., Faivre, R., "Use of Differential Thermal Analysis for Presentation of Austenite, Cementite and Graphite Deposits During Solidification of Pig Fe-C, Fe-Cr-C and Fe-C-Si Alloys" (in French), *Compt. Rend. Acad. Sci. Paris, Ser. C*, **273**(16), 943–945 (1971) (Phase Relations, Experimental, 2)

[1972Bow] Bowman, A.W., Arnold, G.P., Storms, E.K., Nereson, N.G., "The Crystal Structure of $Cr_{23}C_6$", *Acta Crystallogr. B*, **28**, 3102–3103 (1972) (Crys. Structure, Experimental, 3)

[1972Foo] Foo, E.H., Lupis, C.H.P., "Activity of Carbon in Liquid Iron Alloys at 1550°C", *Metall. Trans.*, **3**, 2125–2131 (1972) (Phase Relations, Experimental, 18)

[1972Gor] Gorev, K.V., Shevchuk, L.A., Dudetskaya, L.R., Gurinovich, V.I., "Crystallization and Structure of Hypereutectic Fe-C-Cr Alloys" (in Russian), *Vestsi Akad. Navuk BSSR Fiz.-Tekh.*, **2**, 32–34 (1972) (Morphology, Phase Diagram, Phase Relations, Experimental, 3)

[1972Jel] Jellinghaus, W., Keller, H., "On the Iron-Chromium-Carbon System and Distribution of Chromium Between Ferrite and Special Carbides" (in German), *Arch. Eisenhuettenwes.*, **43**(4), 319–328 (1972) (Morphology, Phase Relations, Experimental, Mechan. Prop., 20)

[1972Pre] Preisendanz, H., Schmuelling, W., Schueler, P., "Thermodynamic Studies of Fe-C-X Alloys by Means of Gas-Metal Reactions and their Importance for the Development and Further Improvement of Steels" (in German), *DEW-Techn. Ber.*, **12**(1), 45–53 (1972) (Phase Diagram, Thermodyn., Review, 18)

[1972Wad] Wada, T., Wada, H., Elliott, J.F., Chipman. J., "Activity of Carbon and Solubility of Carbides in the FCC Fe-Mo-C, Fe-Cr-C and Fe-V-C Alloys", *Metall. Trans.*, **3**(11), 2865–2872 (1972) (Phase Diagram, Thermodyn., Experimental, 21)

[1973Gor1] Gorev, K.V., Shevchuk, L.A., Dudetskaya, L.R., Gurinovich, V.I., "Equilibria Between Carbides and Solid Solutions in the Fe-C-Cr System", (in Russian), *Vestsi Akad. Navuk BSSR Fiz.-Tekh.*, (2), 40–44 (1973) (Phase Diagram, Phase Relations, Experimental, 4)

[1973Gor2] Gorev, K.V., Shevchuk, L.A., Dudetskaya, L.R., Gurinovich, V.I., "Phase Equlibria in the High-Carbon Fe-C-Cr Alloys" (in Russian), *Vestsi Akad. Navuk BSSR Fiz.-Tekh.*, **2**, 45–48 (1973) (Phase Diagram, Phase Relations, Experimental, 5)

[1973Mir] Mirzaev, D.A., Morozov, O.P., Schteinberg, M.M., "On Relation of the γ→α Transformation in Low-Carbon Iron and Iron Base Alloys", (in Russian), *Fiz. Met. Metalloved.* **36**(3), 560–568 (1973) (Phase Relations, Experimental, 24)

[1973Tar] Taran, Yu.N., Novik, V.I., Nesterenko, A.M., Terentyev, V.T., "Structure of Iron-Chromium Carbide Crystals $(Cr, Fe)_7C_3$", *Dop. Akad. Nauk Ukrain. RSR, Ser. A, Fiz.-Mat. Tekh. Nauki*, **9**, 851–854 (1973) (Crys. Structure, Morphology, Experimental, 7)

[1974Ben] Benz, R., Elliott, J.E., Chipman, J., "Thermodynamics of the Carbides in the System Fe-Cr-C", *Metall. Trans.*, **5**, 2235–2240 (1974) (Crys. Structure, Morphology, Phase Diagram, Thermodyn., Experimental, 23)

[1975Cos] Cost, J.R., Blazek, K.E., "Determination of the Solubility of Carbon in Iron-Chromium Alloys", *Trans. Jpn. Inst. Met.*, **16**(3), 177–179 (1975) (Phase Relations, Experimental, 8)

[1974Kun] Kunaev, A.M., Shabdenov, B.A., Levintov, B.L., Geev, O.V., Iliev, A.A., Khobot, V.I., "Study of Some Thermodynamic Properties of the High-chomium Melts of the Fe-Cr-C and Fe-Cr-C-Si Systems" (in Russian), *Deposited Doc. 1974, VINITI 2627-74, 10pp. (Russ.). Avail.Blld.*, 2627–74 (1974) (Thermodyn., Experimental, 4)

[1974Pet] Petrova, E.F., Shvartsman, L.A., "Effect of Chromium Subgroup Elements on Thermodynamic Activity of Carbon Dissolved in Solid Iron" (in Russian), *Dokl. Akad. Nauk SSSR*, **217**(2), 383–385 (1974) (Thermodyn., Theory, 4)

[1974She] Shevchuk, L.A., Dudetskaya, L.R., "On the Stable Fe-C-Cr Phase Diagram" (in Russian), *Izvest. Akad. Nauk Beloruss. SSR, Fiz. -Tekhn.*, (1), 19–21 (1974) (Phase Diagram, Phase Relations, Experimental, 4)

[1975Shi] Shigematsu, T., "Invar Properties of Cementite $(Fe_{1-x}Me_x)_3C$, Me = Cr, Mn, Ni", *J. Phys. Soc. Jpn.*, **39**(4), 915–920 (1975) (Crys. Structure, Phase Relations, Phys. Prop., 14)

DOI: 10.1007/978-3-540-74196-1_3

[1975Kan] Kaneko, K., Sano, N., Matsushita, Y., "Decarburization and Denitrogenization of Iron And Iron-Chromium Alloys by Hydrogen Plasma" (in Japanese), *J. Fac. Eng., Univ. Tokyo*, **A-13**, 60–61 (1975) (Phase Relations, Thermodyn., Experimental, 2)

[1975Str] Straube, H., Bloech, R., Ploeckinger, E., "Dependence of Carbon Distribution in Ternary System Iron-Chromium-Carbon on Crystal Segregation Due to Solidification" (in German), *Metall*, **29**(2), 130–137 (1975) (Phase Diagram, Phase Relations, Experimental, 33)

[1976Cho] Choudary, U.V., Belton, G.R., "Thermodyn. of the Iron-Chromium-Carbon Melts at 1630° C", *J. Metals*, **28**(12), A33 (1976) (Thermodyn., Abstract, 0)

[1976Gor] Gorev, K.V., Shevchuk, L.A., "Phase Equilibria in Fe-C and Fe-C-Cr Alloys" (in Russian), *Vestsi Akad. Navuk BSSR Fiz.-Tekh.*, **2**, 32–35 (1976) (Phase Diagram, Phase Relations, Review, 9)

[1976Kle] Kleemola, H.J., Kuusisto, E.A., "The Effect of Cr, Mn and Ni on the Solubility and Precipitation of Carbon in Ferritic Iron", *Scand. J. Met.*, **5**, 151–158 (1976) (Phase Relations, Experimental, 20)

[1976Ko] Ko, M., Sakuma, T., Nishizawa, T., "Effect of Magnetism on the Partition of Alloying Elements between Cementite and Ferrite" (in Japanese), *J. Jpn. Inst. Met.*, **40**(6), 593–601 (1976) (Phase Relations, Thermodyn., Experimental, 37)

[1976She1] Shevchuk, L.A., Dudetskaya, L.P., Gurinovich, V.I., Tkacheva, V.A., "Carbide Phases in Fe-C-Cr Alloys with High C Content" (in Russian), *Vestsi Akad. Navuk BSSR Fiz.-Tekh.*, **3**, 45–47 (1976) (Crys. Structure, Morphology, Phase Relations, Experimental, 1)

[1976She2] Shevchuk, L.A., Dudetskaya, L.R., Tkacheva, V.A., "Stable Phase Diagram of Fe-C-Cr Alloys" (in Russian), *Vestsi Akad. Navuk BSSR Fiz.-Tekh.*, (2), 36–38 (1976) (Morphology, Phase Relations, Experimental, 5)

[1976Woo] Woodyatt, L.R., Krauss. G., "Iron-Chromium-Carbon System at 870°C", *Metall. Trans. A*, **7A**, 983–989 (1976) (Crys. Structure, Morphology, Phase Diagram, Phase Relations, Experimental, 13)

[1977Lun] Lundberg, R., Waldenstroem, M., Uhrenius, B., "Isothermal Sections of the Fe-Cr-C System in the Temperature Range 873–1373K", *Calphad*, **1**(2), 159–199 (1977) (Phase Diagram, Thermodyn., Calculation, 2)

[1977Nis1] Nishizawa, T., "An Experimental Study of the Fe-Mn-C and Fe-Cr-C Systems at 1000° C", *Scand. J. Met.*, **6**, 74–78 (1977) (Crys. Structure, Morphology, Phase Diagram, Phase Relations, Experimental, 18)

[1977Nis2] Nishizawa, T., Uhrenius, B., "A Thermodynamic Study of the Fe-Cr-C system at 1000°C", *Scand. J. Met.*, **6**, 67–73 (1977) (Phase Diagram, Thermodyn., Calculation, 24)

[1977Pou] Poubeau, J.J., "Solubility of Carbon in Chromium and Precipitation of Carbides in Metal (in French)", *Thesis Doct. Ing*., Univ. Paris, (1977) (Phase Relations, Experimental)

[1977Uhr1] Uhrenius, B., "Optimization of Parameters Describing the Interaction Between Carbon and Alloying Elements in Ternary Austenite", *Scand. J. Metall.*, **6**(2), 83–89 (1977) (Thermodyn., Calculation, 24)

[1977Uhr2] Uhrenius, B., "A Compendium of Ternary Iron Base Phase Diagrams", *The Hardenability of Steels*, 28–81 (1977) (Phase Diagram, Thermodyn., Calculation, 53)

[1977Wal] Waldenstroem, M., Uhrenius, B., "A Thermodynamic Analysis of the Fe-Cr-C System", *Scand. J. Met.*, **6**, 202–210 (1977) (Phase Diagram, Thermodyn., Calculation, 43)

[1978Uhr] Uhrenius, B., "A Compendium of Ternary Iron Base Phase Diagrams", in "*Hardenability Concepts with Applications to Steel*", Doane, D.V., Kirkaldy, J.S. (Eds.), Proc. Symp. Held Sheraton-Chicago Hotel, Oct. 24–26, 1977, Metall. Soc. AIME Heat Treat. Com. / Amer. Soc Met. Activ. Phase Trans., 28–81 (1978) (Phase Diagram, Thermodyn., Calculation, 53)

[1979Bee] Bee, J.V., Howell, P.R., Honeycombe, R.W.K., "Isothermal Transformations in Iron-Chromium-Carbon Alloys", *Metall. Trans. A*, **10A**(9), 1207–1212 (1979) (Morphology, Phase Relations, Experimental, Interface Phenomena, 17)

DOI: 10.1007/978-3-540-74196-1_3

[1979How] Howell, P.R., Bee, J.V., Honeycombe, R.W.K., "The Crystallography of the Austenite-Ferrite/Carbide Transformation in Fe-Cr-C Alloys", *Metall. Trans. A*, **10A**(9), 1213–1222 (1979) (Morphology, Experimental, 14)

[1979Kag] Kagawa, A., Okamoto, T., "Lattice Parameters of Cementite in Fe-C-X (X = Cr, Mn, Mo, and Ni) Alloys", *Trans. Jpn. Inst. Met.*, **20**(11), 659–666 (1979) (Crys. Structure, Experimental, 11)

[1979Sha1] Sharma, R.C., Purdy, G.R., Kirkaldy, J.S., "Thermodyn. and Phase Equilibria for the Fe-C-Cr System in the Vicinity of the Eutectoid Temperature", *Metall. Trans. A*, **10A**(8), 1119–1127 (1979) (Morphology, Phase Diagram, Phase Relations, Thermodyn., Calculation, Experimental, 39)

[1979Sha2] Sharma, R.C., Purdy, G.R., Kirkaldy, J.S., "Kinetics of the Pearlite Reaction in Fe-C-Cr", *Metall. Trans. A*, **10A**(8), 1129–1139 (1979) (Phase Relations, Experimental, Calculation, Kinetics, Interface Phenomena, 32)

[1980Bra] Brandis, H., Presendanz, H., Schueler, P., "Investigations on the Influence of the Alloy Elements Chromium, Molybdenium and Tungsten on the Activity of Carbon in Fe-X-C Alloys in the Temperature Range from 900 to 1100°C" (in German), *Thyssen Edelst. Techn. Ber.*, **6**(2), 155–167 (1980) (Thermodyn., Experimental, 28)

[1980Iwa] Iwadachi, T., Inoue, A., Minemura, T., Masumoto, T., "Nonequilibrium Phases in Fe-X-C (X = Cr, Mo, W) Ternary Alloys Quenched Rapidly from Melts" (in Japanese), *Nihon-Kinzoku-Gakkai-Shi*, **44**(3), 245–254 (1980) (Morphology, Phase Relations, Experimental, 30)

[1980Pot] Potapova, M.S., Golubeva, T.I., "Influence of Carbon and Cromium on Strength and Structure of Cast Iron" (in Russian), *Izv. Vyss. Uchebn. Zaved., Chern. Metall.*, **9**, 131–134 (1980) (Morphology, Experimental, Mechan. Prop., 4)

[1981Ino] Inoue, A., Iwadachi, T., Minemura, T., Masumoto, T., "Nonequilibrium Phases in Fe-X-C (X = Cr, Mo or W) Ternary Alloys Quenched Rapidly from Melts", *Trans. Jpn. Inst. Met.*, **22**(3), 197–209 (1981) (Crys. Structure, Morphology, Phase Relations, Thermodyn., Experimental, 31)

[1981Kno] Knotek, O., Lugscheider, E., Reimann, H., Sasse, H.G., "High-Temperature Differential Thermal Analysis with Optical Measurement of Temperature" (in German), *Metal*, **35**(2), 130–132 (1981) (Phase Diagram, Experimental, 9)

[1981Nis] Nishizawa, T., Hasebe, M., "Computer Calculation of Phase Diagrams of Iron Alloys" (in Japanese), *Tetsu to Hagane*, **67**(14), 2086–2097 (1981) (Thermodyn., Review, 110)

[1981Ogi] Ogilvy, A.J.W., Ostrowski, A., Kirkwood, D.H., "Correction to Solid-Liquid Partition Coefficients in Fe-Cr-C Alloys", *Met. Sci.*, **15**(4), 168–174 (1981) (Phase Diagram, Phase Relations, Thermodyn., Calculation, Experimental, 16)

[1982Hor] Hornbogen, E., Schmidt, I., "Microstructures of Glassy and Metastable Crystalline Phases Formed from Fe-C- Ternary Alloys", *Rapidly Solidified Amorphous Crystalline Alloys*, 199–204 (1982) (Morphology, Phase Diagram, Phase Relations, Thermodyn., Experimental, 7)

[1982Kag] Kagawa, A., Moriyama, S., Okamoto, T., "Partition of Solute Elements During Solidification of Iron-Carbon-Chromium Alloys", *J. Mater. Sci.*, **17**(1), 135–144 (1982) (Phase Diagram, Phase Relations, Thermodyn., Experimental, 19)

[1982Kun] Kunaev, A.M., Geev, O.V., Shabdenov, B.A., Levintov, B.L., Chobot, V.I., "A Study of Thermodynamic Behavior of Carbon in the Fe-Cr-C Melts", (in Russian), *Izv. Vyss. Uchebn. Zaved., Chern. Metall.*, **1**(1), 1–4 (1982) (Thermodyn., Experimental, 10)

[1982Sil] Sil'man, G.I., Bolkhovitina, N.A., "Eutectic Polihedration of Phase Diagrams of the Fe-C-Cr and Fe-C-Cr-Si Systems", (in Russian), *Izv. Vyss. Uchebn. Zaved., Chern. Metall.*, **11**, 99–103 (1982) (Phase Diagram, Experimental, 5)

[1982Yak] Yakel, H.L., Brynestad, J., "Non-random Site-occupation Parameters in $(Cr,Fe)_{23}C_6$ Phases", *Scr. Metall.*, **16**(4), 453–454 (1982) (Crys. Structure, Thermodyn., Calculation, Experimental, 6)

DOI: 10.1007/978-3-540-74196-1_3

[1983Ber] Bergmann, H.W., Brokmeier, U., Fritsch, H.U., "Experimental Investigation on the Thermal Stability of Metallic Glasses", *Ber. Bunsen-Ges. Phys. Chem.*, **87**, 757–761 (1983) (Phase Relations, Mechan. Prop., 15)

[1983Jan] Janas, M., Mamro, K., Jowsa, J., Ludwikowski, S., "Assessment of Ferrous Alloy Component Influence on Carbon Solubility" (in Polish), *Metal. Odlew.*, **9**(3), 213–228 (1983) (Phase Diagram, Phase Relations, Thermodyn., Experimental, 28)

[1983Mol] Molian, P.A., Wood, W.E., "Ferrite Morphology in Rapidly Solidified Ferritic Fe-Cr-C Steels", *Scr. Metall.*, **17**(4), 431–434 (1983) (Morphology, Experimental, 1)

[1983Pol] Polischuk, V.S., Nalivka, G.D., Kisel', N.G., "Composite Magnito-Abrasive Powders Based on Iron, Carbides of Titanium, Vanadium and Chromium" (in Russian), *Poroshk. Metall.*, **3**, 94–100 (1983) (Phase Relations, Morphology, Experimental, Mechan. Prop., 15)

[1983Sil] Sil'man, G.I., "Method of Calculating the Phase Diagrams of Ternary Systems by Using the Interphase Distribution Coefficients of the Elements. II. Three-Phase and Four-Phase Equilibria", *Russ. J. Phys. Chem.*, **57**, 334–337 (1983) (Phase Diagram, Thermodyn.,Theory, 4)

[1983Ume] Umemoto, M., Yoshitake, E., Tamura, I., "The Morphology of Martensite in Fe-C, Fe-Ni-C and Fe-Cr-C Alloys", *J. Mater. Sci.*, **18**(10), 2893–2904 (1983) (Morphology, Phase Relations, Experimental, Mechan. Prop., 32)

[1984Hol] Holleck, H., "C-Cr-Fe" (in German), *Binaere und Ternaere Carbid- und Nitridsysteme der Aebergangsmetalle, (Hrsg.)*, Borntraeger, Berlin, 1984, **6**, 161–161 (1984) (Phase Diagram, Abstract, 1)

[1984Kun] Kundrat, D.M., Chochol, M., Elliott, J.F., "Phase Relationships in the Fe-Cr-C System at Solidification Temperatures", *Metall. Trans. B*, **15B**, 663–676 (1984) (Phase Relations, Thermodyn., Experimental, 33)

[1984Pro] Prokoshkin, S.D., Kaputkina, L.M., Bernsteyn, M.L., Mozzhukhin, V.Ye., Andreeva, S.A., "On the Mechanism of the Development of Abnormally Low Tetragonality and Orthorhombicity in the Lattice of Fe-C, Fe-Mn-C, Fe-Cr-C, Fe-Mn-Cr-C Martensites", *Phys. Met. Metallogr. (Engl. Transl.)*, **58**(4), 114–125 (1984) (Crys. Structure, Phase Relations, Experimental, 17)

[1984Riv] Rivlin, V.G., "Phase Equilibria in Iron Ternary Alloys.14. Critical Review of Constitution of Carbon-Cromium-Iron and Carbon-Iron-Manganese Systems.", *Int. Met. Rev.*, **29**(4), 299–327 (1984) (Crys. Structure, Phase Diagram, Review, #, 91)

[1985Koc] Kocherzhinsky, Yu.A., Vasilenko, V.I., Kulik, O.G., "Construction of the Melting Diagrams of Some Mo-Containing Systems and the Metastable Melting Diagram of the Cr-C System Using DTA-Technique up to 3000 K", *Thermochim. Acta*, **93**, 649–652 (1985) (Experimental, Phase Diagram, 0)

[1985Kow] Kowalski, M., "Polytypic Structures of $(Cr,Fe)_7C_3$ Carbides", *J. Appl. Crystallogr.*, **18**, 430–435 (1985) (Crys. Structure, Experimental, 14)

[1985Pou] Poubeau, J.J., Bigot, J., "Determination of Carbon Solubility in Chromium with Measurement of Electrical Resistivity at Low Temperature (in French)," *Acta Metall.*, **33**(6), 1137–1141 (1985) (Crys. Structure, Phase Diagram, Experimental, 20)

[1985Tho] Thorpe, W.R., Chicco, B., "The Fe-Rich Corner of the Metastable C-Cr-Fe Liquidus Surface", *Metall. Trans. A*, **16A**, 1541–1549 (1985) (Crys. Structure, Morphology, Phase Relations, Experimental, 31)

[1985Vit] Vityaz, P.A., Nasybulin, A.Kh., "Homogenization in Sintering and Its Influence on Mechanical Properties of Fe-Cr-C and Fe-Ni-C Steels", *Powder Met.*, **28**(3), 166–168 (1985) (Morphology, Experimental, Mechan. Prop., 5)

[1985Wad] Wada, H., "Thermodynamics of the Fe-Cr-C System at 985 K", *Metall. Trans. A*, **16A**(8), 1479–1490 (1985) (Morphology, Phase Diagram, Phase Relations, Thermodyn., Experimental, 33)

[1986Dan] Danilenko, V.M., Kocherzhinskii, I.A., Kulik, O.G., "Metastable Melting-Temperature Chart of the Chromium-Carbon System (in Russian)", *Dokl. Akad. Nauk SSSR*, **287**(4), 895–899 (1986) (Phase Diagram, Calculation, Experimental, 7)

DOI: 10.1007/978-3-540-74196-1_3

[1986Kli] Klimenko, V.N., Maslyuk, V.A., Sambros, Y.V., "Sintering, Structurization, and Properties of Powdered Materials of the System Chromium Carbide-Iron", *Sov. Powder Metall. Met. Ceram. (Engl. Transl.)*, **25**(8), 642–646 (1986) (Morphology, Experimental, Mech. Prop., 7)

[1986Mir] Mirzaev, D.A., Karzunov, S.E., Schastlivtsev, V.M., Yakovleva, I.L., Kharitonova, E.V., "γ-α Transformation in Low-Carbon Fe-Cr base Alloys", (in Russian), *Fizika Metallov Metalloved.*, **61**(2), 331–338 (1986) (Phase Relations, Experimental, 21)

[1986Pea] Pearce, J.T.H., Elwell, D.W.L., "Duplex Nature of Eutectic Carbides in Heat Treated 30% Chromium Cast Iron", *J. Mater. Sci. Lett.*, **5**, 1063–1064 (1986) (Morphology, Phase Relations, Experimental, 10)

[1986Sch] Schuermann, E., von Schweinichen, J., "Investigation of the Melting Equilibria of Iron Rich Ternary Fe-C-X_i Alloys with X_i = Al,Cu, Ni and Cr" (in German), *Giessereiforschung*, **38**(4), 125–132 (1986) (Phase Diagram, Phase Relations, Experimental, 63)

[1986Vit] Vitusevich, V.T., Biletskii, A.K., Shumikhin, V.S., "Effect of Chromium on Enthalpy of Graphite Dissolution in Melted Iron" (in Russian), *Izv. Akad. Nauk SSSR, Met.*, (3), 47–49 (1986) (Thermodyn., Experimental, 9)

[1987And] Andersson, J.-O., Sundman, B., "Thermodynamic Properties of the Cr-Fe System", *Calphad*, **11**(1), 83–92 (1987) (Phase Diagram, Calculation, Thermodyn., 51)

[1987Ber] Berkane, R., Gachon, J.C., Charles, J., Hertz, J., "A Thermodynamic Study of the Chromium-Carbon System", *Calphad*, **11**(4), 375–382 (1987) (Crys. Structure, Phase Relations, Thermodyn., 14)

[1987Ere] Eremenko, V.N., Velikanova, T.Y., Bondar, A.A., "Phase Diagram of the Cr-Mo-C System. 1. Phase Equilibria in the Area of Crystallization of Alloys of the Mo-Mo_2C-Cr_7C_3-Cr Partial System," *Sov.Powder Metal. Met. Ceram.*, **26**(5), 409–414 (1987), translated from *Poroshk. Metall., (Kiev)*, (5), 70–76 (1987) (Crys. Structure, Phase Diagram, Experimental, 14)

[1987Kag] Kagawa, A., Okamoto, T., Goda, S., "Youngs Moduli of Iron-Carbon-Chromium Alloy Castings", *J. Mater. Sci.*, **22**(11), 4165–4172 (1987) (Phase Relations, Experimental, Mechan. Prop., 6)

[1987Sch] Schuermann, E., Schweinichen, J., Voelker, R., Fischer, H., "Calculation of the α/δ resp γ-Liquidus of Iron and of the Liquidus of Carbon as well as of the Univariant Reaction Lines in Iron-Rich, Carbon Containing Three-Component and Multicomponent Fe-C-X_1-X_2-Systems. MEMO" (in German), *Giessereiforschung*, **39**(3), 104–113 (1987) (Phase Diagram, Phase Relations, Thermodyn., Calculation, 19)

[1987Vit] Vitusevich, V.T., Biletskii, A.K., Shumikhin, V.S., "Enthalpy of Formation of Iron-Chromium-Carbon Melts", *Russ. J. Phys. Chem.*, **61**, 323–326 (1987), translated from *Zh. Fiz. Khimii*, **61**(3), 623–629, (1987) (Thermodyn., Experimental, 16)

[1987Yak] Yakel, H.L., "Atom Distributions in Tau-Carbide Phases: Fe and Cr Distributions in $(Cr_{23-x}Fe_x)C_6$ with x = 0, 0.74, 1.7, 4.13 and 7.36", *Acta Crystallogr. B.*, **43B**, 230–238 (1987) (Crys. Structure, Experimental, 25)

[1988Mag] Magnin, P., Kurz, W., "Stable and Metastable Eutectic Temperatures of Fe-C with Small Additions of a Third Element", *Z. Metallkd.*, **79**(5), 282–284 (1988) (Phase Relations, Experimental, 5)

[1988And] Andersson J.-O., "A Thermodynamic Evaluation of the Fe-Cr-C System", *Metall. Mater. Trans. A*, **19A**, 627–636 (1988) (Phase Diagram, Assessment, Calculation, 50)

[1988Fra] Fras, E., Guzik, E., Lopez, H.F., "Structure and Mechanical Properties of Unidirectionally Solidified Fe-Cr-C and Fe-Cr-X-C Alloys", *Metall. Trans. A*, **19A**(5), 1235–1241 (1988) (Morphology, Phase Relations, Experimental, Mechan. Prop., 60)

[1988Pil] Pillai, S.R., Mathews, C.K., "Measurement of the Carbon Activity of 18/8 Austenitic Steel and the Free Energy of Formation of the Metal Carbides $Fe_xCr_{23-x}C_6$", *High Temp.-High Pressures*, **20**(3), 263–270 (1988) (Thermodyn., Experimental, 12)

[1988Ray] Raynor, G.V., Rivlin, V.G., "C-Cr-Fe", *Phase Equilibria in Iron Ternary Alloys*, Institute of Metals, London, 143–156 (1988) (Phase Diagram, Review, 45)

DOI: 10.1007/978-3-540-74196-1_3

[1989Age] Ageev, Yu.A., Mizin, V.G., Makeeva, I.A., Pankrashkin, Yu.A., "Carbon Activity in Iron-Chromium Carbon Alloys", *Russ. Metall.*, (3), 26–29 (1989) (Thermodyn., Calculation, 12)

[1989Bat] Battle, T.P., Pehlke, R.D., "Equilibrium Partition Coefficients in Iron-Based Alloys", *Metall. Trans. B*, **20B**, 149–160 (1989) (Thermodyn., Calculation, 61)

[1989Gri] Gridnev, V.N., Ivanchenko, V.G., Pogorelaya, V.V., "Phase Diagram of the Chromium-Carbon System" (in Russian), *Metallofizika*, **11**(5), 129 (1989) (Phase Diagram, Experimental, 0)

[1989Leo1] Leonovich, B.I., Serebryakov, V.E., Frage, N.R., Kartavtsev, A.P., "Thermodynamic Analisis of the System Iron-Cromium-Carbon" (in Russian), *Izv. Vyss. Uchebn. Zaved., Chern. Metall.*, **1**, 4–10 (1989) (Phase Diagram, Thermodyn.,Theory, Calculation, 12)

[1989Leo2] Leonovich, B.I., Frage, N.R., Il`chuk, V.S., Gurevich, Yu.G., Underskaya, S.V., "Phase Equilibria in Fe-Cr-C Alloys", *Russ. Metall.*, (1), 84–87 (1989) (Phase Diagram, Thermodyn., Calculation, 9)

[1989Zhu1] Zhukov, A.A., Shilina, E.P., Archipova, T.F., "Adaptation of new Design Procedures for more Precise Definition of the Fe-C-Cr and Fe-C-Mn Phase Diagrams in the Eutectic Domain" (in Russian), *Izv. Vyss. Uchebn. Zaved., Chern. Metall.*, **3**, 4–9 (1989) (Phase Diagram, Theory, 12)

[1989Zhu2] Zhukov, A.A., Shilina, E.P., Arkhipova, T.F., "New Computation Methods in the Analysis of the Fe-C-Cr and Fe-C-Mn Systems in the Eutectic Range", *Calphad*, **13**(1), 23–32 (1989) (Calculation, Phase Diagram, Phase Relations, Thermodyn., 12)

[1990Ata] Atamert, S., Bhadeshia, H.K.D.H., "Microstructure and Stability of Fe-Cr-C Hardfacing Alloys", *Mater. Sci. Eng. A*, **A130**(1), 101–111 (1990) (Calculation, Experimental, Morphology, Phase Diagram, Phase Relations, Thermodyn., 10)

[1990Ere] Eremenko, V.N., Velikanova, T.Ya., Kharykova, A.M., Velikanova, T.A., "Role of Metallochemical Factors in Formation of Ternary Interstitial Phases", (in Russian), *Ukr. Khim. Zh.*, **56**(4), 356–363 (1990) (Crys. Structure, Phase Relations, Theory, 11)

[1990Gol] Goldenstein, H., Aaronson, H.I., "Overall Reaction Kinetics and Morphology of Austenite Decomposition Between the Upper Nose and the Ms of a Hypoeutectoid Fe-C-Cr Alloy", *Metall. Trans. A*, **21A**(6), 1465–1478 (1990) (Morphology, Phase Relations, Experimental, Kinetics, 65)

[1990Kaj] Kajihara, M., Hillert, M., "Thermodynamic Evaluation of the Cr-Ni-C System", *Metall. Trans. A*, **21A**(10), 2777–2787 (1990) (Phase Diagram, Phase Relations, Thermodyn., Assessment, 36)

[1990Pow] Powell, G.L.F., "Solidification of Undercooled Bulk Melts of Fe-Cr-C, Co-Cr-C and Ag-Ge Alloys of Near-Eutectic Composition", *Mater. Trans., JIM*, **31**(2), 110–117 (1990) (Morphology, Phase Relations, Experimental, 21)

[1990Ven] Venkatraman, M., Neumann, J.P., "The C-Cr (Carbon-Chromium) System", *Bull. Alloy Phase Diagr.*, **11**(2), 152–159 (1990) (Crys. Structure, Phase Diagram, Thermodyn., Review, 76)

[1991Eno] Enomoto, M., Tsubakino, H., "Morphology and Thermodynamics of Bainitic Transformation in Ferrous and Non-Ferrous Alloys", *Mater. Trans., JIM*, **32**(8), 642–657 (1991) (Phase Relations, Thermodyn., Kinetic, Abstract, 114)

[1991Gui] Guillermet, A.F., "Predictive Approach to Thermodynamic Properties of Metastable Cr_3C Carbide", *Int. J. Thermophys.*, **12**(5), 919–936 (1991) (Phase Diagram, Thermodyn., Theory, Calculation, 31)

[1991Hil] Hillert, M., Qui, C., "A Thermodynamic Assesment of the C-Cr-Fe-Ni System", *Metall. Trans. A*, **22A**(10), 2187–2198 (1991) (Phase Diagram, Thermodyn., Calculation, 30)

[1991Kan] Kano, M., Tanimoto, I., "Wear Mechanism of High Wear-Resistans Materials for Automotive Valve Trains", *Wear*, **151**(2), 229–243 (1991) (Abstract, Mech. Prop., 14)

[1991Leo] Leonovich, B.I., Kochurina, O.I., Mikhailov, G.G., Kozyreva, T.D., "Thermodynamic Stability of Phases in Alloys of the Iron-Chromium-Carbon System" (in Russian), *Izv. Vyss. Uchebn. Zaved., Chern. Metall.*, **3**, 4–7 (1991) (Phase Relations, Thermodyn., Calculation, 4)

DOI: 10.1007/978-3-540-74196-1_3

[1991Liu1] Liu, Z.K., Hoeglund, L., Joensson, B., Agren, J., "An Experimental and Theoretical Study of Cementite Dissolution in an Fe-Cr-C Alloy", *Metall. Trans. A*, **22A**(8), 1745–1752 (1991) (Morphology, Phase Diagram, Phase Relations, Thermodyn., Calculation, Experimental, Kinetics, 18)

[1991Liu2] Liu, Z.K., Agren, J., "Morphology of Cementite Decomposition in an Fe-Cr-C Alloy", *Metall. Trans. A*, **22A**(8), 1753–1759 (1991) (Morphology, Phase Diagram, Phase Relations, Experimental, 18)

[1991Mor] Morozov, O.P., "Relation Between Excess Ferrite Precipitation and the Upper Bainite Transformation of Austenite in Steels" (in Russian), *Fiz. Met. Metalloved.*, (8), 154–162 (1991) (Morphology, Phase Relations, Experimental, Kinetics, 24)

[1991Nis] Nishizawa, T., Ishida, K., Ohtani, H., Kami, C., Suwa, M., "Experimental Study on Interaction Parameter for Carbon and Alloying Elements in Austenite and Ferrite", *Scand. J. Metall.*, **20**, 62–71 (1991) (Phase Diagram, Phase Relations, Thermodyn., Calculation, Experimental, 34)

[1991Skr] Skrotzki, B., "The Course of the Volume Fraction of Martensite *vs* Temperature Function Mx(T)", *J. Phys. III (France)*, **1**(4), 367–372 (1991) (Experimental, Mechan. Prop., 10)

[1991Vod] Vodarek, V., Pahuta, P., "Precipitation of ε (2)-Carbide During the First Stage of Martensite Tempering", *Met. Mater. (Czech.)*, **29**(3), 151–159 (1991) (Phase Relations, Experimental) cited from abstract

[1992Lee] Lee, B.J., "On the Stability of Cr Carbides", *Calphad*, **16**(2), 121–149 (1992) (Phase Diagram, Phase Relations, Calculation, 83)

[1992Pow] Powell, G.L.F., Laird, G.II., "Structure, Nucleation, Growth and Morphology of Secondary Carbides in High Chromium and Cr-Ni White Cast Irons", *J. Mater. Sci.*, **27**(1), 29–35 (1992) (Crys. Structure, Morphology, Phase Relations, Experimental, 24)

[1992Sop] Sopousek, J., Komurka, J., "Phase Analysis and Phase Composition Computation of the Fe-20Cr-0.4C Alloy in Equilibrium at 1073°C", *Kovove Mater.*, **30**(5), 412–418 (1992) (Crys. Structure, Morphology, Phase Relations, Experimental, 6)

[1993Itk] Itkin, V.P., "Cr-Fe (Chromium-Iron)" in *"Phase Diagrams of Binary Iron Alloys"*, Okamoto, H. (Ed.), ASM International, Materials Park, Ohio, 102–129 (1993) (Phase Diagram, Thermodyn., Assessment, 232)

[1993Kha] Khayenko, B.V., Golub, S.Ya., Velikanova, T.A., Kuprin, V.V., "Formation of Phases with α-Mn and β-Mn Structures in Iron-based Alloys", *Phys. Met. Metallogr. (Engl. Transl.)*, **75**(1), 86–91 (1993) (Crys. Structure, Phase Relations, Experimental, 14)

[1993Sch] Schon, C.G., Rechenberg, H.R., Goldenstein, H., "Mössbauer Study of an Iron-Chromium-Carbon Austenite", *Scr. Metall. Mater.*, **29**(11), 1483–1488 (1993) (Crys. Structure, Electronic Structure, Experimental, 10)

[1993Zha] Zhao, J., Notis, M.R., "Phase Transformation Kinetics and the Assessment of Equilibrium and Metastable States", *J. Phase Equilib.*, **14**(3), 303–315 (1993) (Phase Diagram, Phase Relations, Assessment, Kinetics, 50)

[1994Kow] Kowalski, M., Spencer, P.J., Granat, K., Drzeniek, H., Lugscheider, E., "Phase Relations in the C-Cr-Fe- System in the Vicinity of the /Liquid+bcc+$M_{23}C_6$+M_7C_3/ Invariant Equilibrium - Experimental Determinations and Thermodynamic Modelling", *Z. Metallkd.*, **85**(5), 359–364 (1994) (Phase Diagram, Thermodyn., Calculation, Experimental, 11)

[1994Pee] Peev, K., Radulovic, M., Fiset, M., "Modification of Fe-Cr-C Alloys Using Mischmetal", *J. Mater. Sci. Lett.*, **13**, 112–114 (1994) (Experimental, Mechan. Prop., Morphology, 19)

[1994Pow] Powell, G.L.F., Carlson, R.A., Randle, V., "The Morphology and Microtexture of M_7C_3 Carbides in Fe-Cr-C and Fe-Cr-C-Si Alloys of Near Eutectic Composition", *J. Mater. Sci.*, **29**(18), 4889–4896 (1994) (Morphology, Phase Relations, Experimental, 18)

[1994Prz] Przylecka, M., Kulka, M., Gestwa, W., "The Activity of Carbon in the Two-Phase Fields of the Fe-Cr-C, Fe-Mn-C and Fe-Si-C Alloys at 1173 K", *Mater. Sci. Forum*, **163–165**, 87–92 (1994) (Thermodyn., Experimental, 10)

DOI: 10.1007/978-3-540-74196-1_3

[1994Rag] Raghavan, V., "The C-Cr-Fe System.", *J. Phase Equilib.*, **15**(4), 418–419 (1994) (Phase Diagram, Review, 26)

[1994Sop] Sopousek, J., Vrestal, J., "Phase Equilibria in the Fe-Cr-Ni and Fe-Cr-C Systems", *Z. Metallkd.*, **85**(2), 111–115 (1994) (Morphology, Phase Diagram, Experimental, 20)

[1994Wit] Witusiewicz, V.T., "Thermodynamic Properties of Liquid Alloys of 3d Transition Metals with Metalloids (Silicon, Carbon and Boron)", *J. Alloys Compd.*, **203**, 103–116 (1994) (Thermodyn., Experimental, Review, 89)

[1995Lee] Lee, B.J., "Thermodynamic Calculations in Stainless Steels Alloy Systems" (in Korean), *J. Korean Inst. Met.*, **33**(6), 766–775 (1995) (Phase Relations, Thermodyn., Calculation, 53)

[1995Mil] Million, B., Bacilek, K., Kucera, J., Michalicka, P., Rek, A., Stransky, K., "Carbon Diffusion and Thermodynamic Characteristics in Chromium Steels", *Z. Metallkd.*, **86**(10), 706–712 (1995) (Phase Relations, Thermodyn., Experimental, Kinetics, 17)

[1995Par] Park, H.S., Lee, B.J., "Computer Graphics of Isoplethic Phase Diagram of Fe-Cr-C System" (in Korean), *J. Korean Inst. Met.*, **33**(9), 1227–1234 (1995) (Phase Relations, Theory, 16)

[1995Pop] Popov, V.V., "Determining Interdiffusion Coefficient for Metal Elements in Austenite and Ferrite of Fe-Cr-C, Fe-Mo-C, and Fe-W-C Systems", *Phys. Met. Metallogr. (Engl. Transl.)*, **79**(4), 418–424 (1995) (Experimental, Morphology, Phase Relations, 23)

[1995Wit] Witusiewicz, V.T, "Thermodynamics of Formation of Binary and Ternary Melts of the 3d Transition Metals with Metalloid" (in Ukrainian), Summary of Thesis, National Academy of Science of Ukraine, Kiev, pp. 55 (1995) (Experimental, Thermodyn., 0)

[1996Bon] Bondar, A.A., Velikanova, T.Ya., "Aspects of Construction of the Constitution Diagrams of Ternary Systems Formed by Chromium with Carbon and d-Transition Metals", *Powder Metall. Met. Cer.*, **35**(7–8), 484–496 (1996), translated from Poroshk. Metall., (7–8), 182–196 (1996) (Phase Relations, Review, 40)

[1996Jun] Jung, Y.-C., Ohtsubo, H., Nakai, K., Ohmori, Y., "Isothermal Decomposition Processes of Austenite in Fe-Cr-C Alloy Steels", *Mater. Trans., JIM*, **37**(4), 676–683 (1996) (Phase Relations, 22)

[1996Kob] Kobayashi, Y., Morita, K., Sano, N., "Thermodyn. of Molten Fe-Cr-C-satd. Alloy", *ISIJ Int.*, **36**(8), 1009–1013 (1996) (Phase Relations, Thermodyn., Experimental, 13)

[1996Ran] Ranganathan, S., "The Technique of Successive Partial Equilibria to Predict Precipitation of Carbides in Equilibrium With a Solution Phase", *Calphad*, **20**(4), 461–470 (1996) (Phase Diagram, Phase Relations, Calculation, 8)

[1996Sop] Sopousek, J., Vrestal, J., "$M_{23}C_6$ Carbide Equilibria in the Fe-Cr-C System", *Metall. Mater. Trans. B*, **27B**, 701–704 (1996) (Phase Relations, Experimental, 14)

[1996Tab] Tabrett, C.P., Sare, I.R., Ghomashchi, M.R., "Microstructure-Property Relashionships in High Chromium White Iron Alloys", *Int. Mater. Rev.*, **41**(2), 59–82 (1996) (Morphology, Phase Relations, Review, Mech. Prop., Interface Phenomena, 191)

[1996Jun] Jung, Y.-C., Ohtsubo, H., Nakai, K., Ohmori, Y., "Isothermal Decomposition Processes of Austenite in Fe-Cr-C Alloy Steels", *Mater. Trans., JIM*, **37**(4), 676–683 (1996) (Crys. Structure, Morphology, Phase Relations, Experimental, 22)

[1997Akt] Aktuerk, S., Gencer, A., Durlu, T.N., "Studies on the Magnetic Properties of Martensitic Phase in an Fe-Cr-C Alloy", *J. Mater. Sci. Lett.*, **16**(5), 389–391 (1997) (Phase Relations, Experimental, Magn. Prop., Mechan. Prop., 9)

[1997Dog] Dogan, O.N., Hawk, J.A., Laird, G., "Solidification Structure and Abrasion Resistance of High Chromium White Irons", *Metall. Mater. Trans. A*, **28A**(6), 1315–1328 (1997) (Morphology, Phase Relations, Experimental, Mechan. Prop., 70)

[1997Hil] Hillert, M., "How to Select Axes for a Phase Diagram", *J. Phase Equilib.*, **18**(3), 249–263 (1997) (Phase Diagram, Phase Relations, Theory, 1)

[1997Miz] Mizuno, M., Tanaka, I., Adachi, H., "Effect of Solute Atoms on the Chemical Bonding of Fe_3C (cementite)", *Philos. Mag. B*, **75**(2), 237–248 (1997) (Electronic Structure, Calculation, 28)

DOI: 10.1007/978-3-540-74196-1_3

[1997Sil] Sil'man, G.I., "Refinement of the Fe-C Diagram on the Basic of Results of a Thermodynamic Analysis and Generalization of Data for Fe-C and Fe-C-Cr Systems", *Metal Sci. Heat Treatm.*, **39**, 451–456 (1997) (Phase Diagram, Phase Relations, Calculation, 20)

[1997Tab] Tabrett, C.P., Sare, I.R., "The Effect of Heat Treatment on the Abrasion Resistance of Alloy White Irons", *Wear*, **203–204**, 206–219 (1997) (Morphology, Experimental, Interface Phenomena, Mechan. Prop., 28)

[1998Hin] Hino, M., Higuchi, K.-I., Nagasaka, T., Ban-Ya, S., "Thermodynamic Estimation on the Reduction Behavior of Iron-Chromium Ore with Carbon", *Metall. Mater. Trans. B*, **29B**, 351–360 (1998) (Phase Relations, Thermodyn., Calculation, 19)

[1998Kay] Kaya, A.A., Edmonds, D.V., "Nonclassical Decomposition Products of Austenite in Fe-C-Cr Alloys", *Metall. Mater. Trans. A*, **29A**(12), 2913–2934 (1998) (Morphology, Phase Relations, Experimental, 37)

[1998Par] Park, J.-H., Min, D.-J., Rhee, C.-H., "Activities of Chromium in Molten Fe-Cr-C Alloy", *ISIJ Int.*, **38**, 1287–1291 (1998) (Thermodyn., Experimental, 10)

[1999Ma] Ma, Z., Janke, D., "Activities of Carbon and Nitrogen in Fe-Cr and Fe-Cr-Ni Melts", *Steel Res.*, **70**, 491–495 (1999) (Thermodyn., Calculation, 25)

[1999Mas] Maslyuk, V.A., Napara-Volgina, S.G., "Wear-resistant and Corrosion-Resistant Carbide-Steel Type Materials Having Different Matrices", *Powder Metall. Met. Ceram.*, **38**(9–10), 521–525 (1999) (Phase Relations, Experimental, Mechan. Prop., Interface Phenomena, 7)

[1999Nak] Nakai, K., Shtansky, D.V., "Evolution During Reverse Phase Transformations in Alloyed Steels Using Calculated Phase Diagrams" (in Japanese), *Materia Japan*, **38**, 975–981 (1999) (Phase Relations, Calculation, 41)

[1999Per] Pero-Sanz, J.A., Plaza, D., Verdeja, J.I., Asensio, J., "Metallographic Characterization of Hypoeutectic Martensitic White Cast Irons: Fe-C-Cr System", *Mater. Charact.*, **43**, 33–39 (1999) (Morphology, Phase Relations, Experimental, Mechan. Prop., 4)

[1999Pop] Popov, V.V., "Diffusion Interaction of Carbides, Nitrides and Carbonitrides With Iron and Steels", *Metallofizika Nov. Tekhnol.*, **21**(2), 99–103 (1999) (Phase Relations, Experimental, Transport Phenomena, 11)

[1999Qia] Qian, M., "In-situ Observations of the Dissolution of Carbides in an Fe-Cr-C Alloy", *Scr. Mater.*, **41**(12), 1301–1303 (1999) (Morphology, Phase Relations, Experimental, 2)

[1999Sht1] Shtansky, D.V., Nakai, K., Ohmori, Y., "Crystallography and Interface Boundary Structure of Pearlite with M_7C_3 Carbide Lamellae", *Acta Mater.*, **47**(4), 1105–1115 (1999) (Crys. Structure, Morphology, Experimental, 42)

[1999Sht2] Shtansky, D.V., Nakai, K., Ohmori, Y., "Pearlite to Austenite Transformation in an Fe-2.6Cr-1C Alloy", *Acta Mater.*, **47**(9), 2619–2632 (1999) (Morphology, Phase Relations, Thermodyn. Calculation, Experimental, Kinetics, 40)

[1999Sht3] Shtansky, D.V., Nakai, K., Ohmori, Y., "Formation of Austenite and Dissolution of Carbides in Fe-8.2Cr-C Alloys", *Z. Metallkd.*, **90**(1), 25–37 (1999) (Morphology, Phase Relations, Thermodyn. Calculation, Experimental, Kinetics, 47)

[1999Sht4] Shtansky, D.V., Nakai, K., Ohmori, Y., "Mechanism and Crystallography of Ferrite Precipitation from Cementite in an Fe-Cr-C Alloy During Austenitization", *Philos. Mag. A*, **79**(7), 1655–1669 (1999) (Crys. Structure, Morphology, Phase Diagram, Phase Relations, Calculation, Experimental, 20)

[2000Abe] Abe, T., Onodera, H., Kimura, K., Kushima, H., "Effect of M-C (M = Mo, Mn,and Cr) Atomic Pairs on Creep Properties of Fe-M-C Ternary Alloys", *Key Eng. Mater.*, **171–174**, 461–468 (2000) (Experimental, Mechan. Prop., 24)

[2000Bor] Borgenstam, A., Engstroem, A., Hoeglund, L., Agren, J., "DICTRA, a Tool for Simulation of Diffusional Transformations in Alloys", *J. Phase Equilib.*, **21**(3), 269–280 (2000) (Thermodyn., Calculation, Kinetics, 59)

[2000Iwa] Iwanaga, K., Tsuchiyama, T., Takaki, S., "Strengthening Mechanisms in Heat-Resistant Martensitic 9Cr Steel", *Key Eng. Mater.*, **171–174**, 477–482 (2000) (Phase Relations, Experimental, Mechan. Prop., 4)

DOI: 10.1007/978-3-540-74196-1_3

[2000Koz1] Kozeschnik, E., Vitek, J.M., "Ortho-Equilibrium and Para-Equilibrium Phase Diagrams for Interstitial/Substitutional Iron Alloys", *Calphad*, **24**(4), 495–502 (2000) (Phase Diagram, Phase Relations, Thermodyn., Calculation, 10)

[2000Koz2] Kozeschnik, E., "A Scheil-Gulliver Model with Back-Diffusion Applied to the Microsegregation of Chromium in Fe-Cr-C Alloys", *Metall. Mater. Trans. A*, **31A**(6), 1682–1684 (2000) (Phase Diagram, Phase Relations, Calculation, 10)

[2000Kun] Kunze, J., Beyer, B., "Thermodynamical Calculation of Martensite Start Temperatures in the System FeCrMnNiC", *Z. Metallkd.*, **91**(2), 106–113 (2000) (Phase Relations, Thermodyn., Calculation, 35)

[2000Oht] Ohta, J., Kako, K., Mayuzumi, M., Kusanagi, H., Abiko, K., "In Situ Transmission Electron Microscopy of Carbide Precipitation in Fe-50%Cr Alloys at Elevated Temperatures", *Mater. Trans., JIM*, **41**(1), 130–135 (2000) (Morphology, Phase Relations, Experimental, 10)

[2000Ran] Ranganathan, S., "Prediction of Phase Equilibria by the Technique of Successive Partial Equilibration- the General Algorithm", *Calphad*, **24**(3), 285–294 (2000) (Phase Diagram, Phase Relations,Theory, 6)

[2001Goe] Gödecke, T., "Delineation of Crystallization Paths in Ternary As-Cast Alloys" (in German), *Z. Metallkd.*, **92**(8), 966–978 (2001) (Phase Diagram, Theory, 37)

[2001Mie] Miettinen, J., Howe, A.A., "Estimation of Liquidus Temperatures for Steels Using Thermodynamic Approach", *Ironmaking Steelmaking*, **27**(3), 212–227 (2000) (Calculation, Experimental, Phase Relations, Thermodyn., 53)

[2001Mor] Morra, P.V., Boettger, A.J., Mittemeijer, E.J., "Decomposition of Iron-based Martensite. A Kinetic Analysis by Means of Differential Scanning Calorimetry and Dilatometry", *J. Therm. Anal. Calorim.*, **64**(3), 905–914 (2001) (Phase Relations, Experimental, Kinetics, 21)

[2001Sht] Shtanskii, D.V., "Analysis of Phase and Structural Transformations in Ternary Systems by the Computer-Thermodynamic Methods: A Review", *Phys. Met. Metallogr. (Engl. Transl.)*, **92**(2), 133–152 (2001) (Phase Diagram, Phase Relations, Thermodyn., Calculation, Review, 108)

[2001Ume] Umemoto, M., Liu, Z.G., Masuyama, K., Tsuchiya, K., "Influence of Alloy Additions on Production and Properties of Bulk Cementite", *Scr. Mater.*, **45**(4), 391–397 (2001) (Crys. Structure, Phase Relations, Experimental, Mechan. Prop., Phys. Prop., 13)

[2001Wan] Wang, H., Wang, S., Yue, K., Dong, Y., Li, W., "The Rules of Thermodynamic Properties in Fe-C-j (j = Ti, V, Cr, Mn) Melts", *Acta Metall. Sin. (China)*, **37**(9), 952–956 (2001) (Thermodyn., Calculation, 13)

[2002Him] Himemiya, T., Wolczynski, W., "Solidification Path and Solute Redistribution of an Iron-Based Multi-Component Alloy with Solute Diffusion in the Solid", *Mater. Trans.*, **43**(11), 2890–2896 (2002) (Phase Relations, Calculation, 12)

[2002Rag] Raghavan, V., "C-Cr-Fe (Carbon-Chromium-Iron)", *J. Phase Equilib.*, **23**(6), 513–514 (2002) (Phase Diagram, Phase Relations, Review, 10)

[2002Shi] Shin, H.D., Min, D.J., Song, H.S., "Influence of Copper on Decarburization Kinetics of Stainless Steel Melt at High Temperatures", *ISIJ Int.*, **42**(8), 809–815 (2002) (Thermodyn., Experimental, Theory, Kinetics, 15)

[2002Wan] Wang, H., Wang, S., Dong, Y., Li, W., "A Data Treatment Method of Carbon Saturated Solubility in Fe-C-Cr Melt", *J. Univ. Sci. Technol. Beijing*, **9**(1), 16 (2002) (Thermodyn., Experimental, 10)

[2003Car1] Carpenter, S.D., Carpenter, D., "Stacking Faults and Superlattice Observations During Transmission Electron Microscopy of a $(Fe,Cr)_7C_3$ Carbide", *Mater. Lett.*, **57**(28), 4460–4465 (2003) (Crys. Structure, Morphology, Experimental, 9)

[2003Car2] Carpenter, S.D., Carpenter, D., "X-Ray Diffraction Study of M_7C_3 Carbide within a High Chromium White Iron", *Mater. Lett.*, **57**(28), 4456–4459 (2003) (Crys. Structure, Experimental, 12)

DOI: 10.1007/978-3-540-74196-1_3

[2003Gav] Gavriljuk, V., Rawers, J., Shanina, B., Berns, H., "Nitrogen and Carbon in Austenitic and Martensitic Steels: Atomic Interaction and Structural Stability", *Mater. Sci. Forum*, **426–432**, 943–950 (2003) (Phase Relations, Calculation, 11)

[2003Kat] Kato, T., Jones, H., Kirkwood, D.H., "Segregation and Eutectic Formation in Solidification of Fe-1C-1.5Cr Steel", *Mater. Sci. Technol.*, **19**, 1070–1076 (2003) (Morphology, Phase Relations, Calculation, Experimental, 21)

[2003Kud] Kudoh, M., Wo, B., "Effects of Solute Elements on Primary and Secondary Dendrite Arm Spacings in Fe-based Alloys", *Steel Res.*, **74**(3), 161–167 (2003) (Phase Relations, Calculation, Experimental, 14)

[2003Lin] Lin, X., Zhang, Y., Gu, N., Meng, Z., "Crystallographic Analysis of (225)f Martensite Transformation in Fe-Cr-C Alloy", *ISIJ Int.*, **43**(7), 1073–1079 (2003) (Crys. Structure, Phase Relations, Theory, 13)

[2003Lu] Lu, L., Soda, H., McLean, A., "Microstructure and Mechanical Properties of Fe-Cr-C Eutectic Composites", *Mater. Sci. Eng. A*, **A347**(1–2), 214–222 (2003) (Phase Diagram, Phase Relations, Experimental, Mechan. Prop., 26)

[2003Nes] Nesterenko, A.M., Kucova, V.Z., Kovzel, M.A., "Crystal Structure of the Carbides of the Me_7C_3 Type" (in Russian), *Metallofizika Nov. Tekhnol.*, **25**(1), 99–106 (2003) (Crys. Structure, Phase Relations, Experimental, 13)

[2003Yam] Yamamoto, K., Liliac, M.M., Ogi, K., "Thermodynamic Evaluation of Solidification Structure of High Chromium White Cast Iron", *Inter. J. Cast Met. Res.*, **16**(4), 435–440 (2003) (Morphology, Thermodyn, Calculation, 16)

[2003Yin] Yin, Y.F., Faulkner, R.G., "Modelling the Effects of Alloying Elements on Precipitation in Ferritic Steels", *Mater. Sci. Eng. A*, **A344**, 92–102 (2003) (Morphology, Calculation, 27)

[2004Aar] Aaronson, H.I., Reynolds, W.T., Purdy, G.R., "Coupled-Solute Drag Effect on Ferrite Formation in Fe-C-X Systems", *Metall. Mater. Trans. A*, **35a**(4), 1187–1210 (2004) (Morphology, Phase Relations, Experimental, Interface Phenomena, Kinetics, 148)

[2004Bon1] Bonade, R., Spaetig, P., Schaeublin, R., Victoria, M., "Plastic Flow of Martensitic Model Alloys", *Mater. Sci. Eng. A*, **387–389**, 16–21 (2004) (Phase Relations, Experimental, Mechan. Prop., 18)

[2004Bon2] Bonade, R., Spaetig, P., Victoria, M., Yamamoto, T., Odette, G.R., "Tensile Properties of a Tempered Martensitic Iron-Chromium-Carbon Model Alloy", *J. Nucl. Mater.*, **329–333**, 278–282 (2004) (Phase Relations, Experimental, Mechan. Prop., 19)

[2004Bra] Bratberg, J., Frisk, K., "An Experimental and Theoretical Analysis of the Phase Equilibria in the Fe-Cr-V-C System", *Metall. Mater. Trans. A*, **35A**(12), 3649–3663 (2004) (Phase Diagram, Phase Relations, Thermodyn., Calculation, Experimental, 43)

[2004Ten] Teng, L., "Thermodynamic Investigation of Transition Metal Systems Containing Carbon and Nitrogen", Thesis Royal Institute of Technology, Stockholm, Sweden, 1–58 (2004) (Calculation, Experimental, Crys. Structure, Thermodyn., Phase Diagram, #, 106)

[2004Sai] Saitoh, H., Yoshinaga, N., Ushioda, K., "Influence of Substitutional Atoms on the Snoek Peak of Carbon in b.c.c. Iron", *Acta Mater.*, **52**(5), 1255–1261 (2004) (Phase Relations, Experimental, 37)

[2004Wie] Wiengmoon, A., Chairuangsri, T., Pearce, J.T.H., "A Microstructural Study of Destabilished 30wt.%Cr-2.3wt.%C High Chromium Cast Iron", *ISIJ Int.*, **44**(2), 396–403 (2004) (Crys. Structure, Morphology, Phase Relations, Experimental, Mechan. Prop., 19)

[2005Als] Al'shevskii, Yu.L., Baklanova, O.N., Zaitsev, A.I., Mal'tsev, V.V., Rodionova, I.G., Rybkin, A.N., Shaposhnikov, N.G., "Thermodynamic Analysis of Equilibria in Fe-Cr-C Alloys and Evaluation of their Dusting Stability in Aggressive Carboniferous Atmospheres", *Inorg. Mater. (Engl. Trans.)*, **41**(2), 133–139 (2005), translated from *Neorg. Mater.*, **41**(2), 177–184 (2005) (Phase Relations, Thermodyn., Calculation, 15)

[2005Bal] Balitchev, E., Hallstedt, B., Neuschuetz, D., "Thermodynamic Criteria for the Selection of Alloys Suitable for Semi-Solid Processing", *Steel Res.*, **76**(2–3), 92–98 (2005) (Phase Relations, Calculation, 22)

DOI: 10.1007/978-3-540-74196-1_3

[2005Bed] Bedolla-Jacuinde, A., Hernandez, B., Bejar-Gomez, L., "SEM Study on the M_7C_3 Carbide Nucleation During Eutectic Solidification of High-Chromium White Irons", *Int. J. Mater. Res. (Z. Metallkd.)*, **96**(12), 1380–1385 (2005) (Experimental, Morphology, Phase Relations, 20)

[2005Bon] Bonade, R., Spatig, P., "On the Strain-hardening of Tempered Martensitic Alloys", *Mater. Sci. Eng. A*, **400–401**, 234–240 (2005) (Morphology, Phase Relations, Calculation, Experimental, Mechan. Prop., 18)

[2005Kun] Kunieda, T., Nakai, M., Murata, Y., Koyama, T., Morinaga, M., "Estimation of the System Free Energy of Martensite Phase in an Fe-Cr-C Ternary Alloy", *ISIJ Int.*, **45**(12), 1909–1914 (2005) (Morphology, Thermodyn., Calculation, Experimental, 14)

[2005Sch] Schneider, A., Inden, G., "Simulation of the Kinetics of Precipitation Reactions in Ferritic Steels", *Acta Mater.*, **53**(2), 519–531 (2005) (Phase Relations, Thermodyn., Calculation, Kinetics, 28)

[2005Ten] Teng, L.D., Aune, R.E., Selleby, M., Seetharaman, S., "Thermodynamic Investigations of the C-Cr-Fe System by Galvanic Cell Technique", *Metall. Mater. Trans. B*, **36B**(2), 263–270 (2005) (Thermodyn., Experimental, 17)

[2005Wie] Wiengmoon, A., Chairuangsri, T., Pearce, J.T.H., "An Unusual Structure of an As-cast 30% Cr Alloy White Iron", *ISIJ Int.*, **45**(11), 1658–1665 (2005) (Morphology, Phase Relations, Experimental, 23)

[2006MSIT] "C-Fe (Iron-Carbon)", Diagrams as Published, in *MSIT Workplace*, Effenberg, G. (Ed.), Materials Science International Services, GmbH, Stuttgart; Document ID: 30.13598.1.20 (2006) (Crys. Structure, Phase Diagram, Phase Relations, 2)

[Mas2] Massalski, T.B. (Ed.), *Binary Alloy Phase Diagrams*, 2nd edition, ASM International, Metals Park, Ohio (1990)

[V-C2] Villars, P. and Calvert, L.D., *Pearson's Handbook of Crystallographic Data for Intermetallic Phases*, 2nd edition, ASM, Metals Park, Ohio (1991)

DOI: 10.1007/978-3-540-74196-1_3

Carbon – Copper – Iron

Nataliya Bochvar, Rainer Schmid-Fetzer, Elena Semenova, Elena Sheftel

Introduction

The C-Fe phase diagram is the base of industrial steels and cast-irons. There are two types of the phase diagram, stable and metastable. The Fe-C (graphite) diagram is related to the alloys which are crystallized at very slow cooling rate with the formation of graphite. Such system is stable. The Fe-Fe_3C system is related to the alloys which are crystallized at ordinary, relatively not high cooling rate with the formation of iron carbide (cementite). Such system is considered as metastable. Copper is a graphitizing element, it promotes a dispergation of the eutectic structure. The additions of Cu in C-Fe alloys raise the mechanical properties of steel and cast-iron, increase the corrosion resistance, improve the formability of steel and wear resistance of cast-iron. On the other hand, this alloying element may be the reason of hot cracking during rolling. Therefore, the investigations of the phase equilibria in stable C-Cu-Fe and metastable Fe-Fe_3C-Cu systems are essential for the estimation of Cu content improving mechanical and technological characteristics of steel and cast-iron. Literature on experimental and thermodynamic studies of phase relations in the C-Cu-Fe system are summarized in Table 1.

The liquidus surface in the C-Cu-Fe system is characterized by a miscibility gap established by [1926Ish, 1936Mad, 1938Iwa, 1959Per, 1961Sch, 1965Loe, 1979Par] and confirmed by [1986Sch, 1987Sch, 1991Sch1, 1991Sch2, 1999Ama]. The compositions of two liquids being in equilibrium were determined at 1600°C [1959Per, 1961Sch, 1975Cho], at 1540 and 1450°C [1938Iwa]. The solubility of graphite in C-Cu-Fe melt was determined at 1600°C [1956Kor], 1550°C [1960Mor, 2001Ma], 1500 and 1600°C [1983Jan1, 1983Jan2], 1200 to 1500°C [1959Per, 1961Sch], 1450°C [1960Fuw], 1300, 1350 and 1400°C [1961She], 1490 and 1300°C [1959Sim], 1300°C [1957Lan], 1270 to 1360°C [1986Zhu]. The solid-state phase relationships in the C-Cu-Fe system were investigated by thermodynamic calculations [1979Cha, 2003Sil] and experiments [1968Wil, 1970Mor, 1972Wil, 1975Lar]. Using as initial data both the thermochemical and experimental phase equilibrium information, the isothermal sections of the iron rich part of the C-Cu-Fe system at 600, 800, 900, 1000 and 1100°C were calculated by [1978Uhr].

There are a number of reviews on the C-Cu-Fe system [1949Jae, 1979Cha, 1984Riv, 1988Ray, 1994Rag, 2002Rag]. [1949Jae] described the results [1926Ish, 1936Mad, 1938Iwa] obtained for the Fe rich part of C-Cu-Fe system characterized by the extensive liquid miscibility gap.

[1979Cha] discussed the literature information on the phase equilibria and thermodynamic characteristics of the C-Cu-Fe system and accepted the following data: [1965Loe, 1975Mor] for liquidus projection and four-phase invariant stable and metastable equilibria; data of [1959Per, 1961Sch, 1975Cho, 1938Iwa, 1957Lan, 1936Mad, 1959Sim, 1960Fuw, 1960Mor, 1956Kor] for liquidus isotherms and tie-lines at different temperatures; data of [1972Wil, 1975Lar, 1971Gre, 1972Wil, 1975Cho, 1975Mos] for the solid-state phase relationships involving the (γFe) phase as well own thermodynamic calculations of the phase boundaries (γFe)/(Cu), (γFe)/(C)gr, (γFe)/Fe_3C. [1979Cha] analyzed and compared the available data and specified certain temperatures and compositions for the ternary system for which they developed a series of stable and metastable sections of the phase diagram.

[1984Riv, 1988Ray] described liquid phase equilibria based on the data of [1926Ish, 1965Loe, 1975Lar] for metastable liquidus and data of [1936Mad, 1965Loe, 1979Par] for stable liquidus. These reviews also contain data about tie-lines in the liquid miscibility gap at 1550°C from [1959Per], isothermal sections at 1172, 1050, 925 and 850°C from [1979Par], vertical sections at 4.5 mass% C from [1965Loe] and a solubility C in (γFe)-(Cu) solid alloys from [1972Wil, 1975Mos, 1979Par].

A short description of the liquid miscibility gap in stable and metastable C-Cu-Fe systems adopted from [1986Sch, 1987Sch, 1991Sch1, 1991Sch2] was presented by [1994Rag] and that adopted from [1999Ama] was presented by [2002Rag].

DOI: 10.1007/978-3-540-74196-1_4

[1990Gus] carried out thermodynamic calculations of phase equilibria in the C-Cu-Fe system which were compared with the experimental data of [1965Loe, 1975Lar, 1975Mos, 1979Cha, 1979Par]. The calculated and experimental data are in very good agreement.
[2003Sil] using the thermodynamic parameters of C-Fe and Cu-Fe systems and magnitude of the phase distribution coefficients of the elements calculated the temperatures and constitutions of four-phase invariant eutectoid equilibria in stable and metastable C-Cu-Fe systems and constructed some isothermal sections.

Binary Systems

The binary C-Fe phase diagram (stable and metastable) is accepted from [2006MSIT]. It is based on [Mas2], however the stable eutectic constitution (17.73 at.% C, or 4.43 mass% C) and temperature (1153.5 ± 5°C) are taken from [2000Fen, 2001Fen].
The binary C-Cu system is accepted from [1994Sub] except for the solubility of C in solid (Cu) which was accepted from [2004Lop]. In accordance with [2004Lop] the solubility varies from $4.8 \pm 0.5 \cdot 10^{-4}$ at.% ($0.9 \pm 0.1 \cdot 10^{-4}$ mass%) at 870°C till $7.4 \pm 0.5 \cdot 10^{-4}$ at.% ($1.4 \pm 0.1 \cdot 10^{-4}$ mass%) at 1020°C. The solubility of C in (Cu) at invariant temperature (~1100°C) was estimated by extrapolation to be $10 \cdot 10^{-4}$ at.% ($1.88 \cdot 10^{-4}$ mass%). The binary Cu-Fe system is accepted from [2007Tur].

Solid Phases

There is no ternary compound in the C-Cu-Fe system. The unary phases and the metastable phases discussed in this assessment are listed in Table 2.

Quasibinary Systems

[1926Ish] theoretically assumed the existence of a quasibinary Fe_3C-Cu system with the miscibility gap in liquid as well two invariant reactions L′ + L′′ ⇌ Fe_3C and L′′ + Fe_3C ⇌ (Cu) in the metastable Fe-Fe_3C-Cu ternary phase diagram. [1991Sch1, 1991Sch2] discussed the quasibinary Fe_3C-Cu system accepted from [1926Ish] and estimated the temperature of the monotectic reaction L′ + L′′ ⇌ Fe_3C of about 1230°C.

Invariant Equilibria

Stable Invariant Equilibria

Three four-phase invariant equilibria were established in the stable C-Cu-Fe system. In accordance with [1936Mad, 1965Loe, 1979Par, 1999Ama, 1991Sch2] one of the invariant equilibria is a transition equilibrium L′ + L′′ ⇌ (γFe) + (C)gr. It stems from the three-phase equilibrium e_1 (1153.5°C) in the binary C-Fe system with increasing temperature into the ternary C-Cu-Fe system. The temperature of the four-phase invariant reaction is 1184, 1172, 1158 and 1160°C in accordance with [1965Loe], [1979Par], [1991Sch2] and [1999Ama], respectively. However, the invariant monotectic temperature determined by thermal analysis [1965Loe, 1979Par, 1999Ama] is not sufficiently precise because the four-phase monotectic reaction occurs on the boundary between two liquid and two solid phases. In order to obtain more accurate values for this temperature the samples must be equilibrated in a temperature gradient, such that the centre of the sample was at the invariant temperature (where austenite, graphite, iron rich liquid and copper rich liquid were present). Although [1979Par] took this into account, he nevertheless obtained experimentally that the temperature of the invariant reaction was not constant and varied from 1163 to 1172°C.
The temperature of this invariant reaction determined by the thermodynamic calculation [1990Gus] is 1165°C. However, determining the compositions of both liquid phases after saturation during exposition at different temperatures, [1991Sch2] established that two immiscible liquids exist yet at the temperature 1164°C, while at 1146°C Fe rich liquid disappears and Cu rich liquid and two solid phases, (γFe) and (C)gr educe. Therefore the temperature of the invariant reaction must be between 1164 and 1146°C. [1991Sch2] estimated it as 1158°C by extrapolating the monotectic line constructed in dependence of the components

DOI: 10.1007/978-3-540-74196-1_4

logarithm from the reciprocal temperature. This temperature might be assumed to be more exact because it was established by a combination of experimental data and thermodynamic calculations.
During the present assessment we carried out thermodynamic calculations for comparison, using a simple extrapolation from the binary edge systems as present in the database [2005Pan]; these gave the invariant reaction temperature 1150.8°C, which is 2.7°C *below* the temperature of the binary eutectic, L′ ⇌ (γFe) + (C)gr, thus indicating that this four-phase invariant reaction is altered to be of *eutectic type*, L′ ⇌ L′′ + (γFe) + (C)gr. The compositions of L′ and (γFe) phases at invariant temperature reported by different investigators are shown in Table 3. In accordance with [1965Loe, 1979Par, 1991Sch2, 1990Gus] the Cu/Fe ratio in (γFe) is larger than in L′, resulting in the transition reaction type with L′ being located outside of the three-phase triangle of L′′ + (γFe) + (C)gr. By contrast, in the simple extrapolation the Cu/Fe ratio is slightly smaller in (γFe) compared to L′, as necessary for the eutectic reaction type with L′ being located just inside the three-phase triangle of L′′ + (γFe) + (C)gr. It should be noted that the difference between these reaction types (eutectic or transition) is not too significant in this case, with L′ being located extremely close to the tie line (γFe) + (C)gr. However, the comparison demonstrates that a simple extrapolation from the binary systems and no ternary interactions does not describe these phase relations precisely. Thus, the calculation by [1990Gus], using ternary interactions and reproducing the experimental temperature, is superior. Thus, from consistency, the compositions calculated by [1990Gus] should also be correct and they indeed agree with most of the experimental data.
The solidification of copper rich liquid (L′′) leads to a second four-phase invariant equilibrium of the transition type, L′′ + (γFe) ⇌ (Cu) + (C)gr. The temperature of this reaction was determined as 1094, 1096, 1095, 1091, 1094 and 1090°C by [1936Mad], [1965Loe], [1976Maj, 1977Maj2], [1979Par], [1991Sch2] and [1999Ama], respectively. According to the thermodynamic calculation by [1990Gus] this temperature is 1095°C which is very close to the invariant temperature in the Cu-Fe binary system.
The following four-phase equilibrium occurs in the solid state (γFe) ⇌ (αFe) + (Cu) + (C)gr. The temperature and composition of the phases were obtained by thermodynamic calculations. The temperature of this reaction is 720, 731 and 726°C according to [1979Cha], [1990Gus] and [2003Sil]. These temperatures agree well. The difference in the chemical compositions of the (γFe) phase (about 0.62 mass% C and about 1.1 mass% Cu) obtained in these works is negligible.
A reaction scheme is given in Fig. 1. Table 4 specifies the invariant equilibria accepted in the present assessment of the C-Cu-Fe system.

Metastable Invariant Equilibria

Three four-phase invariant equilibria have been established in the Cu-Fe-Fe_3C metastable system. The monotectic reaction of eutectic type L′ ⇌ L′′ + (γFe) + Fe_3C is at the temperature 1134°C [1965Loe, 11991Sch2, 1979Cha]. The composition of L′ (Fe rich liquid phase) is about 4.3% C and about 3.3% Cu (mass%) according to [1926Ish, 1965Loe, 1991Sch2, 1990Gus]. The contents of Cu in L′′ (Cu rich liquid phase) is about 96-98 mass% and the contents of carbon is very small [1990Gus, 1991Sch2]. According to [1926Ish, 1990Gus] there are about 2 mass% C and 4.5 to 5.5 mass% Cu in austenite (γFe). [1991Sch1, 1991Sch2] assumed a second invariant transition reaction with participation of liquid phase, L′′ + (γFe) ⇌ (Cu) + Fe_3C. The temperature and constitution of phases were not established experimentally. [1990Gus] calculated the temperature of this reaction as 1095°C and the composition of the phases which were presented in Table 4.
The temperature of the solid-state invariant reaction (γFe) ⇌ (αFe) + (Cu) + Fe_3C was calculated as ~710 by [1975Lar] and 715°C by [1978Uhr, 1979Cha] and agreed well with 717°C calculated by [2003Sil]. The difference in the compositions of phases is more considerable. The calculated composition of (γFe) was 0.83 mass% C and 1.1 mass% Cu in accordance with [2003Sil] instead of 0.68 mass% C and 0.9 mass% Cu according to [1979Cha]. [1978Uhr] estimated the content of Cu in (γFe) about 1.3 mass%.
There are two three-phase invariant equilibria, l′ ⇌ l′′ + Fe_3C, at ~ 1230°C and l′′ + Fe_3C ⇌ (Cu) in the metastable Cu-Fe-Fe_3C system [1926Ish, 1991Sch1, 1991Sch2].
A reaction scheme for the metastable equilibria, that is suspending the graphite phase, is given in Fig. 2. Table 4 specifies invariant equilibria in the metastable Cu-Fe-Fe_3C system.

DOI: 10.1007/978-3-540-74196-1_4

Liquidus, Solidus and Solvus Surfaces

Stable Liquidus Surface

In the C-Cu-Fe ternary system the miscibility gap in the liquid state is well established. There are two liquids, Fe rich (L′) and Cu rich (L′′), presented over a wide composition range. Early investigators [1926Ish, 1936Mad, 1938Iwa] noted that even very small additions of carbon to Cu-Fe alloys caused liquid immiscibility. [1936Mad, 1979Par, 1987Sak, 1988Sak, 1991Sch2] gave clear microscopic evidence of a liquid separation. [1959Per] obtained tie-lines at 1550 and 1500°C for the miscibility gap using chill-cast alloys which found to have separated into Fe rich and Cu rich layers in a morphology quite comparable with that observed by [1936Mad] in cooling-curve ingots. There is no evidence of a change in the magnitude of the miscibility gap boundary between 1550 and 1500°C. However, the composition of the Fe rich liquid (L′), which is in equilibrium with L′′, Cu rich liquid, and (C)gr, is extrapolated from the extensive measurement of [1961Sch] from 1200 to 1500°C. [1959Per] noted that in the composition range 20 to 85 mass% Cu the results were not reproducible and concluded that at low carbon contents either the liquid phase is homogeneous or the separation is too incomplete for accurate analysis of composition. In any case it is clear that the boundary for the miscibility gap at 1550°C approaches the Cu-Fe axis very close. The tie-lines shown in the 1600°C isotherm are taken to be the same as those at 1550 and 1500°C [1959Per]. The tie-line determined at lower temperature by [1938Iwa] at 1450 and 1540°C and by [1957Lan] at 1300°C are in reasonable accord with those in the temperature interval 1200 to 1500°C of [1961Sch]. The solubility of graphite in the C-Cu-Fe melts determined by [1959Sim] at 1300 and 1490°C, by [1960Fuw] at 1450°C and by [1970Mor] at 1550°C agree with the data of [1959Per, 1961Sch], except the data reported by [1956Kor] at 1600°C.

The liquidus surface in the Fe rich corner was calculated by [1990Gus] and [1991Sch2]. The results of [1990Gus] are in very good agreement with most experimental data [1959Sim, 1960Mor, 1959Per, 1986Sch]. For calculation of the liquidus surface, [1991Sch2] used data of [1959Per, 1986Sch, 1987Sch] as well own experimental results. [1991Sch2] constructed the miscibility gap and the liquidus surface of (γFe) and of (C)gr which are shown in Fig. 3. Two upper critical points c_1 and c_2 were identified on the liquid surface. The c_1 point at the graphite side is at about 2000°C (extrapolated value) at 57.5 mass% Cu (49.8 at.%) and 2.34 mass% C (10.7 at.% C). The c_2 point at the austenite side is at 1425°C and at 50.1 mass% Cu (46.9 at.%) and 0.008 mass% C (0.04 at.%). [1936Mad] gives the temperature and composition of c_2 as 1430°C and 50 mass% Cu, < 0.1 mass% C, which confirm the data of [1991Sch2]. The liquidus surfaces in the Fe corner calculated by [1991Sch2] and [1990Gus] agree very well.

The primary crystallization fields of (Cu) and (γFe) in the Cu rich corner are practically merged with the Cu-Fe edge and were not investigated. A schematic sketch of the liquidus surface for the whole system is shown in Fig. 4 with exaggerated solubility.

Metastable Liquidus Surface

The liquidus surface of the metastable Cu-Fe-Fe_3C is not constructed. A schematic sketch of the liquidus surfaces at the Fe rich and Cu rich sides were presented by [1991Sch1, 1991Sch2] and shown in Figs. 5a, 5b. The (γFe) and (Cu) liquidus surfaces are retained in the metastable system as well as the stable position of the double saturation line, L′ + L′′ + (γFe), with the critical point c_2. The miscibility gap is arranged on both sides of the quasibinary Fe_3C-Cu system (dash-dot lines in Figs. 5a, 5b) and so it extends wider at higher carbon content compared with the miscibility gap in the stable system, that is cut off by graphite saturation.

The projections of the eutectoid lines in the Fe corner of the C-Cu-Fe system for stable and metastable conditions are shown in Figs. 6 and 7.

Isothermal Sections

The isothermal sections at 1600, 1400 and 1180°C constructed by [1979Cha] based on [1959Per, 1961Sch] for 1600°C and on [1965Loe, 1975Mor] for 1400 and 1180°C are presented in Figs. 8, 9 and 10. The small correction was made at the binary sides according to the accepted C-Fe and Cu-Fe systems. Figure 11 shows the calculated solubility of graphite and copper in (γFe) at the temperatures between 750 and 1050°C

DOI: 10.1007/978-3-540-74196-1_4

[1990Gus]. The calculated solubility of graphite is in good agreement with the data by [1975Mos] but not so well with the data by [1979Par]. The experimental data by [1979Par] indicate a strong effect of Cu on the carbon activity in the (γFe) phase which is not supported by the direct measurements by [1972Wil]. The isothermal sections in the regions of the eutectoid equilibrium at 726°C for the stable system and at 717°C for the metastable system constructed by [2003Sil] are sketched in Figs. 12 and 13, respectively. The dashed lines indicate the tie lines originating from the (γFe) phase point in the four-phase equilibrium.

Temperature – Composition Sections

The calculated vertical section at 4.5 mass% C is shown in Fig. 14, after [1990Gus] with some correction of the monotectic invariant temperature according to [1991Sch2]. The partial vertical section showing the equilibria between 50Cu/50Fe and graphite (mass%) developed by [1979Cha] is presented in Fig. 15. The invariant temperatures were corrected in accordance with [1991Sch2].

Thermodynamics

From a review of the thermodynamic aspects [1959Per] commented that dissolved copper displaced carbon from liquid iron in equilibrium with graphite, in agreement with the slope of the liquidus isotherms of (C)gr shown in Fig. 3. The same effect of copper additions on carbon solubility in liquid iron was observed in the temperature range of 1200 to 1500°C by [1956Kor, 1961Sch, 1960Mor, 1960Fuw, 1986Zhu]. It was found to decrease linearly with increasing copper content for all temperatures studied. The solubility of carbon in the Cu-Fe melts in the region up to 3.8 mass% Cu at 1550°C was calculated by [2001Ma], using the first order interaction parameters and the activity coefficients at infinite dilution taken from literature data. Comparison of the calculated and experimental results of [1959Neu] showed that the approach developed by [2001Ma] is reliable for thermodynamic analysis of these melts. Based on the determination of carbon solubility in Cu-Fe alloys with ≤ 5.39 at.% Cu within the temperature range 1500 to 1600°C, [1983Jan1, 1983Jan2] evaluated the parameters of the carbon solubility variation.

The activity coefficients of the components of the C-Cu-Fe system were calculated by [1956Kor, 1970Bel, 1978Uhr, 1983Pen, 2000Hug]. The activity coefficient of copper in graphite-saturated iron at 1600°C according to [1956Kor] decreases with increasing copper content. In the dilute (as to copper) graphite-saturated ternary solution it was found to be 16.8. In a good agreement with this is the value of 16.4, obtained for the same temperature by [1975Cho] using the data from mass spectrometry of liquid alloys saturated with carbon at 1600°C. The activity coefficient of iron is 0.69±0.05 at this temperature [1975Cho]. It decreases with the increasing carbon content in the melt at 1550°C according to the calculation of [1983Pen]. By this calculation the experimental data of [1961Sch] regarding the slope of the curves describing carbon solubility in the C-Cu-Fe melt in the temperature range of 1200 to 1600°C were confirmed. The estimation of the first and the second order interaction parameters, parameters of free energy, enthalpy at constant activity as well as the partial molar heat of mixing of carbon affected by copper additions was made by [1983Pen].

The activity of copper in the C-Fe alloys was measured by [2000Hug] using method of distribution of copper between molten silver and C-Fe melts. Under infinite dilution, the copper activity coefficient in graphite-saturated iron at 1550°C was found to be 28.5. The dependence of the copper activity coefficient on temperature in the graphite-saturated iron melt was determined as $\ln\gamma_{Cu}^{0(Fe\text{-}C)} = 1.11 + 4100/T$ and in the alloy with 2 mass% C as $\ln\gamma_{Cu}^{0(Fe\text{-}C)} = 0.72 + 3840/T$. The activity coefficient of copper increases with increasing carbon concentration in the melt and decreasing copper content.

The thermodynamic properties of C-Cu-Fe dilute liquid alloys of system at 1600°C were compiled and evaluated by [1974Sig]. The first-order free energy interaction coefficients for the C-Cu-Fe melts at 1600°C showing the effect of copper on solubility of carbon in the melt and *vice versa* are 0.066 and –0.06, respectively (the composition was expressed in mass%).

[1979Cha] compiled thermodynamic information for the C-Cu-Fe alloys in the solid state using data of [1971Gre, 1972Wil, 1975Mos]. According to [1971Gre] additions of copper slightly increase the activity of carbon in austenitic alloys at 1050°C. By the method of equilibration of graphite with Cu-Fe strips

DOI: 10.1007/978-3-540-74196-1_4

and pure iron strips at 850, 925 and 1050°C [1972Wil] determined the carbon content in the C-Cu-Fe specimens up to 6.74 mass% Cu. The carbon activity calculated based on these results was found to increase with increasing copper concentration. Using gas mixtures of the H_2-H_2O-CO-CO_2-CH_4 type of controlled composition the copper effect on carbon activity in austenite containing up to 7.4 mass% Cu was determined by the method of dynamic equilibrium in the temperature range of 950 to 1100°C by [1975Mos]. Again, it was shown that copper increases the carbon activity both in dilute carbon solutions and concentrated carbon solutions close to saturated. The copper effect was explained by increasing partial enthalpy of carbon in the C-Cu-Fe system. The activity coefficient of carbon was shown to be almost independent of carbon concentration.

An attempt to consider the effect of small amounts of carbon on the C-Cu-Fe liquid phase using the thermodynamic analysis was made in [1976Wag]. When the dependence of liquidus temperature on concentration is small it indicates considerable positive deviations from ideal solution; in case of the C-Cu-Fe system somewhat larger amounts of carbon result in the formation of two liquid phases.

Based on an analysis of the experimental data on the carbon activity the parameters describing the interaction between copper and carbon in the C-Cu-Fe system were evaluated by [1977Uhr]. The parameter values calculated depend linearly on temperature within the range of 850 to 1050°C for this system. Using thermodynamic models, [1996Fri] assessed and analyzed the molar volumes of solid and liquid phases in the C-Cu-Fe system. The available experimental data permitted an evaluation of the temperature and composition dependence of the molar volumes of the various phases in limited ranges of the C-Cu-Fe system. Good agreement between experiments and calculations was obtained.

Notes on Materials Properties and Applications

The copper containing low carbon steels are attractive for application in heavy engineering for excellent combination of good toughness, strength, weldability and corrosion resistance. [2000Hsi] studied the effect of cooling treatment on the transformation of austenite and of subsequent isothermal aging on the precipitation of copper particles in the industrial steel, NAK80, containing 1.08 Cu, 0.13 C, 0.58 Si, 3.09Ni, 0.33 Cr, 0.26 Mo, 0.83 Al (mass%). It was found that depending on the cooling rate (very slow, about 0.05°C·s^{-1}, or ranging from 30 to 0.3°C·s^{-1}) the steel can transform to bainite completely or gives a mixture of martensite and bainite, respectively. After annealing at 900°C for 15 min followed by cooling with rates of 120, 5 and 1°C·s^{-1}, the specimens consisted of 100% martensite, 58% martensite+42% bainite and 42% martensite+58% bainite, respectively. The hardness of the first specimen was found to be the lowest. In contrast, the two others, being aged at 400 and 500°C, demonstrated practically the same value of hardness, significantly higher than the first one. [2000Kre] studied the copper effect on the structure and mechanical properties of cast irons containing in addition to copper (0.02 to 0.78 mass%) the following elements (in mass%) 2.90 to 3.43 C, 1.60 to 2.65 Si, 0.06 to 0.33 Mn and 0.010 to 0.085 Mg. Copper was found to promote formation of the pearlite fraction in the eutectoid composition. Alloys with 0.78% Cu and 3.3% C are characterized by a completely fine pearlite matrix that results in increasing tensile strength up to 1000 MPa and yield strength up to 550 MPa. [2003Des], taking into account a wide industrial application of high strength low alloy steels, compared the precipitation kinetics and mechanical properties of the Cu-Fe binary alloy with those of the low carbon (0.065 mass%) steel containing, except the same quantity of copper (0.78 mass%), some additions of other elements, the most of which was manganese about 0.35 mass%. The precipitation kinetics during aging at 500°C was shown to be qualitatively identical for both samples. The effect of precipitates on the mechanical properties is also similar. Whereas the precipitate growth was much faster in the steel, maximum of changing in hardness (or yield stress) with time was much smaller here. However in absolute value the steel had a higher strength, 300MPa, (Cu-Fe alloy 170 MPa), that was attributed to the presence of carbon and manganese in the steel.

The studies of [2005Wan, 2004Bat] concern the effect of copper on microstructure of industrial steels both sintered and isothermally transformed, their mechanical properties and mechanism of phase transformations in them. In [2005Wan] the effect of copper on the microstructure and microhardness of the carbon compacts sintered at 1140°C, containing 0.4 to 0.6 mass% C and 2 to 8 mass% Cu was investigated. It was found that increasing copper content resulted in refining of ferrite, in decreasing of its volume fraction and in strengthening of the ferrite and pearlite phases. The C-Cu-Fe system is a basis of the C-Cu-Fe-P quaternary system that is now of a great interest for structural applications.

DOI: 10.1007/978-3-540-74196-1_4

The effect of tempering temperature (270, 330 and 380°C) and time (30 to 150 min) on the tensile properties and the correlation of the properties with structural constituents of the commercial foundry alloy, containing 0.6 mass% Cu, which was the most among the other alloying metals (0.22 Mn, 0.05 Cr, 0.06 Ni, 0.04 Ti, 0.03 Mo, 0.0079 Sn) as well as 3.48 mass% C and 2.028 mass% Si was studied by [2004Bat]. The 0.2% proof stress and ultimate tensile strength were found to decrease while the elongation and quality index increased monotonically with increasing tempering temperature from 270 to 380°C. Comparison of the values obtained with standards for austenite red ductile iron showed that majority of them were close, except those obtained for tempering time less than 30 min.

[1968Wil] estimated the mechanical properties of C-Cu-Fe alloys with up to 6 mass% Cu and 0.015 mass% C as well with 8.5 mass% Cr and 1.5 mass% Ni after quenching or air-cooled from 1050°C and subsequent aging at 485°C for 0.1 to 100 h. Massive ferrite and massive martensite structures were obtained depending on composition and cooling rate. The precipitation occurred in the form of spheres and rods, and the precipitate was identified as the copper rich phase (Cu). The ultimate tensile strength of the alloys was considerably less than that to be expected from the hardness data. This is thought to be due to the low rate of work hardening of the alloys. On aging embrittlement occurs with intergranular fracture. This is thought to be due to the segregation of copper to grain boundaries.

[1987Sak, 1988Sak] studied the effect of copper (0 to 60 mass%) on the electrical resistivity of the C-Cu-Fe melts containing 2 or 0.5 mass% C in the temperature range 1200 to 1600°C. The polytherms $\rho(T)$ demonstrated a sharp bend, the temperature of what was attributed to onset of the melt stratification. With increasing copper content this temperature was shifted to the higher temperature region. The temperature coefficient of the electrical resistivity for immiscible melt is higher. In the alloy with 0.5 mass% C the stratification took place at $\geq$ 40 mass% Cu, while in the alloys with 2 mass% C it started at 12 mass% Cu.

[2005Oki] investigated the thermal conductivity of a functionally graded C-Cu-Fe alloy prepared by liquid phase sintering and the subsequent carburization. The microstructure model in which ellipsoidal copper particles are embedded in the iron matrix was employed. The thermal conductivity of the studied alloy was improved by about 20% owing to the graded structure. These alloys may find an application for automobile valve sheets.

[2005Car, 2004Cor] studied the phases and their properties of C-Cu-Fe nanocomposites produced by high energy milling of the powder mixture of 22.5 mass% Fe, 1.6 mass% C, bal. Cu, followed by annealing at 600°C. [2004Cor] found the carbide phase with the Fe_3C crystal structure in a copper matrix after annealing. Hardness of as-milled powders was about 507 VHN. The cementite phase with grains sized from 10 to 50 nm after milling and from 30 to 160 nm after annealing as well as the disperse copper nanoparticles (5 to 10 nm) in cementite were determined by [2005Car] using TEM. A higher growth of carbide phase than copper was attributed to minor mutual solubility of the components, Cu and Fe_3C, and quite low diffusivity. This contributed in increasing of the copper thermal stability.

Taking into account the problem of processing of the steel scraps, containing copper the study of isothermal oxidation and step-oxidation in air at 980, 1120 and 1220°C of the steels with 0.16-0.30 mass% Cu among other residual elements (Ni, Mn, Al, Sn, Cr, P, S, N) was undertaken by [2005Che] with the aim to find out the way to prevent the surface hot shortness. It was shown that at 980°C the copper additions in steel increase oxidation resistance, while at 1120°C reduce it. At 1220°C the effect of copper is minor.

The technological properties of steels were investigated by [1938And, 1977Maj1, 1977Maj2, 1998Tan]. According to [1938And] fluidity of the steels with 0.2 and 0.4 mass% C, Cu up to 5 mass%, about 0.4 mass% Si and 0.7 mass% Mn increases only very slightly with copper content at temperatures of 50°C above the liquidus. [1977Maj1] investigated the difference between the hardenability of the normal wrought steel and that of the sintered steel using the continuous cooling transformation diagram of the eutectoid carbon steel practically free from impurities. The critical cooling rate of the normal wrought Fe-0.77% C -6.5% Cu with 0.75% Mn and 0.2% Si (mass%) was 150°C·s^{-1}, while it was 900°C·s^{-1} in the case of steel practically free from impurities. Using mixed powder compacts of the Fe-8% Cu -C (up to 1.5 % graphite), and Fe-Cu-1% C (up to 12% Cu) (mass%) [1977Maj2] studied the effect of graphite content on the elimination of the abnormal expansion during the heating process. The maximum expansion was observed at temperature slightly higher than 1090°C and decreased at higher temperatures. [1998Tan] measured the wettability of graphite substrate by carbon saturated Cu-Fe melts using the sessile drop method. The segregation of copper both at the interface between the liquid alloy and graphite substrate and at the surface of the

DOI: 10.1007/978-3-540-74196-1_4

liquid alloy caused by the surface activity of copper was thought to result in decreasing of the work of adhesion and, correlating with it, the decreasing carbon solubility when the copper content increases in the melt.

Miscellaneous

The copper addition of 1 mass% accelerates the process of decarburization of iron melts at 1560 to 1650°C substantially as found by [1974Ela]. [1975Sil] proposed to determine the degree of metastability of the cementite phase in the ternary iron systems by an estimation of an influence of the alloying element on mutual solubility of the stable and metastable phases of the C-Fe system, analyzing and calculating a change in the free energy values of the phases. As copper increases the solubility of cementite in austenite and decreases the solubility of graphite in austenite, it was concluded that copper promotes metastability of cementite.
[1968Rep] studied the particular exfoliation of Cu in surplus and eutectic austenite of iron-cast alloys. They established that the exfoliation effects were connected with the structure transformations at the formation and dissociation of austenite, carburization of eutectoid graphite and other transformation which determine the structure and properties of alloys.
[1954Lan] proposed to add in melts different sulphides (Cu_2S, Ni_2S, Na_2S) in order to remove residual-copper content in scrap since this improves hot working of some steel.
[1970Lan] studied transfer processes and phase boundary reactions during the carbon exchange between the carbon containing gas phase and solid Cu-Fe alloy with 4 at.% Cu at 900 to 1000°C in H_2-CH_4 mixtures. The diffusion coefficient, transition coefficient and the Biot index were determined.
The Snoek peak of internal friction of the Fe-0.21C-0.2 Cu (mass%) alloy, neutron-irradiated at 330 to 341°C, was measured by [1978Yam]. It was shown that the resolution temperature of carbon atoms in the neutron-irradiated alloy is about 400°C, but that in the unirradiated alloy is about 200°C.
The kinetics of the isothermal transformation of austenite to bainite and to pearlite were studied by a number of investigators [1990Rey, 1995Fou, 1997Lac, 1997Fou, 2000Cha1, 2000Cha2] and generalized by [2004Aar]. [1990Rey] established that the pearlite reaction was particularly competitive with the bainite reaction in high purity Fe-0.41C-3.01Cu (mass%) alloy after austenitization at 1300°C and annealing at 450, 500 and 550°C. Using TEM [1990Rey] showed also that bainite precipitation initiated at austenite grain boundaries and cementite precipitation was observed both within and between the ferrite plates. [1995Fou] investigated the isothermal pearlitic transformation in medium or high carbon copper steels and established that the decomposition of austenite leads apart from the formation of proeutectoid phases and pearlite, to the precipitation of the (Cu) phase. According to TEM and SEM examinations the (Cu) precipitation occurs within proeutectoid ferrite (medium carbon steels), within grain boundary proeutectoid cementite (high carbon steels) and both pearlite ferrite and cementite. [1997Fou] designing the suitable tempering treatment (within the temperature range 200 to 400°C) of hypereutectoid copper steel (2.73 mass% Cu) after its austenitization at 1050°C observed copper precipitations within supersaturated in copper bainitic ferrite and bainitic cementite. According to [1997Fou] the process of bainitic formation (both the constituents) is controlled by shear mechanism. The appearance of abnormal ferrite in hypereutectoid carbon steels alloyed with copper after their austenitization at 1150°C for 30 min followed by isothermal transformation at 670 to 710°C for 72 to 240 h was investigated by [2000Cha1]. The abnormal ferrite was found to be not due to alloying but to be a characteristic microstructural constituent of the hypereutectoid steels at transformation temperature. The amount of it was higher when the transformation temperature was closer to eutectoid. It forms on the proeutectoid cementite by coarsening. [2000Cha2] proceeded the investigation of the objects of [2000Cha1], which underwent the same heat treatment, characterizing the morphology of the copper precipitations both within pearlite and abnormal ferrite by TEM. [1997Lac] investigated the effect of various additions of Cu and Mn and the cooling rate on the temperature of the onset of stable and metastable eutectoid reactions. A description of the conditions for growth of ferrite and of pearlite is given and shows that these reactions can develop only when the temperature of alloy is below the lower boundary of the ferrite/austenite/graphite or ferrite/austenite/cementite related three-phase field.
The secondary precipitation in C-Cu-Fe alloys were investigated by [1983Sch, 2004Gag, 1973Jeg]. Using Mössbauer spectroscopy [1983Sch] investigated the formation of carbide precipitations in Cu matrix of C-Cu-Fe alloys with low Fe concentration. It was found that repeated melting and holding for up to 2 weeks

DOI: 10.1007/978-3-540-74196-1_4

in graphite crucibles under vacuum did not result in the formation of carbides. Only after remelting in a graphite crucible in H_2 atmosphere did carburization of the alloy occur. The structural transformations of C-Fe precipitates observed after annealing at 400 to 800°C for 25 h are in agreement with the phase diagram. The nucleation and growth of Cu precipitates in ferrite for low carbon steels were studied by [2004Gag] in samples cooled directly to the desired aging temperature from austenitizing temperature. The maximum nucleation and growth rates for Cu were determined to be $8.0 \cdot 10^{21}$ nuclei$\cdot m^{-3} \cdot s^{-1}$ at 612°C and 0.12 nm$\cdot s^{-1}$ at 682°C, respectively. TEM analysis for isothermal aging at 550°C showed that the average Cu precipitate sizes for low-C Cu steels were comparable for all aging times. [1973Jeg] showed that when the third component (for example, Cu) is insoluble in cementite in the ternary Fe-Fe_3C-Cu system two-phase aggregate of ferrite and carbide from austenite form instead of single-phase secondary cementite.

The improvement of the quality of powder during sintering was examined by [1995Bar, 1995Han, 2001Ped] based on the analysis of the physicochemical properties of the melt and the structure of solid metal revealed the effect of the temperature on the pattern of existence of carbon in liquid iron on heating and cooling. The results showed that the lack of uniformity of carbon concentration causes the solution-reprecipitation phenomena leading to the rearrangement of particles and the shrinkage or the suppressed expansion of compacts. Taking into account that the metal matrix composites with graphite are important as frictional materials [2001Ped] studied those containing more graphite (up to 32 mass%) than it was done previously (≤10 mass%). Except graphite powder, the alumina powder, iron fibres, Fe+0.6P powder and bronze powder were included in the eight various compositions studied by dilatometric analysis with the aim to determine the effect of graphite on the expansion of the compacts. The expansion was observed during sintering at the temperature below 500°C. Its degree was linearly dependent on graphite content. [1974Ang] proposed to use mixtures of elemental and Cu-Fe prealloyed powders to improve dimensional stability of C-Cu-Fe compacts. The compacts were presintered for 6 min at 650°C, cooled to room temperature and sintered for 30 min at 1120°C in an atmosphere of 40% H_2, 40% N_2 and 20 % CO.

Introduction of graphite to Cu-Fe powders is a way for both reducing volume growth of the compacts and increasing strength of the sintered materials. Studies of the mechanism of swelling and explanation of the phenomenon are varied. Discussing the numerous views on the problem and analyzing their own experimental data [1999Kur] came to conclusion that the difference in concentration of carbon in iron particles leads to increasing driving force. Under their influence the liquid copper forms a semi-permeable layer preventing carbon atoms from diffusing and allowing iron atoms to be transported between particles. The latter was thought to enhance sintering and to control the process of copper-growth. According to [1985Jam] the extent of the volume after sintering is a result of the liquid copper penetration into particle boundaries and pores inside iron grains. The effect of carbon is in concentrating of copper at the grain corners by increasing of dihedral angle. Additions of graphite (≤1 mass%) to the 10Cu -Fe (mass%) mixtures pressed at 141 to 680 MPa and then sintered at 1140°C for 60 min was shown by [1985Jam] to reduce the degree of the volume growth of the compacts the stronger the more carbon was added. As the copper content in iron was not decreased on addition of carbon it was suggested that carbon affects the kinetics of copper dissolution inside iron grains. [2002Liu] applied the three-dimensional Monte Carlo model to simulate the microstructure characteristics of sintering process in the C-Cu-Fe powder compacts and based on results obtained showed why addition of carbon to Cu-Fe powder prevents the volume expansion. They concluded that carbon promotes lowering of the grain boundary energy of iron and is a cause for increasing of the dihedral angle at the grain boundaries.

[1980Ost] investigated the copper solubility in ferrite and eutectoid cementite of gray iron and constructed the curves of the distribution copper in these phases.

The evaporation rate of Cu in molten C-Fe alloys were investigated under pressures of several hundred Pa in the temperature range from 1500 to 1600°C by [1995Che] and under pressure of 133 Pa at 1700°C by [2003Ono]. It was shown that the apparent rate constant of copper evaporation monotonically increases with increasing carbon content and with decreasing pressure.

[2004Wan] investigated the effect of C on the macroscopic morphologies in Cu-Fe alloys and established that the core-type macroscopic morphology is formed by the addition of C due to the stable miscibility gap in the liquid phase in the C-Cu-Fe system.

DOI: 10.1007/978-3-540-74196-1_4

Table 1. Investigations of the C-Cu-Fe Phase Relations, Structures and Thermodynamics

Reference	Method/Experimental Technique	Temperature/Composition/Phase Range Studied
[1926Ish]	Theoretical consideration and experimental data. Thermal analysis, light microscopy, Expansion-temperature, magnetic analysis. Independence of temperature. The alloys were melted in alumina tubes in kryptol furnace. Cast-iron saturated with gas carbon and electrolytic copper.	The Fe-Fe_3C-Cu system. From 1500 to 670°C, Fe corner (0 to 5 C and 0 to 30 Cu, mass%). Metastable liquidus and liquidus contours for metastable liquidus surface. Quasibinary Fe_3C-Cu system.
[1936Mad]	Thermal analysis, light microscopy, chemical analysis of layers. Armko Fe and electrolitic Cu. The alloys were melted in a vertical molybdenum-wire furnace in an atmosphere of cracked ammonia.	Alloys with 50 mass% Cu and Fe and from 0.05 to 2.0 mass% C. Stable C-Cu-Fe diagram, miscibility gap, the compositions of two liquid layers at 1150°C (invariant monotectic equilibrium), temperature and constitution of critical point on the miscibility curve.
[1938Iwa]	Method of quenching the melt in ice water after heating at different temperature over liquidus and investigation of structure under light microscopy. Tammann carbon resistance furnace, electrolytic Fe and Cu, master alloy with 4.25 mass% C and graphite powder.	Isothermal equilibria of two liquids at 1450 and 1540°C in Fe corner at 0 to 4 mass% C and 0 to 30 mass% Cu
[1956Kor]	The method of copper distribution between liquid silver and the C-Fe melts. Calculation of the activity coefficient of Cu in liquid Fe	Solubility of copper up to 3 at.% and graphite in liquid iron at 1600°C
[1959Neu]	Experiment and thermodynamic calculation	Solubility of carbon at 0 to 7 mass% Cu and 1600°C
[1959Per]	Experiment with use chill-cast alloys and thermodynamic calculation	Tie-lines at 1550 and 1500°C for miscibility gap. Activity of carbon and copper in liquid iron.
[1959Sim]	not quoted by [1979Cha]	Solubility of graphite in C-Cu-Fe melts at 1490 and 1300°C
[1960Mor]	Thermodynamic calculation of the activity coefficient of carbon in C-Cu-Fe solution	Solubility of copper and carbon in liquid iron at 1550°C
[1960Fuw]	Thermodynamic calculation	Solubility of copper and carbon in liquid iron at 1450°C

(*continued*)

DOI: 10.1007/978-3-540-74196-1_4

Reference	Method/Experimental Technique	Temperature/Composition/Phase Range Studied
[1961Sch]	Chemical analysis of probe after casting into permanent mould with thin walls. Pure Fe and Cu were melted in graphite crucibles in electrical furnace in Ag atmosphere and kept at different temperatures. Thermodynamic calculation	Solubility of copper and carbon (graphite) in liquid iron at 1200, 1300, 1400 and 1500°C
[1961She]	Chemical analysis of quenched probes. Electrolytic Cu and cast-iron, produced by graphite saturation of steel were melted in graphite crucibles in cryptole furnace. The contents of steel: 0.12% C, 0.55% Mn, 0.15% Si, 0.04% P and S (mass%)	Solubility of Cu in cast-iron at 1300, 1350 and 1400°C
[1965Loe]	Thermal analysis, light microscopy, chemical analysis of quenched probe. Carbon iron, high purity graphite, electrolytic Cu.	Stable and metastable C-Cu-Fe phase diagram. Vertical sections at compositions 2 to 4.5 mass% C and 0 to 8 mass% Cu. Reaction Scheme. Stable liquidus. Temperatures and constitutions of invariant equilibria in stable and metastable systems.
[1970Bel]	Measurements of the activity of Cu in Fe rich C-Cu-Fe alloys using the Knudsen cell-mass spectrometer.	Determination of copper and carbon solubility in liquid iron at 1600°C
[1971Gre]	Measurement of carbon content using Woesthoff conductimetric apparatus with methane-hydrogen mixtures.	Determination of carbon solubility in Fe alloy with 1.91 mass% Cu at 1050°C and calculation of the interaction parameter.
[1972Wil]	Chemical analysis of carbon content and calculation of carbon activity in (γFe) phase. Pure iron-copper strip and metastable iron carbide as a carbon source placed in the sealed tubes were heated in furnace from 24 h at 1050°C to 7 d at 850°C, then the tubes were quenched to room temperature.	Fe-alloys with 0.72, 1.36, 3.13, 5.61, 6.74 mass% Cu and 0.2 to 1.5 mass% C. Measurements at 850, 925 and 1050°C.
[1975Cho]	The Knudsen cell-mass spectrometer for measurements of the activity of Cu in Fe rich C-Cu-Fe alloys. Alloys were prepared by melting together Cu (99.99% pure) and eutectic composition C-Fe prepared from Fe (99.99% pure) and high purity C. Carbon saturation was ensured by holding at 1660°C for 15 min.	Isotherm at 1600°C. The thermodynamic properties of liquid alloys saturated with graphite.
[1975Lar]	DTA, microprobe analysis, quantitative metallography, light microscopy, microhardness measurements, calculation.	Fe corner of C-Cu-Fe system. The alloys with 0.5 to 4 mass% Cu and 0.2 and 0.4 mass% C.

(*continued*)

DOI: 10.1007/978-3-540-74196-1_4

Reference	Method/Experimental Technique	Temperature/Composition/Phase Range Studied
	The samples were prepared from mixtures of elemental powders sintered at 1100°C in dry hydrogen. Then homogenization in pure Ar at 1250°C for 100 h, cooling with furnace and heat treatment for 16 h at different temperatures in (αFe) + (γFe) range.	The equation for the determination of solubility of Cu in (γFe) at eutectoid temperature. The temperature and constitution of eutectoid reaction.
[1975Mos]	Chemical analysis for determination of equilibrium carbon concentrations in the alloys. Dynamic method for equilibration of alloys with gas mixtures of type H_2-H_2O-CO-CO_2-CH_4	Alloys with Cu contents from 1.95 to 7.4 mass%. Calculation of carbon activity at 950, 1000, 1050, 1100°C.
[1976Maj] [1977Maj2]	DTA with the heating and cooling rates 5 $K \cdot min^{-1}$ after isothermal sintering. The powders of Fe, Cu, graphite were compacted at pressure of 588 MPa.	Alloys Fe-8 mass% Cu-C with up to 1.5 mass% C and Fe-Cu-1 mass% C with up to12 mass% Cu. The temperature of transition invariant reaction
[1977Uhr]	Thermodynamic calculation based on a model of interstitial solution	Optimization at 850, 925, 1050°C
[1978Uhr]	Thermodynamic calculation	Isothermal sections in the temperature region 600 to 1100°C in Fe corner with 0 to 2.4 mass % C and 0 to 8 mass% Cu
[1979Par]	DTA with cooling and heating rates of 0.5 to 3°C·min^{-1}, EMPA, light microscopy. The mixed powder were pressed and then held in a graphite crucibles at different temperatures above liquidus for different times.	Fe rich corner at 0 to 24 mass% Cu and 0 to 5 mass% C. Isothermal section at 950, 1000, 1150, 1155, 1172, 1200, 1400, 1450°C. Temperatures and constitutions of two invariant equilibria.
[1983Jan1] [1983Jan2]	Holding liquid alloys in graphite crucible inserted into a Tamman furnace, quenching and chemical analysis. Equations for calculation of carbon solubility	Solubility of C in liquid Cu-Fe alloys with ≤5.39 at.% Cu at 1500 and 1600°C. Construction of isolines of carbon activity
[1983Pen]	Experiment and thermodynamic calculation	Solubility of C and the activity coefficient of Cu and Fe in C-Cu-Fe melts with (4.8 to 5.3) mass% C and (0 to 4) mass% Cu at 1550°C
[1986Sch]	DTA, method of saturated melts	Fe corner at 0 to 20 mass% Cu and 0 to 6 mass% C. Liquidus surface
[1986Zhu]	Experiment and thermodynamic calculation	Carbon solubility, 0 to $1.6 \cdot 10^{-2}$ at.% Cu, 1500 to 1600°C
[1987Sak] [1988Sak]	Measurement of the electrical resistivity optical microscopy after quenching from liquid state	The temperature dependence of electrical resistivity of Fe-(2 to 90) Cu-0.5C (mass%) at 1350 to 1550°C

(*continued*)

DOI: 10.1007/978-3-540-74196-1_4

Reference	Method/Experimental Technique	Temperature/Composition/Phase Range Studied
[1987Sch]	Thermodynamic calculation	Liquidus surface
[1991Sch1]	Theoretical idea about a construction of C-Cu-Fe system based on the known binary systems	Schematic equilibria in the stable C-Cu-Fe and metastable Fe-Cu-Fe_3C systems
[1991Sch2]	Chemical analysis of compositions of two liquid layers after exposition at certain temperatures and quenching. Tammann furnace, graphite crucibles, electrolytic Fe and Cu. Thermodynamic calculation	The liquidus surfaces with the miscibility gap and liquidus isotherms. The melting equilibria in stable and metastable systems.
[1996Fri]	Thermodynamic calculation	Recalculation of molar volumes of solid and liquid phases and their variation with composition and temperature
[1999Ama]	DTA with cooling and heating rates of 10 $K \cdot min^{-1}$, SEM, EPMA, light microscopy. Arc melting in Ag atmosphere from electrolytic Fe, pure Cu and C.	Fe rich alloys with up to 34 mass% Cu and 5 mass% C. The liquidus surface in stable system. The stable and metastable equilibria.
[2000Hug]	Method of distribution copper between liquid silver and C-Cu melts. Thermodynamic calculation of interaction parameters	The activity of copper in melt (0 to 25) mass% C-(0 to 25) mass% Cu-Fe, 1550°C
[2001Ma]	Thermodynamic calculation	Calculation of carbon in C-Cu-Fe melts with up to 3.8 mass% Cu at 1550°C
[2003Sil]	The calculation of the phase equilibria using of coefficients of interphase distribution of the elements.	The temperatures and constitutions of invariant equilibria in the stable and metastable systems in the solid state. Isothermal sections at 717, 726 and 900°C.

Table 2. Crystallographic Data of Solid Phases

Phase/ Temperature Range [°C]	Pearson Symbol/ Space Group/ Prototype	Lattice Parameters [pm]	Comments/References
(Cu) < 1084.62	*cF*4 $Fm\bar{3}m$ Cu		dissolves up to 5 at.% Fe at 1095°C [2007Tur] and up to 0.1 at.% C at ~1100°C [2004Lop]
		a = 361.46	at 25°C [Mas2]
(αFe) < 912	*cI*2 $Im\bar{3}m$ W	a = 286.65	at 25°C [Mas2] dissolves up to 1.6 at.% Cu at 847°C [2007Tur] and 0.096 at.% C at 740°C [1992Oka]

(*continued*)

DOI: 10.1007/978-3-540-74196-1_4

Phase/ Temperature Range [°C]	Pearson Symbol/ Space Group/ Prototype	Lattice Parameters [pm]	Comments/References
(δFe) 1538 - 1394	*cI*2 $Im\bar{3}m$ W	a = 293.15	[Mas2] dissolves up to 5.8 at.% Cu at 1487°C [2007Tur] and 0.4 at.% C at 1493°C [1992Oka]
(γFe) 1394 - 912	*cF*4 $Fm\bar{3}m$ Cu		dissolves ~13 at.% Cu at 1450°C [2007Tur] and 9.06 at.% C at 1153°C [1992Oka]
		a = 364.67	at 915°C [Mas2, V-C2]
(C)d	*cF*8 $Fd\bar{3}m$ C (diamond)	a = 356.69	at 25°C [Mas2]
(C)gr < 3827	*hP*4 $P6_3/mmc$ C (graphite)	 a = 246.12 c = 670.90	[Mas2, 1992Oka] at 25°C [Mas2, 1994Sub]
Fe_3C (metastable phase, cementite) ≲ 1252	*oP*16 *Pnma* Fe_3C	 a = 452.6 b = 508.7 c = 674.4	[Mas2, 1992Oka] [1992Oka]
Martensite (metastable phase)	*tI*4 *I*4/*mmm* -	a = 285.8 c = 293.5 a = 284.6 c = 301.1	at 2.69 at.% C [1992Oka] at 6.36 at.% C [1992Oka]

Table 3. Comparison of Type, Temperature and Composition of Phases of "Monotectic" Invariant Reaction in Stable C-Cu-Fe System

Reaction	T [°C]	Type	Phase	Composition (mass%)			Reference
				C	Cu	Fe	
L′+ L′′ ⇌ (C)gr+(γFe)	1184	U	L′ (γFe)	4.0 1.9	4.2 4.7	91.8 93.4	[1965Loe]
L′+ L′′ ⇌ (C)gr+(γFe)	1172	U	L′ (γFe)	4.0 1.6	3.7 7.3	92.3 91.1	[1979Par]
L′+ L′′ ⇌ (C)gr+(γFe)	1160	U	-	-	-	-	[1999Ama]
L′+ L′′ ⇌ (C)gr+(γFe)	1158	U	L′ (γFe)	4.015 -	3.956 -	92.029 -	[1991Sch2]

(*continued*)

DOI: 10.1007/978-3-540-74196-1_4

Reaction	T [°C]	Type	Phase	Composition (mass%)			Reference
				C	Cu	Fe	
L′+ L′′ ⇌ (C)gr+(γFe)	1165	U	L′	4.07	4.0	91.93	[1990Gus]
			(γFe)	1.83	5.06	93.11	calculation
L′ ⇌ L′′+(C)gr+(γFe)	1150.8	E	L′	4.09	4.05	91.86	Simplified
			(γFe)	1.67	3.96	94.37	calculation, extrapolation

Table 4. Invariant Equilibria

Reaction	T [°C]	Type	Phase	Composition (mass%)			Composition (at.%)		
				C	Cu	Fe	C	Cu	Fe
Stable									
L′+L′′⇌	1158 [3]	$U_{1(s)}$	L′ [3]	4.015	3.856	92.029	16.349	2.968	80.683
(γFe)+(C)gr			L′′ [3]	0.008	97.50	2.492	0.042	97.133	2.825
			(γFe) [1]	1.83	5.06	93.11	8.022	4.193	87.785
			(C)gr	100	0	00	100	0	0
L′′⇌(γFe)	~1095 [1]	$U_{2(s)}$	L′′	?	97.2	?	?	96.826	?
+(Cu)+(C)gr			(γFe)	1.61	4.55	93.84	7.107	3.797	89.096
			(Cu)	?	96.4	?	?	95.924	?
			(C)gr	100	0	0	100	0	0
(γFe)⇌(αFe)	726 [2]	$E_{1(s)}$	(γFe) [2]	0.64	1.24	98.12	2.912	1.066	96.021
+(Cu)+(C)gr			(αFe) [1]	0.016	0.8	99.184	0.074	0.703	99.222
			(Cu) [1]	?	99.6	?	?	99.545	?
			(C)gr	100	0	0	100	0	0
Metastable									
L′ ⇌ L′′	1134 [3]	$E_{1(m)}$	L′ [3]	4.28	3.28	92.44	17.271	2.502	80.227
+(γFe)			L′′ [3]	<0.008	98.34	~1.652	<0.042	98.083	~1.875
+Fe_3C			(γFe) [1]	2	4.65	93.35	8.712	3.829	87.459
			Fe_3C	6.689	0	93.311	25	0	75
L′′+ (γFe) ⇌	~1095 [1]	$U_{1(m)}$	L′′	?	97.3	?	?	96.939	?
(Cu)+Fe_3C			(γFe)	1.83	4.47	93.88	8.017	3.701	88.282
			(Cu)	?	96.4	?	?	95.924	?
			Fe_3C	6.689	0	93.311	25	0	75
(γFe) ⇌	717 [2]	$E_{2(m)}$	(γFe) [2]	0.83	1.1	98.07	3.751	0.94	95.31
(αFe)+(Cu)			(αFe) [1]	0.018	0.71	99.272	0.084	0.624	99.292
+Fe_3C			(Cu) [1]	?	99.6	?	?	99.545	?
			Fe_3C	6.689	0	93.311	25	0	75

[1] [1990Gus], [2] [2003Sil], [3] [1991Sch2]

DOI: 10.1007/978-3-540-74196-1_4

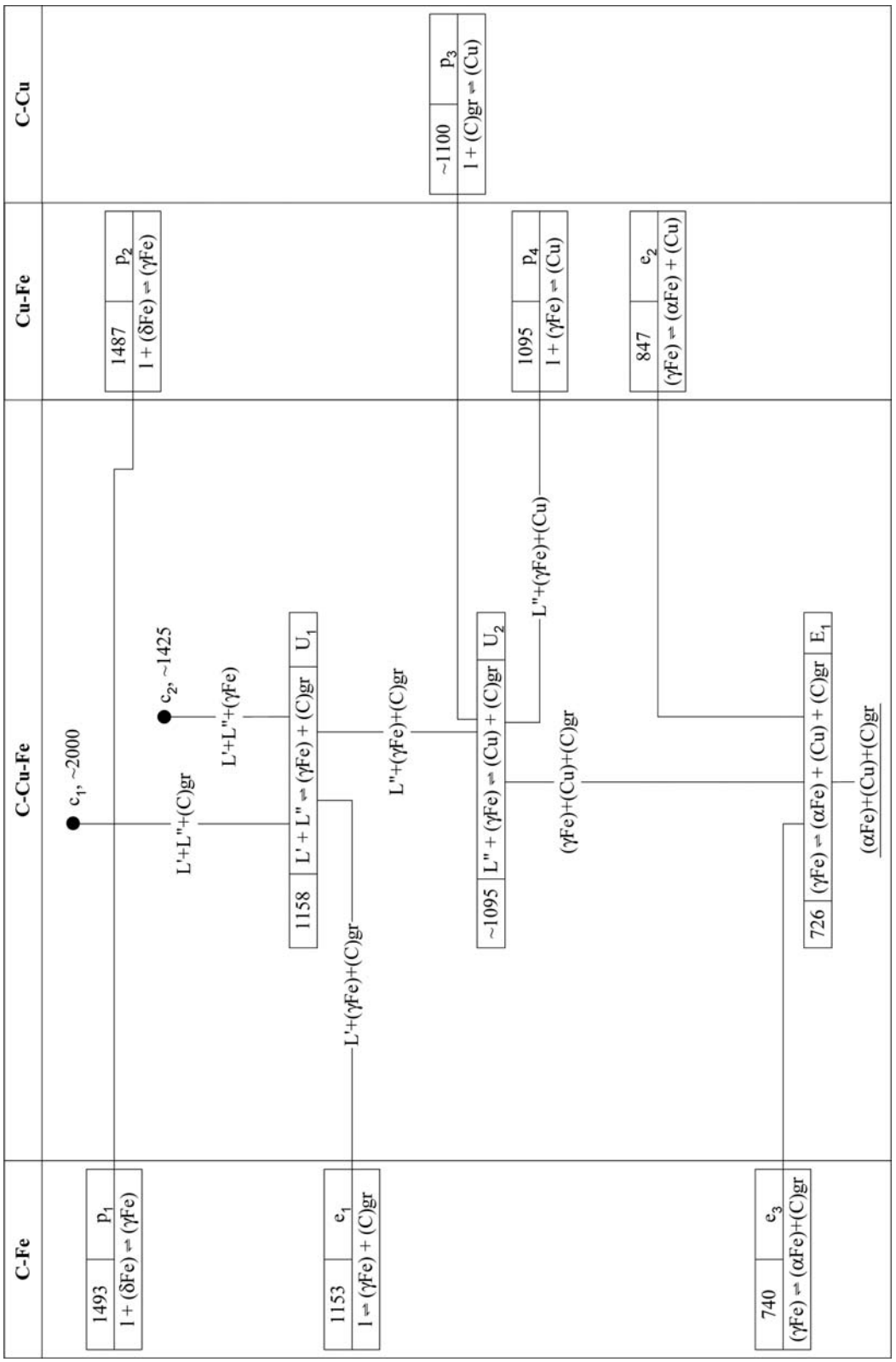

Fig. 1. C-Cu-Fe. Reaction scheme for the stable C-Cu-Fe system

DOI: 10.1007/978-3-540-74196-1_4

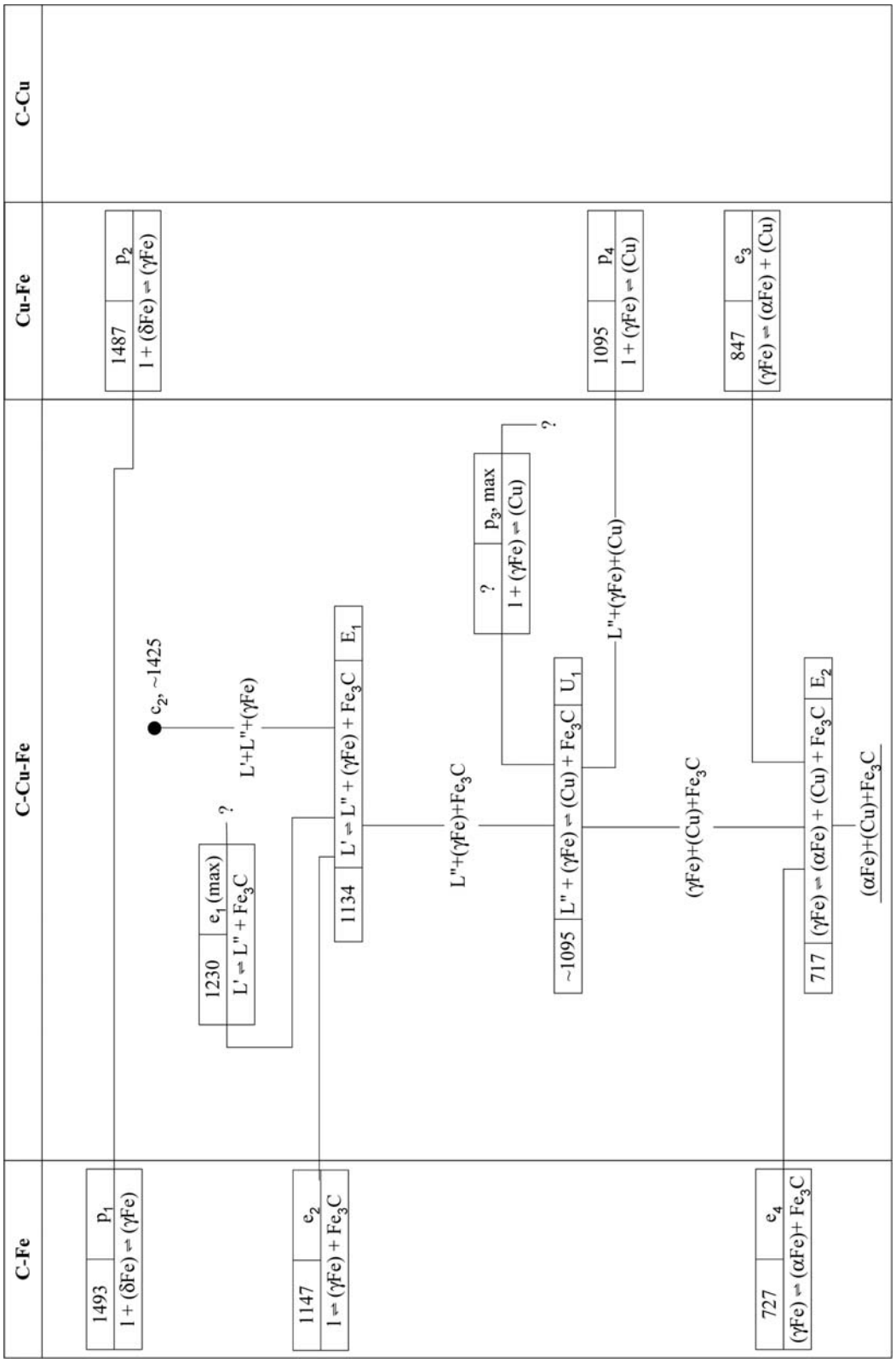

Fig. 2. C-Cu-Fe. Partial reaction scheme for the metastable Cu-Fe-Fe_3C phase diagram

DOI: 10.1007/978-3-540-74196-1_4

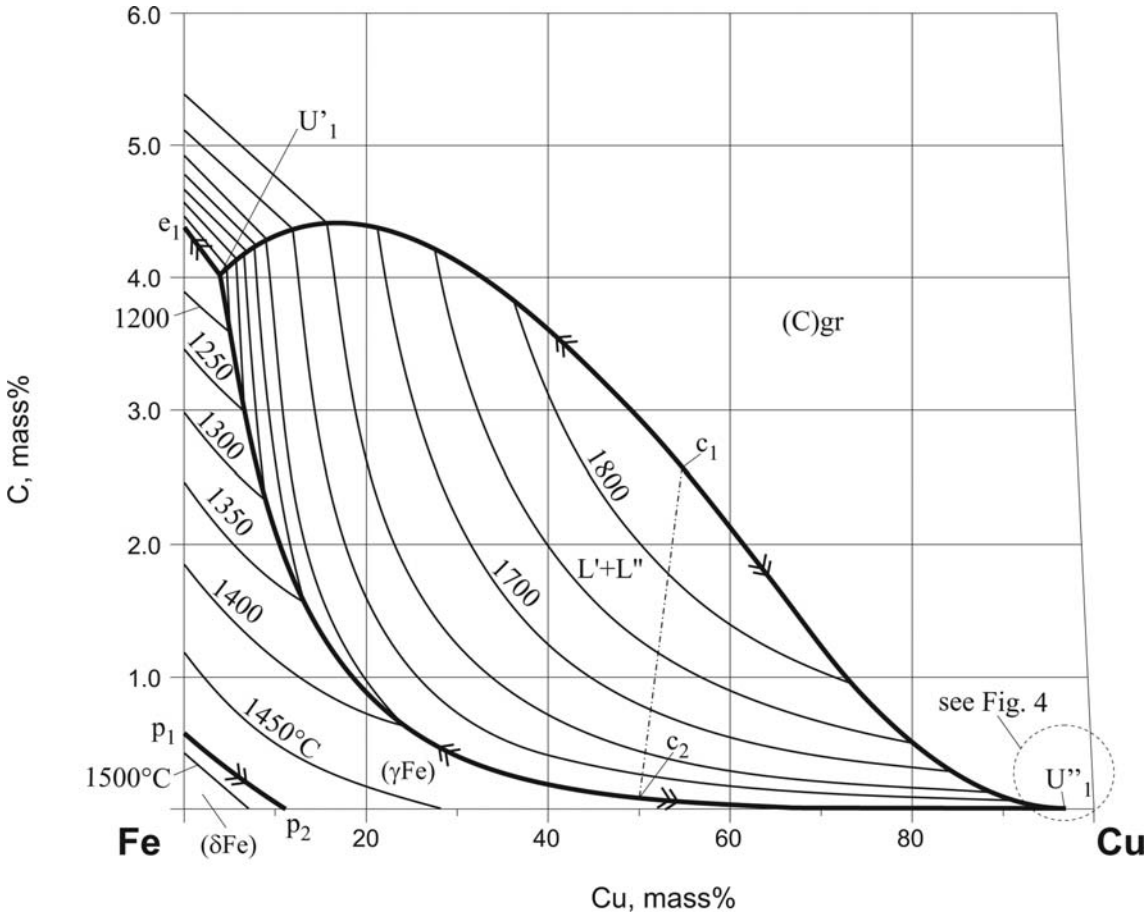

Fig. 3. C-Cu-Fe. Stable liquidus surface and liquidus isotherms

DOI: 10.1007/978-3-540-74196-1_4

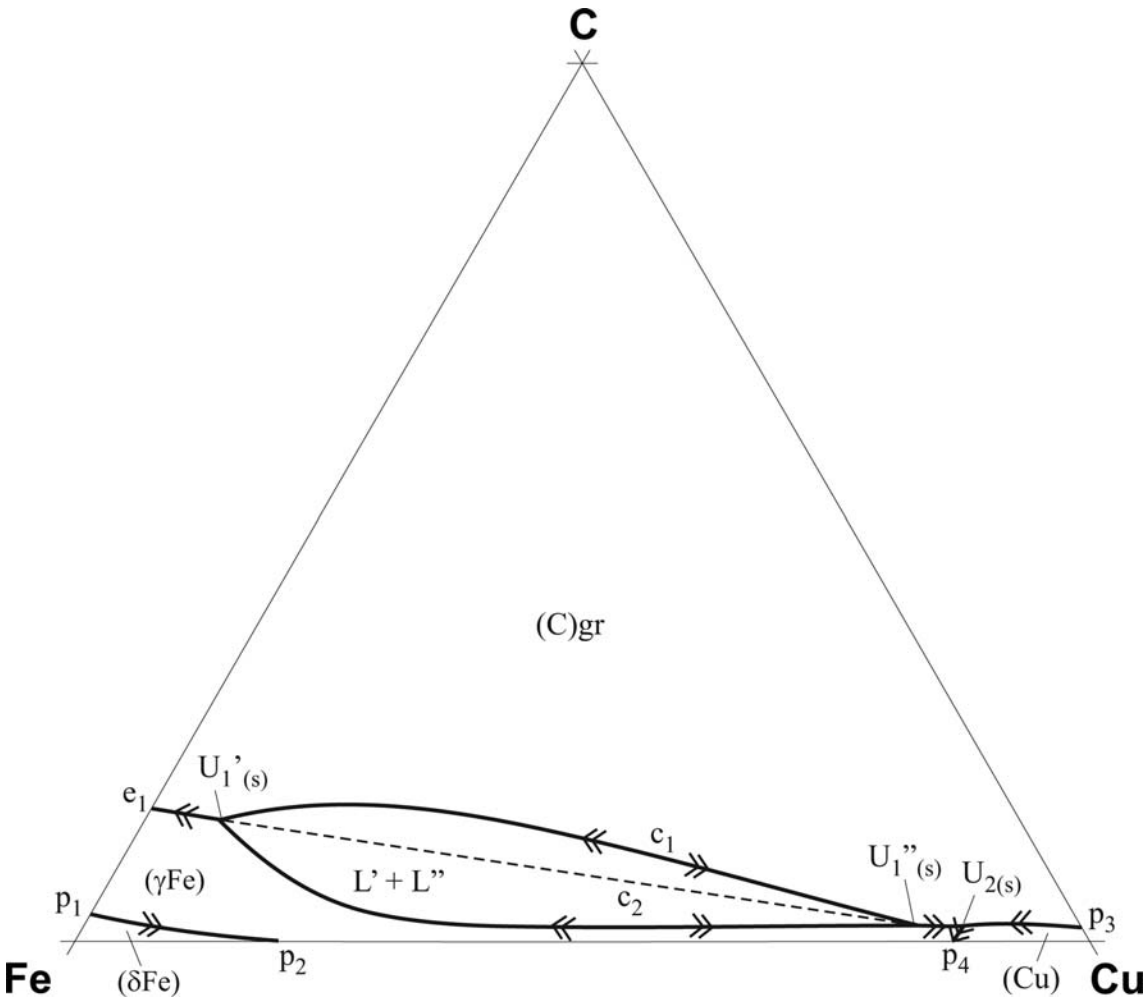

Fig. 4. C-Cu-Fe. Schematic sketch of the stable liquidus surface in the Cu corner

DOI: 10.1007/978-3-540-74196-1_4

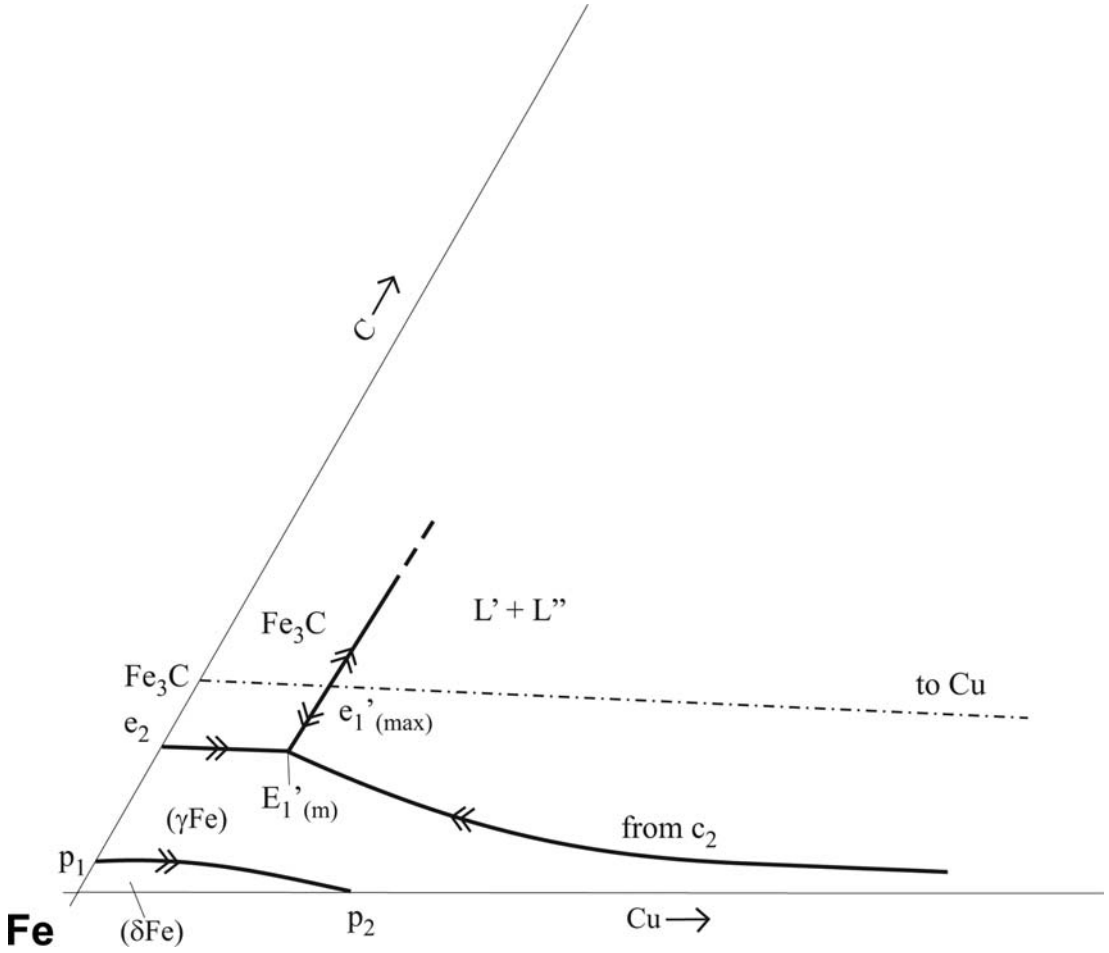

Fig. 5a. C-Cu-Fe. Schematic sketch of the metastable liquidus surface in the Fe rich side of the Cu-Fe-Fe_3C system

DOI: 10.1007/978-3-540-74196-1_4

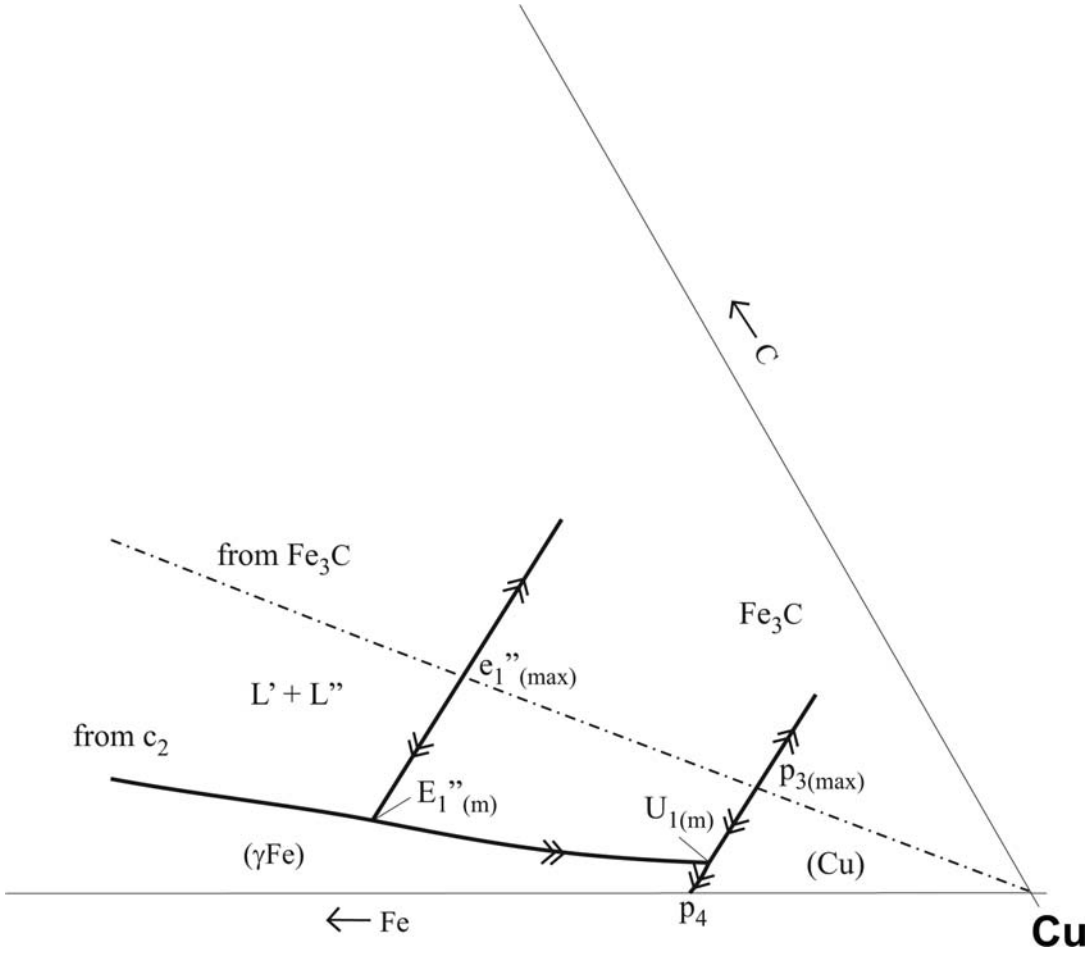

Fig. 5b. C-Cu-Fe. Schematic sketch of the liquidus surface in the Cu rich side of the metastable Cu-Fe-Fe_3C system

DOI: 10.1007/978-3-540-74196-1_4

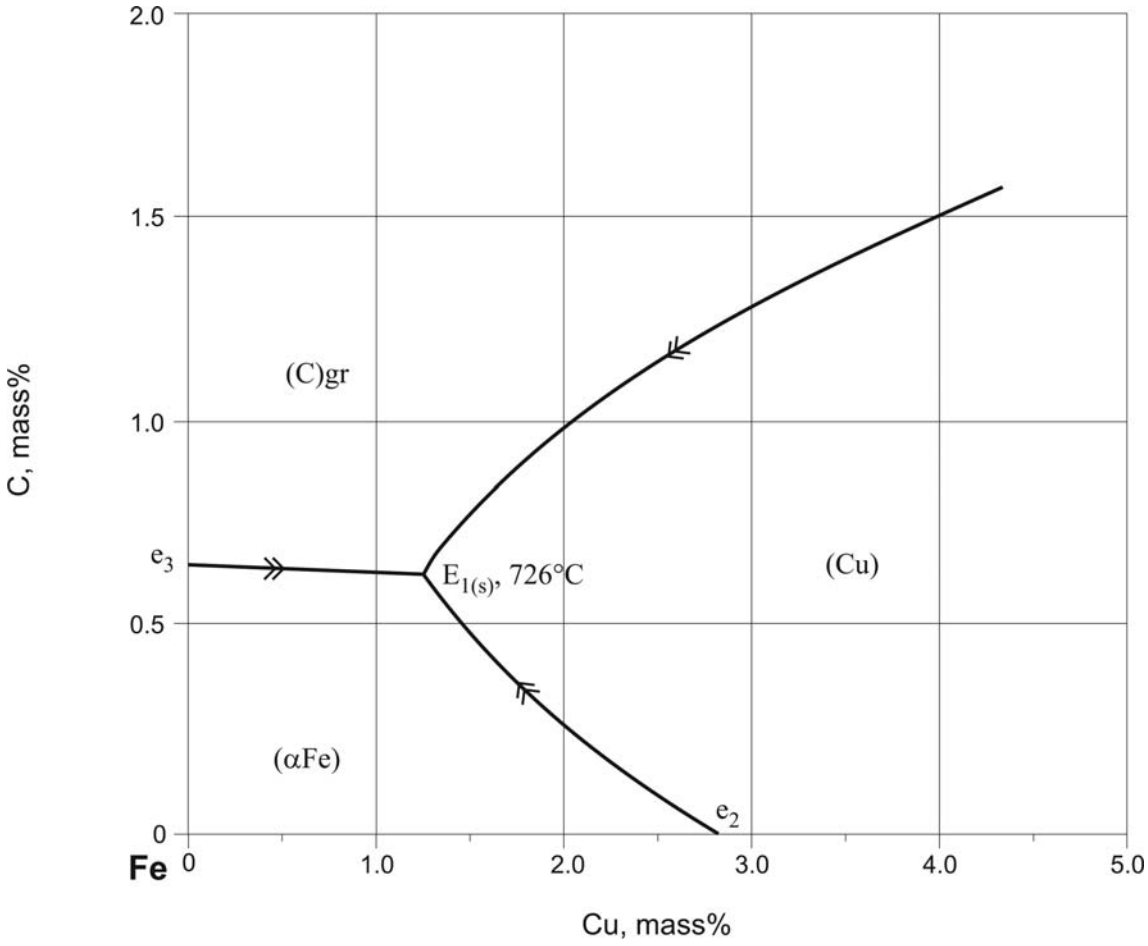

Fig. 6. C-Cu-Fe. (γFe) projection with lines of double saturation in the C-Cu-Fe stable phase diagram

DOI: 10.1007/978-3-540-74196-1_4

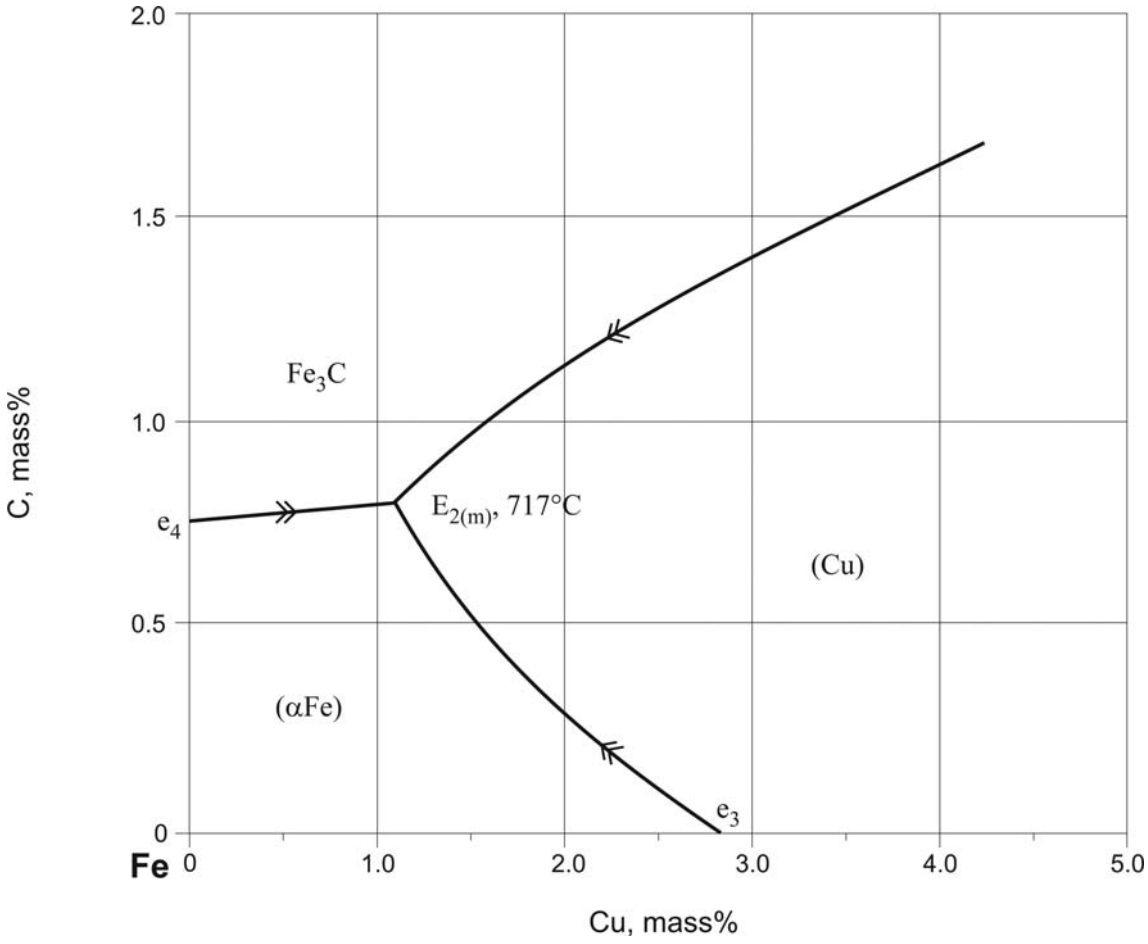

Fig. 7. C-Cu-Fe. (γFe) projection with lines of double saturation in the Cu-Fe-Fe_3C metastable phase diagram

DOI: 10.1007/978-3-540-74196-1_4

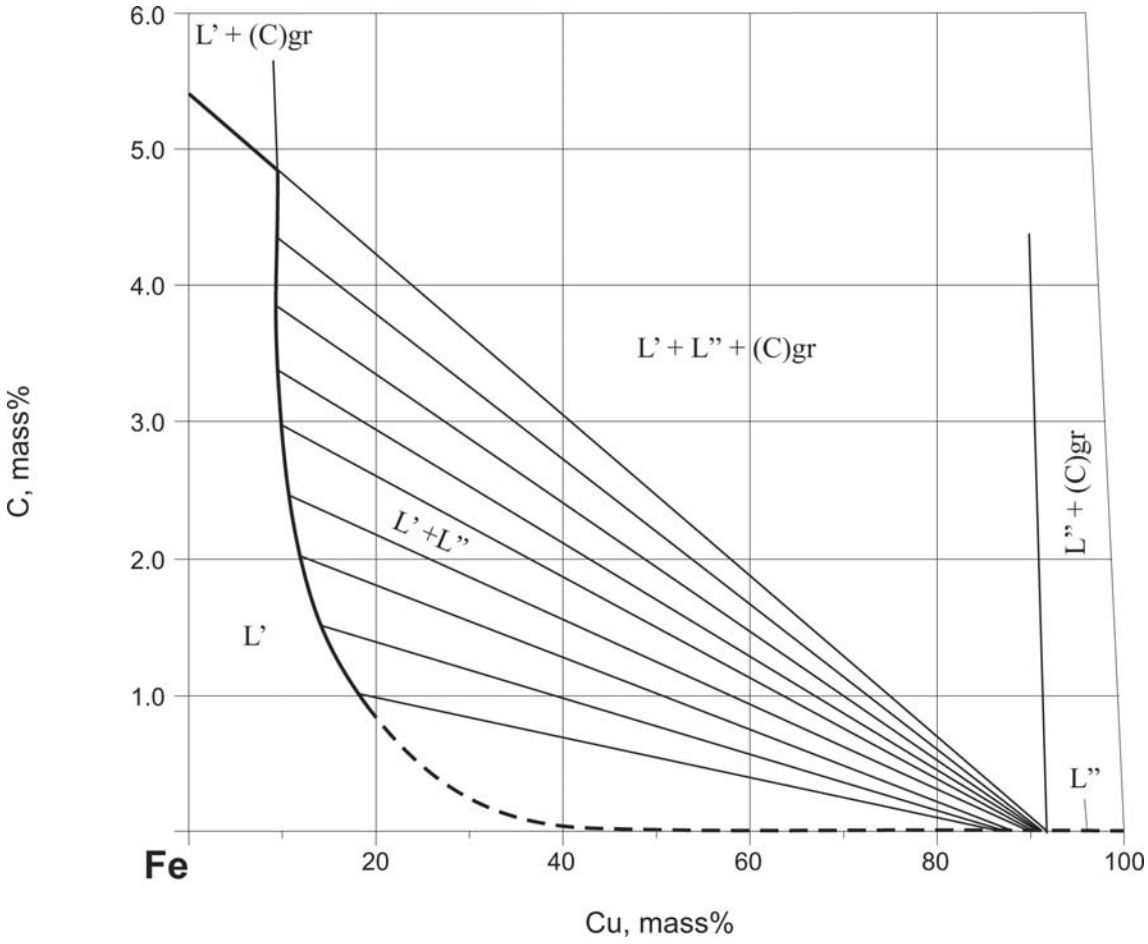

Fig. 8. C-Cu-Fe. Isothermal section at 1600°C

DOI: 10.1007/978-3-540-74196-1_4

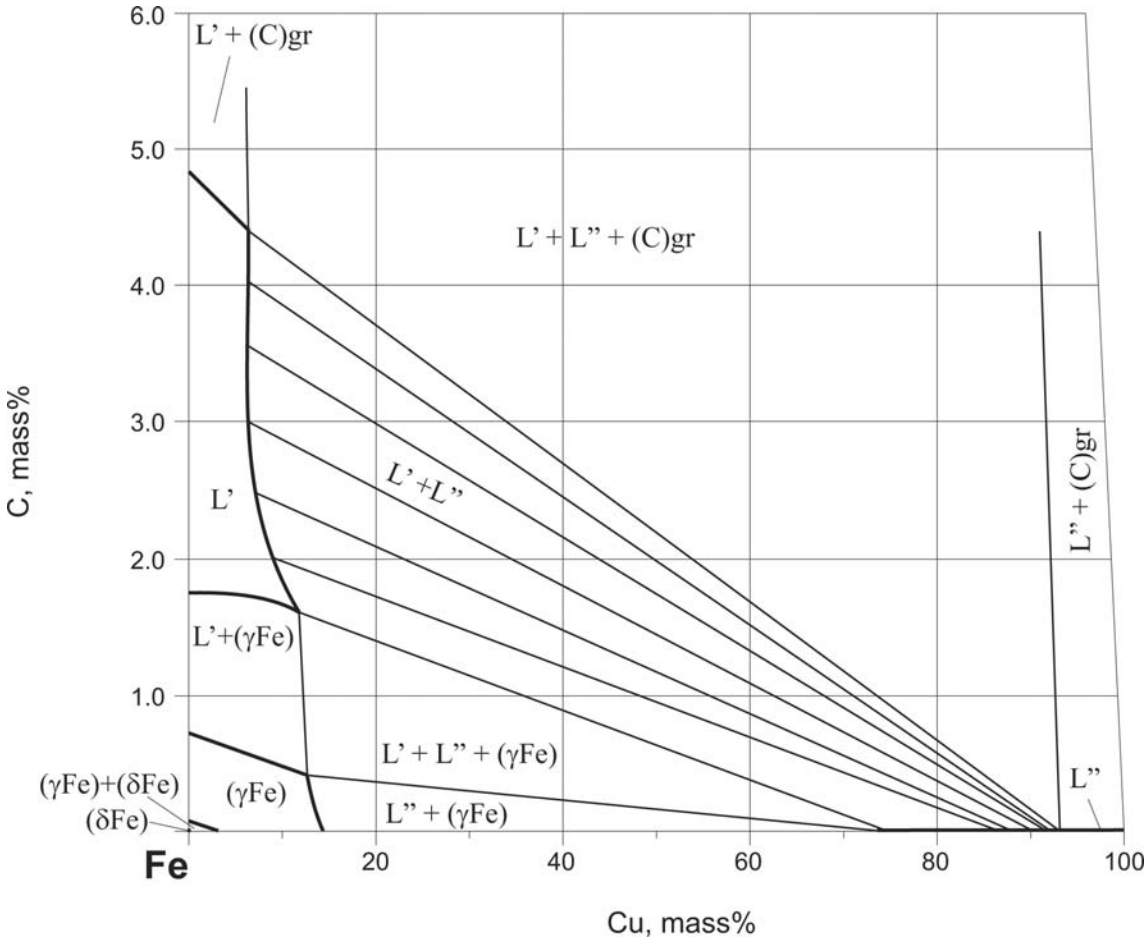

Fig. 9. C-Cu-Fe. Isothermal section at 1400°C

DOI: 10.1007/978-3-540-74196-1_4

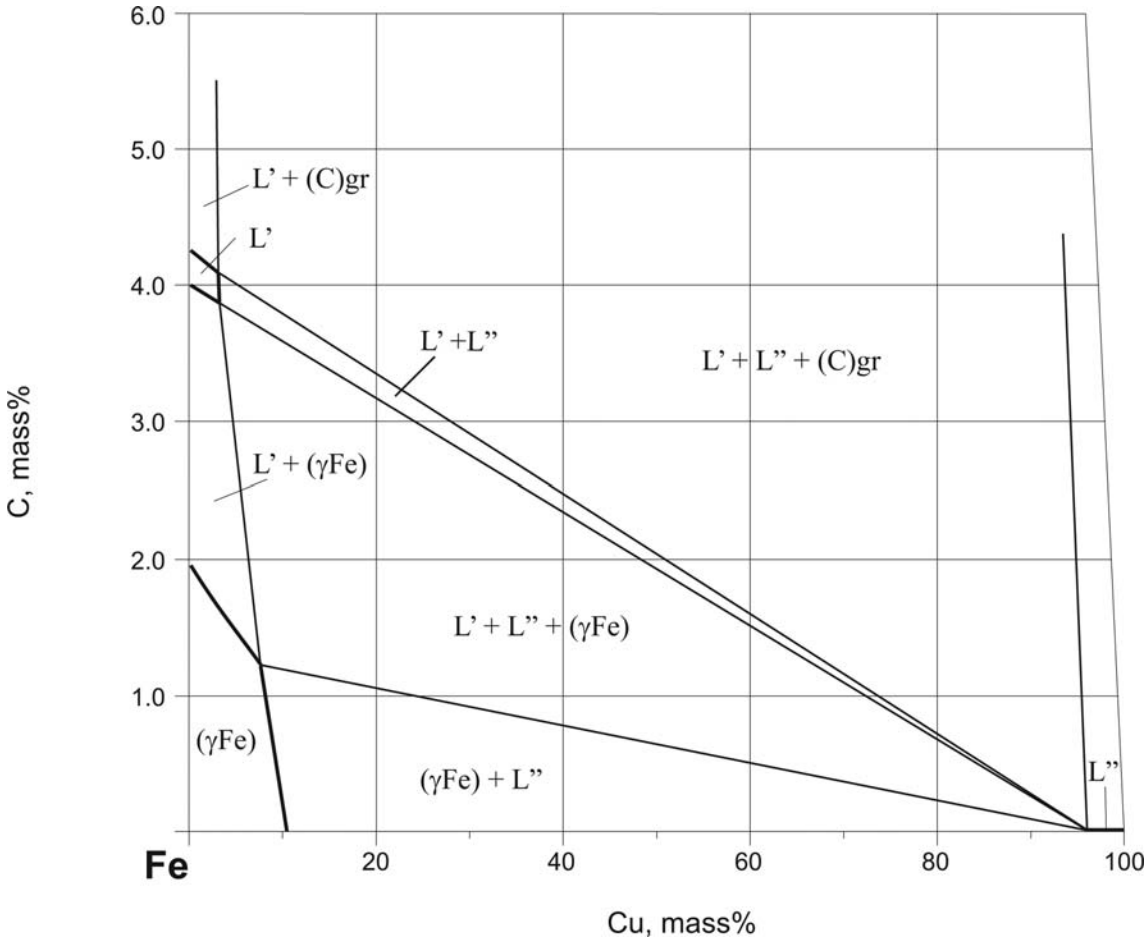

Fig. 10. C-Cu-Fe. Isothermal section at 1180°C

DOI: 10.1007/978-3-540-74196-1_4

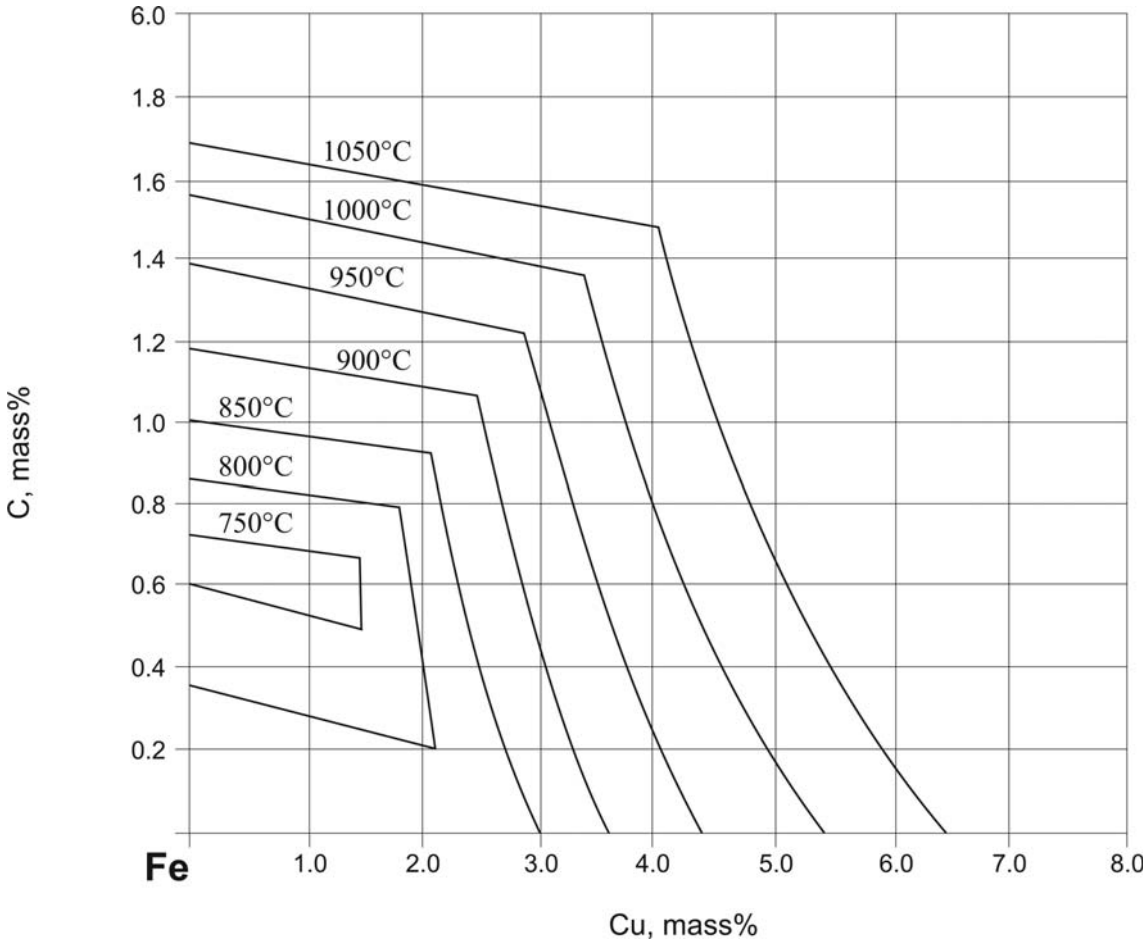

Fig. 11. C-Cu-Fe. Calculated solubility of C and Cu in (γFe)

DOI: 10.1007/978-3-540-74196-1_4

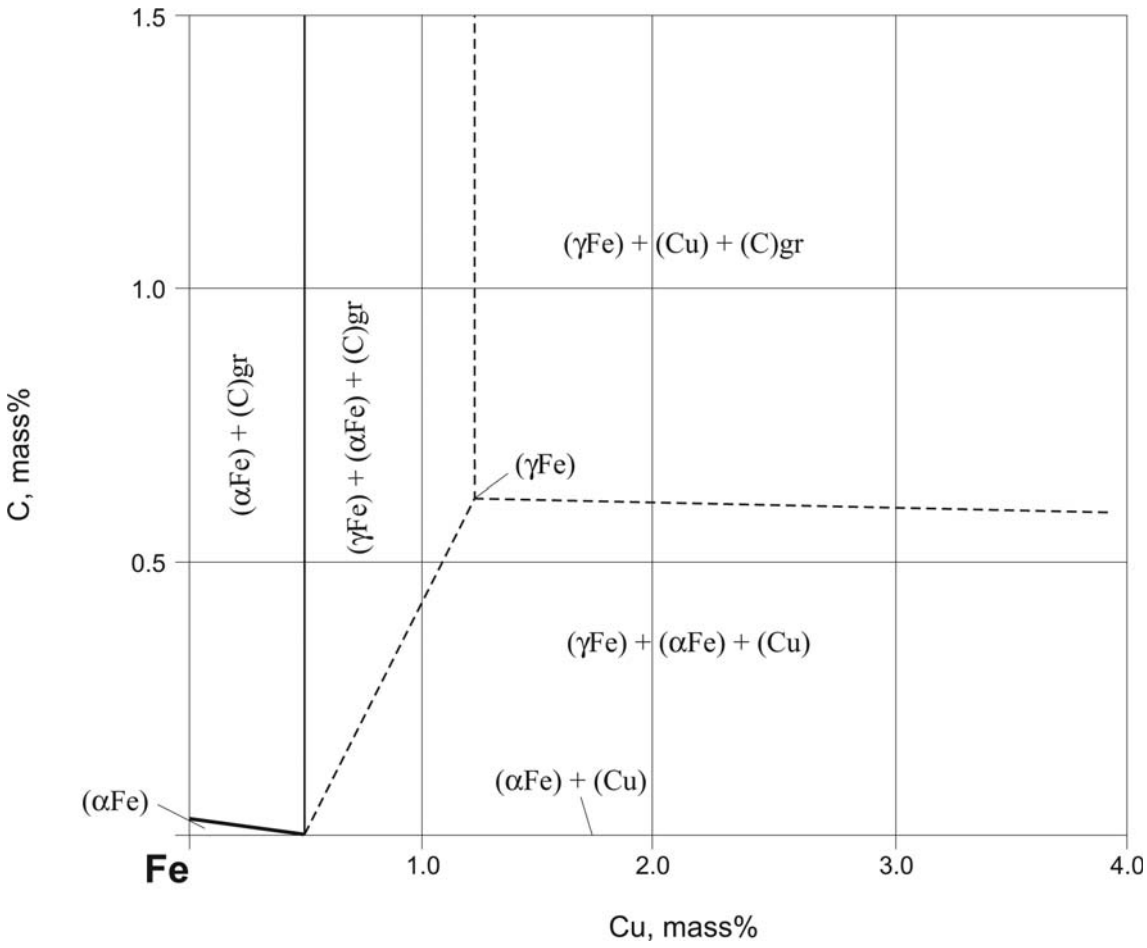

Fig. 12. C-Cu-Fe. Isothermal section of the stable C-Cu-Fe diagram at the eutectoid temperature 726°C

DOI: 10.1007/978-3-540-74196-1_4

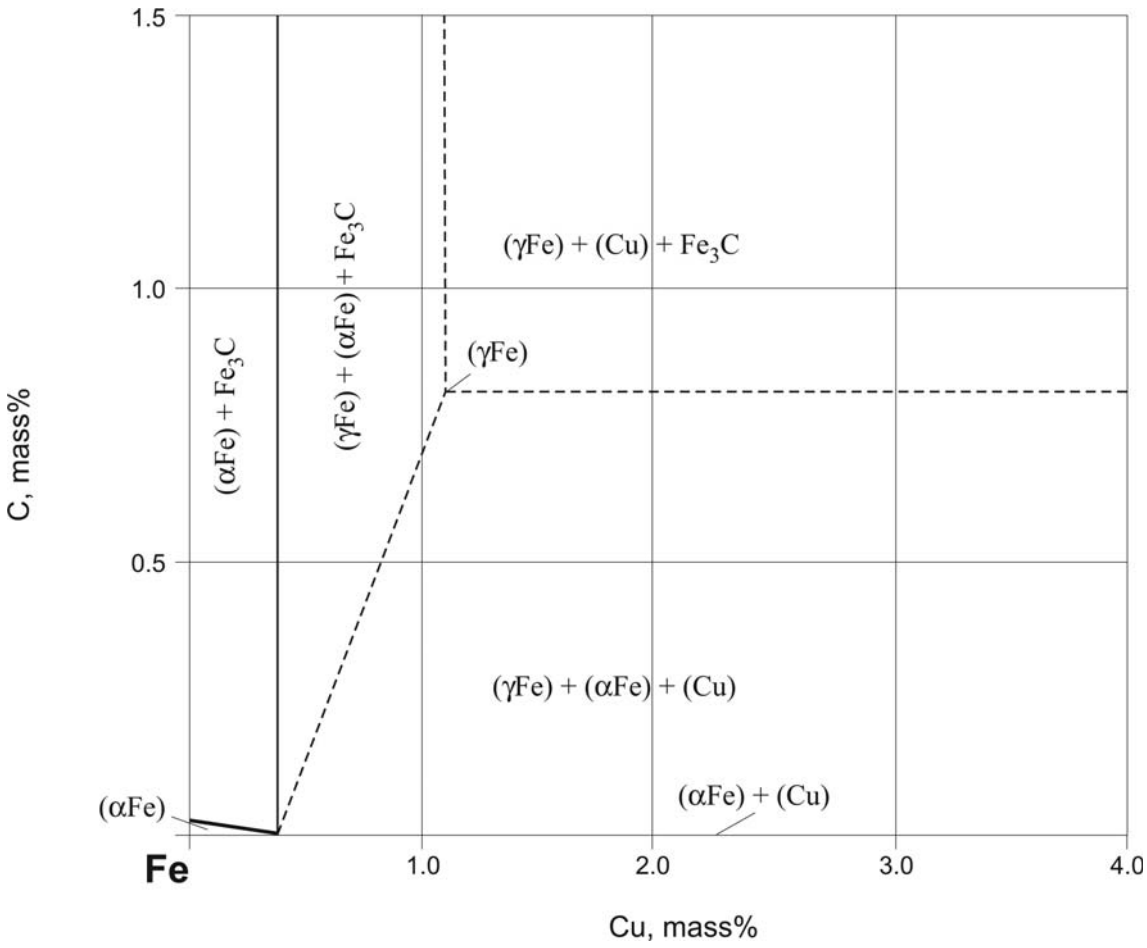

Fig. 13. C-Cu-Fe. Isothermal section of the metastable Cu-Fe-Fe_3C diagram at the eutectoid temperature 717°C

DOI: 10.1007/978-3-540-74196-1_4

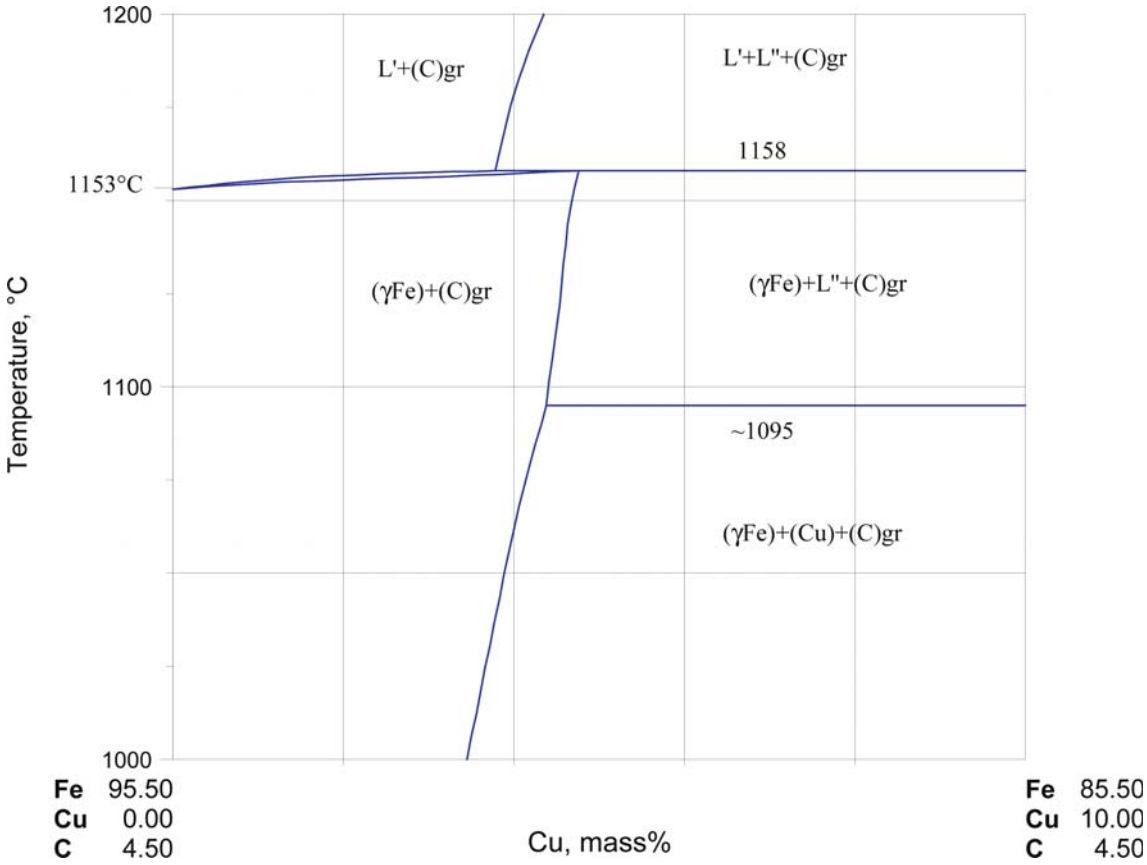

Fig. 14. C-Cu-Fe. Calculated vertical section at 4.5 mass% C

DOI: 10.1007/978-3-540-74196-1_4

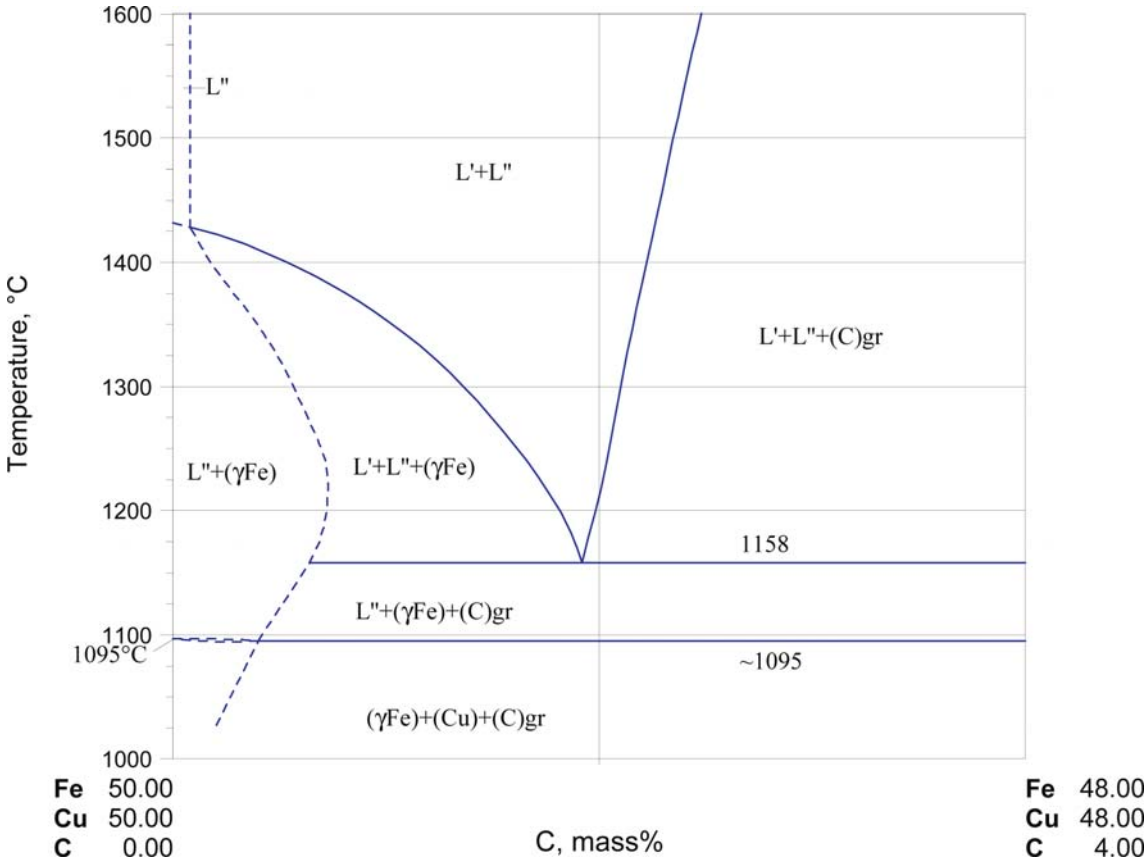

Fig. 15. C-Cu-Fe. Partial vertical section from 50Cu-50Fe to C (mass%)

DOI: 10.1007/978-3-540-74196-1_4

References

[1926Ish] Ishiwara, T., Yonekura, T., Ishigaki, T., "On the Diagram of the System Iron, Carbon and Copper", *Sci. Rep. Tohoku Imp. Univ.*, **15**, 81–114 (1926) (Phase Diagram, Phase Relations, Experimental, Theory, 7)

[1936Mad] Maddocks, W.R., Claussen, G.E., "Section VIII – Alloys of Iron-Copper-Carbon-Cobalt", *Iron Steel Inst., Special Rep.*, **14**, 97–124 (1936) (Phase Diagram, Phase Relations, Morphology, Experimental, 12)

[1938And] Andrew, J.H., Bottomley, G.T., Maddocks, W.R., Percival, R.T., "The Fluidity of Iron-Carbon and other Iron Alloys", Iron Steel Inst., 3th Rep. Steel Castings Research Committee, Publ. Offices Iron Steel Inst. 4, Grosvenor Gardens, London, S.W.1, (23), 5–32 (1938) (Experimental, Mechan. Prop., 9)

[1938Iwa] Iwase, K., Okamoto, M., Amemiya, T., "On the Formation of Two Liquid Layers in Copper-Iron Alloys", *Sci. Rep. Tohoku Imp. Univ.*, **26**, 618–640 (1938) (Phase Diagram, Phase Relations, Morphology, Experimental, 32)

[1949Jae] Jänecke, E., "C-Fe-Cu" (in German), *Kurzgefasstes Handbuch Aller Legierungen*, Winter, Heidelberg, 681–684 (1949) (Phase Diagram, Phase Relations, Review, 2)

[1954Lan] Langenberg, F.C., Lindsay, R.W., "Removal of Copper from Iron-Copper-Carbon Alloys", *J. Metals*, **200**(9), 967–968 (1954) (Experimental, 6)

[1956Kor] Koros, P.J., Chipman, J., "Activity Coefficient of Copper in Liquid Iron, Fe-C, and Fe-C-Si Alloys at 1600°C", *Trans. AIME*, **206**, 1102–1104 (1956) (Phase Diagram, Phase Relations, Experimental, Thermodyn., Calculation, 12)

[1957Lan] Langenberg, F.C. Lindsay, R.W., *Contributions to the Metallurgy of Steel, No. 51*, (1957), as quoted by [1979Cha]

[1959Neu] Neumann, F., Schenck, H., Patterson, W., *Giesserei*, **23**, 1217–1246 (1959) (Thermodyn., Experimental, 74)

[1959Per] Perbix, G., "On Thermodynamics and Technology of Removing of Copper, Tin and Antimony from Iron and Lead" (in German), *Thesis*, Aachen, 1–145 (1959) (Phase Diagram, Experimental, Morphology, Themodyn., 163)

[1959Sim] Simkovich, G., Ph.D. Thesis, Pennsylvania State University (1959) as quoted by [1979Cha]

[1960Fuw] Fuwa, T., Fujikura, M., Matoba, S., "Effect of Elements on the Solubility of Graphite in Liquid Iron" (in Japanese), *Tetsu to Hagane (J. Iron Steel Inst. Jpn)*, **46**, 235–237 (1960) (Phase Relations, Experimental, Thermodyn., 16)

[1960Mor] Mori, T., Aketa, K., Ono, H., Sugita, H., "Effects of Molybdenum, Wolfram and Copper on Solubility of Graphite in Liquid Iron and the Method of Calculation for the Activity of Carbon in a Multicomponent Solution" (in Japanese), *Tetsu-to-Hagane (J. Iron Steel Inst. Jpn)*, **46**, 1429–1439 (1960) (Phase Relations, Thermodyn., 24) as quoted by [1979Cha]

[1961Sch] Schenck, H., Perbix, G., (in German), *Arch. Eisenhuettenwes.*, **32**(2), 123–127 (1961) (Phase Diagram, Phase Relations, Experimental, Thermodyn., 22)

[1961She] Sheludyakov, L.N., Kip'yakov, G.Ye., Lyubimova, L.S., "Solubility of Copper in Carbon-Reach Cast Iron" (in Russian), *Izv. Akad. Nauk Kaz. SSR, Ser. Khim.*, **1**(19), 60–62 (1961) (Phase Diagram, Phase Relations, Experimental, 7)

[1965Loe] Loehberg, K., Roehrig, K., "The Stable and Metastable Solidification Equilibria of Iron Rich Iron-Carbon-Copper-Alloys" (in German), *Giesserei Tech.-Wiss. Beih.*, **17**(3), 91–98 (1965) (Phase Diagram, Phase Relations, Experimental, 15)

[1968Rep] Repina, N.I., Lev, I.E., Yatsenko, A.I., Martsiniv, B.F., "The Transcrystalline Segregation of Copper and Nickel in Iron-Carbon Alloys", *Russ. Metall.*, (2), 100–105 (1968), translated from *Izv. Akad. Nauk, Met.*, (2), 153–160 (1968) (Experimental, 14)

[1968Wil] Wilson, E.A., "Copper Maraging Steels", *J. Iron Steel Inst., London*, **206**, 164 (1968) (Experimental, Mechan. Prop., Morphology, 23)

[1970Bel] Belton, G.R., Serkin, J.A., "A Mass Spectrometric Study of Liquid Fe-Cu and Fe-Cu-C Alloys", *J. Metals*, **22**(12), A18 (1970) (Experimental, Phase Relations, Thermodyn., Abstract)

DOI: 10.1007/978-3-540-74196-1_4

[1970Lan] Lange, K.W., Schenck, H., "Effect of Phase Limit Reaction on Carbon Transfer in Solid Iron-Copper Alloys" (in German), *Arch. Eisenhuettenwes.*, **41**(5), 413–420 (1970) (Experimental, 58)

[1970Mor] Morris, A.E., Annual Report, INCRA Project 156A, Univ. of Missouri-Rolla, (1970), as quoted by [1979Cha]

[1971Gre] Greenbank, J.C., "Carbon Solute Interactions in Fe-Ni-C Alloys", *J. Iron Steel Inst., London*, **209**, 819–825 (1971) (Calculation, Experimental, Thermodyn., Phase Relations, 18)

[1972Wil] Williams, R., Bordsworth, C., "Effect of Cobalt, Copper and Manganese on the Thermodynamic Activity of Carbon in Iron-Base Austenites", *J. Iron Steel Inst., London*, **210**, 106–110 (1972) (Experimental, Phase Relations, Thermodyn., Calculation, 11)

[1973Jeg] Jeglitsch, F., Maier, K., "Secondary Precipitation in Fe-Fe_3C-X Alloys" (in German), *Z. Metallkd.*, **64**(8), 539–545 (1973) (Experimental, Morphology, Phase Relations, 31)

[1974Ang] Angers, R., Trudel, Y., "Dimensional Changes During Sintering of Prealloyed Fe-Cu-C Powders", *Int. J. Powder Met.*, **10**(2), 111–112 (1974) (Experimental, 1)

[1974Ela] Elanskii, G.N., Akinfiev, S.I., Kudrin, V.A., Babich, V.K., "Relationship Between Rate of decarburization of Fe-C-Ni and Fe-C-Cu Melts and Their Structure", *Steel USSR*, **4**(9), 722–723 (1974), translated from *Izv. Vyssh. Ucheb. Zaved. Chern. Metall.*, **9**, 22–25 (1974) (Thermodyn., Kinetics, Experimental, 11)

[1974Sig] Sigworth, G.K., Elliott, J.F., "The Thermodynamics of Liquid Dilute Iron Alloys", *Met. Sci.*, **8**, 298–310 (1974) (Review, Thermodyn., 249)

[1975Cho] Choudary, U.V., Serkin, J.A., Belton, G.R., "A Mass-Spectrometric Study of the Thermodynamics of the Fe-Cu and Fe-Cu-C(sat) Systems at 1600°C", *Metall. Trans. B*, **6**, 399–403 (1975) (Phase Diagram, Phase Relations, Experimental, Thermodyn., Calculation, 28)

[1975Lar] Larsson, L.-E., "On the Effect of Cu on the Fe-C Diagram", *Z. Metallkd.*, **66**(4), 220–223 (1975) (Experimental, Phase Diagram, Phase Relations, Morpholory, 15)

[1975Mor] Morris, A.E., Final Report, INCRA Project 156B, Univ. of Missouri-Rolla, (1975), as quoted by [1979Cha]

[1975Mos] Moskalenko, I.A., Ostrik, P.N., "Effect of Copper on the Thermodynamic Activity of Carbon in Austenite", *Russ. J. Phys. Chem. (Engl. Transl.)*, **49**(7), 1073–1074 (1975), translated from *Zh. Fiz. Khim.*, **49**, 1824–1825 (1975) (Phase Relations, Experimental, Thermodyn., 5)

[1975Sil] Silman, G.I., "Effect of Alloying Elements on the Metastability of Cementite and its Solubility in Austenite" (in Russian), *Metalloved. Term. Obrab. Met.*, (5), 24–27 (1975) (Thermodyn., Phase Relations, Calculation, 9)

[1976Maj] Majima, K., Mitani, H., "On the Sintering Mechanism of Fe-Cu-C Ternary Mixed Powder Compacts" (in Japanese), *J. Jpn. Inst. Met.*, **40**, 327–333 (1976) (Phase Relations, Morphology, Experimental, 5)

[1976Wag] Wagner, C., "Thermodynamic Analysis of the Liquidus in Ternary Systems Involving Small Contents of One Component", *Metall. Trans. B*, **7B**(3), 485–488 (1976) (Phase Diagram, Phase Relations, Thermodyn., 30)

[1977Maj1] Majima, K., Mitani, H., "Hardenability of the Sintered Copper Steel" (in Japanese), *J. Jpn. Inst. Met.*, **41**, 352–358 (1977) (Experimental, Mechan. Prop., 13)

[1977Maj2] Majima, K., Mitani, H., "Sintering Mechanism in Mixed Powder Compacts of the Fe-Cu-C Ternary System", *Trans. Jpn. Inst. Met.*, **18**(10), 663–672 (1977) (Phase Relations, Morphology, Experimental, 17)

[1977Uhr] Uhrenius, B., "Optimization of Parameters Describing the Interaction Between Carbon and Alloying Elements in Ternary Austenite", *Scand. J. Metall.*, **6**(2), 83–89 (1977) (Thermodyn., Calculation, 24)

[1978Uhr] Uhrenius, B., "A Compendium of Ternary Iron-base Phase Diagrams", in "*Hardenability Concepts with Applications to Steel*", Doane, D.V., Kirkaldy, J.S. (Eds.), Proc. Symp. Held Sheraton-Chicago Hotel, Oct. 24–26, 1977, Metall. Soc. AIME Heat Treat. Com./ Amer. Soc Met. Activ. Phase Trans., 28–81 (1978) (Phase Diagram, Phase Relations, Thermodyn., Calculation, 53)

DOI: 10.1007/978-3-540-74196-1_4

[1978Yam] Yamane, T., Minamino, Y., Hirao, K., Takahashi, J., "Resolution of Carbon Atoms in Neutron-Irradiated Fe-0.21wt%C-0.2wt%Cu Alloy", *Radiat. Eff.*, **35**(1–2), 101–103 (1978) (Experimental, 3)

[1979Cha] Chang, Y.A., Neumann, J.P., Mikula, A., Goldberg, D., "C-Cu-Fe", *INCRA Monograph Series 6. Phase Diagrams and Thermodynamic Properties of Ternary Copper-Metall Systems*, NSRD, Washington, **6**, 367–386 (1979) (Phase Diagram, Phase Relations, Thermodyn., Review, 26)

[1979Par] Parameswaran, K., Metz, K., Morris A., "Phase Equilibria for Iron rich Fe-Cu-C Alloys: 1500 to 950°C", *Metall. Trans*, **10A**, 1929–1939 (1979) (Experimental, Morphology, Phase Diagram, Phase Relations, 41)

[1980Ost] Ostrowski, R. Podrzucki, C., "Solubility of Nickel, Copper, Tin and Phosphorus in Ferrite and Eutectoid Cementite in Gray Iron", *Pr. Kom. Metal.-Odlew., (Ser.) Metal. (Pol. Akad. Nauk)*, **28**, 77–102 (1980) (Experimental, Morphology, 17)

[1983Jan1] Janas, M., Mamro, K., Ludwikowski, S., Jowsa, J., "Carbon Solubility in Fe-C(max)-Al, Fe-C(max)-Co, Fe-C(max)-Cu Alloys", *Metal. Odlew.*, **9**(2), 99–118 (1983) (Thermodyn., Experimental, 7)

[1983Jan2] Janas, M., Mamro, K., Jowsa, J., Ludwikowski, S., "Assessment of Ferrous Alloy Component Influence on Carbon Solubility" (in Polish), *Metal. Odlew.*, **9**(3), 213–228 (1983) (Thermodyn., Experimental, 28)

[1983Pen] Peng, P., Wang, G., Zhang, J., "Thermodynamic Properties of Fe-Cu-C and Melts" (in Chinese), *Acta Metall. Sin., Ser. A*, **19**(3), A237–A243 (1983) (Thermodyn., Experimental, 10)

[1983Sch] Schneeweis, O., Gonser, U., Wagner, H.G., "On the Formation of Iron Carbides in Copper-Iron and Copper-Gold-Iron Alloys", *Scr. Metall.*, **17**(4), 463–466 (1983) (Experimental, 5)

[1984Riv] Rivlin, V.G., "Phase Equilibria in Iron Ternary Alloys -(13)- Critical Evaluation of the Constitution of Ternary Systems C-Fe-X (X=Co, Ni, Cu)", *Int. Met. Rev.*, **29**(2), 96–121 (1984) (Phase Diagram, Phase Relations, Review, 76)

[1985Jam] Jamil, S.J., Chadwick, G.A., "Investigation and Analysis of Liquid Phase Sintering of Fe-Cu and Fe-Cu-C Compacts", *Powder Met.*, **28**(2), 65–71 (1985) (Experimental, Morphology, Phase Relations, Experimental, Kinetics, 16)

[1986Sch] Schuermann, E., von Schweinichen, J., "Study of Liquid Phase Equilibria in Iron Corner of Fe-C-X Ternary System with X = Al, Cu, Ni and Cr" (in German), *Giessereiforschung*, **38**(4), 125–132 (1986) (Experimental, Phase Diagram, Phase Relations, 63)

[1986Zhu] Zhu, Xunyun, "Thermodynamic Equilibrium between Lead-Copper System and Iron-Copper-Carbon System" (in Japanese), *Shanghai Jiaotong Daxue Xuebao (J. Shanghai Jiaotong Univ.)*, **20**(2), 132–137 (1986) (Thermodyn., Experimental, 14)

[1987Sak] Sakun, G.V., Singer, V.V., Radovskii, I.Z., Kudryavtseva, E.D., Gel'd, P.V., "Stratification of Liquid Alloys of the Systems Fe-Cu and Fe-Cu-C", *Russ. Metall. (Engl. Transl.)*, **6**, 166–168 (1987), translated from *Izv. Akad. Nauk SSSR. Met.*, **6**, 162–164, 1987 (Experimental, Phase Relations, Electr. Prop., 7)

[1987Sch] Schuermann, E., Schweinichen, J., Voelker, R., Fischer, H., "Calculation of the α/δ Resp γ-Liquidus of Iron and of the Liquidus of Carbon as well as of the Univariant Reaction Lines in Iron-Rich, Carbon Containing Three-Component and Multicomponent Fe-C-X_1-X_2-Systems. MEMO" (in German), *Giessereiforschung*, **39**(3), 104–113 (1987) (Experimental, Phase Diagram, Phase Relations, Thermodyn., 19)

[1988Ray] Raynor, G.V., Rivlin, V.G., "C-Cu-Fe", *Phase Equilibria of Iron Ternary Alloys*, The Institute of Metals, London, **4**, 157–167 (1988) (Phase Diagram, Phase Relations, Review, 15)

[1988Sak] Sakun, G.V., Singer, V.V., Kudryavtseva, E.D., Radovski, I.Z., Shmiuke, A.B., Geld, P.V., "Phase Separation of Iron-Copper-Carbon $(Fe_{1-x}Cu_x)_{0.98}C_{0.02}$ Melts" (in Russian), *Rasplavy*, **2**(3), 125–128 (1988) (Phase Relations, Experimental, Electr. Prop., 8)

[1990Gus] Gustafson, P., "Study of the Thermodynamic Properties of the C-Cu-Fe-P, Fe-Mo-P and Fe-Ni-P System", *Inst. Met. Res. (IM-2549)* (1990) (Thermodyn., Phase Diagram, Phase Relations, 52)

DOI: 10.1007/978-3-540-74196-1_4

[1990Rey] Reynolds, W.T. Jr., Liu, S.K., Li, F.Z., Hartfield, S., Aaronson, H.I., "An Investigation of the Generality of Incomplete Transformation to Bainite in Fe-C-X Alloys", *Metall. Trans. A*, **21A**(6), 1479–1491 (1990) (Experimental, Phase Relations, 56)

[1991Sch1] Schuermann, E., Fischer, H., "Stable and Metastable Melting Equilibria of the Three Component Iron-Copper-Carbon System. Part 1. Discussion of the Possible Melting Equilibria in the Stable Fe-Cu-C System and the Metastable Fe-Cu-Fe_3C System as well as the Current Literature" (in German), *Giessereiforschung*, **43**(2), 84–89 (1991) (Phase Diagram, Phase Relations, Theory, 15)

[1991Sch2] Schuermann, E., Fischer, H., Degen, T., "Stable and Metastable Melting Equilibria of the Three Component Fe-Cu-C System. Part 2. Experimental Results from the Melting Equilibria of the Miscibility Gap and the Iron Rich and Copper Rich Corner in the Stable Fe-Cu-C System and Metastable Fe-Cu-Fe_3C" (in German), *Giessereiforschung*, **43**(3), 91–100 (1991) (Experimental, Phase Diagram, Phase Relations, Thermodyn., Calculation, 7)

[1992Oka] Okamoto, H., "The C-Fe (Carbon-Iron) System", *J. Phase Equilib.*, **13**(5), 543–565 (1992) (Phase Diagram, Phase Relations, Crys. Structure, Thermodyn., Assessment, 252)

[1994Rag] Raghavan, V., "C-Cu-Fe (Carbon-Cooper-Iron)", *J. Phase Equilib.*, **15**(4), 420–421 (1994) (Phase Diagram, Phase Relations, Review, 8)

[1994Sub] Subramanian, P.R., Laughlin, D.E., "C-Cu (Carbon-Copper)" in "*Phase Diagrams of Binary Copper Alloys*", Subramanian, P.R., *et al.* (Eds.), ASM Intl., Materials Park, OH, 109–111 (1994) (Phase Diagram, Crys. Structure, Thermodyn., Review, 15)

[1995Bar] Baryshev, E.E., Tret'yakova, E.E., Baum, B.A., Kostina, T.K., Murav'eva, E.L., Tyagunov, G.V., "Structural Features of Liquid and Solid Hypereutectic Copper Iron", *Russ. Metall. (Engl. Transl.)*, **2**, 82–86 (1995) (Experimental, Phase Relations, 9)

[1995Che] Chen, X., Ito, N., Nakashima, K., Mori, K., "Evaporation Rate of Cupper in High Carbon Iron Melt under Reduced Pressure" (in Japanese), *Tetsu to Hagane*, **81**(10), 959–964 (1995) (Experimental, 14)

[1995Fou] Fourlaris, G., Baker, A.J., Papadimitriou, G.D., "Microscopic Characterisation of epsilon-Cu Interphase Precipitation in Hypereutectoid Fe-C-Cu Alloys", *Acta Metall. Mat.*, **43**(7), 2589–2604 (1995) (Phase Relations, Experimental, 46)

[1995Han] Han, G., Kuroki, H., Shinozaki, K., Sano, Y., "Effect of Carbon Distribution on Copper-Growth of Fe-Cu-C Compacts" (in Japanese), *J. Jpn. Inst. Met.*, **59**(11), 1165–1171 (1995) (Phase Relations, Experimental, 26)

[1996Fri] Frisk, K., "Molar Volumes in the Fe-Cu-C System", *Gov. Rep. Announce. Index (U.S.)*, (4), 1–7 (1996) (Thermodyn., 28)

[1997Fou] Fourlaris, G., Baker, A.J., "Bainite Formation in High Carbon Copper Bearing Steels", *J. Phys. IV, France*, **7**(C5), 389–394 (1997) (Phase Relations, Experimental, Theory, 23)

[1997Lac] Lacaze, J., Boudot, A., Gerval, V., Oquab, D., Santos, H., "The Role of Manganese and Copper in the Eutectoid Transformation of Spheroidal Graphite Cast Iron", *Metall. Mater. Trans. A*, **28**(10), 2015–2025 (1997) (Experimental, Morphology, 24)

[1998Tan] Tanaka, T., Haka, S., Okamoto, M., "The Wettabilites of Graphite by Liquid Carbon-Saturated Fe-Cu, Fe-Sn and Fe-S Alloys" (in Japanese), *Tetsu to Hagane*, **84**(1), 25–30 (1998) (Thermodyn., Experimental, 15)

[1999Ama] Amara, S.-E., Belhadj, A., Kesri, R., Hamar-Thibault, S., "Stable and Metastable Equilibria in the Binary Fe-Cu and Ternary Fe-Cu-C Systems", *Z. Metallkd.*, **90**(2), 116–123 (1999) (Experimental, Phase Diagram, Phase Relations, Morphology, 33)

[1999Kur] Kuroki, H., Han, G., Shinozaki, K., "Solution-Reprecipitation Mechanism in Fe-Cu-C During Liquid Phase Sintering", *Int. J. Powder Met.*, **35**(2), 57–62 (1999) (Phase Relations, Thermodyn., Calculation, 14)

[2000Cha1] Chairuangsri, T., Edmonds, D.V., "The Precipitation of Copper in Abnormal Ferrite and Pearlite in Hyper-Eutectoid Steels", *Acta Mater.*, **48**(15), 3931–3949 (2000) (Phase Relations, Experimental, Morphology, 39)

DOI: 10.1007/978-3-540-74196-1_4

[2000Cha2] Chairuangsri, T., Edmonds, D.V., "Abnormal Ferrite in Hyper-Eutectoid Steels", *Acta Mater.*, **48**(7), 1581–1591 (2000) (Phase Relations, Experimental, Morphology, 15)

[2000Fen] Fenstad, J., "Liquidus Relations and Thermochemistry Within the System Fe-Mn-C-O", *Thesis 2000:126 (2000:23) Dept. Mater. Elchem., NTNU*, (2000) (Experimental, Phase Relations, Thermodyn.)

[2000Hsi] Hsiao, C.N., Yang, J.R., "Age Hardening in Martensitic/Bainitic Matrices in a Copper-Bearing Steel", *Mater. Trans., JIM*, **41**(10), 1312–1321 (2000) (Experimental, Morphology, Mechan. Prop., 25)

[2000Hug] Hug, K.H., Min, D.J., "Thermodynamic Behaviour of Cu in Molten Fe-C-S Alloys at High Temperatures", *Steel Res.*, **71**(1–2), 9–14 (2000) (Experimental, Thermodyn., Theory, 28)

[2000Kre] Krestyanov, V.I., Bakuma, S.S., Brodova, I.G., Yakovleva, I.L., Mirzaev, D.A., "Effect of Copper on the Structure and Properties of High-Carbon Iron Alloys", *Phys. Met. Metallogr. (Engl. Transl.)*, **90**(2), 153–158 (2000) (Phase Relations, Experimental, Morphology, Mechan. Prop., 13)

[2001Fen] Fenstad, J., Tuset, J.Kr., "The Binary Diagram Within the System Fe-Mn-C-O, and the Thermal Properties of Elemenyal Manganese", *INFACON 9: Proceedings of the 9th International Ferro-Alloys Congress*, June 2001, Quebes, Canada, **9**, (2001) (Experimental, Phase Relations, Thermodyn., 25)

[2001Ma] Ma, Z., "Thermodynamic Description for Concentrated Metallic Solutions Using Interaction Parameters", *Metall. Trans. B*, **32B**, 87–103 (2000) (Calculation, Phase Relations, Thermodyn., 70)

[2001Ped] Pedersen, L.M., Bentzen, J.J., Bramso, N., "Dimensional Response of Metal Matrix Graphite Particle Composites to Sintering", *Scr. Mater.*, **44**(5), 743–749 (2001) (Experimental, 13)

[2002Liu] Liu, P.-L., Lin, S.-T., "Relation between Widths of the Grain Boundary Energy Cusps at Special Misorientations and the Microstructural Characteristics in the Sintering of a Fe-Cu-C Alloy", *Mater. Trans.*, **43**(3), 544–550 (2002) (Thermodyn., Calculation, Experimental, 32)

[2002Rag] Raghavan, V., "C-Cu-Fe (Carbon-Copper-Iron)", *J. Phase Equilib.*, **23**(3), 251–252 (2002) (Phase Relations, Review, 7)

[2003Des] Deschamps, A., Militzer, M., Poole, W.J., "Comparison of Precipitation Kinetics and Strengthening in an Fe-0.8%Cu Alloy and a 0.8%Cu-Containing Low-Carbon Steel", *ISIJ Int.*, **43**(11), 1826–1832 (2003) (Phase Relations, Experimental, Kinetics, Mechan. Prop., Morphology, 20)

[2003Ono] Ono-Nakazato, H., Taguchi, K., Seike, Y., Usui, T., "Effect of Silicon and Carbon on the Evaporation Rate of Copper in Molten Iron", *ISIJ Int.*, **43**(11), 1691–1697 (2003) (Experimental, 21)

[2003Sil] Sil'man, G.I., Kamynin, V.V., Tarasov, A.A., "Effect of Copper on Structure Formation in Cast Iron", *Met. Sci. Heat Treat.*, **45**(7–8), 254–258 (2003), translated from Metalloved. Term. Obrab. Met., **7**, 15–20 (2003) (Phase Diagram, Phase Relations, Thermodyn., Calculation, 16)

[2004Aar] Aaronson, H.I., Reynolds, W.T., Purdy, G.R., "Coupled-Solute Drag Effect on Ferrite Formation in Fe-C-X Systems", *Metall. Mater. Trans. A*, **35A**(4), 1187–1210 (2004) (Experimental, Interface Phenomena, Kinetics, Morphology, Phase Relations, Review, 148)

[2004Bat] Batra, U., Ray, S., Prabhakar, S.R., "Tensile Properties of Copper Alloyed Austempered Ductile Iron: Effect of Austempering Parameters", *J. Mater. Eng. Perform.*, **13**(5), 537–541 (2004) (Phase Relations, Morphology, Experimental, Mechan. Prop., 10)

[2004Cor] Correia, J.B., Marques, M.T., "Production of a Copper- Iron Carbide Nanocomposite Via Mechanical Alloying", *Mater. Sci. Forum*, **455–456**, 501–504 (2004) (Phase Relations, Experimental, Mechan. Prop., 8)

DOI: 10.1007/978-3-540-74196-1_4

[2004Gag] Gagliano, M.S., Fine, M.E., "Characterization of the Nucleation and Growth Behavior of Copper Precipitates in Low-Carbon Steels", *Metall. Mater. Trans. A*, **A35**(8), 2323–2329 (2004) (Experimental, 30)

[2004Lop] Lopez, G.A., Mittemeijer, E.J., "The Solubility of C in Solid Cu", *Scripta Mater.*, **51**, 1–5 (2004) (Phase Relations, Experimental, 11)

[2004Wan] Wang, C.P., Liu, X.J., Takaku, Y., Ohnuma, I., Kainuma, R., Ishida, K., "Formation of Core-Type Macroscopic Morphologies in Cu-Fe Base Alloys With Liquid Miscibility Gap", *Metall. Mater. Trans. A*, **35A**(4), 1243–1253 (2004) (Calculation, Experimental, Morphology, Phase Relations, Thermodyn., 31)

[2005Car] Carvalho, P.A., Fonseca, I., Marques, M.T., Correia, J.B., Almeida, A., Vilar, R., "Characterization of Copper-Cementite Nanocomposite Produced by Mechanical Alloying", *Acta Mater.*, **53**(4), 967–976 (2005) (Experimental, Morphology, 46)

[2005Che] Chen, R.Y., Yuen, W.Y.D., "Isothermal and Step Isothermal Oxidation of Copper-Containing Steels in Air at 980–1220°C", *Oxid. Met.*, **63**(3–4), 145–168 (2005) (Experimental, Kinetics, Mechan. Prop., 28)

[2005Oki] Okita, Y., Yamada-Pittini, Y., Watanabe, R., "Thermal Conductivity of Functionally Graded Fe-Cu-C Alloy Processed by Liquid Phase Sintering and Carburization", *Z. Metallkd.*, **96**(2), 135–140 (2005) (Experimental, Phys. Prop., Morphology, Calculation, 15)

[2005Pan] PanIron5.0, Thermodynamic Database for Iron-Based Alloys, and Pandat, Thermodynamic Calculation Software, CompuTherm, LLC, Madison, WI 53719, U.S.A. (2005)

[2005Wan] Wang, W.-F., "Effect of Alloying Elements and Processing Factors on the Microstructure and Hardness of Sintered and Induction-Hardened Fe-C-Cu Alloys", *Mater. Sci. Eng. A*, **402**(1–2), 92–97 (2005) (Experimental, Morphology, Phys. Prop., 26)

[2006MSIT] "C-Fe (Iron-Carbon)", Diagrams as Published, in *MSIT Workplace*, Effenberg, G. (Ed.), Materials Science International Services, GmbH, Stuttgart; Document ID: 30.13598.1.20 (2006) (Crys. Structure, Phase Diagram, Phase Relations, 2)

[2007Tur] Turchanin, M., Agraval, P., "Cu-Fe (Copper-Iron)", MSIT Binary Evaluation Program, in *MSIT Workplace*, Effenberg, G. (Ed.), MSI, Materials Science International Services GmbH, Stuttgart; to be published (2007) (Phase Diagram, Crys. Structure, Thermodyn., Assessment, 31)

[Mas2] Massalski, T.B. (Ed.), *Binary Alloy Phase Diagrams*, 2nd edition, ASM International, Metals Park, Ohio (1990)

[V-C2] Villars, P. and Calvert, L.D., *Pearson's Handbook of Crystallographic Data for Intermetallic Phases*, 2nd edition, ASM, Metals Park, Ohio (1991)

DOI: 10.1007/978-3-540-74196-1_4

Carbon – Iron – Hydrogen

Pierre Perrot

Introduction

Steels, mainly constituted of C and Fe, in presence of H do not form hydrides, but interstitial solid solutions which play an important role in steelmaking because of undesirable effects in the embrittlement of steel products. Most of the investigations have been directed towards the solubility of H in ferrite, austenite and liquid alloys, and on the effects of hydrogen on the mechanical properties of steels. The main experimental results are gathered in Table 1.

Binary Systems

The C-Fe phase diagram accepted from [2006MSIT] is mainly based on the assessment by [1992Oka]. The properties of metastable carbides such as $Fe_{2.2}C$ (Haegg carbide) and $Fe_{2.4}C$ (known as "ε carbide" are well discussed in [1972Chi] which proposes also simple expressions for carbon activities in austenite and thermodynamic properties of carbides. These expressions may be useful because they are in good agreement with more recent and more sophisticated relationships. The Fe-H system under 0.1 MPa of hydrogen pressure is accepted from [1990San]. The Fe-H system has been carefully investigated by [2003Fuk] up to 10 GPa of hydrogen pressure and 1500°C. The hydrogen pressure-temperature diagram presents a drastic lowering of the melting point down to 800°C at 3 GPa. The triple point α-γ-ε of iron is shifted from 8.4 GPa and 430°C for pure iron to 5 GPa and 260°C for the Fe-H system. The hydrogen solubility under high pressure has been investigated by [2005Hir] in the γ region. Under 2.5 GPa, the hydrogen solubility increases with the temperature (from H/Fe = 0.12 at 700°C to H/Fe = 0.2 at 1000°C; under 4 GPa, H/Fe = 0.4 between 400 and 1000°C; under 6 GPa, the hydrogen solubility decreases when the temperature increases (from H/Fe = 0.7 at 700°C to H/Fe = 0.6 at 1000°C. The main compound of interest in the C-H system is CH_4. Mixtures H_2-CH_4 are often used as a source of carbon whose potential is imposed. Under 10 MPa of hydrogen pressure pure graphite may adsorb up to 0.5 mass% H at 800°C.

Solid Phases

Crystallographic data of solid phases are presented in Table 2.

Liquidus, Solidus and Solvus Surfaces

Hydrogen is known to decrease the carbon solubility in solid [1971Vor, 1973Sha, 1978Sha1, 1978Sha3] and liquid [1972Ngi, 1981Sch] iron. For instance, at temperatures above 1050°C the solubility of carbon in austenite, measured at 1.62 mass% C under argon goes down to 1.47 mass% C under 0.1 MPa H_2 and 1.37 mass% C under 0.3 MPa H_2. Unfortunately, the hydrogen content of these alloys was not analyzed. The solubility of C in austenite at 1100°C goes from 1.9 mass% in the Fe-C binary to 1.78 mass% under 50 MPa of hydrogen pressure [1978Sha1]. The eutectic and eutectoid temperatures of the C-Fe binary are also lowered by the insertion of hydrogen [1978Sha1].
Carbon increases slightly the solubility of hydrogen in solid phase [1965Sch] and decreases its solubility in liquid phase [1981Sch]. Under 0.1 MPa of hydrogen pressure at 1600°C, the hydrogen solubility goes from $1.9 \cdot 10^{-3}$ mol% for pure iron to $0.6 \cdot 10^{-3}$ mol% for a liquid of composition Fe_3C.

Isothermal Sections

Isothermal sections at 820 and 715°C from [1978Sha1, 1978Sha2, 1978Sha3] reviewed by [1981Rag] are presented in Figs. 1 and 2. Cementite Fe_3C is known to be metastable and decomposes at 640°C under vacuum whereas, under hydrogen pressure, forms CH_4 above 350°C [1984Fru].

DOI: 10.1007/978-3-540-74196-1_5

Thermodynamics

The Wagner first order interaction parameter $e_H^{(C)}$ has been experimentally determined between 1570 and 1720°C in liquid (Fe,C) alloys by [1961Mae], at 1592°C by [1963Wei] and between 1550 and 1700°C by [1972Ngi]. It is defined by

$$e_H^{(C)} = [\partial \log_{10} f_H / \partial (\%\,C)]$$

where (% C) represents the carbon content of the alloy expressed in mass% and f_H the activity coefficient of H in the alloy defined by

$$f_H = (\%C \text{ in pure iron}) / (\%C \text{ in the alloy}).$$

It is calculated from the solubility measurements at constant temperature and hydrogen pressure. It may be expressed by: $e_H^{(C)} = 0.297 - 1.267 \cdot 10^{-4}\, T$ in the temperature range 1570-1720°C for less than 5 mass% C in the alloy. The careful investigation of [1963Wei] leads to $e_H^{(C)} = 0.060$ at 1592°C for less than 1 at.% C in good agreement with the preceding relation and with the mean value of 0.064 proposed by [1972Ngi] between 1550 and 1700°C. The interaction coefficient may also be defined by $\varepsilon_H^{(C)} = [\partial \ln f_H / \partial x_C]$. Its accepted value is $\varepsilon_H^{(C)} = 3.0$ at 1592°C [1963Wei, 1965Bur] and 3.8 at 1600°C [1999Din]. Experimental data are well-fitted with a statistical model developed by [1980Fro] in order to calculate the hydrogen solubility in the whole concentration range from the solubility in pure metals and the first order Wagner interaction parameters.
In the solid state, it is possible to use the evaluations $\varepsilon_H^{(C)} = \varepsilon_C^{(H)} = 6.2$ and 3.8 at 400 and 700°C respectively [2000Pil], and 2.56 at 1100°C [1999Pil].
Thermodynamics of the reaction between CH_4 and (αFe) has been investigated by [1973Gra]. Main results are shown in Table 3.

Notes on Materials Properties and Applications

Hydrogen is characterized by a high diffusivity in steels, which is the highest of all interstitial elements, so that it can move without having any significant effect on the distribution of other interstitial elements (B,C,N) [1999Pil]. However, it has a strong effect on the embrittlement of martensitic-bainitic and ferritic-bainitic structures in heat affected zones of the welded joints. Hydrogen is thus important owing its influence on the embrittlement of steels and the basic principles, typical reaction mechanism and properties change of metals caused by dissolved non metal atoms have been well summarized in [1980Fro]. Hydrogen diffusion in steels is well theorized in [1999Pil, 2000Pil]. Hydrogen has little effect on the tensile strength, but reduce significantly the ductility of steels. [1986Cha]. Hydrogen greatly impairs the quality of welded joints [1999Pil] and, consequently, is one of the factors causing the formation of cold cracks. In pure C-Fe alloys, the ferrite-pearlite and the pearlite-pearlite interfaces are source of hydrogen trapping whereas the ferrite-cementite interface has little effect on the hydrogen occlusivity, even if cementite lamellae interfere on the hydrogen diffusion path. Hydrogen was shown to increase the pearlite formation in eutectoid steels [1978Sha2] and to decrease the eutectoid temperature, from 740°C for pure C-Fe alloy to 700°C under 30 MPa of hydrogen pressure. Cathodic hydrogen charging at low current density at room temperature induce a martensitic transformation as checked by Mössbauer spectroscopy [1990Uwa]. The spectra observed at room temperature present all the feature of an already aged martensite. Cold working of C-Fe alloys was found to increase greatly the hydrogen solubility and to decrease the hydrogen diffusivity at temperatures up to 400°C [1959Hil]. The hydrogen behavior is consistent with the fact that cold working creates microcracks which act as traps in which hydrogen is chemisorbed.

Miscellaneous

H_2-CH_4 gaseous mixtures may be used to measure carbon activity in steels [1969Bun] by equilibrating the carbon potential in gaseous and solid phases. The kinetics of carburization and decarburization of steels with methane according to the reaction: $CH_4 \rightleftharpoons$ C (dissolved in Fe) + 2 H_2 was measured at 928°C by [1965Gra] on austenite and at 786°C by [1973Gra] on the ferrite. The kinetics of the carburization at 786°C is characterized by a rate constant $k = 5.75 \cdot 10^{10}$ mol·cm^{-3}·s^{-1} which is independent of the carbon

DOI: 10.1007/978-3-540-74196-1_5

content (< 0.012 mass% C). The carburization reaction has an activation energy of 6.850 kJ whereas the reverse reaction (decarburization) has an activation energy of 25.7 kJ.
[1975Kan] demonstrated the possibility of decarburizing (< 0.002 mass% C) and denitrizing (< 0.0015 mass% N) liquid iron at 1700°C by blowing an Ar-H_2 plasma jet on the surface of the molten metal with a blowing rate of 8 $L \cdot min^{-1}$, and an electric power consumption of 15 to 30 kVA for a melt of 2 to 3 kg. The porosity of activated carbon is increased by the presence of iron acting as a catalyst [1999Sta]. The pore structure may be controlled by heat treatment during hydrogenation. An increase of the catalyst concentration is not accompanied by an increase of the hydrogenation rate [1997Sta], but by a change of the pore structure of the adsorbant.

Table 1. Investigations of the C-Fe-H Phase Relations, Structures and Thermodynamics

Reference	Method/Experimental Technique	Temperature/Composition/Phase Range Studied
[1959Hil]	Solubility and diffusion coefficient measurement after cold working	< 0.25 mass% C, < 200 ppm H, < 120 bar, < 400°C
[1961Mae]	Hydrogen solubility measurement by the sampling method	1570-1720°C, 0.1 MPa, liquid (Fe,C) alloy (< 5 mass% C)
[1963Wei]	Hydrogen solubility measurement by the Sievert's method	1592°C, 0.1 MPa, liquid (Fe,C) alloy (< 3.5 mass% C)
[1965Gra]	Kinetics of carburization - decarburization of iron under CH_4	928°C, < 0.1 MPa
[1965Sch]	Solubility and mobility measurement by an effusion method	350-1050°C, < 2 mass% C
[1969Bun]	Carbon activity measurements by equilibrium with H_2/CH_4 mixtures	1000-1100°C, < 8 mol% (2 mass%) C
[1971Vor]	Solubility measurements in γFe by X-ray diffraction measurements	900-1150°C, < 1.7 mass% C, < 3 bar of hydrogen pressure
[1972Ngi]	Solubility and activity measurements in liquid Fe by the Sievert's method	1550-1700°C, < 0.5 mass% C, 6500-13000 Pa of hydrogen pressure
[1973Gra]	Kinetics and thermodynamics of the reaction between αFe and CH_4	650-800°C, < 0.012 mass% C < 0.1 MPa of hydrogen pressure
[1973Sha]	Solubility of hydrogen in steel and cementite	600-1000°C, 6.7 mass% C, < 10 MPa of hydrogen pressure, < 0.01 mass% H
[1975Kan]	Improving intergranular corrosion resistance	Decarburizing and denitrizing molten iron at 1700°C under Ar-H_2 plasma jet
[1975Sha]	Solubility of hydrogen in steel	600-1000°C, 3.1 mass% C, < 10 MPa of hydrogen pressure, < 0.01 mass% H
[1978Sha1] [1978Sha3]	Phase diagram determination in the iron rich corner	690-720, 1100°C, < 1.9 mass% C, < 50 MPa of hydrogen pressure

(*continued*)

DOI: 10.1007/978-3-540-74196-1_5

Reference	Method/Experimental Technique	Temperature/Composition/Phase Range Studied
[1978Sha2]	Microscopic examination	Hydrogen influence on the pearlite formation and on the eutectoid temperature
[1984Fru]	Neutron diffraction, Curie temperature	20-650°C, Fe_3C under < 1 bar hydrogen pressure
[1986Cha]	Ductility, embrittlement, tensile strength measurements	Heat treatment < 1200°C, < 0.8 mass% C, < 1 bar of hydrogen pressure
[1990Uwa]	Mössbauer spectroscopy, martensitic transformation induced by hydrogen	25-140°C, < 1.9 mass% C, < 1 bar of hydrogen pressure
[1997Sta, 1999Sta]	Pore structure investigation by gas adsorption measurements	Fe-activated carbon, annealing < 850°C under 1 bar of hydrogen pressure

Table 2. Crystallographic Data of Solid Phases

Phase/ Temperature Range [°C]	Pearson Symbol/ Space Group/ Prototype	Lattice Parameters [pm]	Comments/References
(C) gr < 4492	*hP*4 $P6_3/mmc$ C (graphite)	*a* = 246.12 *c* = 670.9	pure C at 25°C [Mas2, V-C2] Sublimates at 3827°C
(C)d	*cF*8 $Fd\bar{3}m$ C (diamond)	*a* = 356.69	at 25°C, 60 GPa [Mas2]
α, (αδFe) (αFe) < 912	*cI*2 $Im\bar{3}m$ W	*a* = 286.65	pure Fe at 20°C [Mas2, V-C2]. Dissolves up to 0.096 at.% C at 740°C
(δFe) 1538 - 1394		*a* = 293.15	pure Fe at 1480°C [Mas2] Dissolves up to 0.40 at.% C at 1493°C
γ, (γFe) 1394 - 912	*cF*4 $Fm\bar{3}m$ Cu	*a* = 364.67	at 915°C [Mas2, V-C2] dissolves up to 9.06 at.% C at 1153°C
(εFe)	*hP*2 $P6_3/mmc$ Mg	*a* = 246.8 *c* = 396.0	at 25°C, 13 GPa [Mas2] Triple point α-γ-ε at 8.4 GPa, 430°C
α' (Fe,C)	*tI*4 *I*4/*mmm*	-	martensite, metastable [Mas2]
θ, Fe_3C 1252 - 230	*oP*16 *Pnma* Fe_3C	*a* = 452.48 *b* = 508.96 *c* = 674.43	[1972Chi, 1997Miz] Cementite, high pressure phase. Curie point at 214°C [1984Fru]

(*continued*)

DOI: 10.1007/978-3-540-74196-1_5

Phase/ Temperature Range [°C]	Pearson Symbol/ Space Group/ Prototype	Lattice Parameters [pm]	Comments/References
$\chi Fe_{2.2}C$ (or χFe_5C_2) < 230	*mC*28 *C*2/*c* B_2Pd_5	*a* = 1156.2 *b* = 457.27 *c* = 505.95 β = 97.74°	[1972Chi, V-C2] "Haegg carbide", metastable but more stable than cementite below 230°C
$\varepsilon Fe_{2.4}C$	*hP** $P6_322$	-	[1972Chi, Mas2] "ε carbide", metastable. Curie point at 370°C

Table 3. Thermodynamic Data of Reaction or Transformation

Reaction or Transformation	Temperature [°C]	Quantity, per mol of atoms [J, mol, K]	Comments
(C)gr ⇌ C(dissolved in αFe)	650-800°C	$\Delta_r G° = 68200 - 12.5\ T$	[1973Gra]
CH_4 ⇌ C(dissolved in αFe) + 2 H_2	650-800°C	$\Delta_r G° = 158200 - 121.78\ T$	[1973Gra]

DOI: 10.1007/978-3-540-74196-1_5

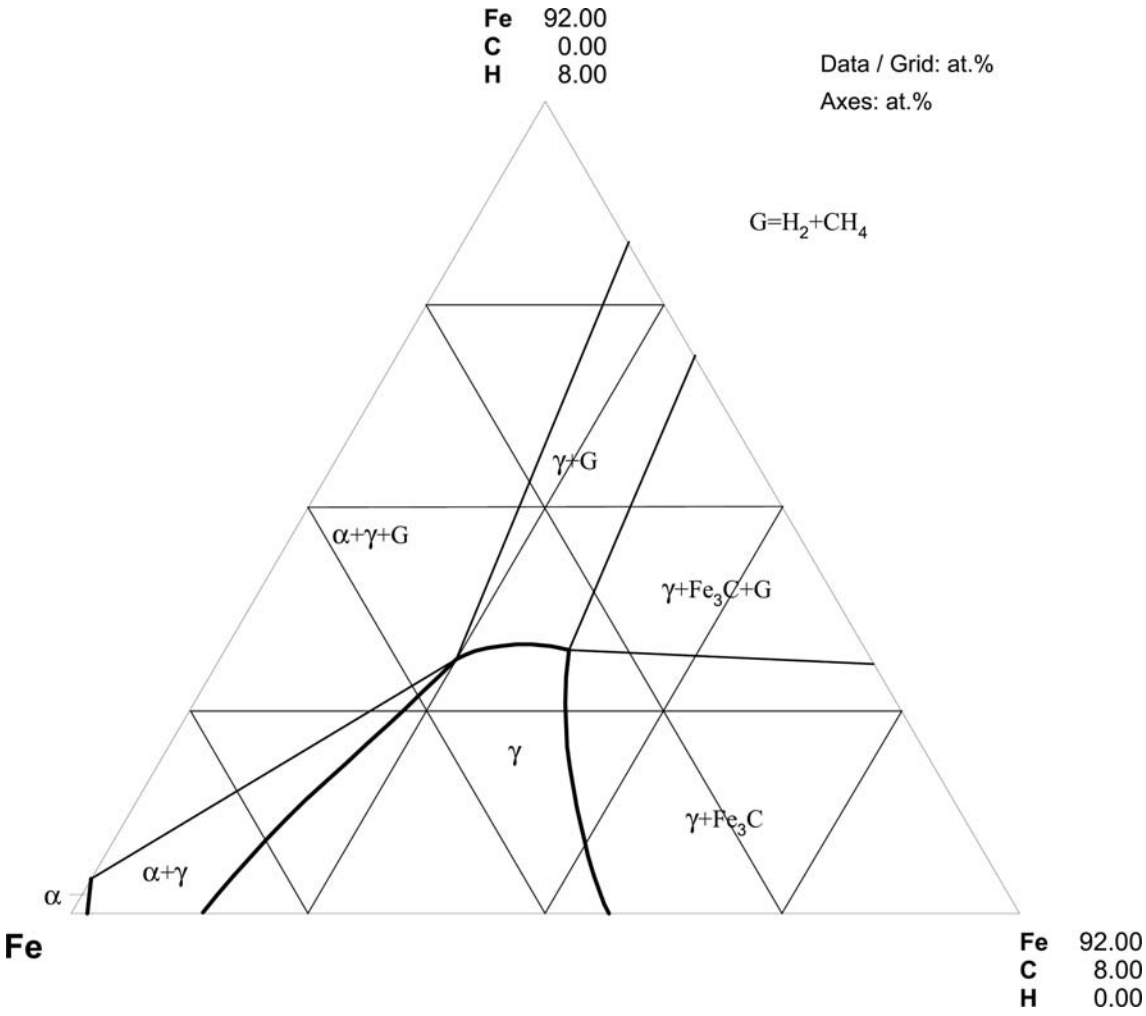

Fig. 1. C-Fe-H. Isothermal section at 820°C

DOI: 10.1007/978-3-540-74196-1_5

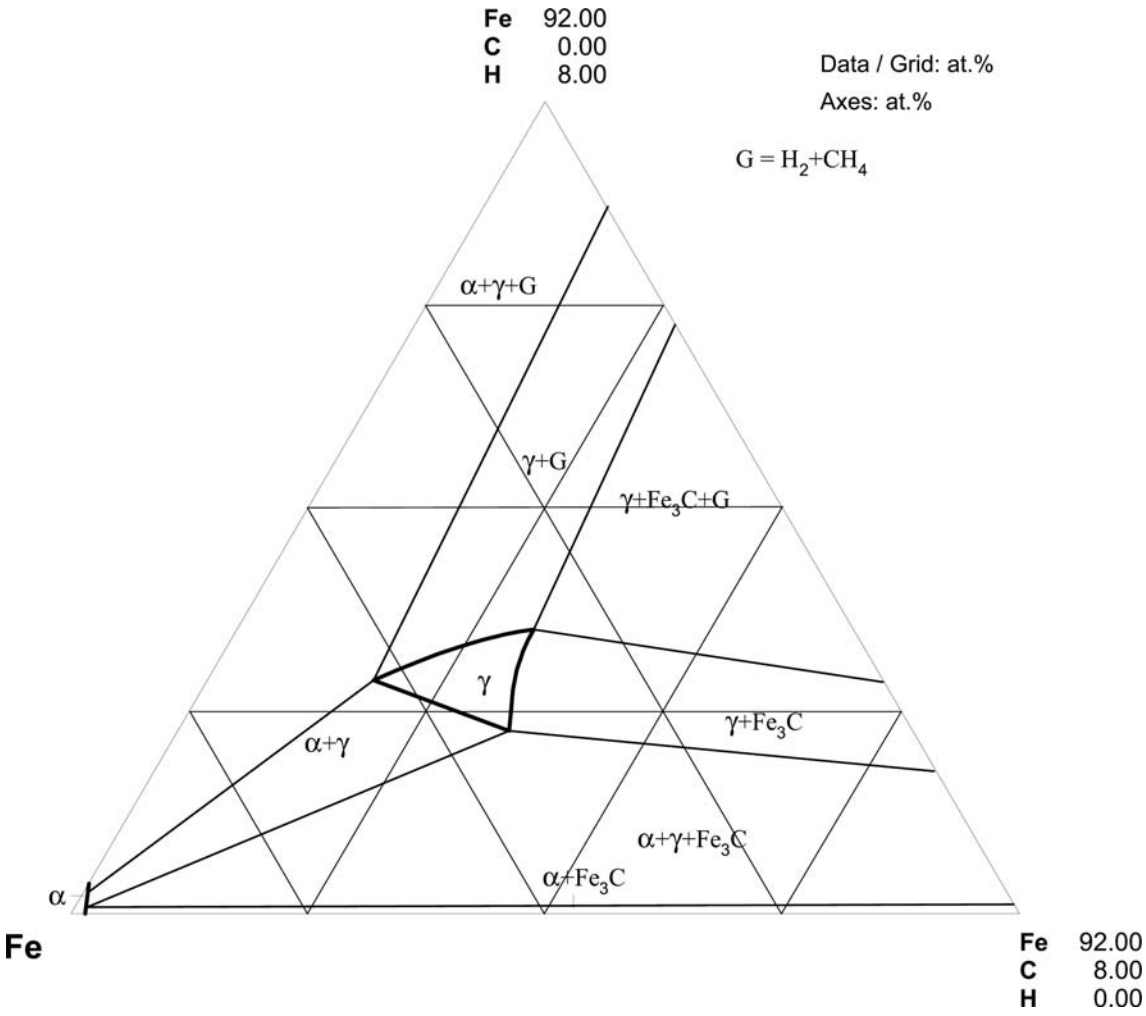

Fig. 2. C-Fe-H. Isothermal section at 715°C

DOI: 10.1007/978-3-540-74196-1_5

References

[1959Hil] Hill, M.L., Johnson, E.W., "Hydrogen in Cold Worked Iron-Carbon Alloys and the Mechanism of Hydrogen Embrittlement", *Trans. Metall. Soc. AIME*, **215**(4), 717–725 (1959) (Experimental, Morphology, Transport Phenomena, 33)

[1961Mae] Maekawa, S., Nakagawa, Y., "The Effect of Some Alloying Elements on the Solubility of Hydrogen in Liquid Iron" (in Japanese), *Nippon Kinzoku Gakkai-shi*, **25**(9), 577–580 (1961) (Experimental, Phase Relations, Thermodyn., 6)

[1963Wei] Weinstein, M., Elliott, J.F., "Solubility of Hydrogen in Liquid Iron Alloys", *Trans. Met. Soc. AIME*, **227**, 382–393 (1963) (Calculation, Experimental, Thermodyn., 27)

[1965Bur] Burylev, B.P., "Solubility of Hydrogen in Liquid Iron Alloys" (in Russian), *Izv. Vyss. Uchebn. Zaved., Chern. Metall.*, **8**(2), 17–22 (1965) (Phase Relations, Thermodyn., Review, 13)

[1965Gra] Grabke, H.-J., "The Kinetic of Decarbonization and Carbonization of (γ-Iron in Methane-Water-Mixture" (in German), *Ber. Bunsen-Ges. Phys. Chem.*, **69**(5), 409–414 (1965) (Kinetics, Experimental, 17)

[1965Sch] Schwarz, W., Zittter H., "Solubility and Diffusion of Hydrogen in Iron Alloys" (in German), *Arch. Eisenhuettenwes.*, **36**(5), 343–349 (1965) (Experimental, Thermodyn., Transport Phenomena, 16)

[1969Bun] Bungardt, K., Schuermann, E., Preisendanz, H., Schueler, P., Psing, H.-J., "Determinartion of the Solubility of C and of Phase Boundaries in the Fe-Mo-C System by Activity Measurements in the Temperature Region 1000-1100°C" (in German), *DEW Techn. Ber.*, **9**(4), 439–462 (1969) (Experimental, Phase Relations, Thermodyn., 65)

[1971Vor] Vorob'ev, G.M., Grechny, Ya.V., Rufanov, Yu.G., "The Influence of Hydrogen to the Solubility of Carbon in γ-Iron" (in Russian), *Izv. Vyss. Uchebn. Zaved., Chern. Metall.*, **14**(6), 124–127 (1971) (Experimental, Morphology, Phase Relations, 15)

[1972Chi] Chipman, J., "Thermodynamics and Phase Diagram of the Fe-C System", *Metall. Trans.*, **3**, 55–64 (1972) (Thermodyn., Phase Diagram, Review, 66)

[1972Ngi] Ngia, N., Yavoyskiy, V.I., Kosterev, L.B., Afanas'yev, M.I., "Hydrogen Solubility in Binary Iron-Base Alloys", *Russ. Metall.*, (4), 11–15 (1972), translated from *Izv. Akad. Nauk SSSR, Met.*, (4), 18–22 (1972) (Experimental, Phase Relations, Thermodyn., 19)

[1973Gra] Grabke, H.J., Martin, E., "Kinetics and Thermodynamics of the Carburisation and Decarburisation of α-Iron in CH_4-H_2 Mixtures" (in German), *Arch. Eisenhuettenwes.*, **44**(11), 837–842 (1973) (Calculation, Experimental, Kinetics, Thermodyn., 16)

[1973Sha] Shapovalov, V.I., Grechnyi, Ya.V., Ksaverchuk, L.P., "Solubility of Hydrogen in Solid Iron-Carbon Alloys", *Steel USSR*, **3**(9), 789–791 (1973) (Experimental, Phase Relations, 10)

[1975Kan] Kaneko, K., Sano, N., Matsushita, Y., "Decarburization and Denitrogenization of Iron And Iron-Chromium Alloys by Hydrogen Plasma" (in Japanese), *J. Fac. Eng., Univ. Tokyo*, **A-13**, 60–61 (1975) (Experimental, Phase Relations, Thermodyn., 2)

[1975Sha] Shapovalov, V.I., "Thermodynamics of the Solubility and the Effect of H on the Phases of Fe-C Alloys", *Termodinam. Svoistva Metal. Splavov*, 270–274 (1975) (Experimental, Phase Relations, Thermodyn., 8)

[1978Sha1] Shapovalov, V.I., Poltoratskij, L.M., "On Fe-C-H Phase Diagram" (in Ukrainian), *Dop. Akad. Nauk Ukr. RSR, A*, (6), 566–569 (1978) (Experimental, Crys. Structure, Phase Diagram, 10)

[1978Sha2] Shapovalov, V.I., "Influence of Hydrogen on the Eutectoid Transformation in Iron-Carbon Alloys", *Phys. Met. Metallogr.*, **46**(3), 183–185 (1978), translated from *Fiz. Metal. Metalloved*, **46**(3), 664–666 (1978) (Experimental, Phase Relations, Morphology, 8)

[1978Sha3] Shapovalov, V.I., Poltoratskii, L.M., "The Iron-Carbon-Hydrogen Phase Diagram", *Steel USSR*, **8**(6), 356–357 (1978), translated from *Izv. VUZ. Chern. Met.*, **6**, 117–120 (1978) (Experimental, Phase Diagram, 14)

[1980Fro] Fromm, E., Hoerz, G., "Hydrogen, Nitrogen, Oxygen, and Carbon in Metals", *Int. Mater. Rev.*, (5/6), 269–312 (1989) (Kinetics, Phase Diagram, Review, Thermodyn., 255)

DOI: 10.1007/978-3-540-74196-1_5

[1981Rag] Raghavan, V., "The C-Fe-H (Carbon-Iron-Hydrogen) System", in "*Phase Diagrams of Ternary Iron Alloys*", Indian Inst. Met., **6A**, 505–507 (1981) (Phase Diagram, Phase Relations, Review, #, 4)

[1981Sch] Schuermann, E., Kaettlitz, W., "Equivalent Effect of the Alloying Elements on the Concentration- and Temperature-Dependent Hydrogen Solubility in Iron-Rich Ternary and Multicomponent Melts" (in German), *Arch. Eisenhuettenwes.*, **52**(8), 295–301 (1981) (Calculation, Experimental, Phase Diagram, 20)

[1984Fru] Fruchart, D., Chaudouet, P., Fruchart, R., Rouault, A., Senateur, J.P., "Structural Studies on Cementite-Type Compounds: Effects of Hydrogen on Fe_3C Followed by Neutron Diffraction. Moessbauer Spectroscopy on $FeCo_2B$ et Co_3B Doped with Fe-57", *J. Solid State Chem.*, **51**, 246–252 (1984) (Crys. Structure, Experimental, 35)

[1986Cha] Chan, S.L.I., Charles, J.A., "Effect of Carbon Content on Hydrogen Occlusivity and Embrittlement of Ferrite-Pearlite Steels", *Mater. Sci. Technol.*, **2**, 956–962 (1986) (Experimental, Mechan. Prop., 26)

[1990San] San Martin, A., Manchester, F.D., "The Fe-H (Iron-Hydrogen) System", *Bull. Alloys Phase Diagrams*, **11**(2), 173–184 (1990) (Phase Diagram, Review, Thermodyn., 86)

[1990Uwa] Uwakweh, O.N.C., Bauer, Ph., Genin, J.M.R., "Moessbauer Study of the Hydrogen Induced Martensitic Transformation in High Carbon Fe-C Martensite and its Ageing Behaviour", *Hyperfine Interact.*, **54**, 877–882 (1990) (Experimental, Electrochemistry, Electronic Structure, 4)

[1992Oka] Okamoto, H., "The C-Fe (Carbon-Iron) System", *J. Phase Equilib.*, **13**(5), 543–564 (1992) (Phase Diagram, Crys. Structure, Thermodyn., Review, #, 242)

[1997Miz] Mizuno, M., Tanaka, I., Adachi, H., "Effect of Solute Atoms on the Chemical Bonding of Fe_3C (Cementite)", *Philos. Mag. B*, **75**(2), 237–248 (1997) (Crys. Structure, Mechan. Prop., Theory, 28)

[1997Sta] Stavinskaya, O.N., Shklovskaya, N.I., "Variations in the Porous Structure of Iron-Containing Carbons During Hydrogenation", *Russ. J. Phys. Chem.*, **71**(9), 1497–1503 (1997), translated from *Zh. Fiz. Khim.*, **71**(9), 1665–1671 (1997) (Experimental, Catalysis, Morphology, 9)

[1999Din] Ding, X., Fan, P., Wang, W., "Thermodynamic Calculations for Alloy Systems", *Met. Mat. Trans., B*, **30B**(2), 271–277 (1999) (Thermodyn., Calculation, Assessment, Review, 17)

[1999Pil] Pilous, V., Foret, R., Stransky, K., "Redistribution of Hydrogen in Steel Weldments Part. 1. Fe-H-C-i Austenite/Austenite Type Weldments", *Met. Mater.*, **37**(2), 61–67 (1999), translated from *Kovove Mater.* **37**(2), 85–95 (1999) (Transport Phenomena, Theory, 10)

[1999Sta] Stavinskaya, O.N., Shklovskaya, N.I., "Some Features of Activation of Synthetic Carbons by Iron-Catalyzed Hydrogenation", *Russ. J. Appl. Chem.*, **72**(5), 783–787 (1999), translated from *Zh. Prikl. Khim.*, **72**(5), 751–755 (1999) (Experimental, Catalysis, Phys. Prop., 13)

[2000Pil] Pilous, V., Foret, R., Stransky, K., "Redistribution of Hydrogen in Steel Weldments Part II. Fe-H-C-i Ferrite-Austenite Type Weldments", *Metal. Mater.*, **38**(2), 82–91 (2000), translated from *Kovove Mater.*, **38**(2), 116–129 (2000) (Transport Phenomena, Phys. Prop., Theory, 11)

[2003Fuk] Fukai, Y., Mori, K., Shinomiya, H., "The Phase Diagram and Superabundant Vacancy Formation in Fe-H Alloys under High Hydrogen Pressures", *J. Alloy Compd.*, **348**, 105–109 (2003) (Phase Relations, Experimental, 42)

[2005Hir] Hiroi, T., Fukai, Y., Mori, K., "The phase Diagram and Superabundant Vacancy Formation in the Fe-H Alloy Revisited", *J. Alloys Compd.*, **404/406**, 252–255 (2005) (Phase Relations, Experimental, 42)

[2006MSIT] "C-Fe (Iron-Carbon)", Diagrams as Published, in *MSIT Workplace*, Effenberg, G. (Ed.), Materials Science International Services, GmbH, Stuttgart; Document ID: 30.13598.1.20 (2006) (Crys. Structure, Phase Diagram, Phase Relations, 2)

[Mas2] Massalski, T.B. (Ed.), *Binary Alloy Phase Diagrams*, 2nd edition, ASM International, Metals Park, Ohio (1990)

[V-C2] Villars, P., and Calvert, L.D., *Pearson's Handbook of Crystallographic Data for Intermetallic Phases*, 2nd edition, ASM, Metals Park, Ohio (1991)

DOI: 10.1007/978-3-540-74196-1_5

Carbon – Iron – Manganese

Viktor Kuznetsov

Introduction

Manganese is one of the most common alloying elements in steels. There is a very large number of investigations of the system C-Fe-Mn. First investigations of phase equilibria were performed as early as 1909 [1909Goe, 1909Wue] and much work was done since that. The results obtained until the end of 40th [1910Arn, 1932Bai, 1933Eck, 1933Gen, 1933Wel, 1935Wel, 1936Wal, 1937Tof] were briefly reviewed by [1949Jae]. Unfortunately, as it is known now, early investigations were based on incomplete versions of binary edges, especially for the C-Mn. More results were obtained by [1951Iso, 1954Kuo, 1964Koc, 1974Sil, 1976Kle, 1976She, 1977Nis, 1977Sch, 1985Koc, 1988Mag, 2005Sil1]. Solubility of C in liquid Fe-Mn alloys also was measured by many authors [1952Chi, 1952Tho, 1955Tur, 1956Tur, 1957San, 1959Pet, 1963Sch, 1969Sch, 1977Sos, 1980Tan4, 1990Ni1, 1990Ni2]. [2005Wan] measured it under reduced pressure (1 Pa) at 1300 and 1400°C. Nevertheless, some important features of the system remain rather unclear.

[1990Put] studied phase equilibria in the carbon rich part of the system (70 to 100 at.% C) at 827°C under pressures of 5 and 6 GPa.

Elder data on phase relations were reviewed and critically assessed by Raynor and Rivlin [1988Ray], who in turn refer to several older reviews and assessments. They suggested best choice versions of liquidus projection, including position of tie-triangles for some solid-liquid monovariant equilibria, Scheil scheme and a number of isothermal sections for 1100 to 600°C. This assessment was updated by [1994Rag], who included literature up to 1991.

Being close chemical analogues, Fe and Mn do not form ternary compounds. Moreover, for all rather numerous Mn carbides, except $Mn_{23}C_6$, their Fe counterparts are known, though either as metastable phases (cementite Fe_3C, Haegg carbide Fe_5C_2) or under high pressure (Fe_7C_3). Analogous carbides of Mn and Fe form continuous solid solutions provided both binary compounds exist, *i.e.* either in metastable systems like one with Fe_3C, or under high pressure conditions. Large solubility of Fe in manganese carbides is observed in all the cases.

Lattice parameters of the ternary χ carbide $(Mn,Fe)_5C_2$ were measured by [1944Oeh, 1966Dug, 1966Jac], for ε phase and $(Mn,Fe)_{23}C_6$ by [1973Ben] and for ternary cementite phase $(Fe,Mn)_3C$ by [1966Dug, 1973Ben, 1977Arb, 1979Kag]. [1990Put] determined lattice parameters for continuous solid solution Fe_7C_3-Mn_7C_3 obtained at 6 GPa at 827°C (measurements were done under atmospheric pressure at room temperature).

Numerous thermodynamic studies of C-Fe-Mn alloys are discussed below in the Thermodynamics section.

Martensite transformations also attracted much attention. The interest to those is to some extent due to the existence of a series of transitions γ → α, γ → ε and ε → α in a narrow concentration range. Structural aspects were studied by [1958Mas] as well as by [1971Izo, 1972And, 1972Dua] (orientation relations), [1976Bog, 1978Shi, 1980Tan1, 1985Nik] (formation of multilayered 15*R*2-packing), [2002Sah] (structure of athermal martensite) and [2005Mor] (influence of grain size of austenite on morphology and structure of resulting martensite). Kinetics and mechanisms were studied by [1947Hul, 1972Oka, 1973Oka]. Various aspects of martensite transformations were also studied by [1976Osh, 1980Tan2, 1984Pro, 1984Sch, 1992Kak, 2000Lu]. [2003Kap] reviews a series of investigations of structure and phase transformations under quenching and tempering during heat and thermomechanical treatment of Mn containing steels.

Mechanisms and kinetics of ordinary (non-martensitic) phase transformations were studied in a number of works. Kinetics of formation of various carbide phases was investigated by [1963Bor, 1973Gri, 1981Tan] (from martensite during tempering at 85°C), [1982Sar, 1987Spa, 1990Rey, 2006Aar] (effect of incompleteness of bainite transformation), [1998Vya] (crystallography and morphology of Widmanstaetten cementite), [2002Cap] (model description of kinetics of pearlite formation), [2004Hut1, 2004Hut2] (kinetics of formation and growth of pearlite). Transformations of non-equilibrium (quenched, including martensitic) phases

DOI: 10.1007/978-3-540-74196-1_6

were studied kinetically by [1965Sai, 1981Wyc, 1982Kaj, 1982Sou, 1983Pri, 1983Sha, 1984Est, 1986Eno, 2004Aar, 2005Mas]. [1998Zha] discovered new orientation relation between Widmanstaetten cementite and austenite matrix. [1989Liu] and [2000Koz1] investigated whether the equilibrium conditions on moving boundaries is a local equilibrium or paraequilibrium. The data for the latter were obtained by calculation based on CALPHAD assessment. [2002Lee] used high-temperature metallography for direct observation of α to γ transformation. [2001Cha] and [2005Cha] used phase field model for simulation of microstructure formation during solidification. [2005Gam] performed calculation of $\gamma \rightarrow \alpha$ transformation kinetics in low-alloyed Fe basing on models accounting for interface mobility and bulk diffusion.
[1964Bro] and [1971Shc] measured diffusion of C in austenite. [1979Ben] did so for Mn diffusion in liquid phase; [1981Wan] studied interdiffusion in melts. Various aspects of interplay of diffusional effects and phase equilibria were studied by [2001Lee] and [2003Gam].
[1990Put] tested mixed carbide $(Fe,Mn)_7C_3$ for catalytic activity in the synthesis of diamond.
Recent (appeared after 1990, *i.e.* after assessment [1994Rag]) investigations of phase equilibria, structures and thermodynamic properties are reviewed in Table 1.

Binary Systems

Phase diagrams for the C-Mn and Mn-Fe binary systems are accepted from [Mas2]. The C-Fe system, as suggested by MSIT very recently [2006MSIT], differs from [Mas2] only in the position of liquidus of the fcc phase, which is accepted from [2001Fen].

Solid Phases

Crystallographic data for solid phases and their temperature ranges of stability are listed in Table 2. No ternary phases are known in the system. The Fe counterparts of Mn carbides, which are known in metastable or pressure stabilized forms, are included in Table 2 as end-members of the corresponding phases, even when concentration range of stability of the phase does not reach C-Fe side.
The ε phase in the C-Mn binary is accepted to be an interstitial solid solution of C in a virtual hcp modification of Mn, as follows from the lattice parameters data of [1973Ben] and was accepted in the calculation [1990Hua2], on which [Mas2] is based. The suggestion of the NiAs structure, made for this phase by the editor in [V-C2], seems to be erroneous.
Concentration dependencies of the lattice parameters for $(Fe,Mn)_{23}C_6$ [1973Ben], $(Fe,Mn)_5C_2$ (χ-carbide) [1966Dug, 1966Jac] and for $(Fe,Mn)_7C_3$ [1990Put] are listed in Table 2. They seem to be linear within experimental errors, especially in the latter case.
Neutron diffraction study of χ-carbide $(Fe_{0.22}Mn_{0.78})_5C_2$ and alloyed cementite $(Fe_{0.6}Mn_{0.4})_3C$ [1966Dug] revealed a virtually random distribution of Fe and Mn atoms in the crystal structure.
[1966Jac] noted a similarity of structures of cementite and χ-carbide, which consist in approximate equalities $a(\text{cem}) \approx b(\chi)$ and $b(\text{cem}) \approx c(\chi)$. A review of crystal structures of Fe and Mn carbides is presented in [1977Nov, 1977Tar].
Structural and lattice space data for non-equilibrium martensite phases are given in [1968Als, 1976Bog, 1980Tan1, 1985Nik, 2002Sah].

Invariant Equilibria

The CALPHAD calculation [1990Hua1], accepted in this evaluation for the system for reasons discussed below (see *Liquidus, Solidus and Solvus Surfaces*), does not contain any information about either calculated invariant equilibria or reaction scheme, though those in principle could be obtained from published model parameters. Fortunately, [1994Rag] presented a version of the Scheil reaction scheme based on the earlier assessment by [1988Ray] but modified to bring it into agreement with [1990Hua1]. This version is accepted and presented in Fig. 1 with small corrections to achieve reasonable agreement with [1990Hua1].
Data for invariant reactions with the participation of the liquid phase, presented in Table 3, are taken from the reaction scheme (temperatures) and from the temperature projection of liquidus [1990Hua1]. Unfortunately, no data seem to be published for the compositions of the solid phases participating in any of invariant

DOI: 10.1007/978-3-540-74196-1_6

reaction, so the phase compositions in Table 3 are given for the liquid phase only. For reactions U_5 to U_7 taking place in the solid state only the temperatures are presented for the same reason.
Figures 2 and 3 present calculated compositions of the γ phase participating in the monovariant eutectoid reaction $\gamma \rightleftharpoons \alpha + M_3C$ [1990Hua1]. Figure 3 is constructed in the coordinates *T*/K *vs* mass% Mn in γ phase, whereas in Fig. 4 the same calculated data are presented on a plane mass% C - mass% Mn in γ phase.

Liquidus, Solidus and Solvus Surfaces

Calculated liquidus projection achieved in the computer assessment of [1990Hua1] is not in a very good agreement with its assessed version presented by [1988Ray]. The latter is based almost solely on the results of [1977Sch]. However, [1990Hua1] showed that liquidus data of [1977Sch] are not compatible with corresponding assessed and experimentally well supported data [Mas2, 1993Oka] for the Fe-Mn binary system. Moreover, parameters of models of the phases obtained by [1990Hua1] provide good description of thermodynamic properties of both liquid and solid phases. For these reasons we prefer the results of [1990Hua1] and recommend those against [1988Ray]. Of course, a new experimental investigation of melting equilibria is highly desirable.
Figure 4 presents a calculated liquidus surface projection onto the composition plane, and in Fig. 5 the same liquidus surface is projected in the direction of the ratio of C content to the total contents of metals, *i.e.* onto the plane *T*/K *vs* mass ratio of metals $x_{Mn}/(x_{Mn}+x_{Fe})$ (x_{Mn}, x_{Fe} are mass% of components). Both are taken from [1990Hua1]; the latter is modified to get a better agreement with the reaction scheme.
Figure 6 displays calculated solubility of graphite in Fe-Mn melts at 1290 to 1690°C [1990Hua1]. They show good agreement with experimental data presented as points.

Isothermal Sections

Isothermal sections calculated by [1990Hua1] from optimized parameters of models of phases are generally in fairly good agreement with corresponding published experimental data. [1990Hua1] noticed also good agreement of the calculated and experimental distribution coefficients for γ and M_3C as well as α and M_3C phases. Very good agreement was noticed also between the calculated and experimental positions of the above mentioned monovariant eutectoid line of $\gamma \rightleftharpoons \alpha + M_3C$, though the experimental data for the latter were not included in the optimization. So, these calculated results are accepted.
Figures 7 to 11 present isothermal sections respectively at 1100, 1000, 900, 800 and 600°C. Newer distribution data by [2005Sil1] as well as the calculations of various sections of phase diagram based on them [2005Sil2, 2005Sil3] are in strong disagreement with the accepted version. These data are rejected as experimental technique used (chemical analysis of carbides in the samples quenched from different temperatures to distinguish between the primary and the eutectoid cementite) is hardly more reliable than EPMA used in all other works.
Figure 12 presents a partial isothermal section at 927°C under a pressure of 5 GPa for the compositions above 30 at.% C [1990Put]. Information for the C content below 30 at.% is absent. Analogous partial section at the same temperature under 6 GPa obtained for the same concentration region in this work contains only continuous solid solution between stable under those conditions Fe_7C_3 and Mn_7C_3 and a two-phase region M_7C_3 + (C)d.

Temperature – Composition Sections

The data for a number of partial vertical sections of the system presented in [1936Wal] were not mentioned anyhow in the assessments [1988Ray, 1994Rag]. [1990Hua1] also did not included them in optimization. The reason of that seems to be the absence of any carbide phases in the region where M_3C should exist as indicated by all other data. So the results of [1936Wal] are not presented here.

Thermodynamics

First thermodynamic study of the system was performed by [1939Sch] by equilibrating Fe-Mn alloys with a mixture H_2/CH_4. Activities of carbon were also measured using the same method by [1948Smi] at 1000°C,

DOI: 10.1007/978-3-540-74196-1_6

by [1960Pet, 1971Tum, 1972Wad] at 850-1147°C, and by [1972Wil] and [1994Prz] who used different carburizing mixtures. All these data were obtained in the solid state. For liquid alloys these values were measured by [1989Dre] and [2003Kim]. [1959Neu] gives a general review of thermodynamic data of carbon in iron and its alloys. Activity of Mn for solid alloys was determined by [1974Ben] and for liquid alloys by [1966Pet, 1980Tan3, 1995Eno]. [1988Hea] compared results of integration of Gibbs-Duhem equation for published data for C activity against published Mn activity in liquid alloys and found satisfactory agreement. Enthalpy of formation was determined for melts by [1993Wit] at 1627°C in the whole range of existence of the liquid phase at this temperature. The results of investigations of solubility of C are usually treated in thermodynamic terms [1955Tur, 1956Tur, 1959Pet, 1990Ni1, 1990Ni2, 2005Wan].

[1978Cho] used phase equilibria in the ternary and data for the C-Fe binary to derive model free estimates of thermodynamic properties of Mn_3C, $Mn_{23}C_6$ and ternary cementite phase.

The system was extensively studied by CALPHAD method. Early calculations (some of which appeared before invention of the term "CALPHAD") include calculations of graphite solubility [1958Koz, 1977Sos] (see also the above mentioned thermodynamic treatment of graphite solubility data). [1977Uhr, 1978Uhr] performed systematic least squares analysis of published data for C activity for austenite, and [1977Hil1, 1977Hil2] assessed the properties of α, γ, M_3C (cementite) and $M_{23}C_6$ phases using experimental information on phase equilibria and thermodynamic properties and calculated phase equilibria between them. The latter authors applied trial and error approach. [1989Lee] revised their description including all stable solid phases. [1990Hua1] performed detailed CALPHAD assessment of the system, basing on his thorough revision of the C-Mn system [1990Hua2] and on cautious analysis of published data. He achieved good general description of thermodynamic data and of solid state phase equilibria, though difficulties arose in reproducing melting equilibria. As corresponding published data proved to be poorly compatible with accepted Fe-Mn binary, which had experimental support, the liquidus projection [1988Ray] had to be rejected. In addition, critical analysis of data of [1973Ben] revealed that diffusional length of Mn during applied annealing time is quite insufficient for achieving equilibrium, and these data were rejected.

There exist also other assessments of thermodynamic properties of the liquid phase [1995Bou] (simultaneous assessments of several systems), and [1997Li, 2003Lee1]. [1995Lee] successfully used the results of [1990Hua1] to calculate multicomponent stainless steels. Results of the CALPHAD type calculations were also used for analysis of paraequilibria in a course of the studies of mechanisms of some phase transformations [1972Gil, 1989Liu, 2000Koz2], and for rationalization and prediction of temperature A_s of martensite transformations [1986Cha, 2000Kun]. They were used also to calculate coherent equilibria [1991Liu]. Some calculations were performed just for testing theoretical models and methods as examples [1985Eno, 1987Sch, 1988Zhu, 1989Zhu, 1998Lee, 2001Ma, 2001Wan, 2003Zhu]. A calculation [2005Sil2, 2005Sil3], based on distribution coefficients of Mn between solid solutions and carbides, is performed with incomplete set of carbide phases (only cementite and χM_5C_2 were taken into account).

[1988Dur] suggested polynomial description of Fe rich part of liquidus surface.

Figure 13 presents calculated but having experimental support Mn activities in the liquid phase in the Mn rich region of the system at 1400°C [1990Hua1]. Newer measurements by [1961But, 1995Eno] seem not to contradict with these results.

New data for C activities in liquid alloys [1989Dre, 1994Prz, 2003Kim] also seem to be in general agreement with the accepted calculation.

Enthalpies of formation of liquid at 1627°C measured by [1993Wit] and reproduced by [1994Wit] are presented only on a small scale graph. This graph is reproduced in Fig. 14. It should be noted, that these results are not in good agreement with more recent binary data for the Fe-Mn system obtained by the same author [2004Wit], so their real precision is not clear. For this reason we did not include the data for partial enthalpies of components, which were also presented in the original paper (also on a small scale graphs), as partial values are usually more error prone.

Calculated by [1990Hua1] carbon activities in the fcc phase, which also have good experimental support are presented in Fig. 15 for 1147°C and in Fig. 16 for 1000°C.

DOI: 10.1007/978-3-540-74196-1_6

Notes on Materials Properties and Applications

[1927Had] studied mechanical properties of manganese steel. [1968Grz] suggested to use C-Fe-Mn alloys for brazing; he studied wettability, as well as morphology and mechanical properties of joins. [1968Jol] studied impact properties of manganese steels. [1979Bul] investigated effect of superplasticity.
[1979Kor] studied relations of stability of ferromanganese containing carbon against water vapor during storage with its phase composition. They found that Haegg carbide Mn_5C_2 formed in ferromanganese with < 5% Fe reacts with H_2O and makes the alloy unstable, whereas cementite does not. Chemical composition of gaseous products of reaction was also studied.
[1985Kho] investigated mechanical properties of manganese austenitic steels under cryogenic conditions.
Damping capacity of manganese steels were investigated by [1998Jun] and [2003Lee2].
[1999Owe] and [2000Abe] studied processes during strain hardening of Hadfield steel, including influence of distribution of C atoms on dislocation mobility. Analysis of plasticity mechanisms of manganese steel was performed also by [2004All].
[2003Roc] tested mechanical properties of the mechanically alloyed Mn steels.
Various aspects of interplay of morphology and mechanical (including tensile) properties of alloys of the system are discussed by [1977Sil, 2004Fu, 2006Sil].
[1990Put] found that mixed carbide $(Fe,Mn)_7C_3$ exhibit catalytic effect on transformation of graphite to diamond at 6 GPa and 1427°C.
A number of electrical properties of C-Fe-Mn alloys were measured by [1939Nem] in a course of physico-chemical study of phase relations. [1968Aks] studied resistivity of C-Fe-Mn alloys in the temperature range 1000 to 1500°C. [1940Wev] measured magnetic properties of alloys. Interplay of magnetization and thermal expansion of Fe-Mn and C-Fe-Mn alloys was investigated by [1988Sta].

Miscellaneous

Data for lattice parameters of cementite $(Fe,Mn)_3C$ are summarized in Fig. 17. They are close to linearity, but closer look reveals a slight minima of parameters a and c (but not b) at about 10 mol.% Mn_3C, noted by [1966Dug] and confirmed by all other data. These minima correspond to composition, at which Curie point of cementite reaches room temperature [1966Dug, 1979Kag].
[1985Liu] briefly presents results of the investigation of banding phenomena in the C-Fe-Mn alloys which arise during hot rolling.
[1989Bug] studied distribution of C atoms in austenite phase using theoretical treatment of Mössbauer data.
[1992Gav] studied mechanisms of internal friction in ferrous martensite. [1992Joa] studied morphology of bainite in a 0.2C-1.5Mn steel. [1996Vya] and [1998Vya] investigated surface phase transitions appearing in a course of phase transformations.
[1986Lad] performed Mössbauer study of austenite retained after martensitic transformation. [1986Lad] and [1994Oda] investigated distribution of C in austenite between positions with various number of Fe and Mn neighbor atoms and estimated difference of interaction energies C-Fe and C-Mn. [1988Sum] used neutron diffraction for investigation of local oscillations of C atoms in austenite. [1990Sum] used the same technique to study lattice dynamics of austenite phase.
[1974Arb] used X-ray spectroscopy to study electronic structure of Mn and several its compounds, $(Fe_{0.64}Mn_{0.36})_3C$ among them. [1975Shi1] and [1975Shi2] measured thermal expansion and Invar properties of alloyed cementite $(Fe,Mn)_3C$. [2001Ume] reported synthesis of bulk cementite and measured some its physical properties, such as hardness, Young modulus for $(Fe_{1-x}Mn_x)_3C$ with x = 0 to 0.3, as well as thermal expansion coefficient for 25 to 1000°C and C_p at –100 to 800°C on a sample with x = 0.2.

DOI: 10.1007/978-3-540-74196-1_6

Table 1. Recent Investigations of the C-Fe-Mn Phase Relations, Structures and Thermodynamics

Reference	Method / Experimental Technique	Temperature / Composition / Phase Range Studied
[1989Dre]	C activity from equilibration of liquid with MnO containing slag and with CO containing gas phase	1400 to 1800°C, 70 and 80 mass% Mn, to 8 mass% C
[1990Ni1], [1990Ni2]	C solubility in melts	1400 and 1500°C, 0 to ~9 mass% Mn
[1990Put]	Metallography, XRD	827°C, 5 and 6 GPa, 70 to 100 at.% C
[1993Wit]	C partial enthalpy, enthalpy of formation, isoperibolic calorimetry	1627°C, 0 to 100% Mn, C up to saturation
[1994Prz]	C activities by equilibration with gas phase	900°C, to 1.55% C, 1.7% Mn
[1995Eno]	Mn activities by distribution between Fe and Ag	1463, 1500 and 1550°C, 0 to 0.45 Mn, C up to saturation
[1998Zha]	XRD, orientation relation	13 to 29 mass% Mn, 380 to 600°C
[2000Cho]	Metallography, SEM	0.44 and 0.95 mass% C, 1.25% Mn
[2000Lu]	Resistivity, dilatometry, tensile properties, metallography	Fe-24Mn alloys, C 0.014 to 0.9%
[2001Ume]	Mechanical alloying plus spark plasma sintering (synthesis); XRD, metallography, SEM, TEM, DSC	$(Fe,Mn)_3C$ with Mn to 30%; hardness and Young modulus at room temp., thermal expansion at 20% Mn, 25 to 1027°C, heat capacity at 20% Mn, –100 to 800°C
[2002Cap]	Metallography, XRD	0.4C-1.6Mn steel
[2002Lee]	Optical microscopy	0.004% C, 1 to 6% Mn, cooling rate 0.5 to 18 °C/s
[2002Sah]	Athermal martensite transition, XRD, microhardness	5.6 to 6% Mn, transformation temperature 77 to 200 K
[2003Kim]	Equilibration of melt with MnO containing slag and CO containing gas mixture with known C activity	1400 to 1500°C, 4.5 to app. 28 mass% Mn, up to 7 mass% C
[2004Hut1]	Metallography	0.85 mass% C, 11.56 mass% Mn, 640 to 675°C
[2004Hut2]	TEM, EPMA (analytical TEM)	0.85 mass% C, 11.56 mass% Mn, 575 to 650°C
[2005Mor]	Optical microscopy, SEM with electron backscattered diffraction pattern detector (electronography), TEM	0.2% C, Mn to 2%

(*continued*)

DOI: 10.1007/978-3-540-74196-1_6

Reference	Method / Experimental Technique	Temperature / Composition / Phase Range Studied
[2005Sil1]	Mn distribution between metal phases and cementite by chemical analysis of carbide phases	White iron with 0.26 to 35.7 mass% Mn, ~2.7 mass% C; also contained ~0.2 to 0.76 mass% Si and small amounts of S and P (~10^{-5}%)
[2005Wan]	Chemical analysis of samples quenched after equilibration with graphite in vacuum ~1 Pa	1300 and 1400°C, Mn to app. 66 mass%

Table 2. Crystallographic Data of Solid Phases

Phase/ Temperature Range [°C]	Pearson Symbol/ Space Group/ Prototype	Lattice Parameters [pm]	Comments/References
(C)d	*cF*8 $Fd\bar{3}m$ C (diamond)	a = 356.69	at 25°C, 60 GPa [Mas2]
(C)gr < 3827	*hP*4 $P6_3/mmc$ C (graphite)	a = 246.12 c = 670.90	at 25°C [Mas2] sublimation point
(δFe) 1538 - 1394	*cI*2 $Im\bar{3}m$ W	a = 293.15	dissolves up to 10 at.% Mn, up to 0.4 at.% C [Mas2]
γ, $(Mn_{1-x}Fe_x)C_y$	*cF*4 $Fm\bar{3}m$ Cu		$0 < x < 1$ at $y = 0$ [Mas2]
			0-9 at.% C at x = 1
(γFe) 1394 - 912		a = 364.67	pure Fe at 915°C [V-C2, Mas2] 13 at.% C at $x = 0$ [Mas2]
(γMn) 1138 - 1100		a = 386.0 a = 363.3 a = 367.7 a = 369.5 a = 372.7	pure Mn [Mas2] at $x = 0.10$, $y = 0.09$ at $x = 0.50$, $y = 0.09$ at $x = 0.79$, $y = 0.09$ at $x = 1.0$, $y = 0.09$ [1973Ben]
(αFe) < 912	*cI*2 $Im\bar{3}m$ W	a = 286.65	at 25°C [Mas2] dissolves up to 3 at.% Mn, 0.096 at.% C [Mas2]
(δMn) 1246 - 1138	*cI*2 $Im\bar{3}m$ W	a = 308.0	[Mas2] dissolves up to 9 at.% Fe, 0.1 at.% C [Mas2]

(*continued*)

DOI: 10.1007/978-3-540-74196-1_6

Phase/ Temperature Range [°C]	Pearson Symbol/ Space Group/ Prototype	Lattice Parameters [pm]	Comments/References
(βMn) 1100 - 727	*cP*20 $P4_132$ βMn	a = 631.52	1155~730°C at 13 at.% Fe dissolves up to 35 at.% Fe, 0.1 at.% C [Mas2]
(αMn) < 727	*cI*58 $I\bar{4}3m$ αMn	a = 891.26	at 25°C [Mas2] dissolves up to 35 at.% Fe, 6.5 at.% C [Mas2]
ε, $(Mn_{1-x}Fe_x)C_y$ 1308 - 990	*hP*2 $P6_3/mmc$ Mg		
εMnC_y 1308 - 1243			$0.156 < y < 0.325$ (13.5-24.5 at.% C) at x = 0 [Mas2]
		a = 270.9 ± 0.1 c = 442.9 ± 0.1	for $MnC_{0.21}$ [V-C2][a)]
$\varepsilon(Mn_{1-x}Fe_x)$			metastable phase, $0.88 > x > 0.70$ (12 to 30 at.% Mn) [Mas2]
		a = 268.4 c = 439.7	at x = 0.1, y = 0.26 [1973Ben]
		a = 269.2 c = 441.0	at x = 0.1, y = 0.27 [1973Ben]
$(Mn_{1-x}Fe_x)_{23}C_6$ < 1034	*oP*116 $Fm\bar{3}m$ $Cr_{23}C_6$		[Mas2]
$Mn_{23}C_6$ < 1034		a = 1058.5 ± 0.6	pure $Mn_{23}C_6$ [1973Ben]
		a = 1055.3 ± 0.6	at x = 0.3 [1973Ben]
		a = 1054.4 ± 0.6	at x = 0.4 [1973Ben]
		a = 1053.5 ± 0.6	at x = 0.5 [1973Ben]
θ, $(Mn,Fe)_3C$	*oP*16 *Pnma* Fe_3C		
Mn_3C 1052 - 971		a = 508.0 b = 677.2 c = 453.0	pure Mn_3C [V-C2]
Fe_3C		a = 507.87 b = 672.97 c = 451.44	pure Fe_3C [V-C2] for intermediate compositions see Fig. 1
χ, $(Mn_{1-x}Fe_x)_5C_2$	*mC*28 *C*2/*c* B_2Pd_5		
Mn_5C_2		a = 1167.2	pure Mn_5C_2 [V-C2]

(*continued*)

DOI: 10.1007/978-3-540-74196-1_6

Phase/ Temperature Range [°C]	Pearson Symbol/ Space Group/ Prototype	Lattice Parameters [pm]	Comments/References
1171 - 428		b = 458.18 c = 509.41 β = 97.69°	
		a = 1156.2 b = 457.27 c = 505.95 β = 97.74°	pure Fe_5C_2 [2006MSIT]
		a = 1164.6 b = 457.0 c = 507.8 β = 97.70°	at x = 0.22 [1966Dug]
		a = 1163.14 b = 456.79 c = 507.54 β = 97.71°	at x = 0.5 [1966Jac]
$(Mn_{1-x}Fe_x)_7C_3$	*oP*40 *Pnma* Cr_7C_3		
Mn_7C_3 < 1333		a = 454.2 ± 0.1 b = 696.5 ± 0.3 c = 1195.5 ± 0.8	at x = 0
Fe_7C_3 metastable at pressures up to 5GPa stable at 827°C, 6 GPa		a = 454.0 ± 0.1 b = 692.8 ± 0.5 c = 1197.7 ± 0.9	at x = 0.167
		a = 453.9 ± 0.2 b = 691.5 ± 0.3 c = 1197.9 ± 0.8	at x = 0.25
		a = 453.5 ± 0.3 b = 685.5 ± 0.4 c = 1197.0 ± 0.9	at x = 0.5
		a = 453.0 ± 0.2 b = 679.3 ± 0.3 c = 1196.2 ± 0.9	at x = 0.75
		a = 452.9 ± 0.3 b = 676.0 ± 0.4 c = 1195.8 ± 0.9	at x = 0.833
		a = 452.5 ± 0.3 b = 674.1 ± 0.1 c = 1195.5 ± 0.8	at x = 1 [1990Put] samples obtained at 6 GPa and 823°C, measured at room temp. and atmospheric pressure

a) note: in [V-C2] structure type is erroneously given as NiAs

DOI: 10.1007/978-3-540-74196-1_6

Table 3. Invariant Equilibria

Reaction	T [°C]	Type	Phase	Composition (at.%)		
				C	Fe	Mn
$L + C(gr) + M_7C_3 \rightleftharpoons M_5C_2$	1274	P_1	L	24	54	22
$L + M_7C_3 \rightleftharpoons M_5C_2 + \varepsilon$	1240	U_1	L	22	69	9
$L + M_5C_2 + \varepsilon \rightleftharpoons M_3C$	1188	P_2	L	17	59	24
$L + M_5C_2 \rightleftharpoons C(gr) + M_3C$	1169	U_2	L	20	31	49
$L + C(gr) \rightleftharpoons \gamma + M_3C$	1139	U_3	L	17	3	80
$L + \varepsilon \rightleftharpoons M_3C + \gamma$	1129	U_4	L	15	57	28
$\varepsilon + M_3C \rightleftharpoons M_{23}C_6 + \gamma$	~1025	U_5	-	-	-	-
$M_{23}C_6 + M_3C \rightleftharpoons \gamma + M_5C_2$	$800 > T > 600$	U_6	-	-	-	-
$\gamma + C(gr) \rightleftharpoons \alpha + M_3C$	$738 > T > 600$	U_7	-	-	-	-

DOI: 10.1007/978-3-540-74196-1_6

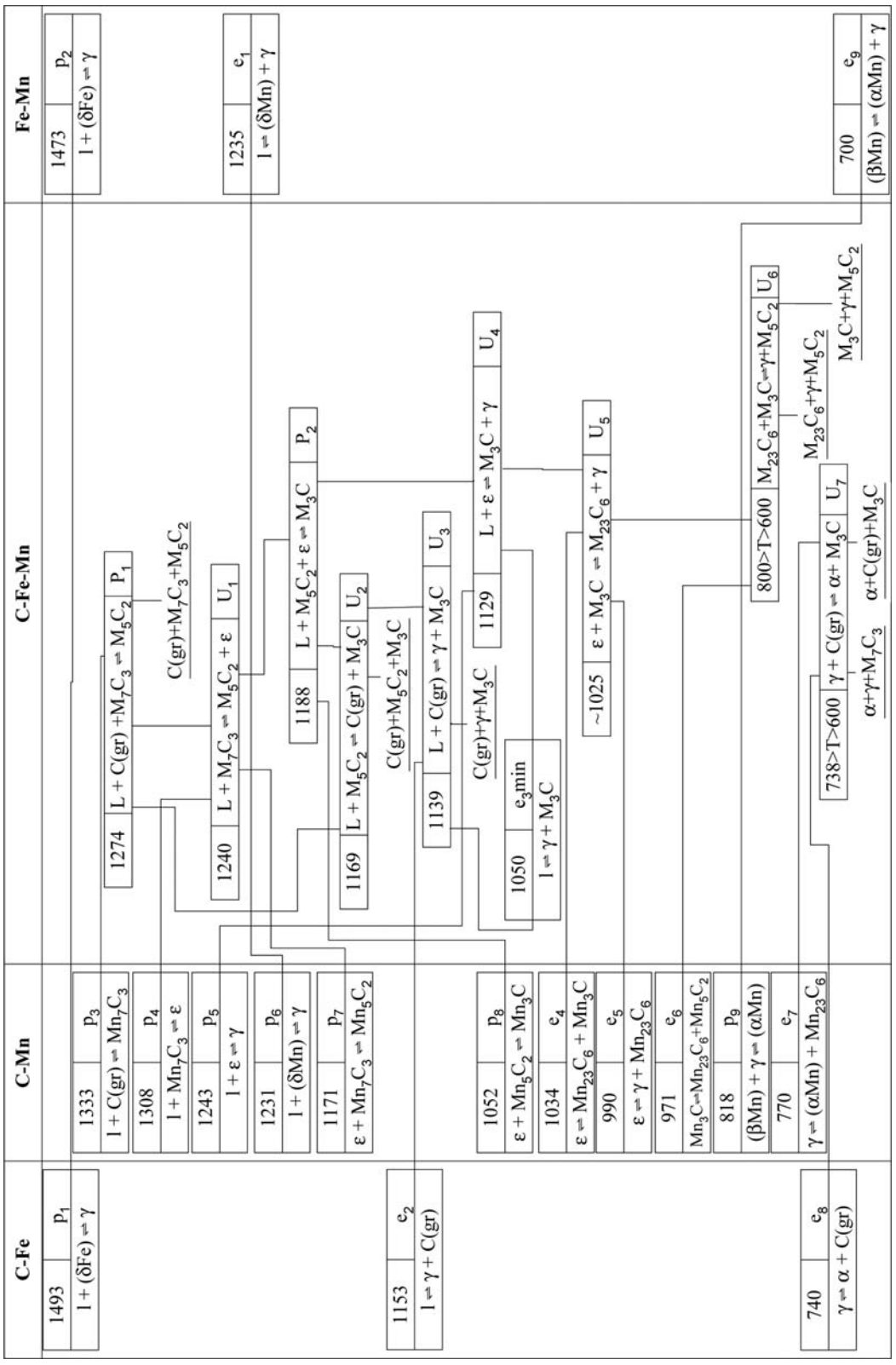

Fig. 1. C-Fe-Mn. Partial reaction scheme

DOI: 10.1007/978-3-540-74196-1_6

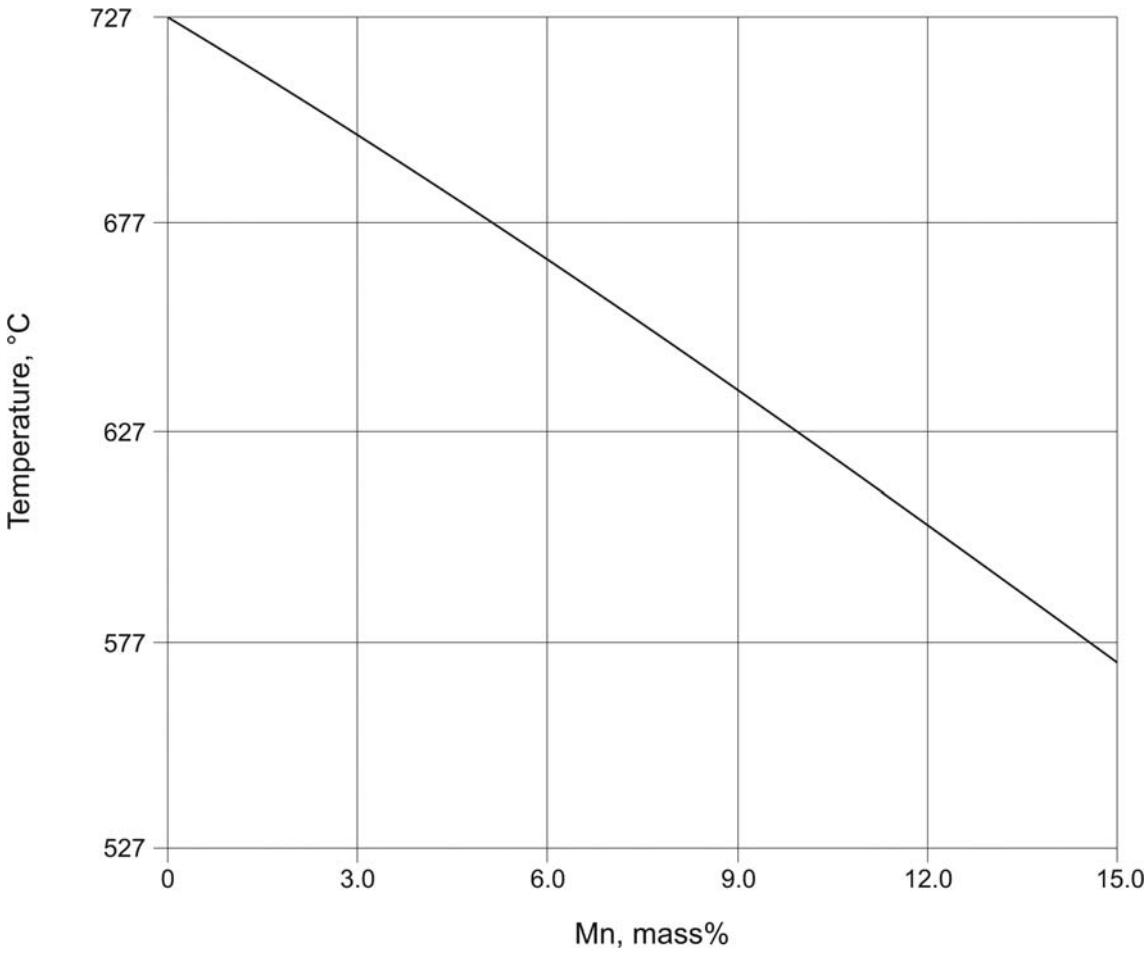

Fig. 2. C-Fe-Mn. Calculated compositions of the γ phase and temperature in the eutectoid reaction $\gamma \rightleftharpoons \alpha + M_3C$

DOI: 10.1007/978-3-540-74196-1_6

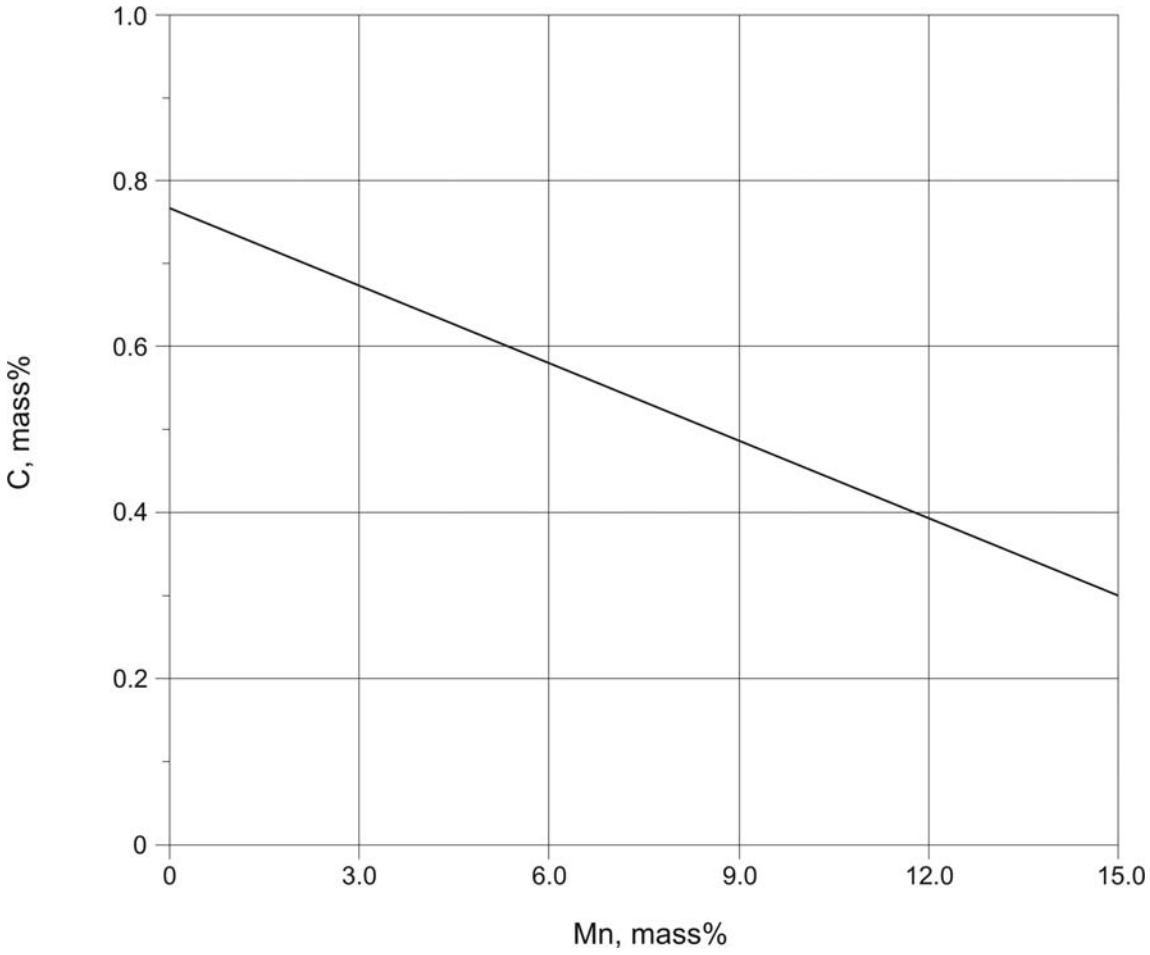

Fig. 3. C-Fe-Mn. Calculated compositions of the γ phase in the eutectoid reaction $\gamma \rightleftharpoons \alpha + M_3C$

DOI: 10.1007/978-3-540-74196-1_6

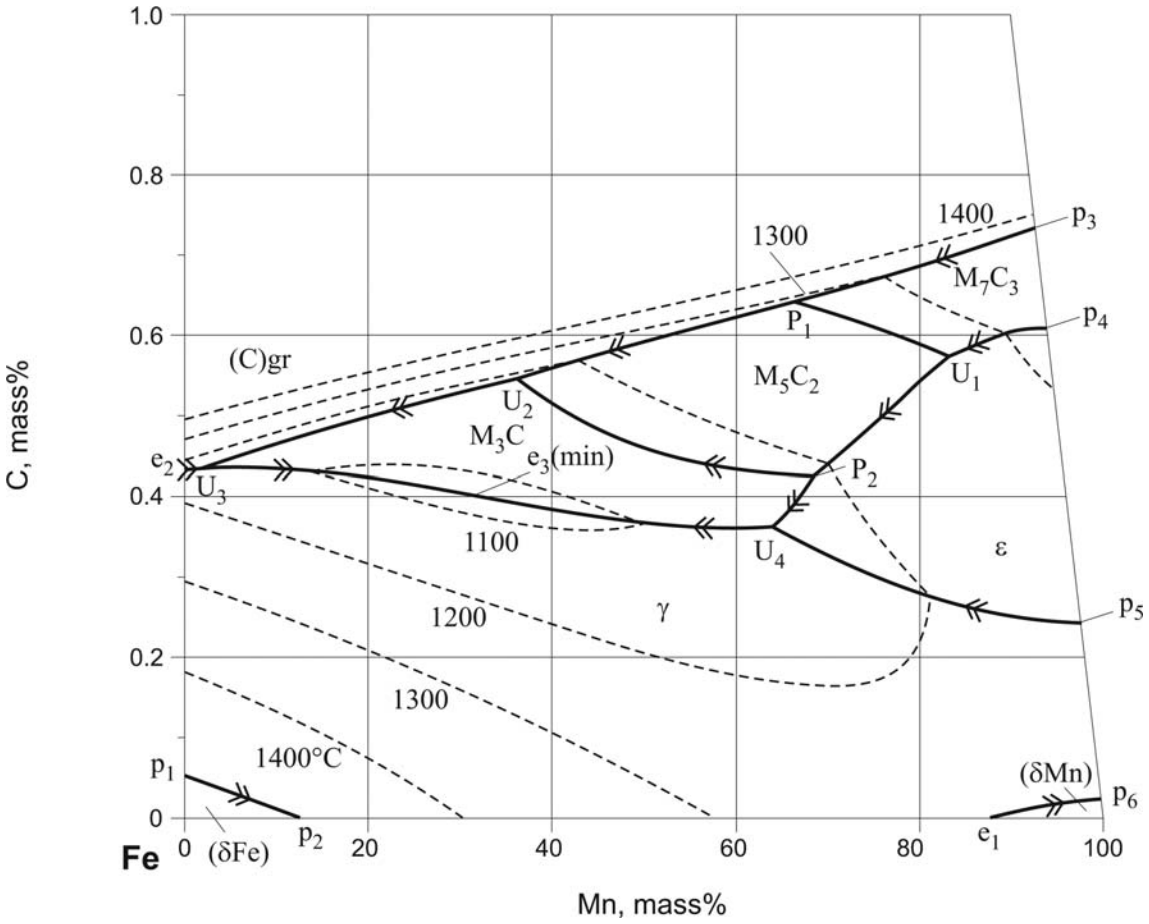

Fig. 4. C-Fe-Mn. Liquidus surface projection on the concentration plane

DOI: 10.1007/978-3-540-74196-1_6

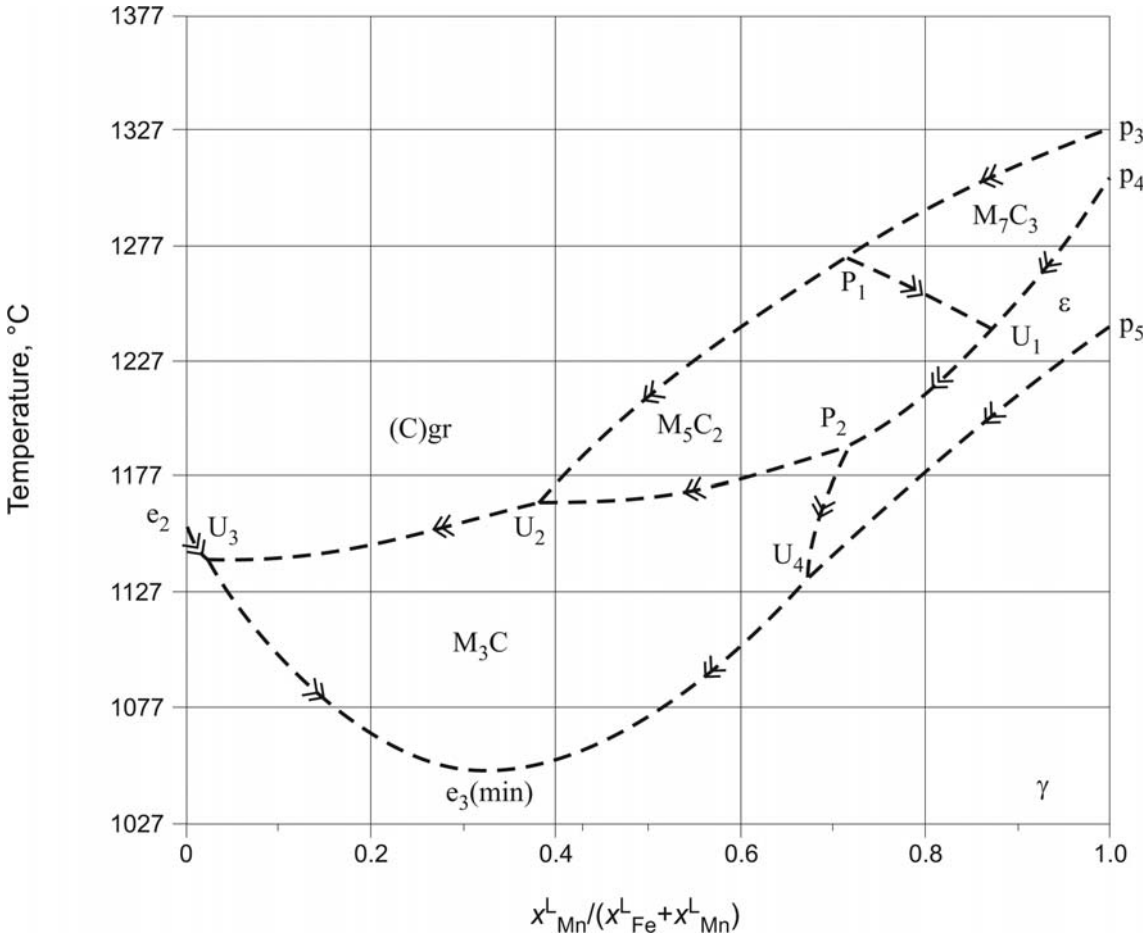

Fig. 5. C-Fe-Mn. Liquidus surface projection on the plane $T - x_{Mn}/(x_{Mn} + x_{Fe})$

DOI: 10.1007/978-3-540-74196-1_6

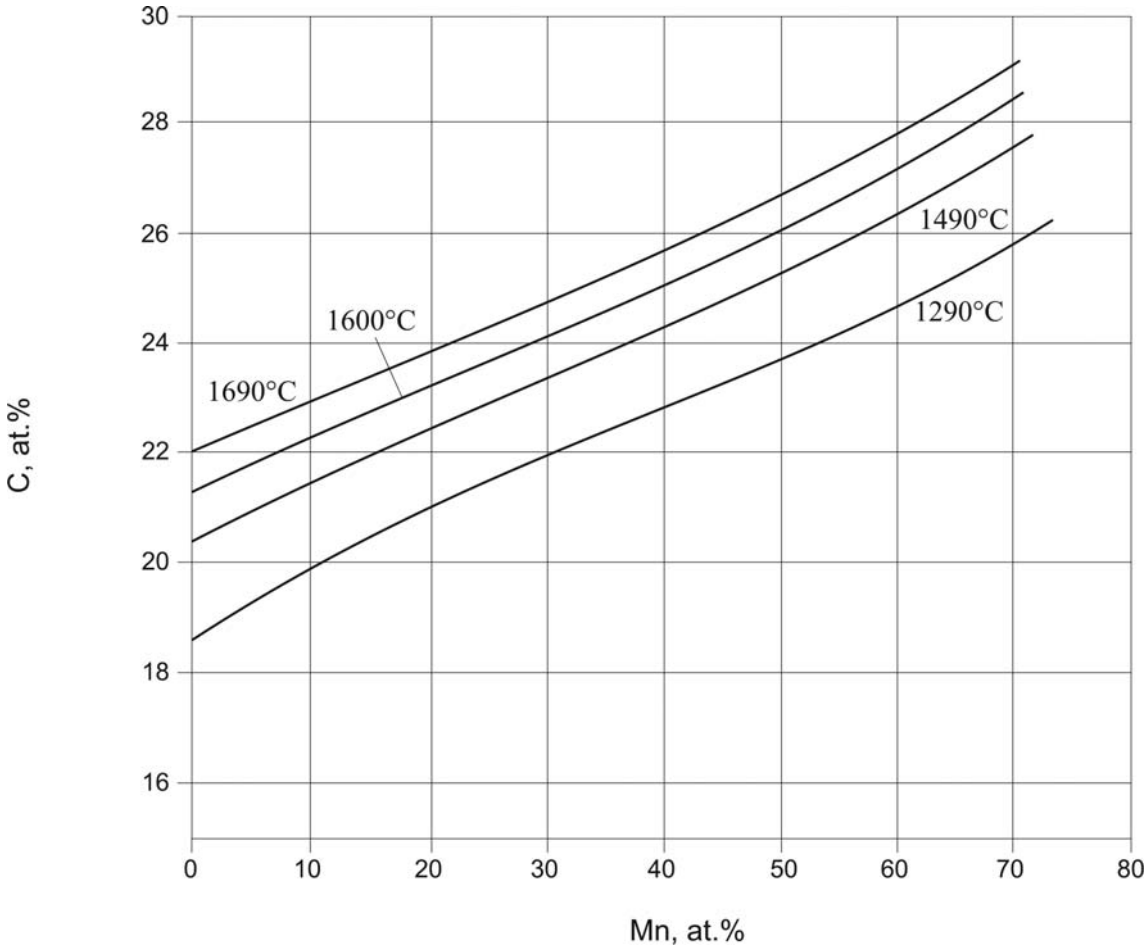

Fig. 6. C-Fe-Mn. Solubility of graphite in Fe-Mn melts

DOI: 10.1007/978-3-540-74196-1_6

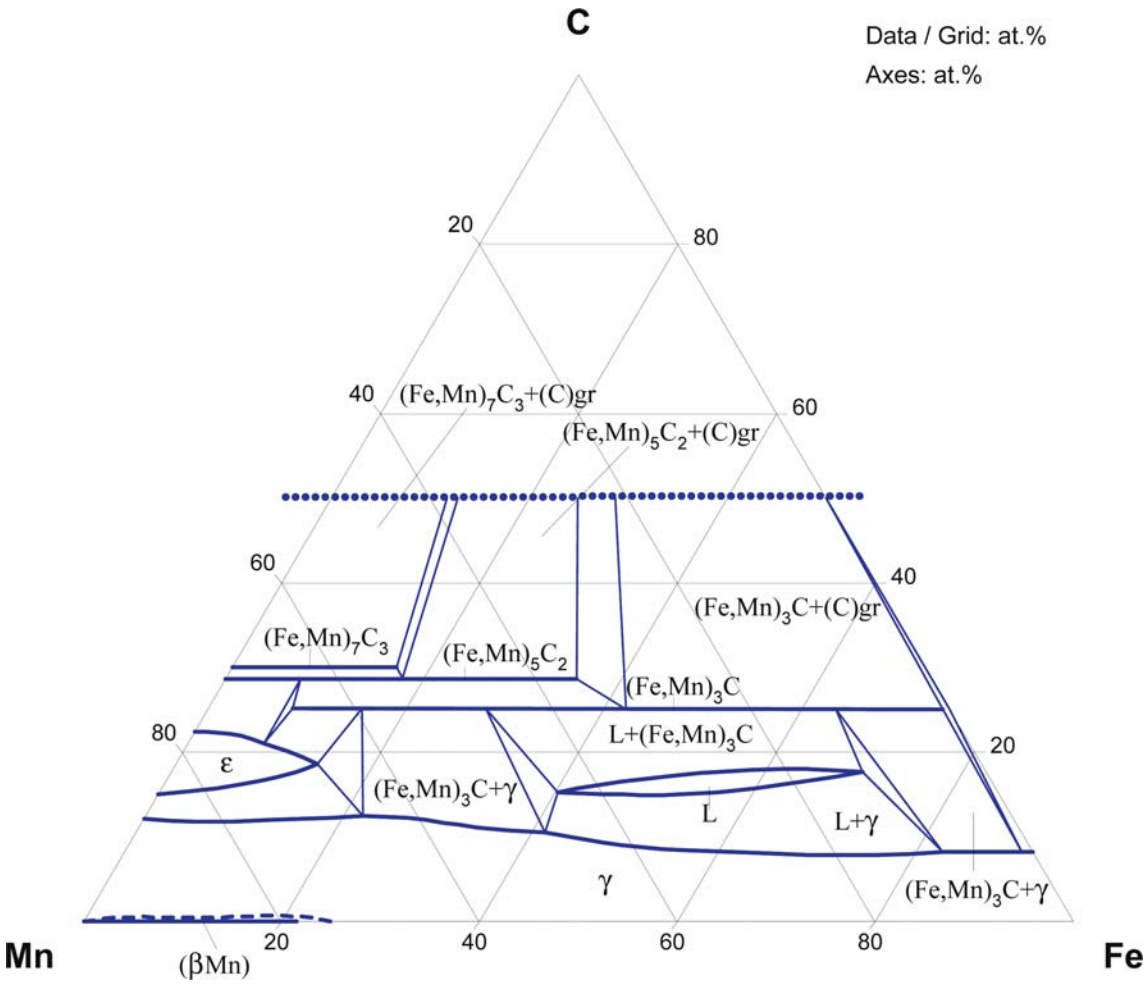

Fig. 7. C-Fe-Mn. Isothermal section at 1100°C

DOI: 10.1007/978-3-540-74196-1_6

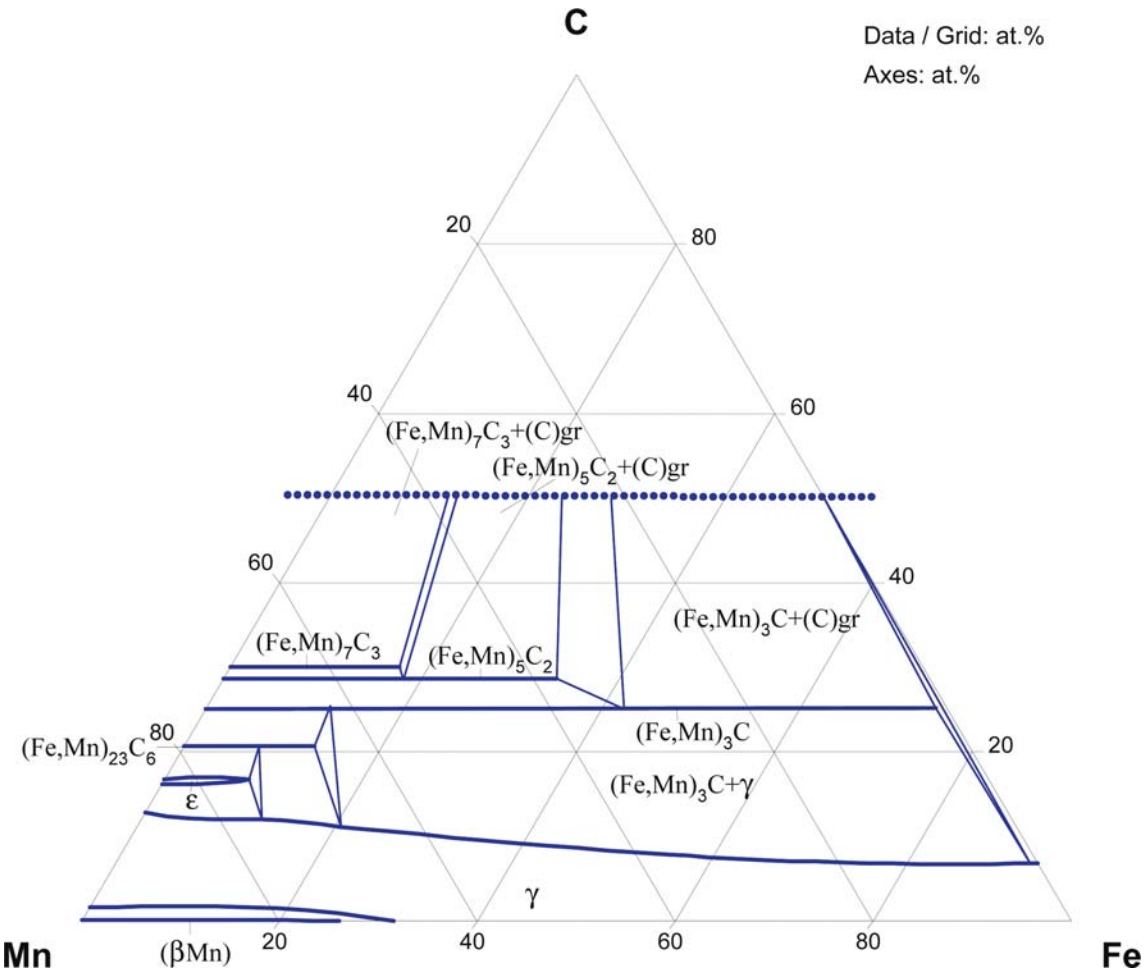

Fig. 8. C-Fe-Mn. Isothermal section at 1000°C

DOI: 10.1007/978-3-540-74196-1_6

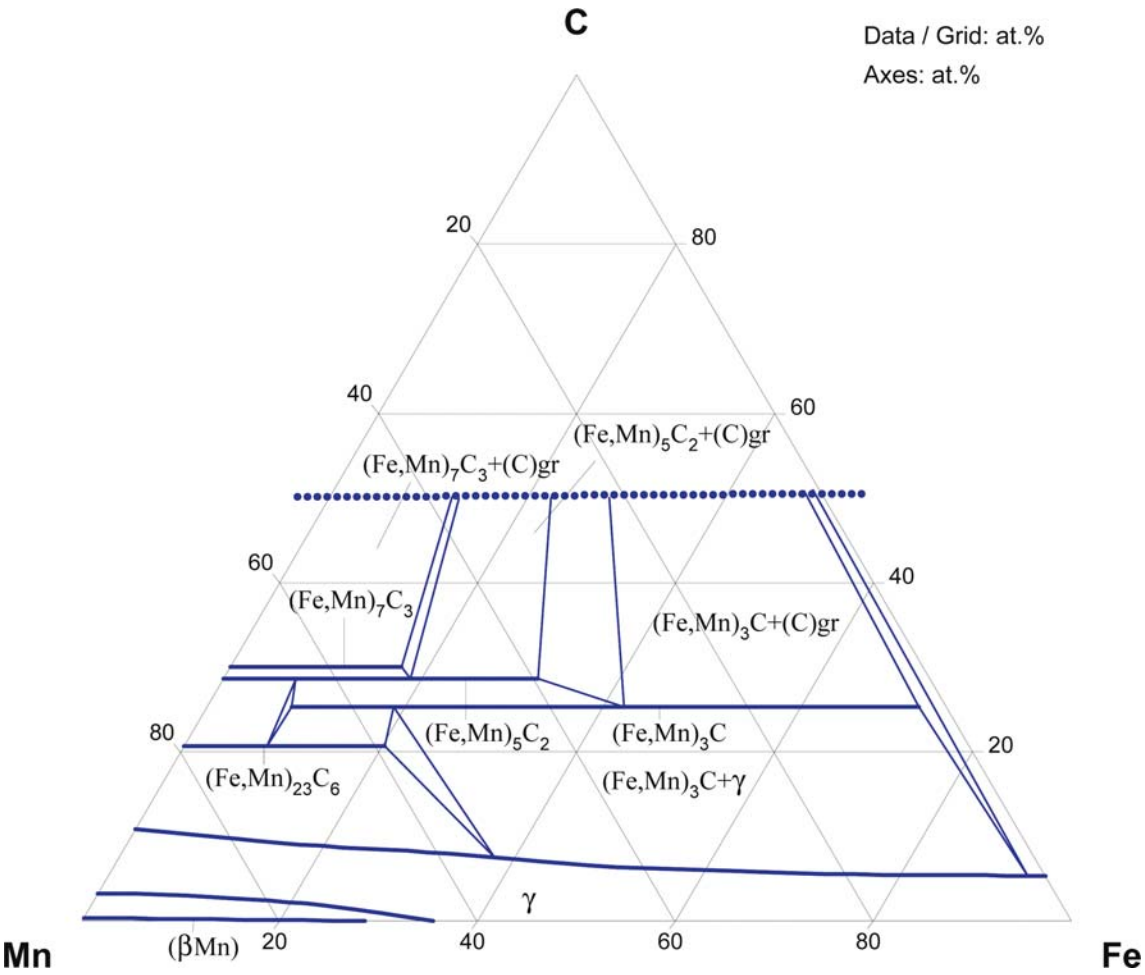

Fig. 9. C-Fe-Mn. Isothermal section at 900°C

DOI: 10.1007/978-3-540-74196-1_6

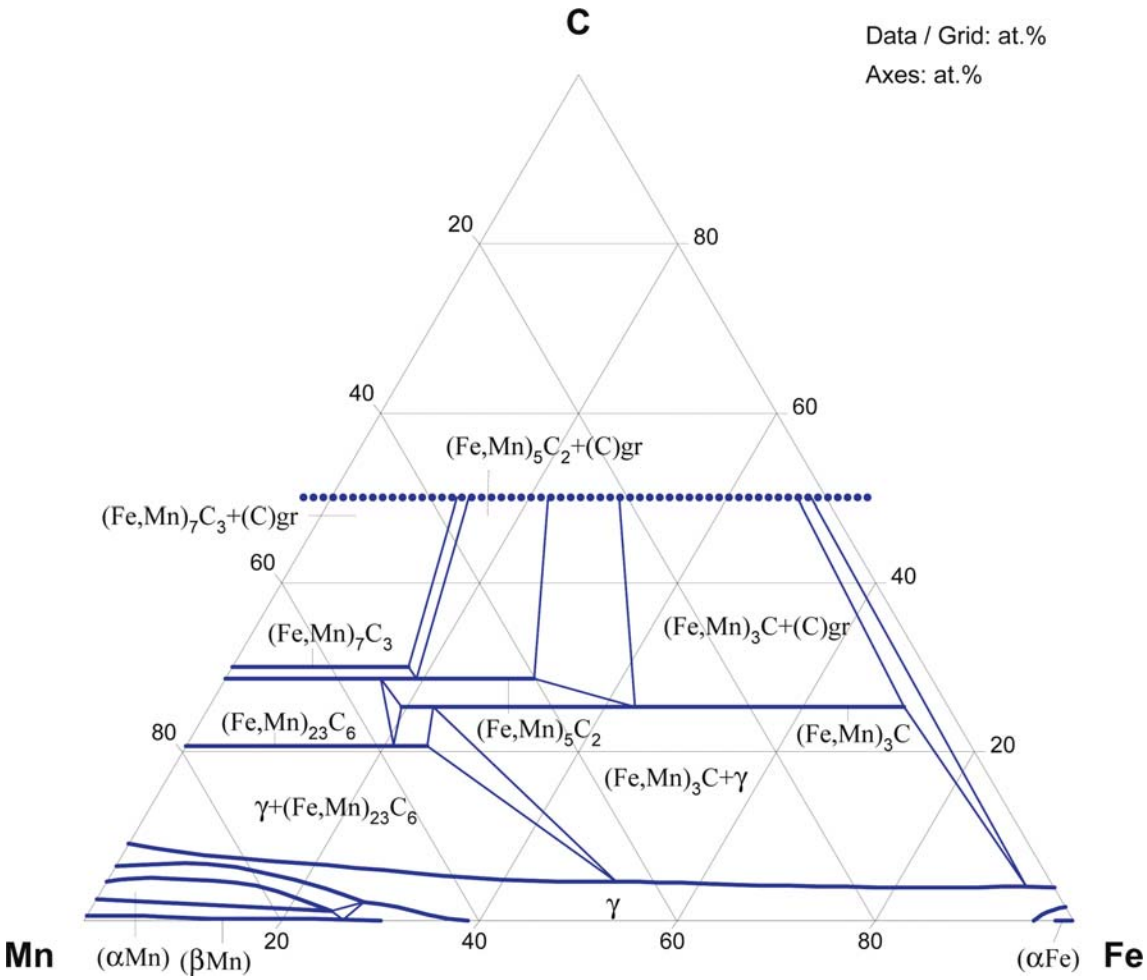

Fig. 10. C-Fe-Mn. Isothermal section at 800°C

DOI: 10.1007/978-3-540-74196-1_6

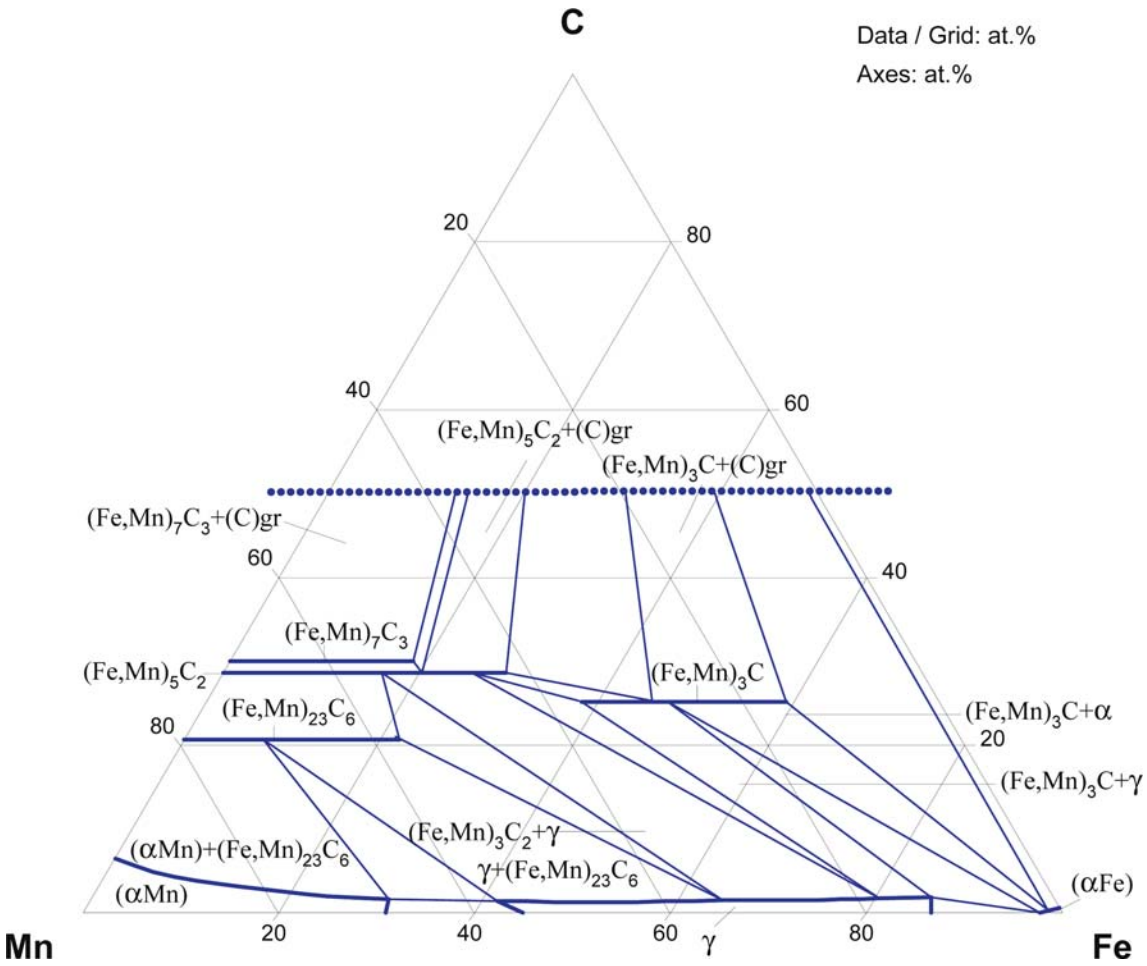

Fig. 11. C-Fe-Mn. Isothermal section at 600°C

DOI: 10.1007/978-3-540-74196-1_6

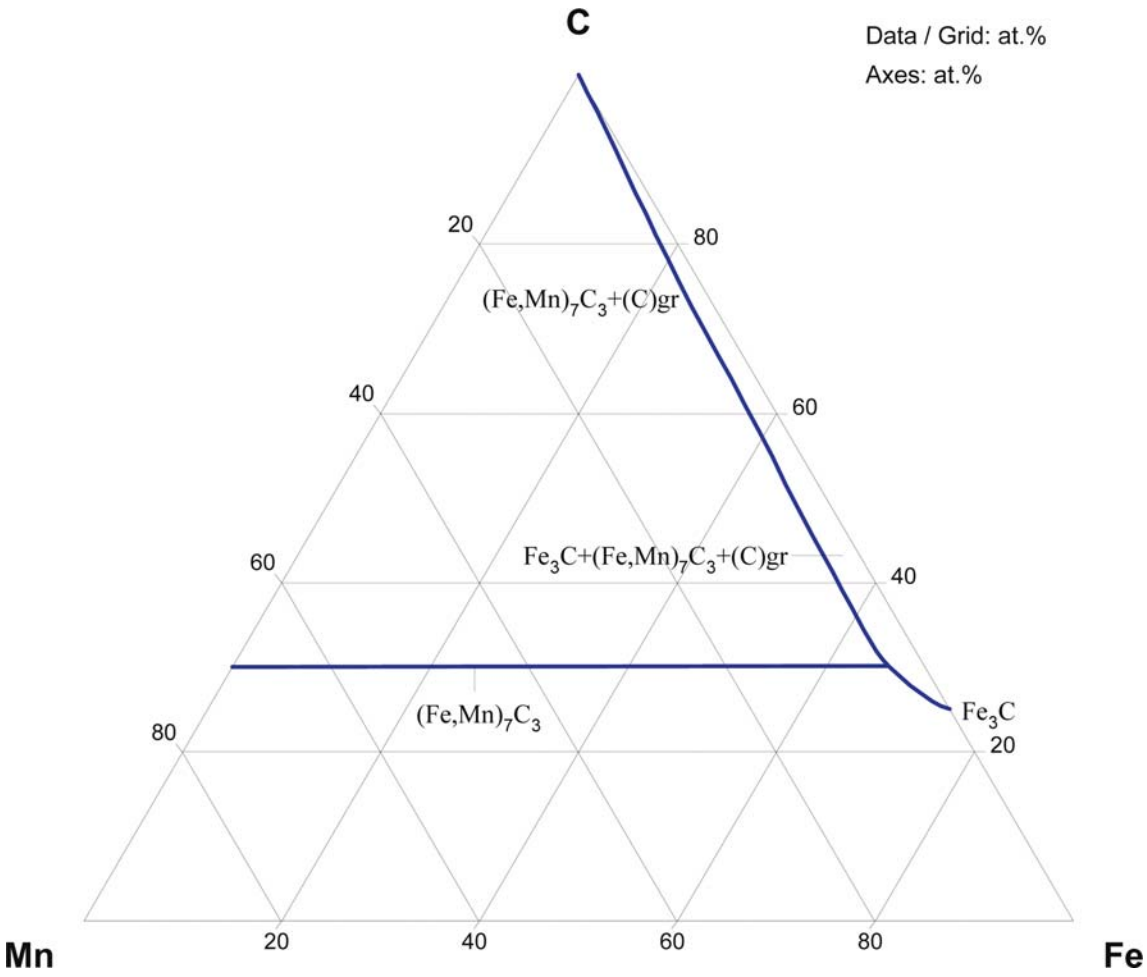

Fig. 12. C-Fe-Mn. Partial isothermal section at 827°C, 5GPa

DOI: 10.1007/978-3-540-74196-1_6

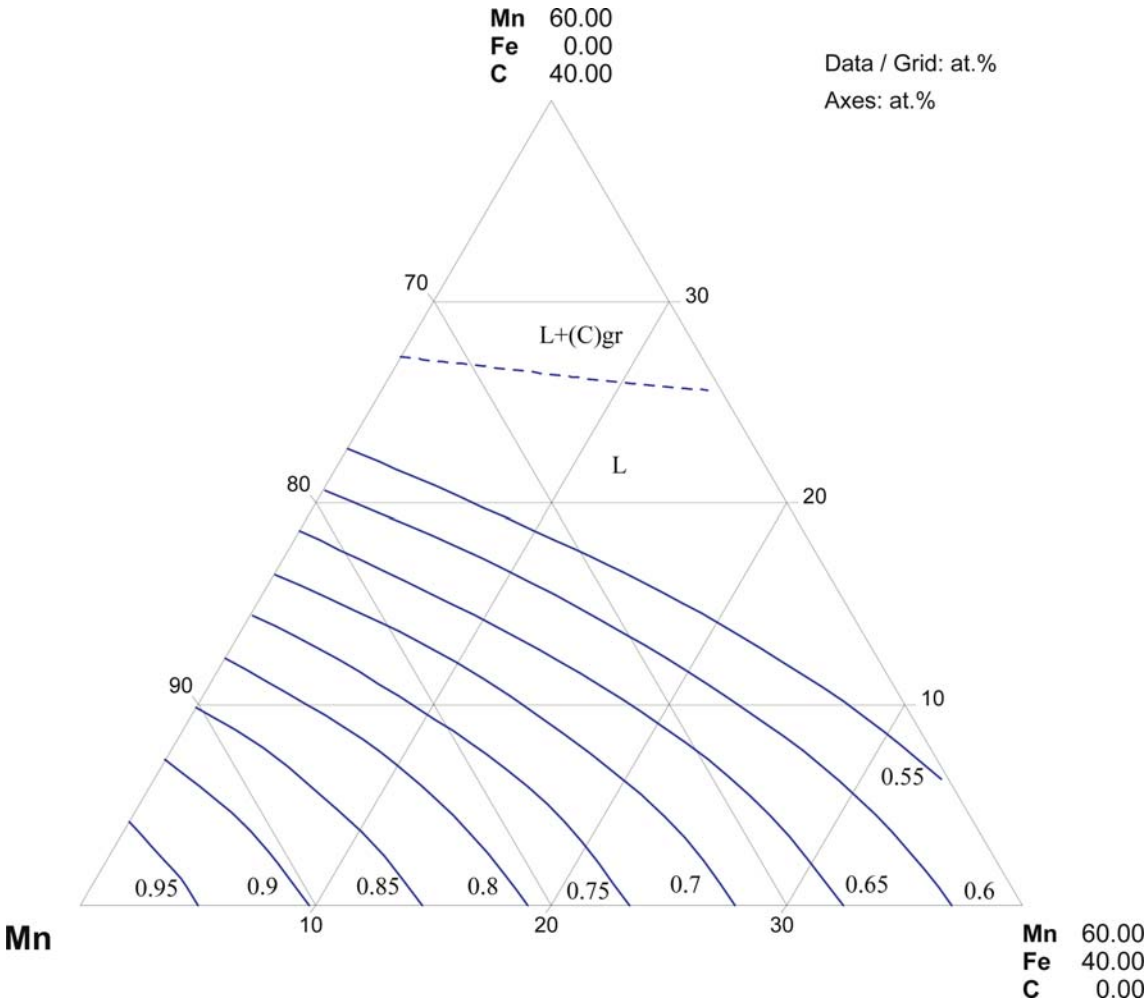

Fig. 13. C-Fe-Mn. Activity of Mn in liquid phase at 1400°C

DOI: 10.1007/978-3-540-74196-1_6

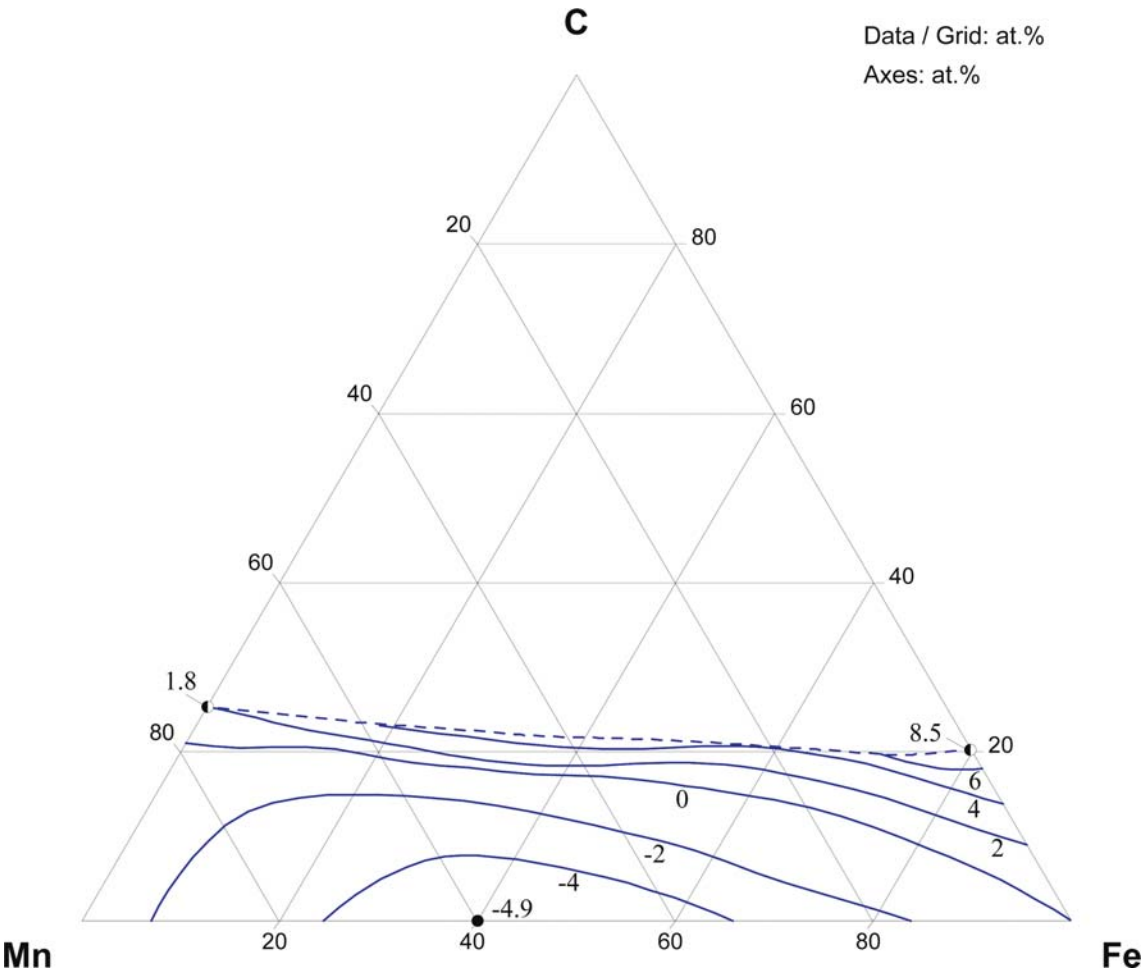

Fig. 14. C-Fe-Mn. Enthalpy of formation of liquid alloys ($kJ \cdot mol^{-1}$)

DOI: 10.1007/978-3-540-74196-1_6

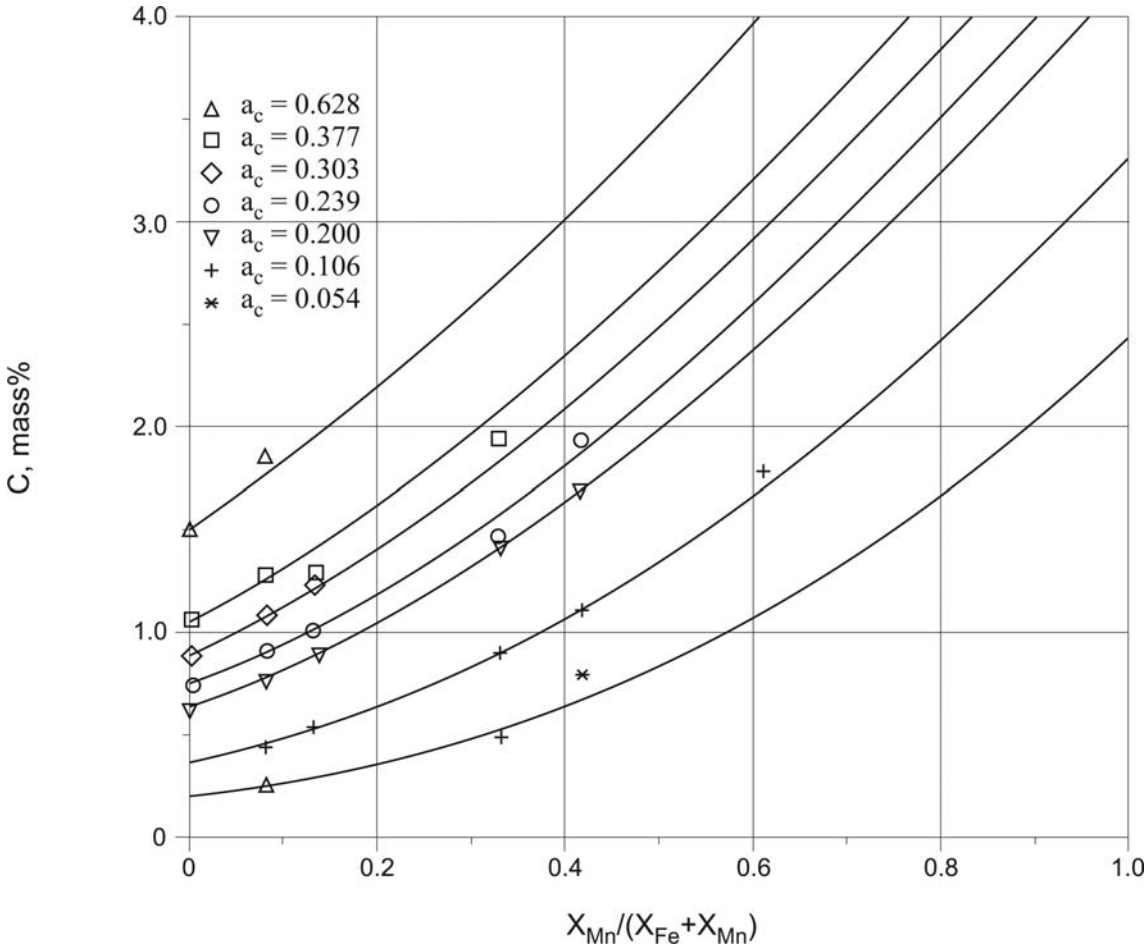

Fig. 15. C-Fe-Mn. Carbon activities in the γ phase at 1147°C with experimental points

DOI: 10.1007/978-3-540-74196-1_6

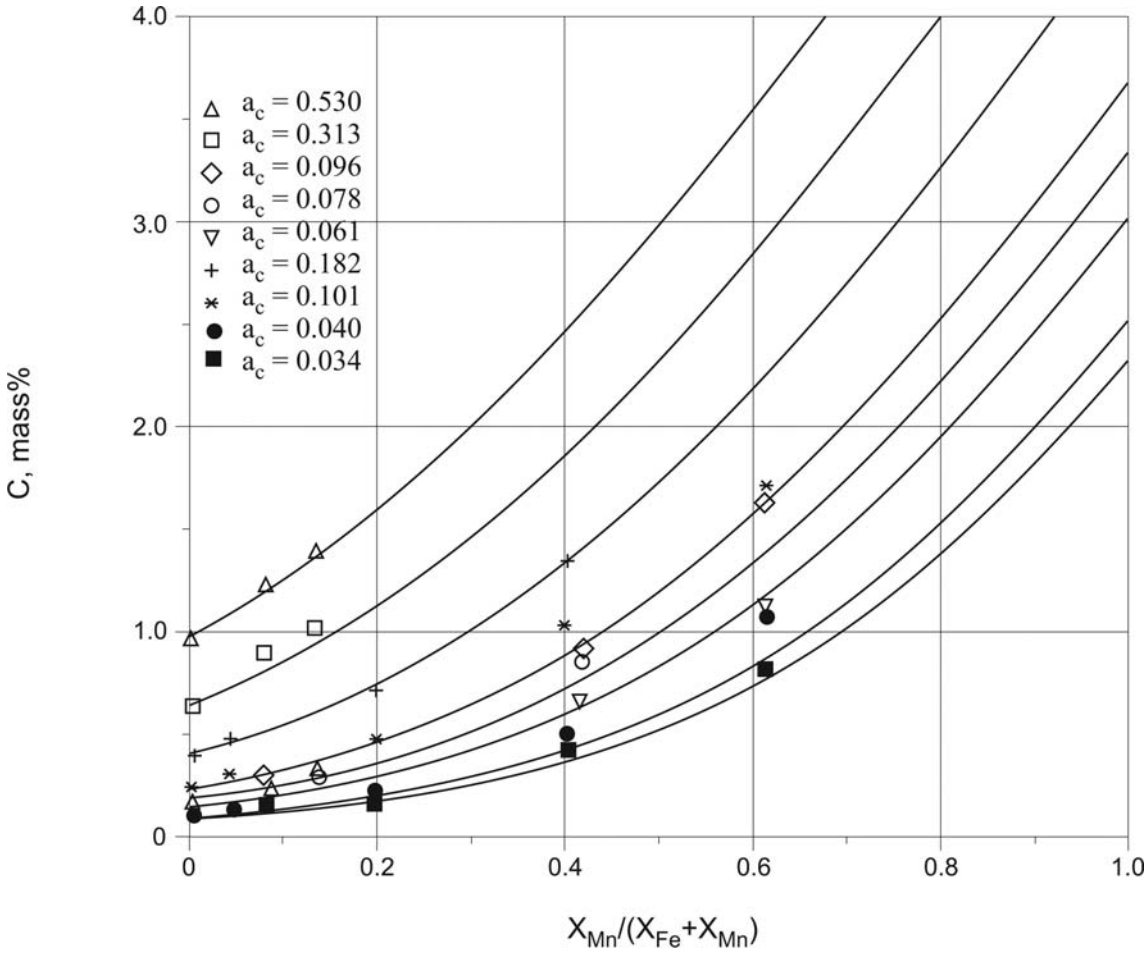

Fig. 16. C-Fe-Mn. Carbon activities in the γ phase at 1000°C with experimental points

DOI: 10.1007/978-3-540-74196-1_6

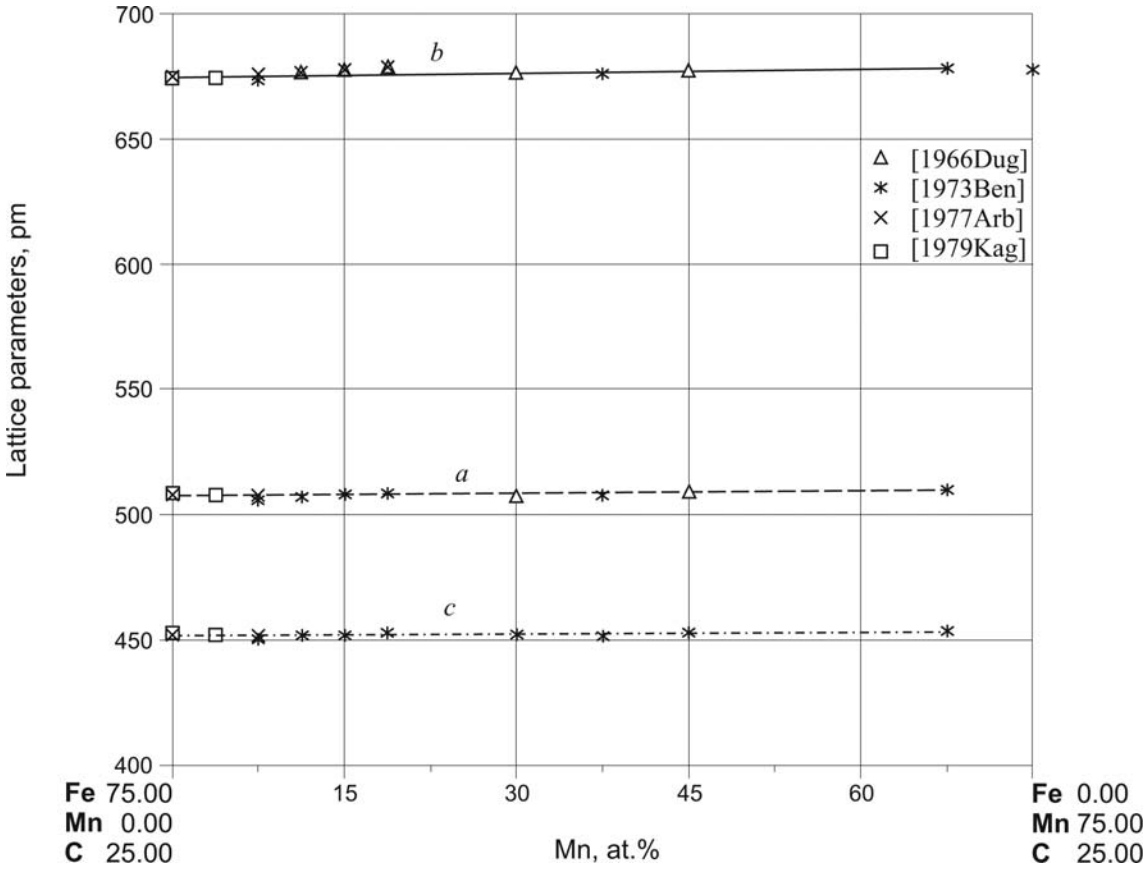

Fig. 17. C-Fe-Mn. Lattice parameters of cementite

DOI: 10.1007/978-3-540-74196-1_6

References

[1909Goe] Goerens, P., "About the Influence of Alloying Substances on Phase Diagram of Alloys of Iron and Carbon" (in German), *Metallurgie*, **6**, 537–550 (1909) (Phase Relations, Experimental, 16)

[1909Wue] Wuest, F., "Investigation of Influence of Manganese on the Phase Diagram Iron-Carbon" (in German), *Metallurgie*, **6**, 3–14 (1909) (Phase Relations, Phase Diagram, Morphology, Experimental, 54)

[1910Arn] Arnold, J.O., Read, A.A., "The Chemical and Mechanical Relations of Iron, Manganese, and Carbon", *J. Iron Steel Inst.*, **81**, 169–184 (1910) (Phase Relations, Mechan. Prop., Experimental, 12)

[1927Had] Hadfield, R.A., Met, D., "Iron-Manganese Alloys Low in Carbon", *Trans. Am. Inst. Min. Metall. Eng.*, **75**, 440–442 (1927) (Mechan. Prop., Experimental, 1)

[1932Bai] Bain, E.C., Davenport, E.S., Waring, W.S.N., Kearny, N.J., "The Equilibrium Diagram of Iron-Manganese-Carbon Alloys of Commercial Purity", *Trans. Am. Inst. Min. Metall. Eng.*, **100**, 228–256 (1932) (Phase Relations, Phase Diagram, Morphology, Experimental, 15)

[1933Eck] Eckel, J.F., Krivobok, V.N., "Alloys of Iron, Manganese and Carbon - Part VIII. Influence of Carbon on 10°C Manganese Alloys", *Trans. Amer. Soc. Steel Treat.*, **21**, 846–864 (1933) (Phase Relations, Experimental, 4)

[1933Gen] Gensamer, M., "Alloys of Iron and Manganese - Part XII. Alloys of Iron and Carbon with 2.5 and 4.5°C Manganese", *Trans. Amer. Soc. Steel Treating*, **21**, 1028–1034 (1933) (Phase Relations, Experimental, 4)

[1933Wel] Wells, C., Walters, F.M., "Alloys of Iron, Manganese and Carbon - Part VII. Influence of Carbon on Thirteen Percent Manganese Alloys", *Trans. Amer. Soc. Steel Treat.*, **21**, 830–845 (1933) (Phase Relations, Experimental, 3)

[1935Wel] Wells, C., Walters, F.M., "Alloys of Iron, Manganese and Carbon-Part XIV. Iron-Carbon Alloys Containing 7% Manganese", *Trans. Amer. Soc. Met.*, **23**, 751–761 (1935) (Phase Relations, Experimental, 6)

[1936Wal] Walters, F.M., Wells, C., "Alloys of Iron, Manganese and Carbon-Part XV. The Ternary Diagram and General Summary", *Trans. Amer. Soc. Metals*, **24**, 359–374 (1936) (Phase Relations, Experimental, 25)

[1937Tof] Tofaute, W., Linden, K., "Transformations in Solid State of Manganese Steels Containing to 1.2%C and 17% Mn" (in German), *Arch. Eisenhuettenwes.*, **10**, 515–524 (1937) (Phase Relations, Experimental, 18)

[1939Nem] Nemilov, V.A., Putsykina, M.M., "About Iron Alloys with Manganese and Carbon" (in Russian), *Zh. Prikl. Khim.*, **12**, 398–405 (1939) (Electr. Prop., Experimental, Mechan. Prop., Morphology, Phase Relations, 15)

[1939Sch] Schenck, R., Meyer, K., Mayer, K., "Investigation of Carbides by Method of Formation of Methane. III" (in German), *Z. Anorg. Chem.*, **243**, 17–31 (1939) (Thermodyn., Phase Relations, Experimental, 8)

[1940Wev] Wever, F., Mathieu, K., "About Transformations in Manganese Steels" (in German), *Mitt. K. W. Inst. Eisenforschung*, **22**(2), 9–18 (1940) (Phase Relations, Mechan. Prop., Magn. Prop., 16)

[1944Oeh] Oehman, E., "The Carbides in the System Iron-Manganese-Carbon" (in Swedish), *Jernkontorets Ann.*, **128**, 13–16 (1944) (Crys. Structure, Experimental, 1)

[1947Hul] Hultgren, A., "Isothermal Transformation of Austenite", *Trans. Am. Soc. Met.*, **39**, 915–989 (1947) (Kinetics, Experimental, 62)

[1948Smi] Smith, R.P., "Equilibrium of Iron-Carbon-Silicon and of Iron-Carbon-Manganese Alloys with Mixtures of Methane and Hydrogen at 1000°C", *J. Am. Chem. Soc.*, **70**, 2724–2729 (1948) (Thermodyn., Experimental, 20)

[1949Jae] Jänecke, E., "C-Fe-Mn" (in German), *Kurzgefasstes Handbuch aller Legierungen*, Winter, Heidelberg, 677–679 (1949) (Phase Diagram, Review, 0)

DOI: 10.1007/978-3-540-74196-1_6

[1951Iso] Isobe, M., "On the Equilibrium Diagram of Ternary Alloy System of Iron, Manganese and Carbon", *Sci. Rep. Res. Inst. Tohoku Univ. A*, **A3**, 540–621 (1951) (Phase Relations, Experimental, 5)

[1952Chi] Chipman, J., Alfred, R. M., Gott, L. W., Small, R. B., Wilson, D. M., Thomson, C. N., Gue, D.L., "The Solubility of Carbon in Molten Iron and Iron-Silicon and Iron-Manganese Alloys", *Trans. Amer. Soc. Metals*, **44**, 1215–1232 (1952) (Experimental, Phase Relations, 16)

[1952Tho] Thomson, C., "Effect of Manganese on the Solubility of Graphite in Liquid Iron", *Trans. ASM*, **44**, 1222–1224 (1952) (Phase Relations, Experimental)

[1954Kuo] Kuo, K., Persson, L.E., "A Contribution to the Constitution of the Ternary System Fe-Mn-C. Isothermal Sections at 1050°, 910°, and 690°C", *J. Iron Steel Inst.*, **178**, 39–44 (1954) (Phase Relations, Experimental, 22)

[1955Tur] Turkdogan, E. T., Leake, L. E., "Thermodynamics of Carbon Dissolved in Iron Alloys. Part I: Solubility of Carbon in Iron-Phosphorus, Iron-Silicon, and Iron-Manganese Melts", *J. Iron Steel Inst., London*, **179**, 39–43 (1955) (Experimental, Phase Diagram, Phase Relations, 15)

[1956Tur] Turkdogan, E. T., Hancock, R. A., Herlitz, S. I., Dentan, J., "Thermodynamics of Carbon Dissolved in Iron Alloys. Part V: Solubility of Graphite in Iron-Manganese, Iron-Cobalt, and Iron-Nickel Melts", *J. Iron Steel Inst., London*, **183**, 69–72 (1956) (Experimental, Phase Relations, Thermodyn., 17)

[1957San] Sanbongi, K., Ohtani, M., Toita, K., "On the Effect of Alloying Elements on the Solubility of Carbon in Molten Iron", *Sci. Rep. Res. Inst. Tohoku Univ. A*, **9**, 147–158 (1957) (Phase Relations, Experimental, 20)

[1958Koz] Kozheurov, V.A., Burylev, B.P., "Carbon Solubility in Liquid Iron in Presence of Manganese and Silicon" (in Russian), *Izv. Vyssh. Uchebn. Zaved., Chernaya Metall.*, (1), 83–93 (1958) (Calculation, Phase Relations, Thermodyn., 12)

[1958Mas] Masin, A., "Crystal Structure of the Non-needle Structure of the Fe-Mn-C Alloy and Hanke-Henkel X-Phases" (in German), *Naturwissenschaften*, **45**, 182–183 (1958) (Crys. Structure, Experimental, 5)

[1959Neu] Neumann, F., Schenck, H., Patterson, W., "Iron-Carbon Alloys in Thermodynamic Consideration" (in German), *Giesserei Tech.-Wiss. Beih.*, **23**, 1217–1246 (1959) (Experimental, Phase Diagram, Phase Relations, Theory, Thermodyn., 72)

[1959Pet] Petrushevskii, M.S., Gel'd, P.V., "Equilibrium of Carbon in Molten Alloys of Fe, Mn, Si and C", *Russ. J. Phys. Chem. (Engl. Transl.)*, 32, 86–94 (1959) (Experimental, Phase Diagram, Phase Relations, Thermodyn., 18)

[1960Pet] Petrova, E.F., Lapshina, M.I., Shvartsman, L.A., "Influence of the Alloying Elements on the Thermodynamic Activity and Carbon Solubility in α-Iron" (in Russian), *Metalloved. Term. Obrab. Met.*, (4), 22–25 (1960) (Experimental, Phase Relations, Thermodyn., 2)

[1961But] Butler, J.F., McCabe, C.L., Paxton, H.W., "Thermodynamic Activities in the Fe-Mn-C System", *Trans. Metall. Soc. AIME*, **221**, 479–484 (1961) (Thermodyn., Experimental, 14)

[1963Bor] Borchers, H., Koenig, M.W., "Cementite Creation in Steels Containing small Quantity of Carbon" (in German), *Arch. Eisenhuettenwes.*, **34**, 453–463 (1963) (Experimental, Morphology, Phase Relations, Thermodyn., 31)

[1963Sch] Schenck, H., Frohberg, M.G., Steinmetz, E., "Investigations on the Mutual Activities Influence in Homogeneous Metallic Substances Solubility. Part I. Experimental Investigations of Manganese-Carbon-X, Cobalt-Carbon-X, Nickel-Carbon-X Systems in Liquid State" (in German), *Arch. Eisenhuettenwes.*, **34**, 37–42 (1963) (Experimental, Phase Diagram, Review, Thermodyn., 30)

[1964Bro] Brown, L.C., Kirkaldy, J.S., "Carbon Diffusion in Dilute Ternary Austenites", *Trans. Metall. Soc. AIME*, **239**, 223–226 (1964) (Experimental, Kinetics, 15)

[1964Koc] Koch, W., Keller, H., "Equilibrium Investigations in the System Iron-Manganese-Carbon as an Example for the Use of Separating Methods for Establishing and Checking Constitutional Diagrams" (in German), *Arch. Eisenhuettenwes.*, **35**, 1173–1180 (1964) (Phase Relations, Experimental, 9)

DOI: 10.1007/978-3-540-74196-1_6

[1965Sai] Saito, T., "The ε Phase Formation Range of Fe-C-Mn Alloys under Quenching Conditions", *Trans. Jpn. Inst. Met.*, **6**, 240–246 (1965) (Phase Relations, Experimental, 15)

[1966Dug] Duggin, M.J., Cox, D., Zwell, L., "Structural Studies of the Carbides $(Fe,Mn)_3C$ and $(Fe,Mn)_5C_2$", *Trans. Metall. Soc. AIME*, **236**, 1342–1346 (1966) (Crys. Structure, Experimental, *, 15)

[1966Jac] Jack, K.H., Wild, S., "Nature of χ-Carbide and its Possible Occurrence in Steels", *Nature*, **212**, 248 (1966) (Crys. Structure, Experimental, Magn. Prop., 19)

[1966Pet] Petot, C., Durand, F., Bonnier, E., "Electrochemical Determination of the Activity of Manganese and its Interaction with Iron in the System Mn-Fe-C Saturated with Carbon at 1320°C" (in French), *Compt. Rend. Acad. Sci. Paris, Ser. C*, **262**, 819–821 (1966) (Thermodyn., Experimental, 4)

[1968Aks] Akshentsev, Yu.N., Baum, B.A., "Resistivity of Manganese-Iron-Carbon and Manganese-Iron-Silicon-Carbon Alloys in the Temperature Range 1000–1500°C", *Russ. J. Phys. Chem.*, **42**, 1388–1390 (1968) (Electr. Prop., Phase Relations, Experimental, 4)

[1968Als] Al'shevskiy, Yu.L., Kurdyumov, G.V., "Crystal Structure of the Martensite of Fe-Mn-C Steels", *Phys. Met. Metallogr. (Engl. Transl.)*, **25**, 156–158 (1968), translated from *Fiz. Met. Metalloved.*, **25**, 172–175 (1968) (Crys. Structure, Experimental, 5)

[1968Grz] Grzhimal'skii, L.L., "An Fe-C-Mn Brazing Alloy", *Weld. Prod.*, **15**, 89–93 (1968) (Morphology, Mechan. Prop., Experimental, 5)

[1968Jol] Jolley, W., "Effect of Mn and Ni on Impact Properties of Fe and Fe-C Alloys", *J. Iron Steel Inst., London*, **206**, 170–173 (1968) (Experimental, Mechan. Prop., 16)

[1969Sch] Schuermann, E., Kramer, D., "Investigations on the Influence of Temperature and on the Equivalent Effect of the Alloy Elements on the Solubility of Carbon in Iron Rich Carbon-Saturated Ternary and Multicomponent Meltings" (in German), *Giessereiforschung*, **21**, 29–42 (1969) (Phase Relations, Experimental, 35)

[1971Izo] Izotov, V.I., Khandarov, P.A., "Structural Features of the Martensitic Transformation in Iron-Manganese-Carbon Alloys", *Phys. Met. Metall.*, **32**, 138–144 (1971) (Crys. Structure, Experimental, 16)

[1971Shc] Shcherbedinskii, G.V., Shaidurov, V.I., "Diffusion Coefficients and Thermodynamic Activity of Carbon in Iron-Manganese-Carbon Alloys", *Russ. J. Phys. Chem.*, **45**, 1113–1115 (1971) (Kinetics, Experimental, 4)

[1971Tum] Tuma, H., "Activity and Solubility of Carbon in the Fe-Mn-C System with Mn Content up to 20% at 1000°C", *Kovove Mat.*, **9**, 99–109 (1971) (Thermodyn., Experimental, 24)

[1972And] Andryushenko, L.N., Georgiyeva, I.Ya., "Investigation of Martensitic Transformations in Iron-Manganese and Iron-Manganese-Carbon Alloys", *Phys. Met. Metallogr. (Engl. Transl.)*, **33**, 156–165 (1972), translated from *Fiz. Met. Metalloved.*, **33**, 1285–1296 (1972) (Experimental, Phase Diagram, Phase Relations, 9)

[1972Dua] Duatovich, D.P., Bowles, J.S., "The Orientation Relationship of the ^{225}F Martensitic Transformation in an Fe-Mn-C Alloy", *Acta Metall.*, **20**, 1137–1142 (1972) (Crys. Structure, Morphology, Experimental, 11)

[1972Gil] Gilmour, J.B., Purdy, G.R., Kirkaldy, J.S., "Thermodynamics Controlling the Proeutectoid Ferrite Transformations in Fe-C-Mn Alloys", *Metall. Trans.*, **3**, 1455–1464 (1972) (Kinetics, Experimental, 36)

[1972Oka] Oka, M., Tanaka, Y., Shimizu, K., "Phase Transitions in a Thermally Cycled Fe-Mn-C Alloy", *Acta Crystallogr., Sect. A: Fund. Crystallogr.*, **28**, 177 (1972) (Crys. Structure, Morphology, Abstract, 0)

[1972Wad] Wada, T., Wada, H., Elliott, J.F., Chipmann, J., "Thermodynamics of the FCC Fe-Mn-C and Fe-Si-C Alloys", *Metall. Trans.*, **3**, 1657–1662 (1972) (Thermodyn., Experimental, 12)

[1972Wil] Williams, R., Bordsworth, C., "Effect of Cobalt, Copper and Manganese on the Thermodynamic Activity of Carbon in Iron-base Austenites", *J. Iron Steel Inst., London*, **210**, 106–110 (1972) (Experimental, Phase Diagram, Phase Relations, 11)

DOI: 10.1007/978-3-540-74196-1_6

[1973Ben] Benz, R., Elliott, J.F., Chipman, J., "Thermodynamics of the Solid Phases in the System Fe-Mn-C", *Metall. Trans.*, **4**, 1975–1986 (1973) (Thermodyn., Experimental, 26)

[1973Gri] Grigorkin, V.I., Korotushenko, G.V., "Influence of Carbon on the Rate of Bainite Transformation in Iron-Manganese Alloys", *Steel USSR*, **3**, 1034–1035 (1973) (Kinetics, Experimental, 12)

[1973Oka] Oka, M., Tanaka, Y., Shimizu, K., "Phase Transitions in a Thermally Cycled Fe-Mn-C Alloy", *Trans. Jpn. Inst. Met.*, **14**, 148–153 (1973) (Crys. Structure, Morphology, Experimental)

[1974Arb] Arbuzov, M.P., Zhurakovsky, E.A., Zolotareva, G.V., Kotlyar, B.I., "Electron Structures and Compositions of the Phase $(Fe, Mn)_3C$ and of Certain Carbides of Manganese", *Inorg. Mater. (Engl. Trans.)*, **10**, 1246–1250 (1974), translated from *Izv. Akad. Nauk SSSR, Neorg. Mater.*, **10**, 1449–1453 (1974) (Electronic Structure, Experimental, 19)

[1974Ben] Benz, R., "Thermodynamics of the Fe-Mn-C System from Solid State EMF Measurements", *Metall. Trans.*, **5**, 2217–2224 (1974) (Thermodyn., Experimental, 20)

[1974Sil] Sil'man, G.I., Tejkh, V.A., "Phase Diagram and Formation of Structures in the Fe-C-Mn System" (in Russian), *Struktura Faz, Fazovye Prevrashchenija i Diagrammy Sostojanija Metallicheskikh Sistem*, Nauka, Moscow, 103–107 (1974) (Phase Relations, Calculation, Experimental, 6)

[1975Shi1] Shigematsu, T., "Invar Properties of Cementite $(Fe_{1-x}Me_x)_3C$, Me = Cr, Mn, Ni", *J. Phys. Soc. Jpn.*, **39**, 915–920 (1975) (Crys. Structure, Phys. Prop., Experimental, 14)

[1975Shi2] Shigematsu,T., Ohmori, S.-I., Nakanishi, N., Kachi, S., "Thermal Expansion of $(Fe_{1-x}Mn_x)_3C$", *J. Phys. Soc. Jpn.*, **38**, 1213 (1975) (Phys. Prop., Crys. Structure, Experimental, 2)

[1976Bog] Bogachev, I.N., Charushnikova, G.A., Chumakova, L.D., "Investigation of the Crystal Structure and Properties of Low-carbon Fe-Mn and Fe-Ni Martensitic Alloys", *Phys. Met. Metallogr. (Engl. Transl.)*, **41**, 97–103 (1976), translated from *Fiz. Met. Metalloved.*, **41**, 1238–1244 (1976) (Crys. Structure, Experimental, 12)

[1976Kle] Kleemola, H.J., Kuusisto, E.A., "The Effect of Cr, Mn and Ni on the Solubility and Precipitation of Carbon in Ferritic Iron", *Scand. J. Met.*, **5**, 151–158 (1976) (Phase Relations, Experimental, 20)

[1976Osh] Oshima, R., Azuma, H., Fujita, F.E., "The Formation of Intermediate Phase in Martensite Transformation of Fe-Mn-C and Fe-Mn-Cr-C Steel", *Scr. Metall.*, **10**, 1011–1014 (1976) (Crys. Structure, Experimental, 16)

[1976She] Shevchuk, L.A., Dudetskaya, L.R., Tkacheva, V.A., "Phase Equilibria in the Fe-C-Mn System" (in Russian), *Liteinoe Proizvod.*, (2), 7–8 (1976) (Experimental, Phase Diagram, Phase Relations, 0)

[1977Arb] Arbuzov, M.P., Dobrovolskaya, L.G., Kotlyar, B.I., "X-Ray Structure Study of the Carbide Phase Precipitated from Tempered Mn Steel" (in Russian), *Akad. Nauk Ukr. SSR, Metallofizika*, **70**, 91–93 (1977) (Crys. Structure, Experimental, 4)

[1977Hil1] Hillert, M., Waldenstroem, M., "A Thermodynamic Analysis of the Fe-Mn-C System", *Metall. Trans. A*, **8A**, 5–13 (1977) (Phase Relations, Phase Diagram, Thermodyn., Calculation, 39)

[1977Hil2] Hillert, M., Waldenstroem, M., "Isothermal Sections of the Fe-Mn-C System in the Temperature Range 873K-1373K", *Calphad*, **1**, 97–132 (1977) (Phase Diagram, Thermodyn., Experimental, Calculation, 1)

[1977Nis] Nishizawa, T., "An Experimental Study of the Fe-Mn-C and Fe-Cr-C Systems at 1000°C", *Scand. J. Met.*, **6**, 74–78 (1977) (Phase Relations, Thermodyn., Experimental, Calculation, 18)

[1977Nov] Novik, V.I., Taran, Yu.N., "Atomic-Interaction Structure in Carbides of the System Fe-Mn-C", *Inorg. Mater. (Engl. Transl.)*, **13**, 825–828 (1977), translated from *Izv. Akad. Nauk SSSR, Neorg. Mater.*,**13**, 1013–1017 (1977) (Crys. Structure, Review, 16)

DOI: 10.1007/978-3-540-74196-1_6

[1977Sch] Schuermann, E., Geissler, I.K., "Melting Equilibria in the Ternary System Fe-C-Mn" (in German), *Giessereiforschung*, **29**, 153–159 (1977) (Phase Relations, Experimental, *, 19)

[1977Sil] Sil'man, G.I., Pristuplyuk, N.I., Frol'tsov, M.S., "Some Characteristics of Structure Formation in Manganese Cast Irons and Steels", *Met. Sci. Heat Treat.*, **2**, 91–95 (1977), translated from *Metalloved. Term. Obrab. Met.*, **2**, 6–10 (1977) (Morphology, Experimental, 7)

[1977Sos] Sosnowski, R., Latusek, J., "Solubility of C in Multicomponent Fe-based Melts" (in Polish), *Hutnik*, **44**, 434–438 (1977) (Phase Relations, Calculation, 5)

[1977Tar] Taran, Ju.N., Novik, V.I., Shestopalenko, R.E., "Crystallochemical Structure of the Carbides $(Fe,Mn)_3C$, $(Fe,Mn)_5C_2$ and $(Fe, Mn)_7C_3$" (in Ukrainian), *Dopov. Akad. Nauk Ukrain. RSR*, **A3**, 272–275 (1977) (Crys. Structure, Review, 11)

[1977Uhr] Uhrenius, B., "Optimization of Parameters Describing the Interaction Between Carbon and Alloying Elements in Ternary Austenite", *Scand. J. Metall.*, **6**, 83–89 (1977) (Thermodyn., Calculation, 24)

[1978Cho] Choudary, U.V., Chang, Y.A., "Gibbs Energies of Formation of Mn_3C, $M(Fe,Mn)_3C$ and $Mn_{23}C_6$ from the Ternary Phase Equilibria in the Fe-Mn-C System", *Calphad*, **2**, 169–185 (1978) (Phase Diagram, Phase Relations, Thermodyn., Theory, 34)

[1978Shi] Shimizu, K., Tanaka, Y., "The γ-ε-α Martensitic Transformations in an Fe-Mn-C Alloy", *Trans. Jpn. Inst. Met.*, **19**, 685–693 (1978) (Phase Relations, Kinetics, Morphology, Crys. Structure, Experimental, 22)

[1978Uhr] Uhrenius, B., "A Compendium of Ternary Iron-Base Phase Diagrams", in "*Hardenability Concepts with Applications to Steel*", Doane, D.V., Kirkaldy, J.S. (Eds.), Proc. Symp. Held Sheraton-Chicago Hotel, Oct. 24–26, 1977, Metall. Soc. AIME Heat Treat. Com./ Amer. Soc Met. Activ. Phase Trans., 28–81 (1978) (Phase Relations, Phase Diagram, Assessment, Review, 53)

[1979Ben] Benesch, R., Javorski, M., Kopec, R., Simon, A., "Diffusion of Manganese in Liquid Iron Saturated with Carbon in the System FeC(sat)-blast Furnace Type Slag", *Thermochim. Acta*, **34**, 221–231 (1979) (Kinetics, Transport Phenomena, Interface Phenomena, Experimental, 18)

[1979Bul] Bulat, S.I., Molochnikova, A.L., "Structural Superplasticity of Fe-Mn-C Alloys", *Met. Sci. Heat Treat.*, **21**, 420–423 (1979) (Mechan. Prop., Experimental, 3)

[1979Kag] Kagawa, A., Okamoto, T., "Lattice Parameters of Cementite in Fe-C-X (X = Cr, Mn, Mo, and Ni) Alloys", *Trans. Jpn. Inst. Met.*, **20**, 659–666 (1979) (Crys. Structure, Magn. Prop., Experimental, 11)

[1979Kor] Kor, G.J.W., "Phase Instability of Manganes-Iron-Carbides", *Metall. Trans. B*, **10B**, 397–400 (1979) (Experimental, Mechan. Prop., 9)

[1980Tan1] Tanaka, Y., Shimizu, K., "Anomalous Changes in Austenite and Martensite Lattice Parameters of Fe-Mn-C Alloys", *Trans. Jpn. Inst. Met*., **21**, 42–50 (1980) (Phys. Prop., Experimental, 22)

[1980Tan2] Tanaka, Y., Shimizu, K., "A Variation of Martensite Morphology with Manganese and Carbon Compositions in Fe-Mn-C Alloys", *Trans. Jpn. Inst. Met.*, **21**, 34–41 (1980) (Morphology, Experimental, 11)

[1980Tan3] Tanaka, A., "Activities of Manganese in Mn-Fe-C, Mn-Si-C and Mn-Fe-Si-C Melts at 1673 K", *Trans. Jap. Inst. Met.*, **21**,27–33 (1980) (Thermodyn., Experimental, 2)

[1980Tan4] Tanaka, A., "Carbon Solubilities in Mn, Mn-Fe, Mn-Si and Mn-Fe-Si Alloy Solutions" (in Japanese),*Muroran Kogyo Daigaku Kenkyu Hokoku, Riko Hen*, **10**, 19–31 (1980) (Phase Relations, Experimental, 8)

[1981Tan] Tanaka, Y., Shimizu, K., "Carbide Formation upon Tempering at Low Temperatures in Fe-Mn-C Alloys", *Trans. Jpn. Inst. Met.*, **22**, 779–788 (1981) (Phase Relations, Kinetics, Experimental, 27)

[1981Wan] Wanibe, Y., Kawashima, N., Fujisawa, T., Sakao, H., "Interdiffusion in Molten Fe-C-Si and Fe-C-Mn Alloys", *Trans. Iron Steel Inst. Jpn.*, **21**, 243–249 (1981) (Experimental, Kinetics, Phase Relations, 28)

DOI: 10.1007/978-3-540-74196-1_6

[1981Wyc] Wycliffe, P.A., Purdy, G.R., Embury, J.D., "Growth of Austenite in the Intercritical Annealing of Fe-C-Mn Dual Phase Steels", *Can. Metall. Quart.*, **20**, 339–350 (1981) (Kinetics, Experimental, 15)

[1982Kaj] Kajatkari, M., Ullakko, K., Pietikaeinen, J., "On the Aging of Fe-Ni-C and Fe-Mn-C Martensites", *J. Phys. (France)*, **43(C4)**, 461–466 (1982) (Kinetics, Experimental, Morphology, 19)

[1982Sar] Sarma, D.S., Song, J.T., Bernstein, I.M., Aaronson, H.I., "The Bainite and Pearlite Reactions in a Hypereutectoid Fe-C-Mn Alloy", *J. Metals*, **34**, A33-A34 (1982) (Morphology, Experimental, 0)

[1982Sou] Souza, M.M., Guimaraes, J.R.C., Chawla, K.K., "Intercritical Austenitization of Two Fe-Mn-C Steels", *Metall. Trans. A*, **13**, 575–579 (1982) (Phase Relations, Morphology, Kinetics, Experimental, 9)

[1983Pri] Prib, V.E., Paskal, Yu.I., "Features of the f.c.c.-f.c.t. Transition in the Paramagnetic Range of the γ Phase in Fe-Mn-C Alloys", *Phys. Met. Metallogr. (Engl. Transl.)*, **55**, 179–183 (1983), translated from *Fiz. Met. Metalloved.*, **55**, 195–198 (1983) (Phase Relations, Experimental, 15)

[1983Sha] Shah, A.K., Sharma, R.C., "Ferrite Transformation in Fe-C-Mn Alloys", *Z. Metallkd.*, **74**, 394–401 (1983) (Kinetics, Experimental, 15)

[1984Est] Estay, S., Chengji, L., Purdy, G.R., "Carbide Dissolution and Austenite Growth in the Intercritical Annealing of Fe-C-Mn Dual Phase Steels", *Canad. Metall. Quart.*, **23**, 121–130 (1984) (Experimental, Phase Diagram, Phase Relations, Thermodyn., 16)

[1984Pro] Prokoshkin, S.D., Kaputkina, L.M., Bernsteyn, M.L., Mozzhukhin, V.Ye., Andreeva, S.A., "On the Mechanism of the Development of Abnormally Low Tetragonality and Orthorhombicity in the Lattice of Fe-C, Fe-Mn-C, Fe-Cr-C, Fe-Mn-Cr-C Martensites", *Phys. Met. Metallogr. (Engl. Transl.)*, **58**, 114–125 (1984), translated from *Fiz. Met. Metalloved.*, **58**, 745–765 (1984) (Crys. Structure, Experimental, 17)

[1984Sch] Schmidt, I., "Friction-Induced Martensite in Austenitic Fe-Mn-C Steels" (in German), *Z. Metallkd.*, **75**, 747–754 (1984) (Phase Relations, Experimental, 20)

[1985Eno] Enomoto, M., Aaronson H.I., "Calculation of α+γ Phase Boundaries in Fe-C-X Systems from the Central Atoms Model", *Calphad*, **9**, 43–58 (1985) (Phase Relations, Calculation, 31)

[1985Kho] Khoroshailov, V.G., Ermakov, B.S., Kolchin, G.G., Korolev, N.V., "Mechanical Properties of Alloyed Fe-C-Mn Alloys at Cryogenic Temperatures", *Steel USSR*, **15**, 236–238 (1985) (Mechan. Prop., Experimental, 2)

[1985Koc] Kocherzhinskiy, Yu.A., Kulik, O.G., Dragunov, V.V., Demyanchuk, A.V., "Melting Diagram of the Fe-Mn-C System" (in Russian), *Stable and Metastable Phase Equilibria in Metallic Systems*, Nauka, Moscow, 124–128 (1985) (Experimental, Phase Diagram, Review, 15)

[1985Liu] Liu, K.-H., Marder, A., Notis, M.R., "Banding Structure in Fe-Mn-C Alloys", *J. Metals*, **37**, 2 (1985) (Kinetics, Abstract, 0)

[1985Nik] Nikolin, B.I., Sizova, T.L., "About formation of 15R2-Martensite in C-Fe-Mn Steels" (in Russian), *Akad. Nauk Ukr. SSR, Metallofizika*, **7**, 108–110 (1985) (Phase Relations, Experimental, 3)

[1986Cha] Chang, H., Hsu, T.Y., Zuyao, X.U., "Thermodynamic Prediction of M_s and Driving Force for Martensitic Transformation in Fe-Mn-C Aalloys", *Acta Metall.*, **34**, 333–338 (1986) (Kinetics, Calculation, Theory, 23)

[1986Eno] Enomoto, M., Aaronson, H.I., "On the Critical Nucleus Composition of Ferrite in an Fe-C-Mn Alloy", *Metall. Mater. Trans. A*, **17**, 1381–1384 (1986) (Phase Relations, Kinetics, Calculation, 12)

[1986Lad] Ladriere, J.H., He, X.J., "Moessbauer Study on Retained Austenite in an Fe-Mn-C Dual-Phase Steel", *Mater. Sci. Eng.*, **77**, 133–138 (1986) (Phys. Prop., Experimental, 13)

[1987Sch] Schuermann, E., Schweinichen, J., Voelker, R., Fischer, H., "Calculation of the α/δ Resp γ-Liquidus of Iron and of the Liquidus of Carbon as well as of the Univariant Reaction Lines

DOI: 10.1007/978-3-540-74196-1_6

in Iron-Rich, Carbon Containing Three-component and Multicomponent Fe-C-X1-X2 Systems. MEMO" (in German), *Giessereiforschung*, **39**, 104–113 (1987) (Experimental, Phase Diagram, Phase Relations, Thermodyn., 19)

[1987Spa] Spanos, G., Fang, H.S., Aaronson, H.I., "The Bainite Reaction in Hypereutectoid Fe-C-Mn Alloys", *J. Met.*, **39**, A58-A59 (1987) (Kinetics, Abstract, 0)

[1988Dur] Durisinova, D., Durisin, J., Repiska, L., "Mathematical Description of Liquidus Surface in Fe-C-Mn System", *Kovove Mater.*, **5**, 547–560 (1988) (Phase Relations, Phase Diagram, Calculation, 22)

[1988Hea] Healy, G.W., "Thermodynamics of Liquid Manganese-Iron-Carbon Alloys", *CIM Bull.*, **81**, 86–87 (1988) (Thermodyn., Theory, Abstract, 0)

[1988Mag] Magnin, P., Kurz, W., "Stable and Metastable Eutectic Temperatures of Fe-C with Small Additions of a Third Element", *Z. Metallkd.*, **79**, 282–284 (1988) (Phase Relations, Experimental, 5)

[1988Ray] Raynor, G.V., Rivlin, V.G., "C-Fe-Mn", *Phase Equilibria in Iron Ternary Alloys*, The Institute of Metals, London, 168–176 (1988) (Phase Relations, Crys. Structure, Assessment, *, 24)

[1988Sta] Stamm, W., Zaehres, H., Acet, M., Schletz, K., Wassermann, E.F., "Magnetization and Thermal Expansion in Fe-Mn and Fe-Mn-C Alloys", *J. Phys. (France)*, 49(C8), 315–316 (1988) (Experimental, Magn. Prop., Phys. Prop., 6)

[1988Sum] Sumin, V.V., Morozov, S.I., Natkanets I., Petru, D., "Inelastic Scattering of Slow Neutrons Study of Local Oscillations of Carbon Atoms in Fe-Mn-C and Fe-Ni-C Alloys", *Phys. Met. Metallogr.*, **65**, 155–159 (1988), translated from *Fiz. Met. Metalloved.*, **65**, 168–172 (1988) (Experimental, Phys. Prop., 16)

[1988Zhu] Zhukov, A.A., Shilina, E.P., Arkhipova, T.F., "New Calculation Methods for Refining the State Diagram of Fe-C-Mn in the Region of the Rutectic", *Russ. Metall. (Engl. Transl.)*, (2), 191–195 (1988), translated from *Izv. Akad. Nauk SSSR, Met.*, (2), 200–203 (1988) (Phase Relations, Calculation, Theory, 9)

[1989Bug] Bugayev, V.N., Gavrilyuk, V.G., Nadutov, V.M., Tatarenko, V.A., "Carbon Distribution in Fe-Ni-C and Fe-Mn-C Alloys with an FCC Lattice", *Phys. Met. Metallogr. (Engl. Transl.)*, **68**, 93–102 (1989), translated from *Fiz. Met. Metalloved.*, **68**, 931–940 (1989) (Crys. Structure, Experimental, Theory, 19)

[1989Dre] Dresler, W., "Activities of Manganese and Carbon in the Liquid System Fe-Mn-C", *Trans. Inst. Min. Metall., Sect. C.*, **98**, C61-C67 (1989) (Phase Relations, Thermodyn., Experimental, Calculation, 17)

[1989Lee] Lee, B.-J., Lee, D.N., "A Thermodynamic Study on the Fe-Mn-C System", *Calphad*, **13**, 355–365 (1989) (Phase Diagram, Thermodyn., Assessment, Calculation, 16)

[1989Liu] Liu, Z.K., Agren, J., "On the Transition from Local Equilibrium to Paraequilibrium During the Growth of Ferrite in Fe-Mn-C Austenite", *Acta Metall.*, **37**, 3157–3163 (1989) (Phase Relations, Kinetics, Theory, 16)

[1989Zhu] Zhukov, A.A., Shilina, E.P., Arkhipova, T.F., "New Computation Methods in the Analysis of the Fe-C-Cr and Fe-C-Mn Systems in the Eutectic Range", *Calphad*, **13**, 23–32 (1989) (Calculation, Phase Diagram, Theory, Thermodyn., 12)

[1990Hua1] Huang, W., "A Thermodynamic Assessment of the Fe-Mn-C System", *Metall. Trans. A*, **21**, 2115–2123 (1990) (Phase Diagram, Phase Relations, Thermodyn., Assessment, Calculation, *, #, 40)

[1990Hua2] Huang, W., "Thermodynamic Assessment of the Mn-C System", *Scand. J. Metall.*, **19**, 26–32 (1990) (Phase Diagram, Phase Relations, Thermodyn., Assessment, Review, Calculation, 37)

[1990Ni1] Ni, R., Ma, Z., Wei, S., "Thermodynamics of Mn-Fe-C and Mn-Si-C System", *Steel Res.*, **61**, 113–116 (1990) (Phase Relations, Phase Diagram, Thermodyn., Experimental, Calculation, 12)

DOI: 10.1007/978-3-540-74196-1_6

[1990Ni2] Ni, R., Ma, Z., Wei, S., "Thermodynamics of Mn-Fe-C and Mn-Si-C Systems" (in Japanese), *J. Iron Steel Res.*, **2**, 17–22 (1990) (Phase Relations, Thermodyn., Experimental, Calculation, 11)

[1990Put] Putyatin, A.A., Kozlovskij, V.F., "Pressure Effect on the Phase Relations in the Alloys of the Fe-(Mn, Co)-C Systems" (in Russian), *Vestn. Mosk. Univ., Ser. 2: Khim.*, **31**, 367–369 (1990) (Phase Relations, Experimental, *, #, 8)

[1990Rey] Reynolds, W.T., Jr., Liu, S.K., Li, F.Z., Hartfield, S., Aaronson, H.I., "An Investigation of the Generality of Incomplete Transformation to Bainite in Fe-C-X Alloys", *Metall. Trans. A*, **21A**, 1479–1491 (1990) (Experimental, Kinetics, 56)

[1990Sum] Sumin, V.V., Zemlyanov, M.G., Kaputkina, L.M., Parshin, P.P., Prokoshkin, S.D., Shoklo, A.I., "Slow Neutron Scattering Study of the Structure and Dynamics of the Crystal Lattice of Fe-Mn-C Alloys", *Phys. Met. Metallogr. (Engl. Transl.)*, **70**, 119–124 (1990), translated from *Fiz. Met.Metalloved.*, **70**, 122–127 (1990) (Phys. Prop., Crys. Structure, Experimental, 14)

[1991Liu] Liu, Z.-K., Agren, J., "Two-Phase Coherent Equilibrium in Multicomponent Alloys", *J. Phase Equilib.*, **12**, 266–274 (1991) (Phase Relations, Theory, 13)

[1992Gav] Gavriljuk, V., Duz, V., Ullako, K., "Internal Friction of Ferrous Martensite", *Scr. Metall. Mater.*, **26**, 667–672 (1992) (Phys. Prop., Abstract, 0)

[1992Joa] Joarder, A., Sarma, D.S., "Bainite Morphologies in a 0.2C-1.5Mn Steel", *Steel Res.*, **66**, 33–38 (1992) (Morphology, Experimental, 29)

[1992Kak] Kakeshita, T., Shimizu, K., Ono, M., Date, M., "Effect of Magnetic Field on Successive α, γ, ε Martensitic Transformations in an Fe-Mn-C Alloy", *Mater. Trans. JIM*, **33**, 461–465 (1992) (Magn. Prop., Kinetics, Phase Relations, 19)

[1993Wit] Witusjevich, V.T., Shumikhin, V.S., "Enthalpy of Formation of Molten Fe-Mn(Co, Ni)-C Systems" (in Russian), *Rasplavy*, (5), 78–80 (1993) (Thermodyn., Experimental, *, 13)

[1994Oda] Oda, K., Fujimura, H., Ino, H., "Local Interactions in Carbon-Carbon and Carbon-M (M: Al, Mn, Ni) Atomic Pairs in FCC γ-iron", *J. Phys.: Condens. Matter*, **6**, 679–692 (1994) (Phys. Prop., Experimental, 32)

[1993Oka] Okamoto, H., "Fe-Mn (Iron-Manganese)", *Phase Diagrams of Binary Iron Alloys*, ASM International, Materials Park. OH, 203–213 (1993) (Phase Diagram, Phase Relations, Crys. Structure, Thermodyn., Magn. Prop., Assessment, 180)

[1994Prz] Przylecka, M., Kulka, M., Gestwa, W., "The Activity of Carbon in the Two-phase Fields of the Fe-Cr-C, Fe-Mn-C and Fe-Si-C Alloys at 1173 K", *Mater. Sci. Forum*, **163–165**, 87–92 (1994) (Experimental, Thermodyn., 10)

[1994Rag] Raghvan, V., "Carbon-Iron-Manganese", *J. Phase Equilib.*, **15**, 421–424 (1994) (Assessment, Phase Relations, *, #, 31)

[1994Wit] Witusiewich, V.T., "Thermodynamic Properties of Liquid Alloys of 3*d* Transition Metals with Metalloids (Silicon, Carbon and Boron)", *J. Alloys Compd.*, **203**, 103–116 (1994) (Review, Thermodyn., 89)

[1995Bou] Bouchard, D., Bale, C.W., "Simultaneous Optimization of Thermochemical Data for Liquid Iron Alloys Containing C, N, Ti, Si, Mn, S, and P", *Metall. Mater. Trans. B*, **26B**, 467–484 (1995) (Thermodyn., Assessment, Calculation, 85)

[1995Eno] Enokido, H., Moro-Oka, A., Ichise, E., "Thermo-Chemical Activities of Liquid Fe-Mn-C Alloy" (in Japanese), *Tetsu to Hagane*, **81**, 619–624 (1995) (Thermodyn., Experimental, 26)

[1995Lee] Lee, B.-J., "Thermodynamic Calculations in Stainless Steels Alloy Systems" (in Korean), *J. Korean Inst. Met.*, **33**, 766–775 (1995) (Calculation, Thermodyn., Phase Relations, Phase Diagram, 3)

[1996Vya] Vyatkin, G.P., Morozov, S.I., Privalova, T.P., Alekseeva, T.O., "The Surface Phases During Mn Segregation in Fe-Mn-C Alloys" (in Russian), *Dokl. Akad. Nauk*, **351**, 773–775 (1996) (Phase Relations, Experimental, 14)

DOI: 10.1007/978-3-540-74196-1_6

[1997Li] Li, H., Morris, A., "Evaluation of Unified Interaction Parameter Model Parameters for Calculating Activities of Ferromanganese Alloys: Mn-Fe-C, Mn-Fe-Si, and Mn-Fe-C-Si Systems", *Metall. Mater. Trans. B*, **28**, 553–562 (1997) (Thermodyn., Calculation, 41)

[1998Jun] Jun, J.-H., Baik, S.-H., Lee, Y.-K., Choi, C.-S., "The Influence of Aging on Damping Capacity of Fe-17%Mn-X%C Alloys", *Scr. Mater.*, **39**, 39–44 (1998) (Experimental, Phase Relations, Mechan. Prop.)

[1998Lee] Lee, Y.E., "Thermodynamic Assessment of Liquid Fe-Mn-C System", *Metall. Mater. Trans. B*, **29B**, 397–403 (1998) (Thermodyn., Assessment, Phase Diagram, Phase Relations, Calculation, Theory, 18)

[1998Vya] Vyatkin, G.P., Morozov, S.I., Privalova, T.P., "The Surface Phase Transitions During the Segregation of Carbon and Manganese in Fe-Mn-C Alloys" (in Russian), *Dokl. Akad. Nauk*, **359**, 46–47 (1998) (Phase Relations, Experimental, 9)

[1998Zha] Zhang, M.X., Kelly, P.M., "Crystallography and Morphology of Widmanstaetten Cementite in Austenite", *Acta Mater.*, **46**, 4617–4628 (1998) (Crys. Structure, Morphology, Experimental, 28)

[1999Owe] Owen, W.S., Grujicic, M., "Strain Aging of Austenitic Hadfield Manganese Steel", *Acta Mater.*, **47**, 111–126 (1999) (Calculation, Thermodyn., Mechan. Prop., 42)

[2000Abe] Abe, T., Onodera, H., Kimura, K., Kushima, H., "Effect of M-C (M = Mo, Mn, and Cr) Atomic Pairs on Creep Properties of Fe-M-C Ternary Alloys", *Key Eng. Mater.*, **171–174**, 461–468 (2000) (Calculation, Thermodyn., Mechan. Prop., 24)

[2000Cho] Choi, J.K., Ohtsuka, H., Xu, Y., Choo, W.Y., "Effects of a Strong Magnetic Field on the Phase Stability of Plain Carbon Steels", *Scr. Mater.*, **43**, 221–226 (2000) (Phase Relations, Magn. Prop., Theory, 16)

[2000Koz1] Kozeschnik, E., "A Discussion of Phase Transformations in Fe-C-Mn as Affected by Para-equilibrium Constrains", *J. Phase Equilib.*, **21**, 336–341 (2000) (Kinetics, Phase Relations, Theory, Calculation, 20)

[2000Koz2] Kozeschnik, E., Vitek, J.M., "Ortho-Equilibrium and Para-Equilibrium Phase Diagrams for Interstitial/Substitutional Iron Alloys", *Calphad*, **24**, 495–502 (2000) (Calculation, Phase Relations, Thermodyn., 10)

[2000Kun] Kunze, J., Beyer, B., "Thermodynamical Calculation of Martensite Start Temperatures in the System FeCrMnNiC", *Z. Metallkd.*, **91**, 106–113 (2000) (Phase Relations, Calculation, 35)

[2000Lu] Lu, X., Qin, Z., Zhang, Y., Wang, X., Li, F., Ding, B., Hu, Z., "Effect of Carbon on the Paramagnetic-Antiferromagnetic Transition and γ - ε Martensitic Transformation of Fe-24Mn Alloys", *J. Mater. Sci. Technol.*, **16**, 297–301 (2000) (Phase Relations, Experimental, 18)

[2001Cha] Cha, P.R., Yeon, D.H., Yoon, J.K., "A Phase Field Model for Isothermal Solidification of Multicomponent Alloys", *Acta Mater.*, **49**, 3295–3307 (2001) (Phase Relations, Kinetics, Calculation, Theory, 38)

[2001Fen] Fenstad, J., Tuset, J.Kr., "The Binary Diagrams within the System Fe-Mn-C-O, and the Thermal Properties of Elemental Manganese", *INFACON 9: Proceedings of the International Ferro-Alloys Congress, June 2001, Quebec, Canada*, **9**, 1–11 (2001) (Experimental, Phase Relations, Thermodyn., 25)

[2001Lee] Lee, B.-J., "Evaluation of Off-Diagonal Diffusion Coefficient from Phase Diagram Information", *J. Phase Equilib.*, **22**, 241–246 (2001) (Kinetics, Calculation, Theory, 9)

[2001Ma] Ma, Z., "Thermodynamic Description for Concentrated Metallic Solutions Using Interaction Parameters", *Metall. Trans. B*, **32B**, 87–103 (2000) (Calculation, Thermodyn., 70)

[2001Ume] Umemoto, M., Liu, Z.G., Masuyama, K., Tsuchiya, K., "Influence of Alloy Additions on Production and Properties of Bulk Cementite", *Scr. Mater.*, **45**, 391–397 (2001) (Crys. Structure, Experimental, Mechan. Prop., Phase Relations, Phys. Prop., 13)

[2001Wan] Wang, H., Wang, S., Yue, K., Dong, Y., Li, W., "The Rules of Thermodynamic Properties in Fe-C-j (j=Ti, V, Cr, Mn) Melts", *Acta Metall. Sin. (China)*, **37**, 952–956 (2001) (Calculation, Thermodyn., 13)

DOI: 10.1007/978-3-540-74196-1_6

[2002Cap] Capdevila, C., Caballero, F.G., Garcia de Andres, C., "Kinetics Model of Isothermal Pearlite Formation in a 0.4C-1.6Mn Steel", *Acta Mater.*, **50**, 4629–4641 (2002) (Kinetics, Theory, 38)

[2002Lee] Lee, J., Shibata, K., Asakura, K., Masumoto, Y., "Observation of α - γ Transformation in Ultralow-Carbon Steel Under a High Temperature Optical Microscope", *ISIJ Int.*, **42**, 1135–1143 (2002) (Experimental, Morphology, Kinetics, 30)

[2002Sah] Sahu, P., De, M., Kajiwara, S., "Microstructural Characterization of Fe-Mn-C Martensites Athermally Transformed at Low Temperature by Rietveld Method", *Mater. Sci. Eng. A*, **333**, 10–23 (2002) (Crys. Structure, Experimental, 36)

[2003Gam] Gamsjaeger, E., Fischer, F.D., Svoboda, J., "Interaction of Phase Transformation and Diffusion in Steels", *J. Eng. Mater. Technol. (Trans. ASME)*, **125**, 22–26 (2003) (Kinetics, Experimental, 25)

[2003Kap] Kaputkina, L.M., Kaputkin, D.E., "Structure and Phase Transformations under Quenching and Tempering During Heat and Thermomechanical Treatment of Steels", *Mater. Sci. Forum*, **426–432**, 1119–1126 (2003) (Crys. Structure, Review, Kinetics, Morphology, Phase Relations, 7)

[2003Kim] Kim, E.-J., You, B.-D., Pak, J.-J., "Thermodynamics of Carbon in Liquid Manganese and Ferromanganese Alloys", *Metall. Mater. Trans. B*, **34B**, 51–59 (2003) (Experimental, Thermodyn., 24)

[2003Lee1] Lee, Y.E., "Thermodynamics Assessment of Liquid Mn-Fe-C System by Unified Interaction Parameter Model", *ISIJ Int.*, **43**, 144–152 (2003) (Assessment, Calculation, Thermodyn., 22)

[2003Lee2] Lee, Y.-K., Baik, S.-H., Kim, J.-C., Choi, C.-S., "Effects of Amount of Epsilon Martensite, Carbon Content and Cold Working on Damping Capacity of an Fe-17% Mn Martensitic Alloy", *J. Alloys Compd.*, **355**, 10–16 (2003) (Crys. Structure, Experimental, Morphology, Phase Relations, Phys. Prop., 13)

[2003Roc] Rochman, N.T., Kuramoto, S., Fujimoto, R., Sueyoshi, H., "Effect of Milling Speed on an Fe-C-Mn System Alloy Prepared by Mechanical Alloying", *J. Mat. Proc. Tech.*, **138**, 41–46 (2003) (Experimental, Mechan. Prop., Morphology, 10)

[2003Zhu] Zhu, H.T., Chang, H.B., Xu, Z.Y.Hsu, T.Y., "Simplified Thermodynamic Model for Proeutectoid Ferrite Formation in Multicomponent Structural Steel", *J. Iron Steel Res. Int.*, **10**, 33–37 (2003) (Thermodyn., Calculation, 21)

[2004Aar] Aaronson, H.I., Reynolds, W.T., Purdy, G.R., "Coupled-solute Drag Effect on Ferrite Formation in Fe-C-X Systems", *Metall. Mater. Trans. A*, **35A**, 1187–1210 (2004) (Interface Phenomena, Kinetics, Morphology, Phase Relations, Review, 148)

[2004All] Allain, S., Chateau, J.-P., Bouaziz, O., Migot, S., Cuelton, N., "Correlations Between the Calculated Stacking Fault Energy and the Plasticity Mechanisms in Fe-Mn-C Alloys", *Mater. Sci. Eng. A*, **387**, 158–162 (2004) (Mechan. Prop., Theory, 26)

[2004Fu] Fu, W., Furuhara, T., Maki, T., "Effect of Mn and Si Addition on Microstructure and Tensile Properties of Cold-rolled and Annealed Pearlite in Eutectoid Fe-C Alloys", *ISIJ Int.*, **44**, 171–178 (2004) (Crys. Structure, Experimental, Mechan. Prop., Morphology, Phys. Prop., 32)

[2004Hut1] Hutchinson, C.R., Shiflet, G.J., "The Formation of Partitioned Pearlite at Temperatures above the Upper Ae1 in an Fe-C-Mn", *Scr. Mater.*, **50**, 1–5 (2004) (Experimental, Morphology, Phase Relations, 5)

[2004Hut2] Hutchinson, C.R., Hachenberg, R.E., Shiflet, G.J., "The Growth of Partitioned Pearlite in Fe-C-Mn Steels", *Acta Mater.*, **52**, 3565–3585 (2004) (Morphology, Experimental, 41)

[2004Wit] Witusiewicz, V.T., Sommer, F., Mittemeijer, E.J., "Reevaluation of the Fe-Mn Phase Diagram", *J. Phase Equilib. Diffus.*, **25**, 346–354 (2004) (Phase Diagram, Thermodyn., Assessment, Calculation, 34)

[2005Cha] Cha, P.-R., Yeon, D.-H., Yoon, J.-K., "Phase-field Model for Multicomponent Alloy Solidification", *J. Cryst. Growth*, **274**, 281–293 (2005) (Phase Relations, Morphology, Theory, 40)

DOI: 10.1007/978-3-540-74196-1_6

[2005Gam] Gamsjaeger, E., Svoboda, J., Fischer, F.D., "Austenite-to-ferrite Phase Transformation in Low-Alloyed Steels", *Comput. Mater. Sci.*, **32**, 360–369 (2005) (Phase Relations, Calculation, 16)

[2005Mas] Massardier, V., Patezour, E.L., Soler, M., Merlin, J., "Mn-C Interaction in Fe-C-Mn Steels: Study by Thermoelectric Power and Internal Friction", *Metall. Mater. Trans. A*, **36A**, 1745–1755 (2005) (Phys. Prop., Experimental, 28)

[2005Mor] Morito, S., Saito, H., Ogawa, T., Furuhara, T., Maki, T., "Effect of Austenite Grain Size on the Morphology and Crystallography of Lath Martensite in Low Carbon Steels", *ISIJ Int.*, **45**, 91–94 (2005) (Electronic Structure, Experimental, Morphology, 17)

[2005Sil1] Sil'man, G.I., "Phase Diagram of Alloys of the Fe-C-Mn System and Some Structural Effects in This System. Part I. Interphase Distribution of Manganese", *Met. Sci. Heat Treat.*, **47**, 48–52 (2005) (Experimental, Phase Relations, 14)

[2005Sil2] Sil'man, G.I., "Phase Diagram of Alloys of the Fe-C-Mn System and Some Structural Effects in This System. Part II. Calculation and Construction of Isothermal Sections of the Diagram", *Met. Sci. Heat Treat.*, **47**, 123–130 (2005) (Phase Relations, Phase Diagram, Calculation, 12)

[2005Sil3] Sil'man, G.I., "Phase Diagram of the Fe-C-Mn System and Some Structural Effects in This System. Part 3. Polythermal Sections and Projections of the Diagram", *Met. Sci. Heat Treat.*, **47**, 397–401 (2005) (Phase Relations, Calculation, 4)

[2005Wan] Wang, H., Wang, S., Zhou, Y., Gao, L., Dong, Y., Sun, H., "The Thermodynamic Properties of Fe-Mn-C Melt at Reduced Pressure", *Steel Res. Int.*, **76**, 731–734 (2005) (Thermodyn., Experimental, 7)

[2006Aar] Aaronson, H.I., Reynolds, W.T., Purdy, Jr., G.R., "The Incomplete Transformation Phenomenon in Steel", *Metall. Mater. Trans. A*, **37A**, 1731–1745 (2006) (Kinetics, Review, 89)

[2006MSIT] "C-Fe (Carbon - Iron)", Diagrams as Published in MSIT Workplace, Effenberg, G. (Ed.), MSI, Materials Science International Services GmbH, Stuttgart; Document ID: 30.13598.1.20, (2006) (Phase Diagram, Phase Relations, Crys. Structure, 2)

[2006Sil] Sil'man, G.I., "Alloys of the Fe-C-Mn System. Part 4. Peculiarities of Formation of Structure in Manganese and High-Manganese Ateels" (in Russian), *Metalloved. Term. Obrab., Met.*, (1), 3–7 (2006) (Morphology, Phase Relations, Experimental, 7)

[Mas2] Massalski, T.B. (Ed.), *Binary Alloy Phase Diagrams*, 2nd edition, ASM International, Metals Park, Ohio (1990)

[V-C2] Villars, P. and Calvert, L.D., *Pearson's Handbook of Crystallographic Data for Intermetallic Phases*, 2nd edition, ASM, Metals Park, Ohio (1991)

DOI: 10.1007/978-3-540-74196-1_6

Carbon – Iron – Molybdenum

Tamara Velikanova, Mikhail Turchanin, Tatyana Dobatkina, Tatyana Velikanova

Introduction

The constitution of the C-Fe-Mo system is of great interest not only because molybdenum is one of the main alloying elements in tool and heat-resisting steels, but also because the complete C-Fe-Mo phase diagram is required in many other applications. Most of the available literature on the C-Fe-Mo system is devoted to investigation of the structure and properties of molybdenum steels. The data on phase relations and crystal structure of phases are presented mainly in the works listed in Table 1.

The earliest works mostly deal rather with the effect of molybdenum on the structure and properties of steels containing typically Mn, Si, Cr and Ni than information on the ternary C-Fe-Mo system itself. Stable, metastable or partly metastable states, in particular, involving cementite, which is realized in steels were considered. The first investigations concerning the C-Fe-Mo alloy system are stimulated by widening incorporation of Mo in steel production carried out independently by [1932Tak1, 1932Tak2] and [1936Sve]. A very detailed study of the system in the Fe-Mo-Mo_2C-Fe_3C range was carried out by Takei [1932Tak1, 1932Tak2]. The ternary M_6C type phase, denoted as τ_1 in the current assessment, was found and shown in the proposed liquidus projection. Evidence for the existence of another ternary phase Fe_2MoC, sometimes named molybdenum cementite phase (τ_2 here), has also been obtained by Takei. A number of vertical sections and a complex reaction scheme have been constructed.

The phase relationships in the Fe corner of the ternary system up to 10 mass% Mo and 2.2 mass% C were investigated by [1936Sve] using alloys of commercial purity. Six vertical sections, from the liquidus down to about 600°C, showing phase equilibria of liquid, (αFe), (γFe), (C) and ternary carbide (denoted in [1936Sve] by ω) are reported. A schematic diagram of metastable states of alloys in the composition triangle including the Fe_3C phase is given. The results are in reasonable agreement with the later data.

Subsequently, the structure and properties of the C-Fe-Mo alloys of different purity, including phase relationships, crystal structure of ternary phases and thermodynamic behavior of alloys, were experimentally investigated in a number of works [1953Kuo1, 1953Kuo2, 1953Kuo3, 1959Fuw, 1959Neu, 1960Cam, 1962Sat, 1968Jel, 1969Bun1, 1969Bun2, 1970Sav, 1970Suz, 1971Gre, 1971Kin, 1972Foo, 1972Hof, 1972Nis, 1972Pet, 1972Sav, 1972Wad, 1975Uhr, 1976Lob1, 1976Lob2, 1976Niz, 1976Sna, 1976Tar, 1977Cha, 1977Fri, 1977She, 1977Uhr, 1980Bra, 1986Wad, 1990Ips, 1991Sch, 1994Sch, 1995Dan, 1995Gir] and phase equilibria were critically reviewed by [1985Riv, 1988Ray, 1994Rag, 2002Rag]. The reaction scheme of [1932Tak1, 1932Tak2] modified by [1968Jel] was adopted later by [1985Riv, 1988Ray]. Partly metastable equilibria including the metastable binary cementite phase are presented in this scheme. Two stable ternary phases: τ_1 (formed by a peritectic reaction) and τ_2 (formed by a peritectoid reaction) are considered. A partly metastable reaction scheme of the C-Fe-Mo system is given also by [1991Sch] on the basis of the results of own experimental investigation of the C-Fe-Mo phase diagram over the whole concentration range. The metastable binary Fe_3C phase, coexisting with (αFe), (γFe), τ_2, Mo_2C, $M_{23}C_6$ (τ_4) and graphite phases are showed in the reaction scheme.

The crystal structure of τ_1 was established by [1933Ade] to be complex cubic and of the τ_2 phase was reported by [1964Dys] to be orthorhombic, different from that of the binary cementite Fe_3C (see Table 2). A peritectoid reaction of formation was assumed for τ_2 by [1964Dys]. For the latter a monoclinic structure and composition Fe_2MoC were obtained from more precise data of [1983Way, 1985Rap]. [1983Way] has found a field of primary crystallization for this phase. Peritectic crystallization of τ_2 was established by [1988And1, 1991Sch, 1995Dan, 1995Gir].

A thermodynamic modeling of the equilibria of austenite with carbides at 1000°C was performed earlier by [1972Nis]. The obtained results differed from those reported before by [1960Cam] and [1969Bun1] but later were confirmed by [1975Uhr] and [1986Wad]. The results of [1975Uhr] were combined with the available information on other temperatures and own experimental data over the temperature range 700 to 1000°C by [1977Cha] in order to obtain a thermodynamic description of the iron rich corner in the C-Fe-Mo system.

DOI: 10.1007/978-3-540-74196-1_7

The invariant reactions, isothermal and vertical sections including the stable ternary phases τ_1, τ_2 and τ_3 are reported in the thermodynamic assessment by [1988And1]. In this case, the ternary solid solution based on the Fe_3C (τ_3) is considered as a separate ternary stable phase. The $M_{23}C_6$ phase (τ_4) is ignored because its existence is not evident in the ternary C-Fe-Mo without additions, which could stabilize this carbide. The results of the calculation by [1988And1] were adopted by [1994Rag] with some corrections and reported as a reaction scheme. The results of the calculation of the liquidus surface and isothermal section at 1000°C by [1988And1] were confirmed experimentally by [1995Gir] for the composition range up to 35 at.% Mo.

Many data on the structure and properties of so-called molybdenum steels, including complex alloyed steels, are available. It is briefly reviewed in the section Notes on Materials Properties and Application of the present assessment.

The constitution of the system being rather complicated, in general is established, however some details need further investigation, as discussed below.

Binary Systems

The C-Fe system is accepted from [2006MSIT]. The C-Mo and Fe-Mo systems are accepted from [Mas2]. In the thermodynamic assessment by [1988And1], the binary phase diagrams of the C-Fe and C-Mo systems are taken from [1985Gus] and [1988And2], respectively. The Fe-Mo system is taken according to the thermodynamic assessment by [1982Gui] updated by [1988And1]. The calculated phase diagrams differ only in some details from that in [Mas2], and these differences do not influence the type of the invariant equilibria obtained by calculation.

Solid Phases

Crystallographic data on the C-Fe-Mo phases and their temperature ranges of stability, if available, are listed in Table 2. Iron and molybdenum form extended fields of solid solution, carbon is markedly dissolved in (δFe) and much more in (γFe), but the solubility of carbon in (αFe) and especially in (Mo) and in Fe-Mo intermetallics is negligible. Some increase in both the solubility of carbon in (αFe) and the temperature of the eutectoid decomposition is observed by [1976Lob1, 1976Lob2]. Solid solution of iron in the β phase extends into the ternary system to 6 at.% after [1988And1] at 1000°C (10 ± 3 at.% after [1991Sch]).

Solution of small amounts of molybdenum in the metastable binary Fe_3C stabilizes this carbide. As a result, $(Fe_{1-x}Mo_x)_3C$ solid solution, τ_3, exists in the ternary system as a separate ternary phase in the temperature range from 1126°C, the temperature of its peritectic formation down to 910°C, the temperature of the eutectoid decomposition after [1988And1].

In addition to this ternary phase, two other stable carbides are well established. The τ_1 phase, f.c.c. Mo_6C (η-carbide"), was observed for the first time by [1932Tak1]. Its structure was determined by [1933Ade] as a structure of the Fe_3W_3C type containing 96 metal atoms in the unit cell. Its composition is $(Fe_{1-x}Mo_x)_6C$ at $x = 0.33$-0.66. The τ_2 carbide was found by [1953Kuo1] (denoted by him as Fe_aMo_bC), and its stoichiometry (Fe_2MoC) and structure as orthorhombic (a = 1627.6 ± 0.2, b = 1003.4 ± 0.1, c = 1132.3 ± 0.1, pm) related to cementite Fe_3C were reported by [1964Dys]. The same structure for the Fe_2MoC (τ_2) phase (a = 1613, b = 996, c = 1109, pm) was found by [1979Woo]. In both cases, of [1964Dys] and [1979Woo], the alloys contained Mn, Cr and Si. From the single crystal X-ray data of [1983Way] crystal structure of τ_2 is monoclinic of its own type. This carbide, sometimes referred to as ξ-carbide, has rather restricted homogeneity range. According to the calculation by [1988And1], it forms through the peritectic reaction L + C + β ⇌ τ_2 at 1086°C and exists down to 653°C, where it decomposes. After [1962Sat] it is stable at 700°C. Contrary to that, [1991Sch] supposes that, being stable at 1000°C, τ_2 is already metastable at 800°C. Both τ_1 and τ_2 carbides have been confirmed by a number of investigators as stable phases. The question whether the $M_{23}C_6$ carbide (τ_4) is stable has not been solved yet, so in the current assessment it is not accepted. The metastable phases τ_5, τ_6 (ε with hcp structure, χ of the αMn type) and τ_7 (π of the βMn type) were found in alloys rapidly quenched from the melts [1980Iwa, 1981Ino] and [1993Kha], respectively.

DOI: 10.1007/978-3-540-74196-1_7

Invariant Equilibria

The reaction scheme in Fig. 1 and the data on the invariant equilibria in the system over the whole composition range given in Table 3 are mainly based on the calculation by [1988And1] who accumulated the earlier information on the thermodynamic properties and phase equilibria [1985Riv, 1986Wad]. They were generally supported by the later experimental investigation of [1995Gir] in the Fe rich part of the system. Some necessary corrections and additions to the reaction scheme proposed by [1994Rag], who adopted the results of [1988And1], have been made in the present assessment based on the recalculation of the phase equilibria using the data set of [1988And1]. Recent data for the boundary binary systems concerning the temperature and the type of invariant reactions, and a new version of the C-Mo phase diagram [1988Vel, Mas2] were taken into account.

A reaction scheme was first proposed by [1932Tak2]. It appears again in the work of [1968Jel] with some modifications. The latter was adopted by [1985Riv, 1988Ray] and reproduced together with the corresponding list of ternary reactions. Taking into account the new version of the C-Mo phase diagram accepted by [Mas], the authors of [1985Riv, 1988Ray] assumed two additional invariant equilibria with the participation of the high temperature δ and η phases to obtain the monovariant equilibrium L ⇌ β + C needed for the reaction assumed by [1985Riv] as L ⇌ γ + β + C to occur. The equilibrium of α, γ, β and carbon was established later by [1988And1] as L + β + C ⇌ τ_2. The above mentioned high temperature reactions are U_1 and U_2 in Fig. 1: L + η ⇌ β + δ and L + δ ⇌ β + C, respectively. They seem to be the most logical reactions in the ternary system from the viewpoint of the catatectic reaction δ ⇌ *l* + η existing in the binary C-Mo system. The same hypothetical equilibria with the η and δ participation were considered by [1985Riv], however they were not included in his reaction scheme.

There are significant difficulties in the results of experimental investigation of phase relationships in the composition range close to the Mo corner of the Gibbs triangle because of the high temperature and extremely high rate of the phase transformation processes. The reaction scheme given by [1985Riv, 1988Ray] differs from that proposed by [1994Rag] because metastable equilibria with the participation of Fe_3C and a peritectoid reaction of the τ_2 phase formation in the ternary system are accepted by [1994Rag]. The τ_2 phase was established later by [1988And1, 1991Sch, 1995Gir] to crystallize from liquid by a peritectic reaction at 1087°C, P_2, as well as τ_3 by P_1 at 1126°C by [1988And1, 1995Gir]. It is interesting to note that [1991Sch] found the invariant point of the liquid phase at 1123°C and a composition coinciding with P_1, however he treated it as a metastable eutectic L ⇌ γ + Fe_3C + τ_2. The reaction of the τ_1 carbide formation should not be considered as established. This phase coexists with liquid, β and (Mo) at 1626°C in an invariant equilibrium of the transition type, U_4, according to the calculated by [1988And1] composition of the phases. The reported by [1968Jel, 1985Riv, 1988Ray, 1991Sch, 1994Rag] peritectic reaction of the τ_1 phase formation is impossible because of the relative positions of the calculated phase compositions, as seen in Table 3. It is important to note that for the U_4 reaction a temperature maximum must exist on the monovariant equilibrium line L ⇌ τ_1 + β (Fig. 2). According to our calculation made using the data set of [1988And1] the maximum lies at 34.41 at.% Mo, 17.5 at.% C and 2063°C. The existence of the maximum can indicate either a congruent melting of τ_1 carbide L ⇌ τ_1 or a quasibinary reaction of a congruent melting in transition point L, β ⇌ τ_1, as it is given in Fig. 1. This question should be investigated additionally because the obtained results of the computation in this area do not give a definitive answer. The thermodynamic model of the liquid phase does not seem to be adequate to solve this question. Not taking into account the homogeneity range of the τ_1 phase concerning carbon content can also negatively influence the results of the computation. The maximum on the solidus of the τ_1 phase in equilibrium with the β carbide, was not confirmed experimentally [1991Sch]. Thus, further experimental work is needed here as well.

The calculated invariant reactions P_1, P_2, U_8, U_{10}, U_{11}, U_{12} and E_1, in the iron rich part of the system were confirmed by the experiments of [1995Gir]. Especially good agreement for the compositions of the liquid phase and temperatures of invariant equilibria U_{11} and E_1 has been found: 17.5C, 9.0Mo (at.%) at 1080°C after [1995Gir] compared to 17.4C, 8.8Mo (at.%) at 1078°C after [1988And1] and 17.3C, 8.0Mo (at.%) at 1065°C [1988And1], compared to 18.1C, 7.7Mo (at.%) at 1065°C [1988And1], respectively. However, the concentration of iron along the τ_1/α and τ_1/γ boundaries is markedly less than the computed values. At the point U_8, it is 77 at.% Fe after [1995Gir] compared to 82.0 at.% Fe after [1988And1].

DOI: 10.1007/978-3-540-74196-1_7

Stable and metastable versions of the equilibria in the system have also been proposed by [1977She], without experimental support. They gave metastable reactions at 1150°C, L + C ⇌ β + M_3C and L ⇌ γ + β + M_3C accepted by [1985Riv] in his reaction scheme. The stable version of [1977She] includes the reactions L + δ ⇌ γ + τ_1 and L + τ_1 ⇌ γ + β in agreement with U_8 and U_{10}, respectively as the calculated by [1988And1] (Table 3), but at slightly different temperatures. Equilibrium between the phases L, β, γ and C at 1150°C was proposed by [1977She, 1981She] instead of an equilibrium reaction including the τ_2 and τ_3 phases.
The reaction schemes reported by [1932Tak2, 1968Jel, 1985Riv, 1977She, 1991Sch] include reactions with the participation of the metastable binary Fe_3C phase. There is an opinion that the metastable phase diagram should serve as a better guide to phase behavior in practical situations because molybdenum stabilizes cementite in the ternary system and graphitization may be prevented by raising the rate of cooling. However, since there is no agreement between different suggestions concerning the type and the sequence of reactions, including metastable ones, they are not discussed in the current assessment in detail.
The presence of the Fe_3C based phase in as-cast and annealed ternary C-Fe-Mo alloys in the corresponding composition range may be related to the equilibrium existence of the stable τ_3 solid solution. Experimental difficulties in distinguishing closely related crystal structures of Fe_3C cementite and τ_3 on one hand and molybdenum cementite, τ_2, on the other hand may explain why the phase relations in the composition range of the τ_3 and τ_2 coexistence have not been established experimentally for a long time notwithstanding a great number of works. Below 1087°C, the temperature of a peritectic formation of the τ_2 phase, the reaction scheme calculated by [1988And1] is not consistent with earlier experimental findings, because the latter were obtained without taking into account the existence of τ_2 (and τ_3 also) fields of the primary crystallization on the liquidus made using the data set of [1988And1].
The β, β' and β" phases are indistinct because of their very close relationship and therefore possible solid phase equilibria with the β' and β" participation are not considered in the present assessment.
The reaction β + C ⇌ τ_2 + MoC reported by [1994Rag] within 700-1000°C range is not confirmed and four new solid state reactions, U_{17}, E_3, U_{18} and D_4, are revealed by the calculation in the current assessment, made using the data set of [1988And1].

Liquidus, Solidus and Solvus Surfaces

A liquidus surface projection is given in Figs. 2a and 2b. There is general agreement between the shape of the τ_1 liquidus surface as calculated by [1988And1] and [1995Dan] and that estimated by [1973Wad, 1985Riv, 1988Ray], mainly on the basis of the experimental results of [1932Tak1, 1932Tak2, 1968Jel]. There are differences in the type, temperature and compositions of the four-phase equilibria introduced by [1985Riv] to link different experimentally investigated parts of the system. Some disagreement between the calculated and assessed [1985Riv] features is not essential taking into account that [1985Riv] considered only the experimental works of [1932Tak1, 1932Tak2, 1968Jel] to estimate liquidus. The liquidus surface projection recently calculated by [1988And1] has been confirmed experimentally by [1995Gir] for the Fe rich part of the system, at above 70 at.% Fe. The reported boundaries of the primary crystallization fields, *e.g.* monovariant lines τ_1/α and τ_1/γ, as well as the disposition of primary crystallization fields of the τ_2 and τ_3 phases after [1995Gir] agree satisfactory with computed ones. The location of the monovariant lines on the liquidus projection was established by microstructure investigation of slowly cooled or quenched alloys for definition of the primary crystallized phase and the crystallization paths. The liquidus temperatures corresponding to the peaks during the cooling process by DTA were established with a cooling rate of 5 $K \cdot min^{-1}$. The structure of samples was determined using metallography and X-ray methods. Under these conditions, experimental results were well reproducible and accurate. The maximum temperature on the monovariant line L ⇌ β + τ_1 and liquidus surfaces of δ, η and β near the C-Mo side were established by calculation only. In Fig. 3 the liquidus isotherms after [1988And1] are given. As can be seen in Fig. 3, the liquidus temperatures of the τ_1 phase monotonously rises with increasing Mo content in the alloys in such a way that temperature maximum is attained at some point on the monovariant line of the liquid phase in the L ⇌ τ_1 + β equilibrium. From this critical point, the monovariant line L ⇌ τ_1 + β steeply drops to U_{10} as well as to U_4 points. The maximum seems to be reliable, but its coordinates should be examined. A temperature maximum on the solidus of the τ_1 phase was not found in the experiments of [1991Sch]. [1991Sch, 1994Sch]

DOI: 10.1007/978-3-540-74196-1_7

reported τ_2 phase liquidus surface with a wider extension compared with the calculation, covering the liquidus field of molybdenum cementite after [1988And1, 1995Gir]. The wide field of the primary crystallization of the Fe_3C phase adjoining the C-Fe boundary system axis is shown by [1991Sch, 1994Sch] in the liquidus projection, which contradicts the known fact that Fe_3C carbide is metastable in the binary C-Fe. Thus, these results can not be accepted.

The data on the liquidus isotherms reported by [1985Riv] have been derived from the primary thermal arrests tabulated by [1932Tak1, 1932Tak2]. Satisfactory agreement was reported for temperature and composition of points, where the binary axis (both C-Fe and Fe-Mo accepted by the authors) are intersected by the constructed liquidus isotherms, however the location of the invariant reaction points did not always agree with [1932Tak1, 1932Tak2]. Notwithstanding a good reproduction, the measured temperatures do not agree with today's data being about 100°C lower. The experimental liquidus isotherms on the surface of the primary graphite crystallization assessed by [1985Riv] are given in Fig. 4. The experimental data are available for three temperatures: 1550°C [1960Mor], 1450°C [1960Fuw, 1973Rim] and 1350°C [1963Yag, 1973Rim]. The points obtained by [1960Fuw] show marked scatter and are considered less reliable than those of [1973Rim] at the same temperature. The data of [1963Yag] and [1973Rim] for 1350°C are in good agreement. Therefore the data of [1973Rim] for 1350°C and 1450°C are preferred and given in Fig. 4 together with the data of [1960Mor] for 1550°C. The intercepts of the isotherms with the C-Fe binary axis agree fairly well with the carbon contents expected from the graphite liquidus of the C-Fe binary system.

The solidus projection of the ternary system and solvus projection of the γ phase are given in Figs. 5 and 6 according to [1988And1]. Three ternary phases τ_1, τ_2 and τ_3 appear on the solidus. The experimental data on the extension of the τ_2 and τ_3 phases on the solidus surface are not available, thus they are shown in Fig. 5 as calculated. The calculated limits of molybdenum content in the τ_1 phase (34.4 to 48.0 at.%) are in good agreement with experimentally defined values of about 35 to 48 at.% obtained on alloys quenched from the solidus [1991Kha]. The projection of solvus of the γ phase given in Fig. 6 shows that all carbides coexist in equilibrium with this phase in wide temperature intervals from the solidus down to low temperature.

Isothermal Sections

Isothermal sections at 1250, 1000, 900, 800, 700 and 550°C are given in Figs. 7 to 12 according to [1988And1] (for 1250, 900, 800, 700 and 550°C as calculated in the current assessment). One can see that the homogeneity ranges of the ternary τ_1 and τ_2 phases reduce with decreasing temperature and the composition of stable ternary cementite solid solution, τ_3, draws to the C-Fe axis of the composition triangle with decreasing temperature from 3.77 at.% Mo at 1076°C to 1.8 at.% at 910°C, near the point of the eutectoid decomposition of the phase. Both $\gamma + \beta$ and $\alpha + \beta$ equilibria are exposed in the section at 800°C together with three-phase fields $\gamma + \beta + \tau_2$ and $\alpha + \beta + \tau_1$. The γ phase in equilibria with β and τ_2 existing at 800°C is replaced by α in the section at 700°C. The same feature exists at 739 to 680°C. In addition, the equilibrium of α with MoC carbide appeared at 684°C is exposed in the isothermal section at 550°C, Fig. 12.

The calculated phase equilibria for 1000°C given in Fig. 8 are generally consistent with the data of the earlier experiments of [1972Nis, 1969Fra]. The equilibria with the participation of the metastable Fe_3C are revised in the current assessment. The calculation has been confirmed by the recent work of [1995Gir] in the range Fe-τ_1-Mo_2C-C perfectly. The section at 1000°C after [1972Nis, 1985Riv] represents the phase equilibria covering the whole composition range based on data obtained for the alloys equilibrated at 1000°C for 100 h. At 1000°C α, γ, τ_1, τ_2, (Mo), β, μ and Fe_3C phases are shown in [1972Nis, 1985Riv]. However, the Fe_3C solid solution is not separated from the binary C-Fe side as that is required according to the known fact that Fe_3C is not stable in the binary system. The extension of the homogeneity range of the β phase computed according by [1988And1] agrees with that experimentally determined. After [1995Gir], the content of iron in β is limited to 6 at.% in as-cast alloys. According to [1991Sch], the solubility at 1000°C is 10 ± 3 at.%, which may be considered as being in agreement with [1995Gir] and the calculation. The isothermal section at this temperature reported by [1991Sch] generally agrees with the above. However, they concluded that the carbides β, τ_1 and τ_2 form tie-lines with ferrite but do not form them with austenite, which contradicts the above experimental results and calculation. This result may have been obtained because austenite containing a significant amount of dissolved carbon at 1000°C

DOI: 10.1007/978-3-540-74196-1_7

could transform under quenching martensitically and XRD could not give correct data [1994Rag]. [1991Sch] treats cementite as a stable phase in the same way as [1972Nis] and [1985Riv] do. Equilibria $\gamma + C$ and $\gamma + C + \tau_3$ are not shown in the section. The experimental data of [1962Sat] on the phases coexisting in the system at 900 and 700°C and the proposed isothermal sections are in conflict with both the results given in Figs. 9 and 11, and differs from [1991Sch]. The equilibrium of τ_1 and τ_2 phases is reported by [1962Sat] instead of $\gamma + \beta$ at 900°C or $\alpha + \beta$ at 700°C after [1988And1]. These results should be treated as metastable, because of an evidential lack of equilibrium (even upon 500 h annealing at 700°C in that work). For more details see section Miscellaneous.

The isothermal sections at 871, 927 and 982°C in the Fe rich part of the system given in Fig. 13 were proposed by [1979Woo] based on a very detailed study. The coexistence of the τ_1 and τ_2 ternary carbides with the γ and Fe_3C based phases was established. The $M_{23}C_6$ phase was not found. In case of treating the reported Fe_3C based phase as τ_3 the obtained results fall in agreement with the calculated section at 900°C, shown in Fig. 9.

When the solubility of Mo in the γ phase was investigated in the narrow temperature ranges by [1960Cam, 1962Sat, 1972Wad, 1972Nis, 1975Uhr] the same phases coexisting in equilibria were observed in alloys, though solubility was found to be significantly different. Bearing in mind the conditions of the experiments, one should suppose that these results are due to impurities, which may accelerate the transformation under quenching. The results of [1979Woo] are considered to be closer to equilibrium [1985Riv].

The isothermal section at 800°C reported by [1991Sch] markedly differs from that given in Fig. 10 after [1988And1] and data of earlier investigators. The $M_{23}C_6$ based carbide of the composition $Fe_{21}Mo_2C_6$ is reported to coexist in equilibria with Fe_3C, α, β phases and admittedly with graphite. In the isothermal section the τ_2 phase is not shown. No τ_2 phase was found by X-ray analysis, in the alloys prepared by sintering at 800°C for 600 h, but it was always present in the alloys melted before annealing at 800°C for 1000 h. From this it was concluded that τ_2 is metastable at 800°C, which is an important conclusion that requires verification. The question whether the $M_{23}C_6$ carbide is stable in the ternary C-Fe-Mo alloys without contaminations, such as Mn, Cr and Si, is not solved yet. As mentioned above, it was omitted in the thermodynamic assessment by [1988And1].

The sections at 1250 and 550°C given in Figs. 7 and 12 are of interest as the technology deals with these temperatures (see section Notes on Materials Properties and Applications). The wide homogeneity regions of the γ solid solution at 1250°C in the Fe rich alloys are replaced the equilibria of the α phase with three carbides τ_1, β and MoC in the section at 550°C as the result of series of phase transformations, finishing at 653°C. Such a kind of equilibria remains down to 347°C. The phase transformations of alloys austenized at 1250°C and tempered at 510-570°C forming precipitates of ternary and molybdenum carbides are the ways of fabricating high strength steels.

Two partial isothermal sections at 1200 and 1800°C in the molybdenum corner reported by [1970Sav] are given in Figs. 14 and 15 in comparison with the calculated ones. The experimental results were obtained on alloys with up to 12 mass% Mo and up to 0.5 mass% C annealed at 1200 and 1800°C for 120 and 25 h, respectively, then reheated electrically at the same temperatures and quenched in liquid nitrogen at an average rate of 600 $K \cdot s^{-1}$. One can see that the phase relationships shown in Fig. 15 cannot be considered as a stable diagram, taking into account the accepted in the current assessment reaction scheme. The (Mo) + β + σ ternary phase field can be realized only if the reaction of the τ_1 phase crystallization at 1629°C, P_1, is suppressed.

Temperature – Composition Sections

Vertical sections at 85 at.% Fe, 2, 5 and 10 mass% Mo, 1 and 2 mass% C are given in Figs. 16 to 19, 21, 22a, 22b as calculated using the thermodynamic model of [1988And1] and at 0.48 and 1.16 mass% C for the Fe rich part in Fig. 20 after the experimental data of [1976Lob1, 1976Lob2]. The sections show a very complex constitution of the phase diagram owing to a number of invariant transformations sometimes with very close temperatures and compositions of the phases coexisting in equilibrium. Because of these complications and difficulties in interpretation of experimental data concerning phase transformations in alloys, thermodynamic calculation as a method for construction of temperature-composition sections is preferred. In the calculations, the $M_{23}C_6$ type carbide is not taken into account.

DOI: 10.1007/978-3-540-74196-1_7

The section at 85 at.% Fe represents phase equilibria with the α and γ based phases participation in a wide temperature range. The other sections are shown in mass%, which is more suitable for practical application. The isopleths at constant molybdenum and carbon content descriptively demonstrate a very strong influence of the third component on the phase transformations in C-Fe alloys, resulting in the formation of very stable binary and ternary carbides capable of additionally strengthening steels. The isopleth at 2 mass% Mo (Fig. 17) demonstrates, among the others, isotherm of equilibrium $\gamma + \tau_1 \rightleftharpoons \alpha + \beta$, U_{14} at 810°C as the highest temperature of coexistence of α and β phases. It is in contradiction at 1190°C according to the version of [1991Sch] for the same equilibrium.
One can see in Fig. 20 that molybdenum additions increase the temperature of the eutectoid decomposition of γ and respectively the carbon solubility in iron. The solubility maximum at 1.15 mass% Mo as read from the figure is 0.02 mass% C. A number of publications are devoted to the investigations of the α and γ ranges of solubility, and their data are represented in the isothermal and vertical sections in [1932Tak1, 1960Cam, 1962Sat, 1969Bun1, 1970Sav, 1970Zem, 1972Nis, 1972Wad, 1975Uhr, 1976Lob1, 1976Lob2, 1979Woo]. There are noticeable discrepancies in the results, which are debatable. They may be caused by a different degree of equilibrium achieved in the samples and/or by unsuspected impurities.

Thermodynamics

The effect of molybdenum on the activity of carbon in liquid iron alloys has been investigated by [1959Fuw, 1960Mor, 1970Suz, 1972Foo], Table 1. The interaction parameter obtained at 1560°C in low-carbon melts by [1959Fuw] was determined as $\varepsilon_C^{Mo} = -3.5$. This value was not referred to fixed carbon concentration. The effect of molybdenum on the solubility of graphite in liquid iron was studied at 1550°C by [1960Mor], and interaction parameter $\varepsilon_C^{Mo} = -3.20$ at $x_C = 0.207$ was given. In [1970Suz], a more negative value of $\varepsilon_C^{Mo} = -6.15$ was obtained at 1560°C for alloys of 0 to 20 mass% Mo and 0.5 to 0.7 mass% C. The first order interaction parameter of molybdenum was found equal to $\varepsilon_C^{Mo} = -4.0 \pm 0.2$ by [1972Foo] at 1550°C, 0 to 6.3 mass% Mo and 0.2 to 0.4 mass% C. The second order interaction parameters $\rho_C^{Mo} = 0.65 \pm 0.15$ and $\rho_C^{Mo,C} = -2.6 \pm 0.2$ were deduced by [1972Foo] using the central atom statistical model. All the above mentioned results point out a decrease in the activity of carbon with adding molybdenum into liquid alloys.
The experimental works [1969Bun1, 1969Bun2, 1971Gre, 1972Nis, 1972Wad, 1975Uhr, 1976Lob2, 1980Bra] were devoted to the study of carbon activity in γ, Table 1. Measurements by [1969Bun1, 1969Bun2] have revealed that molybdenum reduces the carbon activity in this phase proportionally to the molybdenum content added. The interaction parameter ε_C^{Mo} was established to be –9.63 over the temperature interval from 1000°C to 1100°C, carbon concentration from 0 to 7.6 mass% and $x_C = 0$ to 0.11. Based on carbon isoactivities and Gibbs' phase principle, the isothermal sections were build in the iron rich part of the system [1969Bun1, 1969Bun2]. The section qualitatively corresponds to metallographically established phase regions [1960Cam] in areas of low carbon concentrations only.
The activity of carbon in the γ phase has been studied over the temperature range 848 to 1197°C for alloys with 0.33 to 1.33 mass% C and x_{Mo} changing from 0 to 0.025, and the interaction parameter $\varepsilon_C^{Mo} = -11.4$ has been obtained at 1000°C by [1972Wad]. The effect of molybdenum on the activity of carbon in austenite has been determined between 975 and 1125°C for alloys with 0 to 6.68 mass% Mo and 0.015 to 0.587 mass% C [1971Gre]. The temperature dependence of the interaction parameter was expressed as $\varepsilon_C^{Mo} = 7.83 - 15930 \cdot T^{-1}$ (±6%).
The interaction parameter $\varepsilon_C^{Mo} = -7.91$ was established by [1972Nis] at 1000°C, 0 to 2.67 mass% Mo and 0.22 to 1.15 mass% C. On the basis of measurements of carbon activity in [1972Nis], isoactivity lines for carbon in the C-Fe-Mo system at 1000°C were built and solubility lines of carbides were proposed. According to the measurements, the $\alpha + \gamma + \tau_1$ equilibrium takes please at $a_C = 0.05$, $\gamma + \beta + \tau_1$ at $a_C = 0.40$, $\gamma + \tau_2 + \beta$ at $a_C = 0.66$ and $\gamma + Fe_3C + \tau_2$ at $a_C = 0.93$. These findings correlate well with the results of [1975Uhr], where carbon activity was established for alloys with 0.5 to 40 mass% Mo and $a_C = 0$ to 1 at 1000°C. As it follows from the above mentioned works, the activity of carbon in austenitic alloys of the C-Fe-Mo system is depressed by molybdenum.
The experimental works of [1972Pet, 1976Lob1, 1984Wad, 1986Wad] were devoted to the study of carbon activity in α, Table 1. The activity coefficient of carbon in ferritic alloys containing 0.42 to 1.23 mass% Mo was investigated at 800 to 900°C by [1972Pet]. The value of interaction parameter $\varepsilon_C^{Mo} = -64$ was

DOI: 10.1007/978-3-540-74196-1_7

obtained. The results of [1972Pet] indicate an absence of temperature dependence of the activity coefficient of carbon and demonstrate more significant influence of molybdenum on carbon activity in α in comparison with γ.

The activity of carbon in α was investigated by [1976Lob1] at 682 to 848°C and 0 to 1.16 mass% Mo for alloys with 0.003 to 0.017 mass% C. The equations for temperature dependence of partial molar Gibbs free energy of solution of carbon in ferrite were determined. The effect of molybdenum on the thermodynamic properties of carbon was evaluated. The value of the activity coefficient during infinite dilution decreases progressively from pure iron to Fe-1.16Mo (mass%) over the temperature range 750 to 848°C and the reverse occurs for the temperature range 682 to 727°C. Thus ε_C^{Mo} changes from –24.2 at 848°C to 29.0 at 682°C [1976Lob1], and molybdenum increases the solubility of carbon in ferrite relative to the C-Fe system at temperatures above the eutectoid temperature and decreases it below the latter.

The thermodynamic activity of carbon in ferrite alloys were measured at 712°C, 0.24 to 2.93 mass% Mo and 0 to 0.2 mass% C by [1986Wad]. The molybdenum-carbon interaction in the α was analyzed using the central atoms model, and the interaction parameter was determined as $\varepsilon_C^{Mo} = -100 \pm 2$. The τ_1 phase was in equilibrium with α phase over the carbon activity range from 0.045 to 0.156. The β phase was in equilibrium with ferrite at the carbon activity of 0.51. According to the measurements, the α + β + τ_1 equilibrium takes place at $a_C = 0.45$.

The α+γ boundaries in the C-Fe-Mo system were calculated by [1985Eno] using the central atom model.

Gibbs energies of formation of τ_1 (Fe_3Mo_3C) and τ_2 (Fe_2MoC) phases at 1000°C were determined by electromotive force measurements on galvanic cells with solid oxide electrolytes by [1978Kle]. The values of standard Gibbs energies of formation ${}_fG(Fe_3Mo_3C) = -96 \pm 5$ kJ·mol^{-1} and ${}_fG°(Fe_2MoC) = -35 \pm 5$ kJ·mol^{-1} were obtained.

Thermodynamic properties of carbides were evaluated on the basis of the thermodynamic investigation of the molybdenum partitioning between them and γ [1972Nis, 1975Uhr] and α [1986Wad]. The standard free energies of formation of the carbides were expressed by a regular solution model [1972Nis, 1975Uhr, 1986Wad].

Thermodynamic evaluation of the C-Fe-Mo system has been made by [1988And1]. The excess Gibbs energy for ternary liquid alloys was described according to the Redlich-Kister polynomial with ternary Muggianu extrapolation taking into account a single ternary parameter. The Gibbs energy for the ferrite and austenite phases in the ternary system was described with a two-sublattice model assuming that iron and molybdenum can substitute for each other in a metal sublattice and for carbon and vacancies in an interstitial sublattice. The Gibbs energy for the τ_2 phase and Fe_3C was described with a two-sublattice model where iron and molybdenum are mixed in one sublattice and the other sublattice is filled with carbon. The Gibbs energy for the τ_1 phase was described with a four-sublattice model where the iron and molybdenum atoms are mixed in the third sublattice, $Fe_2Mo_2(Fe,Mo)_2C$ and the fourth sublattice is filled with carbon. In such a way, [1988And1] accepts that the τ_1, τ_2 and Fe_3C phases are stoichiometric with respect to carbon but varies in metal content. In order to optimize thermodynamic parameters, the following experimental data were used by [1988And1]: [1972Wad] at 848 and 997°C, [1971Gre] at 975, 1050 and 1125°C, [1980Bra] at 1000 and 1100°C and [1972Nis] at 1000°C. The strong negative interaction parameter of [1986Wad] contradicts the results of calculations by [1988And1].

Notes on Materials Properties and Applications

Molybdenum plays a unique and important role among the common alloying elements added to steels being one of the main alloying elements in tool and heat-resisting steels because of the complex constitution exhibited by steels containing this element. It is a ferrite and cementite stabilizer and forms the so-called molybdenum cementite Fe_2MoC, additionally it is a strong carbide-forming element (MC, M_2C, M_6C). Among the numerous types of the so-called Mo-steels, the *Mo-high speed steels* for application in special cutting tools operating at high speed and high temperature ≤ 600°C and have such useful properties as hot hardness, toughness, high wear resistance, grindability, dimensional stability and high shock resistance related to their structure features, namely the strength of martensite or martensite-bainite matrix and complex carbides distributed in the matrix [1977Tar, 1991Wis, 1996Cha, 2001Mar, 2002Mus]. In the *ferritic steels*, such as ~0.2 mass% C, ~3.5 mass% Mo with other additions [1962Rid], 0.03 at.% C, 0.2 at.% Mo

DOI: 10.1007/978-3-540-74196-1_7

[2000Abe], the main useful property is long term creep strength. The largest strengthening effect is obtained by the addition of Mo to the C-Fe alloys; the molybdenum carbide transformation in ferritic steels has been investigated by [1962Rid]. In the *molybdenum microalloyed low carbon steels* such as 0.25 mass% C, 0.2 mass% Mo with additions of Mn, S, Sb, Si, Sn, As [1994Din], useful properties are high ultimate tensile strength and impact resistance. *Explosively welded molybdenum-steel composites* [1992Cha] are used for the fabrication of heat-resistant vessels and high temperature reactors; the main structural particularity is the ability to form different carbide layers in the molybdenum-steel interface, for example two layers of carbides, M_6C and M_2C, at 1000°C, one M_2C layer at 750°C and two Fe_2MoC and M_2C layers at 700°C. Novel (under development) *hydrogen resistant C-Fe-Mo martensitic steels* with needle shaped Mo_2C particles as hydrogen trapping sites are enhancing the resistance to elastic fracture of components, such as springs, bolts and power plant items [2003Yam]. *Irradiated austenitic steel layered systems* [1994Gau] obtained by e-beam irradiation of Mo sheets mechanically clamped to ARMCO Fe, plain carbon steel and high alloy austenitic steel substrates, are used to improve the corrosion resistance of steels. *Secondary hardened steels*, in which ultra high strength can be obtained by a fine dispersion of M_2C type carbides, have attracted a significant attention for high-performance application and are used at elevated temperatures [2004Hou], the peak hardness observed in C-Fe-Mo and low alloying steel 0.25 C, 0,1 to 2.0 Mo, 2.1 Mn, 0.3 Cr mass% results from Mo-precipitation, and the correlation between secondary hardening and thermoelectric variations exists; ultra-fine precipitates at the peak hardening stage in a tempered C-Fe-Mo alloy have been also examined by [1966Ray1, 1966Ray2, 1991Uem]. *Sintered Mo-steels* [1999Wri, 1999Can, 2000You, 2002Sim, 2005Can] are very promising class of industrial materials due to at least, two reasons: as sintered and potentially sinterable materials, replacing wrought or cast products in more demanding applications in the conditions of a steady market growth (automotive drivetrain systems, main bearing caps, transmission drive and driven sprockets, *etc*.) and as alternative to Ni and Cu alloyed powder metallurgical (PM) steels due to lower production cost of Mo-PM-steels [2000You]. Recent studies involved supersolidus liquid phase sintering of high speed steel and in particular computer aided design of sinterable alloys containing 1.25 C, 12.7 Mo mass% [1999Wri], fracture mechanisms in sintered steels with 3.5 mass% Mo [1999Can], effect of carbon content, sintering temperature, density and cooling rate upon properties of prealloyed Fe-1.5Mo (mass%) powder with and without additions of 0.5-1.2C (mass%) [2000You], sintering mechanism and microstructural changes in low alloyed PM Mo-steels in the temperature range 600 to 1300°C and the effect of Mo on electrical conductivity [2002Sim], the influence of microstructure on mechanical properties of molybdenum alloyed PM steels [2005Can]. *Rapidly quenched Mo-alloys* are produced, for example, via splat-cooling [1978Sar], melt-spinning [1980Iwa, 1981Ino, 1993Kha] and REP-atomization with water cooling on the Cu-screen [1996Fom] methods. *Nanostructured C-Fe-Mo based powders are prepared by mechanical alloying* and subsequent annealing [1996Kuh] with a high-resistant secondary carbide phase; the nanostructure of these powders is similar to that of the high-performance soft magnetic thin films and not accessible by melt quenching methods. Amorphized C-Fe-Mo powders prepared by mechanical alloying [1994Omu] reveal a slight temperature dependence of the resistivity. A Fe_3Mo_3C based hard magnet synthesized by mechanical alloying of elemental powder blends with subsequent heat treatment [2001Zhu, 2001Tsu, 1995Di] has a saturation magnetization of 0.4 emu·g^{-1}, remanence of 0.13 emu·g^{-1} and coercivity of 200 Oe [2001Tsu]. Metallic ferromagnetic $Fe_{21}M_2C_6$ based materials can be applied in thermomagnetic recording media.

For C-Fe-Mo commercial alloys, austenite decomposition reactions are fundamental phase transformations and thus are of great interest for metallurgists. Since Davenport's and Bain's original work [1930Dav] numerous investigations aimed at determining the effect of molybdenum on the isothermal transformation of austenite at subcritical temperatures have been widely carried out. The effect of Mo on the austenite decomposition in low and medium carbon steels [1941Bla] has been studied. The partition of molybdenum in approximately eutectoid [1944Bow] and hypoeutectoid [1946Bow] C-Fe-Mo alloys has been determined and the importance of the proeutectoid reaction for hardening is recognized [1946Bow]. The isothermal decomposition of austenite in high purity C-Fe-Mo alloys in the range 600-900°C with detailed study of the structural changes has been examined by [1970Ber, 1971Ber], and has been discussed by [1971Neh]. The dynamic response and structure of ferrite-austenite interface in dilute C-Fe-Mo and C-Fe alloys has been studied by [1978Pur1] and the growth of ferrite in C-Fe-Mo alloys at intermediate transformation temperatures, characteristic of the bay in the TTT-curve has been observed by [1978Pur2].

DOI: 10.1007/978-3-540-74196-1_7

The morphology of ferrite and carbides in the vicinity of and below the TTT-diagram bay of the Fe-0.19C-2.3Mo (mass%) alloy, in the temperature range 575°C to 475°C [1987Tsu] and the stasis or incomplete transformation phenomenon in 19Fe-C-Mo alloy at three levels of carbon concentration, nominally 0.15; 0.20 and 0.25 mass%, and at Mo concentrations varying from 2.3 to 4.3 mass% [1990Shi] have been studied. The overall kinetics of isothermal transformation of austenite to bainite was studied in a series of high-purity C-Fe-Mo alloys containing from 0.6 to 0.27 mass% C and from 0.23 to 4.28 mass% Mo at reaction temperature mainly below that of the bay in the TTT-curve for initiation of transformation [1990Rey].

The occurrence of this *incomplete transformation phenomenon* known as *transformation stasis phenomenon* [1990Rey, 1990Shi, 2004Aar] has been ascribed to a "solute drag like effect", caused by the segregation of C and Mo atoms at the α/γ and α/α' (martensite) boundaries, for example in ultra low carbon alloy steels containing as little as 0.03 mass% C [1997Men].

The Zener theory of the incomplete transformation phenomenon sometimes attending the bainite reaction in steel, as described by the overall reactions kinetics definition, has been shown by [2001Aar] to be able to describe neither the upper temperature limit for bainite formation in C-Fe-Mo alloys nor the average carbon concentration in retained austenite at the beginning of incomplete transformation.

A modified solute drag model, taking into account the interfacial segregation of alloy elements, is applied to the decomposition of austenite into ferrite in the C-Fe-Mo alloys [1997Liu]. The calculations are performed with assessed thermodynamic and kinetic data stored in a database. The solute drag-like effect suggested in the literature is discussed in comparison with the quantitative calculation by [1997Liu].

A STEM method for investigation of alloying element accumulation at austenite-ferrite boundaries in C-Fe-Mo alloys has been used as a method capable of yielding results combining high accuracy with sufficient rate to permit the analysis of many such boundaries in a given specimen within a reasonable period of time [2001Fle].

Molybdenum accumulation at ferrite/austenite boundaries below the TTT diagram bay in an Fe-0,28C-3Mo (mass%) alloy has been examined in [2003Eno] using a STEM-energy dispersive X-ray analysis. It is concluded that Mo-accumulation at ferrite/austenite boundaries may have a major influence on the growth of ferrite in the bay region. The three-dimensional morphology of degenerate ferrite formed below the bay of the TTT diagram in an C-Fe-Mo alloys was observed by serial sectioning and computer-aided reconstruction [2002Wu, 2003Wu].

A microanalysis study of the eutectoid decomposition of austenite into ferrite and M_2C (to bainite) at the bay in Fe-0.24C-4Mo is reported by [2003Hac1]. It was concluded that alloy element partition between ferrite and alloy carbides at the reaction front is largely responsible for the slow kinetics in this and related alloys. A thermodynamic analysis showed that ferrite-carbide interfacial energy and nonequilibrium carbide compositions reduce the thermodynamic driving force for diffusion processes (Mo partition) by up to 20% further slowing the kinetics.

A reassessment of bainite thickening kinetics data has resulted in a new appreciation for the role of crystallographic effects [2003Hac2], which were ignored or downplayed earlier.

The influence of alloying elements (x) upon proeutectoid ferrite/microstructurally defined bainite formation in C-Fe-Mo alloys, where X is Co, Cr, Cu, Mo, Ni, Si, or V, which was examined in terms of the competing influence of the coupled-solute drag effect and the shifting in the paraequilibrium curve are discussed by [2004Aar].

Molybdenum accumulation at ferrite / austenite interfaces during isothermal transformation of an Fe-0.24C-0.93Mo (mass%) alloy partially transformed at 650, 630, and 610°C has been measured by [2004Hum] using scanning transmission electron microscope and connection between Mo accumulation at α: γ boundaries and couple solute drag effect was tested.

In the review [2004Tak], two models of the overall kinetics of the bainite transformation, one of which is the diffusion controlled growth model of the bainitic laths and the other is the nucleation of bainite ferrite plates controlled model, have been discussed. It was shown that formation and competition of bainitic ferrite and cementite can be predicted quantitatively.

Investigation data on peritectic reaction of austenite formation from the liquid and the δ-ferrite (σ-ferrite + α⇌ γ) in the ternary systems C-Fe-X (X = Mo, W, Cr, Si, Al and others) have been summarized by [2001Kal]. It was proposed to name all steels undergoing peritectic reaction the *peritectic type steels*.

DOI: 10.1007/978-3-540-74196-1_7

Miscellaneous

The problem of equilibrium or of the degree of nonequilibrium for the C-Fe-Mo alloys is of high importance because of their practical application, as a rule, in non-equilibrium state. In most cases, it is unknown if Fe_3C coexisting with the other phases in the alloy is stable or metastable phase. Once formed, cementite can survive anneals for thousands of hours, as for example, after [1953Kuo2] at 700°C for 5000 h. In the alloys annealed both at 900°C for 5 to 50 h and at 700°C for 24 to 500 h, [1962Sat] found the same set of the phases in the alloys α, γ, τ_1, τ_2 and Fe_3C in contradiction with the accepted C-Fe-Mo phase diagram. Based on these results, [1985Riv] came to the conclusion that the reaction $\gamma + \beta \rightleftharpoons \tau_1 + \tau_2$ took place with all the consequences. The metastable reaction scheme after [1985Riv] including the above reaction is given in Fig. 23.

Measurements of the influence of molybdenum and tungsten on the diffusion rate of carbon in face-centered iron at 1000°C have been reported by [1943Smo]. Effective interdiffusion coefficients for metal elements in austenite and ferrite of C-Cr-Fe, C-Fe-Mo, and C-Fe-W systems have been determined by [1995Pop1, 1995Pop2]. Investigation of diffusion interaction of carbides, nitrides and carbonitrides with iron and steels has been carried out on welded diffusion couples interstitial phase - Fe (steel), for example, Mo_2C-Fe [1999Pop]. The effects of intrinsic factors on primary and secondary arm spacings of dendrites have been investigated, and changes in the microsegregation index with changing in primary arm spacings and equilibrium distribution coefficient of each solute element have been also examined [2003Kud]. Grain size and phase arrangement influence on Young's modulus (E) for C-Fe-Mo alloys have been investigated in [2001Hil], and it was shown that there exist a possibility to raise and to reduce E by alloying and by heat treatment due to apparent equilibrium and non-equilibrium stages, the elastic properties can be changed, and E can become a material characteristic for the elastic range.

Specific electric resistivity of the C-Fe-Mo melts was measured by [1985Ver].

The orientation relationship $\{100\}_B$ // $\{2110\}_H$ and $\{011\}_B$ // $\{0001\}_H$ between hexagonal Mo_2C precipitates (H) in ferrite (B) Fe - 4.0 mass% Mo - 0.20 mass% C steel homogenized in an argon atmosphere at 1300°C for about 1 h, brine quenched, and aged at 710°C for up to 10 h have been determined by [2002Shi].

DOI: 10.1007/978-3-540-74196-1_7

Table 1. Investigations of the C-Fe-Mo Phase Relations, Structures and Thermodynamics

Reference	Method/Experimental Technique	Temperature/Composition/Phase Range Studied
[1932Tak1] [1932Tak2]	Thermal, dilatometric, magnetic analysis, microscopic examination	< 6 mass% C, phase diagram.
[1933Ade]	XRD	$Mo_{2-3}Fe_{3-4}C$
[1936Sve]	Tamman furnace, thermal, dilatometric, magnetic analysis, light microscopy, hardness	0 to10 Mo, 0 to 3 C, 0 to 0.485 impurity (Si+Mn+P+S), mass%; R.T. vertical sections at compositions 0.25; 0.5; 1.2; 2.5; 5.5; 10 mass% Mo and 0 to 2.2 mass% C; liquidus surface
[1939Bla]	Induction melting, light microscopy, hardness (Rockwell) examination	735, 790, 845, 900, 955, 1010°C; 0 to 6.0 mass% Mo, 0 to 1.2 mass% C
[1944Bow]	Induction melting, light microscopy, chemical analysis, XRD	$(Mo,Fe)_{23}C_6$
[1950Kra]	XRD	R.T., 720°C, Fe-30Mo-3C, mass%
[1951Las]	XRD, chemical extraction	600°C, Fe-(0.35-4.13) mass% Mo-(0.29-0.33) mass% C, Mo_mFe_nC, Mo_2C
[1952Edw]	Induction melting, light microscopy, XRD	Solid solubility Mo_2C in (αFe) at 1250°C
[1953Kuo1] [1953Kuo2] [1953Kuo3]	XRD, chemical extraction technique	700°C, $M_aC_b(\xi)$, $M_6C(\eta)$, $M_{23}C_6(\tau_4)$
[1959Fuw]	Equilibration of alloys with controlled mixtures of CO and CO_2	ε_C^{Mo} in liquid phase, 1560°C, 8 to 25 mass% Mo
[1960Cam]	XRD, chemical analyses, light microscopy hardness, chemical extraction	721°C - 1316°C 0 to 6.0 mass% Mo, 0.05 to 1.33 mass% C vertical sections at 0.4; 0.8; 1.5; 3.0; 6.0 mass% Mo and 0 to 1.6 mass% C; 0.4; 0.87; 1.1 mass% C and 0 to 8 mass% Mo
[1960Fuw]	Determination of the activity coefficient of carbon	1450°C, 8.72-45.04 mass% Mo, 5.16-5.76 mass% C
[1960Mor]	Determination of the activity coefficient of carbon in multicomponent solution	1550°C, Fe corner
[1962Sat]	XRD, chemical, electron microscopy, thermo-magnetic analysis	700°C, 900°C, isolated $M_aC_b(\xi)$, $M_6C(\eta)$, $M_{23}C_6(\tau_4)$
[1963Yag]	Method of measurement the solubility of carbon in the melt	1350°C, 3 to 25 mass% Mo
[1964Dys]	XRD using quadrupole focusing camera, chemical analysis	550, 700°C, $MoFe_2C$ carbide residues separated by electrolysis of molybdenum steel

(*continued*)

DOI: 10.1007/978-3-540-74196-1_7

Reference	Method/Experimental Technique	Temperature/Composition/Phase Range Studied
[1968Jel]	XRD, light microscopy, magnetic examination, melting temperature by visual observation	700°C, 2.5 to 26.2 at.% C, 2.6 to 65.0 at.% Mo, reaction scheme, liquidus surface
[1969Bun1] [1969Bun2]	Induction furnace melting, chemical analysis, light microscopy, XRD, microprobe, equilibration of alloys with controlled mixtures of H_2 and CH_4	Isothermal sections at 1000, 1100°C, ε_C^{Mo}, 0 to 7.6 at.% Mo, 0 to 11 at.% C
[1969Fra]	Arc melting, XRD, light microscopy	1000°C, Mo-Fe-60 at.% C
[1970Ett]	Powder metallurgical method or melting, XRD	900, 1100, 1300°C, Mo_3Fe_3C
[1970Sav]	Arc melting, XRD, light microscopy, thermal analyses, microhardness	1800, 1200°C, 0 to 11.54 mass% Fe, 0 to 0.5 mass% C, vertical sections at 0.8, 2.0 mass% Fe and 0 to 0.4 mass% C
[1970Suz]	Method of equilibration with controlled mixtures of CO and CO_2	ε_C^{Mo}, 1560°C, 0 to 20 mass% Mo, 0.5 to 0.7 mass% C
[1970Zem]	Radioisotope method, light microscopy, microhardness	500, 550, 600, 620, 650, 680, 700, 720°C, 0 to 1.25 mass% Mo, 0 to 0.02 mass% C, vertical sections at 0.4; 1.25 mass% Mo and 0 to 0.02 mass% C
[1971Gre]	Induction melting, Woesthoff conductimetric instrument, equilibration of alloys with mixtures of CH_4 and H_2	975, 1050, 1125°C, $\varepsilon_C^{Mo} = f(T)$, 0.015 to 0.587 mass% C, 0 to 6.68 mass% Mo
[1972Foo]	Equilibration of alloys with mixtures of CO and CO_2	ε_C^{Mo} in liquid phase, 1550°C, 0 to 6.3 mass% Mo, 0.2 to 0.4 mass% C
[1972Nis]	Sealed capsule technique, equilibration of alloys with hydrogen, microprobe (CAMECA), XRD examination electrochemical extraction technique	Isothermal section at 1000°C, ε_C^{Mo}, 0 to 2.67 mass% Mo, 0.22 to 1.15 mass% C
[1972Pet]	Radiometric method of determination of activity coefficient of carbon, equilibration of alloys with hydrogen	800, 850, 900, 950,1000, 1050°C, ε_C^{Mo}, 0.42 to 1.23 mass% Mo
[1972Sav]	Arc melting, XRD, light microscopy, optical pyrometer, DTA, microprobe (CAMECA), microhardness	1800, 1200°C, 0 to 11.54 Fe, 0 to 0.5 C, mass%
[1972Wad]	Induction melting, metallographic linear Analyses, equilibration of alloys with controlled mixtures CH_4 and H_2	848°C to 1197°C, 0.33 to 1.33 mass% C, 0 to 2.5 at.% Mo
[1975Uhr]	Microprobe measurement, optical microscopy, XRD, equilibration of alloys with hydrogen	Isothermal section at 1000°C, 0.5 to 40 mass% Mo at a_C = 0.03 to 1

(*continued*)

DOI: 10.1007/978-3-540-74196-1_7

Reference	Method/Experimental Technique	Temperature/Composition/Phase Range Studied
[1976Lob1]	Equilibration of alloys with controlled CH_4/H_2 atmosphere, balance method of control	682 to 900°C, $\varepsilon_C^{Mo} = f(T)$ in ferrite, 0 to 1.16 mass% Mo, 0.003 to 0.017 mass% C
[1976Lob2]	Equilibration of alloys with controlled CH_4/H_2 atmosphere, balance method of control	783, 813, 848°C, $\varepsilon_C^{Mo} = f(T)$ in austenite, Fe-0.48 mass% Mo; Fe-1.16 mass% Mo
[1976Sch]	XRD	1150°C, 35 to 42 at.% Mo, 40 to 56 at.% C
[1977She]	Induction melting, light microscopy, XRD	1000°C and above, 1 to 5 mass% C, 0 to 40 mass% Mo
[1978Kle]	Electromotive force measurements on galvanic cells with solid oxide electrolytes	1000°C, ${}_fG(Fe_3Mo_3C)$ and ${}_fG(Fe_2MoC)$
[1979Kag]	XRD, chemical analysis, electron microprobe, Curie temperature measurements, carbides extracted	300°C, $x = 0.0075$, $x = 0.0084$, $x = 0.0196$; RT, $(Mo_xFe_{1-x})_3C$
[1979Woo]	XRD, quantitative metallography, chemical, SEM	870, 925, 980°C, 0 to 5.0 mass% Mo, 1.0 mass% C. $MoFe_2C$, M_6C
[1980Iwa]	Rapid quenching from melts, XRD, TEM	6 to 27 at.% Mo, 13 to 22 at.% C
[1981She]	XRD, light microscopy	700-1420°C, 1 to 25 mass% Mo, 0.5 to 1.2 mass% C
[1983Bus]	Arc melting, XRD, magnetic, Kerr effect measurements	800°C, $Mo_2Fe_{21}C_6$
[1983Jan]	Tamman' furnace, chemical analyses, conventional method, thermodynamic description	1450-1600°C, Fe corner of the system
[1985Rap]	Single crystal XRD, EDAX, light microscopy	1150°C, $Mo_{12}Fe_{22}C_{10}(\xi)$
[1986Wad]	Equilibration of alloys with mixtures of CH_4 and H_2 (a sealing method and a gas flowing method), SEM-EDX, EPMA, TEM	712°C, ε_C^{Mo}, 0.24 to 2.93 mass% Mo, 0 to 0.2 mass% C, homogeneity range of τ_1
[1990Ere]	Arc melting, spun melting, XRD	12 to 50 at.% Mo, 4.6 to 13 at.% C
[1990Ips]	Arc melting, XRD, light microscopy, DTA	1000°C, 0 to 40 at.% Mo, 0 to 20 at.% C (14 samples), liquidus surface
[1991Kha]	Arc melting, XRD, light microscopy, Pirani-Altertum method	1280-1410°C, Fe- Mo_2C-Mo range
[1991Sch]	DTA, XRD, metallography (SEM), Pirani-Altertum method, microprobe	Liquidus surface corner, >50 at.% Fe, 800, 1000°C, vertical sections at 55, 85 at.% Mo and 0 to 25 at.% C
[1992Cha]	Diffusion couple method, light microscopy, microprobe analysis (Camebax-Micro)	700, 750 and 1000°C

(*continued*)

DOI: 10.1007/978-3-540-74196-1_7

Reference	Method/Experimental Technique	Temperature/Composition/Phase Range Studied
[1993Kha]	XRD, light microscopy, Pirani-Altertum method, DTA, spun melting, arc melting	9 to 19 at.% Mo, 5.4 to 21 at.% C spun melted; solidus surface at Fe-17 at.% C-60 at.% Mo field
[1994Sch]	DTA, XRD, light microscopy, microprobe analysis (CAMECA)	0 to 50 at.% Mo, 0 to 50 at.% C liquidus surface
[1995Di]	XRD, SEM-EDX, TEM, DTA, Mössbauer spectroscopy, mechanical alloying	Mo_3Fe_3C
[1995Gir]	DTA, microprobe analysis (CAMECA), XRD, TEM	1000°C, 2.4 to 13.0 at.% Mo, 5.3 to 19.5 at.% C, liquidus surface
[1997Sht1] [1997Sht2]	TEM- EDS, XRD, calculation	700-1000°C, Fe corner
[1999Wri]	DTA, metallography (SEM), SEM-EDX, WDS techniques, calculation	13.0 mass% Mo and 0 to 2.5 mass% C
[2001Tsu]	XRD, light microscopy, SEM, EPMA, TG-DTA, mechanical alloying	Mo_3Fe_3C
[2001Ume]	XRD, light microscopy, SEM, TEM, DSC	900°C, $(Mo_xFe_{1-x})_3C$ at $x = 0.0667$
[2001Zhu]	XRD, Mössbauer spectroscopy, mechanical alloying	Mo_3Fe_3C
[2002Shi]	XRD, TEM, Moire fringe technique	710°C, Fe-4 mass% Mo-0.2 mass% C, $(Mo_{1-x}Fe_x)_3C$, at $0 < x < 1$,
[2003Eno]	STEM- EDX	570°C, α/γ phase boundaries
[2003Wu]	Light microscopy, calculation	810°C and 530°C, α/γ phase boundaries

Table 2. Crystallographic Data of Solid Phases

Phase/ Temperature Range [°C]	Pearson Symbol/ Space Group/ Prototype	Lattice Parameters [pm]	Comments/References
(C)gr < 3827	*hP*4 $P6_3/mmc$ C (graphite)	$a = 246.12$ $c = 670.9$	at 25°C [Mas2] sublimation point
(C)d	*cF*8 $Fd\bar{3}m$ C (diamond)	$a = 356.69$	at 25°C, >60 GPa [Mas2]

(*continued*)

DOI: 10.1007/978-3-540-74196-1_7

Phase/ Temperature Range [°C]	Pearson Symbol/ Space Group/ Prototype	Lattice Parameters [pm]	Comments/References
(Mo), $Mo_{1-x-y}Fe_xC_y$ < 2623	*cI*2 *Im*$\bar{3}$*m* W		$0 < y < 0.011$, $0 < x < 0.313$ [Mas2]
		$a = 314.70$	$x = 0$, $y = 0$ at 25°C [Mas2]
		$a = 311.8$	$x = 0.2$, $y = 0$ [1982Gui, V-C2]
		$a = 312.8$	in alloy $Mo_{52}Fe_{35}C_{13}$ quenched from 1410°C [1991Kha]
α, $Fe_{1-x-y}Mo_xC_y$ < 1538	*cI*2 *Im*$\bar{3}$*m* W		$0 < x < 0.244$ at $y = 0$ $0 < y < 0.004$ at $x = 0$
(δFe), $Fe_{1-x-y}Mo_xC_y$ 1538 - 1394		$a = 293.15$	$x = 0$, $y = 0$ at 1394°C [Mas2, 2006MSIT]
(αFe), $Fe_{1-x-y}Mo_xC_y$ < 912		$a = 286.65$	$x = 0$, $y = 0$ at 25°C [Mas2, 2006MSIT]
		$a = 286.5$	ARMCO Fe [1994Gau]
		$a = 288.15$	$x = 0.422$, $y = 0$ [1982Gui, V-C2]
		$a = 290.98$	$x = 0.1255$, $y = 0$ [1982Gui, V-C2]
		$a = 286.1$	in alloy Fe-4 Mo-0.2 C, mass%, homogenized at 1300°C for 1 h, brine quenched and annealed at 710°C (10 h) [2002Shi]
		$a = 287.7$	in alloy $Mo_{52}Fe_{35}C_{13}$, quenched from 1410°C [1991Kha]
γ, $Fe_{1-x-y}Mo_xC_y$ (γFe) 1393 - 740	*cF*4 *Fm*$\bar{3}$*m* Cu		0 to 9.06 at.% C, 0 to 1.7 at.% Mo [Mas2, 2006MSIT]
		$a = 364.67$	$x = 0$, $y = 0$ at 915°C [Mas2, V-C2, 2006MSIT]
		$a = 363.38$	8.18 C, 0 Mo, at.% [1992Oka]
α, martensite	*tI*4 *I*4/*mmm*		metastable, 0 to 9 at.% C, [Mas2]
		$a = 285.8$ $c = 293.5$	2.69 at.% C [1992Oka, Mas2]
		$a = 285.5$ $c = 296.8$	4.01 at.% C [1992Oka, Mas2]

(*continued*)

DOI: 10.1007/978-3-540-74196-1_7

Phase/ Temperature Range [°C]	Pearson Symbol/ Space Group/ Prototype	Lattice Parameters [pm]	Comments/References
		a = 284.9 c = 298.5	5.26 at.% C [1992Oka, Mas2]
		a = 284.6 c = 301.1	6.36 at.% C [1992Oka, Mas2]
Fe_3C, $(Fe_{1-x}Mo_x)_3C$ < 1252	*oP*16 *Pnma* Fe_3C		metastable, 25 at.% C, 0 to 0.93 at.% Mo [1988And1]; [V-C2, 2006MSIT] ($D0_{11}$ type)
		a = 507.9 b = 673.0 c = 451.4	x = 0, heat treated at 700°C for a long time [1953Kuo1, 1953Kuo3, V-C2, 2006MSIT]
		a = 508.90 b = 674.33 c = 452.35	x = 0 [1985Riv]
		a = 509.0 b = 675.1 c = 452.8	x = 0.0075 (0.56 at.% Mo) annealed at 600°C [1979Kag], from graph
		a = 509.3 b = 678.0 c = 454.4	x = 0.0075 (0.56 at.% Mo), 300°C [1979Kag], from graph
		a = 508.6 b = 675.9 c = 451.9	x = 0.0084 (0.63 at.% Mo) annealed at 900°C [1979Kag], from graph
β, $(Mo_{1-x}Fe_x)_2C$ 2527 - 1220	*hP*3 $P6_3/mmc$ Fe_2N		27 - 36 at.% C at x = 0 [1988Vel, Mas2], 0 to 19.5 at.% Fe at 33 at.% C [1988And1] $0 < x < 0.121$ (0 to 8 at.% Fe), as cast [1995Gir]
		a = 299.8 c = 473.3	31 at.% C, x = 0 at 1700°C [V-C2]
		a = 300.7 c = 472.6	33.5 at.% C, x = 0 [1980Fer]
		a = 301.1 c = 477.1	34.1 at.% C, x = 0 at 1700°C [V-C2]
		a = 301.0 c = 478.0	34.4 at.% C, x = 0 [1980Fer]
		a = 299.8 c = 473.1	x = 0, annealed at 1300-1450°C quenched in gallium [1988Vel, Mas2]

(*continued*)

DOI: 10.1007/978-3-540-74196-1_7

Phase/ Temperature Range [°C]	Pearson Symbol/ Space Group/ Prototype	Lattice Parameters [pm]	Comments/References
		a = 301.2 c = 478.6	x = 0, annealed at 1800°C, quenched in gallium [1988Vel, Mas2]
		a = 300.67 c = 472.83	$Mo_2Fe_{0.17}C_{0.83}$, (x = 0.085, 5.67at.% Fe), annealed at 1000°C [1995Gir]
		a = 300.0 c = 472.0	x = 0.106 (7.1 at.% Fe), heat treatment at 700°C, 900°C [1962Sat]
		a = 299.79 c = 472.16	x = 0.121 (8 at.% Fe), $Mo_{1.9}Fe_{0.24}C_{0.86}$ as cast [1995Gir]
		a = 297.7 c = 472.6	in alloy Fe-4 Mo-0.2 C, mass%, brine quenched from 1300°C and annealed at 710°C 10 h [2002Shi]
		a = 298.9 ± 0.1 c = 472.5 ± 0.1	in alloy $Mo_{52}Fe_{35}C_{13}$ quenched from 1410°C [1991Kha]
		a = 301.2 c = 471.4	in alloy Mo-3.43 Fe-0.39 C, mass%, quenched from 1800°C [1970Sav]
		a = 299.8 c = 473.2	in alloy Mo-11.54 Fe-0.33 C, mass%, quenched from 1200°C [1970Sav]
β', β'Mo_2C < 1440	*oP*12 *Pbcn* V_2C (?) or *oP*12 *Pbcn* PbO_2	$a = 473.0 \not\approx c_0$ $b = 602.7 \not\approx 2a_0$ $c = 519.8 \not\approx \sqrt{3}a_0$ a = 473.3 b = 604.2 c = 520.2 a = 472.4 b = 600.4 c = 519.9	32.5 at.% C at 25°C [1988Vel, Mas2] 32.5 at.% C [V-C2] 33.5 at.% C [1980Fer]
β", β"Mo_2C ≲ 1220	o^{**} -	$a = 946.6 = 2c_0$ $b = 2415.2 \not\approx 8a_0$ $c = 4167.5 \not\approx 8\sqrt{3}a_0$	ca. 33.5 at.% C at 25°C [1988Vel, Mas2]
η, ηMo_3C_2 2530 - 1647	*hP*8 $P6_3/mmc$ TiAs or *hP*12 $P6_3/mmc$	a = 300.0 c = 1458.0 a = 301.2 c = 1463.4 a = 301.8 c = 1463.0	37.5 to 39.7 at.% C [1988Vel, Mas2] 38 at.% C [1988Vel] 39 at.% C, annealed at above 1650°C, quenched in gallium [1988Vel] 38 at.% C, ηMoC_{1-x} according to [1980Fer]

(*continued*)

DOI: 10.1007/978-3-540-74196-1_7

Phase/ Temperature Range [°C]	Pearson Symbol/ Space Group/ Prototype	Lattice Parameters [pm]	Comments/References
δ, δMo_3C_2 2605 - 1956	*cF*8 $Fm\bar{3}m$ NaCl	 a = 428 a = 426.6 a = 426.6 a = 427.4	37 to 43 at.% C [1988Vel, Mas2] [V-C2] 39.7 at.% C [1967Rud] 40 at.% C [1988Vel] 42 at.% C [1967Rud]
MoC ≲ 1220	*hP*2 $P\bar{6}m2$ WC	 a = 290.6 c = 282.2 a = 289.8 c = 280.9 a = 289.9 c = 282.0	50 at.% C [1988Vel, Mas2] [1988Vel] [1980Fer] in alloy Mo-25 Fe-40 C, at.%, annealed at 1150°C 300 h [1976Sch]
λ, $MoFe_2$ < 927	*hP*12 $P6_3/mmc$ $MgZn_2$	 a = 475.5 c = 776.7 a = 474.4 c = 772.5	33.3 at.% Mo [Mas2] [V-C2] [V-C2]
R, Mo_2Fe_3 1488 - 1200	*hR*159 $R\bar{3}$ $Mo_3Cr_2Co_5$	- a = 1091.0 c = 1935.4 a = 1095.6 c = 1935.3	33.9 to 38.5 at.% Mo [Mas2] $Mo_{1.9}Fe_{3.1}$ at 1250 to 1490°C [V-C2] annealed at 1250°C [V-C2]
σ, MoFe 1611 - 1235	*tP*30 $P4_2/mnm$ σCrFe	 a = 921.8 c = 481.3 a = 912.3 c = 482.9 a = 922.6 c = 483.2	42.9 to 56.7 at.% Mo [Mas2] [V-C2] in alloy Mo-11.54 Fe-0.33 C, mass%, quenched from 1200°C [1970Sav] in alloy $Mo_{42}Fe_{48}C_{10}$ quenched from 1390°C [1991Kha]
μ, Mo_6Fe_7 < 1370	*hR*39 $R\bar{3}m$ Fe_7W_6	 a = 475.46 c = 257.16 a = 475.1 c = 256.8	39.0 to 44.0 at.% Mo [Mas2] [V-C2] [1982Gui]
* τ_1, $(Mo_{1-x}Fe_x)_6C$ < 2063	*cF*112 $Fd\bar{3}m$ W_3Fe_3C	a = 1109.8 a = 1109 a = 1112	$Mo_3Fe_{3.1}C$ annealed at 1250°C for 20 h and 1000°C for 150 h [1969Fra, V-C2] Mo_2Fe_4C [1933Ade]

(*continued*)

DOI: 10.1007/978-3-540-74196-1_7

Phase/ Temperature Range [°C]	Pearson Symbol/ Space Group/ Prototype	Lattice Parameters [pm]	Comments/References
		a = 1126	Mo_3Fe_3C [1933Ade]
		a = 1110 to 1111	Mo_4Fe_2C annealed at 1000°C for 50 h [1953Kuo2]
		a = 1111.7±0.5	Mo_3Fe_3C, quenched from 900-1300°C [1970Ett]
		a = 1109.3	in alloy $Mo_{24.5}Fe_{71}C_{4.5}$ quenched from 1280°C [1991Kha]
		a = 1111.6	$Mo_{2.85}Fe_{3.2}C_{0.95}$ as-cast [1995Gir]
			$Mo_3Fe_{3.1}C_{0.9}$ annealed at 1000°C [1995Gir]
* τ_2, $(Fe_{1-x}Mo_x)_3C$ 1087 - 653	*mC*44 *C2/m* $Mo_6Fe_{11}C_5$		25 at.% C 20.8 to 23.4 at.% Mo at 25 at.% C [1988And1], $M_6Fe_{11}C_5$ [1985Rap], $MoFe_2C$, ξ [1964Dys]
		a = 1086.5 ± 0.3 b = 776.7 ± 0.2 c = 655.9 ± 0.2 β = 120.13° ± 0.2	$Mo_{12}Fe_{22}C_{10}$, single crystal XRD [1985Rap, 1986Rap]
		a = 1087.0 b = 767.1 c = 656.3 β = 120.1°	$MoFe_2C$ annealed at 1150°C 24 h, single crystal XRD [1983Way, V-C2]
		a = 1083.30 b = 769.96 c = 651.56 β = 119.31°	$Mo_{8.4}Fe_{27.4}C_{8.2}$ as cast [1995Gir],
		a = 1086.48 b = 767.46 c = 655.98 β = 120.076°	$Mo_{10.6}Fe_{24.3}C_{9.1}$ annealed at 1000°C [1995Gir]
* τ_3, $(Fe_{1-x}Mo_x)_3C$ 1126 - 910	*oP*16 *Pnma* Fe_3C		25C, 0.93 - 3.77Mo, at.% [1988And1]
		a = 508 b = 674 c = 451	x = 0.0125, annealed at 700°C or 900°C, M_3C according to [1962Sat]
		a = 509.3 b = 676.7 c = 453.3	x = 0.0196 (1.47 at.% Mo), annealed at 600°C [1979Kag], from graph

(*continued*)

DOI: 10.1007/978-3-540-74196-1_7

Phase/ Temperature Range [°C]	Pearson Symbol/ Space Group/ Prototype	Lattice Parameters [pm]	Comments/References
* τ_4, $Mo_2Fe_{21}C_6$	*cF*116 $Fm\bar{3}m$ $Cr_{23}C_6$		metastable?
		a = 1052.5	$(Fe,Mo)_{23}C_6$ tempered at 705°C [1944Bow]
		a = 1052	in C-Fe-Mo isothermal transformed at 700°C for 10 h [1953Kuo1, 1953Kuo3]
		a = 1053	metastable 5.0 to 6.0 C, 6.0 to 13.5 Mo, mass%, tempered at 700°C 500 h, [1962Sat]
		a = 1054.6	in C-Fe-Mo annealed at 800°C 18 days [1983Bus, V-C2]
		a = 1063	annealed at 700°C 10 days [1968Aro, V-C2]
* τ_5, ε	*h***	a = 268 c = 427	metastable, rapidly quenched from melts of Fe-6 to 27 Mo-13 to 22 C at.%, ε according to [1980Iwa, 1981Ino]
* τ_6, χ	*cI*58 $I\bar{4}3m$ αMn		metastable, rapidly quenched from melts [1980Iwa, 1981Ino]:
		a = 897.2	in alloy $Fe_{76}Mo_{12}C_{12}$
		a = 899.8	in alloy $Fe_{72}Mo_{16}C_{12}$
* τ_7, π	*cP*20 $P4_132$ βMn		metastable, rapidly quenched from melts [1993Kha]:
		a = 633.3 ± 0.1	in alloy $Fe_{78}Mo_{11}C_{11}$
		a = 636.1 ± 0.1	in alloy $Fe_{75.5}Mo_{10}C_{14.5}$

Table 3. Invariant Equilibria

Reaction	T [°C]	Type	Phase	Composition (at.% / mass%)		
				C	Fe	Mo
L + η ⇌ β + δ	?	U_1	-	-	-	-
L + δ ⇌ β + C	?	U_2	-	-	-	-
δ + β ⇌ η + C	?	U_3	-	-	-	-
L + (Mo) + β ⇌ τ_1	1626	U_4	L	7.64/1.26	42.05/32.37	50.31/66.42
			(Mo)	0.06/0.01	10.15/6.17	89.79/93.82
			β	1.83/3.02	19.48/14.95	62.23/82.03
			τ_1	14.29/2.62	45.99/39.21	39.72/58.17
L + (Mo) ⇌ σ + τ_1	1538	U_5	L	4.39/0.74	52.66/41.34	42.95/57.92
			(Mo)	0.03/0.01	16.91/10.59	83.06/89.40
			σ	0/0	43.90/31.30	56.10/68.70
			τ_1	14.29/2.62	45.85/39.05	39.87/58.33

(*continued*)

DOI: 10.1007/978-3-540-74196-1_7

Reaction	T [°C]	Type	Phase	Composition (at.% / mass%)		
				C	Fe	Mo
$L + \sigma \rightleftharpoons R + \tau_1$	1457	U_6	L	2.75/0.49	65.64/54.46	31.61/45.05
			σ	0/0	56.38/42.93	43.62/57.07
			R	0/0	61.21/47.88	38.79/52.12
			τ_1	1.43/2.63	46.72/40.01	38.99/57.36
$L + R \rightleftharpoons \alpha + \tau_1$	1400	U_7	L	2.31/0.43	73.33/63.40	24.36/36.17
			R	0/0	63.92/50.77	36.08/49.23
			α	0.06/0.02	77.71/67.04	22.23/32.94
			τ_1	14.29/2.64	47.34/40.70	38.37/56.66
$R + \sigma \rightleftharpoons \mu, \tau_1$	1368	D_1	R	0/0	61.50/48.18	38.50/51.82
			σ	0/0	54.93/41.50	45.07/58.50
			μ	0/0	58.60/45.17	41.40/54.83
			τ_1	14.29/2.60	44.81/37.93	40.90/59.47
$L + \alpha \rightleftharpoons \gamma + \tau_1$	1347	U_8	L	6.41/1.34	82.01/79.41	11.58/19.26
			α	0.50/0.10	93.03/89.24	6.47/10.66
			γ	1.63/0.34	92.59/90.00	5.78/9.66
			τ_1	14.29/2.71	51.31/45.21	34.41/52.09
$\tau_1 + \sigma \rightleftharpoons (Mo) + \mu$	1240	D_2	τ_1	14.29/2.53	40.27/33.17	45.44/64.30
			σ	0/0	43.46/30.91	56.54/69.09
			(Mo)	0/0	6.68/4.00	93.32/96.00
			μ	0/0	56.62/43.17	43.38/56.83
$R + \tau_1 \rightleftharpoons \alpha + \mu$	1201	U_9	R	0/0	66.91/54.06	33.09/45.94
			τ_1	14.29/2.59	44.33/37.41	41.39/60.00
			α	0.04/0	85.97/78.15	13.99/21.85
			μ	0/0	61.27/47.94	38.73/52.06
$L + C + \gamma \rightleftharpoons \tau_3$	1126	P_1	L	17.71/4.35	80.13/91.42	2.16/4.23
			C	100/100	0/0	0/0
			γ	8.60/1.98	90.94/97.17	0.46/0.85
			τ_3	25.00/6.63	74.07/91.39	0.93/1.98
$L + \tau_1 \rightleftharpoons \gamma + \beta$	1093	U_{10}	L	16.86/3.88	73.92/79.16	9.22/16.95
			τ_1	14.29/2.67	49.04/42.60	36.67/54.73
			γ	6.75/1.51	91.04/94.55	2.21/3.94
			β	33.19/6.34	13.04/11.58	53.77/82.08
$L + C + \beta \rightleftharpoons \tau_2$	1087	P_2	L	18.92/4.46	72.53/79.46	8.55/16.08
			C	100/100	0/0	0/0
			β	33.23/6.39	13.93/12.45	52.84/81.16
			τ_2	25.00/5.55	51.89/53.51	23.11/40.94
$L + \beta \rightleftharpoons \gamma + \tau_2$	1078	U_{11}	L	17.39/4.04	73.82/79.67	8.79/16.29
			β	33.21/6.35	13.09/11.63	53.70/82.02
			γ	7.15/1.60	90.84/94.78	2.01/3.62
			τ_2	25.00/5.53	51.60/53.09	23.40/41.38

(*continued*)

DOI: 10.1007/978-3-540-74196-1_7

Reaction	T [°C]	Type	Phase	Composition (at.% / mass%)		
				C	Fe	Mo
$L + C \rightleftharpoons \tau_3 + \tau_2$	1076	U_{12}	L	18.70/4.42	73.30/80.49	8.00/15.09
			C	100/100	0/0	0/0
			τ_3	25.00/6.47	71.2385.73	3.77/7.8
			τ_2	25.00/5.56	52.13/53.85	22.87/40.59
$L \rightleftharpoons \tau_3 + \tau_2 + \gamma$	1065	E_1	L	18.06/4.25	74.25/81.29	7.69/14.46
			τ_3	25.00/5.56	52.21/53.97	22.79/40.47
			τ_2	25.00/6.48	71.39/86.05	3.61/7.47
			γ	7.78/1.76	90.57/95.24	1.66/3.00
$\tau_3 \rightleftharpoons \tau_2 + \gamma + C$	910	E_2	τ_3	25.00/6.58	73.22/89.67	1.78/3.75
			τ_2	25.00/5.61	53.38/55.67	21.62/38.73
			γ	5.55/1.25	93.8/97.75	0.54/1.00
			C	100/100	0/0	0/0
$\alpha + \mu \rightleftharpoons \lambda, \tau_1$	900	D_3	α	0/0	94.80/91.38	5.20/8.62
			μ	0/0	60.53/47.16	39.77/52.84
			λ	0/0	66.67/53.79	33.33/46.21
			τ_1	14.29/2.50	37.83/30.71	47.89/66.79
$\beta + C \rightleftharpoons \tau_2 + MoC$	890	U_{13}	β	33.32/6.17	7.83/6.75	58.85/87.08
			C	100/100	0/0	0/0
			τ_2	25/5.56	52.23/54.00	22.77/40.44
			MoC	50/11.13	0/0	50/88.87
$\gamma + \tau_1 \rightleftharpoons \alpha + \beta$	810	U_{14}	γ	1.65/0.36	97.80/98.69	0.55/0.95
			τ_1	14.29/2.54	40.60/33.51	45.11/63.95
			α	0.07/0.02	99.18/98.70	0.75/1.28
			β	33.32/6.04	4.21/3.55	62.47/90.41
$\gamma + \beta \rightleftharpoons \alpha + \tau_2$	786	U_{15}	γ	2.04/0.44	97.55/98.85	0.41/0.71
			β	33.32/6.04	4.29/3.62	62.38/90.34
			α	0.07/0.01	99.40/99.08	0.53/0.91
			τ_2	25.00/5.55	52.13/53.85	22.87/40.60
$\gamma + \tau_2 \rightleftharpoons \alpha + C$	739	U_{16}	γ	3.13/0.69	96.73/99.07	0.14/0.24
			τ_2	25.00/5.65	54.28/56.98	20.72/37.37
			α	0.08/0.02	99.76/99.71	0.16/0.27
			C	100/100	0/0	0/0
$\tau_2 + \beta \rightleftharpoons MoC + \alpha$	684	U_{17}	τ_2	25.00/5.58	52.78/54.79	22.22/39.63
			β	33.33/5.97	2.37/1.98	64.30/92.05
			MoC	50.00/11.13	0/0	50.00/88.87
			α	0.02/0.01	99.75/99.60	0.23/0.39
$\tau_2 \rightleftharpoons \alpha + MoC + C$	653	E_3	τ_2	25.00/5.64	54.25/56.94	20.75/37.42
			α	0.03/0.01	99.88/99.83	0.09/0.16
			MoC	50.00/11.13	0/0	50.00/88.87
			C	100/100	0/0	0/0

(*continued*)

DOI: 10.1007/978-3-540-74196-1_7

Reaction	T [°C]	Type	Phase	Composition (at.% / mass%)		
				C	Fe	Mo
$\alpha + \beta \rightleftharpoons \tau_1 + MoC$	347	U_{18}	α	0/0	99.99/99.99	0.01/0.01
			β	33.33/5.89	0/0	66.67/94.11
			τ_1	14.29/2.37	28.94/22.34	56.77/75.29
			MoC	50.0/11.13	0	50.0/88.87
$\alpha + \beta \rightleftharpoons \tau_1 + MoC$	347	U_{18}	-	-	-	-
$\lambda, \tau_1 \rightleftharpoons \alpha + \mu$	312	D_4	λ	0/0	66.67/53.79	33.33/46.21
			τ_1	14.29/2.37	28.58/22.02	57.13/75.61
			α	0/0	99.88/99.80	0.12/0.20
			μ	0/0	54.32/40.90	45.68/59.10

DOI: 10.1007/978-3-540-74196-1_7

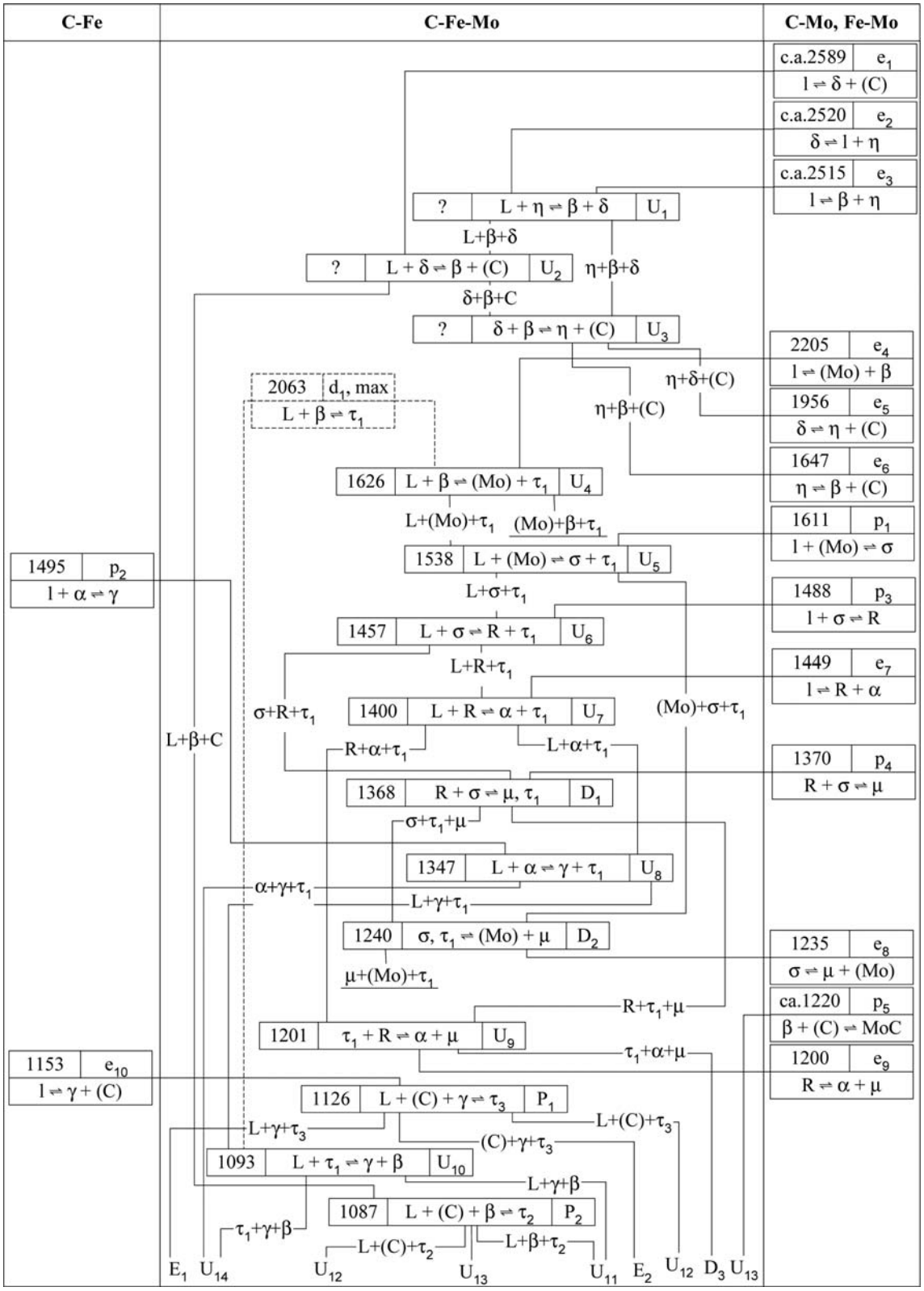

Fig. 1a. C-Fe-Mo. Reaction scheme, part 1

DOI: 10.1007/978-3-540-74196-1_7

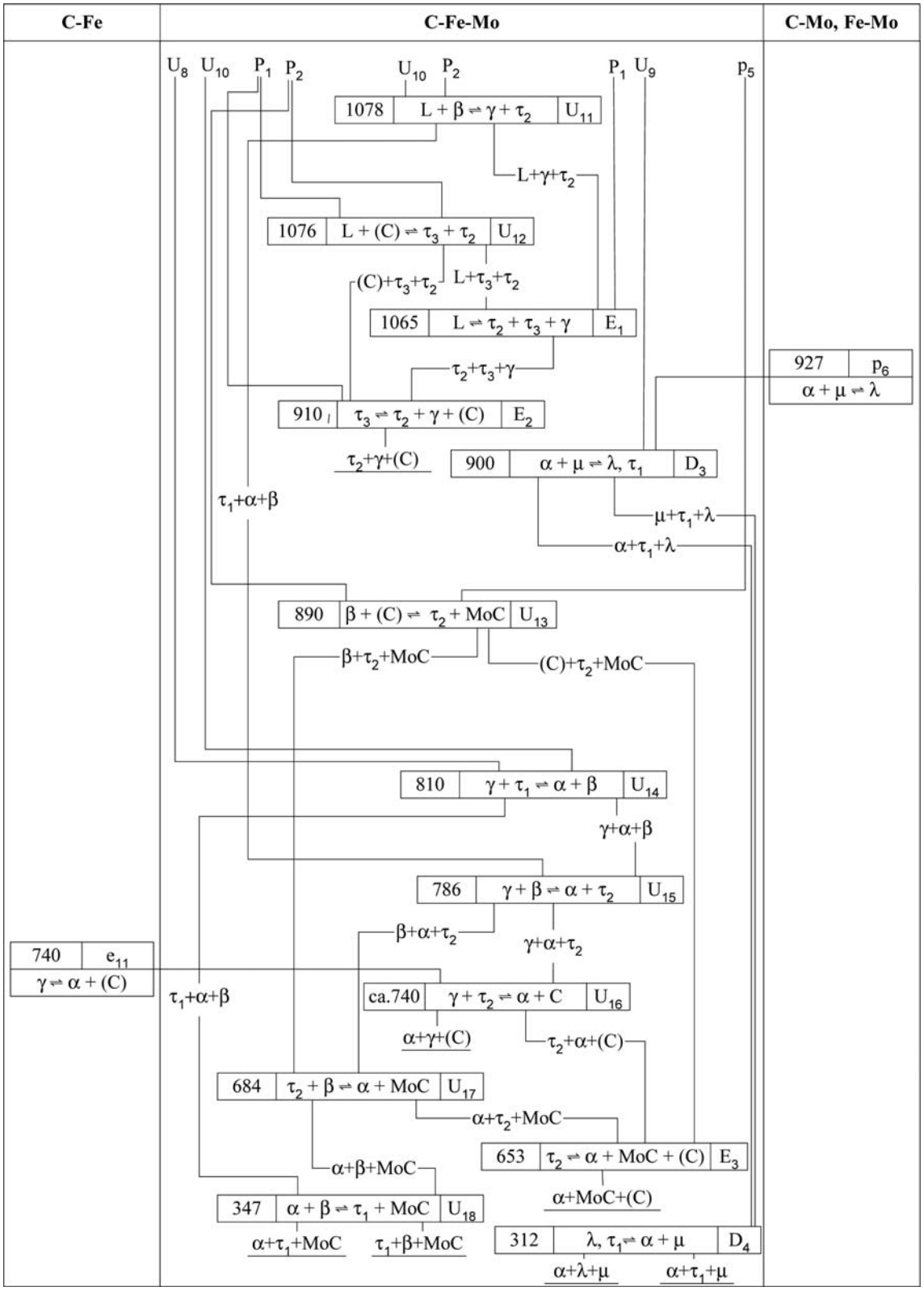

Fig. 1b. C-Fe-Mo. Reaction scheme, part 2

DOI: 10.1007/978-3-540-74196-1_7

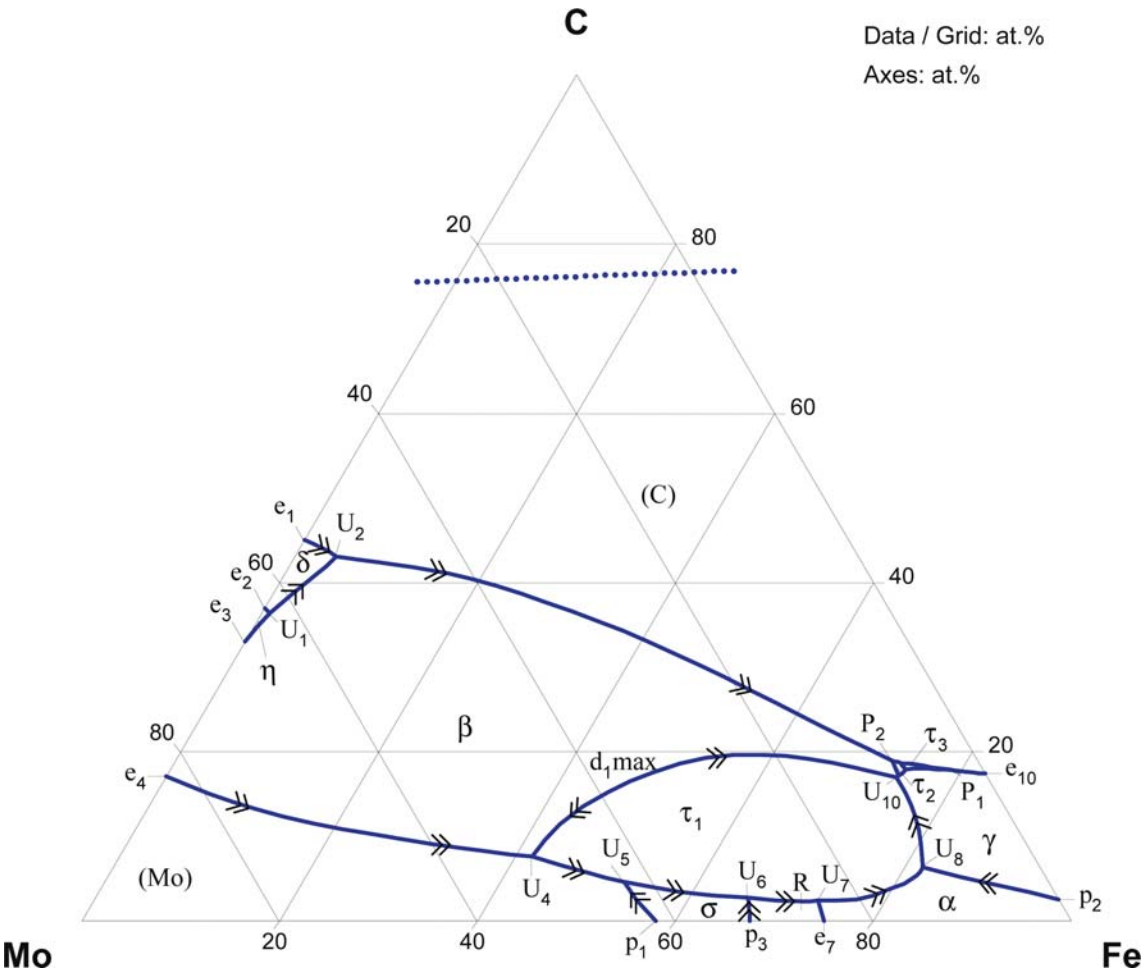

Fig. 2a. C-Fe-Mo. Calculated liquidus surface projection

DOI: 10.1007/978-3-540-74196-1_7

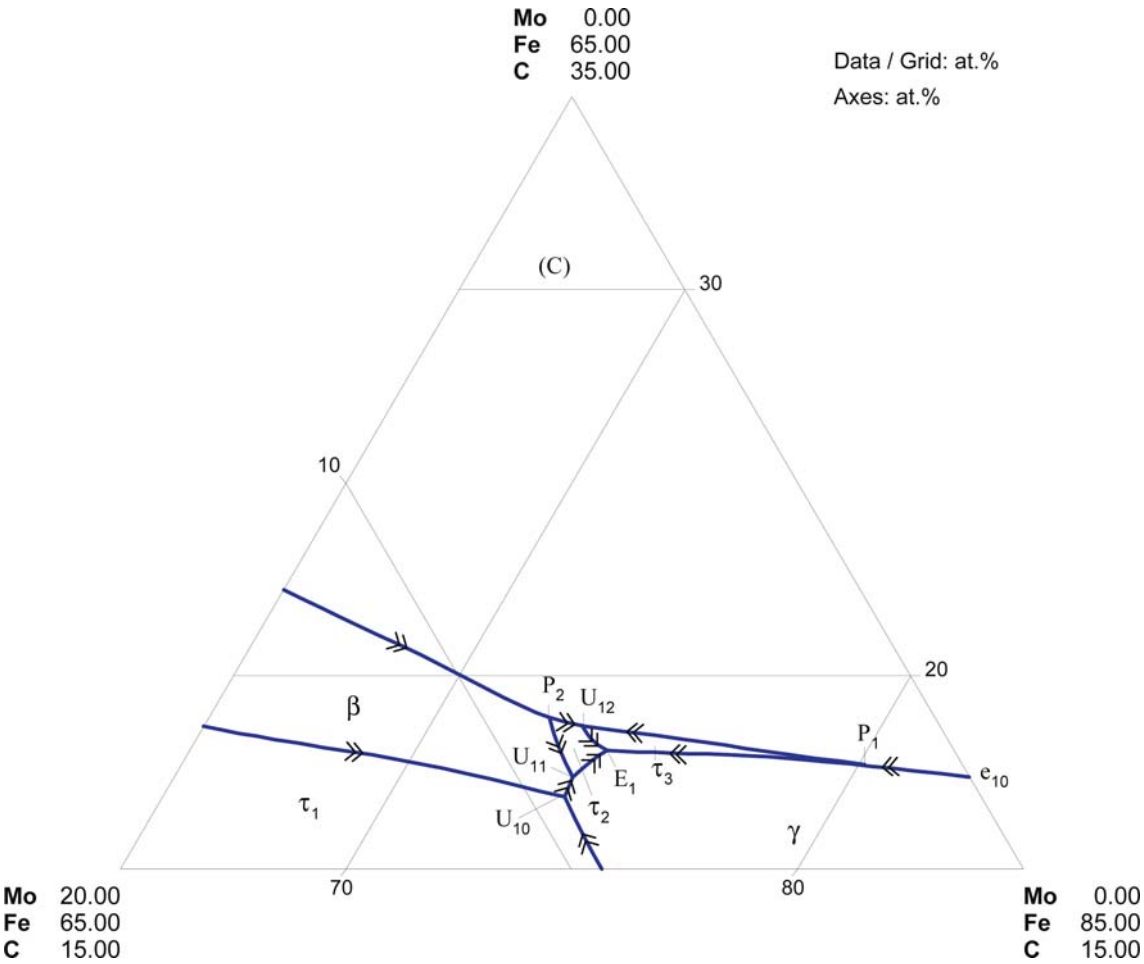

Fig. 2b. C-Fe-Mo. Enlarged part of the calculated liquidus surface projection

DOI: 10.1007/978-3-540-74196-1_7

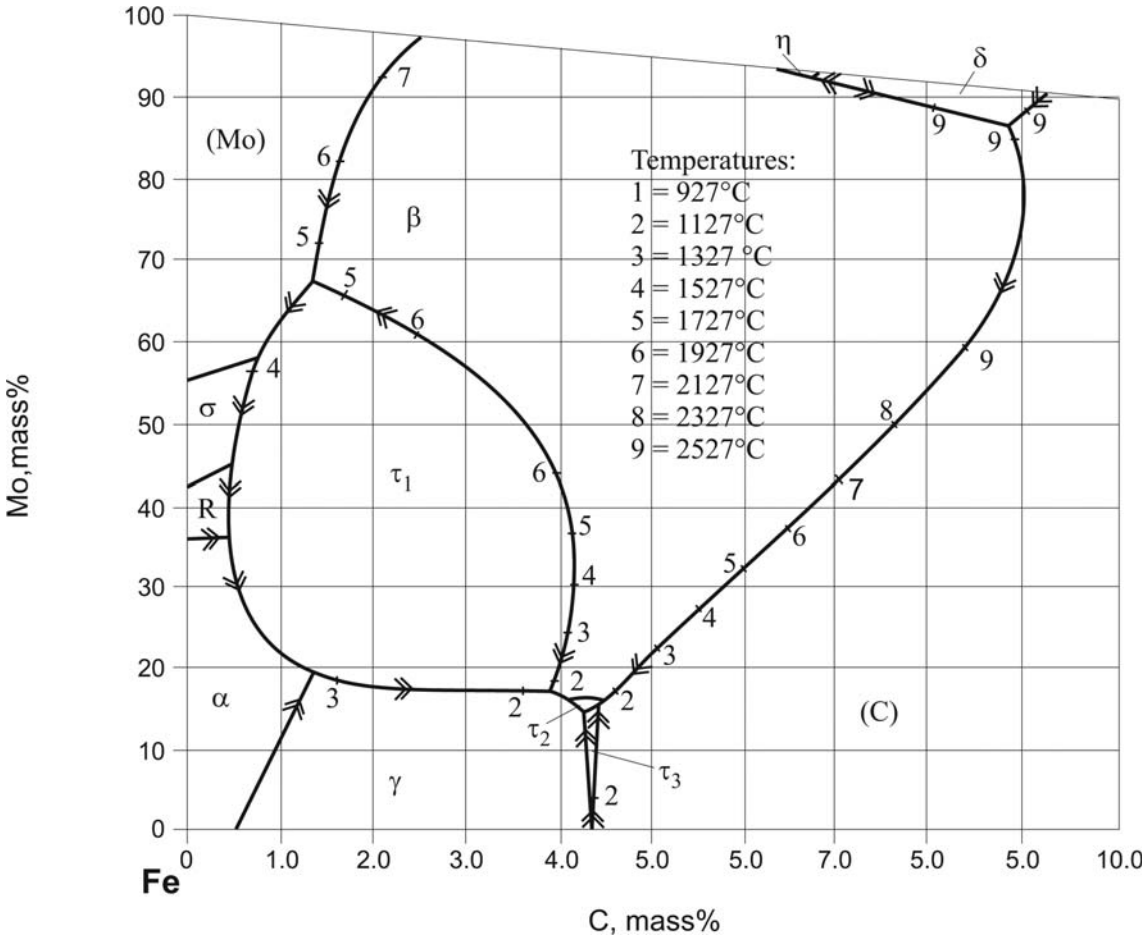

Fig. 3. C-Fe-Mo. Isotherms on the liquidus surface projection

DOI: 10.1007/978-3-540-74196-1_7

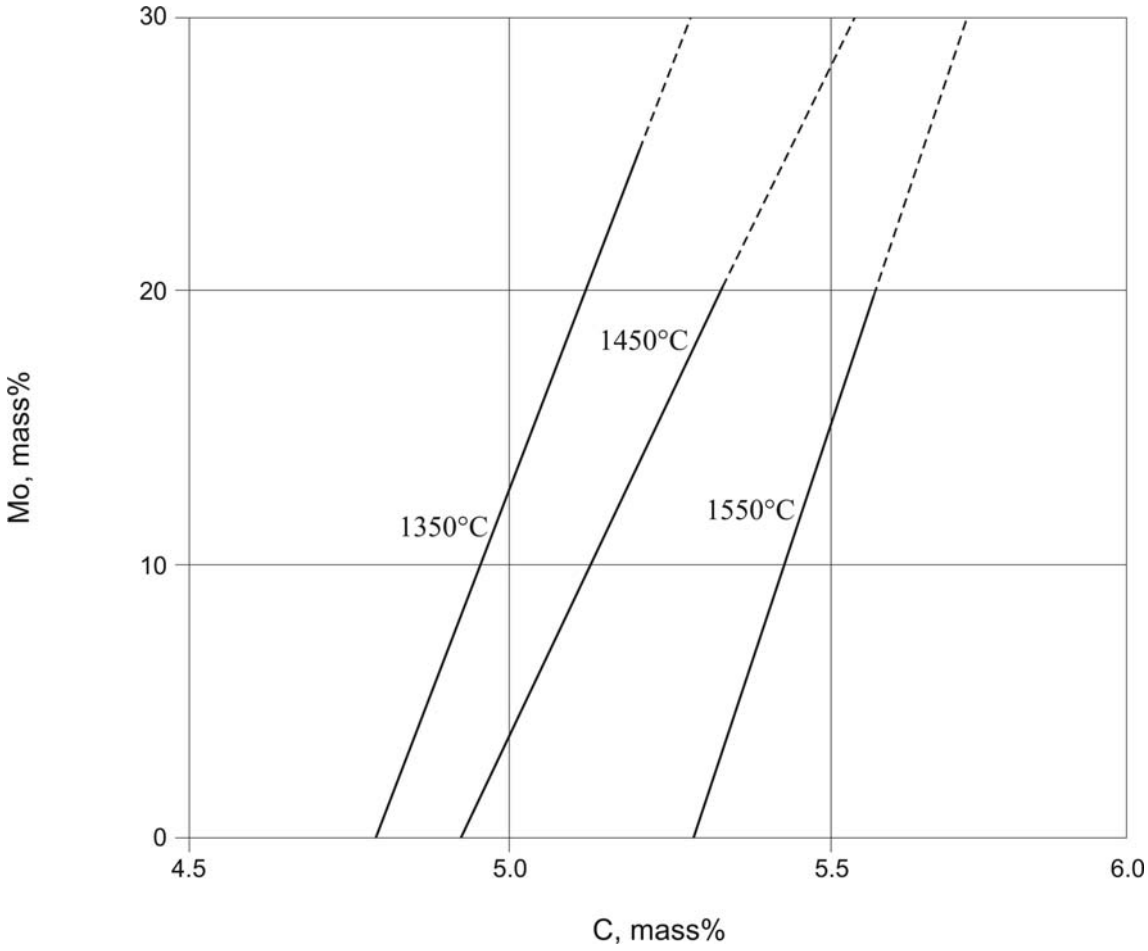

Fig. 4. C-Fe-Mo. Experimental isotherms on the liquidus surface of graphite

DOI: 10.1007/978-3-540-74196-1_7

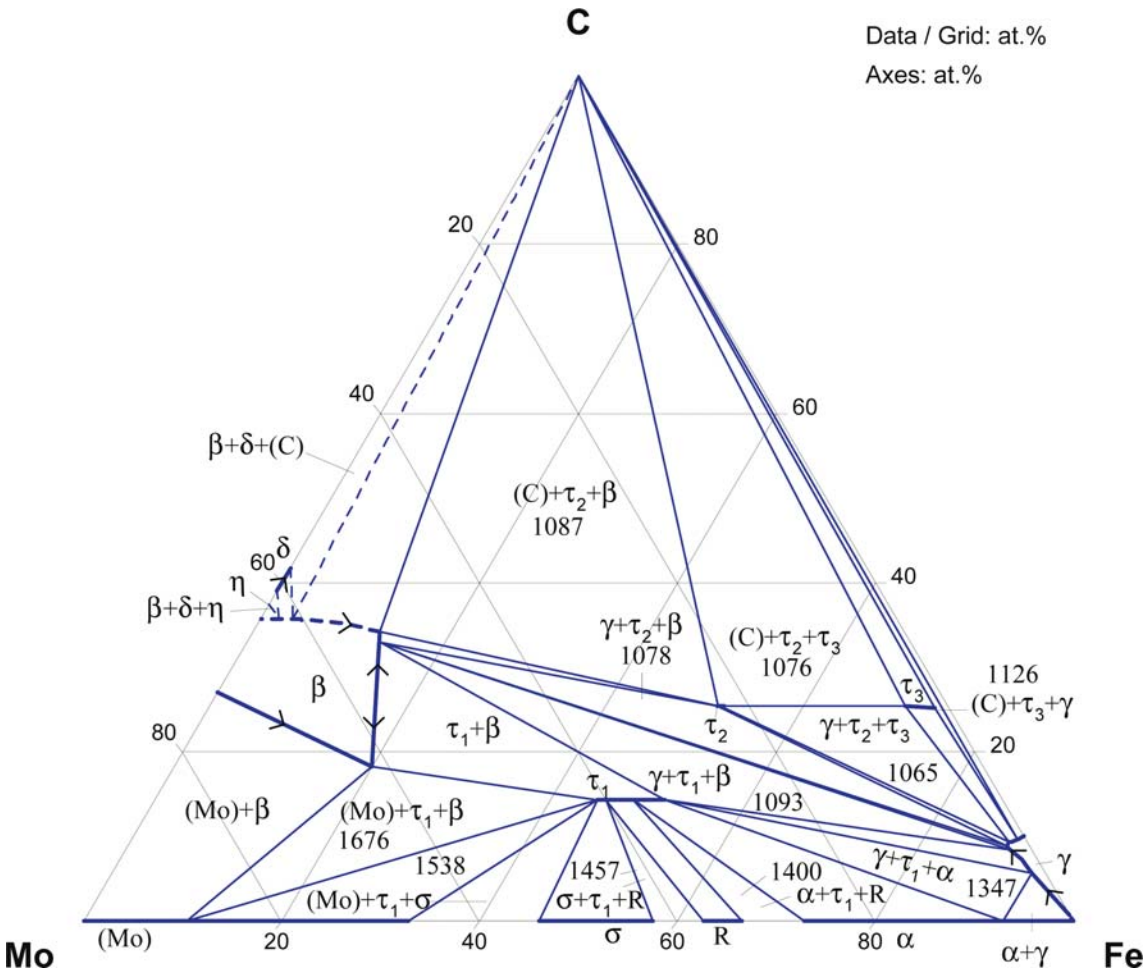

Fig. 5. C-Fe-Mo. Solidus surface projection

DOI: 10.1007/978-3-540-74196-1_7

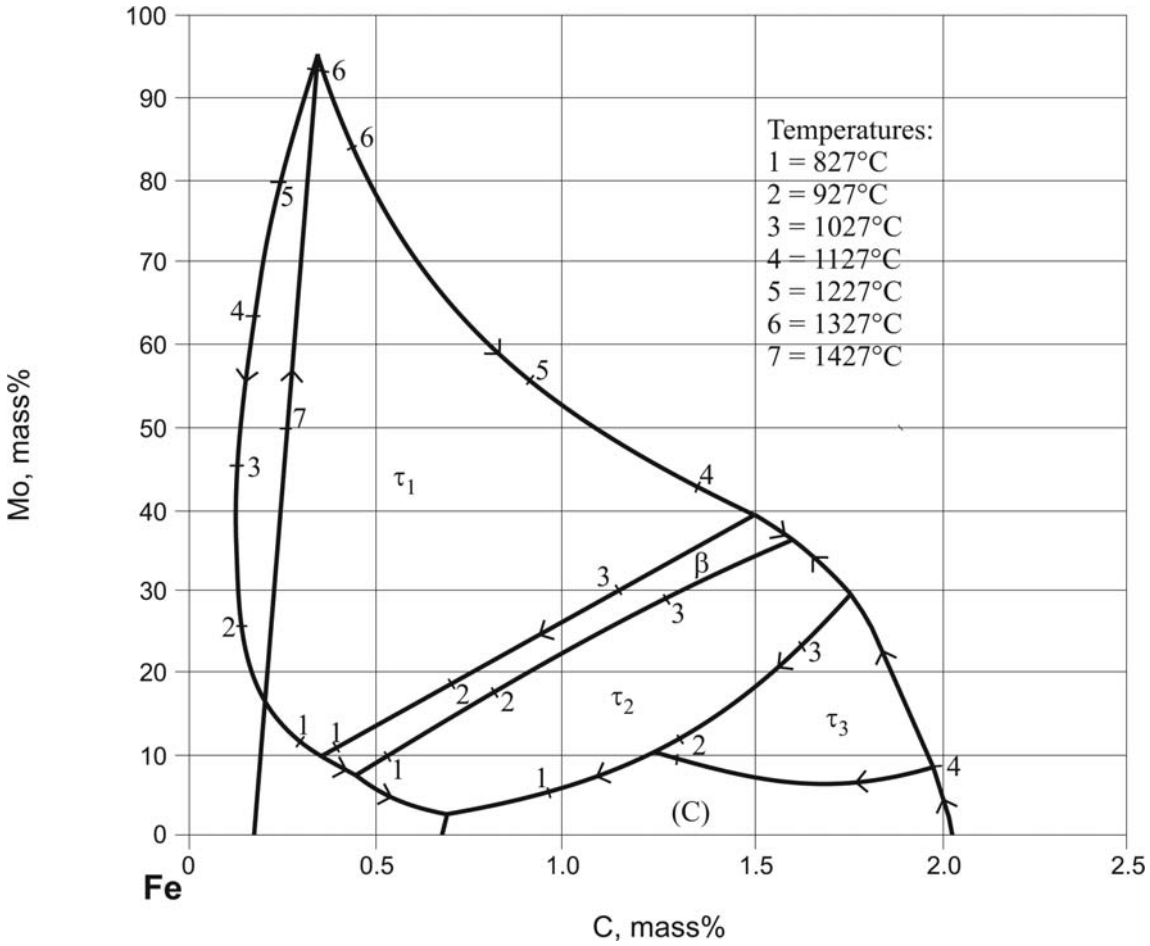

Fig. 6. C-Fe-Mo. Projection of solidus and solvus of γ phase

DOI: 10.1007/978-3-540-74196-1_7

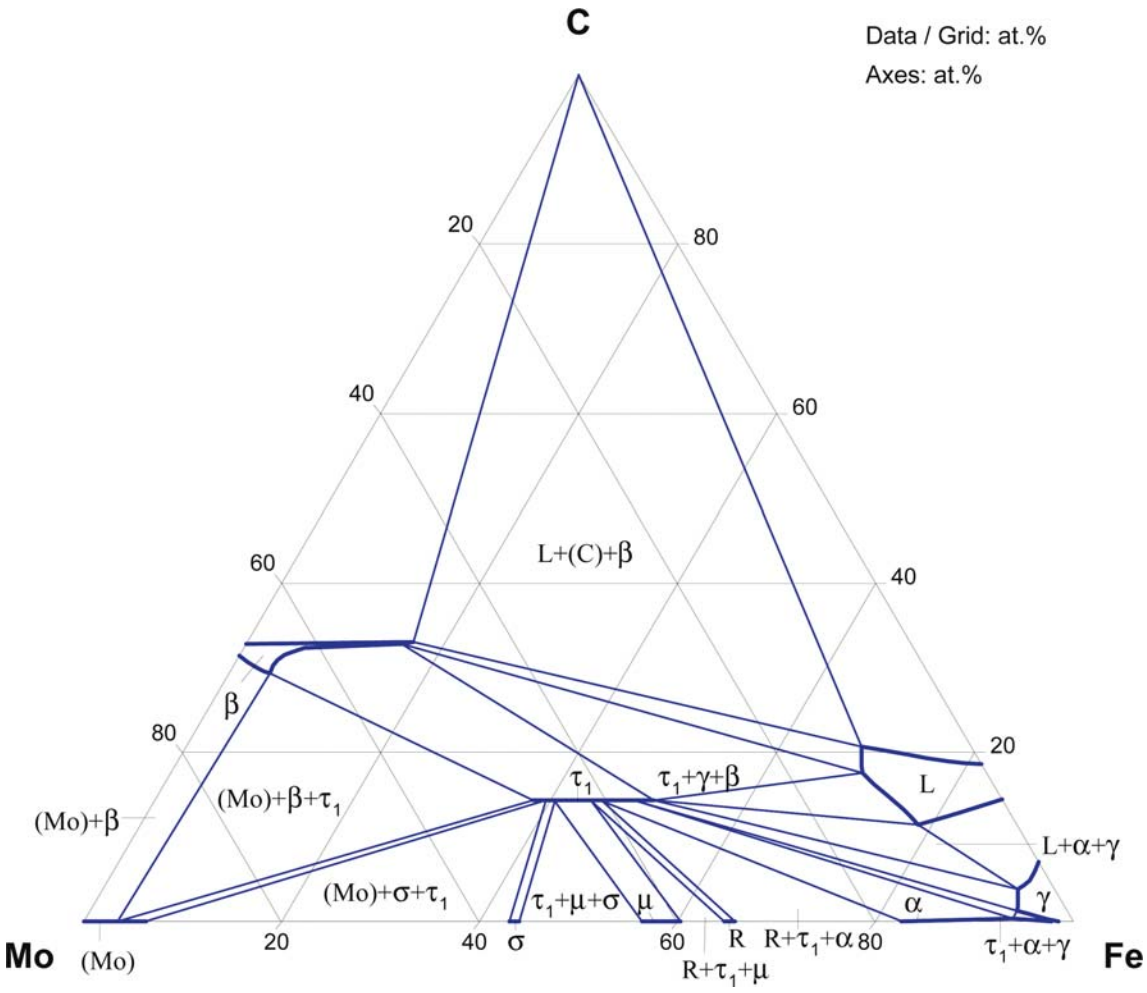

Fig. 7a. C-Fe-Mo. Calculated isothermal section at 1250°C

DOI: 10.1007/978-3-540-74196-1_7

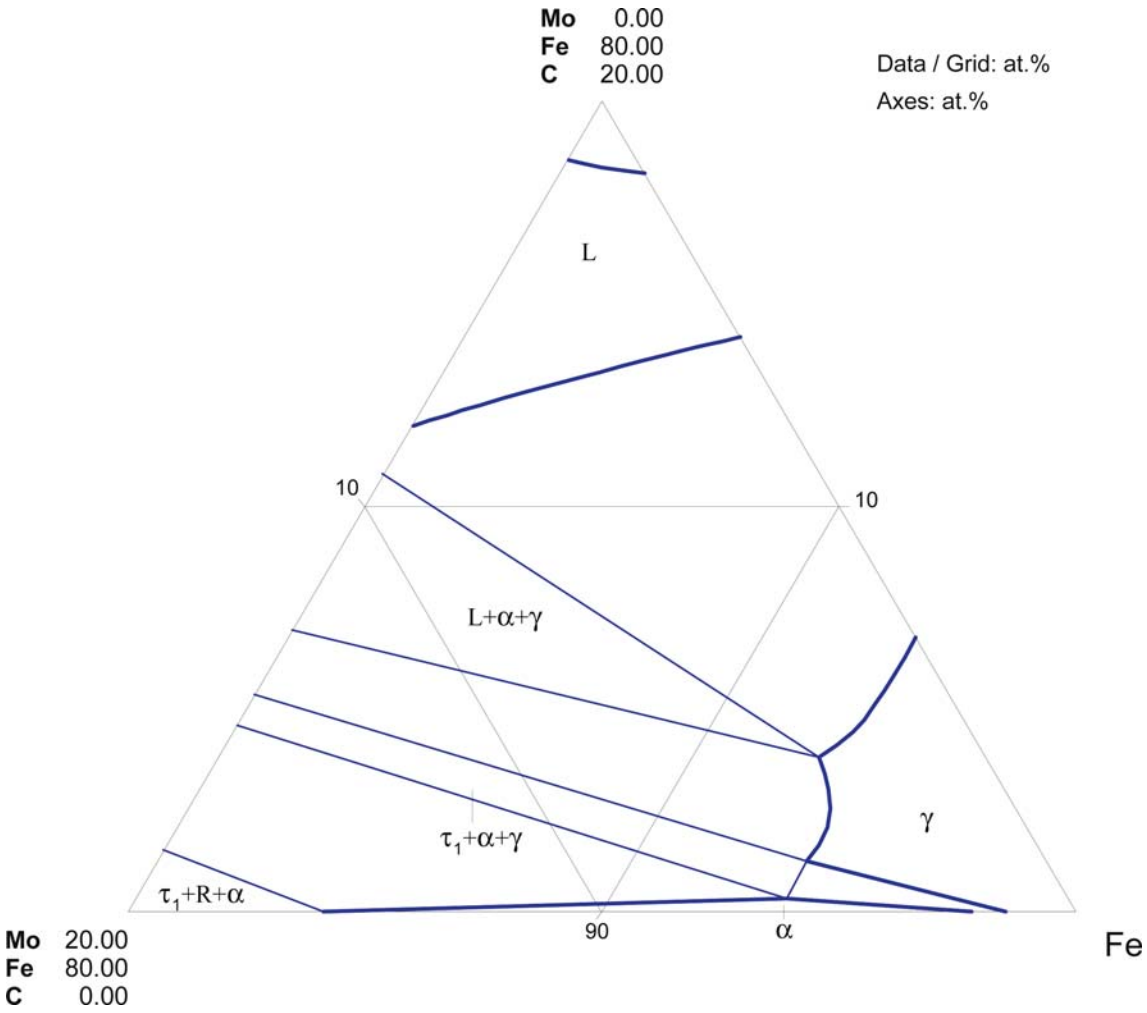

Fig. 7b. C-Fe-Mo. Enlarged part of calculated isothermal section at 1250°C

DOI: 10.1007/978-3-540-74196-1_7

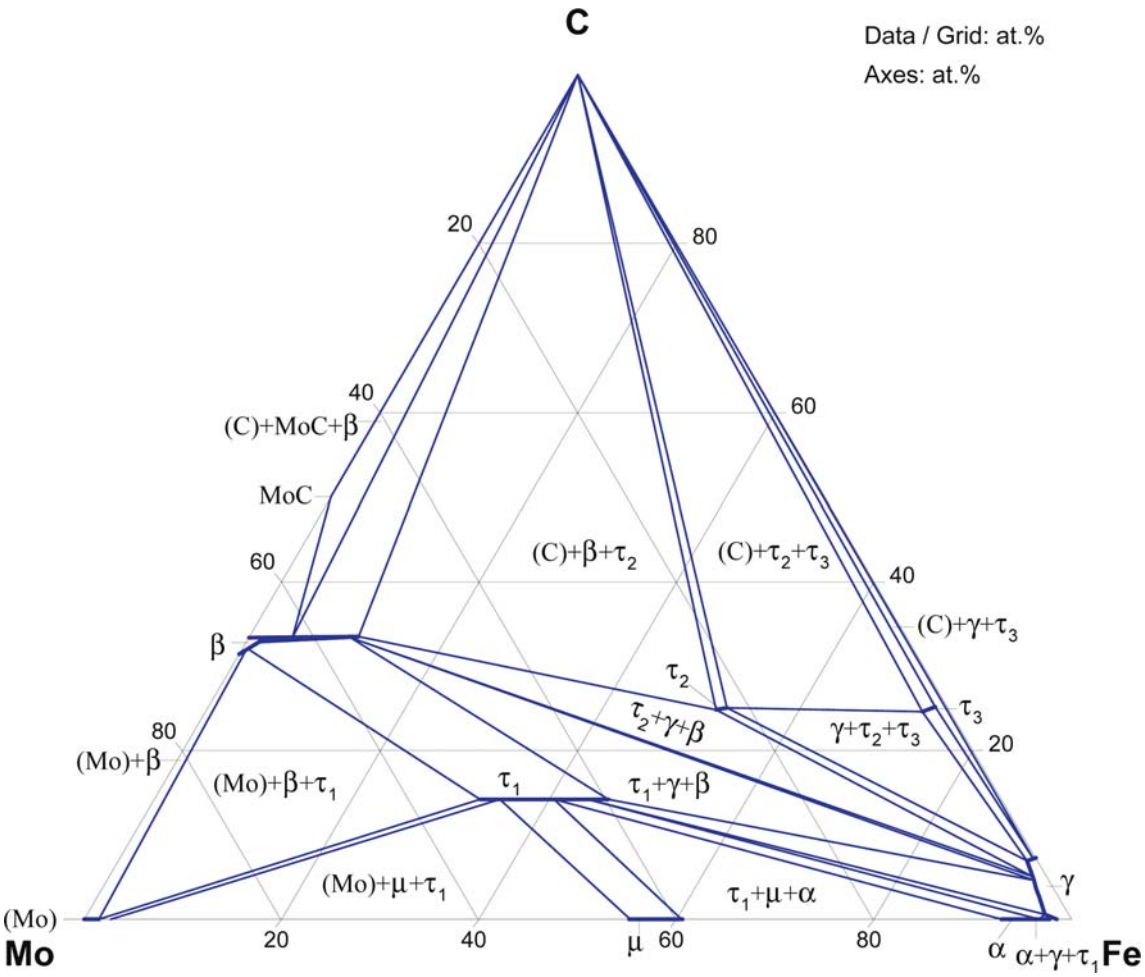

Fig. 8a. C-Fe-Mo. Calculated isothermal section at 1000°C

DOI: 10.1007/978-3-540-74196-1_7

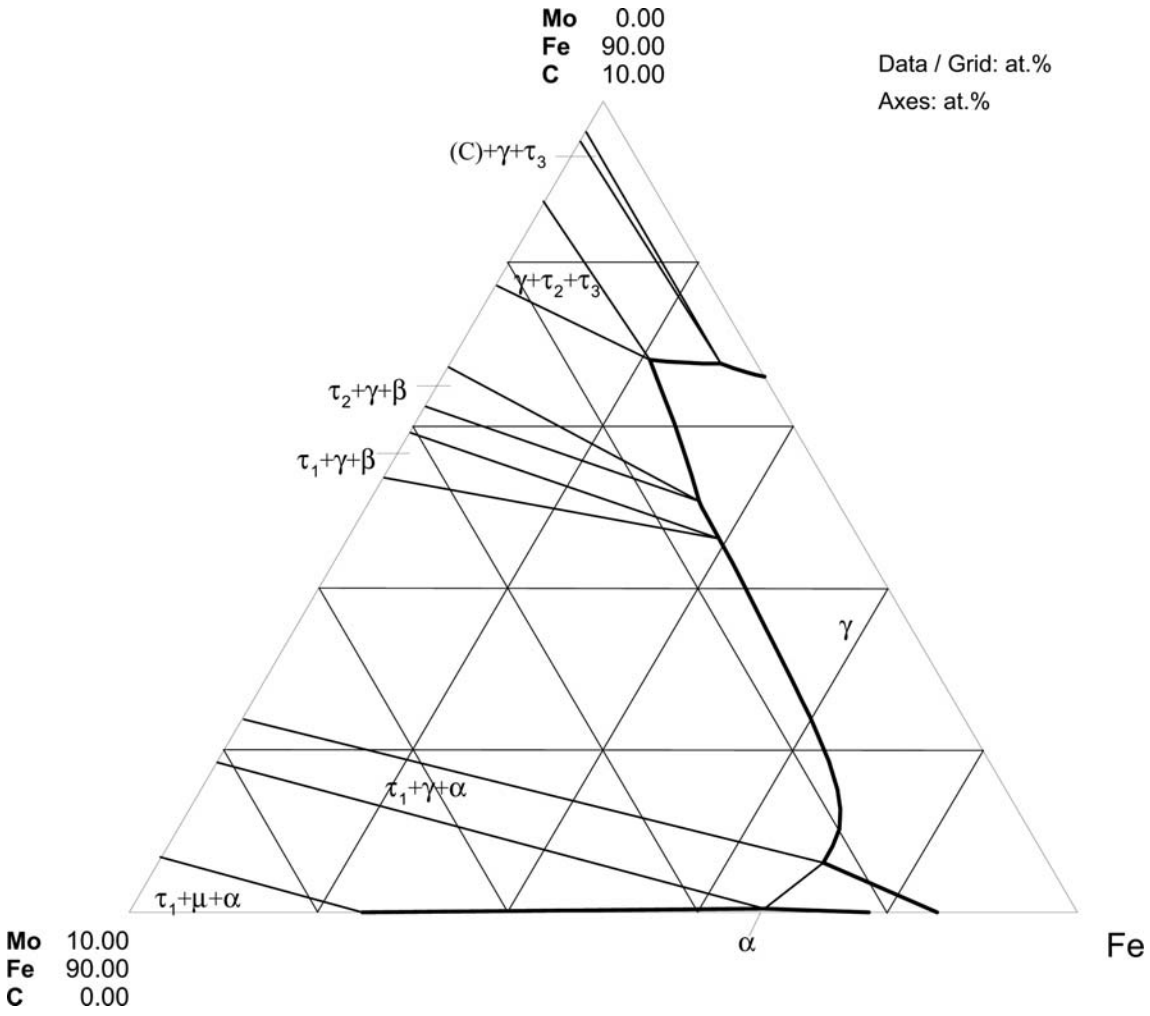

Fig. 8b. C-Fe-Mo. Enlarged part of the calculated isothermal section at 1000°C

DOI: 10.1007/978-3-540-74196-1_7

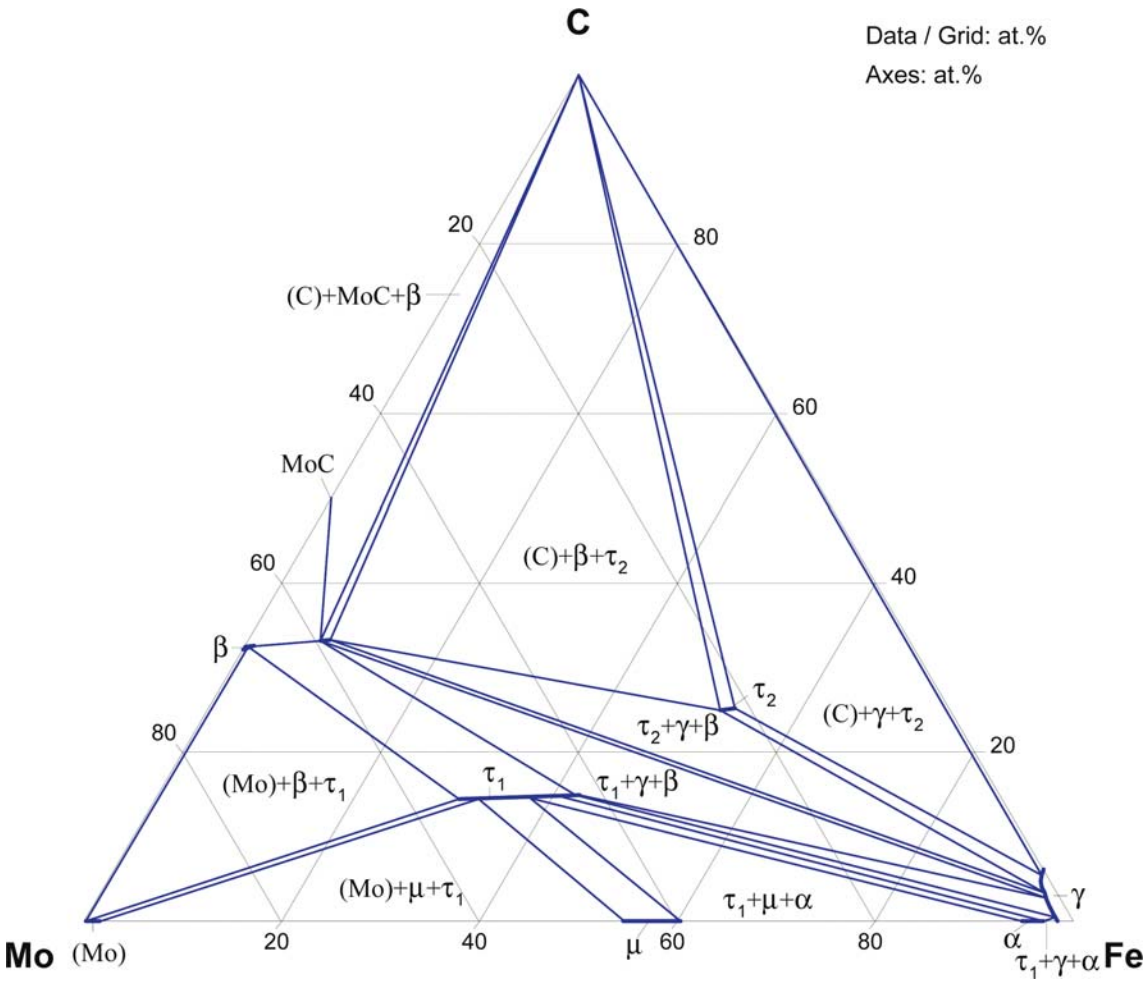

Fig. 9. C-Fe-Mo. Calculated isothermal section at 900°C

DOI: 10.1007/978-3-540-74196-1_7

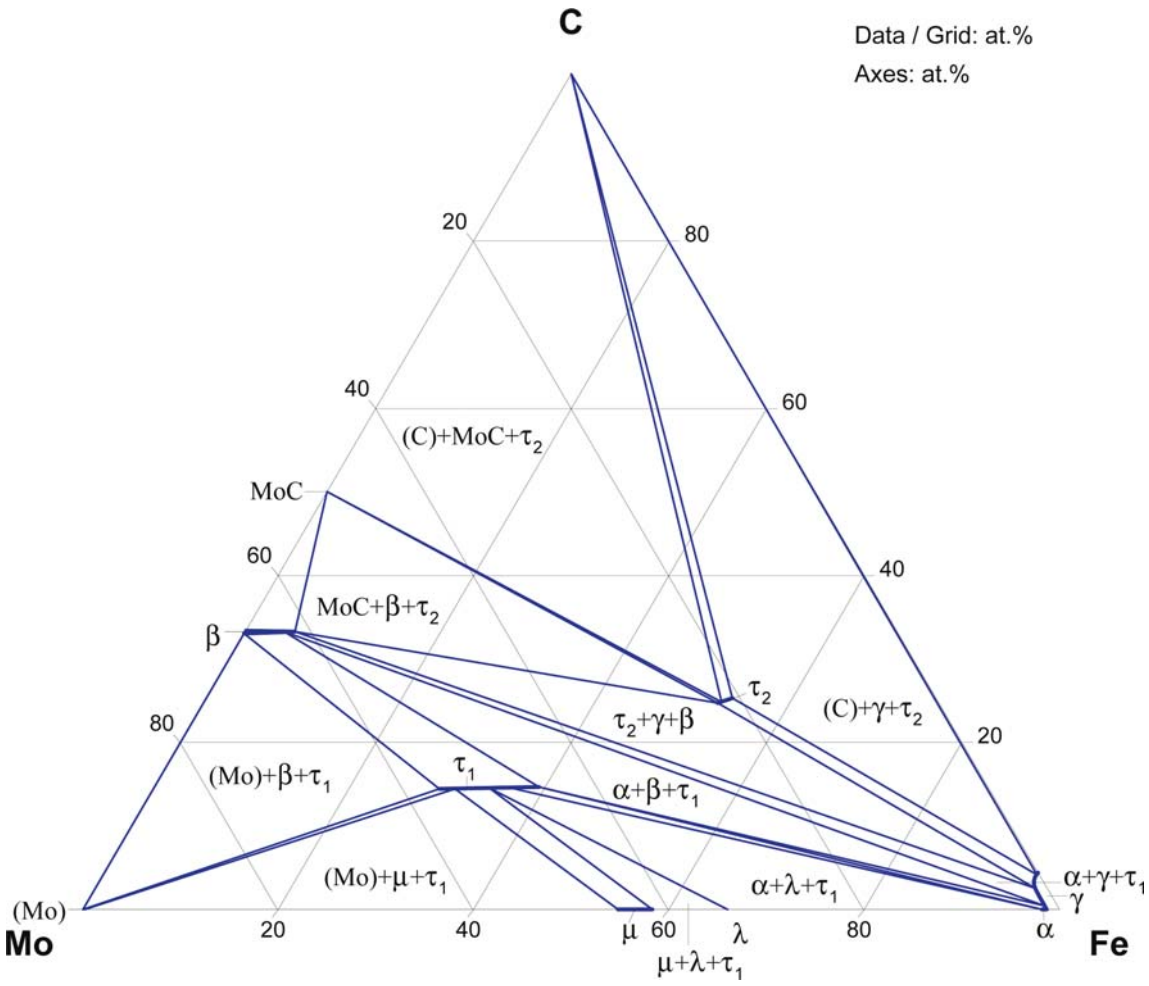

Fig. 10. C-Fe-Mo. Calculated isothermal section at 800°C

DOI: 10.1007/978-3-540-74196-1_7

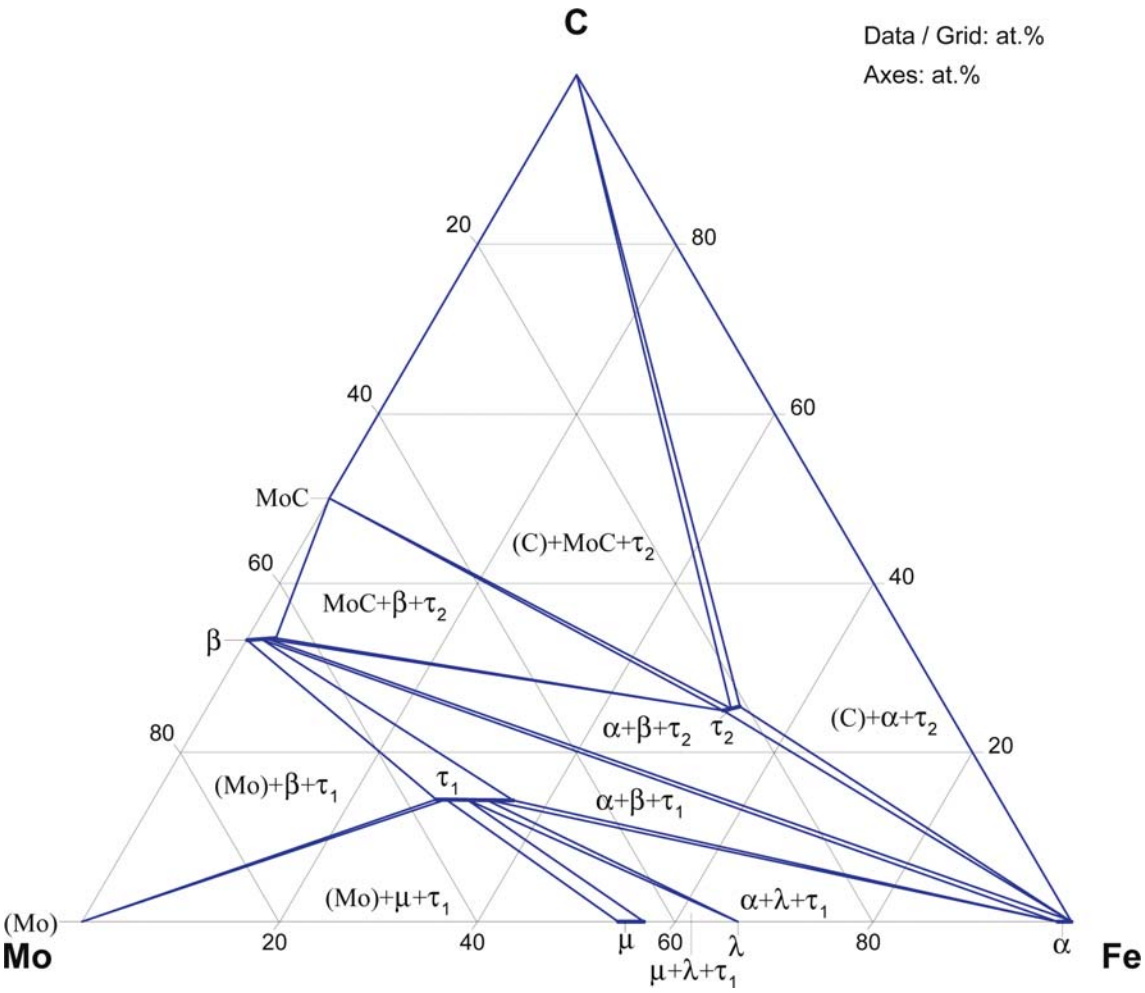

Fig. 11. C-Fe-Mo. Calculated isothermal section at 700°C

DOI: 10.1007/978-3-540-74196-1_7

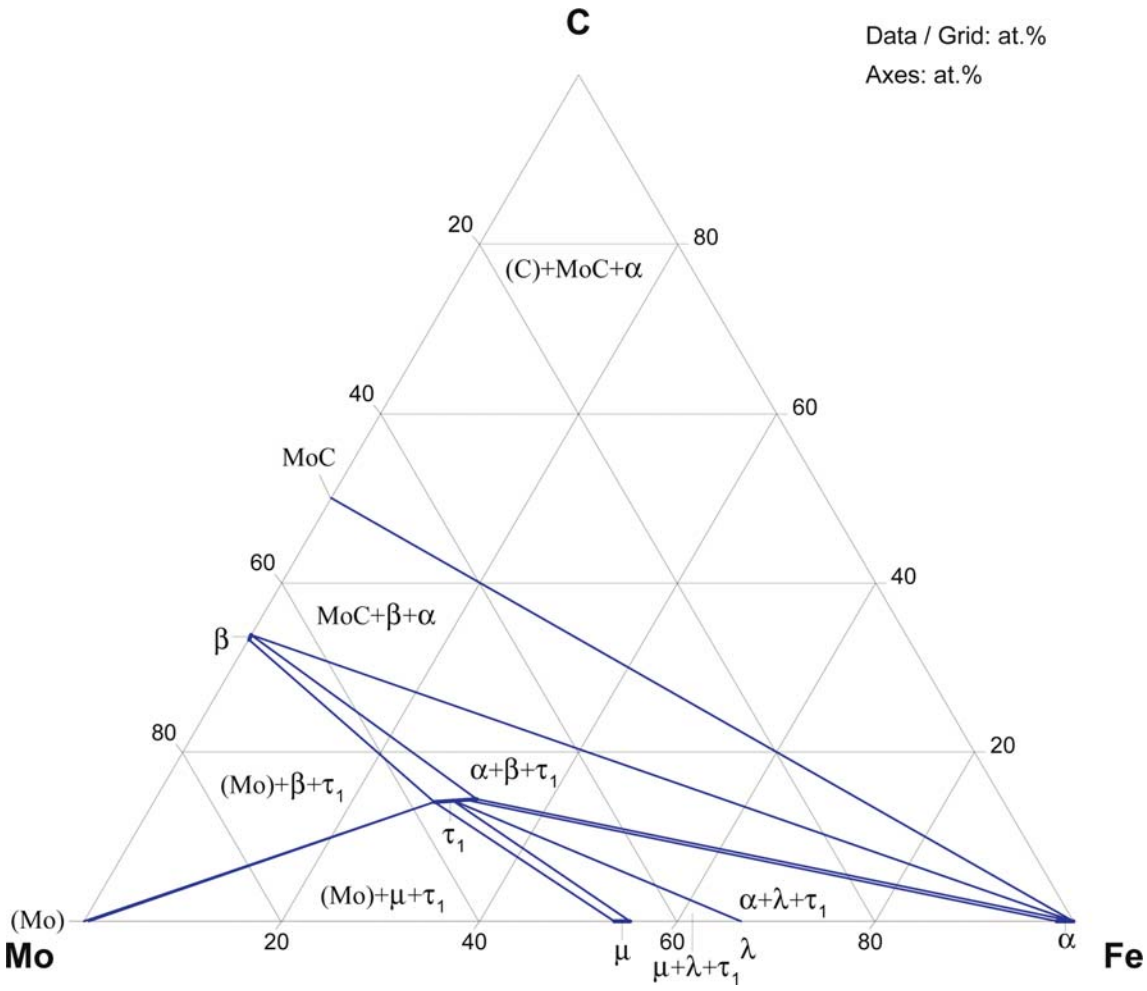

Fig. 12. C-Fe-Mo. Calculated isothermal section at 550°C

DOI: 10.1007/978-3-540-74196-1_7

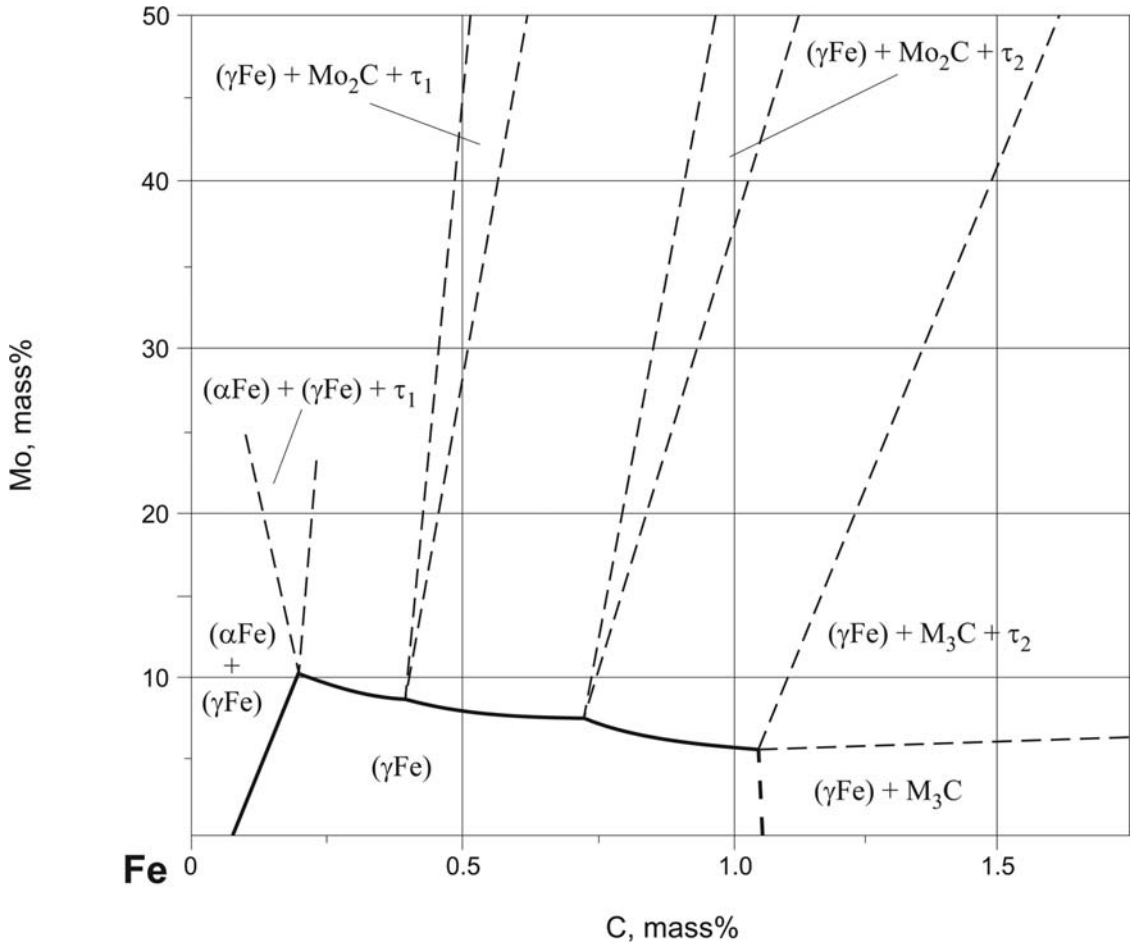

Fig. 13a. C-Fe-Mo. Experimental isotherm of the (γFe) solubility at 871°C

DOI: 10.1007/978-3-540-74196-1_7

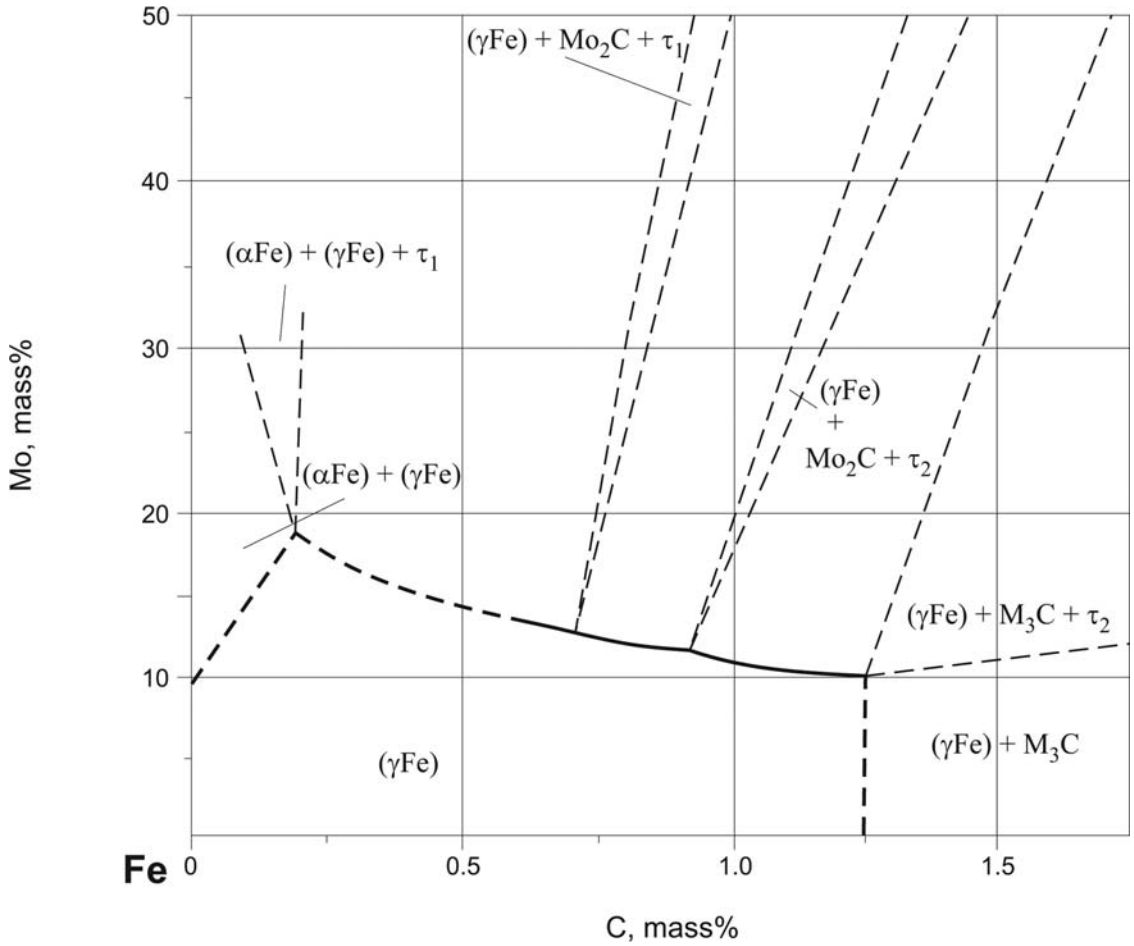

Fig. 13b. C-Fe-Mo. Experimental isotherm of the (γFe) solubility at 927°C

DOI: 10.1007/978-3-540-74196-1_7

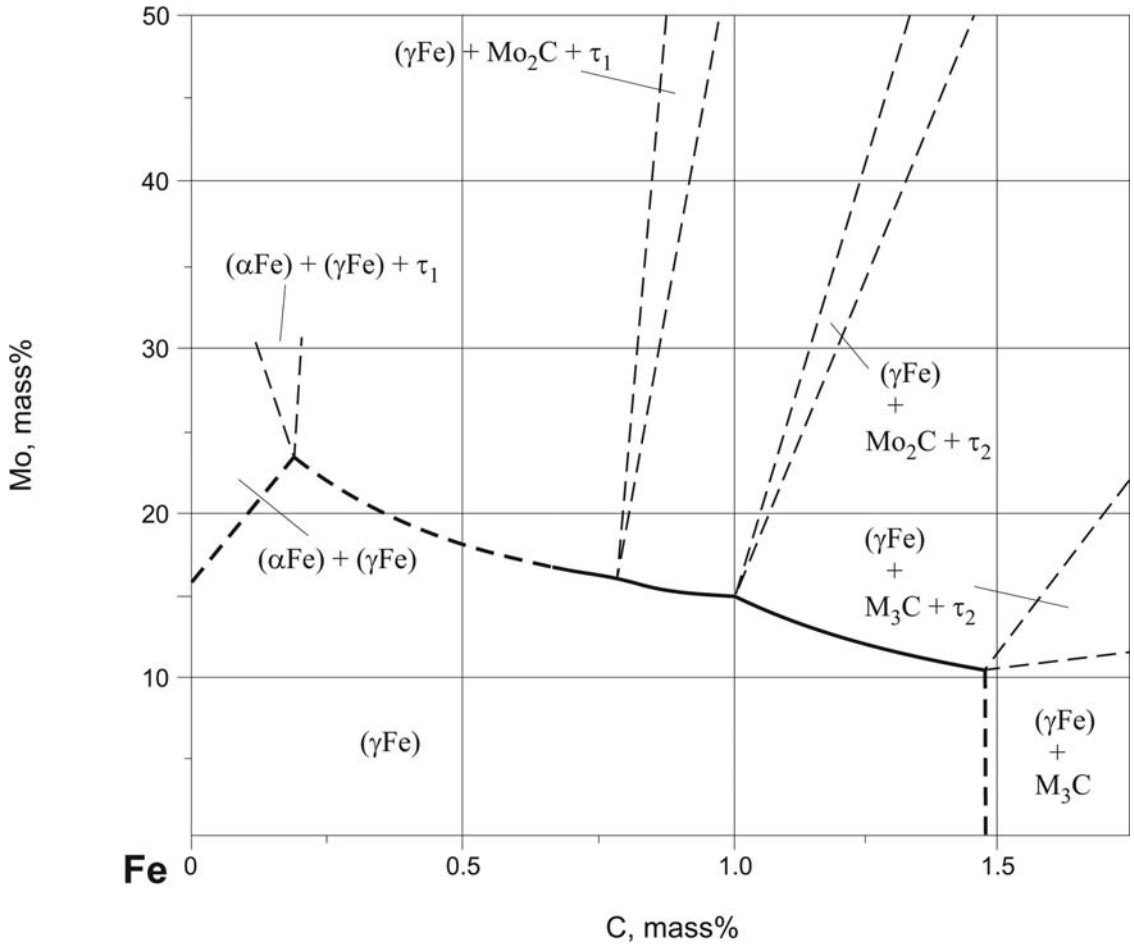

Fig. 13c. C-Fe-Mo. Experimental isotherm of the (γFe) solubility at 982°C

DOI: 10.1007/978-3-540-74196-1_7

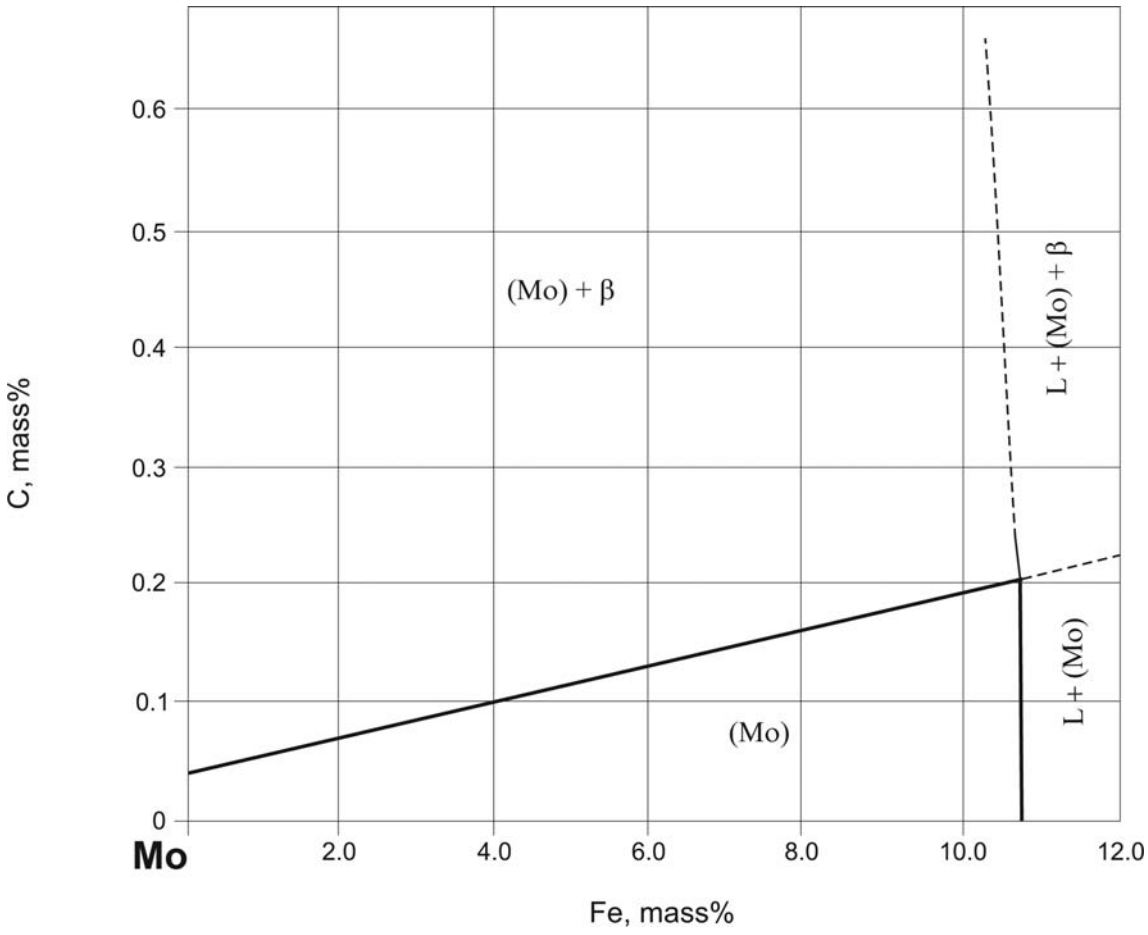

Fig. 14a. C-Fe-Mo. Experimental isothermal section at 1800°C in the molybdenum corner

DOI: 10.1007/978-3-540-74196-1_7

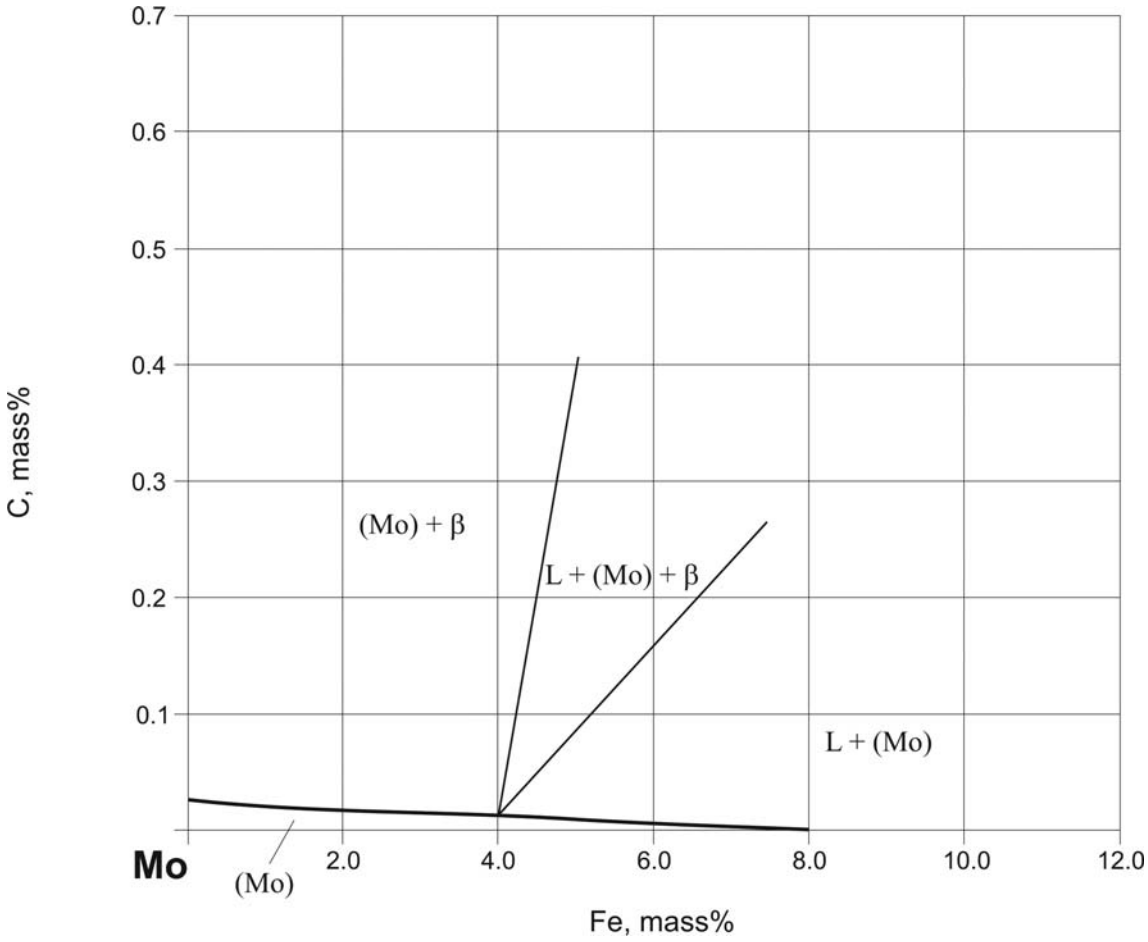

Fig. 14b. C-Fe-Mo. Calculated isothermal section at 1800°C in the molybdenum corner

DOI: 10.1007/978-3-540-74196-1_7

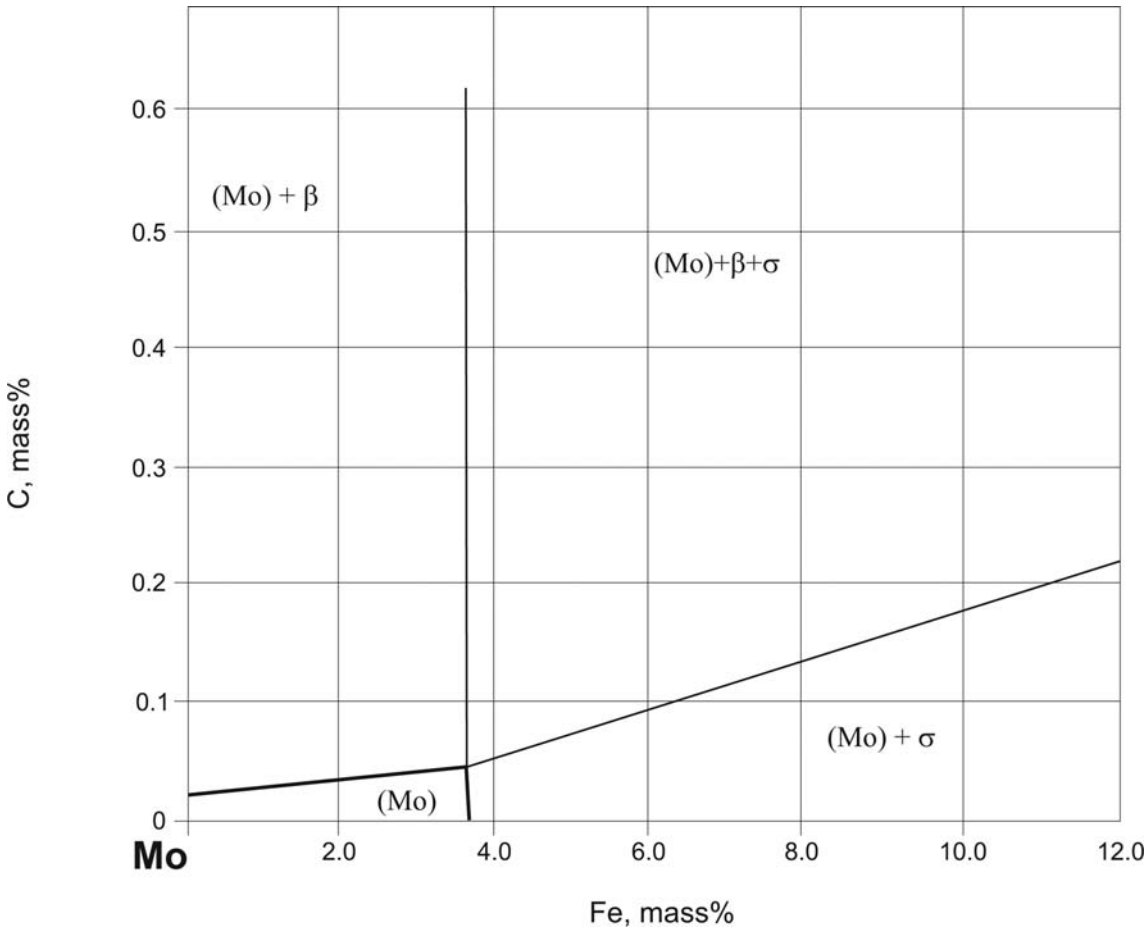

Fig. 15a. C-Fe-Mo. Experimental isothermal section at 1200°C in the molybdenum corner

DOI: 10.1007/978-3-540-74196-1_7

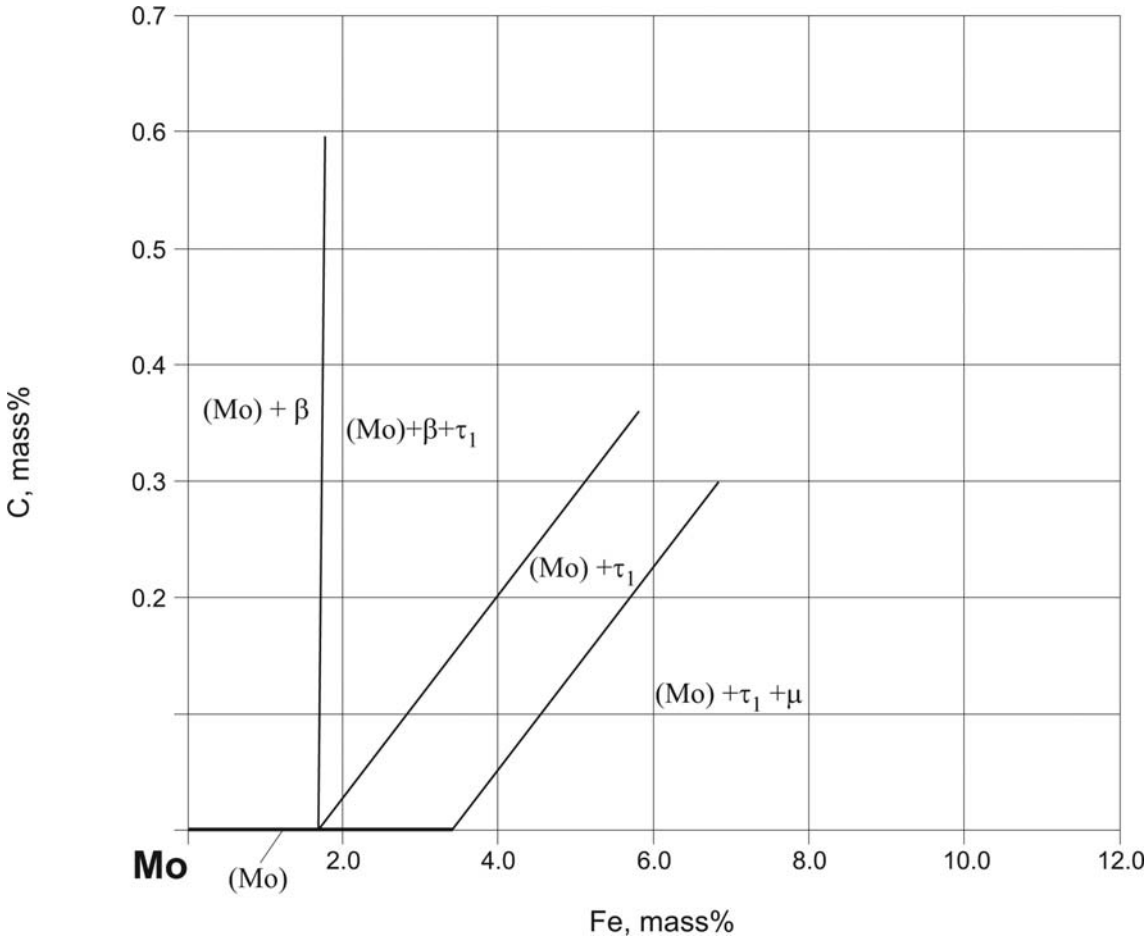

Fig. 15b. C-Fe-Mo. Calculated isothermal section at 1200°C in the molybdenum corner

DOI: 10.1007/978-3-540-74196-1_7

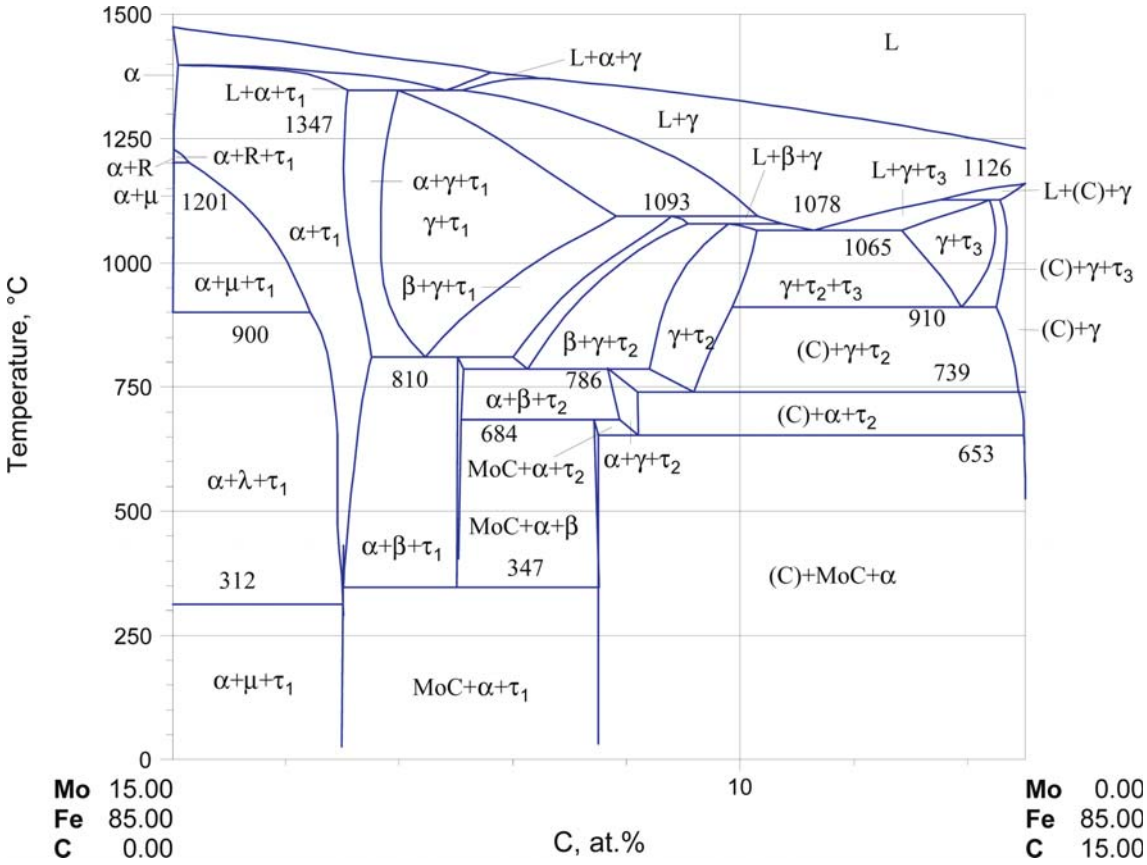

Fig. 16. C-Fe-Mo. Calculated vertical section at 85 at.% Fe

DOI: 10.1007/978-3-540-74196-1_7

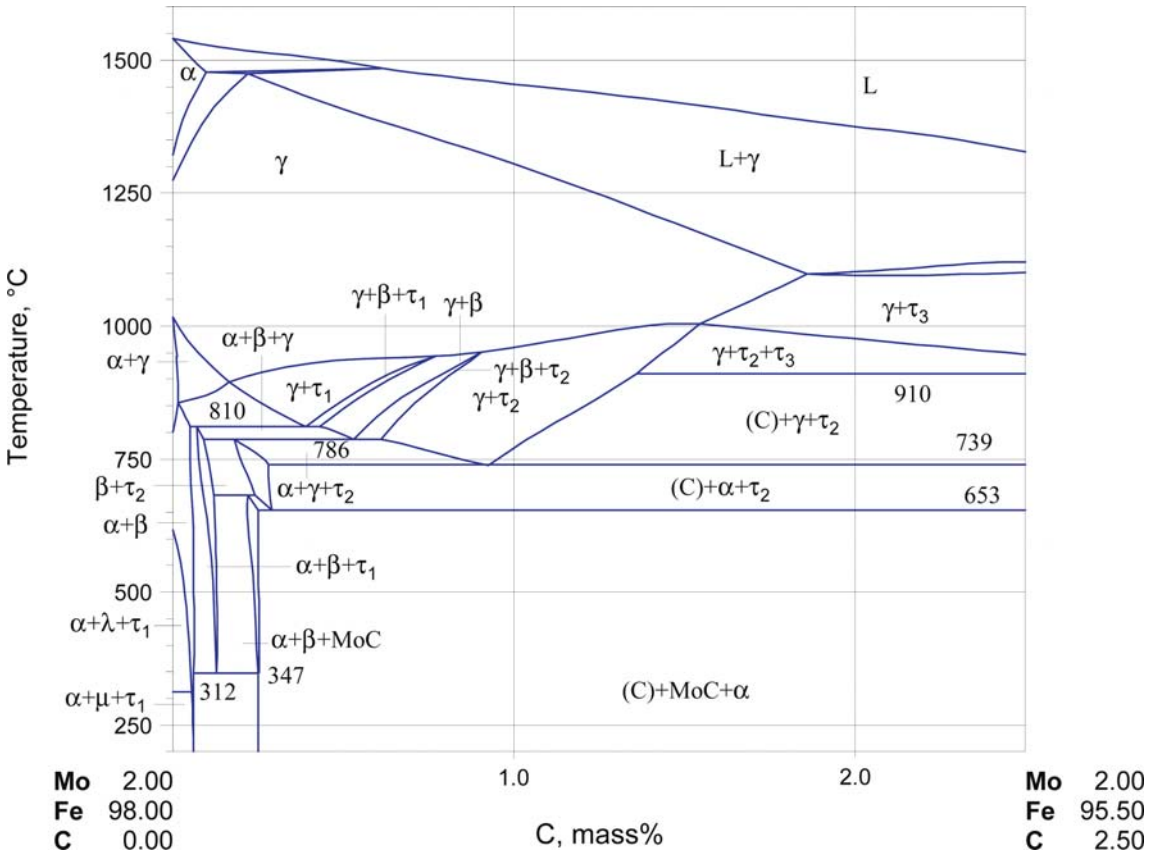

Fig. 17. C-Fe-Mo. Calculated vertical section at 2 mass% Mo

DOI: 10.1007/978-3-540-74196-1_7

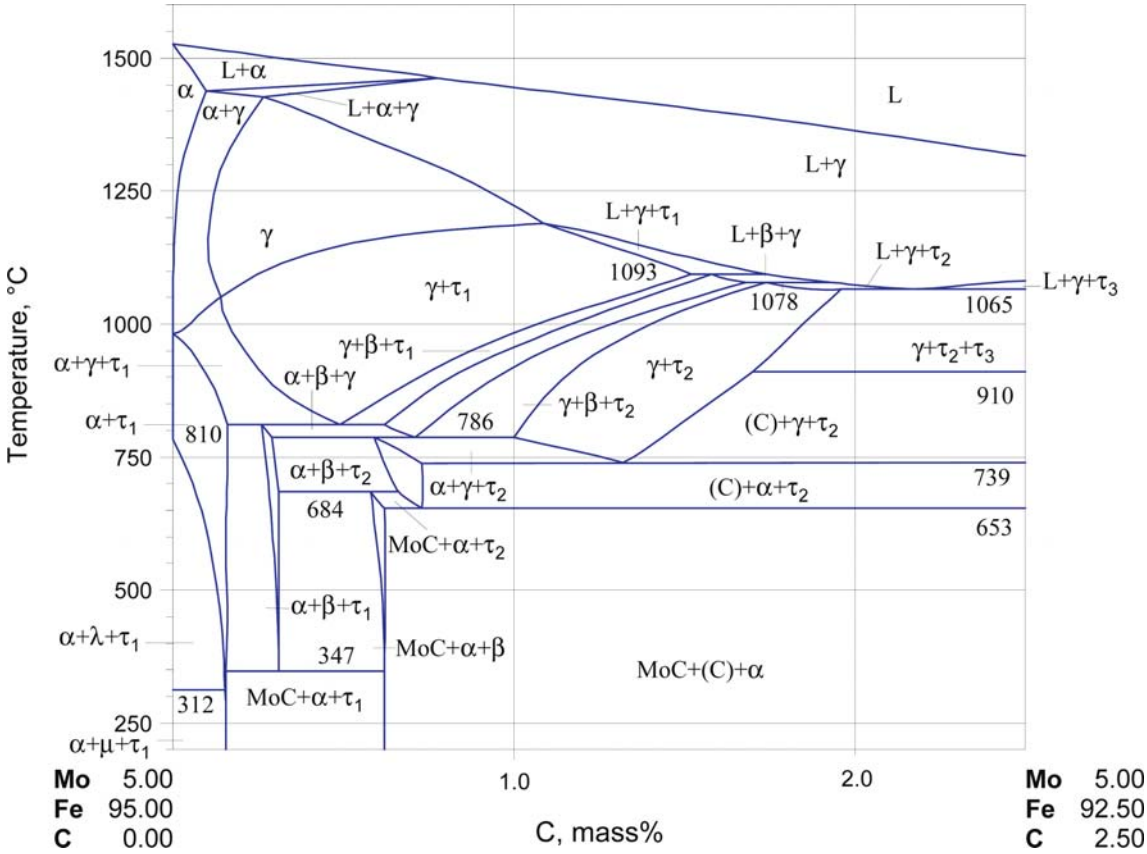

Fig. 18. C-Fe-Mo. Calculated vertical section at 5 mass% Mo

DOI: 10.1007/978-3-540-74196-1_7

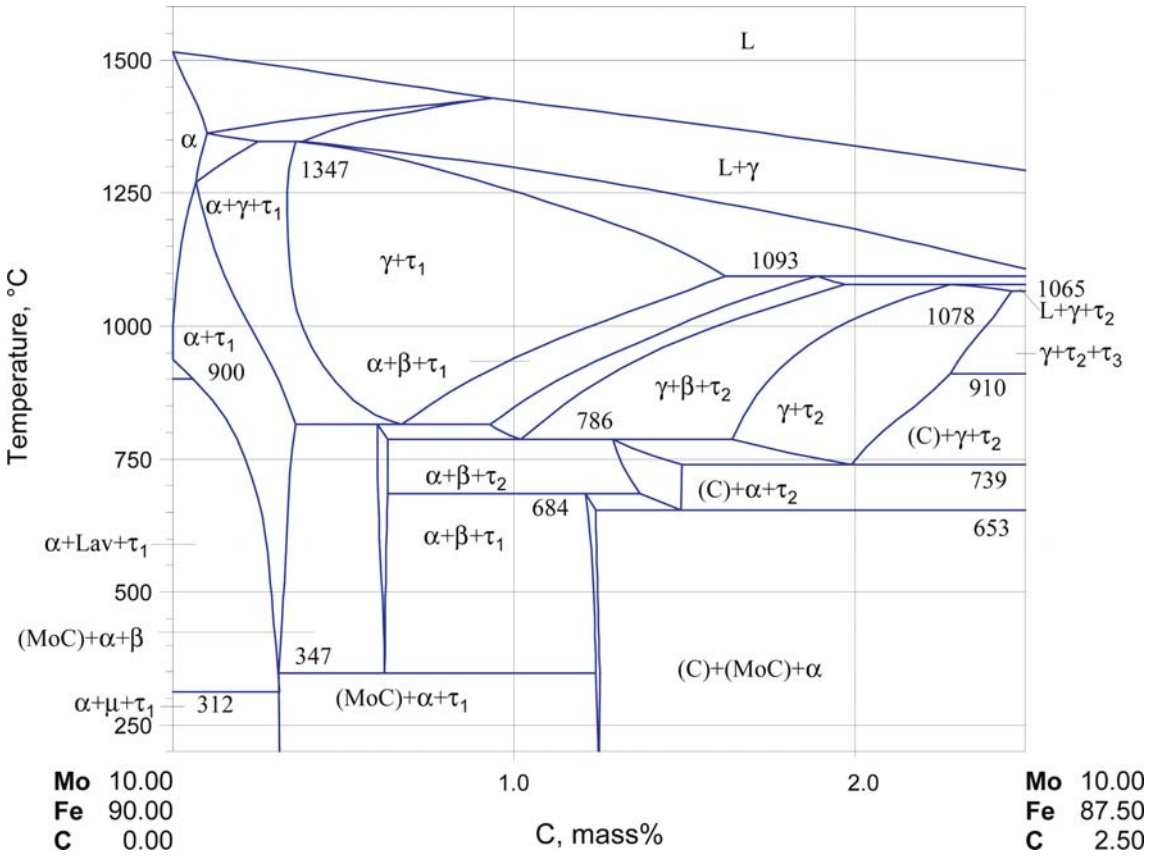

Fig. 19. C-Fe-Mo. Calculated vertical section at 10 mass% Mo

DOI: 10.1007/978-3-540-74196-1_7

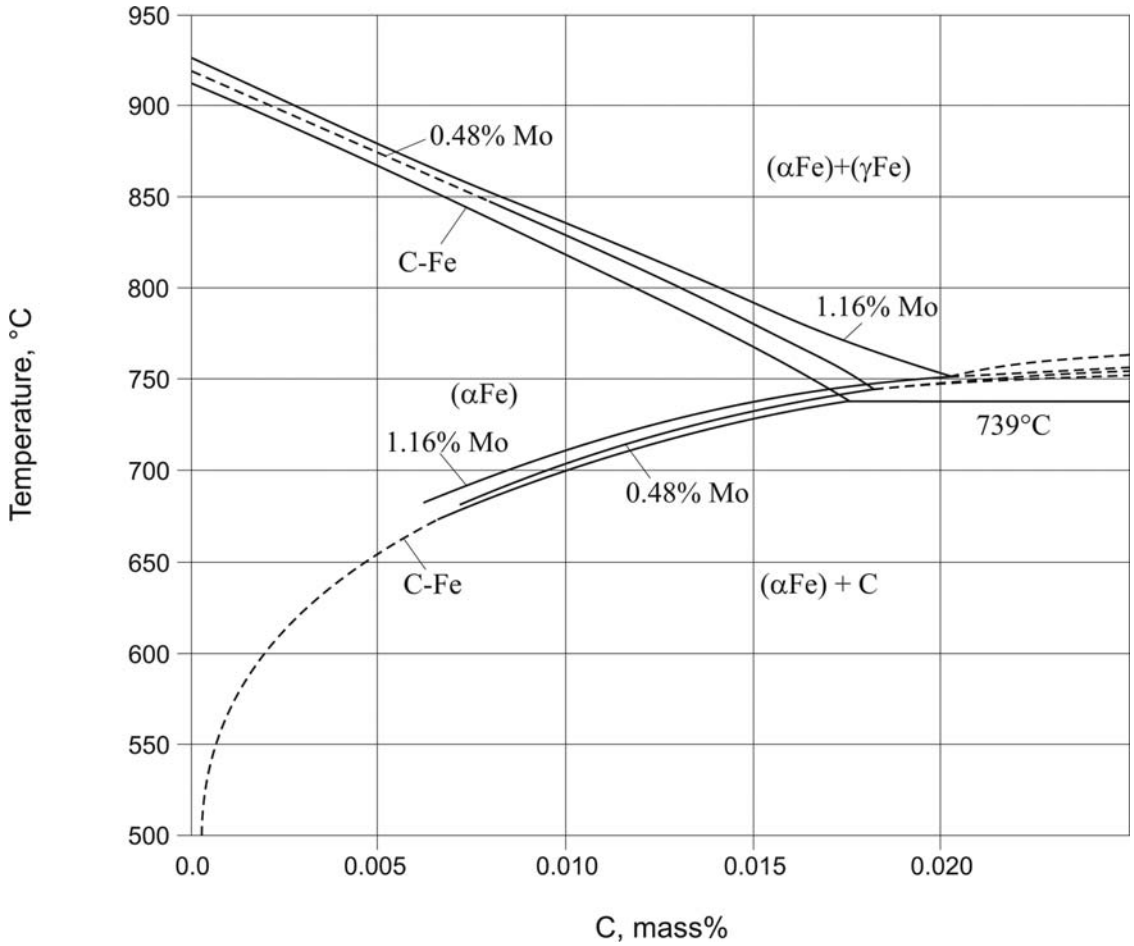

Fig. 20. C-Fe-Mo. Calculated vertical sections at 0.48 and 1.16 mass% C

DOI: 10.1007/978-3-540-74196-1_7

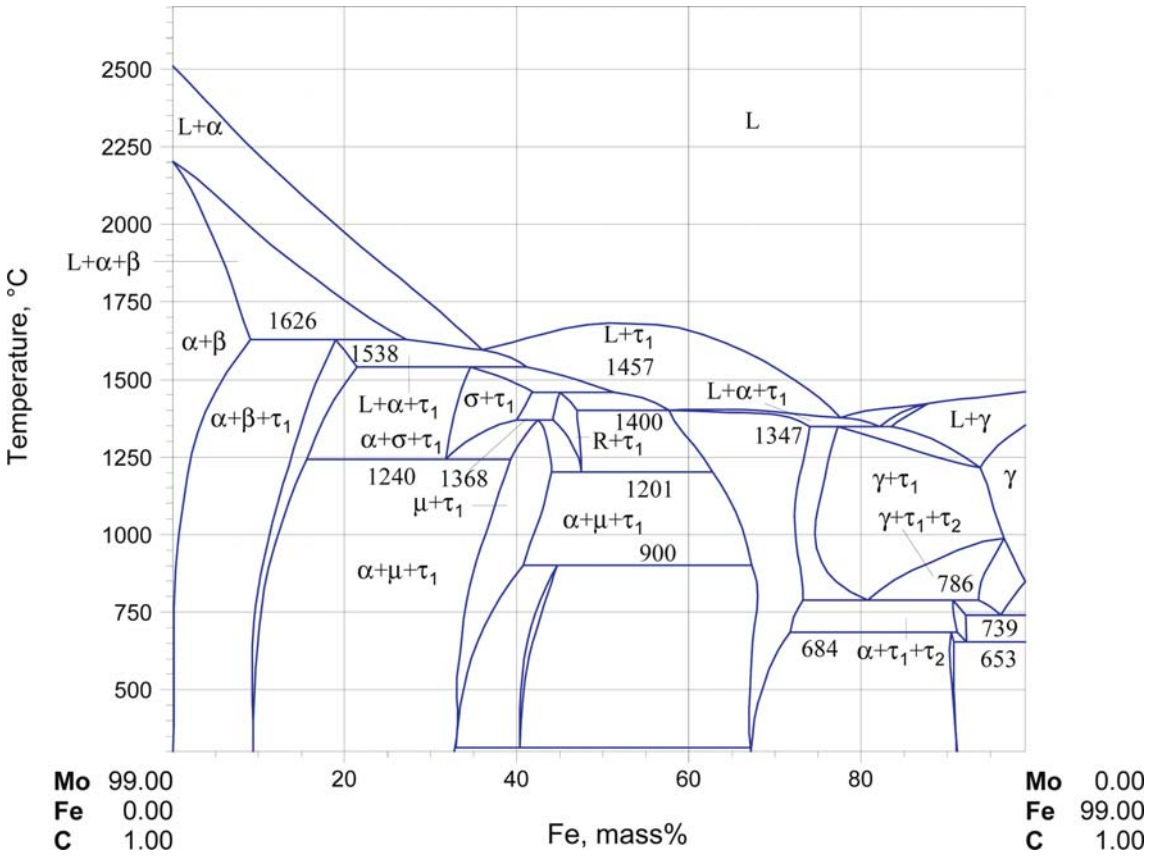

Fig. 21. C-Fe-Mo. Calculated vertical section at 1 mass% C

DOI: 10.1007/978-3-540-74196-1_7

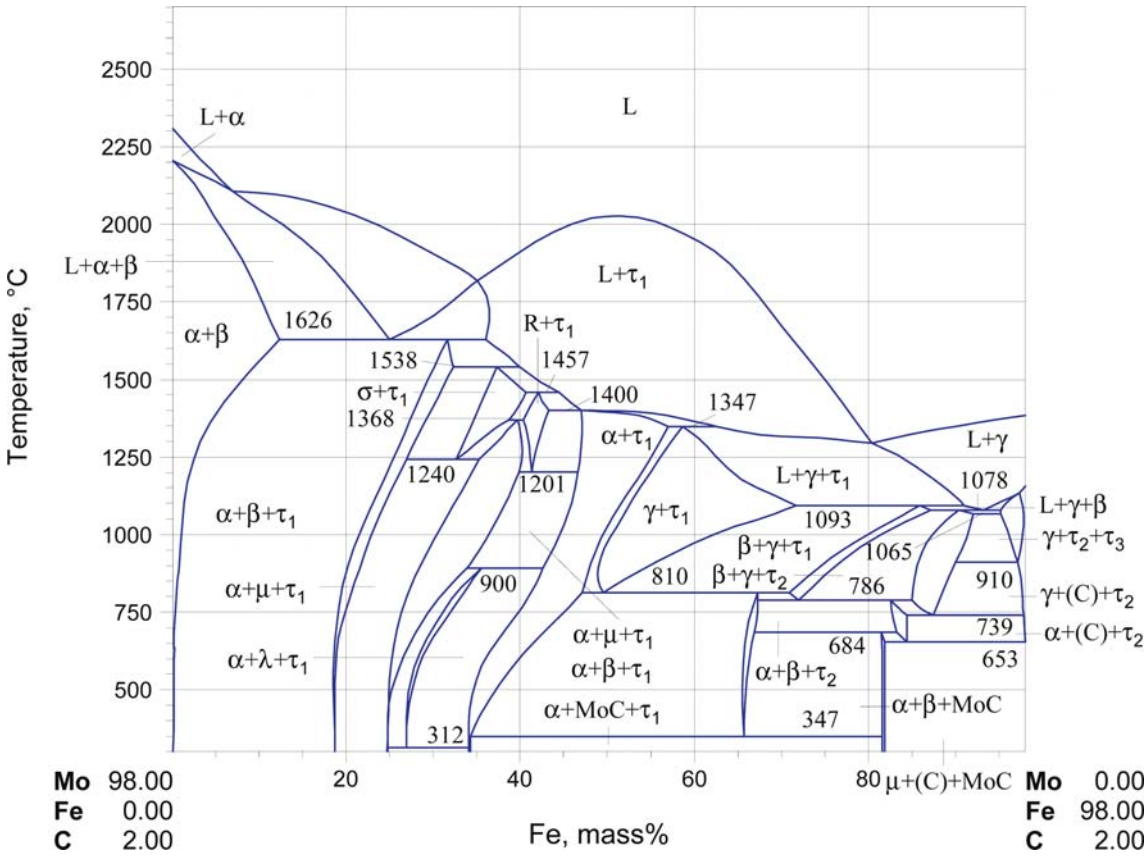

Fig. 22a. C-Fe-Mo. Calculated vertical section at 2 mass% C

DOI: 10.1007/978-3-540-74196-1_7

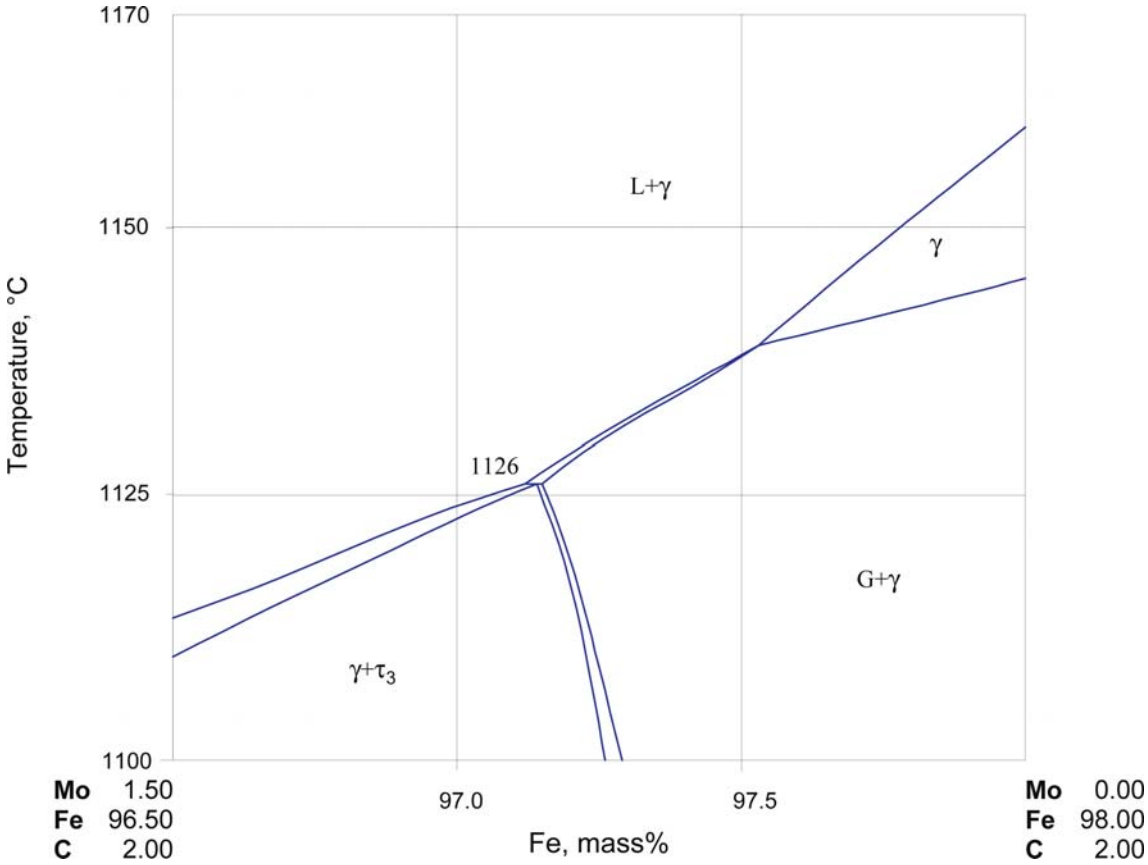

Fig. 22b. C-Fe-Mo. Enlarged part of the calculated vertical section at 2 mass% C

DOI: 10.1007/978-3-540-74196-1_7

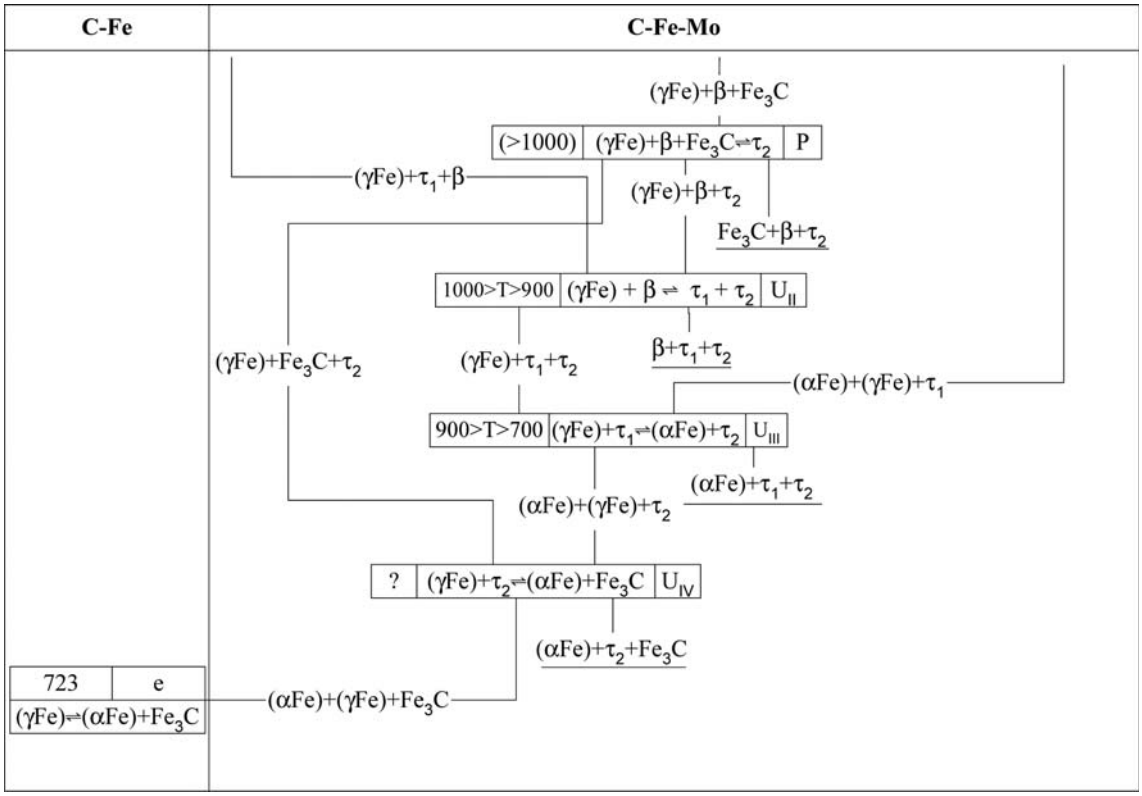

Fig. 23. C-Fe-Mo. Possible partial metastable reaction scheme for the solid state transformations

DOI: 10.1007/978-3-540-74196-1_7

References

[1930Dav] Davenport, E.S., Bain, E.C., "Transformation of Austenite at Constant Subcritical Temperatures", *Transactions Amer. Inst. of Mining and Met. Eng. Iron and Steel Div.*, 117. (1930)

[1932Tak1] Takei, T., "On the Ferromagnetic Carbides in Molybdenum Steels", *Kinzoku no Kenkyu*, **9**, 97–124 (1932) (Phase Diagram, Experimental, 5)

[1932Tak2] Takei, T., "On the Equilibrium Diagram of Fe-Mo-C System", *Kinzoku no Kenkyu*, **9**, 142-173 (1932) (Phase Diagram, Experimental) (as quoted by *Abstract Journal Metals and Alloys*, **3**, MA334 (1932))

[1933Ade] Adelskoeld, V., Sundelin, A., Westgren, A., "Carbides in Carbon Containing Alloys of Tundsten and Molybdenum with Chromium, Manganese, Iron, Cobalt and Nickel" (in German), *Z. Anorg. Chem.*, **212**, 401–409 (1933) (Experimental, Crys. Structure, 11)

[1936Sve] Svechnikov, V.N., Alferova, N.S., "Investigation of the Alloys of the Fe-C-Mo System" (in Russian), *Teor. Prakt. Metall.*, **4**, 72–84 (1936) (Experimental, Magn. Prop., Phase Diagram, Phase Relations, Morphology, 15)

[1939Bla] Blanchard, J.R., Parke, R.M., Herzig, A.J., "Constitution Diagrams for Iron-Carbon-Molybdenum Alloys", *Trans. ASM*, **27**, 697–718 (1939) (Experimental, Phase Diagram, Mechan. Prop., 13)

[1941Bla] Blanchard, J.R., Parke, R.M., Herzig, A.J., "The Effect of Molybdenum on the Isothermal, Subcritical Transformation of Austenite in Low and Medium Carbon Steels", *Trans. Am. Soc. Met.*, **29**, 317–335 (1941) (Experimental, Phase Relations, Morphology, 5)

[1943Smo] Smoluchowski, R., "Diffusion Rates of Carbon in Iron-Molybdenum and Iron-Tungsten Alloys", *Phys. Rev.*, **63**(11/12), 0438–0440 (1943) (Experimental, Phys. Prop., 7)

[1944Bow] Bowman, F.E., Parke, R.M., "The Partition of Molybdenum in Iron-Carbon-Molybdenum Alloys at 1300 Degrees Fahr. and the Nature of the Carbides Formed", *Trans. ASM*, **33**, 481–493 (1944) (Experimental, Crys. Structure, 16)

[1946Bow] Bowman, F.E., "Partition of Molybdenum in Hypoeutectoid Iron-Carbon-Molybdenum Alloys", *Trans. Am. Soc. Met.*, **36**, 61–80 (1946) (Experimental, Phase Relations, 10)

[1950Kra] Krainer, H., (in German), "X-Ray Study of Carbides in W-, Mo-, and V-Steels", *Arch. Eisenhuettenwes.*, **21**(1–2), 39–41 (1950) (Experimental, Crys. Structure, 6)

[1951Las] Lashko, N.F., Nesterova, M.D., "Stable and Metastable Phases in Middle Carbon Steels with Chromium and Molybdenum" (in Russian), *Izv. Akad. Nauk SSSR, Ser. Fiz.*, **15**(1), 67–71 (1951) (Experimental, Crys. Structure, Phase Relations, 0)

[1952Edw] Edwards, R., Raine, T., "The Solid Solubilities of Some Stable Carbides in Cobalt, Nickel and Iron at 1250°C", Pulvermetallurgie, 1. Plansee Seminar, De Re Metallica, 22–26 Juni, 1952, Reutte/Tirol, (Hrsg.) Benesovsky, F., Springer-Verlag, Wien, (1), 232–242 (1952) (Experimental, Phase Relations, Morphology, 5)

[1953Kuo1] Kuo, K., "Carbides in Chromium, Molybdenum, and Tungsten Steels", *J. Iron Steel Inst.*, **173**, 363–375 (1953) (Experimental, Crys. Structure, Phase Relations, 45)

[1953Kuo2] Kuo, K., "The Formation of η Carbides", *Acta Metall.*, **1**, 301–304 (1953) (Experimental, Crys. Structure, 20)

[1953Kuo3] Kuo, K., "X-Ray Investigation of Carbides in Molybdenum Steels" (in Swedish), *Jernkontorets Ann.*, **137**(5), 141–148 (1953) (Experimental, Crys. Structure, Phase Diagram, 17)

[1959Fuw] Fuwa, T., Chipman J., "Activity of Carbon in Liquid-Iron Alloys", *Trans. AIME*, **215**, 708 (1959) (Thermodyn., Experimental, Calculation, Phase Relations, 22)

[1959Neu] Neumann, F., Schenck, H., Patterson, W., "Iron-Carbon Alloys in Thermodynamic Consideration" (in German), *Giesserei Tech.-Wiss. Beih.*, **23**, 1217–1246 (1959) (Thermodyn., Experimental, Phase Relations, Theory, 72)

[1960Cam] Campbell, R.F., Reynolds, S.H., Ballard, L.W., Carroll, K.G., "Constitution of FeCMo Alloys Containig 0.05–1.3pct C and 0.03–6.0 pct Mo", *Trans. AIME*, **218**, 723–732 (1960) (Experimental, Phase Diagram, Crys. Structure, Mechan. Prop., 7)

DOI: 10.1007/978-3-540-74196-1_7

[1960Fuw] Fuwa, T., Fujikura, M., Matoba, S., "Effect of Elements on the Solubility of Graphite in Liquid Iron" (in Japanese), *Tetsu to Hagane (J. Iron Steel Inst. Jpn)*, **46**, 235–237 (1960) (Experimental, Phase Relations, Thermodyn., 8)

[1960Mor] Mori, T., Aketa, K., Ono, H., Sugita, H., "Effects of Molybdenum, Wolfram and Copper on Solubility of Graphite in Liquid Iron and the Method of Calculation for the Activity of Carbon in a Multicomponent Solution" (in Japanese), *Tetsu-to-Hagane (J. Iron Steel Inst. Jpn)*, **46**, 1429–1439 (1960) (Thermodyn., Experimental, Calculation, 24)

[1962Rid] Ridal, K.A., Quarrell, A.G., "The Molybdenum Carbide Transformation in Ferritic Steels", *J. Iron Stell Inst.*, **200**, 359–365 (1962) (Experimental, Phase Relations, 13)

[1962Sat] Sato, T., Nishizawa, T., Tamaki, K., "Carbides in Molybdenum Steels", *Trans. Jpn. Inst. Met.*, **3**, 196–202 (1962) (Phase Diagram, Experimental, Crys. Structure, Morphology, Magn. Prop., 10)

[1963Yag] Yagi, T., Ono, Y., "Effect of Mo, Ti and Zr on the Solubility of Carbon in Molten Iron" (in Japanese), *Tetsu-to-Hagane (J. Iron Steel Inst. Jpn.)*, **49**, 660–665 (1963) (Thermodyn., Experimental, Phase Relations, 23)

[1964Dys] Dyson, D.J., Andrews, K.W., "The Structure and Metallurgical Significance of the Iron-Molybdenum Carbide Fe_2MoC (MaCb)", *J. Iron Steel Inst., London*, **202**, 325–329 (1964) (Crys. Structure, Experimental,10)

[1966Ray1] Raynor, D., Whiteman, J.A., Honeycombe, R.W.K., "In-Situ Transformation of Fe_3C to Mo_2C in Iron-Molybdenum-Carbon Alloys", *J. Iron Steel Inst., London*, **204**, 1114–1116 (1966) (Experimental, Phase Relations, Morphology, 6)

[1966Ray2] Raynor, D., Whiteman, J.A., Honeycombe, R.W.K., "Precipitation of Molybdenum and Vanadium Carbides in High-Purity Iron Alloys", *J. Iron Steel Inst., London*, **204**, 349–354 (1966) (Experimental, Phase Relations, Mechan. Prop., 9)

[1967Rud] Rudy, E., Windisch, St., Stosick, A.J., Hoffman, J.R., "The Constitution of Binary Molybdenum-Carbon Alloys", *Trans. Met Soc. AIME*, **239**(8), 1247–1267 (Experimental, Phase Diagram, Crys. Structure, 38)

[1968Aro] Aronsson, B., Lundstroem, T., Engstroem, I., "Some Aspects of the Crystal Chemistry of Borides, Boro-Carbides and Silicides of the Transition Metals", *Anisotropy in Single-Crystal Refractory Compounds*, Vahldiek, F.W., Mersol, S.A., (Eds.), Proc. Int. Symp., Dayton, Ohio, June 13–15, 1967, Plenum Press, New York, **1**, 3–22 (1968) (Crys. Structure, Review, 19)

[1968Jel] Jellinghaus, W., "Powder-Metallurgical Contributions to the Ternary Systems Iron-Tungsten-Carbon and Iron-Molybdenum-Carbon" (in German), *Arch. Eisenhuettenwes.*, **39**(9), 705–718 (1968) (Phase Diagram, Experimental, Morphology, Magn. Prop., 15)

[1969Bun1] Bungardt, K., Schuermenn, E., Preisendanz, H., Schueler, P., Osing, H.-J., "Determinartion of the Solubility of C and of Phase Boundaries in the Fe-Mo-C System by Activity Measurements in the Temperature Region 1000–1100°C" (in German), *DEW Techn. Ber.*, **9**(4), 439–462 (1969) (Experimental, Thermodyn., Phase Diagram, Phase Relations, 65)

[1969Bun2] Bungardt, K., Preisendanz, H., Schueler, P., Osing, H.J., "Assay of Carbon Activity in Fe-Mo-C and Fe-Mo-Cr-C Systems at Temperatures Between 1000 and 1100°C Over a Gas Equilibrium" (in German), *Chemie - Ing. - Techn.*, **41**(20), 1136–1137 (1969) (Abstract, Thermodyn., 0)

[1969Fra] Fraker, A.C., Stadelmaier, H.H., "The η Carbides of Molybdenum-Iron, Molybdenum-Cobalt and Molybdenum-Nickel", *Trans. AIME*, **245**, 847–850 (1969) (Phase Diagram, Crys. Structure, Experimental, Morphology, 20)

[1970Ber] Berry, F.G., Honeycombe, R.W.K., "The Isothermal Decomposition of Austenite in Fe-Mo-C Alloys", *Metall. Trans.*, **1**(12), 3279–3286 (1970) (Experimental, Phase Relations, 14)

[1970Ett] Ettmayer, P., Suchentrunk, R., "About the Thermal Stability of Eta-Carbides" (in German), *Monatsh. Chem.*, **101**(4), 1098–1103 (1970) (Experimental, Crys. Structure, Phase Relations, 14)

DOI: 10.1007/978-3-540-74196-1_7

[1970Sav] Savitskii, E.M., Zakharov, A.M., Burkhanov, G.S., Kataev, R.S., "The Ternary System Molybdenum-Iron-Carbon" (in Russian), *Izv. VUZ. Tsvetn. Met.*, **13**(6), 113–115 (1970) (Experimental, Phase Diagram, Cry. Structure, Mechan Prop., 10)

[1970Suz] Suzuki, Y., Ban-ya, S., Fuwa, T., "Activity of Carbon and Oxygen in Liquid Iron Alloys" (in Japanese), *Tetsu-to-Hagane (J. Iron Steel Inst. Jpn)*, **56**(14), 23–32 (1970) (Experimental, Thermodyn., Calculation, 15)

[1970Zem] Zemskii, S.V., Gruzin, P.L., "Investigation of the Fe-C and Fe-C-M Systems by Raioisotope Methods" (in Russian), *Optimizatsiya Met. Protsesov*, Metallurgiya, Moscow, **4**, 54–64 (1970) (Experimental, Phase Diagram, Phase Relations, Mechan Prop., 18)

[1971Ber] Berry, F.G., Honeycombe, R.W.K., "Authors' Reply", *Metall. Trans.*, **2**(8), 2284–2284 (1971) (Review, Phase Relations, 8)

[1971Gre] Greenbank, J.C., "Carbon Solute Interactions in Fe-Cr-C, Fe-Mo-C and Fe-W-C Alloys", *J. Iron Steel Inst., London*, **209**, 986–990 (1971) (Experimental, Phase Relations, Thermodyn., #, 16)

[1971Kin] Kinsman, K.R., Eichen, E., Aaronson, H.I., "Electron Microprobe Study of the Carbon Content of Ferrite and Bainite in Fe-C-Mo and Fe-C-Cr Alloys", *Metall. Trans.*, **2**(1), 346–348 (1971) (Experimental, Morphology, Phase Relations, 26)

[1971Neh] Nehrenberg, A.E., "Discussion of the Isothermal Decomposition of Austenite in Fe-Mo-C Alloys", *Metall. Trans.*, **2**(8), 2283–2284 (1971) (Review, Phase Relations, 8)

[1972Foo] Foo, E-H., Lupis, C.H.P., "Activity of Carbon in Liquid Iron Alloys at 1550°C", *Metall. Trans*., **3**, 2125–2131 (1972) (Thermodyn., Experimental, Phase Relations, 18)

[1972Hof] Hoffmeister, H., "Microsegregations and Eutectic Carbide Precipitations in Iron-Carbon-Molybdenum Alloys" (in German), *Arch. Eisenhuettenwes.*, **43**(9), 689–692 (1972) (Experimental, Phase Relations, 9)

[1972Nis] Nishizawa, T., "Thermodynamic Study of the Fe-Mo-C System", *Scand. J. Metall.*, **1**, 41–48 (1972) (Phase Diagram, Phase Relations, Experimental, Thermodyn., Calculation, Morphology, #, 20)

[1972Pet] Petrova, E.F., Shvartsman, L.A., "Influence of Molybdenum on Thermodynamic Activity of Carbon in Solid Iron" (in Russian), *Dokl. Akad. Nauk SSSR*, **205**(6), 1404–1406 (1972) (Experimental, Thermodyn., 3)

[1972Sav] Savitskii, E.M., Zacharov, A.M., Burchanov G.S., Kataev, R.S.V., "Interaction of Molybdenum with the Fe-Group Elements and Carbon" (in Russian), *Metallovedenie Tsvet. Met. Splavov*, Nauka, Moscow, 17–22 (1972) (Experimental, Phase Diagram, Phase Relations, 14)

[1972Wad] Wada, T., Wada, H., Elliott, J.F., Chipman. J., "Activity of Carbon and Solubility of Carbides in the FCC Fe-Mo-C, Fe-Cr-C and Fe-V-C Alloys", *Metall. Trans.*, **3**(11), 2865–2872 (1972) (Experimental, Morphology, Phase Relations, #, 21)

[1973Rim] Rimkus, H.J., "Contribution to Thermodynamics of Carbon in Iron-Carbon, as well as in Iron Rich Ternary and Multicomponent Meltsn" (in German), Dissertation Uni. Clausthal, (1973) (Experimental, Thermodyn., 77)

[1973Wad] Wada, T., "C-Fe-Mo (Carbon-Iron-Molybdenum)", *Metals Handbook*, 8th Edition, Metals Park, Ohio, American Society for Metals, **8**, 409–411 (1973) (Review, Phase Diagram, Phase Relations, 21)

[1975Uhr] Uhrenius, B., Harvig, H., "A Thermodynamic Evaluation of Carbide Solubilities in the Fe-Mo-C, Fe-W-C and Fe-Mo-W-C Systems at 1000°C", *Met. Sci.*, **9**(2) 67–82 (1975) (Thermodyn., Phase Diagram, Phase Relations, Experimental, Calculation, 43)

[1976Lob1] Lobo, J.A., Geiger, G.H., "Thermodynamics and Solubility of Carbon in Ferrite and Ferritic Fe-Mo Alloys", *Metall. Mater. Trans. A*, **7A**, 1347–1357 (1976) (Thermodyn., Experimental, Calculation, 20)

[1976Lob2] Lobo, J.A., Geiger, G.H., "Thermodynamics of Carbon in Austenite and Fe-Mo Austenite", *Metall. Mater. Trans. A*, **7A**, 1359–1364 (1976) (Thermodyn., Experimental, Calculation, 19)

DOI: 10.1007/978-3-540-74196-1_7

[1976Niz] Nizhnikovskaya, P.E., Taran, Yu.N., Grishina, O.N., "Carbide Transformation in Fe-C-W and Fe-C-Mo Alloys" (in Russian), *Karbidy i Splavy Ikh Osn.*, IPM, Kiev, 76–80 (1976) (Experimental, Morphology, Phase Relations, Kinetics, 4)

[1976Sch] Schuster, J., Rudy, E., Nowotny, H., "The "MoC" - Phase with the WC-Structure", *Monatsh. Chem.*, **107**, 1167–1176 (1976) (Crys. Structure, Experimental, 20)

[1976Sna] Snagovskii, V.M., Pirogova, E.K., Snagovskii, L.M., Nizhnikovskaya, P.F., "Structure Formation during Eutectic Soidification of Fe-C-W and Fe-C-Mo Alloys" (in Russian), *Karbidy i Splavy ikh Osn.,* IPM, Kiev, 73–76 (1976) (Experimental, Morphology, Phase Relations, 16)

[1976Tar] Taran, Yu.N., Nesterenko, A.M., Vukelich, S.B., Novik, V.I., "Formation of Fe_3Mo_3C Crystals During Growth in a Melt" (in Russian), *Strukt. Mekh. Fazovikh Prevrashch. Met. Splavov*, Nauka, Moscow, 177–182 (1976) (Morphology, Experimental, Phase Relations, 15)

[1977Cha] Chatfield, C., Hillert, M., "A Thermodynamic Analysis of the Fe-Mo-C System Between 973 and 1273 K", *Calphad*, **1**(3), 201–223 (1977) (Thermodyn., Phase Diagram, Calculation, Experimental, 26)

[1977Fri] Fridberg, J., Hillert, M., "On the Eutectoid Transformation of δ-Ferrite in Fe-Mo-C Alloys", *Acta Metall.*, **25**(1), 19–24 (1977) (Phase Relations, Experimental, Transport Phenomena, Thermodyn., Calculation, 17)

[1977She] Shevchuk, L.A., Dudetskaya, L.R., Gurinovich, V.I., Tkacheva, V.A., "Phase Equilibria in Fe-C-Mo Alloys" (in Russian), *Vestsi Akad. Nauk BSSR, Fiz. Tekh.*, (2), 46–49 (1977) (Phase Diagram, Morphology, Experimental, 3)

[1977Tar] Taran, Yu.N., Nesterenko, A.M., "Structure of M_6C Carbide in Cast High-Speed Steels of the Fe-Mo-C System", *Met. Sci. Heat Treat.*, **19**(11–1), 970–973 (1977) (Experimental, Morphology, Interface Phenomena, 12)

[1977Uhr] Uhrenius, B., "Optimization of Parameters Describing the Interaction Between Carbon and Alloying Elements in Ternary Austenite", *Scand. J. Metall.*, **6**(2), 83–89 (1977) (Thermodyn., Calculation, 24)

[1978Kle] Kleykamp, H., "Thermodynamics of the Mo-Fe-C and W-Fe-C Systems", *Contemporary Inorg. Mater. 1978*, Proc. 3rd Germ.-Yugosl. Meet., Stuttgart, 27–31 (1978) (Thermodyn., Calculation, 12)

[1978Pur1] Purdy, G.R., "The Dynamic of Transformation Interfaces in Steels-I. The Ferrite-Austenite Interface in Fe-C-Mo Alloys", *Acta Metall.*, **26**(3), 477–486 (1978) (Experimental, Phase Relations, Interface Phenomena, Kinetics, 23)

[1978Pur2] Purdy, G.R., "The Dynamics of Transformation Interfaces in Steels -II. Transformations in Fe-C-Mo Alloys at Intermediate Temperatures", *Acta Metall.*, **26**(3), 487–498 (1978) (Experimental, Morphology, Phase Relations, Interface Phenomena, 24)

[1978Sar] Sare, I.R., Honeycombe, R.W.K., "Splat Cooling of Iron-Molybdenum-Carbon Alloys", *J. Mater. Sci.*, **13**(9), 1991–2002 (1978) (Phase Relations, Morphology, Experimental, 34)

[1979Kag] Kagawa, A., Okamoto, T., "Lattice Parameters of Cementite in Fe-C-X (X=Cr, Mn, Mo, and Ni) Alloys", *Trans. Jpn. Inst. Met.*, **20**(11), 659–666 (1979) (Crys. Structure, Experimental, Magn. Prop., 11)

[1979Woo] Woodyatt, L.R., Krauss, G., "Phase Equilibria in the Iron-Molybdenum-1 % Carbon System Between 1143 and 1253 K", *Metall. Mater. Trans. A*, **10A**(12), 1893–1900 (1979) (Phase Diagram, Phase Relations, Crys. Structure, Experimental, 20)

[1980Bra] Brandis, H., Preisendanz, H., Schueler, P., "Studies on the Effect of the Alloying Elements, Chromium, Molybdenum and Tungsten, on the Activity of Carbon in Fe-X-C Alloys from 900 to 1100°C" (in German), *Thyssen Edelstahl Technische Berichte*, **6**(2), 155–167 (1980) (Experimental, Thermodyn., Calculation, 28)

[1980Fer] Ferro, R., Marassa, R., III. Crystal Structure and Density Data, III-1. Alloys and Compounds other than Halides and Chalcogenides" in "Molybdenum, Phys.-Chem. Properties of its Compounds and Alloys", *Atomic Energy Rev.*, Spec. Issue N7 359–507 (1980) (Crys. Structure, Review, 961)

DOI: 10.1007/978-3-540-74196-1_7

[1980Iwa] Iwadachi, T., Inoue, A., Minemura, T., Masumoto, T., "Nonequilibrium Phases in Fe-X-C (X=Cr, Mo, W) Ternary Alloys Quenched Rapidly from Melts" (in Japanese), *Nihon-kinzoku-gakkai-shi*, **44**(3), 245–254 (1980) (Crys. Structure, Experimental, Morphology, Phase Relations, 30)

[1981Ino] Inoue, A., Iwadachi, T., Minemura, T., Masumoto, T., "Nonequilibrium Phases in Fe-X-C (X=Cr, Mo or W) Ternary Alloys Quenched Rapidly from Melts", *Trans. Jpn. Inst. Met.*, **22**(3), 197–209 (1981) (Crys. Structure, Experimental, Morphology, Phase Relations, Thermodyn., 31)

[1981She] Shevchuk, L.A., Dudetskaya, L.R., Tkacheva, V.A., "Investigation of Phase Equilibria in the Austenite Range of the Ternary Systems Fe-C-Mo and Fe-C-W", in "*Phase Equilibria in Metallic Alloys*", Nauka, Moscow, 225–229 (1981) (Experimental, Phase Diagram, Phase Relations, 3)

[1982Gui] Guillermet, A.F., "The Fe-Mo (Iron-Molybdenum) System", *Bull. Alloy Phase Diagrams*, **3**(3), 359–367 (1982) (Phase Diagram, Phase Relations, Crys. Structure, Thermodyn., Review, 40)

[1983Bus] Buschow, K.H.J., van Engen, P.G., Jongebreur, R., "Magneto-Optical Properties of Metallis Ferromagnetic Materials", *J. Magn. Magn. Mater.*, **38**, 1–22 (1983) (Magn. Prop., Optical Prop., Experimental, Crys. Structure, 23)

[1983Jan] Janas, M., Mamro, K., Jowsa, J., Ludwikowski, S., "Assessment of Ferrous Alloy Component Influence on Carbon Solubility" (in Polish), *Metal. Odlew.*, **9**(3), 213–228 (1983) (Phase Relations, Experimental, Thermodyn., Calculation, 28)

[1983Way] Wayne, S.F., Nowotny, H., "The Molybdenum Cementite $MoFe_2C$", *Rev. Chim. Miner.*, **20**(4–5), 528–532 (1983) (Crys. Structure, Experimental, #, 16)

[1984Wad] Wada, H., "Thermodynamics and Solubility of Carbides in the Ferretic Fe-Mo-C Alloys at 712°C", *J. Metals*, **36**(12), 46–46 (1984) (Abstract, Thermodyn., 1)

[1985Eno] Enomoto, M., Aaronson H.I., "Calculation of $\alpha+\gamma$ Phase Boundaries in Fe-C-X Systems from the Central Atoms Model", *Calphad*, **9**(1), 43–58 (1985) (Thermodyn., Calculation, 31)

[1985Gus] Gustafson, P., "A Thermodynamic Evaluation of the Iron-Carbon System", *Scand. J. Metall.*, **14**(5), 259–267 (1985) (Assessment, Thermodyn., Phase Diagram, Calculation, 66)

[1985Rap] Rapposch, M., Kostiner, E., Wayne, S.F., Nowotny, H., "The Crystal Structure of the Molybdenum Cementite $Mo_{12}Fe_{22}C_{10}$ (ξ-Phase)", *Monatsh. Chem.*, **116**(11), 1237–1245 (1985) (Crys. Structure, Experimental, Theory, #, 10)

[1985Riv] Rivlin, V.G., "Critical Review of Constitution of Carbon-Iron-Molybdenum System", *Int. Met. Rev.*, **30**(3), 109–124 (1985) (Review, Phase Diagram, Phase Relations, 54)

[1985Ver] Verzhbolovich, S.A., Kudryavtseva, Y.D., Singer, V.V., Radovskii, I.V., "Specific Electric Resistivity of Fe, Mo and Fe, C, Mo Melts" (in Russian), *Izv. Vyss. Uchebn. Zaved., Fiz.*, **28**(7), 115–116 (1985) (Experimental, Electr. Prop., 5)

[1986Rap] Rapposch, M., Kostiner, E., Wayne, S.F., Nowotny, H., "The Crystal Structure of the Molybdenum Cementite $Mo_{12}Fe_{22}C_{10}$ (ξ-Phase)" (in German), *Monatsh. Chemie*, **117**(1), 55 (1986) (Abstract, Crys. Structure, 0)

[1986Wad] Wada, H., "Thermodynamics of the Fe-Mo-C System at 985 K", *Metall. Mater. Trans. A*, **17A**(7–12), 391–398 (1986) (Thermodin., Experimental, Phase Relations, 22)

[1987Tsu] Tsubakino, H., Aaronson, H.I., "Ferrite and Carbide Morphologies in and below the "Bay Region" of an Fe-0.19%C-2.30%Mo Alloy", *Metall. Trans. A*, **18**(12), 2047–2060 (1987) (Phase Relations, Experimental, Morphology, Interface Phenomena, Kinetics, 49)

[1988And1] Andersson, J.-O., "A Thermodynamic Evaluation of the Fe-Mo-C System", *Calphad*, **12**(1), 9–23 (1988) (Thermodyn., Phase Diagram, Phase Relations, Calculation, #, 45)

[1988And2] Andersson, J.-O., "Thermodynamic Properties of Mo–C", *Calphad*, **12**(1), 1–8 (1988) (Thermodyn., Calculation, 29)

[1988Ray] Raynor, G.V., Rivlin, V.G., "C-Fe-Mo", in "*Phase Equilibria in Iron Ternary Alloys*", Inst. Met., London, **4**, 177–191 (1988) (Phase Diagram, Phase Relations, Review, 31)

DOI: 10.1007/978-3-540-74196-1_7

[1988Vel] Velikanova, T.Ya., Kublii, V.Z., Khaenko, B.V., "Solid State Transformation and Phase Equilibria in the Molybdenum-Carbon System" (in Russian), *Powder Metall.*, **11**, 61–67 (1988) (Crys. Structure, Experimental, Phase Diagram, #, 11)

[1990Ere] Eremenko, V.N., Velikanova, T.Ya., Kharykova, A.M., Velikanova, T.A., "Metallid Based Interstitial Phases in Ternary Systems of Containing Transition Metals and Carbon" (in Russian), *Ukr. Khim. Zhur.*, **56**(4), 356–363 (1990) (Experimental, Crys. Structure, Theory, 11)

[1990Ips] Ipser, H., Schuster, J.C., Nowotny, H., "The Iron-Rich Corner of the Ternary System Fe-Mo-C", *Thermochim. Acta*, **160**, 93–96 (1990) (Experimental, Phase Diagram, Phase Relations, 18)

[1990Rey] Reynolds, W.T., Li, Jr., Li, F.Z., Shui, C.K., Aaronson, H.I., "The Incomplete Transformation Phenomenon in Fe-C-Mo Alloys", *Metall. Trans. A*, **21**(6), 1433–1463 (1990) (Experimental, Phase Relations, Kinetics, Morphology, 101)

[1990Shi] Shiflet, G.J., Aaronson, H.I., "Growth and Overall Transformation Kinetics above the Bay Temperature in Fe-C-Mo Alloys", *Metall. Trans. A*, **21**(6), 1413–1432 (1990) (Experimental, Phase Relations, Kinetics, Morphology, 102)

[1991Kha] Khaenko, B.V., Golub, C.Ya., Velikanova, T.A., Artyukh, L.V., "Investigation of the Phase Constitution in the Fe-Mo-C and Fe-Mo-Cr-C Alloy Systems in Regions of the Assumed Existence of λ and π Phases" (in Russian), *Diagramy Sostoyaniya v Materialoved.*, Nauch. Sov. Akad. Nauk Ukr. SSR po Probl. "Khim. Thermodyn. Term. Anal.", Akad. Nauk Ukr. SSR., IPM, Kiev, 143–146 (1991) (Crys. Structure, Experimental, Phase Diagram, Phase Relations, 7)

[1991Sch] Schuster, J.C., Nowotny, H., Ipser, H., Gupta, H., "The Construction of the Ternary System Iron-Molybdenum-Carbon", *Z. Metallkd.*, **82**(7), 539–543 (1991) (Crys. Structure, Experimental, Phase Diagram, Phase Relations, 23)

[1991Uem] Uemori, R., Tanino, M., "AP-FIM Study of Ultra-Fine Precipitates at the Peak Hardening Stage in a Tempered Fe-Mo-C Alloy" (in Japanese), *J. Jpn. Inst. Met.*, **55**(2), 141–150 (1991) (Experimental, Phase Relations, Morphology, 23)

[1991Wis] Wisell, H., "An Experimental Study of Carbide/Austenite Equilibria in the High-Speed Steel Alloy System", *Metall. Trans. A*, **22**(6), 1391–1405 (1991) (Experimental, Crys. Structure, Morphology, 6)

[1992Cha] Changqing, X., Zhanpeng, J., "Evolution of Microstructure and Diffusion Parts in the Molybdenum-Steel Explosion Weld Interface during Heat Treatment", *Mater. Sci. Eng. A*, **158**(2), 235–239 (1992) (Experimental, Phase Diagram, Phase Relations, Thermodyn., Morphology, 7)

[1992Oka] Okamoto, H., "The C-Fe (Carbon-Iron) System", *J. Phase Equilib.*, **13**(5), 543–565 (Phase Diagram, Phase Relations, Crys. Structure, Thermodyn., Assessment, 242)

[1993Kha] Khayenko, B.V., Golub, S.Ya., Velikanova, T.A., Kuprin, V.V., "Formation of Phases with α-Mn and β-Mn Structures in Iron-based Alloys", *Phys. Met. Metallogr. (Engl. Transl.)*, **75**(1), 86–91 (1993) (Experimental, Crys. Structure, Phase Diagram, Phase Relations, 14)

[1994Din] Din, S.-U., Ikram, N., Suleman, M., "Auger Electron Spectroscopy Study of the Microstructure of Hot Rolled Molybdenum and Vanadium Microalloyed Low Carbon Steels", *J. Mater. Sci. Lett.*, **13**(14), 1004–1006 (1994) (Experimental, Morpology, 15)

[1994Gau] Gauzzi, F., Principi, G., Hu, W.X., "Structural Analysis of Electron Beam Irradiated Steel/Molybdenum Systems", *Hyperfine Interact.*, **92**(1–4), 975–979 (1994) (Experimental, 6)

[1994Omu] Omuro, K., Miura, H., Ogawa, H., "Amorphization in Iron-Carbon Systems with Transition Metals by Mechanical Alloying", *Mater. Sci. Eng. A*, **182**, 1281–1284 (1994) (Experimental, Electr. Prop., 13)

[1994Rag] Raghavan V., "The C-Fe-Mo System", *J. Phase Equilib.*, **15**(4), 425–427 (1994) (Phase Diagram, Phase Relations, Review, 11)

DOI: 10.1007/978-3-540-74196-1_7

[1994Sch] Schuster, J.C., Giron, G., Durand-Charre, M., "On The Liquidus Surface Involving γ-Iron in the System Fe-Mo-C", *Exp. Methods Phase Diagram Determ., Proc. Symp.,* 1993, 133–140 (1994) (Experimental, Phase Diagram, Phase Relations, Morphology, 9)

[1995Dan] Danilenko, V.M., Rubaschevskii, A.A., Velikanova, T.A., "Computer Calculation of Liquidus of Mo-Fe-C Phase Diagram" (in Russian), *Achivements in the Field of the Physical Material Science.*, Akad. Nauk. SSR., IPM, Kiev, 110–126 (1995) (Thermodyn., Phase Diagram, Phase Relations, 16)

[1995Di] Di, L.M., Calka, A., Li, Z.L., Williams, J.S., "The Formation of Ternary Compound Fe_3Mo_3C by Ball Milling", *J. Appl. Phys.*, **78**(6), 4118–4122 (1995) (Experimental, Crys. Structure, 17)

[1995Gir] Giron, G., Durand-Charre, M., "High Temperature Phase Equilibria in the System Fe-Mo-C", *Z. Metallkd.*, **86**(1), 15–21 (1995) (Phase Diagram, Morphology, Crys. Structure, Experimental, Phase Relations, #, 14)

[1995Pop1] Popov, V.V., "Determining Interdiffusion Coefficient for Metal Elements in Austenite and Ferrite of Fe-Cr-C, Fe-Mo-C, and Fe-W-C Systems", *Phys. Met. Metallogr. (Engl. Transl.)*, **79**(4), 418–424 (1995) (Experimental, Morphology, Phase Relations, 23)

[1995Pop2] Popov, V.V., "Determination of Mutual Diffusion-coefficients of Metallic Elements in Austenite and Ferrite of Fe-Cr-C, Fe-Mo-C and Fe-W-C Systems" (in Russian), *Fiz. Met. Metalloved.*, **79**(4), 94–103 (1995) (Experimental, Transport Phenomena, 23)

[1996Cha] Chaix, J.-M., Yang, P.H., Ardin, M., Durand-Charre, M., "Image Analysis of Austenite and Carbides Coarsening in a Fe-Mo-C Steel", *Microscopy Microanalysis Microstructures*, **7**(5–6), 387–392 (1996) (Experimental, Morphology, 9)

[1996Fom] Fomichov, A.S., Karpets, M.V., Velikanova, T.A., Khaenko, B.V., "Metastable Phase Formation During Ultrarapid Crystallization from the Melts of High-Speed Steels and Fe-Mo-C Alloys", 5th International School "*Phase Diagrams in Materials Science*", Katsyvely, Crimea, Ukraine, September 23–29 Abstracts, 45–46 (1996) (Abstract, Crys. Structure, 0)

[1996Kuh] Kuhrt, C., "Magnetic Properties of Nanocrystalline Mechanically Alloyed Fe-TM-C Powder (TM=Ta, Hf, W, Mo, Nb, Zr, and Ti)", *J. Magn. Magn. Mater.*, **158**, 235–236 (1996) (Magn. Prop., Experimental, Morphology, 6)

[1997Liu] Liu, Z.-K., "The Transformation Phenomenon in Fe-Mo-C Alloys: A Solute Drag Approach", *Metall. Mater. Trans. A*, **28**(8), 1625–1631 (1997) (Calculation, Phase Relations, 26)

[1997Men] Menon, E.S.K., Fox, A.G., Reynolds, W.T., Spanos, Jr., "Peels of Steels", *Inst. Phys. Conf. Ser.*, **153**(8), 315–318 (1997) (Experimental, Interface Phenomena, 13)

[1997Sht1] Shtansky, D.V., Inden, G., "Phase Transformation in Fe-Mo-C and Fe-W-C Steels-II. Eutectoid Reaction of $M_{23}C_6$ Carbide Decomposition During Austenitization", *Acta Mater.*, **45**(7), 2879–2895 (1997) (Calculation, Crys. Structure, Experimental, Phase Diagram, Phase Relations, Thermodyn., 26)

[1997Sht2] Shtansky, D.V., Inden, G., "Phase Transformation in Fe-Mo-C and Fe-W-C Steels-I. The Structural Evolution During Tempering at 700°C", *Acta Mater.*, **45**(7), 2861–2878 (1997) (Crys. Structure, Experimental, Phase Relations, 47)

[1999Can] Candela, N., Velasco, F., Torralba, J.M., "Fracture Mechanisms in Sintered Steels with 3.5 (mass%) Mo", *Mater. Sci. Eng. A*, **259**(1), 98–104 (1999) (Mechan. Prop., Phys. Prop., Experimental, Morphology, 11)

[1999Pop] Popov, V.V., "Diffusion Interaction of Carbides, Nitrides and Carbonitrides with Iron and Steels", *Metallofizika Nov. Tekhnol.*, **21**(2), 99–103 (1999) (Experimental, Phase Relations, Transport Phenomena, 11)

[1999Wri] Wright, C.S., Youseffi, M., Wronski, A.S., Ansara, I., Durand-Charre, M., Mascarenhas, J., Oliveira, M.M., Lemoisson, F., Bienvenu, Y., "Supersolidus Liquid Phase Sintering of High Speed Steels. Part 3: Computer Aided Desing of Sinterable Alloys", *Powder Met.*, **42**(2), 131–146 (1999) (Calculation, Experimental, Phase Relations, Thermodyn., 32)

DOI: 10.1007/978-3-540-74196-1_7

[2000Abe] Abe, T., Onodera, H., Kimura, K., Kushima, H., "Effect of M-C (M=Mo, Mn,and Cr) Atomic Pairs on Creep Properties of Fe-M-C Ternary Alloys", *Key Eng. Mater.*, **171–174**, 461–468 (2000) (Experimental, Mechan. Prop., 24)

[2000You] Youseffi, M., Wright, C.S., Jeyacheya, F.M., "Effect of Carbon Content, Sintering Temperature, Density, and Cooling Rate Upon Properties of Prealloyed Fe-1.5Mo Powder", *Powder Met.*, **43**(3), 270–274 (2000) (Experimental, Morphology, Mechan. Prop., Phys. Prop., 9)

[2001Aar] Aaronson, H.I., Purdy, G.R., Malakhov, D.V., Reynolds, W.T., "Tests of the Zener Theory of the Incomplete Transformation Phenomenon in Fe-C-Mo and Related Alloys", *Scr. Mater.*, **44**, 2425–2430 (2001) (Theory, 24)

[2001Fle] Fletcher, H.A., Garratt-Reed, A.J., Aaronson, H.I., Purdy, G.R., Reynolds, W.T., Smith, G.D.W., "A STEM Method for Investigating Alloying Element Accumulation at Austenite-Ferrite Boundaries in an Fe-C-Mo Alloy", *Scr. Mater.*, **45**(5), 561–567 (2001) (Experimental, Interface Phenomena, Morphology, 25)

[2001Hil] Hildebrand, H., Hildebrand, M., "Microstructural Influences on Young's Modulus for Fe-V-C and Fe-Mo-C Alloys", *Materialwiss. Werkst*., **32**(9), 701–711 (2001) (Phys. Prop., Morphology, Experimental, Transport Phenomena, 40)

[2001Kal] Kalinushkin, E.P., Sitalo, Yu.A., "Fe-based Alloys and Other Techniques", *Metallofizika Nov. Tekhnol.*, **23** 235–241 (2001) (SI), (Morphology, Experimental, Interface Phenomena, 4)

[2001Mar] Marsh, P., Wood, J.V., Moon, J.R., "Diffusion between High Speed Steel and Iron Powders", *Powder Met.*, **44**(3), 205–210 (2001) (Experimental, Kinetics, Phase Relations, Transport Phenomena, Thermodyn., 4)

[2001Tsu] Tsuchida, T., "Formation of Ternary Carbide Fe_3Mo_3C by Mechanical Activation and Subsequent Heat Treatment", *J. Mater. Sci.*, **36**, 1735–1740 (2001) (Crys. Structure, Experimental, Magn. Prop., 12)

[2001Ume] Umemoto, M., Liu, Z.G., Masuyama, K., Tsuchiya, K., "Influence of Alloy Additions on Production and Properties of Bulk Cementite", *Scr. Mater.*, **45**(4), 391–397 (2001) (Crys. Structure, Experimental, Mechan. Prop., Phase Relations, Phys. Prop., 13)

[2001Zhu] Zhu, J.J., Jiang, J., Jacobsen, C.J.H., Lin, X.P., "Preparation of Fe-Mo-C Ternary Carbide by Mechanical Alloying", *J. Mater. Chem.*, **11**, 864–868 (2001) (Crys. Structure, Experimental, Magn. Prop., Phase Relations, 31)

[2002Mus] Muscalu, M., Fatu, D., "Physico-Chemical Study of High Speed Steel Structural Components", *Int. J. Mater. Prod. Technol.*, **17**(7), 557–567 (2002) (Experimental, Morphology, Mechan. Prop., 8)

[2002Rag] Raghavan, V., "C-Fe-Mo (Carbon-Iron-Molybdenum)", *J. Phase Equilib.*, **23**(6), 515–516 (2002) (Phase Diagram, Phase Relations, Review, 10)

[2002Shi] Shi, Y.-N., Kelly, P.-M., "The Crystallography and Morphology of Mo_2C in Ferrite", *J. Mater. Sci.*, **37**(10), 2077–2085 (2002) (Crys. Structure, Morphology, Experimental, Calculation, 16)

[2002Sim] Simchi, A., Danninger, H., "Microstructural Changes in Mo Steels During Sintering and Effect on Electrical Conductivity", *Powder Met.*, **45**(4), 307–314 (2002) (Morphology, Electr. Prop., Experimental, 25)

[2002Wu] Wu, K.M., Enomoto, M., "Thee-Dimensional Morphology of Degenerate Ferrite in an Fe-C-Mo Alloy", *Scr. Mater.*, **46**(8), 569–574 (2002) (Experimental, Kinetics, Morphology, Phase Relations, 29)

[2003Eno] Enomoto, M., Maruyama, N., Wu, K.M., Tarui, T., "Alloying Element Accumulation at Ferrite/Austenite Boundaries Below the Time-Temperature-Transformation Diagram Bay in an Fe-C-Mo Alloy", *Mater. Sci. Eng. A*, **343**, 151–157 (2003) (Calculation, Experimental, Kinetics, Phase Diagram, Phase Relations, 27)

[2003Hac1] Hackenberg, R.E., Shiflet, G.J., "A Microanalysis Study of the Bainite Reaction at the Bay in Fe-C-Mo", *Acta Mater.*, **51**(8), 2131–2147 (2003) (Experimental, Kinetics, Phase Relations, Thermodyn., Morphology, 67)

DOI: 10.1007/978-3-540-74196-1_7

[2003Hac2] Hackenberg, R.E., Shiflet, G.J., "The Influence of Morphology on Grain-Boundary and Twin-Boundary Bainite Growth Kinetics at the Bay in Fe-C-Mo", *Philos. Mag.*, **83**(29), 3367–3385 (2003) (Experimental, Interface Phenomena, Morphology, 35)

[2003Kud] Kudoh, M., Wo, B., "Effects of Solute Elements on Primary and Secondary Dendrite Arm Spacings in Fe-based Alloys", *Steel Res.*, **74**(3), 161–167 (2003) (Calculation, Experimental, Phase Relations, 14)

[2003Wu] Wu, K.M., Kagayama, M., Enomoto, M., "Kinetics of Ferrite Transformation in an Fe-0.28mass%C-3mass%Mo Alloy", *Mater. Sci. Eng. A*, **343**(1–2), 143–150 (2003) (Calculation, Experimental, Kinetics, Morphology, Phase Diagram, Phase Relations, Thermodyn., 37)

[2003Yam] Yamasaki, S., Bhadeshia, H.K.D.H., "Modelling and Characterisation of Mo_2C Precipitation and Cementite Dissolution during Tempering of Fe-C-Mo Martensitic Steel", *Mater. Sci. Technol.*, **19**(6), 723–731 (2003) (Morphology, Phase Relations, Experimental, Calculation, 27)

[2004Aar] Aaronson, H.I., Reynolds, W.T., Purdy, G.R., "Coupled-Solute Drag Effect on Ferrite Formation in Fe-C-X Systems", *Metall. Mater. Trans. A*, **35a**(4), 1187–1210 (2004) (Experimental, Interface Phenomena, Kinetics, Morphology, Phase Relations, 148)

[2004Hou] Houze, M., Kleber, X., Fouquet, F., Delnondedieu, M., "Study of Molybdenum Precipitation in Steels Using Thermoelectric Power Measurement", *Scr. Mater.*, **51**(12), 1171–1176 (2004) (Experimental, Electr. Prop., 14)

[2004Hum] Humphreys, E.S., Fletcher, H.A., Hutchins, J.D., Garrat-Reed, A.J., Reynolds, W.T., Aaronson, H.I., Purdy, G.R., Smith, G.D.W., "Molybdenum Accumalation at Ferrite: Austenite Interfaces During Isothermal Transformation of an Fe-0.24 % C-0.93 % Mo Alloy", *Metall. Mater. Trans. A*, **35A**(4), 1223–1235 (2004) (Phase Relations, Morphology, Kinetics, Experimental, 59)

[2004Tak] Takahashi, M., "Recent Progress: Kinetics of the Bainite Transformation in Steels", *Curr. Opin. Solid State Mater. Sci.*, **8**(3–4), 213–217 (2004) (Phase Relations, Kinetics, Calculation, 45)

[2005Can] Candela, N., Velasco, F., Martinez, M.A., Torralba, J.M., "Influence of Microstructure on Mechanical Properties of Molybdenium Alloyed P/M Steels", *J. Mat. Proc. Tech.*, **168**(3), 505–510 (2005) (Mechan. Prop., Experimental, 16)

[2006MSIT] "C-Fe (Carbon - Iron)", *Diagrams as Published* in MSIT Workplace, Effenberg, G. (Ed.), MSI, Materials Science International Services GmbH, Stuttgart; Document ID: 30.13598.1.20, (2006) (Phase Diagram, Phase Relations, Crys. Structure, 2)

[Mas] Massalski, T.B. (Ed.), *Binary Alloy Phase Diagrams*, ASM, Metals Park, Ohio (1986)

[Mas2] Massalski, T.B. (Ed.), *Binary Alloy Phase Diagrams*, 2nd edition, ASM International, Metals Park, Ohio (1990)

[V-C2] Villars, P. and Calvert, L.D., *Pearson's Handbook of Crystallographic Data for Intermetallic Phases*, 2nd edition, ASM, Metals Park, Ohio (1991)

DOI: 10.1007/978-3-540-74196-1_7

Carbon – Iron – Nitrogen

K.C. Hari Kumar

Introduction

Phase equilibria in C-Fe-N system is of fundamental interest to the development of technology related to nitriding, nitrocarburizing, and manufacturing of steels. Most of the investigations reported in the literature are concerned with experiments conducted in iron rich alloys under conditions suitable for nitriding and nitrocarburizing. Those studies in general represent metastable conditions, where graphite phase is not observed.

A critical review of the system was reported by [1984Rag], with an update by [1993Rag].

[1930Koe] reported an isothermal section at 100°C, showing a three-phase field comprising of cementite (θ), (αFe) and Fe_4N (γ′). A detailed study of lattice parameters of carbonitrides and phase relationships in the system at 450°C was presented by [1948Jac]. Using thermo-magnetic measurement [1951Pom] established that the eutectoid transformation temperature of (γFe) containing 0.9 mass% C and 0.56-1.25 mass% N is between 595 to 600°C. Details of lattice parameters and Curie temperatures of various carbonitrides were reported by [1954Bri1, 1954Bri2, 1955Bri].

[1962Sch] presented isothermal sections at 600, 650, and 700°C. Most comprehensive study of the system was undertaken by [1965Nau1, 1965Nau2], who investigated the phase relationships in the system from 500 to 700°C, using XRD of specimens obtained by nitriding mixtures of iron powder and graphite. At 500°C the isothermal section indicated two three-phase fields very close to each other, *viz*. θ+(αFe)+γ′ and γ′+ε+θ, thus establishing the presence of a narrow γ′+θ two-phase field. In the 550°C isothermal section these phase fields are still present, but closer than at 500°C, indicating one is approaching the invariant reaction (αFe) + ε ⇌ γ′ + θ. At 580°C four specimens were reported to contain (αFe)+ε+θ, meaning the four-phase reaction has passed. However, this reaction was not accounted for by [1965Nau2] since one specimen at 580°C reported to have (γFe), thereby proposing the eutectoid reaction (γFe) ⇌ (αFe) + γ′ + θ at 565°C. Data of [1965Nau2] also indicated that χ phase replaced the θ phase in equilibrium with ε phase at high nitrogen and carbon content in the ε phase.

[1983Wel, 1985Wel] reported concentration depth profile of nitrogen and carbon in their nitrocarburized iron samples at 580°C. Their study showed that the compound layers after nitrocarburizing contain ε, γ′, and θ. Most significantly, they have found single ε phase to be present in two phase region (ε+γ′) proposed by [1965Nau2]. They also reported two data points representing (αFe)+ε/ε phase boundary. These were further confirmed by [1987Som, 1990Som]. It should be noted that these studies do not indicate presence of any (γFe) at 580°C or below. A supporting evidence for the presence of (γFe) at about 580°C and the eutectoid reaction (γFe) ⇌ (αFe) + γ′ + θ is due to [1994Rus], who performed XRD of powdered samples between 550-650°C.

Solubility of nitrogen in C-Fe melts was studied by several investigators [1941Koo, 1950Sai, 1959Sch, 1960Mae, 1968Gom, 1969Opr, 1977Pom, 1982Ish, 1999Svy]. Experimental data indicate that carbon increases the activity of nitrogen in the melt and reduces the amount of nitrogen that dissolves for a given nitrogen gas pressure. Most of these investigations are up to a pressure of 101325 Pa and confirm that nitrogen solubility follows Siverts' law.

A concise summary of various experimental investigations is listed in Table 1.

Binary Systems

The binary systems accepted in the present evaluations are: C-Fe [2006MSIT] and Fe-N [1993Du].

DOI: 10.1007/978-3-540-74196-1_8

Solid Phases

No ternary compounds are known to exist in this system. [1948Jac] indicated that there is considerable solubility for carbon in Fe_2N (ξ) and Fe_3N_{1+x} (ε) nitrides, but there is only negligible solubility for nitrogen in θ and in the Hägg carbide (χ). According to [1948Jac] nearly two-thirds of nitrogen atoms can be replaced by carbon at 450°C. With increase in temperature the carbon solubility in nitrides decreases [1965Nau2]. According to [1987Som] the solubility of nitrogen in cementite in equilibrium with ε phase is about 0.3 mass% at 570°C.
[1983Bur] established that lattice parameters of ε carbonitride varies linearly with (C+N) content, whereas [1990Che] reported that lattice parameter of (γFe) has a non-linear dependence on the interstitial atom content. [2001Lei] reported that ε-$Fe_3(C_{0.8},N_{0.2})_{1.38}$ exhibits an $P\bar{3}1m$ type ordering. This type of ordering was not observed in the case of binary ε nitride. Details of crystallographic data of solid phases of the system are given in Table 2.

Invariant Equilibria

There are no accurate measurements of coordinates of the invariant reactions reported in the literature. Information is available concerning invariant reactions relevant to the nitrocarburizing process, occurring close to the Fe rich side, by means of calculations performed using Gibbs energy functions. There are four such invariant reactions. Their coordinates obtained by calculations performed using Gibbs energy functions reported by [1993Du] are listed in Table 3. Figure 1 is the corresponding reaction scheme. Note that the eutectoid reaction at 565°C (γFe) ⇌ (αFe)+γ′+θ proposed by [1965Nau2, 1994Rus] is not included in the current scheme since majority of the experimental data up to 580°C do not indicate presence of (γFe).

Isothermal Sections

Figures 2 to 7 are partial isothermal sections corresponding to 700, 600, 590, 580, 550, and 500°C, respectively. These are calculated using the Gibbs energy functions reported by [1993Du]. They can be considered as the best representation of experimental data discussed in the section "Introduction". Most notable feature of these diagrams is that (γFe) is present only in sections above 586°C, the temperature of the eutectoid (γFe) ⇌ ε + γ′ + (αFe). This agrees with most of the nitrocarburizing data. Note also that ((αFe)+ε) phase-field is present in sections close to 580°C, the most common nitrocarburizing temperature.

Temperature – Composition Sections

A vertical section for the system at 0.5 mass% C is presented in Fig. 8. Again, this is calculated using the thermodynamic functions reported by [1993Du].

Thermodynamics

Following equilibrium constant (K_N) and interaction parameters (e_N^C, r_N^C) are recommend for solubility of nitrogen in iron-carbon melts [1999Svy]:

$$\log K_N = -850/T - 0.905$$
$$e_N^C = 100/T + 0.045$$
$$r_N^C = 90/T - 0.036$$

These expressions are valid for the temperature range 1250 to 2300°C.
Gibbs energy modelling of the phases in the system was attempted by [1987Xu], [1988Sly], [1991Du], and [1993Du]. Amongst various sets of thermodynamic functions reported, the one by [1993Du] is the most reliable and it is accepted here for generating phase equilibria information.

Notes on Materials Properties and Application

The phase equilibria in this system between 550°C and 600°C are of relevance to nitrocarburizing of steels. From the point of tribological performance, it is desirable to have a layer of ε carbonitride as the outermost

DOI: 10.1007/978-3-540-74196-1_8

layer of the carbonitrided steel. Information such as the solubility of nitrogen in melts under varying nitrogen pressures are of great value in steelmaking operations such as degassing.

Miscellaneous

Figure 9 is the calculated nitrogen solubility in C-Fe melts from 1450 to 1750°C under a N_2 pressure of 101325 Pa, which is the best representation of the experimental data.

Table 1. Investigations of the C-Fe-N Phase Relations, Structures and Thermodynamics

Reference	Method/Experimental Technique	Temperature/Composition/Phase Range Studied
[1930Koe]	Magnetic flux density measurements	100°C, < 0.04 mass% C, < 0.085 mass% N
[1941Koo]	Gas equilibration	Solubility of N in liquid
[1948Jac]	Chemical analysis, XRD	450°C, ξ, χ, ε
[1950Sai]	Gas equilibration	Solubility of N in liquid
[1951Pom]	Thermo-magnetic measurements	< 700°C, < 0.9 mass% C, < 1.25 mass% N
[1954Bri1]	XRD, Curie temperature measurements	< 600°C, ε, ξ, γ′, χ
[1954Bri2]	XRD, Curie temperature measurements	< 600°C, ε
[1955Bri]	XRD, Curie temperature measurements	< 600°C, ε, ξ, γ′, χ
[1959Sch]	Gas equilibration	1600°C, solubility of N in liquid
[1962Sch]	XRD, metallography	600-850°C, <1.4 mass% C, < 2.4 mass% N
[1960Mae]	Gas equilibration	Solubility of N in liquid
[1965Nau1]	XRD, metallography	500-850°C, < 8 mass% C, < 11 mass% N
[1965Nau2]	XRD, metallography	500-700°C, < 8 mass% C, < 11 mass% N
[1968Gom]	Gas equilibration	1450-1750°C, < 5 mass% C Solubility of N in liquid
[1969Opr]	Gas equilibration	Solubility of N in liquid
[1977Pom]	Gas equilibration	Solubility of N in liquid, 1600-2100°C
[1982Ish]	Gas equilibration	Solubility of N in liquid 1540-1630°C, < 4 mass% C
[1983Bur]	XRD	ε

(*continued*)

DOI: 10.1007/978-3-540-74196-1_8

Reference	Method/Experimental Technique	Temperature/Composition/Phase Range Studied
[1983Wel]	Chemical analysis, metallography, XRD	580°C, (αFe), ε, γ′, θ
[1985Wel]	Chemical analysis, metallography, XRD	580°C, (αFe), ε, γ′
[1987Som]	EPMA, XRD	570°C, (αFe), ε, γ′, θ
[1990Che]	XRD	780°C, < 0.55 mass% C, < 1.7 mass% N
[1990Som]	Metallography, XRD, SEM, EPMA	570°C, (αFe), ε, γ′, θ
[1994Rus]	Thermal analysis, XRD	550-700°C, < 0.46 mass% C, <3.9 mass% N
[1995Jac]	XRD, Neutron diffraction	γ′, ε
[1999Svy]	Gas equilibration	Solubility of N in liquid
[2001Lei]	Neutron diffraction, Magnetization	ε ($Fe_3(N_{0.80}C_{0.20})_{1.38}$)

Table 2. Crystallographic Data of Solid Phases

Phase/Temperature Range [°C]	Pearson Symbol/ Space Group/ Prototype	Lattice Parameters [pm]	Comments/References
(γFe) 1394 - 912	*cF*4 $Fm\bar{3}m$ Cu	a = 364.67	at 915°C [V-C2, Mas2]
		a = 361.87	[1990Che], 780°C 0.2 mass% C, 1.7 mass% N
(αFe) < 912	*cI*2 $Im\bar{3}m$ W	a = 286.65	at 25°C [Mas2]
γ', Fe_4N < 680	*cP*5 $Pm\bar{3}m$ Fe_4N	a = 379.00	19.3 - 20.0 at.% N [1995Jac], 5 mass% Ni
ε, Fe_3N_{1+x} < 1310	*hP*10 $P6_322$ Fe_3N	a = 469.38 c = 437.48	$-0.471 < x < 0.478$ [1999Lei], for Fe_3N Lattice parameters decrease slightly with decrease in nitrogen content [1948Jac, 2001Lei]
		a = 477.70 c = 440.70	[2001Lei] $Fe_3(C_{0.2},N_{0.8})_{1.38}$

(*continued*)

DOI: 10.1007/978-3-540-74196-1_8

Phase/Temperature Range [°C]	Pearson Symbol/ Space Group/ Prototype	Lattice Parameters [pm]	Comments/References
ξ, Fe_2N	*oP*12 *Pbcn* $Fe_2N_{0.94}$	 *a* = 554.13 *b* = 484.29 *c* = 443.73	33.2 - 33.7 at.% N [1996Rec]
		a = 549.0 *b* = 484.1 *c* = 437.4	[1948Jac], 450°C at.% C = 23.8, at.% N = 10.8
θ, Fe_3C (cementite)	*oP*16 *Pnma* Fe_3C	*a* = 507.87 *b* = 672.97 *c* = 451.44	[V-C2] metastable
χ, Fe_5C_2, (Hägg carbide)	*mC*28 *C*2/*c* Mn_5C_2	*a* = 1156.2 *b* = 457.27 *c* = 505.95 β = 97.74°	[V-C2] metastable

Table 3. Invariant Equilibria

Reaction	*T* [°C]	Type	Phase	Composition (at.%)		
				C	Fe	N
θ + (γFe) ⇌ (αFe) + ε	594	U_1	θ	24.0	75.0	1.00
			(γFe)	1.60	91.1	7.30
			(αFe)	8.10	83.7	8.20
			ε	3.60	79.8	16.6
(γFe) ⇌ ε + γ′ + (αFe)	586	E_1	(γFe)	0.50	90.8	8.70
			ε	2.00	81.2	16.8
			γ′	0.50	80.7	18.8
			(αFe)	~0.0	99.6	0.40
(αFe) + ε ⇌ γ′ + 2	509	U_2	(αFe)	~0.0	99.8	0.20
			ε	4.60	75.6	19.8
			γ′	1.50	80.3	18.2
			2	23.9	75.0	1.10
θ + γ′ ⇌ (αFe) +ε	392	U_3	θ	24.2	75.0	0.80
			γ′	0.90	80.1	19.0
			(αFe)	~0.0	99.9	0.10
			ε	6.00	70.8	23.2

DOI: 10.1007/978-3-540-74196-1_8

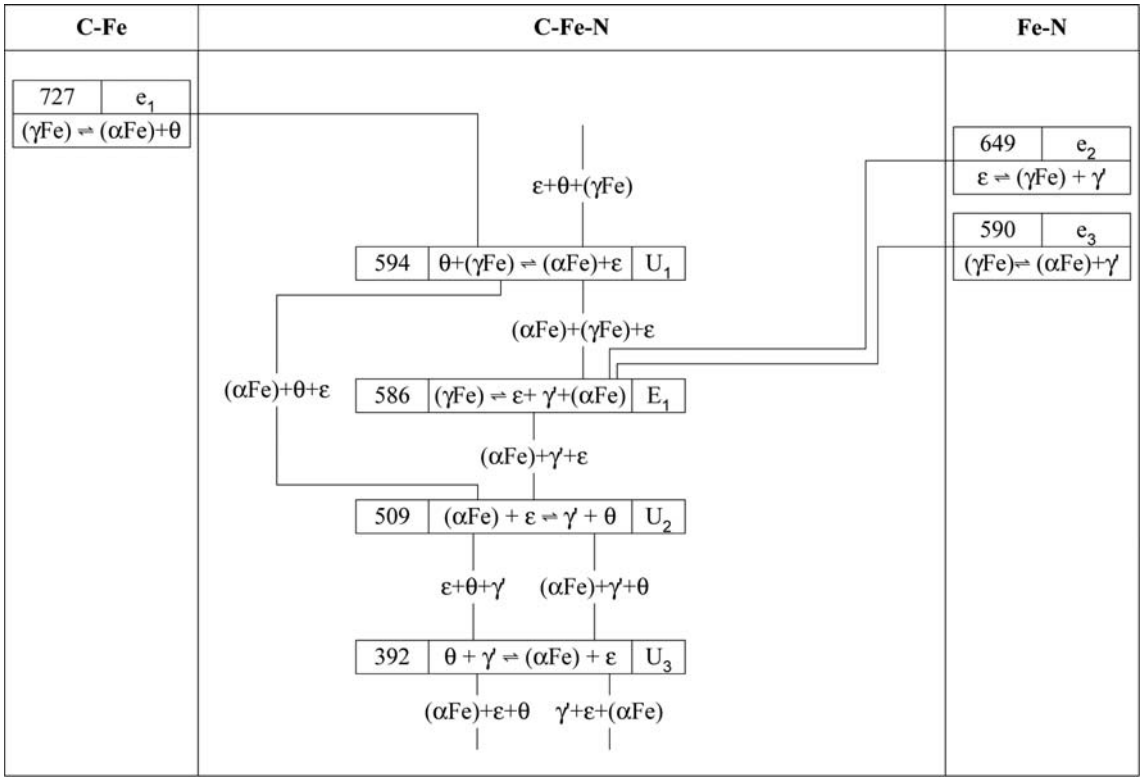

Fig. 1. C-Fe-N. Reaction scheme

DOI: 10.1007/978-3-540-74196-1_8

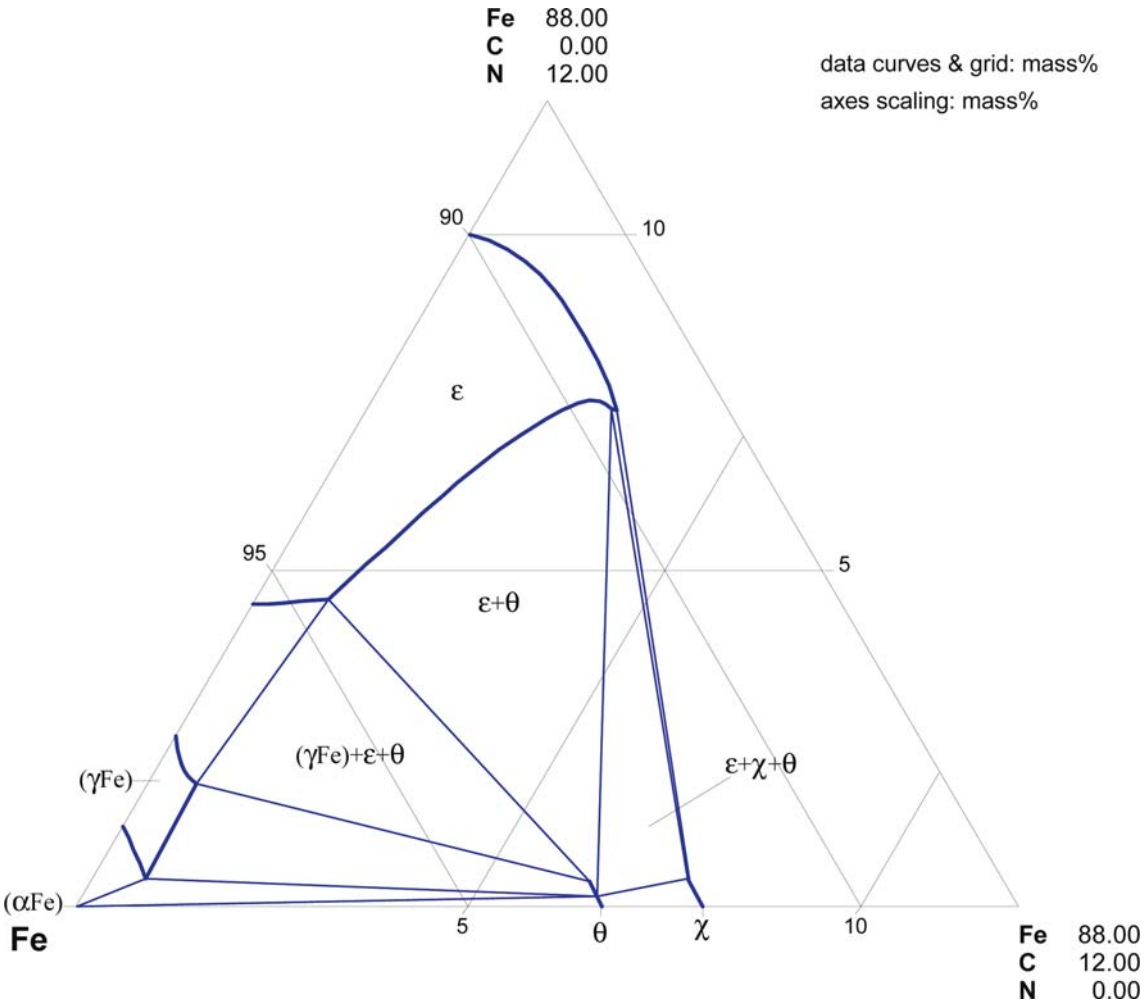

Fig. 2. C-Fe-N. Partial metastable isothermal section at 700°C

DOI: 10.1007/978-3-540-74196-1_8

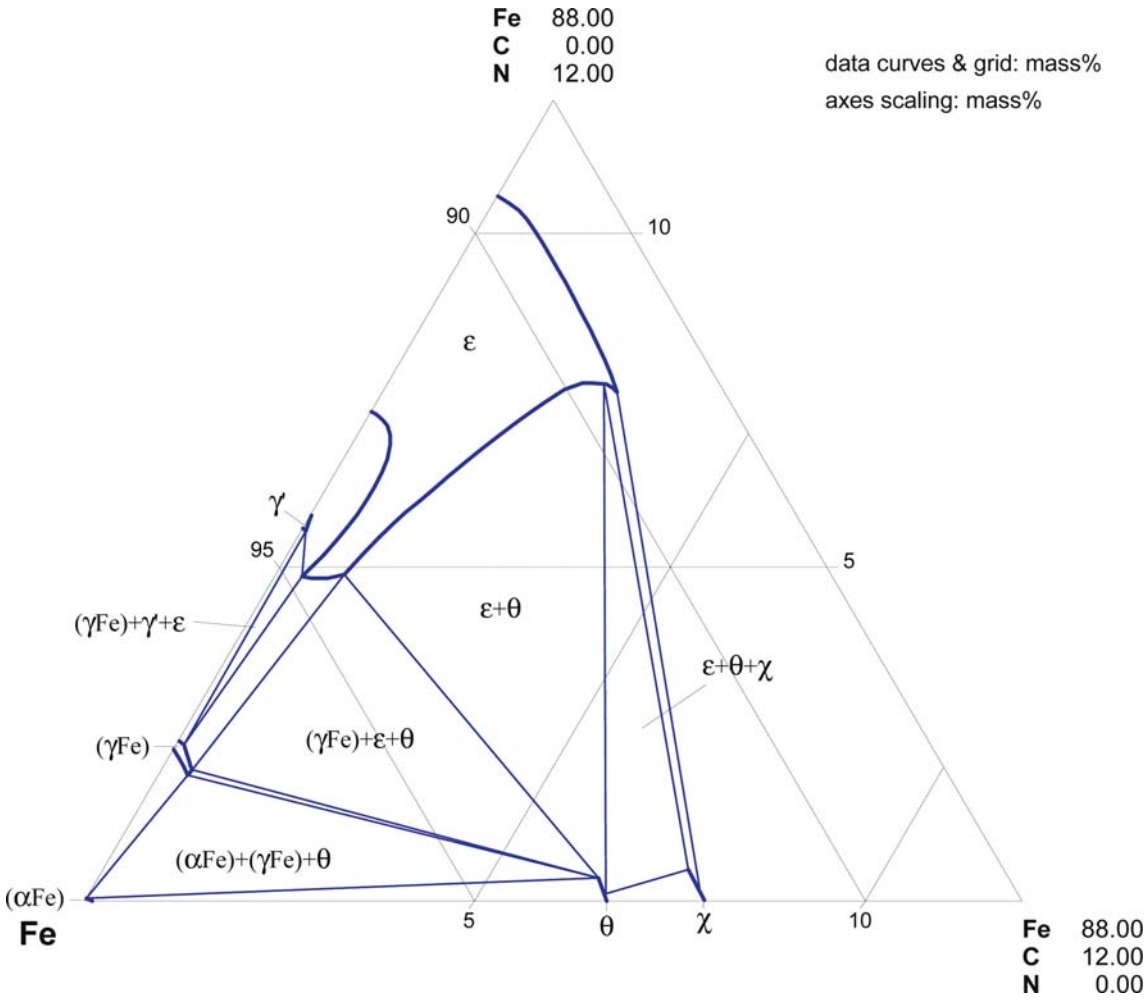

Fig. 3. C-Fe-N. Partial metastable isothermal section at 600°C

DOI: 10.1007/978-3-540-74196-1_8

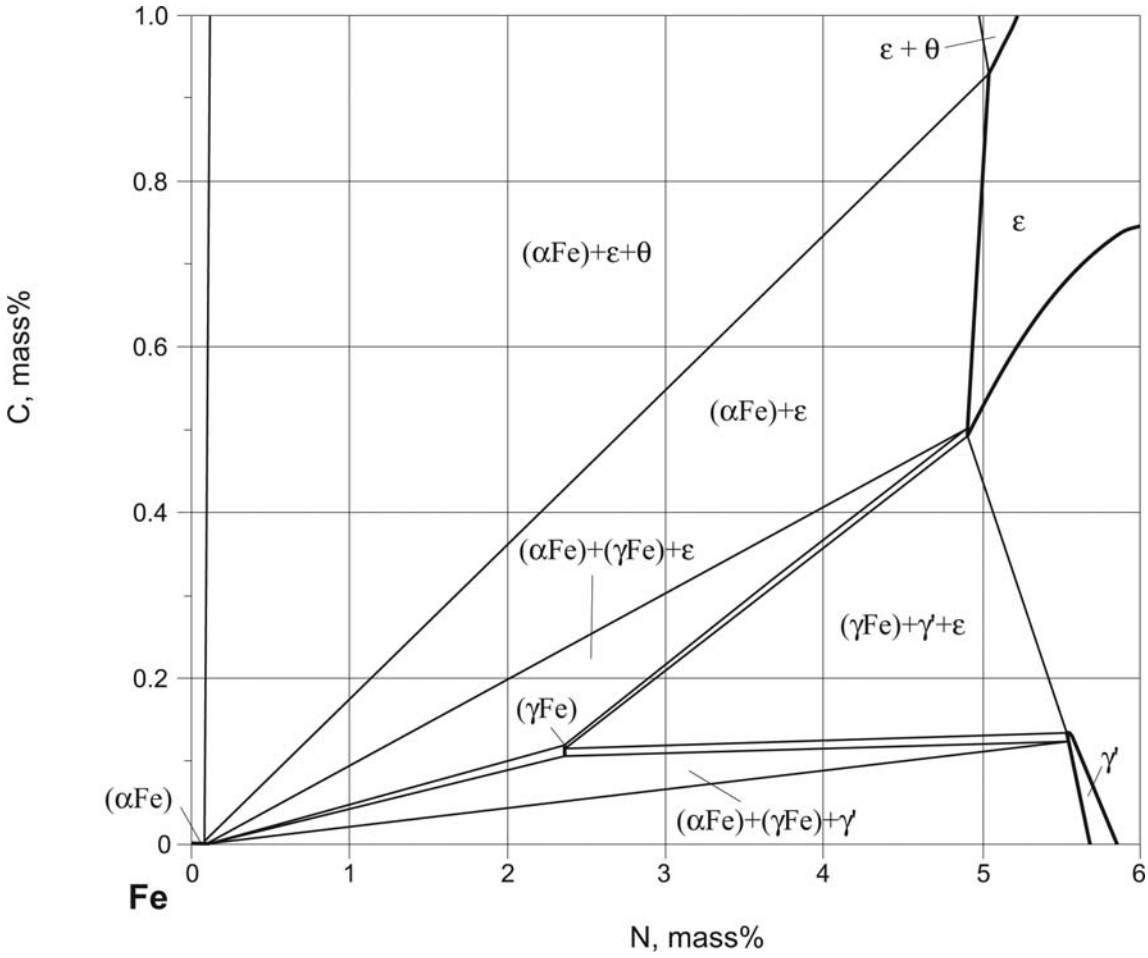

Fig. 4. C-Fe-N. Partial metastable isothermal section at 590°C

DOI: 10.1007/978-3-540-74196-1_8

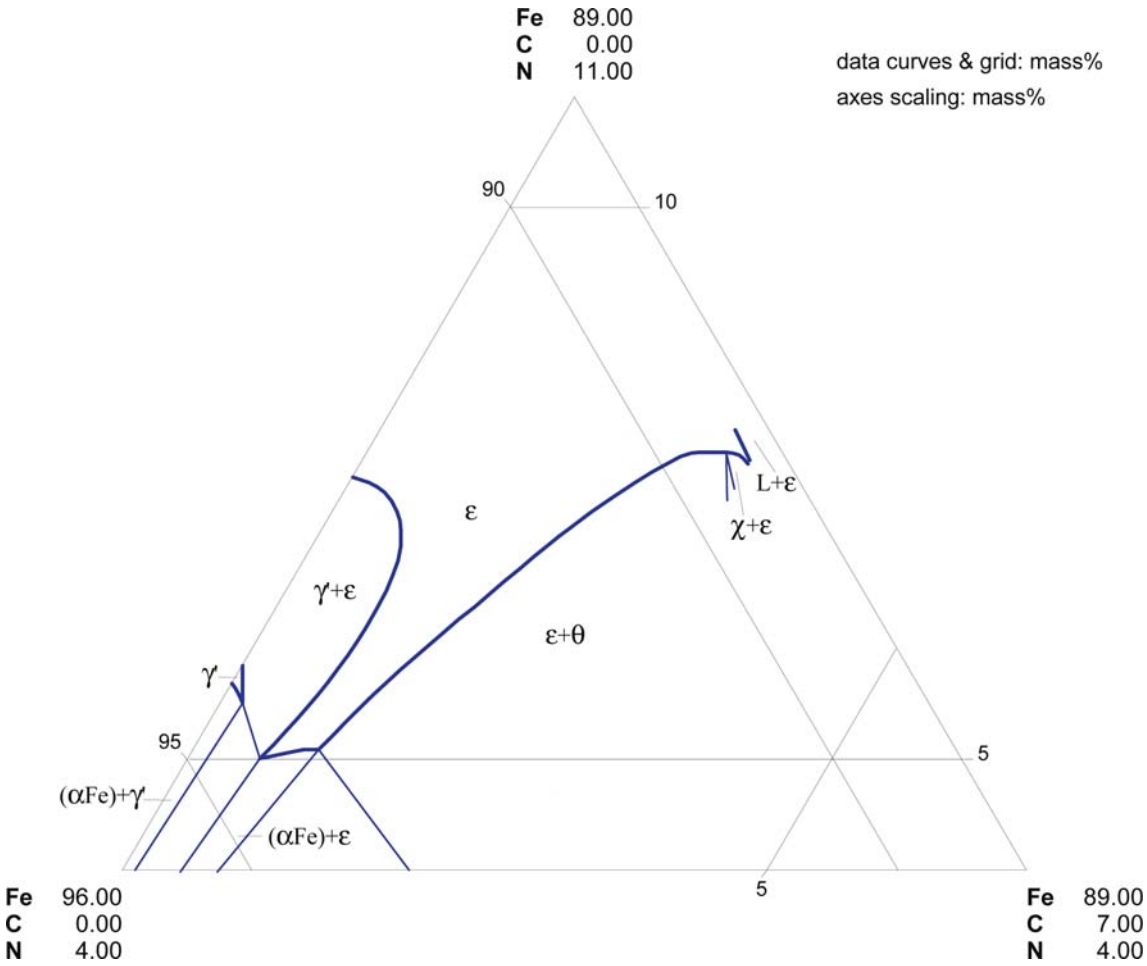

Fig. 5. C-Fe-N. Partial metastable isothermal section at 580°C

DOI: 10.1007/978-3-540-74196-1_8

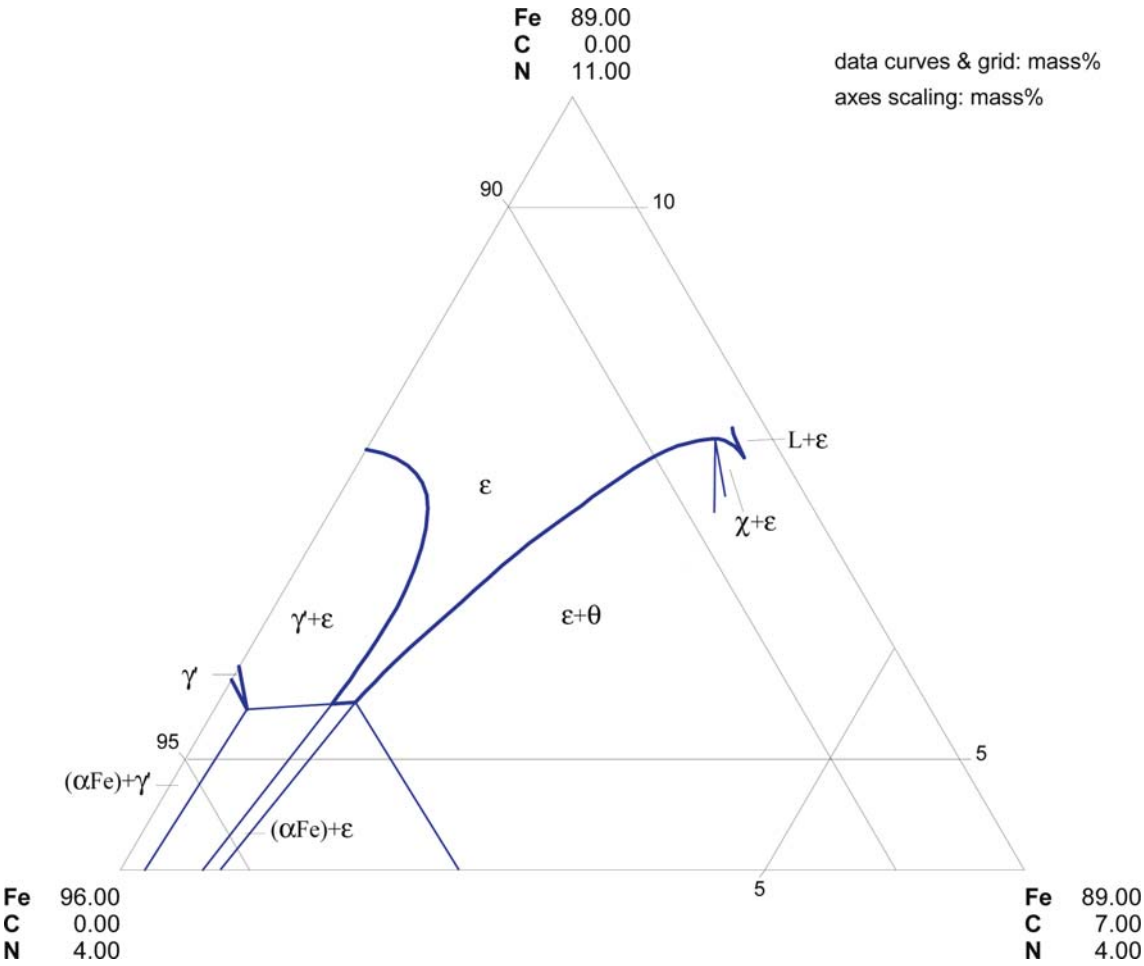

Fig. 6. C-Fe-N. Partial metastable isothermal section at 550°C

DOI: 10.1007/978-3-540-74196-1_8

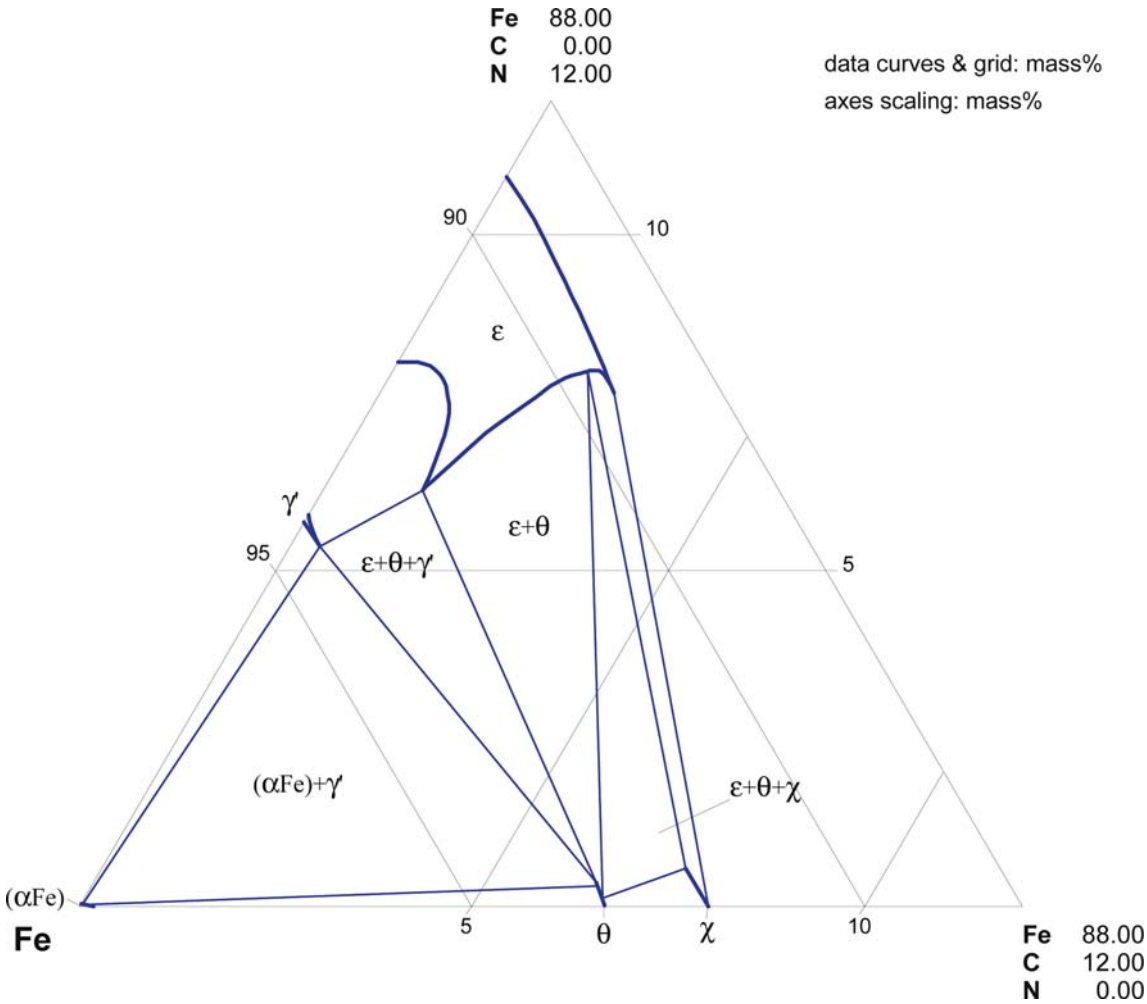

Fig. 7. C-Fe-N. Partial metastable isothermal section at 500°C

DOI: 10.1007/978-3-540-74196-1_8

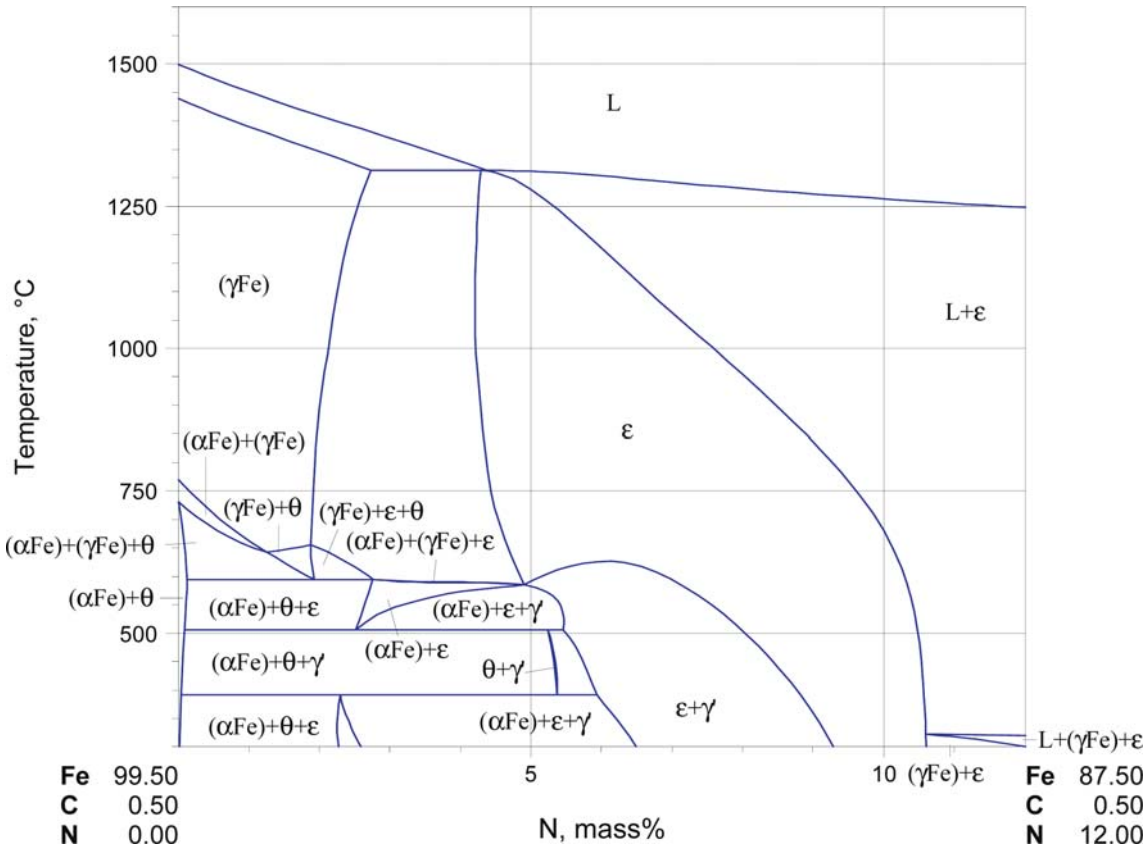

Fig. 8. C-Fe-N. Vertical section at 0.5 mass% C

DOI: 10.1007/978-3-540-74196-1_8

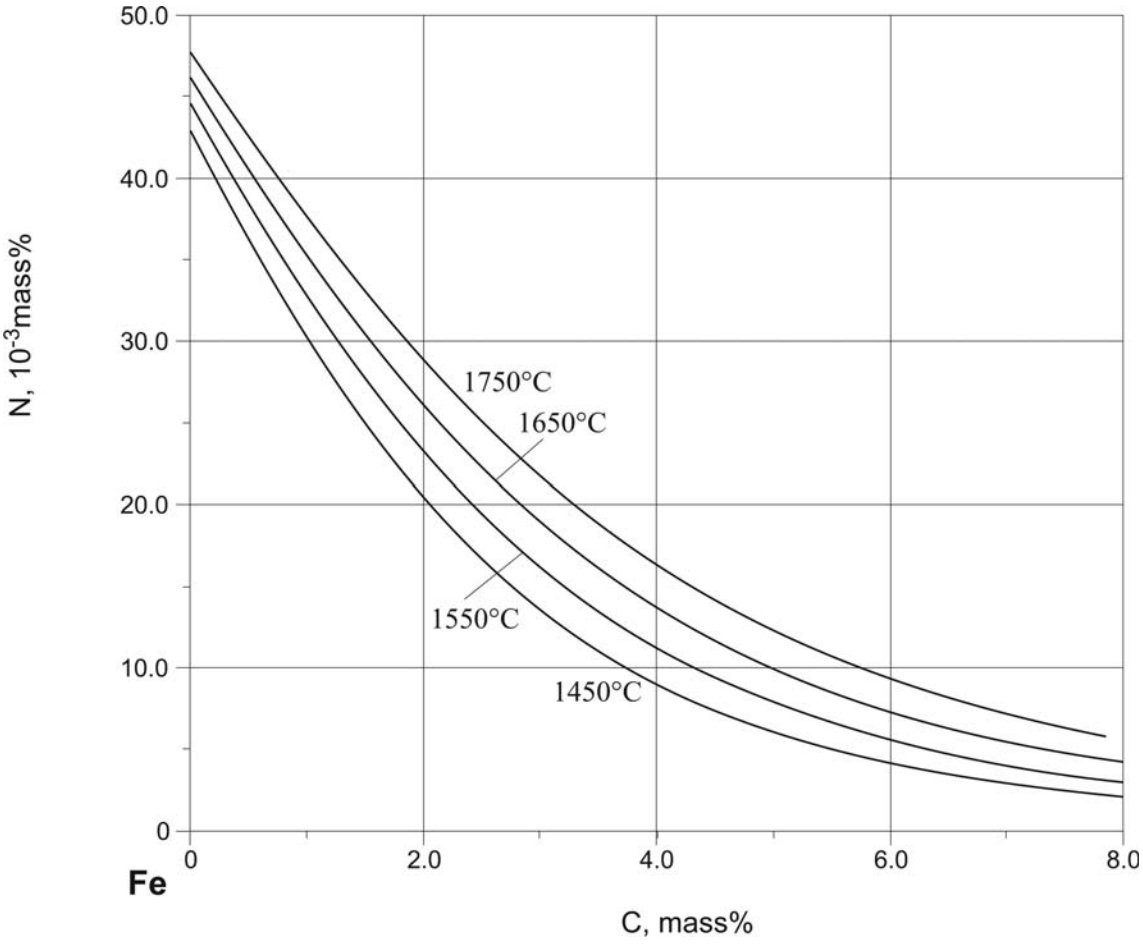

Fig. 9. C-Fe-N. Solubility of N in C-Fe melts at N_2 pressure of 101325 Pa and indicated temperatures

DOI: 10.1007/978-3-540-74196-1_8

References

[1930Koe] Köster, W., "The Question of Nitrogen in Commercial Iron" (in German), *Arch. Eisenhüttenwes.*, **4**(3), 145–150 (1930) (Experimental, Phase Diagram, Phase Relations, 6)

[1941Koo] Kootz, T., "Study of Solubility of Nitrogen in Pure Liquid Iron and Fe-C, Fe-P and Fe-Cr Alloys" (in German), *Archiv. Eisenhüttenwes*., **15**(2), 77–83 (1941) (Experimental)

[1948Jac] Jack, K.H., "Binary and Ternary Interstitial Alloys. II. The Iron-Carbon-Nitrogen System", *Proc. Roy. Soc. (London) A*, **195A**, 41–55 (1948) (Experimental, Phase Diagram, Crys. Structure, 29)

[1950Sai] Saito, T., "Absorption of Nitrogen by Molten Iron Alloys. III. Study on Fe-C and Fe-Si Alloys" (in Japanese), *Sci. Rep. Res. Inst. Tohoku Univ. Ser. A*, **2**, 909–916 (1950) (Phase Relations, Experimental)

[1951Pom] Pomey, J., Coudray, R., Moulin, J., "Magnetic Properties of Fe-C-N" (in French), *Rev. Metall.*, **48**(7), 552–560 (1951) (Experimental, Magn. Properties, 0)

[1954Bri1] Bridelle, R., Michel, A., "Physicochemical Characteristics of Carbonitrides of Iron" (in French), *Compt. Rend. Acad. Sci. Paris*, **239**, 274–275 (1954) (Experimental, Crys. Structure, 8)

[1954Bri2] Bridelle, R., Michel, A., "Study of Hexagonal Carbonitride of Iron (Type Fe_3N)" (in French), *Rev. Metall.*, **51**(4), 278–281 (1954) (Experimental, Crys. Structure, 4)

[1955Bri] Bridelle, B., Michel, A., "Properties of Carbonitrides of Iron" (in French), *Rev. Metall.*, **52**(5), 397–400 (1955) (Experimental, Crys. Structure, 14)

[1959Sch] Schenk, H., Frohberg, M.G., Graf, H., "Influencing the Equilibrium of Nitrogen with Liquid Iron Melts by the Addition of Other Elements II" (in German), *Archiv. Eisenhüttenwes.*, **30**(9), 533–537 (1959) (Experimental, Phase Relations, 22)

[1960Mae] Maekawa, M., Nakagawa, Y., "Solubility of Nitrogen in Liquid Iron and Effect of C, Si and Mn on the Solubility" (in Japanese), *Tetsu to Hagane*, **46**(7), 748–753 (1960) (Experimental, Phase Relations, 14)

[1962Sch] Scheil, E., Mayr, W., Muller, J., "Production of Fe-C-N Alloys and Determination of Some Equilibria in this System" (in German), *Archiv. Eisenhüttenwes.*, **33**(6), 385–392 (1962) (Experimental, Phase Diagram, 10)

[1965Nau1] Naumann, V.F.K., Langenscheid, G., "The Nitriding and Carburizing Capacity of Ammonia-Carbon Monoxide-Hydrogen Mixtures", (in German), *Arch. Eisenhuttenwes.*, **36**(8), 583–590 (1965) (Experimental, Crys. Structure)

[1965Nau2] Naumann, V.F.K., Langenscheid, G., "Contribution to the Investigation into the Iron-Nitrogen-Carbon System", (in German), *Arch. Eisenhuttenwes.*, **36**(9), 677–682 (1965) (Experimental, Phase Diagram, *, 21)

[1968Gom] Gomersall, D.W., McLean, A., Ward, R.G., "The Solubility of Nitrogen in Liquid Iron and Liquid Iron-Carbon Alloys", *Trans. Met. Soc. AIME*, **242**(7), 1309–1315 (1968) (Experimental, Phase Relations, 24)

[1969Opr] Opravil, O., Pehlke, R.S., "Solubility of Nitrogen in Carbon-saturated Liquid Iron Alloys", *Trans. Am. Foundrymens' Soc*., **77**, 415–421 (1969) (Experimental, Phase Relations)

[1977Pom] Pomarin, Yu.M., Grigorenko, G.M., Lakomskiy, V.I., "The Effect of C on the Solubility of N in Fe Alloys at High Temperatures" (in Russian), *Probl. Spets. Elektrometall.*, **6**, 81–85 (1977) (Experimental, Phase Relations, 11)

[1982Ish] Ishii, F., Banya, S., Fuwa, T. "Solubility of Nitrogen in Liquid Iron Alloys" (in Japanese), *Tetsu to Hagane*, **68**(10), 1551–1559 (1982) (Experimental, Phase Relations, 43)

[1983Bur] Burdese, A., Firrao, D., Rosso, M., "On Crystal Structure of ε-Iron Carbonitrides with High Interstitial Element Content" (in Italian), *Gazz. Chim. Ital.*, 113, 265–268 (1983) (Experimental, Crys. Structure)

[1983Wel] Wells, A., Bell, T., "Structural Control of the Compound Layers Formed During Ferritic Nitrocarburising in Methanol/Ammonia Atmospheres", *Heat Treat. Met.*, **10**(2), 39–44 (1983) (Experimental, 12)

DOI: 10.1007/978-3-540-74196-1_8

[1984Rag] Raghavan, V., "The C-Fe-N (Carbon-Iron-Nitrogen) System", *Trans. Ind. Inst. Met.*, **37**(4), 293–301 (1984) (Phase Diagram, Review, *, 38)

[1985Wel] Wells, A., "Metallographic Analysis of Compound Layers on Ferritic Nitrocarburized Plain Low Carbon Steel", *J. Mater. Sci..*, **20**(12), 2439–2445 (1985) (Experimental, 13)

[1987Som] Somers, M.A.J., Mittemeijer, E.J., "Formation and Growth of Compound Layer on Nitrocarburizing Iron: Kinetics and Microstructural Evolution", *Surf. Eng.*, **3**, 123–137 (1987) (Experimental, Morphology, Kinetics)

[1987Xu] Zuyao, X., Lin, L., "Phase Boundaries of Single-phase ε- and γ′-field in Fe-C-N Ternary Phase Diagram", *Mater. Sci. Tech.*, **3**(5), 325–328 (1987) (Theory, Thermodyn., Phase Diagram, 10)

[1988Sly] Slycke, J., Sproge, L., Agren, J., "Nitrocarburizing and the Ternary Fe-N-C Phase Diagram", *Scand. J. Metall.*, **17**, 122–126 (1988) (Theory, Thermodyn., Phase Diagram, 18)

[1990Che] Chen, S.R., Tang, D., "Effect of Interstitial Atom Concentration on Lattice Parameters of Martensite and Retained Austenite in Iron-Carbon-Nitrogen Alloys", *Mater. Sci. Forum*, **56–58**, 201–206 (1990) (Crys. Structure, Experimental, 17)

[1990Som] Somers, M.A.J., Colijin, P.F., Sloof, W.G., Mittemeijer, E.J., "Microstructural and Compositional Evolution of Iron Carbonitride Compound Layers During Salt Bath Nitrocarburizing", *Z. Metallkd.*, **81**(1), 33–43 (1990) (Experimental, Morphology, 28)

[1991Du] Du, H., Hillert, M., "An Assessment of the Fe-C-N System", *Z. Metallkd.*, **82**(4), 310–316 (1991) (Calculation, Crys. Structure, Experimental, Phase Diagram, Thermodyn., 20)

[1993Du] Du, H., "A Reevaluation of the Fe-N and Fe-C-N Systems", *J. Phase Equilib.*, **14**(6), 682–693 (1993) (Theory, Thermodyn., Phase Diagram, Calculation, 61)

[1993Rag] Raghavan, V., "C-Fe-N (Carbon-Iron-Nitrogen)", *J. Phase Equilib.*, **14**(5), 620–621 (1993) (Phase Diagram, Phase Relations, Review, 13)

[1994Rus] Russev, R., Malinov, S., "Some More Data for the Eutectoid Equilibrium of the Fe-N-C System", *Mater. Sci. Forum*, **163–165**, 285–292 (1994) (Theory, Phase Diagram, 6)

[1995Jac] Jacobs, H., Rechenbach, D., Zachwieja, U., "Structure Determination of ξ-Fe_4N and ε-Fe_3N", *J. Alloys Compd.*, **227**(1), 10–17 (1995) (Experimental, Crys. Structure, Magn. Properties, 20)

[1996Rec] Rechenbach, D., Jacobs, H., "Structure Determination of ξ-Fe_2N by Neutron and Synchrotron Powder Diffraction", *J. Alloys Compd.*, **235**(1), 15–22 (1996) (Experimental, Crys. Structure, 19)

[1999Lei] Leineweber, A., Jacobs, H., Hüning, F., Lueken, H., Schilder, H., Kockelmann, W., "ε-Fe_3N: Magnetic Structure, Magnetization and Temperature Dependent Disorder of Nitrogen", *J. Alloys Compd.*, **288**(1–2), 79–87 (1999) (Experimental, Crys. Structure, 40)

[1999Svy] Svyazhin, A.G., Kindop, V.E., El Gammal, T., "Solubility of Nitrogen in Liquid Iron-Carbon Alloys", *Mater. Sci. Forum*, **318-320**, 81–88 (1999) (Experimental, Review, Phase Diagram, 21)

[2001Lei] Leineweber, A., Jacobs, H., Hünning, F., Luecken, H., Kockelmann, W., "Nitrogen Ordering and Ferromagnetic Properties of ε-Fe_3N_{1+x} ($0.10 < x < 0.39$) and ε-$Fe_3(N_{0.80}C_{0.20})_{1.38}$", *J. Alloys Compd.*, **316**, 21–38 (2001) (Experimental, Crys. Structure, 47)

[2006MSIT] "C-Fe (Iron-Carbon)", Diagrams as Published, in *MSIT Workplace*, Effenberg, G. (Ed.), Materials Science International Services, GmbH, Stuttgart; Document ID: 30.13598.1.20 (2006) (Crys. Structure, Phase Diagram, Phase Relations, 2)

[Mas2] Massalski, T.B. (Ed.), *Binary Alloy Phase Diagrams*, 2nd edition, ASM International, Metals Park, Ohio (1990)

[V-C2] Villars, P. and Calvert, L.D., *Pearson's Handbook of Crystallographic Data for Intermetallic Phases*, 2nd edition, ASM, Metals Park, Ohio (1991)

DOI: 10.1007/978-3-540-74196-1_8

Carbon – Iron – Niobium

Lesley Cornish, Andy Watson

Introduction

The C-Fe-Nb system is important for the development of low alloyed C steels and ferritic stainless steels as Nb is a very strong carbide former and since many of the properties of these materials are defined by the solubilities of the carbonitrides in the austenite phase (as well as solid solution strengthening). The earliest work [1952Edw] gave the solubility of Fe in NbC_{1-x} as 1 mass% based on studies involving the milling of powders, and [1966Man] plotted the partition coefficient of Nb between the carbonitrides and (γFe) for temperatures between 950 and 1225°C. The solubility of NbC in (γFe) was derived by [1966Smi, 1967Mey] assuming NbC_{1-x} stoichiometry, and subsequently, [1968Nor] recalculated the values for $NbC_{0.87}$ and presented them in their review. [1984Lak] (reviewed by [1986Das]) used the sealed capsule technique to derive the solubility limit. Binary Fe-C and Fe-Nb alloys were sealed in similar silica ampoules and the C transferred across the samples in the vapor phase during heat treatment. Carbon activities were calculated from known activity-composition relationships, leading to a composition of $NbC_{0.87}$ for the C-deficient carbide and an empirical equation for the limiting solubility for temperatures between 1000 and 1250°C and up to 0.4 mass% C. [1984Sha] compared these data with information available in the literature and found close agreement. Using diffusion couples, [1985Oht] derived new solubility values for temperatures between 1000 and 1200°C and up to 1 mass% C. The values were higher than those of [1984Lak] and also the solubility of Nb increased at C contents above 0.5 mass% - *i.e.* not in agreement with the usual hyperbolic curve. However, the carbon contents used were higher than those by [1984Lak], which may explain why the latter might not have found this relationship. [1988Bal] used a dynamic gas equilibrium method at temperatures between 1000 and 1200°C with 0.2 to 2.0 mass% C and derived a ternary interaction parameter for the NbC_{1-x} carbide. Later, [1992Bal] used the same technique employing methane/hydrogen mixtures of a known C activity to determine the solubility limit. The same temperature range was also used but C contents of only up to 1.6 mass%. A minimum in the Nb content of between 0.4 and 0.5 mass% was found in agreement with [1985Oht], but the values of [1992Bal] were higher at higher temperatures (*e.g.* 1200°C). The results of [1966Smi, 1984Lak] agreed with the calculation of [1986Bal] which suggested a non-stoichiometric niobium carbide. [1986Bal] used the calculations to deduce the optimum temperature range for precipitation. [1991Fan] also measured the solubility, but did not compare with many other workers. The results of the thermodynamic assessment of [1990Hua] agreed better with the data of [1984Lak] than those of [1985Oht, 1988Bal]. In their review, [1994Wil] correlated the microstructures obtained in binary alloys and those observed in C-Fe-Nb alloys with commercial HSLA steels.

[1995Tay] calculated the solubility relationships for NbC_x and ferrite, using austenite solubility data, and gave x as being close to 0.9. The solubilities were found to be much less in ferrite than in austenite.

The earliest phase diagram study was undertaken by [1938Egg] for high Fe contents, and a space diagram, a projection of the primary phase fields and five vertical sections were derived. A space diagram was also given by [1949Jae] using the work of [1938Egg]. The system has been assessed by [1990Hua], and this calculation has been used for a solubility study of the C-Fe-N-Nb system by [1998Zaj] and a calculation of the quinary C-Fe-N-Nb-Ti system by [2001Lee].

The system has been reviewed by [1986Das, 2003Rag]. Details of studies of phase equilibria and thermodynamics are given in Table 1.

Binary Systems

The C-Fe system has stable (Fe-graphite) and metastable (Fe-cementite) versions and is accepted from [2006MSIT]. The C-Nb and Fe-Nb systems are accepted from [Mas2]. In the C-Nb system, the phase previously designated as Nb_4C_3 is given as Nb_4C_{3-x}.

DOI: 10.1007/978-3-540-74196-1_9

Solid Phases

Crystallographic data are given in Table 2. The NbC_{1-x} phase has been described in the literature as NbC, NbC_{1-x} [Mas2] and $NbC_{0.87}$ [1984Lak]. Using TEM and DTA, [1989Kes] suggested that the NbC_{1-x} phase shows long range order at lower temperatures. This phase was designated as Nb_6C_5, and the transition temperature from the NbC_{1-x} phase, which shows short range ordering of vacancies to the Nb_6C_5 phase is ~1025°C.

Invariant Equilibria

Solid state invariant equilibria were determined by [1938Egg]. However, the eutectoid at 920°C involved the Fe_3Nb_2 phase, which is not present in the accepted binary Fe-Nb phase diagram. Owing to uncertainties in the binary systems available at that time these ternary invariants are ignored in this assessment.
As a consequence of their assessment of the ternary system, [1990Hua] calculated invariant equilibria, and these are listed in Table 3.

Liquidus, Solidus and Solvus Surfaces

No experimental liquidus surface has been determined. [1990Hua] calculated a partial liquidus surface for the system for C contents up to 18 mass% and also for Fe rich alloys for metastable equilibria (cementite). These are given in Figs. 1 and 2, respectively.

Isothermal Sections

[1986Das] constructed tentative isothermal sections between 800 and 1700°C, but these contained the phase Fe_3Nb_2 which does not exist. Isothermal sections for the metastable state were calculated by [1989Oht] in the temperature range from 800 to 1500°C at 100°C intervals showing the C solubility limit in austenite to be retrograde at higher C levels.
[1965Fed] reported an isothermal section at 1050°C. [1990Hua] assumed that the Fe solubility in the Nb carbide phases is negligible, as is the C solubility in the Laves and μ Fe-Nb phases and by thermodynamic assessment, calculated isothermal sections for the stable system at 800, 1000, 1200, 1500 and 2000°C. Figures 3-7 show isothermal sections for 800, 1000, 1200, 1500 and 2000°C, taken essentially from this work. Figure 8 shows the solubility of Nb in (αFe) from the (γFe) solubility product and activity coefficients of the Nb solute calculated by [1995Tay]. Amendments have been made to the isothermal sections in Figs. 3-8 in order to maintain consistency with the accepted binaries, particularly where the calculations have assumed that the intermetallic phases do not exhibit a range of homogeneity.
The Nb_4C_{3-x} and Nb_6C_5 phases have not been included in the isothermal sections owing to uncertainties regarding them in the C-Nb binary phase diagram.

Temperature – Composition Sections

Figure 9 shows the Fe-NbC vertical section as calculated by [1990Hua] following the thermodynamic assessment of the system. Using DTA measurements with metallography confirming the microstructures, [1975Fre] suggested that this section was quasibinary with a eutectic composition of ~97.5 at.% Fe and temperature of ~1420 ± 20°C. However, this cannot be the case as from the accepted binary phase diagram, the congruent melting point of the NbC_{1-x} compound does not occur at the stoichiometric composition. Also, in their quasibinary section, there is no distinction between (γFe) and (δFe). Intriguingly, there is a maximum on the monovariant connecting U_2 and E_3, as shown in Fig. 1. This would suggest the possibility of a quasibinary section between Fe and NbC_{1-x} at an off-stoichiometric composition ($x > 0$) corresponding to the congruent melting of this phase. But even if the primary solidification behavior of this section was quasibinary, the involvement of both (γFe) and (δFe) would make this unlikely below the "quasibinary eutectic" temperature.
Figure 10 shows the vertical sections at 0.02 mass% and 0.1 mass% Nb for Fe rich alloys taken from the thermodynamic assessment by [1990Hua]. [1938Egg] derived vertical sections at Nb contents of 0.3, 0.5,

DOI: 10.1007/978-3-540-74196-1_9

1.0, 1.5 and 2.0 mass% Nb but they have been ignored in this assessment as an incorrect version of the Fe-Nb phase diagram was used, as outlined above.

Thermodynamics

The effect of niobium on the activity coefficient of C in liquid Fe was obtained by [1959Fuw]. The activity coefficient of C in liquid Fe-Nb at 1560°C was plotted by [1963Ell] for up to ~5 mass% Nb. The activity coefficient was derived for a range of C-Fe-Nb steels, but in association with other alloying elements, for 0.004-0.005 mass% C and 0.10-1.02 mass% Nb, at 900°C, 1000°C and 1100°C.

[1985Oht] modelled the equilibrium of (γFe) and NbC_{1-x} with a single thermodynamic description showing a miscibility gap since they both have the same crystal structure. NbC_{1-x} has Fe and Nb atoms on the fcc sites and C in the octahedral vacancies. A negative interaction parameter gave the experimentally observed increase in Nb solubility with increasing C in (γFe) at higher C contents. The work was continued in [1989Oht]. [1986Bal] calculated molar free energies of NbC_x and partial free energies of Nb as a function of x between 0.65 and 1.0 at 1000°C. The resulting non-stoichiometric NbC_x-(γFe) equilibria agreed well with the experimental results then available [1966Smi, 1984Lak]. [1988Hon] also studied the thermodynamic properties of NbC_{1-x} and the extent of the phase field.

[1992Bal] calculated a strong interaction between Nb and C in (γFe), the wagner interaction parameter being –50, –46 and –43 at 1000°C, 1100°C and 1200°C respectively. This successfully gave the observed increase in Nb solubility with increasing C in (γFe) at higher C contents.

[1990Hua] undertook a complete thermodynamic evaluation of the system, after modelling the binary systems and estimated ternary interaction parameters. [1990Hua] could not totally reproduce experimental results of Nb solubility in (γFe) with a hyperbolic curve simultaneously with a negligible solubility of Fe in NbC, and deduced that there were problems in the data of [1985Oht, 1988Bal]. [2001Lee] deduced that the Laves phase in the Fe-Nb description had to be changed by adding a temperature dependent term ([1990Hua] used a temperature independent term) when comparing the results of [1990Hua] with experimental values for solubility product *vs* inverse temperature plots. Hyperbolic behavior for the solubility of C in (γFe) was found.

[2004Sho] analyzed equilibrium C solubility data for the austenite phase, described as $Fe_{1-x}Nb_yC_x$, in order to deduce the dipole formation to give a higher affinity between C-Nb atoms than C-Fe atoms.

Notes on Materials Properties and Applications

The major reason for interest in the system is in relation to steels research. Since the 1930s, the benefit of Nb additions to low carbon steels was recognized, and the first Nb-microalloyed steel hot strip was manufactured in 1958 [2001DeA] and grain refinement by carbonitrides was achieved. Since the metal became readily available in 1965, Nb has been an important alloying element (1500 - 5000 ppm) for ferrite pearlite steels. Grain refinement is important because it improves properties such as yield point and impact resistance [1967Irv], and could also offset the deleterious effects that solution hardening has on impact resistance. One of the first studies on the effect of grain refining was based on C-Mn steels, but also included the effect of the solubility product in Nb steels. Nb strengthens in at least two ways: by grain refining and also allowing for the precipitation of fine niobium carbonitrides [1967Irv]. By the early 1980s, controlled rolling and austenite conditioning were well understood in terms of mechanism and alloys design, and the applications were extended to sheet, bars, shapes and castings [2001DeA]. Subsequent improvements included steels with low temperature transformation phases (accicular ferrite and bainite) resulting from accelerated cooling and/or alloying additions. Another important application is as a microalloying (100 - 300 ppm) addition, often with Ti, to act as a stabilizing element in ultra-low C steels and ferritic stainless steels; this has led to the HSLA (high strength low-alloy) steels, which are based on C-Fe-N-Nb-Ti-V. [1998Hil] studied precipitation and recrystallization characteristics, and related the findings to the Hall-Petch relationship. Diffusion studies were carried out by [1999Pop] to derive the diffusion interaction of carbides, nitrides and carbonitrides with Fe in steels during various thermal operations (*e.g.* thermochemical, heat treatment, sintering carbonitride coating).

DOI: 10.1007/978-3-540-74196-1_9

[1994Ji, 2002Yu] measured the internal friction from ambient to 180°C of two steels {Fe-(<0.05%-0.43%) Nb-(0.036%-0.125%)C}, revealing the Snoek peak and a damping peak. It was assumed that the deformation peak was related to dislocation-Cottrell atmosphere interactions. [2004Bem] showed that niobium carbide precipitates already existed in C-Fe-Nb alloys quenched from 1240°C. Samples aged at 750°C had two types of niobium carbide precipitates with different carbon contents. Also, the direction of the habit plane for the matrix/niobium carbide interface was found.
Hot corrosion studies were undertaken on a variety of Fe-5 mass% M - C alloys with different C contents (0.1, 0.4, 0.8 and 1.2 mass%) compared with plain carbon steels. The Nb steels were only marginally better than the plain carbon steels and not as good as W, Cr or Ni-containing steels.
[1993Ber] studied the growth of the solid interface in conditions suitable for composite manufacture. To optimize the application of carbide coatings, [2000Bya] studied a range of parameters for the most widely-used carbide layers, including NbC_{1-x}. It was found that the microhardness and fracture toughness were more dependent on composition than structure. [1988Uhb] measured the electrical resistivity at low temperatures and used these measurements to study precipitation. The system is also of interest because it comprises some of the components of cermets [1940Kie]. Additionally, the NbC_{1-x} carbide is useful in composite materials, where it acts as the hard phase, conferring strength.
The magnetic properties are also very important. Microcrystalline films of C-Fe-M (M = Ti, Zr, Hf, V, Nb and Ta) are suitable for magnetic recording heads [1991Has]. Crystallization is assumed to nucleate on very fine carbides and the supersaturated Fe rich phase produced has a tetragonally deformed structure, which reverts to bcc as the annealing temperature increases. The change in structure occurred at 736K. [1991Has] deduced that the change in soft magnetic behavior is affected by grain structure, rather than crystal structure changes or magnetostriction.
Details of studies on materials properties are given in Table 4.

Miscellaneous

Ordering studies were undertaken by [1989Kes] using TEM and DTA on alloys with vanadium, and for "Chinese script" NbC_x there was short range ordering (SRO) below 1100°C between ~0.75 - ~0.92 C/Nb. Various amorphous and nanocrystalline phases have been produced by mechanical alloying of elemental powders [1996Lou].

DOI: 10.1007/978-3-540-74196-1_9

Table 1. Investigations of the C-Fe-Nb System Phase Relations, Structures and Thermodynamics

Reference	Method / Experimental Technique	Temperature / Composition / Phase Range Studied
[1938Egg]	Metallography, thermal analysis	up to 1050°C; up to 2 mass% Nb and 2 mass% C
[1959Fuw]	Measurement of activity coefficient from passing CO-CO_2-Ar mixture over Fe-Nb melts	1560°C (liquid)
[1966Man]	Residual electrolytic extraction	950-1225°C; multi-component alloy
[1966Smi]	Equilibration with Methane-H_2 mixtures	997-1318°C; < 0.005 mass% C, 0.0-0.8 mass% Nb in multi-component alloy
[1967Irv]	TEM	900-1300°C; 0.025-0.28 mass% Nb
[1975Fre]	DTA	25-1550°C; "NbC"
[1981Bra]	Recirculation of methane-H_2 gases to obtain equilibrium	900, 1000 and 1100°C
[1984Lak]	Sealed capsule technique to derive solubility limits	1000-1250°C; up to 0.4 mass% C; (γFe)-NbC_{1-x}
[1985Oht]	Diffusion couples technique to derive solubility limits	1000-1200°C; up to 1 mass% C; (γFe)-NbC_{1-x}
[1988Bal]	Dynamic gas equilibrium technique to derive solubility limits	1000-1200°C; 0.2 - 2.0 mass% C; (γFe)-NbC_{1-x}
[1988Hon]	Galvanic cell technique using calcia stabilized zirconia (CSZ) and yttria stabilized zirconia (YSZ) solid electrolytes	827-1087°C for compositions varying from $NbC_{0.72}$ and $NbC_{0.98}$
[1989Kes]	TEM, DTA	1000-1400°C; multi-component alloy
[1990Hua]	Calculation	Complete system
[1992Bal]	Dynamic gas equilibrium technique to derive solubility limits, cahn microbalance	1000-1200°C; up to 1.6 mass% C; (γFe)-NbC_{1-x}
[1995Tay]	Calculation	Solubilities of $NbC_{0.9}$ in (αFe)

Table 2. Crystallographic Data of Solid Phases

Phase/ Temperature Range [°C]	Pearson Symbol/ Space Group/ Prototype	Lattice Parameters [pm]	Comments/References
(δFe) 1538 - 1394	*cI2* $Im\bar{3}m$ W	a = 293.15	[Mas2]

(*continued*)

DOI: 10.1007/978-3-540-74196-1_9

Phase/ Temperature Range [°C]	Pearson Symbol/ Space Group/ Prototype	Lattice Parameters [pm]	Comments/References
(γFe) 1394 - 912	*cF*4 $Fm\bar{3}m$ Cu	a = 364.67	at 915°C [V-C2, Mas2]
(αFe) < 912	*cI*2 $Im\bar{3}m$ W	a = 286.65	at 25°C [Mas2]
(C)d	*cF*8 $Fd\bar{3}m$ C (diamond)	a = 356.69	at 25°C, 60 GPa [Mas2]
(C)gr < 3827	*hP*4 $P6_3/mmc$ C (graphite)	a = 246.12 c = 670.90	at 25°C [Mas2] sublimation point
(Nb) < 2469	*cI*2 $Im\bar{3}m$ W	a = 330.4	at 25°C [Mas2]
γNb_2C 3080 - 2450	*hP*9 $P\bar{3}1m$ εFe_2N	a = 540.7 c = 496.8	[Mas2, 1987Smi] ~28-33.3 at.% C
βNb_2C < 2530	*oP*12 $Pmc2_1$ Nb_2C	a = 1091.0 ± 0.1 b = 497.46 ± 0.06 c = 309.54 ± 0.06	[V-C2]
	*hP*3 $P6_3/mmc$ W_2C	a = 312.0 to 312.8 c = 495.7 to 497.0	[1987Smi]
Nb_4C_{3-x} < 2360	*cP*7 $Pm\bar{3}m$ U_4S_3	a = 444.5 ± 0.1	[V-C2]
	*hR*60 $R\bar{3}m$ V_4C_{3-x}	a = 314 c = 3010	[1987Smi]
NbC_{1-x} < 3600	*cF*8 $Fm\bar{3}m$ NaCl	a = 444.7	[V-C] 38-49 at.% C [Mas2]
Nb_6C_5 < 1050	*mC*? *C*2/*m* V_6C_5	a = 546.05 b = 945.79 c = 546.05 β = 109.471°	[1987Smi]
	*hP*11 $P3_1$ or $P3_2$ -	a = 1087 c = 3076	[1987Smi]

(*continued*)

DOI: 10.1007/978-3-540-74196-1_9

Phase/ Temperature Range [°C]	Pearson Symbol/ Space Group/ Prototype	Lattice Parameters [pm]	Comments/References
λ, Fe_2Nb < 1627	*hP*12 $P6_3/mmc$ $MgZn_2$	*a* = 483.8 *c* = 788.9	[V-C]. 27-38 at.% Nb
μ, FeNb < 1611	*hR*39 $R\bar{3}m$ Fe_7W_6	*a* = 492.8 *c* = 2683.0	[V-C, 1990Hua] 47-49 at.% Nb designated $Fe_{21}Nb_{19}$ or Fe_7Nb_6
Metastable / high pressure phases			
(εFe)	*hP*2 $P6_3/mmc$ Mg	*a* = 246.8 *c* = 396.0	at 25°C, 13 GPa [Mas2]
Martensite	*tI*4 *I*4/*mmm*	-	[Mas2]
Fe_4C	*cP*5 $P\bar{4}3m$ Fe_4C	*a* = 387.8	[V-C2]
θ, Fe_3C	*oP*16 *Pnma* Fe_3C	*a* = 507.87 *b* = 672.97 *c* = 451.44	[V-C2]
χ, Fe_5C_2	*mC*28 *C*2/*c* B_2Pd_5	*a* = 1156.2 *b* = 457.27 *c* = 505.95 β = 97.74°	[V-C2]
Fe_7C_3	*hP*20 $P6_3mc$ Fe_3Th_7	*a* = 688.2 *c* = 454.0	[V-C2]
Fe_7C_3	*oP*40 *Pnma* Cr_7C_3	*a* = 454.0 *b* = 687.9 *c* = 1194.2	[V-C2]
η, Fe_2C	*oP*6 *Pnnm* Fe_2C	*a* = 470.4 *b* = 431.8 *c* = 283.0	[V-C2]
ε, Fe_2C	*hP** $P6_322$	-	[Mas2]
Fe_2C	*hP** $P\bar{3}m1$	-	[Mas2]

DOI: 10.1007/978-3-540-74196-1_9

Table 3. Invariant Equilibria

Reaction	T [°C]	Type	Phase	Composition (at.%)		
				Fe	Nb	C
Stable:						
$L \rightleftharpoons \mu + \lambda + Nb_2C$	1595	E_1	-	-	-	-
$L + Nb_2C \rightleftharpoons NbC_{1-x} + \lambda$	1466	U_1	-	-	-	-
$L + (\delta Fe) \rightleftharpoons NbC_{1-x} + (\gamma Fe)$	1463	U_2	-	-	-	-
$L \rightleftharpoons \mu + Nb_2C + (Nb)$	1398	E_2	-	-	-	-
$L \rightleftharpoons (\delta Fe) + NbC_{1-x} + \lambda$	1368	E_3	-	-	-	-
$L + (C)gr + NbC_{1-x} + (\gamma Fe)$	1152	D	-	-	-	-
Metastable:						
$L + (\delta Fe) \rightleftharpoons NbC_{1-x} + (\gamma Fe)$	1463	U	-	-	-	-
$L \rightleftharpoons (\gamma Fe) + Fe_3C + NbC_{1-x}$	1147	E	-	-	-	-

Table 4. Investigations of the C-Fe-Nb Materials Properties

Reference	Method / Experimental Technique	Type of Property
[1967Irv]	Variation of rolling variables and cooling rates	Yield strength; tensile strength; elongation and grain size
[1989Mal]	Hot corrosion tests	Corrosion rates and scale morphologies
[1991Has]	Film manufacture, XRD, DSC	Crystal structure; grain size; thermal stability
[1993Ber]	Liquid metal-graphite contact formation of carbides, metallography	Carbide growth characteristics, C distribution
[1994Ji]	Magnetomechanical hysteresis	Internal friction at 400-850°C
[1996Lou]	Mechanical alloying	Phase structures
[1998Hil]	Magnetic field strength; SEM	Precipitation, distribution and dissolution
[1999Pop]	Welded diffusion couples, XRD, metallography	Concentration-penetration profiles; boundary microstructures
[2000Bya]	Metallography, SEM, EPMA, XRD, diffractometry, impression tests using Palmqvist cracks	Composition; structure; fracture toughness; microhardness
[2002Mar]	3-dimensional atom probe (3DAP); TEM; compression tests	Recrystallization characteristics

(*continued*)

DOI: 10.1007/978-3-540-74196-1_9

Reference	Method / Experimental Technique	Type of Property
[2001Yu]	TEM	Dislocation interactions
[2002Yu]	TEM	Dislocation interactions
[2004Bem]	Field ion microscopy and atom probe tomography	Precipitate type and habit plane

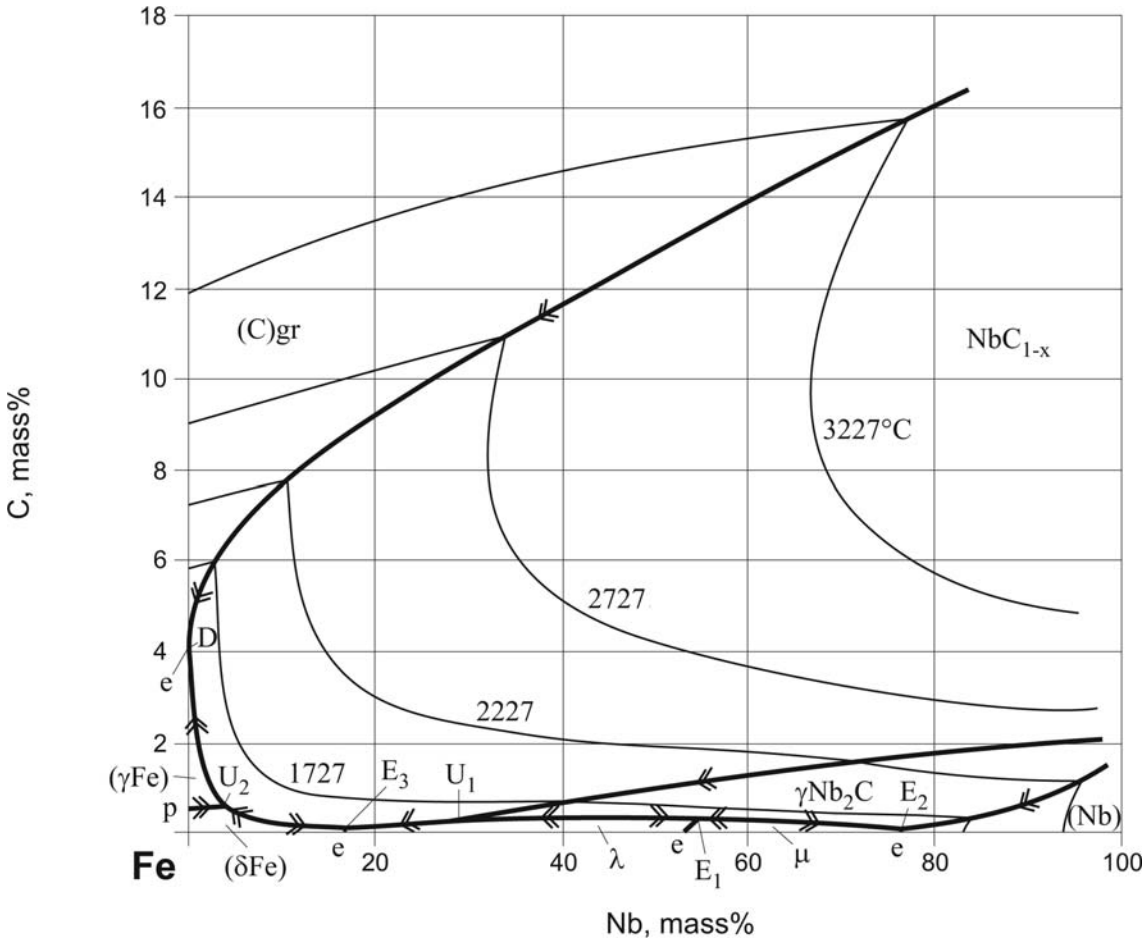

Fig. 1. C-Fe-Nb. Calculated partial liquidus surface

DOI: 10.1007/978-3-540-74196-1_9

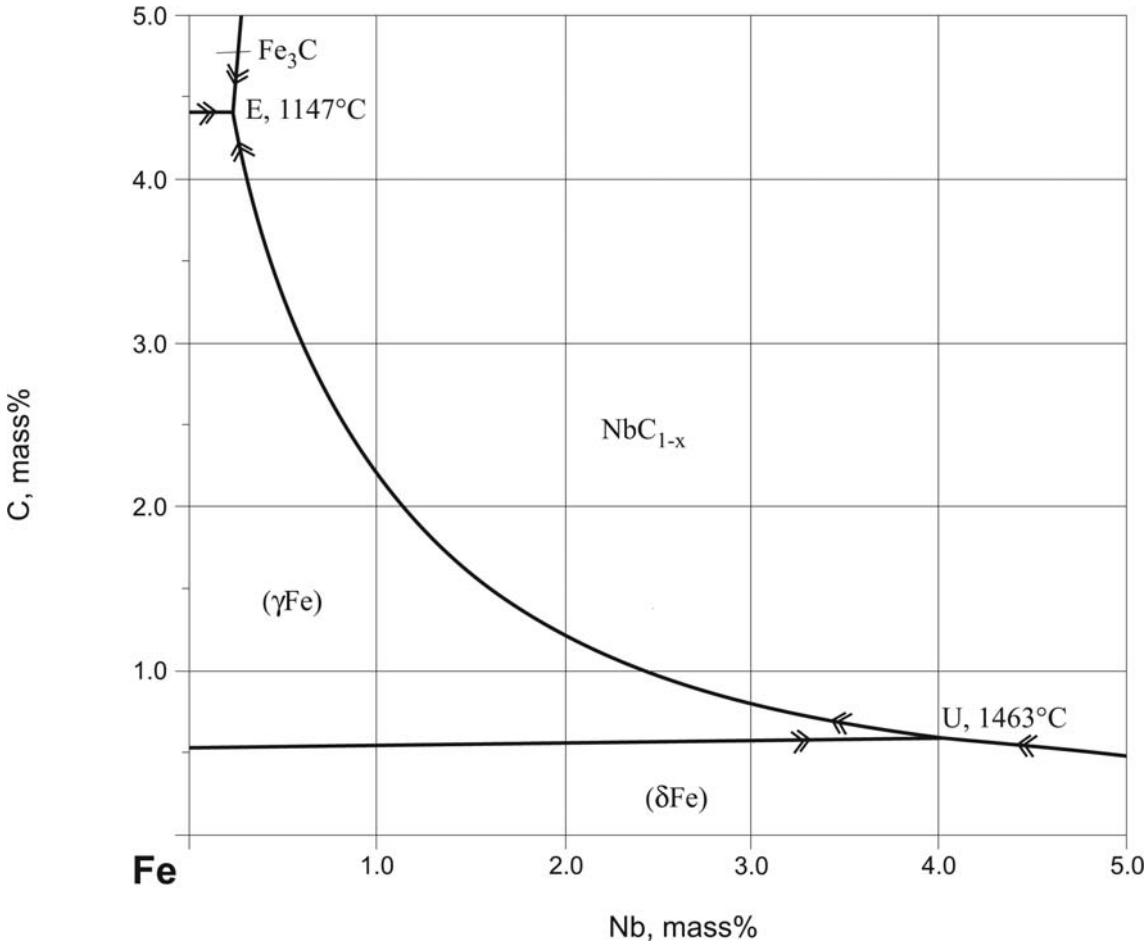

Fig. 2. C-Fe-Nb. Calculated partial liquidus projection for Fe rich alloys with metastable cementite

DOI: 10.1007/978-3-540-74196-1_9

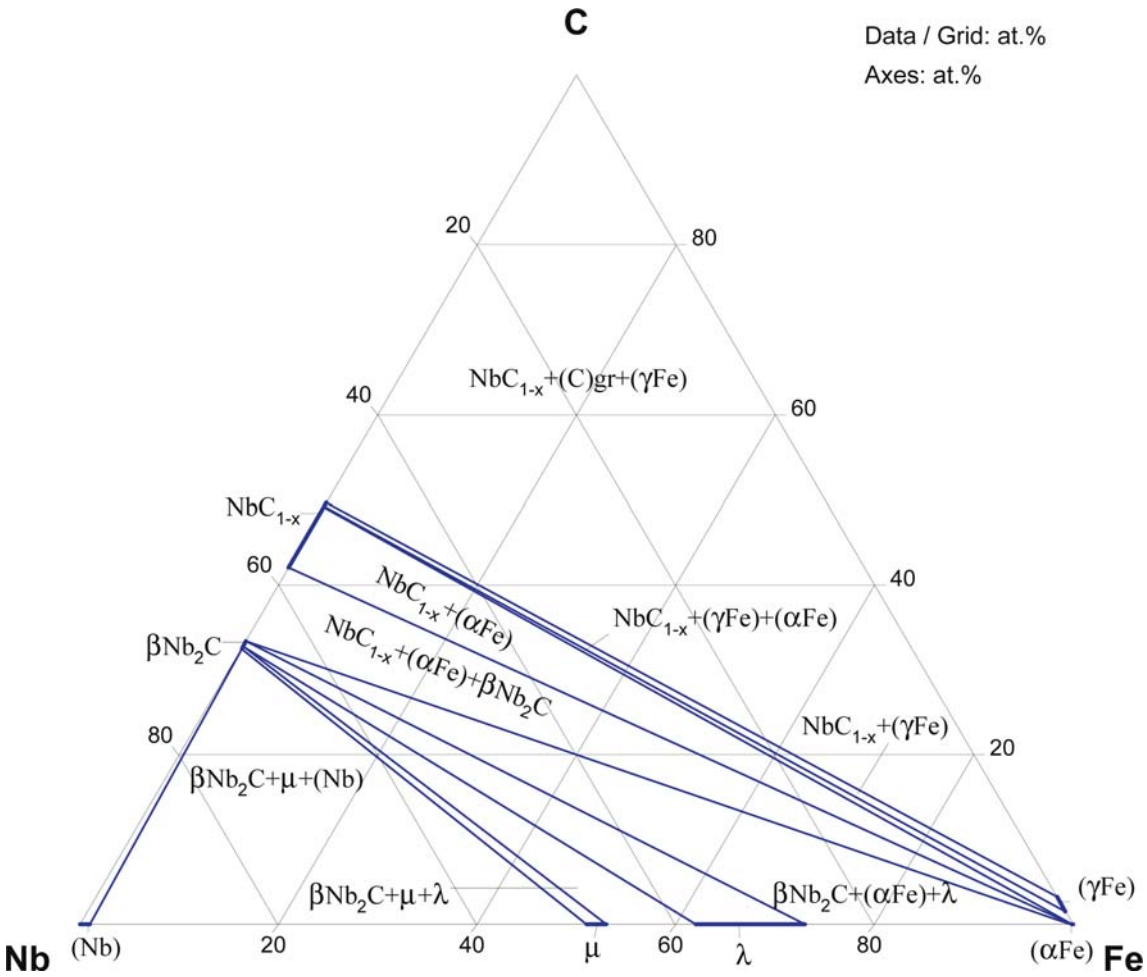

Fig. 3. C-Fe-Nb. Calculated isothermal section at 800°C

DOI: 10.1007/978-3-540-74196-1_9

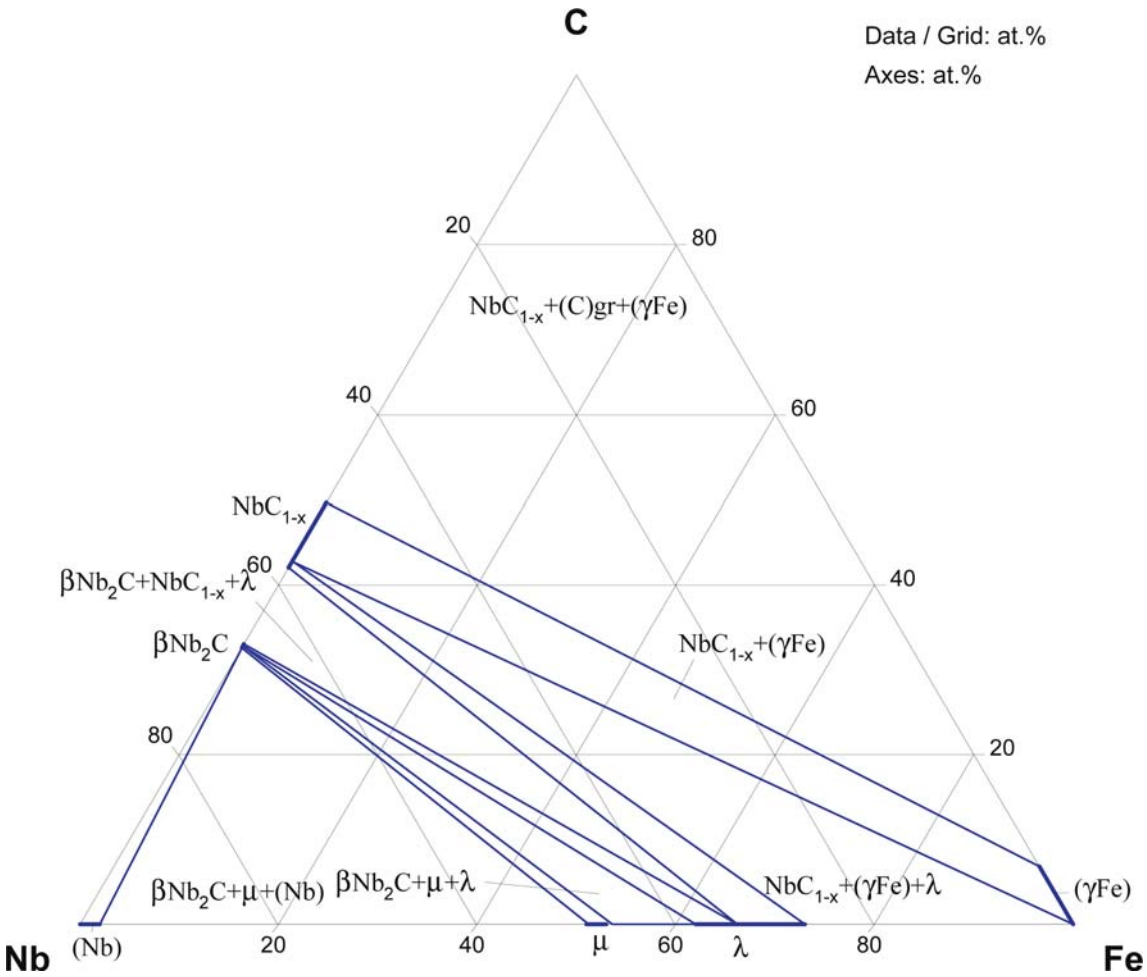

Fig. 4. C-Fe-Nb. Calculated isothermal section at 1000°C

DOI: 10.1007/978-3-540-74196-1_9

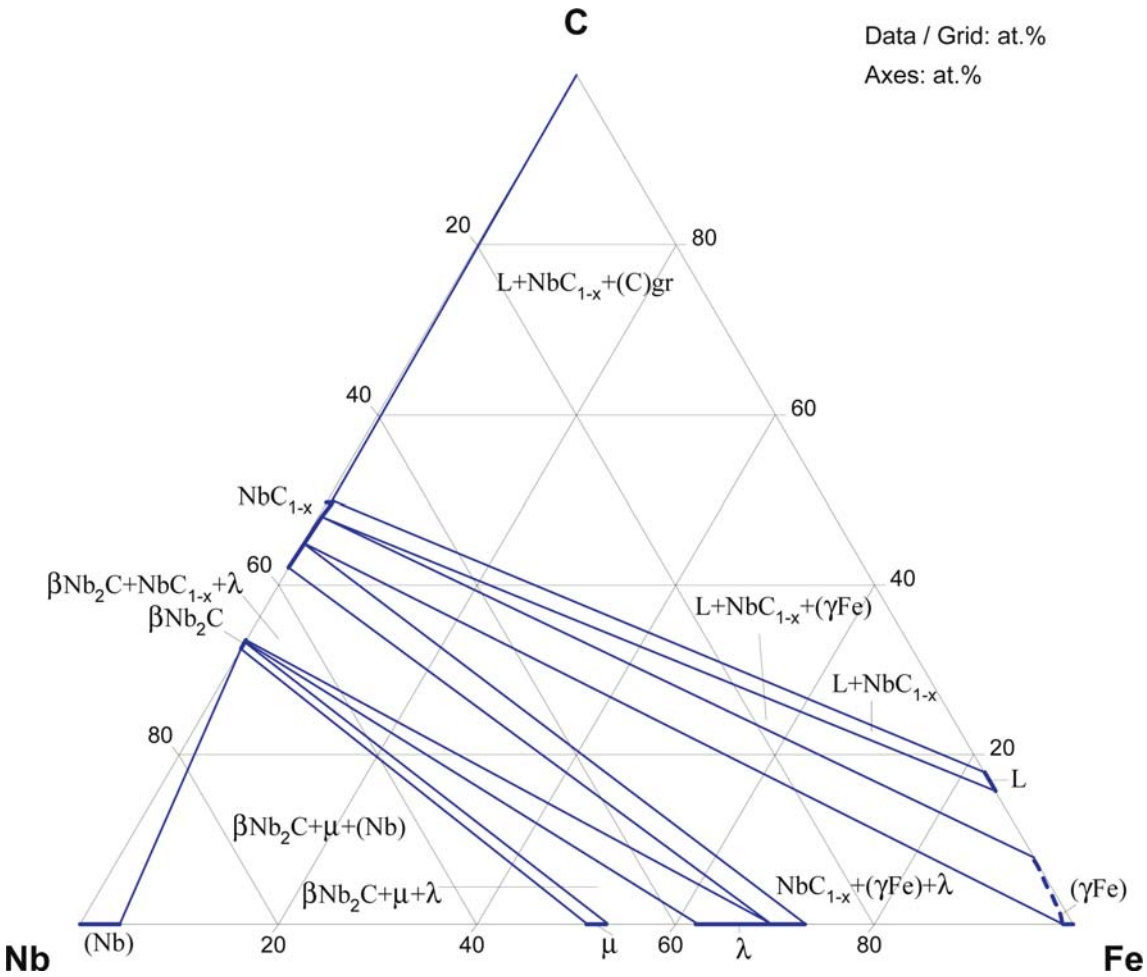

Fig. 5. C-Fe-Nb. Calculated isothermal section at 1200°C

DOI: 10.1007/978-3-540-74196-1_9

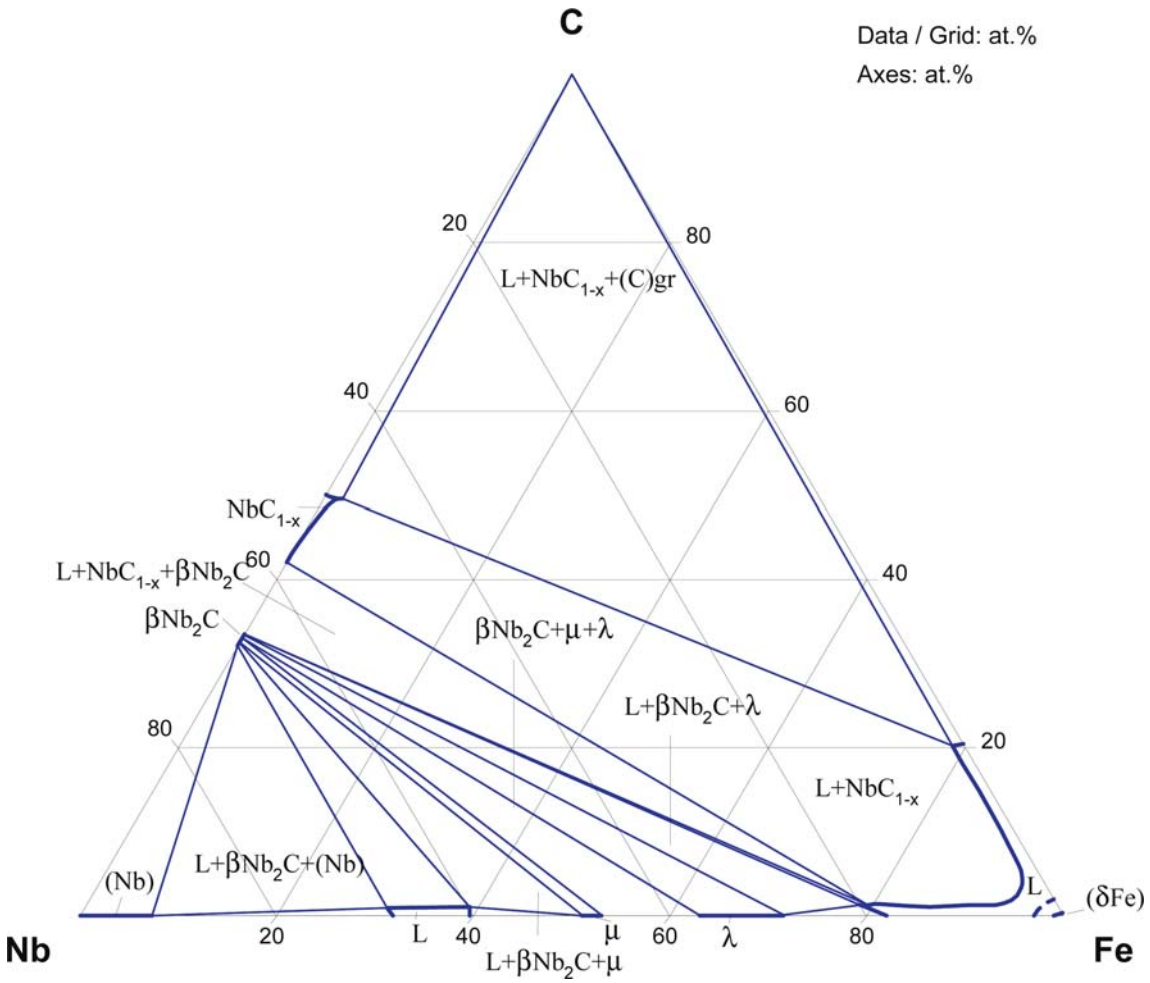

Fig. 6. C-Fe-Nb. Calculated isothermal section at 1500°C

DOI: 10.1007/978-3-540-74196-1_9

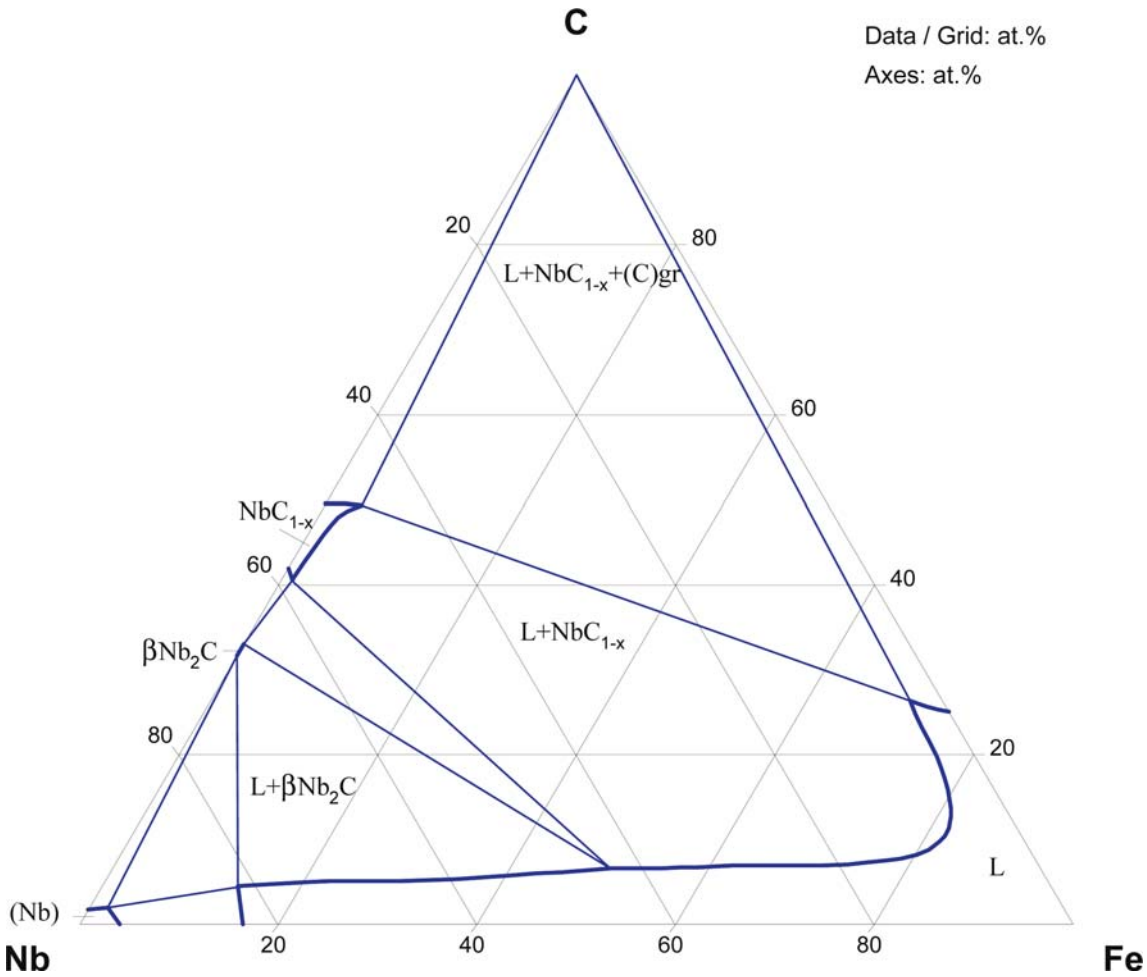

Fig. 7. C-Fe-Nb. Calculated isothermal section at 2000°C

DOI: 10.1007/978-3-540-74196-1_9

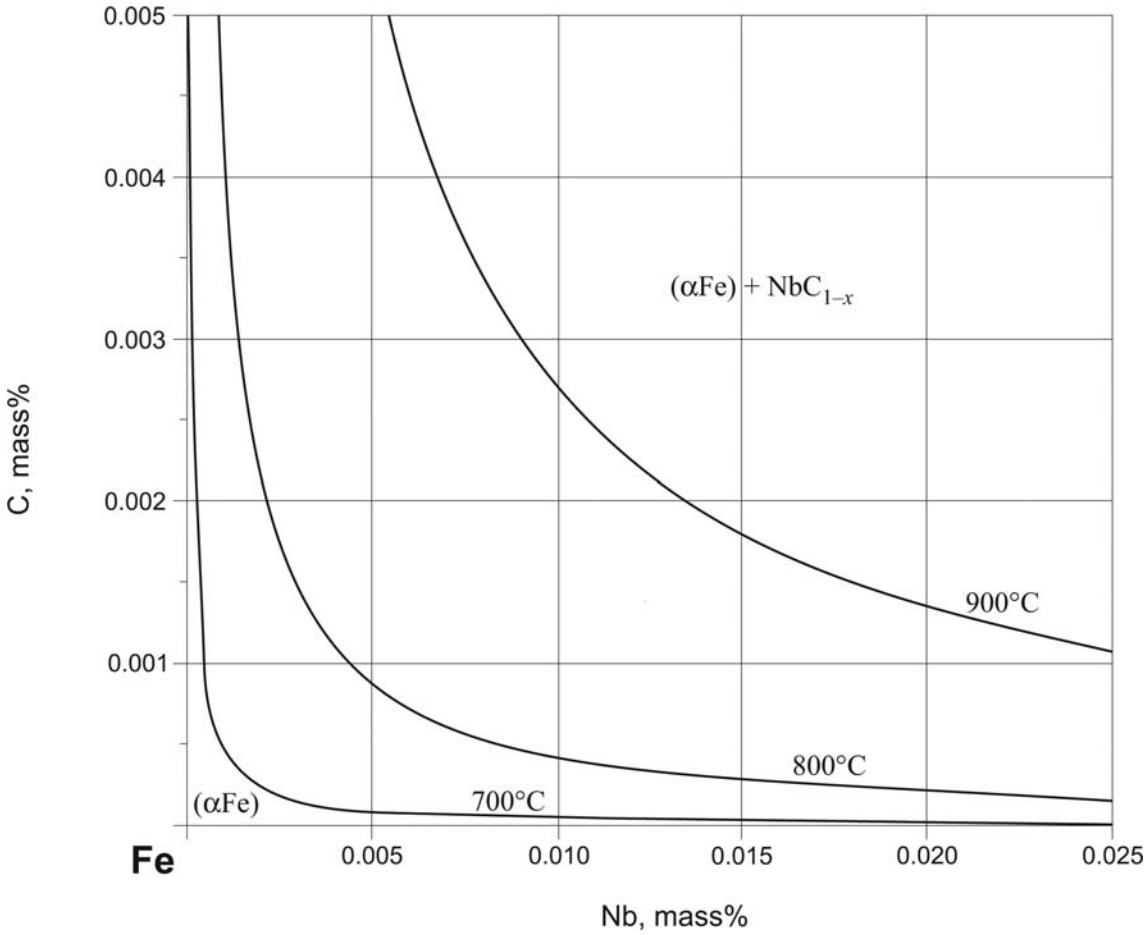

Fig. 8. C-Fe-Nb. Calculated solubility of NbC in ferrite

DOI: 10.1007/978-3-540-74196-1_9

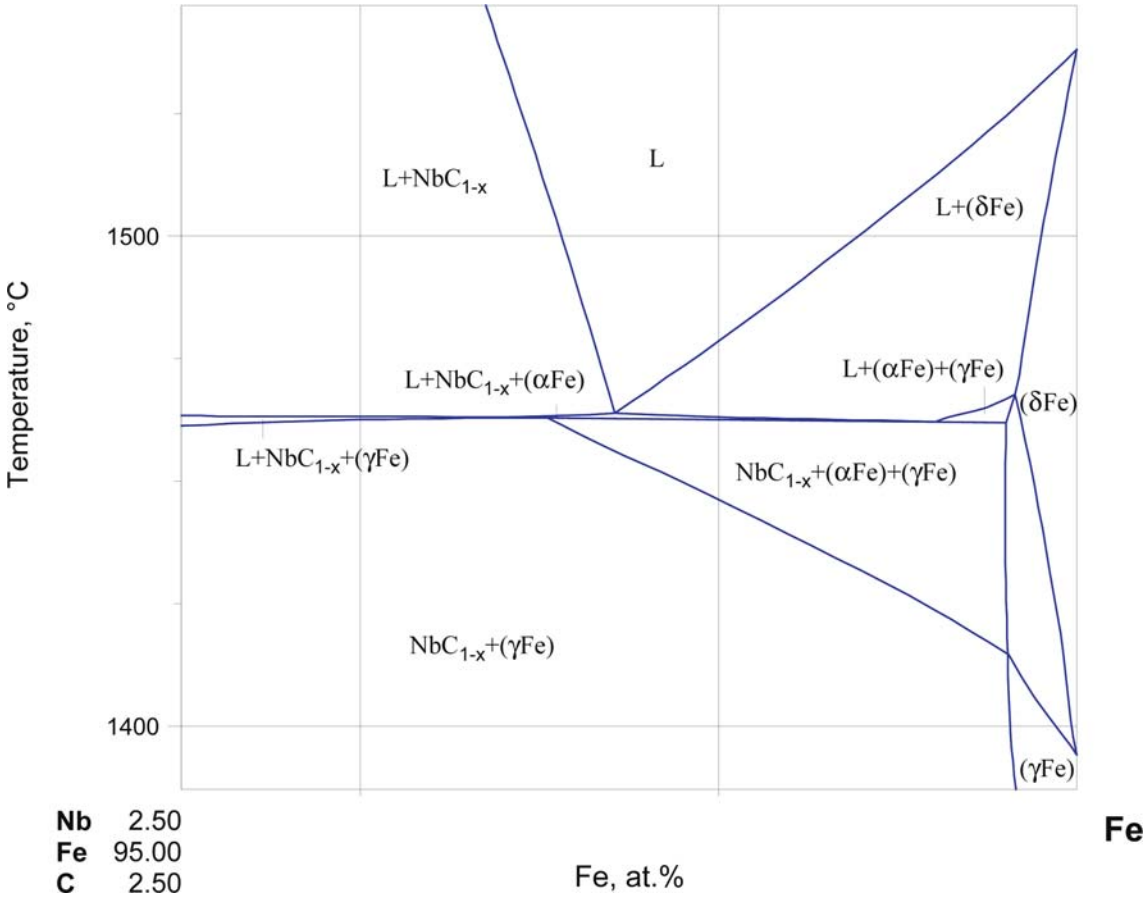

Fig. 9. C-Fe-Nb. Calculated Fe-NbC section

DOI: 10.1007/978-3-540-74196-1_9

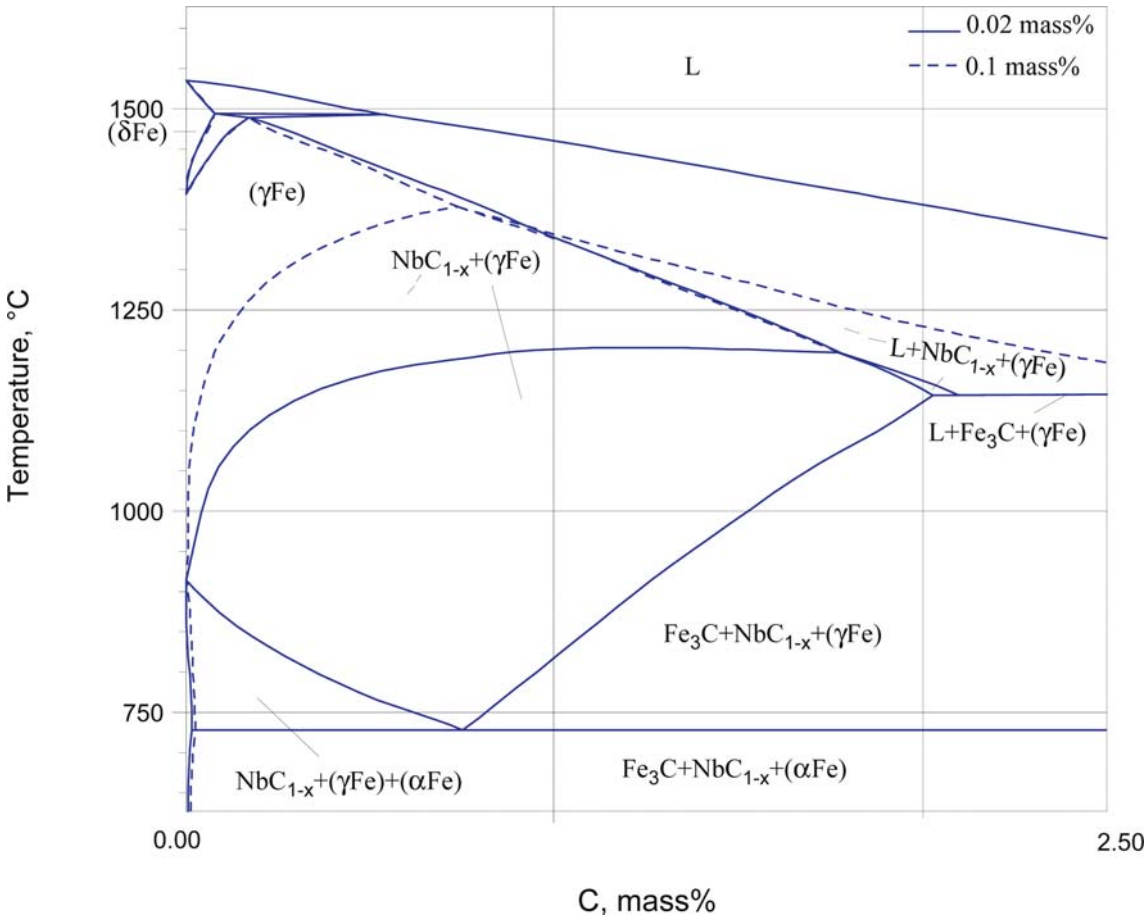

Fig. 10. C-Fe-Nb. Calculated metastable vertical sections for 0.02 and 0.1 mass% Nb

DOI: 10.1007/978-3-540-74196-1_9

References

[1938Egg] Eggers, H., Peter, W., "The Iron-Rich Corner of the Iron-Niobium-Carbon Phase Diagram Lower 1050°C" (in German), *Mitt. K. W. Inst. Eisenforschung*, **20**, 205–211 (1938) (Crys. Structure, Experimental, Morphology, Phase Diagram, 13)

[1940Kie] Kieffer, R., Hotop, W., "The Present Position of the Cermet" (in German), *Stahl Eisen*, **60** (24), 517–527 (1940) (Experimental, Morphology, Phase Diagram, 26)

[1949Jae] Jaenecke, E., "C-Fe-Nb" (in German), *Kurzgefasstes Handbuch aller Legierungen*, Winter Verlag, Heidelberg, 685–686 (1949) (Phase Diagram, Phase Relations, Review)

[1952Edw] Edwards, R., Raine, T., "The Solid Solubilities of Some Stable Carbides in Cobalt, Nickel and Iron at 1250°C", *Pulvermetallurgie, 1. Plansee Seminar, De Re Metallica, 22-26 Juni, 1952, Reutte/Tirol, (Hrsg.)* Benesovsky, F. (Ed.), Springer-Verlag, Wien, (1), 232–242 (1952) (Crys. Structure, Phase Relations, Experimental, 5)

[1959Fuw] Fuwa, T., Chipman, J., "Activity of Carbon in Liquid Iron Alloys", *Trans. Metall. Soc. AIME*, **215**, 708–716 (1959) (Calculation, Experimental, Phase Relations, Thermodyn., 22)

[1963Ell] Elliott, J.F., Gleiser, M., Ramakrishna, V., "Iron-Carbon-j Alloys", *Thermochemistry for Steelmaking*, Addision Wesley, Reading, MA, **2**, 531 (1963) (Review, Thermodyn.)

[1965Fed] Fedorov, T.F., Kuz'ma, Yu.B., Skolozdra, R.V., Popova, N.M., "Phase Equilibria in the Ternary Systems Zr-Co-C and Nb-Fe-C", *Powder Metall. Met. Ceram.*, **4**(12), 1010–1014 (1965), translated from *Poroshkov. Metall.*, **36**(12), 63–68 (1965) (Phase Diagram, Phase Relations, Morphology, 20)

[1966Smi] Smith, R.P., "The Solubility of Niobium (Columbium) Carbide in Gamma Iron", *Trans. Metall. Soc. AIME*, **236**, 220–221 (1966) (Experimental, Phase Diagram, Phase Relations, 8)

[1966Man] Mandry, P., Dornelas, W., "Solubility of Precipitates of Nb in Austenite in the Case of low Construction Steels Containing Very Quantities of Nb" (in French), *Compt. Rend. Acad. Sci. Paris, Ser. C*, **263C**, 1118–1121 (1966) (Crys. Structure, Experimental, Phase Relations, Phys. Prop., 7)

[1967Mey] Meyer, L., "On the Dissolution, Precipitation, and Age Hardening Effect of Niobium in Plain Carbon Steel" (in German), *Z. Metallkd.*, **58**(5), 334–339 (1967) (Experimental, Morphology, Phase Relations, Thermodyn., 21)

[1967Irv] Irvine, K.J., Pickering, F.B., Gladman, T., "Grain-Refined C-Mn Steels", *J. Iron Steel Inst., London*, **205**, 161–182 (1967) (Experimental, Mechan. Prop., Morphology, Phase Relations, 16)

[1968Nor] Nordberg, H., Aronsson, B., "Solubility of Niobium Carbide in Austenite", *J. Iron Steel Inst., London*, **206**, 1263–1266 (1968) (Calculation, Experimental, Mechan. Prop., Phase Relations, Thermodyn., 25)

[1975Fre] Frey, H., Holleck, H., "DTA Investigations of High Temperature Phase Equilibria in Ternary Transition Metal-Carbon Systems", *Thermal Analysis*, Proc. Internat. Conf., 4th, 8-13 July, 1974, Buzas, I., (Ed.), Akad. Kiado, Budapest, **1**, 339–348 (1975) (Experimental, Morphology, Phase Diagram, Phase Relations, 3)

[1981Bra] Brandis, H., Preisendanz, H., Schueler, P., "The Influence of Alloying Elements Titanium, Vanadium and Niobium on the Activity of Carbon in Fe-X-C Alloys in the Temperature Range from 900 to 1100°C" (in German), *Thyssen Edelst. Techn. Ber.*, **7**(1), 92–104 (1981) (Experimental, Thermodyn., 32)

[1984Lak] Lakshmanan, V.K., Kikaldy, J.S., "Solubility Product for Niobium Carbide in Austenite", *Metall. Trans. A.*, **15A**, 541–544 (1984) (Experimental, Morphology, Phase Diagram, Phase Relations, 32)

[1984Sha] Sharma, R.C., Lakshmanan, V.K., Kirkaldy, J.S., "Solubility of Niobium Carbide and Niobium Carbonitride in Alloyed Austenite and Ferrite", *Metall. Trans. A*, **15A**, 545–553 (1984) (Phase Relations, Experimental, 27)

DOI: 10.1007/978-3-540-74196-1_9

[1985Oht] Ohtani, H., Nishizawa, T., Tanaka, T., Hasebe, M., *Proceedings of the Japan-Canada Seminar on Secondary Steelmaking*, The Canadian Steel Industry Association and the Iron and Steel Institute of Japan, Tokyo, J-7-1 - J-7-12 (1985) as quoted by Raghavan, V., "C-Fe-Nb", *J. Phase Equilib.*, **24**(1), 57–61 (2003) (Phase Relations, Review, 12)

[1986Das] Das, R.C., Jha, R., Mukherjee, T., "The Carbon-Iron-Niobium System", *J. Alloy Phase Diagrams*, **2**(2), 131-140 (1986) (Phase Diagram, Thermodyn.)

[1986Bal] Balasubramanian, K., Kirkaldy, J.S., "Austenite-Nonstoichiometric Precipitate Equilibria in Microalloyed Steels. Part I: Fe-Ti-C and Fe-Nb-C Systems", *Calphad*, **10**(2), 187–202 (1986) (Phase Relations, Thermodyn., Calculation, 27)

[1987Smi] Smith, J.F., Carlson, O.N., de Avillez, R.R., "The Niobium-Carbon System: a Review", *J. Nucl. Mater.*, **148**(1), 1–16 (1987) (Crys. Structure, Phase Diagram, Phase Relations, Review, 116)

[1988Bal] Balasubramanian, K., Kirkaldy, J.S., "Thermodynamics of Fe-Ti-C and Fe-Nb-C Austenites and Nonstoichiometric Titanium and Niobium Carbides", *Advances in Phase Transitions*, Proc. Int. Symp., Ontario, Canada, 22-23 Oct., (1987), Embury, J.D., (Ed.), Pergamon Pr., Oxford, 37–51 (1988) (Phase Relations, Thermodyn., 37)

[1988Hon] Hong , Y., "Study on $\gamma/\gamma+NbC_x$ Phase Boundary in Fe-Nb-C System", *Acta Metall. Sin.*, **24**(1), B44–B48 (1988) (Experimental, Thermodyn., 19)

[1988Uhb] Ubhi, H.S., Baker, T.N., "Electrical Resistivity Contribution from Niobium in Dilute Fe-Nb Alloys at 77 K (for use in precipitation studies)", *J. Mat. Sci. Lett.*, **7**(5), 466 (1988) (Experimental, Magn. Prop., 5)

[1989Kes] Kesri, R., Hamar-Thibault, S., "MC Carbides in Ternary Fe-M-C System (M = V, Nb) - Composition, Morphology and Order", *Z. Metallkd.*, **80**(7), 502–510 (1989) (Crys. Structure, Experimental, Morphology, Phase Diagram, 19)

[1989Mal] Malik, A.U., Ishaq, M., Ahmad, Sh., Ahmad, Su., "Influence of Carbon on the Hot Corrosion Behaviour of Fe-base Alloys", *Mater. Trans., JIM*, **30**(9), 707–716 (1989) (Crys. Structure, Experimental, Kinetics, Morphology, 14)

[1989Oht] Ohtani, H., Hasebe, M., Nishizawa, T., "Calculation of the Fe-C-Nb Ternary Phase Diagram", *Calphad*, **13**(2), 183–204, (1989) (Assessment, Calculation, Phase Diagram, Thermodyn., 36)

[1990Hua] Huang, W., "A Thermodynamic Evaluation of the Fe-Nb-C System", *Z. Metallkd.*, **81**(6), 397–404 (1990) (Assessment, Calculation, Phase Diagram, Phase Relations, Thermodyn., #, *, 49)

[1993Ber] Bergman, A., Jarfors, A., Liu, Z., Fredriksson, H., "In-situ Formation of Carbide Composites by Liquid/Solid Reactions", *Key Eng. Mater.*, **79–80**, 213–233 (1993) (Experimental, Phys. Prop., 9)

[1991Fan] Fan, P., Zhou, Y., Yang, T., Dong, Y., Wei, S., "Solubility of Nb in Carbon Saturated Liquid Iron", *Acta Metall. Sin.*, **27**(2), B143–B145 (1991) (Experimental, Phase Diagram, Phase Relations, 3)

[1991Has] Hasegawa, H., Saito, M., Kojima, A., Makino, A., Misaki, Y., Watanabe, T., "Crystallization Behavior of Fe-M-C (M = Ti, Zr, Hf, V, Nb, Ta) Films", *IEEE Trans. J. Magn. Jpn.*, **6**(2), 120–126 (1991) (Crys. Structure, Experimental, Phase Relations, 6)

[1992Bal] Balasubramanian, K., Kroupa, A., Kirkaldy, J.S., "Experimental Investigation of the Thermodynamics of Fe-Nb-C Austenite and Nonstoichiometric Niobium and Titanium Carbides (T = 1273 to 1473 K)", *Metall. Trans. A*, **23A**(3), 729–744 (1992) (Calculation, Crys. Structure, Experimental, Phase Diagram, Phase Relations, Theory, Thermodyn., 51)

[1994Ji] Ji, J., Sun, Y., Liu, Y., "High Temperature Internal Friction for Fe-Nb-C Alloys", *Acta Metall. Sin.*, **30**(5), A210–A216, (1994) (Experimental, Phys. Prop., 15).

[1994Wil] Wilson, E.A., "The γ-α-Transformation in Low Carbon Irons", *ISIJ Int.*, **34**(8), 615–630, (1994) (Review, 124)

[1995Tay] Taylor, K.A., "Solubility Products for Titanium-, Vanadium-, and Niobium-Carbide in Ferrite", *Scr. Metall. Mater.*, **32**(1), 7–12 (1995) (Experimental, 13)

DOI: 10.1007/978-3-540-74196-1_9

[1996Lou] Lou, T.P., Ding, B.Z., Gu, X.J., Li, G.S., Hu, Z.Q., "Mechanical Alloying of Fe-Nb-C Materials", *Mater. Lett.*, **28**(1–3), 129–132 (1996) (Experimental, Phys. Prop., 7)

[1998Hil] Hildebrand, H., Heinzel, G., Schreiber, G., "Characterization of Dual Phase/Dispersion Mixed Microstructure in a Fe-Nb-C Alloy", *Prakt. Metallogr.*, **35**(5), 255–266, (1998) (Experimental, Phys. Prop., 17)

[1998Zaj] Zajac, S., Jansson, B., "Thermodynamics of the Fe-Nb-C-N System and the Solubility of Niobium Carbonitrides in Austenite", *Metall. Mater. Trans. B*, **29B**, 163–176 (1998) (Calculation, Phase Relations, Thermodyn., 33)

[1999Pop] Popov, V.V., "Diffusion Interaction of Carbides, Nitrides and Carbonitrides With Iron and Steels", *Metallofizika Nov. Tekh.*, **21**(2), 99–103 (1999) (Experimental, Phase Relations, Transport Phenomena, 11)

[2000Bya] Byakova, A.V., "Structural Aspects of Strength and Methods to Increase the Serviceability of Carbide Coatings", *Powder Metall. Met. Ceram.*, **39**(1–2), 85–91 (2000) (Crys. Structure, Experimental, Mechan. Prop., 13)

[2001DeA] DeArdo, A.J., "Fundamental Metallurgy of Niobium in Steel", *Niob. Sci. Tech.*, 427–500 (2001) (Calculation, Experimental, Kinetics, Morphology, Phase Diagram, Phase Relations, Phys. Prop., Review, Thermodyn., 226)

[2001Lee] Lee, B.-J., "Thermodynamic Assessment of the Fe-Nb-Ti-C-N System", *Metall. Mater. Trans. A*, **32A**, 2423–2439 (2001) (Assessment, Calculation, Phase Diagram, Phase Relations, Thermodyn., 90)

[2001Yu] Yu, N., Ji, J.W., "Medium Temperature Internal Friction of the Fe-Nb-C Alloys", *Acta Metall. Sin.* **37**(11), 1169–1173 (2001) (Experimental, Phys. Props., 12)

[2002Mar] Maruyama, N., Smith, G.D.W., "Effect of Nitrogen and Carbon on the Early Stage of Austenite Recrystallisation in Iron-Niobium Alloys", *Mater. Sci. Eng. A- Struct. Mater. Prop. Microstruct. Process*., **327** (1 Special Issue SI), 34–39, (2002) (Experimental, Phys. Prop., 25)

[2002Yu] Yu, N., Ji, J.W., "The Internal Friction of Deformed Fe-Nb-C Alloys in the Range from Room Temperature to 180°C", *Acta Metall. Sin.* **38**(3), 230–234 (2002) (Experimental, Phys. Prop., 11)

[2003Rag] Raghavan, V., "C-Fe-Nb", *J. Phase Equilib.*, **24**(1), 57–61 (2003) (Phase Relations, Review, 12)

[2004Bem] Bemont, E., Cadel, E., Maugis, P., Blavette, D., "Precipitation of Niobium Carbides in Fe-C-Nb Steel", *Surf. Interface Anal*., **36**(5-6), 585–588, (2004) (Experimental, Phys. Prop., 12)

[2004Sho] Shohoji, N., "M-C Dipole Formation in fcc (Face Centered Cubic) $Fe_{1-y}M_yC_x$ Solid Solution (M = Ti, Nb)", *Mater. Sci. Technol*., **20**(3), 301–306 (2004) (Calculation, Thermodyn., 16)

[2006MSIT] "C-Fe (Iron-Carbon)", Diagrams as Published, in *MSIT Workplace*, Effenberg, G. (Ed.), Materials Science International Services, GmbH, Stuttgart; Document ID: 30.13598.1.20 (2006) (Crys. Structure, Phase Diagram, Phase Relations, 2)

[Mas2] Massalski, T.B. (Ed.), *Binary Alloy Phase Diagrams*, 2nd edition, ASM International, Metals Park, Ohio (1990)

[V-C] Villars, P. and Calvert, L.D., *Pearson's Handbook of Crystallographic Data for Intermetallic Phases*, ASM, Metals Park, Ohio (1985)

[V-C2] Villars, P. and Calvert, L.D., *Pearson's Handbook of Crystallographic Data for Intermetallic Phases*, 2nd edition, ASM, Metals Park, Ohio (1991)

DOI: 10.1007/978-3-540-74196-1_9

Carbon – Iron – Nickel

Nathalie Lebrun, Pierre Perrot

Introduction

The C-Fe-Ni system has raised much interest as a basis of stainless steels. The first realistic diagram was proposed by [1925Kas1, 1925Kas2] which presents liquidus lines up to 1700°C and, often reproduced [1949Jae, 1984Riv, 1985Riv, 1988Ray]. It is actually in good agreement with the more recent determination of [1986Sch] and calculations of [1987Sch]. The main investigations on the ternary system concern the solubility measurements of carbon in the γ and liquid phases which go always with activity measurements, the determination of the phase diagram under high pressure (~6 GPa) because of the interest of such diagrams in the crystal growth of industrial diamonds and the kinetics studies of the austenite transformation in martensite or bainite because these phases are important in the forecast of mechanical properties of steel. The main experimental investigations on the crystal structure, phase equilibria and thermodynamics are gathered in Table 1.

Binary Systems

The C-Fe phase diagram accepted from [2006MSIT] is based mainly on [Mas2] except for the liquid composition in the eutectic reaction L ⇌ (γFe) + (C). This composition is taken from the data of [2000Fen, 2001Fen]. The C-Ni diagram is accepted from [Mas2] and has been assessed by [1989Sin]. The solubility of C in liquid Ni has been determined by [1963Sch] which proposes the following expression:
$\log_{10} x_C = -0.462 - (895.7 / T)$
The binary Fe-Ni phase diagram is accepted from [2007Kuz].

Solid Phases

There is no ternary phase in this system. The details of the crystal structure and lattice parameters of the unary and binary phases are listed in Table 2 for the stable, metastable and high pressure phases. Metastable carbides such as cementite are well known. Other metastable carbides such as ε, γ and θ may be observed during the ageing of martensite [1997Gen]. [1975Shi] measured the thermal expansion coefficients of the lattice parameters in its stable domain leading a higher value along the *c* axis ($\alpha_c = 15.10^6$ deg^{-1}) than along the *a* and *b* axis ($\alpha_a = \alpha_b = 7 \cdot 10^6$ deg^{-1}). Pressure stabilizes the $(Fe,Ni)_3C$ carbide [1991Pav, 1993Pav]. The lattice parameters of ferromagnetic cementite were measured up to 300°C in ternary C-Fe-Ni alloys annealed at temperatures of 600-1000°C [1979Kag]. Nickel decreases all the lattice parameters and makes cementite less stable.
A martensite α' phase is observed in the quenched austenite (γFe) in Fe rich alloys [2003Dan, 2003Kap] and in quenched CFeNi specimens [1997Gen]. During the first (γFe) - α' - (γFe) cycle of 76.0Fe-23.5Ni-0.5C (mass%) steel, the amount of martensite formed during cooling run diminishes by 12% and it further decreases by 7% after 100 additional cycles. An orthorhombic body centered structure of martensite was observed by [2003Dan] at –185°C with lattice parameters *a* = 285.5, *b* = 284.9 and *c* = 294.0 (in pm) and a tetragonal degree *c/a* = 1.03. On heating from –185°C to room temperature, the lattice parameter *c* reaches its minimum value at –50°C and then increases, whereas *a* and *b* remain almost unchanged. Similar thermal behaviors have been observed after four (γFe) - α' - (γFe) cycles but the lattice parameter *c* increases less than during the first cycle. A body centered tetragonal strain-induced martensite α' has also been obtained by [2003Kap] under cold rolling conditions with about 20 and 40% reduction in studied C-Fe-Ni alloys (79.4Fe - 20.0Ni - 0.6C and 86.7Fe - 12.0Ni - 1.3C).

MSIT®
DOI: 10.1007/978-3-540-74196-1_10

The crystal lattice of the carbide, precipitating during tempering of the martensite in Fe-20.3Ni-0.52C alloy, slightly deviates from the hexagonal symmetry at 200°C [1991Vod] with an orthorhombic distortion of 2.8%. As no superstructure spots were observed in the diffraction patterns, it is impossible to determine whether the carbide was isomorphous with Co_2N or the hexagonal lattice of the carbide was distorted by the carbon atoms ordered in octahedral positions.

Invariant Equilibria

The monovariant equilibrium L ⇌ (γFe,Ni) + C exists in the system C-Fe-Ni at atmospheric pressure [1993Koc]. From C-Fe-Ni melts, the graphite and the diamond phases undergo respectively a ternary eutectic L ⇌ (γFe,Ni) + Fe_3C + (C)gr (below 4.9 GPa) [2002Sol] and L ⇌ (γFe,Ni) + Fe_3C + (C)d (above 4.9 GPa) [1991Pav, 2002Sol]. The eutectic involving the diamond phase was observed at 4.7 and 6 GPa in the work done by [1993Koc, 1996Koc]. The melting temperature of these ternary reactions strongly depends on the experimental conditions and rather contradictory values are observed in the literature. From quenching method, [1991Pav] measured a melting at 1392°C under 5.7 GPa. A lower temperature (1057°C under 6 GPa) has been found by [1993Koc]. More recently, [2002Sol] measured the melting temperature of these ternary eutectics in Fe60Ni40C20 (mass%) alloy under 4.6, 5 and 5.2 GPa leading to a pressure dependence of the eutectic temperature as followed: Te (K) = 1346 + 30p (GPa). [1993Koc, 1991Pav] reported the composition of the eutectic E (L ⇌ (γFe,Ni) + Fe_3C + (C)d) to be 71.72Fe-24.03Ni-4.25C (mass%) under 6 GPa and 73.25Fe - 22Ni - 4.75C under 5.7 GPa, respectively. A U type ternary reaction L + Fe_7C_3 ⇌ Fe_3C +(C)d has also been measured by [1993Koc] at 1312°C with the following composition at 86.18Fe-8.37Ni-5.45C (mass%). Invariant equilibria investigated under 6 GPa [1993Koc] are reported in Table 3.

Liquidus, Solidus and Solvus Surfaces

[1925Kas1, 1925Kas2] first reported a partial liquidus surface along the Fe-Ni side up to 6 mass% C showing non accurate isothermal lines. Nevertheless, general consistencies were observed with the more accurate work done by [1964Buc, 1986Sch]. Partial results of carbon solubility in molten Fe-Ni alloys were also reported by [1956Tur, 1960Mil, 1960War, 1963Sch]. The results of [1956Tur] at 1350 and 1550°C deviate from results given by [1960War] and are not consistent with the binaries. The 1600°C contour of [1963Sch] overlaps with the isothermal line at 1550°C reported by [1960War]. Consequently data reported by [1956Tur, 1963Sch] have not been retained in the present evaluation. The isotherms of the (γFe) and (C)gr liquidus surfaces calculated from 1200 up to 1700°C by [1987Gab, 1987Sch] are in good agreement with the experimental curves. The assessed liquidus surface is shown in Fig. 1 and is mainly based on the review of [1984Riv, 1985Riv, 1988Ray] with slight modification according to the accepted binary systems. The reviews of [1984Riv, 1985Riv, 1988Ray] suggested the existence of a minimum on the e_1-e_2 eutectic valley with no experimental evidence. Since the existence of this minimum is doubtful, it has been not reported on the accepted liquidus surface.

A liquidus surface of the C-Fe-Ni system was reported by [1991Pav] under 5.7 GPa and by [1993Koc] under 6 GPa. Large discrepancies are observed concerning the shape of the curves. [1993Koc] suggested the existence of a ternary reaction involving the Fe_7C_3 phase not reported in [1991Pav]. Based on experimental measurements, the liquidus surface proposed by [1993Koc] seems to be more realistic. Moreover, the calculation undertaken by [1991Pav] lead to a large discrepancies between the melting temperatures of the ternary eutectic deduced from different methods of calculation (variation more than 100°C). Consequently, the liquidus proposed by [1993Koc] has been reported in Fig. 2 with slight modifications according to the C-Fe and Fe-Ni binaries determined at 5.9 and 5.4 GPa, respectively [1996Koc]. The isothermal line at 1737°C has been added as well as the solvus of the (γFe,Ni) domain. The liquidus surface has also been determined under 4.7 GPa where only the eutectic ternary reaction L ⇌ (γFe,Ni) + Fe_3C + (C)d exits [1993Koc] with a melting temperature at about 1077°C.

A solidus map in the iron rich part with 15 mass% Ni and 1 mass% C has been measured by [1964Buc] and is shown in Fig. 3. The (δFe) solidus surface is planar and the limit of its solubility follows a straight line course. The (γFe) solidus surface falls very steeply from the nickel rich side to the carbon rich side of the system.

DOI: 10.1007/978-3-540-74196-1_10

The solubility of C in (γFe) has been extensively measured at 800, 1000 and 1200°C [1969Fra, 1971Wad, 1976Tom] and calculated at 800, 1000 and 1200°C [1968Chi, 1971Gre, 1971Wad, 1984Riv, 1985Riv]. Results of [1971Gre] have been rejected since they found a limited solubility of nickel in (γFe) in disagreement with the accepted Fe-Ni binary. Moreover, the isothermal line at 1200°C could not be extrapolated to the C-Fe boundary since the eutectic reaction involving (γFe) and (C)gr occurs at 1153°C. All the results are in general agreement and show that the (γFe) field is reduced in extent as the Ni content rises and the temperature falls. At Ni contents of 70-80 mass%, the composition effect is reversed. The (γFe) / (γFe)+C boundary at 800, 1000 and 1200°C are reproduced in Fig. 4 from [1984Riv, 1985Riv, 1988Ray] with slight modifications concerning the isothermal line at 1200°C.
The extension of the austenite field in the C-Fe-Ni system below 900°C has been calculated [1977Uhr, 1978Uhr] and was reported in Fig. 5. The line with an arrow indicates the composition of the austenite (γFe,Ni) in simultaneous equilibrium with $(Fe,Ni)_3C$ and ferrite (αFe). Slight modifications have been done according to the binary edges.

Isothermal Sections

The equilibrium of (γFe) and liquid have been measured at 1450°C [1964Buc] and between 1200 and 1400°C by [1983Mor]. Results were well reproduced by calculation involving thermochemical data. [1964Buc] also calculated the isothermal section in the Fe rich corner at 1500°C involving the (δFe), (γFe) and the liquid phases. The two isothermal sections are reported in Figs. 6 and 7.
Several partial metastable isothermal sections in the iron rich corner are available in the literature from 390°C to 1127°C [1973Sha, 1976Kle, 1978Rom, 1977Uhr, 1978Uhr, 1992Gon, 1994Rag]. The diagrams showing a domain of the cementite $(Fe,Ni)_3C$ phase are metastable as pointed out by [1978Kri] who showed that the carbon solubility in (γFe,Ni) alloy is lower when the alloy is in equilibrium with pure graphite than when the alloy is in equilibrium with cementite. General good agreements are observed between the calculated curves and the measured ones. Some of them are reported in the review done by [1988Ray, 1994Rag]. Nickel depressed the solubility of carbon in ferrite (αFe). At 1.4 mass% Ni, the solubility value varies between $5 \cdot 10^{-4}$ mass% C at 390°C and 0.01 mass% C at 670°C [1976Kle]. Some isothermal sections are shown in Figs. 8 to 13. The solubility ranges of the binary phases were adjusted in the isothermal sections according to the accepted binaries. As a consequence, the location of the three-phase field (αFe) + $(Fe,Ni)_3C$ + (γFe, i) was changed at 450 and 550°C.
Using sublattice model, thermodynamic calculations of the ferrite-austenite equilibrium have been carried out by [2001Qui] and isothermal sections in the iron rich corner at 300 and 450°C have been computed at atmospheric pressure.
Based on experimental data of [1971Str], [1996Koc] proposed an isothermal section at 1400°C and 5.7 GPa showing the three-phase equilibria L + (γFe,Ni) + (C)gr and L + Fe_3C + (C)gr, shown in Fig. 14.

Temperature – Composition Sections

The isopleths at 1 mass% Ni and 0.3 mass% C have been experimentally determined in the iron rich corner of the C-Fe-Ni system [1970Zem]. The polythermal section proposed at 0.3 mass% by [1970Zem] does not fit well with the binary C-Fe and has been rejected. The accepted isopleth at 1 mass% Ni from [1970Zem] shown in Fig. 15 matches well with the Fe-Ni binary system. The solubility of C in (αFe,Ni) (1 mass% Ni) presents a maximum of 0.022 mass% at 800°C
The solubility of carbon in (αFe) in metastable equilibrium with (γFe) was calculated by [1967Rao]. Increasing of Ni content leads to smaller solubility.
Using the computer program MatCalc, [2000Koz] calculated the *para*-equilibrium and the *ortho*-equilibrium phase diagram $Fe_{97.14}Ni_{2.86}$ - $Ni_{0.63}C_{99.37}$. It shows that Ni is a very effective austenite stabilizer and opens a wide austenite / ferrite / cementite three-phase field as indicated in Fig. 16. Under more metastable (*para*-equilibrium) conditions, the region is reduced to a quasi-eutectoid temperature at about 675°C.
The polythermal section from 58.80Fe-41.20Ni to 54.23Fe-38Ni-7.78C was also calculated at 5.2 GPa [2002Sol] from experimental measurements of [1993Koc] and is drawn in Fig. 17.

DOI: 10.1007/978-3-540-74196-1_10

Thermodynamics

The carbon activity in (γFe,Ni) has been experimentally determined by means of H_2-CH_4 equilibria at 800, 1000 and 1200°C [1971Wad], at 750, 825, 900, 975, 1050 and 1125°C [1971Gre], at 700, 800, 900, 1000 and 1060°C [1973Nat], by means of CO-CO_2 equilibria at 1000°C [1960Smi, 1980Ram] and by equilibration of carbon between specimens of different nickel content within a sealed silica capsule at 800, 1000 and 1200°C [1963Hec, 1969Fra, 1976Tom]. In the temperature range 800-1200°C, up to 30 at.% Ni in the alloy, the interaction parameter determined by [1963Hec] is: $\varepsilon_C^{(Ni)} = (\partial \ln f_C / \partial x_{Ni}) = 1.3 + (3500/T)$, which may be compared to the interaction parameter proposed by [1973Nat] and accepted by [1985Eno]: $\varepsilon_C^{(Ni)} = -2.2 + (7600/T)$. Both expressions agree at 900°C, but their slopes differ. The analysis of [1971Gre] suggests two temperature dependent parameters; the second order parameter becomes of importance at low temperatures. The activity coefficient presents a clear maximum towards 70 at.% Ni, where the carbon solubility is at minimum [1975Sri, 1980Ram]. For instance, [1980Ram] measures at 1000°C the carbon solubility in various (γFe,Ni) alloys in equilibrium with a CO-CO_2 atmosphere which imposes a constant carbon activity ($a_C = 0.72$ with reference to graphite). The carbon solubility, 1.20 mass% in pure iron, decreases with the nickel content down to a minimum of 0.09 mass% for 70 mass% Ni in the alloy, then increases to reach 0.18 mass% for pure nickel. [2004Tao] presents a statistical model of carbon behavior in the Fe-Ni solid solution, which evaluates the excess entropy and the enthalpy of solids by mean of new expressions of the configurational partition functions of solid solutions derived from statistical thermodynamics. This model introduces less empirical parameters than the preceeding ones [1968Zup, 1977Ach, 1977Eli, 1977Uhr], presents a clearer physical meaning and agrees well with the experimental determinations of [1971Wad]. The central atom model was also used by [1985Eno] to calculate the stable equilibrium and the *para*-equilibrium in the (α + γ) two-phase domain. Paraequilibrium diagrams may be seen in [2000Koz]. Cementite was shown to be the only stable carbide under paraequilibrium conditions. An evaluation of the C-Fe-Ni was carried out by [1987Gab] using a two sublattice subregular model for the interstitial solution phase taking into account the magnetic contribution. A sublattice model was also used by [1995Lee] to describe the Gibbs energy of individual phases present in basic stainless steels. The liquid phase is described by an ordinary subregular solution model.

The carbon activity in liquid alloys has been experimentally determined by means of CO-CO_2 equilibrium at 1560°C [1959Fuw] and by equilibrating C-Fe binary alloys with C-Fe-Ni ternary alloys in an isothermal closed chamber through transport in the gas phase [1972Foo], then modeled with a Redlich-Kister development [1977Eli] and calculated in the temperature range 1300-1700°C. At low nickel content, the interaction parameter in the liquid phase is:

$e_C^{(Ni)} = (\partial \log_{10} f_C / \partial (\text{mass\% Ni})) = 0.01$ or $\varepsilon_C^{(Ni)} = (\partial \ln f_C / \partial x_{Ni}) = 2.4$ at 1550°C [1972Foo], in good agreement with the values of 0.012 and 2.9 at 1560°C proposed by [1959Fuw] for $e_C^{(Ni)}$ and $\varepsilon_C^{(Ni)}$ respectively and with the value $\varepsilon_C^{(Ni)} = 2.637$ accepted by [2001Ma]. [1972Foo] suggested the introduction of second order parameters (based on mass%):

$e_C^{(Ni,\ Ni)} = (\partial^2 \log_{10} f_C / \partial (\text{mass\% Ni})^2) = 1.5 \cdot 10^{-3} e_C^{(Ni,C)} = (\partial^2 \log_{10} f_C / \partial (\text{mass\% Ni})\ \partial (\text{mass\% C})) = 2.6 \cdot 10^{-4}$.

Nickel decreases the solubility of carbon in liquid alloys. That trend is expected to continue up to 75 at.% Ni, where the carbon solubility is at minimum according to the experimental observations [1956Tur, 1959Neu, 1960Mil, 1960War]. The minimum of solubility is probably due to the ordering of (γFe,Ni) alloys around the composition Fe_3Ni, even in the liquid phase. The integral enthalpy of mixing of liquid alloy presents a minimum of -5.6 kJ·mol^{-1} at 75 at.% Fe [1960War, 1962Pet].

Empirical expressions calculated from the experimental data of [1963Hec, 1966Smi] have been proposed to describe the carbon activity in the γ phase [1967Rao]:

In the γ phase: $a_C = x_C \exp \{7.48\ x_C + (1.26 + (3530 / T))\ x\}$

Where x_C represents the mole fraction of carbon and $x = x_{Ni} / (x_{Fe} + x_{Ni})$. The reference state, for which $\gamma_C = a_C / x_C = 1$ for carbon is the carbon at infinite dilution in pure γFe. That expression applies for $1073 < T < 1473$ K ($800 < T < 1200$°C). Starting from the [1966Smi] data at 1000°C, [1968Chi] uses a somewhat different model and proposes:

$a_C = x_C \exp (2.84\ z_C + 1.80\ z_{Ni} + 2.80\ z_C z_{Ni})$

with $z_C = x_C / (x_{Fe} + x_{Ni} - x_C)$ and $z_{Ni} = x_{Ni} / (x_{Fe} + x_{Ni} - x_C)$

DOI: 10.1007/978-3-540-74196-1_10

That expression agrees well with the later measurements of [1969Fra] at 1000°C.
Mössbauer studies on (γFe,Ni,C) alloys [1994Oda] showed interactions C-C strongly repulsive between nearest and second nearest neighbor which agrees well with other thermodynamic evaluations. The C-Ni interactions are very weak.
The integral enthalpy of formation of the liquid solution determined at 1627°C (1900 K) by [1993Vit, 1994Wit] is reproduced in Fig. 18.
Activities of iron and nickel has been measured at 1500°C in the iron rich corner (5 to 8 at.% Ni, 6-9 at.% C [1976Rus]. The pure Fe-Ni alloys are ideal for this composition range. Carbon addition has an effect to decrease iron activity and to increase nickel activity. This is the expected behavior taking into account the strong C-Fe interaction compared with the weak C-Ni interactions.

Notes on Materials Properties and Applications

The iron rich (< 30 at.% Ni) alloys undergo a martensitic transformation due to the fact that carbon presents a high solubility in the γ phase (austenite), stable at high temperature, which cannot be quenched and a low solubility in the α phase (ferrite), stable at low temperature. As a result, quenching austenite gives a hardened phase, generally tetragonal, known as martensite. The ratio austenite/martensite in a steel strongly depends on the heat treatment and the result is presented on so called TTT (Temperature-Time-Transformation) diagrams. One of the first TTT diagrams was given in [1932Bai]. In the C-Fe-Ni system, the martensite presents various morphologies called lath, butterfly or lenticular which have been well described in [1983Ume, 2001Zha] and the factors controlling the various morphologies have been well explicited. A mechanism of the α-γ transformation in C-Fe-Ni alloys is given in [1934Deh, 2003Kap]. The Ms (Martensite start) temperature depends weakly on the carbon content of the alloy, but more strongly on its nickel content. It has been measured at 650°C for 5 mass% Ni and at 500°C for 10 mass% Ni [1938Lan] and below 0°C when the Ni content is higher than 25 mass% [1983Ume, 2001Gho]. A model for predicting the Ms temperature from thermodynamics has been presented in [2001Gho], which match pretty good with observation. The behavior of martensite phase upon tempering shows a complex pattern [1997Gen]. For instance, for an alloy Fe-15Ni-0.5C (mass%), a carbon redistribution may be observed up to 150°C followed by a precipitation of metastable carbides such as ε and η up to 250°C, and by the precipitation of the metastable θ carbide up to 450°C. Above that temperature, austenite is reformed from ferrite and cementite. The crystal structure of the martensite is unstable as pointed out by [2003Dan] and evolves when internal stress is relaxed at the interface martensite-retained austenite. A thermally prepared martensite is energy consuming and environmentally unfriendly. Electrodeposited C-Fe or C-Fe-Ni may achieve hardness (about 800 HV) similar to that of a high temperature martensite [2001Has].
The stabilization of austenite by nickel was also investigated by [1955Sam] on (γFe,Ni) up to 16 mass% Ni, alloys added with 1 mass% C and 0.3 mass% Mn. Undercooling to liquid helium temperature [1990Gav] stabilizes the retained austenite and prevents the isothermal martensitic transformation taking place during subsequent heating. The TTT diagrams were also used to investigate the austenite-bainite transformation [1990Rey]. Bainite is an intimate mixture of ferrite and cementite which forms below a Bs (Bainite start) temperature. The transformation proceeds quickly after an induction period and may be incomplete [2006Aar]. The Bs temperature has been measured around 500°C for an alloy with 9 mass% Ni and < 0.28 mass% C [1991Tsu] and seems independent of the C content and around 550°C for an alloy with 3.28 mass% Ni and 0.12 mass% C [1992Spa]. The formation of bainite, in (Fe,Ni,C) alloys, well investigated in [2001Qui, 2004Aar] appears as intermediate between diffusive high temperature transformation and displacive, such as martensitic low temperature transformation. A theory of the nucleation and growth of bainite was proposed in [2002Qui].
Nickel is known to improve both toughness and strength as measured by impact and room temperature tension stress [1968Jol]. For a particular heat treatment, nickel refines the ferrite grain size as compared with that of a plain carbon steel of similar composition. This grain refinement would produce an improvement of the yield strength and a better resistance to brittle fracture.
The presence of Ni decreases the Vicker's hardness of Fe_3C [1997Miz]. The hardness of the solid solution is determined by the strength of the M-C bond rather than by the M-M bond. Experimental investigations on materials properties are summarized in Table 4.

DOI: 10.1007/978-3-540-74196-1_10

Miscellaneous

Solid solutions $(Fe,Ni)_3C$, probably metastable, have been prepared [1951Ber] reacting H_2+CO mixtures on dispersed alloys between 170 and 560°C. The solid solution $(Fe_{1-x}Ni_x)_3C$ ($x < 0.4$) has the cementite (Fe_3C) structure with a Curie point starting from 210°C for Fe_3C, going up to 234°C for $(Fe_{0.75}Ni_{0.25})_3C$, then going down to 150°C for $(Fe_{0.6}Ni_{0.4})_3C$. The solid solution $(Fe_{1-x}Ni_x)_3C$ ($x > 0.7$) is hexagonal and paramagnetic. Both phases coexist at $0.4 < x < 0.7$. The influence of C on the Curie temperature of (Fe,Ni) alloys has been determined [1968Bol] in the composition range 22-34 mass% Ni, which corresponds to the domain of Invar alloys. Ni has been shown [2001Ume] to partition in ferrite rather than in cementite, and thus to stabilize the ferrite.

The flux of interstitial carbon (element 1) with respect to a fixed framework can be written as:
$J_1 = - D_{11} \nabla c_1 - D_{12} \nabla c_2$ where ∇c_1 and ∇c_2 represent the concentration gradient of elements 1 and 2. [1964Bro] measured experimentally the diffusion coefficient ratio D_{12} / D_{11} over the temperature range 800-1050°C and showed that, within a good approximation, this ratio may be deduced from thermodynamic considerations. The diffusion coefficient of carbon in an (αFe,Ni) alloy has been measured by [1964Hel] which proposes the following relationship:
$D/cm^2 \cdot s^{-1} = 2.9 \cdot 10^{-3} \exp(-9950 / T)$, nearly independent of the nickel content (< 5 mass% Ni).

By a more complete investigation of carbon diffusion (0.1 mass% C) in (γFe,Ni) alloys extending on the whole composition range between 860 and 1100°C, [1966Smi] showed that the diffusion coefficient D presents a maximum near 60 mass% Ni; the preexponential factor D_o and the activation energy presents a maximum and a minimum, respectively near 45 mass% Ni and minimum and a maximum respectively near 85 mass% Ni, as shown in Fig. 19. Under a temperature gradient, carbon was found to migrate toward higher temperatures in the low carbon single-phase alloys [1982Oka]. In the higher carbon content, an abrupt jump in the carbon concentration is observed when a part of the specimen is in a two phase-region.

Diamond crystals up to 1 carat (0.2 g) size have been grown in the C-Fe and C-Fe-Ni systems at 57 kbar (5.7 GPa) [1971Str, 2000Yin]. In the C-Fe system, Fe_3C is stable up to 1415°C, preventing diamond growth below this temperature. Addition of Ni lowers the melting temperature of Fe_3C and widens the temperature range for diamond growth [1996Koc].

Nickel accelerates the process of removing carbon in liquid steel [1974Ela], observation explained by the fact that nickel increases the iron activity in steels.

Magnetic transitions were shown to affect strongly the thermodynamic properties such as the partition coefficient of nickel between ferrite and cementite or between cementite and austenite [1976Ko].

Laser treatment used for surface hardening of the (γFe,Ni,C) [1994Dan] was shown to cause irregular carbon distribution in depth together with formation of zones characterized by abnormally high carbon content.

DOI: 10.1007/978-3-540-74196-1_10

Table 1. Investigations of the C-Fe-Ni Phase Equilibria

Reference	Method/Experimental Technique	Temperature/Composition/Phase Range Studied
[1925Kas1] [1925Kas2]	Thermal analysis, liquidus determination	700-1600°C, < 6 mass% C
[1931Soe]	Carbon solubility in (γFe,Ni) alloys	800-1150°C, < 4 mass% C
[1951Ber]	Structural determinations	170-560°C, $(Fe,Ni)_3C$
[1955Sam]	α-γ transition determination	550-1000°C, < 16 mass% Ni, 1 mass% C
[1956Tur]	Carbon solubility in liquid (γFe,Ni) alloys	1350-1550°C, < 4.1 mass% C
[1959Fuw]	Carbon activity measurements in liquid (Fe,Ni) alloys, CO-CO_2 equilibrium	1560°C, < 25 mass% Ni, < 4 mass% C
[1960Mil]	Carbon solubility in liquid (γFe,Ni) alloys	1350-1550°C, < 5.2 mass% C
[1960Smi]	Carbon activity measurements in (γFe,Ni) alloys, CO-CO_2 equilibrium	1000°C, < 1.4 mass% C
[1960War]	Carbon solubility measurements in liquid (Fe,Ni) alloys	1350°C, < 4.3 mass% C
[1963Hec]	Solubility and Carbon activity measurements in γFe,Ni) alloys	800-1200°C, < 30 mass% Ni, < 1.4 mass% C
[1964Buc]	Liquidus surface, γ-liquid equilibria	1400-1520°C, <40 mass% Ni, <5 mass% C
[1969Fra]	Solubility measurements in (γFe,Ni) alloys	1000°C, < 30 mass% Ni, < 1.5 mass% C
[1970Zem]	Solubility measurements in (αFe,Ni) alloys	300-900°C, < 1 mass% Ni, < 0.3 mass% C
[1971Gre]	Carbon activity measurements in (γFe,Ni) alloys, H_2-CH_4 equilibrium	750-1125°C, < 42 mass% Ni, < 1.2 mass% C
[1971Wad]	Carbon activity measurements in (γFe,Ni) alloys, H_2-CH_4 equilibrium	800-1200°C, < 2 mass% C.
[1972Foo]	Carbon activity measurements in liquid (Fe,Ni) alloys	1550°C, < 25 mass% Ni, < 5.2 mass% C
[1973Nat]	Interaction parameters in (γFe,Ni) alloys, H_2-CH_4 equilibrium	700-1060°C, 8-16 mass% Ni
[1973Sha]	Carbon diffusion in a (γFe,Ni) framework	730°C, paraequilibrium diagram
[1975Shi]	Thermal expansion coefficient measurements	0-200°C, $(Fe_{1-x}Ni_x)_3C$ (x = 0.02, 0.07)
[1976Kle]	Solubility measurements in (αFe) alloys	390-670°C, < 2 mass% Ni, < 120 ppm C
[1976Rus]	Activity measurements in liquid (Fe,Ni,C) alloys. Equilibrium method	1500°C, 5-8 at.% Ni, < 9 at.% C
[1976Tom]	Carbon activity measurements in (γFe,Ni) alloys	500-1200°C, 75-82 mass% Ni, < 0.2 mass% C

(*continued*)

DOI: 10.1007/978-3-540-74196-1_10

Reference	Method/Experimental Technique	Temperature/Composition/Phase Range Studied
[1977Rom] [1978Rom]	Electron microprobe analysis. α-γ and γ-cementite tie lines determination	500-730°C, < 20 mass% Ni, < 7 mass% C
[1979Kag]	Lattice parameters measurements	0-300°C, $(Fe_{1-x}Ni_x)_3C$ ($x < 0.03$)
[1980Ost]	Solubility measurements in (γFe,Ni) alloys	390-670°C, < 3 mass% Ni, < 10 mass% C
[1980Ram]	Carbon activity measurements in (γFe,Ni) alloys. Equilibrium method	1000°C, < 1.2 mass%, $a_C = 0.71$ by means of a CO-CO_2 atmosphere
[1983Mor]	Two phase equilibria between (γFe,Ni) alloy and liquid	1180-1420°C, < 1.1 mass% Ni, < 4 mass% C
[1986Sch]	Thermal analysis, liquidus determination	1100-1700°C, < 50 mass% Ni, < 6 mass% C
[1991Pav] [1993Pav]	Liquidus determination under pressure	1000-1300°C, 5.7 GPa, < 0.3 mass% C
[1992Gon]	Phase equilibria analysis	450-550°C, < 30 mass% Ni, < 7 mass% C
[1993Koc]	Thermal analysis	1075-1730°C, C-Fe-Ni diagram under 4.4 and 6 GPa
[1993Vit] [1994Wit]	Integral enthalpy of mixture in the liquid phase	1627°C, < 7 mass% C
[1996Koc]	Phase equilibria under high pressure	1400°C, 5.7 GPa, < 7 mass% C
[2000Yin]	Diamond synthesis in a Fe-Ni solvent catalyst	1300°C, 5.5 GPa, synthesis of $(Fe,Ni)_{23}C_6$ together with diamond
[2002Sol]	Diamond synthesis in a liquid solution	1240-1420°C, C-$Fe_{0.6}Ni_{0.4}$, 5-6 GPa
[2003Dan]	Crystal structure of a martensite	88-293 K, 25 mass% Ni, 0.5 mass% C

Table 2. Crystallographic Data of Solid Phases

Phase/ Temperature Range [°C]	Pearson Symbol/ Space Group/ Prototype	Lattice Parameters [pm]	Comments/References
(C)gr < 4492	*hP*4 $P6_3/mmc$ C (graphite)	$a = 246.12$ $c = 670.90$	at 25°C [Mas2] sublimation point at 3827°C
(C)d	*cF*8 $Fd\bar{3}m$ C (diamond)	$a = 356.69$	at 25°C, 60 GPa [Mas2] Stable at 1600°C, > 6 GPa
(εFe)	*hP*2 $P6_3/mmc$ Mg	$a = 246.8$ $c = 396.0$	at 25°C, > 13 GPa [Mas2]

(*continued*)

DOI: 10.1007/978-3-540-74196-1_10

Phase/ Temperature Range [°C]	Pearson Symbol/ Space Group/ Prototype	Lattice Parameters [pm]	Comments/References
(αδFe)	*cI*2	*a* = 293.15	[Mas2]
(δFe)	$Im\bar{3}m$		dissolves up to 0.4 at.% C at 1493°C [2006MSIT]
1538 - 1394	W		dissolves up to 3.8 at.% Ni at 1517°C [2007Kuz]
(αFe)		*a* = 286.65	at 25°C [Mas2]
< 912			dissolves up to 0.096 at.% C at 740°C [2006MSIT]
			dissolves up to 4.6 at.% Ni at 495°C [2007Kuz]
			ferrite
γ, (γFe,Ni)	*cF*4		complete solubility range
	$Fm\bar{3}m$		
(γFe)	Cu	*a* = 364.67	at 915°C [V-C2, Mas2]
1394 - 912			dissolves up to 9.06 at.% C at 1153°C [2006MSIT]
			austenite
(Ni)		*a* = 352.41	at 25°C [1989Sin]
< 1455			dissolves up to 2.7 at.% C at 1326.5°C [1989Sin]
			below critical temperature: γ_1 - paramagnetic, Fe enriched γ_2 - ferromagnetic, Ni enriched
γ', $FeNi_3$	*cP*4	*a* = 355.23	ordered phase
< 517	$Pm\bar{3}m$		63 to 85 at.% Ni [2007Kuz]
	$AuCu_3$		
γ", FeNi	*tP*4	*a* = 357.9	[V-C2] Metastable ordered phase below 320°C at 51.2 at.% Ni [2007Kuz]
	*P*4/*mmm*		
	AuCu		
Martensite α'	*tI*4		metastable [Mas2]
	*I*4/*mmm*		
Fe_4C	*cP*5	*a* = 387.8	metastable [V-C2]
	$P\bar{4}3m$		
	Fe_4C		
$(Fe,Ni)_3C$	*oP*16		carbide phase cohenite
	Pnma		
Fe_3C	Fe_3C	*a* = 452.48	[1997Miz]
		b = 508.96	cementite, high pressure phase
		c = 674.43	
Ni_3C		*a* = 264.6	[1951Ber]
		c = 432.0	prepared by CO over Ni
			determined for *hP*4

(*continued*)

DOI: 10.1007/978-3-540-74196-1_10

Phase/ Temperature Range [°C]	Pearson Symbol/ Space Group/ Prototype	Lattice Parameters [pm]	Comments/References
χ, Fe_5C_2	*mC*28 *C*2/*c* B_2Pd_5	*a* = 1156.2 *b* = 457.27 *c* = 505.95 β = 97.74°	metastable [V-C2]
Fe_7C_3	*hP*20 $P6_3mc$ Fe_3Th_7	*a* = 688.2 *c* = 454.0	metastable [V-C2]
Fe_7C_3 (HP)	*oP*40 *Pnma* Cr_7C_3	*a* = 454.0 *b* = 687.9 *c* = 1194.2	high pressure phase [V-C2]
η, Fe_2C	*oP*6 *Pnnm* Fe_2C	*a* = 470.4 *b* = 431.8 *c* = 283.0	metastable [V-C2]
ε, Fe_2C	*hP** $P6_322$	-	metastable [Mas2]
Fe_2C	*hP** $P\bar{3}m1$	-	metastable [Mas2]
$(Fe,Ni)_{23}C_6$	*cF*116 $Fm\bar{3}m$ $Cr_{23}C_6$	*a* = 1065	metastable [2000Yin]

Table 3. Invariant Equilibria in the C-Fe-Ni System Under a Pressure of 6 GPa

Reaction	*T* [°C]	Type	Phase	Composition (mass%)		
				Fe	Ni	C
L ⇌ Fe_3C + γ + (C)d	1077	E	L	71.7	24.0	4.3
			Fe_3C	84.8	8.5	6.7
			γ (C)d	66.8	26.0	7.2
				0	0	100
L + Fe_7C_3 ⇌ Fe_3C + (C)d	1312	U	L	86.2	8.4	5.4
			Fe_7C_3	91.6	0	8.4
			Fe_3C	89.9	3.5	6.6
			(C)d	0	0	100

DOI: 10.1007/978-3-540-74196-1_10

Table 4. Investigations of the C-Fe-Ni Materials Properties

Reference	Method / Experimental Technique	Type of Property
[1926Osa]	Density and hardness measurements	Brinell hardness, 25°C, < 0.8 mass% C
[1926Rib]	Electrical resistivity	0-1000°C, < 0.3 mass% C
[1938And]	Fluidity evaluation (qualitative)	1400-1500°C, 0.4 mass% C, < 17 mass% Ni
[1938Lan]	Magnetic measurements	Phase transformation, 400-700°C, < 12 at.% Ni, < 1.5 at.% C
[1964Bro]	Carbon diffusion in a (γFe,Ni) framework	800-1050°C, diffusion coefficient ratio
[1964Hel]	Carbon diffusion in an (αFe,Ni) framework	0-500°C, diffusion coefficient measurement
[1966Smi]	Carbon diffusion in a (γFe,Ni) framework	860-1100°C, < 0.1 mass% C, diffusion coefficient measurements
[1968Bol]	Curie temperature determination	0-200°C, < 0.66 mass% C, 22-34 mass% Ni
[1976Ko]	Magnetic transition influence	Partition coefficient of Ni between ferrite and cementite or cementite and austenite
[1982Kaj]	Dilatometric and Mössbauer study	80 +100°C, Ageing behavior of martensite
[1982Oka]	Diffusion under a temperature gradient	750-1150°C, 32.5 mass% Ni, < 0.8 mass% C
[1983Ume]	Martensite morphology, optical means	0-400°C, < 30 mass% Ni, < 2 mass% C
[1985Vit]	Tensile strength and hardness measurements	880-1280°C, 20 mass Ni, C not given, sintered samples
[1988Sum]	Inelastic scattering of slow neutrons in Fe-Ni austenite	Energy of local oscillation of C atoms measured at 75.8 meV
[1989Bug]	Mössbauer spectroscopy	C distribution in Fe-25% Ni-0.5% C
[1990Gav]	Mössbauer and magnetic susceptibility	4-293 K, 25 mass% Ni, 0.6 mass% C
[1990Rey]	Optical metallography, transmission electron microscopy	Austenite-Bainite transformation, 3 mass% Ni, < 0.6 mass% C
[1991Tsu]	Metallographic study	500°C, 9 mass% Ni, < 0.28 mass% C
[1992Men]	Microhardness measurements after heat treatment of melt spun alloys	< 12 mass% Ni, < 4 mass% C
[1992Run]	Small angle scattering of neutrons	Ageing of a martensite Fe-25% Ni-0.7% C formed at 77 K
[1992Spa]	Optical metallography, transmission electron microscopy	Austenite-Bainite transformation, 3.2 mass% Ni, 0.12 mass% C
[1994Dan]	X-ray powder diffraction, scanning electron microscopy	Surface analysis (0-60 μm in depth) after laser treatment
[1994Oda]	Mössbauer spectroscopy on γ alloy	Interaction between C-C nearest and second neighbor

(*continued*)

DOI: 10.1007/978-3-540-74196-1_10

Reference	Method / Experimental Technique	Type of Property
[1997Gen]	X-ray powder diffraction, scanning electron microscopy	20-700°C, aging and tempering of an alloy Fe-14.4Ni-2.35C (at.%)
[2001Has]	Mössbauer spectroscopy on electrodeposited Fe-C or Fe-Ni-C layers	Fe-15Ni-0.7C (mass%) electrodeposited at 50°C
[2001Qui] [2002Qui]	Dilatometry, microscopic observations	Austenite-Bainite transformation, 4.9 mass% Ni, 0.49 mass% C
[2001Zha]	Electron diffraction, optical microscopy	Deformation twinning of martensite 20 mass% Ni, 0.8 mass% C
[2003Kap]	Thermomechanical treatment	< 750°C, < 20 mass% Ni, < 1.3 mass% C
[2004Hut]	Kinetics measurements of the α-γ transformation	700°C, < 3.4 mass% Ni, 0.1 mass% C

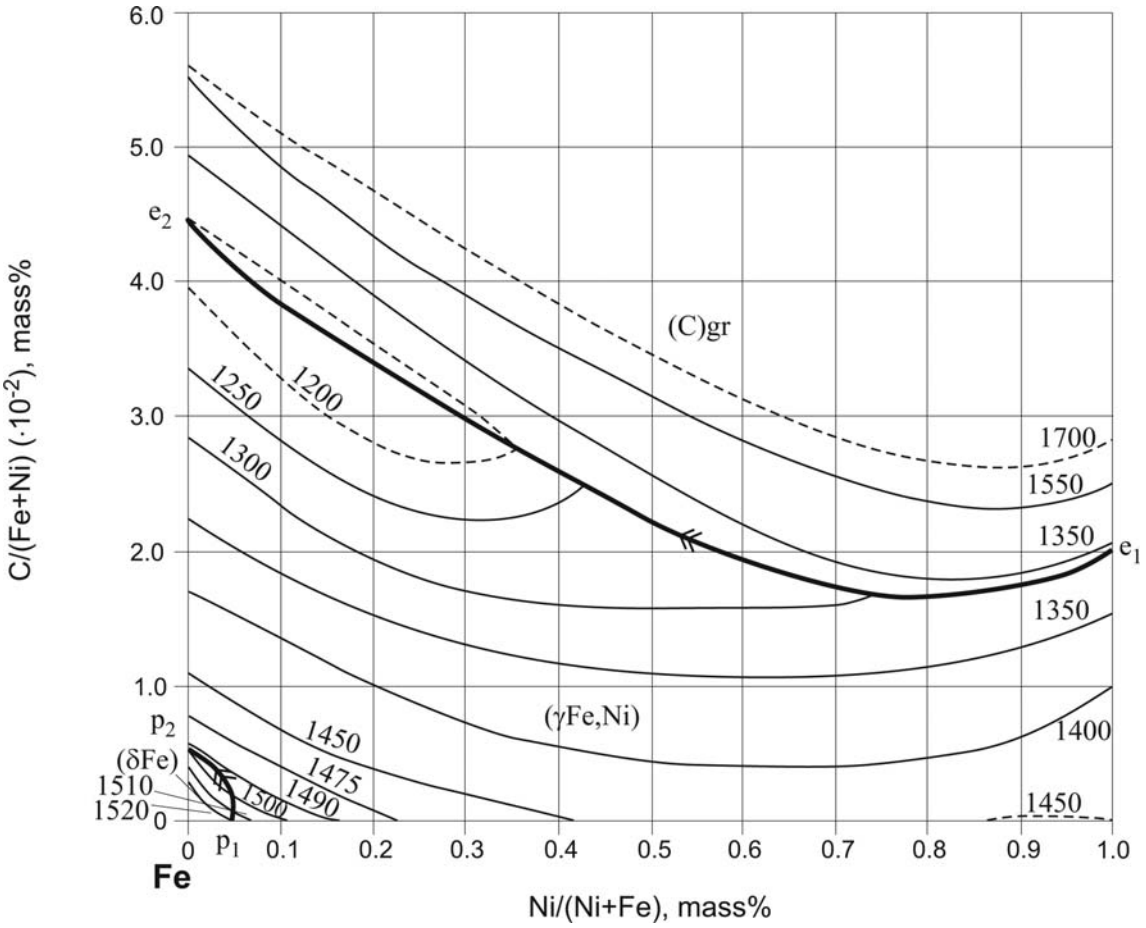

Fig. 1. C-Fe-Ni. Partial liquidus surface under 0.1 MPa

DOI: 10.1007/978-3-540-74196-1_10

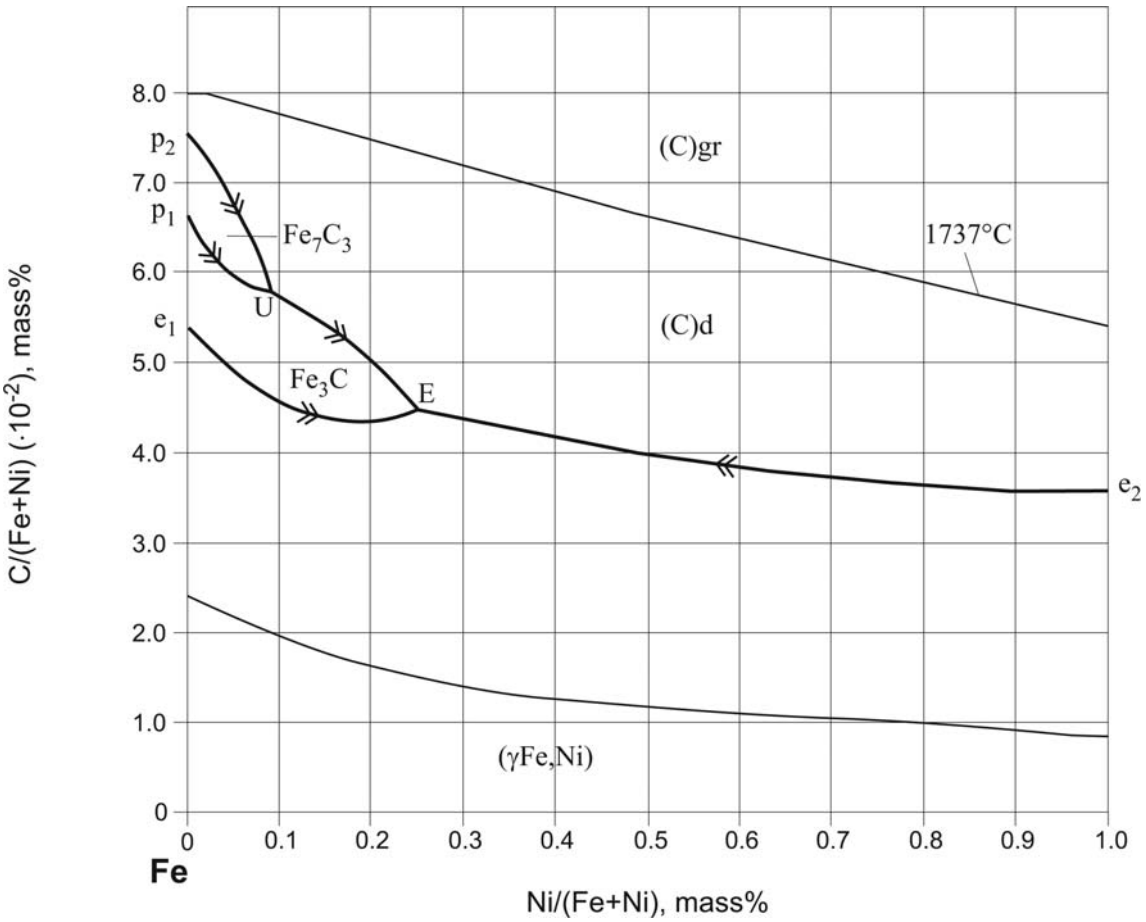

Fig. 2. C-Fe-Ni. Partial liquidus surface under 5.7 GPa

DOI: 10.1007/978-3-540-74196-1_10

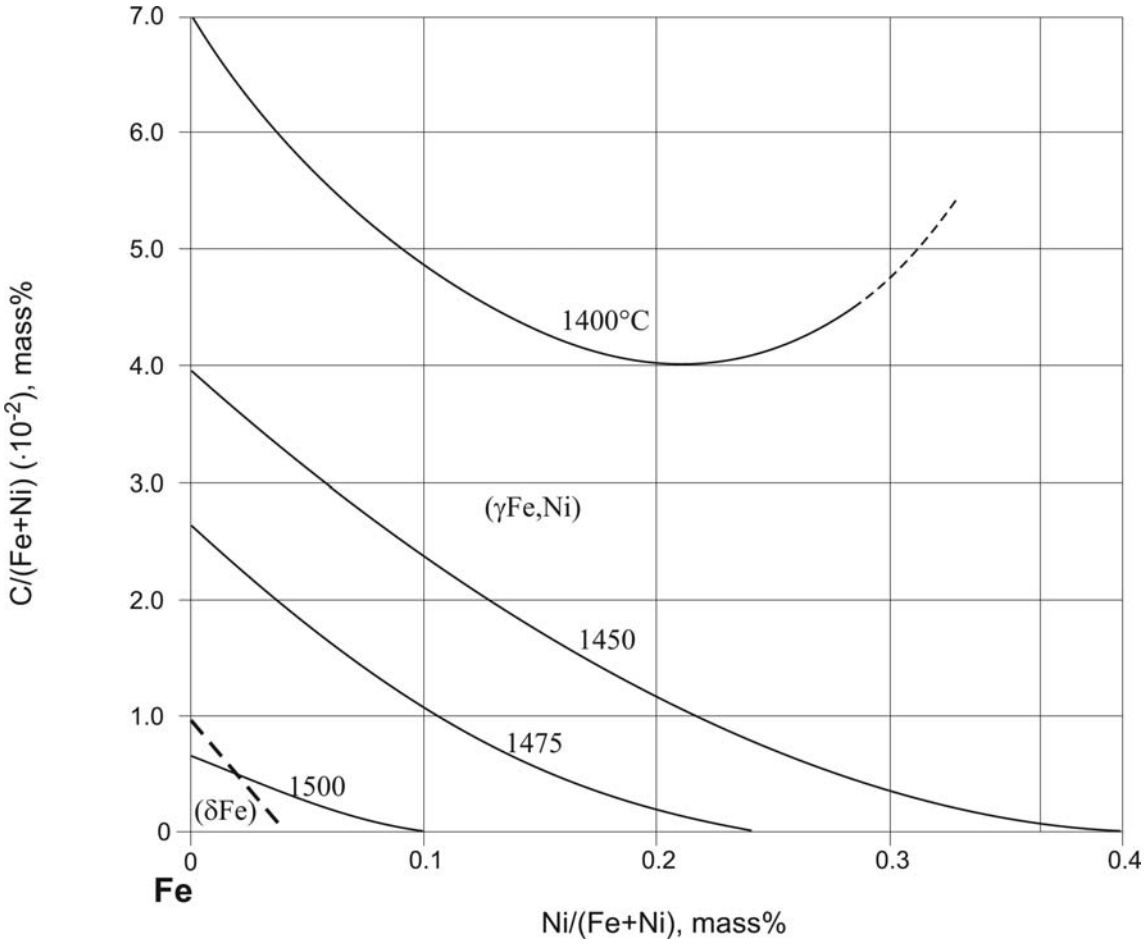

Fig. 3. C-Fe-Ni. Partial solidus surface under 0.1 MPa

DOI: 10.1007/978-3-540-74196-1_10

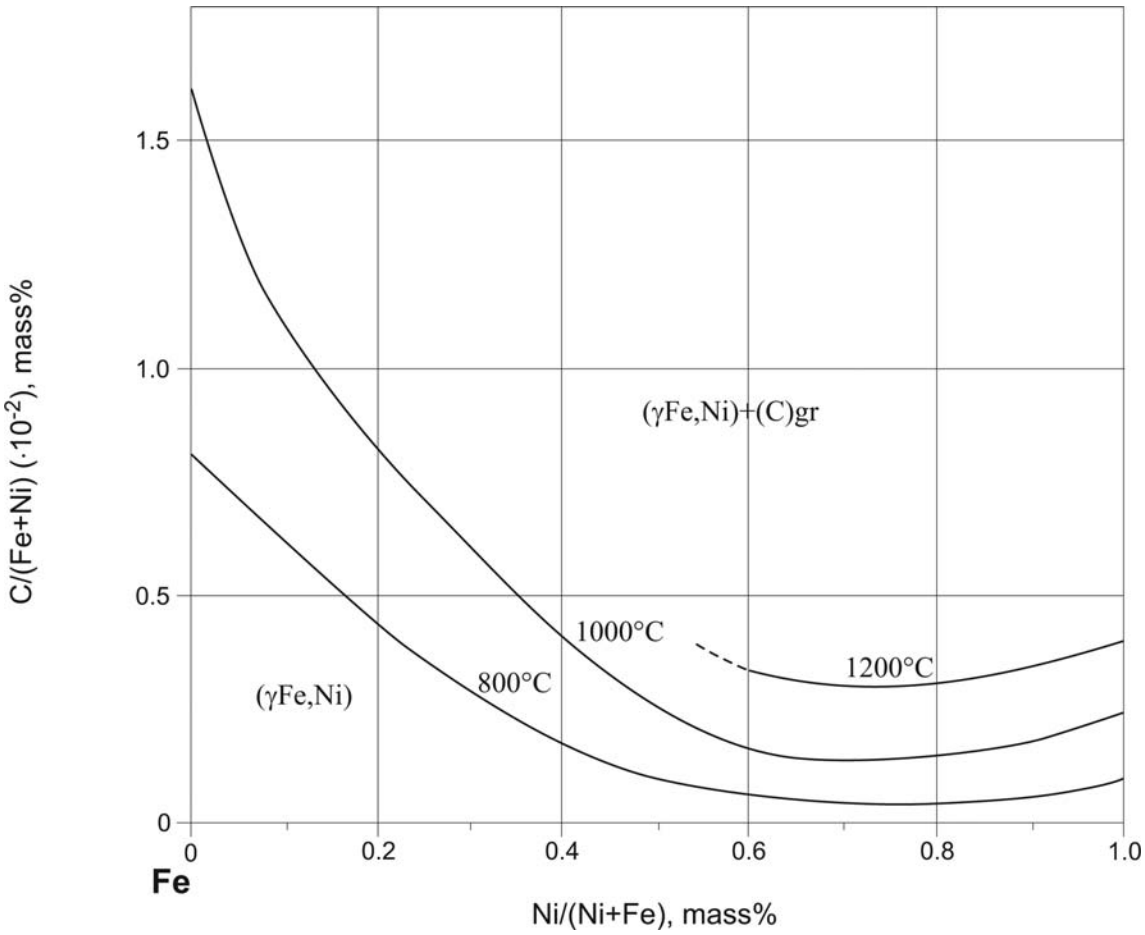

Fig. 4. C-Fe-Ni. Carbon solubility in (γFe,Ni) alloys

DOI: 10.1007/978-3-540-74196-1_10

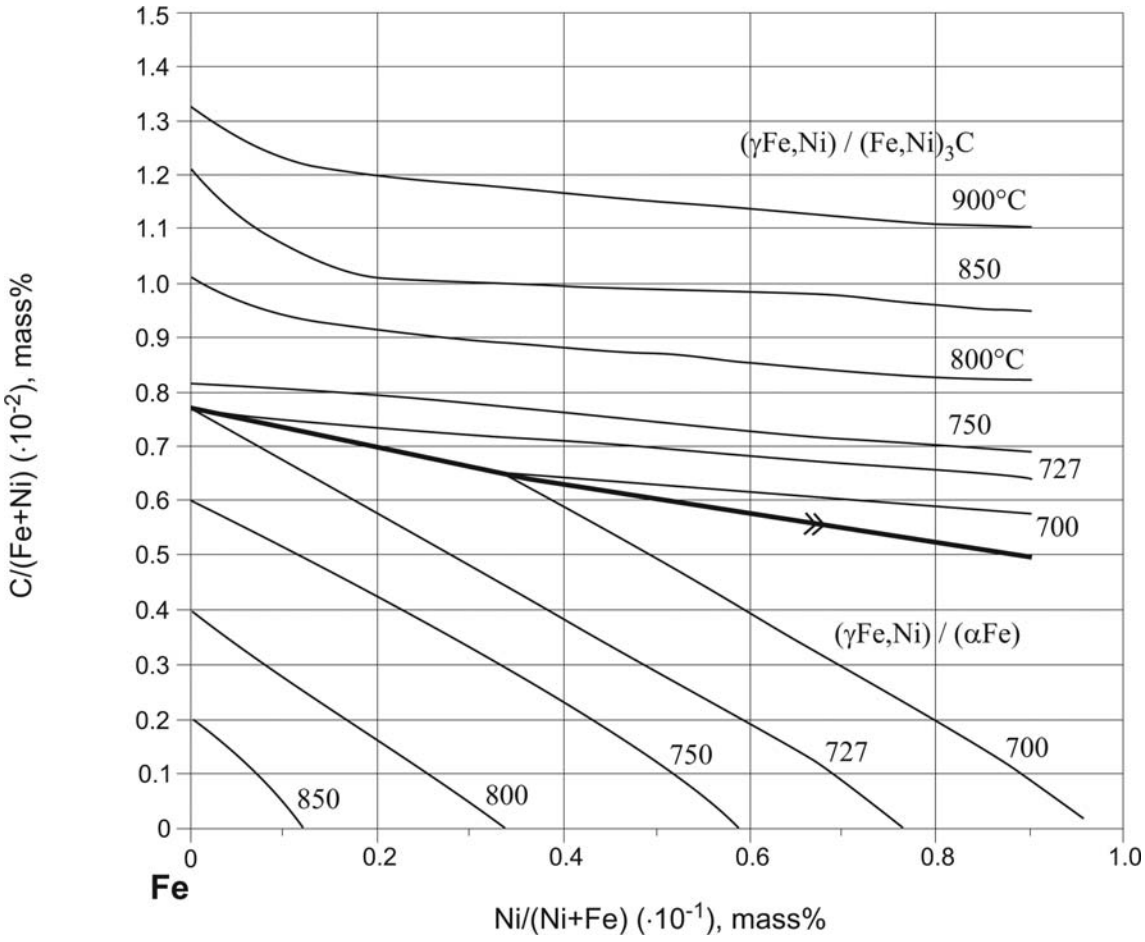

Fig. 5. C-Fe-Ni. Austemite field below 900°C

DOI: 10.1007/978-3-540-74196-1_10

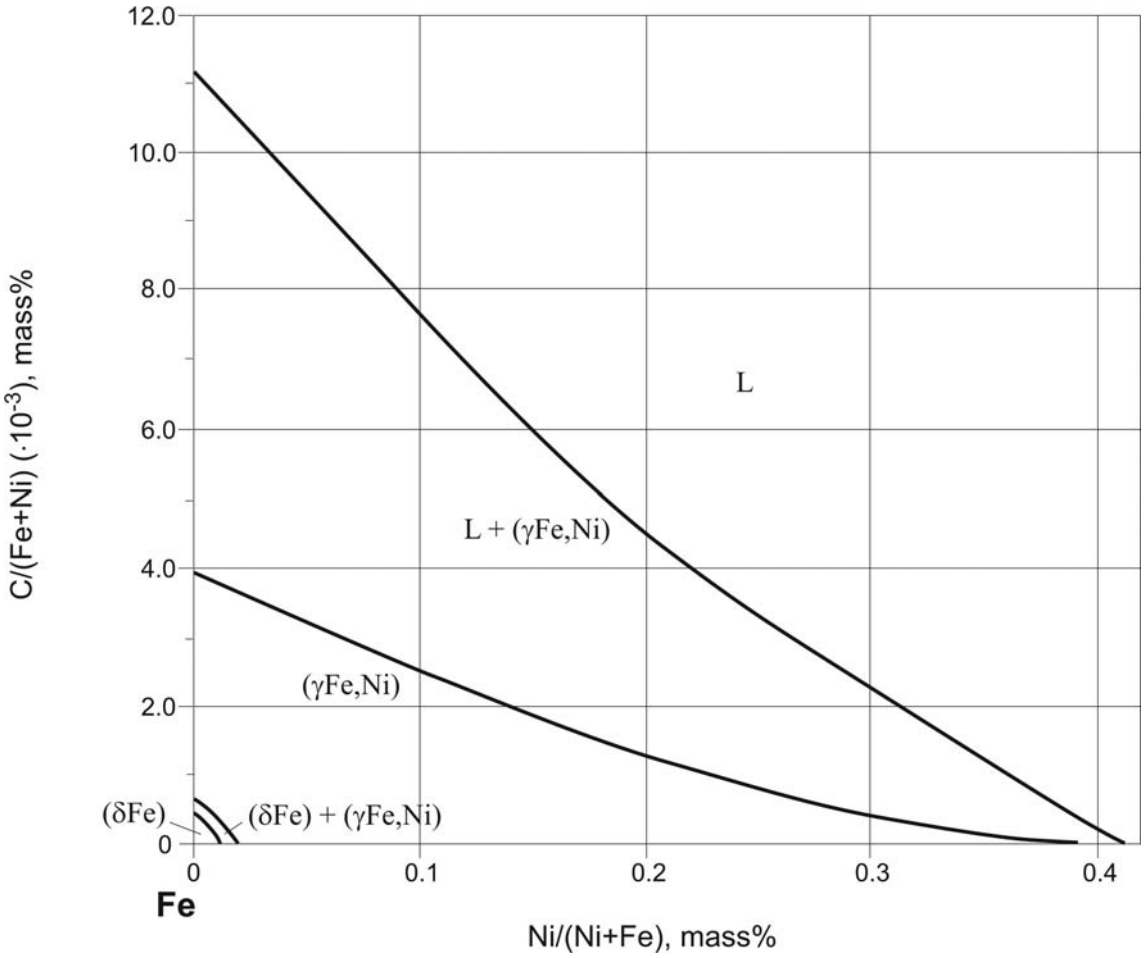

Fig. 6. C-Fe-Ni. Partial isothermal section at 1450°C

DOI: 10.1007/978-3-540-74196-1_10

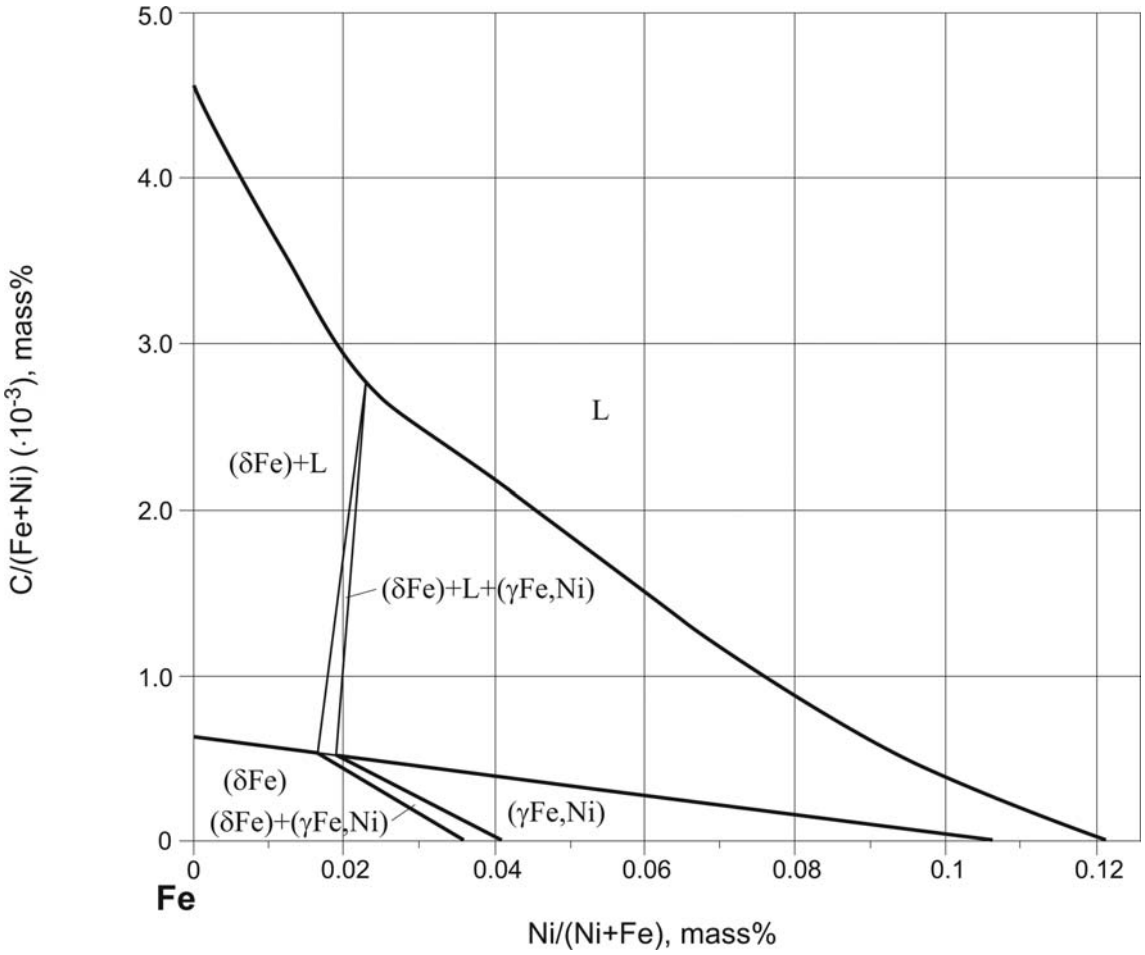

Fig. 7. C-Fe-Ni. Calculated partial isothermal section at 1500°C

DOI: 10.1007/978-3-540-74196-1_10

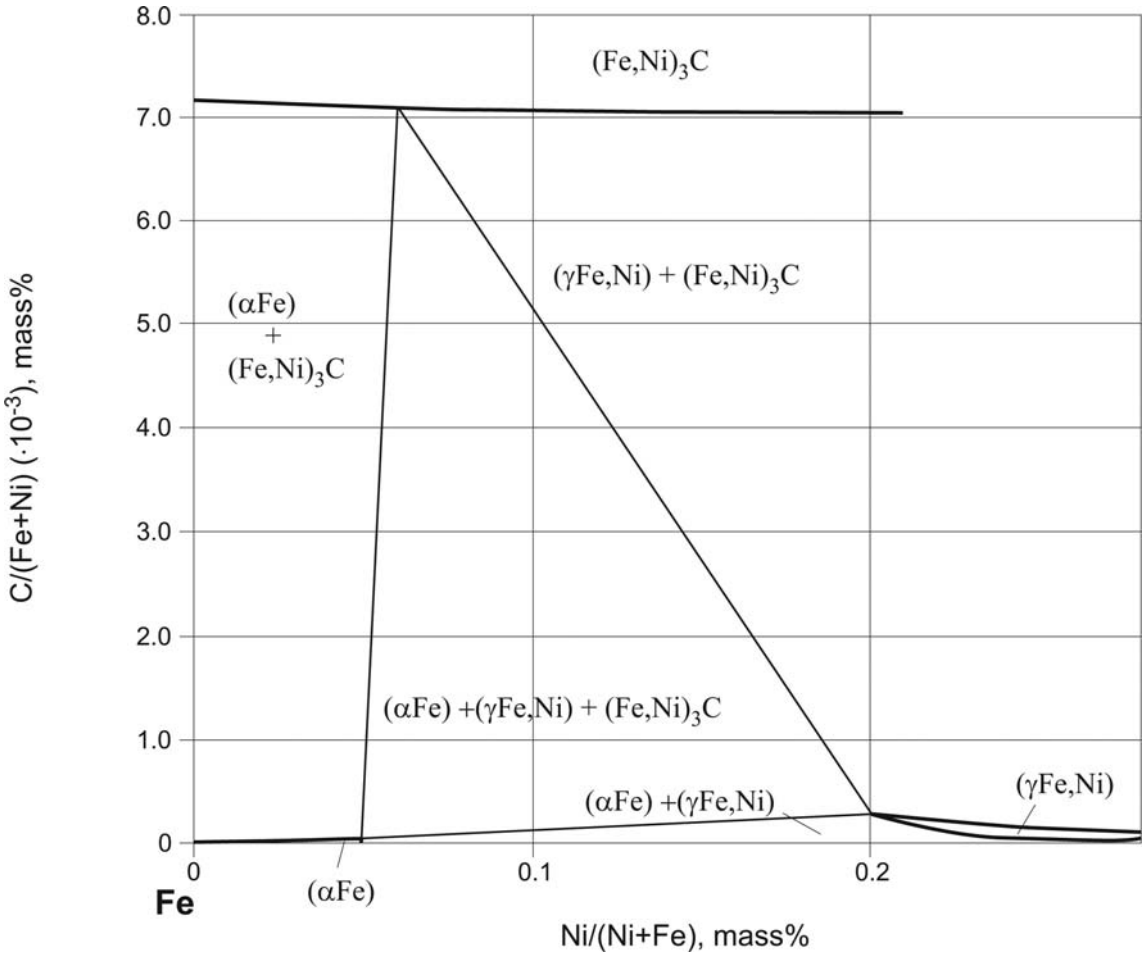

Fig. 8. C-Fe-Ni. Partial metastable isothermal section at 450°C

DOI: 10.1007/978-3-540-74196-1_10

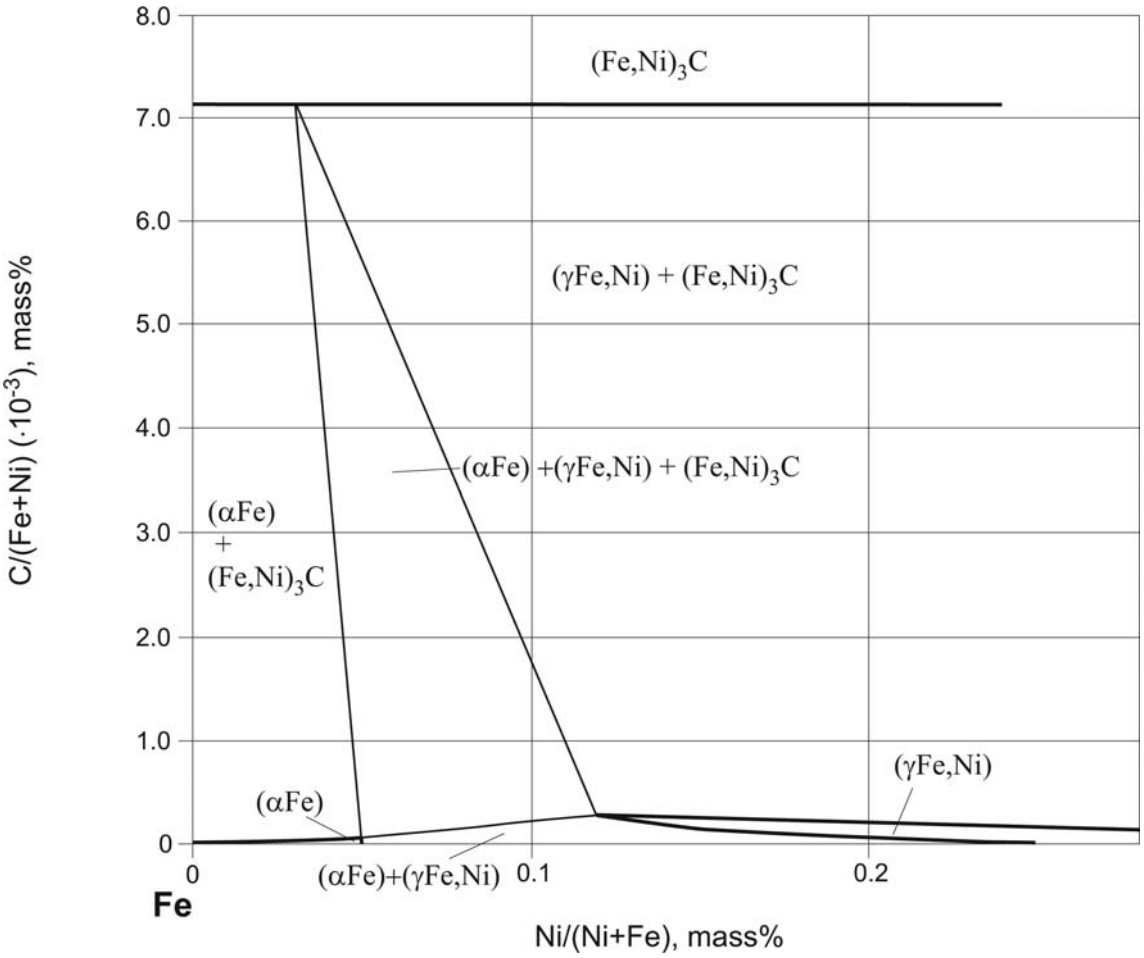

Fig. 9. C-Fe-Ni. Partial metastable isothermal section at 550°C

DOI: 10.1007/978-3-540-74196-1_10

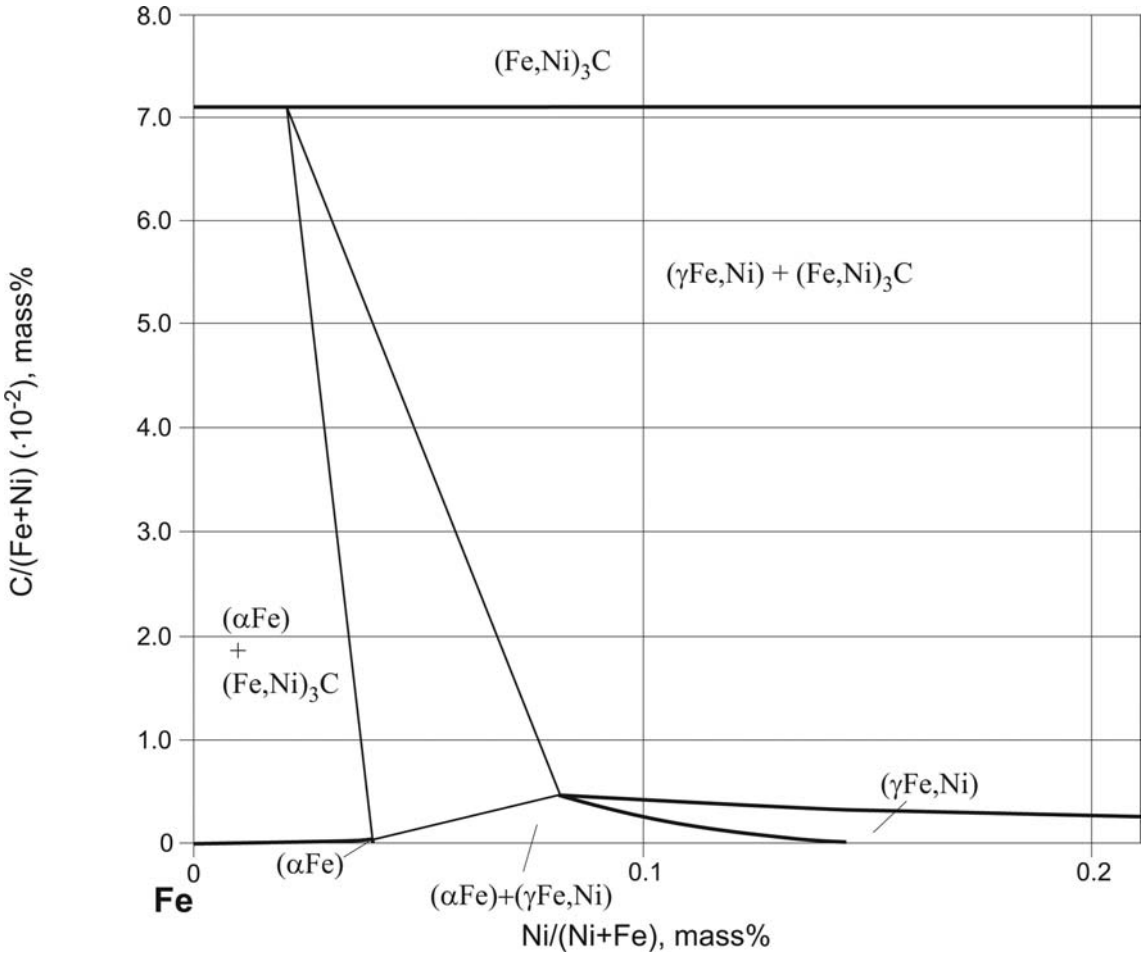

Fig. 10. C-Fe-Ni. Partial metastable isothermal section at 650°C

DOI: 10.1007/978-3-540-74196-1_10

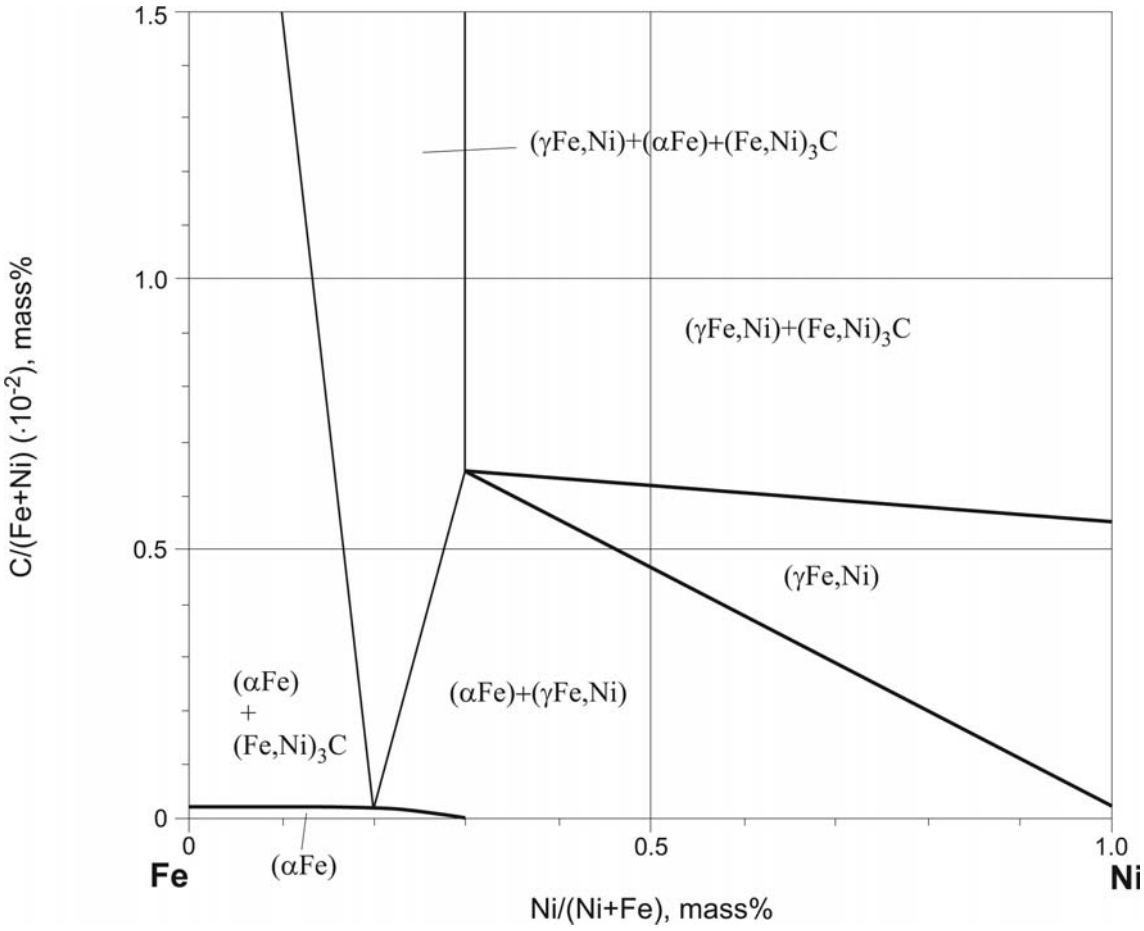

Fig. 11. C-Fe-Ni. Partial metastable isothermal section at 700°C

DOI: 10.1007/978-3-540-74196-1_10

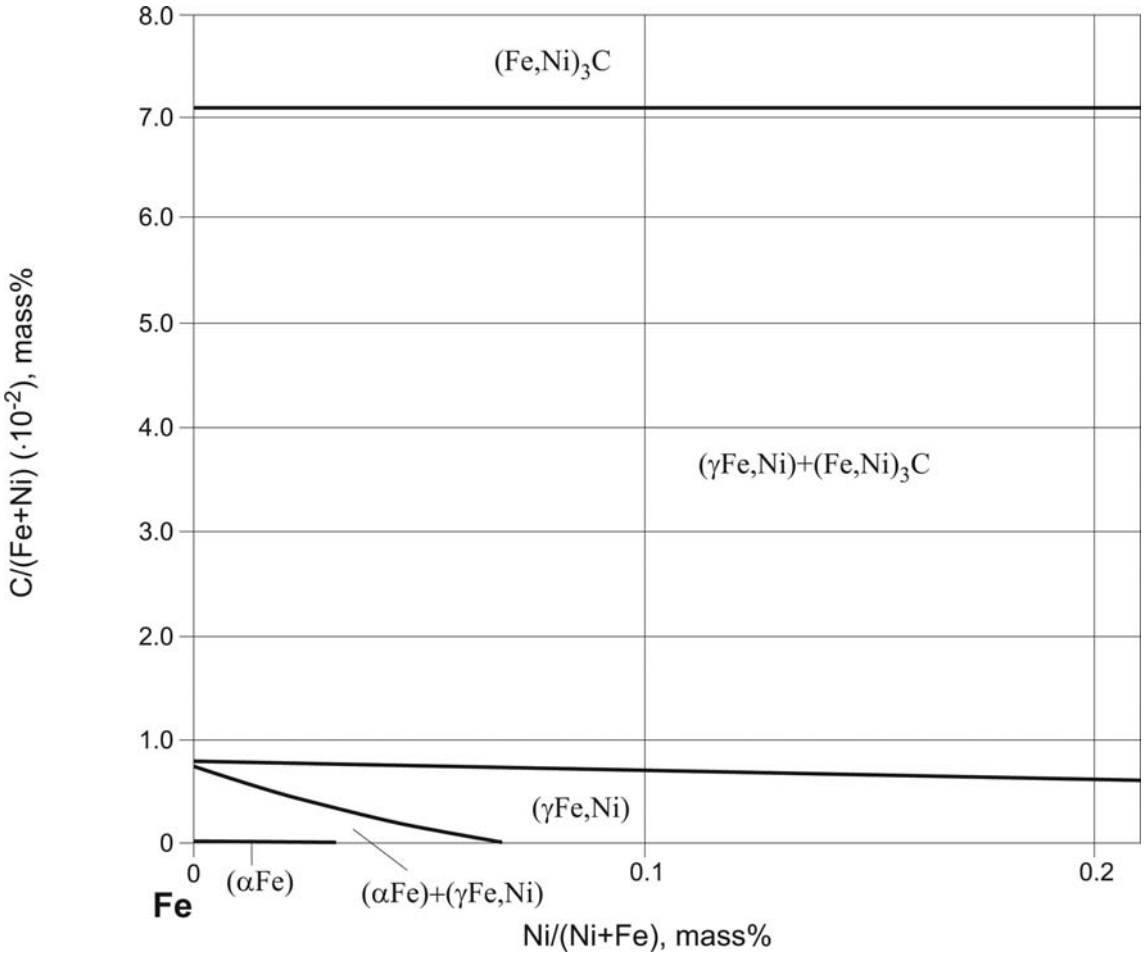

Fig. 12. C-Fe-Ni. Partial metastable isothermal section at 730°C

DOI: 10.1007/978-3-540-74196-1_10

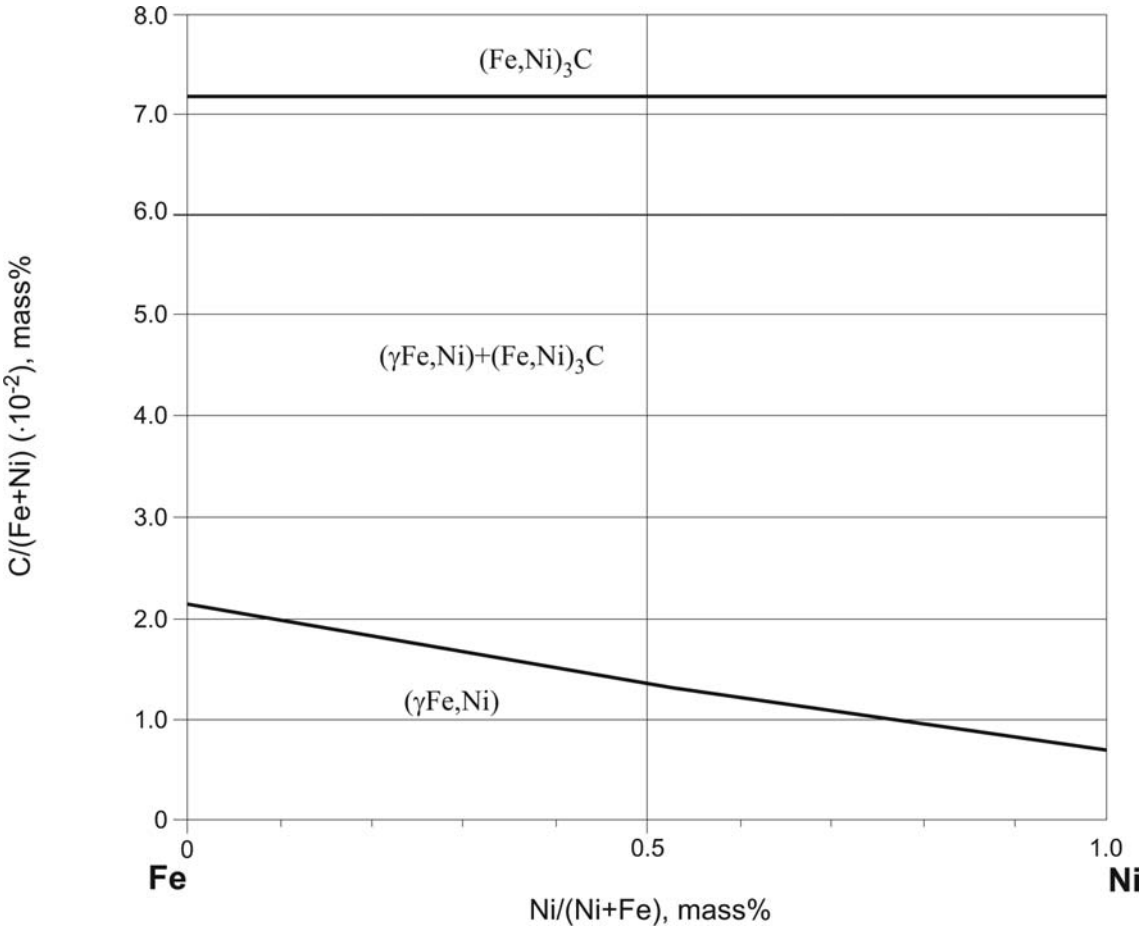

Fig. 13. C-Fe-Ni. Partial metastable isothermal section at 1127°C

DOI: 10.1007/978-3-540-74196-1_10

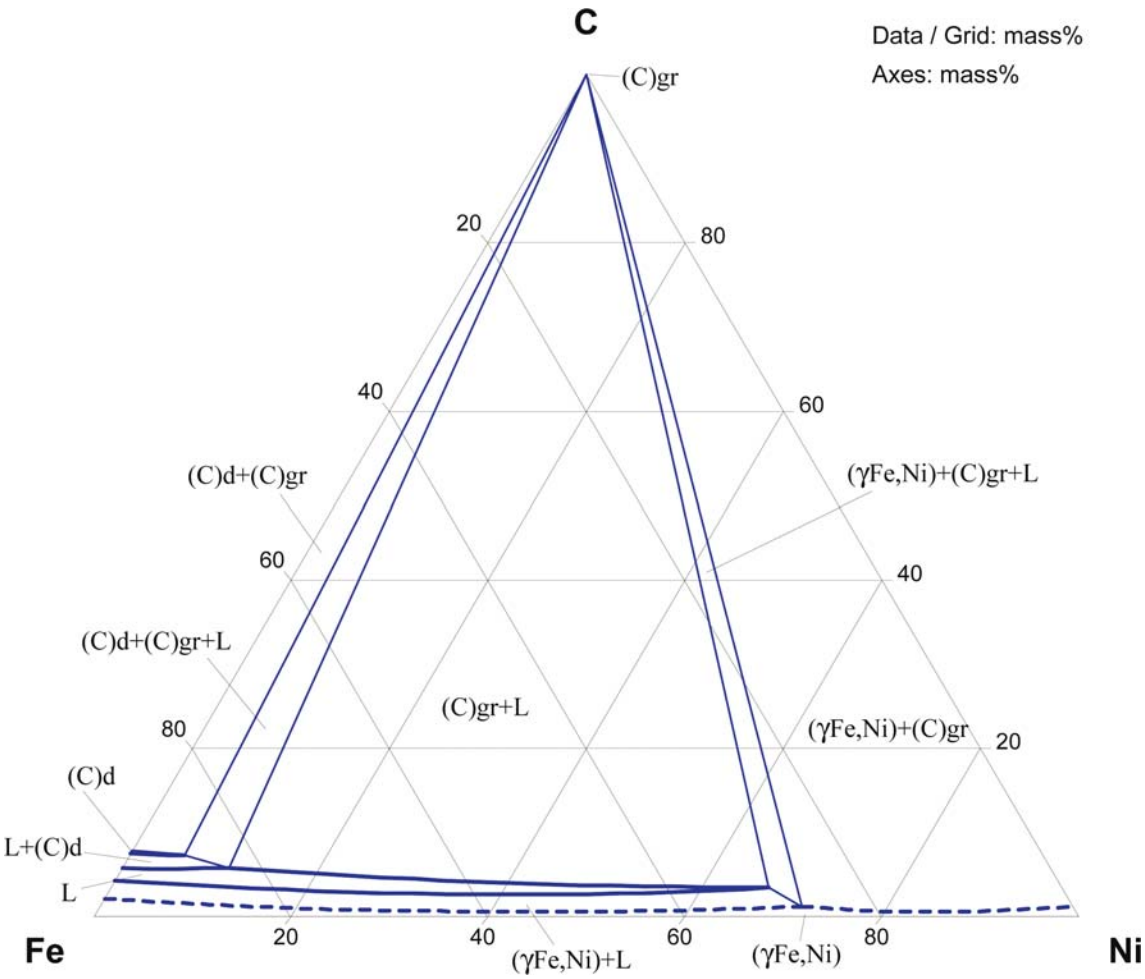

Fig. 14. C-Fe-Ni. Isothermal section at 1397 °C under 5.7 GPa

DOI: 10.1007/978-3-540-74196-1_10

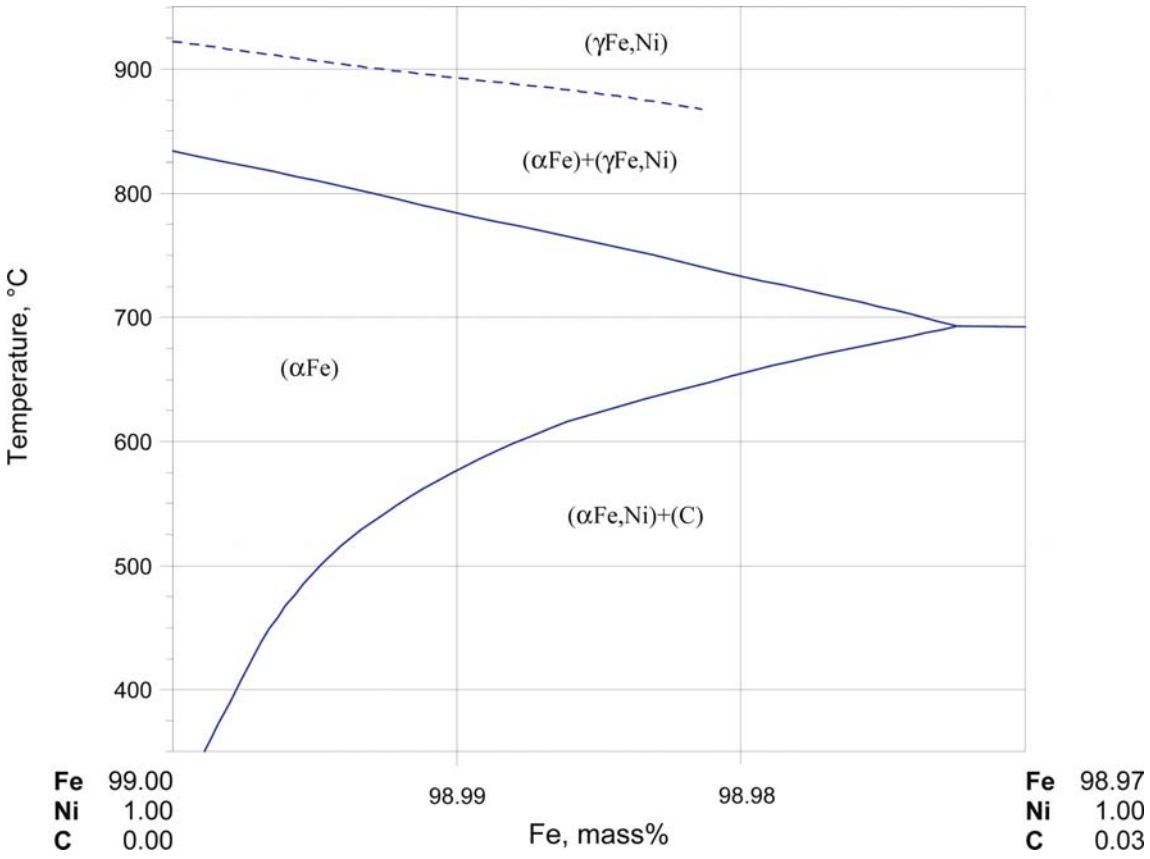

Fig. 15. C-Fe-Ni. Vertical section at 1 mass% Ni

DOI: 10.1007/978-3-540-74196-1_10

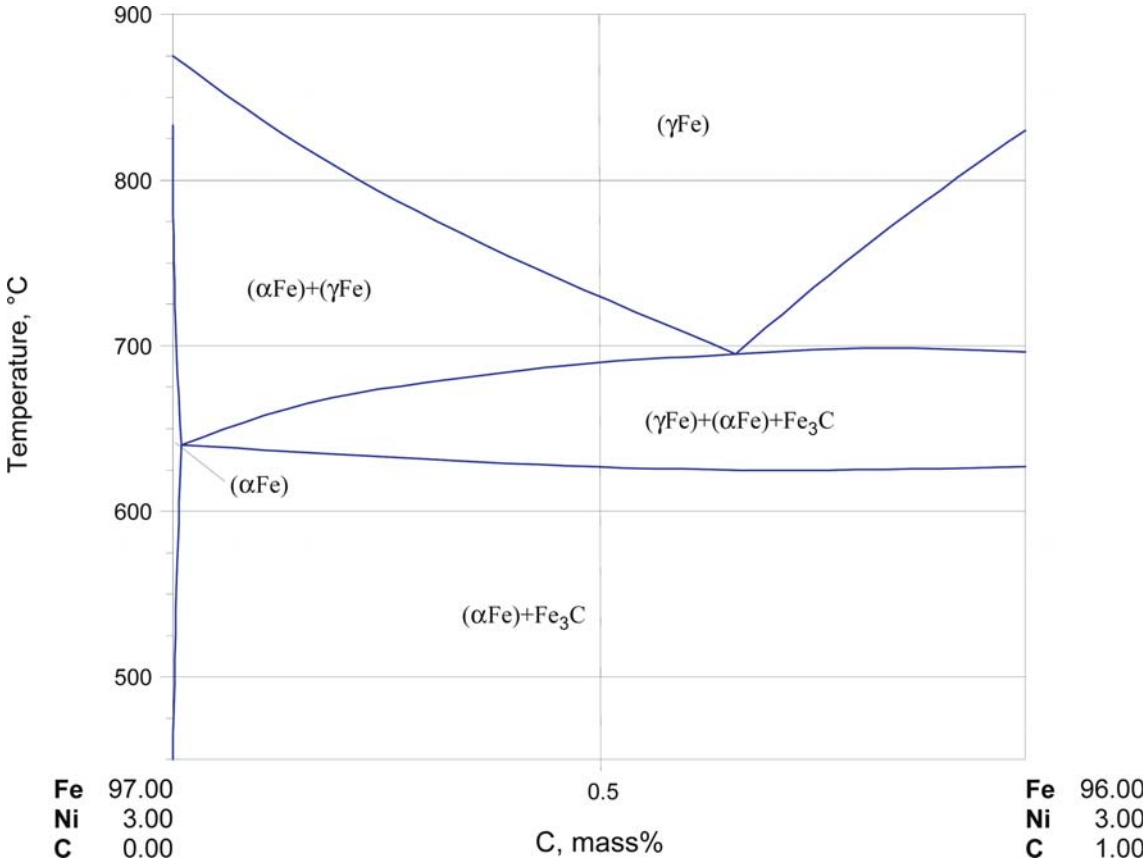

Fig. 16. C-Fe-Ni. Vertical section at 3 mass% Ni

DOI: 10.1007/978-3-540-74196-1_10

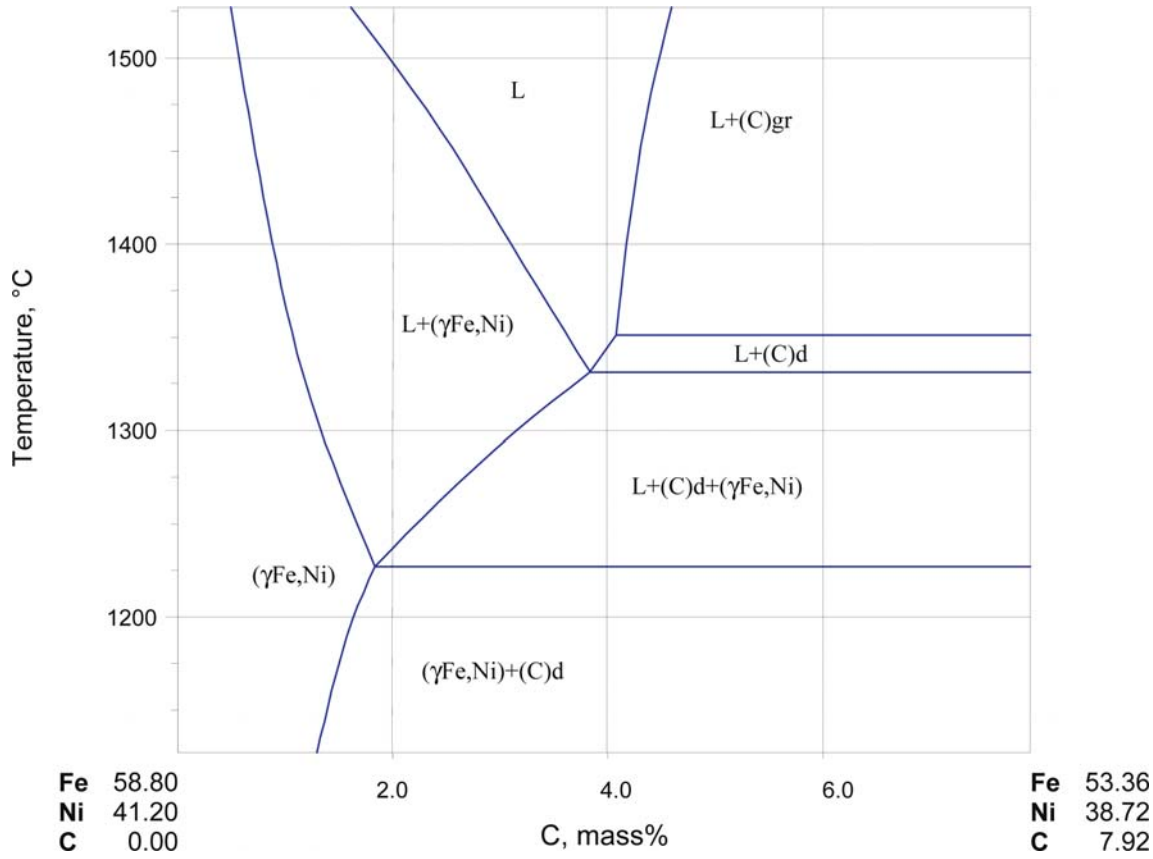

Fig. 17. C-Fe-Ni. Vertical section C-$Fe_{0.6}Ni_{0.4}$ under 5.2 GPa, plotted in mass%

DOI: 10.1007/978-3-540-74196-1_10

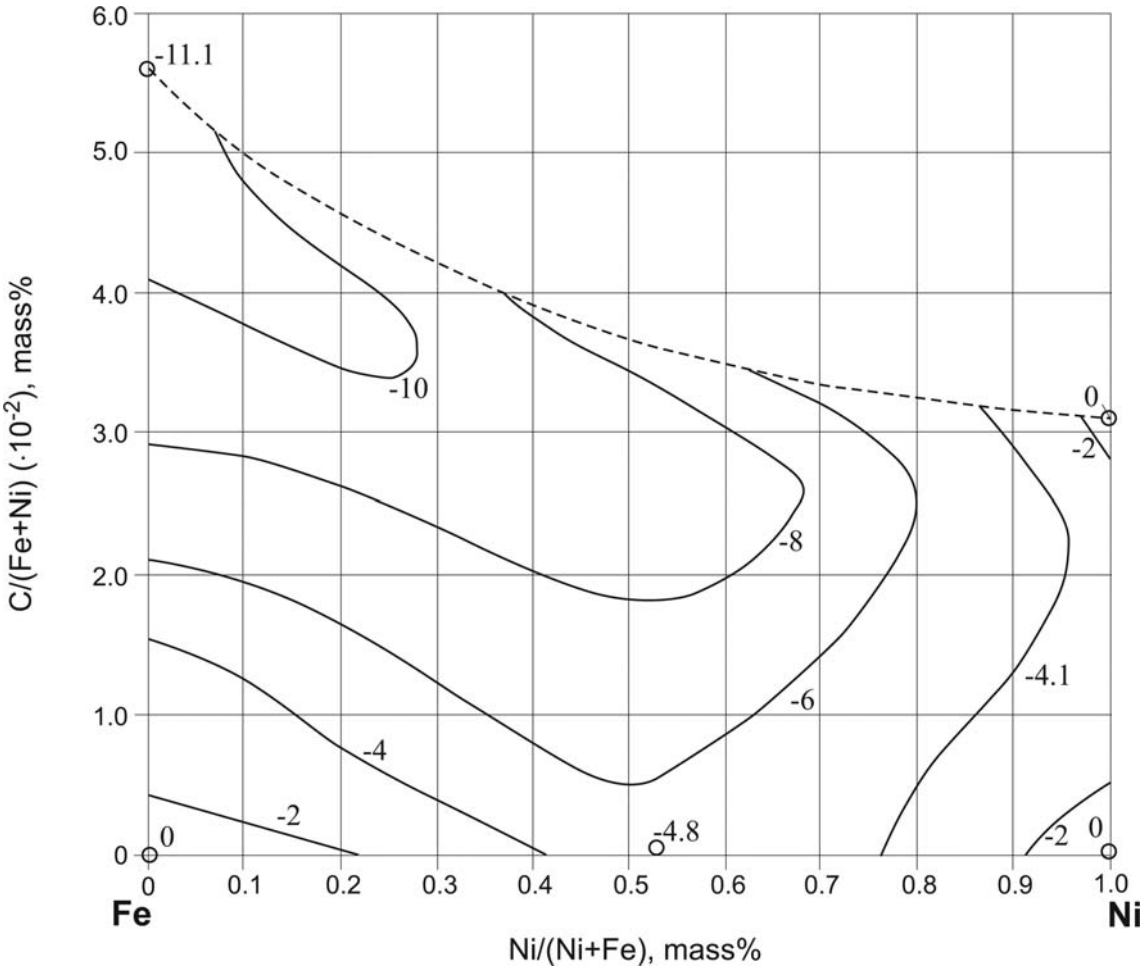

Fig. 18. C-Fe-Ni. Integral enthalpy of mixing (in $kJ \cdot mol^{-1}$) in liquid alloys

DOI: 10.1007/978-3-540-74196-1_10

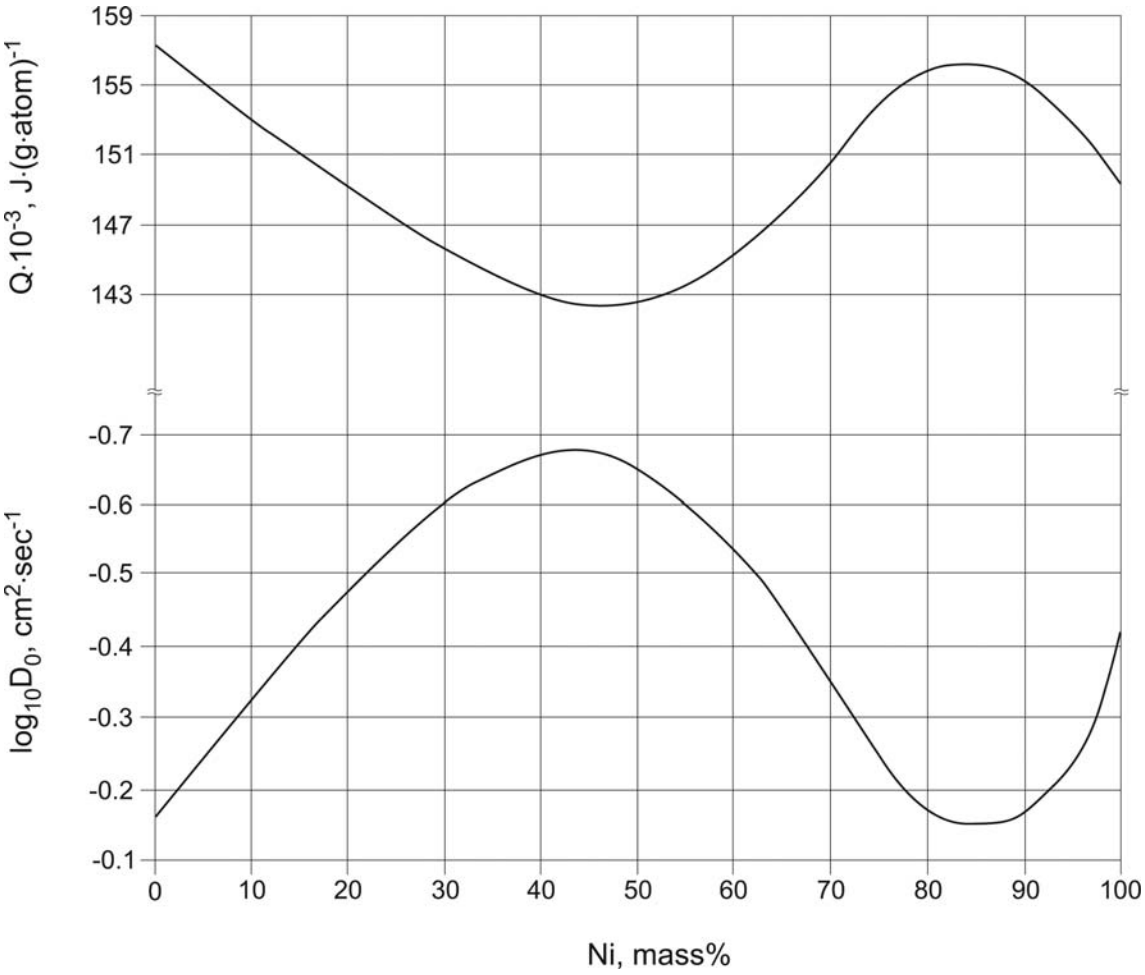

Fig. 19. C-Fe-Ni. Activation energy and diffusivity of C in (γ Fe,Ni) alloys

DOI: 10.1007/978-3-540-74196-1_10

References

[1925Kas1] Kase, T., "Ternary System of Iron-Carbon-Nickel", *Sci. Rep. Tohoku Imp. Univ.*, **1**(14), 193–217 (1925) (Phase Diagram, Phase Relations, Morphology, Experimental, 5)

[1925Kas2] Kase, T., "On the Equilibrium Diagram of the Iron-Carbon-Nickel System", *Sci. Rep. Tohoku Imp. Univ.*, **1**(14), 173–217 (1925) (Phase Diagram, Phase Relations, Experimental, 25)

[1926Osa] Osawa, A., "The Relation Between Lattice Constants and Densities in Nickel-Steels", *Sci. Rep. Tohoku Imp. Univ.*, **15**(1), 619–630 (1926) (Crys. Structure, Mechan. Prop., Phys. Prop., Experimental,4)

[1926Rib] Ribbeck, F., "About Dependence of Nickel's Steel Electrical Resistivity from Composition, Temperature and Heat Treatment" (in German), *Z. Physik*, **39**, 787–812 (1926) (Electr. Prop., Experimental, Phase Diagram, 10)

[1931Soe] Soehnchen, V.E., Piwowarsky, E., "About the Influence of Alloying Elements Nickel, Silicon, Aluminium and Phosphorus on the Carbon Solubility in Liquid and Solid Iron" (in German), *Arch. Eisenhuettenwes.*, **5**(2), 111–121 (1931) (Experimental, Morphology, Phase Diagram, 51)

[1932Bai] Bain, E.C., Kearny, N.J., "On the Rates of Reactions in Solid Steel", *Trans. Amer. Inst. Min. Met. Eng.*, 100, 13–46 (1932) (Kinetics, Phase Relations, Review, 0)

[1934Deh] Dehlinger, U., Bumm, H., "Kinetics and Phase Diagram of Irreversible Transformations in Iron-Nickel System" (in German), *Z. Metallkd.*, **26**(5), 112–116 (1934) (Experimental, Morphology, Phase Diagram, 10)

[1938And] Andrew, J.H., Bottomley, G.T., Maddocks, W.R., Percival, R.T., "The Fluidity of Iron-Carbon and other Iron Alloys", Iron Steel Inst., 3th Rep. *Steel Castings Research Committee*, Publ. Offices Iron Steel Inst. 4, Grosvenor Gardens, London, S.W.1, 1938, (23), 5–32 (1938) (Phys. Prop., Experimental, 9)

[1938Lan] Lange, H., Mathieu, K., "About Evolution of the Austenite Transformation in Supercool State of Iron-Nickel-Carbon Alloys" (in German), *Mitt. K. W. Inst. Eisenforschung*, **20**, 125–134 (1938) (Experimental, Phys. Prop., Morphology, 17)

[1949Jae] Jänecke, E., "C-Fe-Ni" (in German), *Kurzgefasstes Handbuch Aller Legierungen*, Winter, Heidelberg, 674–675 (1949) (Phase Diagram, Review, 2)

[1951Ber] Bernier, R., "Thermomagnetic Study of Iron and Nickel Carbides" (in French), *Ann. Chim. (Paris)*, **6**(12), 104–161 (1951) (Crys. Structure, Experimental, Magn. Prop., Review, 66)

[1955Sam] Samuel, P., Finch, L.G., Rait, J.R., "A Phase Diagram for I per Cent Carbon-Iron Alloys Containing up to 16 % Nickel", *Nature*, **175**, 37–38 (1955) (Experimental, Phase Diagram, Phase Relations, 4)

[1956Tur] Turkdogan, E.T., Hancock, R.A., Herlitz, S.I., Dentan, J., "Thermodynamics of Carbon Dissolved in Iron Alloys. Part V: Solubility of Graphite in Iron-Manganese, Iron-Cobalt, and Iron-Nickel Melts", *J. Iron Steel Inst., London*, **183**, 69–72 (1956) (Experimental, Phase Relations, Thermodyn., 17)

[1959Fuw] Fuwa, T., Chipman, J., "Activity of Carbon in Liquid Iron Alloys", *Trans. Metall. Soc. AIME*, **215**, 708–716 (1959) (Calculation, Experimental, Phase Relations, Thermodyn., 22)

[1959Neu] Neumann, F., Schenck, H., Patterson, W., "Iron-Carbon Alloys in Thermodynamic Consideration" (in German), *Giesserei Tech.-Wiss. Beih.*, **23**, 1217–1246 (1959) (Phase Diagram, Phase Relations, Theory, Thermodyn., 72)

[1960Mil] Miller, K.O., Elliott, J.F., "Phase Relationship in the Systems Fe-Pb-Ni, Fe-Ni-C(Sat), Fe-Pb-Ni-C; 1300 to 1550°C", *Trans. Metall. Soc. AIME*, **218**, 900–910 (1960) (Phase Diagram, Experimental, 12)

[1960Smi] Smith, R.P., "Activity of Carbon in Iron-Nickel Alloys at 1000°C", *Trans. Metall. Soc. AIME*, **218**, 62–64 (1960) (Experimental, Phase Relations, Thermodyn., 4)

[1960War] Ward, R.G., Wright, J.A., "The Solubility of Carbon in Molten Iron-Nickel Alloys", *J. Iron Steel Inst., London*, **194**, 304–306 (1960) (Experimental, Phase Diagram, Phase Relations, Thermodyn., 10)

DOI: 10.1007/978-3-540-74196-1_10

[1962Pet] Petrova, E.F., Shvartsmann, L.A., "On the Thermodynamics of the Fe-Ni Solid Solutions" (in Russian), *Dokl. Akad. Nauk SSSR*, **146**(3), 646–648 (1962) (Calculations, Thermodyn., 5)

[1963Hec] Heckler, A.J., Winchell, P.G., "The Activity of Carbon in Iron-Nickel-Carbon Austenite", *Trans. Metall. Soc. AIME*, **227**, 732–736 (1963) (Experimental, Phase Relations, Thermodyn., 3)

[1963Sch] Schenck, H., Frohberg, M.G., Steinmetz, E., "Investigations on the Mutual Activities Influence in Homogeneous Metallic Substances Solubility. Part I. Experimental Investigations of Manganese-Carbon-X, Cobalt-Carbon-X, Nickel-Carbon-X Systems in Liquid State" (in German), *Arch. Eisenhuettenwes.*, **34**(1), 37–42 (1963) (Experimental, Phase Diagram, Thermodyn., Review 30)

[1964Bro] Brown, L.C., Kirkaldy, J.S., "Carbon Diffusion in Dilute Ternary Austenites", *Trans. Metall. Soc. AIME*, **239**, 223–226 (1964) (Experimental, Transport Phenomena, Interface Phenomena, Kinetics, 15)

[1964Buc] Buckley, R.A., Hume-Rothery, W., "Liquidus and Solidus Relations in Iron-Rich Iron-Carbon-Nickel Alloys", *J. Iron Steel Inst., London*, **202**, 895–898 (1964) (Experimental, Phase Diagram, Phase Relations, 16)

[1964Hel] Heller, W., Brauner, J., "Investigations on the Diffusion and Precipitation of Carbon in Ferritic Iron-Nickel Alloys by Measuring the Damping Capacity" (in German), *Arch. Eisenhuettenwes.*, **35**(11), 1105–1110 (1964) (Experimental, Kinetics, Interface Phenomena, Phase Relations, 13)

[1966Smi] Smith, R.P., "The Diffusivity of Carbon in γ Iron-Nickel Alloys", *Trans. Metall. Soc. AIME*, **236**, 1224–1227 (1966) (Experimental, Kinetics, Thermodyn., 15)

[1967Rao] Rao, M.M., Russell, R.J., Winchell, P.G., "A Correlation of Thermodynamic Variables for Iron-Rich Iron-Nickel-Carbon Alloys", *Trans. Metall. Soc. AIME*, **239**, 634–642 (1967) (Calculation, Phase Relations, Thermodyn., 35)

[1968Bol] Bolling, G.F., Arrott, A., Richman, R.H., "A Study of Curie Temperatures and the Effect of Carbon in Face-Centered Cubic Iron-Nickel Alloys", *Phys. Status Solidi*, **26**, 743–750 (1968) (Calculation, Experimental, Magn. Prop., 14)

[1968Chi] Chipman, J., Brush, E.F., "The Activity of Carbon in Alloyed Austentite at 1000°C", *Trans. AIME*, **242**, 35–41 (1968) (Calculation, Phase Relations, Thermodyn., 21)

[1968Jol] Jolley, W., "Effect of Mn and Ni on Impact Properties of Fe and Fe-C Alloys", *J. Iron Steel Inst., London*, **206**, 170–173 (1968) (Experimental, Morphology, Mechan. Prop., 16)

[1968Zup] Zupp, R.R., Stevenson, D.A., "Statistical Thermodynamics of Carbon in Ternary Austenitic Iron-Base Alloys", *Trans.Metall. Soc. AIME*, **242**, 862–869 (1968) (Thermodyn., Calculation, Phase Relations, 35)

[1969Fra] Fray, D.J., Chipman, J., "The Solubility of Graphite in Fe-Ni and Fe-Co Alloys at 1000°C", *Trans. Metall. Soc. AIME*, **245**, 1143–1144 (1969) (Experimental, Phase Relations, 4)

[1970Zem] Zemskii, S.V., Gruzin, P.L., "Investigation of the Fe-C and Fe-C-M Systems by Raioisotope Methods" (in Russian), *Optimizatsiya Metallurgicheskikh Protsesov*, Metallurgiya, Moscow, **4**, 54–64 (1970) (Experimental, Phase Diagram, Phase Relations, 18)

[1971Gre] Greenbank, J.C., "Carbon Solute Interactions in Fe-Ni-C Alloys", *J. Iron Steel Inst., London*, **209**, 819–825 (1971) (Calculation, Experimental, Phase Diagram, Phase Relations, 18)

[1971Str] Strong, H.M., Chrenko, R.M., "Further Studies on Diamond Growth Rates and Physical Properties of Laboratory-made Diamond", *J. Phys. Chem.*, **78**(12), 1838–1843 (1971) (Experimental, Phase Diagram, 30)

[1971Wad] Wada, T., Wada, H., Elliott, J.F., Chipmann, J., "Thermodynamics of the fcc Fe-Ni-C and Ni-C Alloys", *Metall. Trans.*, **2**, 2199–2208 (1971) (Experimental, Thermodyn., 25)

[1972Foo] Foo, E.H., Lupis, C.H.P., "Activity of Carbon in Liquid Iron Alloys at 1550°C", *Metall. Trans.*, **3**, 2125–2131 (1972) (Experimental, Thermodyn., Phase Relations, 18)

[1973Nat] Natesan, K., Kassner, T.F., "Thermodynamics of Carbon in Nickel, Iron-Nickel and Iron-Chromium-Nickel Alloys", *Metall. Trans.*, **4**, 2557–2566 (1973) (Experimental, Phase Diagram, Thermodyn., 39)

DOI: 10.1007/978-3-540-74196-1_10

[1973Sha] Sharma, R.C., Kirkaldy, J.S., "Thermodynamics and Kinetics of the Proeutectoid Ferrite Reaction in Fe-C-Ni in the Vicinity of 730°C", *Canad. Metall. Quart.*, **12**(4), 391–401 (1973) (Calculation, Experimental, Kinetics, Phase Relations, Thermodyn., 24)

[1974Ela] Elanskii, G.N., Akinfiev, S.I., Kudrin, V.A., Babich, V.K., "Relationship Between Rate of decarburization of Fe-C-Ni and Fe-C-Cu Melts and Their Structure", *Steel USSR*, **4**(9), 722–723 (1974), translated from *Izv. VUZ Chern. Metall.*, (9), 22–25 (1974) (Experimental, Kinetics, 11)

[1975Shi] Shigematsu, T., "Invar Properties of Cementite $(Fe_{1-x}Me_x)_3C$, Me = Cr, Mn, Ni", *J. Phys. Soc. Jpn.*, **39**(4), 915–920 (1975) (Experimental, Mechan. Prop., 14)

[1975Sri] Srinivasan, S.R., Grabke, H.J., "Interpretation of Thermodynamic Data of Fe-Ni-C and Fe-Ni-N Alloys", *Scr. Metall.*, **9**(4), 387–390 (1975) (Calculation, Phase Relations, Thermodyn., 5)

[1976Kle] Kleemola, H.J., Kuusisto, E.A., "The Effect of Cr, Mn and Ni on the Solubility and Precipitation of Carbon in Ferritic Iron", *Scand. J. Met.*, **5**, 151–158 (1976) (Experimental, Phase Diagram, Kinetics, 20)

[1976Ko] Ko, M., Sakuma, T., Nishizawa, T., "Effect of Magnetism on the Partition of Alloying Elements between Cementite and Ferrite" (in Japanese), *J. Jpn. Inst. Met.*, **40**(6), 593–601 (1976) (Experimental, Phase Relations, Thermodyn., Magn. Prop., 37)

[1976Rus] Rusin, V.A., Onishchin, B.P., Gran, N.I., "Activity of Iron and Nickel in Ferronickel" (in Russian), *Nauchn. Issl. Metall. Ni i Co.* Nauchn. Trud. Gos. Proektn. Nauchno-Issled. Inst. 'Gipronikel', Leningrad, **1**(65), 12–18 (1976) (Calculation, Experimental, Thermodyn., 9)

[1976Tom] Tomilin, I.A., Konnova, I.Yu., Golovanenko, S.A., "The Activity of Carbon in Ni-Fe Alloys at 500-1200°C", *Russ. Metall. (Engl. Transl.)*, (4), 24–27 (1976) (Experimental, Thermodyn., 8)

[1977Ach] Achar, B.S., Miodownik, A.P., "The Effect of Two γ States on the Activity of Carbon in FCC Iron-Nickel-Carbon Alloys", *Calphad*, **1**(3), 275–280 (1977) (Phase Diagram, Theory, Thermodyn., 14)

[1977Eli] Eliezer, I., Howald, R.A., "A Systematic Treatment of the Three-Compenent System Fe-Ni-C", *High Temp. Sci.*, **9**, 119–130 (1977) (Calculation, Phase Relations, Thermodyn., 33)

[1977Rom] Roming, A.D., Goldstein, J.I., "Experimental Determination of Phase Diagrams with the Electron Microprobe and Scanning Transmission Electron Microscope", *Nat. Bur. Stand. Special Publ.* N° 496, **Vol. 1**, 462–482 (1977) (Experimental, Phase Diagram, Phase Relations, 33)

[1977Uhr] Uhrenius, B., "Optimization of Parameters Describing the Interaction Between Carbon and Alloying Elements in Ternary Austenite", *Scand. J. Metall.*, **6**(2), 83–89 (1977) (Assessment, Calculation, 24)

[1978Uhr] Uhrenius, B., "A Compendium of Ternary Iron-base Phase Diagrams", *The Hardenability of Steels*, *Proc. Symp. AIME-ASM,* Chicago, Oct. 24-26, 1977*,* 28–81 (1978) (Assessment, Thermodyn., Calculation, 53)

[1978Kri] Kripakaran, R., Winchell", P.G., "Discussion of "Determination of the Fe-Rich Portion of the Fe-Ni-C Phase Diagram", *Metall. Trans. A*, **9A**, 1687–1688 (1978) (Phase Relations, Thermodyn., Review, 7)

[1978Rom] Romig, A.D., Goldstein, J.I., "Determination of the Fe-Rich Portion of the Fe-Ni-C Phase Diagram", *Metall. Trans. A*, **9A**, 1599–1609 (1978) (Experimental, Morphology, Phase Diagram, 30)

[1979Kag] Kagawa, A., Okamoto, T., "Lattice Parameters of Cementite in Fe-C-X (X=Cr, Mn, Mo, and Ni) Alloys", *Trans. Jpn. Inst. Met.*, **20**(11), 659–666 (1979) (Crys. Structure, Experimental, 11)

[1980Ost] Ostrowski, R., Podrzucki, C., "Solubility of Nickel, Copper, Tin and Phosphorus in Ferrite and Eutectoid Cementite in Gray Iron" (in Polish), *Prace Komisji Metallurgiczno-Odlewniczej, Metallurgia*, **28**, 77–99 (1980) (Phase Relations, Experimental, 17)

DOI: 10.1007/978-3-540-74196-1_10

[1980Ram] Ramanathan, R., Oates, W.A., "Activity Coefficient of Carbon In Fe-Co-Ni-C Alloys at 1273 K", *Metall. Trans. A*, **11A**, 459–466 (1980) (Experimental, Thermodyn., Phase Relations, 24)

[1982Kaj] Kajatkari, M., Ullakko, K., Pietikaeinen, J., "On the Aging of Fe-Ni-C and Fe-Mn-C Martensites", *J. Phys. (France)*, **43**(C4), 461–466 (1982) (Experimental, Morphology, Mechan. Prop., 19)

[1982Oka] Okafor, I.C.I., Carlson, O.N., Martin, D.M., "Mass Transport of Carbon in One and Two Phase Iron-Nickel Alloys in a Temperature Gradient", *Metall. Trans. A*, **13A**, 1713–1719 (1982) (Calculation, Experimental, Morphology, Phase Diagram, Transport Phenomena, 21)

[1983Mor] Morita, Z.-I., Tanaka, T., "Thermodynamics of Solute Distributions Between Solid and Liquid Phases in Iron-base Ternary Alloys", *Trans. Iron Steel Inst. Jpn.*, **23**(1), 824–833 (1983) (Experimental, Thermodyn., Phase Relations, 30)

[1983Ume] Umemoto, M., Yoshitake, E., Tamura, I., "The Morphology of Martensite in Fe-C, Fe-Ni-C and Fe-Cr-C Alloys", *J. Mater. Sci.*, **18**(10), 2893–2904 (1983) (Experimental, Mechan. Prop., Morphology, Phase Relations, 32)

[1984Riv] Rivlin, V.G., "Phase Equilibria in Iron Ternary Alloys –(13)- Critical Evaluation of the Constitution of Ternary Systems C-Fe-X (X=Co, Ni, Cu)", *Int. Met. Rev.*, **29**(2), 96–121 (1984) (Phase Diagram, Phase Relations, Review, 76)

[1985Eno] Enomoto, M., Aaronson H.I., "Calculation of $\alpha+\gamma$ Phase Boundaries in Fe-C-X Systems from the Central Atoms Model", *Calphad*, **9**(1), 43–58 (1985) (Theory, Calculation, Thermodyn., 31)

[1985Riv] Rivlin, V.G., "Assessment of Phase Equilibria in Ternary Alloys of Iron", *J. Less-Common Met.*, **114**, 111–121 (1985) (Assessment, Phase Diagram, Phase Relations, 4)

[1985Vit] Vityaz, P.A., Nasybulin, A.Kh., "Homogenization in Sintering and its Influence on Mechanical Properties of Fe-Cr-C and Fe-Ni-C Steels", *Powder Metal.*, **28**(3), 166–168 (1985) (Experimental, Mechan. Prop., Morphology, 5)

[1986Sch] Schuermann, E., von Schweinichen, J., "Investigations on Equilibria in the Liquid State in the Iron Rich Corner of the Ternary Systems Fe-C-X with X = Al, Cu, Ni und Cr" (in German), *Giessereiforschung*, **38**(4), 125–132 (1986) (Experimental, Phase Diagram, Phase Relations, 63)

[1987Gab] Gabriel, A., Gustafson, P., Ansara, I., "A Thermodynamic Evaluation of the C-Fe-Ni System", *Calphad*, **11**(2), 203–218 (1987) (Assessment, Phase Diagram, Thermodyn., Phase Relations, 41)

[1987Sch] Schuermann, E., Schweinichen, J., Voelker, R., Fischer, H., "Calculation of the α/δ Resp γ Liquidus of Iron and of the Liquidus of Carbon as well as of the Univariant Reaction Lines in Iron-Rich, Carbon Containing Three Component and Multicomponent Fe-C-X_1-X_2-Systems" (in German), *Giessereiforschung*, **39**(3), 104–113 (1987) (Phase Diagram, Phase Relations, Calculation, Thermodyn., 19)

[1988Ray] Raynor, G.V., Rivlin, V.G., "C-Fe-Ni" in "*Phase Equilibria in Iron Ternary Alloys*", Inst. Metals, London, **4**, 192–200 (1988) (Phase Diagram, Review, 27)

[1988Sum] Sumin, V.V., Morozov, S.I., Natkanets, I., Petru, D., "Inelastic Scattering of Slow Neutrons Study of Local Oscillations of Carbon Atoms in Fe-Mn-C and Fe-Ni-C Atoms", *Phys. Met. Metallogr.*, **65**(1), 155–159 (1988), translated from *Fiz. Metal. Metalloved.*, **65**(1), 168–172 (1988) (Crys. Structure, Experimental, Thermodyn., 16)

[1989Bug] Bugayev, V.N., Gavrilyuk, V.G., Nadutov, V.M., Tatarenko, V.A., "Carbon Distribution in Fe-Ni-C and Fe-Mn-C Alloys with an FCC Lattice", *Phys. Met. Metallogr.*, **68**(5), 93–102 (1989), translated from *Fiz. Metal. Metalloved.*, **68**(5), 931–940 (1989) (Crys. Structure, Experimental, 19)

[1989Sin] Singleton, M., Nash, P., "The C-Ni System", *Bull. Alloy Phase Diagrams*, **10**(2), 121–126 (1989) (Crys. Structure, Phase Diagram, Review, Thermodyn., 44)

[1990Gav] Gavrilyuk, V.G., Nadutov, V.M., Oshkaderov, S.P., Pietikainen, J., Ullakko, K., "Phase and Magnetic Transformations in the Fe-Ni-C Alloy at Low Temperatures", *Phys. Met. Metall.*,

DOI: 10.1007/978-3-540-74196-1_10

70(1), 120–125 (1990), translated from *Fiz. Met. Metalloved*, (7), 128–133 (1990) (Crys. Structure, Experimental, Magn. Prop., 14)

[1990Rey] Reynolds, W.T. Jr., Liu, S.K., Li, F.Z., Hartfield, S., Aaronson, H.I., "An Investigation of the Generality of Incomplete Transformation to Bainite in Fe-C-X Alloys", *Metall. Trans. A*, **21A**(6), 1479–1491 (1990) (Experimental, Kinetics, Phase Relations, 56)

[1991Pav] Pavel, E., Pintiliescu, L., Baluta, Gh., Giurgiu, C., Barb, D., Lazar, D.P., Morariu, M., "The Ternary Constitution Diagrams for the Fe-Ni-C and Fe-Co-C Systems at 5.7 GPa", *Physica B*, **175**(4), 354–360 (1991) (Experimental, Morphology, Phase Diagram, Phase Relations, Thermodyn., 21)

[1991Tsu] Tsuzaki, K., Fujiwara, K., Maki, T., "Bainite Reaction in Fe-Ni-C Alloys", *Mater. Trans., JIM*, **32**(8), 667–678 (1991) (Experimental, Kinetics, 24)

[1991Vod] Vodarek, V., Pahuta, P., "Precipitation of ε (η)-Carbide During the First Stage of Martensite Tempering", *Met. Mater. (Czech.)*, **29**(3), 151–159 (1991) (Abstract)

[1992Gon] Gong, F., Goldstein, J., "550 and 450°C Isothermal Sections of Fe-Ni-C Phase Diagram", *Acta Metall. Sin.., Ser. B*, **5**(6), 471–475 (1992) (Experimental, Morphology, Phase Diagram, 4)

[1992Men] Mencl, J., Mordike, B.L., Riehemann, W., "Isothermal Ageing of Fine Grained Supersaturated Fe-C-Ni Alloys", *Int. J. Rapid Solidif.*, **7**(1), 1–16 (1992) (Experimental, Mechan. Prop., 9)

[1992Run] Runov, V.V., Okorokov, A.I., Tretjakov, A.D., Grigorjev, L.V., Uljanov, V.A., Ullakko, K., Gavriljuk, V.G., "Observation of a Relaxation Phenomenon During Ageing of Fe-Ni-C Martensite by Means of Small Angle Neutron Scattering", *Scr. Metall. Mater.*, **26**(4), 661–665 (1992) (Experimental, Mechan. Prop., Abstract)

[1992Spa] Spanos, G., "The Morphology, Crystallography, and Mechanism of Carbide Precipitation in an Fe-0.12C-3.28Ni Alloy", *Metall. Trans. A*, **23A**(1), 171–181 (1992) (Experimental, Mechan. Prop., Morphology, 44)

[1993Koc] Kocherzhinskii, Y.A., Kulik, O.G., Turkevich, V.Z., "Phase Equilibria in the Fe-Ni-C and Fe-Co-C Systems under High Temperatures and High Pressures", *High Temp. - High Pres.*, **25**, 113–116 (1993) (Experimental, Phase Diagram, 9)

[1993Pav] Pavel, E., Baluta, G., Giurgiu, C., Barb, D., Sandu, V., "Effects of Pressure, Time, and Various Additives of the Crystallization of Graphite and $(Fe_{1-x}Ni_x)_3C$ Carbide in the Fe-Ni-C System", *Mater. Charact.*, **30**, 107–112 (1993) (Experimental, Phase Diagram, 7)

[1993Vit] Vitusevich, V.T., Shumikhin, V.S., "Enthalpy of Formation of Molten Fe-Mn(Co, Ni)-C Systems" (in Russian), *Rasplavy*, (5), 78–80 (1993) (Thermodyn., Experimental, 13)

[1994Dan] Danilchenko, V.E., Nedolya, A.V., "Carbon Solubility in Laser Treated Zone of Fe-Based Alloys", *Mater. Sci. Forum*, **166–169**, 427–432 (1994) (Mechan. Prop., Crys. Structure, Experimental, 5)

[1994Oda] Oda, K., Fujimura, H., Ino, H., "Local Interactions in Carbon-Carbon and Carbon-M (M: Al, Mn, Ni) Atomic Pairs in FCC γ-Iron", *J. Phys.: Condens. Matter*, **6**(3), 679–692 (1994) (Experimental, 32)

[1994Rag] Raghavan V., "C-Fe-Ni (Carbon-Iron-Nickel)", *J. Phase Equilib.*, **15**(4), 428–429 (1994) (Phase Diagram, Review, 12)

[1994Wit] Witusiewicz, V.T., "Thermodynamic Properties of Liquid Alloys of 3d Transition Metals with Metalloids (Silicon, Carbon and Boron)", *J. Alloys Compd.*, **203**, 103–116 (1994) (Theory, Thermodyn., Review, 89)

[1995Lee] Lee, B.-J., "Thermodynamic Calculations in Stainless Steels Alloy Systems" (in Korean), *J. Korean Inst. Met.*, **33**(6), 766–775 (1995) (Calculation, Phase Relations, Phase Diagram, Thermodyn., 53)

[1996Koc] Kocherzhinski, Yu.A., Kulik, O.G., "Equilibrium Phase Diagrams and Manufacture of Synthetic Diamond", *Powder Metall. Met. Cer.*, **35**(7–8), 470–483 (1996) (Experimental, Phase Relations, 37)

DOI: 10.1007/978-3-540-74196-1_10

[1997Gen] Van Genderen, M.J., Isac, M., Boettger, A., Mittemeijer, E.J., "Aging and Tempering Behavior of Iron-Nickel-Carbon and Iron-Carbon Martensite", *Metall. Mater. Trans. A*, **28**(3), 545–561 (1997) (Experimental, Kinetics, Phase Relations, 51)

[1997Miz] Mizuno, M., Tanaka, I., Adachi, H., "Effect of Solute Atoms on the Chemical Bonding of Fe_3C (Cementite)", *Philos. Mag. B*, **75**(2), 237–248 (1997) (Crys. Structure, Mechan. Prop., Theory, 28)

[2000Fen] Fenstad, J., "Liquidus Relations and Thermochemistry within the System Fe-Mn-C-O", Thesis 2000:126 (2000:23) Dept. Mater. Elchem., NTNU, (2000) (Experimental, Phase Relations, Thermodyn.)

[2000Koz] Kozeschnik, E., Vitek, J.M., "Ortho-Equilibrium and Para-Equilibrium Phase Diagrams for Interstitial/Substitutional Iron Alloys", *Calphad*, **24**(4), 495–502 (2000) (Calculation, Phase Diagram, Phase Relations, Thermodyn., 10)

[2000Yin] Yin, L.-W., Li, M.-S., Liu, Y.-X., Hao, Z.-Y., "Direct Microscopic Observation of Metallic Impurities in Synthetic Diamonds Produced from Fe-Ni-C System", *J. Mater. Sci. Lett.*, **19**(22), 2001–2002 (2000) (Crys. Structure, Morphology, Experimental, 13)

[2001Fen] Fenstad, J., Tuset, J.Kr., "The Binary Diagrams within the System Fe-Mn-C-O, and the Thermal Properties of Elemental Manganese", *INFACON 9: Proceedings of the International Ferro-Alloys Congress,* June 2001, Quebec, Canada, 9, (2001) (Experimental, Phase Relations, Thermodyn., 25)

[2001Gho] Ghosh, G., Olson, G.B., "Computational Thermodynamics and the Kinetics of Martensitic Transformation", *J. Phase Equilib.*, **22**, 199–207 (2001) (Calculation, Phase Relations, Thermodyn., 65)

[2001Has] Haseeb, A.S.M.A., Nishida, T., Masuda, M., Hayashi, Y., "Moessbauer Investigation on Electrodeposited Fe-C and Fe-Ni-C Alloys", *Scr. Mater.*, **44**(3), 519–524 (2001) (Experimental, 12)

[2001Ma] Ma, Z., "Thermodynamic Description for Concentrated Metallic Solutions Using Interaction Parameters", *Metall. Trans. B*, **32B**, 87–103 (2000) (Calculation, Phase Relations, Thermodyn., 70)

[2001Qui] Quidort, D., Brechet, Y.J.M., "Isothermal Growth Kinetics of Bainite in 0.5 C Steels", *Acta Mater.*, **49**, 4161–4170 (2001) (Experimental, Kinetics, Phase Relations, 42)

[2001Ume] Umemoto, M., Liu, Z.G., Masuyama, K., Tsuchiya, K., "Influence of Alloy Additions on Production and Properties of Bulk Cementite", *Scr. Mater.*, **45**(4), 391–397 (2001) (Crys. Structure, Experimental, Mechan. Prop., Phase Relations, Phys. Prop., 13)

[2001Zha] Zhang, M.-X., Kelly, P.M., "Deformation Twinning of Martensite in an Fe-Ni-C Alloy", *Scr. Mater.*, **44**(11), 2575–2581 (2001) (Crys. Structure, Experimental, 15)

[2002Qui] Quidort, D., Brechet, Y.J.M., "A Model of Isothermal and Non Isothermal Transformation Kinetics of Bainite in 0.5% C Steels", *ISIJ Int.*, **42**(9), 1010–1017 (2002) (Calculation, Kinetics, Phase Relations, Theory, Thermodyn., 36)

[2002Sol] Solozhenko, V.L., Turkevich, V.Z., Kurakevych, O.O., Crichton, W.A., Mezouar, M., "Kinetics of Diamond Crystallization from the Melt of the Fe-Ni-C System", *J. Phys. Chem. B*, **106**(26), 6634–6637 (2002) (Experimental, Kinetics, Phase Diagrams, Phase Relations, 24)

[2003Dan] Danil'chenko, V.E., Sagaradze, V.V., L'Heritier, Ph., "Martensite Crys. Structure of Nickel Steel at Cryogenic Temperatures", *Mater. Sci. Eng. A*, **358**, 26–31 (2003) (Crys. Structure, Experimental, Phase Relations, 25)

[2003Kap] Kaputkina, L.M., Kaputkin, D.E., "Structure and Phase Transformations under Quenching and Tempering During Heat and Thermomechanical Treatment of Steels", *Mater. Sci. Forum*, **426–432**, 1119–1126 (2003) (Crys. Structure, Experimental, Morphology, Phase Relations, 7)

[2004Aar] Aaronson, H.I., Reynolds, W.T., Purdy, G.R., "Coupled-Solute Drag Effect on Ferrite Formation in Fe-C-X Systems", *Metall. Mater. Trans. A*, **35A**(4), 1187–1210 (2004) (Experimental, Interface Phenomena, Kinetics, Morphology, Phase Relations, 148)

DOI: 10.1007/978-3-540-74196-1_10

[2004Hut] Hutchinson, C.R., Fuchsmann, A., Brechet, Y., "The Diffusional Formation of Ferrite from Austenite in Fe-C-Ni Alloys", *Metall. Mater. Trans. A*, **35A**(4), 1211–1221 (2004) (Experimental, Kinetics, Mechan. Prop., Morphology, Phase Relations, Interface Phenomena, 29)

[2004Tao] Tao, D.P., "A Thermodynamic Model for Solid Solutions and ist Application to the C-Fe-Co, C-Fe-Ni and Mn-Cr-Pt Solid Dilutions", *Mater. Sci. Eng. A*, **366**(2), 239–274 (2004) (Calculation, Theory, Thermodyn., 26)

[2006Aar] Aaronson, H.I., Reynolds, W.T., Purdy, Jr. G.R., "The Incomplete Transformation Phenomenon in Steel", *Metall. Mater. Trans. A*, **37A**(6), 1731–1745 (2006) (Experimental, Phase Relations, Kinetics, 89)

[2006MSIT] "C-Fe (Carbon Iron)", *Diagrams as Published in MSIT Workplace*, Effenberg, G. (Ed.), MSI, Materials Science International Services GmbH, Stuttgart; Document ID: 30.13598.1.20, (2006) (Phase Diagram, Phase Relations, Crys. Structure, 2)

[2007Kuz] Kuznetsov, V., "Fe-Ni (Iron-Nickel)", MSIT Binary Evaluation Program, in MSIT Workplace, Effenberg, G. (Ed.), MSI, Materials Science International Services, GmbH, Stuttgart; to be published (2007) (Crys. Structure, Phase Diagram, Phase Realtions, Assessment, 41)

[Mas2] Massalski, T.B. (Ed.), *Binary Alloy Phase Diagrams*, 2nd edition, ASM International, Metals Park, Ohio (1990)

[V-C2] Villars, P. and Calvert, L.D., *Pearson's Handbook of Crystallographic Data for Intermetallic Phases*, 2nd edition, ASM, Metals Park, Ohio (1991)

DOI: 10.1007/978-3-540-74196-1_10

Carbon – Iron – Phosphorus

Pierre Perrot

Introduction

Phosphorus is known to be a deleterious element in steels because of the formation of a low melting eutectic, so the C-Fe-P system raised much interest. The first tentative diagrams were proposed by [1908Goe, 1908Wue] who measured the position of the ternary eutectic. The values obtained by [1908Wue] (2 mass% C, 6.7 mass% P and 950°C), confirmed by [1915Ste, 1930Kue], then later accepted by [1949Jae] are astonishingly close to its actual values (1.95 mass% C, 6.75 mass% P and 955°C) [1987Sch, 1988Rag, 2004Rag]. The main investigations on the ternary system concern the stable and metastable phase equilibria and the segregation of phosphorus during solidification which governs the crack formation. Thermodynamic assessment of the C-Fe-P ternary system has been carried out in [2000Shi]. Experimental investigations on the crystal structure, phase equilibria and thermodynamics are gathered in Table 1.

Binary Systems

The C-Fe phase diagram accepted from [2006MSIT] is mainly based on the assessment by [1992Oka]. The properties of metastable carbides such as $Fe_{2.2}C$ (Haegg carbide) and $Fe_{2.4}C$ (know as "ε carbide" are well discussed in [1972Chi] which proposes also simple expressions for carbon activities in austenite and thermodynamic properties of carbides, which may be useful because they are in good agreement with more recent and more sophisticated relationships. The Fe-P diagram is mainly accepted from [2002Per].

Solid Phases

Crystallographic data of solid phases are shown in Table 2. No ternary compound is known.

Invariant Equilibria

Details of invariant equilibria are shown in Table 3. The compositions of the liquids given in the table are taken from experimental determinations of [1984Sch] and Calphad assessment from [2000Shi] reproduced in [2004Rag]; the compositions of the solid phases are calculated by [1990Gus].

Liquidus, Solidus and Solvus Surfaces

Earlier studies [1930Kue] showed that C-Fe-P system may be presented in the form of a metastable Fe-Fe_3C-Fe_3P phase diagram or in the form of a stable Fe-C-Fe_3P diagram. The liquidus lines have been experimentally determined by [1984Sch, 1985Sch] for the stable and metastable diagrams, accepted by [1988Rag]. They are in good agreement with the Calphad assessment of [1990Gus, 2000Shi] and are shown in Figs. 1 and 2, respectively, after substantial adjustments to the accepted binary systems. The addition of phosphorus has an effect to decrease the eutectic temperature of the stable (C-Fe) and metastable (Fe-Fe_3C) binary diagrams [1988Mag]. The reaction schemes for the stable and metastable diagrams are shown in Figs. 3 and 4, respectively.

The distribution coefficient of phosphorus between the α and liquid phases, measured by [1986Mor], is given by:

$k_{P,\alpha} = x_P$ (sol) / x_P (liq) = $0.715 - 3.20 \cdot 10^{-4} T$ (infinite dilution). At the melting point of Fe, $k_{P,\alpha} = 0.136$.

Expressed in mass%:

$k_{P,\alpha}$ = (mass% P, sol) / (mass% P, liq) = $0.643 - 2.80 \cdot 10^{-4} T$

$k_{P,\gamma}$ has been measured between 2 and 4 mass% C, composition for which the liquid phase may be in equilibrium with the γ phase. $k_{P,\gamma} \approx 0.09$ and decreases with the carbon content. By extrapolation, $k_{P,\gamma} \approx 0.06$ for pure Fe.

MSIT®
DOI: 10.1007/978-3-540-74196-1_11

Isothermal Sections

The α-γ, γ-Fe_3C and γ-Fe_3P two-phase equilibria in the iron rich corner were investigated by [1970Hof] between 600 and 900°C and by [1970Lan] at 900, 950 and 1000°C. Figure 5 shows the stable and metastable equilibria at 950°C. The presence of phosphorus decreases the carbon solubility in the γ phase as well as in the liquid phase. For instance, at 1400°C, [1992Yan] proposes the following relationship: $x_C = 0.1937 - 1.1028\ x_P + 3.093\ x_P^2$ ($x_P < 0.1$), x_C and x_P being the mole fractions of C and P respectively in the liquid phase in equilibrium with solid graphite.

Temperature – Composition Sections

The calculated (metastable) vertical section Fe_3P-Fe_3C from [2000Shi] is presented in Fig. 6.

Thermodynamics

The interaction coefficient between C and P in liquid iron has been calculated by [1997Wan] from a new model and found to be $\varepsilon_C^{(P)} = \varepsilon_P^{(C)} = (\partial \ln x_P / \partial x_C) = 17.86$ at 1600°C, which is to be compared with the experimental value of 4.2 at an unknown temperature [1959Neu], 4.72 at 1600°C [1975Ban], 12.8 at 1515°C [1966Sch], 5.43 at 1400°C [1983Ban] and 7.84 at 1400°C [1992Yan] and 7.0 at 1600°C [1999Din]. The most credible experimental result is the last one. [1992Yan] proposes, in addition, an evaluation of the carbon auto interaction parameter ($\varepsilon_C^{(C)} = 11.51$) and an evaluation of the second order interaction parameters. [1993Din, 1999Din] calculate $\varepsilon_P^{(C)} = 20$ at 1600°C, value not very credible when compared to the accepted experimental values $\varepsilon_P^{(C)} \approx 7$. The addition of one element (C or P) in liquid iron has an effect to decrease the solubility of the other element, a fact already observed by [1955Tur, 1963Bur, 1969Sch] and investigated at 1400°C by [1992Yan]. Two Calphad assessments [2000Shi, 1990Gus] which are in good agreement with the experimental liquidus given by [1984Sch] have been presented. The description of [2000Shi] is more elaborate than that of [1990Gus] and takes into account the magnetic order contribution to the Gibbs energy.

Notes on Materials Properties and Applications

Main experimental investigations are gathered in Table 4. A comprehensive review of the solidification process in the C-Fe base alloys has been presented in [1982Fre]. The segregation of a third element is much smaller when the primary crystallization phase is ferritic than when it is austenitic and increases drastically when increasing the cooling rate. Phosphorus segregation to austenite grain boundary, investigated by [1988Paj] is mainly at equilibrium, even if some segregation is observed during quenching. Phosphorus enhances the austenite γ grains in steels [2004Yos] by lowering the γ/δ transition temperature. Carbon, which segregates at equilibrium in austenite as well as during quenching, was shown to decrease the grain boundary concentration of phosphorus. The Gibbs energy of segregation of phosphorus in grain boundaries has been evaluated by [1981Ehr] between 400 and 800°C:

$$\Delta_{segr}G/\left(\mathrm{J\cdot mol^{-1}}\right) = -34\,300 - 21.5(T/K).$$

For a given amount of C in a steel, the recrystallization of a steel after annealing is delayed when increasing the P concentration [1989Ina]. High level of phosphorus (~20 mass%) have been found in grain boundaries of an alloy (Fe-0.06% P-0.002% C) after annealing at 600°C [1998Cow]. A more complete investigation of [2002Cow] showed that P and C concentration at grain boundaries depends on both dislocation density and time. The diffusion coefficient of P and C in the alloy are respectively:

$$D_P/\left(\mathrm{m^2\cdot s^{-1}}\right) = 2.5 \cdot 10^{-5} \exp(-24\,000/T)$$
$$D_C/\left(\mathrm{m^2\cdot s^{-1}}\right) = 6.2 \cdot 10^{-7} \exp(-9600/T)$$

Phosphorus is considered as a graphitizing element when added in small amount, but as a carbide stabilizing element in large amount [1918Ste]. It does not concentrate in the austenite, neither in the cementite phase, but segregates in the last part to solidify, known as steadite, which is composed of Fe, Fe_3C and Fe_3P. Such effects lead to solidification structures which differ considerably from the expected ones [1954Mor].

DOI: 10.1007/978-3-540-74196-1_11

Although phosphorus does not stabilize the pearlite (eutectoid cementite) at high temperature, it increases the durability of this constituent in cast iron [1979Ost]. P does not affect the C concentration at the interface of a diffusion couple Fe-0.01% C / Fe-0.01% C-0.2% P [1991Ray], which means that P does not affect the carbon activity in ferrite, but it is effective in delaying the coarsening of cementite particles at higher aging temperatures. The survival of liquid rich in tramp elements such as phosphorus enhances the solidification cracking and their level have to be limited at 0.03 mass% in attempt to eliminate cracking. A model developed by [1982Cly] shows that cracking may be limited by increasing the carbon level from 0.1 to 0.25 mass%. Anomalous grain growth after annealing may be caused by an inhomogeneous distribution of phosphorus [2004Wil]. A short annealing may improve the fracture resistance of such alloys.

Miscellaneous

Crystalline order is not necessary for the existence of ferromagnetism and Fe based amorphous alloys possesses attractive soft magnetic properties and are functional materials for motors, transformers, high frequency transducers, *etc*., The Curie temperature and the magnetization contribution to heat capacity has been measured by [1973Che]. These values increase with the concentration of P and C in the alloy. At fixed phosphorus concentration, a rapid decrease is observed when decreasing the carbon content. Amorphous ribbons $Fe_{80}P_{13}C_7$ prepared by a centrifugal solidification technique [1976Obi] present a low coercive force and a high permeability after magnetic annealing. [2001Cha] shows that bulk ferromagnetic $Fe_{80}P_{13}C_7$ amorphous rods, compacted together, may be fused perfectly at 410°C, under 2.5 to 4 GPa during 5 min. $Fe_{75}P_{15}C_{10}$ amorphous ribbons prepared by centrifugation present the same magnetic moment by iron atom than Fe_3P (1.8 μB); Mössbauer investigation [1979Ama] shows that short range order in $Fe_{75}P_{15}C_{10}$ is predominantly that of Fe_3P. Amorphous $Fe_{76}P_{16}C_8$ alloys embedded in C nanotubes have been prepared by a rapid solidification process [2003Wei]. The embedding in C nanotubes can efficiently inhibit the nucleation and growth of Fe_3P, which resulted in an improved thermal stability of Fe-P alloys.

DOI: 10.1007/978-3-540-74196-1_11

Table 1. Investigations of the C-Fe-P Phase Relations, Structures and Thermodynamics

Reference	Method/Experimental Technique	Temperature/Composition/Phase Range Studied
[1906Fet]	Solubility measurements of P in liquid (Fe,C)	Temperature unknown (probably 1600°C), < 4.5 mass% C, < 16 mass% P
[1908Goe]	Simple thermal analysis, melting points measurements	700-1400°C, < 12 mass% P, < 12 mass% C
[1908Wue]	Simple thermal analysis, melting points measurements	700-1350°C, < 15 mass% P, < 5 mass% C
[1929Vog]	Thermal analysis, vertical sections determination	700-1500°C, Fe-Fe_3C-Fe_3P
[1930Kue]	Thermal analysis, eutectic valley determination	950-1100°C, < 7 mass% C, < 12 mass% P
[1955Tur]	Carbon solubility measurements in Fe-P melts	1290-1575°C, < 4.18 mass% P < 5.25 mass% C
[1963Bur]	Solubility measurements in C-Fe-P melts	1290°C, 1.42-5.52 mass% P 2.88-5.00 mass% C
[1966Sch]	Solubility measurements in C-Fe-P melts	1515°C, < 30 mass% P, < 3.3 mass% C
[1969Sch]	Solubility measurements in C-Fe-P melts	1350-1550°C, < 14.5 mass% P, < 5.0 mass% C.
[1970Hof]	Electron microprobe, diffusion couples, microhardness measurements	600-900°C, < 3.0 at.% P, < 0.7 at.% C
[1970Lan]	Electron microprobe measurements, morphology, solid phase equilibria	900-1000°C, < 5.20 mass% P, < 3.52 mass% C
[1975Ban]	Phosphorus activity by distribution equilibrium measurements	1300-1600°C, < 21 mass% P, < 20 at.% C
[1983Ban]	Phosphorus activity by vapor pressure measurements with a transport method	1400°C, < 15 at.% C, < 30 at.% P
[1984Sch, 1985Sch]	Thermal analysis, determination of stable and metastable diagrams	1000-1500°C, Fe-Fe_3C-Fe_3P triangle
[1986Mor]	Distribution coefficient of phosphorus between α-liq and γ-liq phases	1150-1500°C, < 4 mass% C, < 0.5 mass% P
[1988Mag]	Thermal analysis, eutectic valley determination	1145-1155°C, 4.23-4.26 mass% C, < 0.1 mass% P
[1992Yan]	Interaction coefficients measurements by a carbon isoactivity method	1400°C, < 7 mass% C, < 5 mass% P

DOI: 10.1007/978-3-540-74196-1_11

Table 2. Crystallographic Data of Solid Phases

Phase/ Temperature Range [°C]	Pearson Symbol/ Space Group/ Prototype	Lattice Parameters [pm]	Comments/References
(C) gr < 4492	*hP*4 $P6_3/mmc$ C (graphite)	a = 246.12 c = 670.9	pure C at 25°C [Mas2, V-C2] Sublimates at 3827°C
(C)d	*cF*8 $Fd\bar{3}m$ C (diamond)	a = 356.69	at 25°C, 60 GPa [Mas2]
P (red) < 417	*c**66	a = 1131	sublimation at 1 bar. Stable form or P. Triple point at 576°C, > 36.3 bar [Mas2, V-C2]
P (white) < 44.14	*c*** P (white)	a = 718	common form of P [Mas2, V-C2]
P (black)	*oC*8 *Cmca* P (black)	a = 331.36 b = 1047.8 c = 437.63	at 25°C [Mas2, V-C2]
α, (αδFe) (αFe) < 912	*cI*2 $Im\bar{3}m$ W	a = 286.65	pure Fe at 20°C [Mas2, V-C2] dissolves up to 0.096 at.% C at 740°C and 4.52 at.% P at 1048°C
(δFe) 1538 - 1394		a = 293.15	at 1394°C dissolves up to 0.40 at.% C at 1493°C
γ, (γFe) 1394 - 912	*cF*4 $Fm\bar{3}m$ Cu	a = 364.67	at 915°C [Mas2, V-C2] dissolves up to 9.06 at.% C at 1153° C and 0.5 at.% P at 1150°C
(εFe)	*hP*2 $P6_3/mmc$ Mg	a = 246.8 c = 396.0	at 25°C, 13 GPa [Mas2] triple point (αFe)-(γFe)-(εFe) at 8.4 GPa, 430°C
α', (Fe,C)	*tI*4 *I*4/*mmm*	-	Martensite, metastable [Mas2]
θ, Fe_3C 1252 - 230	*oP*16 *Pnma* Fe_3C	a = 452.48 b = 508.96 c = 674.43	[1972Chi, 1997Miz] cementite, high pressure phase. Curie point at 214°C
χ, $Fe_{2.2}C$ (or χFe_5C_2) < 230	*mC*28 *C*2/*c* B_2Pd_5	a = 1156.2 b = 457.27 c = 505.95 β = 97.74°	[1972Chi, V-C2] "Haegg carbide", metastable but more stable than cementite below 230°C
ε, $Fe_{2.4}C$	*hP** $P6_322$	-	[1972Chi, Mas2] "ε carbide", metastable. Curie point at 370°C
$Fe_2C(\eta)$	*oP*6 *Pnnm*	a = 470.4 b = 431.8	[1988Rag, V-C2]

(*continued*)

DOI: 10.1007/978-3-540-74196-1_11

Phase/ Temperature Range [°C]	Pearson Symbol/ Space Group/ Prototype	Lattice Parameters [pm]	Comments/References
	Fe_2C	c = 283.0	
Fe_3P < 1166	$tI32$ $I\bar{4}$ Ni_3P	a = 910.8 c = 445.5	at 25°C [Mas2, V-C2]
		a = 917.4 c = 453.0	at 678°C [1990Oka]
Fe_2P < 1370	$hP9$ $P\bar{6}2m$ Fe_2P	a = 586.4 c = 346.0	33.3-34.3 at.% P [1988Rag]
Fe_2P (HP)	$oP12$ $Pnma$ Co_2Si	a = 577.5 b = 357.1 c = 664.1	at 800°C under 80 kbar [1988Rag]
FeP < 1370	$oP8$ $Pna2_1$ MnP	a = 519.3 b = 579.3 c = 309.9	[2002Per]
FeP_2	oP6 Pnnm FeS_2 (marcassite)	a = 497.29 b = 565.68 c = 272.30	[1988Rag]
FeP_4	$mP30$ $P2_1/c$ FeP_4	a = 461.9 b = 1367.0 c = 700.2 β = 101.48°	[1988Rag]
Fe_4P (HP)	$oC20$ $C222_1$	a = 500.5 b = 1021.3 c = 553.0	at 1100°C under 60 kbar [1988Rag]

Table 3. Invariant Equilibria

Reaction	T [°C]	Type	Phase	Composition (at.% (mass%))		
				C	Fe	P
L + Fe_2P ⇌ (C) + Fe_3P (stable)	1150	U_1	L Fe_2P Fe_3P (C)	2.10 (0.51) 0 0 100	75.67 (85.55) 66.67 (78.29) 75.0 (84.40) 0	22.23 (13.94) 33.33 (21.71) 25.0 (15.60) 0
L + α ⇌ γ + Fe_3P (stable and metastable)	1006	U_2	L α γ Fe_3P	3.5 (0.83) 0.1 (0.02) 2.4 (0.53) 0	82.5 (90.67) 95.9 (97.72) 95.7 (98.39) 75.0 (84.40)	14.0 (8.50) 4.0 (2.26) 1.9 (1.08) 25.0 (15.60)
l ⇌ Fe_3C + Fe_3P (metastable)	993	e_3	L	13.2 (2.93)	75.2 (88.46)	11.6 (8.61)

(*continued*)

DOI: 10.1007/978-3-540-74196-1_11

Reaction	T [°C]	Type	Phase	Composition (at.% (mass%))		
				C	Fe	P
$L + Fe_3P \rightleftharpoons Fe_2P + Fe_3C$ (metastable)	982	U_3	L	13.84 (3.60)	71.67 (86.68)	14.49 (9.72)
$L \rightleftharpoons \gamma + Fe_3P + (C)$ (stable)	958	E_1	L γ Fe_3P C	6.85 (1.64) 5.23 (1.18) 0 100	82.0 (91.46) 93.57 (98.12) 75.0 (84.40) 0	11.15 (6.89) 1.20 (0.70) 25.0 (15.60) 0
$L \rightleftharpoons \gamma + Fe_3P + Fe_3C$ (metastable)	952	E_2	L γ Fe_3P Fe_3C	8.55 (2.08) 5.53 (1.25) 0 25.0 (6.69)	80.38 (90.97) 93.32 (98.08) 75.0 (80.40) 75.0 (93.31)	11.07 (6.95) 1.15 (0.67) 25.0 (15.60) 0

Table 4. Investigations of the C-Fe-P Materials Properties

Reference	Method / Experimental Technique	Type of Property
[1918Ste]	Thermal analysis, metallographic examination	Phosphorus distribution on melting and cooling
[1919Kon]	Electrical conductivity measurements	< 15 mass% P, < 0.9 mass% C
[1954Mor]	Cooling curves determinations, morphology	Solidification structures, 929-1222°C, 2.15-3.6 mass% C, < 5 mass% P
[1973Che]	Curie temperature and heat capacity measurements on amorphous alloys	15 at.% P, < 0.16 at.% C, < 720°C
[1975Ohi]	Thermal analysis, metallographic examination	Solidification structures of cast iron < 4 mass% C, < 8 mass% P
[1976Gri]	Microprobe analysis, metallographic examination	Solidification structure of the ternary eutectic
[1976Obi]	Pattern of the magnetic domains, magnetization curves	$Fe_{80}P_{13}C_7$ amorphous ribbon prepared by centrifugal solidification
[1979Ama]	Mössbauer, magnetic order determination	$Fe_{75}P_{15}C_{10}$ amorphous ribbon prepared by centrifugal solidification
[1979Ost]	Dilatometry, isothermal annealing, metallographic examination	Eutectoid transformation, < 950°C, < 1.6 mass% P
[1982Cly]	Diffusion measurements. Effect of carbon on solidification cracking	1200-1500°C, < 1 mass% C, < 0.1 mass% P
[1988Paj]	Auger Electron Spectroscopy, phosphorus segregation	825-1100°C, < 0.35 mass% C, < 0.2 mass% P
[1989Ina]	Optical microscopy	Recrystallization of steels, < 1250°C, < 0.2% P, < 0.05% C

(*continued*)

DOI: 10.1007/978-3-540-74196-1_11

Reference	Method / Experimental Technique	Type of Property
[1991Ray]	Transmission and Scanning Electron Microscopy	0.01% C, < 0.2% P, < 700°C, P diffusion measurement
[1998Cow, 2002Cow]	Auger Electron Spectroscopy, phosphorus segregation	< 600°C, 0.002 mass% C, 0.06 mass% P, diffusion measurement
[2001Cha]	Thermal analysis, X-ray diffraction, high pressure experiment	Preparation of ferromagnetic rods, $Fe_{80}P_{13}C_7$, 680-1000°C, 2.5-4 GPa
[2003Wei]	Magnetic measurements, Transition Electron Microscopy	< 1100°C, amorphous $Fe_{78}P_{16}C_8$ alloys embedded in C nanotubes
[2004Sai]	Internal friction, Infra Red Spectroscopy	< 0.21 mass% P, 0.045 mass% C, influence of P on the C Snoek peak in αFe
[2004Wil]	Heat treatment, morphology, grain growth and grain boundary mobility	< 1000°C, < 0.12 mass% P, 0.002 mass% C, fracture resistance
[2004Yos]	Microscopic examination	100-1500°C, 0.1 mass% C, < 0.2 mass% P, γ grain refinement

DOI: 10.1007/978-3-540-74196-1_11

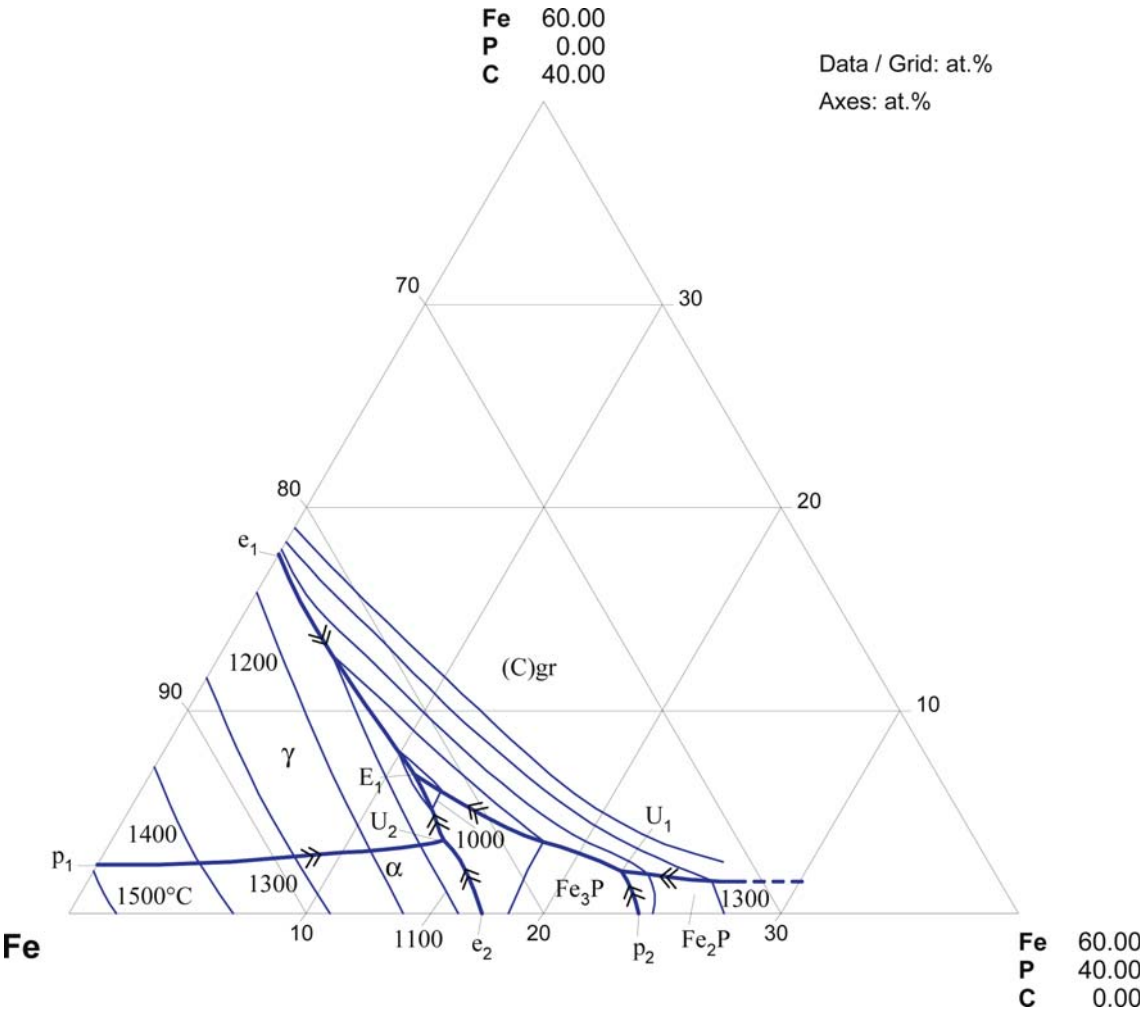

Fig. 1. C-Fe-P. Stable liquidus surface projection

DOI: 10.1007/978-3-540-74196-1_11

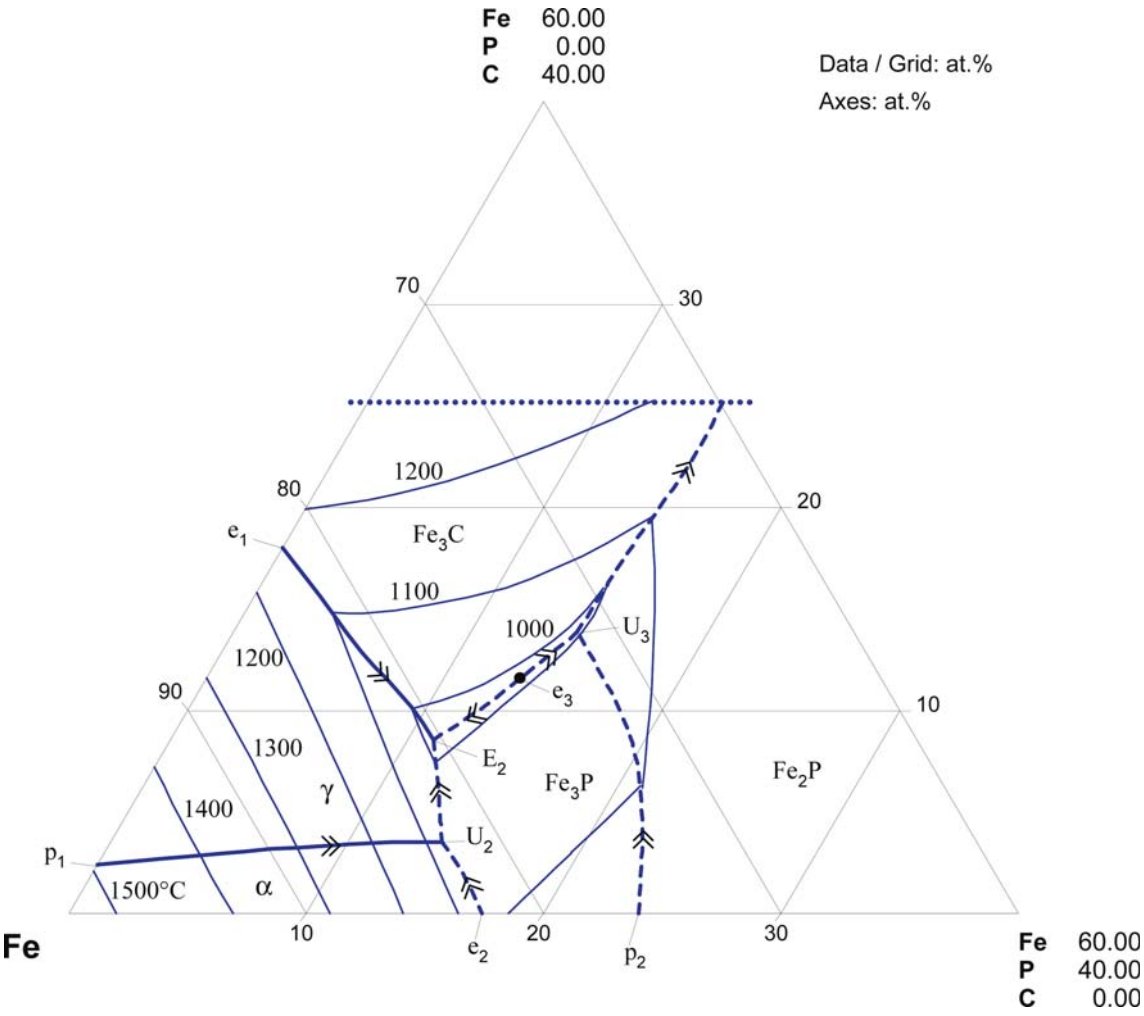

Fig. 2. C-Fe-P. Metastable liquidus surface projection

DOI: 10.1007/978-3-540-74196-1_11

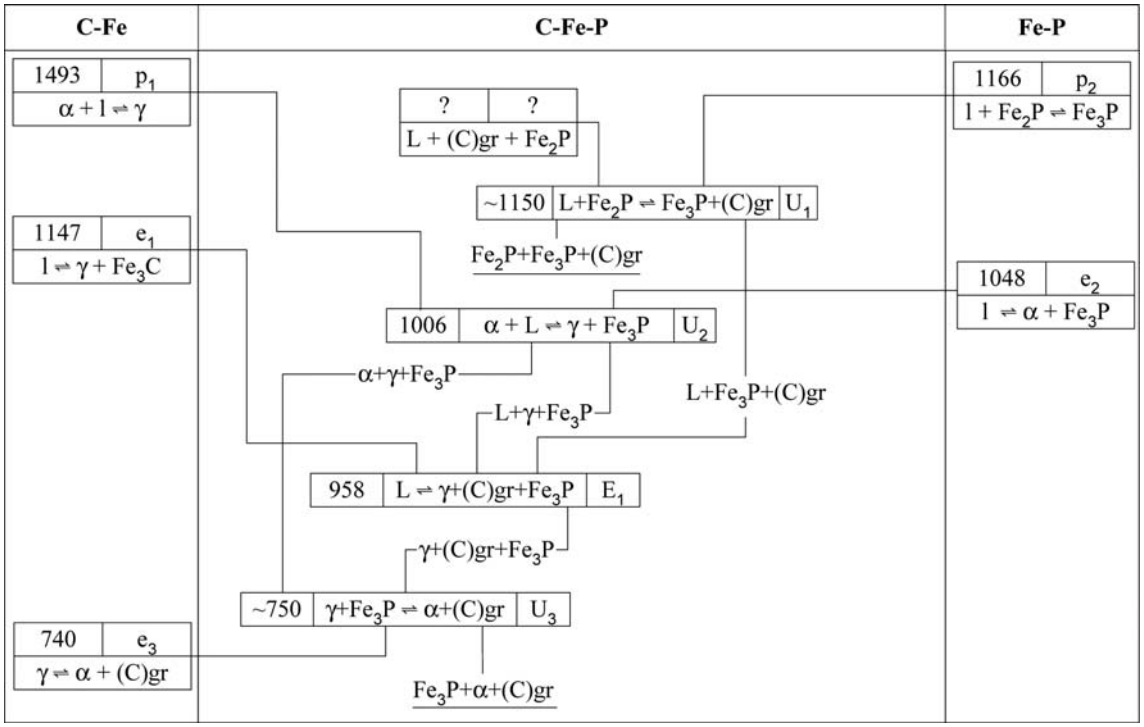

Fig. 3. C-Fe-P. Reaction scheme (stable equilibrium Fe-(C)gr-Fe_2P)

DOI: 10.1007/978-3-540-74196-1_11

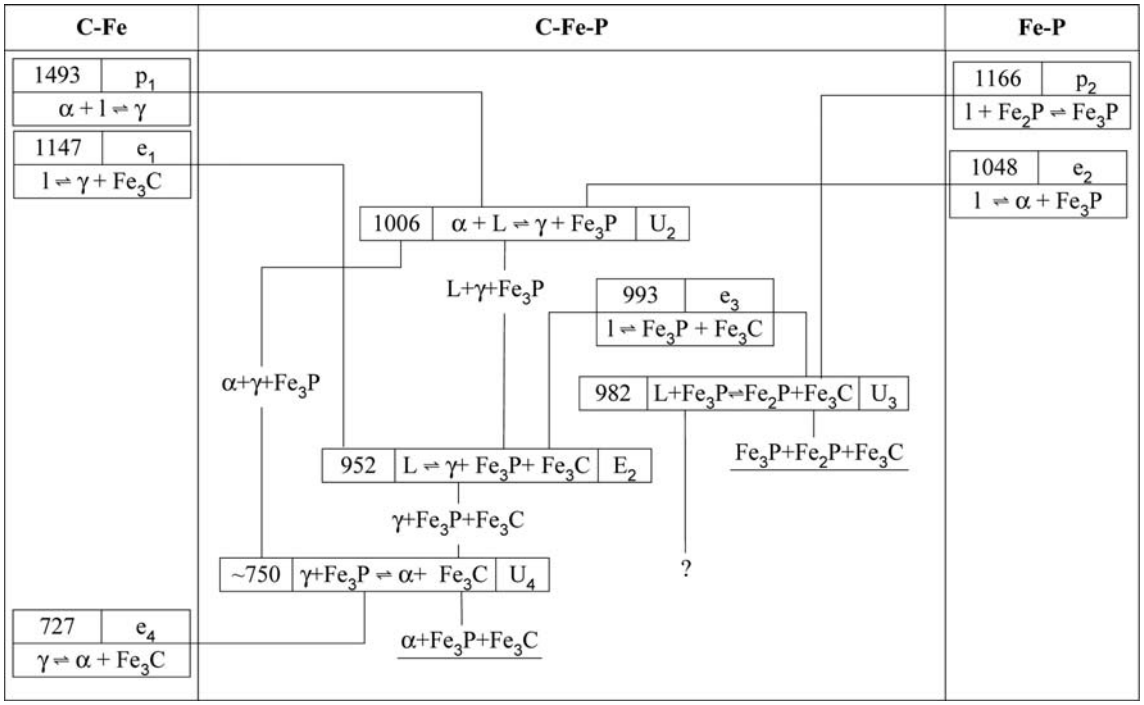

Fig. 4. C-Fe-P. Reaction scheme (metastable equilibrium)

DOI: 10.1007/978-3-540-74196-1_11

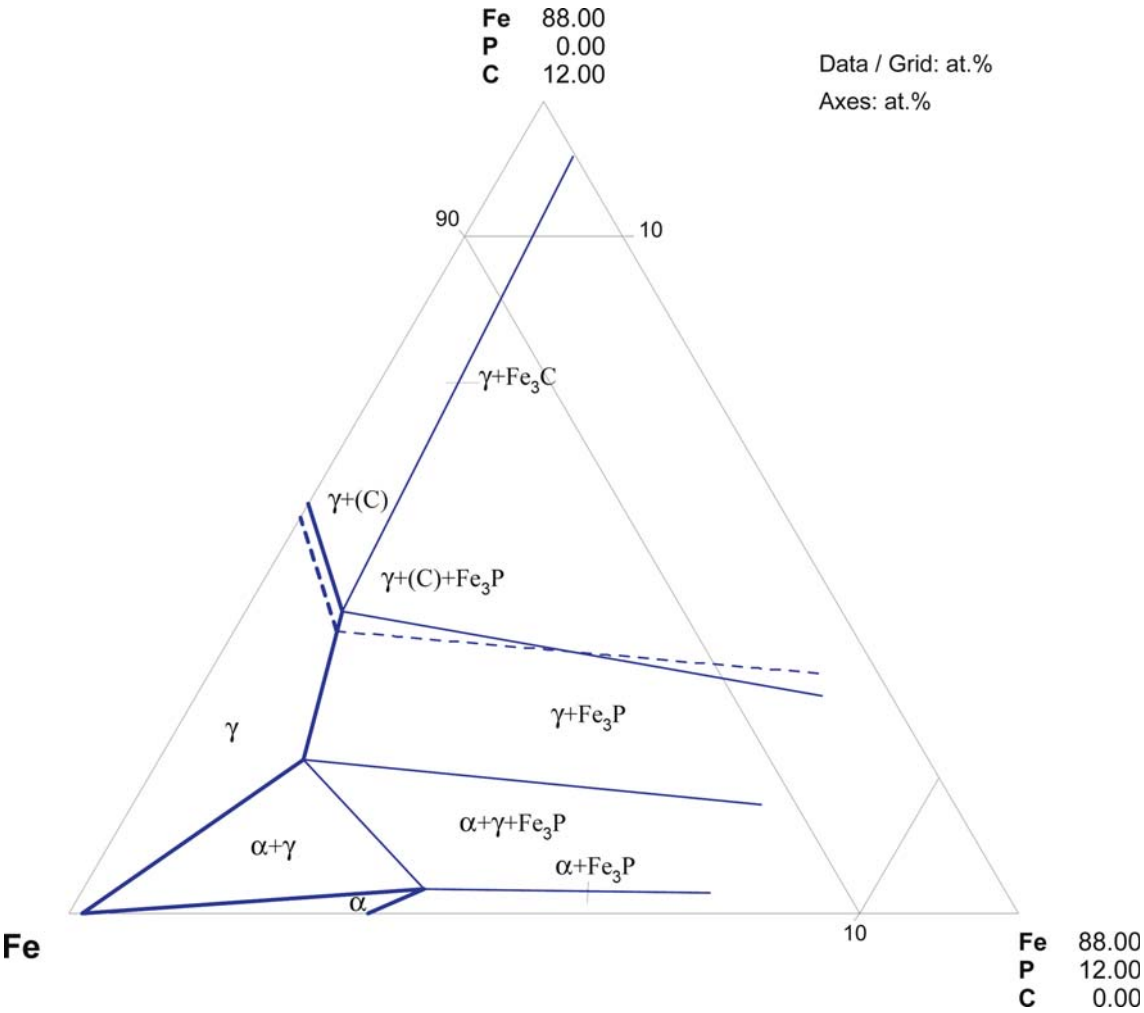

Fig. 5. C-Fe-P. Stable and metastable (dashed lines) isothermal section at 950°C

DOI: 10.1007/978-3-540-74196-1_11

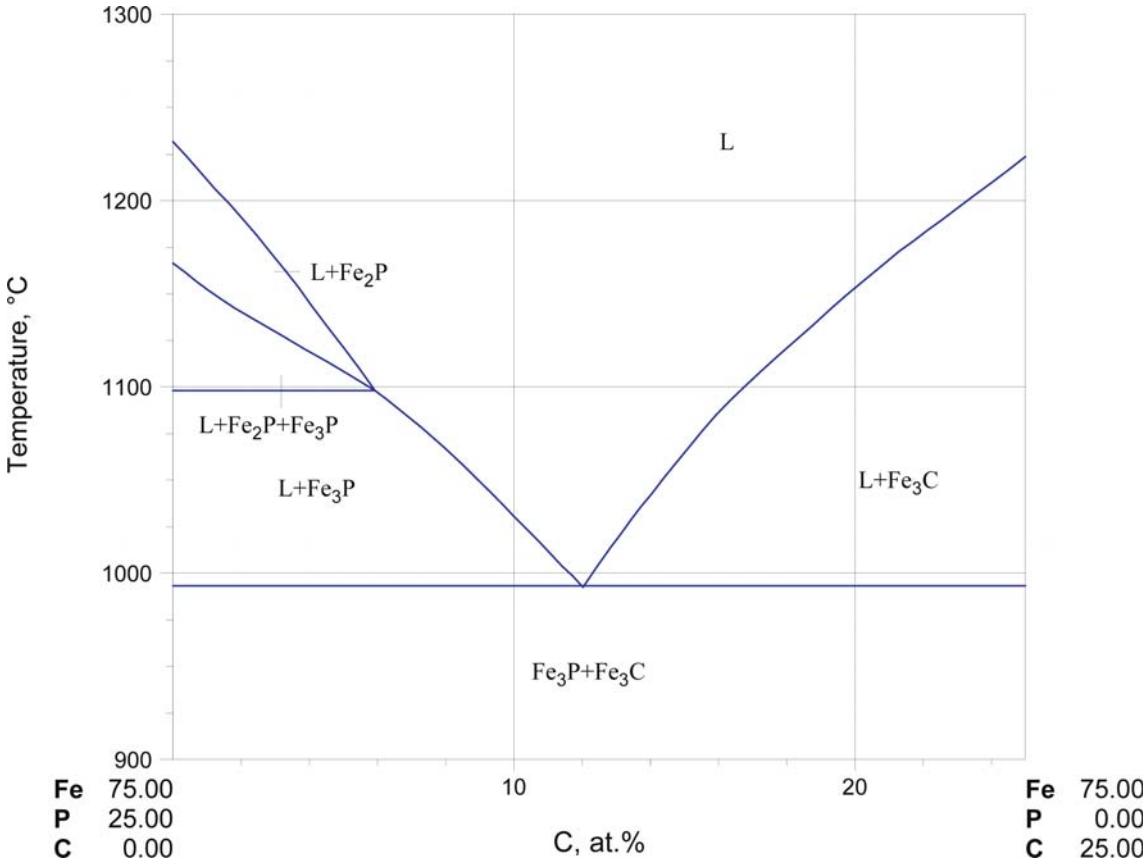

Fig. 6. C-Fe-P. The metastable vertical section Fe_3P-Fe_3C

DOI: 10.1007/978-3-540-74196-1_11

References

[1906Fet] Fettweis, F., "Influence of the Phosphorus on Thesaturation of Liquid Iron by Carbon" (in German), *Metallurgie*, **3**, 60–62 (1906) (Experimental, Phase Relations, 1)

[1908Goe] Görens, P., Dobbelstein, W., "The Fe-P-C Ternary System" (in German), *Metallurgie*, **5**, 561–566 (1908) (Experimental, Morphology, Phase Diagram, Phase Relations, 1)

[1908Wue] Wüst, F., "Influence of Phosphorus to Iron-Carbon" (in German), *Metallurgie*, **5**, 73–87 (1908) (Experimental, Morphology, Phase Diagram, Phase Relations, 16)

[1915Ste] Stead, J.E., "Iron, Carbon, Phosphorus", *J. Iron Steel Inst*., London, **91**, 140–198 (1915) (Experimental, Morphology, Review, 58)

[1919Kon] Konstantinova, N.S., "Physicochemical Investigation of the Ternary Alloys of Iron With Phosphorus and Carbon" (in Russian), *Izv. Inst. Fiziko-Khim. Anal.*, **1**(1), 33–59 (1919) (Electr. Prop., Mechan. Prop., Experimental, Phase Relations, 61)

[1918Ste] Stead, J.E., "Iron, Carbon, Phosphorus", *J. Iron Steel Inst*., London, **97**, 389–415 (1918) (Experimental, Morphology, 1)

[1929Vog] Vogel, R., "The Iron-Phosphorus-Carbon System" (in German), *Arch. Eisenhuettenwes*., **3**(4), 369–381 (1929) (Experimental, Morphology, Phase Diagram, 9)

[1930Kue] Kuenkele, M., "The Constitution and the Formation of Phosphide Eutecticx in Cast Iron", *Mitt. K.-W.-Inst. Eisenforschung*, **12**(4), 23–31 (1930) (Experimental, Phase Diagram, Phase Relations, 34)

[1949Jae] Jänecke, E., "C-Fe-P" (in German), *Kurzgefasstes Handbuch Aller Legierungen*, Winter, Heidelberg, 718–719 (1949) (Phase Diagram, Review)

[1954Mor] Morrogh, H., Tutseh, P.H., "The Soldification of Iron-Phosphorus-Carbon Alloys", *J. Iron Steel Inst., London*, **176**, 382–384 (1954) (Experimental, Morphology, Phase Diagram, Phase Relations, 4)

[1955Tur] Turkdogan, E.T., Leake, L.E., "Thermodynamics of Carbon Dissolved in Iron Alloys. Part I: Solubility of Carbon in Iron-Phosphorus, Iron-Silicon, and Iron-Manganese Melts", *J. Iron Steel Inst., London*, **179**, 39–43 (1955) (Experimental, Phase Diagram, Phase Relations, 15)

[1959Neu] Neumann, F., Schenck, H., Patterson, W., "Iron-Carbon Alloys in Thermodynamic Consideration" (in German), *Giesserei Tech.-Wiss. Beih*., **23**, 1217–1246 (1959) (Review, Phase Diagram, Phase Relations, Theory, Thermodyn., 72)

[1963Bur] Burylev, B.P., "Solubility of Carbon in Liquid Iron in the Presence of Phosphorus" (in Russian), *Izv. Vyss. Uchebn. Zaved., Chern. Metall*., **6**(9), 11–15 (1963) (Calculation, Experimental, Thermodyn., 10)

[1966Sch] Schenk, H., Steinmetz, E., Gohlke, R., "Contribution to the Study of the Chemical Activity of the Elements P, S, Si, Cu and Cr in Molten Iron Solutions Saturated with Carbon" (in German), *Arch. Eisenhuettenwes*., **37**(12), 919–924 (1966) (Calculation, Experimental, Phase Diagram, Thermodyn., 30)

[1969Sch] Schürmann, E., Kramer, D., "Influence of Temperature and the Equivalent Effects of Alloying Elements on Carbon Solubility in Iron-Rich Carbon Saturated Ternary and Multicomponent Melts" (in German), *Giessereiforschung*, **21**(1), 29–42 (1969) (Experimental, 35)

[1970Hof] Hofman, H.P., Lohberg, K., Reif, W., "Solubility of Phosphorus in Fe and Fe-C Alloys below 1000°C" (in German), *Arch. Eisenhuettenwes*., **41**(10), 975–982 (1970) (Experimental, Phase Diagram, Phase Relations, 32)

[1970Lan] Langenscheid, G., Mathesius, H.A., Nauman, F.K., "Use of the Quantitative Television Microscope and of the Electron Beam Microprobe in the Study of the Fe-C-P System at 900–1000°C" (in German), *Arch. Eisenhuettenwes*., **41**(8), 817–824 (1970) (Experimental, Phase Diagram, 4)

[1972Chi] Chipman, J., "Thermodynamics and Phase Diagram of the Fe-C System", *Metall. Trans.*, **3**, 55–64 (1972) (Assessment, Thermodyn., Phase Relations, Review, 66)

[1973Che] Chen, H.S., "Effect of Composition and Structure on Magnetic Properties of Amorphous Fe-P-C Alloys", *Phys. Status Solidi A*, **16**(A), 561–566 (1973) (Crys. Structure, Experimental, Magn. Prop., 25)

DOI: 10.1007/978-3-540-74196-1_11

[1975Ban] Ban-ya S., Suzuki M., "Activity of Phosphorus in Liquid Fe-P and Fe-P-C Alloys" (in Japanese), *Tetsu to Hagane*, **61**(14), 2933–2942 (1975) (Experimental, Kinetics, Phase Relations, Thermodyn., 21)

[1975Ohi] Ohide, T., Ohira, G., "The Solidification Structures of Fe-C-P Ternary Alloys", *Brit. Foundryman*, **68**(4), 106–115 (1975) (Experimental, Morphology, 8)

[1976Gri] Grinberg, B.M., Zhukov, A.A., Sherman, A.D., Dukhin A.I., Durachenko, A.I., "Effect of Cooling Rate on the Phase Compositions of a Ternary Eutectic in the Fe-C-P System" (in Russian), *Fiz. Khim. Obrab. Mater.*, (3), 114–119 (1976) (Morphology, Experimental, 7)

[1976Obi] Obi, Y., Fujimori, H., Saito, H., "Magnetic Domain Structure of an Amorphous Fe-P-C Alloy", *Jap. J. Appl. Phys.*, **15**(4), 611–317 (1976) (Experimental, Magn. Prop., Mechan. Prop., Morphology, 16)

[1979Ama] Amamou, A., "Mossbauer Effect and Short-range Order in Fe-P-B and Fe-P-C Amorphous Alloys", *Phys. Status Solidi A*, **54**, 565–572 (1979) (Crys. Structure, Experimental, Magn. Prop., 31)

[1979Ost] Ostrowski, R., Podrzucki, C., "Effect of Nickel, Copper, Tin, Chromium and Phosphorus on the Durability of the Eutectoid Cementite in Hypoeutectic Cast Iron" (in Polish), *Pol. Akad. Nauk-Oddz. Krak., Pr. Kom. Met.-Od.*, **27**, 33–66 (1979) (Phase Relations, Morphology, Experimental, 30)

[1981Ehr] Erhart, H., Grabke, H.J., "Equilibrium Segregation of Phosphorus at Grain Boundaries of Fe-P, Fe-C-P, Fe-Cr-P, and Fe-Cr-C-P Alloys", *Met. Sci.*, **15**(9) , 401–408 (1981) (Electronic Structure, Experimental, Morphology, 17)

[1982Cly] Clyne, T.W., Wolf, M., Kurz, W., "The Effect of Melt Composition on Solification Cracking of Steel, with Particular Reference to Continuous Casting", *Metall. Trans. B*, **13B**, 259–266 (1982) (Experimental, Phase Diagram, Phase Relations, Thermodyn., 43)

[1982Fre] Fredrikson, H., Stjerndahl, J., "Solidification of Iron Base Alloys", *Met. Sci.*, **16**(12), 575–585 (1982) (Calculation, Theory, Kinetics, Phase Relations, 31)

[1983Ban] Ban-ya, S., Maruyama, N., Fujino, "The Effect of C, Si, Sn and B on the Activity of Phosphorus in Liquid Iron", *Tetsu to Hagane*, **69**, 921–928 (1983) (Experimental, 32)

[1984Sch] Schürmann, E., Hensgen, U., Schweinichen, J., "Melt Equilibrium of the Ternary Systems Fe-C-Si and Fe-C-P" (in German), *Giessereiforschung*, **36**(4), 121–129 (1984) (Experimental, Phase Diagram, #, *, 33)

[1985Sch] Schürmann, E., "New Measurements and Calculations for Stable and Metastable Soldification Equilibria of Fe-C-Si and Fe-C-P Phase Diagrams" (in German), *Giesserei-Rundsch.*, **32**(4), 27–32 (1985) (Phase Diagram, Review, #, 13)

[1986Mor] Morita, Z., Tanaka, T., "Equilibrium Distribution Coefficient of Phosphorus in Iron Alloys", *Trans. Iron Steel Inst. Jpn.*, **26**, 114–120 (1986) (Experimental, Phase Diagram, Phase Relations, 30)

[1987Sch] Schürmann, E., Schweinichen, J., Voelker, R., Fischer, H., "Calculation of the α/δ Resp γ-Liquidus of Iron and of the Liquidus of Carbon as well as of the Univariant Reaction Lines in Iron-Rich, Carbon Containing Three-component and Multicomponent Fe-C-X_1-X_2-Systems" (in German), *Giessereiforschung*, **39**(3), 104–113 (1987) (Experimental, Phase Diagram, Phase Relations, Thermodyn., 19)

[1988Mag] Magnin, P., Kurz, W., "Stable and Metastable Eutectic Temperatures of Fe-C with Small Additions of a Third Element", *Z. Metallkd.*, **79**(5), 282–284 (1988) (Experimental, 5)

[1988Paj] Paju, M., Viefhaus, H., Grabke, H.J., "Phosphorus Segregation in Austenite in Fe-P-C, Fe-P-B and Fe-P-C-B Alloys", *Steel Res.*, **59**(8), 336–343 (1988) (Experimental, Morphology, Thermodyn., 32)

[1988Rag] Raghavan, V., "The C-Fe-P (Carbon-Iron-Phosphorous) System", Phase Diagrams of Ternary Iron Alloys. Part 3; Ternary Systems Containing Iron and Phosphorous, Indian Institute of Metals, **3**, 33–44 (1988) (Phase Diagram, Phase Relations, Review, 22)

DOI: 10.1007/978-3-540-74196-1_11

[1989Ina] Inagaki, H., "Effect of C Concentration on the Recrystallization Behavior and the Recrystallization Texture of Purity Fe-P Alloys", *Z. Metallkd.*, **80**(8), 570–576 (1989) (Crys. Structure, Experimental, Kinetics, 14)

[1990Gus] Gustafson, P., "Study of the Thermodynamic Properties of the C-Cu-Fe-P, Fe-Mo-P and Fe-Ni-P System", Inst. Met. Res. Rept (IM-2549), 1–50 (1990) (Thermodyn., Assessment, Phase Diagram, 52)

[1990Oka] Okamoto, H., "The Fe-P (Iron-Phosphorus) System", *Bull. Alloy Phase Diagrams*, **11**(4), 404–412 (1990) (Phase Diagram, Review, 89)

[1991Ray] Ray, S.K., "Effect of Phosphorus on Carbon Activity, Carbide Precipitation, and Coarsening in Ferritic Fe-C-P Alloys", *Metall. Trans. A*, **22A**(1), 35–43 (1991) (Transport Phenomena, Experimental, Kinetics, Morphology, 40)

[1992Oka] Okamoto, H., "The C-Fe (Carbon-Iron) System", *J. Phase Equilib.*, **13**(5), 543–564 (1992) (Phase Diagram, Crys. Structure, Thermodyn., Review, #, 242)

[1992Yan] Yang, Y.-D., "Interaction Coefficients in Fe-C-P Ternary and Fe-Cr-C-P Quaternary Solutions at 1400°C", *Scand. J. Metall.*, **21**(5), 194–201 (1992) (Thermodyn., Experimental, 23)

[1993Din] Ding, X., Wang, W., Han, Q., "Thermodynamic Calculation of Fe-P-j System Melt" (in Chinese), *Acta Metall. Sin. (China)*, **29**(12), B527–B532 (1993) (Calculation, Theory, Thermodyn., 7)

[1997Miz] Mizumo, M., Tanaka, I., Adachi, H., "Effect of Solute Atoms on the Chemical Bonding of Fe_3C (Cementite)", *Philos. Mag. B*, **75**(2), 237–248 (1997) (Crys. Structure, Mechan. Prop., Theory, 28)

[1997Wan] Wang, F.M., Li, X.P., Han, Q.Y., Zhang, N.X., "A Model for Calculating Interaction Coefficients Between Elements in Liquid and Iron-Base Alloy", *Metall. Trans B*, **28B**(1), 109–113 (1997) (Thermodyn., Theory, Calculation, 11)

[1998Cow] Cowan, J.R., Evans, H.E., Jones R.B., Bowen, P., "The Grain-Boundary Segregation of Phosphorus and Carbon in an Fe-P-C Alloy During Cooling", *Mater. Sci. Technol.*, **46**(18), 6565–6574 (1998) (Transport Phenomena, Experimental, Morphology, 27)

[1999Din] Ding, X., Fan, P., Wang, W., "Thermodynamic Calculations for Alloy Systems", *Met. Mat. Trans.*, B, **30B**(2), 271–277 (1999) (Thermodyn., Calculation, Review, 17)

[2000Shi] Shim, J-H., Oh, C-S., Lee, D.N., "Thermodynamic Assessment of the Fe-C-P System", *Z. Metallkd.*, **91**(2), 114–120 (2000) (Assessment, Phase Relations, Thermodyn., 22)

[2001Cha] Chan, F.W., Ma, N.G., Kui, H.W., "Compaction of Bulk Ferromagnetic $Fe_{80}P_{13}C_7$ Amorphous Alloys", *J. Mater. Res.*, **16**(10), 2767–2769 (2001) (Crys. Structure, Magn. Prop., Experimental, 10)

[2002Cow] Cowan, J.R., Evans, H.E., Jones R.B., Bowen, P., "Role of Dislocation Density and Structure in Grain Boundary Segregation of Phosphorus and Carbon in Model Fe-P-C Alloy", *Mater. Sci. Technol.*, **18**(11), 1305–1313 (2002) (Transport Phenomena, Experimental, Morphology, 27)

[2002Per] Perrot, P., Batista, S., Xing, X., "Fe-P (Iron-Phosphorus)", *Binary Evaluation Program in MSIT Workplace*, Effenberg, G. (Ed.), MSI, Materials Science International Services GmbH, Stuttgart; Document ID: 20.16107.1.20, (2002) (Phase Diagram, Phase Relations, Crys. Structure, Assessment, 23)

[2003Wei] Wei, B.Q., Li, Y.B., Kohler-Redlich, P., Luck, R., Xie, S.S., "Crystallization Behavior of Amorphous Fe-P Strengthened With Embedded Carbon Nanotubes", *J. Appl. Phys.*, **93**(3), 1748–1752 (2003) (Experimental, Magn. Prop., Mechan. Prop., Morphology, 18)

[2004Rag] Raghavan, V., "C-Fe-P (Carbon-Iron-Phosphorus)", *J. Phase Equilib. Diffus.*, **25**(6), 541–542 (2004) (Phase Diagram, Phase Relations, Review, 9)

[2004Sai] Saitoh, H., Yoshinaga, N., Ushioda, K., "Influence of Substitutional Atoms on the Snoek Peak of Carbon in b.c.c. Iron", *Acta Mater.*, **52**(5), 1255–1261 (2004) (Mechan. Prop., Optical Prop., Experimental, 37)

[2004Wil] Williams, G.O., Randle, V., "Grain Boundary Crystallography in Two Fe-C-P Alloys", *Mater. Sci. Technol.*, **20**(5), 599–604 (2004) (Experimental, Mechan. Prop., Morphology, 20)

DOI: 10.1007/978-3-540-74196-1_11

[2004Yos] Yoshida, N., Umezawa, O., Nagai, K., "Analysis on Refinement of Columnary γ Grain by Phosphorus in Continuously Cast 0.1 mass% Carbon Steel", *ISIJ Int.*, **44**(3), 547–555 (2004) (Experimental, Interface Phenomena, Morphology, Phase Relations, 25)

[2006MSIT] "C-Fe (Iron-Carbon)", *Diagrams as Published in MSIT Workplace*, Effenberg, G. (Ed.), Materials Science International Services, GmbH, Stuttgart; Document ID: 30.13598.1.20 (2006) (Crys. Structure, Phase Diagram, Phase Relations, 2)

[Mas2] Massalski, T.B. (Ed.), *Binary Alloy Phase Diagrams*, 2nd edition, ASM International, Metals Park, Ohio (1990)

[V-C2] Villars, P. and Calvert, L.D., *Pearson's Handbook of Crystallographic Data for Intermetallic Phases*, 2nd edition, ASM, Metals Park, Ohio (1991)

DOI: 10.1007/978-3-540-74196-1_11

Carbon – Iron – Silicon

Nathalie Lebrun

Introduction

Because of the great importance of the ternary system C-Fe-Si in ferrous metallurgy a considerable amount of attention has been devoted to the phase relations, particularly those occurring in the solid state. The stable and metastable phase relations have raised much interest as a basis of steelmaking processes and cast iron foundry industry. The knowledge of the various stable and metastable transformations is therefore important for the improvement of the composition and treatment of many engineering alloys and steels. The rapid solidification technologies have particularly attracted much attention for improving the mechanical properties such as mechanical strength, ductility, corrosion resistance and magnetic properties which are far superior to conventional cast irons.
Numerous investigations have been done regarding the liquidus surface, the isothermal sections and the vertical sections in the stable and metastable systems. The other investigations on the ternary system concern the solubility measurements of carbon in the γ and liquid phases which go always with activity measurements, the determination of the phase diagram under high pressures and the kinetics studies of the austenite transformation in martensite or bainite because these phases are important in the forecast of mechanical properties of steel. The main experimental investigations on crystal structure, phase equilibria and thermodynamics are gathered in Table 1.

Binary Systems

The C-Si phase diagram up to 30 at.% (15.49 mass%) C was optimized recently by [1996Gro] using the least square method. Good agreements have been observed with the experimental data available in the literature. The phase diagram shown in Fig. 1 is a compilation of [1996Gro] and [Mas2].
The C-Fe phase diagram accepted from [2006MSIT] is based mainly on [Mas2] except for the liquid composition in the eutectic reaction L ⇌ (γFe) + (C). This composition is taken from the data of [2000Fen, 2001Fen].
After [Mas2], the liquidus and solidus phase boundaries in the Fe rich portion of the Fe-Si phase diagram was measured by [2005Mec] and thermodynamically reassessed by [1998Mie]. The DTA measurements done by [2005Mec] reveal a significant shift compared to [Mas2] in the solidus and liquidus curves in the range between 20 and 25 at.% Si (11.17 and 14.36 mass% Si), suggesting that the *A*2-*B*2 (and perhaps *B*2-$D0_3$) ordering transition occurs in large part through the two-phase temperature regions. Since these careful experimental data are identical to those used by [1998Mie] for a thermodynamic assessment, these data are retained in this assessment. Consequently, the Fe-Si phase diagram accepted in this assessment and shown in Fig. 2, is a compilation of [Mas2] and [2005Mec] for the liquidus and solidus curves in the Fe rich part. Nevertheless, a more sophisticated thermodynamic treatment of the ordering transition is necessary for a better accuracy of the Fe-Si diagram in the range from 20 to 35 at.% Si (11.17 to 21.31 mass% Si).

Solid Phases

Numerous phases could crystallize depending on the thermal treatment of the C-Fe-Si alloys.
[1911Gon, 1916And] were the first to suggest the existence of silico-carbide occurring in C-Fe-Si alloys. [1923Hon, 1924Hon, 1927Han, 1930Kri, 1932Kri] have suggested the existence of complex carbides of iron and silicon. [1944Hur] have also commented upon the occurrence of a carbide phase for which the carbon content may be lower than the cementite. The stability of the carbides may be increased by superheating the melt before casting. Later [1948Mar] confirmed the existence of two carbides and introduced the term iron silico-carbides to describe these phases.
A number of metastable ternary compounds with different compositions and crystal structure has been referred in the literature: orthorhombic [1959Kon, 1975Sch, 1977Dub, 1977Edn, 2006Yel], triclinic [1969Bun,

DOI: 10.1007/978-3-540-74196-1_12

1972Spi, 1991Lac] and hexagonal [1952Owe1, 1952Owe2, 1952Owe3, 1961Hum, 1964Sch2, 1965Del, 1967Tar, 1971Mal, 1971She, 1975Sar, 1983Bas]. Furthermore, various compositions have been reported: Fe_3SiC and Fe_4SiC [1993Sol], Fe_8Si_2C [1969Bun, 1972Spi, 1988Yat, 1991Lac], Fe_9SiC_2 [1983Bas], Fe_5SiC [2006Yel], Fe_6SiC [1994Mch]. The composition of these ternary compounds strongly depends on the process of heat treatment of silicon, iron and steels. The chemical method of silicon carbide extraction from these alloys also strongly affects the composition. For instance, additional hydrogen in the liquid carbon organic media used during the milling process of Fe-Si favours the formation of Fe_8Si_2C instead of Fe_5SiC obtained using liquid without hydrogen [2006Yel]. [2006Yel] determined the lattice parameters of Fe_5SiC in annealed mechanical alloying of C-Fe-Si powder mixtures which are in good agreement with those reported by [1959Kon] on silicon carbide inclusions in annealed low-carbon iron-silicon alloys. The amount of Fe_5SiC is maximum (95%) when the Si content in the initial mixture is equal to 14 at.% (8.75 mass%) in $Fe_{70}Si_xC_{30-x}$ mechanical alloys. The Fe_3C and (αFe) are also present in these alloys with amounts depending on the composition. [1983Bas] investigated the crystal structure of Fe_9SiC_2 in cast microwire of alloys and showed that Fe_9SiC_2 appears involving enrichment of the core periphery with silicon. It was also noticed that the decomposition of this ternary carbide leads to a supersaturated ferrite in the structure (a = 292 pm). The appearance of this metastable phase together with $Fe_2C(\omega)$ phase in rapidly cooled C-Fe-Si alloys can be attributed to the influence of the silicon atoms. It crystallizes directly from the melts since no phase transformation in the solid state has been detected. In rapid super cooled C-Fe-Si alloys until –196°C, the carbide phase $Fe_2C(\omega)$ crystallizes and then transforms into other carbide $Fe_5C_2(\chi)$ leading to the cementite phase at the end of the process of transformation [1967Ben, 1968Ben]. Due to the stabilization of the carbide $Fe_2C(\omega)$ by silicon, the transformation of the residual austenite could be separated from carbides in the martensite phase using isothermal dilatometry [1967Sim].

Cementite, which is considered as metastable phase, does not dissolve any Si [1952Hil, 1953Iba, 1974Mal, 1977Oka]. The variation of the lattice parameters of the cementite is only due to the variation in C concentration of the cementite.

The effect of silicon on the $Fe_2C(\omega)$ metastable carbide has been extensively studied. [1968Fuj, 1983Ray] have reported that silicon decreases the growth rate of $Fe_2C(\omega)$ metastable carbide precipitation. [1983Ray] explained the effect of silicon with the mechanism proposed by [1954Owe] for the $Fe_3C(\theta)$ metastable carbide: silicon is rejected by the carbide leading to an increase of silicon content in the matrix which reduces the gradient activity of carbon. [1968Fuj] considered that silicon atoms act as weak trapping site of carbon atoms, thereby silicon decreases the diffusion rate of carbon. More recently [1993Sai] concludes that this is caused by the decrease of the number of preferred nucleation site of $Fe_2C(\omega)$ due to the decrease in the number of density of carbide particles with the addition of silicon. After partial transformation at 450°C, thin crystals of carbide have been observed in contact with austenite in a Fe-2.06Si-0.63C alloy with the following orientation relationships: {111} austenite // {011} ferrite // {0001} carbide and {10-1} austenite // {11-1} ferrite // {11-20} carbide [1976Guh].

Another hexagonal metastable phase $Fe_{24}C_{10}$ has been found after splat quenching of C-Fe-Si alloys with 2.5 to 5.0 mass% C and 0.3 to 5.1 mass% Si [1969Ruh]. It undergoes a two-stage decomposition upon heating forming first martensite plus carbide (1 hour from 140 to 200°C) and then ferrite plus cementite (1 hour from 330 to 460°C).

Amorphous phase [1987Ino, 1992Tan, 2006Yel] have also been observed. For instance the amorphous alloy formation field from melt quenching method extends in a range above 9 at.% (2.1 mass%) C and 4 at.% (2.3 mass%) Si, with the total metalloid content more than 30 at.% (60.5 mass%) [1987Ino]. This glass formation is favoured by the strong bonding nature between C and Si causes a decrease of atomic mobility in C-Fe-Si supercooled liquid with high metalloid concentration.

All structural data for unary, binary and ternary phases have been indicated in Table 2.

Invariant Equilibria

Inconsistency was observed concerning the nature of the four-phase equilibria L-(αFe)-(γFe)-(C)gr and L-FeSi-(αFe)-(C)gr. [1938Jas, 1932Kri, 1951Owe, 1966Sch1, 1966Sch2] stipulate the existence of a peritectic reaction L + (αFe) ⇌ (γFe) + (C)gr whereas [1952Hil] suggest the eutectic reaction L ⇌ (αFe) + (γFe) + (C)gr. [1968Pat] conclude to a eutectic type ternary reaction L ⇌ (αFe) + (γFe) + (C)gr. [1938Jas] reported the existence of a peritectic reaction L + FeSi ⇌ (αFe) + (C)gr whereas

DOI: 10.1007/978-3-540-74196-1_12

[1968Pat] concluded the existence of a eutectic reaction L ⇌ FeSi + (αFe) + (C)gr. Since the last works were based on microscopic examinations, the nature of the two ternary reactions have been concluded to be a eutectic type reactions, called E_1 and E_2 respectively. Moreover the existence of these two E-type reactions was confirmed by [1984Sch]. Large discrepancies have been observed concerning the silicon concentration of the liquid and the temperature of the ternary reaction E_2 ranging from 6 mass% Si at 1172°C [1938Jas] to 8.35 mass% Si at 1145°C [1952Hil]. On contrary, good agreement has been observed on the liquid composition of the ternary reaction E_1 determined by [1938Jas, 1968Pat]. The more recent data for the liquid composition [1984Sch] and for the solid phases involved [1968Pat] were reported on Table 3.
[1966Sch1, 1966Sch2, 1984Sch] suggested the formation of a ternary reaction U involving the order-disorder transition of the Fe_3Si phase. This reaction is doubtful and has not been accepted.
Later [1991Lac, 1998Mie] have deduced from thermodynamic optimizations the position of E_2 showing large disagreement between the two calculations concerning the liquid composition: Fe-7.06Si-2.40C (mass%) at 1170°C [1998Mie] and Fe-6.16Si-7C (mass%) at 1171°C [1991Lac]. The composition proposed by [1998Mie] seems to be the most reliable since the limit of crystallization regions of different phases involved in this ternary reaction fits well with the experimental data available in the literature. Nevertheless, its calculated value does not fit well with the experimental value measured by [1968Pat].
[1991Lac, 1998Mie] calculated also the position of a U-type ternary reaction (L + β,Fe_2Si ⇌ FeSi + (αFe)) with excellent agreements. Nevertheless, large discrepancies have been observed with the location of this U reaction proposed in the review of [1992Rag]. Because of the position of the binary eutectic reaction L ⇌ (αFe) + β,Fe_2Si, the values reported in [1992Rag] have been retained in this assessment and are reported on Table 3.
Regarding the metastable phase equilibria, two ternary reactions have been measured [1967Mal, 1974Mal]: an E-type and a U-type. The compositions of the phases and the reaction temperatures have been indicated in Table 4 as taken from [1974Mal].
Others four phase equilibria have been calculated by [1991Lac, 1998Mie] for the stable equilibrium (L-(αFe)-(C)gr-SiC and L-(αFe)-Fe_2Si-SiC) and the metastable equilibrium (L-(αFe)-(γFe)-Fe_8Si_2C, L-(αFe)-Fe_8Si_2C-SiC and L-Fe_3C-SiC). [1952Chi] reported the possible existence of a ternary eutectic involving (αFe), FeSi and SiC. Due to the lack of experiment, these four-phase equilibria could not be reported on the liquidus surface diagram. Experimental investigations are needed.
A ternary reaction (γFe) + τ ⇌ (αFe) + Fe_3C occurs in the metastable solid state at 820°C [1968Gor, 1974Mal] with the compositions for the (γFe) and (αFe) phases equal to 3.8 mass% Si - 0.7 mass% C and 5.1 mass% Si - 0.1 mass% C respectively [1974Mal].
The reaction schemes corresponding to the stable and metastable liquidus surface are reported in Figs. 3 and 4.

Liquidus, Solidus and Solvus Surfaces

The stable liquidus surface in the iron rich corner was extensively studied showing the crystallization regions of the (αFe) and the (γFe) phases [1906Wue, 1908Gon, 1911Gon, 1916And, 1923Hon, 1924Hon, 1927Han, 1929Nor, 1930Kei, 1930Kri, 1930Sat, 1932Kri, 1938And, 1938Jas, 1940Jae, 1941Jae, 1962Zhu, 1952Hil, 1966Sch1, 1966Sch2, 1966Sch3, 1968Ole, 1968Pat, 1971Gor, 1972Jeg, 1977Agr, 1980Kag, 1987Hei]. General good agreements were observed except the nature of the ternary reactions as described previously. A transition reaction U is necessary to eliminate the β,Fe_2Si phase as predicted by [1991Lac, 1998Mie] using thermodynamic optimization. This ternary reaction has been added on the liquid surface shown in Fig. 5. The isothermal lines showing the liquid-graphite equilibrium have been measured at 1550 and 1350°C [1952Chi, 1969Sch].
[1987Sch] calculated the liquidus surface in the iron rich corner and [1977Agr, 1977Car] calculated the stable valley between graphite and the (γFe)/(αFe). Calculations reproduce well the experimental data except the one done by [1977Agr] rejected in this assessment. More recently, [1991Lac, 1998Mie] undertook a precise thermodynamic assessment. Disagreements appear between the calculated isothermal lines at 1550 and 1350°C [1991Lac, 1998Mie] with experimental data, in particular at high silicon content. On contrary, the limit of the crystallization regions for the (αFe) and the (γFe) phases are quite well thermodynamically optimized. Nevertheless, the data of [1991Lac] seem slightly to overestimate the stability of the (αFe) phase with respect to the (γFe) phase. The isothermal lines calculated by [1987Sch] reproduce well the experimental results of

DOI: 10.1007/978-3-540-74196-1_12

saturation melts done by [1984Sch]. Small addition of Si on pure C-Fe eutectic alloys leads to a slight increase of the stable eutectic temperature inside the ternary system up to 0.5 mass% Si [1988Mag], 4 at.% (2.4 mass%) Si [1977Car], 22 mass% Si [1923Hon, 1924Hon].
The stable liquidus surface depicted in Fig. 5 is taken from the review of [1992Rag] mainly based on the careful experimental data of [1952Hil, 1968Pat]. Slight modifications have been done on the binary edges according to the accepted binary diagrams.
The metastable liquidus surface was investigated by [1949Jae, 1966Gor, 1967Mal, 1967Zhu, 1969Zhu, 1970Mal, 1972She, 1974Mal, 1984Sch, 1986Kal, 1987Hei]. The liquidus surface shown in Fig. 6 is taken from [1992Rag] based on the experimental work of [1967Mal, 1974Mal]. The eutectic line calculated proposed by [1977Car] is in fairly good agreement with experimental results, whereas the calculated curve proposed by [1977Agr] is in total disagreement on the composition point of view. The cementite and the ternary phase τ appear as primary phases during crystallization. The results of [1949Jae] have not been retained in this assessment since the phase equilibria involving the metastable ternary phase τ have not been taken into account. Small addition of Si to pure C-Fe eutectic alloys leads to a decrease of the metastable eutectic temperature inside the ternary system up to 0.1 mass% Si [1988Mag] and 3 at.% (1.75 mass%) Si [1977Car].
A calculated partial stable liquidus surface in the iron rich corner, shown in Fig. 7, has been reported by [1996Koc] at 8 GPa based on the experimental work done by [1978Kam].
In the review of [1994Mch], tentative subsolidus relations have been suggested showing the following three-phase equilibria: ζ,$FeSi_2$+SiC+ε,FeSi, β,Fe_2Si+SiC+ε,FeSi and ζ,$FeSi_2$+(C)gr+τ. The phase relations in the iron rich corner disobey the phase rule.

Isothermal Sections

The limit of graphite in C-Fe-Si melts has been extensively studied to temperatures as high as 1700°C and to silicon concentration up to 23 mass% or 35 at.% [1922Sch, 1952Chi, 1955Tur, 1958Koz, 1959Neu, 1977Ash, 1977Sos, 1981Sch, 1982Vre, 1983Jan]. [1969Sch] has given an empirical expression in agreement with the experimental data: x_C (mass%) = $1.34 + 2.53\cdot10^{-3}T - 0.2941x_{Si} + 0.725\cdot10^{-2}\cdot x_{Si}^2 - 0.0285\cdot10^{-3}T\cdot x_{Si} - 0.139\cdot10^{-5}T\cdot x_{Si}^2$, where T is temperature in °C and x_{Si} is the silicon composition in mass%. [1977Sos] also proposed another empirical expression which reproduced well the experimental data. For the concentrations higher than 20-23 mass% Si, cooling of a C-Fe-Si liquid alloy leads to the appearance of a second solid phase more stable than graphite [1952Chi, 1954Ful]. This phase, identified as SiC, crystallizes along the graphite domains. The solubility of carbon in silicon-containing austenite and ferrite in equilibrium with each other or with graphite or cementite has been reported in [1934Her, 1948Smi, 1958Lea, 1966Sch1, 1967Sch, 1972Wad, 1977Agr, 1984And, 1984Wri, 1987Chu].
Several partial isothermal sections have been measured in the iron rich corner.
Stable isothermal sections were reported at 800°C [1969Bun], at 1000°C [1948Smi, 1932Kri, 1969Bun], at 1160°C [1932Kri, 1969Bun], at 1170°C [1932Kri], at 1200°C [1969Bun], at 1260°C [1969Bun], at 1300°C [1932Kri] at 1425°C [1969Bun].
Metastable isothermal sections were determined at 1150, 1250, 1350 and 1450°C by [1952Hil].
In his review, [1992Rag] established the stable isothermal sections at 1300 and 1000°C taking into account the solubility of carbon measured by [1952Chi] and the computed isothermal section of [1987Chu]. In the same review, the metastable isothermal sections at 1100 and 900°C were drawn using the vertical sections of [1968Gor, 1974Mal], the computed data of [1977Agr, 1984And] and the fixed composition of τ deduced from [1971Mal].
Composition discrepancies have been noticed between the isothermal proposed by [1932Kri, 1969Bun] and [1992Rag]. Large discrepancies have been observed with the accurate experimental stable vertical sections constructed by [1968Pat]. Consequently the stable isothermal sections have been modified to be in agreement with results of [1968Pat]. Moreover, [1952Hil] did not report the phase equilibria involving the ternary compound τ reported by [1971Mal]. Consequently the isothermal sections proposed by [1952Hil] have are not accepted in this assessment.
[1977Agr, 1977Uhr2, 1978Uhr] calculated partial isothermal section in Fe rich part showing discrepancies with the experimental data on the phase boundaries (γFe) / ((αFe) + (γFe)) [1966Aar1, 1966Aar2,

DOI: 10.1007/978-3-540-74196-1_12

1966Aar3]. Later [1989Eno] undertook calculations with correct values of ${}^{0}G_{(\gamma Fe)}{}^{Si} - {}^{0}G_{(\alpha Fe)}{}^{Si}$ and found a quite good agreement with the experimental data. It confirms the assumption of [1981Bra] who predicts the existence of the (γFe) phase at alloy composition Fe-1.73Si-0.4C (mass%) using a Hillert-Staffanson regular solution model. The stability of the (αFe) phase is overestimated with respect to the (γFe) phase in the calculated iron rich isothermal sections proposed by [1991Lac] at 1350, 1250, 1150 and 1000°C. The optimized sections done by [1998Mie] seem to be more realistic as a better agreement with the experimental data [1948Smi, 1966Fis] is observed. Nevertheless disagreements are observed with the partial isothermal section calculated at 1000°C and at higher temperatures by [1987Chu]. Larger two-phase fields (αFe)+(γFe) regions have been found by [1998Mie] compared to those suggested by [1987Chu].
[1988Sch] calculated the isothermal section at 850°C showing the phase equilibria with the SiC phase.
[1987Chu] calculated metastable sections at 800, 900, 1000 and 1100°C showing large discrepancies to those reported by [1992Rag]. The results of [1987Chu] have not be retained in this assessment since the phase equilibria involving the metastable ternary phase τ have not been taken into account.
Figures 8, 9 and 10 show the accepted stable isothermal sections at 850°C [1988Sch], at 1000°C and 1300°C [1987Chu]. Figures 11 and 12 depict the metastable isothermal sections at 900°C [1992Rag] and 1100°C [1992Rag]. All of them have been slightly modified according to the accepted binary phase diagrams and the accepted vertical sections.

Temperature – Composition Sections

Several vertical sections are available in the literature at fixed silicon contents ranging from 2 to 18.49 mass% [1923Hon, 1924Hon, 1932Kri, 1952Hil, 1968Pat, 1969Bun, 1971Chr, 1974Mal, 1990Jan] and at fixed carbon content 0.05 to 2.54 mass% C [1932Kri, 1935Daw, 1968Gor, 1988Yat]. [1932Kri, 1952Hil, 1968Gor, 1974Mal, 1988Yat] measured metastable phase equilibria and [1923Hon, 1924Hon, 1932Kri, 1968Pat, 1969Bun, 1971Chr, 1990Jan] presented the stable ones.
An addition of silicon to an iron-based alloy stabilizes ferrite relative to austenite [1967Sch] and decreases the graphite solubility [1925Bec, 1948Smi, 1966Sch1, 1967Sch]. The limit of solubility of carbon in ferrite containing silicon increases with the carbon content [1946Ric, 1951Har, 1966Fis]. The vertical section proposed by [1971Chr] has not been retained in this assessment since disagreements are observed with the same vertical section proposed by [1932Kri, 1968Pat, 1990Jan]. The minimum of the carbon solubility in the (γFe) phase was found at about 1000°C whereas [1968Pat] found a minimum at higher temperature (1250-1270°C) and a much higher carbon concentration. Moreover, all the authors, except [1971Chr], indicated that the (αFe) + (γFe) field was of a rather constant width over a wide temperature range. On the contrary, [1971Chr] showed that the (αFe) + (γFe) field narrows markedly at a temperature of about 1050°C. Disagreement is also observed in the stable vertical section regarding the three-phase equilibrium L + (αFe) + (γFe). [1968Pat, 1971Chr, 1990Jan] found a ternary peritectic reaction contrary to the extrapolated results of [1939Sal, 1969Bun]. Because of the careful experimental data of [1968Pat] and the well defined calculated vertical sections of [1990Jan], only these results have been retained in this assessment. Good agreement is observed concerning the eutectic reaction (αFe) + (γFe) + (C)gr at around 800°C except for results of [1939Sal, 1974Mal]. Nevertheless, this lower temperature reaction has not been reported in Figs. 13 to 18 showing stable vertical sections at various Si fixed content based on results of [1968Pat]. This part of the diagram needs more experimental investigations.
Schematic stable vertical sections have been proposed by [1932Kri] at fixed carbon content ranging from 0.1 to 2.54 mass% C. Some of them are reported in Figs. 19 to 22. Experimental results of [1932Kri] are in good agreement with theoretical deductions done by [1928Sch] based on the combination of the system C-Fe and the system Fe-Si with closed (γFe) phase region.
The metastable vertical sections have also been investigated. They present an identical shape that the stable ones with the same type of reactions in the same temperature range: carbon phase is simply replaced by the carbide phase Fe_3C. General good agreement has been observed regarding the shape. Nevertheless, [1932Kri] found systematically higher compositions compared to the ones measured by [1952Hil]. Based on geometrical nature of phase diagram, [1988Luo] drawn schematic vertical sections at fixed silicon content which are in agreement with those reported by [1952Hil]. [1930Kri, 1932Kri, 1988Luo] also reported a lower three-phase field involving (αFe), (γFe), Fe_3C at around 750°C at 1 mass% Si and

DOI: 10.1007/978-3-540-74196-1_12

850°C at 4 mass% Si which becomes larger as Si content increases. The vertical sections reported by [1952Hil] are not in agreement with the metastable liquidus surface accepted in this assessment. More experimental investigations are needed. These vertical sections are not retained in this assessment.
[1968Gor] measured metastable vertical sections at 0.25, 0.5 and 0.8 mass% C with silicon content varying up to 10 mass%. These sections present the same behavior that the one reported by [1922Sch, 1974Mal] for the stable vertical sections. These vertical sections have not been retained in this assessment since both (C)gr (stable system) and cementite phase (metastable system) appear on the same vertical section. From literature data, [1935Daw] made assumption on the constitution of a schematic vertical section at fixed composition of carbon. Since it is not corroborated by experimental data along, all these vertical sections are not retained in this assessment. Further experimental investigations are needed.
A quite large number of computed phase equilibria have been reported for the iron rich corner [1977Agr, 1984And, 1985Ves, 1988Luo, 1991Lac, 1998Mie]. Vertical sections of the stable system were calculated at fixed Si content ranging from 2.08 to 6.12 mass% by [1985Ves]. They reproduce well the experimental results of [1968Pat]. Vertical sections for the metastable system were calculated by [1932Kri, 1988Luo, 1988Yat] at fixed Si and C content ranging from 1 to 8 mass% Si and 0.02 to 0.1 mass% C, respectively. Reasonable agreements have been observed between the calculated vertical section done by [1988Luo, 1991Lac, 1998Mie] and the experimental ones measured at various fixed silicon contents for the metastable [1952Hil] and the stable [1968Pat] phase equilibria. Nevertheless, [1991Lac] found systematically liquidus and solidus calculated curves lower than those optimized more recently by [1998Mie]. [1991Lac] gives also too low values for the peritectic temperatures at high silicon content, whereas at lower silicon contents a better agreement was observed between [1991Lac] and the experimental data compared to the optimized data of [1998Mie]. Comparison of the calculated vertical sections proposed by [1988Luo, 1988Yat] with experimental data is not possible due to the lack of careful experimental data. Anyway the schematic vertical sections proposed by [1988Luo] have been reported in Figs. 23 to 25.
[1906Wue, 1908Gon, 1911Gon, 1923Hon, 1924Hon, 1936Han, 1938Jas, 1952Hil, 1966Sch1, 1966Sch2, 1968Pat] constructed a vertical section along the channel e_8-e_7-E_2-e_6-E_1 of the liquidus surface. As confirmed later by [1988Mag], small addition of Si (<0.6 mass%) in the stable C-Fe eutectic alloys leads to an increase of the eutectic temperature inside the ternary system. Some discrepancies have been noticed regarding the temperature ranging up to 5 mass% Si. Values of [1906Wue] and [1923Hon, 1924Hon] are found respectively larger and lower than those reported by [1908Gon, 1911Gon, 1952Hil]. As already mentioned above, discrepancies have been observed concerning the nature of the ternary reactions found along this vertical section. [1938Jas] mentioned the existence of two peritectic reactions at 5.5 mass% Si (1175°C) and 13.44 mass% Si (1200°C). Later [1966Sch1, 1966Sch2] confirmed the existence of the peritectic reaction at 5 mass% Si but stipulated that the other ternary reaction is a U type reaction due to the existence of a maximum at around 15 mass% Si (1210°C). [1952Hil] investigated the vertical section up to 10 mass% Si and detected the presence of a maximum at around 4.6 mass% Si (1172°C) leading to a change of the nature of the ternary eutectic found by [1938Jas, 1966Sch1, 1966Sch2]. [1968Pat] also detected a E type reaction at 5 mass% Si and replaced the U type reaction found by [1966Sch1, 1966Sch2] by a E type reaction at around 19 mass% Si (1180°C). The two E type ternary reactions have been confirmed by [1984Sch] who presents careful data measurements on the liquidus curve with the existence of two maxima at 5 mass% Si (1168°C) and 14.8 mass% Si (1197°C).
[1952Hil, 1968Pat] concluded that the eutectic valley e_8-E_2 presents a maximum at 1170°C and 5 mass% Si and then decreases to 1153°C again with further increase in Si content. [1998Mie] noticed the existence of this maximum very close to the point E_2 leading to a small eutectic character of the ternary reaction E_2. According to [1966Sch1, 1966Sch3, 1968Pat], the L+(αFe)+(C)gr univariant line also passes through a maximum at 1198°C corresponding to the ordering of the (αFe) to the α_1,Fe_3Si [1992Rag].
Consequently, only the "vertical section" constructed by [1968Pat] is depicted in Fig. 26 showing the two maxima at 1170°C (maximum e_7) and 1198°C (maximum e_6). The liquidus curve has been taken from [1984Sch] who presented more careful and more precise data compared to [1968Pat]. The Fe rich part of the isopleth has been modified to be in agreement with the accepted liquidus surface.

DOI: 10.1007/978-3-540-74196-1_12

Thermodynamics

The activities of carbon and silicon in C-Fe-Si melts have been determined many times [1948Chi, 1954Chi, 1965Rei, 1977Ash, 1977Kul, 1980Mer, 1980Sch, 1981Sch, 1985Chu, 1989Dre, 1990Dre]. Silicon increases the activity coefficient of carbon in melt. [1959Pet] calculated the activity coefficient of carbon at 1460°C using the following equation: $\log(\gamma_C^{Fe,Si}) = 2.15N_{Si}+2.25N_{Si}^2$, where N_{Si} represents atom fraction of silicon. This expression is in fair agreement with the experimental results of [1948Chi]. The isoactivity lines in the liquid phase of C-Fe-Si system have been also experimentally determined at 1550 and 1420°C for carbon [1962Nyq, 1980Sch, 1981Sch] and at 1500 and 1420°C for silicon [1985Chu, 1964Sch1, 1980Sch, 1981Sch, 1990Dre]. [1998Mie] proposed a better thermodynamic assessment than in [1991Lac] since excellent agreements were observed with experimental data even at high silicon content. The experimental data reported by [1985Chu] are twice lower than those found by [1964Sch1]. Consequently, unique parameter optimization could not be found by [1991Lac, 1998Mie] which could well satisfy both of these experimental values. The first-order interaction determined by [1974Sig] is: $e_C^{(Ni)} = (\partial \log f_C / \partial x_{Si}) = -0.008 + (162 / T)$ (T/K and x_{Si}/mass%). The second-order coefficient is found to be 0.0007. Isoactivity lines for Si and C in C-Fe-Si liquid alloys at 1420°C [1980Sch, 1981Sch] in the Fe rich corner is shown in Fig. 27. [1980Mer] found isothermal lines carbon-silicon systematically with higher contents than the those determined by [1980Sch].

The carbon activity coefficient lines have been calculated at various temperatures from 700 to 1100°C in the (αFe) phase of the C-Fe-Si system with fixed silicon contents of 3.14 and 4.95 mass% [1991Lac, 1998Mie] showing excellent agreement with experimental data of [1991Nis]. They have been also optimized in the (γFe) phase at 1147, 1000 and 997°C [1998Mie, 1991Lac, 1994Lee] and reproduced well the experimental data available in the literature [1948Smi, 1967Sch, 1972Wad]. Using a thermodynamic model for interstitial solutions, [1977Uhr1] determined the temperature evolution of the carbon metal interactions. The temperature dependence of the parameter K_2, describing the interaction between carbon and silicon in C-Fe-Si austenite, is found to be $K_2 = -465+0.48\ T$ (kJ·mol^{-1}) for $827 < T < 952$°C and $K_2 = 123$ kJ·mol^{-1} for $952 < T < 1177$°C. The activity of carbon in austenite could be described at 1000°C by the following equation: $\log(a_C/z_C) = 2.84z_C + 3.11z_{Si} + 12.9z_Cz_{Si} + 16.2z_{Si}^2$ with $z_C = n_C / (n_{Fe} - n_C - n_{Si})$ and $z_{Si} = n_{Si} / (n_{Fe} - n_C - n_{Si})$ [1968Chi]. Additional experimental data of the activity of carbon a_C in the (γFe) phase were obtained at 900°C for two fixed silicon compositions (0.64 and 1.53 mass% Si) [1994Prz]. Good agreements were observed with previously calculated and experimental data concerning the slope of the curve $\log_{10}(\gamma_C) = f(y_C)$ with $\gamma_C = a_C / x_C$ and $y_C = x_C / (1-x_C)$ (x_C: mole fraction of carbon atoms). Moreover, for both (γFe) and (αFe) phases, increase of silicon leads to lower carbon activity value [1990Jan]. The same effect has been observed in ledeburite decomposition of the liquid eutectic in the metastable phase diagram C-Fe and hence a decrease of the ledeburite transformation temperature is noticed [1988Mag, 1993Zhu].

The activity of silicon in the graphite-saturated, SiC-saturated solution is: $\log a_{Si} = -5330/T + 1.81$ (T/°C) [1954Chi].

The only known measurements on mixing enthalpy in molten C-Fe-Si alloys are those of [1989Vit, 1994Wit]. Figure 28 reproduces these data at 1587°C. The level agreement with the thermodynamic models used by [2001Sch] is not especially impressive but the regular solution model clearly matches the experimental data better in highly alloyed compositions.

Notes on Materials Properties and Applications

The Vickers hardness of amorphous C-Fe-Si alloys is in the range of $8.43\cdot10^6$ to $10.2\cdot10^6$ kg·m(·s^2)$^{-1}$ [1987Ino] and tends to exhibit higher values for the C rich alloys. The same behavior has been observed in C-Fe-Si powders and in cast iron alloys [1936Thy]. Nevertheless, on contrary to amorphous alloys, the hardness of powder alloys increases as silicon content increases. A lower hardness value was measured in annealed powder (200-300 instead of 1000-1500 kg·mm^{-2}) [1990Yeo]. The increasing annealing temperature up to 650°C of C-Fe-Si steels with small amount of C (0.4 mass%) and Si (0.25 mass%) strongly decreases the hardness values [2005Tek]. The hardness strongly depends on the treatment of the powder alloy. The hardness of the deposit layers tempered at 300-500°C is larger than that of the as-sprayed deposit layers [1989Mur]. It was also shown that the addition of boron in Fe-Si alloys containing up to 5 mass% Si

DOI: 10.1007/978-3-540-74196-1_12

strongly increases the hardness [1968Hof]. Moreover, the yield strength and the ultimated tensile strength decrease with increasing tensile test temperature leading to higher values for quenched alloys. Higher values of the Young's modulus have also been observed in cast alloys than in annealed alloys [2005Liu]. The Fe-2.5Si-C mixed powders, preformed at 1150°C under H_2 atmosphere and compacted at 600 MPa, show high strength (900-1200 MPa) after sintering for a long time or powder-forging. No similar behavior is observed for samples containing more than 2 mass% C [1980Han]. Addition of 1 or 2 mass% Si to a cold-rolled and annealed pearlite in Fe-0.8 mass% C eutectoid alloys reduces less than half the interlamellar spacing of pearlite leading to an increase of the yield strength and the tensile strength whereas the ductility remains almost constant [2004Fu]. The increase of yield strength is observed larger than the tensile strength. The growing of the θ particles of the lamellar cementite, mixed with the ferrite (αFe) in the pearlite, is significantly retarded with increase of Si content and the grains are much finer. Rich iron steels transformed into the lower bainite region show better tensile property than steels transformed into the upper bainite region [1991Kim]. This behavior is directly related to the morphology of the bainite where the retained austenite is finely dispersed film type in the lower region and is a bulky type in the upper region. The tensile strength increased with increasing extrusion rate in Fe-Si alloy powders containing 3.6 mass% C and reached 65∼75 $kg \cdot mm^{-2}$ when extrusion rate was 13 [1990Yeo].

The resistivity of Fe-7Si-16C (in at.%) (Fe-4.2Si-4.1C in mass%) decreases by about 45% during the total decomposition of the Fe_9SiC_2 metastable phase. This reduction is only 25% for Fe-3Si-16C (in at.%) (Fe-1.7Si-4C in mass%) alloys [1983Bas]. No resistivity changes is observed upon changing the aging temperature in Fe-0.38Si-0.0269C (in at.%) (Fe-0.19Si-0.1251C in mass%) [1993Sai]. [1931Soe, 1936Thy] noticed a decrease in the bending resistance with increasing content in carbon and silicon in cast iron alloys.

Cast iron alloys containing carbides and high content of silicon are very brittle in particular when the Fe_3Si_2 phase crystallizes. The hardest cast iron alloys contain pearlitic phase [1936Thy, 1941Boy].

The electrical resistivity in iron rich amorphous alloys is quite constant with silicon and carbon contents [1922Sch, 1987Ino]. Carbon and silicon added together do not have a simple additive effect on the resistivity of molten C-Fe-Si alloys [1976Ono]. The electrical resistivity was also measured in lamellar graphite structure of C-Fe-Si alloys and presents unexpectedly no anisotropy leading to a constant value estimated to be 50-80 μΩ·cm, whereas a large anisotropy exists in the form of layer graphite [1981Yos].

The effect of sintering in Fe-2.5Si-1.4C compacts on microstructure have been studied at various sintering times for temperature ranging from 1140 to 1170°C [1986Cho]. At early stages of sintering, the as-quenched microstructure was fine pearlite and changed to martensite with successive sintering up to 27 h. It is closely related to the homogenization process of Si.

(Si,Fe)C shows apparent ferromagnetic behavior up to approximately –23°C with implant concentration of about 5 at.% (12.8 mass%) Fe [2001The]. The microscopic origin of the ferromagnetism is not well understood at this stage and further work is needed in order to increase the Curie temperature point in these high doses Fe^+ implanted into p-SiC. Higher Curie point is observed in mechanical alloying which increases with Si content [2003Oga, 2006Yel]. For instance, a value of 351°C was measured for the amorphous sample $Fe_{70}Si_{20}C_{10}$ (at.%) ($Fe_{85.4}Si_{2.36}C_{12.24}$ in mass%) [2003Oga], 30°C lower than the extrapolated value of [2006Yel] and 124°C higher than the value measured in amorphous sample $Fe_{70}Si_{12}C_{18}$ (in at.%) ($Fe_{87.60}Si_{7.55}C_{4.85}$ in mass%) [1996Kon]. The Curie temperatures of the amorphous phases obtained by the mechanical alloying [2006Yel] are identical to those measured in amorphous phases obtained in melt quenching [1987Ino] in the same composition range ($Fe_{70}Si_xC_{30-x}$; $5 \le x \le 20$ at.% or $3.2 \le x \le 12.3$ mass%). Identical magnetic properties have been measured in amorphous alloys $Fe_{70}C_{30}$ ($Fe_{91.56}C_{8.44}$ in mass%) with small amount of silicon [2006Yel] whereas large discrepancies are noticed in amorphous alloys $Fe_{70}Si_{30}$ ($Fe_{82.27}Si_{17.73}$ in mass%) with small amount of carbon [2006Yel, 1976Mar]. Numerous magnetic properties were measured and calculated in amorphous alloys by [2006Yel]. The specific saturation magnetization σ_0 presents a maximum for amorphous alloys $Fe_{70}Si_{10}C_{20}$ ($Fe_{85.4}Si_{2.36}C_{12.24}$ in mass%) where the content of (αFe) is maximal. The coercivity H_c of the annealed samples $Fe_{70}Si_xC_{30-x}$ seem to be affected by the Fe_5SiC content and reaches its maximum value (450 Oe) at $x = 14$ at.% (8.75 mass%) and 27°C. Indeed, for instance, [1987Ino] measured a coercivity H_c ranging from 0.37 to 0.28 Oe in samples Fe_{70}-$(Si,C)_{30}$ where the crystallization of the Fe_5SiC is avoided. Fe_5SiC is a ferromagnet with σ_0 varying from 155 to 145 $emu \cdot g^{-1}$ with temperature ranging from 196 to 27°C. The Curie temperature is calculated to be 507°C. The lamellar structure of Fe_5SiC results in a strong anisotropy of magnetic properties leading

DOI: 10.1007/978-3-540-74196-1_12

to a higher external magnetic field for the amorphous samples compared to the annealed ones. Moreover, the coercivity is 18 times lower (25 Oe) than in annealed amorphous samples.
Small amount of Si (3.16 mass%) dissolving in cementite is insufficient to vary significantly the Curie temperature of the cementite due to a slight variation of the free energy [1977Oka].
[2004Aar, 2006Aar] gave a recent overview of the incomplete transformation phenomenon (TTT diagram) observed in C-Fe-X alloys and defined as the temporary cessation of ferrite formation (in the absence of carbide precipitation at (αFe) / (γFe) boundaries) before the fraction of austenite transformed to ferrite. In most cases, ferrite nucleates at the graphite/austenite interface and then grows as halo around graphite nodules. The primary ferrite in the alloys with up to 6 mass% Si is unstable during undercooling and transforms partially or totally in austenite [1988Yat]. [1982San] studied the bainitic ferrite formed in silicon alloyed high-carbon steels in the temperature range 290 to 380°C. It was found that the bainitic ferrite is heavily dislocated, while the surrounding austenite contains thin twins. The carbon content of the austenite in contact with the bainitic ferrite increases with the bulk carbon content [1973Par, 1979Bha]. This is thought to be a result of strain energy accumulation in the austenite [1979Bha]. These phenomena occur below about 420°C for a C-Fe alloy containing 3.9 mass% Si [1970Sch2]. Moreover, at 420°C, the common crystallographic plane between ferrite and austenite is a (253)cfc type with a Wassermann-Nishiyama orientation [1970Sch1]. The second stage of the bainitic transformation consists of the decomposition of austenite leading to an orthorhombic silico-carbide [1975Sch] dispersed in a ferritic matrix [1973Sch1]. Following the heat treatment, the bainite can also precipitate as a mixture of ferrite and cementite which forms below a Bs (Bainite start) temperature [1990Rey]. The transformation proceeds quickly after an induction period and may be complete. From revised thermodynamic data, [1989Eno] confirmed the conclusion of [1981Bra, 1985Liu] that the growth of ferrite in the Fe-1.73Si-0.4C (mass%) alloy ceases well before the carbon concentration of the residual austenite reaches the level given by the extrapolated paraequilibrium (αFe) + (γFe) / (αFe) phase boundary. Nevertheless, [1985Bha1, 1985Bha2, 1987Bha] suspected the data of [1981Bra, 1985Liu] because the experimental method employed certainly favours the decarburization and/or the surface degradation of the alloys. With the heat treatment method used, the C-Fe-Si alloy does not have the hardenability necessary to ensure that transformation occurs only at the isothermal transformation temperature of interest. Moreover [1989Bha] showed that the assumption of [1989Eno] is not justified since the model used (one-dimensional thickening process) is inadequate and only empirical. The model of oblate ellipsoids of revolution reduces the apparent small disagreement between the experiments [1981Bra] and the calculation [1989Eno]. At that time the claim that the observed growth kinetics for alliotriomorphic ferrite are faster than expected from paraequilibrium transformation theory does not seem justified. It is currently not possible to theoretically decide which of the modes (local equilibrium or local paraequilibrium) is favoured. The possible existence of solute-drag and interface pinning effects may further complicate the theoretical interpretation done from experimental evidence.
[1974Met] observed the formation of the martensite from the residual austenite supersaturated in carbon which normally leads to the bainite transformation at 420°C. The common crystallographic plane between ferrite and austenite is a (3,15,10)cfc type with a Greninger-Troïano orientation [1970Met]. The temperature Ms of the martensitic transformation is estimated to be –130°C. The martensitic phase could not be developed if the spheroid graphite is present in the sample [1973Sch2].
For alloys up to 3 mass% Si, the crystallization of a high carbon silicon phase Fe_8Si_2C may be formed from the ferrite in addition to the austenite, as observed in high carbon C-Fe-Si alloys [1969Bun]. The influence of Si upon the morphology of ferrite allotriomorphs is minor and is largely confined to shifting the Ws temperature [2004Aar, 2006Aar]. Austenite formation is favoured by the development of a network of boundaries of ferrite polygonal grains. Silicon influences the nucleation kinetics of grain boundary ferrite allotriomorphs at austenite grain faces by changing the driving force for nucleation.
Mechanical alloying materials $Fe_x(Si,C)_{100-x}$ (x = 65-85 at.%, x = 83.8-94.04 mass%) are easily to amorphize in C rich composition in comparison with the Si rich composition. The amorphization reaction most readily occurs near the composition of x = 70-75 at.% (x = 86.67-89.31 mass%) [2003Oga]. Prolonged mechanical alloying processing favours the amorphization of $Fe_{80}(Si,C)_{20}$ materials whose amorphization is not attained by liquid quenching process. [1992Tan] also prepared amorphous phases using mechanical alloying method suggesting that only the (αFe) phase remained for small amount of silicon ($Fe_{75}Si_8C_{17}$ (at.%) or $Fe_{90.71}Si_{4.87}C_{4.42}$ (mass%) and $Fe_{60}Si_7C_{33}$ (at.%) or $Fe_{84.97}Si_{4.99}C_{10.04}$ (mass%)) even after a long

DOI: 10.1007/978-3-540-74196-1_12

period of milling, whereas amorphous phase appears for alloys such as $Fe_{54}Si_{14}C_{32}$ (at.%) ($Fe_{79.5}Si_{10.37}C_{10.13}$ in mass%), $Fe_{68}Si_{16}C_{16}$ (at.%) ($Fe_{85.55}Si_{10.12}C_{4.33}$ in mass%), $Fe_{45}Si_{25}C_{30}$ (at.%) ($Fe_{70.28}Si_{19.64}C_{10.08}$ in mass%) and $Fe_{56}Si_{29}C_{15}$ (at.%) ($Fe_{75.87}Si_{19.16}C_{4.97}$ in mass%). However, the amorphous phase coexists with Fe_3C or Fe_7C_3 carbides.

The presence of high silicon content in austempered ductile iron retards the formation of cementite in both ferrite and austenite, however the precipitation of cementite in ferrite is possible when the reaction temperature is low enough [1998Cha]. During the crystallization process of bulk cementite made by combining mechanical alloying with the subsequent spark plasma sintering, the alloying addition of Si leads to the complete suppression of the formation of cementite and results in the formation of a (αFe) solid solution and graphite [2001Ume].

The planar Fe-Fe_3C eutectic in C-Fe-Si alloys during laser surface re-melting on alloys containing small amount of Si (1-3 mass%) and C (3.2-4.2 mass%) is destabilized with respect to primary austenite dendrites for a velocity of the laser impulsions of the order of several $mm \cdot s^{-1}$ ($0.44\ mm \cdot s^{-1}$ for Fe-1Si-4.2C (mass%)) [1998Lim].

Addition of small amount of silicon up to 0.832 mass% in very rich iron alloys (0.045 to 0.047 mass% C) reduces the peak height of the internal friction spectra which presents a maximum at around 50°C. The main reason of this drastic decrease should be due to the influence of the strain field generated by a substitutional atom due to the difference in atomic size [2004Sai].

Crystallization of graphite, austenite and cementite could occur in pigs C-Fe-Si alloys [1971Vig]. Various solidification processes have been demonstrated on C-Fe-Si samples undercooled severely at various temperatures below the theoretical freezing point [1972Kos, 1973Kos]. In a “G type non eutectic process”, excess carbon in supersaturated austenite is precipitated on the graphite eutectic phase formed by the graphite eutectic reaction. In a “C type non eutectic reaction”, excess of carbon is precipitated along the austenite-cementite interface formed by the cementite eutectic reaction. In a “K type non eutectic reaction”, graphite nodules which may develop in the melt as non equilibrium phase are immediately surrounded by austenite and their growth results from the diffusion of carbon through austenite shells from the carbon rich melt. [2001Kag, 2002Kag] investigated the influence of pressure on graphite (gray) to carbide (white) transition in C-Fe-Si eutectic alloys. The critical pressure for this transition was estimated to be 2000 bar for commercial grade cast irons. The pressure-induced stable to metastable transition possibly occurs in spheroid cast iron with a pearlitic matrix.

Experimental investigations on material properties are summarized in Table 5.

Miscellaneous

[1938And] pointed out that addition of small amount of silicon in C-Fe alloys leads to the largest decrease of the fluidity in passing from the liquid state to that in which some solid is present. This may be due to an increase in the viscosity of the liquid. These properties lead to a good castability of these alloys and the sheet, wire and powder form samples made by melt quenching. A non monotone progress of structure rearrangements has been observed in molten iron alloys with small content of carbon (3.6 mass%) and silicon (2.3 mass%) [1995Kha, 1991Sly] leading to a steady hysteresis of physical properties. A change of the apparent activation energy is observed [1977Soi] in Fe-2 at.% Si alloys containing 11.7 to 13.6 at.% C (96.08Fe-1.12Si-2.8C to 95.55Fe-1.14Si-3.31C in mass%) heated 150°C above the liquidus line. Inside the liquid phase, the suggested structure is a short range order type (ideal interstitial solution of carbon in (γFe) quasi-lattice). A rearrangement of the structure occurs at 11.5-12 at.% C (96.13Fe-1.12Si-2.75C to 96Fe-1.12Si-2.88C in mass%) at 1420 and 1520°C. Near the melting temperature, the structure of the melts contains microgroups Fe_xSi_y and $Fe_xSi_yC_z$ which inherit the structural features of phases and compounds in the solid alloy [1995Kha]. It was found also that an increase of the maximum alloy preheating temperature from 1350 to 1500°C decreases the temperature interval of precipitation of primary austenite from 68 to 55°C.

Directional solidification of white cast iron has been studied [1996Par]. The primary effect of Si addition on the ledeburite eutectic Fe-Fe_3C induces cell and dendrite formation. The rod morphology of this eutectic is stabilized because the faceting Fe_3C matrix phase is being force to grow in a specific crystallographic direction (perpendicular to the cells or the dendrites). Silicon is dissolved in the ferrite as well as in the carbide in which silicon is insoluble in equilibrium [1973Jeg].

DOI: 10.1007/978-3-540-74196-1_12

Diffusion reactions have been simulated in C-Fe-Si alloys using the software DICTRA [2000Bor] with experimental data of [1949Dar] joining two steels with similar carbon contents (0.49 and 0.45 mass%) but different Si contents (3.8 and 0.05 mass% respectively). Good agreements have been observed. The experimental uphill diffusion of [1949Dar] in the (γFe) C-Fe-Si alloys is well simulated using a diffusion model [1994Lee]. As Si diffuses much lower than C [1962Kir] and also increases the C activity, C will diffuse from high Si side to the lower one up to its own concentration gradient. In Fe-0.38Si-0.0269C (at.%) (Fe-0.19Si-0.1251C in mass%) alloys, the activation energy for diffusion of carbon atoms was estimated to be 83 ± 2 kJ·mol^{-1} [1993Sai], value very close to that one measured in pure C-Fe alloys indicating that addition of small amount of silicon does not affect the activation energy. The carbon dissolution rate into liquid C-Fe alloys is not changed by addition of 1.9 mass% Si to the melt [1998Sun]. Nevertheless, the diffusion rate of carbon in molten iron (1.02 to 3.04 mass% C and 0.98 to 2.06 mass% Si) increases [1981Wan, 1982Ono] with Si content. The diffusion mechanism was also investigated in coupled FeSi-C annealed for 20 h at 850°C under 13 MPa [1988Sch] showing random precipitates of carbon in the (Fe,Si) layer. Marker experiments with aluminium reveal that iron migrates through the reaction layer whereas silicon and carbon are immobile. The diffusivity of carbon in austenite (γFe) has been also studied in Fe rich alloys containing 1, 2, 4 or 6 mass% Si and carbon concentrations between 0 to 1.25 mass% C [1980Roy]. A strongly decelerating effect of silicon on the carbon diffusivity has been observed. [1970Vig2] studied the diffusivity at 1250°C between Fe-50 mass% Si and Fe-4.18 mass% C alloys. The inter-diffusion area is successively formed of a silico-ferrite matrix with inter-dendrite graphite particles, then a lamellar structure Fe_3Si containing graphite spheroids and SiC equi-axis. The graphite spheroids crystallize preferentially in hypereutectic alloys [1970Vig1].

Oxidation behavior of carbon and silicon of molten C-Fe-Si alloys have been carried out [2001Ono] by blowing CO_2 gas into the metal bulk at fixed flow rates ranging from 10 to 50 L·min^{-1}. Desiliconization limit with CO_2 is 9.1.10-4 mass% Si under the conditions of a_C = 1, a_{SiO2} = 1 and p_{CO2} = 1 atm and silicon can be removed up to 1.3.10-3 mass% Si. This process could be improved by removing SiO_2 from the metal bath in desiliconization with CO_2 because SiO_2 is reduced by carbon in the melt and Si is remelted into the metal. The overall rate constants of simultaneous carbon and silicon oxidation under p_{CO2} = 1 atm are $4 \cdot 10^{-6}$ m·s^{-1} and $5 \cdot 10^{-6}$ m·s^{-1} respectively, and are independent of the CO_2 flow rate. The influence of the CO-partial pressure on the C-Si equilibria compositions for p_{CO} = 0.7, 1 and 1.5 bar has been studied at 1450 and 1550°C from thermodynamic calculations [1981Sch]. The lower p_{CO} value shifts the C-Si equilibria to lower carbon and higher silicon contents.

From investigation on solidification in eutectic and hypereutectic C-Fe-Si alloys, [1968Ole] demonstrated the existence of three different eutectic morphologies: divorced dendritic, non-divorced tending to grow dendritically and cellular. [1998Lac] developed a model describing the eutectoid reaction during cooling of C-Fe-Si alloys with spherical graphite cast iron. It was concluded that interfacial reactions at the matrix graphite interface affect the growth of ferrite in cast iron. This explained that grey irons with lamellar graphite are much less prone to give a ferritic matrix than spheroid or compact graphite cast iron.

In austenized samples, the morphology and the chemical composition of the phases produced depend on the transformation temperature and the stress-strain response of the material depends strongly on the austempering treatment [1994Lue]. The heat treatment is also a crucial factor on the morphologies of the iron rich powders. When the substrate is not water cooled, the deposit layer done by spray plasma technique is composed of ferrite and cementite. In the case of water-cooled substrates, the main constituents are retained austenite and the metastable phase $Fe_2C(\omega)$ on the free surface side [1989Mur].

The partition coefficients for silicon between eutectic liquid and solid during austenite-graphite and austenite-cementite eutectic solidifications were measured leading to k_0 = 1.73 for the austenite-graphite eutectic solidification and k_0' = 0.77 for the austenite cementite eutectic solidification [1980Kag]. These values are in good agreement with those determined from thermodynamic evaluation. The calculated partition coefficient strongly depends on silicon content, especially for the austenite-graphite eutectic solidification.

The hydrogen solubility has been investigated in iron rich alloys containing small amount of Si (1.04 to 2.36 mass%) and C (1.03 to 3.54 mass%) [1970Fuk]. This solubility has a linear temperature variation and becomes higher as C and Si contents decrease.

DOI: 10.1007/978-3-540-74196-1_12

Table 1. Investigations of the C-Fe-Si Phase Equilibria

Reference	Experimental Technique	Phase/Temperature/Composition Region Studied
[1906Wue]	Thermal analysis	550-1250°C / Fe rich alloys with 0.13 to 26.93 mass% Si and 4.29 to 0.87 mass% C
[1908Gon], [1911Gon]	Thermal analysis	1100-1500°C / Fe rich alloys with 0.33 to 33.7 mass% Si and 0.07 to 6.67 mass% C
[1922Sch]	Thermal analysis, metallography	1213-1132°C / Fe rich alloy with 2.30 mass% C and 1.2 mass% Si (impurity: 0.29 mass% Mn, 0.156 mass% P, 0.048 mass% S)
[1923Hon], [1924Hon]	Thermal analysis	700-1500°C / C-Fe-Si alloys with up to 80 mass % Si and 4 mass% C
[1925Bec]	Carburised experiments	800-1100°C / Fe rich alloys up to 4.22 mass% Si and 0.1 mass% C (impurity: up to 22 mass% Mn, 0.030 mass% S and 0.032 mass% P)
[1927Han]	Thermal analysis, microscopic analysis	500-1600°C / Fe rich alloys with up to 2 mass% Si and 4 mass% C
[1930Kei]	Thermal analysis, microscopic analysis	Fe rich alloys with up to 5 mass% C and 6 mass% Si
[1930Kri]	Metallographic, thermal and microscopic analyses	600-1000°C / Fe rich alloys with 6 mass% Si and 0.1 to 4 mass% C (purity: up to 0.57 mass% Mn, 0.085 mass% P, 0.021 mass% S)
[1931Soe]	Thermal analysis	700-1200°C / Fe rich alloys with up to 5 mass% C and 6 mass% Si
[1932Kri]	Thermal analysis, metallographic examinations	1000-1500°C / Fe rich alloys with 3.67 to 16.33 mass% Si and 0.11 to 3.30 mass% C (impurity: up to0.51 mass% Mn, 0.130 mass% P and 0.033 mass% S)
[1935Daw]	Metallographic analysis	Fe rich alloys with 3.12-3.41 mass% C and 0.3-1.33 mass% Si (Impurity: up to 0.18 mass% Mn, 0.039 mass% P and mass% 0.04 S)
[1936Han]	Thermal analysis	900-1250°C / Fe alloys with 34 mass% Si and 5 mass% C
[1938Jas]	Thermal analysis	600-1600°C / Fe alloys with 0.03 to 22.30 mass% Si and 0.07 to 4.24 mass% C
[1941Boy]	Emf measurements, microscopic analysis	Fe-2.19Si-2.93C and Fe-2.34Si-3.03C (mass%)
[1946Ric]	Metallographic examination	700-1400°C / Fe rich alloys with 0.20 to 4.05 mass% Si and 0.52 to 0.74 mass% C (Impurity: up to 0.39 mass% Mn, 0.055 mass% P and 0.026 mass% S)
[1948Mar]	Microscopic examination	Fe rich alloys with 1.70-3.06 C and 2.21-6.69 Si (mass%)

(*continued*)

DOI: 10.1007/978-3-540-74196-1_12

Reference	Experimental Technique	Phase/Temperature/Composition Region Studied
[1948Smi]	Equilibrium measurement	1000°C / Fe alloys with Si and C up to 15 mass% and 1.5 mass% respectively
[1951Har]	Microscopic examination	750-1150°C / Fe rich alloy with 4 mass% Si and 0.05 mass% C
[1951Owe]	X-ray diffraction, microstructure analysis	Fe rich alloys with 1-3.49 mass% C and 0.15-3.14 mass% Si (Impurity: up to 0.81 mass% Mn, 0.12 mass% S, 0.06 mass% P, 0.017 mass% Ni and 0.05 mass% Cr)
[1952Chi]	Pyrometric measurement	1300-1700°C / C-Fe-Si solutions up to 13.60 mass% Si melted in graphite under slags
[1952Hil]	Thermal analysis	1000-1500°C / Fe rich alloys with C up to 4 mass% and fixed Si content (mass%): 2.3, 3.5, 5.2 and 7.9
[1952Owe1]	X-ray diffraction	Fe rich alloys with 0.16-2.15 mass% C and 5.12-8.10 mass% Si
[1954Chi]	Vycor tube and pyrometric measurements	1290-1690°C / C-Fe-Si solutions up to 20-44 mass% Si
[1954Ful]	Microscopic investigations and Vycor tube measurements	1205-1690°C / Fe-19.2Si-0.7C and Fe-20.3Si-0.14C (mass%)
[1959Kon]	X ray diffraction	150, 315 and 425°C / Fe-3.51Si-0.062 C (mass%)
[1959Pet]	Optical pyrometer method	1460°C / Fe alloys up to 4 mass% C and 40 mass% Si
[1961Hum]	X-ray diffraction, microscopic examination	Fe alloys with 4.88-12.22 mass% Si and 0.30-1.76 mass% C
[1962Nyq]	Gas equilibrium method	1550°C / Fe alloys up to 12 at.% Si (24.18 mass%) and 4 at.% C (0.89 mass%)
[1964Her]	X-ray diffraction	Fe_7C_3
[1964Sch1]	Equilibrium measurements	1420°C / Fe rich alloys with 0.15-0.25 Si and up to 0.08 C (mass%)
[1966Dug]	X-ray diffraction	Fe_2C
[1966Fis]	Thermal analysis, microscopic analysis	700-1500°C / Fe rich alloys with 0.01-0.35 mass% C and mass% 0-9.9 Si (Impurity: up to 0.08 Mn, 0.03 P, 0.03 S, 0.02 N and 0.1 O, in mass%)
[1966Sch1]	Thermal analysis	600-1200°C / Fe alloys up to 25 Si mass% and 8 mass% C
[1966Sch2]	Thermal analysis	200-1000°C / Fe alloys with 0.05-15.39 Si and 0.85-4.38 C (mass%)
[1967Sch]	Equilibrium measurements	850-1050°C / Fe rich alloys with 0.45-9.60 mass% Si and 0.11-0.22 mass% C (Impurity: up

(*continued*)

DOI: 10.1007/978-3-540-74196-1_12

Reference	Experimental Technique	Phase/Temperature/Composition Region Studied
		to 0.08 Mn, 0.062 P, 0.011 S, 0.28 Al, 0.13 Cu, 0.015 N2, in mass%)
[1967Tar]	Microscopic analysis, X-ray diffraction	Fe alloys with 1.83-2.63 mass% C and mass% 6.60-11.22 Si (Impurity: 0.018 S, 0.008 P, 0.03 Mn, 0.08 Cu, in mass%)
[1968Gor]	Thermal analysis	700-1200°C / Fe rich alloys with 0.24-0.82 mass% C and mass% 0.40-9.73 Si (Impurity: 0.007 S, 0.007 P, 0.06 Cr, 0.1 Mn, 0.13 Ni, in mass%)
[1968Ole]	Microscopic examination	1000-1600°C / Fe rich alloys with 1-2.9 mass% Si and 3.86-4.48 mass% C
[1968Pat]	Thermal analysis, dilatometry, microscopic analysis	1000-1500°C / Fe alloys up to 20 mass% Si and 4 mass% C
[1969Ruh]	X-ray diffraction	Fe rich alloys with 2.5-5 mass% C and 0.3-5.1 mass% Si
[1969Sch]	Equilibrium measurements	1200-1600°C / Fe alloys up to 17.5 mass% Si and 5 mass% C
[1971Chr]	Equilibrium measurements	835-1050°C / Fe-3.38 Si-0.002 C (mass%) (Impurity: 0.04 Cr, 0.003 Cu, 0.01 Mn, 0.009 Mo, 0.004 Ni, 0.003 Ti, in mass%)
[1971Gor]	Microscopic examinations	1160°C / Fe-11Si-3C (mass%)
[1971Mal]	Microscopic analysis, X-ray diffraction	Fe alloys with 1.50-2.76 mass% C and 2.12-11.22 mass% Si
[1971She]	X-ray diffraction	Fe alloys with 0.27-1.76 mass% C and 6.14-11.70 mass% Si
[1972Jeg]	Micro-probe measurements, microscopic analysis	Fe-2.6 mass% Si with 1.7-3.8 mass% C (Impurity: 0.02 Mn, 0.021 P and 0.013 S, in mass%)
[1972Spi]	X-ray diffraction	Fe_8Si_2C
[1972She]	Microscopic examination	Fe alloys up to 12 mass% Si and 6 mass% C
[1972Wad]	Equilibrium measurements, X-ray microanalysis	848-1147°C / Fe-Si alloys up to 7 mass% Si
[1974Mal]	Thermal analysis	700-1100°C / Fe rich alloys up to 2.4 mass% C and 3.6 to 5 mass% Si
[1975Sar]	X-ray diffraction	Fe-1.9Si4.2C (mass%)
[1975Sch]	X-ray diffraction, microscopic analysis, dilatometry	420°C / Fe-4Si-1C (mass%)
[1977Car]	Unidirectional solidification experiments, DTA measurements, microscopic analysis	1120-1200°C / Fe rich alloys with 3.9-4.3 mass% C and mass% 0.21-2.27 Si

(*continued*)

DOI: 10.1007/978-3-540-74196-1_12

Reference	Experimental Technique	Phase/Temperature/Composition Region Studied
[1977Dub]	Electron diffraction, Mössbauer spectroscopy	Fe rich alloys with 2.56-2.418 mass% C and 2.56-6.91 mass% Si
[1977Edn]	X-ray diffraction	Fe-4.7Si-3.8C (mass%)
[1977Oka]	X-ray diffraction	Fe rich alloys with 0.69-4.30 mass% C and 0.94-3.16 mass% Si
[1980Mer]	Floating zone melting method	Eutectic C-Fe alloys with 0.1-0.6 mass% Si
[1983Bas]	X-ray diffraction	400°C / Fe-16C with 3-10 at.% Si (1.76-6.10 mass%)
[1983Ray]	Transmission electron microscopy	Carbon steels with 0.3-1.52 mass% Si
[1984Sch]	Thermal analysis	1150-1210°C / Fe alloys up to 20 mass% Si and 7 mass% C
[1984Wri]	Equilibrium gas method	940-1080°C / Fe rich alloys 0.005-0.053 mass% C and 1.42-2.92 mass% Si
[1987Hei]	Thermal analysis	1050-1300°C / up to 8 mass% C and 10 mass% Si
[1988Luo]	Microscopic analysis	0-1550°C / C-Fe with 1 to 8 mass% Si and Fe-Si with 0.02 to 0.08 mass% C
[1988Mag]	Chemical analysis, DTA/DSC technique	1140-1160°C / C-Fe-Si with up to 0.5 mass% Si
[1988Yat]	Microscopy, thermogravimetry, X-ray microspectral method and X-ray diffraction	1300-1500°C / C-Fe-Si alloys with 0.05 mass% C and 0 to 8 mass% Si
[1988Sch]	Microprobe measurements	850°C / C-Fe-Si alloys
[1991Nis]	Diffusivity measurements	700-1100°C / Fe-Si with 1.03-7.10 mass% Si
[1993Sol]	Microscopic analysis	Fe rich alloys with 3.0-3.3 mass% C and 2.7-3.0 mass% Si (Impurity: up to 0.6 Mn, 0.1 0, 0.02 S, 0.1 Cr, 0.06 Mg)
[1994Prz]	Chemical analysis, equilibration method with control carburizing atmosphere	900°C / Fe alloys in (γFe) up to 1.53 mass% Si and 2 mass% C
[1994Wit]	Isoperibolic high temperature calorimeter	C-Fe-Si

DOI: 10.1007/978-3-540-74196-1_12

Table 2. Crystallographic Data of Solid Phases

Phase/Temperature Range [°C]	Pearson Symbol/Space Group/ Prototype	Lattice Parameters [pm]	Comments/References
(αδFe)	*cI*2	*a* = 286.65	
(αFe)	$Im\bar{3}m$		pure Fe at 20°C [Mas2, V-C2].
< 912	W		Dissolves up to 0.096 at.% C at 740°C [2006MSIT], dissolves up to 10 at.% Si at 500°C [Mas2].
(δFe)		*a* = 293.15	Ferrite at 1394°C
1538 - 1394			dissolves up to 0.40 at.% C at 1493°C [2006MSIT] dissolves up to 19.5 at.% Si at 1280°C [Mas2]
(γFe)	*cF*4	*a* = 364.67	at 915°C [Mas2, V-C2]
1394 - 912	$Fm\bar{3}m$		dissolves up to 9.06 at.% C at 1153°C [2006MSIT] dissolves up to 3.8 at.% Si at 1150°C [Mas2]
	Cu		austenite
(εFe)	*hP*2	*a* = 246.8	at 25°C, > 13 GPa [Mas2]
	$P6_3/mmc$	*c* = 396.0	
	Mg		
(Si)	*cF*8	*a* = 543.06	at 25°C [Mas2]
< 1414	$Fd\bar{3}m$		
	C (diamond)		
(C)gr	*hP*4	*a* = 246.12	at 25°C [Mas2]
< 4492	$P6_3/mmc$	*c* = 670.90	sublimation point at 3827°C
	C (graphite)		
(C)d	*cF*8	*a* = 356.69	at 25°C, 60 GPa [Mas2]
	$Fd\bar{3}m$		Stable at 1600°C, *p* > 6 GPa
	C (diamond)		
ε, FeSi	*cP*8	*a* = 451.7	at 300°C [V-C2, Mas2]
< 1410	$P2_13$		
	FeSi		
β, Fe_2Si	*cP*2	*a* = 282	66 at.% Si [Mas2, V-C2]
1212 - 1040	CsCl		
	or		
	*hP*6	*a* = 405.2	
	Fe_2Si	*c* = 508.55	
α_1, Fe_3Si	*cF*16		10 to 30 at.% Si [Mas2]
	$Fm\bar{3}m$		
	BiF_3		

(*continued*)

DOI: 10.1007/978-3-540-74196-1_12

Phase/Temperature Range [°C]	Pearson Symbol/Space Group/ Prototype	Lattice Parameters [pm]	Comments/References
α_2, Fe_3Si	*cP*2 $Fm\bar{3}m$ CsCl		10 to 22 at.% Si [Mas2]
η, Fe_5Si_3 1060 - 825	*hP*16 $P6_3/mcm$ Mn_5Si_3	a = 675.9 c = 472.0	38.4 at.% Si [V-C2, Mas2]
ζ_1, $FeSi_2$(h) 1220 - 937	*tP*3	a = 269.0 c = 513.4	69.5 to 73.5 at.% Si [Mas2, V-C2]
ζ_2, $FeSi_2$(r) < 982	*oC*48	a = 986.3 b = 779.1 c = 783.3	66.7 at.% Si [Mas2, V-C2]
Fe_2C	*oP*6 *Pnnm* Fe_2C	a = 470.4 b = 431.8 c = 283.0	metastable [V-C2]
ω, Fe_2C	*m** Mn_5C_2 or *hP** $P6_322$ or $P\bar{3}m1$	a = 1156 b = 456 c = 503 β = 98.3°	metastable lattice parameters [1966Dug]
θ, Fe_3C	*oP*16 *Pnma* Fe_3C	 a = 452.48 b = 508.96 c = 674.43	carbide phase cohenite [1997Miz] cementite, high pressure phase
Fe_4C	*cP*5 $P\bar{4}3m$ Fe_4C	a = 387.8	metastable [V-C2]
χ, Fe_5C_2	*mC*28 *C*2/*c* B_2Pd_5	a = 1156.2 b = 457.27 c = 505.95 β = 97.74°	metastable [V-C2]
Fe_7C_3	*hP*20 $P6_3mc$ Fe_3Th_7	a = 688.2 c = 454.0	metastable [V-C2] lattice parameters [1964Her]
Fe_7C_3 (HP)	*oP*40 *Pnma* Cr_7C_3	a = 454.0 b = 687.9 c = 1194.2	High pressure phase [V-C2]
SiC < 2824	*cF*8 $F\bar{4}3m$ ZnS	a = 435.8	[1996Gro]

(*continued*)

DOI: 10.1007/978-3-540-74196-1_12

Phase/Temperature Range [°C]	Pearson Symbol/Space Group/ Prototype	Lattice Parameters [pm]	Comments/References
* τ, Fe_6SiC	*h***	*a* = 1177.4 *c* = 1086.2	At the composition 87.7 mass% Fe (72.4 at.%), 8.9 mass% Si (14.7 at.%) and 3.4 mass% C (12.9 at.%) [1971Mal] *c/a* = 0.922
Fe_5SiC	*o*** *Cmc*2.1	*a* = 1004.3 *b* = 794.4 *c* = 746.9	$Fe_{70}Si_xC_{30-x}$ with $x < 14$ at.%, amorphous phase [2006Yel]
Fe_8Si_2C	*a***	*a* = 634.7 ± 0.4 *b* = 641.4 ± 0.8 *c* = 972 ± 1 α = 84.05 ± 0.04 β = 99.84 ± 0.04 γ = 119.98 ± 0.05	triclinic structure [1972Spi]
Fe_9SiC_2	*o***	*a* = 455 *b* = 424 *c* = 281.4	Fe-16C-7Si (at.%), thermal stability rises 625°C with increasing of Si to 10 at.% [1983Bas]

Table 3. Stable Invariant Equilibria

Reaction	*T* [°C]	Type	Phases	Composition (mass%)		
				C	Fe	Si
L + β,Fe_2Si ⇌ (αFe) + ε,FeSi	1197	U	L	0.1	80.40	19.50
			β,Fe_2Si	~ 0.00	~ 79.50	~ 20.50
			(αFe)	~ 0.00	~ 100.00	~ 0.00
			ε,FeSi	~ 0.00	~ 66.50	~ 33.50
L ⇌ (αFe) + (C)gr	1198	e_6	L	0.8	84.4	14.8
			(αFe)	~ 0.00	~ 100.00	~ 0.00
			(C)gr	~ 100.00	~ 0.00	~ 0.00
L ⇌ (αFe) + ε,FeSi + (C)gr	1182	E_1	L	0.15	80.65	19.20
			(αFe)	~ 0.00	~ 100.00	~ 0.00
			ε,FeSi	~ 0.00	~ 66.50	~ 33.50
			(C)gr	~ 100.00	~ 0.00	~ 0.00
L ⇌ (γFe) + (C)gr	1170	e_7	L	2.80	92.20	5.00
			(γFe)	~ 0.00	~ 100.00	~ 0.00
			(C)gr	~ 100.00	~ 0.00	~ 0.00
L ⇌ (αFe) + (γFe) + (C)gr	1156	E_2	L	1.90	89.40	8.70
			γFe	0.50	91.70	7.80
			αFe	0.08	89.52	10.40
			(C)gr	~ 100.00	~ 0.00	~ 0.00

DOI: 10.1007/978-3-540-74196-1_12

Table 4. Metastable Invariant Equilibria

Reaction	T [°C]	Type	Phases	Composition (mass%)		
				C	Fe	Si
L + (αFe) ⇌ (γFe) + τ	1155	U	L	2.00	89.80	8.20
			(γFe)	0.50	91.00	8.50
			(αFe)	0.30	88.70	11.00
			τ	3.40	87.70	8.90
L ⇌ τ + (γFe) + Fe_3C	1030	E	L	3.90	90.80	5.30
			(γFe)	1.40	94.40	4.20
			τ	3.40	87.70	8.90
			Fe_3C	6.69	93.31	0.00

Table 5. Investigations of the C-Fe-Si Materials Properties

Reference	Method/Experimental Technique	Type of Property
[1922Sch]	Electrical resistance measurements using a Kelvin bridge apparatus	Resistivity, Fe rich alloy with 2.30 mass% C and 1.2 mass% Si (Impurity: 0.29 mass% Mn, 0.156 mass% P, 0.048 mass% S)
[1923Hon], [1924Hon]	Magnetometric method	Magnetization-temperature curves, Fe rich alloys with 0.47 to 27.8 mass% Si and 0.172 to 3.66 mass% C
[1936Thy]	Flowability measurements	Bending strength, hardness, brittleness, corrosion; Fe alloys with up to 20 mass% Si and 6 mass% C
[1941Boy]	Emf measurements, microscopic analysis	Tensile strength, hardness; Fe-2.19Si-2.93C and Fe-2.34Si-3.03 C (mass%)
[1968Hof]	Mechanical and magnetic measurements	Tensile strength, elongation at fracture, reduction of area, modulus of elasticity, coercive force; Fe rich alloys with 0.002 to 0.011 mass% C and up to 5.1 Si mass%
[1976Mar]	Resistance measurements, electron and diffraction microscopy	Hyperfine structure; $Fe_{70}Si_{30}$, $Fe_{65}Si_{35}$
[1976Ono]	Electrodeless, rotating magnetic field method	Electric resistivity; Fe rich alloys with 1 or 3 mass% C and 2, 5, 10 mass% Si
[1981Yos]	Unidirectional solidification measurements	Electrical resistance; Fe-1.72Si-3.91C and Fe-1.77Si-3.75C
[1983Bas]	Resistivity measurements	Resistivity; Fe-16C with 3-10 at.% Si (Fe-1.7Si-4C and Fe-6.10Si-4.17C in mass%)

(*continued*)

DOI: 10.1007/978-3-540-74196-1_12

Reference	Method/Experimental Technique	Type of Property
[1987Ino]	Vickers microhardness tester, Instron-type tensile testing machine, magnetic balance, B-H tracer, impedance analyzer	Hardness, tensile fracture strength, magnetization, Curie temperature, coercive field, permeability; annealed and quenched C-Fe-Si melts
[1989Mur]	Vickers microhardness measurements	Vickers microhardness; Spray powder alloy of Fe-0.85Si-2.20C (mass%) and Fe-0.87Si-4.16C (mass%); water-cooled substrates tempered at 300, 400 and 500°C
[1990Yeo]	Extrusion process, mechanical measurement	Hardness and tensile strength / Fe-3.6% C-Si alloy powders
[1991Kim]	Tensile and deformation tests	Tensile properties; Fe-1.5Si-0.2C (mass%) annealed 8 min at 790°C and isothermally transformed at 320-480°C for various time
[1993Sai]	Electrical resistivity measurements	Electrical resistivity; –196°C; Fe-0.38Si-0.269C (at.%) (Fe-0.19Si-0.1251 C in mass%)
[1996Kon]	Mössbauer (MS), X-ray photoelectron (XPS) and Auger (AS) spectroscopy, X-ray diffraction and magnetic measurements	Curie temperature, Magnetic field / Amorphous $Fe_{70}Si_{12}C_{18}$ obtained from milling of the $Fe_{85}Si_{15}$ powder with liquid hydrocarbon (toluene)
[2001Kag]	Piston-cylinder type high pressure apparatus	Yield strength
[2001The]	Magnetometer apparatus	Magnetization property and Curie point temperature; doped p-SiC samples (2000 Å depth) with 5 at.% (12.8 mass%) Fe maintained at 350°C in order to avoid amorphization and annealed at 700°C
[2001Ume]	X-ray diffraction, SEM, TEM, DSC, SPS	Vickers hardness, Young's modulus; Fe_3C
[2003Oga]	X-ray diffraction and differential scanning calorimetry	Curie point temperature; $Fe_x(Si,C)_{100-x}$ (x = 65-85 at.% or x = 83.8-94.04 mass%)
[2004Fu]	Tensile tests	Yield and tensile strengths, Young's modulus; Fe-0.8mass%C with 1 or 2 mass% Si
[2004Sai]	Inverted torsion pendulum technique, infrared analysis of C using a high frequency combustion technique	Internal friction; cold rolled C-Fe-Si samples with small amount of Si (0.050 to 0.832 mass%) and C (0.45 to 0.47 mass%) and decaburization annealing at 700°C
[2005Liu]	DMA method and Young's modulus measurements	Damping capacity and Young's modulus from annealed samples (2 h at 600°C) slowly cooled to room temperature; measurement between –150 and 100°C at 5°C·min^{-1}

(*continued*)

DOI: 10.1007/978-3-540-74196-1_12

Reference	Method/Experimental Technique	Type of Property
[2005Tek]	Hardness and tensile measurements	Vickers hardness on annealed steel Fe-0.4mass%C-0.25mass%Si between 350 and 650°C for 1 h; yield strength and ultimate tensile strength up to 700°C from quenched and annealed (1 h at 500°C) samples
[2006Yel]	AC magnetic susceptibility device, Mössbauer spectrometer, mechanochemical alloying, X-ray diffraction, Auger Electron Spectroscopy	Magnetic properties: coercivity, specific saturation magnetization, average magnetic moment of Fe per atom and Curie temperature / $Fe_{70}Si_xC_{30-x}$ (x in at.%) on mechanical amorphous alloys and annealed ones (1 h at 500°C)

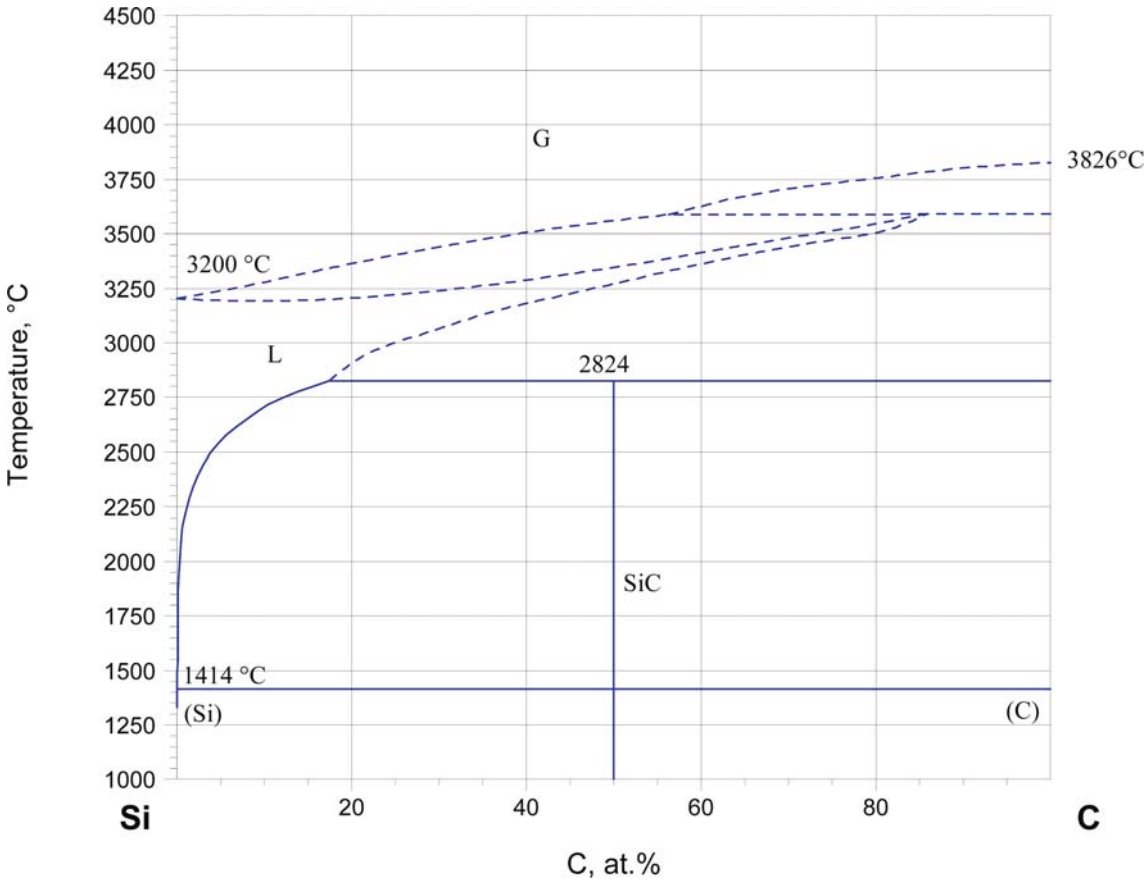

Fig. 1. C-Fe-Si. Phase diagram of C-Si system

DOI: 10.1007/978-3-540-74196-1_12

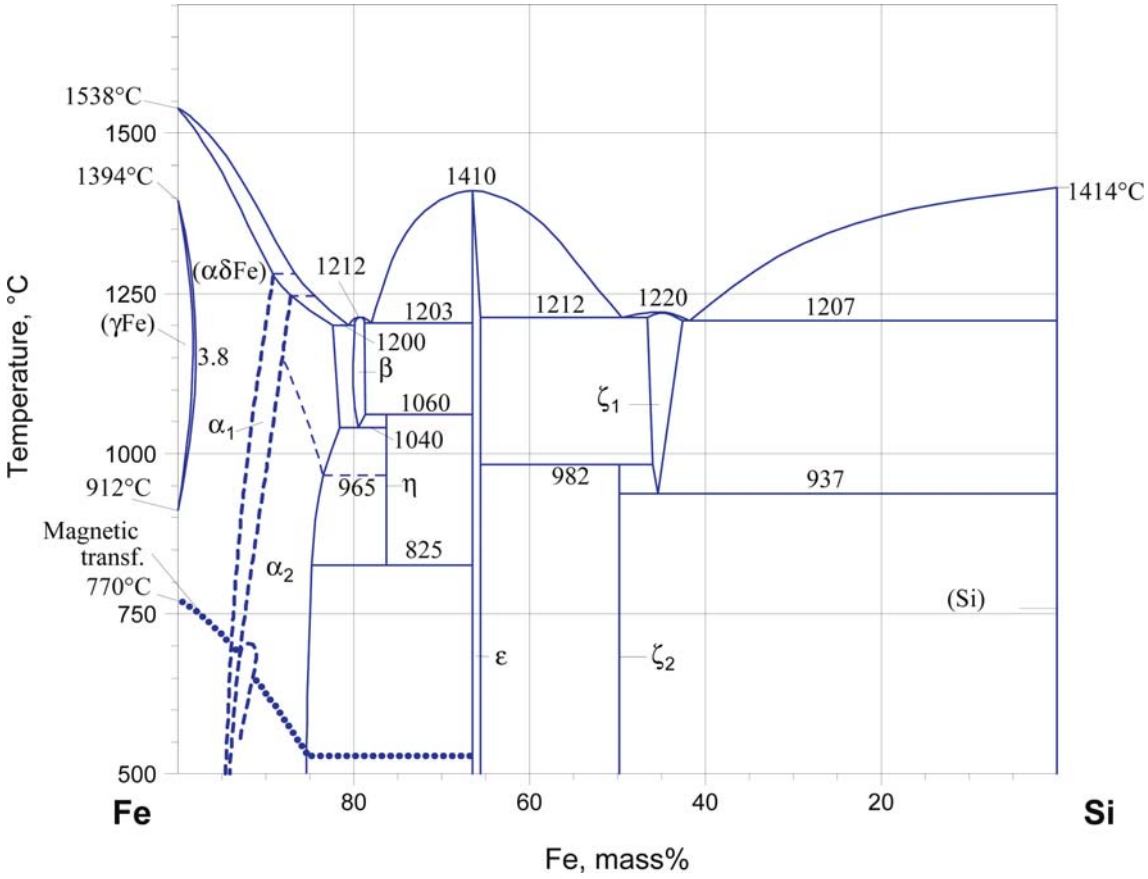

Fig. 2. C-Fe-Si. Phase diagram of the Fe-Si system

DOI: 10.1007/978-3-540-74196-1_12

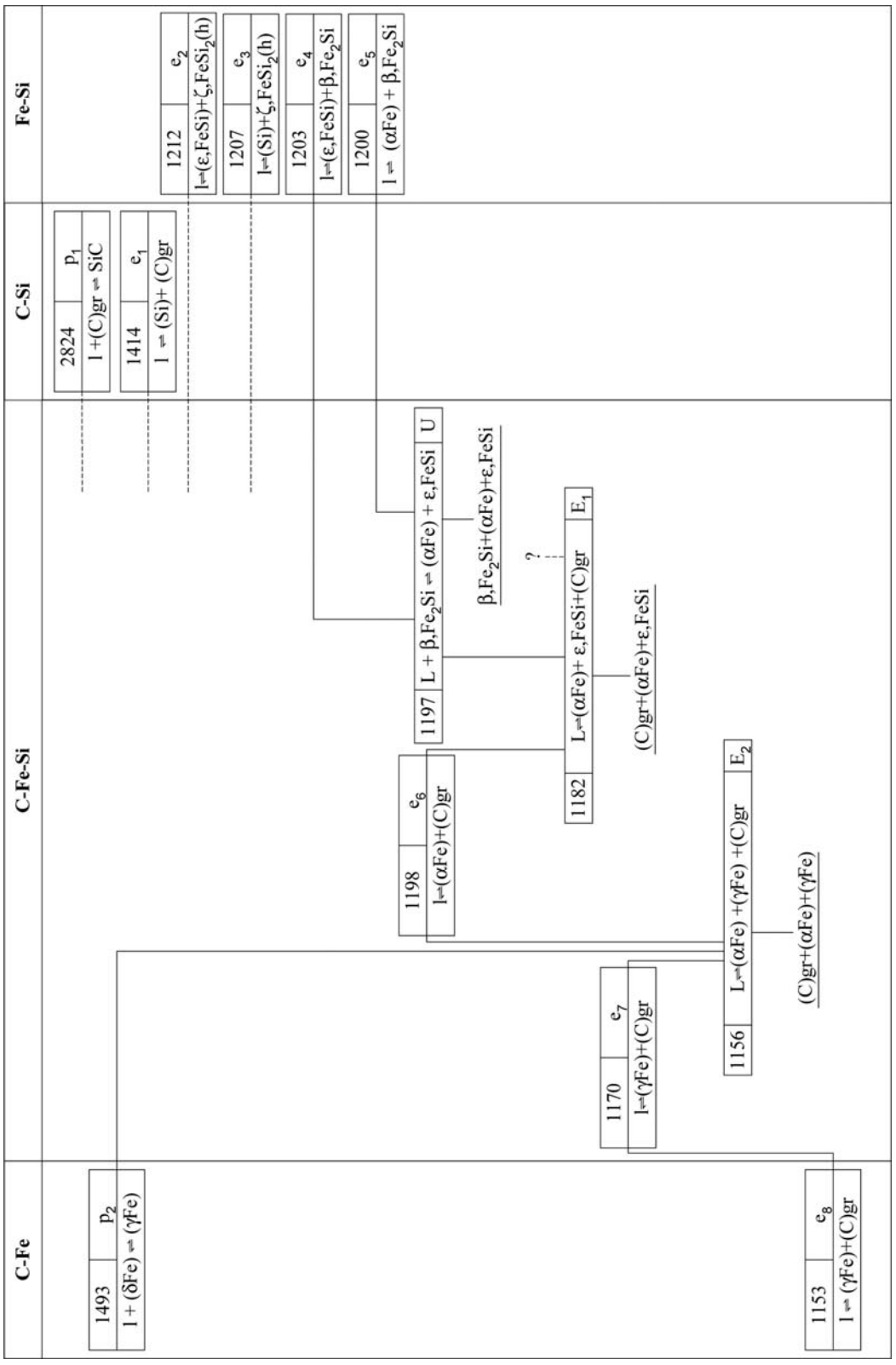

Fig. 3. C-Fe-Si. Reaction scheme of the stable invariant equilibria

DOI: 10.1007/978-3-540-74196-1_12

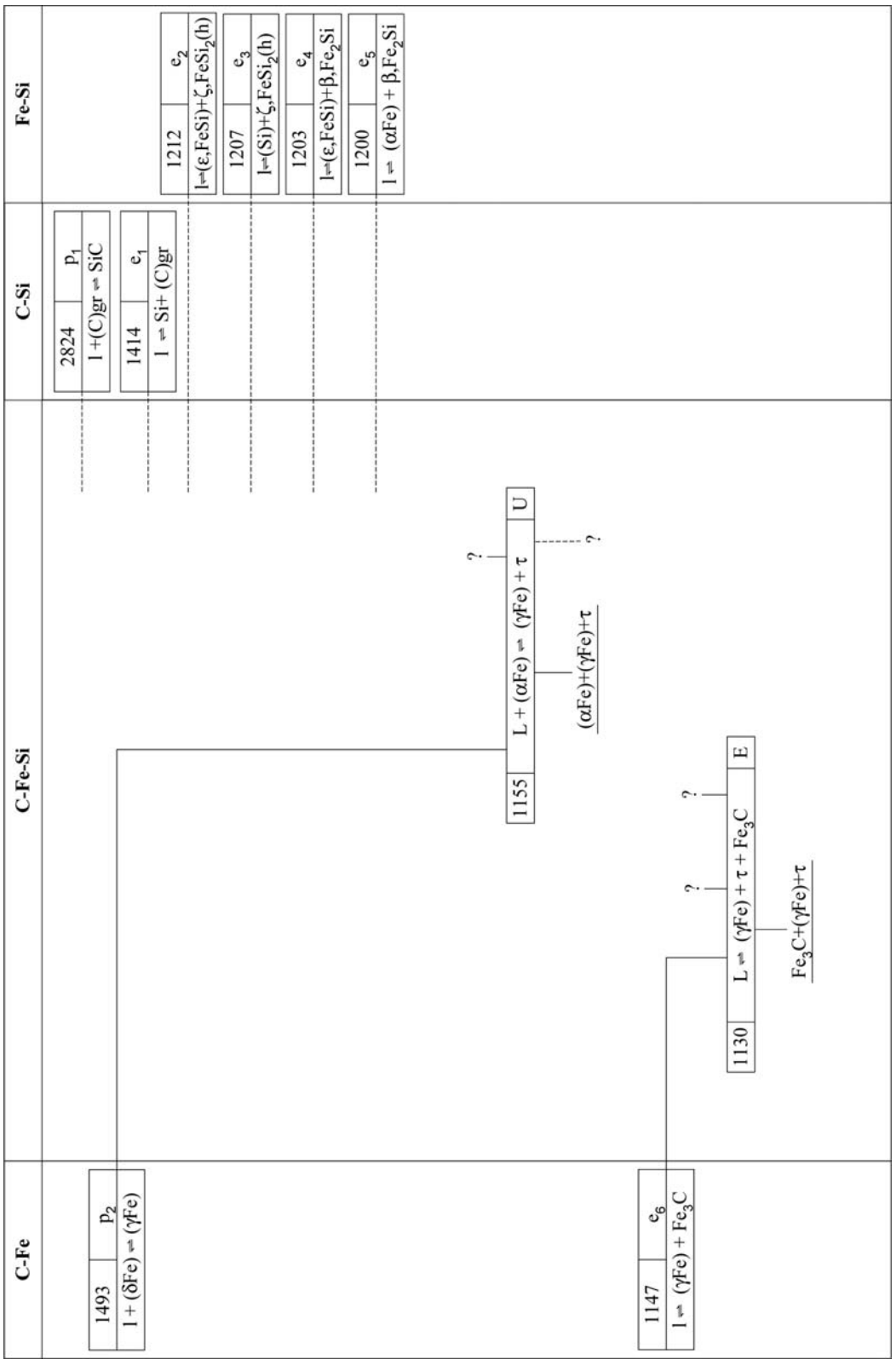

Fig. 4. C-Fe-Si. Reaction scheme of the metastable invariant equilibria

DOI: 10.1007/978-3-540-74196-1_12

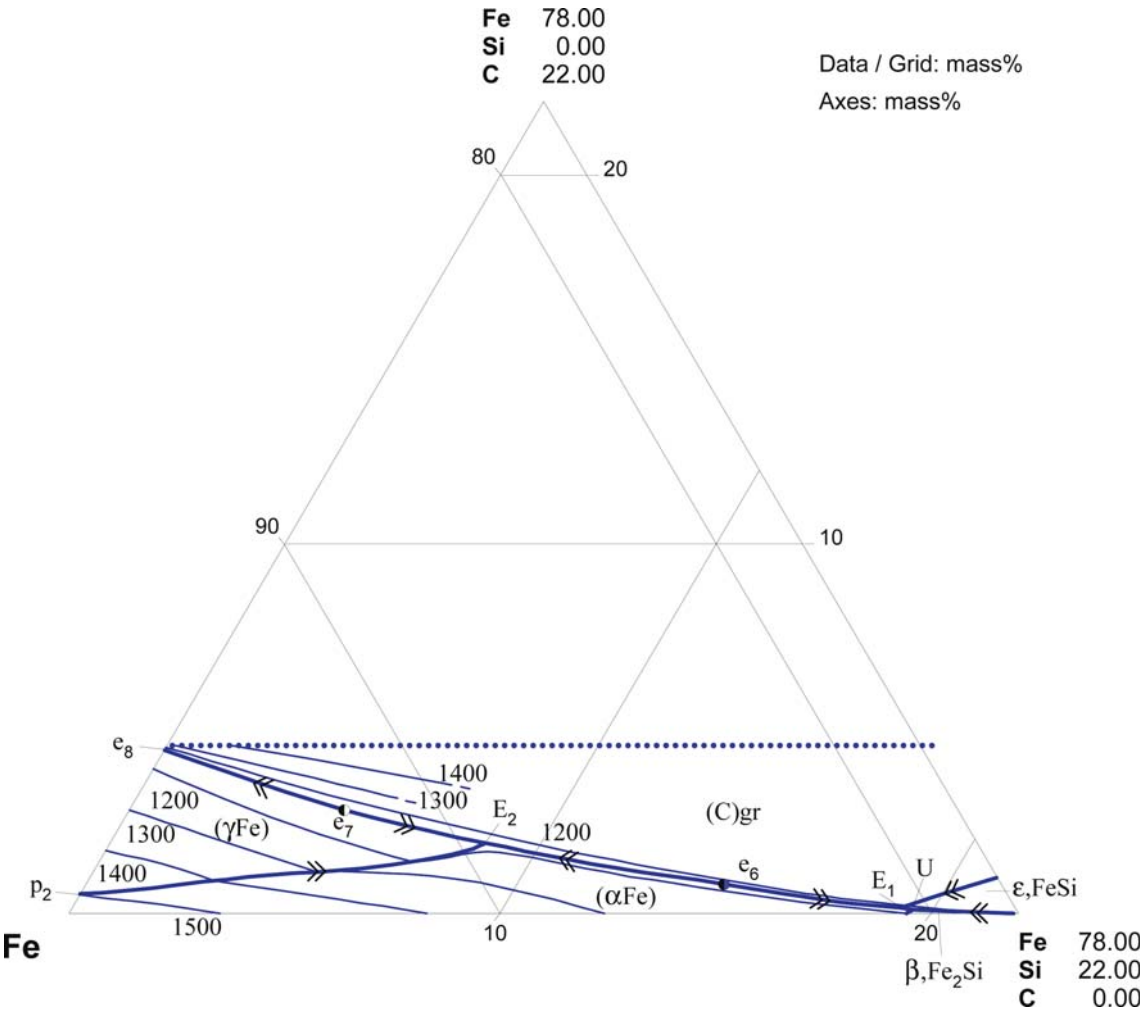

Fig. 5. C-Fe-Si. Stable liquidus surface

DOI: 10.1007/978-3-540-74196-1_12

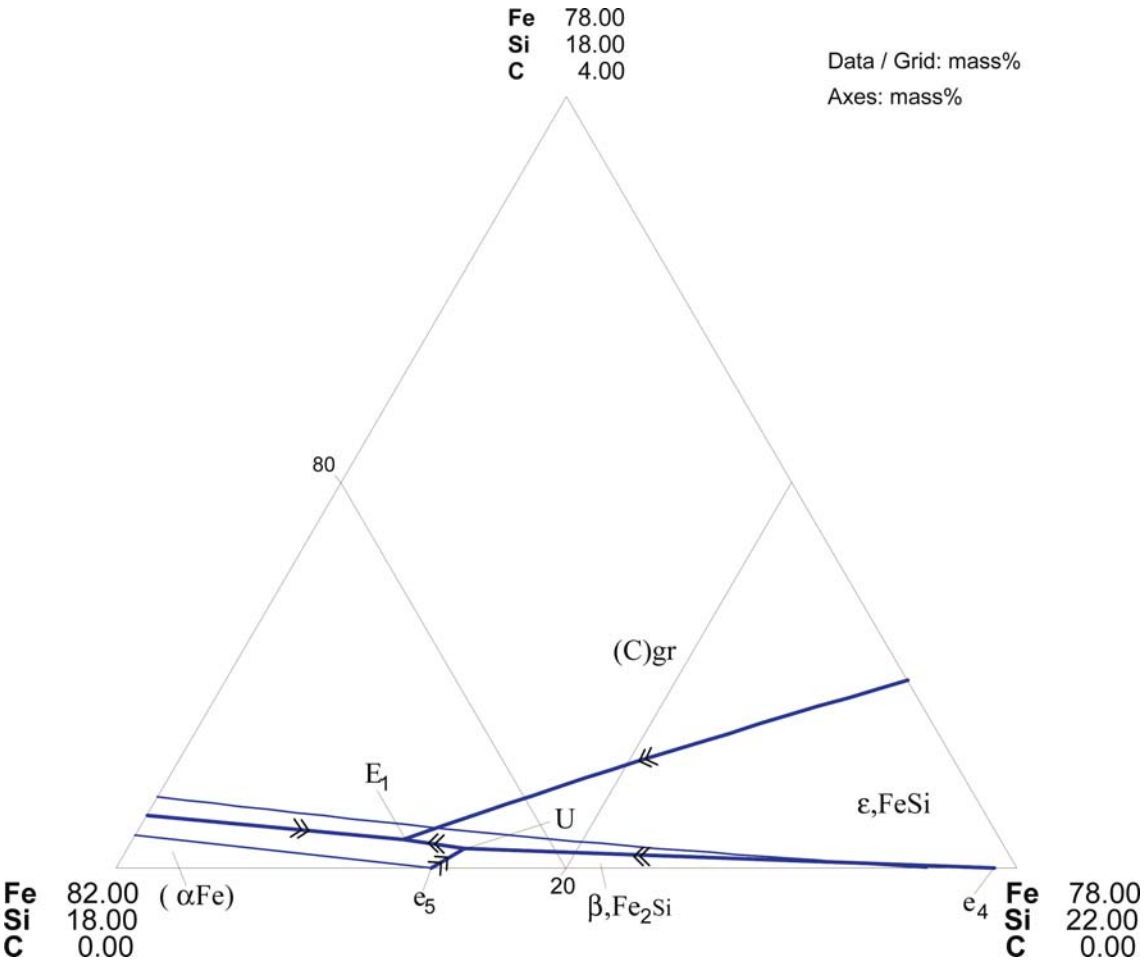

Fig. 5a. C-Fe-Si. Stable liquidus surface

DOI: 10.1007/978-3-540-74196-1_12

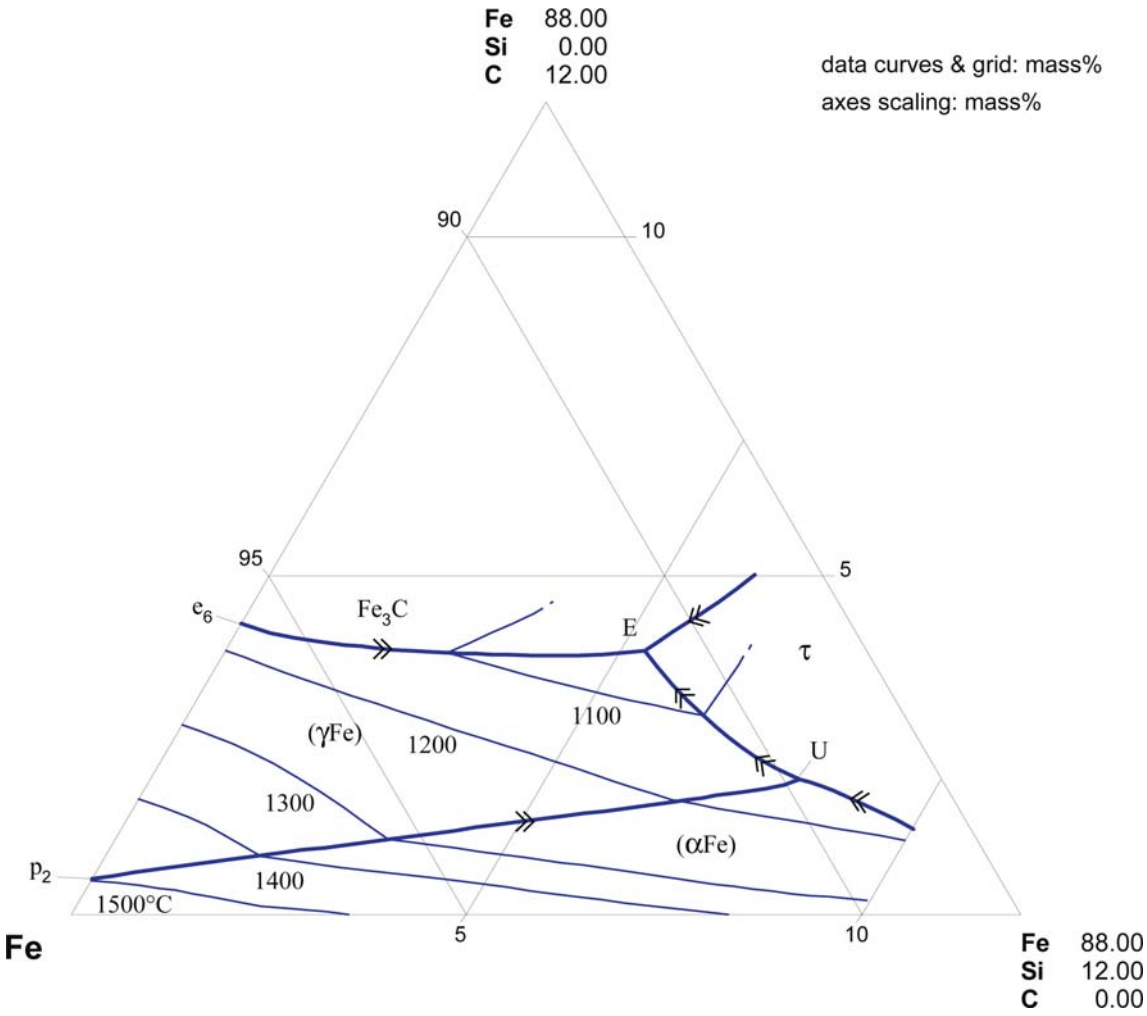

Fig. 6. C-Fe-Si. Metastable liquidus surface

DOI: 10.1007/978-3-540-74196-1_12

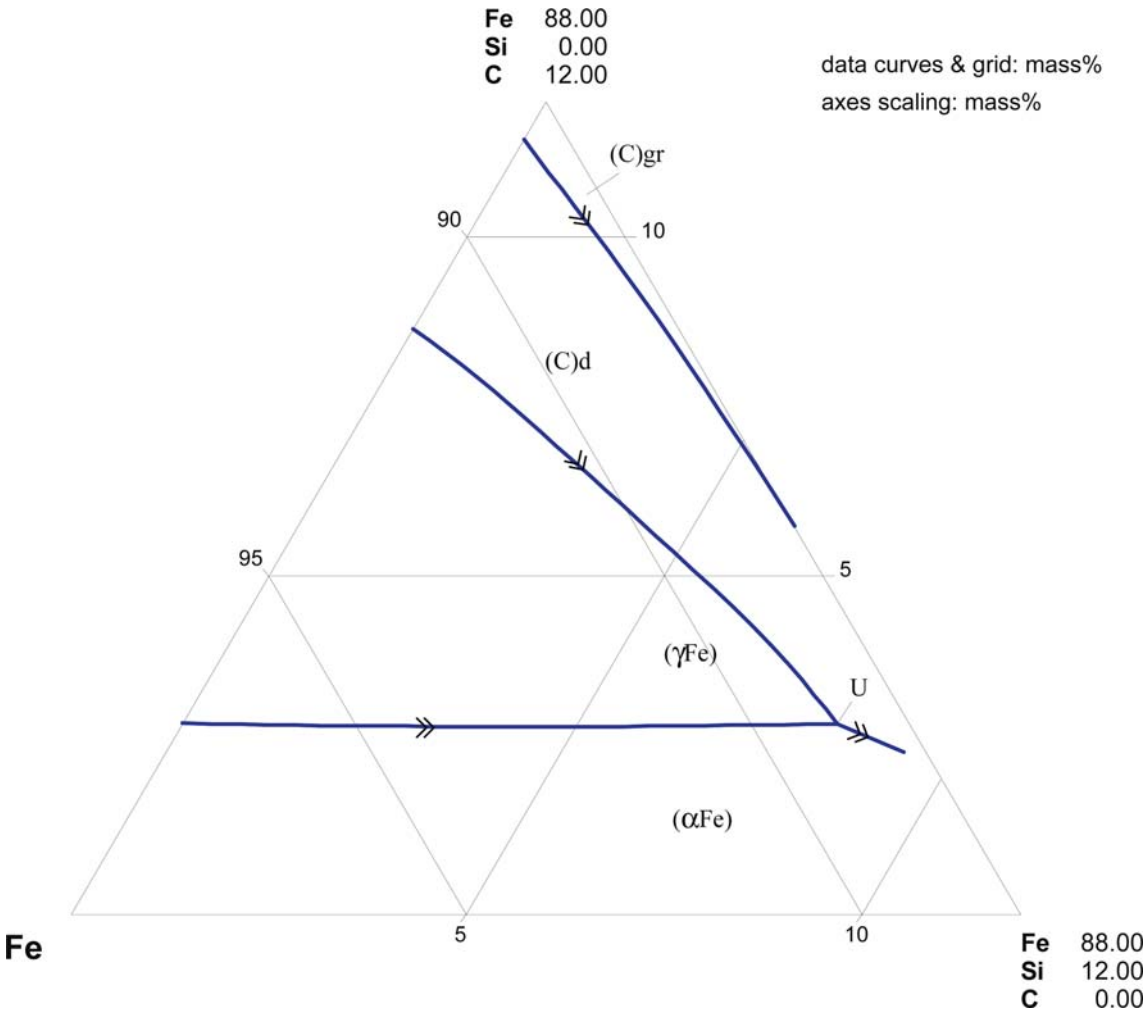

Fig. 7. C-Fe-Si. Partial stable liquidus surface at 8 GPa

DOI: 10.1007/978-3-540-74196-1_12

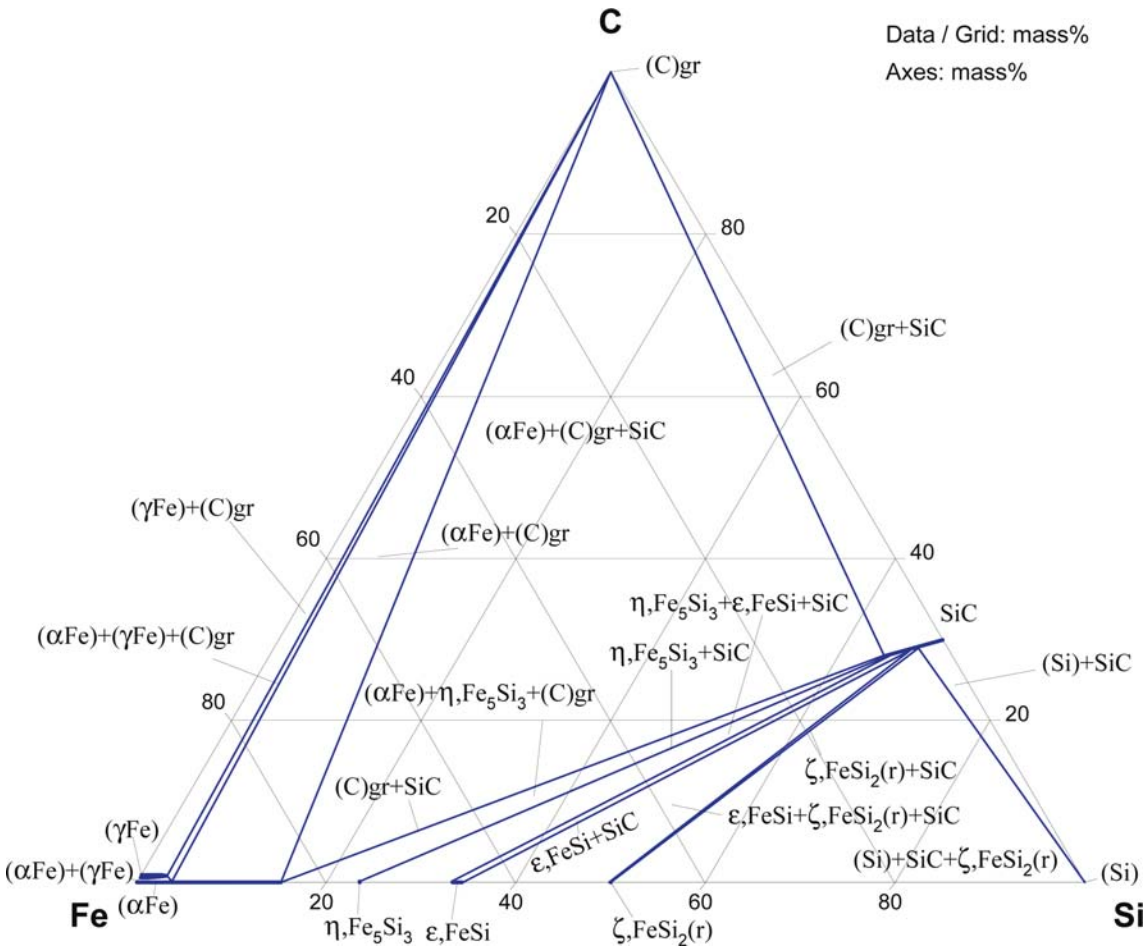

Fig. 8. C-Fe-Si. Calculated stable isothermal section at 850°C

DOI: 10.1007/978-3-540-74196-1_12

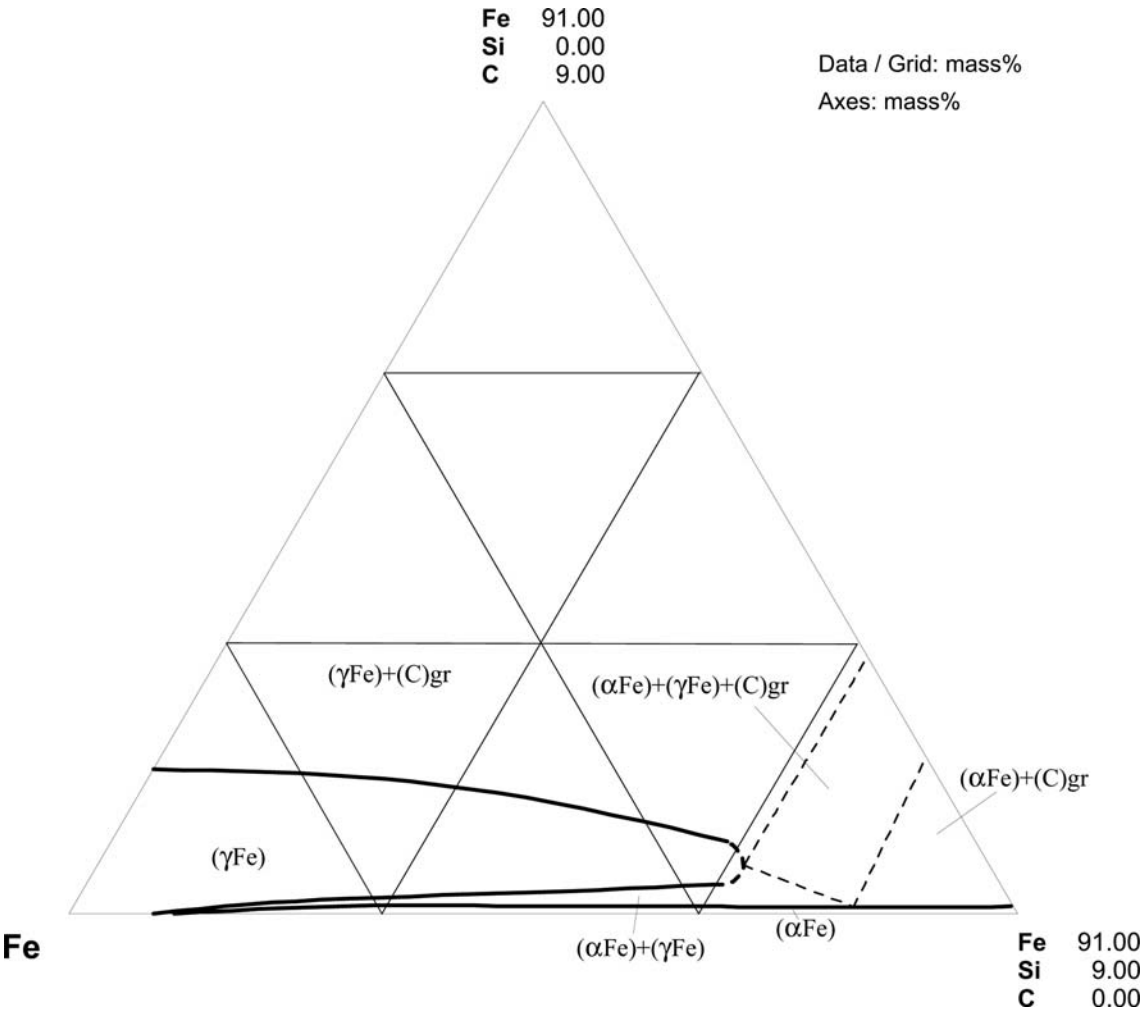

Fig. 9. C-Fe-Si. Stable isothermal section at 1000°C

DOI: 10.1007/978-3-540-74196-1_12

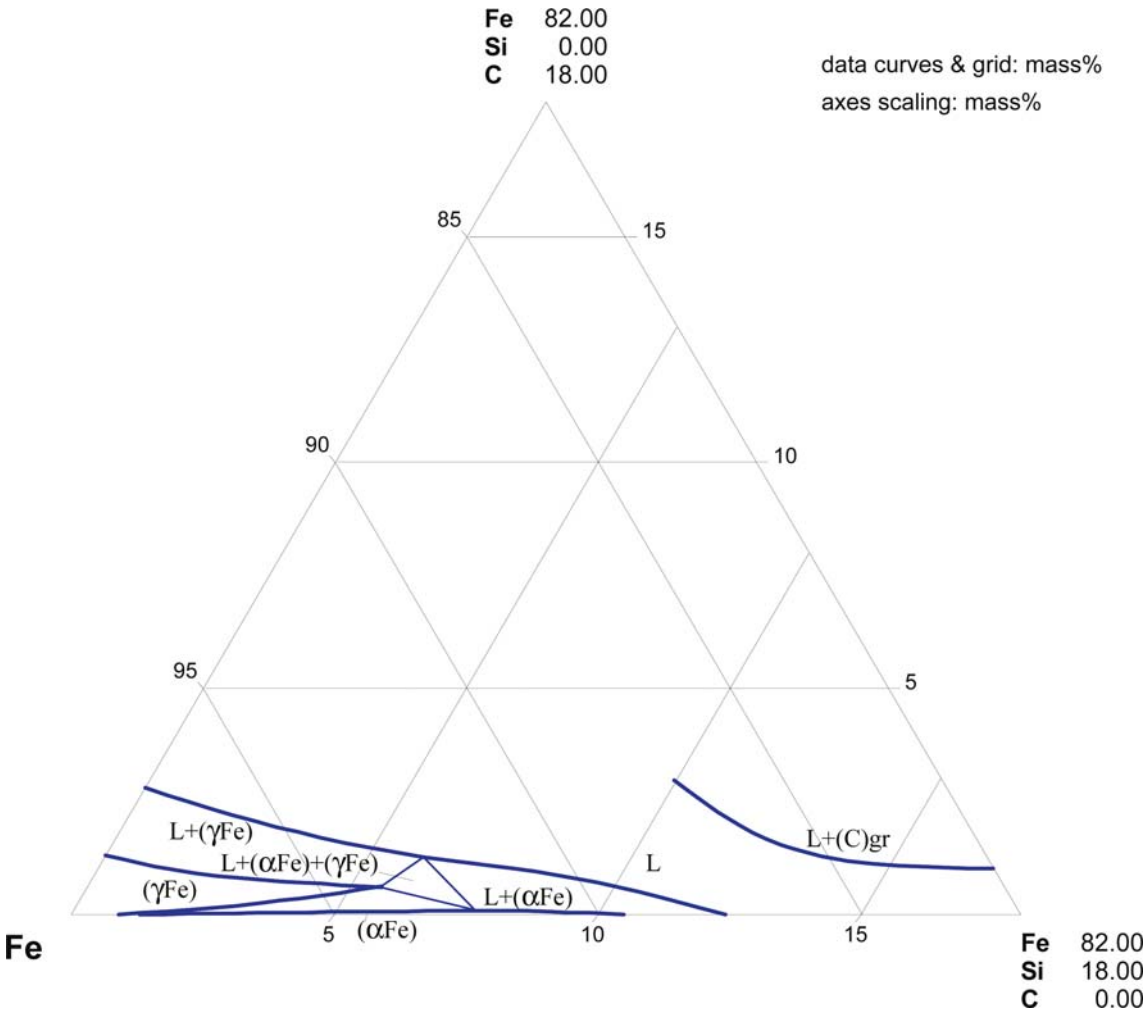

Fig. 10. C-Fe-Si. Stable isothermal section at 1300°C

DOI: 10.1007/978-3-540-74196-1_12

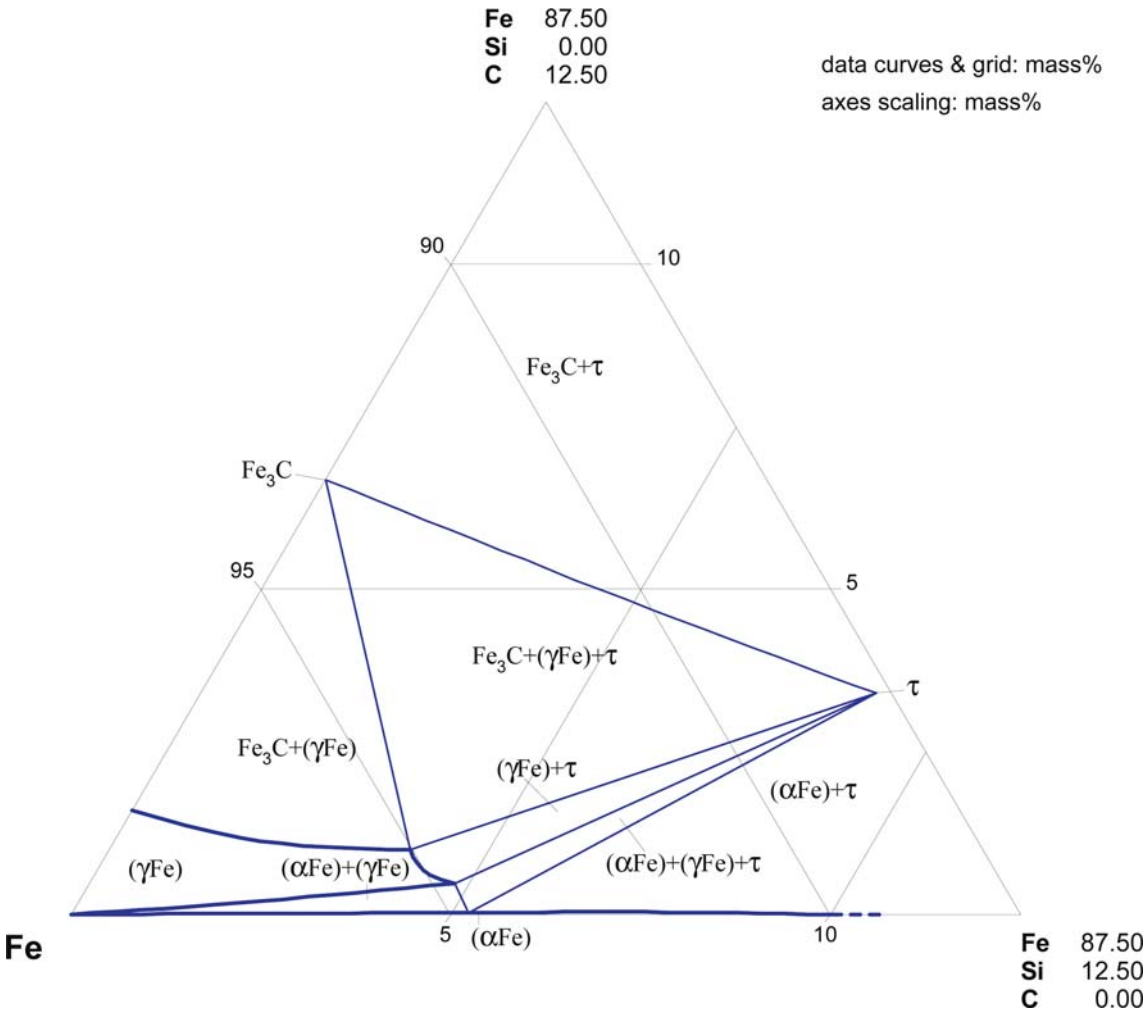

Fig. 11. C-Fe-Si. Metastable isothermal section at 900°C

DOI: 10.1007/978-3-540-74196-1_12

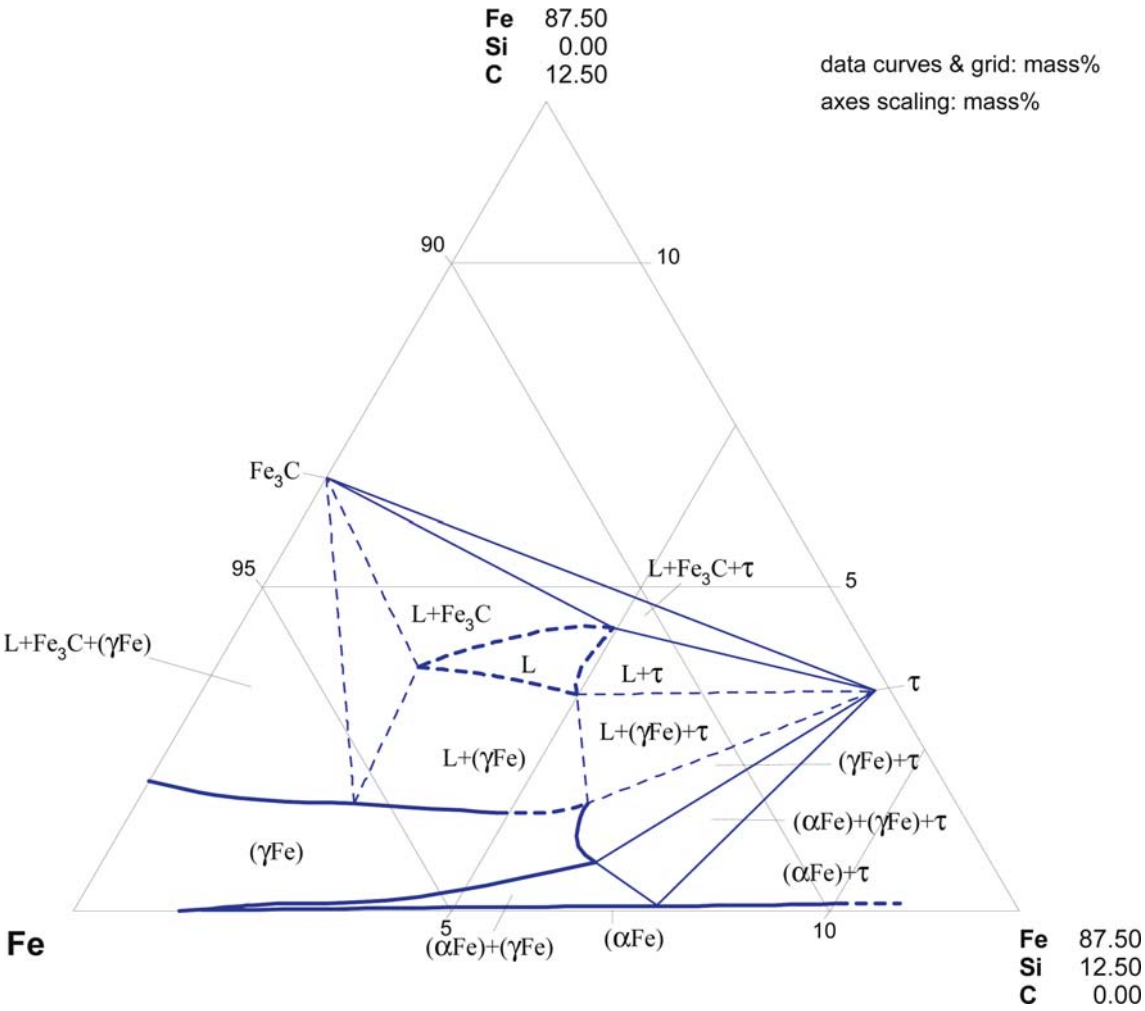

Fig. 12. C-Fe-Si. Metastable isothermal section at 1100°C

DOI: 10.1007/978-3-540-74196-1_12

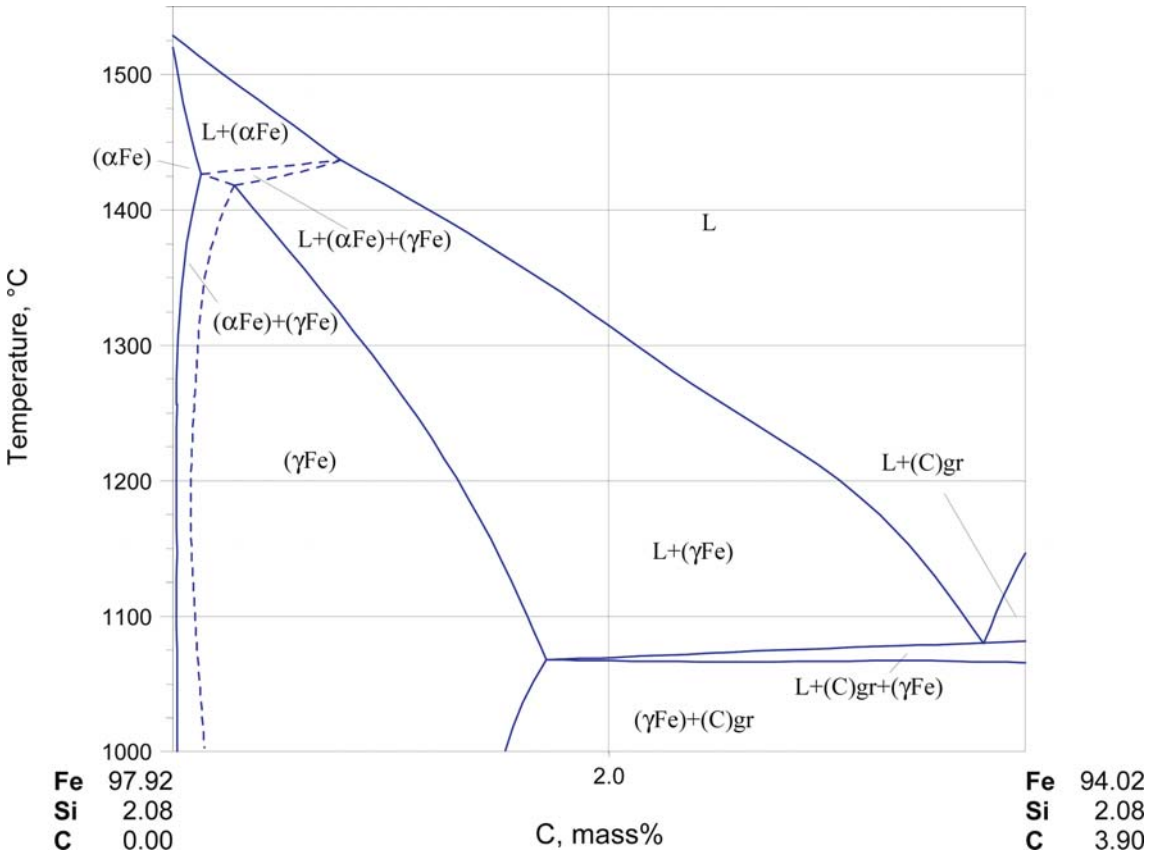

Fig. 13. C-Fe-Si. Stable vertical section at 2.08 mass% Si

DOI: 10.1007/978-3-540-74196-1_12

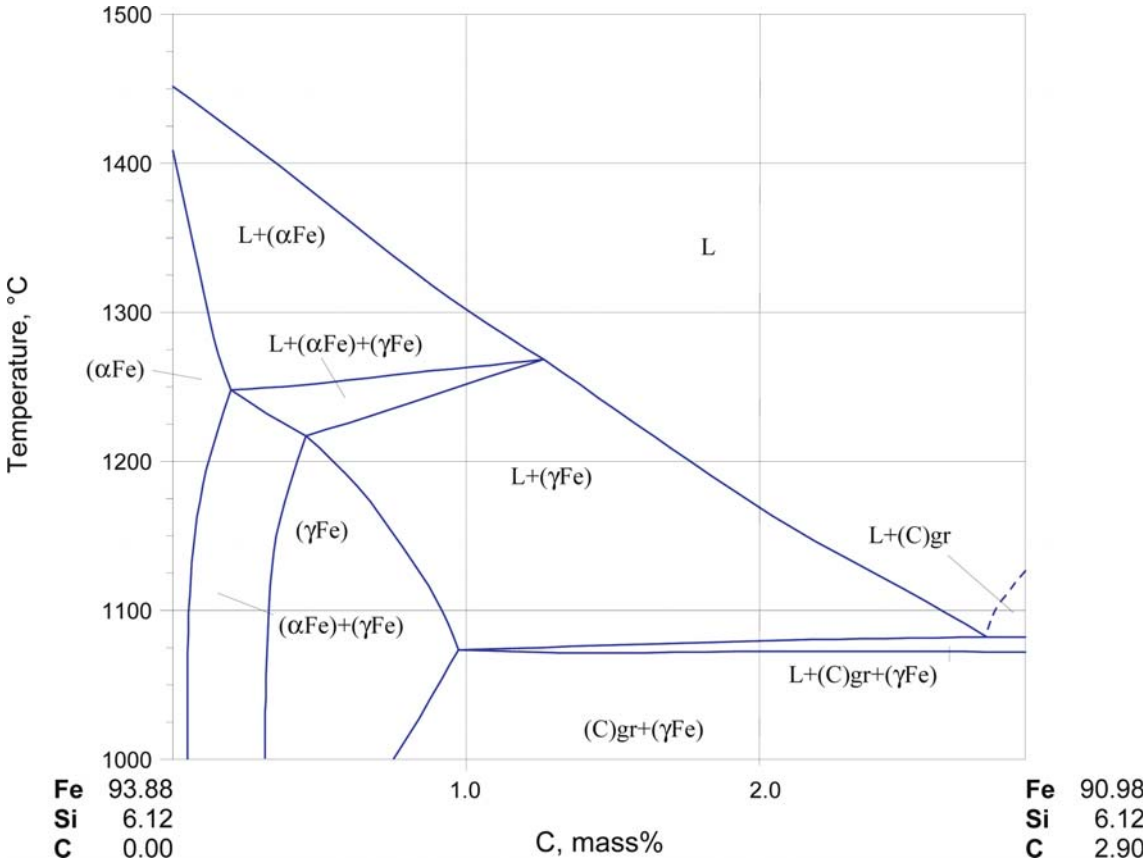

Fig. 14. C-Fe-Si. Stable vertical section at 6.12 mass% Si

DOI: 10.1007/978-3-540-74196-1_12

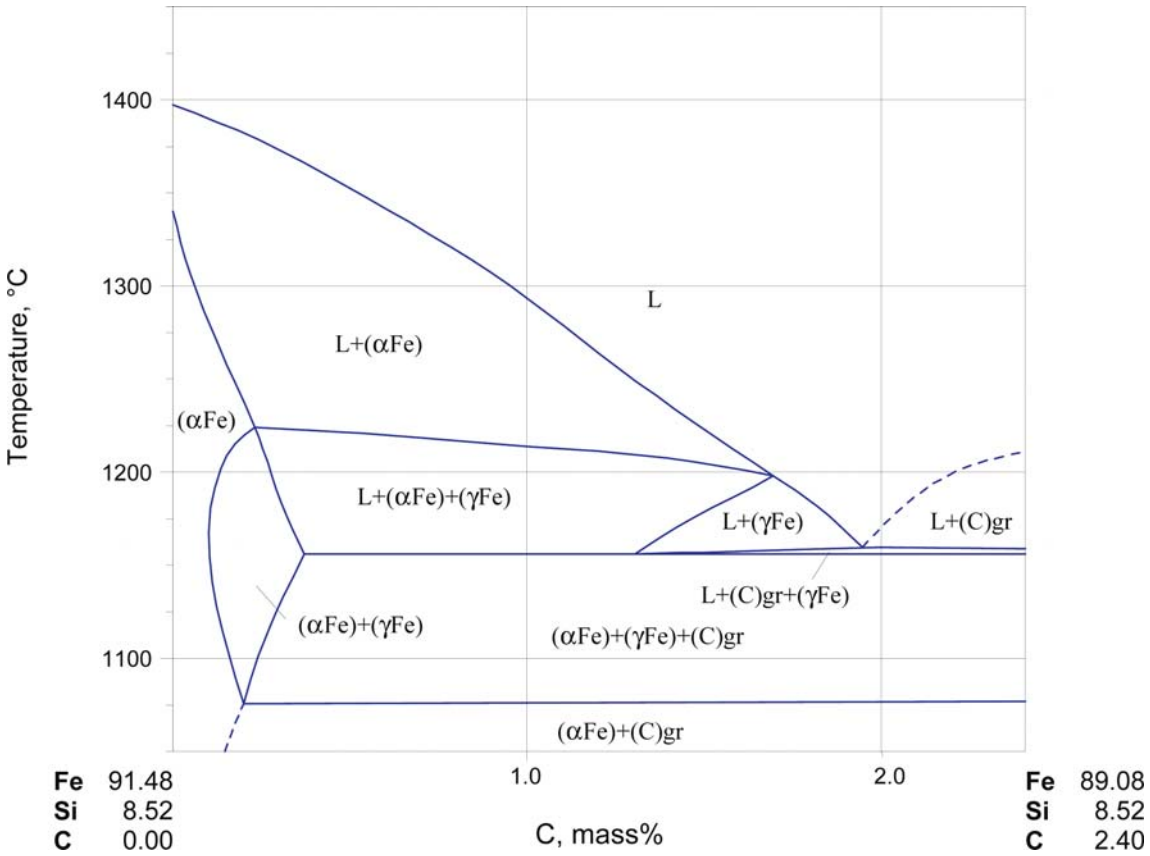

Fig. 15. C-Fe-Si. Stable vertical section at 8.52 mass% Si

DOI: 10.1007/978-3-540-74196-1_12

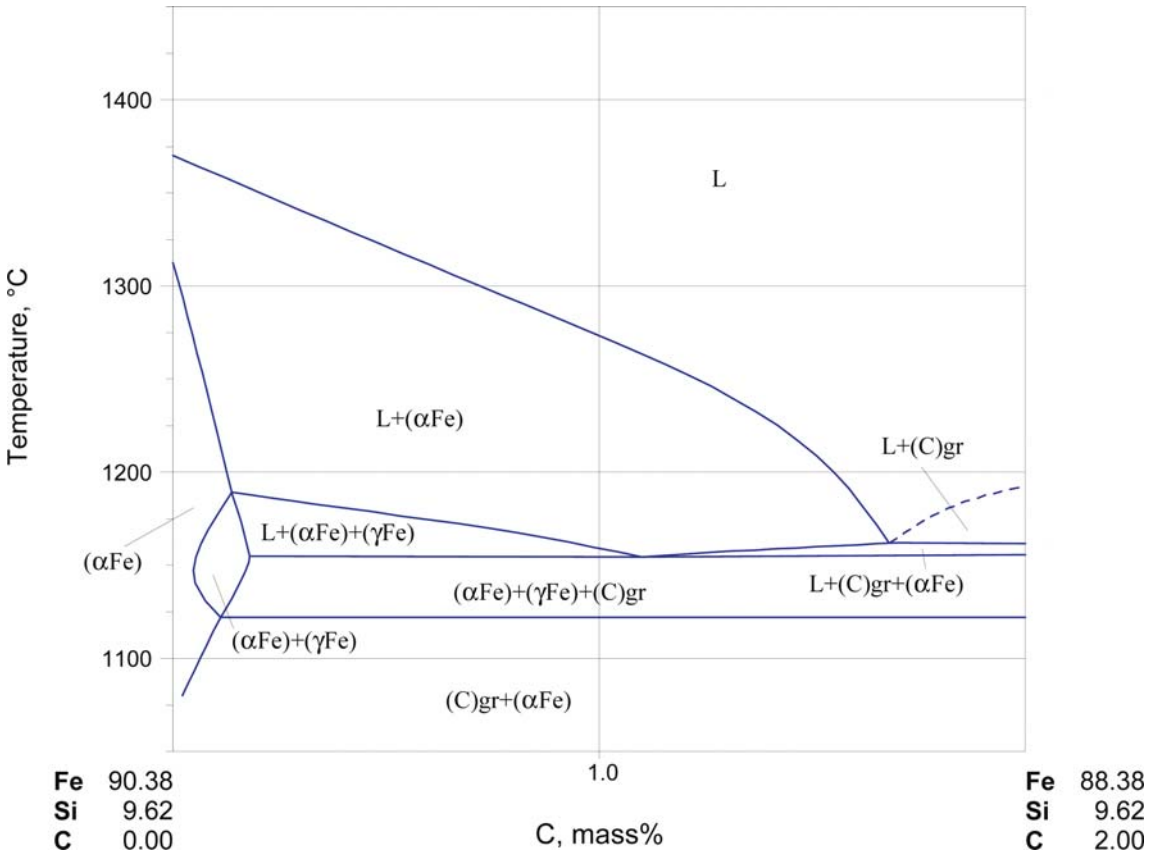

Fig. 16. C-Fe-Si. Stable vertical section at 9.62 mass% Si

DOI: 10.1007/978-3-540-74196-1_12

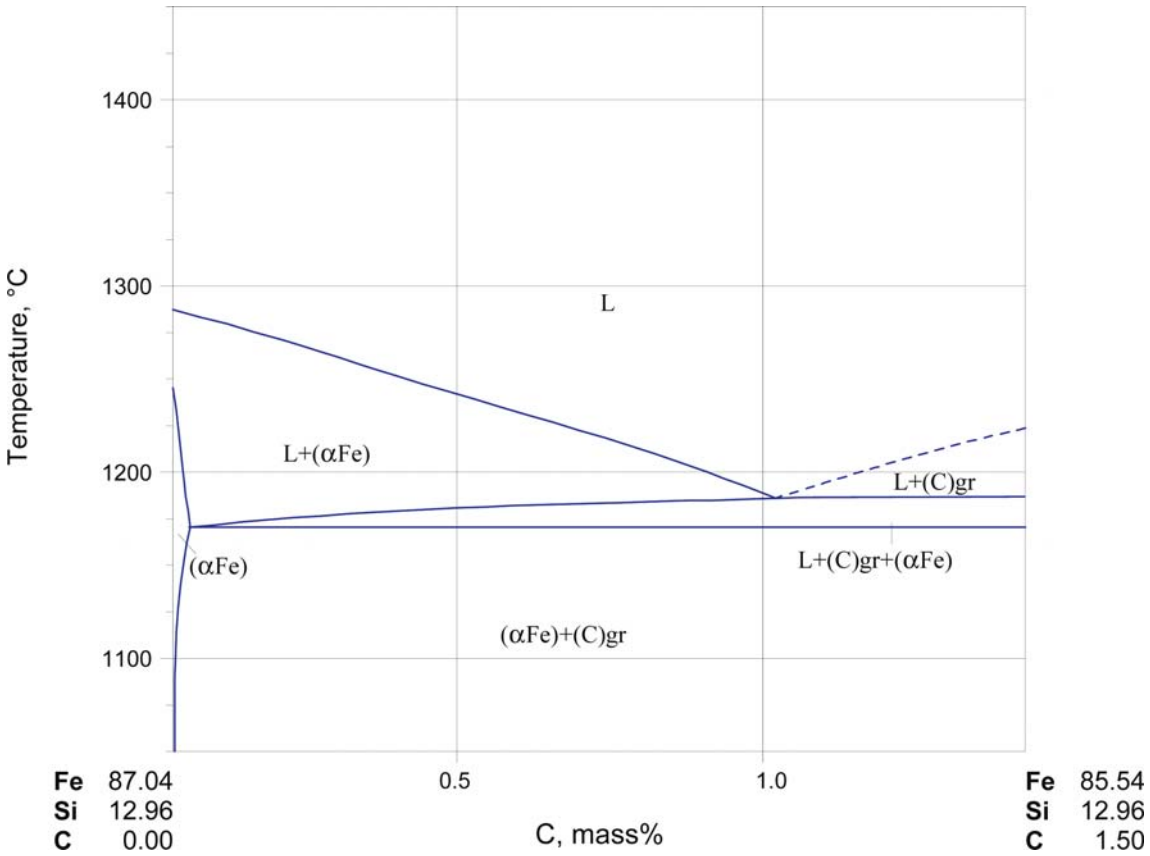

Fig. 17. C-Fe-Si. Stable vertical section at 12.96 mass% Si

DOI: 10.1007/978-3-540-74196-1_12

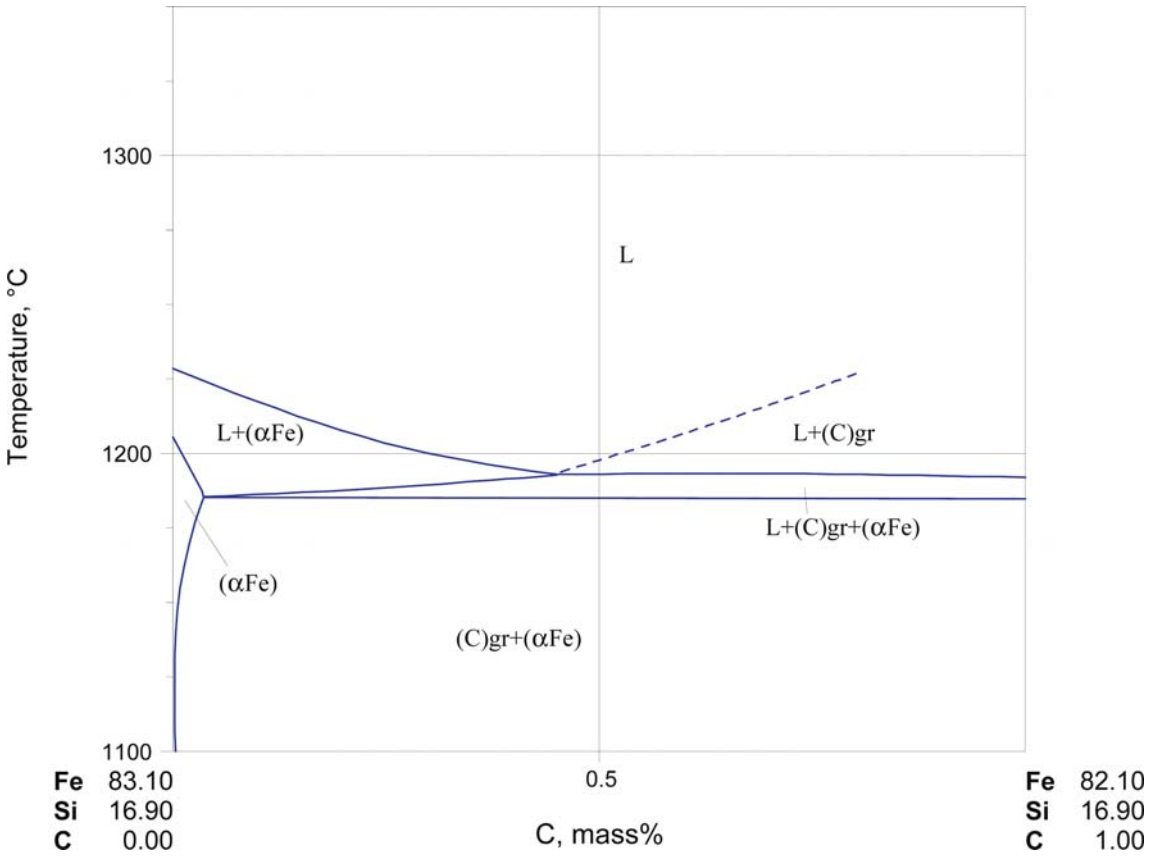

Fig. 18. C-Fe-Si. Stable vertical section at 16.9 mass% Si

DOI: 10.1007/978-3-540-74196-1_12

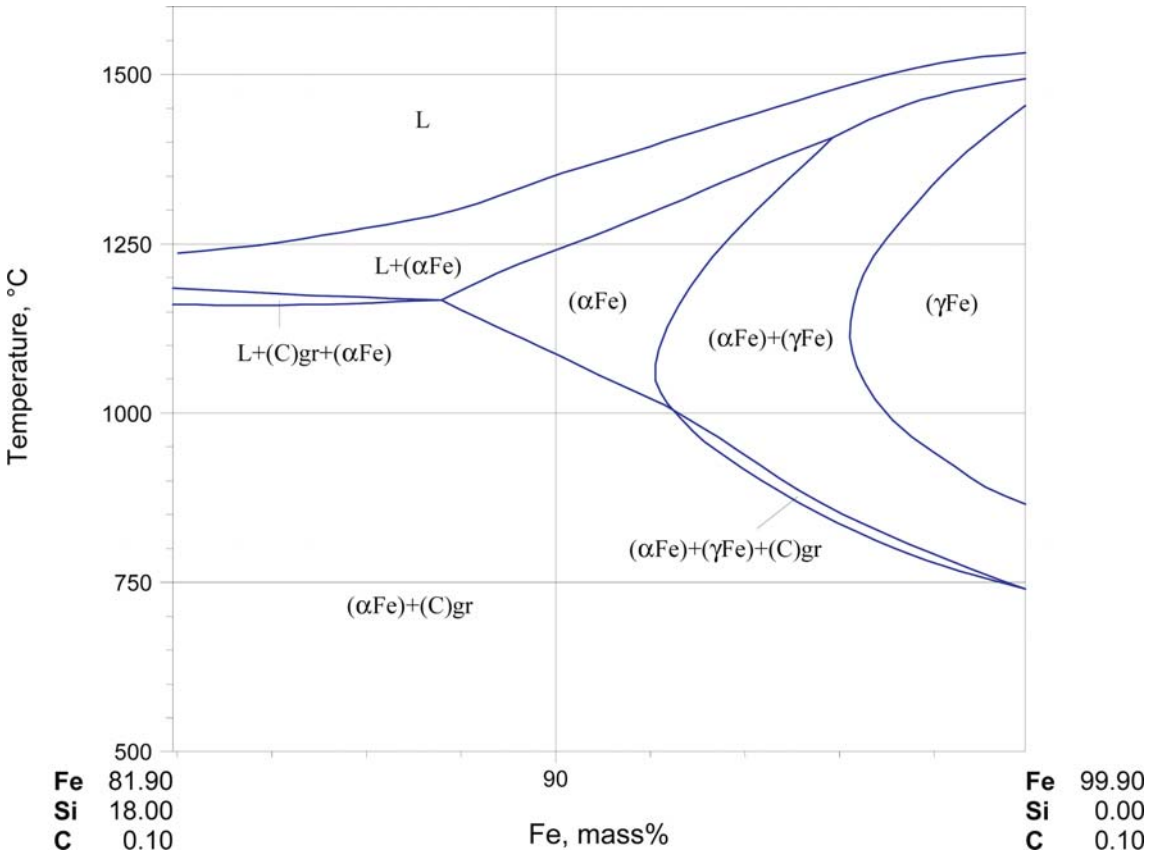

Fig. 19. C-Fe-Si. Stable vertical section at 0.1 mass% C

DOI: 10.1007/978-3-540-74196-1_12

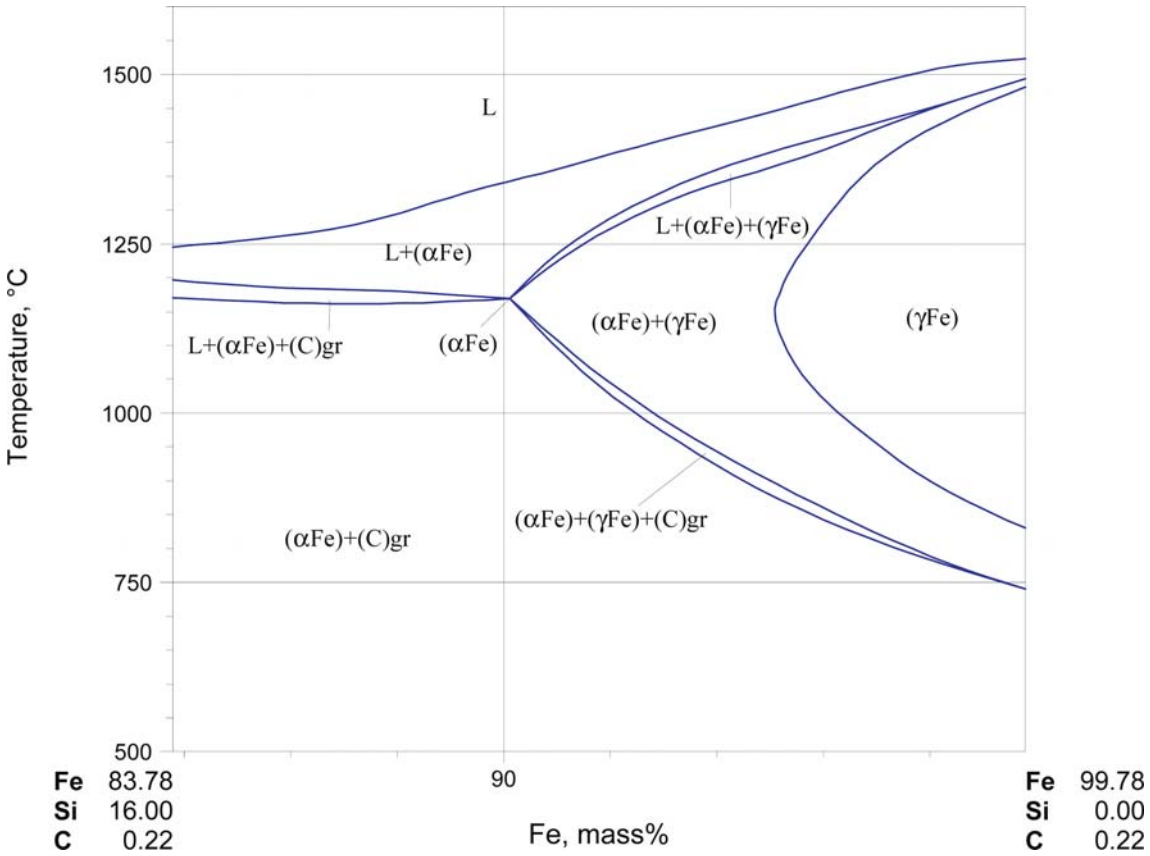

Fig. 20. C-Fe-Si. Stable vertical section at 0.22 mass% C

DOI: 10.1007/978-3-540-74196-1_12

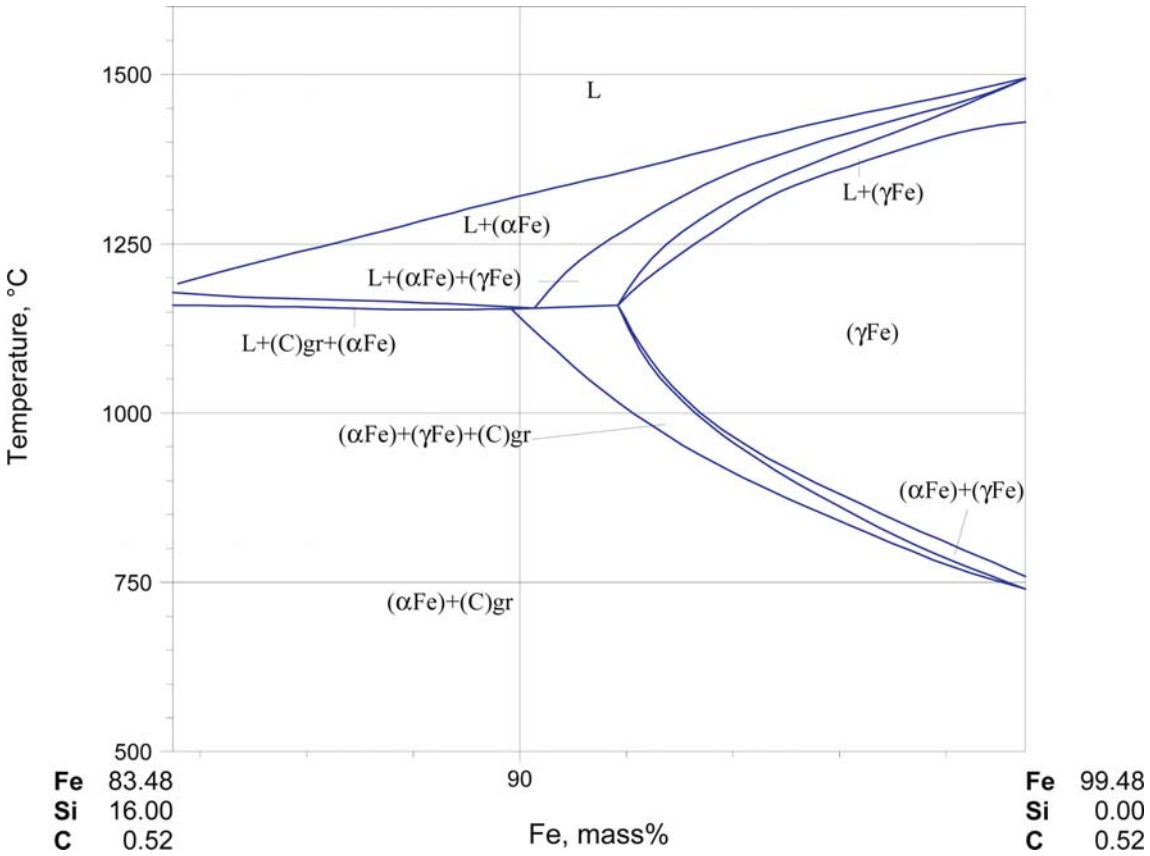

Fig. 21. C-Fe-Si. Stable vertical section at 0.52 mass% C

DOI: 10.1007/978-3-540-74196-1_12

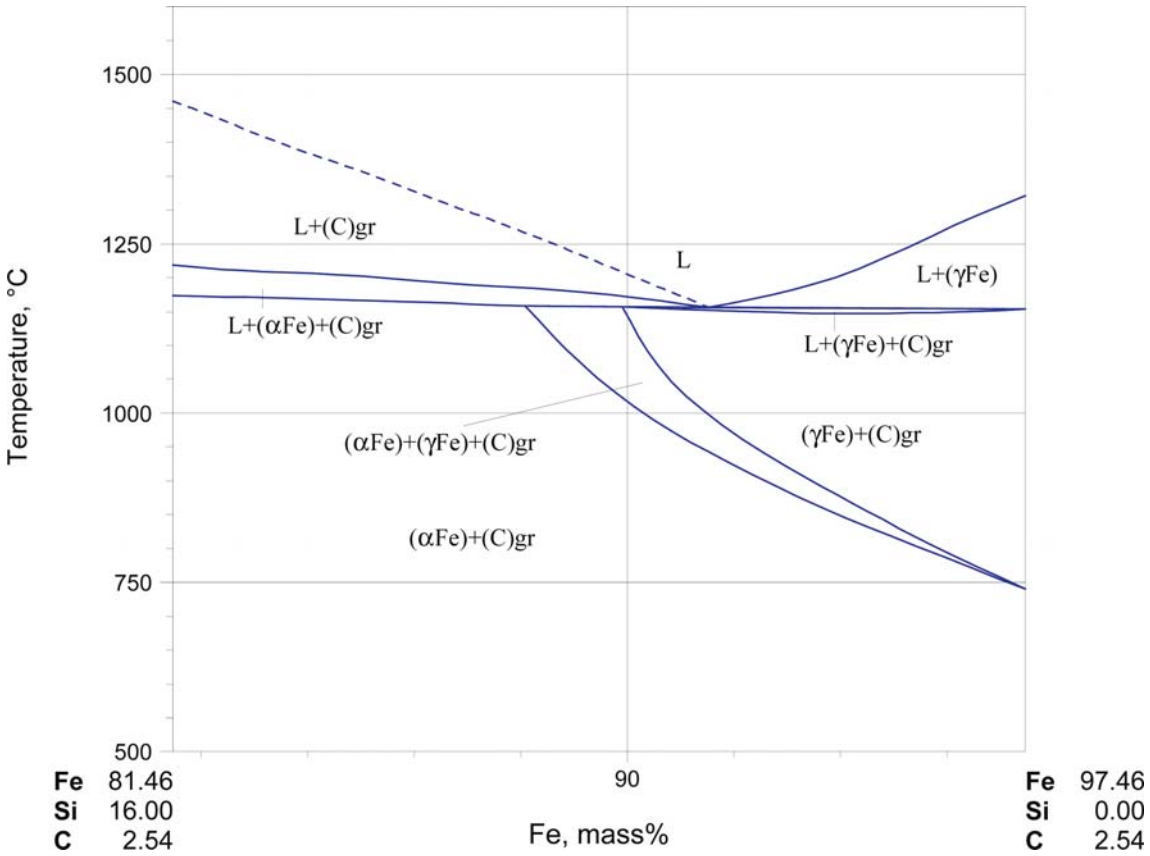

Fig. 22. C-Fe-Si. Stable vertical section at 2.54 mass% C

DOI: 10.1007/978-3-540-74196-1_12

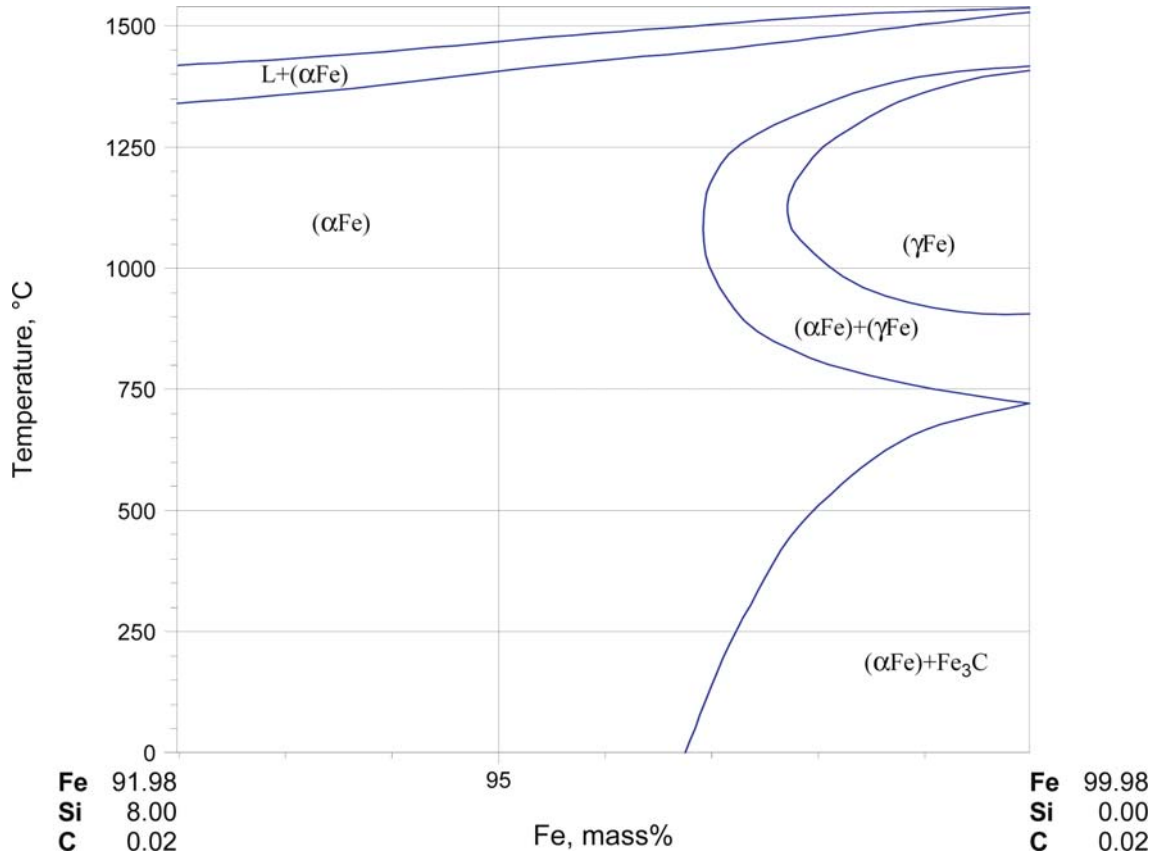

Fig. 23. C-Fe-Si. Metastable vertical section at 0.02 mass% C

DOI: 10.1007/978-3-540-74196-1_12

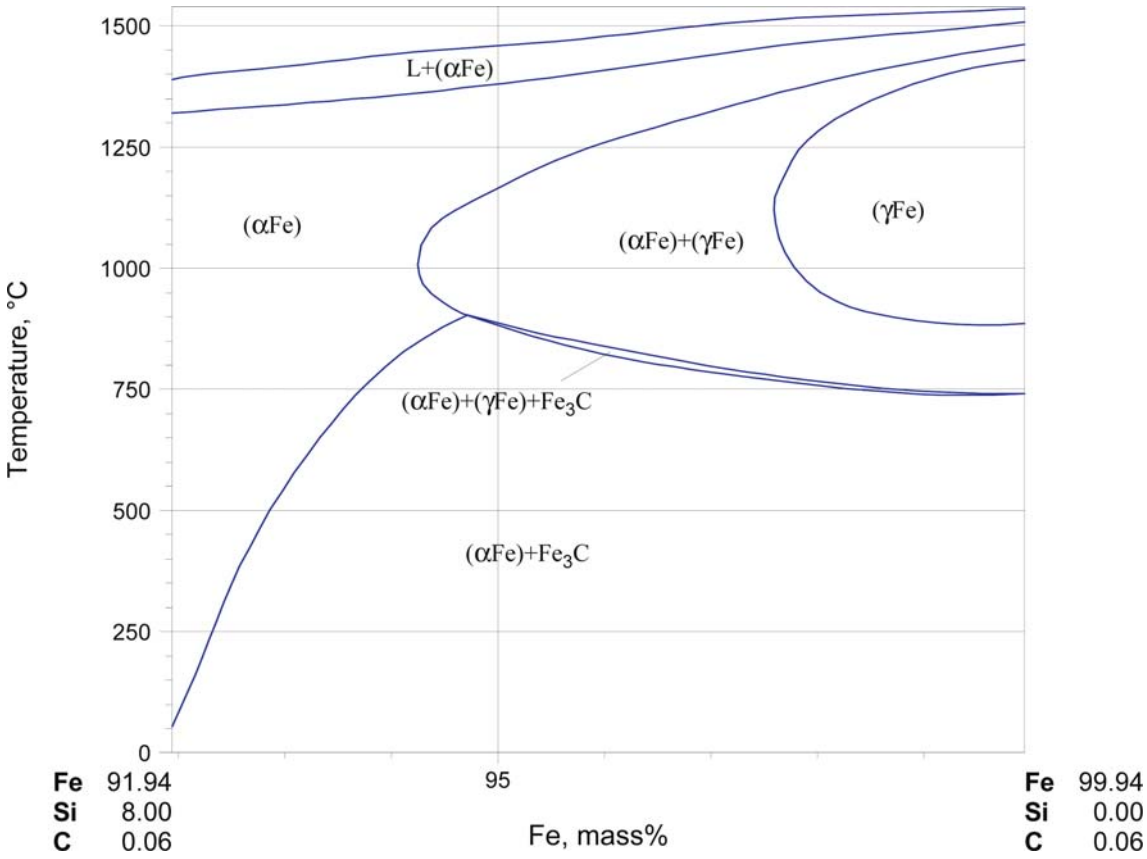

Fig. 24. C-Fe-Si. Metastable vertical section at 0.06 mass% C

DOI: 10.1007/978-3-540-74196-1_12

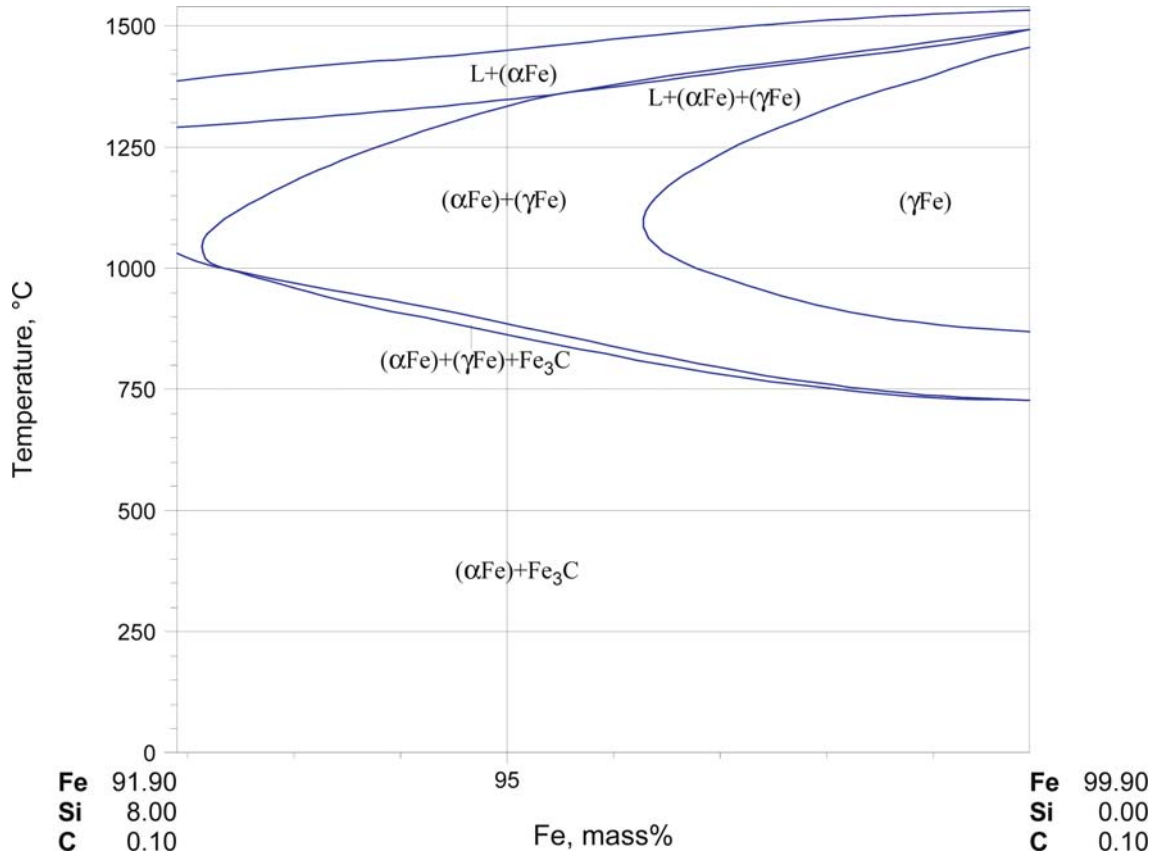

Fig. 25. C-Fe-Si. Metastable vertical section at 0.1 mass% C

DOI: 10.1007/978-3-540-74196-1_12

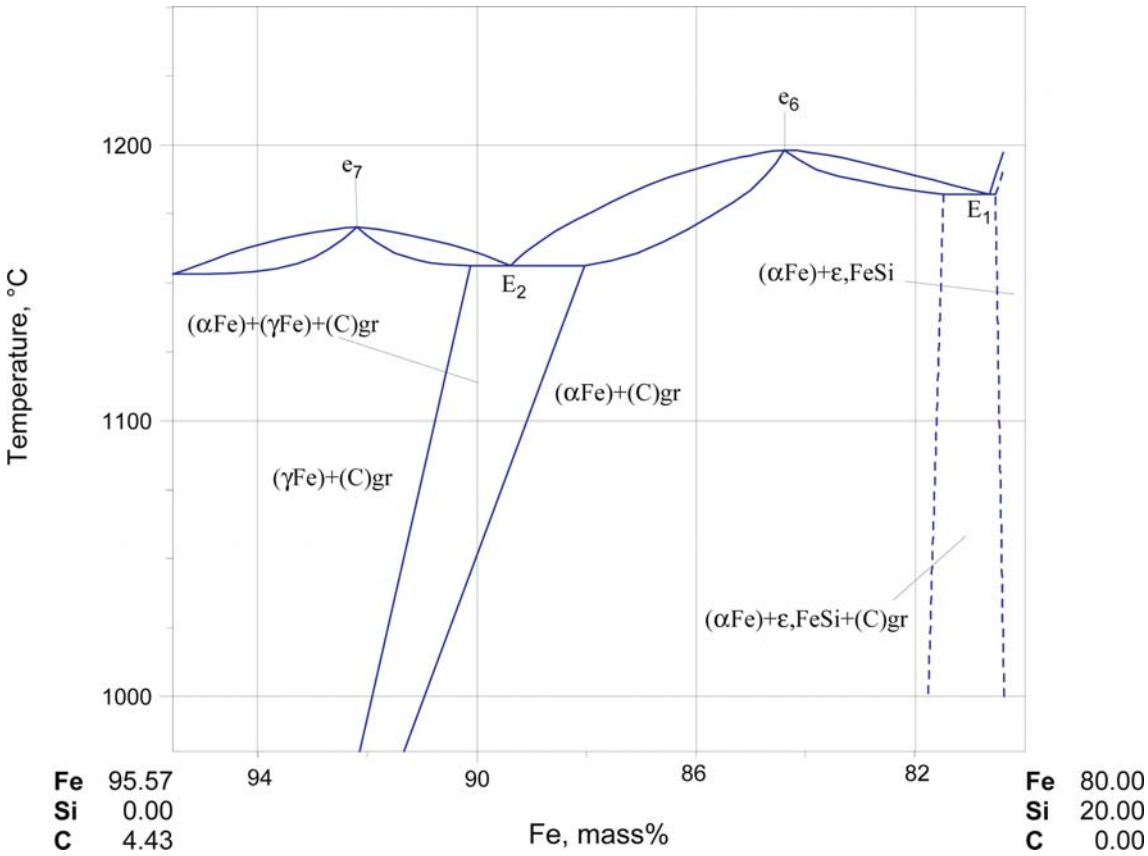

Fig. 26. C-Fe-Si. Vertical section through the invariant points of the liquidus surface

DOI: 10.1007/978-3-540-74196-1_12

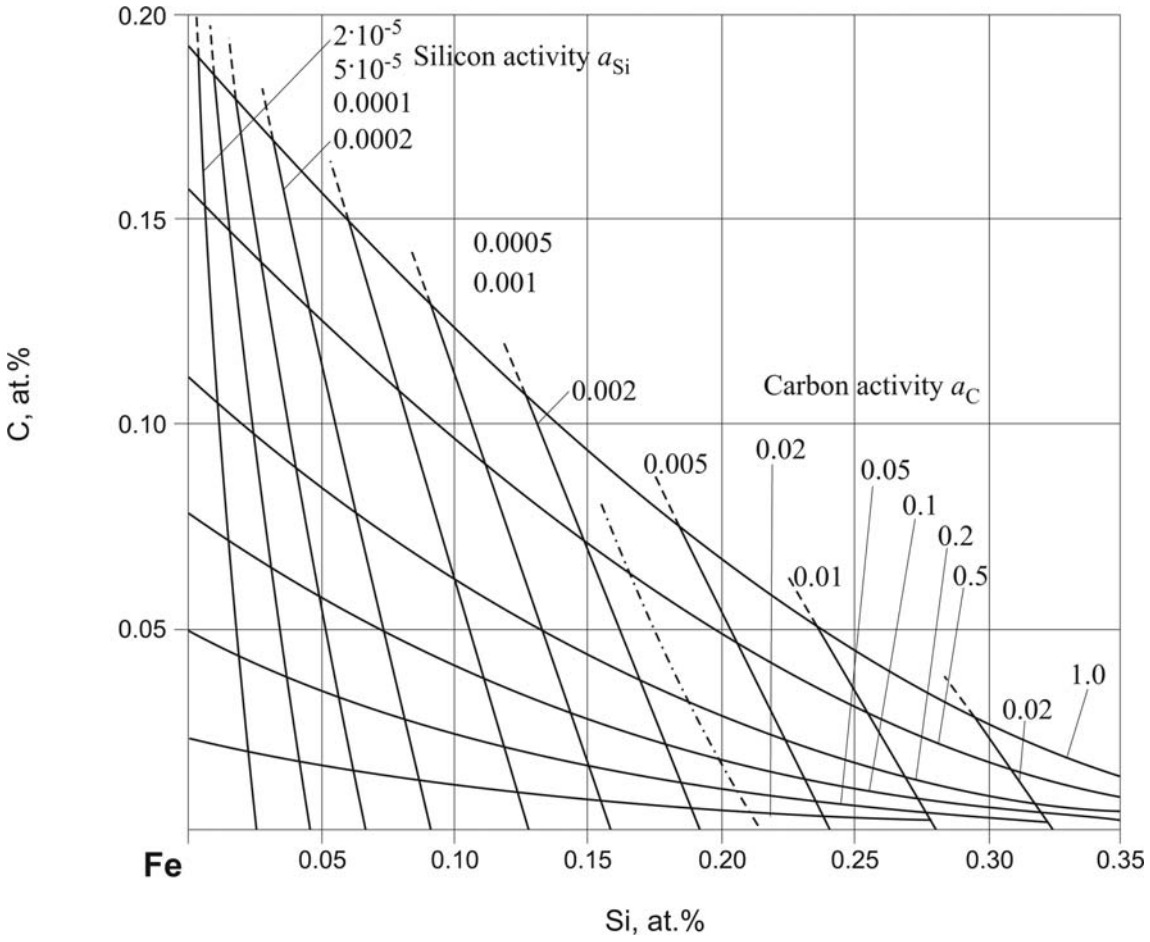

Fig. 27. C-Fe-Si. Isoactivity lines for Si and C in C-Fe-Si liquid at 1420°C

DOI: 10.1007/978-3-540-74196-1_12

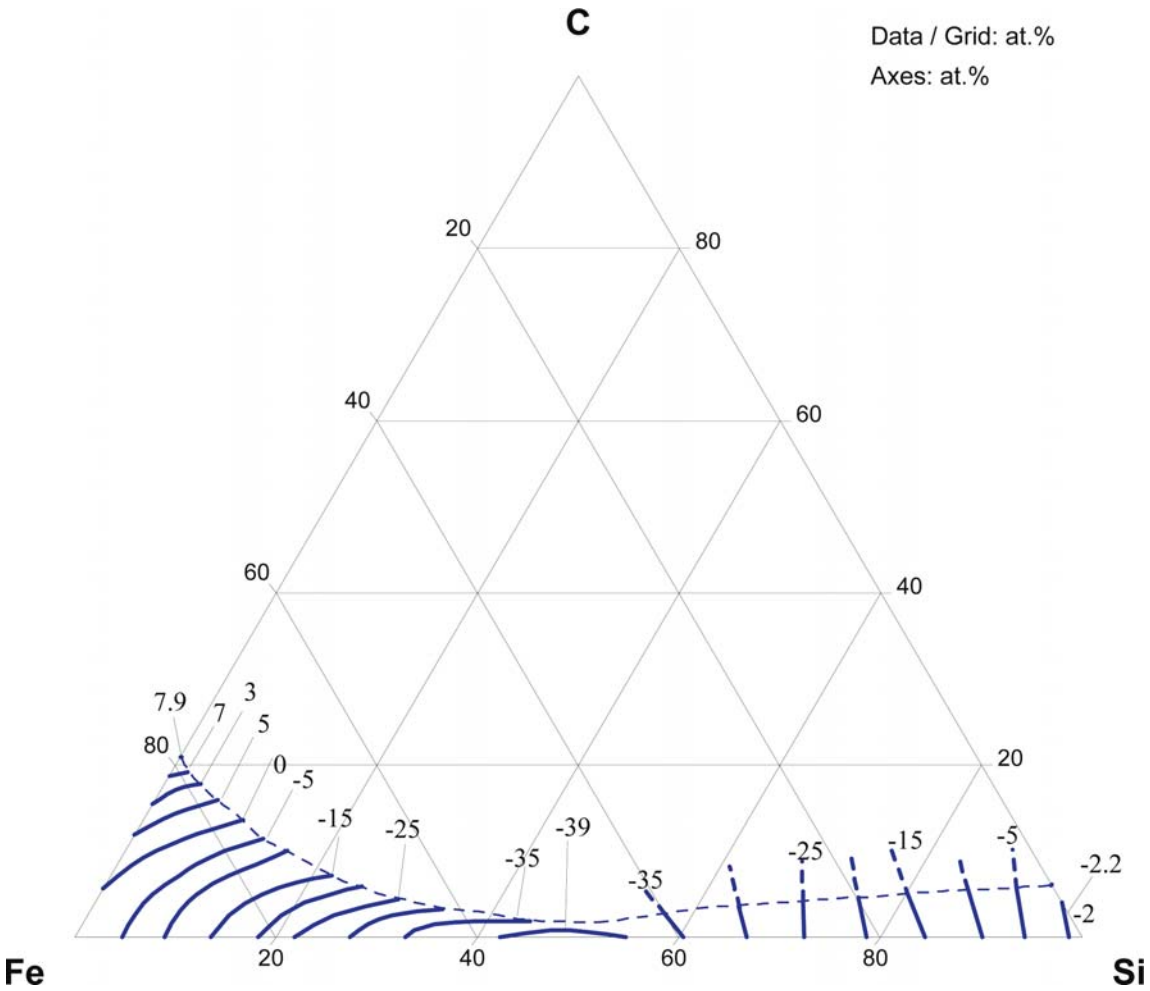

Fig. 28. C-Fe-Si. Mixing enthalpy in molten C-Fe-Si alloys at 1587 °C

DOI: 10.1007/978-3-540-74196-1_12

References

[1906Wue] Wuest, F., Petersen, G., "Contribution for the Influence of the Silicon on the System Iron-Carbon" (in German), *Metallurgie*, **3**, 811–820 (1906) (Experimental, Phase Relations, 20)

[1908Gon] Gontermann, W., "About Some Iron-Silicon-Carbon Alloys" (in German), *Z. Anorg. Chem.*, **59**, 373–413 (1908) (Experimental, Phase Diagram, Phase Relations, Review, 25)

[1911Gon] Gontermann, W., "Iron-Silicon-Carbon Alloys", *J. Iron Steel Inst.*, **83**, 421–475 (1911) (Experimental, Phase Diagram, Phase Relations, 23)

[1916And] Andrew, J.H., "Iron-Carbon-Silicon Alloys", *J. Iron Steel Inst., London*, **94**, 459–460 (1916) (Abstract)

[1922Sch] Schwartz, H.A., Payne, H.R., Gorton, A.F., Austin, M.M., "Conditions of Stable Equilibrium in Iron-Carbon Alloys", *Trans. Amer. Inst. Min. Met. Eng.*, **68**, 916–929 (1922) (Experimental, Phase Diagram, Mechan. Prop., 9)

[1923Hon] Honda, K., Murakami, T., "On the Structural Constitution of Iron-Carbon-Silicon Alloys", *J. Iron Steel Inst.*, **107**, 545–583 (1923) (Magn. Prop., Morphology, Phase Diagram, Thermodyn., 19)

[1924Hon] Honda, K., Murakami, T., "On the Structural Constitution of Iron-Carbon-Silicon Alloys", *Sci. Rep. Tohoku Imp. Univ.*, **1**(12), 257–287 (1924) (Experimental, Magn. Prop., Morphology, Phase Diagram, Thermodyn., 16)

[1925Bec] Becker, M.L., "Equilibrium at High Temperatures in the Iron-Carbon-Silicon System", *J. Iron Steel Inst.*, **112**, 239–253 (1925) (Experimental, Phase Diagram, Phase Relations, 14)

[1927Han] Hanson, D., "The Constitution of Silicon-Carbon-Iron Alloys and a New Theory of the Cast Irons", *J. Iron Steel Inst.*, **116**, 129–183 (1927) (Experimental, Phase Diagram, 1)

[1928Sch] Scheil, E., "Over Ternary Diagrams on the Basis iron-Carbon" (in German), *Mitt. as Forschungs Inst.*, Ver. Stahlwerke A.G., Dortmund, **1**, 1–21 (1928) as quoted in [1932Kri]

[1929Nor] Norbury, A. L., "Constitutional Diagrams for Cast Irons and Quenched Steels", *J. Iron Steel Inst.*, **119**, 443–471 (1929) (Morphology, Phase Diagram, Review, 27)

[1930Kei] Keil, O., Kotyza, F., "The Influence of Silicon and Manganese on the Solidification of Iron-Carbon Alloys" (in German), *Arch. Eisenhuettenwes.*, **4**(6), 295–297 (1930) (Experimental, Morphology, Phase Diagram, 20)

[1930Kri] Kriz, A., Poboril, F., "A Contribution on the Constitution of the Fe-C-Si System", *J. Iron Steel Inst.*, **122**, 191–213 (1930) (Experimental, Phase Diagram, 16)

[1930Sat] Sato, T., "A Metallographic Investigation of the Iron-Silicon-Carbon Alloys", *Tech. Rep. Tohoku Imp. Univ.*, **9**, 515–565 (1930) as quoted in [1951Owe]

[1931Soe] Soehnchen, V.E., Piwowarsky, E., "About the Influence of Alloying Elements Nickel, Silicon, Aluminium and Phosphorus on the Carbon Solubility in Liquid and Solid Iron" (in German), *Arch. Eisenhuettenwes.*, **5**(2), 111–121 (1931) (Experimental, Morphology, Phase Diagram, 51)

[1932Kri] Kriz, A., Poboril, F., "A Further Contribution on the Constitution of the Fe-C-Si System", *J. Iron Steel Inst.*, **126**, 323–349 (1932) (Experimental, Phase Diagram, Phase Relations, 4)

[1934Her] Herty, C.H., Jr., Royer, M.B., *U.S. Bur. Mines, Rep. Invest.* (3230), (1934) as quoted in [1948Smi]

[1935Daw] Dawans, A., "The Fe-C-Si Diagram" (in French), *Rev. Univ. Mines*, **11**(14), 541–552 (1935) (Experimental, Theory, Phase Diagram, Phase Relations, 12)

[1936Han] Hanemann, H., Jass, H., "About the Fe-FeSi-Graphite" (in German), *Anniversary Volume Dedicated to K. Honda (Tohoku Imp. Univ.)*, 793–811 (1936) (Experimental, Phase Diagram, Phase Relations, 13)

[1936Thy] Thyssen, M.H., "Cast Iron in Silicium" (in French), *Rev. Metall.*, **33**, 379–389 (1936) (Experimental, Morphology, Mechan. Prop., Phase Relations, 10)

[1938And] Andrew, J.H., Bottomley, G.T., Maddocks, W.R., Percival, R.T., "The Fluidity of Iron-Carbon and other Iron Alloys", *Iron Steel Inst., 3th Rep. Steel* Castings Research Committee, Publ. Offices Iron Steel Inst. 4, Grosvenor Gardens, London, S.W.1, (23), 5–32 (1938) (Experimental, 9)

DOI: 10.1007/978-3-540-74196-1_12

[1938Jas] Jass, H., Hanemann, H., "About the Iron-Ironsilicon FeSi-Carbon System" (in German), *Giesserei*, **25**(12), 293–299 (1938) (Experimental, Morphology, Phase Diagram, Phase Relations, 23)

[1939Sal] Saltykov, S.A., "Stable Phase Diagram Iron-Carbon Alloys with Silicon" (in Russian), *Liteynoe Delo*, **10–11**, 15–16 (1939) (Review, Phase Diagram, Phase Relations, 4)

[1940Jae] Jaenecke, E., "About 'half' Two Phase Diagrams of the Iron-Carbon System and their Relationships in Ternary Alloys, in Particular by Silicon" (in German), *Z. Metallkd.*, **32**(5), 142–144 (1940) (Abstract, Phase Diagram, Phase Relations, 23)

[1941Boy] Boyles, A., "The Pearlite Interval in Gray Cast Iron", *Trans. Amer. Found. Assoc.*, **48**, 531–573 (1941) (Experimental, Mechan. Prop., Morphology, Phase Diagram, Phase Relations, 9)

[1941Jae] Jaenecke, E., "About a 'Half' of Double Diagram of the Iron-Carbon System etc." (in German), *Z. Metallkd.*, **33**, 186–187 (1941) (Abstract, Phase Diagram, 5)

[1944Hur] Hurst, J.E., Riley, R.V., "The Occurrence of the Carbide Phase in High-Silicon Iron-Carbon Alloys", *J. Iron Steel Inst.*, **149**, 213–219 (1944) (Experimental, Morphology, 1)

[1946Ric] Rickett, R.L., Fick, N.C., "Constitution of Commercial Low-Carbon Iron-Silicon Alloys", *Trans. Amer. Inst. Min. Met. Eng.*, **167**, 346–356 (1946) (Experimental, Morphology, Phase Diagram, 4)

[1948Chi] Chipman, J., "Activities in Liquid Metallic Solutions", *Disc. Farad. Soc.*, **4**, 23–49 (1948) (Experimental, Calculation, Phase Diagram, Thermodyn., 53)

[1948Mar] Marles, D., "The Carbides in Iron Carbon Silicon Alloys and Cast Irons", *J. Iron Steel Inst.*, **158**(4), 433–436 (1948) (Experimental, Morphology, 9)

[1948Smi] Smith, R.P., "Equilibrium of Iron-Carbon-Silicon and of Iron-Carbon-Manganes Alloys with Mixtures of Methane and Hydrogen at 1000°C", *J. Am. Chem. Soc.*, **70**, 2724–2729 (1948) (Experimental, Thermodyn., Phase Diagram, 20)

[1949Dar] Darken, L.S., "Diffusion of Carbon in Austenite with a Discontinuity in Composition", *Trans. AIME*, **180**, 430–438 (1949) (Experimental, Thermodyn., Kinetics, Theory, Interface Phenomena, 11)

[1949Jae] Jaenecke, E., "C-Fe-Si", in "*Kurzgefasstes Handbuch aller Legierungen*", (in German), Winter Verlag, Heidelberg, 707–714 (1949) (Phase Diagram, Phase Relations, Review)

[1951Har] Harry, E.D., "Metallography of Carbon in Silicon-Iron Alloys Containing 4% Silicon", *J. Iron Steel Inst.*, **167**, 241–246 (1951) (Experimental, Morphology, Phase Diagram, Phase Relations,13)

[1951Owe] Owen, W.S., "The Carbide Phase In Iron Carbon Silicon Alloys", *J. Iron Steel Inst.*, **167**(2), 117–120 (1951) (Experimental, Crys. Structure, Phase Diagram, 25)

[1952Chi] Chipman, J., Alfred, R. M., Gott, L.W., Small, R.B., Wilson, D.M., Thomson, C.N., Gue, D.L., "The Solubility of Carbon in Molten Iron and Iron-Silicon and Iron-Manganese Alloys", *Trans. Amer. Soc. Metals*, **44**, 1215–1232 (1952) (Experimental, Phase Relations, 16)

[1952Hil] Hilliard, J.E., Owen, W.S., "A Thermal and Microscopic Study of the Iron-Carbon-Silicon-System", *J. Iron Steel Inst.*, **172**, 268–282 (1952) (Experimental, Morphology, Phase Diagram, 28)

[1952Owe1] Owen, W.S., Street, B.G., "Identification of Certain Iron-Silicon Carbides", *J. Iron Steel Inst.*, **172**, 15–18 (1952) (Crys. Structure, Experimental, Morphology, 10)

[1952Owe2] Owen, W.S., "The Carbide Phase in Iron-Carbon-Silicon Alloys", *J. Iron Steel Inst.*, **171**(1), 74–74 (1952) (Review, 2)

[1952Owe3] Owen, W.S., Street, B.G., Riley, R.V., Taylor, A., Morrogh, H., Allison, A., Hultgren, A., Kuo, K., Petch, N.J., "The Crystal Structure of Graphite in Cast Iron - the Carbide Phase in Iron Carbon Silicon Alloys", *J. Iron Steel Inst*., **170**(3), 237–242 (1952) (Crys. Structure, Review, 15)

[1953Iba] Ibaragi, M., Okumura, T., "On the Solubility of Silicon in Cementite", *Mem. Inst. Sci. Ind. Res. Osaka Univ.*, **10**, 103–105 (1953) as quoted in [1992Rag]

DOI: 10.1007/978-3-540-74196-1_12

[1954Chi] Chipman, J., Fulton, J.C., Gokcen, N., Caskey, G.R., "Activity of Silicon in Liquid Fe-Si and Fe-C-Si Alloys", *Acta Metall.*, **2**, 439–450 (1954) (Calculation, Experimental, Phase Relations, Thermodyn., 28)

[1954Ful] Fulton, J.C., Chipman, J., "Occurrence of Silicon Carbide in the Fe-C-Si System", *Trans. Amer. Inst. Min. Met. Eng.*, **200**, 356–357 (1954) (Experimental, 2)

[1954Owe] Owen, W.S., "The Effect of Silicon on the Kinetics of Tempering", *Trans. ASM*, **46**, 812–828 (1954) (Experimental, 15)

[1955Tur] Turkdogan, E.T., Leake, L.E., "Thermodynamics of Carbon Dissolved in Iron Alloys. Part I: Solubility of Carbon in Iron-Phosphorus, Iron-Silicon, and Iron-Manganese Melts", *J. Iron Steel Inst.*, **179**, 39–43 (1955) (Experimental, Phase Diagram, Phase Relations, Thermodyn., 15)

[1958Koz] Kozheurov, V.A., Burylev, B.P., "Carbon Solubility in Liquid Iron in Presence of Manganese and Silicon" (in Russian), *Izv. Vyssh. Uchebn. Zaved., Chern. Metall.*, **1**, 83–93 (1958) (Calculation, Phase Relations, Thermodyn., 12)

[1958Lea] Leak, D.A., Leak, G.M., "Solubility and Diffusion of Carbon in a Silicon-Iron Alloy", *J. Iron Steel Inst.*, **189**, 256–262 (1958) (Experimental, Kinetics, Interface Phenomena, Transport Phenomena, 23)

[1959Kon] Konoval, G., Zwell, L., Gorman, L.A., Leslie, W.C., "X-Ray Diffraction Pattern of Carbide in Low-Carbon Iron-Silicon Alloys", *Nature*, **184**(4702), 1862–1863 (1959) (Experimental, Crys. Structure, 4)

[1959Neu] Neumann, F., Schenck, H., Patterson, W., "Iron-Carbon Alloys in Thermodynamic Consideration" (in German), *Giesserei Tech.-Wiss. Beih.*, **23**, 1217–1246 (1959) (Experimental, Phase Diagram, Phase Relations, Theory, Thermodyn., 72)

[1959Pet] Petrushevskii, M.S., Gel'd, P.V., "Equilibrium of Carbon in Molten Alloys of Fe, Mn, Si and C", *Russ. J. Phys. Chem.*, **32**, 86–94 (1959) (Experimental, Phase Diagram, Phase Relations, Thermodyn., 18)

[1961Hum] Humphreys, J.G., Owen, W.S., "The Carbide Constituents in Iron-Carbon-Silicon Alloy", *J. Iron Steel Inst.*, **198**, 38–45 (1961) (Crys. Structure, Experimental, 20)

[1962Kir] Kirkaldy, J.S., Purdy, G.R., "Diffusion in Multicomponent Metallic Systems V. Interstitial Diffusion in Dilute Ternary Austenites", *Canad. J. Phys.*, **40**, 208–217 (1962) (Experimental, Theory, Kinetics, 9)

[1962Nyq] Nyquist, O., Lange, K.W.K., Chipman, J., "Influence of Silicon on the Activity of Carbon in Liquid Iron", *J. Trans. Met. Soc. AIME*, **224**, 714–718 (1962) (Thermodyn., Experimental, Calculation, 13)

[1962Zhu] Zhukov, A.A., "Phase Diagram for Iron-Carbon and Iron-Carbon-Silicon Alloys", *Russ. J. Phys. Chem.*, **36**(6), 734–736 (1962) translated from *Zh. Fiz. Khim.*, **36**(6), 1371–1375 (1962) (Review, 8)

[1964Her] Herbstein, F.H., Snyman, J.A., "Identification of Eckstrom-Adcock Iron Carbide as Fe_7C_3", *Inorg. Chem.*, **3**(6), 894–896 (1964) (Crys. Structure, Experimental, 18)

[1964Sch1] Schröder, D., Chipman, J., "The Influence of Carbon on the Activity Coefficient of Silicon in Liquid Iron-Carbon-Silicon", *J. Trans. Met. Soc. AIME*, **230**, 1492–1494 (1964) (Experimental, Thermodyn., 7)

[1964Sch2] Schwaab, P., "A New Ternary Silicon Carbide" (in German), *Naturwiss.*, **51**(15), 356 (1964) (Abstract, 4)

[1965Del] Deliry, J., "A New Iron Carbide in Carbon-Silicon Steels" (in French), *Mem. Sci. Rev. Metall.*, **62**(7–8), 527–550 (1965) (Experimental, Morphology, Crys. Structure, 23)

[1965Rei] Rein, R.H., Chipman, J., "Activities in the Liquid Solution SiO_2-CaO-MgO-Al_2O_3 at 1600°C", *Trans. Metall. Soc. AIME*, **233**, 415–425 (1965) (Phase Diagram, Phase Relations, Thermodyn., 37)

[1966Aar1] Aaronson, H.I., Domian, H.A., Pound, G.M., "Thermodynamics of the Austenite - Proeutectoid Ferrite Transformation. I, Fe-C Alloys", *Trans. AIME*, **236**, 753–767 (1966) (Calculation, Phase Diagram, Thermodyn., Theory, 43)

DOI: 10.1007/978-3-540-74196-1_12

[1966Aar2] Aaronson, H.I., Domian, H.A., "Partition of Alloying Elements Between Austenite and Proeutectoid Ferrite or Bainite", *Trans. AIME*, **236**, 781–796 (1966) (Experimental, Kinetics, Morphology, 27)

[1966Aar3] Aaronson, H.I., Domian, H.A., "Thermodynamics of the Austenite → Proeutectoid Ferrite Transformation. II Fe-C-X Alloys", *Trans. AIME*, **236**, 768–781 (1966) (Calculation, Theory, Thermodyn., Phase Diagram, 52)

[1966Dug] Duggin, M.J., Hofer, L.J.E., "Nature of P-Iron Carbide", *Nature*, **212**(5059), 248 (1966) (Crys. Structure, Experimental, 11)

[1966Fis] Fischer, W.A., Lorenz, K., Fabritius, H., Hoffman, A., Kalwa, G., "Investigation of Phase Transformations in Pure Iron Alloys with Magnetic Balance" (in German), *Arch. Eisenhuettenwes.*, **37**(1), 79–86 (1966) (Calculation, Experimental, Morphology, Thermodyn., 43)

[1966Gor] Gorev, K.V., Shevchuk, L.A., "The Fe-C-Si Metastable State Diagram" (in Russian), *Dokl. Akad. Nauk BSSR*, **10**(10), 778–782 (1966) (Phase Relations, Phase Diagram, Review)

[1966Sch1] Schuermann, E., Hirsch, J., "Contributions to the Heterogeneous Equilibrium of Iron-Silicon-Carbon System" (in German), *Giesserei Tech.-Wiss. Beih.*, **18**(1), 1–16 (1966) (Experimental, Phase Diagram, 29)

[1966Sch2] Schuermann, E., Hirsch, J.V., "Calorimetry in the Stable System Iron-Silicon-Carbon" (in German), *Giesserei Tech.-Wiss. Beih.*, **18**(1), 17–24 (1966) (Experimental, Phase Diagram, Phase Relations, 11)

[1966Sch3] Schuermann, E., Hirsch, J.V., "Solidification and Transformation Equilibria of the Stable Fe-C-Si System" (in German), *Giesserei Tech.-Wiss. Beih.*, **5**3, 398–400 (1966) (Review, Phase Relations, 10)

[1967Ben] Benabder, A., Faivre, R., "A Quantitative Study of Influence of Formation and Decomposition of Tempering Carbides at Low Temperature on Graphitization at 530°C of a Ternary Alloy Fe-C-Si Having Undergone a Martensitic Tempering" (in French), *Compt. Rend. Hebdom. Acad. Sciences Serie C*, **265**(22), 1231–1233 (1967) (Experimental, Phase Relations, 11)

[1967Mal] Malinochka, Y.N., Dolinskaya, V.Z., Lev, L.E., "Ternary Carbide Eutectic in the Fe-C-Si Alloys", *Izv. Akad. Nauk SSSR, Met.*, **2**, 106–107 (1967) (Abstract)

[1967Sch] Schuermann, E., Schmidt, T., Tillmann, F., "Activities of Carbon in γ and α -Mixed Crystal of the Iron-Carbon-Silicon Alloys" (in German), *Giessereiforschung*, **19**(1), 25–34 (1967) (Experimental, Phase Diagram, Thermodyn., 33)

[1967Sim] Simon, A., "Isothermic Dilatometric and Electron Microscopic Study of Decomposition of Residual Austenite in Alloy of Iron-Carbon-Silicon With 2 % Carbon and 0.5 % Silicon Tempered from 1130 to −5°C" (in French), *Compt. Rend. Hebdo. Acad. Sciences Serie C*, **265**(18), 970–973 (1967) (Experimental, Morphology, 3)

[1967Tar] Taran, Y.N., Malinochka, Y.N., Lev, I.E., Dolinskaya, V.Z., "Microscopic and X-ray Spectral Investigation of the Silico-Carbide Eutectics in Fe-C-Si Alloys", *Ivz. Akad. Nauk SSSR, Metally*, **1**, 92–97 (1967) (Experimental, Crys. Structure, Morphology, 6)

[1967Zhu] Zhukov, A.A., Snezhnoy, R.L., "Position of the Ledeburite Valley in the Fe-C-Si System", *Russ. Metall. (Engl. Transl.)*, **2**, 107–108 (1967), translated from *Izv. Akad. Nauk SSSR, Met.*, (**2**) 195–200 (1967) (Abstract, Phase Relations, 1)

[1968Ben] Benabder, A., Faivre, R, "Influence of Formation and Decomposition of Low-Temperature Carbides on Graphitisation of Some Iron-Carbon-Silicon Alloys after a Martensitic-Type Quench" (in French), *Mem. Sci. Rev. Metall.*, **65**(4), 309–315 (1968) (Experimental, Crys. Structure, Morphology, 15)

[1968Chi] Chipman, J., Brush, E.F., "The Activity of Carbon in Alloyed Austentite at 1000°C", *Trans. AIME*, **242**, 35–41 (1968) (Calculation, Thermodyn., 21)

[1968Fuj] Fujita, F.E., Ono, Y., Inokuti, Y., *J. Jpn. Inst. Met.*, **32**, 328 (1968) as quoted in [1983Ray]

[1968Gor] Gorev, K.V., Shevchuk, L.A., Dudetskaya, L.R., "A Study of the Phase Composition of Low-Carbon Iron-Carbon-Silicin Alloys" (in Russian), *Dokl. Akad. Nauk BSSR*, **12**(2), 136–139 (1968) (Experimental, Phase Diagram, 4)

DOI: 10.1007/978-3-540-74196-1_12

[1968Hof] Hoffmann, A., "Properties of Pure Iron-Silicon Alloys Containing Up to 5% Si" (in German), *Arch. Eisenhuettenwes.*, **39**(3), 191–199 (1968) (Experimental, Magn. Prop., Mechan. Prop., Phase Relations, 29)

[1968Ole] Olen, K.R., Heine, R.W., "A Revision of the Fe-C-Si System", *Cast Metals Res. J.*, **4**(1), 28–43 (1968) (Experimental, Morphology, Phase Relations, Phase Diagram, 30)

[1968Pat] Patterson, W., Huelsenbeck, G., Madi, H.A.S., "Contribution to the Solidification Equlibrium in the Iron Corner of the Stable Iron-Carbon-Silicon System" (in German), *Giessereiforschung*, **20**(2), 49–65 (1968) (Electr. Prop., Experimental, Morphology, Phase Diagram, Theory, 36)

[1969Bun] Bunin, K.P., Malinochka, Ya.N., Taran, Yu.N., "The C-Fe-Si System" (in Russian), Principles of Metallography of Cast Iron, Meallurgiya, Moscow, 25–37 (1969) (Phase Diagram, Phase Relations, Review)

[1969Ruh] Ruhl, R.C., Cohen, M., "Splat Quenching of Carbon-Iron Alloys", *Trans. AIME*, **245**, 241 (1969) (Experimental, Crys. Structure, 50)

[1969Sch] Schuermann, E., Kramer, D., "Investigations on the Influence of Temperature and on the Equivalent Effect of the Alloy Elements on the Solubility of Carbon in Iron Rich Carbon-saturated Ternary and Multi-component Meltings" (in German), *Giessereiforschung*, **21**(1), 29–42 (1969) (Experimental, Phase Diagram, Thermodyn., Calculation, 35)

[1969Zhu] Zhukov, A.A., "Improving the Metastable Equilibrium Diagram of the Iron-Carbon-Silicon System" (in Russian), *Izv. Akad. Nauk SSSR, Met.*, **2**, 155–158 (1969) (Phase Diagram, Thermodyn., Calculation, 9)

[1970Fuk] Fukuda, S., Sugiyama, T., Furukawa, T., Kato, E., "Solubility of Hydrogen in Liquid Iron Alloys", *Rep. Casting Research*, Lab./Waseda Univ., (21), 35–46 (1970) (Calculation, Experimental, Phase Relations, Thermodyn., 22)

[1970Mal] Malinochka, Y.N., Dolinskaya, V.Z., "A New Metastable Equilibrium Diagram and Structure of Iron-Carbon-Silicon Alloys" (in Russian), *Liteinoe Proizvod.*, **7**, 26–27 (1970) quoted in [1992Rag]

[1970Met] Metauer, G., Schissle, J.M., "Orientation Relationship Between Austenite with 2.1 C and with 3.9 Si Obtained by Keeping an Alloy Fe-C-Si at 420°C and Martensite Derived from it by Quenching in Liquid Nitrogen" (in French), *Compt. Rend. Hebd. Acad. Sci., Ser. C*, **271**(18), 1123–1126 (1970) (Experimental, Crys. Structure, 7)

[1970Sch1] Schissler, J.M., Metauer, G., "Electron Microscope and Electron Diffraction Studies on the Orientation Relations Between Ferrite and Carbon Enriched Austenite in the Transformation at 420°C of a Fe-C-Si Alloy Containing 1.02% Carbon and 3.9% Silicon" (in French), *Compt. Rend. Hebd. Acad. Sci., Ser. C*, **270**(22), 1785–1787 (1970) (Experimental, Crys. Structure, 6)

[1970Sch2] Schissle, J.M., Metauer, G., "Effect of Elevated Silicon Level on Isothermal Bainite Conversion at 420°C in Fe-C-Si Alloys" (in French), *Compt. Rend. Hebd. Acad. Sci., Ser. C*, **270** (13), 1162–1164 (1970) (Experimental, Crys. Structure, Morphology, 7)

[1970Vig1] Vigneron, B., "Effect of the Composition of Fe-C-Si alloys Containing Less than 7% of Carbon and Less than 15% of Silicon, Cooled very Rapidly by Casting, on the Structure of their Matrix and the Morphology of the Graphite" (in French), *Compt. Rend. Hebd. Acad. Sci., Ser. C*, **270**(24), 1941–1944 (1970) (Experimental, Morphology, Crys. Structure, Phase Relations, 5)

[1970Vig2] Vigneron, B., Faivre, R., "Interpenetration of 2 Iron Alloys with 50 Percent Silicon and 4.18 Percent Carbon at 1250°C" (in French), *Compt. Rend. Hebd. Acad. Sci. Ser. C*, **270**(13), 1159–1161 (1970) (Crys. Structure, Experimental, 3)

[1971Chr] Chraska, P., McLellan, R.B., "Thermodynamic Properties of Carbon in BCC and FCC Iron-Silicon-Carbon Solid Solutions", *Acta Metall.*, **19**, 1219–1225 (1971) (Experimental, Phase Diagram, Phase Relations, Calculation, Thermodyn., 31)

[1971Gor] Gorev, K.V., Shevchuk, L.A., Dudetskaya, L.R., Gurinovich, V.I., "Position of a Peritectic Quadrangle in the Iron-Carbon-Silicon System" (in Russian), *Izv. Akad. Nauk. BSSR*, **1**, 21–27 (1971) (Morphology, Experimental, 13)

DOI: 10.1007/978-3-540-74196-1_12

[1971Mal] Malinochka, Y.N., Taran, Y.N., Lev, I.E., Dolinskaya, V.Z., Vorob'eva, L.N., "Composition and Crystal Structure or Iron Silico- Carbide" (in Russian), *Izv. Akad. Nauk SSSR, Neorg. Mater.*, **7**(4), 614–616 (1971) (Crys. Structure, Experimental, 9)

[1971She] Shevchuk, L.A., Gurinovich, V.I., "Composition and Structure of Fe-Si Carbide in Fe-C-Si Alloys" (in Russian), *Izv. Akad. Nauk. BSSR*, **1**, 28–32(1971) (Crys. Structure, Experimental, 7)

[1971Vig] Vigneron, B., Faivre, R., "Use of Differential Thermal Analysis for Presentation of Austenite, Cementite and Graphite Deposits during Solidification of Pig Fe-C, Fe-Cr-C and Fe-C-Si Alloys" (in French), *Compt. Rend. Hebd. Acad. Sci., Ser. C*, **273**(16), 943–945 (1971) (Experimental, Phase Relations, 2)

[1972Kos] Kosaka, Y., "Non-eutectic Solidification in Fe-C-Si Alloys" (in Japanese), *J. Jpn. Inst. Met.*, **36**(2), 105–112 (1972) (Experimental, Morphology, Kinetics, 9)

[1972Jeg] Jeglitsch, F., Maier, K., "Investigation into the Constitution of Fe-C(Fe_3C)-Si Alloys" (in German), *Berg.-und Huttenmann. Monatsh.*, **117**(1), 381–400 (1972) (Experimental, Phase Diagram, Morphology, 33)

[1972Spi] Spinat, P., Senateur, J.-P., Fruchart, R., Herpin, P., "Characterization of Two Isotypic Phases Mn_8Si_2C and Fe_8Si_2C" (in French), *Compt. Rend. Hebd. Acad. Sci., Ser., C*, **274**(12), 1159–1162 (1972) (Crys. Structure, Experimental, Magn. Prop., 8)

[1972She] Shevchuk, L.A., Dudetskaya, L.R., Gurinovich, V.I., "Structure of Silicon Steels and Metastable Phase Diagram of Iron-Carbon-Silicon Alloys" (in Russian), *Izv. Akad. Nauk BSSR*, **3**, 54–61 (1972) (Experimental, Phase Diagram, Morphology, 9)

[1972Wad] Wada, T., Wada, H., Elliott, J.F., Chipmann, J., "Thermodynamics of the FCC Fe-Mn-C and C-Fe-Si Alloys", *Metall. Trans.*, **3**, 1657–1662 (1972) (Experimental, Thermodyn., Calculation, 12)

[1973Jeg] Jeglitsch, F., Maier, K., "Secondary Precipitation in Fe-Fe_3C-X Alloys" (in German), *Z. Metallkd.*, **64**(8), 539–545 (1973) (Experimental, Morphology, Phase Relations, 31)

[1973Kos] Kosaka, Y., "Isothermal Solidification Diagram for Fe-C-Si Alloys" (in Japanese), *J. Jpn. Inst. Met.*, **37**(8), 820–828 (1973) (Experimental, Morphology, 10)

[1973Par] Paradimitriou, G., Courrier, R., Genin, J-M., "Kinetic Study of the First Stage of Austenite Decomposition of the Bainite Fe-C-Si with 0.9% C and 3.85% Si" (in French), *Compt. Rend. Hebd. Acad. Sci., Ser. C*, **276**(9), 739–742 (1973) (Experimental, Kinetics, Morphology, 12)

[1973Sch1] Schissler, J.-M., Metauer, G., "Dilatometric Study of the Second Stage of the Isothermal Bainitic Transformation at 420°C of Hypereutectoid Fe-C-Si Alloys with 3.9% Silicon. Observation of a New Carbide" (in French), *Compt. Rend. Hebd. Acad. Sci., Ser. C*, **277**(21), 1081–1083 (1973) (Experimental, Crys. Structure, 6)

[1973Sch2] Schissler, J.-M., Metauer, G., "Influence of the Isothermal Bainitic Transformation at 420°C on Graphitization by Ulterior Recovery in Hypereutectoid Fe-C-Si Alloys with 3.9% Silicon" (in French), *Compt. Rend. Hebd. Acad. Sci., Ser. C*, **277**(20), 997–999 (1973) (Experimental, Crys. Structure, 4)

[1974Mal] Malinochka, Ya.N., Kovalchuk, G.Z., Slinkko, L.A., "Experimental Data for Improving the Metastable Equilibrium Diagram of Fe-C-Si Alloys" (in Russian), *Akad. Nauk Ukr. SSR, Metallofizika*, **56**, 91–95 (1974) (Experimental, Morphology, Phase Diagram, Phase Relations, 8)

[1974Met] Metauer, G., Schissle, J.-M., "Study of Mechanism of Martensite Formation in Certain Iron-Carbon-Silicon and Iron-Carbon-Nickel Alloys" (in French), *Mem. Scient. Rev. Metall.*, **71**(5), 295–306 (1974) (Experimental, Crys. Structure, Morphology, 13)

[1974Sig] Sigworth, G.K., Elliott, J.F., "The Thermodynamic of Liquid Dilute Iron Alloys", *Met. Sci.*, **8**, 298–310 (1974) (Calculation, Thermodyn., 249)

[1975Sar] Sare, I.R., "Two Non-Crystalline Phases in a Splat-Cooled Fe-1.9 mass% Si – 4.2 mass% C Alloy", *Scr. Metall.*, **9**, 607–609 (1975) (Experimental, Crys. Structure, 7)

[1975Sch] Schissler, J.M., Arnould, J., Metauer, G., "Study of Decomposition of Post-Bainitic Austenite in Fe-C-Si Alloys with 1 Percent C and 4 Percent Si During Isothermal Holding

DOI: 10.1007/978-3-540-74196-1_12

at 420°C - Influence of an Addition of 1 Percent Mn" (in French), *Mem. Scient. Rev. Metall.*, **72**(11), 779–793 (1975) (Experimental, Crys. Structure, Morphology, 22)

[1976Guh] Guha, A., Aaronson, H.I., Rigsbee, J.M., "Observations on Epsilon Carbide Precipitation at Austenite - Ferrite Boundaries in an Fe-C-Si Alloy", *J. Metals*, **28**(12), A54–A54 (1976) (Abstract)

[1976Mar] Marchal, G., Mangin, Ph., Janot, Chr., "Magnetism in Amorphous Fe-Si Alloys", *Solid State Commun.*, **18**, 739–742 (1976) (Experimental, Magnetic Prop., 13)

[1976Ono] Ono, Y., Hirayama, K., Furukawa, K., "Electric Resistivity of Molten Fe-C, Fe-Si and Fe-C-Si Alloys", *Trans. Iron Steel Inst. Jpn.*, **16**(3), 153–160 (1976) (Experimental, Mechan. Prop., 20)

[1977Agr] Agren, J., "A Thermodynamic Analysis of the C-Fe-Si System Between 973 and 1373 K", *Report TRITA-MAC-0125*, Materials Center, Royal Inst. Technolohy, Stockholm (1977) (Thermodyn., Calculation, 12)

[1977Ash] Ashin, A.K., "Activity of Silicon and Carbon and Fe-Si-Cmax Molten Alloys" (in Russian), *Izv. Akad. Nauk SSSR, Met.*, **4**, 81–84 (1977) (Calculation, Thermodyn., 19)

[1977Car] Carlberg, T., Fredriksson, H., "The Influence of Silicon and Aluminium on the Solidification of Cast Iron", Int. Conf. Solidification Casting, Sheffield, U.K., 115–124 (1977) (Calculation, Experimental, Morphology, Phase Diagram, Thermodyn., 17)

[1977Dub] Dubois, J.M., Caer, G.L.E., "Electron Diffraction and Mossbauer Studies of the Epsilon Phase Retained in Splat-Quenched Fe-C and Fe-C-Si Alloys", *Acta Metall.*, **25**, 609–618 (1977) (Crys. Structure, Experimental, 13)

[1977Edn] Edneral, N.V., Lyakishev, V.A., Skakov, Yu.A., "Investigation of the Structure and Constitution of the Alloy Fe-3.8% C-4.7% Si Quenched from the Liquid State" (in Russian), *Fiz. Met. Metalloved.*, **43**(2), 426–427 (1977) (Crys. Structure, Experimental, 1)

[1977Kul] Kulikov, I.S., "Activity of Components in C-Fe-Si Melts", *Izv. Akad. Nauk SSSR, Met.*, **1**, 89–92 (1977) (Calculation, Thermodyn., 7)

[1977Oka] Okamoto, T., Kagawa, A., "Lattice Parameters of Cementite in Iron-Carbon-Silicon Alloy", *Met. Sci.*, **11**(10), 471–473 (1977) (Experimental, Crys. Structure, Magn. Prop., 19)

[1977Soi] Soifer, L.M., Izmailov, V.A., Kashin, V.I., "The Effect of Si on the Structure of Fe-C Melts", *Russ. J. Phys. Chem.(Engl. Transl.)*, **51**(2), 300–301 (1977), translated from *Zh. Fiz. Khim.*, **51**, 509–510 (1977) (Experimental, Mechan. Prop., Phase Diagram, Phase Relations, 2)

[1977Sos] Sosnowski, R., Latusek, J., "Solubility of C in Multicomponent Fe-base Melts" (in Polish), *Hutnik*, **44**(10), 434–438 (1977) (Thermodyn., Calculation, 5)

[1977Uhr1] Uhrenius, B., "Optimization of Parameters Describing the Interaction Between Carbon and Alloying Elements in Ternary Austenite", *Scand. J. Metall.*, **6**(2), 83–89 (1977) (Calculation, Thermodyn., 24)

[1977Uhr2] Uhrenius, B., "A Compendium of Ternary Iron-Base Phase Diagrams", *The Hardenability of Steels*, 28–81 (1977) (Review, Calculation, 53)

[1978Kam] Kamenetskaya, D.S., Korsunskaya, I.A., Litvin, Y.A., "Effect of Graphitizing Elements on Equilibrium with the Melt in the Iron-Carbon System at High Pressures", *Fiz. Met. Mettaloved.*, **45**(3), 569–579 (1978) (Experimental, Morphology, Phase Diagram, Thermodyn., Calculation, 27)

[1978Uhr] Uhrenius, B., "A Compendium of Ternary Iron-base Phase Diagrams", *Hardenability Concepts with Applications to Steel*, Doane, D.V., Kirkaldy, J.S. (Eds.), Proc. Symp. Held Sheraton-Chicago Hotel, Oct. 24–26, 1977, Metall. Soc. AIME Heat Treat. Com./ Amer. Soc Met. Activ. Phase Trans., 28–81 (1978) (Review, Calculation, Phase Relations, 53)

[1979Bha] Bhadeshia, H.K.D.H., Edmonds, D.V., "The Bainite Transformation in a Silicon Steel", *Metall. Trans. A*, **10A**, 895–907 (1979) (Experimental, Morphology, Kinetics, 33)

[1980Han] Hanawa, K., Akechi, K., Hara, Z., Nakagawa, T., "Study of Cast Iron Powder Sintering Using C-Fe-Si Mixed Powders", *J. Jpn. Inst. Met.*, **44**(8), 943–948 (1980) (Abstract)

[1980Kag] Kagawa, A., Okamoto, T., "Partition of Silicon During Eutectic Solidification of Iron-Carbon-Silicon Alloy", *Metal Sci.*, **14**(11), 519–524 (1980) (Experimental, Calculation, Thermodyn., Kinetics, 21)

DOI: 10.1007/978-3-540-74196-1_12

[1980Mer] Merta, K., Marincek, B., "Thermodynamics of C-Fe-Si Melts" (in German), *Giessereiforsch.*, **32**(4), 157–161 (1980) (Experimental, Thermodyn., Calculation, 16)

[1980Sch] Schmid, R., "Thermodynamic Evaluation of the System on Iron- Carbon-Silicon Within the Range of Steel and Cast Iron Melts" (in German), *Geissereiforsch*, **32**(4), 147–151 (1980) (Calculation, Thermodyn., Phase Diagram, 19)

[1980Roy] Roy, S.K., Grabke, H.J., Wepner, W., "Diffusivity of Carbon in Austenitic C-Fe-Si Alloys", *Arch. Eisenhuettenwes.*, **51**(3), 91–96 (1980) (Experimental, Kinetics, Theory, Calculation, 15)

[1981Bra] Bradley, J.R., Aaronson, H.I., "Growth Kinetics of Grain Boundary Ferrite Allotriomorphs in Fe-C-X Alloys", *Metall. Trans. A*, **12A**, 1729–1741 (1981) (Kinetics, Calculation, Morphology, 78)

[1981Sch] Schmid, R., "Thermodynamics of Fe-C-Si Melts", *Calphad*, **5**(4), 255–266 (1981) (Calculation, Thermodyn., Phase Diagram, 35)

[1981Wan] Wanibe, Y., Kawashima, N., Fujisawa, T., Sakao, H., "Interdiffusion in Molten Fe-C-Si and Fe-C-Mn Alloys", *Trans. Iron Steel Inst. Jpn.*, **21**(4), 243–249 (1981) (Experimental, Kinetics, Phase Relations, 28)

[1981Yos] Yoshida, C., Sakamoto, T., Ito, T., Mori, T., Takada, H., "Anisotropy of Electrical-Resistance in Layer Graphite Fe-C-Si Alloy", *Trans. Iron Steel Inst. Jap.*, **21**(3), 187–191 (1981) (Experimental, Mechan. Prop., Morphology, 19)

[1982Ono] Ono, Y., Hamada, K., "Inter-Diffusion of Carbon in Molten Fe-C and Fe-C-Si Alloys", *Trans. Iron Steel Inst. Jap.*, **22**(3), B41–B41 (1982) (Experimental, Kinetics, Interface Phenomena, Transport Phenomena, 4)

[1982San] Sandvik, B.P.J., "The Bainite Reaction in C-Fe-Si Alloys: the Primary Stage", *Metall. Trans. A (Phys. Metall. Mat. Science)*, **13A**(5), 777–787 (1982) (Experimental, Morphology, Phase Relations, 40)

[1982Vre] Vrestal, J., "The Influence of Small Ammounts of Alloying Elements on the Equilibrium of Eutectic and Eutectoid Point in the Fe-C System" (Polish), *Kovove Mater.*, **20**(4), 417–425 (1982) (Calculation, Thermodyn., 12)

[1983Bas] Bashev, V.F., "Non-Equilibrium Crystallization and Structural Transformations in Microwires of Alloys Fe-C and Fe-C-Si During Heating", *Phys. Met. Metallogr.*, **55**(2), 114–119 (1983), translated from *Fiz. Metal. Metalloved.*, **55**(2), 331–336 (1983) (Experimental, Mech. Prop., 8)

[1983Jan] Janas, M., Mamro, K., Jowsa, J., Ludwikowski, S., "Assessment of Ferrous Alloy Component Influence on Carbon Solubility" (in Polish), *Metal. Odlew.*, **9**(3), 213–228 (1983) (Experimental, Kinetics, 28)

[1983Ray] Ray, S.K., Mohanty, O.N., "TEM Investigation of Carbide Precipitation in Low Carbon Steels Containing Silicon", *Trans. JIM*, **24**, 81–87 (1983) (Experimental, Phase Relations, Morphology, 15)

[1984And] Andersson, J.O., Gustafsson, P., Hillert, M., Jansson, B., Sundman, B., Agren, J., "The Ferrite/Austenite Equilibrium in Silicon Steels", *Met. Sci.*, **18**, 501–502 (1984) (Calculation, Thermodyn., 3)

[1984Sch] Schurman, E., Hensgen, U., Schweinichen, J., "Melt Equilibrium of the Ternary Systems Fe-C-Si and Fe-C-P" (in German), *Giessereiforsch.*, **36**(4), 121–129 (1984) (Experimental, Phase Diagram, 33)

[1984Wri] Wriedt, H.A., Turkdogan, E.T., "Composition Limits of Ferritic Solid Solutions in Silicon Steels at 950-1100°C", *Met. Sci.*, **18**, 27–30 (1984) (Experimental, Thermodyn., Phase Relations, 7)

[1985Bha1] Bhadeshia, H.K.D.H., Edmonds, D.V., "Authors' Reply", *Metall. Trans. A*, **16A**, 466–468 (1985) (Review, 14)

[1985Bha2] Bhadeshia, H.K.D.H., "Diffusional Formation of Ferrite in Iron and Its Alloys", *Prog. Mat. Sci.*, **29**, 321–386 (1985) (Calculation, Experimental, Kinetics, Morphology, Phase Diagram, Theory, Thermodyn., 196)

DOI: 10.1007/978-3-540-74196-1_12

[1985Chu] Ji, C., Qi, G., "Activity Coefficient of Silicon and Its Interaction Coefficients in Fe-C-Si Melts at 1773 K", *Trans. Japan Inst. Metals*, **26**(11), 832–839 (1985) (Experimental, Thermodyn., 13)

[1985Liu] Liu, S.K., Reynolds, W.T., Hu, Jr.H., Shiflet, G.H., Aaronson, H.I., "Discussion of "The Bainite Transformation in a Silicon Steel", *Metall. Trans. A*, **16A**, 457–466 (1985) (Review, Experimental, Kinetics, 66)

[1985Ves] Veselovska, E., Durisin, J., Repiska, L., "Theoretical Examination of Phase Diagrams of Fe-C, Fe-Si and Fe-C-Si Systems" (in Polish), *Kovove Mater.*, **23**(2), 156–166 (1985) (Calculation, Phase Diagram, 16)

[1986Cho] Choi, D.C., Lee, D.J., Lee, B.S., Kang, K.W., "Structure Changes during Sintering of C-Fe-Si Compacts", *J. Korean Inst. Met.*, **24**(2), 149–57 (1986) (Abstract)

[1986Kal] Kalenov, V.P., "Structural Diagrams for Forms of Graphite in Fe-C-Si Alloys" (in Russian), *Steel in the USSR*, **16**(2), 91–93 (1986) (Calculation, Phase Diagram, 5)

[1987Bha] Badeshia, H.K.D.H., "Diffusional Formation of Ferrite in Iron and its Alloys", *Scr. Metall.*, **21**, 1605–1609 (1987) (Review, Kinetics, 23)

[1987Chu] Chueh, S.C., Smith, J.F., "Stable and Metastable Equilibria in the Iron Rich Corner of the Fe-C-Si" System", *Calphad*, **11**(2), 149–158 (1987) (Calculation, Phase Relations, Phase Diagram, 9)

[1987Hei] Heine, R.W., "The Fe-C-Si Solidification Diagram for Cast Iron" (in German), *Geisserei-Prax.*, **17**, 239–247 (1987) (Experimental, Phase Diagram, Phase Relations, 23)

[1987Ino] Inoue, A., Furukawa, S., Masumoto, T, "Amorphous Fe-C-Si Alloys Prepared by Melt Quenching", *Metall. Trans. A- Phys. Metall. Mat. Sci.*, **18**(4), 715–717 (1987) (Experimental, Magn. Prop., Mechan. Prop., 20)

[1987Sch] Schuermann, E., Schweinichen, J., Voelker, R., Fischer, H., "Calculation of the α/δ Resp γ-Liquidus of Iron and of the Liquidus of Carbon as well as of the Univariant Reaction Lines in Iron-Rich, Carbon Containing Three-Component and Multicomponent Fe-C-X_1-X_2-Systems." (in German), *Giessereiforsch.*, **39**(3), 104–113 (1987) (Phase Diagram, Phase Relations, Thermodyn., 19)

[1988Luo] Luo, Y., "Partial Phase Diagram of Fe-Si (≤8 mass% Si)-C(≤0.8 mass% Si) and Pseudobinary Sections of Fe-Si and Fe-C", *Acta Metall. Sin.*, **24**(3), B187–B194 (1988) (Experimental, Theory, Phase Diagram, 8)

[1988Mag] Magnin, P., Kurz, W., "Stable and Metastable Eutectic Temperatures of Fe-C with Small Additions of a Third Element", *Z. Metallkd.*, **79**(5), 282–284 (1988) (Experimental, Phase Relations, 5)

[1988Sch] Schiepers, R.C.J., van Loo, F.J.J., de With, G., "Reactions Between α-Silicon Carbide Ceramic and Nickel or Iron", *J. Am. Ceram. Soc.*, **71**(6), C284–C287 (1988) (Experimental, Phase Diagram, 9)

[1988Yat] Yatsenko, A.I., Doronkin, K.Yu., Grushko, P.D., Repina, N.I., "On the Polymorphic α(δ)-γ Transformation in Low-Carbon Fe-C-Si Alloys", *Phys. Met. Metallogr.*, **66**(6), 117–122 (1988), translated from *Fiz. Met. Metalloved.*, **66**(6), 1172–1176, (1988) (Experimental, Phase Diagram, 4)

[1989Bha] Bhadeshia, H.K.D.H., Edmonds, D.V., "Discussion of the Criticism of Heat-Treatment of an Fe-C-Si Alloy – Authors Reply", *Metall. Trans. A-Phys. Metall. Mat. Sci.*, **20**(2), 333–334 (1989) (Calculation, 8)

[1989Dre] Dresler, W., "Activities of Silicon and Carbon in the Fe-C-Si Liquid System", *Iron Making*, Conf. Proc., 48, 83–88 (1989) as quoted in [1992Rag]

[1989Eno] Enomoto, M., "Discussion of the Criticism of Heat-Treatment of an Fe-C-Si Alloy", *Metall. Trans. A-Phys. Metall. Mat*. Sci., **20**(2), 332–333 (1989) (Calculation, 11)

[1989Mur] Murakam, K., Okamoto, T., Miyamoto, Y., Nakazono, S., "Rapid Solidification and Self-Annealing of Fe-C-Si Alloys by Low-Pressure Plasma Spraying", *Mat. Sci. Eng. A -Struct. Mat. Prop. Microstr. Proc.*, **117**, 207–214 (1989) (Experimental, Mechan. Prop., Morphology, 14)

DOI: 10.1007/978-3-540-74196-1_12

[1989Vit] Vitusevich, V.T., Biletskii, A.K., Shimukhin, V.S., "Heat of Formation of C-Fe-Si Melts" (in Russian), *Rasplavy*, 3, 5–8 (1989) (Experimental, Thermodyn., 18)

[1990Dre] Dresler, W., "Activity of Silicon and Carbon in Liquid Iron-Silicon-Carbon Alloys", *Iron Steel.*, **17**(3), 95–100 (1990) (Thermodyn., Calculation, 20)

[1990Jan] Jansson, B.J., "Thermodynamic Calculations for Tungsten Carbide Tools with an Iron-Based Binder", *High Temp.-High Pres.*, **22**(4), 465–478 (1990) (Assessment, Calculation, Phase Diagram, 9)

[1990Rey] Reynolds, W.T., Jr., Liu, S.K., Li, F.Z., Hartfield, S., Aaronson, H.I., "An Investigation of the Generality of Incomplete Transformation to Bainite in Fe-C-X Alloys", *Metall. Trans. A*, **21A**(6), 1479–1491 (1990) (Experimental, Phase Relations, 56)

[1990Yeo] Yeo, D.H., Kim, D.I., Ra, H.Y., "The Microstructures and Mechanical Properties of Extruded Bars of Rapidly Solidified Fe-3.6% C-Si Alloy Powders" (in Korean), *J. Korean Inst. Met.*, **28**(11), 990–995 (1990) (Abstract)

[1991Lac] Lacaze, J., Sundman, B., "An Assessment of the Fe-C-Si System", *Metall. Trans. A*, **22A**, 2211–2223 (1991) (Experimental, Thermodyn., Phase Diagram, Assessment, 53)

[1991Nis] Nishizawa, T., Ishida, K., Ohtani, H., Kami, C., Suwa, M., "Experimental Study on Interaction Parameter for Carbon and Alloying Elements in Austenite and Ferrite", *Scand. J. Metall.*, **20**, 62 (1991) (Experimental, Thermodyn., Calculation, 34)

[1991Kim] Kim, S.W., Kim, S.H., Hahn, B.H., Park, Y.B., "The Effect of Retained Austenite to the Tensile Property of Intercritically Annealed Fe-0.2C-1.5Si Steel", *J. Korean Inst. Met. Mat.*, **29**(10), 967–972 (1991) (Abstract, Thermodyn., 11)

[1991Sly] Slyusarenko, S.I., Bukhalenko, V.V., Kutuzov, V.P., Rostovskaya, L.A., Romanova, A.V., "X-Ray Diffraction Study of Molten Alloys of Fe-C-Si" (in Russian), *Metallofizika*, **13**(4), 66–73 (1991) (Experimental, Crys. Structure, 10)

[1992Rag] Raghavan, V., "The C-Fe-Si (Carbon-Iron-Silicon) System", Phase Diagrams of Ternary Iron Alloys, Part 6A, Indian Institute of Metals, Calcutta, 523–534 (1992) (Review, Phase Relations, Phase Diagram, 89)

[1992Tan] Tanaka, T., Nasu, S., Nakagawa, K., Ishihara, K.N., Shingu, P.H., "Mechanical Alloying of Fe-C and Fe-C-Si Systems", *Mater. Sci. Forum*, **88–90**, 269–274 (1992) (Experimental, Crys. Structure, Morphology, 8)

[1993Sai] Saito, N., Abiko, K., Kimura, H., "Effect of Silicon on the Kinetics of Epsilon-Carbide Precipitation in High-Purity Fe-C Alloys", *Mat. Trans. JIM*, **34**(3), 202–209 (1993) (Experimental, Mechan. Prop., Calculation, 13)

[1993Sol] Solntzev, L.A., Shifrin, V.D., Miroshnichenko, O.N., Serhovetz, S.I., "A Study of High-Silicon Structural Constituents of Magnesium Iron Cast in Metal Molds", (in Russian), *Metally*, **4**, 102 (1993) (Experimental, Morphology, 5)

[1993Zhu] Zhukov, A.A., Shul'te, G.Yu., Yanchenko, A.B., "Silicon and Sulfur Effects on Activity of Carbon in Cementite Fe_3C", *Russ. J. Phys. Chem. (Engl. Transl.)*, **67**(12), 2235–2237 (1993), translated from *Zh. Fiz. Khim.*, **67**(12), 2480–2482 (1993) (Calculation, Phase Diagram, Phase Relations, Thermodyn., 14)

[1994Lee] Lee, Byeong-Joo, "Ternary Diffusion Coefficients and Phase Diagram in Fe-M-C Systems", *J. Korean Inst. Metal. Mater.*, **32**(2), 214–223 (1994) (Calculation, Thermodyn., Kinetics, 33)

[1994Lue] Luenenbuerger, A. Loehe, D. Macherauch, E., "Elastic Deformation and Phase Transformation of a Metastable Bainitic-Austenitic Fe-C-Si-Alloy", *Strength of Materials. Fundamental Physical Aspects of the Strength of Crystalline Materials*. ICSMA 10. Proceedings of the 10th International Conference, Japan Inst. Metals., Sendai, Japan, 311–314, (1994) (Abstract)

[1994Mch] McHale, A.E., "C-Si-Fe", in "Phase Equilibria Diagrams, Phase Diagrams for Ceramits", **10**, 13 (1994) (Review, Phase Diagram, Phase Relations, 6)

DOI: 10.1007/978-3-540-74196-1_12

[1994Prz] Przylecka, M., Kulka, M., Gestwa, W., "The Activity of Carbon in the Two-Phase Fields of the Fe-Cr-C, Fe-Mn-C and C-Fe-Si Alloys at 1173 K", *Mater. Sci. Forum*, **163–165**, 87–92 (1994) (Experimental, Thermodyn., 10)

[1994Wit] Witusiewicz, V.T., "Thermodynamic Properties of Liquid Alloys of 3d Transition Metals with Metalloids (Silicon, Carbon and Boron)", *J. Alloys Compd.*, **203**, 103–116 (1994) (Experimental, Thermodyn., 89)

[1995Kha] Khakimov, O.P., Tyagunov, G.V., Baryshev, E.E., Kostina, T.K., Baum BA., Silin, A.M., "Effect of Melt State on the Solidification of Fe-C-Si Alloy", *Russ. Metall.*, **6**, 9–12 (1995) (Experimental, 4)

[1996Gro] Gröbner, J., Lukas, H.L., Aldinger, F., "Thermodynamic Calculation of the Ternary System Al-Si-C", *Calphad*, **20**(2), 247–254 (1996) (Phase Diagram, Phase Relations, Thermodyn., Calculation, 37)

[1996Koc] Kocherzhinski, Yu.A., Kulik, O.G., "Equilibrium Phase Diagrams and Manufacture of Synthetic Diamond", *Powder Metall. Met. Cer.*, **35**(7–8), 470–483 (1996) (Calculation, Phase Relations, 37)

[1996Kon] Konygin, G.N., Yelsukov, E.P., Barinov, V.A., "Synthesis of Amorphous C-Fe-Si Alloys by Ball Milling of Fe-Si Powder in Toluene", Conference Proceedings. Vol. **50** International Conference on the Applications of the Mossbauer Effect. ICAME-95. Soc. Italiana di Fisica., Bologna, Italy, 157–60, (1996) (Abstract)

[1996Par] Park, J.S., Verhoeven, J.D., "Directional Solidification of White Cast Iron", *Metall. Mat. Trans. A-Phys. Metall. Mat. Sci.*, **27**(8), 2328–2337 (1996) (Experimental, Morphology, 25)

[1997Miz] Mizuno, M., Tanaka, I., Adachi, H., "Effect of Solute atoms on the Chemical Bonding of Fe_3C (Cementite)", *Philos. Mag. B*, **75**(2), 237–248 (1997) (Electronic Structure, Calculation, 28)

[1998Cha] Chang, L.C., "Carbon Content of Austenite in Austempered Ductile Iron", *Scr. Mater.*, **39**(1), 35–38 (1998) (Calculation, Experimental, Phase Relations, 21)

[1998Lac] Lacaze, J., Gerval, V., "Modelling of the Eutectoid Reaction in Spheroidal Graphite Fe-C-Si Alloys", *ISIJ International*, **38**(7), 714–722 (1998) (Theory, Calculations, Phase Relations, 36)

[1998Lim] Lima, M.S.F., Gilgien, P., Kurz, W., "Microstructure Selection in Laser Remelted Fe-C-Si Alloys", *Z. Metallkd.*, **89**(11), 751–757 (1998) (Experimental, Phase Relations, 21)

[1998Mie] Miettinen, J., "Reassessed Thermodynamic Solution Phase Data for Ternary C-Fe-Si System", *Calphad*, **22**(2), 231–256 (1998) (Calculation, Assessment, Thermodyn., Phase Relations, 36)

[1998Sun] Sun, H.P., Mori, K., Sahajwalla, V., Pehlke, R.D., "Carbon Solution in Liquid Iron and Iron Alloys", *High Temp. Mater. Proc.*, **17**(4), 257–270 (1998) (Experimental, Kinetics, 22)

[2000Bor] Borgenstam, A., Engstroem, A., Hoeglund, L., Agren, J., "DICTRA, a Tool for Simulation of Diffusional Transformations in Alloys", *J. Phase Equilib.*, **21**(3), 269–280 (2000) (Calculation, Kinetics, Thermodyn., 59)

[2000Fen] Fenstad, J., "Liquidus Relations and Thermochemistry within the System Fe-Mn-C-O", Thesis of Dept. Mater. Elchem., NTNU, 1–126, (2000) (Experimental, Phase Relations, Thermodyn.)

[2001Fen] Fenstad, J., Tuset, J.Kr., "The Binary Diagrams within the System Fe-Mn-C-O, and the Thermal Properties of Elemental Manganese", *INFACON 9: Proceedings of the International Ferro-Alloys Congress*, June 2001, Quebec, Canada, **9**, (2001) (Experimental, Phase Relations, Thermodyn., 25)

[2001Kag] Kagawa, A., Imaizumi, T., Mizumoto, M., "Pressure-Induced Transition from Graphite Eutectic to Carbide Eutectic in Iron-Carbon-Silicon Alloys", *Mat. Trans.*, **42**(7), 1385–1391 (2001) (Experimental, Morphology, Mechan. Prop., 20)

[2001Ono] Ono-Nakazato, H., Morita, Y., Tamura, K., Usui, T., Marukawa, K., "Oxidation Behaviour of Silicon and Carbon in Molten Iron-Carbon-Silikon Alloys with Carbon Dioxide", *ISIJ Int.*, **41**, S61–S65 (2001) (Experimental, Phase Relations, Thermodyn., 13)

DOI: 10.1007/978-3-540-74196-1_12

[2001Sch] Schlesinger, M.E., Xiang, Q., "Enthalpies of Mixing in Fe-C-Si Melts", *J. Alloys Compd.*, **321**(2), 242–247 (2001) (Assessment, Calculation, Thermodyn., 15)

[2001The] Theodoropoulou, N., Hebaed, A.F., Chu, S.N.G., Overberg, M.E., Abernathy, C.R., Pearton, S.J., Wilson, R.G., Zavada, J.M., "Magnetic Properties of Fe- and Mn-Implanted SiC", *Electrochem. Solid State Lett.*, **4**(12), G119–G121 (2001) (Experimental, Magn. Prop., 20)

[2001Ume] Umemoto, M., Liu, Z.G., Masuyama, K., Tsuchiya, K., "Influence of Alloy Additions on Production and Properties of Bulk Cementite", *Scr. Mater.*, **45**(4), 391–397 (2001) (Crys. Structure, Experimental, Mechan. Prop., Phase Relations, Phys. Prop., 13)

[2002Kag] Kagawa, A., "Pressure-Induced Stable to Metastable Transition in Eutectic Alloys", *Rep. Faculty Eng.*, *Nagasaki Uni*., **32**(58), 191–197 (2002) (Experimental, Mechan. Prop., 13)

[2003Oga] Ogawa, H., Miura, H., "Compositional Dependence of Amorphization of M-C-Si (M= Fe, Co or Ni) Materials by Mechanical Alloying", *J. Mat. Proc. Tech.*, **143–144**, 256–260 (2003) (Crys. Structure, Experimental, Phase Relations, 14)

[2004Aar] Aaronson, H.I., Reynolds, W.T., Purdy, J.R., "Coupled-Solute Drag Effects on Ferrite Formation in Fe-C-X Systems", *Metall. Mat. Trans. A*, **35A**, 1187–1210 (2004) (Review, 148)

[2004Fu] Fu, W., Furuhara, T., Maki, T., "Effect of Mn and Si Addition on Microstructure and Tensile Properties of Gold-Rolled and Annealed Pearlite in Eutectoid Fe-C Alloys", *ISIJ Int.*, **44**(1), 171–178 (2004) (Crys. Structure, Experimental, Mechan. Prop., Morphology, Phys. Prop., 32)

[2004Sai] Saitoh, H., Yoshinaga, N., Ushioda, K., "Influence of Substitutional Atoms on the Snoek Peak of Carbon in b.c.c. Iron", *Acta Mater.*, **52**(5), 1255–1261 (2004) (Experimental, Mechan. Prop., 37)

[2005Liu] Liu, X., Takamori, S., Osawa, Y., Yin, F., "Low-Temperature Damping Behavior of Cast Iron with Aluminum Addition", *J. Mater. Sci.*, **40**(7), 1773–1775 (2005) (Experimental, Mechan. Prop., Phys. Prop., 12)

[2005Mec] Meco, H., Napolitano, R.E., "Liquidus and Solidus Boundaries in the Vinicity of Order-Disorder Transitions in Fe-Si System", *Scr. Mater.*, **52**, 221–226 (2005) (Experimental, Calculation, Phase Diagram, Thermodyn., 30)

[2005Tek] Tekmen, C., Toparli, M., Ozdemir, I., Kusoglu, I.M., Onel, K., "High Temperature Behaviour of H13 Steel", *Z. Metallkd.*, **96**(12), 1431–1433 (2005) (Experimental, Mechan. Prop., Morphology, Phase Relations, 7)

[2006Aar] Aaronson, H.I., Reynolds, W.T., Purdy, Jr. G.R., "The Incomplete Transformation Phenomenon in Steel", *Metall. Mater. Trans. A*, **37A**, 1731–1745 (2006) (Review, Morphology, Phase Relations, 89)

[2006MSIT] "C-Fe (Carbon Iron)", *Diagrams as Published* in MSIT Workplace, Effenberg, G. (Ed.), MSI, Materials Science International Services GmbH, Stuttgart; Document ID: 30.13598.1.20, (2006) (Phase Diagram, Phase Relations, Crys. Structure, 2)

[2006Yel] Yelsukov, E.P., Maratkanova, A., Lomayeva, S.F., Konygin, G.N., Nemtsova, O.M., Ul'yanov, A.I., Chulkina, A.A., "Structure, Phase Composition and Magnetic Properties of Mechanically Alloyed and Annealed Quasibinary $Fe_{70}Si_xC_{30-x}$ Alloys", *J. Alloys Compd.*, **407**(1–2), 98–105 (2006) (Experimental, Magn. Prop., Crys. Structure, 33)

[Mas2] Massalski, T.B. (Ed.), Binary Alloy Phase Diagrams, 2nd edition, ASM International, Metals Park, Ohio (1990)

[V-C2] Villars, P. and Calvert, L.D., *Pearson's Handbook of Crystallographic Data for Intermetallic Phases*, 2nd edition, ASM, Metals Park, Ohio(1991)

DOI: 10.1007/978-3-540-74196-1_12

Carbon – Iron – Titanium

Nathalie Lebrun, Pierre Perrot

Introduction

The first tentative diagrams were drawn by [1917Vog, 1925Tam, 1938Tof1] in the iron rich corner and show that titanium decreases the stability domain of austenite and accelerates the carbon graphitization, which explain the perlite decomposition. The ability of titanium to form carbide was also well recognized. The state of the art was reviewed by [1939Nor, 1949Jae]. Unfortunately, the proposed ternary diagram rests on inaccurate knowledge of the Fe-Ti binary. Careful examination done by [1942Hum] showed that titanium steels react easily with nitrogen to give titanium nitrides impurities which have to be taken into account when investigating phase equilibria between C, Fe and Ti. More recent reviews of the ternary system were presented by [1985Maz, 2003Rag]. Calphad assessments were carried out mainly by [1988Oht, 2001Lee]. The most recent experimental results on the crystal structure, phase equilibria and thermodynamics are gathered in Table 1.

Binary Systems

The C-Fe phase diagram is mainly accepted from [2006MSIT]. The properties of metastable carbides such as $Fe_{2.2}C$ (Haegg carbide) and $Fe_{2.4}C$ (known as "ε carbide") are well discussed by [1972Chi] who proposed also simple expressions for carbon activities in austenite and thermodynamic properties of carbides, which may be useful because they are in good agreement with more recent and more sophisticated relationships.

Numerous thermodynamic assessments have been recently done for the C-Ti system [1995Alb, 1996Jon, 1996Sei, 1999Dum1, 2001Lee, 2003Fri]. The more recent assessment leads to a better fit of high temperature heat capacity measurements than all previous studies. The phase diagram of [2003Fri] is reproduced with the same accuracy as given by [1999Dum1] and gives a better description of the experimental data than previous assessments. Consequently, it has been accepted and is reproduced in Fig. 1.

The Fe-Ti has been carefully reviewed by [1981Mur] and thermodynamically assessed by [1998Dum]. Although Fe-Ti, shown in Fig. 2, is accepted from [1998Dum], new experimental data are needed in order to improve the thermodynamic assessment. As the TiFe has been taken in [1998Dum] as stoichiometric, the homogeneity range of TiFe has been taken from [1981Mur].

Solid Phases

No ternary compound has been discovered. All structural data for unary and binary phases are indicated in Table 2.

Quasibinary Systems

The vertical section Fe-TiC for the stable system has first been investigated in [1952Edw, 1956Ere] and more precisely in the Fe rich part (up to 7 mass% TiC). A ternary reaction L ⇌ TiC + (γFe) has been located experimentally at 1460°C and 3.8 mass% TiC (3.425 at.% Ti and 3.425 at.% C). More recent data of [1975Fre, 1977Mal] indicate a temperature of 1380 ± 20°C with a lower composition of around 8 mol% TiC. Since reaction with crucible could not be excluded in the work of [1975Fre], the vertical section proposed by [1956Ere] and confirmed by the Calphad assessment of [1988Oht, 2001Lee] has been selected here. The accepted temperature and composition of the ternary reaction has been selected from [1998Jon, 2003Rag] (reaction e_2 in Table 3). The accepted vertical section is depicted in Fig. 3. Modifications have been done in the Fe rich side since the (δFe) and (γFe) phases exist according to the accepted stable liquidus surface. Another solid state reaction has been measured by [1956Ere] inside the ternary system: (γFe) + TiC ⇌ (αFe) at 920°C and 0.15 mass% TiC (0.14 at.% Ti and 0.14 at.% C). Another reaction has been suggested at 768°C.

DOI: 10.1007/978-3-540-74196-1_13

Since no details have been reported in the experimental study this last reaction has not been retained in this assessment. More experimental data are needed. TiC seems to react hardly with liquid iron, even at 1800°C [1967Sto].
The same vertical section has been calculated for the metastable system [1999Dum2] using thermodynamic assessments. This vertical section is not in agreement with the accepted metastable liquidus surface done by [1969Jel], as well as the accepted isothermal sections. Consequently this calculated vertical section has not been retained in this assessment. Experimental investigations are needed.

Invariant Equilibria

[1957Mur, 1998Jon] proposed identical invariant reactions in the TiC-$TiFe_2$-Fe part of the system. Large discrepancies have been observed along the binaries C-Fe and Fe-Ti. The invariant reactions from [1998Jon] are more reliable than those reported by [1957Mur]. Based in these more recent experimental data, [1998Jon] computed the invariant reactions with the simultaneous presence of graphite and cementite. The C-Fe phase diagram accepted here consists of two parts: one including stable equilibria and another one including metastable equilibria. Consequently, [2003Rag] proposed in his review a new reaction scheme consistent with the stable C-Fe phase diagram and the reaction temperatures were taken from those calculated by [1998Jon]. Large discrepancies have been observed regarding the U type reaction ($L + (\gamma Fe) \rightleftharpoons TiC + (\alpha\delta Fe)$) leading to a different pseudo-eutectic reaction: $L \rightleftharpoons TiC + (\gamma Fe)$ in [1998Jon] and $L \rightleftharpoons TiC + (\alpha\delta Fe)$ in [1956Ere, 1957Mur, 1998Jon]. General agreement has been observed regarding the compositions and the temperatures of the other ternary reactions. The careful thermodynamic assessment has been retained in this assessment. Consequently, all the data on ternary reactions indicated in Table 3 are based on [1998Jon, 2003Rag].
A reaction scheme is proposed by [1969Jel] for the metastable system. Three U type ternary reactions have been reported. The corresponding ternary reactions mainly based on [1969Jel] are reported in Table 4. The reaction scheme regarding the stable and the metastable ternary reactions is depicted in Figs. 4a and 4b respectively.

Liquidus, Solidus and Solvus Surfaces

Melting determination have been made by [1957Mur] without any indication of the invariant reaction temperatures except in the TiC-Fe-C partial ternary region. Later [1998Jon] proposed a similar liquidus surface showing a ridge line along TiC-Fe on the liquidus surface. The liquidus temperature close to TiC is 60°C higher in [1957Mur] than the accepted congruent melting point of TiC (3067°C). Consequently these experimental results were not considered in the computed stable liquidus surface thermodynamically assessed by [1998Jon]. The accepted liquidus surface in the Fe rich corner [1998Jon], has been reproduced in Fig. 5 and has been slightly modified in agreement with the binary systems. The liquidus surfaces of graphite and TiC dominate and the extensions of the other phases are limited. However the liquidus surfaces of ($\alpha\delta Fe$) and (γFe) exist. A maximum point exists along the valley which separates the (γFe) and TiC phases. Small addition of Ti on pure C-Fe eutectic alloys leads to a large decrease of the stable eutectic temperatures inside the ternary system up to 0.5 mass% Ti [1988Mag]. This was later confirmed in the review done by [2000Zhu].
The constitution of the ternary system Fe-Fe_3C-Fe_3Ti has been discussed theoretically from the binary systems [1917Vog] leading to the existence of a ternary eutectic inside the system. [1969Jel] measured the metastable liquidus surface up to 42 at.% C and 40 at.% Ti showing three ternary reactions. [1925Tam] noticed that the eutectic temperature of C-Fe increases with increasing titanium content: from 1130°C and 4.3 mass% C to 1180°C and 3.8 mass% C with 4 mass% titanium. More recently, [1988Mag] observed that small addition of Ti on pure C-Fe eutectic alloys leads to a slight decrease of the metastable eutectic temperatures inside the ternary system up to 0.5 mass% Ti. This was later confirmed in the review done by [2000Zhu]. Consequently the nature of the ternary reaction involving the (γFe), Fe_3C and TiC has been change from a U type to a E type to be in agreement with results of [1988Mag] as well as those of [1938Tof1, 1938Tof2] who found a ternary eutectic containing about 3.9 mass% C and 0.9 mass% Ti. The liquidus surface shown in Fig. 6 is in agreement with the binary systems and exhibits a considerable extension of ($\alpha\delta Fe$), (γFe) and cementite primary crystallization fields.

DOI: 10.1007/978-3-540-74196-1_13

Small addition of Ti on pure C-Fe eutectic alloys leads to a decrease of the stable (–18.7 K·(at.%) $^{-1}$) and the metastable (–17.5 K·(at.%)$^{-1}$) eutectic temperatures inside the ternary system up to 0.5 mass% Ti [1988Mag]. The decrease is more pronounced in the stable system [2000Zhu] which seems to be the reason why Ti in cast iron is considered as a weak graphitizer.

Isothermal Sections

In the solid state, TiC was shown to be in equilibrium with TiFe, $TiFe_2$, Fe and Fe_3C [1956Ere, 1985Ram]. The solubility of TiC in (γFe) is negligible, less than 0.5 mass% TiC (0.72 at.% TiC) at 1250°C [1952Edw]. [1992Bal1] measured the solubility of carbide TiC in (γFe) from 1000°C to 1200°C using hydrogen-methane gas mixtures. There is a minimum in the solubility curve (0.02 mass% Ti or 0.023 at.% Ti and 0.4 mass% C or 1.83 at.% C at 1000°C) and at higher carbon content, the solubility increases with increasing carbon content and temperature. Their results are in agreement with those reported by [1988Oht] despite the slight shift towards the low values. Nevertheless the tendency and the position of the minimum solubility are almost the same. Later [1998Jon, 1999Dum2, 2001Lee] carried out a detailed thermodynamic assessment and computed the solubility of TiC in (γFe) at 1000°C, 1100°C and 1200°C in the Fe rich corner, showing a very close agreement with the experimental data of [1988Oht, 1992Bal1]. Results reported in Figs. 7 and 8 are taken from the review of [2003Rag].

Isothermal sections were experimentally investigated by [1957Mur, 1980Sar]. A large Fe solubility in TiC (15 mass% Fe or 8.7 at.% Fe) was suggested by [1957Mur] which has been disproved by later investigators. [1985Ram] found at 1000°C a maximum solubility of Fe in TiC of 1.3 ± 0.2 at.% Fe and the maximum carbon solubility in the TiFe and $TiFe_2$ phases was reported to be 1.7 ± 0.4 and 1.4 ± 0.3 at.% C respectively. From a careful thermodynamic assessment, [1999Dum2] calculated the isothermal section at 1600°C showing the phase equilibria involving liquid, graphite and TiC in the Fe rich corner. Despite the fact that the liquidus limit fits well with most of the experimental data reported in [1999Dum2], large discrepancies have been observed with the calculated isotherm proposed by [1989Fra, 1999Fra] and reproduced by [1994McH]. Since the liquidus border is supported by experimental data by [1990Guo] in [1999Dum2], the isothermal section shown in [1989Fra] was not retained in this assessment.

Others computed isothermal sections are available in the literature: at 25°C [2002Liu], at 1000°C, 1200°C, 1400°C [1998Jon] and 1500°C [1999Fra]. The TiC phase is involved in the equilibria with all the other binary phases at temperatures from 1000 to 1400°C. The isothermal section at 1500°C done by [1999Fra] does not include the (αδFe) phase which normally exists at this temperature according to the binaries Fe-Ti and Fe-C systems. Consequently, this isothermal section has not been retained here. The calculated isothermal sections at 1000°C and 1400°C proposed by [1998Jon] reproduce well the experimental data except the homogeneity range of the binary phases which were not taken into account. Moreover, the measured isothermal section proposed in the review of [1985Maz] does not exhibit phase equilibria involving the $TiFe_2$ and the graphite phases. Consequently the isothermal section at 1400°C proposed by [1998Jon] has been modified to be in agreement with those of [1985Maz] and the accepted binary systems. The isothermal section at 1000°C is taken from [2003Rag] and based on the calculations from [1998Jon]. The isothermal sections at 25°C, 1200°C and 1800°C are taken from [2002Liu], [1998Jon] and [1998Jon] respectively. The isothermal section proposed at 1260°C by [1998Jon] has not been retained in this report since the cementite Fe_3C appears as a metastable phase. All the accepted isothermal sections for the stable system are reported in Figs. 9 to 14.

[1938Tof1, 1938Tof2] measured metastable isothermal sections from 700°C to 1100°C. Later, [1981Bra] proposed schematic isothermal sections at 900, 1000, 1100°C in the Fe rich corner involving the metastable cementite and deduced from activity measurements. A more recent careful thermodynamic assessment [1988Oht] calculated isothermal section from 800°C to 1500°C. General agreement has been observed also with the binary edges. The more recent results have been retained and are reproduced in Figs. 15 to 19. The isothermal section at 1400°C has not been retained since the graphite phase does not crystallize at this temperature in the C-Fe metastable binary system.

All the isothermal sections have been slightly modified to be in agreement with the accepted binary systems.

DOI: 10.1007/978-3-540-74196-1_13

Temperature – Composition Sections

Numerous vertical sections have been calculated for the stable system (Fe-5C (at.%), $Fe_{82.48}C_{17.52}$-$Fe_{82.52}C_{17.28}$ (at.%)) [1998Jon]) using careful thermodynamic assessments.
The computed vertical section at 5 at.% C done by [1998Jon] reproduced well the experimental data done by [1998Jon]. It is shown in Fig. 20.
[1938Tof1, 1938Tof2, 1947Nor, 1988Oht] presented a series of metastable vertical sections parallel to the C-Fe side (from 0 to 5.8 mass% Ti) determined from measurements [1938Tof1, 1938Tof2, 1947Nor] and calculation [1988Oht]. The data of [1938Tof1, 1938Tof2] indicated a much higher solubility of TiC than found in more recent investigations done by [1947Nor, 1988Oht, 1992Bal1]. Consequently the data of [1938Tof1, 1938Tof2] were not retained in this assessment. General good agreement have been observed concerning the phase fields between 900 and 600°C. Some recent vertical sections have been reported in Figs. 21 to 23.

Thermodynamics

The interaction coefficient between C and Ti in liquid iron has been evaluated around 1600°C by [1990Guo, 1996Fra1, 2001Wan1, 2004Red] and may be expressed by the relationship proposed by [1990Guo]:

$$\varepsilon_C^{(Ti)} = \varepsilon_{Ti}^{(C)} = (\partial \ln \gamma_C / \partial x_{Ti}) = -5.374 - (8070 / T),$$

where γ_C = [x_C in pure Fe] / [x_C in the alloy]. This value gives $\varepsilon_C^{(Ti)} = -9.68$ at 1600°C, which differs from $\varepsilon_C^{(Ti)} = -11.93$ accepted by [2004Red].
The interaction coefficient of Ti in Fe saturated with C, expressed by
$e_C^{(Ti)} = (\partial \log_{10} f_C / \partial \{\%Ti\})$ with f_C = {% C in pure Fe} / {% C in the alloy} where {% C} and {% Ti} represents the C and Ti content of the alloy in mass%, was measured by [1958Del] in liquid Fe at 1600°C: $e_C^{(Ti)} = 5.6 \cdot 10^{-3}$.
The interaction coefficient between C and Ti in γ austenite has been calculated by [1968Zup] from a statistical model and found to be $\varepsilon_C^{(Ti)} = \varepsilon_{Ti}^{(C)} = -27.35$ at 1000°C, which must be compared to the experimental value of – 65 [1983Vre]. A thermodynamic analysis carried out by [1986Bal] leads to the expression $\varepsilon_C^{(Ti)} = -79650 / T = -62$ at 1000°C. From a more critical analysis of experimental data, [1992Bal1, 1992Bal2] propose, between 1000 and 1200°C:

$$\varepsilon_C^{(Ti)} = (2.5 \pm 1.0) - (83400 \pm 4000) / T.$$

The interaction coefficient $e_C^{(Ti)}$ determined from carbon solubilities measurements at 1300-1500°C [1981Sum] is given by the relationship:

$$e_C^{(Ti)} = -0.072 - (221 / T)$$

$\varepsilon_C^{(Ti)}$ and $e_C^{(Ti)}$ are negative in both liquid and γ phases, which means that Ti increases the carbon solubility of the alloy as shown in Fig. 24 [1981Sum, 1995Bou].
The carbon activities in the (αFe), (γFe) and (α + γ) domains, investigated by equilibrium measurements at 900°C under (CH_4+H_2) atmospheres [1981Bra] are shown in Fig. 25. A closer investigation of the γ field [1988Bal, 1988Oht, 1992Bal1] shows that the Ti solubility presents a minimum towards 0.5 mass% C between 1000 and 1200°C. The same phenomenon is observed in the liquid phase towards 2 mass% C between 1400 and 1500°C [1988Oht, 1989Fra].

Notes on Materials Properties and Applications

Main experimental investigations are gathered in Table 5. TiC is one of the most suitable compounds for the production of ceramic-metal composite materials. These materials have unique characteristics because they can be annealed, worked by normal machining techniques and hardened by subsequent heat treatment [1996Fra2]. The effect of Ti on steels has since long been recognized [1947Nor] as the result of the strong affinity between Ti and C, the shrinking of the γ region with the increase of Ti and the hardening of ferrite by precipitation of TiC [1970Zbo]. The presence of Ti in steels, even in small amount allows a substantial increase of the hardness of steels. The Fe matrix-TiC composites are characterized by a lower coefficient of

DOI: 10.1007/978-3-540-74196-1_13

friction and lower wear rates than other carbide reinforced material due to unique morphology of the TiC particles: they act as localized bearing surfaces during wear. According to [1996Pop], TiC is one of the most stable carbides in iron during sintering, practically insoluble in iron, and it is not forming ternary phases. The optimal content of titanium carbide in the matrix is about 10 vol.%, that will improve hardness, wear resistance and tensile properties of Fe-TiC composites.

Precipitation of TiC particles in an iron matrix are generally obtained from the melt [1970Zbo, 1992Ter, 2006Wu] following by an annealing. Levitation method [1992Ter], mechanical alloying [2001Wan2], combustion synthesis [2002Liu, 2004Zha] and *in situ* reactions between Fe-Ti and C-Fe alloys [2002Ren, 2003Mei] are alternative methods and may also be used. A rapid solidification [1996Pop] allows the formation of submicronic particles of TiC in the Fe matrix. The processes based on liquid phase synthesis are easier to control and lead to more homogeneous materials [2002Per]. It must be pointed out that the solubility of TiC in iron and its hardness depend strongly on its stoichiometry (a 50% increase of the Rockwell hardness is observed from $TiC_{0.6}$ to TiC and the excess of Ti in $TiC_{0.6}$ is transferred in Fe). As a consequence, it is practically impossible to harden composites prepared with titanium carbide of low carbon concentration [1996Fra2, 2003Mei]. Experimental observations [1999Fra] show that non stoichiometric TiC_x tends towards stoichiometry by reacting with the C of the metallic matrix. Ti may have the drawback to react with nitrogen forming TiN which gives a complete solid solution with TiC [1948Gol]. Small TiC particles act as dislocation traps [1975Dun] and thus significantly increase the coarsening kinetics of fine particles. Fe-TiC mixtures may be used to prepare magneto-abrasive materials [1983Pol] with high service properties which may be used in steel working.

Carbide coatings found their applications to improve the working properties of cutting tools. Their microhardness and plasticity are basically determined by the composition of the carbide whereas the fracture toughness is determined by the structure of the coating [2000Bya].

Although Ti is considered as a rather poor cementite stabilizer in steels, [2001Ume] found that the addition of 5 % Ti in cementite leads to the formation of TiC and αFe owing the strong affinity of Ti for C. The precipitation of TiC may be used to improve the mechanical properties, the corrosion and burn resistance of Ti as shown in [2003Che].

Miscellaneous

Rapid quenching of C-Fe-Ti alloys from the melt by splat cooling [1980Sar] produces stable phases such as ferrite, austenite, TiC and metastable phases such as cementite, martensite and a hexagonal ε phases. Austenite decomposes in the temperature range 200-400°C whereas TiC precipitates at 700°C and coarsens slowly at 700-800°C.

Hot corrosion of C-Fe-Ti alloys has been investigated by [1989Mal] at 700-850°C under Na_2SO_4 and NaCl brines. Hot corrosion rate increases with the temperature and with the carbon content at least up to 0.4 mass% C.

The explosive welding of metals is widely used for the cladding of steel with titanium [1990Xia]. The resulting composite is mainly used for the fabrication of corrosion-resistant reactors for the chemical industry.

Thin films prepared by sputtering are excellent soft magnetic materials [1991Has] combining a high saturation flux density together with a high thermal stability. Laser alloying of TiC on an iron surface forms (αFe), Fe_3C, TiC, martensite, plus two unknown titanium carbides (Ti,Fe)C [1995Ari] whose parameters are given in Table 2.

The transformation Ferrite ⇌ Carbide + Austenite and the influence of an α stabilizer has been observed in [1999Mov].

Calphad assessments [1988Oht, 2001Lee] have been used by [2002Liu] to investigate the influence of Fe content and C/Ti ratio on the adiabatic temperature and equilibrium phase. The (Fe+TiC) equilibrium may be obtained by combustion synthesis with Fe content up to 55 mass%. The graphite content varies from 1 % to 16% when the C/Ti atomic ratio varies from 1 to 1.4 at low combustion temperatures.

An analysis of the carbon activity measurements in the γ austenite made by [1992Bal1] was carried out by [2004Sho] for modelling the γ(Fe,Ti)C solid solution. The model in which Ti atoms are bonded to C was proved to be more realistic than that in which Ti atoms are randomly distributed over the metal sublattice and more in agreement with Ti-C interactions stronger than C-Fe interactions.

DOI: 10.1007/978-3-540-74196-1_13

Table 1. Investigations of the C-Fe-Ti: Phase Diagrams and Thermodynamics

Reference	Method/Experimental Technique	Temperature/Composition/Phase Range Studied
[1952Edw]	Micrographic observation	1250°C, Fe-TiC joint
[1956Ere]	Metallographic and X-ray analysis	700-1500°C, Fe-TiC diagram
[1957Mur]	X-ray and thermal analysis	500-1500°C, liquidus determination
[1958Del]	Ti activity measurements	1500-1600°C, < 6 mass% C
[1967Sto]	X-ray and metallography	1800°C, TiC in liquid iron
[1969Jel]	X-ray and metallography	500-1500°C, < 50 at.% C
[1975Fre]	Metallography, DTA analysis	1300-1500°C, Fe-TiC diagram
[1981Bra]	C activity by equilibrium under CH_4/H_2 atmospheres	900-1100°C, < 1 at.% Ti, < 3 at.% C
[1981Sum]	Carbon solubility measurements, microscopy, chemical analysis	1300-1500°C, < 0.8 at.% Ti, < 5.3 at.% C
[1983Vre]	C equilibria under CH_4/H_2 atmospheres	1000°C, < 1 mass% Ti
[1985Ram]	Electron probe microanalysis (EPMA), optical microscopy	1000°C, < 15 at.% C, diffusion path
[1988Bal]	Carbon solubility measurements, Gas (CH_4/H_2) equilibration technique	1000-1200°C, < 1 mass% Ti, < 0.2 mass% C
[1988Mag]	Eutectic temperatures measurements by thermal analysis	1140-1160°C, < 0.2 mass% Ti, 4.3 mass% C
[1990Guo]	Ti activity measurement	1600°C, < 2.1 mass% Ti, < 2.5 mass% C
[1990Xia]	Optical microscopy, EPMA	650-1000°C, Fe-Ti-TiC triangle, diffusion path measurements
[1992Bal1]	Carbon solubility measurements, Gas (CH_4/H_2) equilibration technique	1000-1200°C, < 1 mass% Ti, < 2 mass% C
[1999Fra]	Scanning electron microscopy, porosity measurements	1500-1600°C, (Fe,C)-TiC_x reactions

Table 2. Crystallographic Data of Solid Phases

Phase/ Temperature Range [°C]	Pearson Symbol/ Space Group/ Prototype	Lattice Parameters [pm]	Comments/References
(C)gr < 3827	*hP*4 $P6_3/mmc$ C (graphite)	a = 246.12 c = 670.9	pure C at 25°C [Mas2, V-C2] sublimation point

(*continued*)

DOI: 10.1007/978-3-540-74196-1_13

Phase/ Temperature Range [°C]	Pearson Symbol/ Space Group/ Prototype	Lattice Parameters [pm]	Comments/References
(C)d	*cF*8 *Fd*3*m* C (diamond)	*a* = 356.69	at 25°C, 60 GPa [Mas2]
(αδFe) (αFe) < 912°C	*cI*2 *Im*3*m* W	*a* = 286.65	pure Fe at 20°C [Mas2, V-C2] dissolves up to 0.096 at.% C at 740°C, 0.40 at.% C at 1493°C and 10 at.% Ti at 1289°C
(δFe) 1538 - 1394		*a* = 293.15	
(γFe) 1394 - 912	*cF*4 *Fm*3*m* Cu	*a* = 364.67	at 915°C [Mas2, V-C2] dissolves up to 9.06 at.% C at 1153°C and 0.8 at.% Ti at 1150°C [1998Dum]
(εFe)	*hP*2 $P6_3/mmc$ Mg	*a* = 246.8 *c* = 396.0	at 25°C, 13 GPa [Mas2]. Triple point (αFe)-(γFe)-(εFe) at 8.4 GPa, 430°C
(βTi) 1670 - 882	*cI*2 *Im*3*m* W	*a* = 330.65	[Mas2] dissolves up to 22 at.% Fe at 1085°C and up to 0.8 at.% C at 1647°C [1996Sei]
(αTi) < 882	*hP*2 $P6_3/mmc$ Mg	*a* = 295.06 *c* = 468.35	[Mas2] dissolves up to 0.05 at.% Fe at 595°C [1998Dum] and 1.5 at.% C at 920°C [1996Sei]
TiFe < 1317	*cP*2 *Pm*3*m* CsCl	*a* = 298.80	from 49.7 to 52.5 at.% Ti [1981Mur]
$TiFe_2$ < 1427	*hP*12 $P6_3/mmc$ $MgZn_2$	*a* = 478.57 *c* = 779.9	from 30.4 to 41.10 at.% Ti [1998Dum] parameter for 26.5 at.% Fe at 1000°C [1981Mur]
α' (Fe,C)	*tI*4 *I*4/*mmm*		martensite, metastable [Mas2]
θ, Fe_3C 1252 - 230	*oP*16 *Pnma* Fe_3C	*a* = 452.48 *b* = 508.96 *c* = 674.43	[1972Chi, 1997Miz] Cementite, high pressure phase. Curie point at 214°C
$\chi Fe_{2.2}C$ (or χFe_5C_2) < 230	*mC*28 *C*2/*c* B_2Pd_5	*a* = 1156.2 *b* = 457.27 *c* = 505.95 β = 97.74°	[1972Chi, V-C2] "Haegg carbide", metastable but more stable than cementite below 230°C
$\varepsilon Fe_{2.4}C$	*hP** $P6_322$ $\varepsilon Fe_{2.4}C$	*a* = 275.2 *c* = 435.3	[1972Chi, 1985Maz] "ε carbide", metastable. Curie point at 370°C

(*continued*)

DOI: 10.1007/978-3-540-74196-1_13

Phase/ Temperature Range [°C]	Pearson Symbol/ Space Group/ Prototype	Lattice Parameters [pm]	Comments/References
η Fe_2C	*oP*6 *Pnnm* Fe_2C	*a* = 470.4 *b* = 431.8 *c* = 283.0	[V-C2] metastable
TiC < 3067	*cF*8 *Fm*3*m* NaCl	*a* = 428.5 *c* = 432.8	31 at.% C at 1645°C 50 at.% C at 2776°C [1996Art]
(Ti,Fe)C	*t***	*a* = 411 ± 4 *c* = 519 ± 6	Metastable, laser alloying [1995Ari]
(Ti,Fe)C	*o***	*a* = 426 ± 2 *b* = 436 ± 1 *c* = 465 ± 0.3	Metastable, laser alloying [1995Ari]

Table 3. Invariant Equilibria for the Stable System C-Fe-Ti

Reaction	*T* [°C]	Type	Phase	Composition (at.%)		
				C	Fe	Ti
L ⇌ TiC + (γFe)	1475	e_2	L	3.09	93.82	3.09
			TiC	47.10	0.00	52.90
			(γFe)	0.54	98.85	0.70
L+(γFe) ⇌ TiC + (δFe)	1451	U_1	L	2.33	93.74	3.93
			(δFe)	0.24	98.52	1.24
			TiC	46.80	0.00	53.20
			(γFe)	0.77	97.92	1.31
L ⇌ TiC + $TiFe_2$	1427	e_3	L	0.50	66.10	33.40
			TiC	41.60	0.10	58.30
			$TiFe_2$	0.00	66.00	34.00
L + $TiFe_2$ ⇌ TiC + TiFe	1318	U_2	L	0.20	48.40	51.40
			$TiFe_2$	0.00	60.90	39.10
			TiC	38.90	0.00	61.10
			TiFe	0.00	50.00	50.00
L ⇌ TiC + (δFe) + $TiFe_2$	1289	D_1	L	0.20	83.40	16.40
			TiC	44.00	0.00	56.00
			(δFe)	0.10	88.80	11.30
			$TiFe_2$	0.00	69.40	30.60
L ⇌ TiC + (γFe) + (C)gr	1150	E_1	L	17.56	81.52	0.92
			TiC	49.20	0.20	50.60
			(γFe)	10.30	89.20	0.50
			(C)gr	100.00	0.00	0.00

(*continued*)

DOI: 10.1007/978-3-540-74196-1_13

Reaction	T [°C]	Type	Phase	Composition (at.%)		
				C	Fe	Ti
L ⇌ TiC + (βTi) + TiFe	1072	E_2	L	0.10	28.10	71.80
			TiC	35.80	0.00	64.20
			(βTi)	0.00	0.00	100.00
			TiFe	0.00	50.00	50.00
TiC + (γFe) ⇌ (αFe) + (C)gr	~750	U_3	TiC	~50.00	~0.00	~50.00
			(γFe)	~0.00	~100.00	~0.00
			(αFe)	~0.00	~100.00	~0.00
			(C)gr	~100.0	~0.00	~0.00
(βTi) + TiC ⇌ (αTi) + TiFe	~590	U_4	(βTi)	~0.00	~0.00	~100.00
			(αTi)	~0.00	~0.00	~100.00
			TiFe	~0.00	~50.00	~50.00
			TiC	~50.00	~0.00	~50.00

Table 4. Invariant Equilibria for the Metastable System C-Fe-Ti

Reaction	T [°C]	Type	Phase	Composition (at.%)		
				C	Fe	Ti
L ⇌ TiC + $TiFe_2$	1470	e_2	L	8.90	55.15	35.95
			TiC	~50.00	~0.00	~50.00
			$TiFe_2$	~0.00	~66.67	~33.33
L + TiC + $TiFe_2$ ⇌ (δFe)	1340	P_1	L	5.66	80.27	14.07
			TiC	~50.00	~0.00	~50.00
			$TiFe_2$	~0.00	~66.67	~33.33
			(δFe)	~0.00	~100.00	~0.00
L ⇌ TiC + Fe_3C	1300	e_3	L	33.02	50.89	16.09
			TiC	~50.00	~0.00	~50.00
			Fe_3C	~25.00	~75.00	~0.00
L + (δFe) ⇌ TiC + (γFe)	1260	U_1	L	8.54	88.33	3.13
			(δFe)	~0.00	~100.00	~0.00
			TiC	~50.00	~0.00	~50.00
			(γFe)	~0.00	~100.00	~0.00
L + TiC ⇌ (γFe) + Fe_3C	1150	U_2	L	16.52	81.24	2.24
			TiC	~50.00	~0.00	~50.00
			(γFe)	~0.00	~100.00	~0.00
			Fe_3C	~25.00	~75.00	~0.00
(γFe) ⇌ Fe_3C + (αFe) + TiC	720	E_1	(γFe)	~0.00	~100.00	~0.00
			Fe_3C	~25.00	~75.00	~0.00
			(αFe)	~0.00	~100.00	~0.00
			TiC	~50.00	~0.00	~50.00

DOI: 10.1007/978-3-540-74196-1_13

Table 5. Investigations of the C-Fe-Ti Materials Properties

Reference	Method / Experimental Technique	Type of Property
[1970Zbo]	Quenching and annealing, hardness measurements	1.32 mass% Ti, 0.33 mass% C. Precipitation of TiC from the melt
[1975Dun]	Metallography, transmission electron microscopy (TEM)	Coarsening measurements, 725°C, 0.38 mass% Ti, 0.42 mass% C
[1976Ciu]	Magnetic permeability, carbon Snoek relaxation	0.10-0.22 mass% Ti, C saturation
[1977Mal]	Metallography, solidification structures examination	0.14-1.69 mass% Ti, 0.19-1.78 mass% C melted, annealing at 300°C
[1980Sar]	Metallography, X-ray diffraction (XRD)	2.0-4.0 mass% Ti, 0.2-1.0 mass% C rapidly quenched from the melt
[1983Pol]	Metallography, microhardness, magnetic measurements	Preparation of magneto-abrasive material, Fe-TiC mixtures
[1989Mal]	Scanning electron microscopy (SEM), kinetics, corrosion studies	700-850°C, < 5 mass% Ti, < 1.2 mass% C, Na_2SO_4, NaCl atmospheres
[1991Has]	Annealing of thin films prepared by sputtering	392-477°C, 10 at.% C, 14 at.% Ti
[1992Ter]	Preparation of Fe-TiC, XRD, microscopic examination	1600°C, Fe-TiC composites prepared by a levitation in melted Fe
[1993Ber]	SEM, kinetics, metallography	1550°C, < 8 mass% Ti, precipitation of TiC from the melt
[1995Ari]	Laser alloying, XRD, TEM	Laser alloying of TiC on Fe surface
[1996Fra2]	Metallography, SEM, hardness measurements	1500°C, Fe + TiC_x ($0.6 < x < 1$)
[1996Liu]	Chemical analysis, SEM	1500°C, 6 to 8 mass% Ti, 3.0 to 4.3 mass% C, microgravity, < 20 s.
[1996Pop]	Metallography	1600°C, 4 mass% Ti, 1 mass% C
[1997Liu]	Chemical analysis, SEM	1550°C, < 8 mass% Ti, 3.0 to 4.3 mass% C, microgravity, < 10 s.
[1999Mov]	Metallography	1100°C, 1.7 mass% Ti, 1.1 mass% C
[2000Bya]	SEM, XRD, metallography	Microhardness, plasticity and fracture thoughness of carbide coatings
[2001Ume]	XRD, SEM, TEM	700-1000°C, Fe_3C-Ti reactions
[2001Wan2]	XRD, TEM, metallography	15 mass% Ti, 1.7 mass% C, ball milling, then annealing 1 h at 800°C
[2002Per]	Porosity, density and hardness measurements, metallography	Fe-TiC composites by liquid phase sintering and high temperature synthesis

(*continued*)

DOI: 10.1007/978-3-540-74196-1_13

Reference	Method / Experimental Technique	Type of Property
[2002Ren]	SEM, energy dispersive X-ray spectroscopy (EDX), Metallography	4.5 mass% Ti, 1.1 mass% C, Fe-TiC composites preparation
[2003Che]	Secondary and backscattered electron imaging, metallography	15 mass% Fe, 0.2 mass% C, hardening of (βTi)
[2003Mei]	TEM, EDX, optical microscopy, metallography	1600°C, 40 mass% Ti, 0.08 mass% C, Fe-TiC composite preparation
[2004Zha]	XRD, TEM, SEM, density measurements	Fe-TiC composites by combustion synthesis, < 40 mass% Fe
[2006Nak]	SEM, atomic field microscopy (AFM)	Carbon nanotubes preparation (C_2H_2 on Fe-Ti catalyst), 500°C
[2006Wu]	Wear measurements, optical microscopy	1620-1680°C, precipitation of TiC from the melt; 0.2 to 1.8 mass% C,

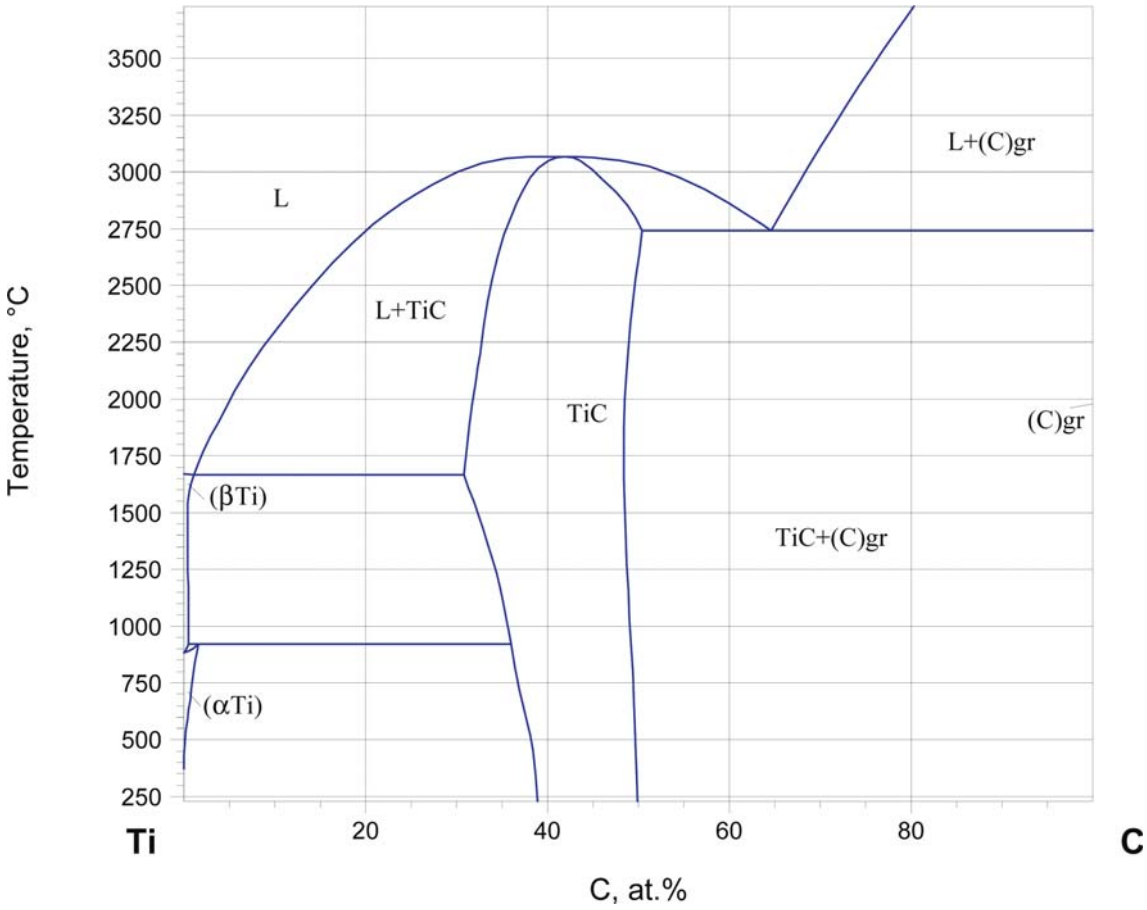

Fig. 1. C-Fe-Ti. C-Ti phase diagram

DOI: 10.1007/978-3-540-74196-1_13

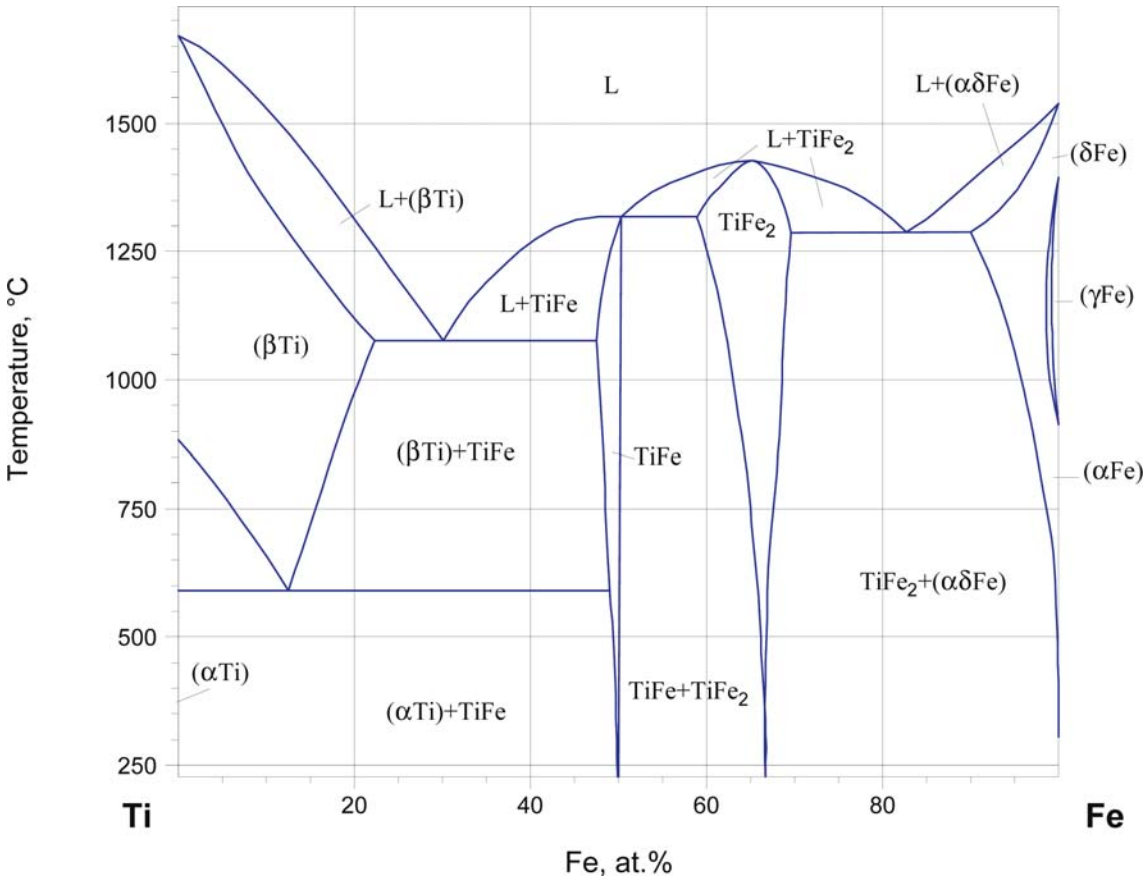

Fig. 2. C-Fe-Ti. Fe-Ti phase diagram

DOI: 10.1007/978-3-540-74196-1_13

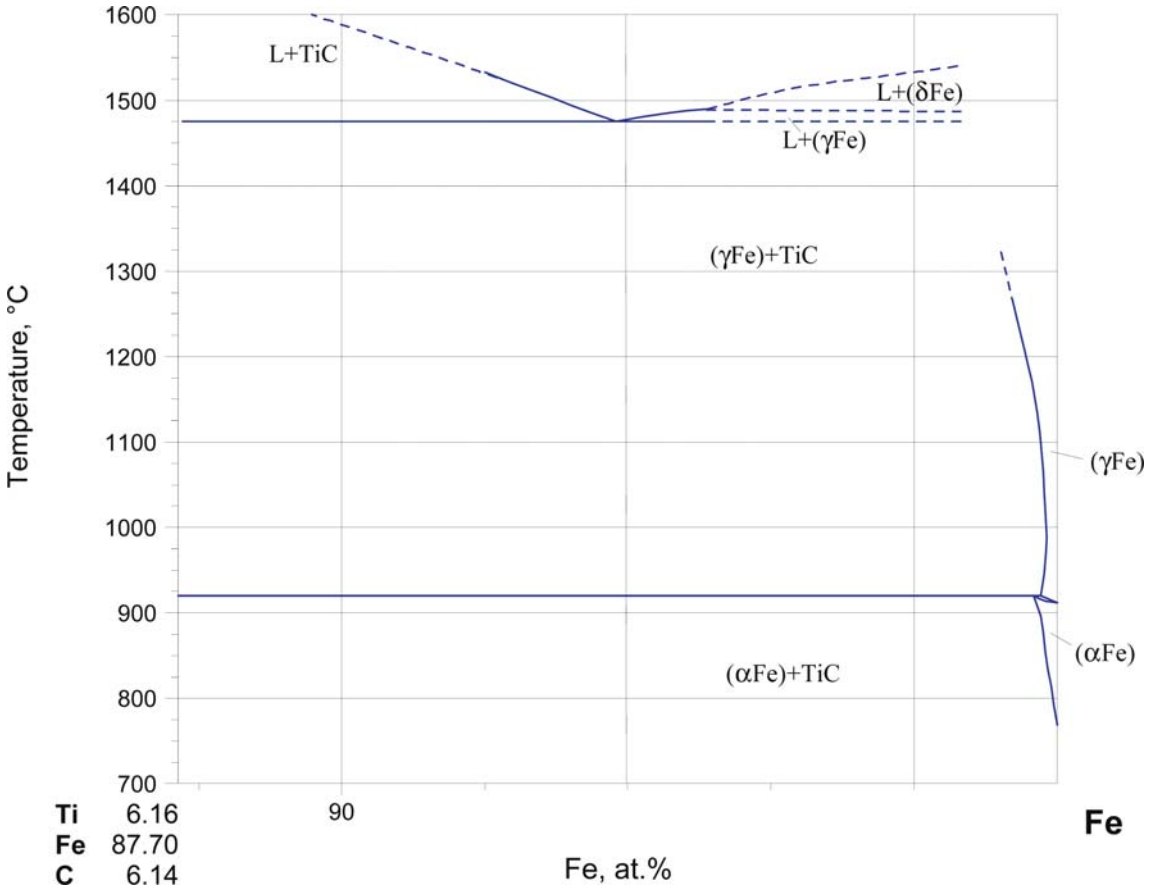

Fig. 3. C-Fe-Ti. Partial vertical section Fe-TiC of the stable system

DOI: 10.1007/978-3-540-74196-1_13

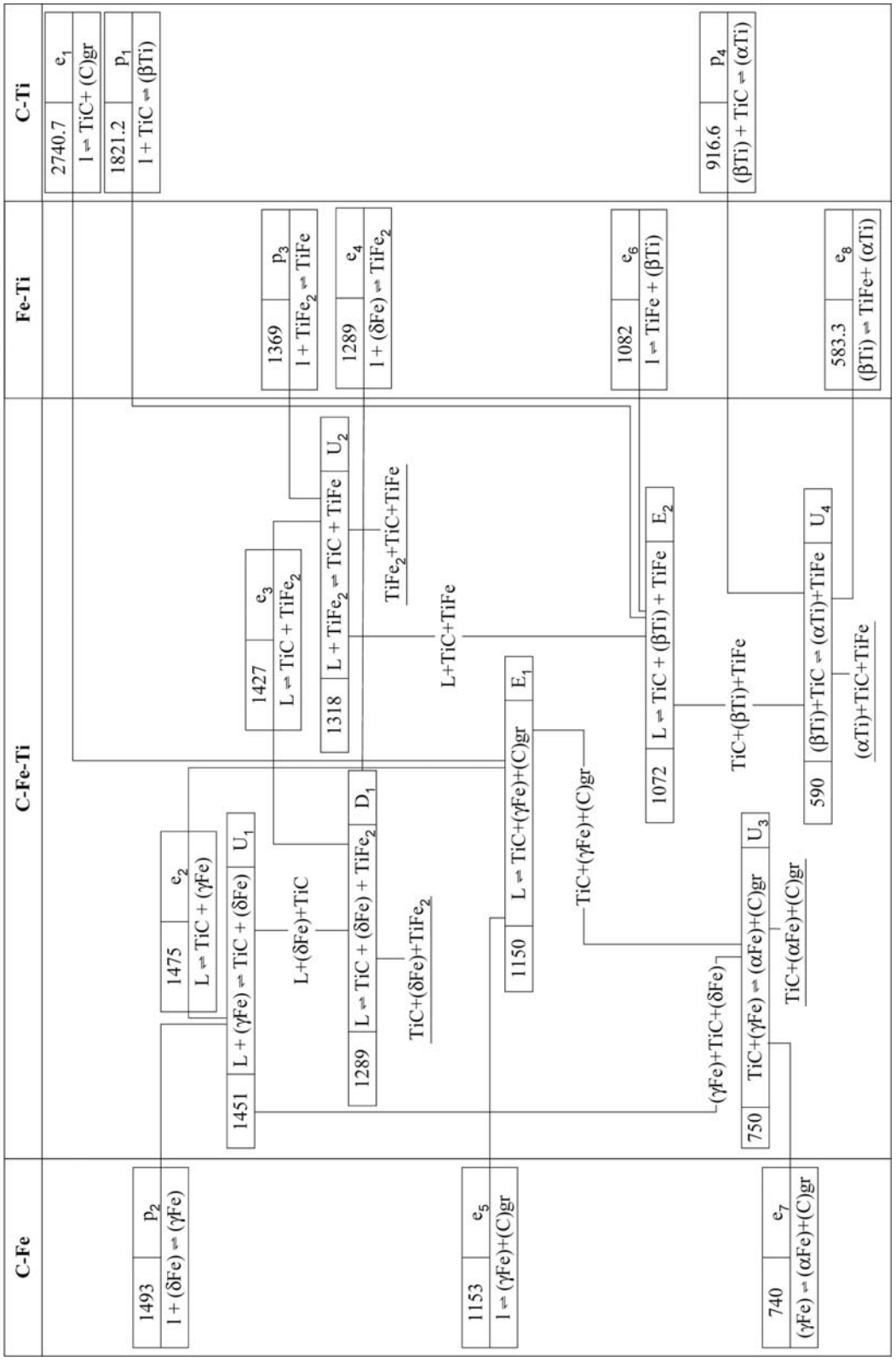

Fig. 4a. C-Fe-Ti. Stable reaction scheme

DOI: 10.1007/978-3-540-74196-1_13

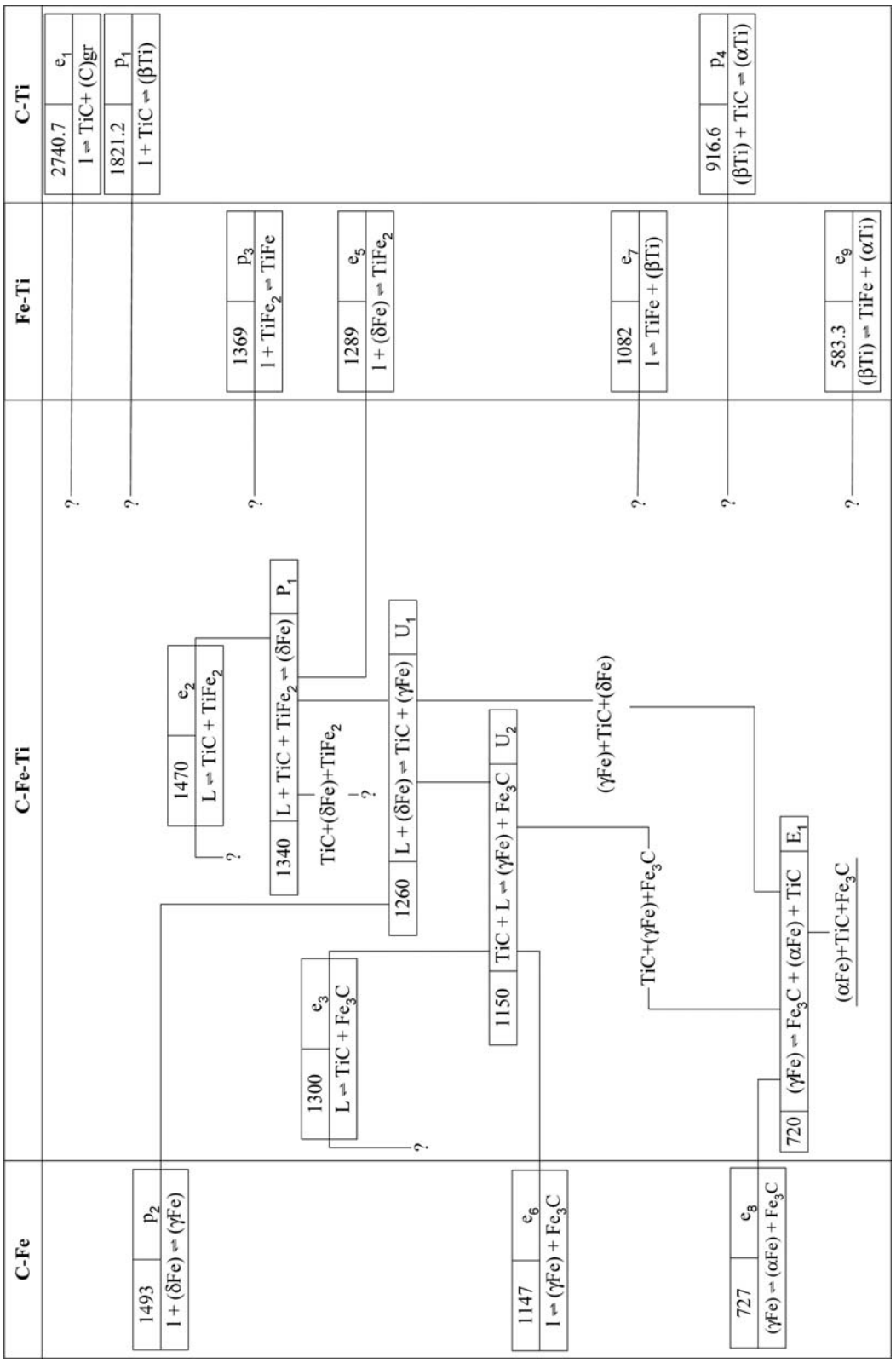

Fig. 4b. C-Fe-Ti. Metastable reaction scheme

DOI: 10.1007/978-3-540-74196-1_13

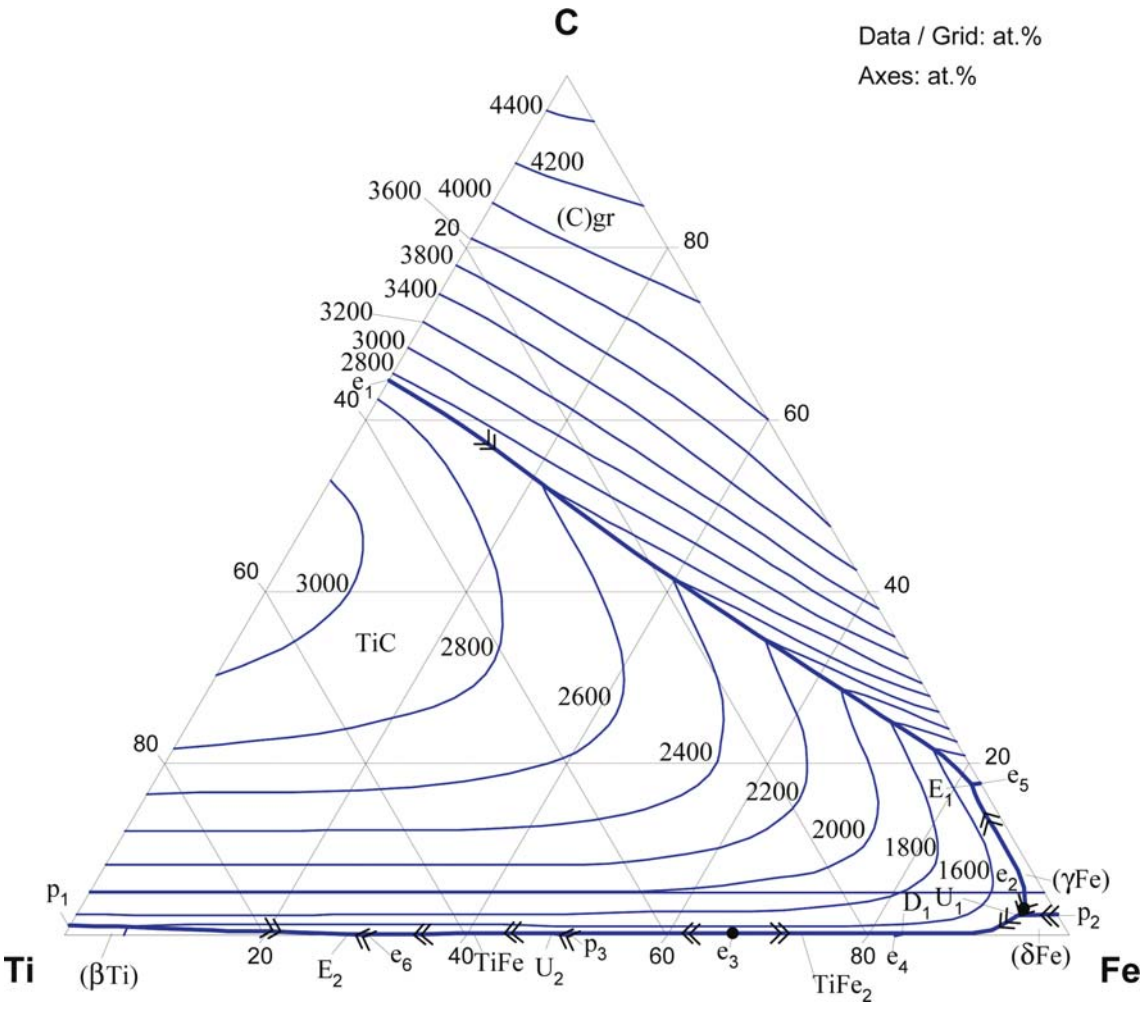

Fig. 5. C-Fe-Ti. Computed liquidus surface

DOI: 10.1007/978-3-540-74196-1_13

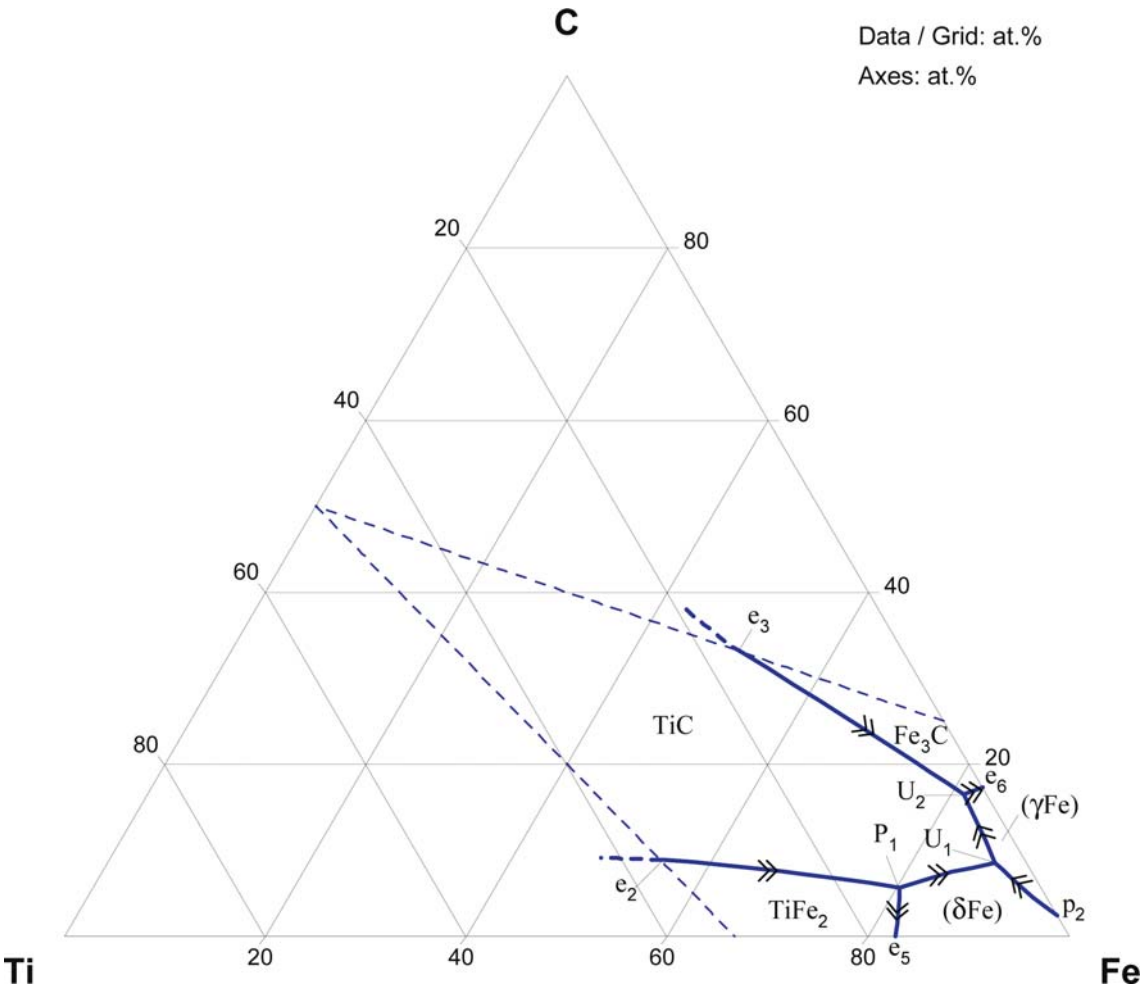

Fig. 6. C-Fe-Ti. Metastable liquidus surface

DOI: 10.1007/978-3-540-74196-1_13

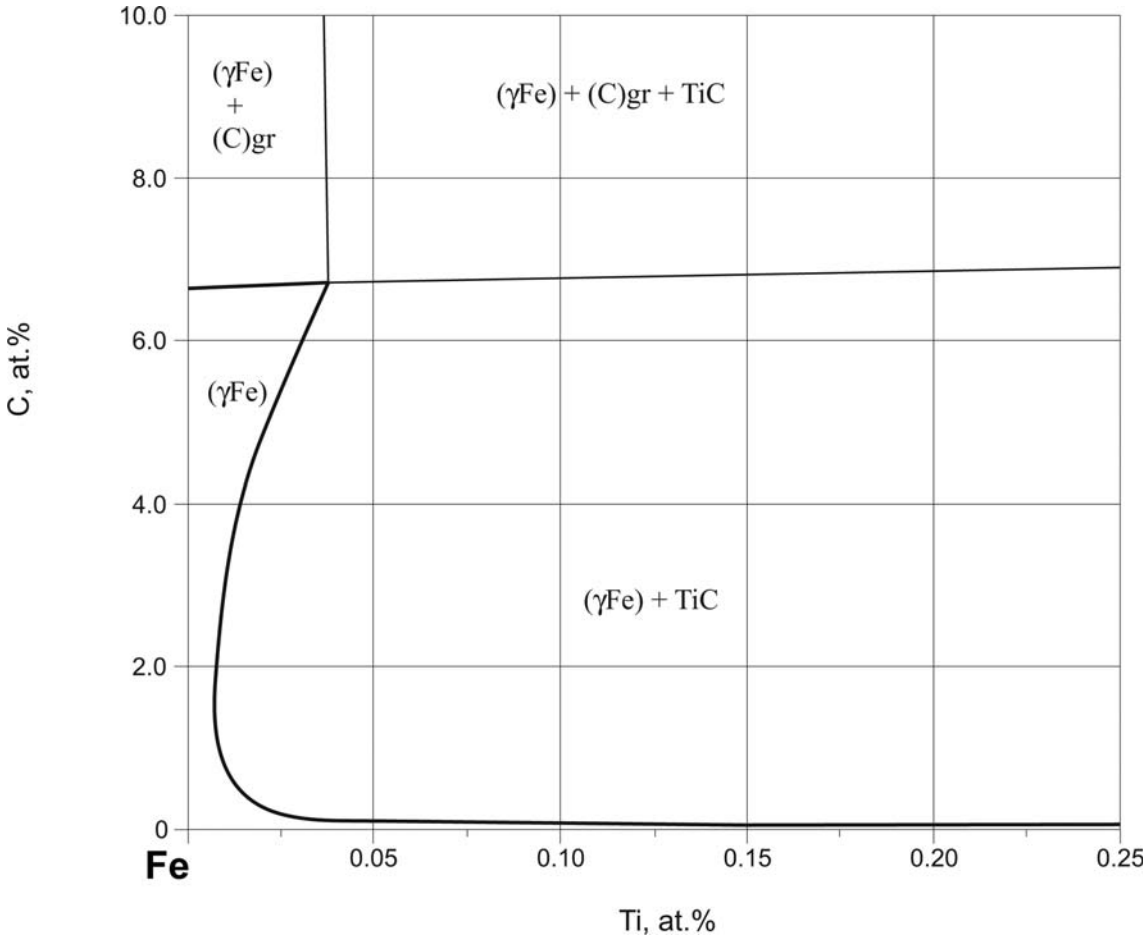

Fig. 7. C-Fe-Ti. Fe-rich corner of the isothermal section at 1000°C

DOI: 10.1007/978-3-540-74196-1_13

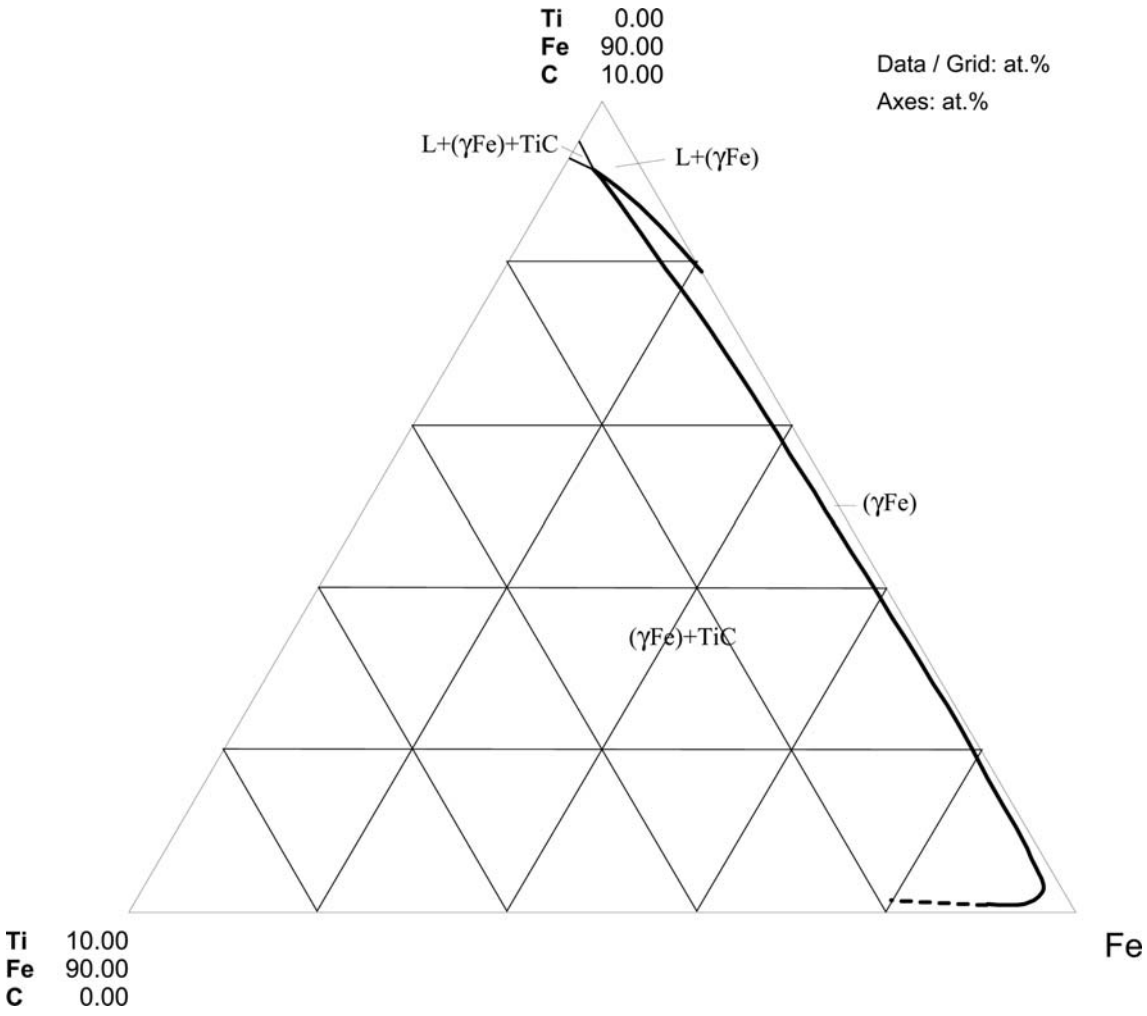

Fig. 8. C-Fe-Ti. Fe rich corner of the isothermal section at 1200°C

DOI: 10.1007/978-3-540-74196-1_13

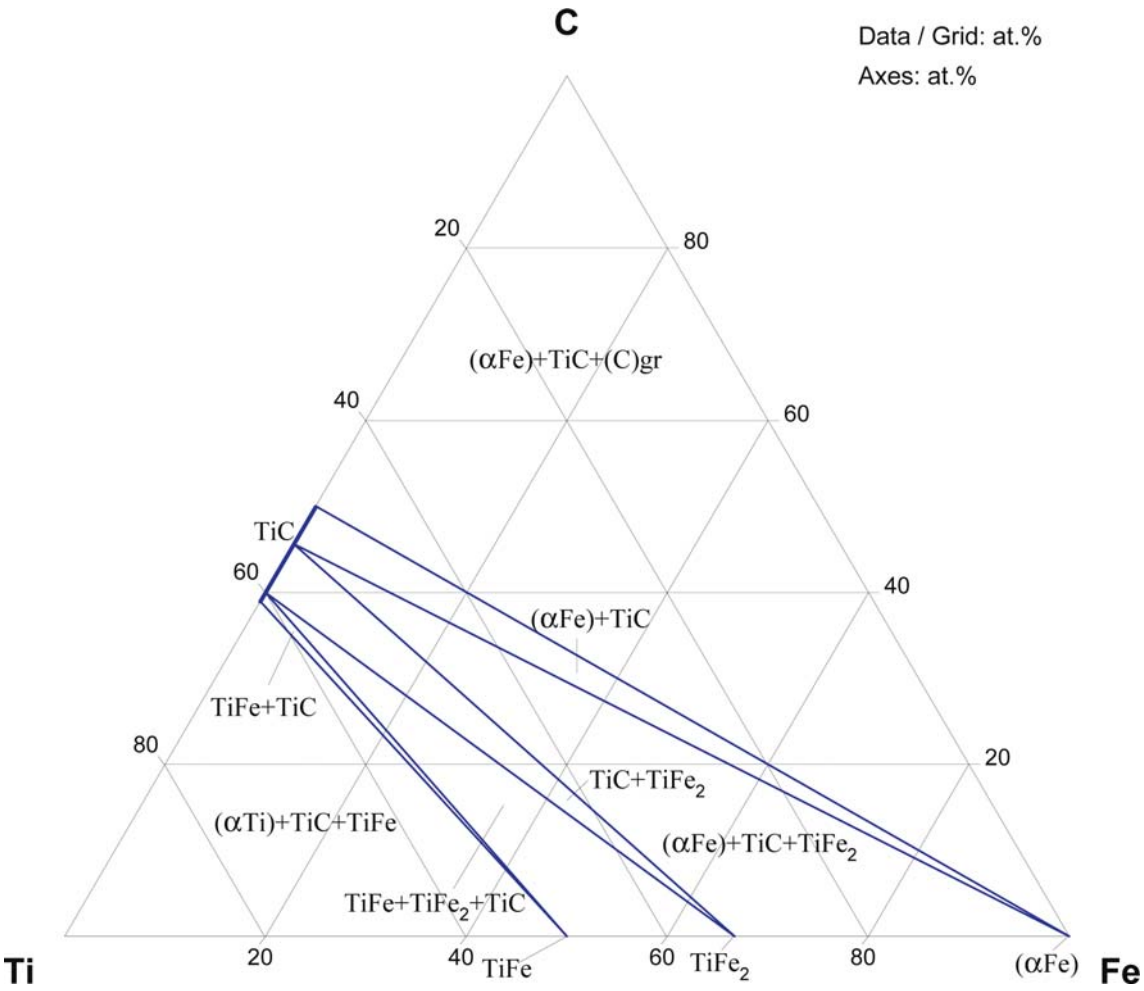

Fig. 9. C-Fe-Ti. Stable isothermal section at 25°C

DOI: 10.1007/978-3-540-74196-1_13

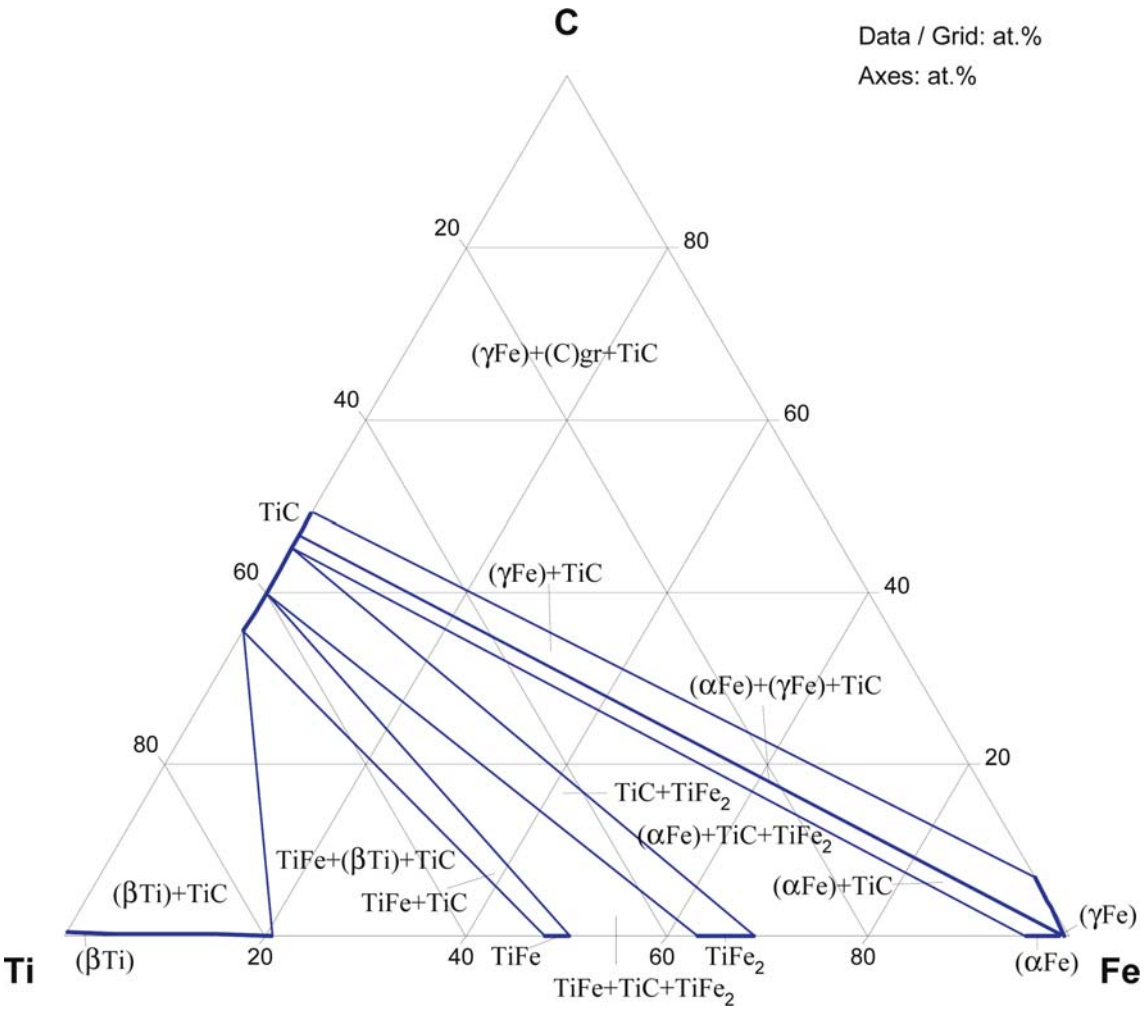

Fig. 10. C-Fe-Ti. Stable isothermal section at 1000°C

DOI: 10.1007/978-3-540-74196-1_13

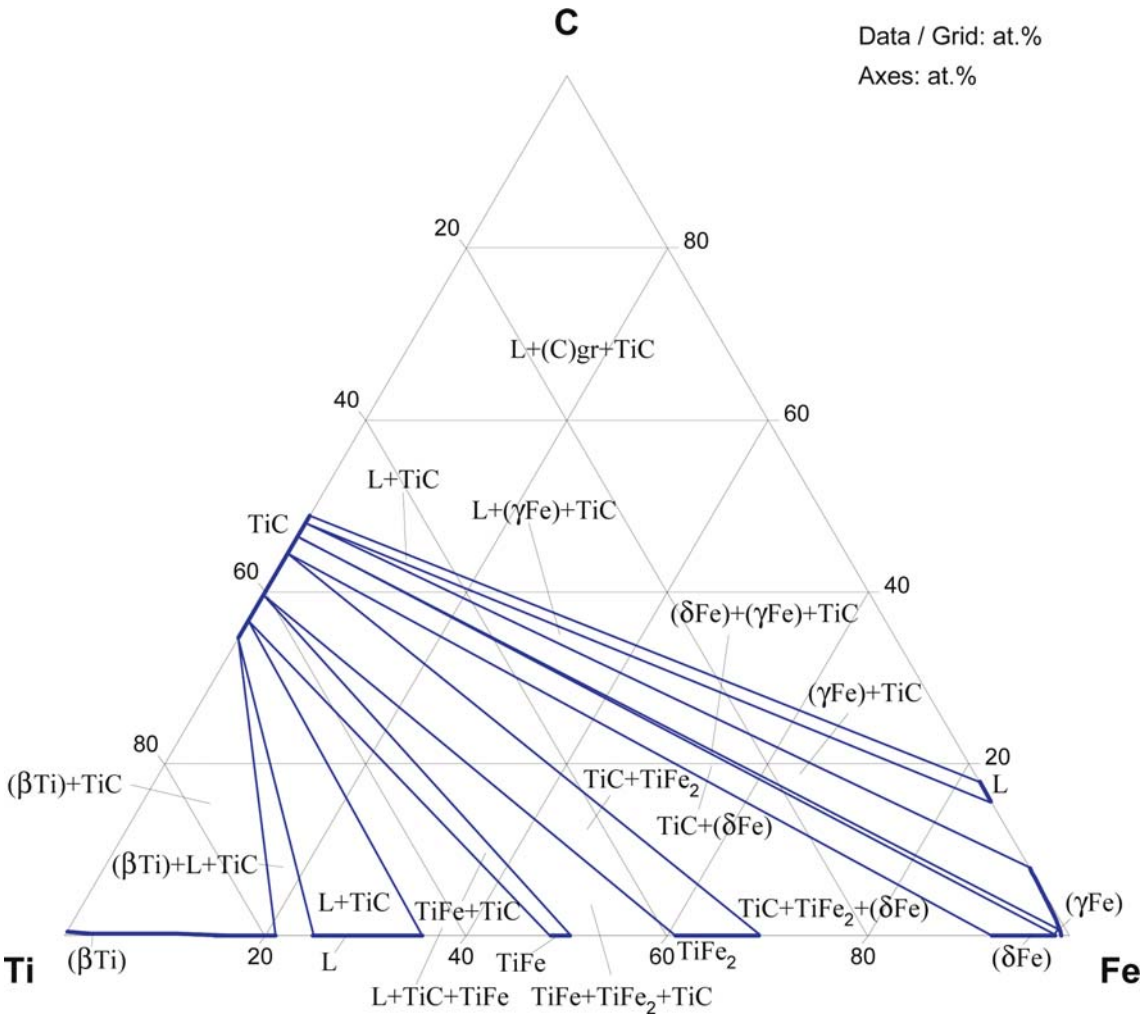

Fig. 11. C-Fe-Ti. Stable isothermal section at 1200°C

DOI: 10.1007/978-3-540-74196-1_13

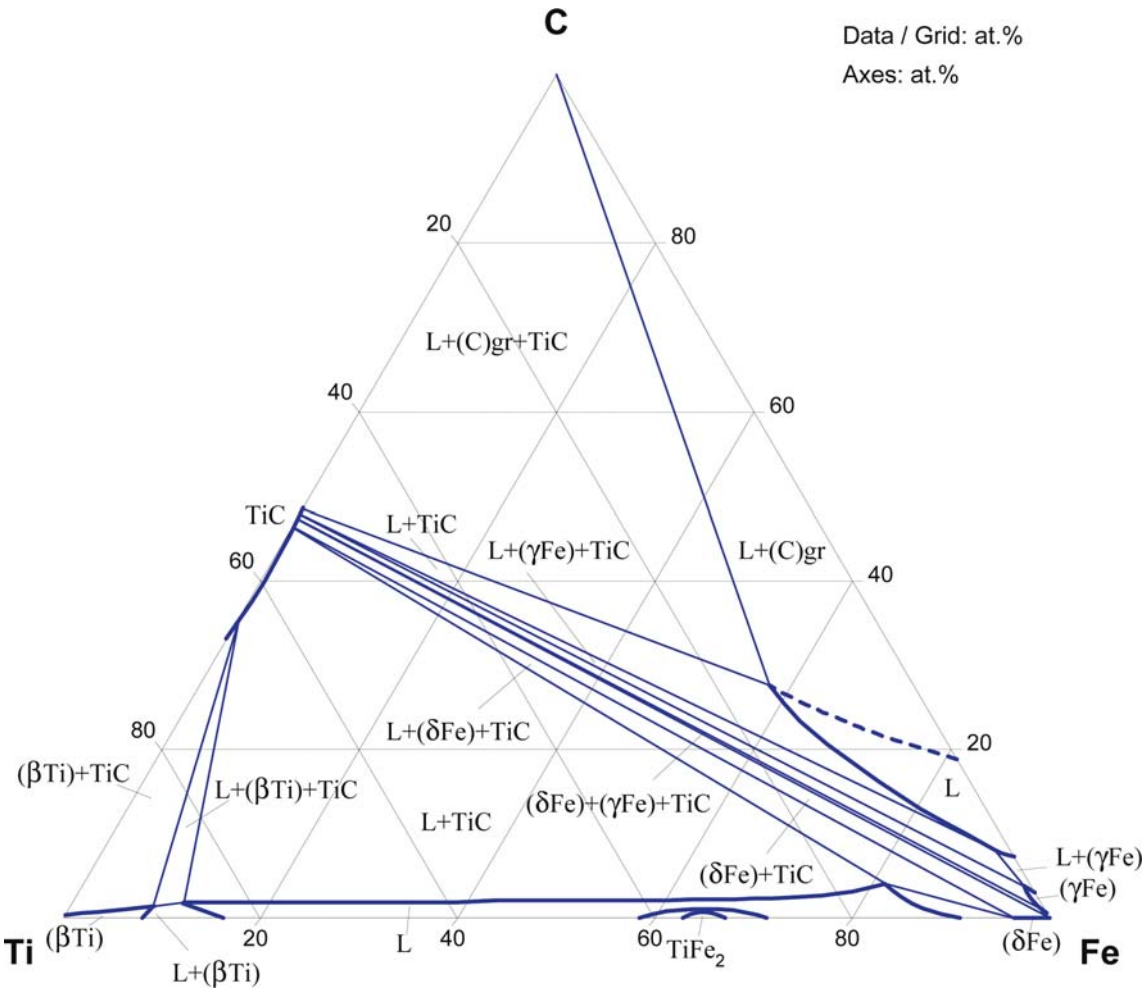

Fig. 12. C-Fe-Ti. Stable isothermal section at 1400°C

DOI: 10.1007/978-3-540-74196-1_13

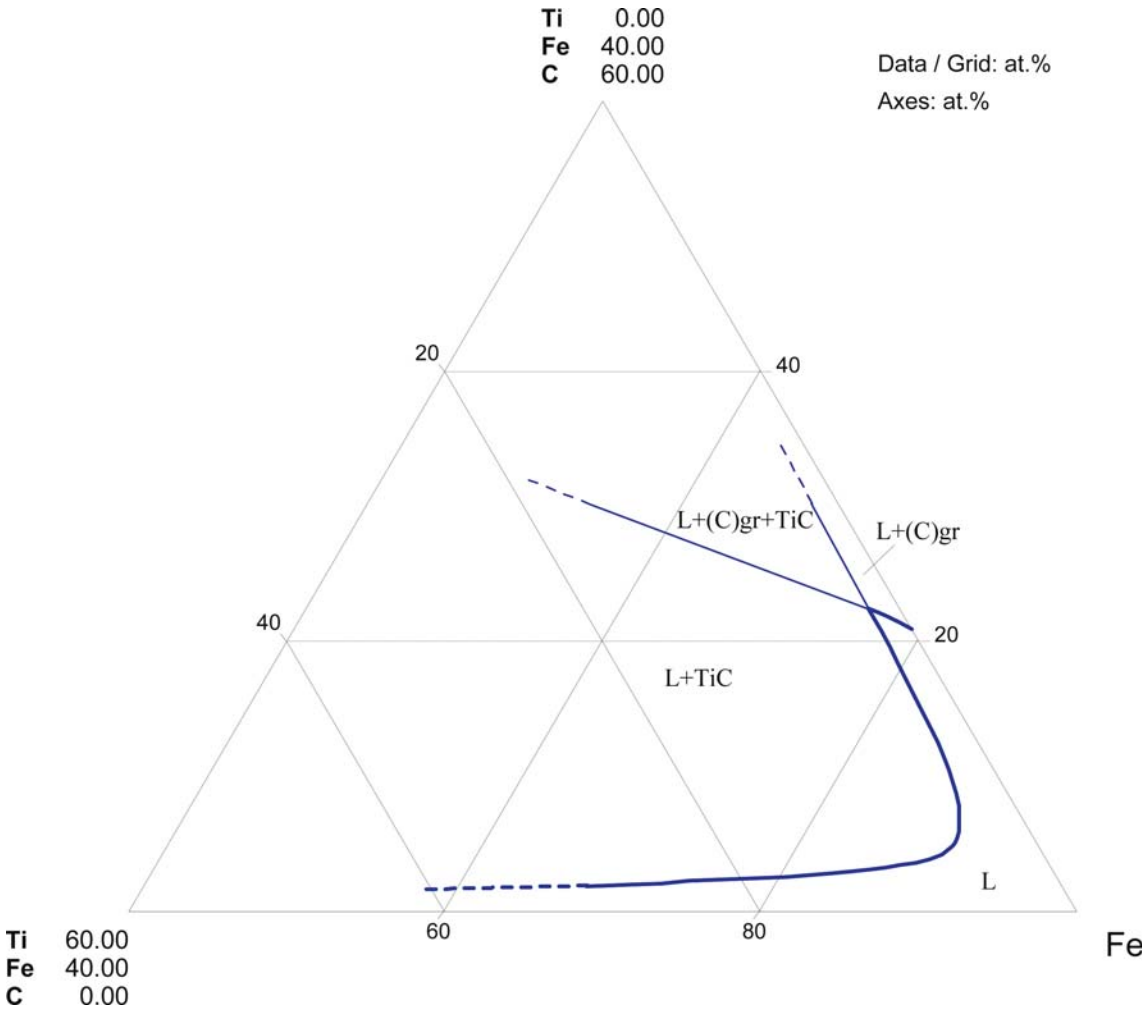

Fig. 13. C-Fe-Ti. Fe rich corner of the stable isothermal section at 1600°C

DOI: 10.1007/978-3-540-74196-1_13

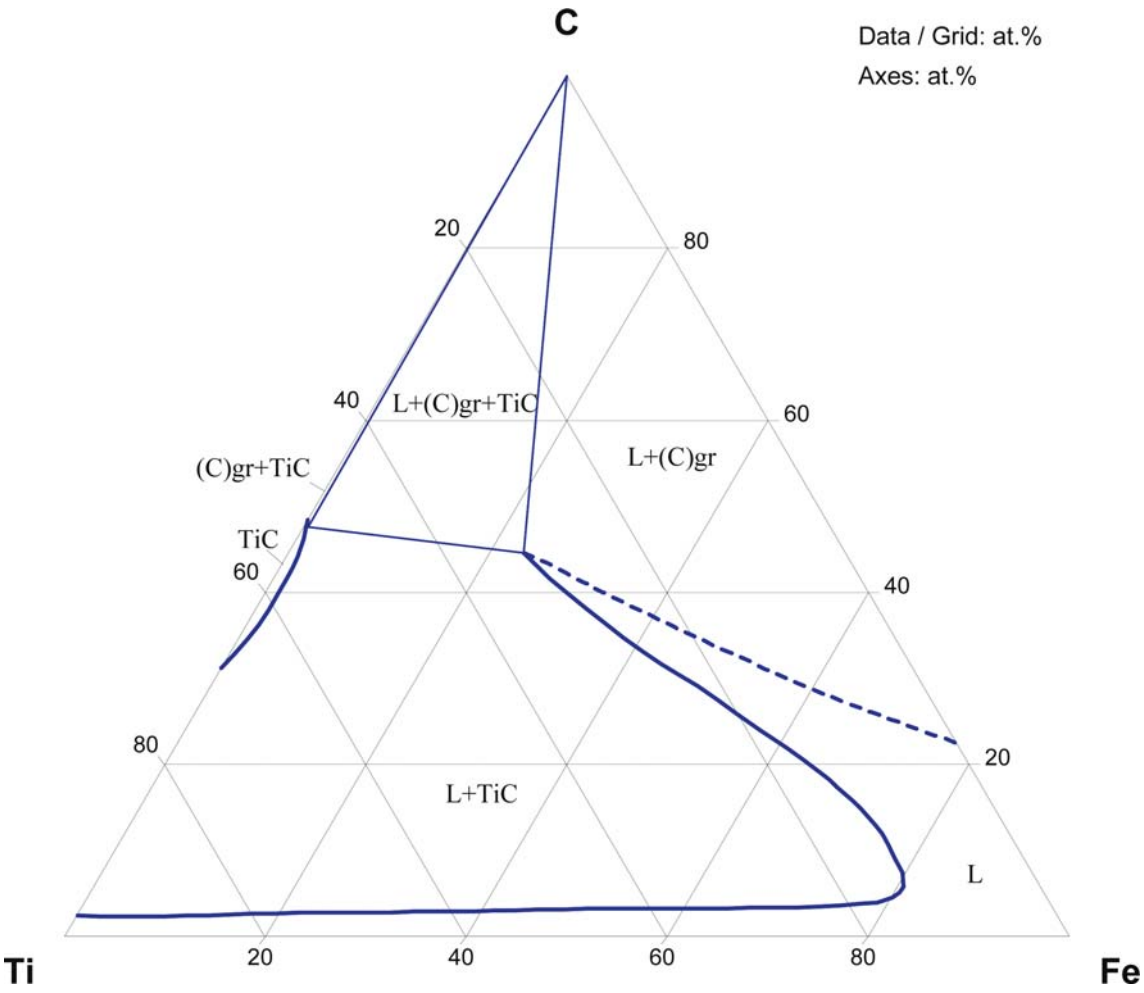

Fig. 14. C-Fe-Ti. Stable isothermal section at 1800°C

DOI: 10.1007/978-3-540-74196-1_13

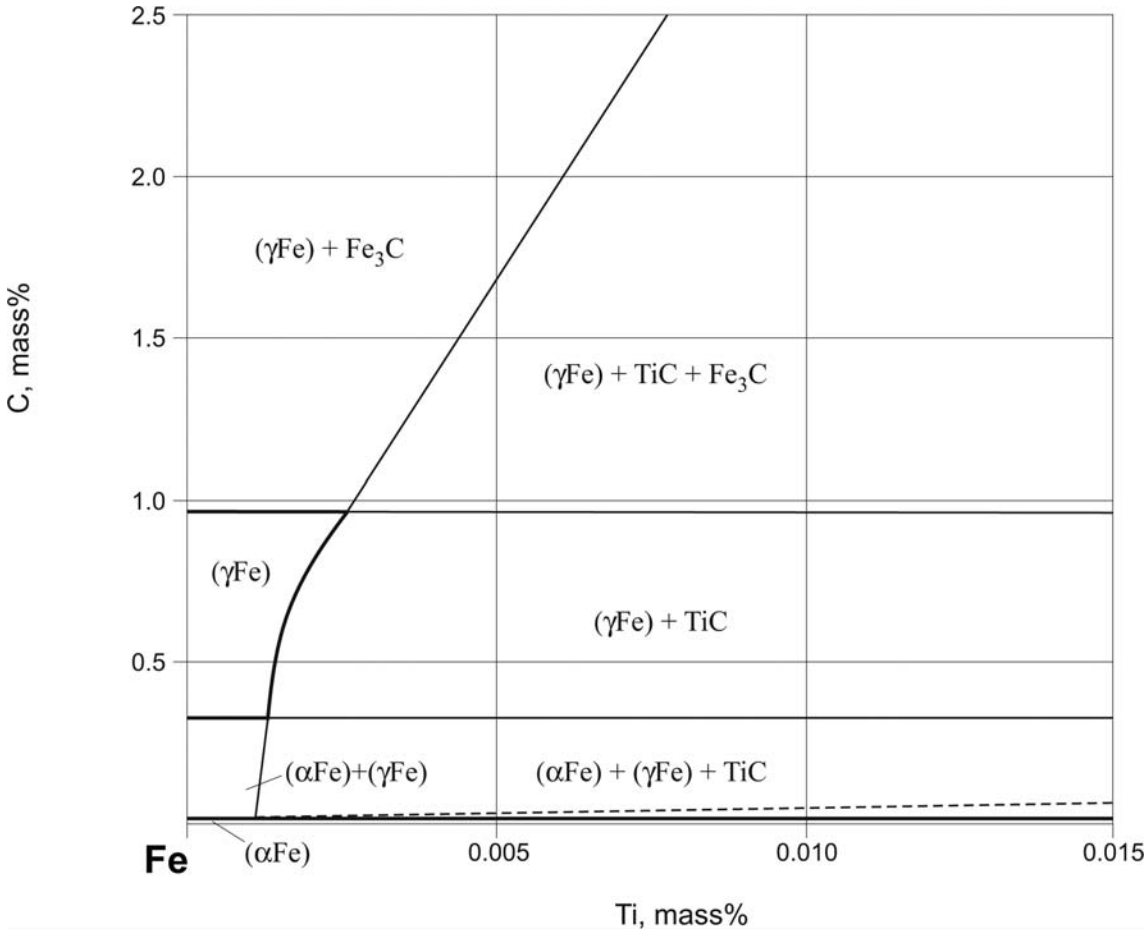

Fig. 15. C-Fe-Ti. Fe rich corner of the metastable isothermal section at 800°C

DOI: 10.1007/978-3-540-74196-1_13

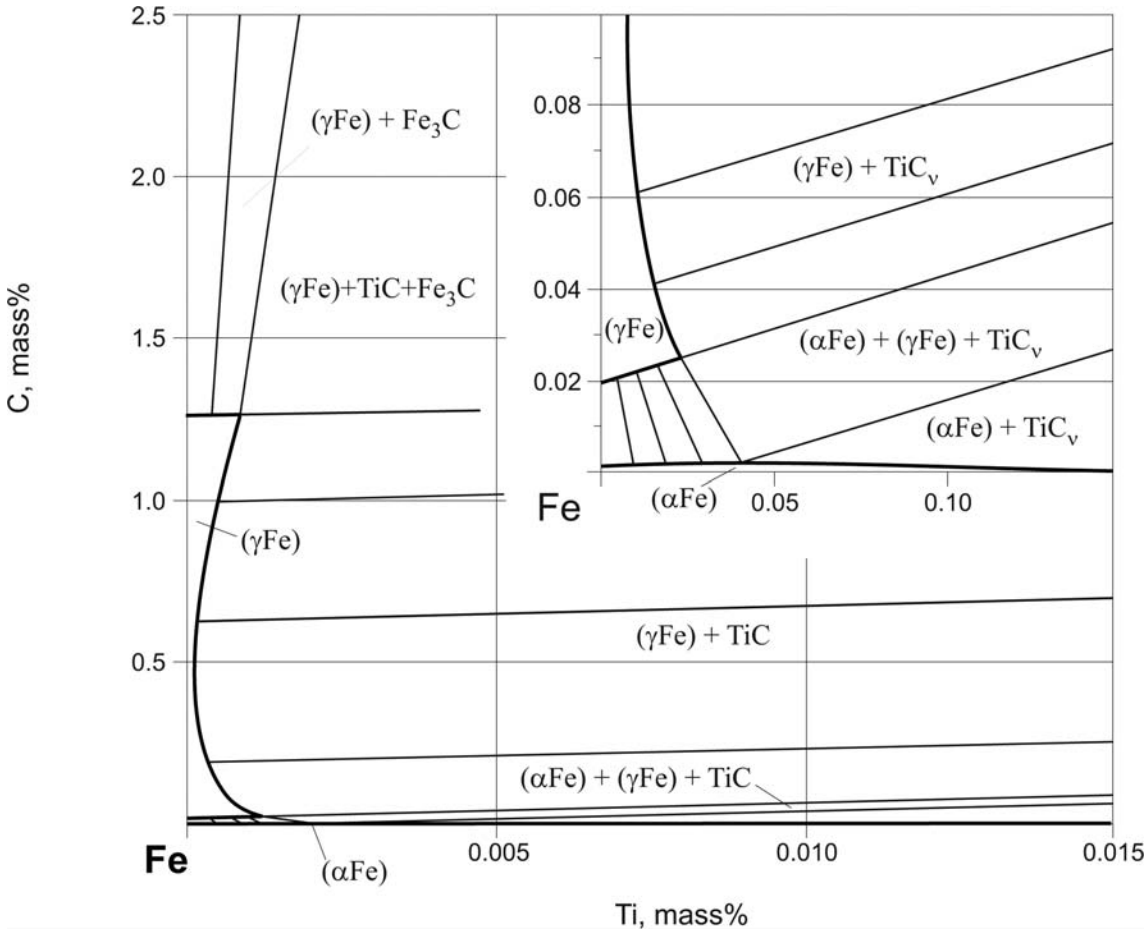

Fig. 16. C-Fe-Ti. Fe rich corner of the metastable isothermal section at 900°C

DOI: 10.1007/978-3-540-74196-1_13

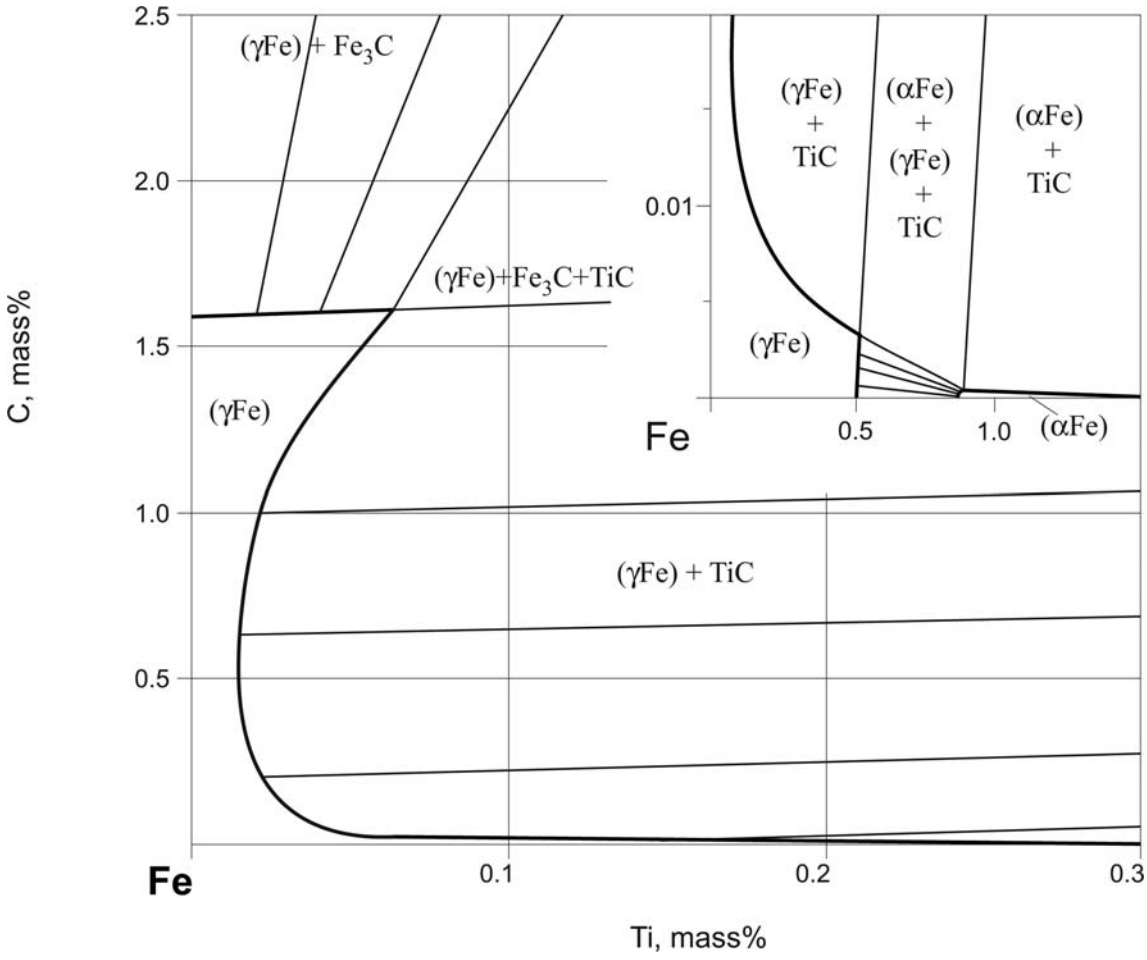

Fig. 17. C-Fe-Ti. Fe rich corner of the metastable isothermal section at 1000°C

DOI: 10.1007/978-3-540-74196-1_13

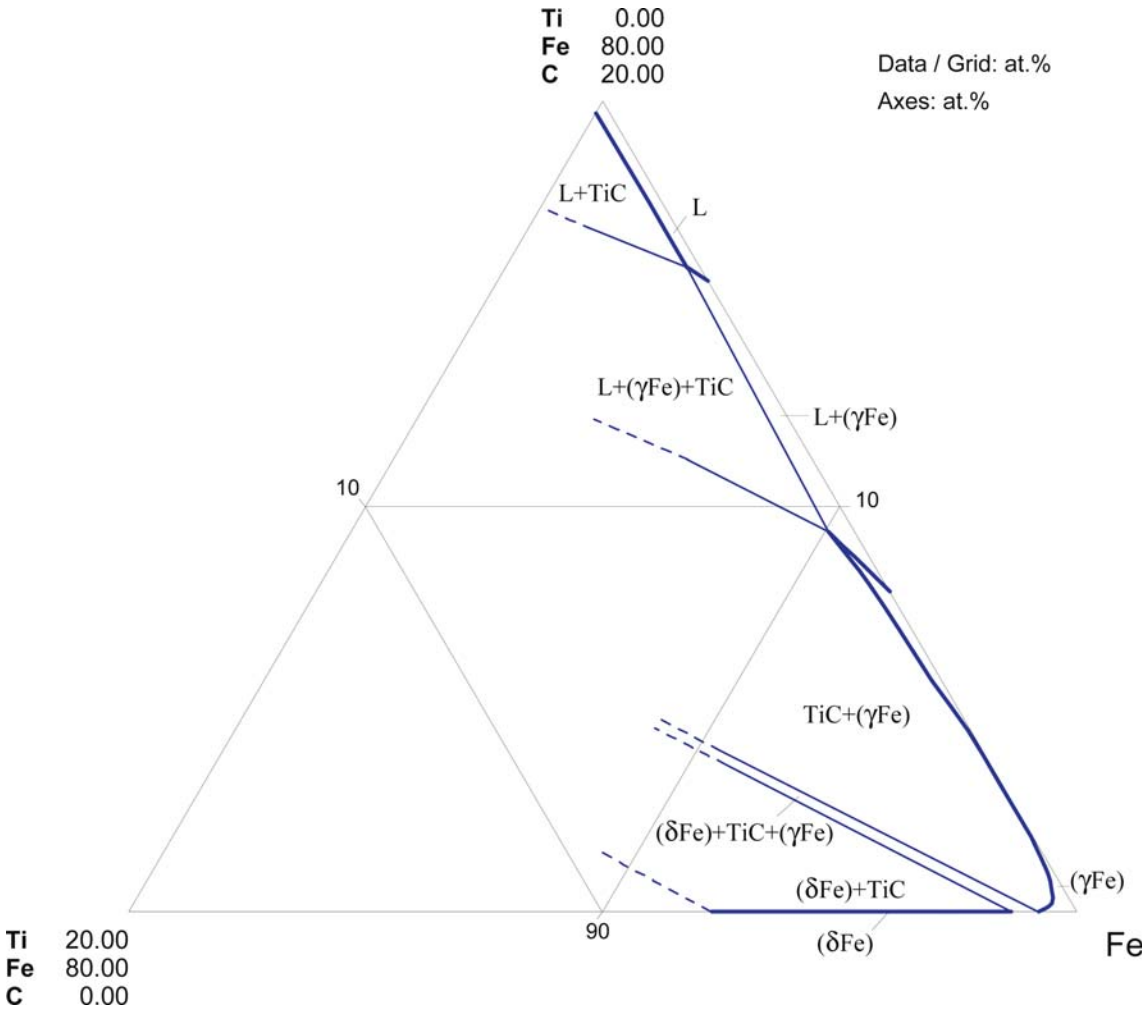

Fig. 18. C-Fe-Ti. Partial metastable isothermal section at 1200°C

DOI: 10.1007/978-3-540-74196-1_13

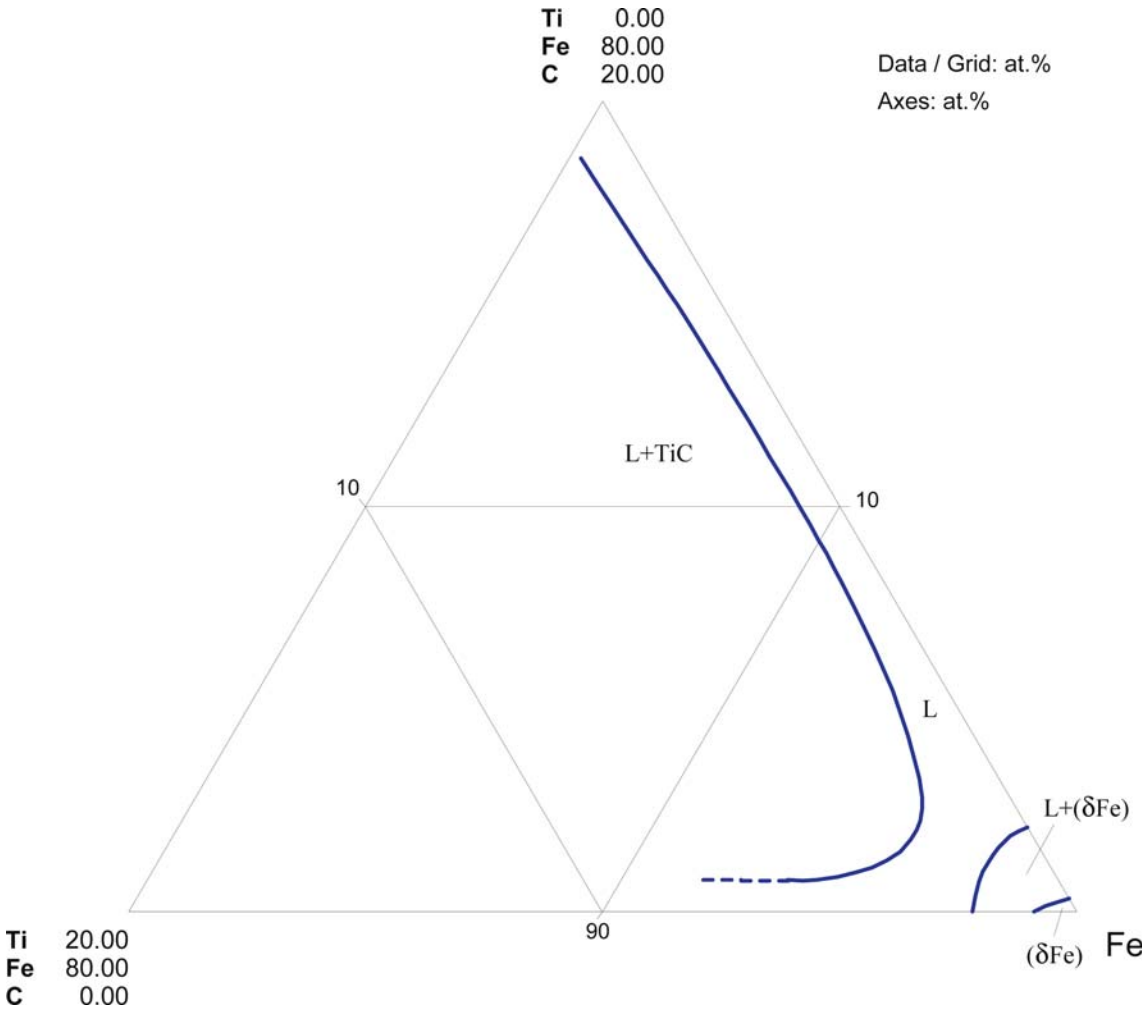

Fig. 19. C-Fe-Ti. Partial metastable isothermal section at 1500°C

DOI: 10.1007/978-3-540-74196-1_13

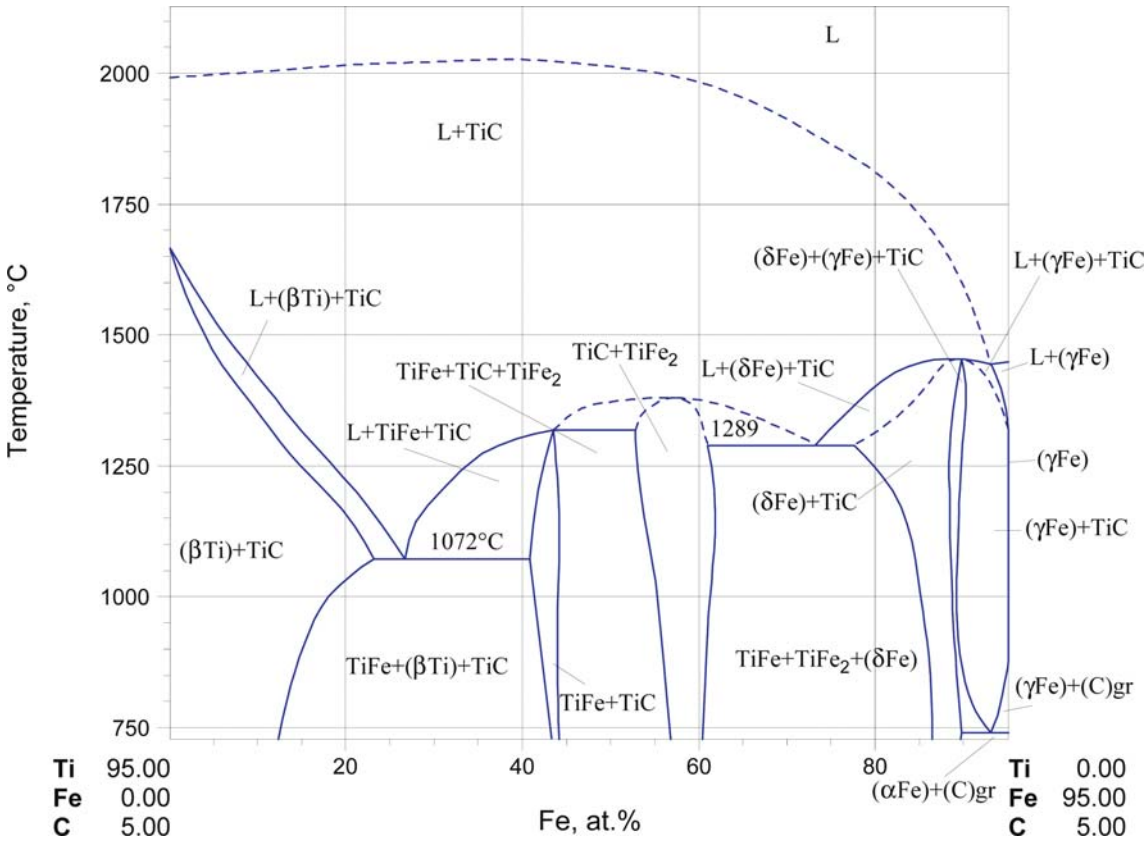

Fig. 20. C-Fe-Ti. Stable vertical section at 5 at.% C

DOI: 10.1007/978-3-540-74196-1_13

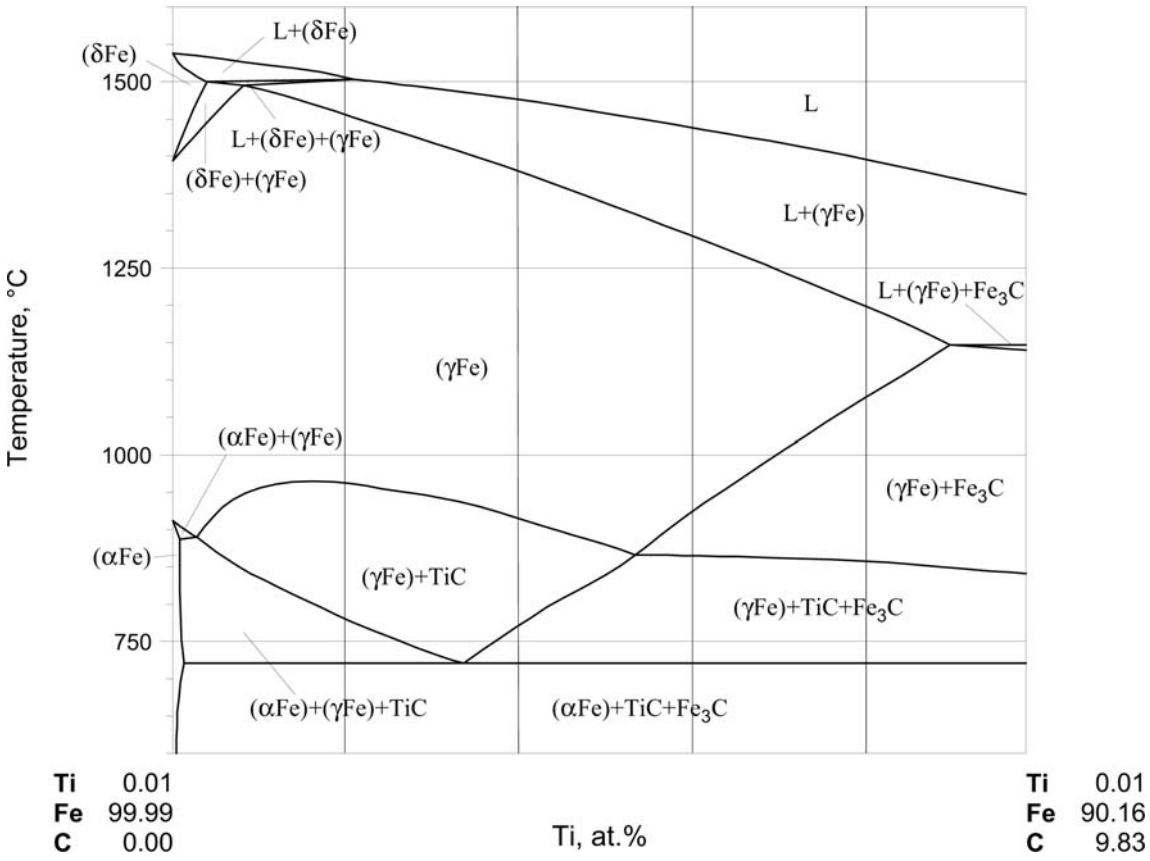

Fig. 21. C-Fe-Ti. Metastable vertical section at 0.01 mass% Ti

DOI: 10.1007/978-3-540-74196-1_13

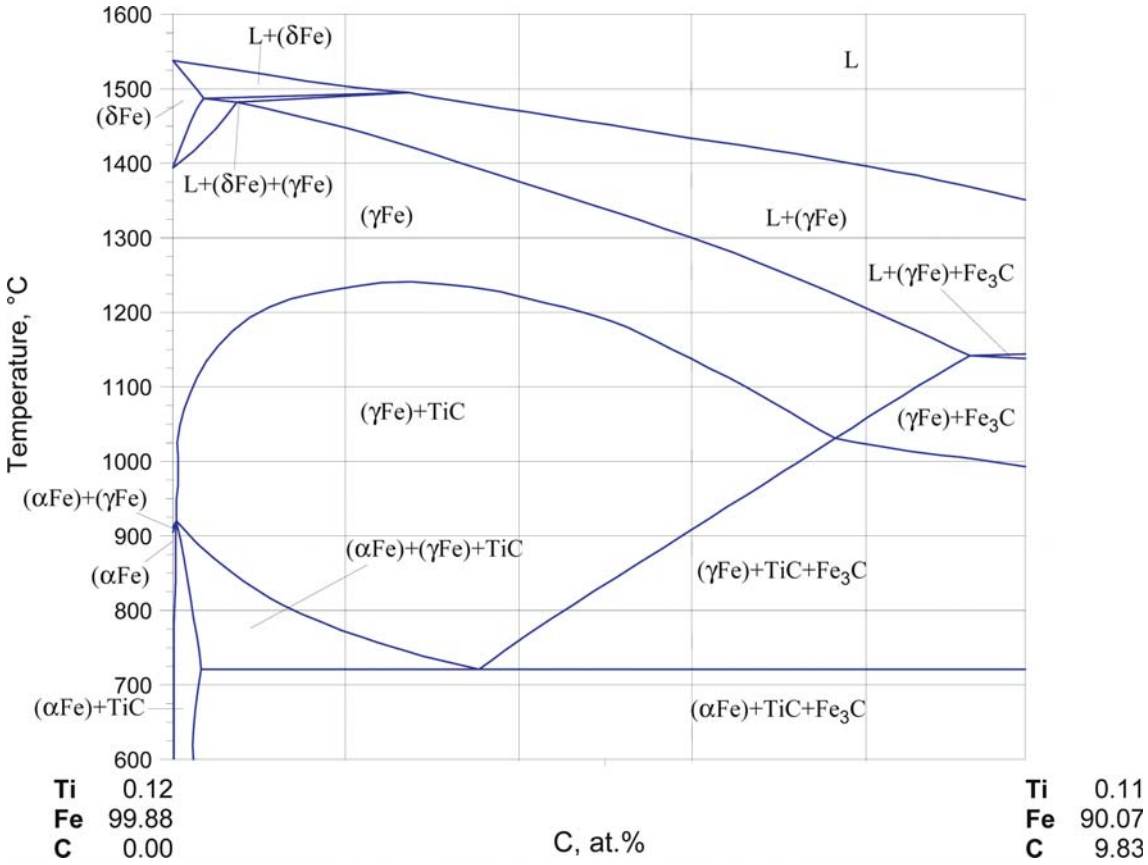

Fig. 22. C-Fe-Ti. Metastable vertical section at 0.1 mass% Ti

DOI: 10.1007/978-3-540-74196-1_13

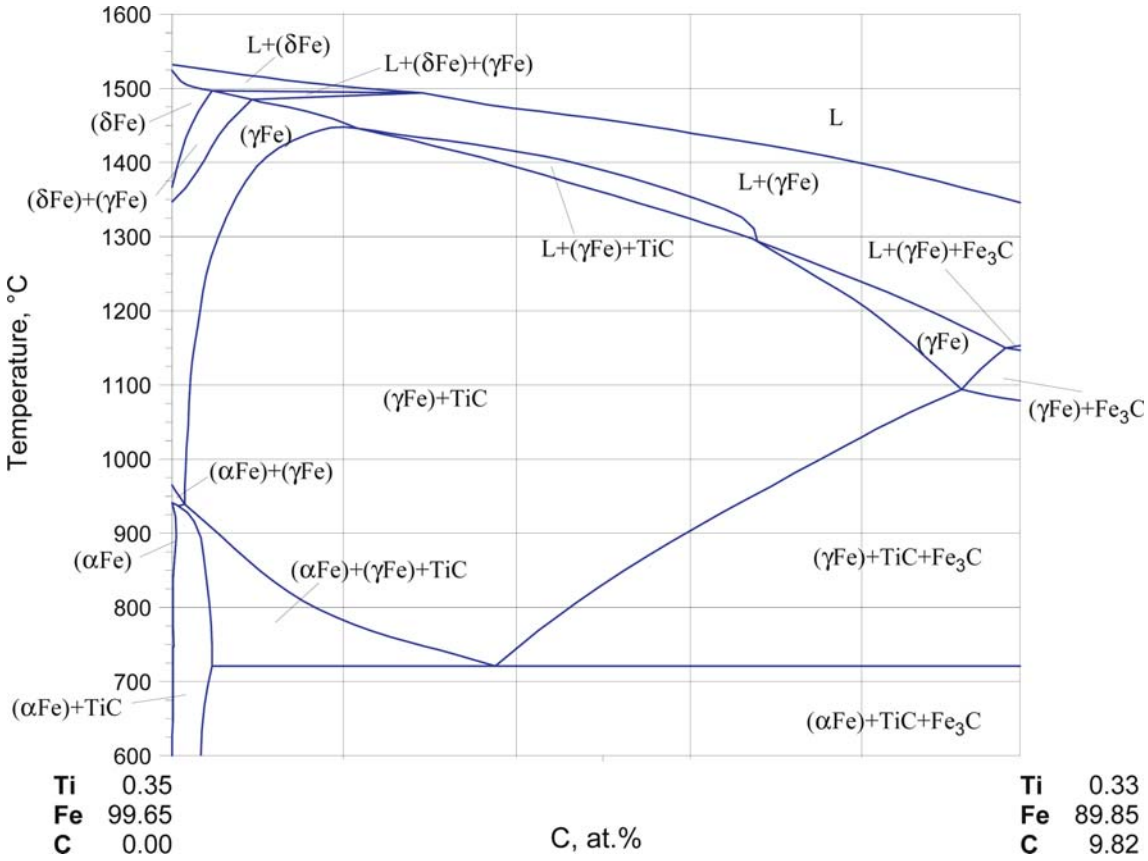

Fig. 23. C-Fe-Ti. Metastable vertical section at 0.3 mass% Ti

DOI: 10.1007/978-3-540-74196-1_13

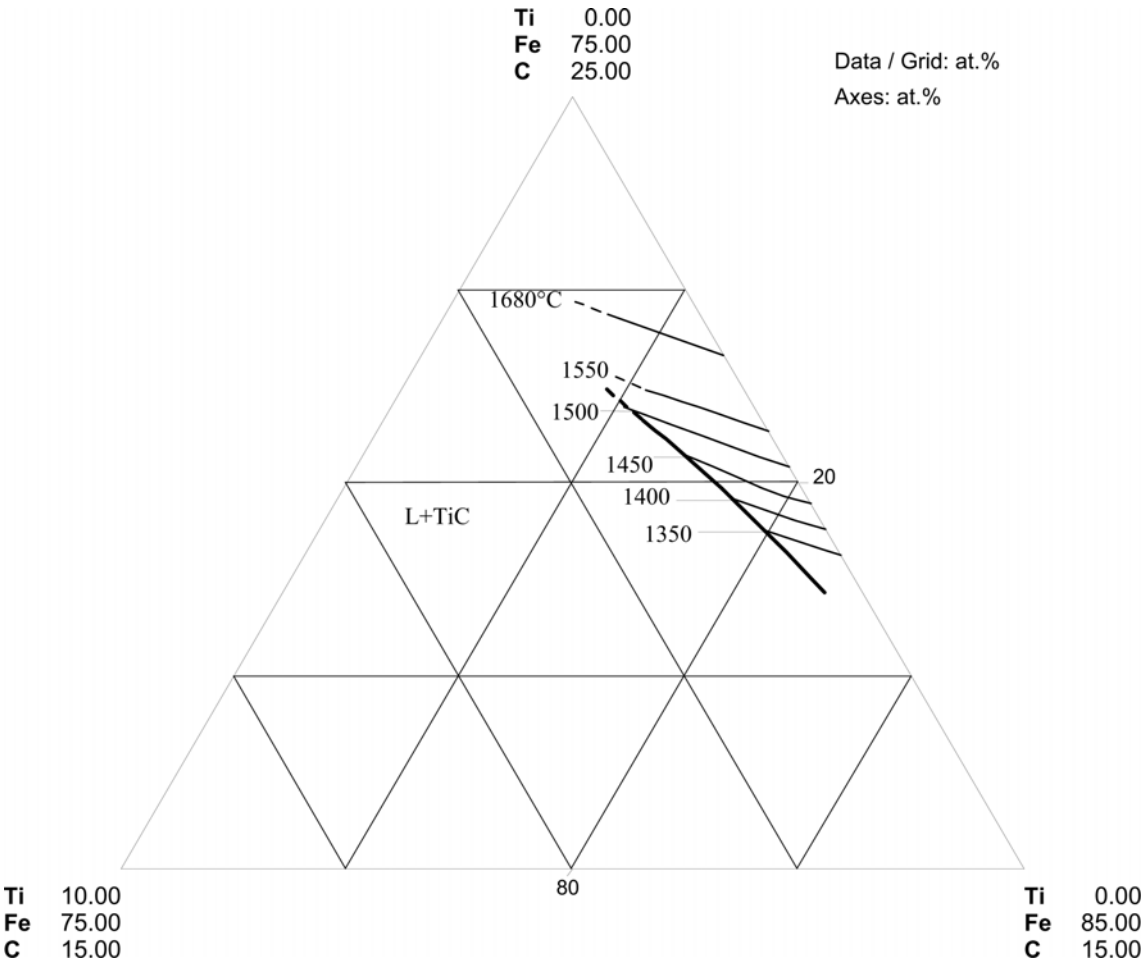

Fig. 24. C-Fe-Ti. Carbon solubility in molten alloys at various temperatures

DOI: 10.1007/978-3-540-74196-1_13

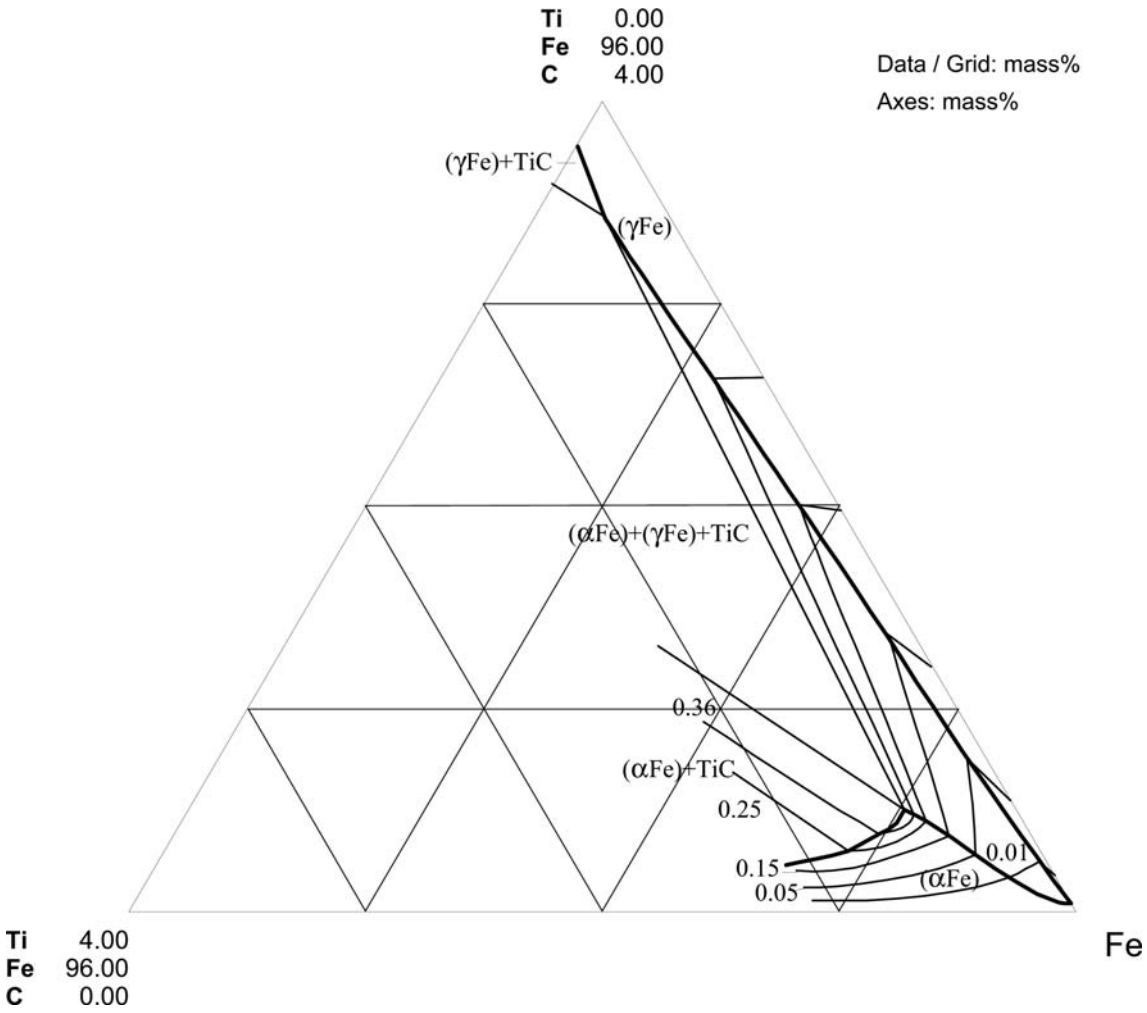

Fig. 25. C-Fe-Ti. Carbon activity at 900°C in the Fe rich corner

DOI: 10.1007/978-3-540-74196-1_13

References

[1917Vog] Vogel, R., "About the Influence of the Titanium on the Perlit Creation in Carbon Steel", *Ferrum*, **14**(11–12), 177–195 (1917) (Experimental, Phase Diagram, Phase Relations, 9)

[1925Tam] Tamaru, K., "On the Equilibrium Diagram of the System Iron-Carbon-Titanium", *Sci. Rep. Tohoku Imp. Univ.*, **14**(1), 25–32 (1925) (Experimental, Morphology, Phase Diagram, Phase Relations, Phys. Prop., 4)

[1938Tof1] Tofaute, W., Buettinghaus, A., "The Iron rich Corner of the Iron-Titanium-Carbon System" (in German), *Arch. Eisenhuettenwes*., **12**(1), 33–37 (1938) (Experimental, Phase Relations, Phase Diagram, 8)

[1938Tof2] Tofaute, W., Buttinghaus, A., "Iron-Titanium-Carbon Alloys", *Metallurgist (Suppl. Engineer)*, **11**, 190–192 (1938) (Crys. Structure, Review, Phase Diagram, 8)

[1939Nor] Northcott, L., "Section V.-Titamium and its Effect Upon Iron and Steel. I.-A. Summary of Published Information", *Iron Steel Inst. Special Rep*., **24**, 107–146 (1939) (Mechan. Prop., Phase Diagram, Phase Relations, Review, 121)

[1942Hum] Hume-Rothery, W., Raynor, G.V., Little, A.T., "On the Carbide and Nitride Particles in Titanium Steels", *J. Iron Steeel Inst*., **145**, 129–141 (1942) (Experimental, Phase Relations, Morphology, 3)

[1947Nor] Northcott, L., McLean, D., "Some Properties of Titanium Steels", *J. Iron Steel Inst., London*, **157**, 492–512 (1947) (Experimental, Mechan. Prop., Morphology, Phase Relations, 12)

[1948Gol] Goldschmidt, H.J., "The Structure of Carbides in Alloy Steels", *J. Iron Steel Inst*., **160**, 345–362 (1948) (Crys. Structure, Phase Diagram, Phase Relations, Phys. Prop., Rewiew, 93)

[1949Jae] Jaenecke, E., "C-Fe-Ti" (in German), *Kurzgefasstes Handbuch aller Legierungen*, Winter Verlag Heidelberg, 714–718 (1949) (Assessment, Phase Diagram, Phase Relations, 1)

[1952Edw] Edwards, R., Raine, T., "The Solid Solubilities of Some Stable Carbides in Cobalt, Nickel and Iron at 1250°C", *Pulvermetallurgie*, Benesovsky, F. (Ed.), Springer-Verlag, Wien, (1), 232–242 (1952) 1. Plansee Seminar, De Re Metallica, 22–26 Juni, 1952, Reutte/Tirol, (Phase Relations, Morphology, Experimental, 5)

[1956Ere] Eremenko, V.N., Bulanov, V.M., Gaevskaya, L.O., "Investigation of the Polythermal Section of the Phase Diagram of the Ternary System Ti-Fe-C" (in Ukrainian), *Kyivskii Derzhavnyi Univ. im T.G. Shevchenka*, *Khim. Zbirnyk*, (7), 119–142 (1956) (Phase Relations, Phase Diagram, Experimental, 15)

[1957Mur] Murakami, Y., Kimura, H., Nishimura, Y., "An Investigation on the Titanium-Iron-Carbon System", *Mem. Fac. Eng. Kyoto Imp. Univ.*, **19**, 302–319 (1957) (Crys. Structure, Experimental, Phase Diagram, Phase Relations, 13)

[1958Del] Delve, F.D., "The Solubility and Activity of Titanium in Carbon-Saturated Iron", *Trans. AIME*, **212**, 183–185 (1958) (Thermodyn., Experimental, 2)

[1967Sto] Storms, E.K., "The Titanium-Titanium Carbide System", *Refr. Mater.*, **2**, 1–17 (1967) (Phase Diagram, Phase Relations, Crys. Structure, Thermodyn., Experimental)

[1968Zup] Zupp, R.R., Stevenson, D.A., "Statistical Thermodynamics of Carbon in Ternary Austenitic Iron-Base Alloys", *Trans. AIME*, **242**, 862–869 (1968) (Thermodyn., Calculation, 35)

[1969Jel] Jellinghaus, W., "Contribution to the Knowledge of the Ternary System Iron-Titanium-Carbon and of the $TiFe_2$ Compound" (in German), *Arch. Eisenhuettenwes*., **40**(10), 843–850 (1969) (Phase Diagram, Phase Relations, Morphology, Experimental, 6)

[1970Zbo] Zboril, J., Posedel, Z., "Microstructure and Hardness of Iron-Molybdenum-Carbon and Iron-Titanium-Carbon Alloys after Rapid Cooling from the Melt" (in German*)*, *Z. Metallkd*., **61**(3), 214–217 (1970) (Mechan. Prop., Experimental,3)

[1972Chi] Chipman, J., "Thermodynamics and Phase Diagram of the Fe-C System", *Metall. Trans*., **3**, 55–64 (1972) (Assessment, Thermodyn., Review, 66)

[1975Dun] Dunlop, G.L., Honeycombe, R.W.K., "The Role of Dislocations in the Coarsening of Carbide Particles Dispersed in Ferrite", *Philos. Mag*., **32**(1), 61–72 (1975) (Mechan. Prop., Experimental, Morphology, 12)

DOI: 10.1007/978-3-540-74196-1_13

[1975Fre] Frey, H., Holleck, H., "DTA Investigations of High Temperature Phase Equilibria in Ternary Transition Metal-Carbon Systems", *Thermal Analysis*, Proc. Internat. Conf., 4th, 8–13 July 1974, Buzas, I. (Ed.), Akad. Kiado, Budapest, **1**, 339–348 (1975) (Experimental, Morphology, Phase Diagram, 3)

[1976Ciu] Ciurzynska, W., Moron, J.W., Zielinska, B., "Magnetic Permeability Disaccommodation in α C-Fe-Ti with Small Titanium Content", *Acta Phys. Pol. A*, **A49**(3), 409–416(1976) (Experimental, Magn. Prop., 21)

[1977Mal] Malinochka, Ya.N., Balakina, N.N., Savich, A.I., "Solidification and Structure of Fe-C-Ti Alloys", *Russ. Metall.*, (3), 80–83 (1977), translated from *Izv. Akad. Nauk SSSR*, *Met.*, (Experimental, Morphology, Phase Relations, 8)

[1980Sar] Sare, I.R., "Splat-Cooled Iron-Titanium-Carbon Alloys", *Met. Sci.*, **14**, 177–183 (1980) (Experimental, Morphology, Phase Relations, 28)

[1981Bra] Brandis, H., Preisendanz, H., Schueler, P., "The Influence of Alloying Elements Titanium, Vanadium and Niobium on the Activity of Carbon in Fe-X-C Alloys in the Temperature Range from 900 to 1100°C" (in German), *Thyssen Edelst. Techn. Ber.*, **7**(1), 92–104 (1981) (Experimental, Thermodyn., Phase Diagram, Phase Relations, 32)

[1981Mur] Murray, J.L., "The Fe-Ti (Iron-Titanium) System", *Bull. Alloy Phase Diagrams*, **2**(3), 320–334 (1981) (Phase Diagram, Phase Relations, Crys. Structure, Thermodyn., Review, 124)

[1981Sum] Sumito, M., Tsuchiya, N., Okabe, K., Sanbongi, K., "Solubility of Titanium and Carbon in Molten Fe-Ti Alloys Saturated with Carbon", *Trans. Iron Steel Inst. Jpn.*, **21**, 414–421 (1981) (Calculation, Experimental, Morphology, Phase Relations, Thermodyn., 16)

[1983Pol] Polischuk, V.S., Nalivka, G.D., Kisel', N.G., "Composite Magneto-Abrasive Powders Based on Iron, Carbides of Titanium, Vanadium and Chromium" (in Russian), *Poroshk. Metall.*, **3**, 94–100 (1983) (Experimental, Mechan. Prop., Morphology, Magn. Prop., 15)

[1983Vre] Vrestal, J., Bechny, L., Cochnar, Z., Petrus, J., Pokarna, A., "Titanium Influence on the Thermodynamic Activity of Carbon in Iron" (in Czech), *Kovove Mater.*, **21**(3), 217–222 (1983) (Experimental, Thermodyn., 7)

[1985Maz] Mazumdar, S., Ramaswamy, V., "The Carbon-Iron-Titanium System", *J. Alloys Phase Diagrams*, **1**, 27–38 (1985) (Phase Diagram, Phase Relations, Crys. Structure, Review, 26)

[1985Ram] Ramaekers, P.P.J., van Loo, F.J.J., Bastin, G.F., "Phase Relations, Diffusion Paths and Kinetics in the System C-Fe-Ti at 1273 K", *Z. Metallkd.*, **76**(4), 245–248 (1985), Erratum published in *Z. Metallkd.*, **76**(9), 639 (1985) (Experimental, Kinetics, Phase Diagram, Phase Relations, Transport Phenomena, 16)

[1986Bal] Balasubramanian, K., Kirkaldy, J.S., "Austenite-Nonstoichiometric Precipitate Equilibria in Microalloyed Steels. Part I: C-Fe-Ti and Fe-Nb-C Systems", *Calphad*, **10**(2), 187–202 (1986) (Thermodyn., Assessment, 27)

[1988Bal] Balasubramanian, K., Kirkaldy, J.S., "Thermodynamics of C-Fe-Ti And Fe-Nb-C Austenites and Nonstoichiometric Titanium and Niobium Carbides", *Advances in Phase Transitions*, Proc. Int. Symp., Ontario, Canada, 22–23 Oct. 1987, Pergamon Pr., Oxford, 37–51 (1988) (Thermodyn., Phase Relations, Experimental, 37)

[1988Mag] Magnin, P., Kurz, W., "Stable and Metastable Eutectic Temperatures of Fe-C with Small Additions of a Third Element", *Z. Metallkd.*, **79**(5), 282–284 (1988) (Phase Relations, Experimental, 5)

[1988Oht] Ohtani, H., Tanaka, T., Hasebe, M., Nishizawa, T., "Calculation of the Fe-C-Ti Ternary Phase Diagram", *Calphad*, **12**(3), 225–246 (1988) (Phase Diagram, Phase Relations, Assessment, Thermodyn., 40)

[1989Fra] Frage, N.R., Gurevich, Yu.G., Sokolova, A.V., Chumanov, V.I., "Stability of Titanium Carbide in Molten Iron and Nickel", *Russ. Metall.*, (3), 30–34 (1989), translated from *Izv. Akad. Nauk SSSR, Met.*, (3), 33–37, (1989) (Phase Relations, Phase Diagram, Thermodyn., Calculations, 8)

DOI: 10.1007/978-3-540-74196-1_13

[1989Mal] Malik, A.U., Ishaq, M., Ahmad, Sh., Ahmad, Su., "Influence of Carbon on the Hot Corrosion Behaviour of Fe-base Alloys", *Mater. Trans., JIM*, **30**(9), 707–716 (1989) (Experimental, Kinetics, Morphology, 14)

[1990Guo] Guo, Y., Wang, C., Yu, H., "Interaction Coefficients in the Iron-Carbon-Titanium and Titanium-Silver Systems", *Metall. Trans. B*, **21B**, 537–541 (1990) (Phase Relations, Thermodyn., Experimental, 33)

[1990Xia] Xia, C., Jin, Z., "On the Evolution of Microstructure and Diffusion Paths in the Titanium-Steel Explosion Weld Interface During Heat Treatment", *J. Less-Common Met.*, **162**(2), 315–322 (1990) (Experimental, Kinetics, Morphology, Phase Relations, 7)

[1991Has] Hasegawa, H., Saito, M., Kojima, A., Makino, A., Misaki, Y., Watanabe, T., "Crystallization Behavior of Fe-M-C (M = Ti, Zr, Hf, V, Nb, Ta) Films", *IEEE Trans. J. Magn. Jpn.*, **6**(2), 120–126 (1991) (Crys. Structure, Surface Phenomena, Morphology, Experimental, 6)

[1992Bal1] Balasubramanian, K., Kroupa, A., Kirkaldy, J.S., "Experimental Investigation of the Thermodynamics of the C-Fe-Ti Austenite and the Solubility of Titanium Carbide", *Metall. Trans. A*, **23A**(3), 709–727 (1992) (Calculation, Experimental, Phase Diagram, Phase Relations, 24)

[1992Bal2] Balasubramanian, K., Kroupa, A., Kirkaldy, J.S., "Experimental Investigation of the Thermodynamics of Fe-Nb-C Austenite and Nonstoichiometric Niobium and Titanium Carbides (T = 1273 to 1473 K)", *Metall. Trans. A*, **23A**(3), 729–744 (1992) (Calculation, Experimental, Phase Relations, Theory, Thermodyn., 51)

[1992Ter] Terry, B.S., Chinyamakobvu, O.S., "Dispersion and Reaction of TiC in Liquid Iron Alloys", *Mater. Sci. Technol.*, **8**, 399–405 (1992) (Experimental, Morphology, Mechan. Prop., 25)

[1993Ber] Bergman, A., Jarfors, A., Liu, Z., Fredriksson, H., "In-situ Formation of Carbide Composites by Liquid/Solid Reactions", *Key Eng. Mater.*, **79–80**, 213–233 (1993) (Kinetics, Experimental, Morphology, Phase Relations, 9)

[1994McH] McHale, A.E., "C-Fe-Ti", *Phase Diagrams for Ceramists*, **10**, fig. 8979, 290–291 (1994) (Phase Diagram, Review, 8)

[1995Alb] Albertsen, K., Schaller, H.J., "Constitution and Thermodynamics of the System Ti-C", *Z. Metallkd.*, **86**(5), 319–325 (1995) (Calculation, Phase Relations, Thermodyn., 46)

[1995Ari] Ariely, S., Bamberger, M., Hugel, H., Schaaf, P., "Phase Investigation in Laser Surface Alloyed Steels With TiC", *J. Mater. Sci.*, **30**(7), 1849–1853 (1995) (Crys. Structure, Experimental, Morphology, 11)

[1995Bou] Bouchard, D., Bale, C.W., "Simultaneous Optimization of Thermochemical Data for Liquid Iron Alloys Containing C, N, Ti, Si, Mn, S, and P", *Metall. Mater. Trans. B*, **26B**, 467–484 (1995) (Phase Relations, Theory, Thermodyn., 85)

[1996Art] Artkyukh, L.V., Ilyenko, S.M., Velikanova, T.Ya., "The Scandium-Titanium-Carbon Phase Diagram", *J. Phase Equilib.*, **17**(5), 403–413 (1996) (Phase Diagram, Phase Relations, Crys. Structure, Experimental, 16)

[1996Fra1] Frage, N., Levin, L., Manor, E., Shneck, R., Zabicky, J., "Iron-Titanium-Carbon System. I. Equilibrium Between Titanium Carbide (TiC_x) of Various Stoichiometries and Iron-Carbon Alloys", *Scr. Mater.*, **35**(7), 791–797 (1996) (Thermodyn., Calculation, Phase Diagrams, Phase Relations, 14)

[1996Fra2] Frage, N., Levin, L., Manor, E., Shneck, R., Zabisky, J., "Iron-Titanium-Carbon System. II. Microstructure of Titanium Carbide (TiC_x) of Various Stoichiometries Infiltrated with Iron-Carbon Alloy", *Scr. Mater.*, **35**(7), 799–803 (1996) (Experimental, Morphology, Mechan. Prop., Phase Relations, 11)

[1996Jon] Jonsson, S., "Assessment of the Ti-C System", *Z. Metallkd.*, **87**(9), 703–712 (1996) (Assessment, Phase Diagram, Phase Relations, Thermodyn., 59)

[1996Liu] Liu, Z., Fredriksson, H., "On the Reaction Between Fe-Ti and Fe-C Liquids under Microgravity", *Metall. Mater. Trans. A*, **27A**, 407–414 (1996) (Kinetics, Phase Relations, Experimental, 10)

DOI: 10.1007/978-3-540-74196-1_13

[1996Pop] Popov, A.A., Gasik, M.M., "Rapidly Solidified Fe-TiC Composites: Thermodynamics and the Peculiarities of Microstructure Formation in situ", *Scr. Mater.*, **35**(5), 629–634 (1996) (Calculation, Experimental, Morphology, Phase Relations, Thermodyn., 17)

[1996Sei] Seifert, H.J., Lukas, H.L., Petzow, G., "Thermodynamic Optimization of the Ti-C System", *J. Phase Equilib.*, **17**(1), 24–35 (1996) (Phase Diagram, Phase Relations, Thermodyn., Assessment, 58)

[1997Liu] Liu, Z., Fredriksson, H., "On the Kinetics of Carbide Precipitation During Reaction Between Graphite and Fe-Ti Liquids Under Microgravity", *Metall. Mater. Trans. A*, **28A**, 707–719 (1997) (Experimental, Kinetics, Morphology, Thermodyn., 19)

[1997Miz] Mizuno, M., Tanaka, I., Adachi, H., "Effect of Solute Atoms on the Chemical Bonding of Fe_3C (Cementite)", *Philos. Mag. B*, **75**(2), 237–248 (1997) (Crys. Structure, Mechan. Prop., Theory, 28)

[1998Dum] Dumitrescu, L.S.F., Hillert, M., Saunders, N., "Comparison of Fe-Ti Assessments", *J. Phase Equilib.*, **19**(5), 441–448 (1998) (Review, Phase Diagram, Phase Relations, Thermodyn., 48)

[1998Jon] Jonsson, S., "Assessment of the C-Fe-Ti System, Calculation of the Fe-Ti-N System, and Prediction of the Solubility Limit of Ti(C,N) in Liquid Fe", *Metall. Mater. Trans. B*, **29B**, 371–384 (1998) (Assessment, Phase Diagram, Phase Relations, Thermodyn., 53)

[1999Dum1] Dumitrescu, L.F.S., Hillert, M., Sundman, B., "A Reassessment of Ti-C-N Based on a Critical Review of Available Assessments of Ti-N and Ti-C", *Z. Metallkd.*, **90**(7), 534–541 (1999) (Assessment, Phase Relations, Thermodyn., 38)

[1999Dum2] Dumitrescu, L.F.S., Hillert, M., "Reassessment of the Solubility of TiC and TiN in Fe", *ISIJ Int.*, **39**(1), 84–90 (1999) (Assessment, Calculation, Phase Diagram, Phase Relations, Thermodyn., 39)

[1999Fra] Frage, N., "Interaction between Nonstoichiometric Titanium Carbide and Fe-C Alloys", *Metall. Mater. Trans. B*, **30B**, 857–863 (1999) (Experimental, Phase Relations, Morphology, 22)

[1999Mov] Movchan, A.V., Pedan, L.G., Bachurin, A.P., "Growth of Austenite-Carbide Colonies on Carburizing Complex Fe-Ti Alloys", *Russ. Metall.*, (5), 66–71 (1999), translated from *Izv. Ross. Akad. Nauk*, (5), 53–57 (1999) (Experimental, Phase Relations, Morphology, 9)

[2000Bya] Byakova, A.V., "Structural Aspects of Strength and Methods to Increase the Serviceability of Carbide Coatings", *Powder Metall. Met. Ceram.*, **39**(1–2), 85–91 (2000) (Crys. Structure, Morphology, Experimental, Mechan. Prop., 13)

[2000Zhu] Zhukov, A.A., Savulyak, V.I., Arkhipova, T.F., "On the Effect of Elements on the Equilibrium Temperature of Eutectic Transformations", *Met. Sci. Heat Treat.*, **42**(1–2), 47–52 (2000) (Thermodyn., Review, 24)

[2001Lee] Lee, B.-J., "Thermodynamic Assessment of the Fe-Nb-Ti-C-N System", *Metall. Mater. Trans. A*, **32A**, 2423–2439 (2001) (Assessment, Calculation, Phase Diagram, Phase Relations, Thermodyn., 90)

[2001Ume] Umemoto, M., Liu, Z.G., Masuyama, K., Tsuchiya, K., "Influence of Alloy Additions on Production and Properties of Bulk Cementite", *Scr. Mater.*, **45**(4), 391–397 (2001) (Crys. Structure, Experimental, Mechan. Prop., Phase Relations, 13)

[2001Wan1] Wang, H., Wang, S., Yue, K., Dong, Y., Li, W., "The Rules of Thermodynamic Properties in Fe-C-j (j = Ti, V, Cr, Mn) Melts" (in Chinese), *Acta Metall. Sin.*, **37**(9), 952–956 (2001) (Calculation, Thermodyn., Review, 13)

[2001Wan2] Wang, C.G., Qi, B.S., Bai, Y.J., Wu, J., Yang, J.F., "Dispersion Strengthened Alloy Due to the Precipitation of Carbide During Mechanical Alloying", *Mater. Sci. Eng. A*, **308**(1–2), 292–294 (2001) (Experimental, Morphology, Mechan. Prop., 7)

[2002Liu] Liu, C.-S., Huang, J.-H., Sheng, Y., "Thermodynamic Analysis of C-Fe-Ti System" (in Chinese), *J. Inorg. Mat.*, **17**(2), 288–292 (2002) (Phase Relations, Calculation, 11)

DOI: 10.1007/978-3-540-74196-1_13

[2002Per] Persson, P., Jarfors, A.E.W., Savage, S., "Self-Propagating High-Temperature Synthesis and Liquid-Phase Sintering of TiC/Fe Composites", *J. Mat. Proc. Tech*., **127**(2), 131–139 (2002) (Experimental, Kinetics, Phys. Prop., 14)

[2002Ren] Ren, Y.L., Qi, L., Fu, L.M., Zhou, X.M., Han, X.L., Jiang, W.H., Pan, W.D., Cai, Q.K., "Microstructural Characteristics of TiC and (TiW)C Iron Matrix Composites", *J. Mater. Sci*., **37**(23), 5129–5133 (2002) (Crys. Structure, Morphology, Experimental, Phase Relations, 7)

[2003Che] Chen, Z.Q., Li, Y.G., Hu, D., Loretto, M.H., Wu, X., "Role of Alloying Elements in Microstructures of β Titanium Alloys with Carbon Additions", *Mater. Sci. Technol*., **19**, 1391–1398 (2003) (Crys. Structure, Experimental, Morphology, Phase Relations, 11)

[2003Fri] Frisk, K., "A Revised Thermodynamic Description of the Ti-C System", *Calphad*, **27**(3), 367–373 (2003) (Phase Diagram, Phase Relations, Thermodyn., Assessment, 22)

[2003Mei] Mei, Z., Yan, Y.W., Cui, K., "Effect of Matrix Composition on the Microstructure of in-situ Synthesized TiC Particulate Reinforced Iron-based Composites", *Mater. Lett*., **57**(21), 3175–3181 (2003) (Experimental, Mechan. Prop., Morphology, Thermodyn., 15)

[2003Rag] Raghavan, V., "C-Fe-Ti (Carbon-Iron-Titanium)", *J. Phase Equilib*., **24**(1), 62–66 (2003) (Phase Diagram, Phase Relations, Review, 19)

[2004Red] Reddy, R.G., Reddy, S.R., "Derivation and Consistency of the Partial Functions of a Ternary System Involving Interaction Coefficients", *Z. Metallkd*., **95**(9), 806–812 (2004) (Calculation, Thermodyn., 21)

[2004Sho] Shohoji, N., "M-C Dipole Formation in FCC (Face Centered Cubic) $Fe_{1-y}M_yC_x$ Solid Solution (M = Ti, Nb)", *Mater. Sci. Technol*., **20**(3), 301–306 (2004) (Calculation, Thermodyn., 16)

[2004Zha] Zhang, W., Zhang, X., Wang, J., Hong, C., "Effect of Fe on the Phases and Microstructure of TiC-Fe Cermets by Combustion Synthesis/Quasi-Isostatic Pressing", *Mater. Sci. Eng. A*, **A381**(1–2), 92–97 (2004) (Experimental, Morphology, Phase Relations, 14)

[2006Nak] Nakayama, Y., Pan, L., Takeda, G., "Low-Temperature Growth of Vertically Aligned Carbon Nanotubes Using Binary Catalysts", *Jpn. J. Appl. Phys*., **45**(1A), 369–371 (2006) (Experimental, Morphology, 16)

[2006Wu] Wu, Q., Sun, Y., Yang, C., Xue, F., Song, F., "Microstructure and Mechanical Properties of Common Straight Carbon Steels Strengthened by TiC Dispersions", *Mater. Trans.*, **47**(9), 2393–2398 (2006) (Phase Relations, Morphology, Mechan. Prop., Experimental, 26)

[2006MSIT] "C-Fe (Iron-Carbon)", Diagrams as Published, in *MSIT Workplace*, Effenberg, G. (Ed.), Materials Science International Services, GmbH, Stuttgart; Document ID: 30.13598.1.20 (2006) (Crys. Structure, Phase Diagram, Phase Relations, 2)

[Mas2] Massalski, T.B. (Ed.), *Binary Alloy Phase Diagrams*, 2nd edition, ASM International, Metals Park, Ohio (1990)

[V-C2] Villars, P. and Calvert, L.D., *Pearson's Handbook of Crystallographic Data for Intermetallic Phases*, 2nd edition, ASM, Metals Park, Ohio (1991)

DOI: 10.1007/978-3-540-74196-1_13

Carbon – Iron – Uranium

Viktor Kuznetsov

Introduction

The system was studied to provide a background for the description of the interaction between carbide fuels and steel canning materials.

Most attention has been paid to the vertical sections. The quasibinary section UC-Fe was studied by [1961Bar, 1963Bri1, 1963Bri2, 1963Nic, 1971Guh] and the results of [1963Bri2, 1963Nic, 1971Guh] are in good agreement. The UC-UFe_2 quasibinary section was studied by [1961Bar] and [1963Nic]. It was found that the section was of a simple eutectic type, but the eutectic temperature presented by [1961Bar] and the eutectic temperature presented by [1963Nic] differed by more than 120°C. The discrepancies in the results may have arisen from differences in the techniques used. [1961Bar] used metallographic observation of melting of powder mixtures of Fe and UC which had been annealed at various temperatures, whereas [1963Nic] used thermal analysis studies of alloys of higher purity which had been prepared by arc melting under an argon atmosphere on a water cooled copper hearth using a tungsten electrode.

The phase equilibria along the Fe-UC_2 tie line were studied by [1962Bal, 1963Bri2, 1963Nic]. [1962Bal] found that the $UFeC_2$ ternary carbide was formed peritectically from UC_2 and liquid [1963Bri2]. The existence of a quasibinary eutectic between Fe and $UFeC_2$ was established by [1963Bri2, 1963Nic]. The UC_2 - Fe section cannot be considered as truly quasibinary because of the eutectoid decomposition of UC_2 at 1516°C in the C-U binary system.

In addition to these sections, thermal analysis studies by [1963Nic] led to the suggestion of a number of invariant four-phase equilibria, but these are very uncertain and in need of further experimental investigation. They also presented a scheme of solid state tie lines for “low temperatures”. Based on these data, [1984Hol1, 1984Hol2] constructed schematic isothermal sections for 1000°C.

Recently, [1990Ale, 1992Ale] investigated the system with special attention to the UC-UC_2-$UFeC_2$ composition region through the study of approximately 10 alloys.

Based on the results of X-ray analysis of annealed and quenched alloys, [1990Ale] reported the existence of two new ternary carbides, namely $U_2Fe_2C_3$ and $U_3Fe_2C_5$. Later, [1995Wac] reported that compound called “$U_2Fe_2C_3$” by [1990Ale] is isotypic with $Th_{11}Fe_{12}C_{18}$. [1986Ger] found the $UFeC_2$ compound to be isostructural with $UCoC_2$.

[1992Ale] presented the liquidus projection, partial isothermal section at 1400°C and isothermal section at 1150°C. In addition to $UFeC_2$, three more ternary phases were found. The solubility of Fe in UC_{1+x} was studied; for compositions with $x \approx 0$ (near UC composition). The homogeneity region stretches towards a carbon content of $\geq$ 50 at.%, so this result does not contradict the absence of Fe solubility in UC found in the Fe-UC and UFe_2-UC sections by earlier investigators. For compositions with $x \approx 1$ (αUC_2), an island phase field of UC_{1+x} is found to exist at both temperatures. [1992Ale] also attempted to make a qualitative description of all topologically different isothermal sections where the liquid phase exists. These results were presented in the review of [2002Rag].

Thermodynamic data exist only for the $UFeC_2$ phase. Its Gibbs energy of formation was obtained by [1973Tan] using emf measurement of U activity in a $UFeC_2$+(C)+(Fe) mixture at 722 to 811°C. CaF_2 was used as solid electrolyte with a U+UF_3 mixture as reference electrode.

The reaction of UC and UC_2 powders with Fe as well as stainless steel at 1000°C was studied by [1962Kat] and [1963Nic]. [1974Mat] studied the influence of Fe on the self-diffusion of C in UC. [1988Jon] determined the products of acid hydrolysis of $UFeC_2$ and some other carbides as a tool for determining whether C atoms form chains.

Experimental investigations of phase relations, crystal structure and thermodynamics are reviewed in Table 1.

DOI: 10.1007/978-3-540-74196-1_14

Binary Systems

The three binary systems are taken from [Mas2]. In the C-U binary system, the UC_{1+x} phase ($x \approx 1$) in equilibrium with graphite should be denoted as the βUC_2 phase with a crystal structure of the CaF_2 type.

Solid Phases

In the C-U binary phase UC_{1+x} at temperatures between 2104 and 1769°C, there exists two separate regions with $x \approx 0$ and at $x \approx 1$ which are often considered as separate carbides, UC and βUC_2 [2001Che]. At 1400°C, the phase dissolves about 10 at.% Fe near the "UC" composition and also exists as a separate region at Fe contents of about 4 to 6 at.% and C contents of about 62 to 65 at.%, *i.e.* close to the "UC_2" binary composition [1992Ale]. At 1150°C, the Fe solubility is smaller, but both solid solutions near "UC" and a small separate region near "UC_2" still exist (see below Isothermal Sections).
Four ternary phases are known, denoted here τ_1 to τ_4. The τ_1 phase with the composition $UFeC_2$ is formed by a peritectic reaction in the section "UC_2"-Fe [1962Bal, 1963Bri1]. [1986Ger] found it to be isostructural with $UCoC_2$. Phase τ_2 was found by [1990Ale] to form peritectoidally at 1500 ± 100°C; a composition close to $U_3Fe_2C_5$ was claimed. Later, [1992Ale] shifted its composition from the section UC-Fe to a higher C content $U_{\sim 32}Fe_{\sim 17}C_{\sim 51}$ (see isothermal section at 1400°C below); this shift is accepted here. X-ray diffraction of this phase suggests it to be a distorted tetragonal solid solution of Fe in UC_{1+x} [1990Ale, 2002Rag]; though no structural studies were performed. The phase τ_3 exists at 1400°C but not at 1150°C in an alloy with a gross composition of $U_{30.6}Fe_{8.6}C_{60.8}$, taken from figure 2 of [1992Ale]; no structural data exist. The phase τ_4 is formed by peritectoid reaction at 1197°C [1992Ale] with a composition close to $U_2Fe_2C_3$; the stoichiometry $U_{11}Fe_{12}C_{18}$ following from its crystal structure was established by [1995Wac].
All of the phases are listed in Table 2.

Quasibinary Systems

The sections between UC-Fe and UC-UFe_2 are quasibinary with simple eutectics [1961Bar, 1963Bri1, 1963Bri2, 1963Nic, 1971Guh]. No solid solubilities were found in either. All data for the eutectic temperature and composition for UC-Fe section are in good agreement. The UC-Fe section is given in Fig. 1. A eutectic temperature of 1117°C was accepted from [1963Nic], where it was measured using TA. The UC-UFe_2 section is presented in Fig. 2 after [1961Bar, 1963Bri1, 1963Bri2, 1963Nic]. A eutectic melting temperature of 1201°C is accepted from [1963Nic]. This value is preferred as the method of observation of melting used by [1961Bar, 1963Bri1] may be too sensitive to admixtures.
The solubility of Fe in UC which was found by [1992Ale] does not lie in either of these sections (see Isothermal Sections below) and so does not contradict these findings.
The UC_2-Fe section, as presented by [1963Bri2], may be regarded as quasibinary but in the Fe-$UFeC_2$ composition region only, since the eutectoid decomposition of αUC_2 at 1516°C takes place in the C-U binary system. The peritectic formation of the τ_1 phase $UFeC_2$ occurs at 1615°C. The region between the τ_1 phase and βUC_2 is unclear. The Fe solid solution (about 3 mass%) is stabilized at low temperatures, and the βUC_2 phase and the τ_3 phase should exist at least around 1400°C according to [1992Ale]. But these results are in contradiction with those presented by [1963Bri2], who reported the decomposition of βUC_2 at temperatures lower than 1516°C. Since additional experimental data in this composition region are absent and the phase equilibria promise to be very complicated and would include the phase relations between solid phases existing at these temperature and composition intervals, the composition region between $UFeC_2$ and UC_2 was deleted from the section and it was bordered by $UFeC_2$ compound. The quasibinary section $UFeC_2$-Fe is presented in Fig. 3.

Invariant Equilibria

The invariant equilibria are listed in Table 3. They are almost confined to those in the quasibinary sections UC-Fe, UC-UFe_2 and the vertical section Fe-"UC_2" (see below).
Also, according to [1963Nic], two eutectic reactions: E_1: L ⇌ UC + (Fe) + UFe_2 at 1037°C and E_2: L ⇌ UC + UFe_2 + U_6Fe with a melting point of 720°C exist in the system. A series of invariant reactions

DOI: 10.1007/978-3-540-74196-1_14

proposed in [1992Ale] was omitted since they have not any experimental confirmation and are only speculative constructions.

Liquidus, Solidus and Solvus Surfaces

The liquidus projection presented by [1992Ale] was omitted since the amount of experimental data associated with its construction was not sufficient.

Isothermal Sections

A partial isothermal section for 1400°C is presented in Fig. 4. It is taken mainly from [1992Ale], but redrawn slightly to bring it into agreement with the accepted binary systems.
The UC phase dissolves up to about 10 at.% Fe. This unary region is directed along and somewhat above the line at 50 at.% C. This is the reason for it being missing in early works where the sections studied were directed from UC to Fe and UFe_2. Another stability region for that phase is near the UC_2 composition.
The isothermal section at 1050°C is presented in Fig. 5. It is also based on the data of [1992Ale]. The composition of the τ_4 phase has been changed slightly to bring it into accordance with the accepted stoichiometry $U_{11}Fe_{12}C_{18}$. Two regions of solid solubility of Fe in UC and βUC_2 still exist at this temperature though with narrower homogeneity ranges. Two three-phase fields with a seemingly identical phase composition of $L+UC+UFe_2$ are separated by the quasibinary section $UC\text{-}UFe_2$ with a maximum on the monovariant line and so differ in the composition of the participating liquid phases.

Thermodynamics

The Gibbs energy of formation of the τ_1 phase is presented in Table 4 as obtained by emf studies [1973Tan].

Notes on Materials Properties and Applications

Uranium monocarbide has received a good deal of attention as a reactor fuel, particularly for fast reactor applications, since it has the advantage over the dioxide UO_2 of possessing a high thermal conductivity and is, therefore, capable of being used at higher ratings with lower centre temperatures [1961Bar]. To elucidate the interaction between UC-base nuclear fuel and canning materials, the underlying phase equilibrium relationships in the system involved have been studied.
[1962Kat] studied the interaction of UC and UC_2 powders with Fe in samples held at 1000°C for 500 h. At these conditions, UC reacted with Fe; however, the UC_2 showed no signs of interaction. A parabolic time dependence was found for the reaction with UC.
[1963Nic] noticed that UC gives a "eutectic" (*i.e.* begins to form liquid) with stainless steel 100°C lower than with pure Fe.
Both UC and UC_2 quickly react with stainless steel after an induction period of 24 h [1962Kat]. [1966Far] noted that in the three-phase region $UC\text{-}UFe_2\text{-}Fe$, a UC-Fe mixture containing less than 50 at.% carbon did not react with type 316 stainless steel after 1500 h at 750°C, whereas unalloyed UC containing less than 50 at.% carbon reacted with stainless steel in 24 h at 750°C.

Miscellaneous

[1988Jon] found that the products of acid hydrolysis of $UFeC_2$ contain only CH_4 and concluded that no C-C bonds exist in crystals of that phase.
The self-diffusion of uranium in stoichiometric UC which was doped with Fe is increased as compared to undoped UC at all temperatures studied (1380 to 2200°C). The increase was most pronounced (by more than a factor of 100) at low temperatures [1974Mat]. Simultaneously, pronounced grain-boundary penetration was observed at low temperatures.

DOI: 10.1007/978-3-540-74196-1_14

Table 1. Investigations of the C-Fe-U Phase Relations, Structures and Thermodynamics

Reference	Method/Experimental Technique	Temperature/Composition/Phase Range Studied
[1961Bar]	Metallography, XRD	Up to 1800°C, sections UC-Fe and UC-UFe_2
[1962Bal]	Metallography, chemical analysis of single-phase specimen, density and microhardness measurements, thermal analysis, XRD	$UFeC_2$ and close compositions
[1963Bri1]	Metallographical and X-ray investigation of annealed mixtures of powders of UC and UC_2 with Fe	Up to 1800°C, sections UC-Fe and UC-UFe_2
[1963Bri2]	Metallographical and X-ray investigation of annealed mixtures of powders of UC and UC_2 with Fe	Up to 1950°C, sections UC-Fe, UC-UFe_2 and UC_2-Fe
[1963Nic]	Thermal analysis, metallography	Up to 1700°C, U_6Fe-UC-UC_2-Fe composition region
[1971Guh]	Metallography, XRD	Section UC-Fe
[1973Tan]	emf	$UFeC_2$ compound, 722 to 811°C
[1986Ger]	Powder XRD	Crystal structure of $UFeC_2$
[1990Ale]	XRD	X-ray data and temperatures of formation of "$U_2Fe_2C_3$" and "$U_3Fe_2C_5$"
[1992Ale]	Metallography, XRD, EPMA	UC-UC_2-Fe region: UC-UC_2-$UFeC_2$ at 1400°C, other at 1050°C
[1995Wac]	XRD	Crystal structure of "$U_2Fe_2C_3$" phase

Table 2. Crystallographic Data of Solid Phases

Phase/ Temperature Range [°C]	Pearson Symbol/ Space Group/ Prototype	Lattice Parameters [pm]	Comments/References
(C) gr < 3827	*hP*4 $P6_3/mmc$ C (graphite)	a = 246.12 c = 670.90	at 25°C [Mas2] sublimation point
(δFe) 1538 - 1394	*cI*2 $Im\bar{3}m$ W	a = 293.15	[Mas2]
(γFe) 1394 - 912	*cF*4 $Fm\bar{3}m$ Cu	a = 364.67	at 915°C [V-C2, Mas2]
(αFe) < 912	*cI*2 $Im\bar{3}m$ W	a = 286.65	at 25°C [Mas2]

(*continued*)

DOI: 10.1007/978-3-540-74196-1_14

Phase/ Temperature Range [°C]	Pearson Symbol/ Space Group/ Prototype	Lattice Parameters [pm]	Comments/References
(γU) 1135 - 776	*cI*2 $Im\bar{3}m$ W	a = 352.4	[Mas2]
(βU) 776 - 668	*tP*30 $P4_2/mnm$ βU	a = 1075.9 c = 565.6	[Mas2]
(αU) < 668	*oC*4 *Cmcm* αU	a = 285.37 b = 586.95 c = 495.48	at 25°C [Mas2]
UC_{1+x} < 2530 (at $x \approx 0$) 2585 - ~2100 (at $x \approx 1$)	*cF*8 $Fm\bar{3}m$ NaCl	a = 496.1 a = 507.5 a = 550.4	x = 0, room temperature [V-C] x = 0, at 2100°C x = 0.9 at 2100°C [1972Ben]
βUC_2 ~2100 - 1768	*cF*12 $Fm\bar{3}m$ CaF_2?	a = 547.5	[2001Che] actually, "βUC_2" phase represents the UC phase in equilibrium with graphite [2001Che]
αUC_2 1793 - 1516	*tI*6 *I*4/*mmm* CaC_2	a = 355.2 c = 598.8	[V-C2] may be stabilized by alloying with Fe up to 1050°C [1992Ale]
U_2C_3 1823 - 850	*cI*40 $I\bar{4}3d$ Pu_2C_3	a = 807.4	[V-C2]
UFe_{2-x} < 1228	*cF*24 $Fd\bar{3}m$ $MgCu_2$	a = 707.2 a = 706.3	x = –0.137 x = 0.048, [V-C2]
U_6Fe < 795	*tI*28 *I*4/*mcm* Mn_6U	a = 1028.63 c = 524.10	[V-C2]
* τ_1, $UFeC_2$ < 1615 ± 10	*tP*8 *P*4/*mmm* $UCoC_2$	a = 349.44 ± 0.06 c = 738.9	[V-C2]
* τ_2, $U_{\sim 32}Fe_{\sim 17}C_{\sim 51}$ < 1500 ± 100	*t***	a = 500.7 c = 508.4	stoichiometry $U_3Fe_2C_5$ [1990Ale] stoichiometry $U_{\sim 32}Fe_{\sim 17}C_{\sim 51}$ [1992Ale]
* τ_3, $U_{30.6}Fe_{8.6}C_{60.8}$ (≥1400) - (>1150)	-	-	[1992Ale]
* τ_4 $U_{11}Fe_{12}C_{18}$ < 1197	*cI*82 $I\bar{4}3m$ $Th_{11}Ru_{12}C_{18}$	a = 1006.8	[1990Ale], [1995Wac]

DOI: 10.1007/978-3-540-74196-1_14

Table 3. Invariant Equilibria

Reaction	T [°C]	Type	Phase	Composition (at.%)		
				C	Fe	U
$1 + UC_2$[a)] $\rightleftharpoons UFeC_2$	1615±10	p_1	L $UFeC_2$	48.8 50	26.8 25	24.4 25
$1 \rightleftharpoons UC + UFe_2$	1201	e_1 (max)	L UC UFe_2	3.8 ~ 50 ~ 0	61.7 ~ 0 ~ 66.7	34.5 ~ 50 ~ 33.3
$1 \rightleftharpoons UFeC_2 + (\gamma Fe)$	1160	e_2 (max)	L $UFeC_2$ (γFe)	14.8 50 ~ 0	70.4 25 ~ 100	14.8 25 ~ 0
$1 \rightleftharpoons UC + (\gamma Fe)$	1117	e_3 (max)	L UC (γFe)	48.8 ~ 50 ~ 0	26.8 ~ 0 ~ 100	24.4 ~ 50 ~ 0
$L \rightleftharpoons UC + (\gamma Fe) + UFe_2$	1037	E_1	UC (γFe) UFe_2	~ 50 ~ 0 ~ 0	~ 0 100 ~ 66.7	~ 50 ~ 0 ~33.3
$L \rightleftharpoons UC + UFe_2 + U_6Fe$	720	E_2	UC UFe_2 U_6Fe	~ 50 ~ 0 ~ 0	~0 ~ 66.7 ~ 7.7	~ 50 ~ 33.3 92.3

a) note: contains some (not determined exactly, probably about 3 mass%) Fe

Table 4. Thermodynamic Data of Reaction or Transformation

Reaction or Transformation	Temperature [°C]	Quantity, per mol [kJ, mol, K]	Comments
$(\alpha Fe) + (\beta U) + 2C(gr) \rightleftharpoons UFeC_2$	722-778	$\Delta G = -139.03 + 0.01448T$	emf [1973Tan]
$(\alpha Fe) + (\gamma U) + 2C(gr) \rightleftharpoons UFeC_2$	778-811	$\Delta G = -146.65 + 0.02172T$	emf [1973Tan]

DOI: 10.1007/978-3-540-74196-1_14

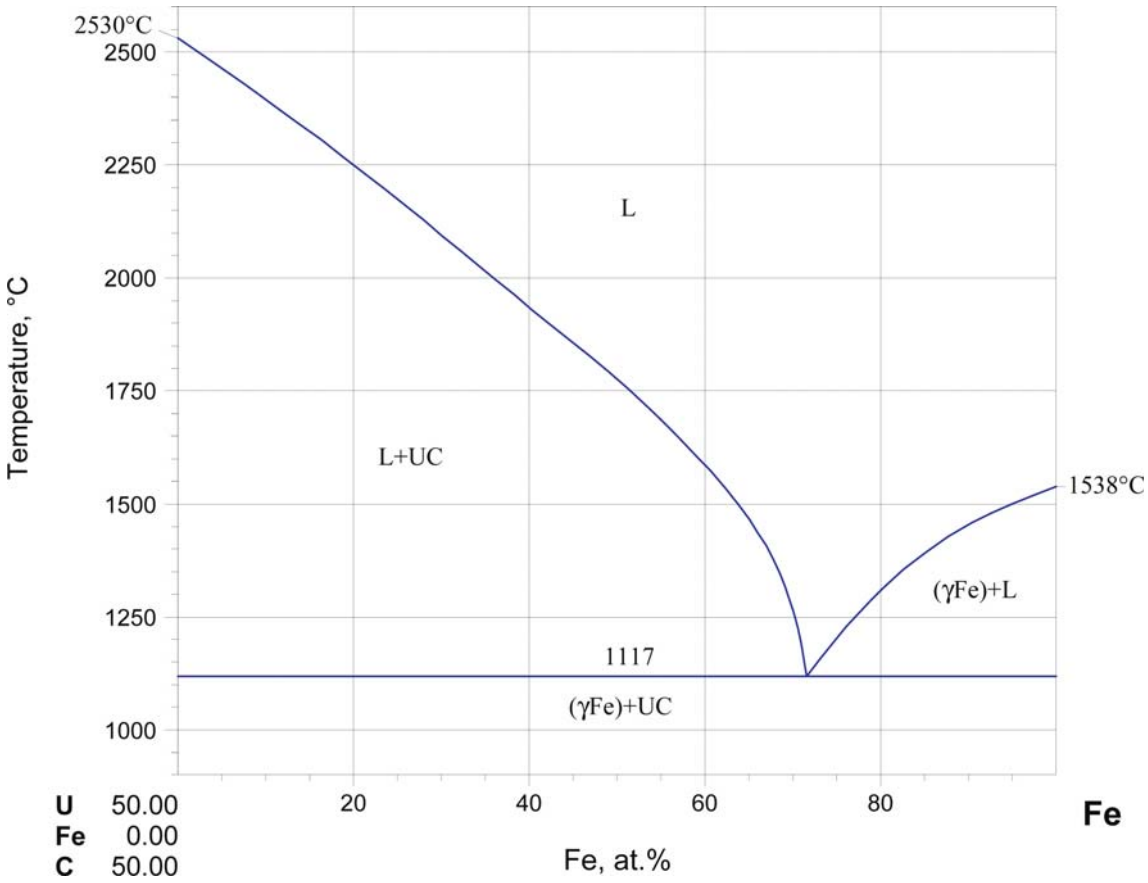

Fig. 1. C-Fe-U. The UC-Fe quasibinary section

DOI: 10.1007/978-3-540-74196-1_14

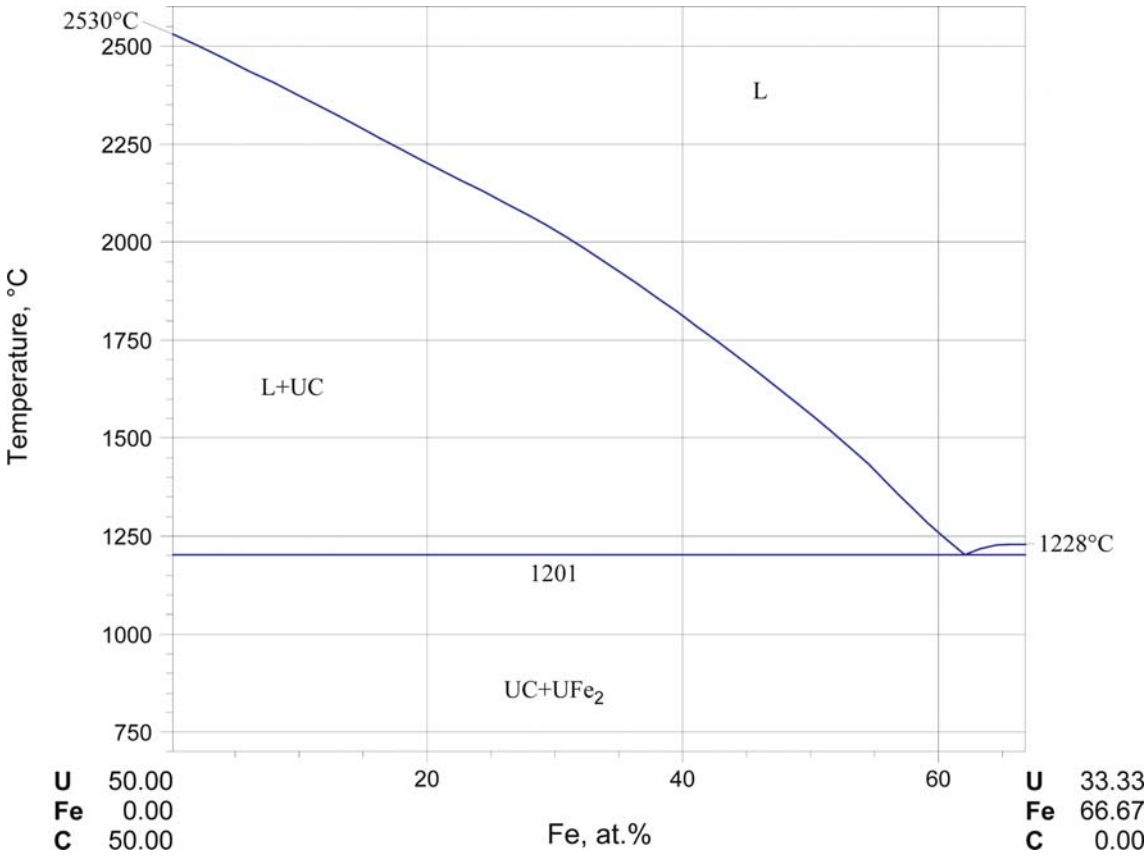

Fig. 2. C-Fe-U. The UC-UFe_2 quasibinary section

DOI: 10.1007/978-3-540-74196-1_14

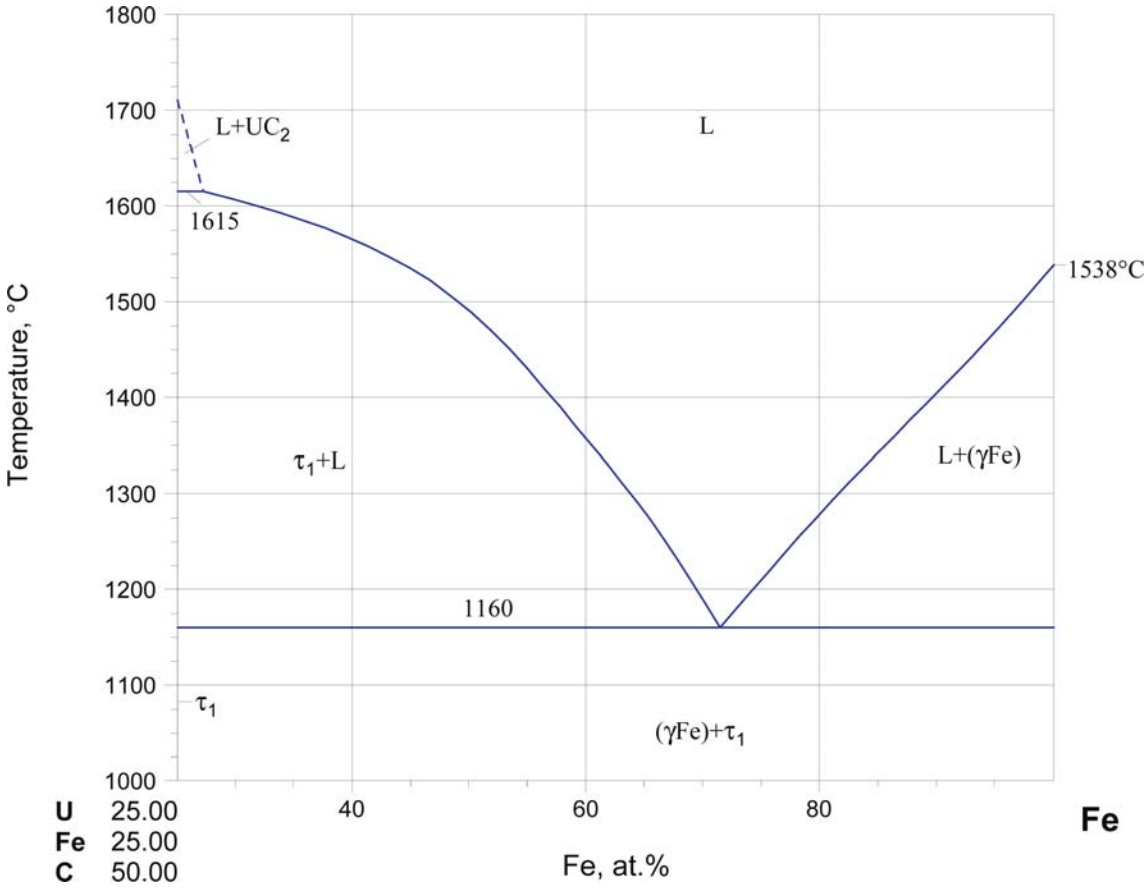

Fig. 3. C-Fe-U. The $UFeC_2$-Fe quasibinary section

DOI: 10.1007/978-3-540-74196-1_14

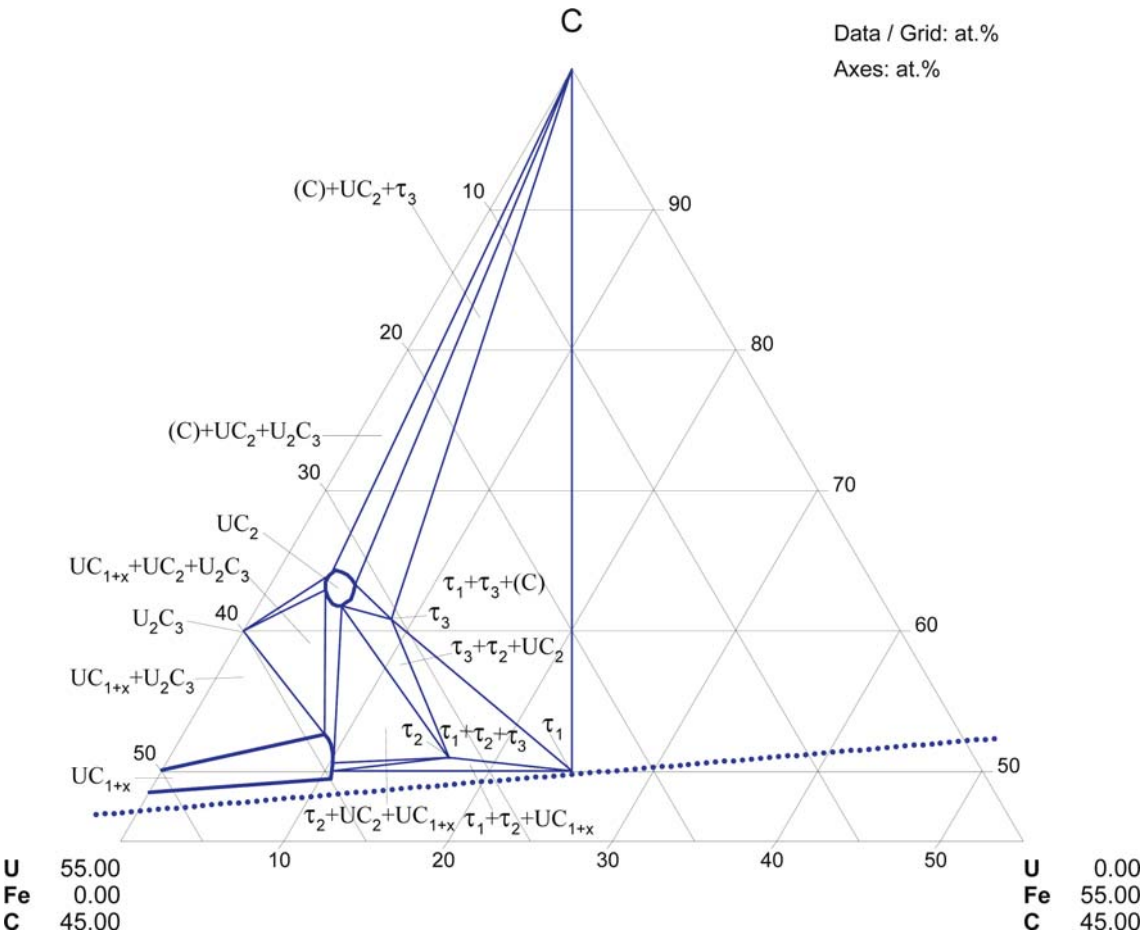

Fig. 4. C-Fe-U. Partial isothermal section at 1400°C

DOI: 10.1007/978-3-540-74196-1_14

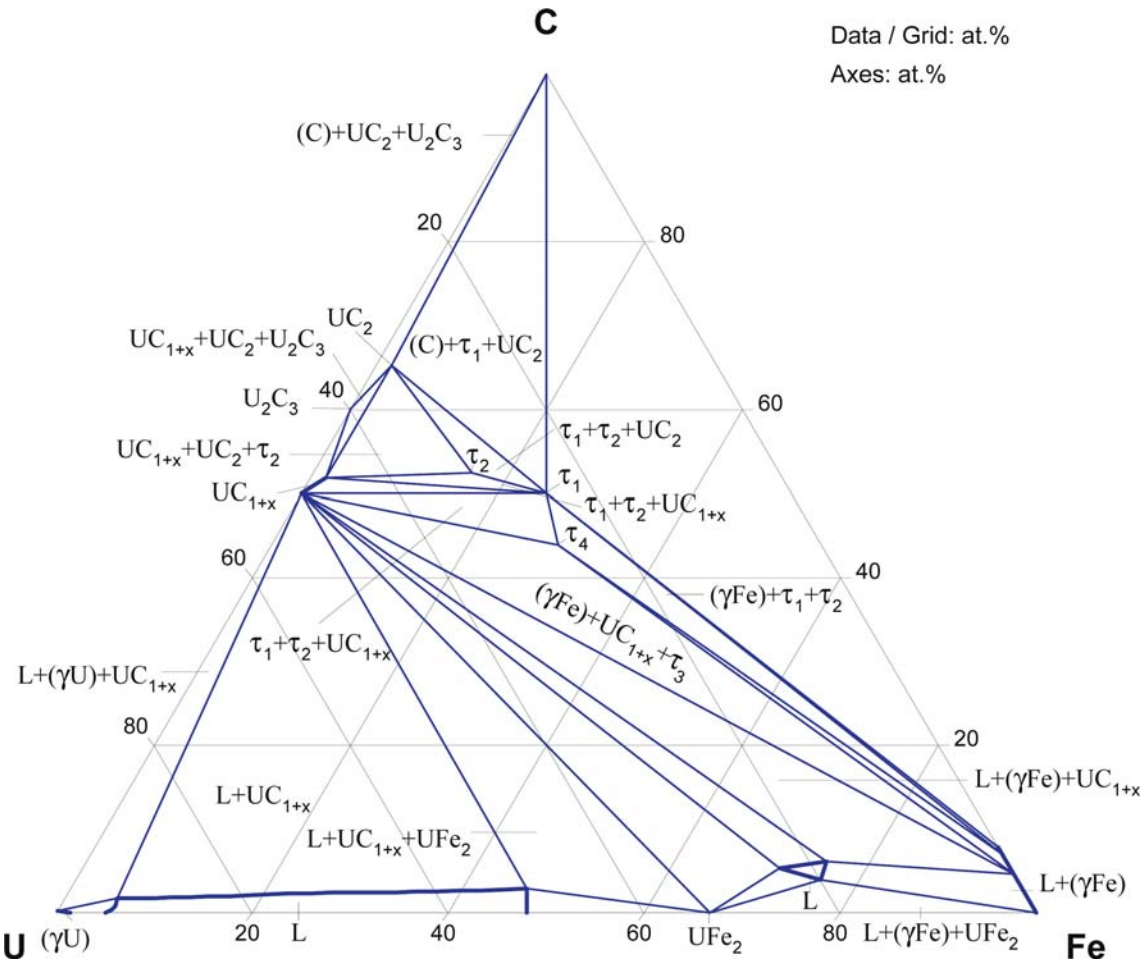

Fig. 5. C-Fe-U. Isothermal section at 1050°C

DOI: 10.1007/978-3-540-74196-1_14

References

[1961Bar] Barta, J., Briggs, G., White, J., "Phase Diagrams of Uranium Monocarbide - Transition Metal Systems", *J. Nucl. Mater.*, **4**, 322–324 (1961) (Experimental, Phase Diagram, Phase Relations, 6)

[1962Bal] Baldock, P., McLaren, J.R., Hedger, H.J., "A Ternary Compound in the U-Fe-C System", *J. Nucl. Mater.*, **5**, 257–258 (1962) (Crys. Structure, Experimental, 2)

[1962Kat] Katz, S., "High Temperature Reactions Between Refractory Uranium Compounds and Metals", *J. Nucl. Mater.*, **6**, 172–181 (1962) (Experimental, Calculation, Phase Relations, 21)

[1963Bri1] Briggs, G., Barta, J., White, J., "Phase Diagrams of Uranium Monocarbide-Transition Metal Systems - the Systems UC-Cr, UC-Fe, UC-UFe_2, and UC-Ni", *Powder Mettalutgy in the Nuclear Technics, 4 Plansee Seminar "De Re Metallica"*, Juni 1961, Reutte, Tirol, Benesovsky, F. (Ed.), Metallwerk Plansee AG., Reutte, Tirol, 1962, 249–278 (1963) (Crys. Structure, Experimental, Morphology, Phase Diagram, Phase Relations, Thermodyn., 12)

[1963Bri2] Briggs, G., Guha, J., Barta, J., White, J., "Systems of UC, UC_2, and UN with Transition Metals", *Trans. Brit. Ceram. Soc.*, **62**, 221–246 (1963) (Experimental, Morphology, Phase Diagram, Phase Relations, Thermodyn., 18)

[1963Nic] Nichols, J.L., Marples, J.A.C., "An Investigation of the U-C-Fe and Pu-C-Fe Ternary Phase Diagram with Some Observations on the U-Pu-C-Fe Quaternary", *Carbides in Nuclear Energy*, Symp. Harwell, England (Publ. 1964), 246–260 (1963) (Crys. Structure, Experimental, Phase Diagram, Phase Relations, 11)

[1966Far] Farkas, M.S., Storhok, V.W., Pardue, W.M., Smith, R.A., Veigel, N.D., Miller, N.E., Wright, T.R., Barnes, R.H., Chubb, W., Lemmon, A.W., Berry, W.E., Rough, F.A., "Fuel and Fertile Materials - Uranium Metal and Alloys - Plutonium - Thorium - Metal-Ceramic Fuels - Coated-Particle Fuel Materials - Uranium and Thorium Oxides - Uranium Carbides, Nitrides, Phosphides, Sulfides and Arsenides - Fuel-Water Reactions", *Reactor Mater.*, **9**(3), 151–165 (1966) (Assessment, Electr. Prop., Mechan. Prop., Phys. Prop., Transport Phenomena, 77)

[1971Guh] Guha, J.P., "Phase Equilibrium Relationships in the System UN-UC-Fe", *J. Nucl. Mater.*, **41**, 187–194 (1971) (Experimental, Phase Diagram, Phase Relations, 15)

[1972Ben] Benz, R., Farr, J.D., "X-ray Diffraction of UC-UC_2 and UC-UN Alloys at Elevated Temperatures", *J. Nucl. Mater.*, **42**, 217–222 (1972) (Crys. Structure, Experimental, 18)

[1973Tan] Tanaka, H., Kishida, Y., Moriyama, J., "Standard Free Energies for the Formation of $UFeC_2$ and UWC_2 by Electro-Motive Force Measurements" (in Japanese), *J. Jpn. Inst. Met.*, **37**, 564–567 (1973) (Crys. Structure, Experimental, Phase Diagram, Phase Relations, Thermodyn., 11)

[1974Mat] Matzke, Hj., "The Effect of Fe, Ni and W Impurities on Uranium Diffusion in Uranium Monocarbide", *J. Nucl. Mater.*, **52**, 85–88 (1974) (Experimental, Optical Prop., Transport Phenomena, 18)

[1984Hol1] Holleck, H., "Ternary Carbide Systems of Actinoids with the Transitions Metals of 4 to 8 Groups", *J. Nucl. Mater.*, **124**, 129–146 (1984) (Assessment, Crys. Structure, Phase Diagram, Phase Relations, 78)

[1984Hol2] Holleck, H., "Ternary Carbide Systems of Actinoids with Transition Metals of Other Groups" (in German), in "*Binary and Ternary Transition Metal Carbide and Nitride Systems*", Petzow, G. (Ed.) Gebrueder Borntraeger Berlin, Stuttgart, 92–111 (1984) (Crys. Structure, Phase Diagram, Phase Relations, Review, 91)

[1986Ger] Gerss, M.H., Jeitschko, W., "The Crystal Structures of Ternary Actinoid Iron (Cobalt, Nickel) Carbides with Composition 1:1:2", *Mater. Res. Bull.*, **21**, 209–216 (1986) (Crys. Structure, Experimental, 29)

[1988Jon] Jones, D.W., McColm, I.J., Yerkess, J., Clark, N.J., "Carbon Species in the Crystal Structures of Uranium-Transition-Element Carbides, UMC_2", *J. Solid State Chem.*, **74**, 304–313 (1988) (Crys. Structure, Experimental, 27)

[1990Ale] Alekseeva, Z.M., "Crystal Structure of Ternary Compounds $C_3Fe_2U_2$ and $C_5Fe_2U_3$", *Sov. Phys.-Crystallogr.(Engl. Transl.)*, **35**, 749–750 (1990), translated from *Kristallografiya*, **35**, 1273–1274 (1990) (Crys. Structure, Experimental, 4)

DOI: 10.1007/978-3-540-74196-1_14

[1992Ale] Alekseyeva, Z.M., "Phase Constitution of C-Fe-U Alloys" (in Russian), *Metally*, (5), 151–157 (1992) (Experimental, Phase Diagram, Phase Relations, 7)

[1995Wac] Wachtmann, K.H., Moss, M.A., Hoffmann, R.-D., Jeitschko, W., "Crystal Structures of Several Ternary Lanthanoid and Aactinoid Ruthenium Carbides", *J. Alloys Compd.*, **219**, 279–284 (1995) (Crys. Structure, Experimental, Phase Diagram, Phase Relations, 32)

[2001Che] Chevalier, P.Y., Fischer, E., "Thermodynamic Modelling of the C-U and B-U Binary Systems", *J. Nucl. Mater.*, **288**, 100–129 (2001) (Phase Relations, Thermodyn., Calculation, Assessment, 97)

[2002Rag] Raghavan, V., "C-Fe-U (Carbon-Iron-Uranium)", *J. Phase Equilib.*, **23**, 521–522 (2002) (Phase Relations, Review, 6)

[Mas2] Massalski, T.B. (Ed.), *Binary Alloy Phase Diagrams*, 2nd edition, ASM International, Metals Park, Ohio (1990)

[V-C] Villars, P. and Calvert, L.D., *Pearson's Handbook of Crystallographic Data for Intermetallic Phases*, ASM, Metals Park, Ohio (1985)

[V-C2] Villars, P. and Calvert, L.D., *Pearson's Handbook of Crystallographic Data for Intermetallic Phases*, 2nd edition, ASM, Metals Park, Ohio (1991)

DOI: 10.1007/978-3-540-74196-1_14

Carbon – Iron – Vanadium

Volodymyr Ivanchenko, Tatyana Pryadko

Introduction

The influence of V on structure and properties of iron and steels was realized in the steelworks of Sheffield University during a series of researches carried out from 1899 to 1902. The first review on the structure, carbide composition, and properties of steels alloyed with vanadium was presented by [1912Arn]. The first fundamental investigation of C-Fe-V alloys was performed by [1930Oya1, 1930Oya2], who presented the phase equilibria in the Fe rich portion of the phase diagram. But raw materials in this work were seriously contaminated with Si and Mn. Phase relations in the Fe rich corner were also determined by [1931Hou] and locations of borders of some phase domains were predicted. [1931Vog] constructed some vertical sections in the C-Fe-V system. The above experimental results were reviewed by [1949Jae]. But these early results are of limited use because they did not include the binary V_2C compound formation. [1955Bun] investigated the solubility of V_4C_3 in austenite by combining experimental study with thermodynamic calculations.

[1963Fle] and [1969Ebe] reported solubility data of VC_y in austenite at 1000°C. Phase equilibria along the Fe-VC quasibinary section have been studied by [1975Fre] and [1978Dmi].

Thermodynamic properties of the liquid C-Fe-V alloys has been studied by [1959Fuw, 1963Ell, 1962Neu, 1963Mor, 1972Foo, 1974Sig, 1983Mor]. Liquid-solid equilibria were studied in the Fe rich corner by [1988Kes]. It was shown that the crystallographic structure and morphology of the VC_y carbides are related to the crystallization path during solidification [1989Kes].

[1993Pol, 1994Pol] determined the compositions of phases presented in C-Fe-V alloys in order to assess which phases are best suited for the C-Fe-V hardfacing materials. In accordance with these results, for the compositions presented in Table 1, $VC_{0.76}$ stoichiometry was in the best agreement between experimental results and calculations. [2001Wan] estimated the influence of V on the C solubility in the C-Fe melt using thermodynamic calculations.

[1968Zup] evolved statistical thermodynamics of C in ternary austenite using the C-Fe-V system as an example. A review of thermodynamic properties of C in alloyed austenite, including C-Fe-V system, was performed by [1968Chi]. [1970Sch] analyzed the literature data on the effect of V, Ga and In on the solubility of C in molten iron and tried to establish a relationship between the solubility or interaction parameters and the structure of the periodic table. The activity of C in (αFe) and (γFe) solid solutions was studied by [1981Bra].

The extension of the austenitic field in the C-Fe-V system was computed by [1977Uhr, 1978Uhr] who also presented the isothermal sections of the Fe rich part at 800, 850, 900, 1000, and 1100°C. The assumption made in the calculations is that the carbides found in steels are the stoichiometric with the composition of $VC_{0.75}$.

A method of calculating the corners of the tie-triangles and quadrilaterals which define the positions of multi-phase equilibrium regions in the isothermal sections of the ternary systems was described by [1983Sil]. Partial isothermal section at 1149.3°C in the region up to 25 at.% V and 1 at.% C was presented. Isothermal sections of the Fe rich corner of the (γFe)+VC_y two-phase region at 900, 1000, 1200, and 1300°C were calculated by [1986Pop]. [1997Du] used Thermo-Calc software to predict the eutectic point $L \rightleftharpoons (\gamma Fe) + M_3C + MC$.

A detailed electron microscopic examination has been made on high purity C-Fe-V alloys with particular reference to the aging behavior prior to the hardness peak in the temperature range of 500-600°C [1966Ray]. Precipitation of vanadium carbide on aging has been studied in a ferritic iron-vanadium alloy containing a small amount of carbon by [1973Hei].

The morphology and growth kinetics of grain boundary ferritic allotriomorphs and the distribution of VC_y particles associated with allotriomorphs were studied in a Fe-0.12C-0.11V (mass%) alloy isothermally reacted at temperatures in the range of 800 to 870°C by [1985Abe]. Some aspects of carbide precipitations

DOI: 10.1007/978-3-540-74196-1_15

under decomposition of ferrite or austenite were presented by [1971Sut, 1973Bat, 1973Edm, 1985Par]. Electrical resistivity measurements at 77 K have been used to follow vanadium carbide precipitation in an Fe-0.12C-0.02Mn-0.46 mass% V alloy during isothermal aging between 598 and 800°C after solution treatment at 1200°C. The contribution in the resistivity from the lattice, grain boundaries, dislocations, carbon, and V were evaluated and found to agree well with the measured values. Based on the obtained earlier theoretical results, a numerical analysis of the experimental isochronal magnetic permeability disaccommodation curves was performed for dilute α-C-Fe-V alloys [1981Kus]. Calculations have been intended to give the optimum values of parameters describing the potential energy of C-atoms in α-C-Fe-V. [1988Tod] successfully explained many observations regarding the interphase precipitation reaction in C-Fe-V alloys under eutectoid decomposition of austenite. [2003Yam] simulated the precipitation of V_4C_3 during tempering of a martensite steel in the C-Fe-V ternary system, taking into account of local equilibrium, the capillarity effect, cementite enrichment and dissolution. Coupled solute drag effects on ferrite formation was studied by [2004Aar]. Recrystallization in cold-rolled C-Fe-V alloy containing fine carbide was studied by [1982Dun]. [1973Hof] discussed the influence of the C content on V segregation and formation of carbides with uniform total V content.

[2000Zhu] studied the effect of elements, including V, on the equilibrium temperature of eutectic austenite-graphite and austenite-cementite transformations to prognosis the driving forces of graphitization. Crystallization behavior of $Fe_{73.1}V_{19.9}C_{14}$ thick films was studied by [1991Has]. The solidification microstructures of hypereutectic alloy powders produced by rapid solidification in gas atomization process were studied by [1997Beh].

Diffusion of C in one- or multiphases C-Fe-V alloys has been examined by [1964Wev]. [1997Pop] determined the mutual diffusion coefficients of V in austenite and ferrite. The diffusional interaction of VC with Fe was studied by [1999Pop]. The diffusion coefficients of V across the interface from H 100 steel into Fe with no added carbon and when 1 mass% carbon has been added were measured by [2001Mar].

The effect of composition and structure on the microhardness, plasticity parameter and fracture toughness of VC layer on high carbon steel was studied by [2000Bya]. The solid solubility of V in cementite at 900°C, as well as mechanical properties of bulk cementite were studied by [2001Ume].

Thermal expansion of Fe-$VC_{0.75}$ alloys was studied by [1997Shu].

Equilibrium surface segregations of V and C on Fe-3V-C (100), (111) and (110) surfaces were studied by [1992Ueb], [1993Ueb], and [1995Ueb], respectively.

Electron structure of Fe-0.2 mass% C melts doped with 0.05-0.45 mass% V was studied by [1978Dov].

Three thermodynamic computations of the C-Fe-V system were performed by [1986Pop, 1991Hua, 1991Lee]. [1986Pop] indicated that the composition of VC_y in equilibrium with austenite varies from $VC_{0.92}$ to $VC_{0.84}$. A more detailed thermodynamic analysis of the system was carried out by [1991Hua] and [1991Lee]. The thermodynamic parameters resented by [1991Hua] were successfully used by [2005Pop] in the thermodynamic calculations of the C-Fe-N-V system.

The comprehensive reviews of phase equilibria in the C-Fe-V system have been presented in [1984Rag, 1987Rag, 1993Rag, 2003Rag].

The data on experimental study of crystal structure and phase equilibria are presented in Table 1.

Binary Systems

The C-Fe phase diagram is accepted as presented in [2006MSIT].

The Fe-V system is taken mainly from [Mas2], except for the Fe rich part of the σ phase region, which is presented in Fig. 1 in accordance with [2005Ust]. [2005Ust] found that the σ phase exists in the temperature range from 1219 to 650°C, and a phase separation is observed below 650°C. In the accepted Fe-V phase diagram the σ phase decomposes eutectoidally into (αFe) and (V) at about 650°C. Because of the contradiction between these results and the shape of the σ phase region presented by [1984Smi], the V rich part needs further experimental work.

In the composition range of 0-34 at.% C the C-V phase diagram is accepted from [1985Car]. In the composition range of 34-55 at.% C the C-V phase diagram is accepted as presented by [1999Lip]. It is given in Fig. 2. The main differences between phase diagram assessed by [1985Car] and experimental data of

DOI: 10.1007/978-3-540-74196-1_15

[1999Lip] obtained with X-ray diffraction and DSC methods are related to the phase relations between disordered VC_y and both V_6C_5 and V_8C_7 ordered phases, and temperature of peritectoid formation of V_4C_{3-x} denoted by [1999Lip] as V_3C_2 and its homogeneity region.

Solid Phases

Table 2 summarizes the crystal structure data of the unary, binary and ternary phases of this system. Vanadium forms a cubic monocarbide VC_y with *B*1 (NaCl) structure and a lower hexagonal carbide V_2C. These carbides possess extended regions of homogeneity, the width of which depends of temperature. For example, at 1800°C a cubic vanadium carbide VC_y and a hexagonal vanadium carbide V_2C_y display the regions of homogeneity $VC_{0.58}$ - $VC_{0.87}$ and $V_2C_{0.74}$ - $V_2C_{1.0}$, respectively. In such strongly no-stoichiometric carbides the carbon atoms may occupy only a fraction of the interstitial sites. At high temperatures (>1250°C) the carbon atoms and unfilled interstitial sites are distributed in the carbon lattice in a random fashion. Lowering the temperature leads to a redistribution of non-metallic interstitial atoms and structural vacancies and results in disorder-order phase transformations that give rise to various ordered structures. A cubic ordered V_8C_7 phase arises in the VC_y carbide over the range $VC_{0.87}$-$VC_{0.875}$ [1999Lip]. This superstructure has a double lattice spacing with respect to the lattice spacing of a disordered phase. An other ordered phase, V_6C_5, may have trigonal (space group $P3_1$) [1968Ven] or monoclinic symmetry (space group $C2$ [1972Bil], or $C2/m$ [1988Kes] and was experimentally observed in vanadium carbide VC_y over the range $VC_{0.75}$ - $VC_{0.83}$. The trigonal and monoclinic superstructures are closely related and are identical in the character of the short-range order. All forms of V_2C are based on a hcp sublattice of V atoms. The disordered hexagonal structure is designated as βV_2C. The evidence for ordering of the C atoms in material, that was equilibrated at 900°C for seven days has been found with neutron diffraction by [1967Yvo]. Composition was not specified. This ordered structure was also hexagonal, with reflections intensities being compatible with an εFe_2N type structure. The *a* parameter of the ordered structure was approximately $\sqrt{3}$ times the *a* parameter of the disordered structure, and the *c* parameters of both the ordered and disordered structures were approximately equal. This hexagonal ordered structure is designated $\beta' V_2C$. The additional ordering occurs in V_2C below ~800°C to produce an orthorhombic structure. Neutron diffraction data [1967Yvo] showed all diffraction maxima from this phase to have intensities and indices compatible with the ξFe_2N type structure. Two or more extraneous maxima detected by X-ray diffraction most likely are arising from contaminations or from twinning or faulting.

In the formula V_4C_{3-x}, *x* is near 1/3 corresponding to 40 at.% C, that was the reason to denote it as V_3C_2 by [1999Lip]. Its trigonal structure with twelve close-packed V layers in the sequence *ABABCACABCBC* has $R\bar{3}m$ space group symmetry. This structure is believed to be isostructural with Sn_4P_3. A ternary carbide, Fe_3V_3C (τ), with a complex fcc structure and 16 formula per unit cell, has been reported by [1966Grd1, 1966Grd2]. It is isostructural with the η carbide (Fe_3W_3C). This carbide was not found at 1100°C by [1981Hol]. It probably exists only in narrow composition and temperature ranges [1987Rag].

Quasibinary Systems

A quasibinary section of Fe_3C - $VC_{0.75}$ reported by [1931Vog] is a simple eutectic system with the eutectic temperature of 1151°C and the eutectic composition of 62 at.% Fe, 28 at.% C and 10 at.% V. [1978Dmi] reported on the existence of a quasibinary section along the Fe-VC vertical section. It is of the eutectic type. The eutectic temperature was reported to be 1350±50°C. The eutectic composition given by [1978Dmi] is 82 at.% Fe. In this section, three invariant reactions similar to those in the C-Fe binary system were presented. With the appreciable solubility of C in (δFe) and (γFe) and keeping in mind the large solubility of V in (αFe), it is doubtful to expect that quasibinary section lies exactly in the Fe-VC plane. This fact was accentuated by [1984Rag]. The calculated vertical section along the Fe-VC join [1991Hua, 1991Lee] shows the existence of a three-phase region under crystallization line of the binary (γFe)+VC eutectic. It agrees well with the C-Fe-V liquidus surface constructed by [1987Rag] based mainly on the results of [1930Oya2]. The existence of a maximum on the univariant line from U_1 to E_1 at about 1415°C (e_3) may be considered as an evidence of the existence of a quasibinary section on the join $Fe_{82}V_{17}$ - $VC_{0.75}$, where

DOI: 10.1007/978-3-540-74196-1_15

the tie-line triangle of the eutectic reaction is degenerated in a straight line. A cross-section point of the interconnection between Fe and $VC_{0.75}$ with the univariant line from U_1 to E_1 gives very close results with respect to the melting temperature and the composition point of the eutectic presented by [1978Dmi] and [1997Shu].

Invariant Equilibria

The accepted reaction scheme (Fig. 3) is a compilation of the reaction scheme constructed by [1987Rag] and the recent data on the decomposition of σ phase presented by [2005Ust]. It is consistent with the invariant reactions on the liquidus surface [1988Kes] and the isotherm at 1100°C from [1981Hol]. [1987Rag] presented the three-phase equilibrium α+V_2C+σ as originated from a maximum point within a triangle. In the solid state, the γ phase decomposition through a ternary eutectoid reaction was presented by [1987Rag] in accordance with [1972Col]. The ternary compound τ was assumed to be formed by a peritectoid reaction between α and V_2C [1987Rag]. A transition reaction U_2 was proposed by [1987Rag] to account for the three-phase fields α+σ+τ and V_2C+σ+τ in the isotherm at 500°C presented by [1966Grd2]. But the decomposition of the σ phase at 650°C reported by [2005Ust] invocates to displace this reaction in the temperature region above 650°C, and leads to include in the reaction scheme two new invariant equilibria at the temperature below 650°C: U_3 and E_2 reactions. It should be noted, that since the Fe_3C phase is metastable in the C-Fe binary system, the reaction scheme presented in Fig. 3 may be regarded as metastable.

In the accepted reaction scheme, temperatures of some invariant equilibria in the binary systems were corrected in accordance with the accepted binary phase diagrams. Invariant equilibria, that included subcarbides of vanadium were omitted due to the absence of experimental data on the influence of alloying with Fe on the ordering of VC_y and V_2C carbides.

The temperatures and the phase compositions associated with the invariant equilibria are presented in Table 3.

Liquidus, Solidus and Solvus Surfaces

[1930Oya2] and [1931Vog] determined the solidification characteristics of alloys in the range Fe-Fe_3C-V_4C_3-V-Fe. The liquidus surface of this partial system is presented in Fig. 4. It was constructed by [1987Rag], who based mainly on the results of [1930Oya2]. The accepted binary data are not in controversion with those accepted by [1987Rag]. The eutectic point e_4 on the Fe_3C-V_4C_3 section is from [1931Vog]. There are five fields of primary crystallization. The three four-phase invariant points are the ternary eutectics E_1, E_2 and the transition reaction U_1. The invariant line from U_1 to E_1 has a maximum at about 1415°C. It should be noted, that since the Fe_3C phase is metastable in the C-Fe binary system, the liquidus surface presented in Fig. 4 may be regarded as metastable. In accordance with calculations of [1991Hua] the alloying with V stabilized the cementite. Though many experiments dealt with the cementite phase, it had not been pointed out whether the cementite phase is stable in the ternary or metastable as in the C-Fe side since the graphite was usually not included.

[1988Kes] redetermined the liquidus surface near the Fe corner. Their results confirm the presence of the transition reaction U_1 and the ternary reaction E_2 near the Fe corner. For compositions lying in the primary crystallization field of austenite, the liquidus temperature was given by the following equation: T(°C) = $1523 - 49.8X - 6.1Y + 3.3XY - 0.2Y^2$, where X and Y are the contents of C and V in mass%. The temperatures of the U_1 and E_2 reactions were determined to be 1370 and 1120°C, as against ~1330 and 1122°C in [1987Rag].

[1969Sch] proposed the following empirical equation to calculate the solubility of C in the Fe-V melts: mass% C = $1.34 + 2.53\cdot10^{-3}T + (1.307\cdot10^{-1} - 2.24\cdot10^{-6}T)\cdot$ (mass% V) + $(4.98\cdot10^{-3} - 4.8\cdot10^{-6}T)\cdot$ (mass% V)^2, where the first two terms refer to the binary alloys and are applicable from the eutectic temperature to 1900°C. For ternary melts, the equation is applicable for V content up to 6 mass% in the temperature range of 1300 to 1600°C. The experimental values of [1956Oht, 1959Fuw, 1963Mor] agree reasonably with the calculations. [1968Sek] studied the solubility of carbon in the Fe-0.5 mass% V alloy quenched from different temperatures. The precipitating phase was V_4C_3. The relation $\{V\}^{4/3}\ \{C\} = 4.5\cdot10^5 exp\{-21620/T\}$ was found for all specimens with V content less than 3 mass%.

DOI: 10.1007/978-3-540-74196-1_15

Isothermal Sections

Figure 5a shows the isothermal section at 1100°C from [1981Hol]. The homogeneity ranges shown for V_2C and VC_y are those reported by [1981Hol] as it was accepted by [1987Rag]. The V_3C_2 (V_4C_{3-x}) phase has not been included in the isothermal sections at 1100°C. The ordered phases V_6C_5 and V_8C_7 are indicated by dashed lines. Their extensions into the ternary region have not been determined. τ phase is not presented at this temperature. [1991Hua] calculated isothermal section at 1100°C, which differs from the experimental results of [1981Hol], as an additional phase V_3C_2 is present in the computed section, which is shown in Fig. 5b.

Using thermodynamic data, the phase equilibria in Fe rich alloys were calculated by [1977Uhr, 1978Uhr]. VC_y was assumed to have a fixed composition of V_4C_3. Its Gibbs energy of formation was evaluated using the austenite solubility data of [1972Wad] at 1000°C. The temperature dependence of its Gibbs energy was chosen to agree with the data of [1970Hul]. Figures 6a, 7, and 8 show the calculated isothermal sections in the Fe rich part at 1100, 1000, and 900°C, respectively. The calculated results at 1000°C are in excellent agreement with the experimental solubility data of [1960Sav, 1972Wad, 1981Wri]. [1991Hua] optimized the thermodynamic parameters for the C-Fe-V system and presented the calculated isothermal section in the Fe rich corner at 1100°C. It is presented in Fig. 6b. The calculation results of [1991Hua] are nearly the same as those by [1977Uhr, 1978Uhr]. Several isothermal sections have been calculated by [1993Sil]. They are very close to those presented by [1991Hua].

Figure 9 shows the isothermal section at 500°C, that is mainly based on the results of [1966Grd2], but differs from the section presented by [1966Grd2], and accepted by [1987Rag], by the absence of the phase regions involving the σ phase. This is consistent with the decomposition of the σ phase at 650°C reported by [2005Ust]. The ordered phases V_6C_5 and V_8C_7 are indicated by dashed lines. Their extensions into the ternary region have not been determined. Also, equilibria with V_3C_2 phase were added.

The solubility of C in Fe-V ferrite was measured by [1968Sek] and [1973Koy]. Their data are in good agreement at 700 and 800°C. The empirical solubility product proposed by [1973Koy] was as follow: $\log \{(\text{mass\% V})\cdot(\text{mass\% C})\} = -6080/T + 2.72$ where T is in K. The $\alpha/(\alpha+VC_y)$ phase boundaries calculated using this equation are given in Fig. 10.

Temperature – Composition Sections

The vertical section along the Fe-VC_y join was calculated by [1991Hua] and [1991Lee]. Both results are nearly the same. It is redrawn in Fig. 11 from [1991Hua]. [1991Hua] calculated vertical sections at 2, 5, and 10 mass% V and at 3 and 4 mass% C. They are presented in Figs. 12, 13, 14, 15 and 16, respectively. They agree well with the experimental results of [1930Oya2].

Thermodynamics

Thermodynamic properties of some unary and binary phases are presented in Table 4 and Table 5. Thermodynamic properties of the ternary C-Fe-V alloys are restricted to the data on carbon solubility in the Fe-V melts and examination of carbon activity in the melt and austenite. The solubility of graphite in liquid has been studied in the temperature range of 1300 to 1600°C and 0 to 10 mass% V by a number of investigators. The most extensive results are from [1962Neu] at 1320 to 1490°C and [1963Mor] at 1350 to 1550°C with good agreement, and from [1987Guo] at 1350 to 1502°C, showing stronger effect of V on the solubility. In dilute solution, the Wagner interaction coefficient ε_V^C was reported to be –8.0 at 1560°C by [1959Fuw] and –6.2 at 1550° by [1972Foo] and –16 at 1600°C by [1974Sig]. The solubility of VC carbide in the austenite has been investigated extensively. [1972Wad] measured the solubility at 1000°C by identifying break points on iso-carbon activity lines and analyzed experiments published before 1970. They found an agreement between their results and those by [1966Zup] after reinterpretation and those by [1960Sav]. Subsequently, [1981Wri] made measurements at 918, 993 and 1150°C and the results are in good agreement with those by [1972Wad]. The experimental data of [1972Wad] were presented by following equation $\log \psi_C = 2300/T - 0.92 + (3860/T)\ Y_C - (10700/T)\ Y_V$, where $\psi_C = a_C/z_C$ and $Z_C = Y_C/(1-Y_C)$ and Y_C and Y_V are atom fractions of carbon and vanadium.

DOI: 10.1007/978-3-540-74196-1_15

Notes on Materials Properties and Applications

As alloying element V is used in manufacturing high-quality steels, its influence is very marked in the presence of Cr, Ni, and W due to the formation of vanadium carbides as strengthening particles [1999Oka, 2003Per]. Low transformation temperatures under decomposition of austenite are associated with very fine carbide distributions which have high strength but very low ductility. At higher transformation temperatures the precipitates coarsen, the strength decreases and the ductility rises. The transformation conditions required for the production of high ductility with reasonable strength are such that it may be possible to obtain useful properties in very large sections [1971Sut]. [1972Edm, 1973Edm] showed, that sheets of vanadium carbides precipitates in ferrite may be obtained by simple cooling of an Fe-1V-0.2 mass% C alloy from the austenitic conditions. The intersheet spacing decreases as the cooling rate is increased. As the cooling rate increases the strength of the alloy increases, but the tensile ductility is reduced. The dispersion strengthening due to precipitation varied with the intersheet spacing as $\sigma_p = k\ \lambda^{-1.1}$ where σ_p is the dispersion strengthening component of the yield strength, and λ is intersheet parameter. [2001Hil] reported, that C-Fe-V alloys showed the dependence of E on microstructure (grain size and phase arrangement) that is connected with deviation scope from equilibrium state. With the specific variation of E it is possible to improve the stiffness of thin steel sheet materials, preferred this is of interest for the car industry.

Due to the high Vickers hardness Fe-VC eutectic alloys (700 HV at 12 mass% VC) are used as abrasion-resistant facing [1978Dmi]. C-Fe-V alloys are used to produce composite magnetoabrasive powders for finishing polysurfaces [1983Pol]. The VC_{1-x} phase possess a highly brittle nature combined with hardness and hence is readily comminuted into irregularly poligonal powders of a desirable size range below 325 mesh (44 μm) by a hammer milling treatment. Annealing at temperatures above 700°C results in the decomposition of the MC phase into an aggregate of stable ferrite, including a uniform dispersion of fine VC carbide accompanied by a remarkable reduction in hardness and a significant increase in ductility. The resulting C-Fe-V and C-Fe-V-X (X = Cr or Mo) powders dissolving C, V and Cr (or Mo) by as much as about 25 to 40 at.%, are highly attractive as raw materials for consolidation into bulk form by conventional powder consolidation techniques, owing to the expectation that their bulk materials exhibit higher strengths and better ductility compared to those of the alloys solidified in the usual manner [1986Ino]. Since the composition dependence of the coefficient of thermal expansion of Fe-$VC_{0.75}$ alloys is not smooth, they can be used as materials with predetermined values of full spelling for CTE. The CTE is increased sharply as the carbide content is less than 3 mass% (in the ternary solid solution domain). When the carbide content is more than 3 mass% in the two-phase (αFe)+$VC_{0.75}$ region the increasing of volume fraction of $VC_{0.75}$ leads to the CTE decreasing [1997Shu].

To develop hot corrosion resistant Fe base alloys for coalfired plants, hot corrosion resistance of some C-Fe-V alloys was studied by [1989Mal]. The hot corrosion products indentified by X-ray diffraction were α Fe_2O_3, FeV_2O_6, VC, and $FeCl_2$. The Fe-VC alloys showed heavy mass losses in the temperature range of 700-850°C. Unlike plane oxidation where alloys have oxidation resistance due to the presence of VC, under ionic salt environment the alloys were corroded catastrophically due to the easy fluxing of VC and conversion of carbide into volatile V_2O_5 and VCl_4.

Microcrystalline C-Fe-V films crystallized from the amorphous state are suitable for use in magnetic heads [1991Has].

V_4C_3 may be introduced into steels as hydrogen trapping sites to enhance the resistance to static fracture of component such as springs, bolts and power plant items [2003Yam].

The data on experimental study of the materials properties are presented in Table 6.

Miscellaneous

Additional Snoek peak has been reported in C-Fe-V system by [1967Sek]. The heights of the normal and additional peaks, *i.e.*, the free carbon content, are significantly reduced by the addition of V, where as the ratio of the additional peak to a normal peak, increases with V content. Thus the additional carbon peak at 75°C suggests the existence of interaction between V and C. [1967Per] showed that it is possible to estimate the value of the interaction energy from the results of [1967Sek].

The vanadium steel (2 mass% V, 0.2 mass% C) quenched from 1300°C and then overaged at 550°C has a structure comprising plates of V_4C_3 lying on cube planes in the ferrite. At the peak hardness (~ 500 HV)

DOI: 10.1007/978-3-540-74196-1_15

after 3 h at 550°C much smaller V_4C_3 plates were observed to form mainly on dislocations. The plates on this stage are about 10 nm diameter and 1 nm thick, and can be indentified as V_4C_3 by electron diffraction. Before peak hardness, indentifiable V_4C_3 has been observed. The orientation relationship V_4C_3 to ferrite was found to correspond $\{100\}_\alpha$ // $\{100\}V_4C_3$, $\{011\}_\alpha$ // $\{001\}V_4C_3$. This relationship gives a misfit of about 3% between the ferrite {010} and V_4C_3 {011} and 31% misfit between ferrite {010} and V_4C_3 {100} directions. This accounts for the occurrence of V_4C_3 as plates on {100} planes [1966Ray]. Fibrous V_4C_3 found after isothermal transformation at temperatures between 500°C and 700°C is not a product of the isothermal transformation but forms in a specific temperature range on cooling to the transformation temperature [1971Sut]. Under austenite decomposition in the range from 600 to 850°C an extremely fine dispersion of plates of V_4C_3 in ferrite is formed [1972Dav]. [1973Bat] showed that the fibre carbides are nucleated in the prior austenite grain boundaries and the amount of fibre carbide does not depend on the isothermal treatment but on the composition and austenite grain size. The strengthening of an C-Fe-V low-alloy steel by carbide precipitation during continuous cooling from austenite region has been studied by [1974Edm]. Parameters of isothermal precipitation of V carbide in ferrite over the temperature range 725-850°C are very sensitive to temperature. The nature of the precipitate orientation concerning the austenite to ferrite+precipitate reaction was studied by [1979Ric]. [1985Par] studied steel containing 1.65 % V with 0.26 % C, which is isothermally transformed in the temperature range 600-750°C. It was shown that ferrite matrix and carbide precipitates possessed the Baker-Nutting orientation relationship with no difference of carbide morphologies.

The elevated temperature coarsening of fine banded dispersions of VC is associated with the presence of dislocations and it was found that the overall kinetics for the coarsening of VC in ferrite at 725°C obeyed a law of the form $\bar{x}^5 ¥ t$ which is in qualitative agreement with the predictions of the theory for the coarsening of particles by dislocation pipe diffusion [1975Dun].

The isothermal magnetic permeability disaccommodation has been investigated in four α C-Fe-V alloys in the region of Snoek relaxation by [1975Ilc, 1976Han]. Besides the Snoek relaxation process two further relaxations were found, originated from directional ordering of point relaxation. In samples aged at room temperature a fourth process occurs. It was suggested that the last relaxation corresponds to thermally activated dislocation movement.

Microstructures of glassy and metastable crystalline phases formed from $Fe_{69}V_{12}C_{19}$ alloy were studied by [1982Hor]. It was shown that the non-stoichiometric monocarbide VC_{1-x} could be modified by splat cooling into a mixed carbide if V was partially substituted by Fe.

Cold rolling an Fe-1V-0.23C alloy containing ~1 vol% of fine interphase V_4C_3 particles results in the formation of shear bands at rolling reductions greater than 20%. These shear bands provide potential sites for nucleation of recrystallization on subsequent annealing. In 60% cold-rolled samples, annealed at 706°C resulted in the onset of recrystallization within 15 min, but the recrystallization process was still incomplete after 100 h. The low rate of recrystallization was associated with the pinning effect of the V_4C_3 precipitates on boundaries of both recrystallized grains and subgrains [1982Dun].

[1985Par] studied steels containing 1.65 mass% V with 0.26 mass% C that were isothermally transformed in the temperature range of 600 to 750°C using TEM and selected electron microdiffraction. On the contrary to the previous reports ferrite matrix and carbide precipitates possessed the Baker's-Nutting orientation relationship with no difference of carbide morphology.

Structure and morphology of $(\gamma Fe)+Fe_3C+V_4C_3$ and $(\alpha Fe)+V_4C_3$ eutectics forming in the C-Fe-V systems have been studied by [1966Tar, 1980Fra, 1997Fra]. A solidification constant for stable eutectic growth under unidirectional solidification process of C-Fe-V eutectics was experimentally determined as $U\,\lambda^2 = 0.202\ mm^3 \cdot s^{-1}$ by [1997Fra].

Mutual diffusion coefficients of V in austenite and ferrite have been presented by [1993Pop] as follows: $D_V^\alpha = 1.17_{-(0.36)}{}^{0.52} \cdot 10^{-4} exp[(228040 \pm 2180)/(RT)]$ for temperature interval from 755 to 1454°C and V concentration in solid solution up to 30 at.%; $D_V^\alpha = exp(-10.73^{\pm 0.44} + 1.51^{\pm 0.11} X_C)\ exp[-(257300 \pm 5200)/(RT)]$ for temperatures from 975 to 1300°C and $X_C \geq 0.95$ mass%. Under diffusion interaction of VC with Fe, V and C pass into solid solution in quantities proportional to their fractions in the interstitial phase [1999Pop].

DOI: 10.1007/978-3-540-74196-1_15

Table 1. Investigations of the C-Fe-V Phase Relations, Structures and Thermodynamics

Reference	Experimental Technique	Temperature/Composition/Phase Range Studied
[1930Oya1]	Light microscopy, dilatometry, magnetic analysis (magnetization-temperature curves)	up to 900°C, 0.75-21.27 V, 0.13-3 mass% C, ferrite, austenite, cementite, martensite, V_4C_3
[1931Hou]	Light microscopy, magnetometry, resistometry, Rockwell hardness (HRC)	up to 1000°C, 0.4-16%V, 0.1-3 mass% C, ferrite, austenite, cementite, vanadium carbide
[1931Vog]	Light microscopy, TA	up to 1500°C, Fe-Fe_3C-V_4C_3-$Fe_{50}V_{50}$, ferrite, austenite, cementite, vanadium carbide and their combinations
[1936Wev]	Light microscopy, TA	up to 1500°C, Fe-Fe_3C-V_4C_3-$Fe_{50}V_{50}$, ferrite, austenite, cementite, vanadium carbide and their combinations
[1952Edw]	Light microscopy, X-ray analysis	1250°C, (γFe)+V_4C_3
[1955Bun]	Light microscopy, X-ray analysis, resistivity	Up to 1310°C, 0.11-3.04 mass% V and 0.12-5.22 mass% C, (γFe)+V_4C_3
[1959Fuw]	Equilibration with controlled mixture CO/CO_2, the solubility of graphite in the melt	1560°C, up to 20 mass% V, liquid
[1963Fle]	Equilibration in a flowing gas mixture CH_4/H_2 over alloy	1000°C, up to 2 mass% V, (γFe)+V_4C_3, (γFe)+V_4C_3+$(Fe,V)_3C$, (γFe)+$(Fe,V)_3C$
[1966Grd1]	Light microscopy, X-ray analysis of chemically extracted carbides, microhardness	annealing at 1050, 750, 550°C, 39.7-76 at.% Fe, 33-52.3 at.% V, 2.8-14 at.% C, V_2C+η+(Fe), σ+η+(Fe), V_2C+σ+η, σ+η
[1966Grd2]	X-ray analysis	500°C, Fe-V-up to 60 at.% C
[1966Zup]	Transfer of C from Fe-C to Fe-V alloy through the vapor phase	1000°C, 0.25-1.98 mass% V, (γFe)+V_4C_3, (γFe)+V_4C_3+$(Fe,V)_3C$, (γFe)+$(Fe,V)_3C$,
[1968Sek]	Vibration type internal friction method	equilibrating at 680°C, followed by brine quenching, up to 5 mass% V and 0.024 mass% C, ferrite
[1968Ven]	TEM, Electron diffraction, nuclear magnetic resonance	V_6C_5
[1969Ebe]	Diffusion couple, X-ray analysis	1000°C, 1050°C, up to 2 at.% V and up to 16 at.% C, (γFe)+VC_y, (γFe)+VC_y+$(Fe,V)_3C$, (γFe)+$(Fe,V)_3C$

(*continued*)

DOI: 10.1007/978-3-540-74196-1_15

Reference	Experimental Technique	Temperature/Composition/Phase Range Studied
[1971Sut]	TEM, X-ray diffraction, dilatometry, mechanical testing	solution treatment at 1150°C and then rapidly transferred to lead or salt bath, tempering at 500, 600, 700, and 800°C, followed by quenching in water, Fe-1.91-0.23 mass%, Fe-1.91V-0.41 mass% (αFe)+V_4C_3
[1971Tel]	X-ray analysis	800°C, 1100°C 20-50 at.%V, 17.5-50 at.% C (α_1Fe)+VC_y, (α_1Fe)+σ+VC_y, σ+VC_y, σ+VC_y+V_2C, σ+V_2C+(α_2Fe), V_2C+(α_2Fe), (α_1Fe)+VC_y+C
[1972Foo]	Equilibrating of Fe-C binary alloys with C-Fe-V ternary alloys in an isothermal closed chamber through transport in the gas phase	1550°C, 0.61-11.8 mass% V, liquid
[1972Wad]	Equilibrium with controlled mixture CH_4/H_2	997, 1201°C, up to 2.11 at.% V, equilibrium of austenite with carbides
[1975Fre]	DTA	up to 1400°C, Fe-VC, (94-97 at.% Fe), eutectic melting temperature on the Fe-VC quasibinary section
[1978Dmi]	Light microscopy, SEM, EPMA, DTA, dilatometry	up to 1550°C, Fe-VC quasibinary section (up to 70 mass% VC)
[1997Fra] [1980Fra]	Light microscopy, SEM	as-cast alloys, up to 14% V and 3.5% C, Near-eutectic alloys
[1981Bra]	Equilibrating of Fe-V alloys with controlled mixture of CH_4/H_2	900, 1000, and 1100°C, 0.3-1.85 mass% V, 0.003-0.014 mass% C, (γFe)+VC_y, (γFe)+VC_y+$(Fe,V)_3C$
[1983Mor]	SEM, EPMA of alloys quenched from liquid state	1180-1420°C, up to 3 mass% V and up to 4 mass% C, (γFe)/liquid
[1986Ino]	Light microscopy, TEM, selected area electron diffraction, X-ray diffraction, Vickers hardness, tensile tests	melt quenched $Fe_{100-2x}V_xC_x$, up to 20 at.% V and 20 at.% C, α' (martensite), α'+MC, (αFe)+MC, (γFe)+MC, (γFe)+M_3C, α'+(γFe)+M_3C
[1987Guo]	Saturation of Fe-V liquid alloys with carbon	1350-1500°C, up to 6 mass% V and 5.82 mass% C, liquid
[1988Kes]	DTA, SEM, TEM, EPMA	up to 1417°C, 0-20 mass% V and 1.5-4.2 mass% C, liquid/(αFe), (γFe), VC_{1-x}, $(Fe,V)_3C$

(*continued*)

DOI: 10.1007/978-3-540-74196-1_15

Reference	Experimental Technique	Temperature/Composition/Phase Range Studied
[1989Kes]	DTA, TEM, SEM, EPMA	slowly cooled and quenched from liquid 5.16-19.18 mass% V and 1.34-3.26 mass% C, (γFe)+VC_{1-x}, (γFe)+VC_{1-x}+$(Fe,V)_3C$, VC_{1-x}→V_6C_5, VC_{1-x}→V_8C_7
[1991Has]	X-ray diffraction, DSC, TEM, Measurement of magnetic properties	up to 600°C, $Fe_{73.1}V_{12..9}C_{14}$ thick films
[1993Pol] [1994Pol]	X-ray diffraction, Mössbauer spectroscopy	as cast, 10.4-62.7 mass% V and 3.1-9.3 mass% C, (αFe)/V_2C,/VC_{1-x}/$(Fe,V)_3C$
[1994Ama]	DTA, EPMA	up to melting, 20-70 at.% V and 6.5-8.4 at.% C, (αFe)/V_2C/VC_{1-x}/σ

Table 2. Crystallographic Data of Solid Phases

Phase/ Temperature Range [°C]	Pearson Symbol/ Space Group/ Prototype	Lattice Parameters [pm]	Comments/References
(C)d	*cF*8 $Fd\bar{3}m$ C (diamond)	a = 356.69	at 25°C, 60 GPa [Mas2]
(C)gr < 3827	*hP*4 $P6_3/mmc$ C (graphite)	a = 246.12 c = 670.90	at 25°C [Mas2] sublimation point
(εFe)	*hP*2 $P6_3/mmc$ Mg	a = 246.8 c = 396.0	at 25°C, 13 GPa [Mas2]
γ, (γFe) 1394 - 912	*cF*4 $Fm\bar{3}m$ Cu	a = 364.67	at 915°C [V-C2, Mas2] 0-1.3 at.% V [Mas2]
α, (α,δ $Fe_{1-x}V_x$) 1538 - ~1270	*cI*2 $Im\bar{3}m$ W	a = 288.8 a = 290.8 a = 292.0 a = 293.3 a = 296.8	x = 0.2, 25°C, [1984Smi] x = 0.4 x = 0.5 x = 0.6 x = 0.8
α_1,(α,δ $Fe_{1-x}V_x$) < 650			$0 < x \lesssim 18$ at.% V
α_2, (α,δ $Fe_{1-x}V_x$) < 650			~75 < x < 100 at.% V
(δFe) 1538 - 1394		a = 293.15	x = 0 [Mas2]

(*continued*)

DOI: 10.1007/978-3-540-74196-1_15

Phase/ Temperature Range [°C]	Pearson Symbol/ Space Group/ Prototype	Lattice Parameters [pm]	Comments/References
(αFe) < 912		a = 286.65	x = 0 at 25°C [Mas2]
(αV) < 1910		a = 302.4	x = 1 [Mas2]
σ, FeV ~1200 - ~650	*tP*30 $P4_2/mnm$ σCrFe	a = 886.5 to 901.5 c = 460.5 to 464.2	at 25°C 29.6-60.1 at.% V, [1984Smi] [2005Ust]
βV_2C_{1-x} < 2210	*hP*3 $P6_3/mmc$ W_2C	a = 288.0 c = 455.6 a = 288.7 c = 456.7 a = 289.6 c = 457.9	29 at.% C 31 at.% C 33 at.% C [1999Lip]
β', V_2C(h) ~1600 -~ 850	*hP*9 $P\bar{3}1m$*(c)* εFe_2N	a = 500.5 c = 455.1	27.5-31.5 at.% C [1985Car]
α V_2C(l) ≲ 1327	*oP*12 *Pbcn* ξFe_2N	a = 457.7 b = 574.2 c = 503.7 a = 455.0 b = 574.5 c = 503.0 a = 457.0 b = 574.2 c = 502.6	31-32 at.% C [1999Lip] [1985Car]
V_3C_2 ≳ 900	*hR*60 $R\bar{3}m$ Sn_4P_3	a = 291.7 c = 2783 a = 291.9 c = 2779	~40 at.% C [1970Yvo] [1985Car] 40.1-41.9 at.% C [1999Lip]
VC_y ~2800 > T ≳ 1060	*cF*8 $Fm\bar{3}m$ NaCl	 a = 412.6 a = 413.8 a = 415.3 a = 417.5	0.58 < y < 0.875 37-47 at.% C [1985Car] 42 at.% C 44 at.% C 46 at.% C 48 at.% C
V_6C_5 < 1212	*mB*44 *B*2	 a = 509 b = 1108 c = 882 γ = 109.47°C	42.8 - 45.3 at.% C at 827°C [1999Lip] [1972Bil], [1985Car]

(*continued*)

DOI: 10.1007/978-3-540-74196-1_15

Phase/ Temperature Range [°C]	Pearson Symbol/ Space Group/ Prototype	Lattice Parameters [pm]	Comments/References
V_8C_7 ~1110 - ~367	*cP*60 $P4_3/mmc$	a = 833.33	46.5-46.7 at.% C [1999Lip] [1985Car]
Fe_3C metastable	*hP*8 $P6_322$ Fe_3C	a = 476.7 c = 435.4	[V-C2]
Fe_3C metastable	*oP*16 *Pnma* Fe_3C	a = 509.0 b = 674.8 c = 452.3	[V-C2]
Fe_2C metastable	*oP*6 *Pnnm* Fe_2C	a = 470.4 ± 0.16 b = 431.8 ± 0.5 c = 283.0 ± 0.6	[V-C2]
Fe_4C metastable	*cP*5 $P\bar{4}3m$ Fe_4C	a = 387.8 ± 0.2	[V-C2]
$Fe_{15}C$ metastable	*cF*4 $Fm\bar{3}m$ Cu	a = 361.8	[V-C2]
Fe_5C_2 metastable	*mC*28 *C*2/*c* Pd_5B_2	a = 1156.2 ± 0.1 b = 457.27 ± 0.05 c = 505.95 ± 0.05 β = 97.74 ± 0.01	[V-C2]
Fe_7C_3 metastable	*oP*40 *Pnma* Cr_7C_3	a = 454.0 b = 687.9 c = 1194.2	[V-C2]
Fe_7C_3 metastable	*hP*20 $P6_3mc$ Th_7Fe_3	a = 688.2 c = 454.0	[V-C2]
$Fe_{20}C_9$ metastable	*o**116	a = 906 ± 3 b = 1569 ± 3 c = 794 ± 1	[V-C2]
*τ, Fe_3V_3C	*cF*112 $Fd\bar{3}m$ Fe_3W_3C	a = 1087.7 to 1089.7	[1966Grd1]

DOI: 10.1007/978-3-540-74196-1_15

Table 3. Invariant Equilibria

Reaction	T [°C]	Type	Phase	Composition (at.%)		
				C	Fe	V
$\alpha + L \rightleftharpoons (\gamma Fe) + VC_y$	~ 1370	U_1	L	9.9	~83	~7.1
$L \rightleftharpoons \alpha + VC_y + V_2C$	~ 1390	E_1	L	~4.5	~59.5	~36
$L \rightleftharpoons (\gamma Fe) + VC_y + Fe_3C$	~ 1120	E_2	L (γFe) VC_{1-x} Fe_3C	17.1 9.27 46 25	80.15 89.8 1 70.8	2.75 0.93 53 4.2
$L \rightleftharpoons \alpha + VC_y$	~ 1415	e_3	L (αFe) VC_{1-x}	~2.9 ~0.3 ~39	~74.2 ~81.9 ~3	~22.9 ~17.8 ~58
$L \rightleftharpoons Fe_3C + V_3C_2$	~ 1151	e_4	L Fe_3C V_4C_3	27.7 ~25 ~40	62.13 ~70 ~3	10.17 ~5 ~57
$\gamma \rightleftharpoons \alpha + Fe_3C + VC_{1-x}$	~ 700	E_3	-	-	-	-
$\alpha + V_2C \rightleftharpoons \sigma + \tau$	> 650	U_2	-	-	-	-
$\sigma + V_2C \rightleftharpoons \alpha_2 + \tau$	< 650	U_3	-	-	-	-
$\sigma \rightleftharpoons \alpha_1 + \alpha_2 + \tau$	< 650	E_4	-	-	-	-

Table 4. Thermodynamic Data of Reaction or Transformation

Reaction or Transformation	T [°C]	Quantity, per mol of atoms [kJ, mol]	Comments
$xV+(1-x)C \rightarrow V_xC_{1-x}$	25	$\Delta_f G^o = -48.300-18\ N_C + (1.59 + 8.14\ N_C)\cdot 10^{-3} T$	[1985Car], VC field N_C - mole fraction of C
$xV+(1-x)C \rightarrow V_xC_{1-x}$	25	$\Delta_f G^o = -42.200-11.500\ N_C + (6.89-7.16\ N_C)\cdot 10^{-3} T$	[1985Car], V_2C field N_C - mole fraction of C
$0.6\ V + 0.4\ C \rightarrow V_{0.60}C_{0.40}$	1320	$\Delta_f G^o = -47.7$	[1985Car], V_4C_{3-x}
$V_6C_5 \rightarrow VC_{0.83}$	1172	$\Delta H_{trans} = 1.16$	[1999Lip]
$V_8C_7 \rightarrow VC_{0.87}$	1085	$\Delta H_{trans} = 2.23$	[1999Lip]
$V_4C_{3-x} \rightarrow VC_{0.79}$	1473	$\Delta H_{trans} = 1.56$	[1999Lip]

DOI: 10.1007/978-3-540-74196-1_15

Table 5. The Heat Capacity of Ordered VC_y Carbides with Different Carbon Contents

Phase	Temperature Range [°C]	Property, per mole of atoms [J, mol, K]	Comments
$VC_{0.79}$	25 - 1027	$C_p = 61.26 - 0.0316\,T + 8.479\cdot10^{-6}T^2 - 8437\,T^{-1}$	[1999Lip], per mol VC_y
$VC_{0.83}$	25 - 1027	$C_p = 68.66 - 0.0212\,T + 1.295\cdot10^{-6}T^2 - 9867\,T^{-1}$	[1999Lip], per mol VC_y
$VC_{0.87}$	25 - 1027	$C_p = 65.31 - 0.0118\,T + 7.562\cdot10^{-6}T^2 - 9041\,T^{-1}$	[1999Lip], per mol VC_y

Table 6. Investigations of the C-Fe-V Materials Properties

Reference	Method / Experimental Technique	Type of Property
[1931Hou]	Rockwell hardness	Hardness
[1966Ray]	Vickers hardness	Hardness
[1971Sut]	Mechanical testing in an Instron tensile mashine fitted with a 500 kg load cell, hardness	0.2%PS, UTS, hardness
[1973Bat]	Mechanical testing in an Instron tensile machine at a constant cross-head speed corresponding to a strain rate of $2.8\cdot10^{-4}\cdot s^{-1}$	0.2% PS, YS, precipitation hardening
[1978Dmi]	Tensile tests at 700 and 900°C, Vickers hardness, microhardness	σ_B, δ (tensile strain), ψ (reduction of area), hardness
[1978Dov]	Magnetic susceptibility measurements of melts	Electron structure of melts
[1989Mal]	The laboratory-made helical thermobalance, light microscopy, SEM, X-ray diffraction	Hot corrosion in saturated solutions of Na_2SO_4 and NaCl as a function of carbon content (Fe-5V-0.1, 0.4, 0.8 and 1.2 mass% C) in temperature range of 700-850°C
[1991Has]	VSM, B-H loop tracer, Coil method, optical cantilever method, four-probe method of resistivity measuring	Saturation flux density (B_S), coercetivity (H_C), relative permeability (μ), Saturation magnetostriction, electroresistivity of $Fe_{73.9}V_{12..9}C_{14}$ thick films
[1992Ueb]	AES (auger electron spectroscopy), XPS (X-ray photo-electron spectroscopy), LEED (Low energy electron diffraction)	Surface cosegregation and surface precipitation on Fe-3V-C {100} single crystals
[1993Ueb]	AES (auger electron spectroscopy), XPS (X-ray photo-electron spectroscopy), LEED (Low energy electron diffraction)	Surface cosegregation and surface precipitation on Fe-3V-C {111} single crystals

(*continued*)

DOI: 10.1007/978-3-540-74196-1_15

Reference	Method / Experimental Technique	Type of Property
[1995Ueb]	AES (auger electron spectroscopy), XPS (X-ray photo-electron spectroscopy), LEED (Low energy electron diffraction)	Surface cosegregation and surface precipitation on Fe-3V-C {110} single crystals
[1997Shu]	Dilatometry	Composition dependencies of CTE of Fe-$VC_{0.75}$ alloys at 20, 100, 200, 400, 600, and 800°C
[2000Bya]	Impression tests, light microscopy, SEM, EPMA	Microhardness and fracture toughness of VC coatings on Fe-0.8 mass% C steel

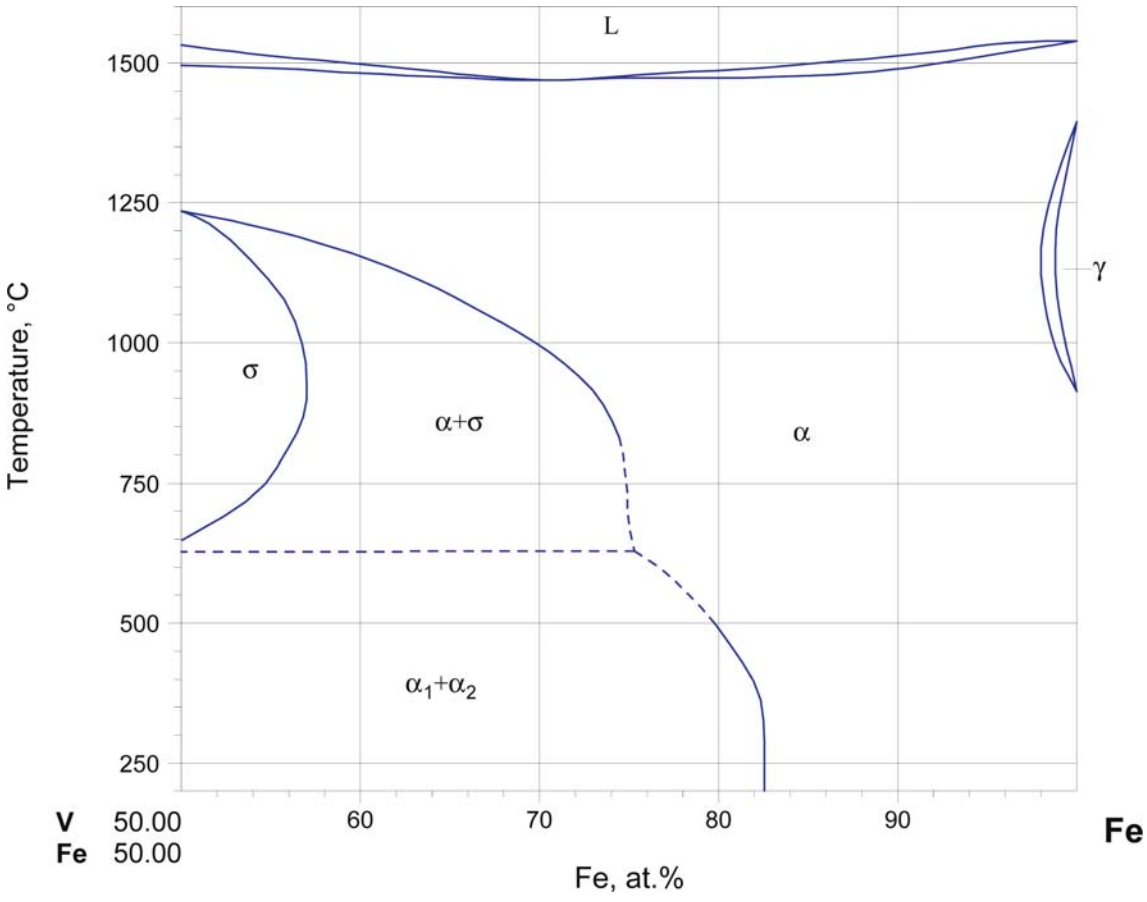

Fig. 1. C-Fe-V. Phase diagram of the Fe-V system

DOI: 10.1007/978-3-540-74196-1_15

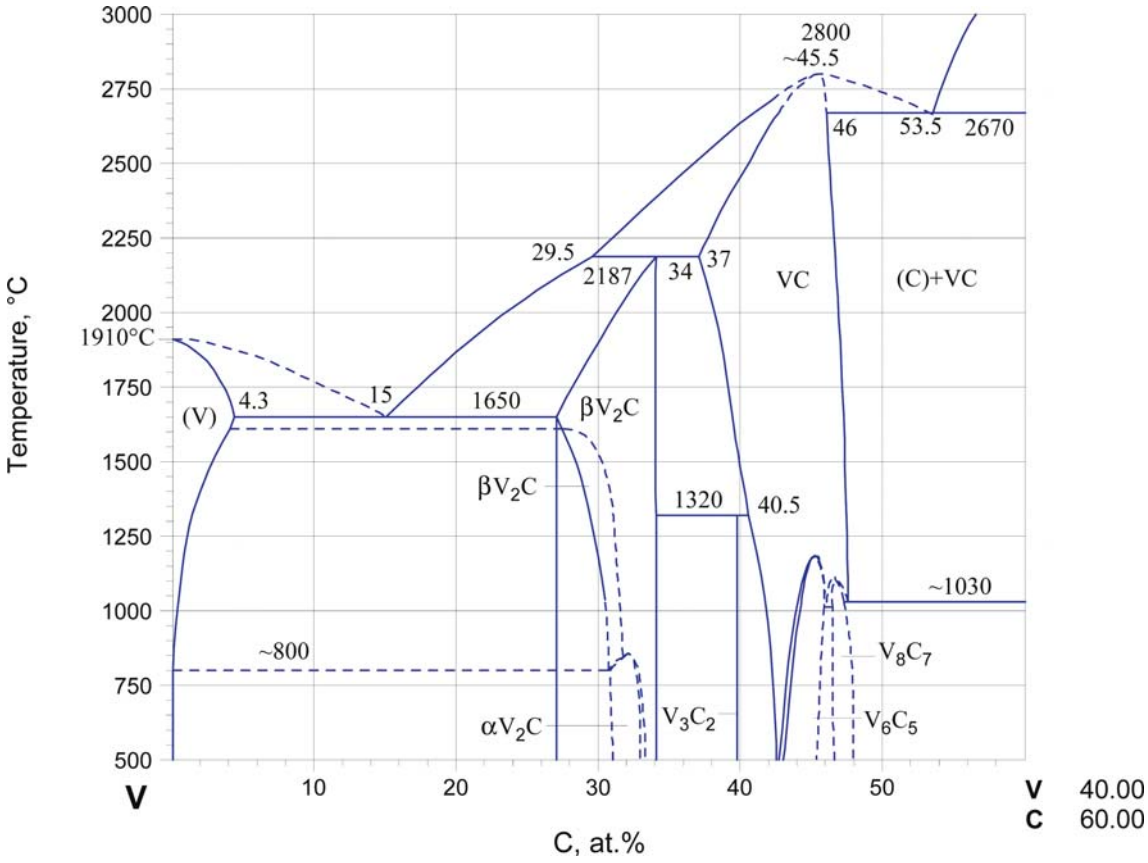

Fig. 2. C-Fe-V. Phase diagram of the C-V system

DOI: 10.1007/978-3-540-74196-1_15

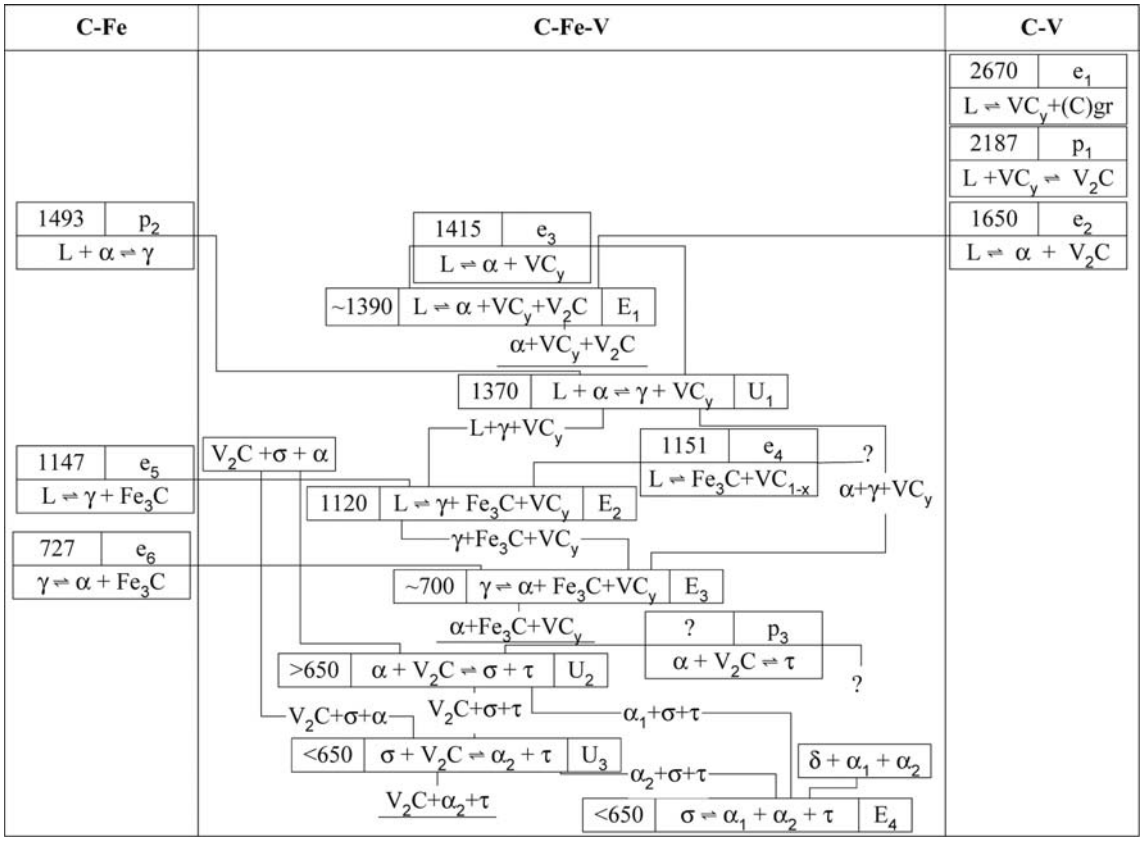

Fig. 3. C-Fe-V. Reaction scheme

DOI: 10.1007/978-3-540-74196-1_15

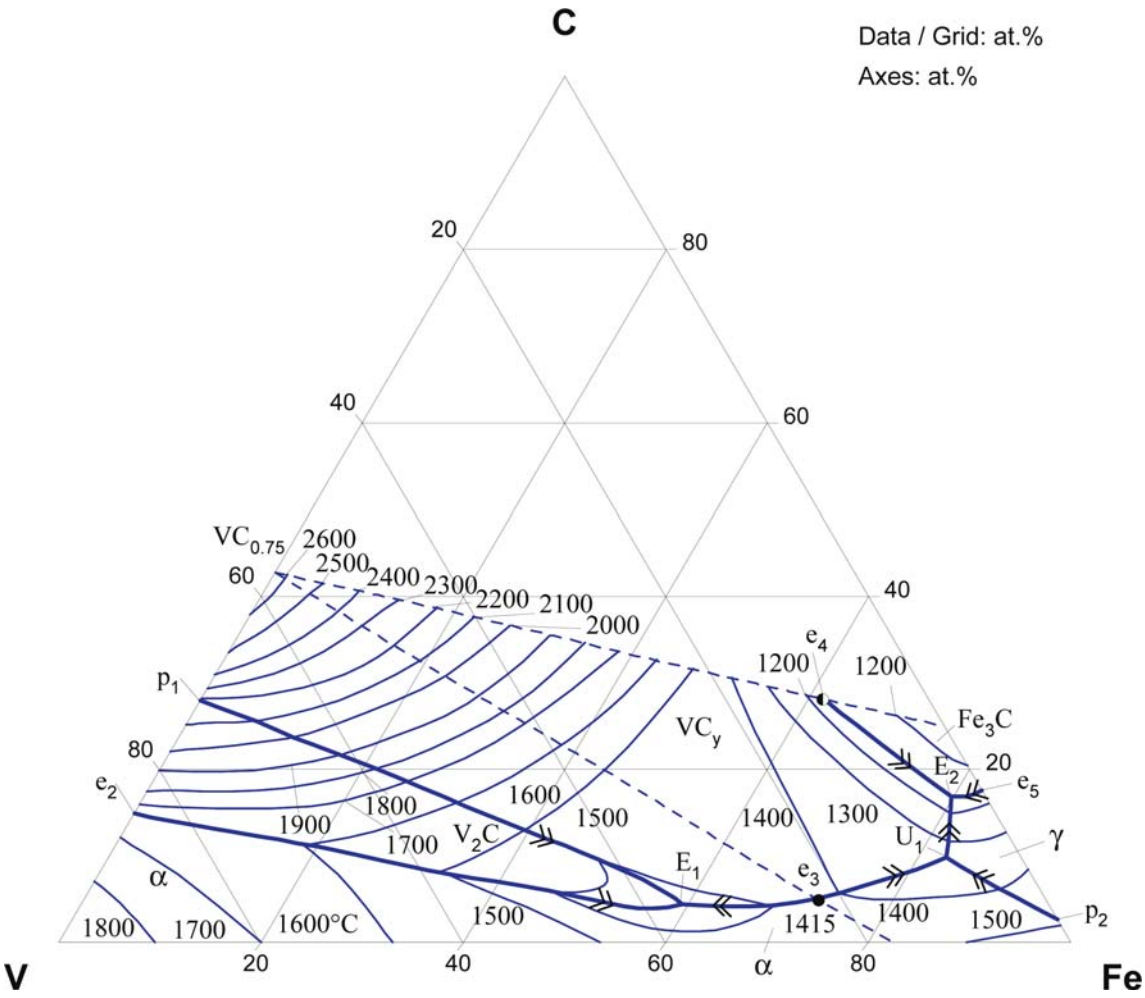

Fig. 4. C-Fe-V. Partial liquidus surface projection

DOI: 10.1007/978-3-540-74196-1_15

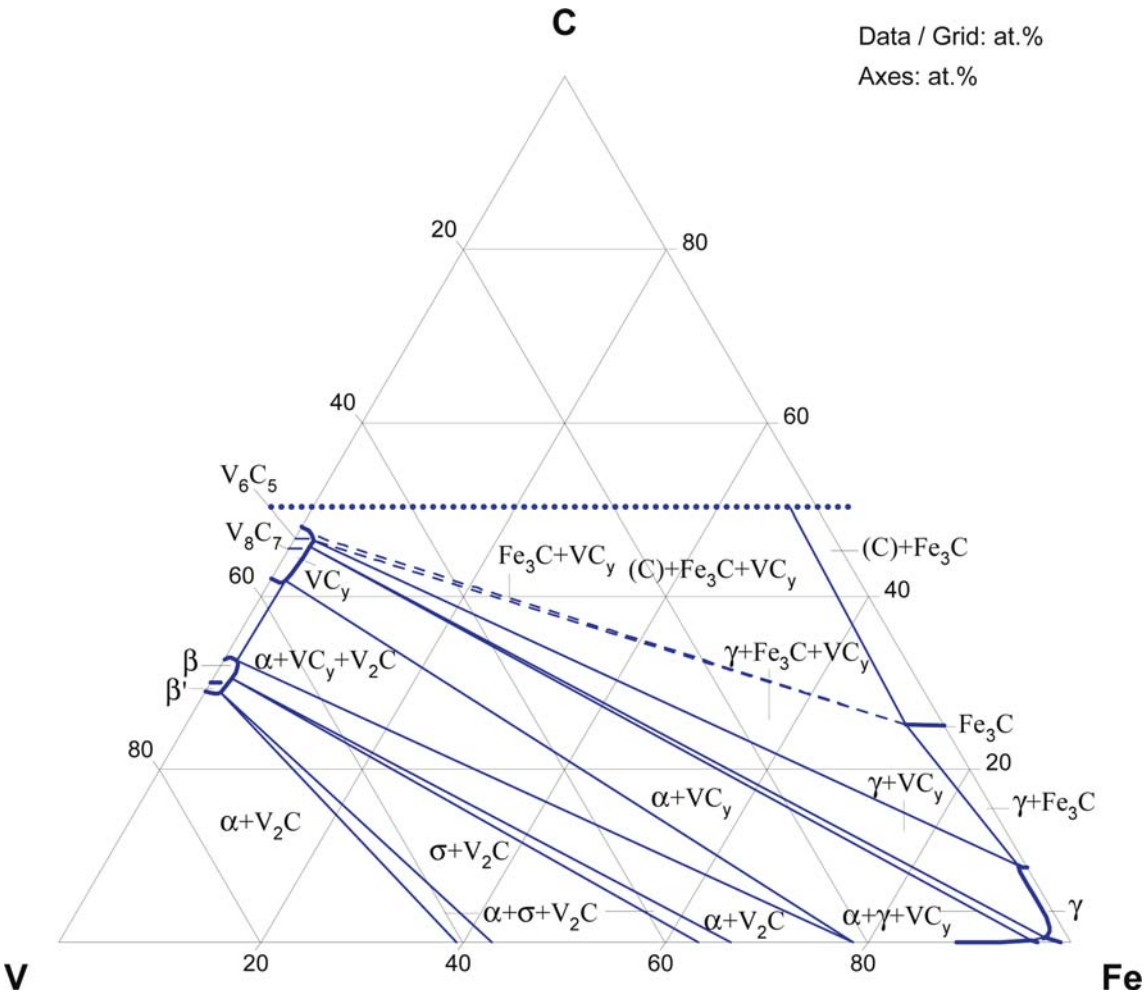

Fig. 5a. C-Fe-V. Experimental isothermal section at 1100°C

DOI: 10.1007/978-3-540-74196-1_15

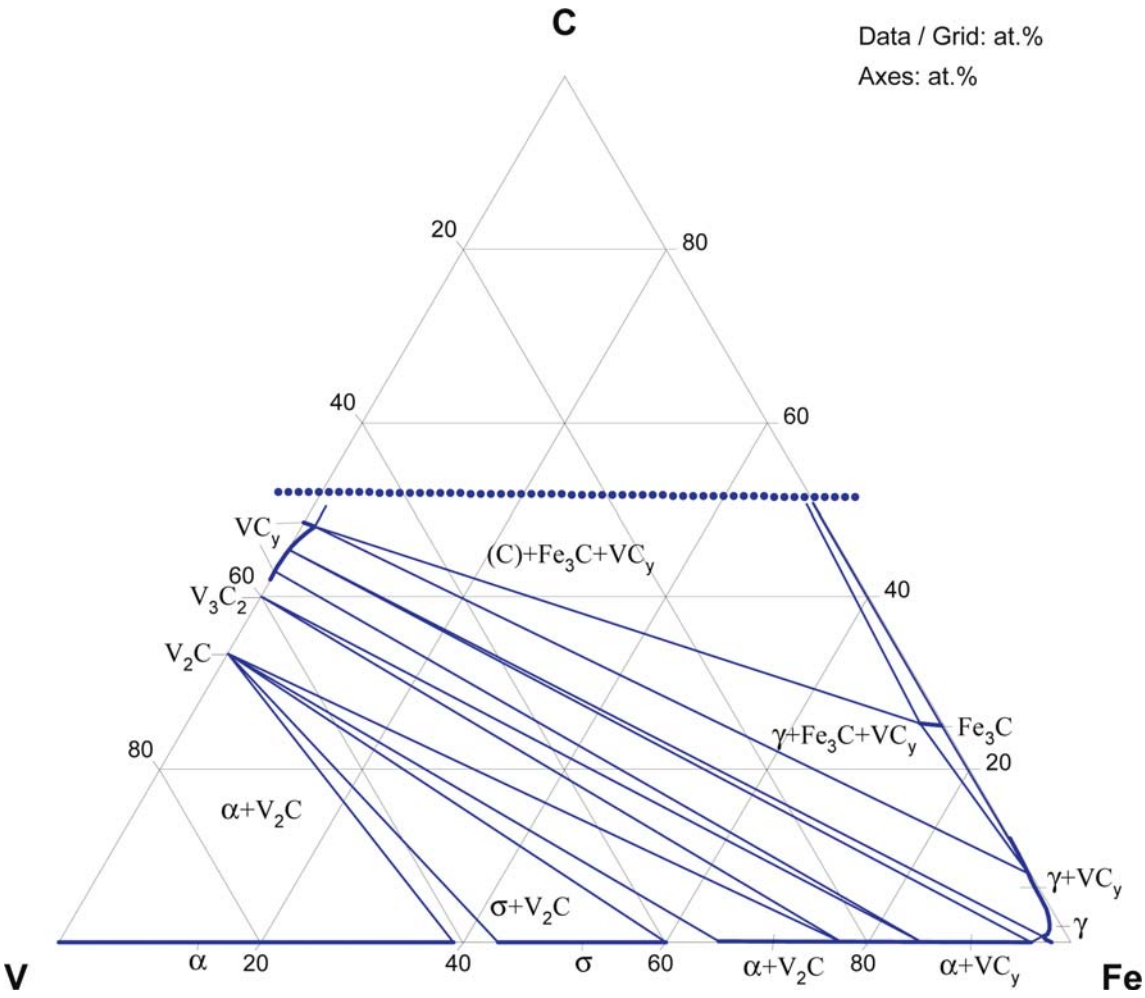

Fig. 5b. C-Fe-V. Computed isothermal section at 1100°C

DOI: 10.1007/978-3-540-74196-1_15

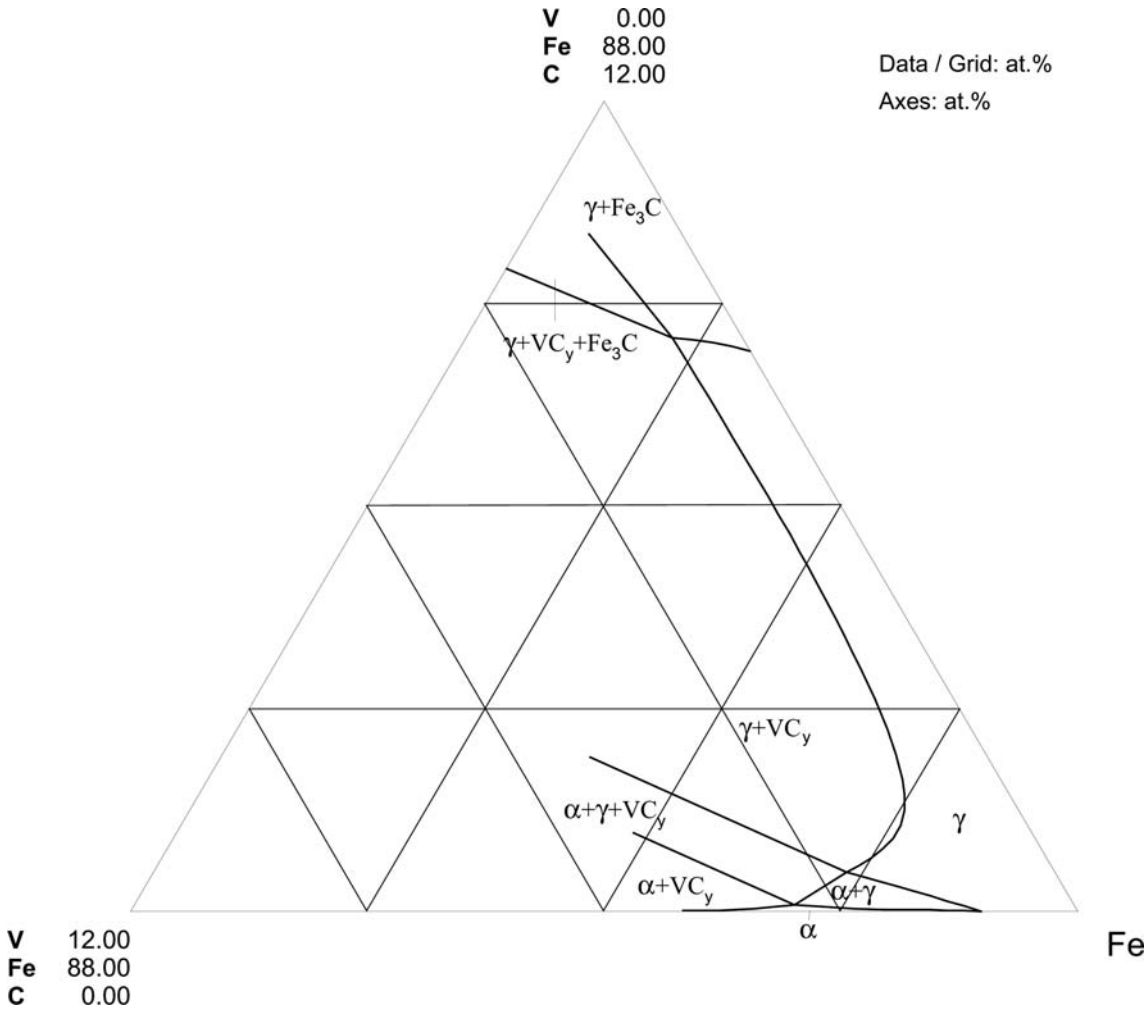

Fig. 6a. C-Fe-V. Isothermal section in the Fe rich part at 1100°C

DOI: 10.1007/978-3-540-74196-1_15

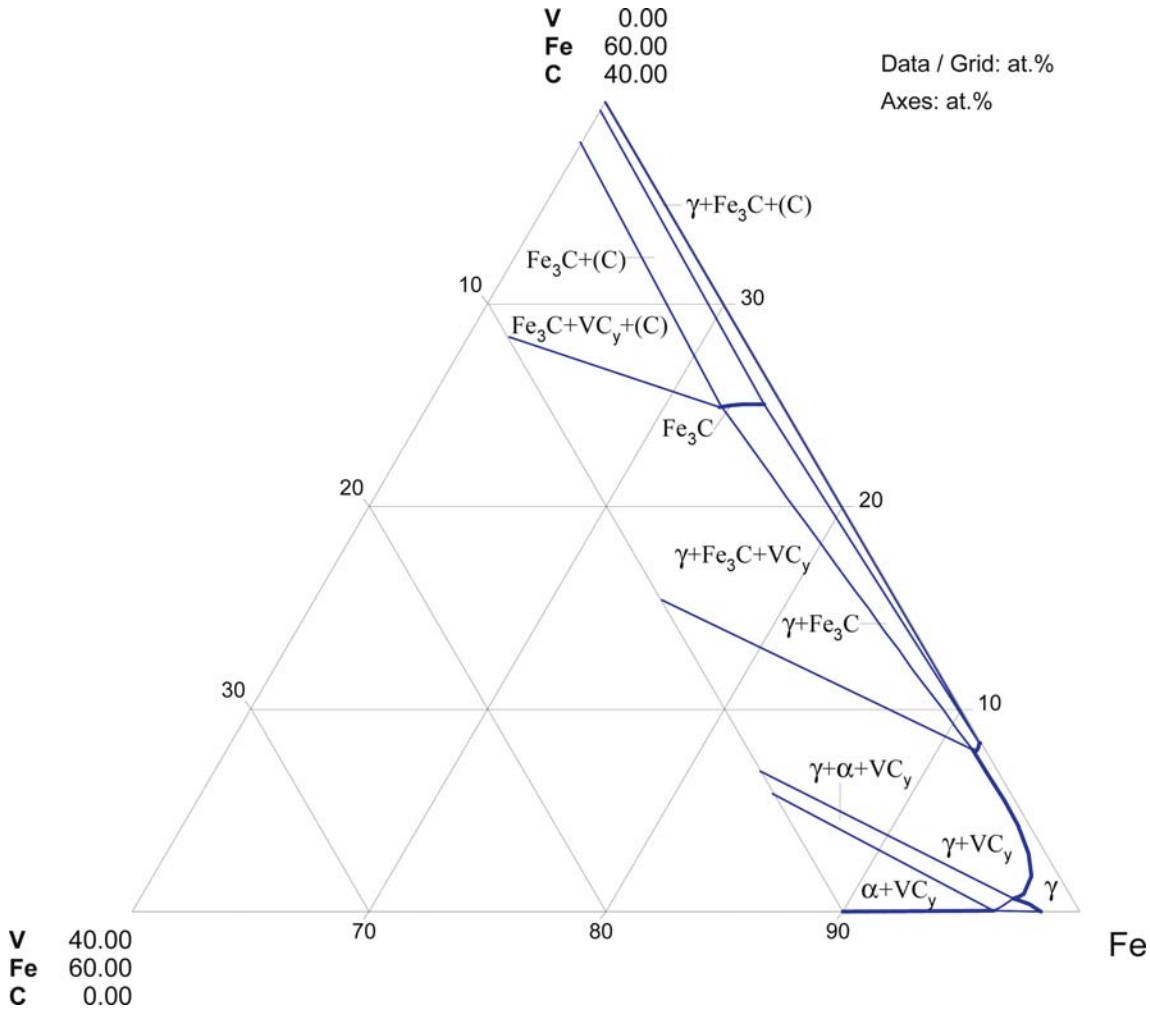

Fig. 6b. C-Fe-V. Isothermal section in the Fe rich part at 1100°C

DOI: 10.1007/978-3-540-74196-1_15

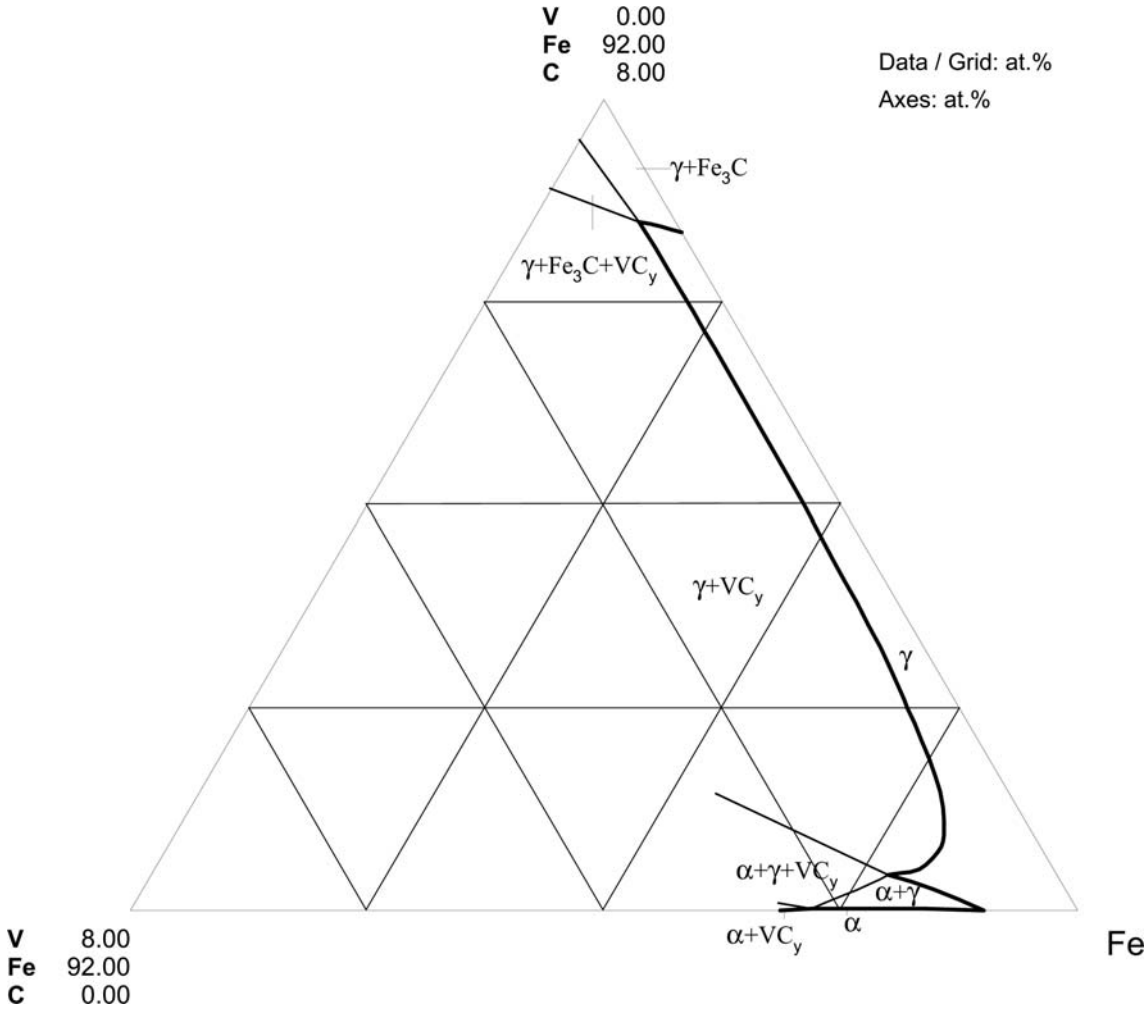

Fig. 7. C-Fe-V. Isothermal section in the Fe rich part at 1000°C

DOI: 10.1007/978-3-540-74196-1_15

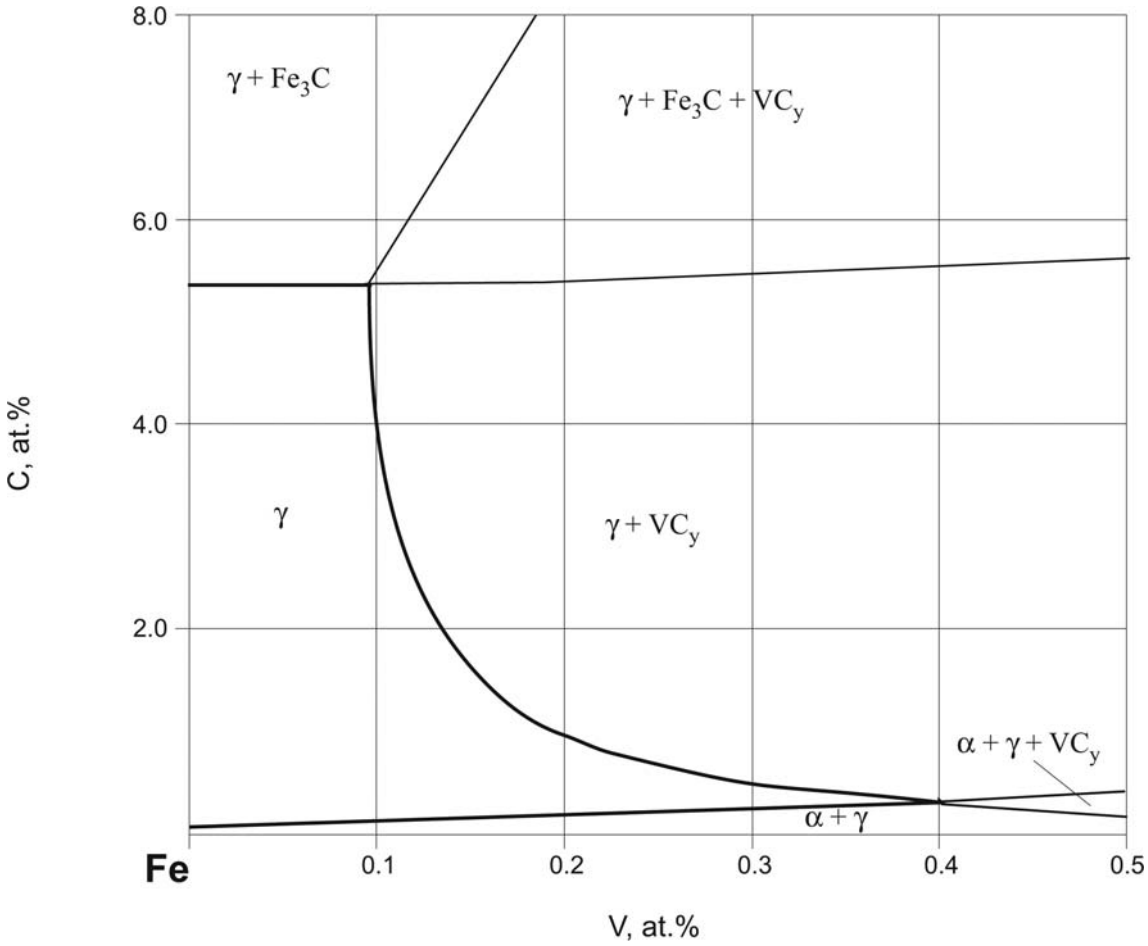

Fig. 8. C-Fe-V. Isothermal section at 900°C

DOI: 10.1007/978-3-540-74196-1_15

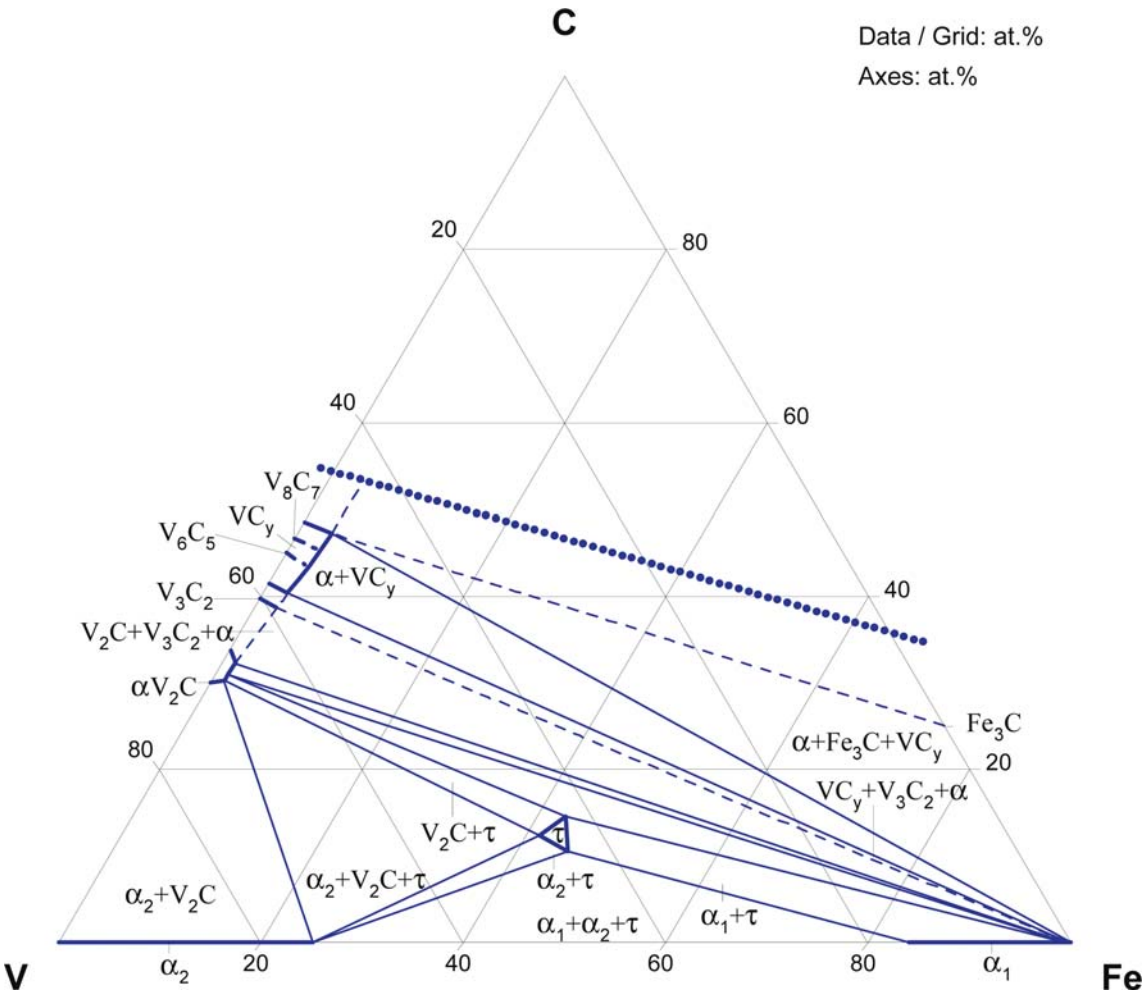

Fig. 9. C-Fe-V. Isothermal section at 500°C

DOI: 10.1007/978-3-540-74196-1_15

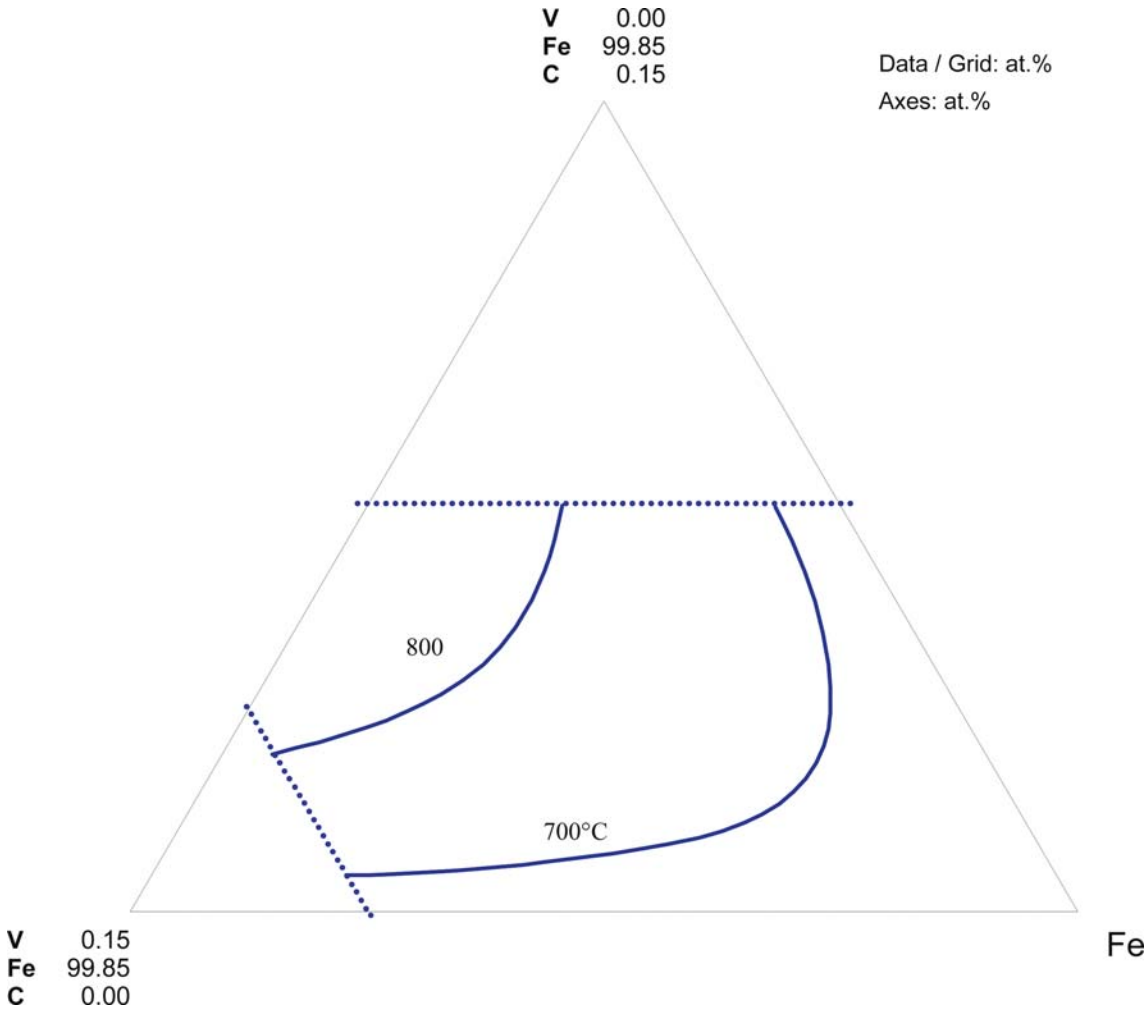

Fig. 10. C-Fe-V. $\alpha/(\alpha + VC_y)$ phase boundaries at 700 and 800°C

DOI: 10.1007/978-3-540-74196-1_15

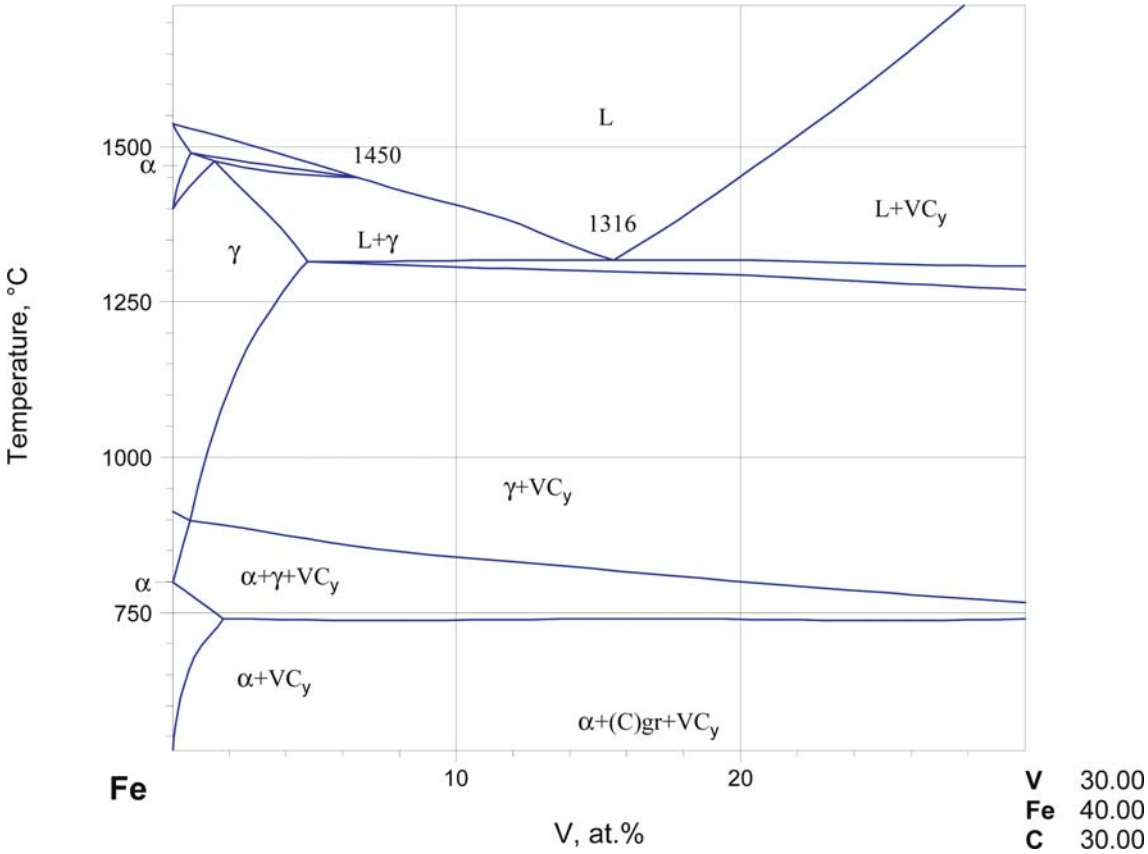

Fig. 11. C-Fe-V. The calculated vertical section Fe-VC_y

DOI: 10.1007/978-3-540-74196-1_15

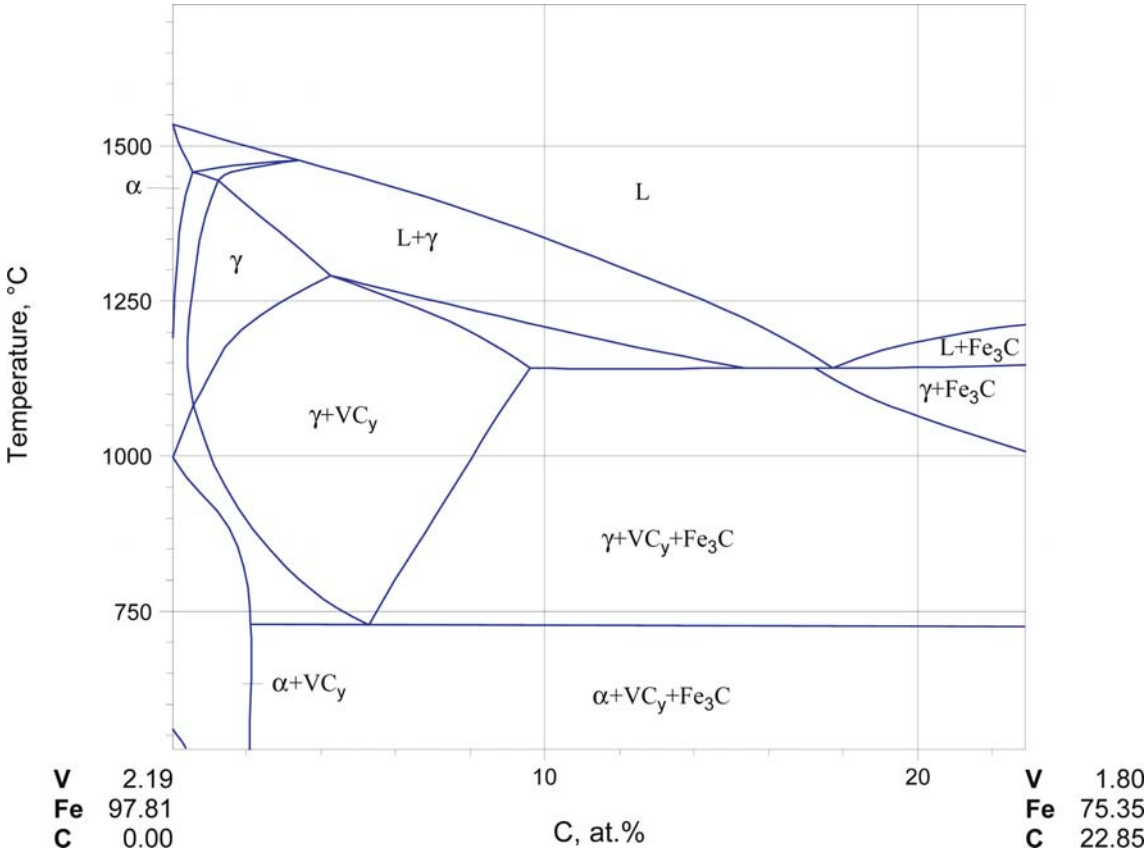

Fig. 12. C-Fe-V. The calculated vertical section at 2 mass% V

DOI: 10.1007/978-3-540-74196-1_15

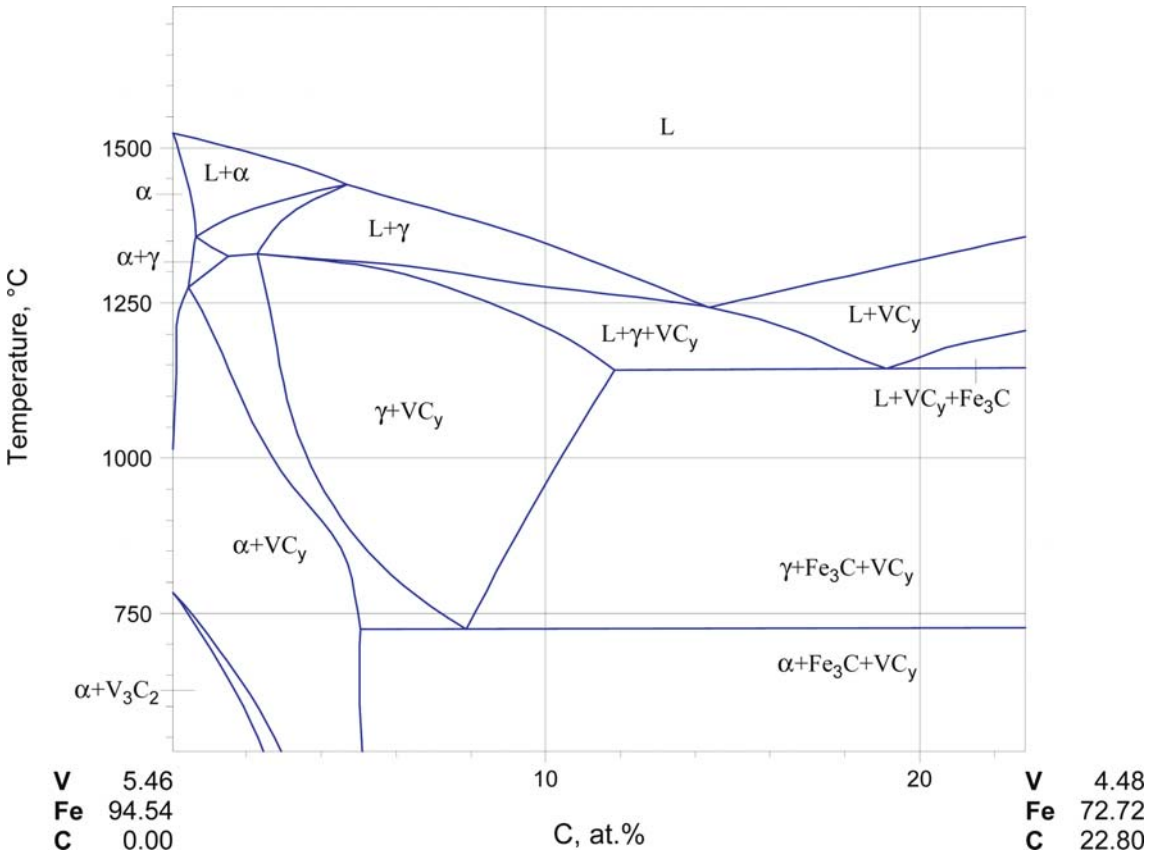

Fig. 13. C-Fe-V. The calculated vertical section at 5 mass% V

DOI: 10.1007/978-3-540-74196-1_15

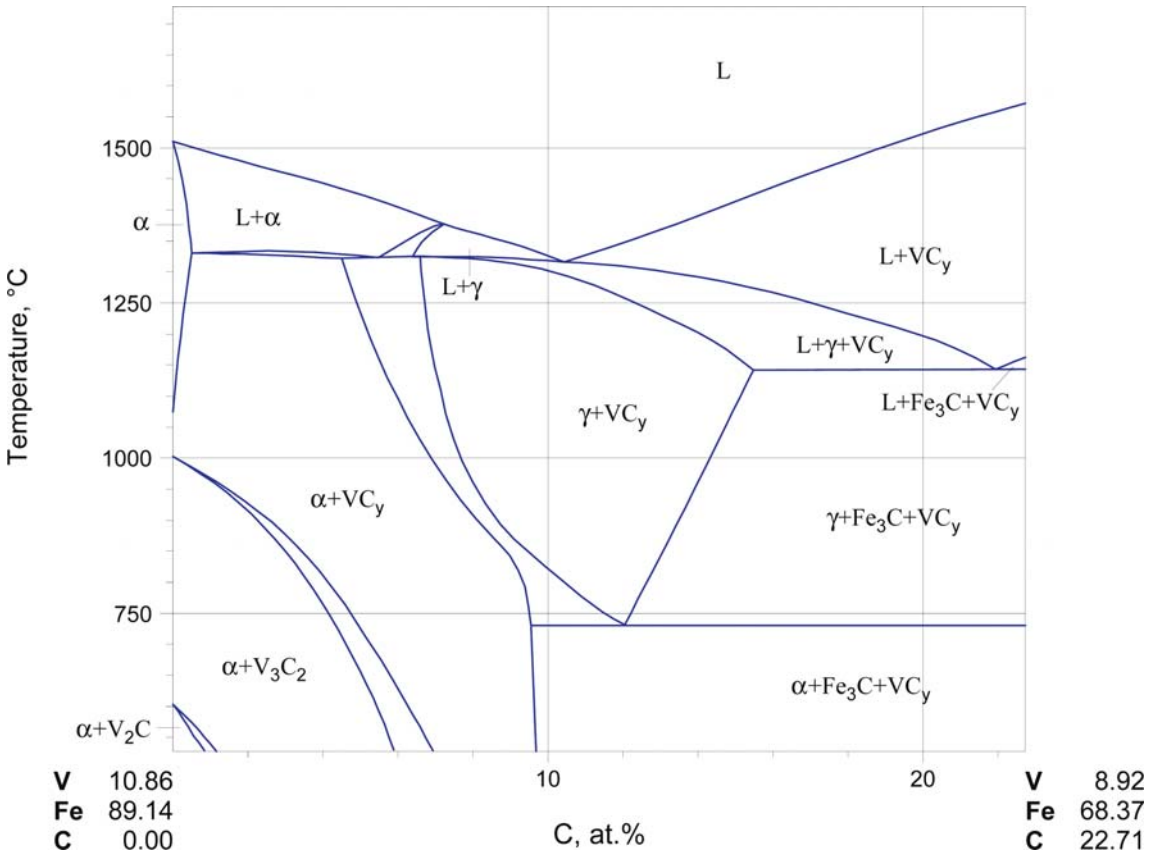

Fig. 14. C-Fe-V. The calculated vertical section at 10 mass% V

DOI: 10.1007/978-3-540-74196-1_15

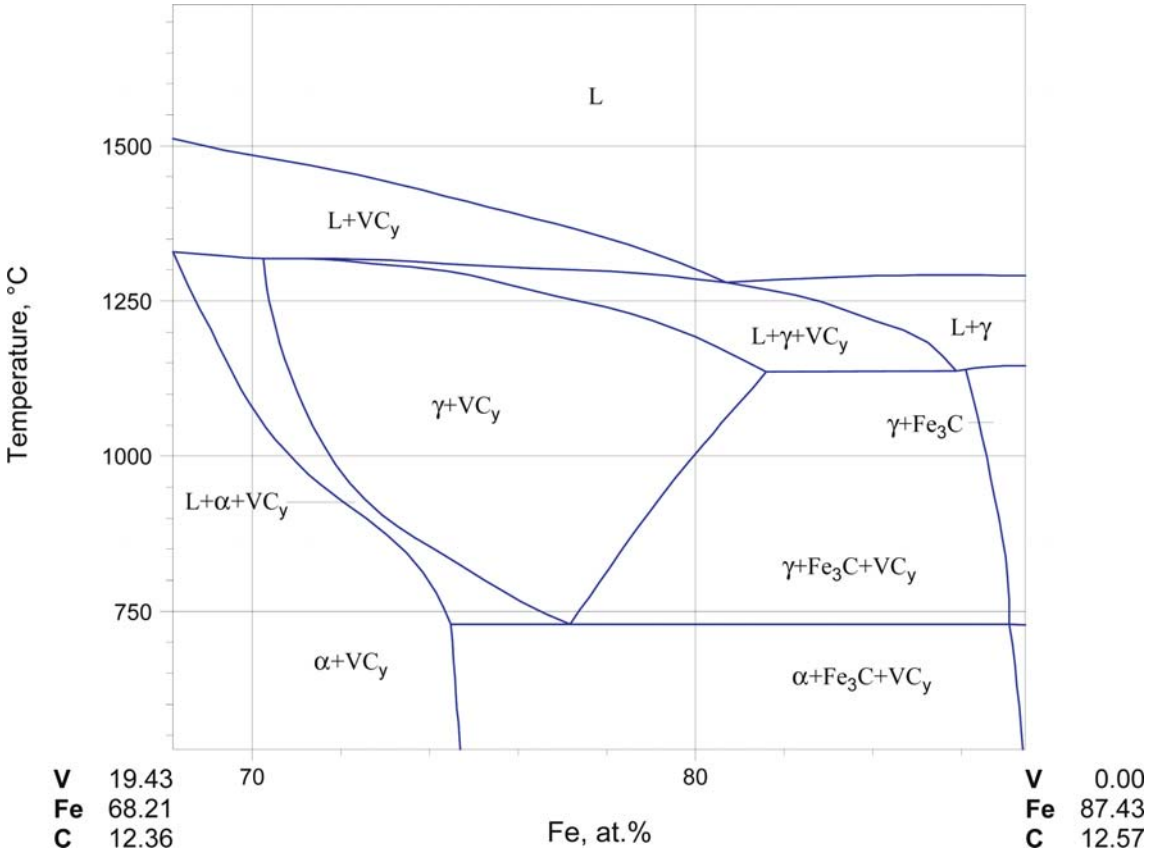

Fig. 15. C-Fe-V. The calculated vertical section at 3 mass% C

DOI: 10.1007/978-3-540-74196-1_15

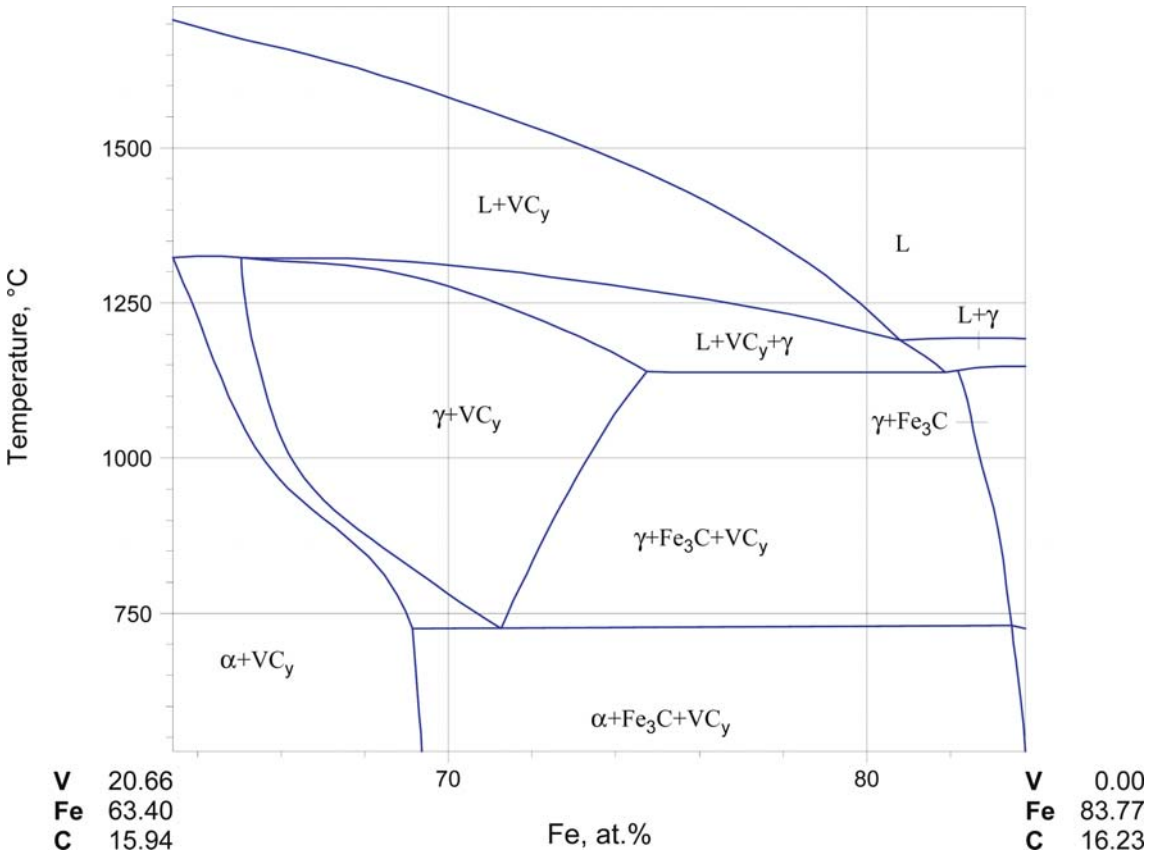

Fig. 16. C-Fe-V. The calculated vertical section at 4 mass% C

DOI: 10.1007/978-3-540-74196-1_15

References

[1912Arn] Arnold, J.O., Read, A.A., "The Chemical and Mechanical Relations of Iron, Vanadium, and Carbon", *J. Iron Steel Inst., London*, **85**, 215–234 (1912) (Morphology, Phase Relations, Review, 16)

[1930Oya1] Oya, M., "Metallographic Investigation of Vanadium Steels", *Sci. Rep. Tohoku Imp. Univ.*, **19**, 331–364 (1930) (Morphology, Phase Diagram, Phase Relations, Thermodyn., Experimental, Magn. Prop., #, 15)

[1930Oya2] Oya, M., "On the Equilibrium Diagram of the Iron-Vanadium-Carbon System", *Sci. Rep. Tohoku Imp. Univ.*, **19**, 449–472 (1930) (Crys. Structure, Morphology, Phase Diagram, Phase Relations, Experimental, #, 6)

[1931Hou] Hougardy, H., "Contribution to the Knowledge of the Iron-Carbon-Vandium System" (in German), *Arch. Eisenhuettenwes.*, **4**(10), 497–503 (1931) (Morphology, Phase Diagram, Experimental, Magn. Prop., Electr. Prop., 15)

[1931Vog] Vogel, V.R., Martin, E., "About the Iron-Carbon-Vanadium Ternary System" (in German), *Arch. Eisenhuettenwes.*, **4**(10), 487–495 (1931) (Morphology, Phase Diagram, Experimental, #, 11)

[1936Wev] Wever, F., Rose, A., Eggers, H., "Contribution to the Iron Corner of the Iron-Vanadium-Carbon Ternary System" (in German), *Mitt. Kaiser Wilhelm Institute Eisenforsch.*, **18**, 239–246 (1936) (Phase Diagram, Phase Relations, Experimental, #, 7)

[1949Jae] Jaenecke, E., "C-Fe-V" (in German), *Kurzgefasstes Handbuch aller Legierungen*, Carl Winter, Heidelberg, 696–699 (1949) (Phase Diagram, Phase Relations, Review, 9)

[1952Edw] Edwards, R., Raine, T., "The Solid Solubilities of Some Stable Carbides in Cobalt, Nickel and Iron at 1250°C", *Pulvermetallurgie, 1. Plansee Seminar, De Re Metallica, 22–26 Juni, 1952*, Reutte/Tirol, Benesovsky, F. (Ed.), Springer-Verlag, Wien, (1), 232–242 (1952) (Morphology, Phase Relations, Experimental, 5)

[1955Bun] Bungardt, V.K., Kind, K., Oelsen, W., "Solubility of Vanadium Carbide in Austenite" (in German), Arch. Eisenhuttenwes., **27**(1), 61–66 (1956) (Phase Diagram, Phase Relations, Thermodyn., Experimental, Calculations, 13)

[1956Oht] Ohtani, M., "On the Effect of Alloying Elements on the Solubility of Carbon in Molten Iron", (in Japanese), *Tetsu to Hagane*, **42**, 169–170 (1956) (Phase Relations, Experimental, 1)

[1959Fuw] Fuwa, T., Chipman, J., "Activity of Carbon in Liquid-Iron Alloys", *Trans. Metall. Soc. AIME*, **215**, 708–716 (1959) (Phase Relations, Thermodyn., Experimental, Calculation, 22)

[1960Sav] Savost'yanova, N.A., Shvartsman, L.A., "The Solubility of Vanadium Carbide in γ Iron" (in Russian), *Fiz. Met. Metalloved*. **9**(4), 515–519 (1960) (Thermodyn., Phase Relations, Review, 11)

[1962Neu] Neumann, F., Schenck, H., "The Influence of Added Elements on the Behavior of Carbon in Molten Iron Alloys and the Relations to Their Position in the Periodic System" (in German), *Giesserei Tech.-Wiss. Beih.*, **14**(1), 21–29 (1962) (Phase Relations, Experimental, 8)

[1963Ell] Elliott, J.F., Gleiser, M., Ramakrishna, V., "Iron-Carbon-j Alloys", *Thermochemistry for Steelmaking*, Addision Wesley, Reading, MA, **2**, 531 (1963) (Thermodyn., Review, 1)

[1963Fle] Flender, V.H., Wever, H., "The Thermodynamic Activity of Carbon in the Iron-Vanadium-Carbon and Iron-Carbon-Chromium Systems" (in German), *Arch. Eisenhuettenwes.*, **34**(10), 727–732 (1963) (Phase Diagram, Thermodyn., Experimental, 23)

[1963Mor] Mori, T., Fujimura, K., Kanoshima, H., "Effects of Aluminium, Sulphur, and Vanadium on the Solubility of Graphite in Liquid Iron", *Mem. Fac. Eng.Kyoto Univ.*, **25**, 83–105 (1963) (Phase Relations, Thermodyn., Experimental, 22)

[1964Wev] Wever, V.H., Flender, H., "The 'Growing'-Diffusion of the Carbon in One- or Multiphases of the Iron-Carbon Alloys" (in German), *Arch. Eisenhuettenwes.*, **35**(1), 65–73 (1964) (Phase Diagram, Thermodyn., Theory, Kinetics, 21)

[1966Grd1] Grdina, Yu.V., Lykhin, I.D., Fedorov, T.F., "Carbides in the C-Fe-V Ternary System", (in Russian), *Izv. V.U.Z. Chern. Metall.* No 4, 124–127 (1966) (Crys. Structure, Morphlogy, Phase Relations, Experimental, 10)

DOI: 10.1007/978-3-540-74196-1_15

[1966Grd2] Grdina, Yu.V., Lykhin, I.D., Fedorov, T.F., "Isothermal Section of the C-Fe-V Ternary System at 500°C" (in Russian), *Izv. V.U.Z. Chern. Metall.*, (6), 156–160, (1966) (Crys. Structure, Phase Relations, Phase Diagram, Experimental, #, 12)

[1966Ray] Raynor, D., Whiteman, J.A., Honeycombe, R.W.K., "Precipitation of Molybdenum and Vanadium Carbides in High-Purity Iron Alloys", *J. Iron Steel Inst., London*, **204**, 349–354 (1966) (Experimental, Phase Relations, 9)

[1966Tar] Taran, Yu.N., Kalinina, L.T., Ivanov, L.I. "Eutectic Structure in the C-Fe-V Alloys", *Izv. VUZ Chern. Metall.*, (in Russian), (6), 145–150 (1966) (Morphology, 18)

[1966Zup] Zupp, R.R., Stevenson, D.A., "The Influence of Vanadium on the Activity of Carbon in the C-Fe-V System at 1000°C; Correlation of the Influence of Substitutional Solutes on the Activity Coefficient of Carbon in Iron-Base Systems", *Trans. AIME*, **236**, 1316–1323 (1966) (Phase Diagram, Thermodyn., Experimental, 35)

[1967Per] Perry, A.J., "Anomalous Snoek Peak in C-Fe-V Alloys", *Jpn., J. Appl. Phys.*, **6**(11), 1340 (1967) (Calculation, Electronic Structure, 4)

[1967Sek] Sekine, H., Inoue, T., Ogasavara, M., "Additional Snoek Peak due to Carbon in C-Fe-V Alloys", *Jpn. J. Appl. Phys.*, **6**(2), 272 (1967) (Experimental, Kinetics, 5)

[1967Yvo] Yvon, K., Nowotny, H., Kieffer, R., *Monatsch. Chem.***98**, 34–44 (1967) (Crys. Structure, Experimental, #) as quoted by [1985Car]

[1968Chi] Chipman, J., Brush, E.F., "The Activity of Carbon in Alloyed Austentite at 1000°C", *Trans. AIME*, **242**, 35–41 (1968) (Thermodyn., Review, 21)

[1968Sek] Sekine, H., Inoue, T., Ogasawara, M., "Solubility of V_4C_3 in α-Iron", *Trans. Iron Steel Inst. Jpn.*, **8**, 101–102 (1968) (Phase Relations, Experimental, 6)

[1968Ven] Venables, J.D., Kahn, D., Lye, R.G., "Structure of the Ordered Compound V_6C_5", *Philos. Mag.*, **18**, 177–192 (1968) (Crys. Structure, Experimental, 10)

[1968Zup] Zupp, R.R., Stevenson, D.A., "Statistical Thermodynamics of Carbon in Ternary Austenitic Iron-Base Alloys", *Trans. AIME*, **242**, 862–869 (1968) (Thermodyn., Theory, 35)

[1969Ebe] Ebeling, V.R., Wever, H., "Contribution to the Cognition of the Iron Corner of the System Iron-Vanadium-Carbon" (in German), *Arch. Eisenhuettenwes.*, **40**(7), 551–555 (1969) (Phase Diagram, Phase Relations, Thermodyn., Experimental, Kinetics, 26)

[1969Sch] Schurmann, V.E., Kramer, D., "The Effect of Temperature and Equivalence of Alloying Elements Effects on the Carbon Solubility in Iron rich Carbon-Saturated Multicomponent Melts" (in German), *Giessereiforschung*, **21**(1), 29–42 (1969) (Thermodyn., Review, Calculation, 35)

[1970Hul] Hultgren, B., Orr, R.L., Kelley, K.K., "*Supplement to Selected Values of Thermodynamic Properties of Metals and Alloys*", Dept. of Mineral Tech., University of California, Berkeley, (1970) (Thermodyn., Review)

[1970Sch] Schenck, V.H., Gloz, M., Steinmetz, E., "Influence of the Elements Vanadium, Gallium, and Indium on the Solubility of Carbon in Molten Iron Alloys" (in German), *Arc. Eisenhuettenwes.*, **41**(1), 1–3 (1970) (Phase Relations, Thermodyn., Calculation, 15)

[1970Yvo] Yvon, K., Parthe, E., "On the Crystal Chemistry of the Close Packed Transition Metal Carbides, 1. The Crystal Structure of the ξ-V, Nb, and Ta Carbides", *Acta Crystall.*, **B26**(1), 149–153 (1970) (Crys. Structure, Experimental, #, 16)

[1971Sut] Sutton, H.C., Whiteman, J.A., "Structure and Mechanical Properties of Isothermally Transformed Iron-Vanadium-Carbon Alloys", *J. Iron Steel Inst.*, **209**(March), 220–225 (1971) (Crys. Structure, Morphology, Experimental, Mechan. Prop., 10)

[1971Tel] Telegus, V.S., Kuzma, Yu.B., "On Interaction of Some Transition Metals with Carbon" (in Ukrainian), *Bull. Lviv State Univ., Ser. Chem., (Visn. L'viv Derzh. Univ., Ser Khim.)*, (12), 28–33 (1971) (Crys. Structure, Phase Diagram, Experimental, 16)

[1972Bil] Billingham, J., Bell, P.S., Lewis, M.H., "Vacancy Short-Range Order in Substoichiometric Transition Metal Carbides and Nitrides with NaCl Structure. 1. Electron Diffraction Studies of Short-Range Ordered Compounds", *Acta Crystallogr., A*, **28**, 602–606 (1972) (Crys. Structure, Experimental, 21)

DOI: 10.1007/978-3-540-74196-1_15

[1972Col] Collins, M.J., "C-Fe-V Phase Diagram", *J. Iron Steel Inst.*, **210**, 284 (1972) (Phase Diagram, Phase Relations, Experimental, 2)

[1972Dav] Davenport, A.T., Honeycombe, R.W.K., "Precipitation of Carbides at α-γ Boundaries in Alloyed Steels", *Proceed. Royal Soc. London, Ser. A*, **322**(1549), 191–205 (1972) (Crys. Structure, Morphology, Phase Relations, Experimental, 23)

[1972Edm] Edmonds, D.V., "Occurrence of Fibrous Vanadium Carbide during Transformation of an C-Fe-V Steel", *J. Iron Steel Inst.*, **210**(5), 363–365 (1972) (Morphology, Phase Relations, Experimental, Mechan. Prop., 7)

[1972Foo] Foo, E.H., Lupis, C.H.P., "Activity of Carbon in Liquid Iron Alloys at 1550°C", *Metall. Trans.*, **3**, 2125–2131 (1972) (Phase Relations, Thermodyn., Experimental, 18)

[1972Wad] Wada, T., Wada, H., Elliott, J.F., Chipman. J., "Activity of Carbon and Solubility of Carbides in the FCC Fe-Mo-C, Fe-Cr-C and C-Fe-V Alloys", *Metall. Trans.*, **3**(11), 2865–2872 (1972) (Phase Relations, Thermodyn., Experimental, 21)

[1973Bat] Batte, A.D., Honeycombe, R.W.K., "Strengthening of Ferrite by Vanadium Carbide Precipitation", *Met. Sci. J.*, **7**, 160–168 (1973) (Morphology, Phase Relations, Mechan. Prop., 19)

[1973Edm] Edmonds, D.V., "The Strengthening of an C-Fe-V Low-Alloy Steel by Carbide Precipitation during Continuous Cooling from the Austenitic Condition", *Metallurg. Trans., A*, **4**(11), 2527–2533 (1973) (Morphology, Phase Relations, Experimental, Mechan. Prop., 19)

[1973Hei] Heikkinen, V.K., Hakkarainen, T.J., "Precipitation Associated with Climb of a {100} Dislocations in a Low-Carbon Iron-Vanadium Alloy", *Philos. Mag*, **28** (1), 237–240 (1973) (Morphology, Phase Relations, Experimental, 5)

[1973Hof] Hoffmeister, H., "Crystal Segregations and Eutectic Carbide Precipitations in Iron-Carbon-Vanadium Alloys" (in German), *Arch. Eisenhuettenwes.*, **44**(5), 349–355 (1973) (Morphology, Phase Relations, Experimental, 7)

[1973Koy] Koyama, S., Ishii, T., Narita, K., "Solubility of Vanadium Carbide and Nitride in Ferritic Iron" (in Japanese), *Nippon Kinzuku Gakkai-Shi*, **37**(2), 191–196 (1973) (Phase Relations, Experimental, 14)

[1974Edm] Edmonds, D.V., "The Strengthening of an C-Fe-V Low-Alloy Steel by Carbide Precipitation during Continuous Cooling from the Austenitic Condition", *Metall. Trans. A*, **4**(11), 2527–2533 (1973) (Morphology, Phase relations, Mechan. Prop., Experimental, 19)

[1974Sig] Sigworth, G.K., Elliott, J.F., *Metall. Sci.*, **8**, 298–310 (1974) as quoted in [1991Hua]

[1975Dun] Dunlop, G.L., Honeycombe, R.W.K., "The Role of Dislocations in the Coarsening of Carbide Particles Dispersed in Ferrite", *Philos. Mag.*, **32**(1), 61–72 (1975) (Crys. Structure, Morphology, Experimental, Kinetics, 12)

[1975Fre] Frey, H., Holleck, H., "DTA Investigations of High Temperature Phase Equilibria in Ternary Transition Metal-Carbon Systems", in "*Thermal Analysis"*, Proc. Internat. Conf., 4th, 8–13 July 1974, Buzas, I. (Ed.), Akad. Kiado, Budapest, **1**, 339–348 (1975) (Morphology, Phase Diagram, Phase Relations, Experimental, 3)

[1975Ilc] Ilczuk, J., Haneczok, G., Moron, J.W., "Isothermal Magnetic Permeability Disaccommodation in α-Fe-V(0.5%)-C in the Region of the Snoek Relaxation", *Acta Physica Polonica A*, **A48**(6), 757–763 (1975) (Morphology, Experimental, 20)

[1976Han] Haneczok, G., Ilczuk, J., Kuska, R., Moron, J.W., "Migrational Relaxations in α-C-Fe-V in the Region of the Snoek Effect", *Phys. Status Solidi A*, **33**(1), 313–324 (1976) (Morphology, Experimental, 22)

[1977Uhr] Uhrenius, B., "Optimization of Parameters Describing the Interaction Between Carbon and Alloying Elements in Ternary Austenite", *Scand. J. Metall.*, **6**(2), 83–89 (1977) (Thermodyn., Calculations, #, 24)

[1978Dmi] Dmitrieva, G.P., Shurin, A.K., Vasilev, A.D., "Mechanicostructural Properties of Iron-Alloys with Vanadium Carbide", *Met. Sci. Heat Treat.*, **20**(3–4), 325–327 (1978) (Phase Diagram, Experimental, Mechan. Prop., 2)

DOI: 10.1007/978-3-540-74196-1_15

[1978Dov] Dovgopol, M.P., Dovgopol, S.P., Radovskii, I.Z., Gel'd, P.V., "Electron Structure of Fe-C Melts, Alloyed with Vanadium" (in Russian), *Izv. Vyss. Uchebn. Zaved., Fiz.*, **2**, 82–86 (1978) (Experimental, Electronic Structure, Magn. Prop., 14)

[1978Uhr] Uhrenius, B., "A Compendium of Ternary Iron-base Phase Diagrams", in "*Hardenability Concepts with Applications to Steel*", Proc. Symp. Held Sheraton-Chicago Hotel, Oct. 24–26, 1977, Doane, D.V., Kirkaldy, J.S. (Eds.), Metall. Soc. AIME Heat Treat. Com./ Amer. Soc Met. Activ. Phase Trans., 28-81 (1978) (Phase Diagram, Phase Relations, Thermodyn., Calculations, #, 53)

[1979Ric] Ricks, R.A., Howell, P.R., Honeycombe, R.W.K., "Crystallographic Studies of Reaction Products in Isothermally Transformed Iron-Base Alloys", *Phase Transformations. Spring Residental Conference*. Inst. Metallurgists, Part II, 84–86 (1979) (Crys. Structure, Morphology, Experimental, 5)

[1980Fra] Fras, E., Guzik, E., "Primary Microstructure of the C-Fe-V Alloys", *Arch. Hutn.*, **25**(4), 757–772 (1980) (Morphology, Phase Relations, Experimental, Mechan. Prop., 24)

[1981Bra] Brandis, V.H., Preisendanz, H., Schuler, P., "Effect of Some Carbide Forming Elements on the Activity of Carbon in Fe-X-C Alloys in the Temperature Range from 900 to 1100°C" (in German), *Hart.-Tech. Mit.*, **35**, 121–128 (1981) (Thermodyn., Experimental, 32)

[1981Hol] Holleck, H., "Binary and Ternary Carbides and Nitrides of Transition Metals and Their Phase Relationships" (in German), *Report KfK 3087B*, Kernforschungszentrum, Karlsruhe, 181–183 (1981) (Phase Diagram, Review, 41)

[1981Kus] Kuska, R., Moron, J.W., "Magnetic Permeability Disaccommodation in αFe-C Type Alloys Containing s-i Pairs. II. Application to α-C-Fe-V Alloys", *Phys. Status Solidi A*, **66**(2), 431–438 (1981) (Calculation, Theory, Phys. Prop., 7)

[1981Wri] Wriedt, H.A., Hu, H., "Solubility Product of Vanadium Carbide in Austenite", "*Chemical Metallurgy – A Tribute to Carl Wagner*", Proc. Symp. Chicago, Feb. 23–25 1981, 171–194 (1981) (Phase Relations, Experimental, #, 18)

[1982Dun] Dunne, D.P., "Recrystallization in Cold-Rolled C-Fe-V Alloy Containing Fine Carbides", *Met. Sci.*, **16**(5), 259–267 (1982) (Morphology, Experimental, Kinetics, 31)

[1982Hor] Hornbogen, E., Schmidt, I., "Microstructures of Glassy and Metastable Crystalline Phases Formed from Fe-C- Ternary Alloys", *Rapidly Solidified Amorphous and Crystalline Alloys*, Thesis, Ruhr-Universität Bochum 199–204 (1982) (Morphology, Phase Diagram, Phase Relations, Thermodyn., Experimental, 7)

[1983Mor] Morita Z.-I., Tanaka, T., "Thermodynamics of Solute Distributions between Solid and Liquid Phases in Iron-base Ternary Alloys", *Trans. Iron Steel Inst. Jpn.*, **23**(1), 824–833 (1983) (Morphology, Phase Relations, Thermodyn., Experimental, 30)

[1983Pol] Polischuk, V.S., Nalivka, G.D., Kisel', N.G., "Composite Magnito-Abrasive Powders Based on Iron, Carbides of Titanium, Vanadium and Chromium" (in Russian), *Poroshk. Metall.*, **3**, 94–100 (1983) (Morphology, Phase Relations, Experimental, Mechan. Prop., 15)

[1983Sil] Sil'man, G.I., "Method of Calculating the Phase Diagrams of Ternary Systems by Using the Inter-Phase Distribution Coefficients of the Elements. II. Three-Phase and Four-Phase Equilibria", *Russ. J. Phys. Chem.*, **57**(3), 334–337 (1983) (Phase Diagram, Phase Relations, Thermodyn., Theory, 4)

[1984Rag] Raghavan, V., "The C-Fe-V (Carbon-Iron-Vanadium) System", *Bull. Alloy Phase Diagrams*, **5**(3), 293–299 (1984) (Crys. Structure, Phase Diagram, Review, 42)

[1984Smi] Smith, J.F., "The Fe-V (Iron-Vanadium) System", *Bull. Alloy Phase Diagrams*, **5**(2), 184–193 (1984) (Crys. Structure, Phase Diagram, Phase Relations, Thermodyn., Assessment, #, 99)

[1985Abe] Abe, T., Aaronson, H.I., Shiflet, G.J., "Growth Kinetics and Morphology of Grain Boundary Ferrite Allotriomorphs in an C-Fe-V Alloy", *Metall. Trans.A*, **16A**(4), 521–527 (1985) (Morphology, Experimental, Kinetics, 50)

[1985Car] Carlson, O.N., Ghaneya, A.H., Smith, J.F., "The C-V (Carbon-Vanadium) System", *Bull. Alloy Phase Diagrams*, **6**(2), 115–124 (Cryst. Structure, Phase Diagram, Phase Relations, Thermodyn., Assessment, #, 77)

DOI: 10.1007/978-3-540-74196-1_15

[1985Par] Park, H.S., Kim, S.J., "The Crystallography of the Ferrite Matrix and Carbides in C-Fe-V Alloy" (in Korean), *J. Korean Inst. Met.*, **23**(10) 1099–1105 (1985) (Crys. Structure, Morphology, Experimental, 10)

[1986Ino] Inoue, A., Harakawa, Y., Oguchi, M., Masumoto, T., "Metastable MC Phase in Melt-Quenched C-Fe-V and Fe-C-V-(Cr or Mo) Alloys-Mechanical Properties and Powder-Forming Tendency by Comminution", *J. Mater. Sci.*, **21**, 1310–1320 (1986) (Crys. Structure, Morphology, Phase Relations, Experimental, Mechan. Prop., 16)

[1986Pop] Popov, V.V., Gol'dshtein, M.I., Emel'yanov, D.A., Kostrov, Yu.N., "Thermodynamic Calculation of the Solubility of Cubic Vanadium Carbide in Austenite", *Russ. Metall. (Engl. Transl.)*, **1**(1), 111–115 (1986), translated from *Izv. Akad. Nauk SSSR. Metally*, (1), 105–109 (1986) (Phase Diagram, Phase Relations, Thermodyn., Calculation, 14)

[1987Guo] Guojun, Q., Chunlin, J., Yinchang, C., "Thermodynamic Activity Interaction Coefficients in C-Fe-V Melts", *Trans. Jpn. Inst. Met.*, **28**(5), 412–423 (1987) (Experimental, Phase Relations, Thermodyn., 42)

[1987Rag] Raghavan, V., "The C-Fe-V (Carbon-Iron-Vanadium) System" in *"Phase Diagrams of Ternary Iron Alloys"*, ASM International, Materials Park, OH, 111–125 (1987) (Phase Diagram, Review, 41)

[1988Kes] Kesri, R., Durand-Charre, M., "Metallurgical Structure and Phase Diagram of C-Fe-V System: Comparison with other Systems Forming *M*C Carbides", *Mat. Sci. Technol.*, **4**(8), 692–699 (1988) (Crys. Structure, Morphology, Phase Diagram, Phase Relations, Experimental, 27)

[1988Tod] Todd, J.A., Copley, S.M., "Cooperative Growth at Interphase Boundaries in Solid-Solid and Solid-Liquid Systems", *Scr. Metall.*, **22**(11), 1771–1774 (1988) (Crys. Structure, Thermodyn., Calculation, Interface Phenomena, 14)

[1989Kes] Kesri, R., Hamar-Thibault, S., "MC Carbides in Ternary Fe-M-C Systems (M = V, Nb) - Composition, Morphology and Order", *Z. Metallkd.*, **80**(7), 502–510 (1989) (Crys. Structure, Morphology, Phase Diagram, Experimental, 19)

[1989Mal] Malik, A.U., Ishaq, M., Ahmad, S., "Influence of Carbon on the Hot Corrosion Behaviour of Fe-base Alloys", *Mater. Trans., JIM*, **30**(9), 707–716 (1989) (Crys. Structure, Morphology, Experimental, Kinetics, 14)

[1991Has] Hasegawa, N., Saito, M., Kojima, A., Makino, A., Misaki, Y., Watanabe, T., "Crystallization Behavior of Fe-M-C (M = Ti, Zr, Hf, V, Nb, Ta) Films", *IEEE Trans. J. Magn. Jpn.*, **6**(2), 120–126 (1991) (Crys. Structure, Phase Relations, Experimental, 6)

[1991Hua] Huang, W., "A Thermodynamic Evaluation of the C-Fe-V System", *Z. Metallkd.*, **82**(5), 391–401 (1991) (Calculation, Phase Diagram, Thermodyn., Experimental, #, 54)

[1991Lee] Lee, B.J., Lee, D.N., "A Thermodynamic Study on the C-Fe-V System", *Calphad*, **15**(3), 293–306 (1991) (Phase Diagram, Thermodyn., Calculation, 31)

[1992Sil] Sil'man, G.I., "Phase Diagram of the C-Fe-V System and its Application to Metallography of Steels and Cast Irons", *Met. Sci. Heat Treat.*, **34**(11–12), 665–670 (1992) (Phase Diagram, Phase Relations, Thermodyn., Experimental, 11)

[1992Ueb] Uebing, C., Viefhaus, H., Grabke, H.J., "Surface Cosegregation and Surface Precipitation on Fe-3%V-C,N(100) Single Crystals", *Surf. Sci.*, **264**(1–2), 114–126 (1992) (Phase Relations, Interface Phenomena, Experimental, 20)

[1993Pol] Pollak, H., Fleischmann, A., Luyckx, S.B., Koursaris, A., "Investigation of the Phases Present in C-Fe-V Alloys by Mössbauer Spectroscopy and X-ray Diffraction", *Nucl. Instrum. Methods Phys. Res., Sec. B., (Beam Interactions with Materials and Atoms), Netherlands*, **B76**(1–4), 270–272 (1993) (Phase Relations, Experimental, 2)

[1993Pop] Popov, V.V., "Determination of Mutual Diffusion Coefficients in Austenite and Ferrite of C-Fe-V System" (in Russian), *Phiz. Met. Metalloved.*, **83**(3), 98–103 (1993) (Transport Phenomena, Experimental, 12)

[1993Rag] Raghavan, V., "C-Fe-V (Carbon-Iron-Vanadium)", *J. Phase Equilib.*, **14**(5), 622–623 (1993) (Phase Diagram, Review, #, 11)

DOI: 10.1007/978-3-540-74196-1_15

[1993Ueb] Uebing, C., Viefhaus, H., Grabke, H.J., "Facetting of Fe-15 %Cr-N, Fe-3 %V-C and Fe-3 % V-C,N (111) Surfaces", *Fresenius Z. Anal. Chem.*, **346**(1–3), 275–280 (1993) (Phase Relations, Interface Phenomena, Experimental, 24)

[1994Ama] Amara, S.E., Kesri, R., Valignat, N., Hamarthibault, S., "Composition of Vanadium Carbides Formed by Solidification in Ternary C-Fe-V Alloys", *Microchimica Acta*, **114**, 157–164 (1994) (Phase Diagram, Phase Relations, Morphology, Experimental, 13)

[1994Pol] Pollak, H., Luyckx, S.B., "The Role of Mössbauer Spectroscopy in the Determination of the Microstructure and Composition of C-Fe-V Alloys", *Hyperfine Interactions*, **84**(1–4), 187–192 (1994) (Phase Relations, Experimental, 12)

[1995Ueb] Uebing, C., Viefhaus, H., Grabke, H.J., "Surface Cosegregation on Fe-3%V-C, Fe-3%V-C,N and Fe-15%Cr-N (110) Single Crystals", *Fresenius J. Anal.Chem.*, **353**(3–4), 254–258 (1995) (Phase Relations, Interface Phenomena, Experimental, 17)

[1997Beh] Behulova, M., Grgac, P., Kabat, E., "The Heat Transfer during Rapid Solidification of Undercooled Hypereutectic Fe-C-X Alloy Droplets", in "*Rapidly Quenched and Metastable Materials*", Proc. of the Ninth International Conference on Rapidly Quenched and Metastable Materials. Supplement, Elsevier, Part Suppl., pp. 10–13. Amsterdam, Netherlands, (1997) (Morphology, Interface Phenomena, 38)

[1997Du] Du, H., Morral, J.E., "Prediction of the Lowest Melting Point Eutectic in the Fe-Cr-Mo-V-C System", *J. Alloys Compd.*, **247**, 122–127 (1997) (Phase Relations, Experimental, Calculation, Review, 20)

[1997Fra] Fras, E., Guzik, E., Kapturkiewicz, W., Lopez, H.F., "Carbide Morphology in Bulk and Unidirectionally Solidified C-Fe-V Eutectics", *Mat. Sci. Technol.*, **13**(12), 989–996 (1997) (Morphology, Phase Diagram, Phase Relations, Experimental, 24)

[1997Pop] Popov, V.V., "Determination of the Interdiffusion Diffusion Coefficients in Austenite and Ferrite of C-Fe-V System", *Phys. Met. Metallogr.*, **83**(3), 299–302 (1997) (Transport Phenomena, Experimental, 12)

[1997Shu] Shurin, A.K., Shishkin, E.A., "Thermal Expansion of Two-Phase Alloys of Iron-Nickel-Vanadium Carbide. 2. Fe-$VC_{0.75}$ System Alloys" (in Russian), *Metallofizika i Noveish. Tekhnologii*, **19**(1), 58–61 (1997) (Thermodyn., Experimental, Phys. Prop., 13)

[1999Lip] Lipatnikov, V.N., Gusev, A.I., Ettmayer, P., Lengauer, W., "Phase transformations in nonstoichiometric vanadium carbide", *J. Phys.: Condens. Matter.*, **11**, 163–184 (1999) (Crys. Structure, Phase Relations, Phase Diagram, Experimental, #, 55)

[1999Oka] Okane, T., Umeda, T., "Microstructure of Unidirectionally Solidified C-Fe-V Alloy and Interface Temperature Measurement of γ+VC Eutectic Carbide", *Inter. J. Cast Metals Res.*, **11**(5), 291–296 (1999) (Crys. Structure, Morphology, Phase Relations, 5)

[1999Pop] Popov, V.V., "Diffusion Interaction of Carbides, Nitrides and Carbonitrides With Iron and Steels", *Metallofizika Nov. Tekhnol.*, **21**(2), 99–103 (1999) (Phase Relations, Transport Phenomena, Experimental, 11)

[2000Bya] Byakova, A.V., "Structural Aspects of Strength and Methods to Increase the Serviceability of Carbide Coatings", *Powder Metall. Met. Ceram.*, **39**(1–2), 85–91 (2000) (Crys. Structure, Experimental, Mechan. Prop., 13)

[2000Zhu] Zhukov, A.A., Savulyak, V.I., Arkhipova, T.F., "On the Effect of Elements on the Equilibrium Temperature of Eutectic Transformations", *Met. Sci. Heat Treat.*, **42**(1–2), 47–52 (2000) (Phase Diagram, Phase Relations, Thermodyn., Calculation, 24)

[2001Hil] Hildebrand, H., Hildebrand, M., "Microstructural Influences on Young's Modulus for C-Fe-V and Fe-Mo-C Alloys", *Materialwissenschaft und Werkstofftechnik*, **32**(9), 701–711, (2001) (Morphology, Mechan. Prop., Experimental, 39)

[2001Mar] Marsh, P., Wood, J.V., Moon, J.R., "Diffusion between High Speed Steel and Iron Powders", *Powder Met.*, **44**(3), 205–210 (2001) (Crys. Structure, Phase Relations, Experimental, Kinetics, 4)

DOI: 10.1007/978-3-540-74196-1_15

[2001Ume] Umemoto, M., Liu, Z.G., Masuyama, K., Tsuchiya, K., "Influence of Alloy Additions on Production and Properties of Bulk Cementite", *Scr. Mater.*, **45**(4), 391–397 (2001) (Crys. Structure, Phase Relations, Experimental, Mechan. Prop., Phys. Prop., 13)

[2001Wan] Wang, H., Wang, S., Yue, K., Dong, Y., Li, W., "The Rules of Thermodynamic Properties in Fe-C-j (j = Ti, V, Cr, Mn) Melts" (in Chinese), *Acta Metall. Sin.*, **37**(9), 952–956 (2001) (Thermodyn., Calculation, 13)

[2003Per] Perepletchikov, E.F., Ryabtsev, I.A., Vasil'ev, V.G., Heinze, H., "Structure and Properties of High-Carbon High-Vanadium Iron-Base Alloys for Surfacing", *Met. Sci. Heat Treat.*, **45**(5–6), 193–196 (2003) (Morphology, Phase Relations, Experimental, Mechan. Prop., 8)

[2003Rag] Raghavan, V., "C-Fe-V (Carbon-Iron-Vanadium)", *J. Phase Equilib.*, **24**(1), 67 (2003) (Phase Relations, Review, #, 7)

[2003Yam] Yamasaki, S., Bhadeshia, H.K.D.H., "Modelling and Characterisation of V_4C_3 Precipitation and Cementite Dissolution During Tempering of C-Fe-V Martensitic Steel", *Mater. Sci. Technol.*, **19**(10), 1335–1343 (2003) (Morphology, Calculation, Experimental, Electronic Structure, 34)

[2004Aar] Aaronson, H.I., Reynolds, W.T., Purdy, G.R., "Coupled-Solute Drag Effects on Ferrite Formation in Fe-C-X Systems", *Metall. Mater. Trans. A.*, **35A**(4), 1187–1210 (2004) (Morphology, Phase Relations, Experimental, Interface Phenomena, Kinetics, 148)

[2005Pop] Popov, V.V., Gorbachev, I.I., "Analysis of Solubility of Carbides, Nitrides, and Carbonitrides in Steels Using Methods of Computer Thermodynamics: II. Solubility of Carbides, Nitrides, and Carbonitrides in the Fe-V-C, Fe-V-N, and Fe-V-C-N Systems", *Phys. Met. Metallogr. (Engl. Transl.)*, **99**(3), 286–299 (2005) (Phase Diagram, Phase Relations, Thermodyn., Calculation, 40)

[2005Ust] Ustinovshikov, Y., Pushkarev, B., Sapegina, I., "Phase Transformations in Alloys of the Fe-V System", *J. Alloys Compd.*, **398**, 133–138 (2005) (Crys. Structure, Morphology, Phase Diagram, Phase Relations, Experimental, #, 9)

[2006MSIT] "C-Fe (Iron-Carbon)", Diagrams as Published, in *MSIT Workplace*, Effenberg, G. (Ed.), Materials Science International Services, GmbH, Stuttgart; Document ID: 30.13598.1.20 (2006) (Crys. Structure, Phase Diagram, Phase Relations, 2)

[Mas2] Massalski, T.B. (Ed.), *Binary Alloy Phase Diagrams*, 2nd edition, ASM International, Metals Park, Ohio (1990)

[V-C] Villars, P. and Calvert, L.D., *Pearson's Handbook of Crystallographic Data for Intermetallic Phases*, ASM, Metals Park, Ohio (1985)

[V-C2] Villars, P. and Calvert, L.D., *Pearson's Handbook of Crystallographic Data for Intermetallic Phases*, 2nd edition, ASM, Metals Park, Ohio (1991)

DOI: 10.1007/978-3-540-74196-1_15

Carbon – Iron – Tungsten

Kostyantyn Korniyenko

Introduction

Phase relations in the C-Fe-W system are of great interest above all because of the importance of tungsten as alloying element in steels. Therefore constitution of this system has been studied quite intensively. Other important aspects of this subject, in particular the dissolution of iron carbides during austenitization of tungsten steels, phase transformations of carbides as well as diffusion interaction of carbides with iron and steels also attract attention of investigators widely. Details of experimental studies of phase relations, crystal structures and thermodynamics as well as applied techniques are presented in Table 1.

From the twenties of the last century interest of investigators was concentrated in the first place on the influence of tungsten on the properties of steels [1918Hon, 1921Dae, 1922Oza, 1924Obe, 1929Zie], and also on phase equilibria in the ternary C-Fe-W system, in particular the Fe-W-WC-Fe_3C partial system was researched actively [1920Hul1, 1921Hul, 1930Tak1, 1930Tak2, 1931Tak]. So, in [1930Tak1, 1930Tak2, 1931Tak] the liquidus surface projection with a series of temperature-composition sections and a reaction scheme were proposed. Later the liquid-solid equilibria and crystallization paths of the alloys were experimentally determined in [1959Fuw, 1960Fuw, 1960Mor, 1966Gob, 1968Jel, 1973Rim, 1976Sna, 1980Ake, 1981She, 1985Gab, 1986Gab]. Information about phase relations at different temperatures, in particular, in the form of isothermal sections was experimentally obtained by [1952Kuo, 1953Kuo, 1957Sat, 1970Pol, 1975Uhr, 1977Ber]. Series of vertical sections were constructed by [1952Edw].

The first detailed studies of crystal structure of the W_2Fe_4C phase were carried out by [1927Wes, 1928Wes]. The data about the crystal structures of the phases, which are present in the C-Fe-W alloys are also reported in [1929Zie, 1930Tak1, 1933Mor, 1947Hul, 1950Kra, 1951Uma, 1952Edw, 1952Kuo, 1953Kuo, 1957Sat, 1964Lec, 1967Boj, 1968Jel, 1970Pol, 1973Rim, 1975Uhr, 1976Lyu1, 1976Lyu2, 1976Niz, 1976Sna, 1977Ber, 1980Iwa, 1981Ino, 1981She, 1982Hor, 1982Lug, 1983Bus, 1983Haa, 1983Jer, 1992Azu, 1994Tri, 1995Tri, 1997Sht1, 1997Sht2, 1998Hac, 1998Tri, 2002Hac1].

Data on thermodynamic properties, mainly on the activity of carbon in liquid iron alloys were experimentally obtained by [1959Fuw, 1960Mor, 1965Kri, 1971Gre]. Reviews of literature data deal with phase equilibria [1920Hul2, 1929Zie, 1949Jae, 1961Eng, 1985Riv, 1988Ray, 1994Rag], crystal structures [1929Zie, 1985Riv, 1988Ray, 1990Ere] and thermodynamics [1963Ell, 1981Nis].

The latest accomplishments in the field of computer thermodynamics as applied to the diffusion transformations in the C-Fe-W system are reviewed in [2001Sht]. Thermodynamic calculations of isothermal sections were carried out by [1978Uhr, 1980Uhr, 1987Gus, 1997Sht2], of temperature-composition sections - by [1987Gus, 1990Jan, 1998Hac], as well as of the liquidus surface - by [1980Uhr, 1987Gus]. Optimization of the parameters describing the interaction between carbon and tungsten in the ternary C-Fe-W austenite was presented by [1977Uhr].

As a whole, the constitution of the C-Fe-W system being rather complicated is, in general, well established. However, some details need further investigations, in particular constitution of the liquidus, solidus and solvus surfaces, as well as the reaction scheme for the whole range of compositions and alloys thermodynamics (see below).

Binary Systems

The C-Fe system is accepted from [2006MSIT]. Data relating to the C-W system constitution at the temperatures higher than 2100°C are taken from [1991Nag], the corresponding phase diagram is presented in Fig. 1. The C-W system at lower temperatures as well as the Fe-W system are accepted from [Mas2].

DOI: 10.1007/978-3-540-74196-1_16

Solid Phases

Crystallographic data on the known unary, binary and ternary C-Fe-W phases and their concentration and temperature ranges of stability are listed in Table 2. Among the pure components, iron and tungsten form the extended fields of solid solutions; in particular, solubility of tungsten in (δFe) reaches 14.3 at.% at 1548°C in the boundary Fe-W system.

According to the literature data, in the C-Fe-W system three stable ternary phases exist, namely τ_1, τ_2 and τ_3 phases (Table 2). The τ_1 phase (so-called M_6C phase), as it was reported by [1927Wes, 1928Wes], lies in the range of compositions varying from W_3Fe_3C to W_2Fe_4C. Probably, this phase is the same like W_2Fe_2C that was found by [1920Hul1, 1921Hul]. The τ_1 phase takes part in the solid-liquid equilibria, melting incongruently at 1668°C [1980Ake, 1980Uhr]. In contrast to the τ_1 phase, the τ_2 and τ_3 phases exist only in the subsolidus region. The τ_2, W_6Fe_6C phase (so-called $M_{12}C$ phase) was claimed by [1982Lug] to be closely related to the τ_1 phase. According to the authors' data, the alloys containing both τ_1 and τ_2 phases have undergone a reversible transformation. But conclusion of [1982Lug] that τ_1 is a high-temperature modification of τ_2 does not, however, seem to be justified in a view of the very different compositions [1988Ray]. It was shown by [1977Ber] that the carbon contents of the τ_1 and τ_2 phases are constant and probably coincide with the stoichiometric ones. The homogeneity region of the τ_1 phase, *i.e.*, Fe:W ratio was observed to be wider than of the τ_2 phase. As for the τ_3 phase stoichiometry, [1970Pol] prefer the W_3FeC formula as more representative than the prototype (9:3:4) declared by [1983Haa] (Table 2), which a comparison with the cobalt isomorph would suggest. This fact is an evidence of a preferential occupancy of octahedral sites in the hexagonal lattice.

The τ_4, τ_5, τ_6 and τ_7 phases are metastable in the ternary C-Fe-W system, but the τ_4, $W_2Fe_{21}C_6$ (so-called $M_{23}C_6$) phase, is stabilized by chromium in the quaternary C-Cr-Fe-W system. This phase was reported first by [1933Mor] being labelled as the $(W,Fe)_4C$ phase with face-centered cubic Cr_4C type structure. It was obtained from tungsten magnet steels by electrolytic dissolution of their iron phases. [1933Mor] also declared the presence of this phase in high-speed steels, but only in a very small amount.

The metastable τ_6, ψ (C-Fe-W) phase has been found by [1980Iwa] and [1981Ino] in the ternary alloys containing 10 to 14 at.% W and 18 to 20 at.% C, quenched rapidly from the melts. This phase was interpreted as a supersaturated solid solution with body-centered cubic structure. A phase of the same type was reported by [1980Iwa, 1981Ino] also in the C-Cr-Fe and C-Fe-Mo ternary systems. Review of structures of implantation metallide-based phases in the ternary systems of transition metals with carbon, including the τ_6 phase, was presented in [1990Ere]. The τ_7, η' (C-Fe-W) metastable ternary phase (so-called η'-$M_{\sim 4}C$ phase) was found by [1982Hor] in the alloys of $W_{11}Fe_{69}C_{20}$ and $W_{11}Fe_{67}C_{22}$ compositions rapidly cooled from the liquid and then reheated from ambient temperature. After annealing of glass the τ_7 phase was observed in the $W_{11}Fe_{69}C_{20}$ alloy. The metastable C-Fe-W films obtained by non-reactive RF magnetron sputtering were studied by [1994Tri]. The results show that their structure at room temperature depends on the percentage of iron in the films, varying from WC_{1-x} to amorphous with the increasing content of this element. The crystallization mechanism of the amorphous films is characterized by the formation of carbon-deficient phases, such as W_2C or M_6C. Structural behavior of the metastable C-Fe-W films was investigated by [1995Tri, 1998Tri].

Invariant Equilibria

Temperatures, types of reactions and known compositions of the phases taking place in the invariant equilibria are listed in Table 3. Conversion of the composition values from mass to atomic per cents was carried out in this report. These data as well as the partial reaction scheme showing the stable and metastable equilibria (Figs. 2 and 3, respectively) are based mainly on the review of [1988Ray] with slight corrections according to the accepted binary systems. Eight four-phase reactions listed in Fig. 2 provide a complete description of the stable ternary liquid-solid equilibria. As to the metastable equilibria, it was assumed by [1988Ray] that the cementite θ phase is metastable both in the binary C-Fe system and in the ternary C-Fe-W system. At the same time, from the measurements of the activity of carbon it was concluded [1975Uhr] that a very small percentage of tungsten will stabilize cementite relative to graphite at 1000°C. This issue needs additional studies.

DOI: 10.1007/978-3-540-74196-1_16

Existence of an invariant equilibrium in the C-Fe-W system was first reported by [1922Oza], namely of the four-phase eutectic reaction L ⇌ θ + λ + (γFe) at 1065°C. A reaction scheme was first published by [1930Tak2] (completed in [1931Tak]), with division of equilibria into metastable (with participation of the metastable θ phase) and stable. Two four-phase invariant reactions corresponding to the stable equilibria and four reactions corresponding to the metastable ones were listed. Later the proposed scheme was reproduced in [1968Jel] with some modifications, in particular, with addition of certain equilibria, temperatures of which were not established. Taking into account the experimental data of [1980Ake], [1980Uhr] corrected some temperatures of reactions and added two metastable equilibria according to the calculation results. The results of [1980Uhr] became a basis for the stable equilibria presentation in the reviews of [1985Riv, 1988Ray] As for the metastable reaction scheme, the authors of the two last works applied mainly the data of [1968Jel]. scheme. [1988Ray] added two hypothetical four-phase invariant reactions with the participation of liquid to the reaction scheme referring incorrectly to [1968Jel]; the κ, WC_{1-x} phase, had been included, which was not known according to the constitution of the C-W system accepted by [1968Jel]. As a whole, the additions made by [1988Ray] are accepted in the present reaction scheme (Fig. 2). The hypothetical solid-solid reaction sequence proposed by [1988Ray] based on the comparison of phase equilibria at different temperatures [1953Kuo, 1957Sat, 1970Pol, 1975Uhr, 1977Ber] does not show temperature any reaction. Therefore further experimental work is necessary. An attempt of thermodynamic evaluation of the temperatures and co-ordinates of the four-phase equilibria with the participation of liquid in the C-Fe-W system was made by [1987Gus], but the obtained results, especially invariant points positions, essentially differ from the experimental literature data and need further experimental verification.

Liquidus, Solidus and Solvus Surfaces

Figure 4 presents liquidus surface projection involving stable phase equilibria, according to the reaction scheme (Fig. 2). It is based mainly on the data of [1980Uhr] reproduced also in the review by [1988Ray]. The reported information is compiled on the basis of a complex analysis of experimental data and thermodynamic evaluations published in the earlier works [1931Tak, 1968Jel, 1975Uhr, 1977Uhr, 1978Uhr, 1980Ake], with addition of the schematic e_1U_1, e_2U_1, U_1U_2 and U_2P curves, in accordance with the reaction scheme. In this assessment slight corrections according to the constitution of the boundary binary systems were carried out. Compositions of the E, P and U_3 to U_6 invariant points are listed in Table 3.
First experimental investigations of the aspects related to the liquidus surface constitution were performed by [1921Dae, 1922Oza, 1930Tak1]. They deal with the constitution and crystallization paths of the as-cast eutectic-containing alloys in the Fe rich corner. Later, results published in the numerous works were reviewed by [1931Tak] and generalized in the form of the liquidus surface projection of the Fe-Fe_3C-WC-W partial system, but the participation of the ternary phases in the equilibria was not taken into account. Isothermal contours for the primary crystallization surfaces of the (γFe), (δFe) and μ phases were shown but their positions contradict to the later data for the invariant reactions involving liquid. In [1930Tak1, 1931Tak, 1968Jel, 1981She] also estimation of phase equilibria with the participation of the metastable θ phase was presented.
The solubilities of graphite in the melt were studied at the temperatures of 1450, 1550 and 1560°C by [1959Fuw, 1960Fuw], [1960Mor] and [1959Fuw], respectively. The reported data do not agree well with the accepted liquidus temperatures in the accepted binary C-Fe system. This conclusion follows from the extrapolation to the C-Fe axis which evidences that carbon compositions are higher by ~0.3 mass% C than those expected than those expected from the iron liquidus curve according to the C-Fe system [1988Ray]. At the same time, the values of solubilities of graphite in the melt at 1550, 1450 and 1350°C obtained by [1973Rim, 1988Ray] agree accurately with the C-Fe system data (to less than 0.1 mass%). Agreement of the [1973Rim, 1988Ray] data with the data of [1960Mor] at 1550°C is quite good but discrepancies may be seen in a comparison with the data of [1959Fuw] at 1450°C.
The liquidus surface projection of the partial Fe-Fe_3C-WC-W system constructed by [1968Jel] contradicts to the constitution of the currently accepted binary systems. In particular, the W_2C phase is presented by one modification; the Fe_3C phase is shown as stable; invariant equilibrium with the participation of the liquid, (δFe) and the μ phase in the Fe-W system is presented as the eutectic one taking place at 1520°C, and the corresponding invariant point is shifted towards the tungsten side. Structure formation of the C-Fe-W alloys

DOI: 10.1007/978-3-540-74196-1_16

during eutectic solidification was studied by [1976Sna] but the proposed character of phase relations is presented schematically, without satisfactory explanations and temperature-composition relations. The position of the $\tau_1 + \gamma$ eutectic valley determined by [1985Gab, 1986Gab] partially agrees with the location of the U_6P monovariant curve (Fig. 4) being slightly shifted to the carbon side. This difference is probably due to a certain inaccuracy in the determination of the primary phases in the alloys adjacent to the eutectic alloy. Liquidus surface projection calculation presented by [1987Gus] on the basis of thermodynamic evaluation essentially contradicts to the data accepted in this assessment. This is mainly due to the different versions of the binary systems accepted by [1987Gus].
As a whole, a continuation of the liquid-solid equilibria investigations, with a goal to construct the liquidus surface of the whole system, is necessary. In particular, positions of the monovariant curves in the range of the compositions close to the C-W system must be established. Furthermore, the solidus and solvus surfaces up to now are not determined and need further experimental studies.

Isothermal Sections

Partial isothermal section of the C-Fe-W system at the temperature of 1500°C in the range of tungsten content up to 50 at.% and carbon content up to 25 at.% was calculated by [1980Uhr]. Later the composition interval was widened by the calculations of [1987Gus] up to 50 at.% of C and W. This section is shown in Fig. 5, with certain corrections according to the accepted binary Fe-W and C-Fe systems. So, the extension of the μ phase homogeneity region in the Fe-W system is increased, and the boundary of the liquid field in the C-Fe system is slightly shifted to the iron side. The calculation demonstrates a good agreement with the experimental results of [1980Ake] concerning the $L/(L + \gamma)$ and $L/(L + \tau_1)$ boundaries. At the same time, position of the $L/(L + \gamma + \tau_1)$ apex contradicts to the experimental data of [1985Gab]. [1987Gus] considered that this disagreement is most likely due to the experimental errors. In Figs. 5 to 9 some tie-lines are prolonged, where it is possible, over the calculated range, assuming the γ phase practically does not dissolve the third component at all temperatures like at 1500°C (Fig. 5).
[1980Uhr] also calculated partial isothermal section in the Fe rich corner (up to 25 at.% C and up to 25 at.% W) at 1400°C (Fig. 6). Comparing with 1500°C, extension of the (αδFe) range from the Fe-W system side decreases. At the same time, the L + (αδFe) phase region from the C-Fe binary system is replaced by the corresponding field containing the (γFe) phase.
Calculated partial isothermal section of the C-Fe-W system at 1320°C was reported by [1980Uhr] in the range of the tungsten content up to 10 at.% and carbon content up to 25 at.%. In [1987Gus] the limit of tungsten content was increased up to 40 mass% (16.8 at.%). The experimental values and their uncertainties were estimated by [1987Gus] using, in particular, the average compositions given by [1980Ake, 1980Uhr]. Figure 7 presents this section on the basis of [1987Gus] data, after the transformation of the concentration values from mass% to at.%. [1980Uhr] also calculated the sections at 1195 and 1145°C in the iron rich corner at carbon content up to 25 at.% and tungsten content up to 5 at.% (Figs. 8 and 9, respectively). The results of the calculations are in a good agreement with the experimental data of [1980Ake] on the W content in the liquid phase in equilibrium with (C) and the γ phase.
[1952Edw] reported that at the temperature of 1250°C Fe dissolves 7 mass% WC. On the basis of experimental investigations [1977Ber] presented the isothermal section at 1250°C for the partial Fe-WC-W system. This section is shown in Fig. 10, with a slight correction of the homogeneity region of the μ phase, between 41 and 44 at.% W at 1250°C, in agreement with the accepted Fe-W binary system, instead of the W_2Fe_3-based phase at 40 at.% Fe accepted by [1977Ber]. Thus, the positions of the $\tau_2 + \mu + (\alpha\delta Fe)$ and $(W) + \tau_2 + \mu$ three-phase regions apexes corresponding to the μ phase are slightly shifted to the tungsten side. It was established that at this temperature the τ_1 and τ_2 phases are stable within their homogeneity ranges, constant by carbon contents, but with mutual solubility of iron and tungsten. Since both the ternary τ_2 and the binary μ phases have homogeneity ranges, a relatively wide two-phase field between them is expected, in contrast to the data of [1977Ber]. The $\tau_2\mu$ boundary tie-lines are shown in Fig. 10 as dotted lines. As to the τ_3 phase, it does not possess a visible homogeneity region, but its composition is shifted to the tungsten side. The participation of the αW_2C phase in the equilibria is not reflected probably because it is already decomposed at this temperature (Table 2).

DOI: 10.1007/978-3-540-74196-1_16

[1920Hul1, 1921Hul, 1924Obe] published a tentative Fe-W-WC-Fe_3C isothermal section corresponding to a temperature of about 1100°C. Two ternary carbides, namely W_2Fe_2C and WFeC, were shown to be stable and metastable phases, respectively.
[1975Uhr] obtained some experimental data about phase relations in the Fe rich corner that serve as an evidence of the participation of the metastable θ phase and the λ phase existing at the temperatures lower than 1060°C in the Fe-W binary system, in the phase equilibria. These data agree satisfactorily with the earlier data of [1970Pol] about phase relations in the Fe-Fe_3C-WC-W partial system at 1000°C. Isothermal section at 1000°C according to the data of [1970Pol] with some corrections according to the Fe-W system is shown in Fig. 11. Three ternary phases, namely τ_1, τ_2 and τ_3 take part in the equilibria.
Isothermal section of the metastable C-Fe-W phase diagram at 910°C was calculated by [1997Sht2]. This section shows equilibria which include the γ and μ phases that have not been observed during experimental study carried out by the same authors.
Isothermally transformed alloys in the range of the compositions rich in iron (see Table 1) were studied at 700°C by [1952Kuo, 1953Kuo] and [1957Sat]. Both stable and metastable equilibria were described.

Temperature – Composition Sections

In [1930Tak2] a series of the temperature-composition sections constructed on the basis of experimental results were presented. They correspond to 2, 4, 6, 8, 10, 12, 14, 16 mass% W (while carbon content was from 0 to 1.6 mass%) as well as to 0.1, 0.3, 0.6, 0.9, 1.2 mass% C (at the same time with the change of tungsten content up to 24 mass%). The character of the phase relations was reflected clearly only in the solid state, because the investigations were carried out at the temperatures below the beginning of melting. Therefore hypothetical boundaries of the liquid-containing ranges were plotted as dotted lines. In [1931Tak] a series of mainly hypothetical sections (at 1.5, 2.0, 3.0, 3.5, 4.0 mass% C; 20 and 35 mass% W) were reported. [1952Edw] established that along the WC-Fe section at 1250°C Fe dissolves 7 mass% of WC.
[1981She] mentioned about a series of the temperature-composition sections but these sections were not presented. [1987Gus] have calculated two vertical sections: at 5 mass% W with C content in the range up to 2 mass% C as well as at 0.6 mass% C with tungsten content changing from 0 to 50 mass%. After conversion to at.% these sections correspond to $W_{1.57}Fe_{98.43}$-$W_{1.46}Fe_{89.58}C_{8.96}$ and $Fe_{97.27}C_{2.73}$-$W_{22.54}Fe_{73.32}C_{4.14}$, respectively (Figs. 12, 13). These sections are generally in good agreement with the experimental data of [1930Tak2]. In Fig. 13 the invariant horizontal at about 727°C is shown by a dotted line as corresponding to the equilibrium with the participation of the metastable θ phase.
[1990Jan] calculated the partial temperature-composition section at 5.5 mass% Fe and 5.7 to 6.1 mass% C (in at.%: $W_{45.74}Fe_{9.33}C_{44.93}$-$W_{44.23}Fe_{9.06}C_{46.71}$). Its constitution contradicts to the liquidus surface projection and the reaction scheme, because in the presented range of compositions graphite must primary crystallize, while [1990Jan] shows primary crystallization of the γ phase and equilibria with its participation at lower temperatures. Isopleth at 6.3 mass% W with up to 1.4 mass% C (W_2Fe_{98}-$W_{1.90}Fe_{91.64}C_{6.46}$ in at.%) was calculated by [1998Hac]. It demonstrates equilibria among liquid, the (αFe), (δFe), (γFe), τ_1, metastable θ, γ and λ phases (Fig. 14). The invariant isothermal line corresponding to the equilibrium with the participation of the θ phase is shown by a dotted line. The character of the phase equilibria in the solid state needs further experimental verification.

Thermodynamics

Experimentally obtained data on the thermodynamic properties of the C-Fe-W alloys are very scarce. The effect of tungsten on the activity of carbon in liquid iron alloys has been studied by [1959Fuw, 1960Fuw, 1960Mor]. The interaction parameter obtained at 1560°C in low-carbon melts by [1959Fuw] was reported as $\varepsilon_C^W = -2.3$. This value was not referred to a fixed carbon concentration. The summarized results of [1959Fuw] were mentioned in the review of [1963Ell].
[1960Mor] studied the effect of tungsten on graphite solubility in liquid iron at 1550°C and used the obtained data for the verification of the general approximate equation for calculation the activity coefficient of carbon in a multicomponent solution deduced by them. The value of interaction parameter $\varepsilon_C^W = -1.31$ at $x_C = 0.207$ was presented. The influence of the tungsten content (up to about 12 mass%)

DOI: 10.1007/978-3-540-74196-1_16

on the thermodynamic activity of carbon in the iron alloys and on the diffusion coefficient of carbon at its content of 0.4 mass% was investigated by [1965Kri] applying the diffusional annealing at 950 and 1150°C. The obtained results show that tungsten decreases these parameters.

Experimental data about the effect of tungsten on the activity of carbon in austenite were reported in [1971Gre, 1975Uhr]. [1971Gre] used the methane-hydrogen atmosphere as environment of the experiment, and determined the corresponding effect at 1050 and 1125°C on the alloys with tungsten content up to 5.86 mass% and carbon content from 0.125 to 0.445 mass%. The obtained values of the interaction parameters were $\varepsilon_C^W = -3.92 \pm 0.96$ at 1050°C and $\varepsilon_C^W = -2.45 \pm 0.44$ at 1125°C. On the basis of the comparison of the obtained results with those for the C-Fe-Cr and C-Fe-Mo systems, a survey of possible factors which may govern interactions between interstitial carbon atoms and alloyed host lattices was carried out. It was suggested that a close correlation between a solute's interaction parameter (1st Long Period) and the thermodynamics of carbide formation exists. In [1975Uhr], the activities of carbon were determined on the encapsulated carburized samples heat treated at 1000°C. These samples contained 0.97 to 40 mass% W, and the values of a_C were in the range from 0.012 to 0.97.

The Gibbs energy of formation of the ternary carbide τ_1, W_3Fe_3C at 1300 K (1027°C) was roughly estimated to be $-(76 \pm 31)$ kJ·mol^{-1} [1980Kle] using a correlation between the Gibbs energies of the phases taking part in the equilibria at this temperature, according to the literature data.

Analyses of the different phase and structural transformations, phase relations and equilibria in the C-Fe-W system using the computer thermodynamic methods were carried out by [1975Uhr, 1977Uhr, 1978Uhr, 1980Uhr, 1984Wad, 1987Gus, 1990Jan, 1997Sht1, 1997Sht2, 1998Hac, 1999Nak, 2002Bab]. [1975Uhr, 1977Uhr, 1978Uhr, 1980Uhr] used a regular solution model for the description of the free energies of ferrite, austenite and carbides. This model was suggested by [1970Hil] and later extended by [1979Sun, 1980Sun] to describe higher-order systems. Thermodynamic calculations were conducted by means of the computer program Letagroup (pit-mapping) which is based on a generalized least square method. As a result, a number of isothermal sections of the Fe rich part of the system in the temperature range from 600 to 1320°C as well as liquidus surface projection were calculated and compared to the available experimental information. The same regular solution model was also used by [1984Wad] to calculate the partial isothermal section at 1000°C in the Fe rich corner (up to 3.5 at.% W and up to 10 at.% C). [1987Gus, 1990Jan, 1997Sht1, 1997Sht2, 1998Hac, 1999Nak, 2002Bab] used the computer program Thermo-calc to phase equilibria calculate. So, thermodynamic evaluation of the phase equilibria at different temperatures was carried out by [1987Gus] using a magnetic two-sublattice subregular model for the interstitial solution phases, a multi-sublattice model for intermetallic phases and ternary carbides, as well as an ordinary subregular solution model for the liquid phase. As it was indicated earlier, the liquidus surface constitution calculated by [1987Gus] essentially contradict to those accepted by [1980Ake, 1980Uhr, 1988Ray] on the basis of experimental data, mainly due to the different applied versions of the binary systems. At the same time, there is a satisfactory accordance of the proposed by [1987Gus] isothermal sections at the temperatures of 1500, 1400, 1320, 1195 and 1145°C (Figs. 5 to 9 in the present evaluation) and two temperature-composition sections with experimental results. Partial temperature-composition section at 5.5 mass% Fe was calculated by [1990Jan]. Mechanism and kinetics of cementite growth in the C-Fe-W steels were considered in [1997Sht1]. For this purpose, the isothermal section at 700°C in the Fe rich corner was calculated. [1997Sht2, 1999Nak] calculated the isothermal section at 910°C in order to analyze the mechanism of the eutectoid reaction of the $M_{23}C_6$ carbide decomposition during austenitization. Both at 700 and 910°C, the presence of the metastable equilibria was considered.

The temperature-composition section at 6.3 mass% W was calculated by [1998Hac] during examination of a ternary C-Fe-W steel with the purpose of characterizing the carbide morphologies that arise during the diffusional decomposition of austenite. Phase stability at the melting point of a low-alloyed steel (1527°C) was estimated by [2002Bab].

A review of the literature data originating from computer calculations of phase equilibria in the iron-containing binary and ternary systems, including C-Fe-W, published up to the 1980, was presented in [1981Nis]. A review of the publications in the field of computer thermodynamics as applied to the diffusion transformations in multicomponent systems, in particular, the C-Fe-W system, was presented by [2001Sht]. The methods of the driving forces determination for the diffusion of carbon and alloying elements upon phase transformations by finding the thermodynamic activity of all moving interfaces with the help of the

DOI: 10.1007/978-3-540-74196-1_16

isothermal sections construction are described. This approach allows one to qualitatively understand the mechanism and kinetics of solid phase transformations without rigorously solving the diffusion equation.

Notes on Materials Properties and Applications

Among the common alloy elements added to steels, tungsten as the chromium group element plays a unique and important role, not only because this is a main alloying element in tool and heat-resistance steels but also because of the complex constitution exhibited by steels containing this element. Tungsten as the transition element on the left side of the chromium group of elements in the Periodic Table has such a high affinity for carbon that it forms with carbon the NaCl type carbide [1953Kuo] (labelled as κ in Table 2). Only when there is carbon in excess after the formation of the NaCl type carbide, cementite will be present in steels, and this fact influences positively on their properties. The M_6C ternary carbide (τ_1, W_3Fe_3C phase) also plays an important role in high speed steels, hot working tool steels and superalloys. Although the typical hot hardness of high speed steels is caused by other carbides in fine precipitation [1953Kuo], the M_6C carbide and its distribution is important for cold wear resistance, toughness and grindability. It constitutes the coarse carbide particles occurring in hardened tool steels. The applied experimental techniques and investigated types of properties of the C-Fe-W alloys are summarized in Table 4. In particular, data about magnetic properties were reported widely by [1918Hon, 1922Oza, 1930Tak1, 1930Tak2, 1947Hul, 1957Sat, 1968Jel, 1983Bus]. In the study of transformations in tungsten steels [1918Hon, 1922Oza, 1930Tak1, 1930Tak2] made measurements of magnetization intensity at different temperatures for the Fe rich alloys. It was concluded by [1930Tak1, 1930Tak2] that in the annealed Fe rich C-Fe-W specimens the magnetic changes of ferromagnetic carbide usually take place in two steps: at about 200 and 400°C. These critical points, however, are variable between 0 and 400°C according to the compositions of the alloys and to the mode of the applied heat treatment (annealing, quenching and tempering). It was concluded that the critical point of the θ, Fe_3C phase depends on the concentration of tungsten and iron in this phase. Namely, tungsten lowers the critical point down to 200°C while iron raises it up to 200°C. [1947Hul] established that the θ and τ_4, $W_2Fe_{21}C_6$ phases are ferromagnetic at lower temperatures, whereas the τ_1 phase is not. [1957Sat] determined magnetic intensities and Curie temperatures for the carbides isolated from tungsten steels, isothermally transformed at 700°C, in particular, for the θ and τ_4 phases. [1983Bus] presented the values of the Curie temperature, saturation moment at 4.2 K, saturation magnetization at 300 K as well as Kerr rotation at two different wavelengths (633 and 830 nm) obtained on the τ_4 phase-based alloy annealed at 800°C. The results of dilatometric investigations were reported by [1929Zie, 1930Tak2].
Information concerned mechanical properties of the C-Fe-W alloys is presented in [1929Zie, 1968Jel, 1976Lyu1, 1976Lyu2, 1977Ber, 1983Kwo, 1998Tri, 1999Xu, 2000Kir, 2002Hac1]. According to the data of [1977Ber], microhardness of the τ_1 phase is generally higher than that of the τ_2 phase. A study on the phenomenon of tempered martensite embrittlement (TME) has been made by [1983Kwo] in experimental C-Fe-W steel containing 0.23 and 5.85 mass% of carbon and tungsten, respectively. The represented TME was correlated with the formation of the interlath cementite, resulting from the decomposition of interlath retained austenite. TME occurred in a limited range of test temperatures where the interlath cementite could act as a source of embrittling cracks. [1999Xu] obtained the iron matrix composites with tungsten carbide particle using the Expendal Pattern Casting with dry sand Vacuum (EPC-V) process. It was determined that these composites possess high hardness, and the abrasive wear resistance of them is higher than that of high chromium cast iron. [1976Lyu1] have analyzed the influence of dispersivity of particles, pressure and temperature of pressing on the parameters of producible resistors using, in particular, tungsten steels. A mathematical model of the heat transfer during rapid cooling and solidification of undercooled hypereutectic C-Fe-W alloy droplets was used by [1997Beh] to explain morphological differences in the rapidly solidified particles assuming Newtonian conditions and solidification of the spherical droplet started from multiple nucleation events randomly distributed inside the droplet. The thermophysical properties and boundary conditions are supposed to be temperature dependent and different for the liquid and solid phases.

Miscellaneous

Wettability of the refractory carbide WC by the molten iron was investigated by [1966Yas] using the resting drop technique described by [1958Ere]. This type of wettability was characterized by the contact angle

DOI: 10.1007/978-3-540-74196-1_16

formed by tangent to drop in the point of its contact with solid surface. In the environment of the experiment it was established that the contact angle was 0°, *i.e.* molten iron actively interacted with WC and wetted its surface well. During this process migration of iron atoms into the WC compound took place. The eutectic A (austenite) + $(W,Fe)_6C$ in high-speed steels was studied by [1972Tar]. In these steels the eutectic transformation L (liquid) A + $(W,Fe)_6C$ is the final step in solidification. It was shown that the form of the eutectic colonies and their internal structure are masked by the previously formed austenite.

[1982Dra] used the published theoretical treatments with a view to analyze the characteristics of grain-boundary segregation of various impurities in the binary and ternary alloys based on refractory VIA group metals. Calculations were made of the binding energy of impurities to grain boundaries, of the segregation isotherms in the case of interaction between atoms of different impurities as well as of the influence of the alloys cooling rate on the segregation process at boundaries. The examples of the C-Fe-W system comparing with those of the C-W-Zr system are used to demonstrate the influence of the different nature of chemical interaction between an impurity and the alloying element on the degree of segregation in refractory metals. The oxidation behavior of the C-Fe-W alloys with tungsten content of 5 mass% and carbon content of 0.1, 0.4, 0.8 or 1.2 mass% was studied by [1985Mal] and [1989Mal] at 1.013 bar pressure of oxygen in the temperature ranges of 600-850°C or 700-850°C, respectively. The samples were used for high temperature oxidation and hot corrosion investigations. The alloys exhibited a parabolic rate law during oxidation, at the same time the oxidation rate increased with increasing carbon content. The carbon provides a carbide network which gives a convenient route for the internal penetration of salt into the alloy. It was concluded that the C-Fe-W alloys are resistant to plain oxidation as well as to hot corrosion. The effect of microdoping with iron (up to 3 at.%) on the enrichment with impurities in the intergrain and intragrain parts of the break in alloys of tungsten fractured under high-vacuum conditions was investigated by [1990Dra] using Auger-electron spectroscopy. It was shown that as the mean content of iron in alloy increased, the concentration of carbon and oxygen on the intergrain surfaces decreased monotonically, while at the intergrain regions it did not change. The correlation in the change of the chemical composition of the fracture surface and the temperature of the brittle-viscous transition was pointed out.

A model C-Fe-W steel was used by [1992Sah] to study the effect of the precipitation of carbides at austenite grain surfaces, on the subsequent formation of allotriomorphic ferrite. It was found that the removal of potential austenite grain boundary nucleation sites by the precipitation of carbides retarded the allotriomorphic ferrite transformation. This effect was found to be most pronounced at small undercoolings below the equilibrium transformation temperature. Diffusion interaction of carbides with iron and tungsten steel was studied by [1995Pop, 1999Pop]. It is concluded that coefficients of mutual diffusion of metallic elements in austenite almost do not depend on the concentration of carbide-forming element and depend weakly on the content of carbon in steel. Analytical expressions describing concentration and temperature dependences of mutual diffusion coefficients of the substituting elements in ferrite are obtained by [1995Pop]. Rates of tungsten diffusion between high speed steel powders and iron powders in the presence of additional carbon have been measured by [2001Mar]. It was shown that the original size of the extra carbon is important and that maximum diffusion rates occur when there is about 1 mass% extra carbon on the iron side of the diffusion interfaces. The fractal of metallographic structure for the original WC and electroslag remelted (ESR) WC in ferrite-cemented tungsten carbide was studied by [2001Ska] in terms of "Sierpinski carpet" of fractal theory applied to this kind of material. Calculation of the kinetics of microstructural evolution in the laser surface alloying (LSA) process, at the same time with experimental phase-stability solidification, was carried out. A rapid dissolution of tungsten carbide particles in Fe rich liquid, as compared with the dissolution rate in Ni rich liquid, was shown. Optical microscopy indicated a heterogeneous microstructure around the tungsten particles that is in agreement with concentration gradients predicted by kinetic calculations. Degenerate ferrite grown below the bay in the Fe-0.3C-6.3W (mass%) (Fe-1.44C-1.98W in at.%) alloy was serially sectioned and reconstructed in a computer by [2002Hac2] with a view to examine its three-dimensional (3D) structure. The 3D reconstruction revealed the true shape, orientation and connectivity of ferrite subunits, highlighting the misleading appearance that two-dimensional (2D) sections can sometimes give.

DOI: 10.1007/978-3-540-74196-1_16

Table 1. Investigations of the C-Fe-W Phase Relations, Structures and Thermodynamics

Reference	Method / Experimental Technique	Temperature / Composition / Phase Range Studied
[1918Hon]	Optical microscopy	< 7 at.% C, < 8 at.% W
[1920Hul1]	Optical microscopy, X-ray diffraction, thermal analysis	Fe-W-WC-Fe_3C partial system
[1921Dae]	Optical microscopy, thermal analysis, chemical analysis	≤ 1500°C, < 7.5 at.% C, < 4.5 at.% W
[1921Hul]	Optical microscopy, thermal analysis	Fe-W-WC-Fe_3C partial system
[1922Oza]	Chemical analysis, thermal analysis, optical microscopy	< 1500°C, < 19 at.% C, < 17 at.% W
[1924Obe]	Optical microscopy, thermal analysis	1100°C, < 7.5 at.% C, < 5 at.% W
[1927Wes]	X-ray Laue powder diffractometry	~ W_2Fe_4C
[1928Wes]	X-ray diffraction studies (Laue, rotation techniques), optical microscopy, chemical analysis	W_2Fe_4C phase containing alloys
[1929Zie]	Arc melting, optical microscopy, X-ray diffraction	< 11 at.% C, < 17 at.% W
[1930Tak1]	Electrolytic extraction, optical microscopy, X-ray diffraction	< 50 at.% W
[1930Tak2]	Tamman furnace melting, optical microscopy	< 1500°C, < 6.5 at.% C, < 6 at.% W
[1931Tak]	Tamman furnace melting, thermal analysis, optical microscopy	< 4.0 mass% C, < 80 mass% W
[1933Mor]	X-ray diffraction, chemical analysis	0-50 at.% C
[1943Smo]	Diffusion rate determination	1000°C, ≤ 4.2 at.% C, ≤ 1.1 at.% W
[1947Hul]	Electrolytic extraction, optical microscopy, X-ray diffraction	≤ 1340°C, Fe rich corner
[1950Kra]	X-ray diffraction	1050°C, 720°C, ~$W_{5.8}Fe_{92.3}C_{1.9}$ - ~$W_{2.8}Fe_{86.4}C_{10.8}$ (at.%)
[1951Uma]	Induction melting, sintering, X-ray diffraction, pycnometry	≤ 1800°C, ≤ 34 at.% C
[1952Edw]	Induction melting, optical microscopy, X-ray diffraction	1250°C, Fe - (5 - 30) mass% WC
[1952Kuo] [1953Kuo]	Electrolytic extraction, X-ray diffraction (Guinier technique)	700°C, ≤ 9.56 mass% W, ≤ 0.32 mass% C
[1957Sat]	Electrolytic extraction, X-ray diffraction, chemical analysis	700°C, ≤ 27.4 mass% W, ≤ 1.13 mass% C

(*continued*)

DOI: 10.1007/978-3-540-74196-1_16

Reference	Method / Experimental Technique	Temperature / Composition / Phase Range Studied
[1959Fuw]	Equilibration of alloys with controlled mixtures of CO and CO_2	ε_C^W in liquid phase, 1560°C, < 30 at.% W
[1960Fuw]	Determination of the carbon solubility in liquid iron	1450°C; 6.07-14.48 mass% W, 4.62-5.01 mass% C
[1960Mor]	Determination of the activity coefficient of carbon in multicomponent solution	1550°C, Fe rich corner
[1964Lec]	Neutron diffraction	W_6Fe_6C
[1965Kri]	Determination of the activity coefficient of carbon	1150°C, 950°C, < 11.6 mass% W
[1966Gob]	Thermal analysis, optical microscopy	700-1500°C, ≤ 20 mass% W, ≤ 2 mass% C
[1967Boj]	Sintering, neutron diffraction	W_3Fe_3C, W_6Fe_6C
[1968Jel]	Sintering, arc melting, thermal analysis, X-ray diffraction, optical microscopy, density measurements	Fe- Fe_3C-WC-W partial system
[1970Pol]	Sintering, arc melting, optical microscopy, X-ray diffraction	1000°C, Fe- Fe_3C-WC-W partial system
[1971Gre]	Induction melting, Woesthoff conductimetric instrument measurements, equilibration of alloys in recirculated CH_4-H_2 atmosphere	1125°C, 1050°C, $\varepsilon_C^W = f$ (T), 0.125 to 0.445 mass% C, ≤ 5.86 mass% W
[1973Rim]	Thermal analysis, optical microscopy, X-ray diffraction	1500°C, 1450°C, 1350°C, surface of primary crystallization of graphite
[1975Uhr]	Melting, capsule technique of carburization, SEM, chemical analysis, Pt-Pt10%Rh thermocouples temperature measurements, conventional etching technique, X-ray powder diffractometry, microprobe analysis	1000°C, Fe rich corner
[1976Lyu1]	Electrolytic extraction, X-ray diffraction, optical microscopy	1000-1800°C, W_3Fe_3C
[1976Lyu2]	X-ray diffraction, optical microscopy, chemical analysis	1000°C, 1200°C, 1400°C, W_3Fe_3C
[1976Niz]	Induction melting technique, annealing, optical microscopy, X-ray diffraction, microprobe analysis	950-1250°C, Fe rich corner
[1976Sna]	Induction melting, optical microscopy, X-ray diffraction	≤ 4.3 mass% C, ≤ 28 mass% W
[1977Ber]	Sintering, hot pressing, arc melting, optical microscopy, X-ray diffraction	1250°C, the Fe-WC-W partial system

(*continued*)

DOI: 10.1007/978-3-540-74196-1_16

Reference	Method / Experimental Technique	Temperature / Composition / Phase Range Studied
	(Guinier-Haegg camera), EMPA, coulometric titration	
[1980Ake]	Optical microscopy, EMPA	1195°C, 1145°C, ≤ 4.6 mass% C, ≤ 20 mass% W
[1980Iwa]	Rapid quenching from melts, X-ray diffraction, TEM	~$W_{10\text{-}14}Fe_{66\text{-}72}C_{18\text{-}20}$ (at.%)
[1981Ino]	Rapid quenching from melts, X-ray diffraction, TEM	~$W_{10\text{-}14}Fe_{66\text{-}72}C_{18\text{-}20}$ (at.%)
[1981She]	Induction melting, chemical analysis, annealing, thermal analysis, X-ray diffraction	≤ 7 mass% C, ≤ 40 mass% W
[1982Hor]	Rapid cooling of liquids, optical microscopy, electron microscopy, electron diffraction	$W_{11}Fe_{67\text{-}69}C_{20\text{-}22}$ (at.%)
[1982Lug]	High-temperature X-ray powder diffraction, DTA	τ_1 and τ_2 phases containing regions
[1983Bus]	Arc melting, vacuum annealing, X-ray diffraction	$W_2Fe_{21}C_6$
[1983Haa]	Annealing, X-ray powder diffraction, neutron powder diffraction, chemical analysis	$W_{9.43}Fe_{3.57}C_{3.54}$
[1983Jer]	Annealing, Mössbauer spectroscopy	$W_{9.43}Fe_{3.57}C_{3.54}$
[1985Gab]	Electromagnetic phase decantation, DTA, chemical analysis, EMPA, optical microscopy	Fe- Fe_3C-WC-W partial system
[1992Azu]	Annealing with quenching, X-ray diffraction, chemical analysis	1200°C, the τ_1 single phase region
[1994Tri]	Magnetron sputtering, X-ray diffraction, EMPA, secondary ion mass spectroscopy	Metastable C-Fe-W films
[1995Tri]	Magnetron sputtering, hot stage TEM, DTA, X-ray diffraction	< ~950°C, amorphous $W_{46}Fe_{13}C_{41}$ and $W_{36}Fe_{31}C_{33}$ films
[1997Sht1]	Induction melting, annealing, quenching, TEM, X-ray diffraction, energy-dispersive spectrometry	700°C, ≤ 0.85 mass% C, ≤ 2.5 mass% W
[1997Sht2]	Induction melting, annealing, quenching, TEM, X-ray diffraction, energy-dispersive spectrometry	700-1400°C, ≤ 0.8 mass% C, ≤ 2.5 mass% W

(*continued*)

DOI: 10.1007/978-3-540-74196-1_16

Reference	Method / Experimental Technique	Temperature / Composition / Phase Range Studied
[1998Hac]	Arc melting, annealing, optical microscopy, SEM, TEM	1200°C, 660-960°C, $W_{6.3}Fe_{93.5}C_{0.2}$ (mass%) ($W_{1.98}Fe_{97.05}C_{0.97}$ in at.%)
[1998Tri]	Magnetron sputtering, X-ray diffraction, laser interferometry	Iron-doped WC_{1-x} thin films
[2002Bab]	Laser surface alloying (LSA), optical pyrometry and microscopy	Fe rich corner
[2002Hac1]	Induction melting, annealing, rapid water quenching, chemical analysis, etching (nital), optical microscopy, TEM, selected-area diffraction (SAD), field-emission gun-transmission electron microscopy (FEG-TEM), energy-dispersive X-ray spectroscopy (EDS)	$W_{6.3}Fe_{93.4}C_{0.3}$ (mass%) ($W_{1.98}Fe_{96.58}C_{1.44}$ in at.%)

Table 2. Crystallographic Data of Solid Phases

Phase/ Temperature Range [°C]	Pearson Symbol/ Space Group/ Prototype	Lattice Parameters [pm]	Comments/References
(C)gr < 3827	*hP*4 $P6_3/mmc$ C (graphite)	a = 246.12 c = 670.90	at 25°C [Mas2] sublimation point
(C)d	*cF*8 $Fd\bar{3}m$ C (diamond)	a = 356.69	at 25°C, 60.78 kbar [Mas2] high-pressure modification
(W), $W_{1-x-y}Fe_xC_y$ < 3422	*cI*2 $Im\bar{3}m$ W	a = 316.52	at 25°C [Mas2] $x = 0, 0 < y \lesssim 0.007$, 2710°C [1991Nag] $y = 0, 0 < x \lesssim 0.026$, 1637°C [Mas2]
(αδFe), $W_xFe_{1-x-y}C_y$	*cI*2 $Im\bar{3}m$ W		$y = 0, 0 < x \leq 0.143$, 1548°C [Mas2] $x = 0, 0 < y \leq 0.004$, 1493°C [Mas2, 2006MSIT]
(δFe), $W_xFe_{1-x-y}C_y$ 1538 - 1394		a = 293.15	$x = 0, y = 0$ [Mas2] $y = 0, T < 1548$°C [Mas2] critical point at $x = 0.044, y = 0$, 1529°C [Mas2]
(αFe) (ferrite), $W_xFe_{1-x-y}C_y$ < 912		a = 286.65	$x = 0, y = 0$, 25°C [Mas2] $x = 0, 0 < y \leq 0.00096$, 740°C [Mas2, 2006MSIT]

(*continued*)

DOI: 10.1007/978-3-540-74196-1_16

Phase/ Temperature Range [°C]	Pearson Symbol/ Space Group/ Prototype	Lattice Parameters [pm]	Comments/References
(γFe) (austenite), $W_xFe_{1-x-y}C_y$ 1394 - 912	*cF*4 *Fm*$\bar{3}$*m* Cu	*a* = 364.67	*x* = 0, *y* = 0, 915°C [V-C2, Mas2]
			x = 0, 740°C ≤ *T* ≤ 1493°C [Mas2, 2006MSIT]
			x = 0, 0 < *y* ≤ 0.0906, 1153°C [Mas2, 2006MSIT]
			y = 0, 0 < *x* ≤ 0.0146 [Mas2]
		a = 363.38	*x* = 0, *y* = 0.0818 [1992Oka]
(εFe) ≥ $1.3 \cdot 10^5$ bar	*hP*2 *P*6_3/*mmc* Mg	*a* = 246.8 *c* = 396.0	at 25°C, $1.3 \cdot 10^5$ bar [Mas2]
			high-pressure modification
α, martensite	*tI*4 *I*4/*mmm* α, martensite		metastable, 0 to 9 at.% C [Mas2]
		a = 285.8 *c* = 293.5	2.69 at.% C [1992Oka]
		a = 284.6 *c* = 301.1	6.36 at.% C [1992Oka]
θ, Fe_3C (cementite)	*oP*16 *Pnma* Fe_3C		metastable phase
		a = 507.87 *b* = 672.97 *c* = 451.44	25 at.% C [V-C2]
		a = 507.9 *b* = 673.0 *c* = 451.4	heat treated at 700°C for a long time [1953Kuo]
			dissolves < 1 mass% W at 700°C [1953Kuo]
			dissolves < 1.3 mass% W at 1000°C [1957Sat]
γW_2C 2776 - 2490	*hP*3 *P*6_3/*mmc* Fe_2N		25.6 to 34.5 at.% C [1991Nag]
		a = 300.0 *c* = 473.0	at 32.8 at.% C [1966Rud, 1991Nag]
		a = 298.5 *c* = 471.6	at 29.5 at.% C [1973Rud, 1991Nag]
βW_2C < 2490	*oP*12 *Pbcn* $PbCl_2$		29.6 to 32.7 at.% C [1991Nag]
		a = 472.8 *b* = 600.9 *c* = 519.3	at 2350°C [1973Rud, 1991Nag]
		a = 472.0 *b* = 601.6 *c* = 518.0	at 30.5 at.% C, 850°C [2000Kub]
αW_2C ~2100 - 1250	*hP*3 *P*$\bar{3}$*m*1 αW_2C	-	29.6 to 32.5 at.% C [1969Rud, 1991Nag]

(*continued*)

DOI: 10.1007/978-3-540-74196-1_16

Phase/ Temperature Range [°C]	Pearson Symbol/ Space Group/ Prototype	Lattice Parameters [pm]	Comments/References
κ, WC_{1-x}	*cF*8		37.5 to 39.5 at.% C at
2747 - 2530	$Fm\bar{3}m$		2720°C [1991Nag]
	NaCl	a = 433.6	[V-C2]
		a = 422.0	at 38 at.% C [1966Rud, 1991Nag]
γ, WC	*hP*2	a = 290.63	50 at.% C [V-C2]
< 2776	$P\bar{6}m2$	c = 283.67	
	WC	a = 290.3	at 700°C; carbide extracted from
		c = 283.2	tungsten steel [1953Kuo]
			dissolves ~ 1 at.% Fe at 1250°C [1977Ber]
δ, WFe	*oP*56		47 to 51.5 at.% Fe [Mas2]
1215 - <400	$P2_12_12_1$	a = 776	at 49.3 at.% Fe [1986Nag]
	MoNi	b = 1248	
		c = 710	
μ, W_6Fe_7	*hR*39		~56 to 59.5 at.% Fe [Mas2]
1637 - 1190	$R\bar{3}m$		
	W_6Fe_7	a = 477.1	in the W rich alloys [1986Nag]
		c = 2596	
		a = 475.5	in the Fe rich alloys [1986Nag]
		c = 2583	
λ, WFe_2	*hP*12		66.7 at.% Fe [Mas2]
≲ 1060	$P6_3/mmc$	a = 473.7	[1986Nag]
	$MgZn_2$	c = 770.0	
* τ_1, W_3Fe_3C	*cF*112	a = 1104	corresponds to the W_2Fe_4C
< 1668	$Fd\bar{3}m$		composition [1927Wes, 1928Wes]
	W_3Fe_3C		[1951Uma]
		a = 1105.0 to 1112.5	from W_4Fe_2C to W_2Fe_4C compositions at 700°C [1952Kuo]
		a = 1108.7	at 1300°C [1967Boj]
			from $W_{2.5}Fe_{3.5}C$ to W_3Fe_3C compositions [1968Jel]
		a = 1100.2 to 1114.6	at 1000°C [1970Pol]
		a = 1105.5 to 1107.8	at 1000°C to 1400°C [1976Lyu1]
		a = 1109.8	at 1400°C [1976Lyu2]
		a = 1106.5 to 1112	at 1250°C, with increasing of W content [1977Ber]
		a = 1109.0 to 1115.6	with increasing of W content, room temperature
		a = 1110.94 to 1115.5	[1982Lug]
			at 1200°C, W_3Fe_3C to W_4Fe_2C [1992Azu]

(*continued*)

DOI: 10.1007/978-3-540-74196-1_16

Phase/ Temperature Range [°C]	Pearson Symbol/ Space Group/ Prototype	Lattice Parameters [pm]	Comments/References
* τ_2, W_6Fe_6C	*cF*96	a = 1093.0	[1951Uma]
≲ 1400	$Fd\bar{3}m$	a = 1093.4	[1964Lec];
	W_6Fe_6C		at 1200°C [1967Boj]
		a = 1095.6 to 1095.8	at 1000°C [1970Pol]
		a = 1096 to 1109	at 25°C to 1200°C [1982Lug]
* τ_3, W_3FeC	*hP**	$a \neq c$ = 780.6 to 781.0	at 1000°C [1970Pol]
≲ 1600	$P6_3/mmc$		
	$W_9Co_3C_4$		
		a = 779.82	$W_{9.43}Fe_{3.57}C_{3.54}$, at 1600°C
		c = 782.98	[1983Haa]
* τ_4, $W_2Fe_{21}C_6$	*cF**		metastable
	$Fm\bar{3}m$	a = 1051	labelled as $(W,Fe)_4C$ [1933Mor]
	$W_2Cr_{21}C_6$		
		a = 1065	$W_{4.82}Fe_{90.36}C_{4.82}$, at 720°C
		a = 1052	[1950Kra]
		a = 1053.3	at 700°C [1953Kuo]
			at 800°C [1983Bus]
* τ_5, WFeC			metastable, at 1100°C [1920Hul1, 1921Hul]
* τ_6, ψ (C-Fe-W)	*cP**		metastable, in ternary alloys (compositions in at.%) rapidly quenched from the melt [1981Ino]:
		a = 892.2	$W_{12}Fe_{78}C_{10}$
		a = 899.6	$W_{12}Fe_{74}C_{14}$
		a = 899.2	$W_8Fe_{74}C_{18}$
		a = 905.3	$W_{12}Fe_{70}C_{18}$
* τ_7, η' (C-Fe-W)	*cF**	a = 1220	in the $W_{11}Fe_{69}C_{20}$ alloy rapidly cooled from liquid and then reheated from ambient temperature [1982Hor]

Table 3. Invariant Equilibria

Reaction	T [°C]	Type	Phase	Composition (at.%)		
				C	Fe	W
Stable equilibria						
L + κ ⇌ γW_2C + γ	?	U_1	-	-	-	-
L + γW_2C ⇌ (W) + γ	?	U_2	-	-	-	-
L + (W) + γ ⇌ τ_1	1668	P	L	15.5	57.1	27.4

(*continued*)

MSIT®
DOI: 10.1007/978-3-540-74196-1_16

Reaction	T [°C]	Type	Phase	Composition (at.%)		
				C	Fe	W
L + (W) ⇌ μ + τ_1	1550	U_3	L	6.9	72.8	20.3
L + μ ⇌ (δFe) + τ_1	1396	U_4	L	6.5	82.1	11.4
L + (δFe) ⇌ (γFe) + τ_1	1371	U_5	L	7.6	82.7	9.7
L + τ_1 ⇌ (γFe) + γ	1291	U_6	L	11.9	81.0	7.1
L ⇌ (C) + γ + (γFe)	1143	E	L	17.5	81.2	1.3
Metastable equilibria						
L + (C) ⇌ γ + θ	?	U_m	-	-	-	-
L ⇌ (γFe) + γ + θ	?	E_m	-	-	-	-

Table 4. Investigations of the C-Fe-W Materials Properties

Reference	Method / Experimental Technique	Type of Property
[1918Hon]	Magnetic measurements (during heating and cooling)	Magnetization
[1922Oza]	Magnetometric method (measurements during heating and cooling)	Magnetization
[1929Zie]	Dilatometry, Brinell hardness measurements	Dilatation, hardness
[1930Tak1]	Magnetometric method (measurements during heating and cooling)	Magnetization
[1930Tak2]	Dilatometry, electric resistance measurements, magnetometric method (measurements during heating and cooling)	Dilatation, electric resistance, magnetization
[1947Hul]	Magnetic measurements (magnetic balance technique)	Curie temperature
[1957Sat]	Thermomagnetic analysis, Rockwell hardness measurements	Magnetic intensity, Curie temperature, hardness
[1968Jel]	Magnetic measurements, Vickers hardness measurements	Magnetization, hardness
[1976Lyu1]	Microhardness measurements	Microhardness
[1977Ber]	Vickers microhardness measurements	Microhardness
[1983Bus]	Kerr effect measurements (HeNe and a solid state GeAs lasers), magnetic measurements (PAR vibrating sample magnetometer)	Curie temperature, magnetization, polar Kerr rotation angle, saturation moment

(*continued*)

DOI: 10.1007/978-3-540-74196-1_16

Reference	Method / Experimental Technique	Type of Property
[1983Kwo]	Charpy impact testing, mechanical tests (on the Instron machine)	Tempered martensite embrittlement (TME), impact toughness, ultimate tensile strength
[1998Tri]	Laser interferometry, ultra-microhardness measurements	Hardness, Young's modulus
[1999Xu]	Hardness measurements	Abrasive wear resistance
[2000Kir]	Davydenkov's technique (described in [1981Dav])	Internal tensile stress
[2002Hac1]	Vickers microhardness measurements	Microhardness

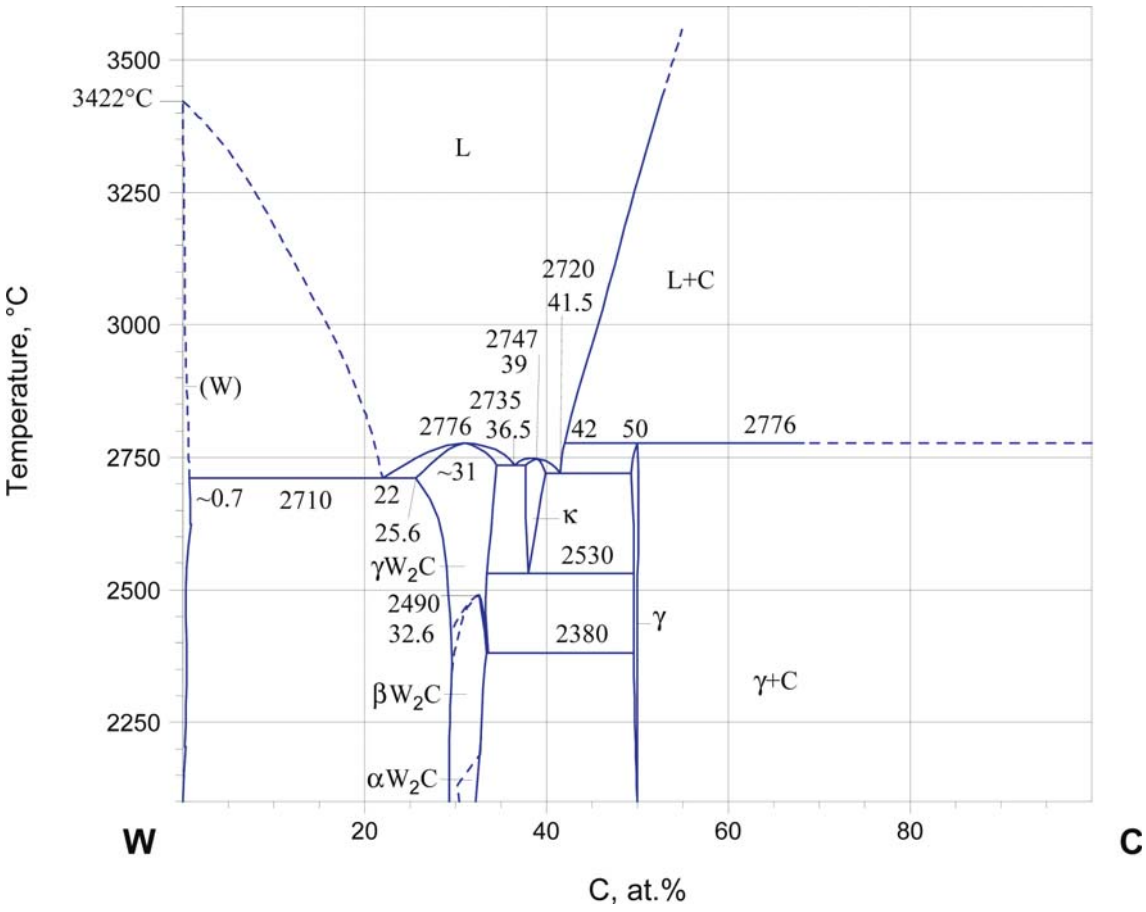

Fig. 1. C-Fe-W. The C-W phase diagram

DOI: 10.1007/978-3-540-74196-1_16

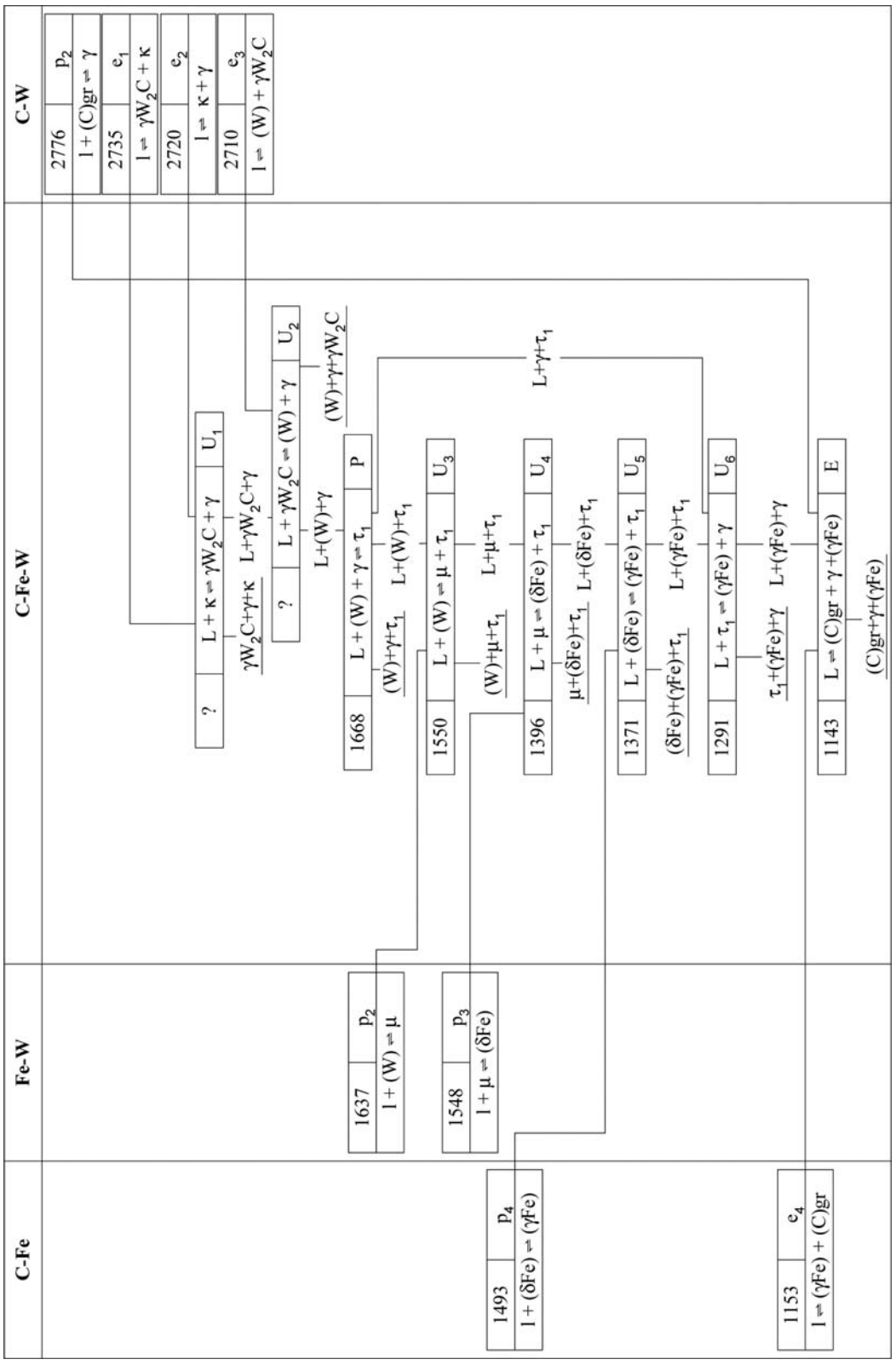

Fig. 2. C-Fe-W. Reaction scheme for stable equilibria

DOI: 10.1007/978-3-540-74196-1_16

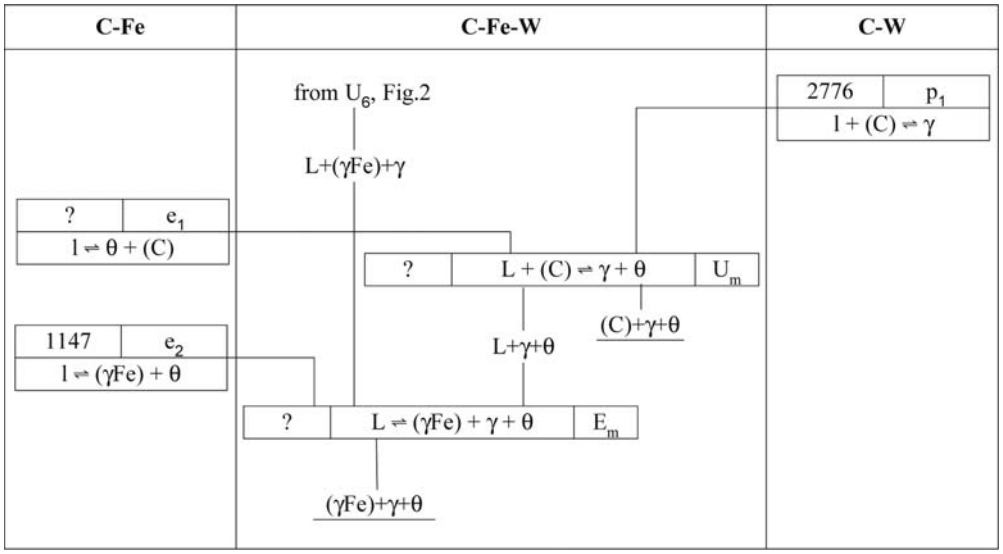

Fig. 3. C-Fe-W. Partial reaction scheme for metastable equilibria

DOI: 10.1007/978-3-540-74196-1_16

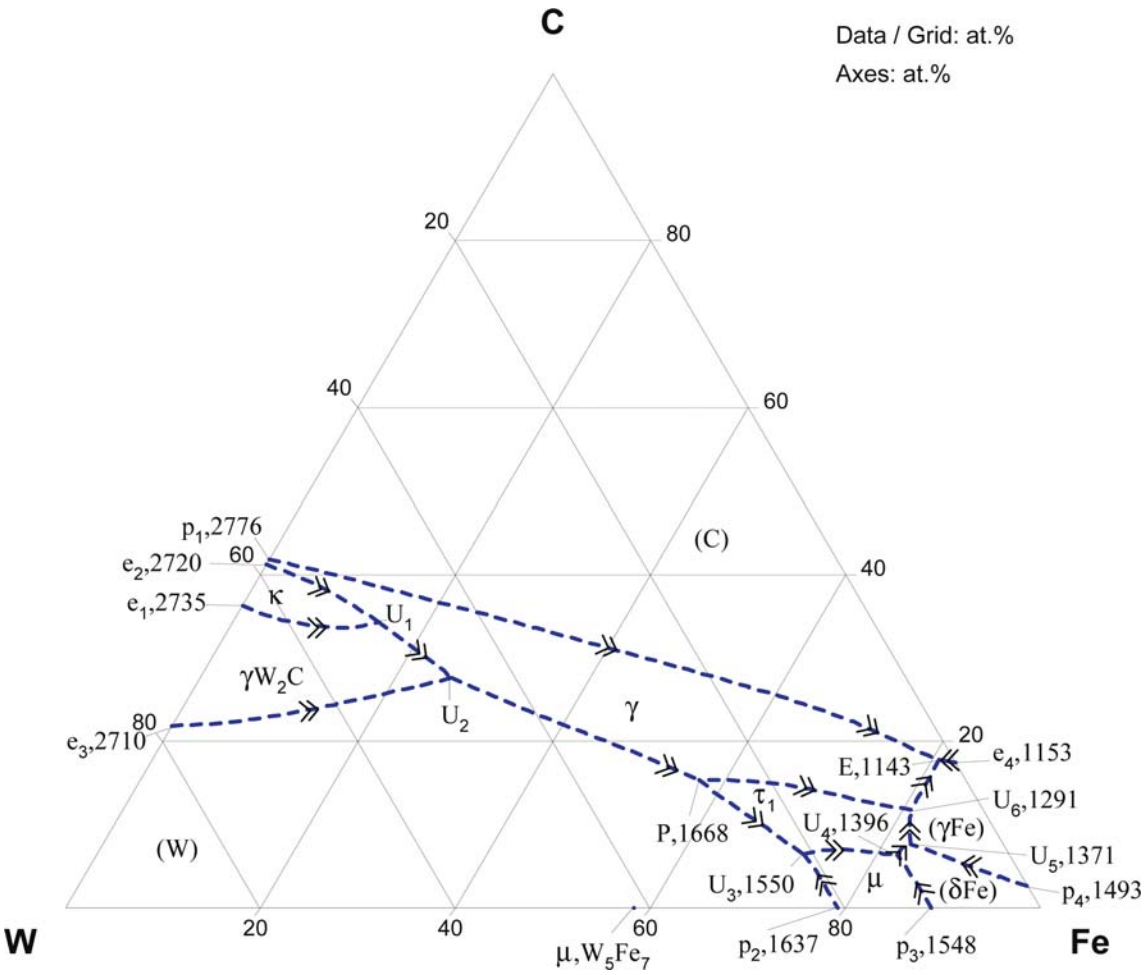

Fig. 4. C-Fe-W. Partial liquidus surface projection. Stable equilibria

DOI: 10.1007/978-3-540-74196-1_16

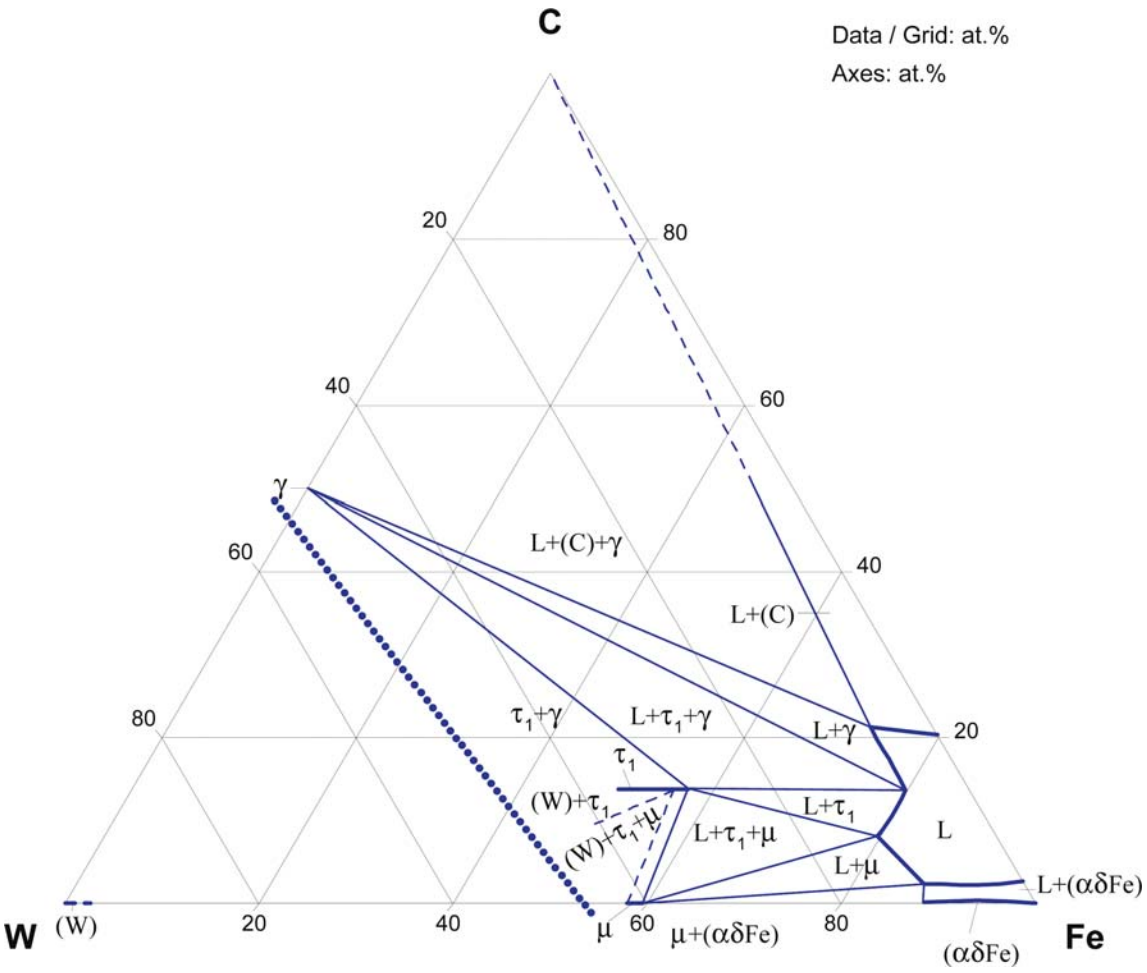

Fig. 5. C-Fe-W. Calculated partial isothermal section at 1500°C

DOI: 10.1007/978-3-540-74196-1_16

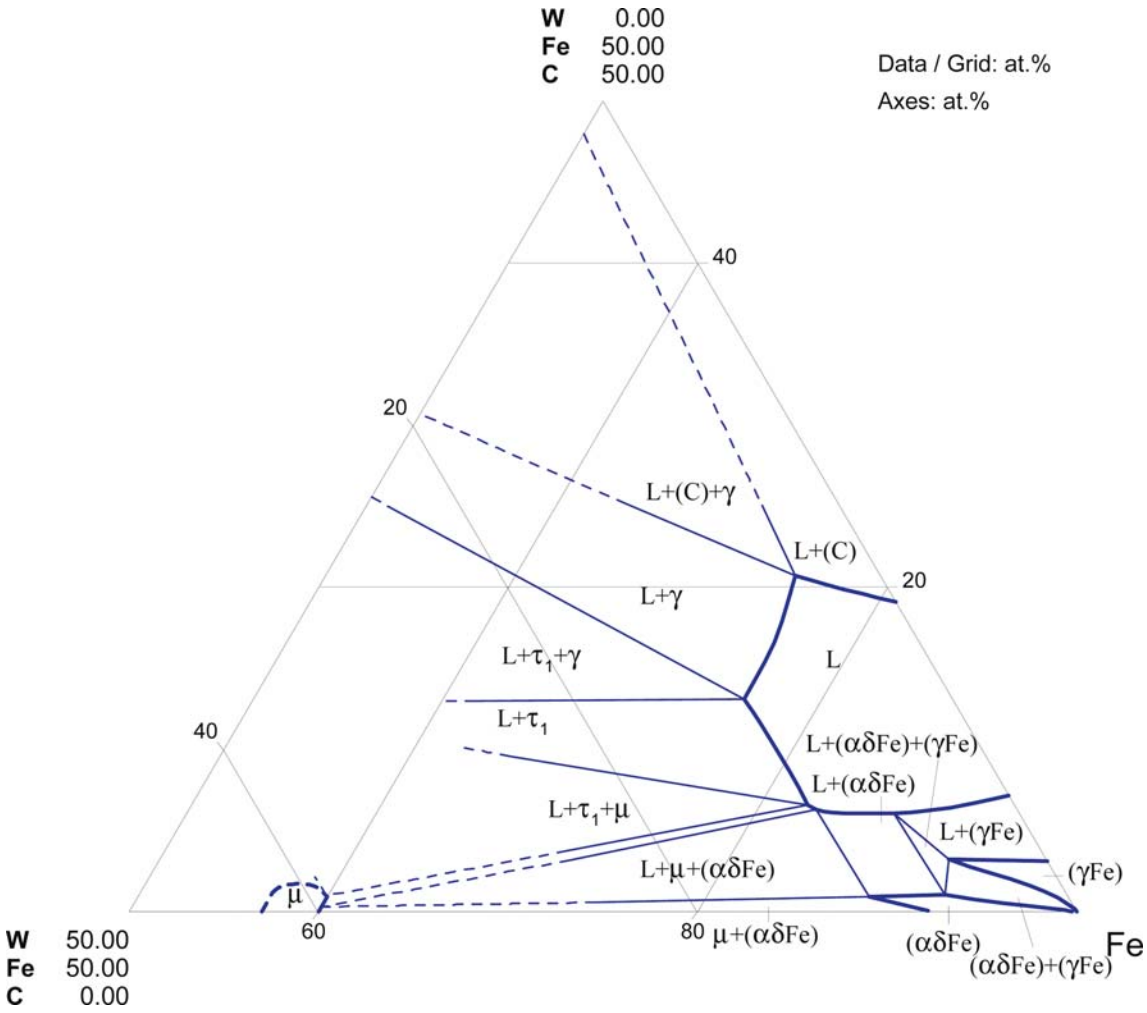

Fig. 6. C-Fe-W. Calculated partial isothermal section at 1400°C

DOI: 10.1007/978-3-540-74196-1_16

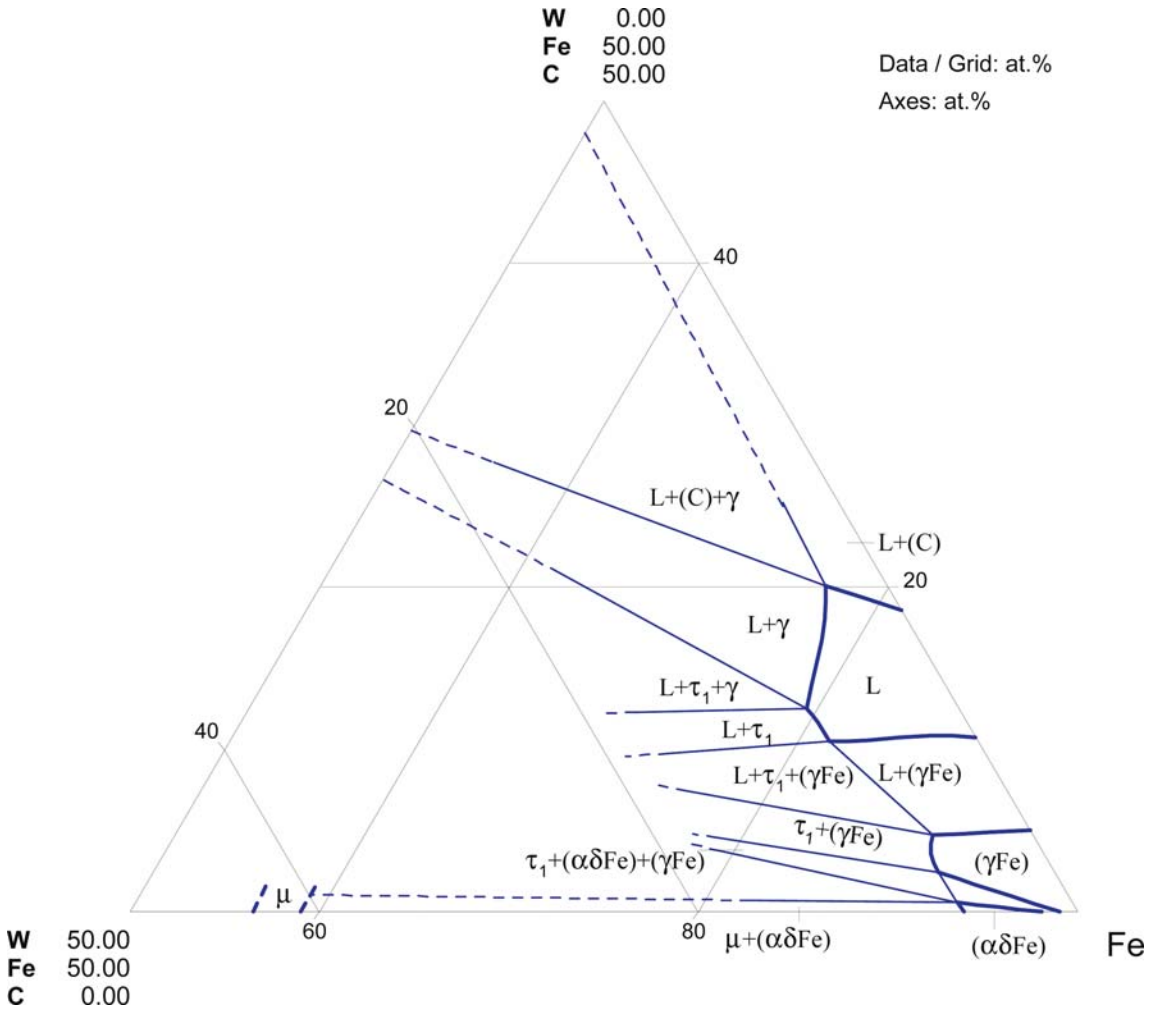

Fig. 7. C-Fe-W. Calculated partial isothermal section at 1320°C

DOI: 10.1007/978-3-540-74196-1_16

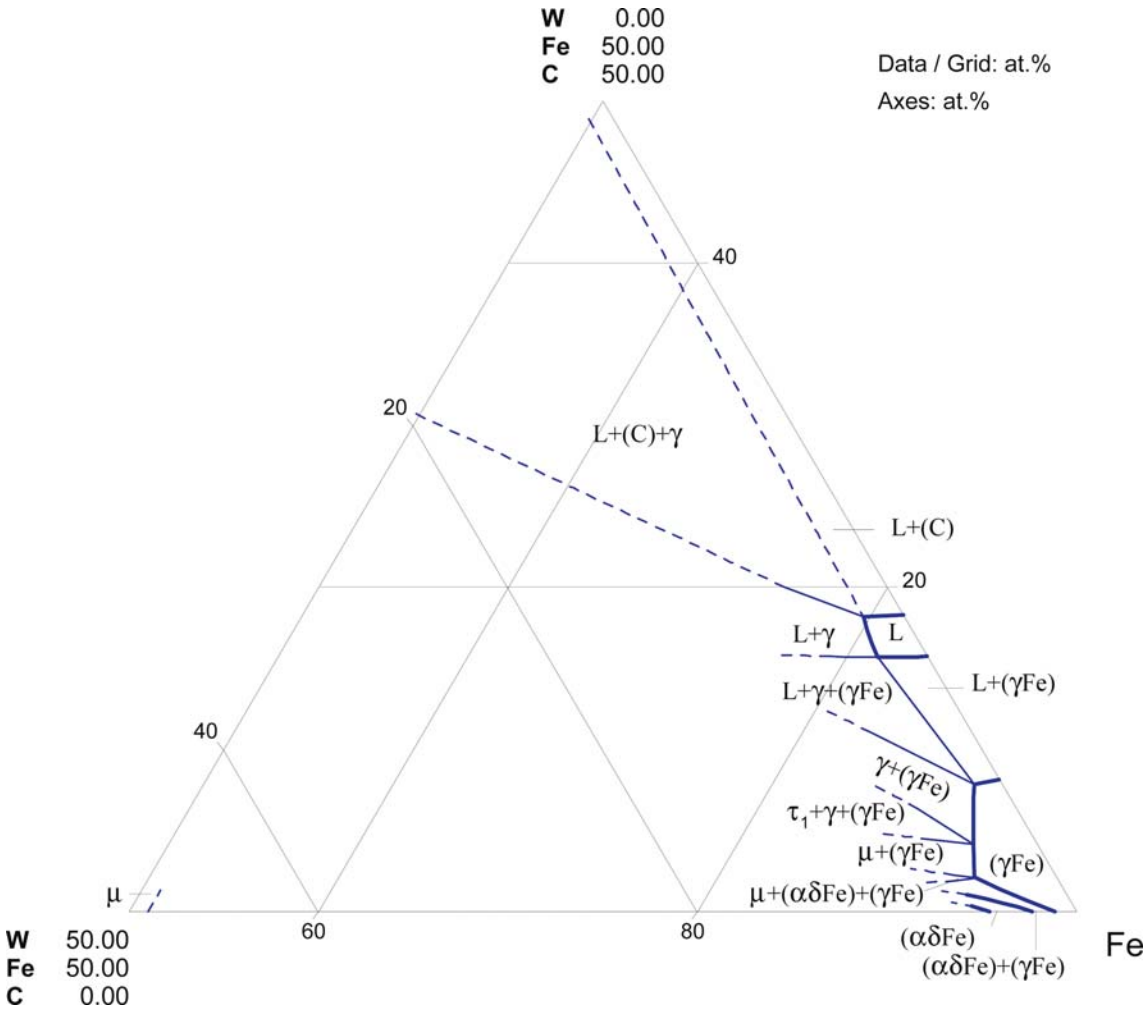

Fig. 8. C-Fe-W. Calculated partial isothermal section at 1195°C

DOI: 10.1007/978-3-540-74196-1_16

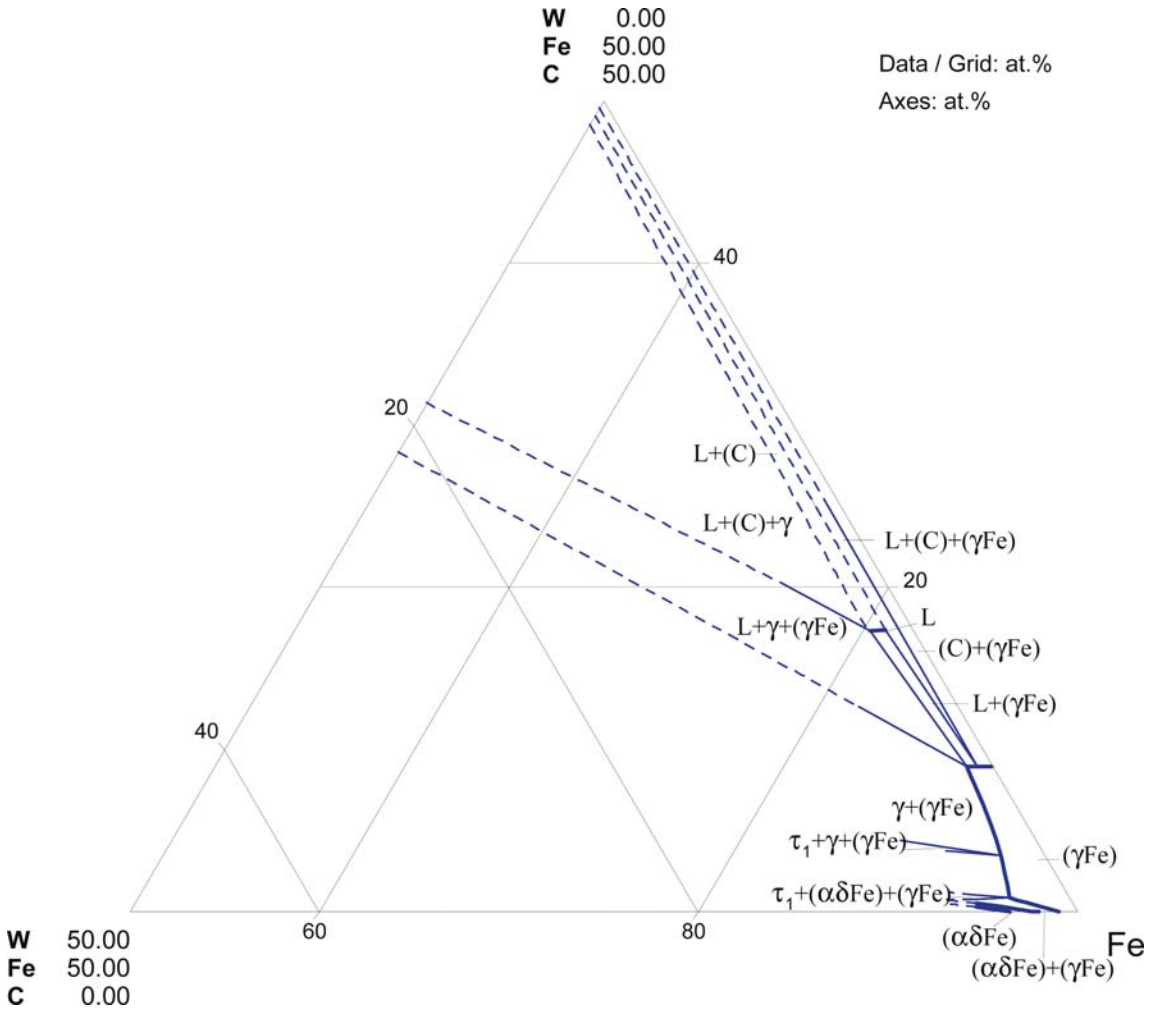

Fig. 9. C-Fe-W. Calculated partial isothermal section at 1145°C

DOI: 10.1007/978-3-540-74196-1_16

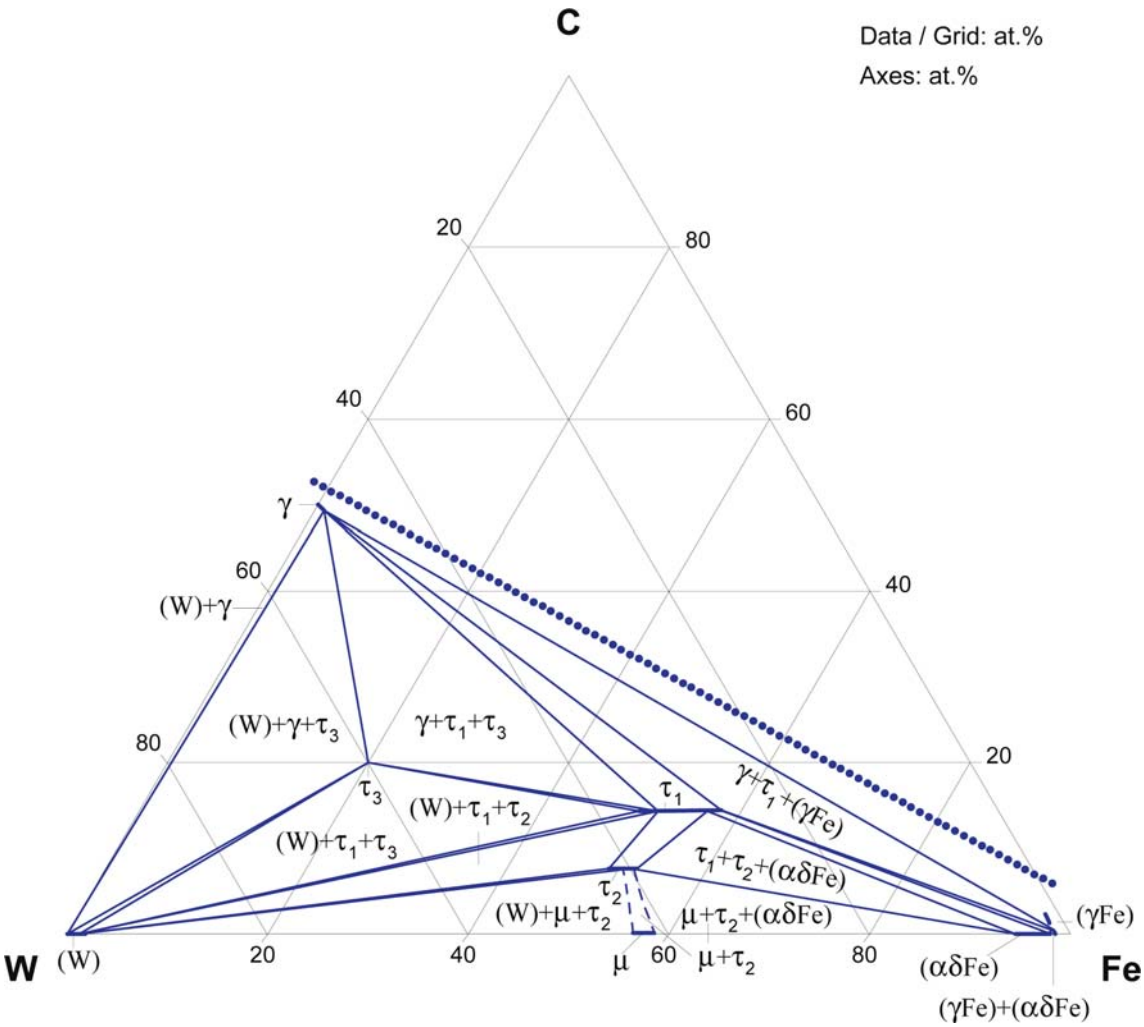

Fig. 10. C-Fe-W. Partial Fe-WC-W isothermal section at 1250°C

DOI: 10.1007/978-3-540-74196-1_16

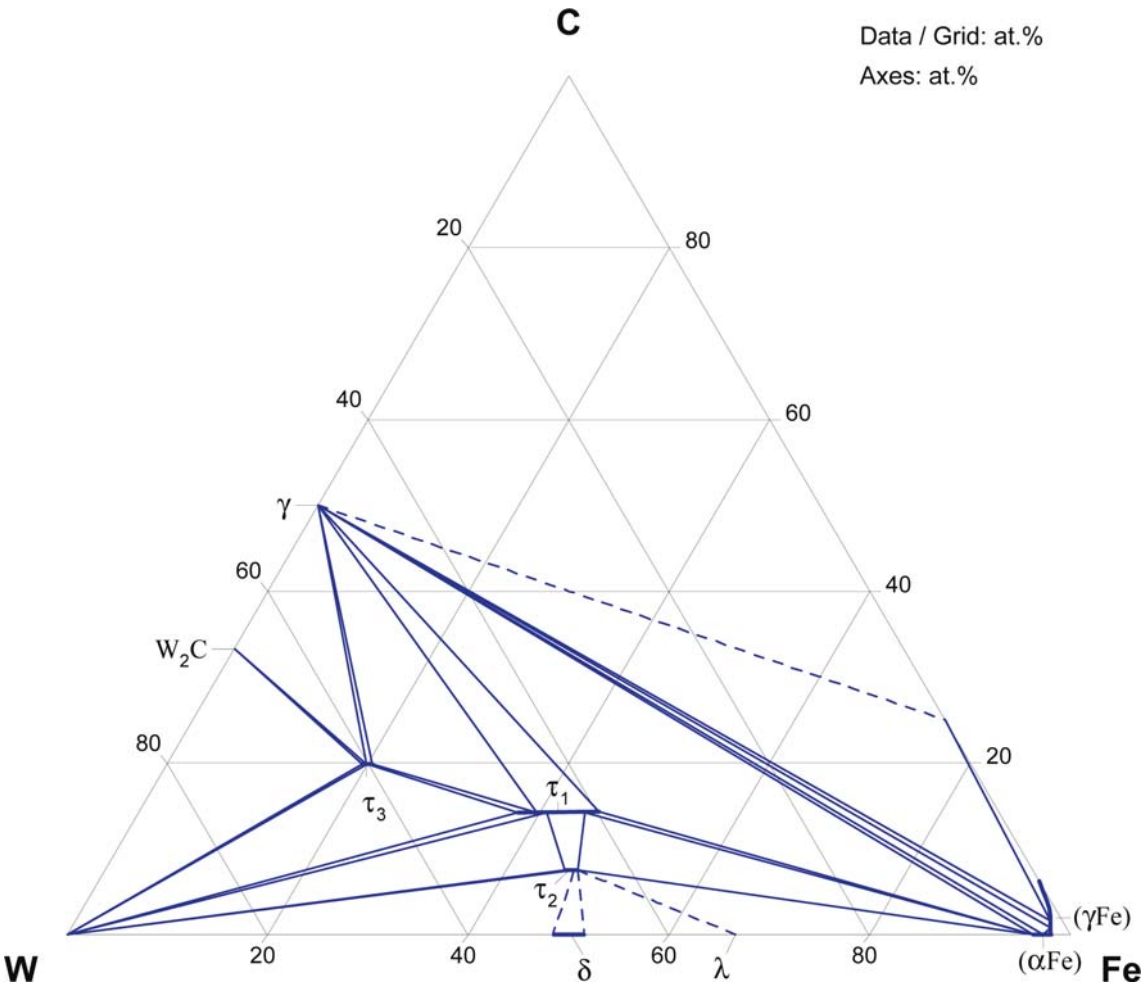

Fig. 11. C-Fe-W. Partial isothermal section at 1000°C

DOI: 10.1007/978-3-540-74196-1_16

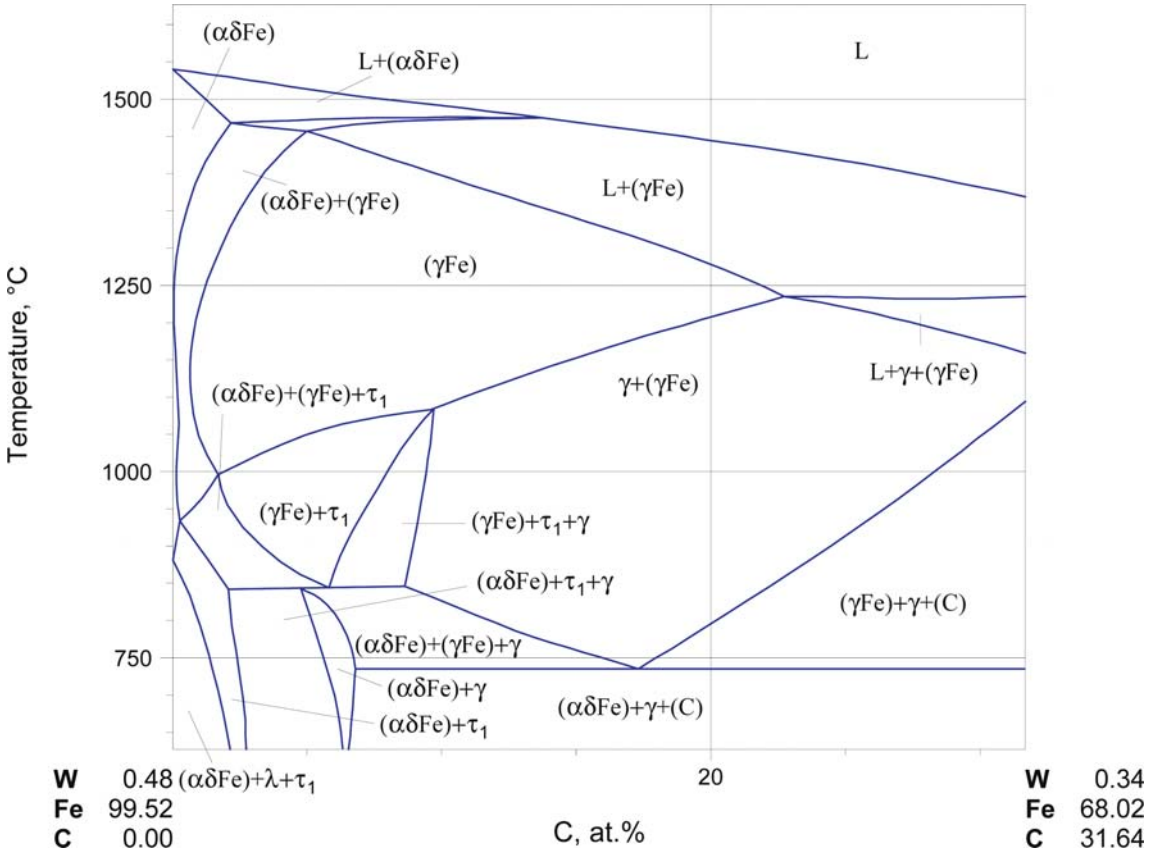

Fig. 12. C-Fe-W. Temperature-composition section $W_{1.57}Fe_{98.43}$-$W_{1.46}Fe_{89.58}C_{8.96}$ (plotted in at.%)

DOI: 10.1007/978-3-540-74196-1_16

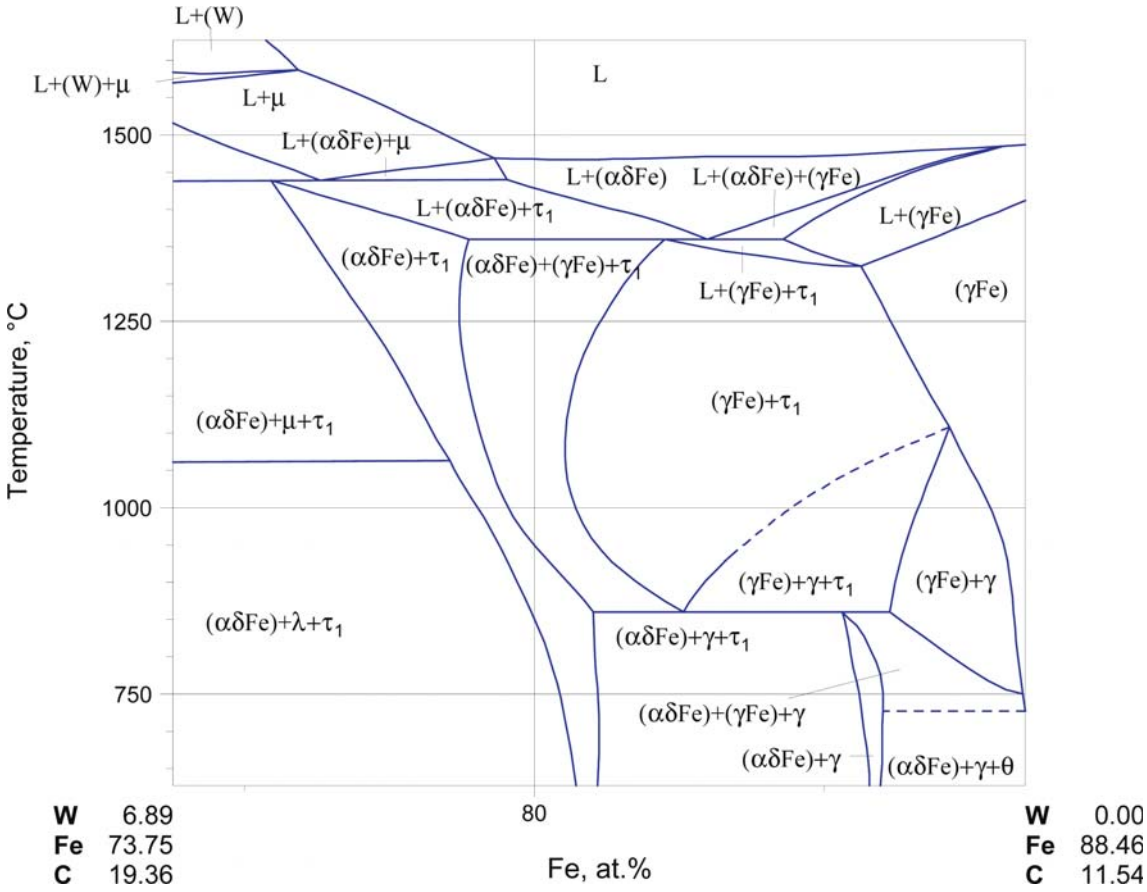

Fig. 13. C-Fe-W. Temperature-composition section $W_{22.54}Fe_{73.32}C_{4.14}$-$Fe_{97.27}C_{2.73}$ (plotted in at.%)

DOI: 10.1007/978-3-540-74196-1_16

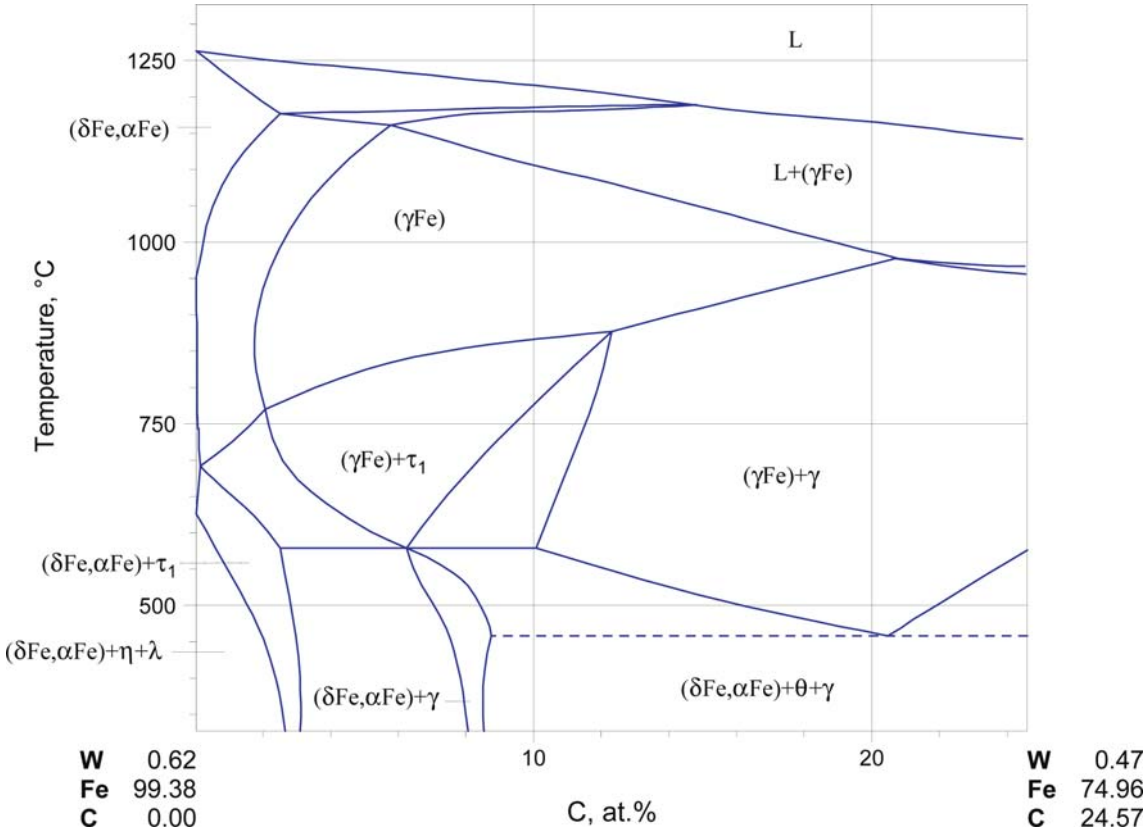

Fig. 14. C-Fe-W. Temperature-composition section W_2Fe_{98}-$W_{1.90}Fe_{91.64}C_{6.46}$ (plotted in at.%)

DOI: 10.1007/978-3-540-74196-1_16

References

[1918Hon] Honda, K., Murakami, T., "On the Structure of Tungsten Steels", *Sci. Rep. Tohoku Imperial Univ.*, **6**(5), 235–284 (1918) (Morphology, Phase Diagram, Experimental, Magn. Prop.) as quoted by [1920Hul2] and [1930Tak1]

[1920Hul1] Hultgren, A., "Tentative Iron-Tungsten-Carbon Diagram", *A Metallographic Study on Tungsten Steels*, John Wiley & Sons, Inc., New York, Chapman & Hall, Limited, London, 63–67 (1920) (Phase Diagram, Experimental, 1)

[1920Hul2] Hultgren, A., "Investigations on Tungsten Steels by Honda and Murakami", *A Metallographic Study on Tungsten Steels*, John Wiley & Sons, Inc., New York, Chapman & Hall, Limited, London, 79–85 (1920) (Morphology, Phase Diagram, Phase Relations, Review, Magn. Prop., 2)

[1921Dae] Daeves, K., "Limits of Solubility for Carbon in Ternary Steels. II. The System Tungsten-Iron-Carbon" (in German), *Z. Anorg. Chem.*, **118**, 67–74 (1921) (Morphology, Phase Diagram, Phase Relations, Experimental, 10)

[1921Hul] Hultgren, A., "Tungsten Steels" (in German), *Stahl Eisen*, **41**(49), 1824–1828 (1921) (Phase Diagram, Phase Relations, Experimental, 1)

[1922Oza] Ozawa, S., "On the Constitutional Diagram of the Iron-Carbon-Tungsten System", *Sci. Rep. Tohoku Univ.*, *Ser. 1*, **11**, 333–350 (1922) (Morpology, Phase Diagram, Experimental, Magn. Prop., *, 15)

[1924Obe] Oberhoffer, P., Daeves, K., Rapatz, F., "Checking of the Solubility Line for Carbon in Chromium and Tungsten Steels" (in German), *Stahl Eisen*, **44**(16), 432–456 (1924) (Morphology, Phase Diagram, Phase Relations, Experimental, 20)

[1927Wes] Westgren, A., Phragmen, G., "About Tungsten Steel Dicarbide" (in Swedish), *Jernkontorets Ann.*, **110**, 535–545 (1927) (Crys. Structure, Experimental, 9)

[1928Wes] Westgren, A., Phragmen, G., "On the Double Carbide of High Speed Steel", *Trans. Amer. Soc. Steel Treat.*, **13** (4), 539–554 (1928) (Crys. Structure, Morphology, Experimental, 10)

[1929Zie] Zieler, W., "Investigations over Tungsten Steel" (in German), *Arch. Eisenhuettenwes.*, **3**(1), 61–78 (1929) (Crys. Structure, Morphology, Phase Diagram, Phase Relations, Experimental, Review, Mechan. Prop., Phys. Prop., 22)

[1930Tak1] Takeda, S., "A Metallographic Investigation of the Ternary Alloys of the Iron-Tungsten-Carbon System. I. On the Carbides in Tungsten Steels", *Tech. Rep. Tohoku Imp. Univ.*, **9**, 483–514 (1930) (Crys. Structure, Morphology, Phase Diagram, Phase Relations, Experimental, Magn. Prop., 21)

[1930Tak2] Takeda, S., "A Metallographic Investigation of the Ternary Alloys of the Iron-Tungsten-Carbon System. II. Transformation and Constitution of Tungsten Steels", *Tech. Rep Tohoku Imp. Univ.*, **9**, 627–664 (1930) (Morphology, Phase Diagram, Phase Relations, Experimental, Electr. Prop., Magn. Prop., *, 1)

[1931Tak] Takeda, S., "A Metallographic Investigation of the Ternary Alloys of the Iron-Tungsten-Carbon System. III. The Equilibrium Diagram of the Fe-W-C System", *Tech. Rep. Tohoku Imp. Univ.*, **10**, 42–92 (1931) (Morphology, Phase Diagram, Phase Relations, Experimental, *, 15)

[1933Mor] Morral, F.R., Phragmén, G., Westgren, A., "Carbides of Low Tungsten and Molybdenum Steels", *Nature*, **132**, 61–62 (1933) (Crys. Structure, Experimental, 3)

[1943Smo] Smoluchowski, R., "Diffusion Rates of Carbon in Iron-Molybdenum and Iron-Tungsten Alloys", *Phys. Rev.*, **63**(11/12), 438–440 (1943) (Phase Relations, Experimental, Transport Phenomena, 7)

[1947Hul] Hultgren, A., "Isothermal Transformation of Austenite", *Trans. Am. Soc. Met.*, **39**, 915–989 (1947) (Crys. Structure, Morphology, Phase Diagram, Phase Relations, Experimental, Magn. Prop., 62)

[1949Jae] Jaenecke, E., "C-Fe-W" (in German), *Kurzgefasstes Handbuch aller Legierungen*, Winter Verlag Heidelberg 699–701 (1949) (Phase Diagram, Review, 1)

DOI: 10.1007/978-3-540-74196-1_16

[1950Kra] Krainer, H., "X-ray Investigation of the Carbides in Tungsten, Molybdenum and Vanadium Steels" (in German), *Arch. Eisenhuettenwes.*, **21**(1–2), 39–41 (1950) (Crys. Structure, Phase Diagram, Experimental, 6)

[1951Uma] Umansky, Ya.S., Chebotarev, N.T., "Structure and Compositions of the Iron-Tungsten Carbides" (in Russian), *Izv. Akad. Nauk SSSR, Ser. Fiz.*, **15**(1), 24–38 (1951) (Crys. Structure, Phase Relations, Experimental, 4)

[1952Edw] Edwards, R., Raine, T., "The Solid Solubilities of Some Stable Carbides in Cobalt, Nickel and Iron at 1250°C", *Pulvermetallurgie, 1. Plansee Seminar, De Re Metallica, 22–26 Juni, 1952, Reutte/Tirol, (Hrsg.)*, Benesovsky, F., Springer-Verlag, Wien, (1), 232–242 (1952) (Crys. Structure, Morphology, Phase Relations, Experimental, 5)

[1952Kuo] Kuo, K., "X-Ray Analysis of Carbides in Tungsten Steel" (in Swedish), *Jernkontorets Ann.*, **136**(6), 156–170 (1952) (Crys. Structure, Phase Relations, Experimental, *, 17)

[1953Kuo] Kuo, K., "Carbides in Chromium, Molybdenum, and Tungsten Steels", *J. Iron Steel Inst.*, **173**, 363–375 (1953) (Crys. Structure, Phase Diagram, Phase Relations, Experimental, *, 45)

[1957Sat] Sato, T., Nishizawa, T., Ohashi, M., "Study on Carbides in Iron and Steel by Electrolytic Separation. VIII. Carbides in Tungsten Steel" (in Japanese), *Nippon Kinzoku Gakkai Shi*, **21**, 662–665 (1957) (Crys. Structure, Phase Diagram, Experimental, Magn. Prop., *, 16)

[1958Ere] Eremenko, V.N., Naidich, Yu.V., "Wetting by Liquid Metals of Refractory Compounds Surfaces" (in Ukrainian), *Kiev, Akad. Nauk URSR*, 1–60 (1958) (Phase Relations, Experimental, Review, Theory, Interface Phenomena, 135)

[1959Fuw] Fuwa, T., Chipman, J., "Activity of Carbon in Liquid-Iron Alloys", *Trans. Metall. Soc. AIME*, **215**, 708–716 (1959) (Phase Relations, Thermodyn., Calculation, Experimental, *, 22)

[1960Fuw] Fuwa, T., Fujikura, M., Matoba, S., "Effect of Elements on the Solubility of Graphite in Liquid Iron" (in Japanese), *Tetsu to Hagane (J. Iron Steel Inst. Jpn.)*, **46**, 235–237 (1960) (Phase Relations, Thermodyn., Experimental, *, 16)

[1960Mor] Mori, T., Aketa, K., Ono, H., Sugita, H., "Effects of Molybdenum, Wolfram and Copper on Solubility of Graphite in Liquid Iron and the Method of Calculation for the Activity of Carbon in a Multicomponent Solution" (in Japanese), *Tetsu-to-Hagane (J. Iron Steel Inst. Jpn.)*, **46**, 1429–1437 (1960) (Phase Relations, Thermodyn., Calculation, Experimental, *, 24)

[1961Eng] English, J.J., "Tungsten-Carbon-Iron System", *Binary Ternary Phase Diagrams, Columbium, Molybdenum, Tantalum, Tungsten*, Apr. 28, (1961), Def. Met. Inf. Cent., Battelle Memor. Inst., Columbus 1, Ohio, **152**, 190–193 (1961) (Phase Diagram, Review)

[1963Ell] Elliott, J.F., Gleiser, M., Ramakrishna, V., "Iron-Carbon-j Alloys", *Thermochemistry for Steelmaking*, Addision Wesley, Reading, MA, **2**, 531 (1963) (Thermodyn., Review, 1)

[1964Lec] Leciejewicz, J., "Positions of the Carbon Atoms in Fe_6W_6C", *J. Less-Common Met.*, **7**, 318–320 (1964) (Crys. Structure, Experimental, 3)

[1965Kri] Krishtal', M.A., Davydov, Yu.I., "Influence of Chromium and Tungsten on the Thermodynamic Activity of Carbon in the Iron Alloys" (in Russian), *Izv. Vyss. Uchebn. Zaved., Chern. Metall.*, 9, 133–138 (1965) (Thermodyn., Experimental, Kinetics, 13)

[1966Gob] Gobin, F., Bouchy, C., "Establishment of Structure Diagrams for Steel With Chromium and Tungsten on Basis of Spatial Extension of Austenite Region in Ternary Alloys Iron - (Chromium or Tunsten)-Carbon" (in French), *Mem. Sci. Rev. Metall.*, **63**(1), 75–80 (1966) (Morphology, Phase Relations, Experimental, 3)

[1966Rud] Rudy, E., Windisch, St., Hoffman, J.R., *Aerojet General Corp. Tech. Rep. No. AFML-TR-65-2,* Part I, Vol. **VI**, (1966) (Phase Diagram, Experimental) as quoted by [1991Nag]

[1966Yas] Yasinskaya, G.A., "Wettability of the Refractory Carbides, Borides and Nitrides by the Molten Metals" (in Russian), *Poroshk. Metall. (Kiev)*, **43**(7), 53–55 (1966) (Morphology, Experimental, Interface Phenomena, 5)

[1967Boj] Bojarski, Z., Leciejewicz, J., "Neutron-Diffraction Study of the Crystal Structures of eta-Type Tungsten Iron Carbides" (in Polish), *Arch. Hutn.*, **12**(3), 255–263 (1967) (Crys. Structure, Experimental, 9)

DOI: 10.1007/978-3-540-74196-1_16

[1968Jel] Jellinghaus, W., "Powder-Metallurgical Contributions to the Ternary Systems Iron-Tungsten-Carbon and Iron-Molybdenum-Carbon" (in German), *Arch. Eisenhuettenwes.*, **39**(9), 705–718 (1968) (Crys. Structure, Morphology, Phase Diagram, Phase Relations, Experimental, Magn. Prop., Mechan. Prop., *, 15)

[1969Rud] Rudy, E., "Compendium of Phase Diagram Data", *Air Force Materials Laboratory, Wright-Patterson Air Force Base, O.H. Rep. No. AFML-TR-65-2,* Part V, 192–197 (May, 1969) (Phase Diagram, Experimental) as quoted by [1991Nag]

[1970Hil] Hillert, M., Staffansson, L.-I., "The Regular Solution Model for Stoichiometric Phases and Ionic Melts", *Acta Chem. Scand.*, **24**, 3618–3626 (1970) (Thermodyn., Calculation) as quoted by [1978Uhr]

[1970Pol] Pollock, C.B., Stadelmaier, H.H., "The η Carbides in the Fe-W-C and Co-W-C Systems", *Metall. Trans.*, **1**(4), 767-770 (1970) (Crys. Structure, Morphology, Phase Diagram, Phase Relations, Experimental, *, 15)

[1971Gre] Greenbank, J.C., "Carbon Solute Interactions in Fe-Cr-C, Fe-Mo-C and Fe-W-C Alloys", *J. Iron Steel Inst., London*, **209**, 986–990 (1971) (Phase Relations, Thermodyn., Experimental, 16)

[1972Tar] Taran, Yu.N., Ivanov, L.I., Moshkevich, L.D., "Morphology of the Eutectic in Fe-W-C Alloys", *Metal Sci. Heat Treatment*, **14**(1–2), 3–6 (1972) (Morphology, Experimental, 8) cited from abstract

[1973Rim] Rimkus, H.R., "Dissertation", *Technische Universitaet Clausthal, FRG* (1973) (Crys. Structure, Phase Diagram, Experimental, *) as quoted by [1988Ray]

[1973Rud] Rudy, E., "Constitution of Ternary Titanium-Tungsten-Carbon Alloys", *J. Less-Common Met.*, **33**, 245–273 (1973) (Phase Diagram, Experimental) as quoted by [1991Nag]

[1975Uhr] Uhrenius, B., Harvig, H., "A Thermodynamic Evaluation of Carbide Solubilities in the Fe-Mo-C, Fe-W-C and Fe-Mo-W-C Systems at 1000°C", *Met. Sci.*, **9**(2), 67–82 (1975) (Crys. Structure, Morphology, Phase Diagram, Phase Relations, Thermodyn., Experimental, *, 43)

[1976Lyu1] Lyudvinskaya, T.A., "Investigation of Possibility of Obtaining a Carbide of the M_6C Type in the Fe-W-C System" (in Russian), *Karbidy i Splavy na ikh Osnove*, IPM Akad. Nauk Ukr. SSR, 86–97 (1976) (Crys. Structure, Experimental, Theory, Phys. Prop., 3)

[1976Lyu2] Lyudvinskaya, T.A., Nizhnikovskaya, P.F., "Interaction of WC Powder with Iron" (in Russian), *Karbidy i Splavy na ikh Osnove*, IPM Akad. Nauk Ukrain. SSR, 80–85 (1976) (Crys. Structure, Morphology, Phase Relations, Experimental, Mechan. Prop., 7)

[1976Niz] Nizhnikovskaya, P.E., Taran, Yu.N., Grishina, O.N., "Carbide Transformations in the Fe-C-W and Fe-C-Mo Alloys" (in Russian), *Karbidy i Splavy na ikh Osnove*, IPM Akad. Nauk Ukrain. SSR, 76–80 (1976) (Crys. Structure, Morphology, Phase Relations, Experimental, 4)

[1976Sna] Snagovskii, V.M., Pirogova, E.K., Snagovskii, L.M., Nizhnikovskaya, P.F., Taran, Yu.N., "Structure Formation During Eutectic Solidification of Fe-C-W and Fe-C-Mo Alloys" (in Russian), *Karbidy i Splavy na ikh Osnove,* IPM Akad. Nauk Ukrain. SSR, 73–76 (1976) (Crys. Structure, Morphology, Phase Relations, Experimental, 16)

[1977Ber] Bergstroem, M., "The η-Carbides in the Ternary System Fe-W-C at 1250°C", *Mater. Sci. Eng.*, **27**, 257–269 (1977) (Crys. Structure, Morphology, Phase Diagram, Phase Relations, Experimental, Mechan. Prop., *, 24)

[1977Uhr] Uhrenius, B., "Optimization of Parameters Describing the Interaction Between Carbon and Alloying Elements in Ternary Austenite", *Scand. J. Metall.*, **6**(2), 83–89 (1977) (Thermodyn., Calculation, 24)

[1978Uhr] Uhrenius, B., "A Compendium of Ternary Iron-base Phase Diagrams", *Hardenability Concepts with Applications to Steel, Doane, D.V., Kirkaldy, J.S. (Eds.), Proc. Symp. Held Sheraton-Chicago Hotel, Oct. 24-26, 1977,* Metall. Soc. AIME Heat Treat. Com./Amer. Soc Met. Activ. Phase Trans., 28–81 (1978) (Phase Diagram, Phase Relations, Thermodyn., Calculation, 53)

DOI: 10.1007/978-3-540-74196-1_16

[1979Sun] Sundman, B., "Gibbs Energy System, User Guide", *Internal Report,* **D5**, Division of Physical Metallurgy, Royal Inst. of Technology, Stockholm, (1979) (Thermodyn., Calculation) as quoted by [1980Uhr]

[1980Ake] Akesson, L., *Sandvik Coromant Research Center,* Stockholm, Internal Report, No.70, (1980) (Phase Relations, Experimental, *) as quoted by [1980Uhr]

[1980Iwa] Iwadachi, T., Inoue, A., Minemura, T., Masumoto, T., "Nonequilibrium Phases in Fe-X-C (X=Cr, Mo, W) Ternary Alloys Quenched Rapidly from Melts" (in Japanese), *Nihon-Kinzoku-Gakkai-Shi*, **44**(3), 245–254 (1980) (Crys. Structure, Morphology, Phase Diagram, Phase Relations, Experimental, 30)

[1980Kle] Kleykamp, H., "Thermodynamics of the Fe-W, Fe-W-O and Fe-W-C Systems" (in German), *J. Less-Common Met.*, **71**(1), 127–134 (1980) (Thermodyn., Calculation, Experimental, 23)

[1980Sun] Sundman, B., Agren, J., *TRITA-MAC-0166*, Royal Inst. of Technology, Stockholm, (1980) (Thermodyn., Calculation) as quoted by [1980Uhr]

[1980Uhr] Uhrenius, B., "Calculation of Phase Equilibria in the Fe-W-C System", *Calphad*, **4**(3), 173–191 (1980) (Phase Diagram, Phase Relations, Thermodyn., Calculation, Review, #, 27)

[1981Dav] Davydenkov, N.N., "Mechanical Properties of Materials and Methods of Strain Measurement" (in Russian), *Kiev, Naukova Dumka*, 1–656 (1981) (Morphology, Phase Relations, Experimental, Review, Mechan. Prop., Phys. Prop., 913)

[1981Ino] Inoue, A., Iwadachi, T., Minemura, T., Masumoto, T., "Nonequilibrium Phases in Fe-X-C (X=Cr, Mo or W) Ternary Alloys Quenched Rapidly from Melts", *Trans. Jpn. Inst. Met.*, **22**(3), 197–209 (1981) (Crys. Structure, Morphology, Phase Diagram, Phase Relations, Experimental, 31)

[1981Nis] Nishizawa, T., Hasebe, M., "Computer Calculation of Phase Diagrams of Iron Alloys" (in Japanese), *Tetsu to Hagane*, **67**(14), 2086–2097 (1981) (Phase Diagram, Thermodyn., Calculation, Review, 110)

[1981She] Shevchuk, L.A., Dudetskaya, L.R., Tkacheva, V.A., "Investigation of Phase Equilibria in the Austenite Range of the Ternary Systems Fe-C-Mo and Fe-C-W", in "*Phase Equilibria in Metallic Alloys*", Nauka, Moscow, 225–229 (1981) (Crys. Structure, Phase Diagram, Phase Relations, Experimental, *, 3)

[1982Dra] Drachinskii, A.S., Krainikov, A.V., Trefilov, V.I., "Some Characteristics of Equilibrium Segregation in Refractory Group VIA Metals" (in Russian), *Fiz. Met. Metalloved.*, **54**(6), 1133–1137 (1982) (Morphology, Calculation, Review, 12) cited from abstract

[1982Hor] Hornbogen, E., Schmidt, I., "Microstructures of Glassy and Metastable Crystalline Phases Formed from Fe-C- Ternary Alloys", *Rapidly Solidified Amorphous Crystalline Alloys*, B.H. Kear, B.C. Giessen, M. Cohen (Eds.), 199–204 (1982) (Crys. Structure, Morphology, Phase Diagram, Phase Relations, Experimental, 7)

[1982Lug] Lugscheider, E., Reimann, H., Pankert, R., "η-Carbides in Co-W-C and Fe-W-C Alloys", *Z. Metallkd.*, **73**(5), 321–324 (1982) (Crys. Structure, Experimental, 17)

[1983Bus] Buschow, K.H.J., van Engen, P.G., Jongebreur, R., "Magneto-Optical Properties of Metallic Ferromagnetic Materials", *J. Magn. Magn. Mater.*, **38**, 1–22 (1983) (Crys. Structure, Experimental, Magn. Prop., Optical Prop., 23)

[1983Haa] Haarsta, A., Rundqvist, S., Thomas, J.O., "A Neutron Powder Diffraction Study of the κ Phase in the Fe-W-C System", *J. Solid State Chem.*, **49**(1), 118–122 (1983) (Crys. Structure, Experimental, 17)

[1983Jer] Jernberg, P., Waeppling, R., "A Mössbauer Study of the 6 Phase in the Fe-W-C System", *J. Solid State Chem.*, **49** (1), 123–125 (1983) (Crys. Structure, Experimental, 5)

[1983Kwo] Kwon, H., Kim, C.H., "Tempered Martensite Embrittlement in Fe-Mo-C and Fe-W-C Steel", *Metall. Trans. A (Physical Metallurgy and Materials Science)*, **14A**(7), 1389–1394 (1983) (Morphology, Experimental, Mechan. Prop., 16)

[1984Wad] Wada, T., Ohriner, E.K., "Phase Equilibria in the Fe-Mo-W-C System Containing $(Mo_{0.7}W_{0.3})C$ Carbide", *Calphad*, **8**(1), 69–74 (1984) (Phase Diagram, Thermodyn., Calculation, 20)

DOI: 10.1007/978-3-540-74196-1_16

[1985Gab] Gabriel, A., Pastor, H., Deo, D.M., Basu, S., Allibert, C.H., "New Experimental Data in the C-Co-W, C-Fe-W, C-Ni-W, C-Fe/Ni-W and C-Co/Ni-W Systems and their Applications to Sintering Conditions", *11th Internatl Plansee Seminar'85, Vol. Ii (Proc.Conf.), Reutte, Austria, 1985*, Metallwerk Plansee Gmbh, Reutte, Tirol, Austria, 509–525 (1985) (Phase Diagram, Phase Relations, Experimental, *, 21)

[1985Mal] Malik, A.U., "High-Temperature Oxidation of Transition Metal, Carbide-Dispersed Iron-Base Alloys", *Oxid. Met.*, **24**(5–6), 233–263 (1985) (Morphology, Experimental, Kinetics, 17) cited from abstract

[1985Riv] Rivlin, V.G., "Critical Review of Constitution of Carbon-Iron-Tungsten System", *Int. Met. Rev.*, **30**(6), 259–274 (1985) (Crys. Structure, Phase Diagram, Phase Relations, Assessment, *, 66) cited from abstract

[1986Gab] Gabriel, A., Pastor, H., Deo, D.M., Basu, S., Allibert, C.H., "New Experimental Data in the C-Fe-W, C-Co-W, C-Ni-W, C-Fe-Ni-W and C-Co-Ni-W Cemented Carbide Systems and their Application to Sintering Conditions", *Int. J. Refract. Met. Hard Mater.*, **5**(4), 215–221 (1986) (Phase Diagram, Phase Relations, Experimental, Magn. Prop., Mechan. Prop., 46)

[1986Nag] Nagender Naidu, S.V., Sriramamurthy, A.M., Rama Rao, P., "Fe-W (Iron-Tungsten)", *J. Alloy Phase Diagrams*, **2**(3), 176–188 (1986) (Crys. Structure, Phase Diagram, Experimental, Review, 80)

[1987Gus] Gustafson, P., "A Thermodynamic Evaluation of the C-Fe-W System", *Metall. Trans. A*, **18A**(2), 175–188 (1987) (Phase Diagram, Thermodyn., Calculation, *, 53)

[1988Ray] Raynor, G.V., Rivlin, V.G., "C-Fe-W" in *"Phase Equilibria in Iron Ternary Alloys",* Institute of Metals, London, **4**, 200–212 (1988) (Crys. Structure, Phase Diagram, Phase Relations, Review, #, 21)

[1989Mal] Malik, A.U., Ishaq, M., Ahmad, Sh., Ahmad, Su., "Influence of Carbon on the Hot Corrosion Behaviour of Fe-Base Alloys", *Mater. Trans., JIM*, **30**(9), 707–716 (1989) (Morphology, Experimental, Kinetics, 14)

[1990Dra] Drachinskii, A.S., Ivashchenko, Yu.N., Krainikov, A.V., "Investigation of Concurrent Segregation of Impurities at Grain Boundaries in W-Fe-C Alloys using Auger-Electron Spectroscopy", *Physics, Chemistry and Mechanics of Surfaces*, **5**(5), 1288–1293 (1990) (Morphology, Experimental, Theory, 4) cited from abstract

[1990Ere] Eremenko, V.N., Velikanova, T.Ya., Khar'kova, A.M., Velikanova, T.A., "Implantation Phases on the Basis of Metallides in the Ternary Systems of Transition Metals with Carbon" (in Russian), *Ukr. Khim. Zh.*, **56**(4), 356–363 (1990) (Crys. Structure, Assessment, Review, 11)

[1990Jan] Jansson, B.J., "Thermodynamic Calculations for Tungsten Carbide Tools with an Iron-Based Binder", *High Temp.-High Pressure*, **22**(4), 465–478 (1990) (Phase Diagram, Phase Relations, Thermodyn., Calculation, *, 9)

[1991Nag] Nagender Naidu, S.V., Sriramamurthy, A.M., Rama Rao, P., "C-W (Carbon-Tungsten)" in "*Phase Diagrams of Binary Tungsten Alloys*", Nagender Naidu, S.V., Rama Rao, P. (Eds.), Indian Institute of Metals, Calcutta, 37–50 (1991) (Crys. Structure, Phase Diagram, Phase Relations, Review, #, 100)

[1992Azu] Azubike, D.C., Chrysanthou, A., Igiehon, U.O., "A Crystallographic Re-Examination of the $(Fe, W)_6C$ Phase Field in the Fe-W-C System", *Powder Diffr.*, **7**(3), 162–163 (1992) (Crys. Structure, Experimental, 5)

[1992Oka] Okamoto, H., "The C-Fe (Carbon-Iron) System", *J. Phase Equilib.*, **13**(5), 543–565 (1992) (Crys. Structure, Phase Diagram, Phase Relations, Thermodyn., Assessment, Review, *, 242)

[1992Sah] Sahay, S.K., Bhadeshia, H.K.D.H., Honeycombe, R.W.K., "Carbide Precipitation and the Nucleation of Allotriomorphic Ferrite in an Fe-W-C Steel", *Mater. Sci. Eng. A (Structural Materials: Properties, Microstructure and Processing)*, **A157**(1), 101–105 (1992) (Morphology, Experimental, 13) cited from abstract

[1994Rag] Raghavan, V., "C-Fe-W (Carbon-Iron-Tungsten)", *J. Phase Equilib.*, **15**(4), 429–430 (1994) (Phase Diagram, Review, 8)

DOI: 10.1007/978-3-540-74196-1_16

[1994Tri] Trindade, B., Vieira, M.T., Bauer-Grosse, E., "Characterization of W-Me-C (Me = Fe, Co) Films and their Structural Behaviour with Temperature", *Mater. Sci. Eng. A (Structural Materials: Properties, Microstructure and Processing)*, **A174**(2), 165–171 (1994) (Crys. Structure, Morphology, Experimental, 24) cited from abstract

[1995Pop] Popov, V.V., "Determination of Mutual Diffusion Coefficients of Metallic Elements in Austenite and Ferrite of the Systems Fe-Cr-C, Fe-Mo-C and Fe-W-C" (in Russian), *Fiz. Met. Metalloved.*, **79**(4), 94–103 (1995) (Morphology, Calculation, Experimental, Transport Phenomena, 23)

[1995Tri] Trindade, B., Vieira, M.T., Grosse, E.B., "In Situ High Temperature Crystallization Study of Sputter Deposited Amorphous W-Fe-C Films", *Acta Metall. Mater.*, **43**(1), 93–99 (1995) (Crys. Structure, Morphology, Experimental, 25) cited from abstract

[1997Beh] Behulova, M., Grgac, P., Kabat, E., "The Heat Transfer During Rapid Solidification of Undercooled Hypereutectic Fe-C-X Alloy Droplets", *Rapidly Quenched and Metastable Materials. Proceedings of the Ninth International Conference on Rapidly Quenched and Metastable Materials.*, Supplement. Elsevier. Part suppl., Amsterdam, Netherlands, 10–13 (1997) (Morphology, Calculation, Experimental, Phys. Prop., 38) cited from abstract

[1997Sht1] Shtansky, D.V., Inden, G., "Phase Transformation in Fe-Mo-C and Fe-W-C Steels. I. The Structural Evolution during Tempering at 700°C", *Acta Mater.*, **45**(7), 2861–2878 (1997) (Crys. Structure, Morphology, Phase Relations, Thermodyn., Calculation, Experimental, *, 47)

[1997Sht2] Shtansky, D.V., Inden, G., "Phase Transformation in Fe-Mo-C and Fe-W-C Steels. II. Eutectoid Reaction of $M_{23}C_6$ Carbide Decomposition during Austenization", *Acta Mater.*, **45**(7), 2879–2895 (1997) (Crys. Structure, Morphology, Phase Relations, Thermodyn., Calculation, Experimental, Transport Phenomena, 26)

[1998Hac] Hackenberg, R.E., Shiflet, G.J., "Transitions in Carbide Morphology in a Ternary Fe-C-W Steel", *Metall. Mater. Trans. A*, **29A**, 2087–2100 (1998) (Crys. Structure, Morphology, Phase Relations, Thermodyn., Calculation, Experimental, Kinetics, *, 63)

[1998Tri] Trindade, B., Vieira, M.T., Amaro, A.M., Cirne, J.S., "Mechanical Behaviour of Sputtered M-Fe-C (M=Cr, Mo, W) Carbides", *Fundamentals of Nanondentation and Nanotribology. Symposium. Mater. Res. Soc.,* 305–310 (1998) (Crys. Structure, Morphology, Experimental, Mechan. Prop., 7) cited from abstract

[1999Nak] Nakai, K., Shtansky, D.V., "Analyses of Microstructure Evolutions During Reverse Phase Transformations in Alloyed Steels Using Calculated Phase Diagrams" (in Japanese), *Materia Japan*, **38**, 975–981 (1999) (Phase Relations, Thermodyn., Calculation, 41)

[1999Pop] Popov, V.V., "Diffusion Interaction of Carbides, Nitrides and Carbonitrides with Iron and Steels", *Metallofizika Nov. Tekhnol.*, **21**(2), 99–103 (1999) (Morphology, Experimental, Transport Phenomena, 11)

[1999Xu] Xu, D.Q., Luo, J.R., Huang, N.Y., "Structures and Properties of Iron Matrix Composites with Tungsten Carbide Particle by EPC-V Process", *J. Iron Steel Res. Int.*, **6**(2), 29–32 (1999) (Morphology, Experimental, Phys. Prop., 3) cited from abstract

[2000Kir] Kirilenko, S.M., "Internal Stress Formation in Spark Coatings and Heat Treatment Effects", *Powder Metall. Met. Ceram.*, **39**(1–2), 29–31 (2000) (Morphology, Experimental, Mechan. Prop., 3)

[2000Kub] Kublii, V.Z., Velikanova, T.Ya., Gnitetskii, O.A., Makhovitskaya, S.I., "Structural Parameters of the Low-Temperature Metastable Form of the Carbide W_2C", *Powder Metall. Met. Ceram.*, **39**(3-4), 151–156 (2000) (Crys. Structure, Experimental, 15)

[2001Mar] Marsh, P., Wood, J.V., Moon, J.R., "Diffusion Between High Speed Steel and Iron Powders", *Powder Met.*, **44**(3), 205–210 (2001) (Morphology, Experimental, Kinetics, 4)

[2001Sht] Shtanskii, D.V., "Analysis of Phase and Structural Transformations in Ternary Systems by the Computer-Thermodynamic Methods: A Review", *Phys. Met. Metallogr. (Engl.*

DOI: 10.1007/978-3-540-74196-1_16

Transl.), **92**(2), 133–152 (2001) (Morphology, Phase Diagram, Phase Relations, Thermodyn., Review, 108)

[2001Ska] Skaojun, C., Sbu-Sheng, D., Yong-Lin, L., Jie, H., "Morphological Fractal Characteristics of WC in Ferrite-Cemented Tungsten Carbide before and after ESR Process" (in Chinese), *J. Iron Steel Res.*, **13**(1), 54–59 (2001) (Morphology, Experimental, Theory, 8) cited from abstract

[2002Bab] Babu, S.S., Martukanitz, R.P., Parks, K.D., David, S.A., "Toward Prediction of Microstructural Evolution During Laser Surface Alloying", *Metall. Mater. Trans. A*, **33**(4), 1189–1200 (2002) (Morphology, Phase Diagram, Thermodyn., Calculation, Experimental, Kinetics, 31)

[2002Hac1] Hackenberg, R.E., Granada, D.G., Shiflet, G.J., "Austenite Decomposition to Carbide rich Products in 0.30C-6.3W", *Metall. Mater. Trans. A*, **33A**(12), 3619–3633 (2002) (Crys. Structure, Morphology, Phase Diagram, Phase Relations, Experimental, Kinetics, Mechan. Prop., 61)

[2002Hac2] Hackenberg, R.E., Nordstrom, D.P., Shiflet, G.J., "Morphology and Three-Dimensional Structure of Ferrite Formed Below the Bay in an Fe-C-W Alloy", *Scr. Mater.*, **47**(6), 357–361 (2002) (Morphology, Experimental, 16)

[2006MSIT] "C-Fe (Iron-Carbon)", Diagrams as Published, in *MSIT Workplace*, Effenberg, G. (Ed.), Materials Science International Services, GmbH, Stuttgart; Document ID: 30.13598.1.20 (2006) (Crys. Structure, Phase Diagram, Phase Relations, 2)

[Mas2] Massalski, T.B. (Ed.), *Binary Alloy Phase Diagrams*, 2nd edition, ASM International, Metals Park, Ohio (1990)

[V-C2] Villars, P. and Calvert, L.D., *Pearson's Handbook of Crystallographic Data for Intermetallic Phases*, 2nd edition, ASM, Metals Park, Ohio (1991)

DOI: 10.1007/978-3-540-74196-1_16

Calcium – Iron – Oxygen

Joachim Gröbner, Simona Delsante, Nuri Solak, Vasyl Tomashik

Introduction

The discussed system is of outstanding importance for steelmaking and also in cement manufacture. Since lime (CaO) is one of the most important additives in steel plant refractions, the reactions and formed compounds of iron with lime are of particular interest. These processes influence the reduction characteristics as well as the slag formation in the blast furnace.

A huge number of studies have been done especially in the region where iron is in equilibrium with the various oxides in the system. First investigations start in the thirties in Germany (Schrenck and Martin *et al.* [1929Sch, 1934Mar, 1937Sch] and Italy (Cirilli and Burdese *et al.* [1947Cir, 1952Cir, 1952Bur, 1954Bur, 1960Bur]. [1961Tur] calculated activities of oxygen in Ca-Fe-O melts from the available experimental data and developed a reactions sequence from theoretical considerations, which is favored by several authors. Very important work was presented by Schürmann and his group [1973Sch, 1976Sch1, 1976Sch2, 1976Sch3, 1976Sch4, 1993Sch]. Some studies reported at higher oxygen content no final equilibria between iron and the oxides. In several investigations the oxygen potential, in equilibria with the reported solid phases, is not measured or not given at all. Reviews of the investigations in phase diagrams in the Ca-Fe-O are given by [1943Whi], [1965Mua], [1976Sch4] and [1989Rag].

Calphad type assessment was performed by [1989Sel, 1990Hil, 1996Sel, 2001Fri]. An independent Calphad assessment was given by [1993Wu]. All calculations reproduce the experimental data only partly. Therefore the assessment of [1989Rag] was favored.

All experimental works and calculations in this system are listed in Table 1.

Binary Systems

Ca-Fe binary system was selected from [1994Oka] which combined iron rich part of [Mas2] with the new data for the Ca corner [1993Gla]. The Ca-O binary system was taken from the new experimental investigation of [2000Zai]. The Fe-O system was taken from critical assessment of [1991Sun].

Solid Phases

In the Ca-Fe-O system four stable binary phase exist with different ternary solubilities. The following notation is used to denote them: C = CaO (lime), F = Fe_2O_3 (hematite), W = FeO (wustite) and WF = Fe_3O_4 (magnetite).

The CaO solubility in $Fe_{1-x}O$ (wustite) is strongly temperature dependent. [1980Lyk] measured this solubility at 850°C as 9.5 mol% and at 1050°C as 29 mol% CaO by emf method, whereas [1975Tar] using emf method, determined at 850°C higher than 10 mol% and at 1050°C this value is much higher than 30 mol%. [1975Abb] found a maximum solubility about 40 mol.% CaO at 1130°C. Other measurements by [1946Pet], [1952Cir], [1955All], [1955Tro], [1970Nek], [1971Ino], [1975Tar] differ in some ranges, which could be explained by the observed temperature dependence. The lattice parameter change of FeO at 1000°C depending on the CaO concentration is given by [2002Ina].

CaO dissolves maximum about 10 mol% FeO at 1130°C [1975Abb]. Whereas the maximal solubility of CaO is less than 1 mol% in Fe_2O_3 and about 2.5 mol% in Fe_3O_4 at 1430°C [1958Phi].

There is a number of ternary compounds in this system. Ternary phases are denoted by combination of the above mentioned notations of the binary compounds (see Table 2).

Three compounds were formed at the CaO-Fe_2O_3 section: $Ca_2Fe_2O_5$ (C_2F), $CaFe_2O_4$ (CF) and $CaFe_4O_7$ (CF_2). $Ca_2Fe_2O_5$ (C_2F) is formed congruently from the melt at 1148°C. Its crystal structure is investigated intensively [1967Hug, 1971Ber, 1976Mus, 1980Har, 1994Gib, 1999Gom, 2004Red].

MSIT®
DOI: 10.1007/978-3-540-74196-1_17

$CaFe_2O_4$ (CF) is formed peritectically at 1228°C. The very similar crystal structure is reported by [1957Dec, 1967Hug, 1976Mus, 1971Apo]. [1963Leo] claims the absence of the appreciable mutual solubility of $CaFe_2O_4$ and $Ca_2Fe_2O_5$ by XRD.
$CaFe_4O_7$ (CF_2) is a high temperature phase, which is stable only between 1226 and 1155°C [1976Sch1]. [1983Mod] found a solubility of FeO in this phase less than 9 mol%. The crystal structure was given by [1962Che, 1967Hug, 1986Mil].
[1980Evr] reported the crystal structure of three other phases: $CaFe_3O_5$ (CWF), $CaFe_4O_6$ (CW_2F) and $CaFe_5O_7$ (CW_3F). Two of them were already found by [1976Mus]. [1982Bau] confirmed the data given by [1980Evr]. $CaFe_5O_7$ is formed peritectically at 1050°C and decomposes eutectoidally at 654°C [1961Tur]. [1995Lyk] found a solid solution from $CaFe_5O_7$ to the composition $CaFe_6O_8$. The estimated decomposition temperature for $CaFe_3O_5$ is 290°C [1967Ree2] and the homogeneity range of this phase extends from $Ca_{0.95}Fe_{3.05}O_{4.95}$ to $Ca_{1.02}Fe_{2.96}O_5$ [1986Mil].
The compound $CaFe_6O_8$ reported by [1995Lyk] corresponds most probably to the solid solution based on $CaFe_5O_7$ the XRD patterns are nearly identical with a shift which is an indication of a solid solution.
In the Fe_3O_4 - $Ca_2Fe_2O_5$ - Fe_2O_3 region [1960Phi] found two additional compounds: $Ca_4Fe_9O_{17}$ (C_4WF_4) and $Ca_4Fe_{17}O_{29}$ (C_4WF_8) which were formed pertectically at 1212°C and 1230°C. The crystal structures were solved by [1982Mal1] and [1986Mil], respectively. For $Ca_4Fe_{17}O_{29}$ (C_4WF_8) a large homogeneity range was reported by [1986Mil]. Two more phases $CaFe_4O_{6.95}$ and $CaFe_4O_{6.86}$ with homogeneity ranges were also reported at 1200°C by [1986Mil].
The compound $Ca_3Fe_{15}O_{25}$ (C_3WF_7) reported by [1983Ara, 1985Kar, 1987Ara, 1987Kar] exists in three poly-types: αCFF, βCFF and βCFF. [1988Ara] gives the crystal structures for these phases. The crystal structure of two additional phases at 1120°C were reported by [1981Mal]: $Ca_2Fe_9O_{13}$ ($C_2W_5F_2$) and $Ca_2Fe_7O_{11}$ ($C_2W_3F_2$). For these phases only the crystal structures are known. No stability and temperature ranges are reported in the literature, therefore these phases are not occurring in the phase diagrams.
[2000Woo] determined the crystal and magnetic structures of $CaFeO_3$ at 300 and 15 K using synchrotron X-ray and neutron powder-diffraction techniques. They found two different distorted perovskite structures at these temperatures. [1970Kan] reported earlier a cubic perovskite formed at high temperature and high pressure.

Quasibinary Systems

The quasibinary section along Fe_2O_3-CaO was determined by [1958Phi, 1976Sch1, 1986Ber] in air and 1 atm of oxygen. Figure 1 gives the phase diagram of this section in air.
Although it was mentioned in some articles, CaO-FeO is not a true quasibinary section since FeO is not a stoichiometric phase and iron is present in this section. This section is reported in the section Temperature-Composition Sections.

Invariant Equilibria

Invariant equilibria are given in Table 3, which is mainly based on the works of [1960Phi], [1961Tur], [1967Ree1], the review of [1989Rag] and the calculation of [1990Hil]. A partial reaction scheme is given in Fig. 2.
[1988Ber] found the CW3F phase stable up to about 1100°C and have questioned the peritectic reaction at 1050°C.

Liquidus, Solidus and Solvus Surfaces

The FeO - Fe_3O_4 (WF) - $Ca_2Fe_2O_5$ (C_2F) - CaO region of the liquidus surface was investigated by several authors [1954Bur, 1961Tur, 1967Ree1, 1976Sch3, 1988Ber]. Many of the invariant reactions listed by [1961Tur] were confirmed experimentally by [1967Ree1, 1967Per, 1976Sch2, 1976Sch3]. The liquidus surface of [1976Sch4] differs from the others because of the use of a different FeO-CaO vertical section.
The solidification of the Fe_2O_3 (F) - Fe_3O_4 (WF) - $Ca_2Fe_2O_5$ (C_2F) region was determined by [1934Mar, 1955Tro, 1960Phi, 1986Ber].

DOI: 10.1007/978-3-540-74196-1_17

The quasiternary liquidus surface FeO - Fe_3O_4 (WF) - CaO in Fig. 3 combines all these results. The type of reaction for the invariant reactions U_4, U_5, U_7 and E_3 given by [1967Ree1] is changed to fit into the sequence of reactions given in the reaction scheme in Fig. 2.

Isothermal Sections

A large number of isothermal sections at different temperatures have been determined. All of them show only a part of the quasiternary system FeO - Fe_3O_4 (WF) - CaO.
Following sections are reported:
565°C: [1973Sch], 600°C: [1952Bur], 625°C: [1973Sch], 650°C: [1973Sch], 690°C: [1973Sch], 700°C: [1952Bur], 800°C: [1952Bur], 840°C: [1973Sch], 850°C: [1983Lyk], 900°C: [1937Sch, 1976Lyk, 1980Lyk, 1981Bur, 1983Lyk], 1000°C: [1976Lyk, 1980Lyk, 1983Lyk], 1027°C: [1984Bjo], 1050°C: [1952Bur, 1980Lyk, 1983Lyk, 1988Ber], 1060°C: [1973Sch], 1085°C: [1967Ree1], 1100°C: [1980Evr, 1988Ber], 1120°C: [1981Mal], 1125°C: [1981Bur], 1135°C: [1960Phi], 1190°C: [1960Phi], 1195°C: [1960Phi], 1200°C: [1960Phi, 1981Tak, 1986Mil], 1210°C: [1960Phi], 1220°C: [1960Phi], 1230°C: [1960Phi], 1300°C: [1981Tak], 1450°C: [1970Tim], 1500°C: [1984Har1], 1550°C: [1953Lar, 1970Tim], 1600°C: [1950Gur].
Here we present isothermal sections at 1450°C (above the formation of the ternary phases, Fig. 4), 1200°C (including the new phases given by [1986Mil], Fig. 5), 1085°C (above the decomposition of CF_2, Fig. 6) and 900°C (with the $CaFe_5O_7$ (CW_3F) phase), Fig. 7). The phase relations at 1200°C given by [1986Mil] are not clear. They report two additional phases, $CaFe_4O_{6.95}$, $CaFe_4O_{6.86}$, and a large homogeneity range of $Ca_4Fe_{17}O_{29}$ (C_4WF_8) at this temperature. Since this homogeneity ranges is only determined by XRD and not confirmed by any other work, we simplified the phase to be stoichiometric in Fig. 5. About the stability of these phases and the $Ca_3Fe_{15}O_{25}$ (CFF) down to lower temperatures no information exists. At lower temperature the phase relations are almost identical with that at 900°C [1971Iml, 1973Sch].

Temperature – Composition Sections

The vertical section along FeO-CaO has been investigated by several authors [1955All, 1955Tro, 1967Ree1, 1973Sch, 1975Abb, 1976Sch3, 1984Bjo, 1987Ber]. There are some discrepancies about the invariant temperatures. Since the terminal solubilities of [1975Abb] reach closer equilibrium, they were preferred against [1973Sch]. As this section is not quasibinary, the peritectic reaction at 1130°C is actually U_6 (see Table 3). The FeO-CaO vertical section in the presence of iron in Fig. 8 is based mainly on the results of [1975Abb].
[1934Mar] show 10 additional vertical sections which are not accepted in the present evaluation because of the disagreement with more recent investigations.

Thermodynamics

There is a number of studies concerning thermodynamic properties of the ternary compounds existing in the Ca-Fe-O system. Thermodynamic properties of the compounds are summarized in Table 4. Heat capacity measurements of $CaFe_2O_4$ and $Ca_2Fe_2O_5$ were conducted throughout the temperature range 52 to 298 K. $CaFe_2O_4$ has an anomalous heat capacity between 150 and 200 K. The entropies of the ferrites at 298.15 K are 34.7±0.2 cal·mol^{-1}·°C^{-1} (145.18 J·(mol·K)$^{-1}$) and 45.1±0.3 cal·mol^{-1}·°C^{-1} (188.69 J·(mol·K)$^{-1}$) respectively, for $CaFe_2O_4$ and $Ca_2Fe_2O_5$ [1954Kin]. High temperature heat content of the compounds between room temperature and 1577°C was measured by [1954Bon] and the heat of fusion of $CaFe_2O_4$ was determined as 108.24 J·mol^{-1} at 1237°C, and that of $Ca_2Fe_2O_5$ as 151.08 J·mol^{-1}at 1477°C. Heat and free energy of formation of $CaFe_2O_4$ and $Ca_2Fe_2O_5$ from oxides and elements in the temperature range of 25-1527°C were determined by [1961Koe].
Activity-composition relation in FeO-CaO system was investigated using emf technique and free energy of formation of $Ca_2Fe_2O_5$ from CaO and FeO was determined by [1986Sha]. Limited mutual solubility and high positive deviation from ideality was reported. Standard free energy of formation of the $Ca_2Fe_2O_5$ compound from the component oxides CaO and FeO was reported as –10.4±1.5 kJ·mol^{-1}. Using same technique, [1987Raj] determined enthalpy of formation of $Ca_2Fe_2O_5$ at room temperature as –2071.4 kJ·mol^{-1}.

DOI: 10.1007/978-3-540-74196-1_17

[1984Iwa] determined activities of CaO and Fe_xO at 1400°C as the function of slag composition which is a mixture of CaO and Fe_xO.
In the temperature range 427-727°C standard free energy of formation of the $Ca_2Fe_2O_5$ compound was also reported. And, using gas equilibration technique activity of iron oxide in the CaO-FeO system was performed in the temperature range 1550-1600°C by [2004Fre]. During the experiment a part of the Fe from the FeO was reduced during the equilibration and got dissolved in the Pt phase which comes from the crucible. The activity of FeO in the slag was calculated from the experimental data. Good agreement between the experimental results and calculated data was observed. [1956New] measured heat of solution of $Ca_2Fe_2O_5$ in HCl, 26.61H_2O (2 *Normal* at 25°C) and from the data together with appropriate heat of dilution measurements heat formation of $Ca_2Fe_2O_5$ was reported as 7.44 kCal·mol^{-1} (31.129 kJ·mol^{-1}).
The free energy of formation of $Ca_2Fe_2O_5$ (from its oxides) calculated from the activity data along the vertical sections Fe_3O_4-$Ca_2Fe_2O_5$ and FeO-$Ca_2Fe_2O_5$ was given at 1550°C as 76.567 (±4) kJ·mol^{-1} in the study of [1961Tur]. These data are in good agreement with the study of [1960Ell] (79.469 (±4) kJ·mol^{-1}). Along the section Fe_3O_4-$CaFe_2O_4$ and FeO-$CaFe_2O_4$ the free energy of formation $CaFe_2O_4$ (from its oxides) was found at the same temperature to be –54.81 kJ·mol^{-1}. Essential data for the computation of the thermodynamic parameters of $CaFe_2O_4$ were obtained from the measurements of the emf of galvanic cells at temperature range between 330 and 730°C. The average value of enthalpy of formation was given as –1552 (±50) kJ·mol^{-1} [1990Raj].
Standard Gibbs energy change for the reactions CaO + Fe_2O_3 ⇌ $CaFe_2O_4$ and 2CaO + Fe_2O_3 ⇌ $Ca_2Fe_2O_5$ was determined from solid state emf measurements, using CaF_2 as a solid electrolyte. By applying *third-law* the standard enthalpy of formation of $CaFe_2O_4$ from constituent oxides at 25°C was evaluated as $\Delta H°_{298}(CaFe_2O_4) = -17.5 \pm 0.4$ kJ·mol^{-1} [2002For].
Activities of FeO at 1100°C in the solid solution in equilibrium with Fe were measured by several authors using gas equilibration [1975Abb, 1970Tim] and galvanic cells with solid electrolytes [1984Bjo]. Activity of FeO in liquid solutions in equilibrium with Fe was reported at 1400°C by [1980Ban]. The CaO and FeO rich solid solutions were treated as one phase with a miscibility gap with $G^E = X_{CaO}\, X_{FeO}$ (22773 – 3140 X_{CaO} + 15522 X^2_{CaO}) J·mol^{-1} was calculated by [1993Wu].
Thermodynamic data in single phase calciowustite solid solution at 1100°C was measured by [1975Tar] using emf method. In the same work lattice parameter change of wustite as a function of CaO was reported and good agreement was obtained with the literature data.
Using emf technique [1984Bjo] measured Gibbs energy: $\Delta G° = -845230 + 227.93T$ (±430)J·mol^{-1} for the equilibrium $2CaO(in(Ca,Fe_{1-x})O)+2Fe_{(s)}+3/2O_{2(g)} = Ca_2Fe_2O_{5(s)}$.
Temperature limit for the equilibrium was given as 1060±7°C. At this temperature the terminal solid solutions $(Fe_{1-x},Ca)O$ and $(Ca,Fe_{1-x})O$ are coexisting with iron. The chemical potentials of CaO in the two-phase fields Fe_2O_3 + $CaFe_2O_4$ and $CaFe_2O_4$ + $Ca_2Fe_2O_5$ of the quasibinary system CaO-Fe_2O_3 have been measured in the temperature range 702-1002°C using solid state galvanic cell. Standard Gibbs energy of formation of $CaFe_2O_4$ and $Ca_2Fe_2O_5$ was derived from the emf data [1999Jac].
Existence of ternary compounds in the FeO-Fe_2O_3-CaO system was established using XRD and emf measurements. In the temperature range 797-1057°C, $CaFe_3O_5$ and $CaFe_6O_8$ compounds were reported. Additionally, in the same temperature range, equilibrium oxygen pressure over the ternary phases was determined and Gibbs energies of formation of the compounds from Fe, O_2 and CaO were calculated [1972Lyk, 1976Lyk, 1980Lyk, 1983Lyk, 1995Lyk].
Calcium ferrite is an important constituent mineral of the sinter following iron oxides. In order to estimate the reduction rate of calcium ferrites and iron oxides at higher temperature range of the blast furnace, the reduction equilibria are of great importance. One of the first detailed oxygen potential diagram studies of the Ca-Fe-O system was done by [1967Ree1]. The system was investigated in the temperature range 1000-1050°C. The proposed diagram contains literature information and theoretical works. In general there is good agreement between this work and the literature data, although two discrepancies were noted in the work and revised. Later, the system was investigated in details by Schürmann *et al.* [1976Sch1, 1976Sch2, 1976Sch3, 1976Sch4] and by [1988Chu]. [1993Sch] revised the published Baur-Glaessner diagrams in the Fe-Fe_2O_3-CaO system as a function of oxygen concentration and in the temperature range 700-1000°C. In Figs. 9a, 9b, 9c Baur-Glaessner diagrams of the system are given. [1980Tak1] determined oxygen isobars and liquidus isotherms of the CaO-FeO-Fe_2O_3 system at 1200 and 1300°C by quenched samples

DOI: 10.1007/978-3-540-74196-1_17

equilibrated with CO_2-CO mixture. [1980Tak1] determined oxygen isobars and liquidus isotherms at 1200 and 1300°C. It was reported in the same work that within the range of Po_2 from one order above that at iron saturation to 10^{-4} atm, the slag composition, po_2, and the temperature are related to each other by the following equation:

$$\log (Fe^{3+}/Fe^{2+}) \sim 0.170 \log p_{O2} + 0.018 \text{ (mass\% CaO)} + 5500 / T - 2.52$$

In the same work also activities of CaO(s), FeO(l) and Fe_3O_4(s) were calculated and activities of FeO(l) along the iron liquidus at both temperatures showed negative deviations from the behavior expected when the slags were ideal binary solutions of FeO and CaO. Isoactivity curves for CaO, FeO and Fe_3O_4 at 1200 and 1300°C are given in Figs. 10a and 10b. Results of vapor pressure measurements are given in Tables 5 and 6.

The first Calphad assessment of the system on CaO-FeO and CaO-Fe_2O_3 sections was done by [1979Kau]. [1990Hil] studied the system in details using the compound energy model with ionic species for all solid solution phases in the temperature range of 25 to 1727°C. Later a reassessment was published by the same group because of the difficulties in higher the order silica containing systems [1989Sel, 1996Sel]. Also [1993Wu] thermodynamically modeled the CaO-FeO section. In all the assessment good agreement with the literature data was obtained.

Notes on Materials Properties and Applications

The Ca-Fe-O system is of central importance for steelmaking. During the reduction of iron oxides in the blast furnace the reactions with CaO (lime), one of the most important additives, is of particular interest. The resulting calcium ferrites are consequentially important slag forming phases. The second industrial field of application of the calcium ferrites is the cement production.

Hardness and magnetic properties of $CaFe_3O_5$ and $CaFe_4O_6$ were reported by [1971Jas]. [1970Kan] measured the magnetic susceptibility of $CaFeO_3$.

Miscellaneous

[1982Mal1] described the kinetics and mechanism of phase formation of calcium ferrites in the temperature range 400 to 900°C.

[1991Har] measured surface tension of melts in the systems FeO-Fe_2O_3-CaO and FeO-Fe_2O_3-2CaO·SiO_2 under air and CO_2 atmosphere in the temperature range 1400-1640°C using the maximum bubble pressure method. A very low temperature dependence of the surface tension in both systems were measured. The surface tension of iron oxide melt under air is 605±7 $mN \cdot m^{-1}$ at 1600°C which suggests that the ferric ion in the iron oxide melt is not surface active, the addition of CaO to the melt decrease the surface tension.

Deoxidation equilibrium of calcium in liquid iron was studied by [1997Ito]. Incomplete expression of the activity of dissolved calcium and oxygen were pointed out and interaction parameters to express the activities were developed.

Optical microscopic investigation of the Ca-Fe-O system is very common method for the characterization of the samples. In earlier times, to etch the minerals an alcoholic hydrofluoric acid solution was used. Later [1960Sno] proposed a method based on etching with an aqueous hydrochloric acid solution which provides separation of six minerals in the polished section by the rate of etching and by the crystal form.

Electronic state of Fe^{4+} ions in perovskite type oxides was investigated by [1983Tak] in the review type Mössbauer effect study. It was reported in the study that the Fe^{4+} ions in $SrFeO_3$ take the high spin state and the electrons are accommodated in the σ* band. When Sr ions are completely replaced by Ca ions to form $CaFeO_3$, the σ* band becomes unstable at 290 K and the Fe^{4+} ions disproportionate into equal numbers of Fe^{3+} and Fe^{5+} ions passing temperature dependent intermediate valance states. [2002Kaw] determined the critical temperatures of the charge disproportionation (CD) and the magnetic order (MO) as a function of pressure. In $CaFeO_3$ the CD ($2Fe^{4+} \rightarrow Fe^{3+}+Fe^{5+}$) occurs at an almost constant temperature of 290 K in the pressure range of 0-17 GPa. Above 20 GPa, the CD is suppressed. The crystal and magnetic

DOI: 10.1007/978-3-540-74196-1_17

structures of $CaFeO_3$ was determined by [2000Woo] at 300 and 15 K using synchrotron X-ray and neutron powder-diffraction techniques. A reasonable fit to the magnetic intensities is seen with the results of [2002Kaw].

Using high temperature X-ray diffraction the structure of molten CaO-Fe_2O_3, with CaO content from 33 to 60 mol%, was studied by [1989Suh]. It is reported that at higher CaO concentrations the iron atoms are found to become more and more tetrahedrally by rather than octahedrally surrounded by oxygens.

[1994Gib] synthesized under high pressure a non-stoichiometric $Ca_2Fe_2O_{5.12}$ and characterized it using Mössbauer spectroscopy. It is reported that at elevated temperature and under high pressure $Ca_2Fe_2O_5$, which contains layers of iron-oxygen octahedra and tetrahedra, takes up additional oxygen. It is also determined in the same study that the Mössbauer spectra in the range 4.2-290 K establish that all the original material was transformed into a new phase which is still structurally related to the original lattice, but features a disordered introduction of oxygen into the tetrahedral layers and oxidation of some of the iron to the +4 oxidation state.

^{119}Sn Mössbauer spectra of tin impurity ions located in the bulk of $Ca_2Fe_2O_5$ particles was investigated over the 77+1070 K temperature range by [2000Min] which allows determining the sign of electric field gradient (EFG) as well as the angle between directions of the main EFG axis and magnetic field induced at ^{119}Sn nuclei. Analysis of the asymmetry of the ^{119}Sn quadrupole doublet at $T > T_N$ showed that the mean-square amplitudes of Sn^{4+} thermal vibrations along the EFG direction are greater than those in the perpendicular direction.

The evolution with pressure of the unit-cell parameters brownmillerite ($Ca_2Fe_2O_5$) was determined to a maximum pressure of 9.46 GPa, by single-crystal X-ray diffraction measurements at room temperature [2002Ros]. No any phase transitions in this pressure range was observed. The stiffest direction (*i.e.* along *a*) coincides with the direction of the FeO_4 tetrahedral chains. Comparison of these data with the elasticity systematics of Ca-perovskites shows that the presence of oxygen vacancies in the brownmillerite structure softens the structure by ~25% and that the ordering of vacancies in the perovskite structure increases the anisotropy of compression.

Synthesis and formation mechanism of calcium ferrite compounds from calcium and iron nitrate were investigated by [2004Sal] using various techniques and it is concluded that the formation mechanism of Ca ferrites depends mainly on the valency of iron cations which in role depends on its molar ratio and the existing atmosphere.

[2002Fuk] studied solid state reaction mechanism of the CaO-FeO system by a diffusion couple method in the temperature range 800-1000°C under controlled oxygen partial pressure. The interdiffusivities and intrinsic diffusivities of Ca^{2+} and Fe^{2+} were reported in the limited FeO solid solution range. The $Ca_2Fe_2O_5$ formed at the interface and grew according to a diffusion-controlled process and simultaneously decomposed at the FeO-$Ca_2Fe_2O_5$ interface because of the dissolution of CaO in the FeO phase. According to the model, the diffusivity of Fe^{3+} in the $Ca_2Fe_2O_5$ phase was estimated at 1000°C.

[2003Kon] proposed a new thermophysicochemical model that reflects the physicochemical structure of the slag. Liquidus surface of “lime ferrite” slag at intermediate oxygen potentials was modeled and effect of silica and Cu_2O was investigated.

DOI: 10.1007/978-3-540-74196-1_17

Table 1. Investigations of the Ca-Fe-O Phase Relations, Structures and Thermodynamics

Reference	Method/Experimental Technique	Temperature/Composition/Phase Range Studied
[1929Sch]	Controlled oxygen partial pressure	Influence of CaO in oxide formation
[1934Mar]	Thermal analysis and optical microscopy	Liquidus surface and 10 vertical sections.
[1936Tav]	Optical microscopy	Fe_2O_3 rich part of the CaO-Fe_2O_3 section
[1937Sch]	Reaction synthesis of Fe_2O_3CaO	900°C, 5 ternary phases were reported and partial isothermal section was constructed.
[1939Cro]	Optical microscopy, chemical analysis	Fe-Fe_2O_3-CaO
[1946Pet]	XRD	Solubility of CaO in FeO
[1947Cir]	XRD, magnetic measurements	reduction equilibrium of $Ca_2Fe_2O_5$ at 1100°C
[1950Gur]	Controlled oxygen partial pressure	1600°C / isothermal section CaO-FeO-Fe_2O_3
[1952Bur]	Controlled oxygen partial pressure, XRD	600-1050°C, CaO-FeO-Fe_2O_3 system.
[1952Cir]	XRD	reduction equilibria of calcium ferrite from 680°C to 1050°C
[1953Lar]	Controlled oxygen partial pressure	1550°C / 10^{-1}-10^{-10} atm.
[1954Kin]	Calorimetry	Heat capacity measurement of $Ca_2Fe_2O_5$ and $CaFe_2O_4$
[1954Bon]	Calorimetry	High temperature heat content of $Ca_2Fe_2O_5$ and $CaFe_2O_4$
[1954Bur]	Controlled oxygen partial pressure XRD, optical microscopy	CaO-Fe-Fe_2O_3 system
[1955All]	XRD, optical microscopy, chemical analysis	CaO-FeO quasibinary section
[1955Tro]	XRD, optical microscopy	Solubility of CaO in FeO up to 50 mass% CaO
[1956New]	Solution calorimetry	Heats of solution
[1957Dec]	XRD	Crystal structure of $CaFe_2O_4$
[1958Eds]	Controlled oxygen partial pressure	Description of reactions
[1958Phi]	XRD, optical microscopy, chemical analysis	CaO-Fe_2O_3 quasibinary section in air and 1 bar O_2 atmosphere
[1960Bur]	XRD, optical microscopy	$3CaO{\cdot}7Fe_2O_3$ - $4CaO{\cdot}FeO{\cdot}9Fe_2O_3$ - Fe_3O_4 section
[1960Hol]	XRD	Two new compounds with unclear compositions
[1960Phi]	XRD, optical microscopy	1130-1408°C / liquidus section Fe_2O_3 rich side 1135-1230°C isothermal section

(*continued*)

DOI: 10.1007/978-3-540-74196-1_17

Reference	Method/Experimental Technique	Temperature/Composition/Phase Range Studied
[1961Koe]	Calorimetry	Heat and free energy of formation of $CaFe_2O_4$, and $Ca_2Fe_2O_5$
[1961Tur]	Calculation	activity of CaO, FeO, Fe_2O_3
[1962Che]	XRD	Lattice constants of $CaFe_4O_7$
[1963Leo]	XRD	Homogeneity range of $CaFe_2O_4$ and $Ca_2Fe_2O_5$
[1967Bra]	Adiabatic calorimetry	Formation of $CaFe_2O_4$ and $Ca_2Fe_2O_5$ at 500-1200°C
[1967Buz]	Calculation	Reaction coefficients of O
[1967Hug]	XRD, optical microscopy	Powder diffraction data of $CaFe_2O_4$, $Ca_2Fe_2O_5$ and $CaFe_4O_7$
[1967Per]	XRD, Controlled oxygen partial pressure	700-1200°C, Solubility CaO in FeO and FeO in CaO, reduction of $Ca_2Fe_2O_5$ and $CaFe_2O_4$.
[1967Rez]	Galvanic cell	Thermodynamic Properties of $CaFe_2O_4$ and $Ca_2Fe_2O_5$
[1967Ree1] [1967Ree2]	XRD, hot stage optical microscopy	1085°C isothermal section, CaO-FeO-Fe_2O_3. liquidus surface.
[1969Duf]	Thermal analysis	Gibbs enthalpies of formation of $CaFe_3O_5$, $CaFe_2O_4$, $CaFe_5O_7$
[1970Aub]	XRD	Solid solution of CaO in FeO between 800-1130°C
[1970Kan]	Phase synthesis, XRD, Mössbauer spectroscopy	Lattice parameter and magnetic properties of $CaFeO_3$
[1970Nek]	XRD, optical microscopy	Variation of lattice parameters in Fe_xO up to 20% CaO
[1970Tim]	XRD, optical microscopy	Isothermal section CaO-FeO-Fe_2O_3 at 1450°C schematic iso-oxygen activity curves
[1971Apo]	Neutron diffraction	crystal structure of $Ca_2Fe_2O_4$
[1971Ber]	XRD	crystal structure of $Ca_2Fe_2O_5$
[1971Iml]	Optical microscopy	subsolidus phase relations
[1971Jas]	Optical and electron microscopy, XRD, microhardness, magnetic measurement	Crystallization of $CaFe_3O_5$ in self fluxing agglomerates.
[1971Miy]	Deoxidation with Ca	Ca solubility in liquid iron at 1600°C
[1972Lyk]	emf	limit solubility of CaO in wustite
[1973Abb1]	XRD, optical microscopy	1100°C / CaO-Fe-FeO-$CaFe_2O_5$
[1973Abb2]	emf	equilibria between FeO, Fe, CaO and $Ca_2Fe_2O_5$

(*continued*)

DOI: 10.1007/978-3-540-74196-1_17

Reference	Method/Experimental Technique	Temperature/Composition/Phase Range Studied
[1973Reg]	Mössbauer spectroscopy	77-300 K / CaO doped by Fe
[1973Sch]	Controlled oxygen partial pressure	10 isothermal section 565-1060°C
[1974Abb]	Gas chromatography	850-1100°C, Fe-Fe_2O_3, Fe-CaO stability.
[1974Sch]	Test heating of slags	Saturations isotherms
[1975Abb]	Spectrometic and microscopic analysis	activity in FeO up to 0.4 at.%CaO
[1975Tar]	XRD, emf, chemical analysis	lattice parameters and solubility of CaO in FeO
[1976Lyk]	emf	800-1100°C, CaO-$Ca_2Fe_2O_5$-Fe-Fe_3O_4
[1976Mus]	XRD	700-1000°C / $CaFe_2O_4$, $CaFe_3O_5$, $Ca_2Fe_2O_5$, $CaFe_5O_7$
[1976Oto]	Deoxidation	Ca solubility in liquid iron at 1600°C
[1976Sch1]	thermal analysis, optical microscopy	CaO-Fe_2O_3 diagram
[1976Sch2]	thermal analysis	liquidus surface and 2 vertical sections
[1976Sch3]	thermal analysis, optical microscopy	CaO-FeO diagram, partial liquidus surface
[1976Sch4]	review, calculation	partial pressure diagrams, between FeO-Fe_2O_3
[1978Spe]	Calphad calculation	CaO-FeO phase diagram
[1979Kau]	Calphad calculation	CaO-Fe_2O_3 phase diagram
[1979Shi]	XRD	Catalytic decomposition of $Ca_2Fe_2O_5$
[1979Ute]	Calculation	Thermodynamic properties
[1980Ban] [1980Ban]	Controlled oxygen partial pressure	Activity of FeO in Fe_xO-CaO section at 1400°C
[1980Evr]	XRD	Crystal structure of $CaFe_3O_5$, $CaFe_4O_6$ and $CaFe_5O_7$ at 1125°C
[1980Gus1] [1980Gus2]	Chemical analysis using atomic absorption method	Equilibrium constant between CaO and Fe at 1600°C
[1980Har]	XRD	Crystal structure, $Ca_2Fe_2O_5$
[1980Lyk]	emf	Phase relations Fe-Fe_3O_4-CaO
[1980Tak1]	Spectrophotometric titration, optical microscopy	Oxygen isobars and liquidus isotherms at 1200 and 1300°C
[1980Tak2]	Controlled oxygen partial pressure	Activities of CaO and FeO at 1200-1300°C
[1981Bur]	emf	CaO-FeO-Fe_2O_3, quasiternary system at 900 and 1125°C
[1981Lyk]	emf	850-1050°C, CaO-Fe-Fe_3O_4 phase relations
[1981Mal]	XRD	Crystal structures of $Ca_2Fe_9O_{13}$ and $Ca_2Fe_7O_{11}$

(*continued*)

DOI: 10.1007/978-3-540-74196-1_17

Reference	Method/Experimental Technique	Temperature/Composition/Phase Range Studied
[1981Tak]	Controlled oxygen partial pressure	Liquidus isotherms
[1981Yaz]	HT-XRD, calculation	1200-1300°C, liquidus surfaces, isoactivity curves, FeO-Fe_2O_3-CaO
[1982Bau]	XRD	Crystal structures of $CaFe_3O_5$, $CaFe_4O_6$, $CaFe_5O_7$
[1982Mal1]	XRD	Crystal structures of $Ca_4Fe_9O_{17}$
[1982Mal2]	XRD, Mössbauer spectroscopy	400-900°C. Kinetic of phase formation of C_2F, CF and CF_2
[1983Ara]	XRD	Crystal structures of $Ca_{2.95}Fe_{14.85}O_{25}$
[1983Lyk]	XRD, emf	800-1100°C / CaO-$Ca_2Fe_2O_5$-Fe-Fe_3O_4
[1983Mod]	XRD, microstructural and chemical analysis, EPMA	1130-1210°C / CaO+$2Fe_2O_3$ /
[1984Bjo]	emf, calculation	Activities in CaO-FeO liquid between 667-1105°C
[1984Har1] [1984Har2]	Galvanic cell	Activities at 1500°C
[1984Iwa]	Galvanic cell	Activities in CaO-Fe_xO liquid at 1400°C
[1984Vid]	Thermal decomposition, XRD	d-values for $Ca_2FeO_{3.5}$
[1985Igu]	Controlled oxygen partial pressure	1000-1200°C, activities of CaO in FeO
[1985Kar]	XRD	Crystal structure of CCF
[1985Kul]	Deoxidation of Iron by Ca	Isotherm of oxygen in iron at 1600°C
[1986Ber]	Diffusion couples	Vertical sections CaO-Fe_2O_3
[1986Mil]	XRD	Isothermal section Fe_3O_4-Fe_2O_3-$CaFe_2O_4$-$CaFe_3O_5$ at 1200°C
[1986Nad]	Controlled oxygen partial pressure	Solution product of Ca and O in liquid steel at 1600°C
[1986Sha]	emf	Free energy of formation of $Ca_2Fe_2O_5$ at 727°C
[1987Ara]	XRD	Crystal structure of $Ca_{3.0}Fe_{14.82}O_{25}$ (γCFF)
[1987Kar]	XRD	Crystal structure of $Ca_{3.0}Fe_{14.82}O_{25}$ (αCFF)
[1987Raj]	emf	Gibbs energy of formation of $Ca_2Fe_2O_5$
[1988Ara]	XRD	Crystal structures of 3 polytypes of CFF
[1988Bag]	Calculation	Enthalpy of oxides
[1988Ber]	SEM, EDX	1050-1100°C / CaO-FeO, decomposition FeO
[1988Chu]	emf measurements	C_2F-CW_3F-W equilibria between 1000-1100°C

(*continued*)

DOI: 10.1007/978-3-540-74196-1_17

Reference	Method/Experimental Technique	Temperature/Composition/Phase Range Studied
[1988Dob]	Calculation	Activity of Ca
[1988Han]	XRD, infrared and mass spectrometry, chemical analysis	1600°C / Fe-Ca-O equilibria in molten iron
[1988Ota]	XRD	Solubility of Fe
[1988Wan]	Controlled oxygen partial pressure	Equilibrium constant at 1600°C
[1989Ber]	Optical microscopy	Congruent melting of $CaFe_5O_7$ at ~1100°C
[1989Bog]	Calculation	Equilibrium constant 1600°C
[1989Sel]	Calphad calculation	Isothermal section and isopleths
[1989Suh]	HT-XRD	Structure of CaO solid solution in FeO and some viscosity data.
[1989Zha]	XRD, microstructural analysis, nuclear γ-resonance spectrometry	1000-1100°C / CaO-FeO
[1990Hil]	Calphad calculation	Isothermal section and isopleths
[1990Raj]	emf	323-723°C, free energy of formation of $CaFe_2O_4$
[1990Rez]	Calculation	Enthalpy of formation of $Ca_2Fe_2O_5$
[1991Har]	Bubble pressure method	1400-1640°C, surface tension of melt
[1993Sch]	Isothermal reduction test	900°C isothemal section, reduction diagrams
[1993Wu]	Assessment and calculation	CaO-FeO system
[1994Cho]	Calculation	Activities and equilibrium constants
[1994Gib]	Mössbauer spectral analysis	Atomic coordination of $Ca_2Fe_2O_5$
[1994Kim]	Controlled oxygen partial pressure	Partial pressure of oxygen over iron melts with CaO
[1995Fuj]	Chemical analysis, gas chromatography	1550°C, solubility and activity of Ca and O in CaO-Ca-O alloy-molten Fe under variable calcium potential.
[1995Jow1, 1995Jow2]	Calculation	Equilibrium constants
[1995Lyk]	XRD	800-1100°C, solid solution between CW_3F-CW_4F
[1996Sel]	Calphad assessment	Reassessment of the Ca-Fe-O system
[1997Elg]	XRD, chemical analysis, optical microscopy, pore size	900-1200°C, effect of CaO on reduction of Fe_2O_3
[1997Ito]	Deoxidation equilibrium	1600-1750°C, Ca and O solubility in liquid iron
[1998Elg]	Reduction test	Effect of CaO on reducibility of Fe_2O_3

(*continued*)

DOI: 10.1007/978-3-540-74196-1_17

Reference	Method/Experimental Technique	Temperature/Composition/Phase Range Studied
[1999Bel]	Calculation	CaO-FeO
[1999Gom]	XRD	Crystal structure of $Ca_2Fe_2O_5$
[1999Jac]	emf	700-1000°C / $CaFe_2O_4$, $Ca_2Fe_2O_5$
[2000Min]	Mössbauer spectral analysis	77-1070 K / $Ca_2Fe_2O_5$
[2000Woo]	Synchrotron x-ray and neutron powder-diffraction techniques	Crystal and magnetic structures of $CaFeO_3$ at 300 and 15 K
[2001Bel]	Calculation	1600°C, CaO-FeO system
[2001Ber]	Calculation	Oxygen diffusion on $CaFeO_3$
[2002For]	emf, XRD	777-1077°C, Gibbs energy of formation of $CaFe_2O_4$ and $Ca_2Fe_2O_5$ from oxides
[2002Fuk]	Diffusion couple, SEM	800-1000°C, interdiffusivity and intrinsic diffusivities of Ca^{2+} and Fe^{2+} in the limited FeO solid solution range
[2002Ina]	XRD	1000°C, lattice parameter change of FeO depending on CaO concentration
[2002Kaw]	Mössbauer spectroscopy	5-304 K high pressure studies of $CaFeO_3$
[2002Ros]	Single crystal XRD, SEM, EPMA, Mössbauer spectroscopy	Pressure dependence of $Ca_2Fe_2O_5$
[2004Fre]		1550-1600°C activity of FeO in CaO

Table 2. Crystallographic Data of Solid Phases

Phase/ Temperature Range [°C]	Pearson Symbol/ Space Group/ Prototype	Lattice Parameters [pm]	Comments/References
(βCa) 842 - 443	*cI*2 *Im*$\bar{3}$*m* W	a = 448.0	[Mas2]
(αCa) < 443	*cF*4 *Fm*$\bar{3}$*m* Cu	a = 558.84	at 25°C [Mas2]
(δFe) (h_2) 1538 - 1394	*cI*2 *Im*$\bar{3}$*m* W	a = 293.15	[Mas2]
(γFe) (h_1) 1394 - 912	*cF*4 *Fm*$\bar{3}$*m* Cu	a = 364.67	at 915°C [V-C2, Mas2]

(*continued*)

DOI: 10.1007/978-3-540-74196-1_17

Phase/ Temperature Range [°C]	Pearson Symbol/ Space Group/ Prototype	Lattice Parameters [pm]	Comments/References
(αFe) < 912	*cI*2 $Im\bar{3}m$ W	*a* = 286.65	at 25°C [Mas2]
(εFe)	*hP*2 $P6_3/mmc$ Mg	*a* = 246.8 *c* = 396.0	at 25°C, 13 GPa [Mas2]
CaO > 2613 (C)	*cF*8 $Fm\bar{3}m$ NaCl	*a* = 480.96	[1985Wri]
CaO_2	*tI*6 *I*4/*mnm* CaC_2	*a* = 356.0 *c* = 595.0	[1985Wri]
$Fe_{1-x}O$ < 912 Wustite (W)	*cF8* $Fm\bar{3}m$ NaCl	*a* = 431.0 *a* = 429.3	*x* = 0.05, *x* = 0.12 [V-C2] 51.15 to 54.6 at.% O dissolves is equal to 9.5 mol% CaO at 850°C and to 29 mol% CaO at 1050°C [1980Lyk]
αFe_2O_3 >1457 Hematite (F)	*hR*30 $R\bar{3}c$ Al_2O_3	*a* = 503.47 *c* = 1367.73	[V-C2]
βFe_2O_3 (l)	*cI*80 $Ia\bar{3}$ Mn_2O_3	*a* = 939.3	[V-C2], low temperature or metastable
γFe_2O_3	*tP*56 $P4_12_12$ Mn_5Si_2	*a* = 833.96 *c* = 832.21	[V-C2], low temperature or metastable
εFe_2O_3 (l)	*m**100	*a* = 1297 *b* = 1021 *c* = 844 β = 95.32°	[V-C2], low temperature or metastable
Fe_3O_4 (LT) > 580	*mC*224 *Cc* Fe_3O_4	-	[Mas2]
Fe_3O_4 1596 - 580 Magnetite (WF)	*cF*56 $Fd\bar{3}m$ Al_2MgO_4	*a* = 841.1	[V-C2], 57.1 - 58.0 at.% O

(*continued*)

DOI: 10.1007/978-3-540-74196-1_17

Phase/ Temperature Range [°C]	Pearson Symbol/ Space Group/ Prototype	Lattice Parameters [pm]	Comments/References
Fe_3O_4 (l)	*oP*56 *Pbcm* Fe_3O_4(LT)	*a* = 1186.8 *b* = 1185.1 *c* = 1675.2	at 10 K [V-C2]
Fe_3O_4(HP)	*m**14	-	Stable at pressures >25 GPa
* $Ca_2Fe_2O_5$ (C_2F)	*oP*36 *Pnma* $Ca_2Al_2O_5$	*a* = 542.68 *b* = 1476.31 *c* = 559.69	[2004Red]
* $CaFe_2O_4$ (CF)	*oP*28 *Pnma*	*a* = 923.0 *b* = 1070.5 *c* = 302.4	[1957Dec]
* $CaFe_4O_7$ (CF_2)	*mC** *C*2	*a* = 1040.9 *b* = 600.5 *c* = 316.4 β = 96.5°	[1986Mil]
* $CaFe_3O_5$ (CWF)	*oC*36 *Cmcm*	*a* = 302.1 *b* = 1000.9 *c* = 1264.3	[1980Evr]
* $CaFe_4O_6$ (CW_2F)	*oC*44 *Cmcm*	*a* = 305.0 *b* = 998.6 *c* = 1532.1	[1980Evr]
* $CaFe_5O_7$ (CW_3F)	*oC*52 *Cmcm*	*a* = 305.2 *b* = 1004.1 *c* = 1796.6	[1980Evr] solid solution to $CaFe_6O_8$ [1995Lyk]
* $Ca_4Fe_9O_{17}$ (C_4WF_4)	*mC*60 *C*2	*a* = 1044.1 *b* = 602.5 *c* = 1138.4 β = 98.8°	[1982Mal1]
* $Ca_4Fe_{17}O_{29}$ (C_4WF_8)	-	-	[1986Mil]
* $CaFe_4O_{6.95}$	-	-	[1986Mil]
* $CaFe_4O_{6.86}$	-	-	[1986Mil]
* $\alpha Ca_3Fe_{15}O_{25}$ (C_3WF_7) (αCFF)	*R*32	*a* = 601.1 *c* = 9469.0	[1988Ara], [1985Kar]
* $\beta Ca_3Fe_{15}O_{25}$ (C_3WF_7) (βCFF)	$P\bar{3}c1$	*a* = 598.6 *c* = 3138.8	[1988Ara], [1983Ara]
* $\gamma Ca_3Fe_{15}O_{25}$ (C_3WF_7) (γCFF)	*P*321	*a* = 598.5 *c* = 1574.8	[1988Ara], [1987Ara]

(*continued*)

DOI: 10.1007/978-3-540-74196-1_17

Phase/ Temperature Range [°C]	Pearson Symbol/ Space Group/ Prototype	Lattice Parameters [pm]	Comments/References
* $Ca_2Fe_9O_{13}$ ($C_2W_5F_2$)	*mC*48 *C*2/*m*	*a* = 1002.2 *b* = 304.7 *c* = 1687.7 β = 99.2°	[1981Mal]
* $Ca_2Fe_7O_{11}$ ($C_2W_3F_2$)	*mC*40 *C*2/*m*	*a* = 996.0 *b* = 303.0 *c* = 1577.0 β = 118°	[1981Mal]
* $CaFeO_3$(HP)	perovskite	*a* = 377.0	[1970Kan] High temperature, high pressure phase
* $CaFeO_3$	*Pbnm* $GdFeO_3$	*a* = 553.26 *b* = 553.52 *c* = 575.39	at 300 K [2000Woo]
	*P*21/*n*	*a* = 553.11 *b* = 553.47 *c* = 575.20 β = 90.065°	at 15 K [2000Woo]

Table 3. Invariant Equilibria

Reaction	*T* [°C]	Type	Phase	Composition (mass%)		
				CaO	FeO	Fe_2O_3
L + αFe_2O_3 + Fe_3O_4 ⇌ $Ca_4Fe_{17}O_{29}$	1230	P_1	L	17.0	3.5	79.5
L + αFe_2O_3 ⇌ $CaFe_4O_7$ + $Ca_4Fe_{17}O_{29}$	1220	U_1	L	18.5	2.5	79.0
L + Fe_3O_4 + $Ca_2Fe_2O_5$ ⇌ $Ca_4Fe_9O_{17}$	1212	P_2	L	23.0	5.0	72.0
L + $Ca_2Fe_2O_5$ ⇌ $CaFe_2O_4$ + $Ca_4Fe_9O_{17}$	1210	U_2	L	23.0	2.0	75.0
L ⇌ $CaFe_4O_7$ + $CaFe_2O_4$ + $Ca_4Fe_9O_{17}$	1200	E_1	L	19.5	2.0	78.5
L + $Ca_4Fe_9O_{17}$ ⇌ $CaFe_2O_4$ + Fe_3O_4	1197	U_3	L	20.0	4.0	76.0
L ⇌ $CaFe_2O_4$ + Fe_3O_4 + $Ca_4Fe_{17}O_{29}$	1194	E_2	L	19.5	3.5	77.0
L + Fe_3O_4 ⇌ $Ca_2Fe_2O_5$ + $CaFe_3O_5$	1189	U_4	L	18	25	56
L + Fe_3O_4 ⇌ FeO + $CaFe_3O_5$	1150	U_5	L	18	27	55

(*continued*)

DOI: 10.1007/978-3-540-74196-1_17

Reaction	T [°C]	Type	Phase	Composition (mass%)		
				CaO	FeO	Fe_2O_3
L + (Fe) ⇌ FeO + CaO	1130	U_6	-	-	-	-
L + CaO ⇌ FeO + $Ca_2Fe_2O_5$	1115	U_7	L	23	50	27
L ⇌ FeO + $Ca_2Fe_2O_5$ + $CaFe_3O_5$	1110	E_3	L	23	22	55

Table 4. Thermodynamic Properties of Single Phases

Phase	Temperature Range [°C]	Property, per mole of atoms [J, mol, K]	Comments
$CaFe_5O_7$	703 - 1059	$\Delta_f G°(CaFe_5O_7) = -2242.084\ 10^3 + 127.086\ T + 53.853\ T\ln(T)$ J·mol^{-1}	Gibbs energy of formation from oxides [1984Bjo]
$CaFe_3O_5$	703 - 1059	$\Delta_f G°(CaFe_3O_5) = -1826.311\ 10^3 + 487.8703T$ J·mol^{-1}	Gibbs energy of formation from oxides [1984Bjo]
	827 - 1077	$\Delta_f G°(CaFe_3O_5) = -63.05\ 10^3 + 40.759\ T$ (±700) J·mol^{-1}	Gibbs energy of formation from CaO and Fe_3O_4 [1995Lyk]
$CaFe_6O_8$	827 - 1077	$\Delta_f G°(CaFe_6O_8) = -17.82\ 10^3 + 19.422\ T$ (±350) J·mol^{-1}	Gibbs energy of formation from $CaFe_3O_5$ and FeO [1995Lyk]
$Ca_2Fe_2O_5$	867 - 1067	$\Delta_f G°(Ca_2Fe_2O_5) = -2049.9\ 10^3 - 12.84\ T + 55.91\ T\ln(T)$ (±2800) J·mol^{-1}	Gibbs energy of formation from oxides [2002For]
$Ca_2Fe_2O_5$	703 - 1059	$\Delta_f G°(Ca_2Fe_2O_5) = -2091.01\ 10^{-3} + 236.36\ T + 25.35\ T\ln(T)$ J·mol^{-1}	Gibbs energy of formation from oxides [1984Bjo]
	702 - 1002	$\Delta_f G°(Ca_2Fe_2O_5) = -45.280\ 10^3 - 13.51\ T$ (±275) J·mol^{-1}	Gibbs energy of formation from oxides [1999Jac]
	727	$\Delta_f G°(Ca_2Fe_2O_5) = -47.8$ (±5.5) 10^3 J· mol^{-1}	Gibbs energy of formation from oxides [1963Ell]
	727	$\Delta_f G°(Ca_2Fe_2O_5) = -46.4$ (±5.0) 10^3 J· mol^{-1}	Gibbs energy of formation from oxides [1986Sha]
	25	$\Delta_f H°(Ca_2Fe_2O_5) = -2071.4$ kJ·mol^{-1}	Enthalpy of formation [1987Raj]
	427 - 727	$\Delta_f G_T(Ca_2Fe_2O_5) = -2259.3 + 0.2187\ T$ kJ·mol^{-1}	Gibbs energy of formation [1987Raj]

(*continued*)

DOI: 10.1007/978-3-540-74196-1_17

Phase	Temperature Range [°C]	Property, per mole of atoms [J, mol, K]	Comments
	427 - 727	$\Delta_f G_T(Ca_2Fe_2O_5) = -2283.4 + 0.5864\ T$ kJ·mol^{-1}	Gibbs energy of formation [1987Raj]
	25	$\Delta_f H°(Ca_2Fe_2O_5) = -44.14$ kJ·mol^{-1}	Enthalpy of formation from oxides [1961Koe]
	1550	$\Delta_f G°(Ca_2Fe_2O_5) = -76.567\ (\pm 4.0)\ 10^3$ J·mol^{-1}	Gibbs energy of formation from oxides [1961Tur]
	25	$\Delta_f H°(Ca_2Fe_2O_5) = -44.6$ kJ·mol^{-1}	Enthalpy of formation from oxides [1990Rez]
	927 827 - 1077 827 - 1077	 $\Delta_f G°(Ca_2Fe_2O_5) = -58.98$ kJ·mol^{-1} $\Delta S°(Ca_2Fe_2O_5) = 23.0$ J·mol^{-1}·K^{-1} $\Delta H°(Ca_2Fe_2O_5) = -31.58$ kJ·mol^{-1}	Thermodynamic properties from oxides [1967Rez]
	25	$\Delta H°(Ca_2Fe_2O_5) = 32993$ J·mol^{-1}	Adiabatic calorimetry [1967Bra]
	51 - 298 K	$S_{298}(Ca_2Fe_2O_5) = 188.69$ J·mol^{-1}·K^{-1}	Adiabatic calorimetry [1954Kin]
	51 - 298 K	C_p	Adiabatic calorimetry [1954Kin]
	25	$\Delta_f H°(Ca_2Fe_2O_5) = -61.856$ kJ·mol^{-1}	Heat of formation from oxides [1956New]
$CaFe_2O_4$	757 - 1007	$\Delta_f G°(CaFe_2O_4) = -1448.4\ 10^3 + 128\ T + 27.95\ T \ln(T)\ (\pm 1800)$ J·mol^{-1}	Gibbs energy of formation from oxides [2002For]
	25	$\Delta H°(CaFe_2O_4) = -17500\ (\pm 400)$ J·mol^{-1}	The standard enthalpy of formation from oxides [2002For]
	702 - 1002	$\Delta_f G°(CaFe_2O_4) = -37.48\ 10^3 + 1.16\ T\ (\pm 250)$ J·mol^{-1}	Gibbs energy of formation from oxides [1999Jac]
	25	$\Delta H°(CaFe_2O_4) = -61086$ J·mol^{-1}	Heat of formation from oxides [1961Koe]
	330 - 730	$\Delta_f G°(CaFe_2O_4) = -642.0\ 10^3 + 0.055\ T$ J·mol^{-1}	Gibbs energy of formation from oxides [1990Raj]
	927 827 - 1077	$\Delta_f G°(CaFe_2O_4) = -35.47$ kJ·mol^{-1} $\Delta S°(CaFe_2O_4) = 4.81$ J·mol^{-1}·K^{-1}	

(*continued*)

DOI: 10.1007/978-3-540-74196-1_17

Phase	Temperature Range [°C]	Property, per mole of atoms [J, mol, K]	Comments
	827 - 1077	$\Delta H°(CaFe_2O_4) = -29.69$ kJ·mol^{-1}	Thermodynamic properties from oxides [1967Rez]
	25	$\Delta H°(CaFe_2O_4) = -22769$ J·mol^{-1}	
	51 - 298 K	C_p	Adiabatic calorimetry [1967Bra]
	51 - 298 K	$S_{298}(CaFe_2O_4) = 145.18$ J·mol^{-1}·K^{-1}	Adiabatic calorimetry [1954Kin]
			Adiabatic calorimetry [1954Kin]

Table 5. Vapor Pressure Measurements

Phase(s)	Temperature [°C]	Pressure –log pO_2 [Pa]	Comments
Fe + CaO + $Ca_2Fe_2O_5$	897	12.118	[1995Lyk]
		12.155	[1967Per]
		12.165	[1981Bur]
		12.219	[1988Chu]
Fe + FeO + $Ca_2Fe_2O_5$		11.837	[1995Lyk]
		11.777	[1967Per]
		11.855	[1981Bur]
		11.901	[1988Chu]
$Ca_2Fe_2O_5$ + $CaFe_6O_8$ + FeO		11.463	[1995Lyk]
		11.328	[1967Per]
		11.405	[1981Bur]
		11.230	[1988Chu]
$Ca_2Fe_2O_5$+$CaFe_6O_8$+ $CaFe_3O_5$		10.742	[1995Lyk]
		10.984	[1967Per]
		10.935	[1981Bur]
		10.742	[1988Chu]
Fe_3O_4 + $CaFe_3O_5$ + FeO		9.857	[1995Lyk]
		9.953	[1967Per]
		9.862	[1988Chu]

DOI: 10.1007/978-3-540-74196-1_17

Table 6. Monovariant Equilibria in the Ca-Fe-O System in the Temperature Range of 839-1057°C. ($\log p_{O2}$ [Pa] = –A/T + B)

Equilibrium	A	B	Comments
$Fe_3O_4 + FeO + CaFe_3O_5$	33410	18.62	[1981Lyk,
$Ca_2Fe_2O_5 + CaFe_6O_8 + CaFe_3O_5$	32700	17.13	1995Lyk]
$Ca_2Fe_2O_5 + FeO + CaFe_6O_8$	34730	18.14	
$Ca_2Fe_2O_5 + Fe + FeO$	26700	10.92	
$Ca_2Fe_2O_5 + Fe + CaO$	29810	13.29	

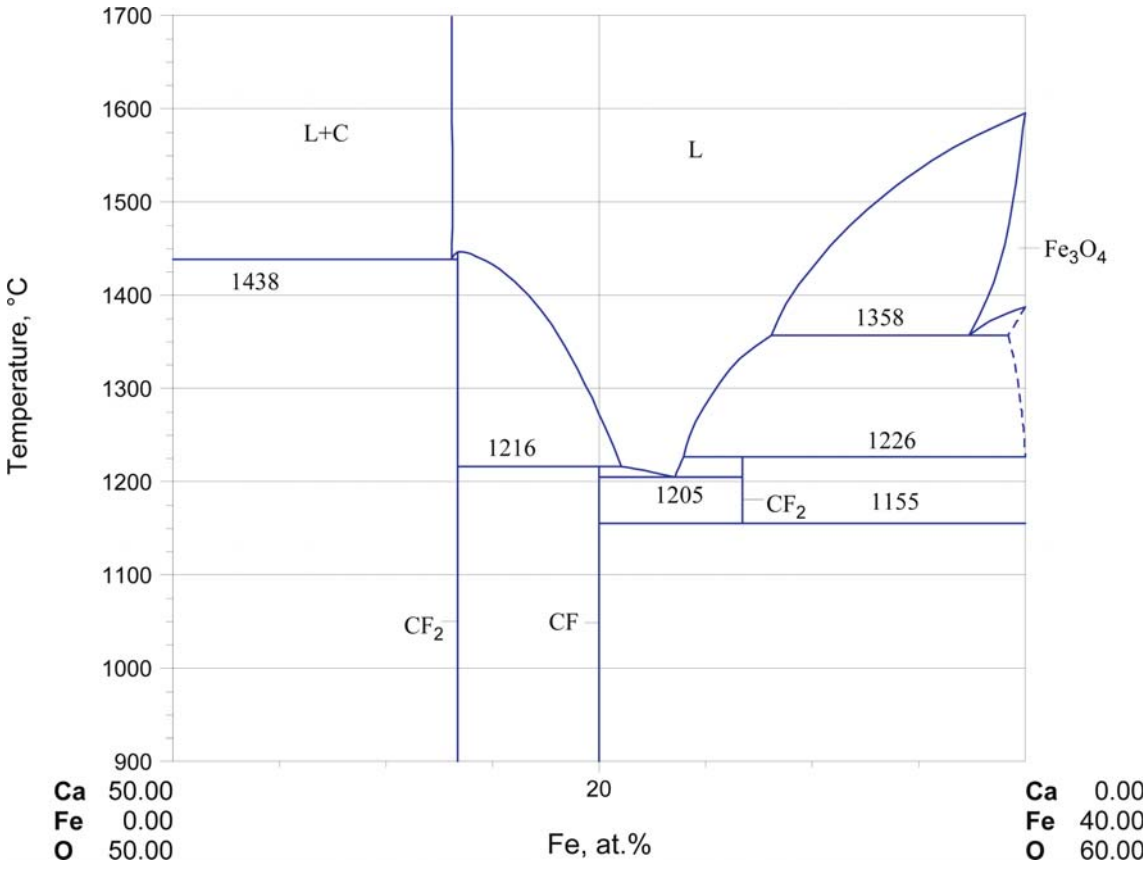

Fig. 1. Ca-Fe-O. The quasibinary section along Fe_2O_3-CaO in air

DOI: 10.1007/978-3-540-74196-1_17

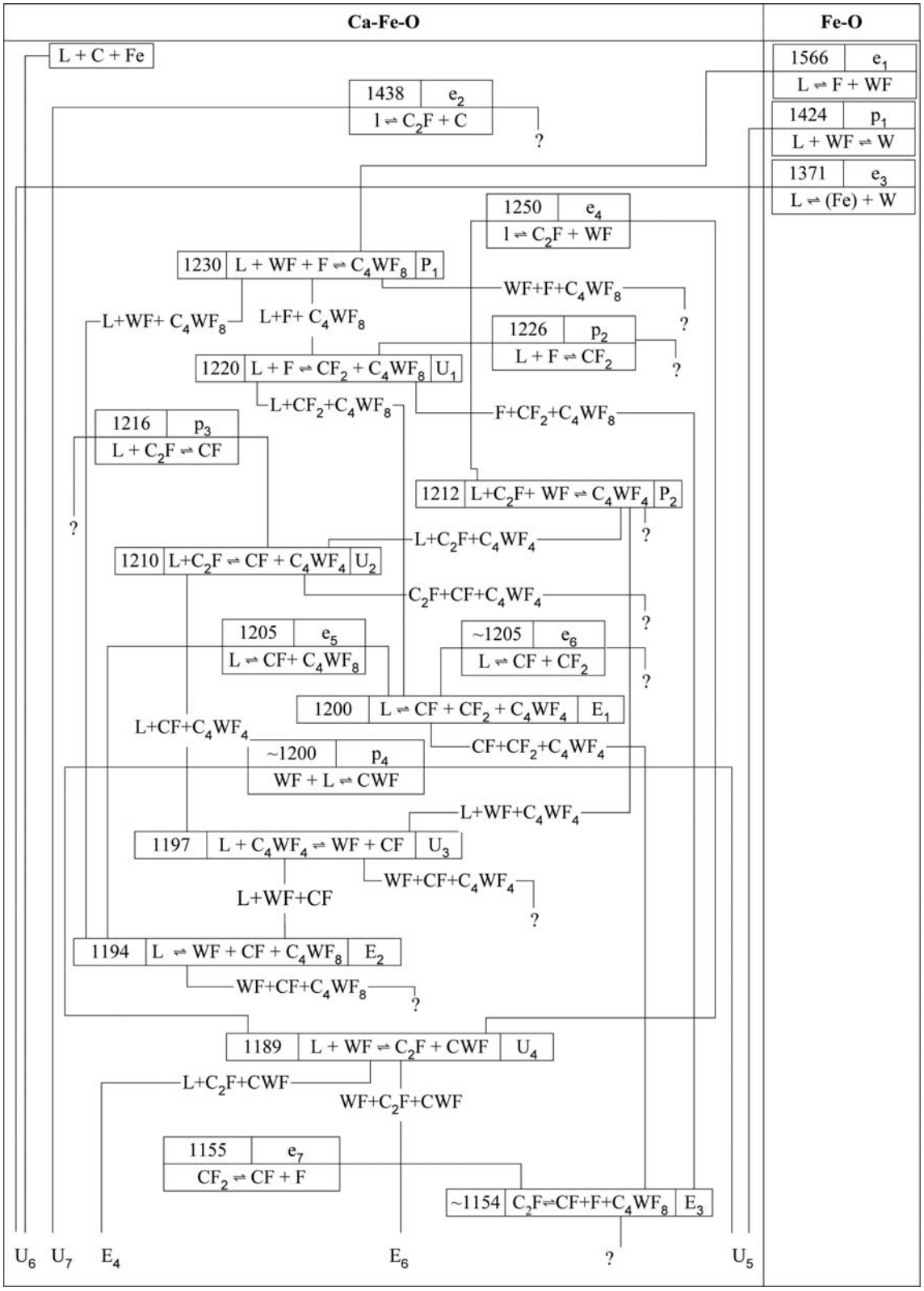

Fig. 2a. Ca-Fe-O. Partial reaction scheme for the Fe-Fe_2O_3-CaO region

DOI: 10.1007/978-3-540-74196-1_17

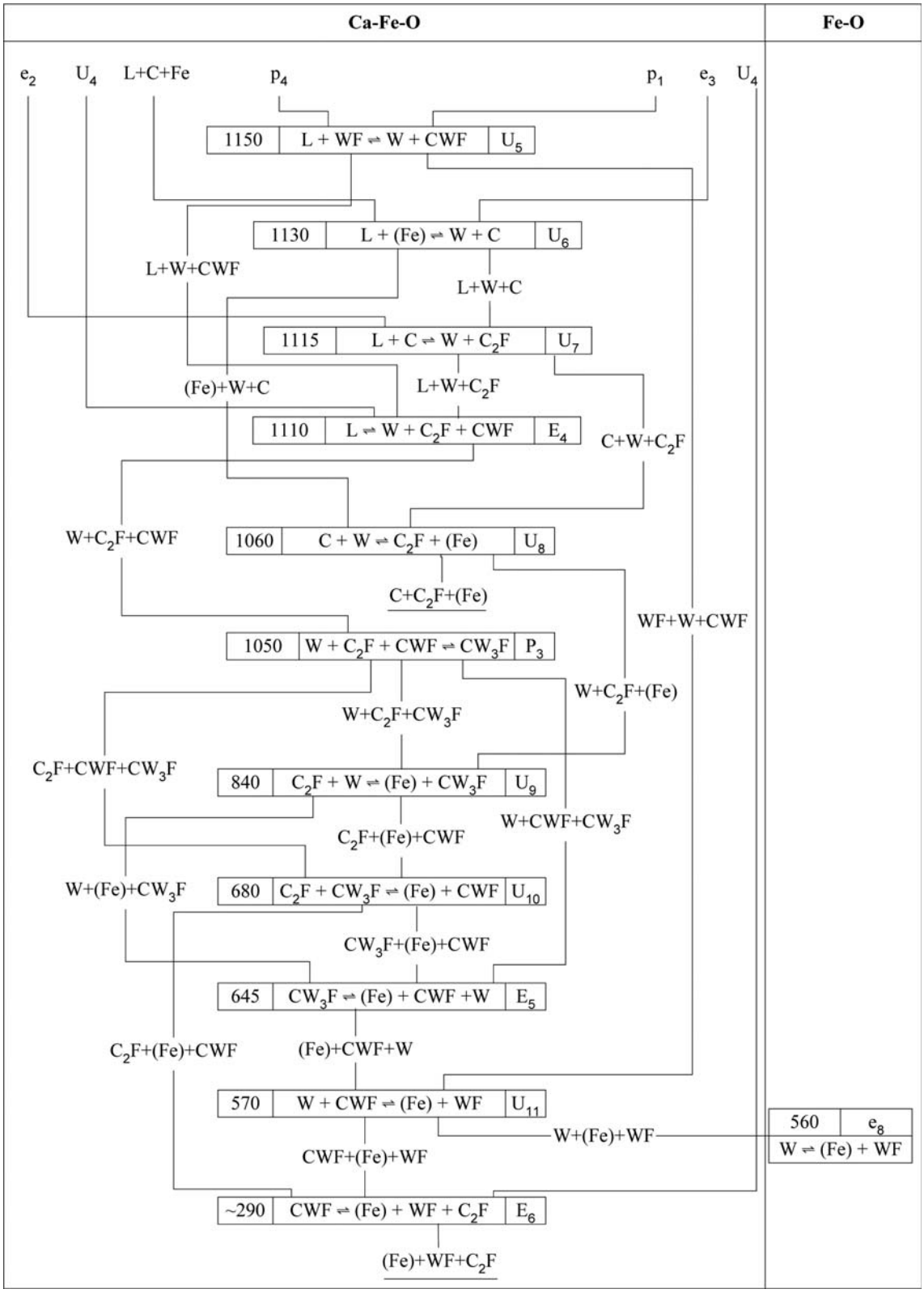

Fig. 2b. Ca-Fe-O. Partial reaction scheme for the Fe-Fe_2O_3-CaO region. C = CaO; W = FeO (Wustite); F = Fe_2O_3; WF = Fe_3O_4

DOI: 10.1007/978-3-540-74196-1_17

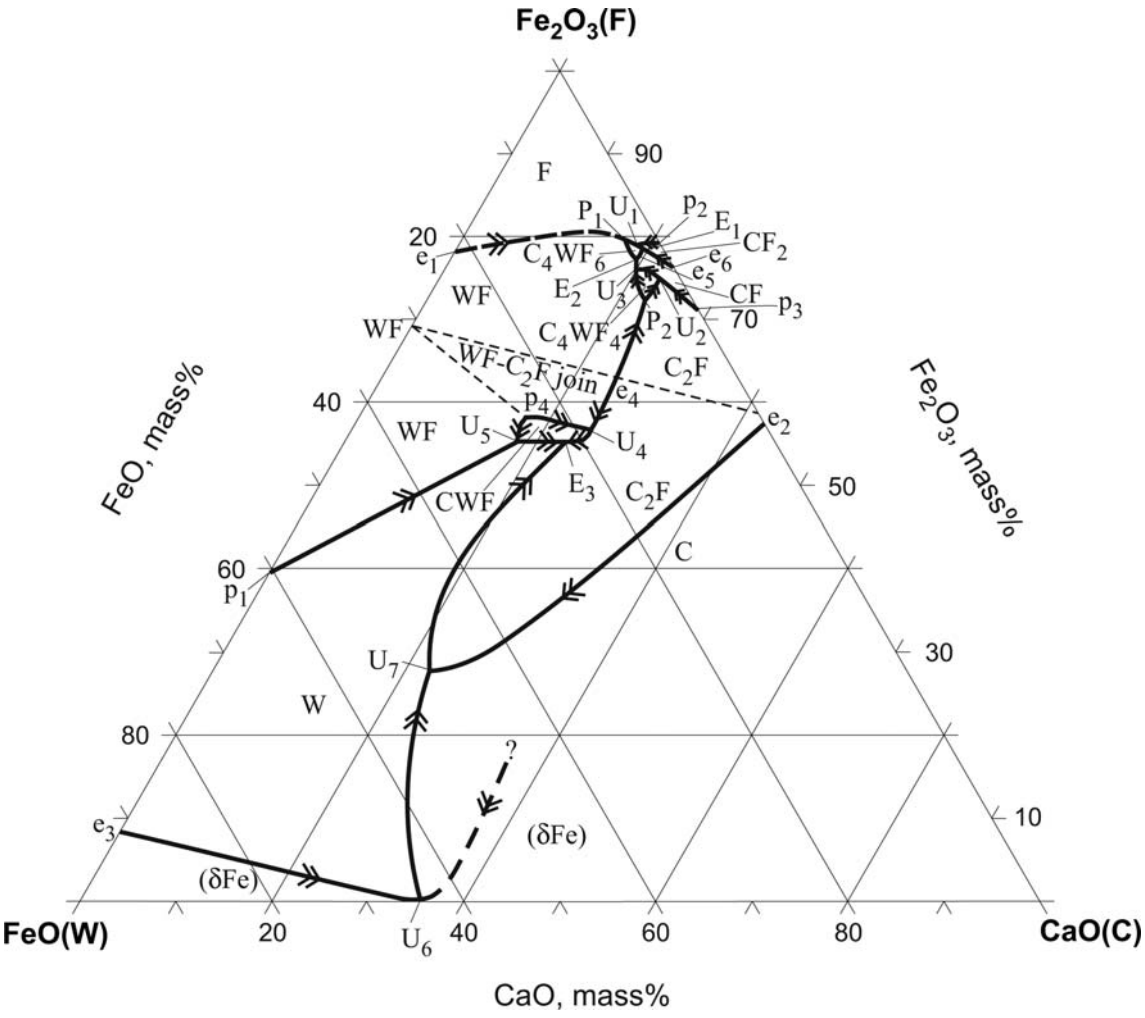

Fig. 3. Ca-Fe-O. The liquidus surface of the quasiternary FeO - Fe_2O_3 (F) - CaO system

DOI: 10.1007/978-3-540-74196-1_17

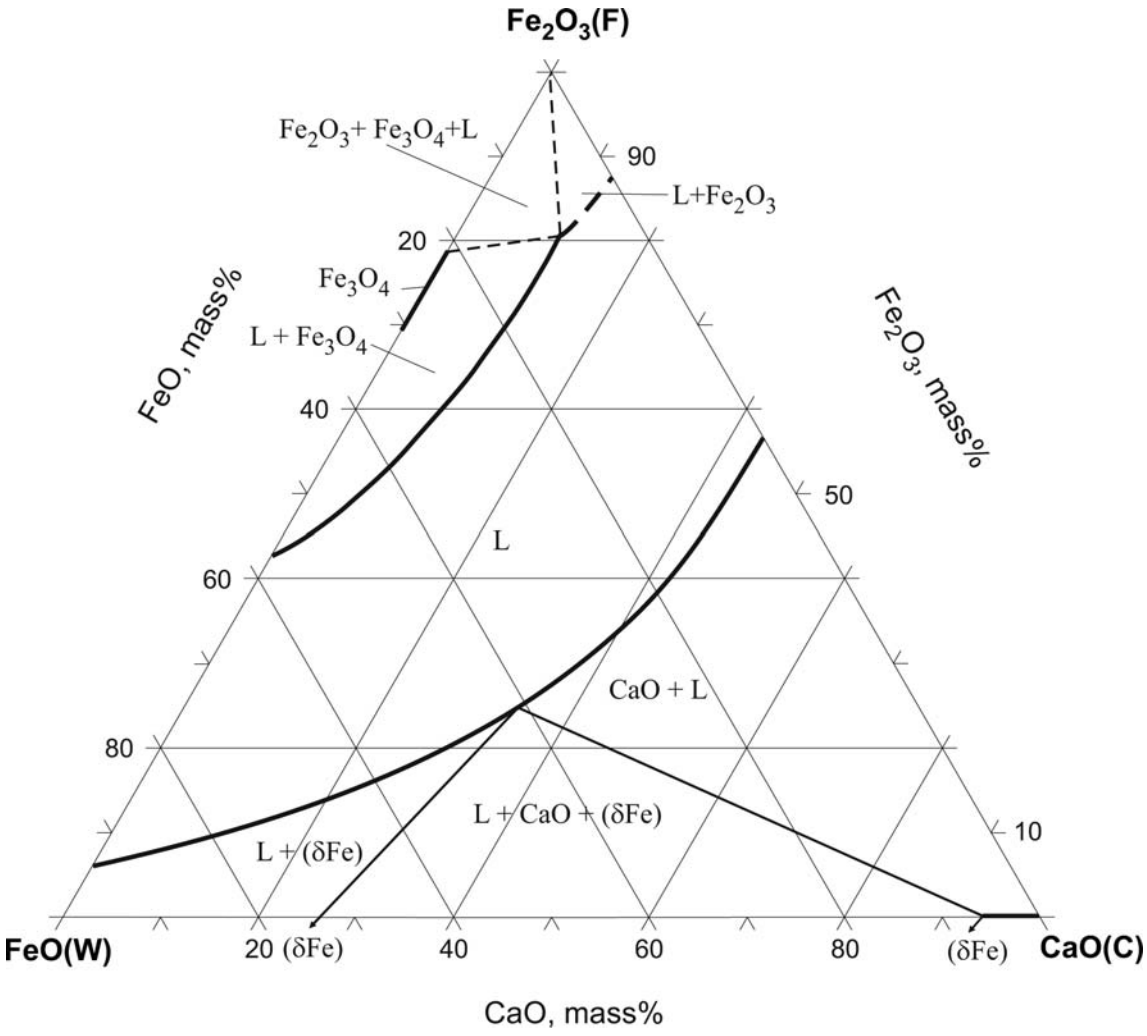

Fig. 4. Ca-Fe-O. Isothermal section of the quasiternary FeO - Fe_2O_3 (F)- CaO system at 1450°C

DOI: 10.1007/978-3-540-74196-1_17

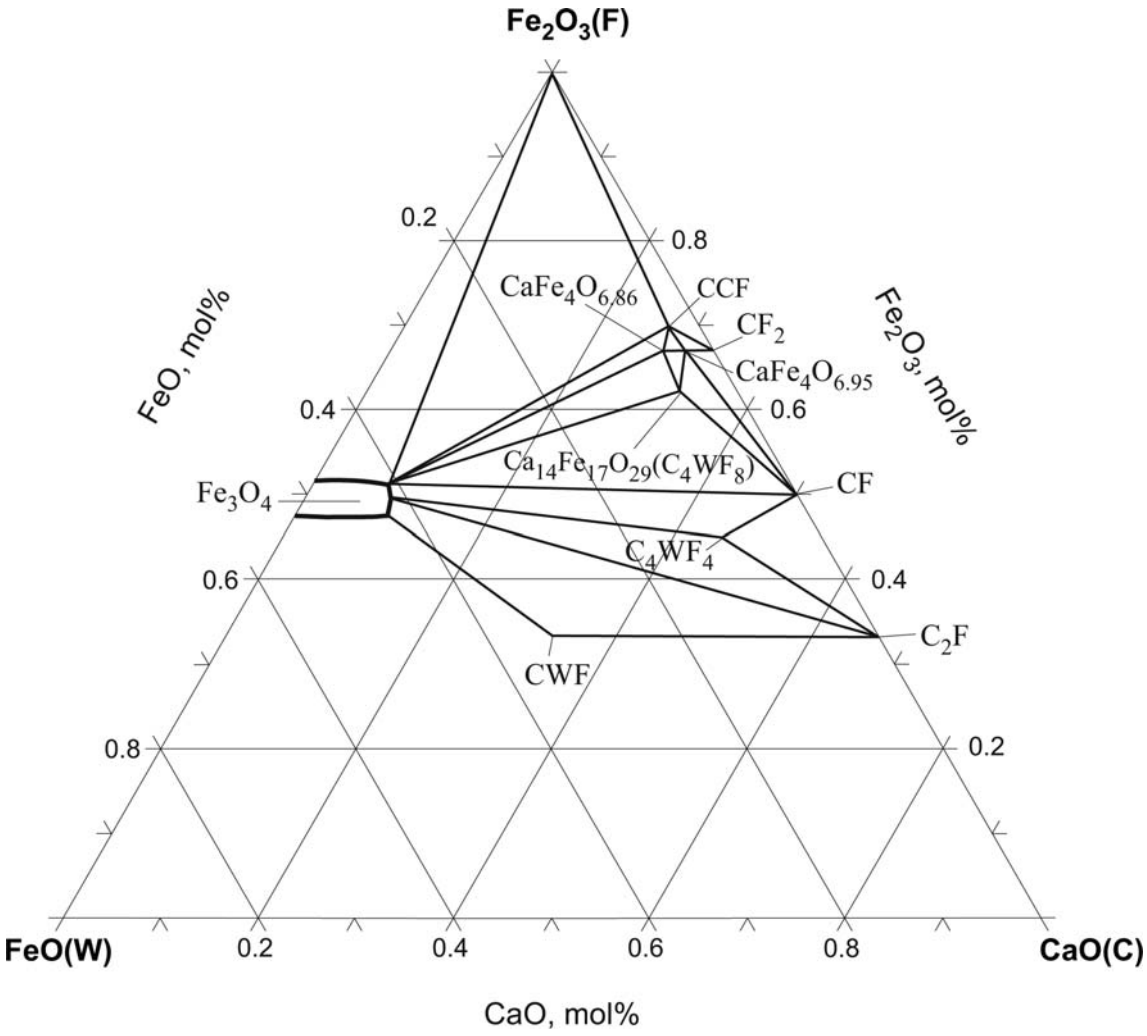

Fig. 5. Ca-Fe-O. Schematic isothermal section of the quasiternary FeO - Fe_2O_3(F) - CaO system at 1200°C

DOI: 10.1007/978-3-540-74196-1_17

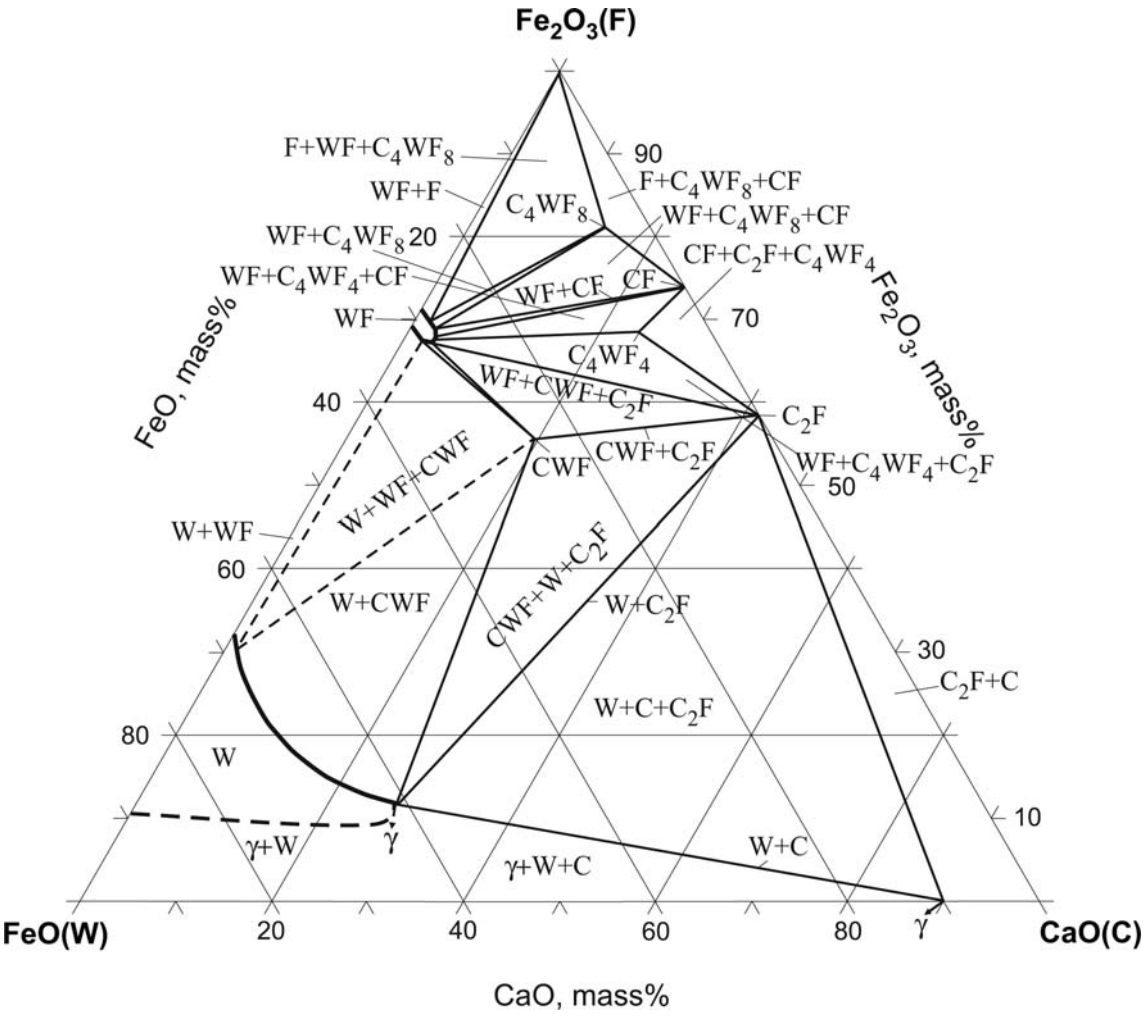

Fig. 6. Ca-Fe-O. Isothermal section of the quasiternary FeO - Fe_2O_3 - CaO system at 1085°C

DOI: 10.1007/978-3-540-74196-1_17

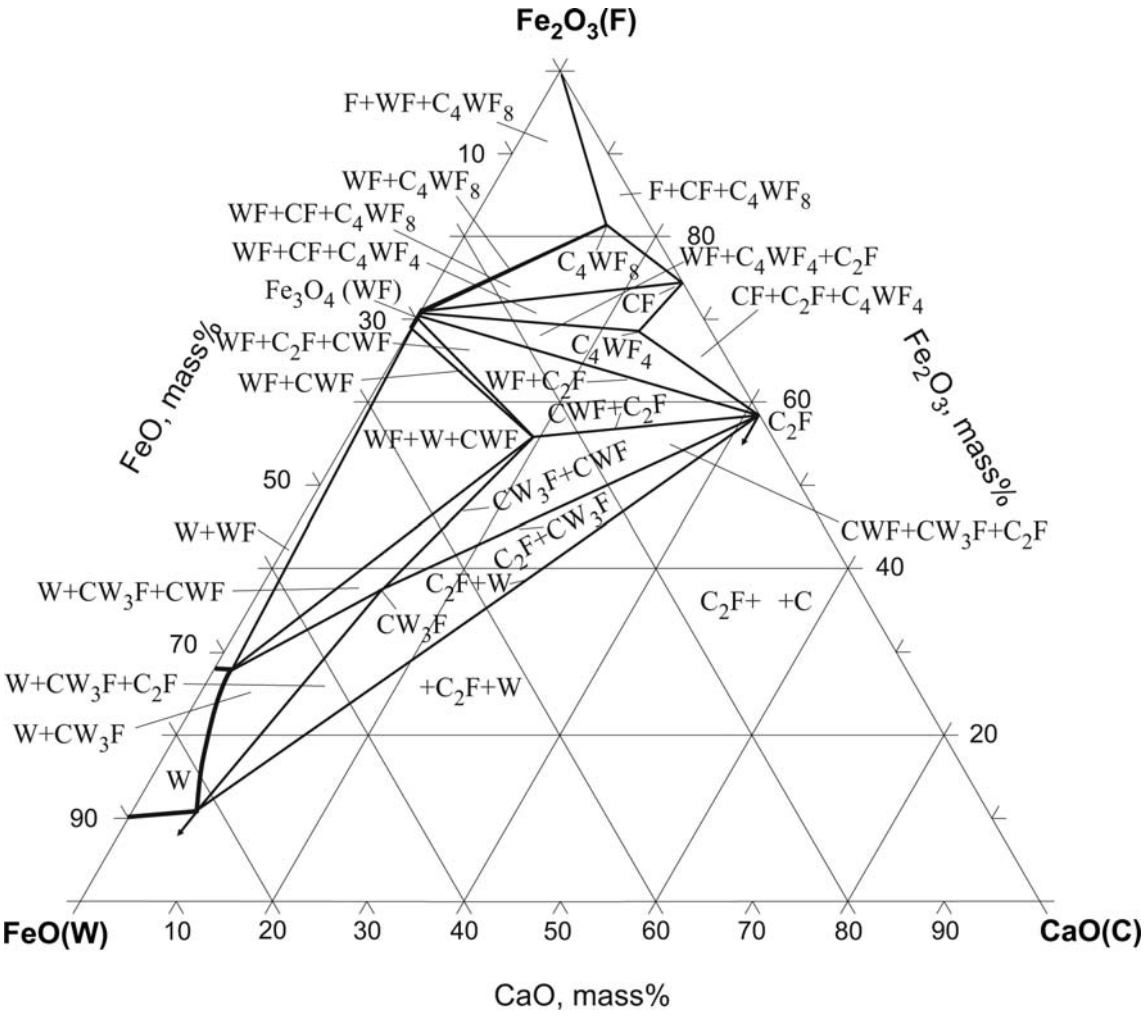

Fig. 7. Ca-Fe-O. Isothermal section of the quasiternary FeO - Fe_2O_3 - CaO system at 900°C

DOI: 10.1007/978-3-540-74196-1_17

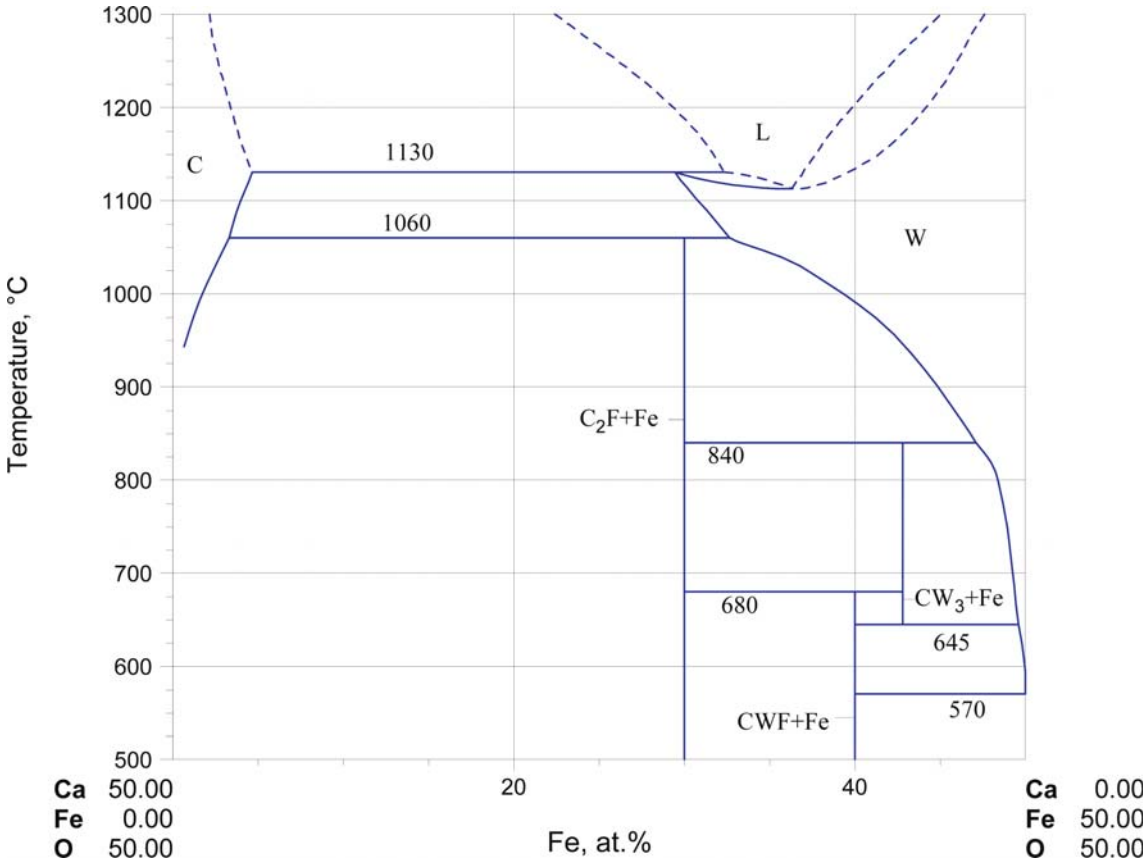

Fig. 8. Ca-Fe-O. The FeO-CaO vertical section in the presence of iron

DOI: 10.1007/978-3-540-74196-1_17

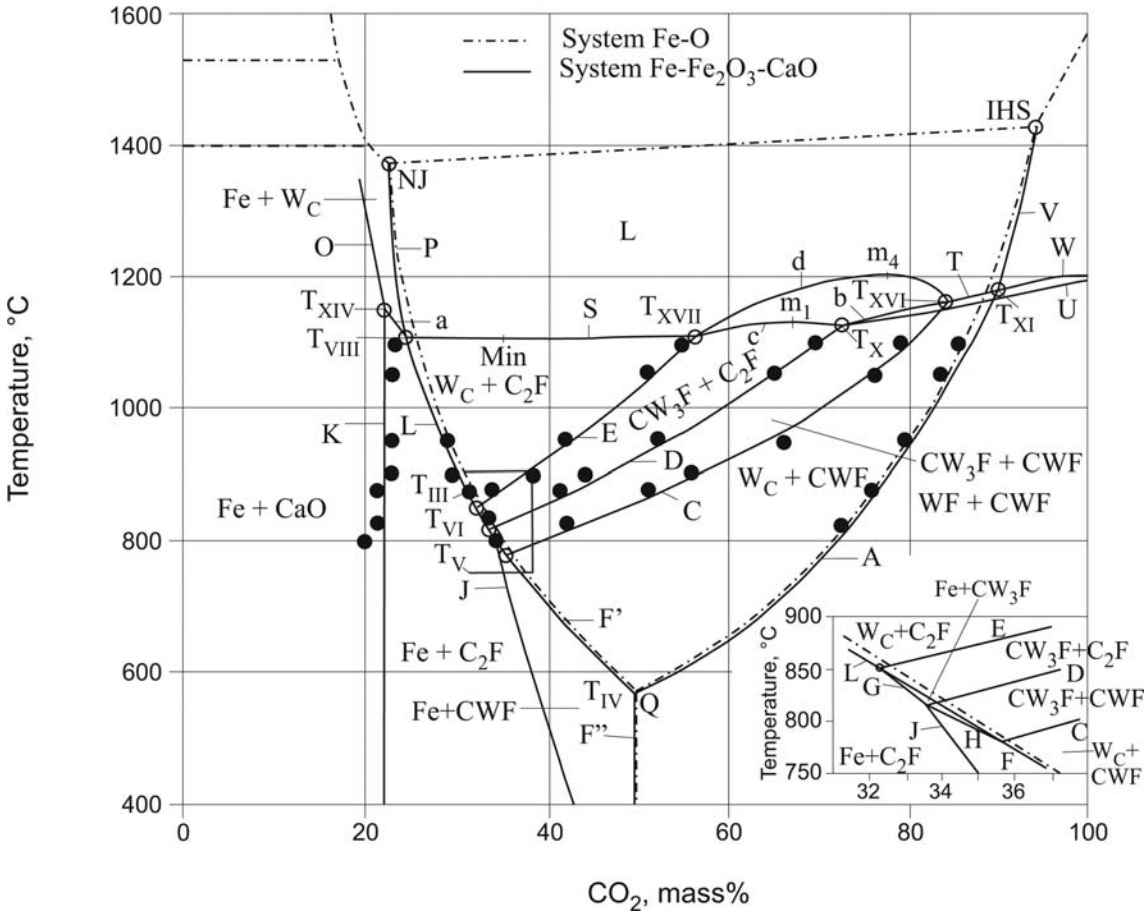

Fig. 9a. Ca-Fe-O. Baur-Glaessner diagram for iron oxides with lime, corresponding to the reduction route CF_2

DOI: 10.1007/978-3-540-74196-1_17

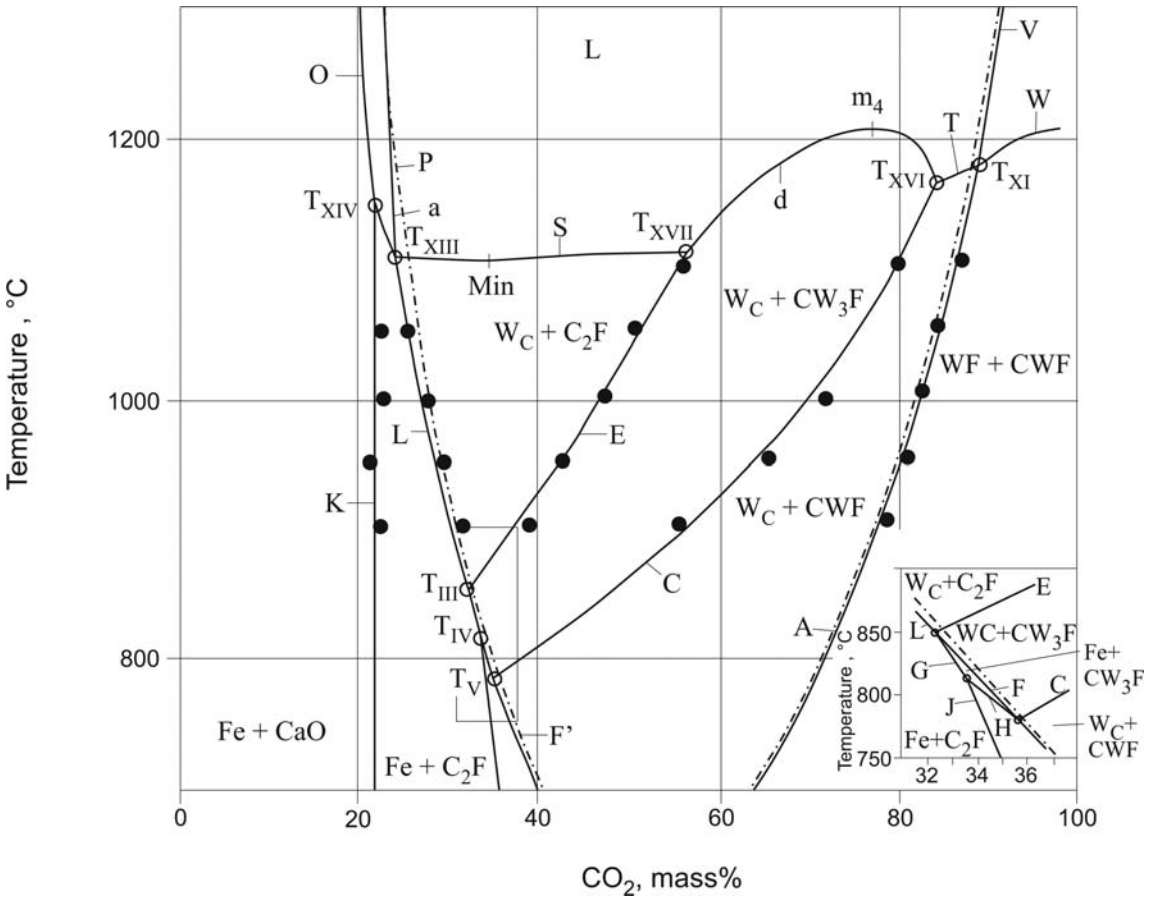

Fig. 9b. Ca-Fe-O. Baur-Glaessner diagram for iron oxides with lime, corresponding to the reduction route CF_2+F

DOI: 10.1007/978-3-540-74196-1_17

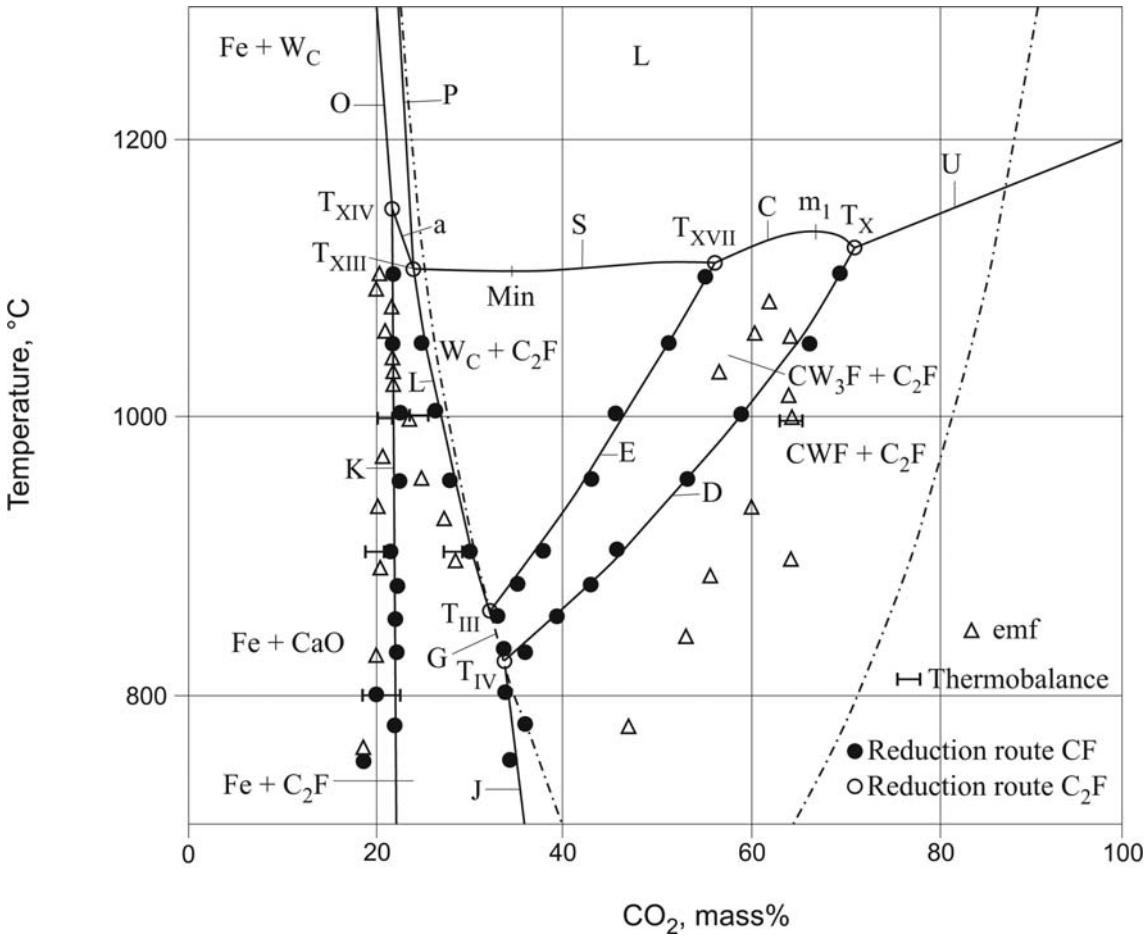

Fig. 9c. Ca-Fe-O. Baur-Glaessner diagram for iron oxides with lime, corresponding to the reduction route CF and C_2F

DOI: 10.1007/978-3-540-74196-1_17

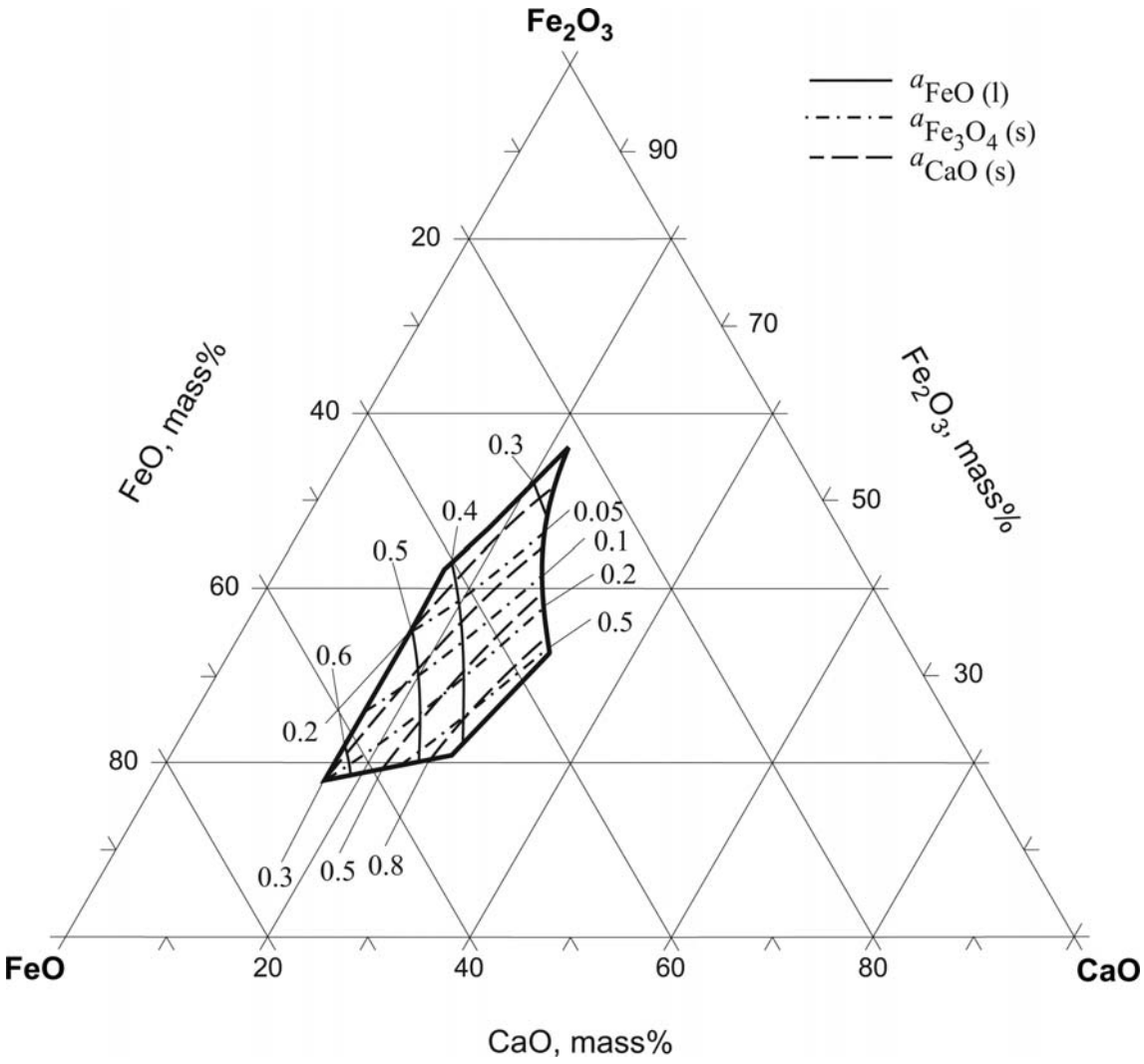

Fig. 10a. Ca-Fe-O. Isoactivity curves for CaO, FeO and Fe_3O_4 at 1200°C

DOI: 10.1007/978-3-540-74196-1_17

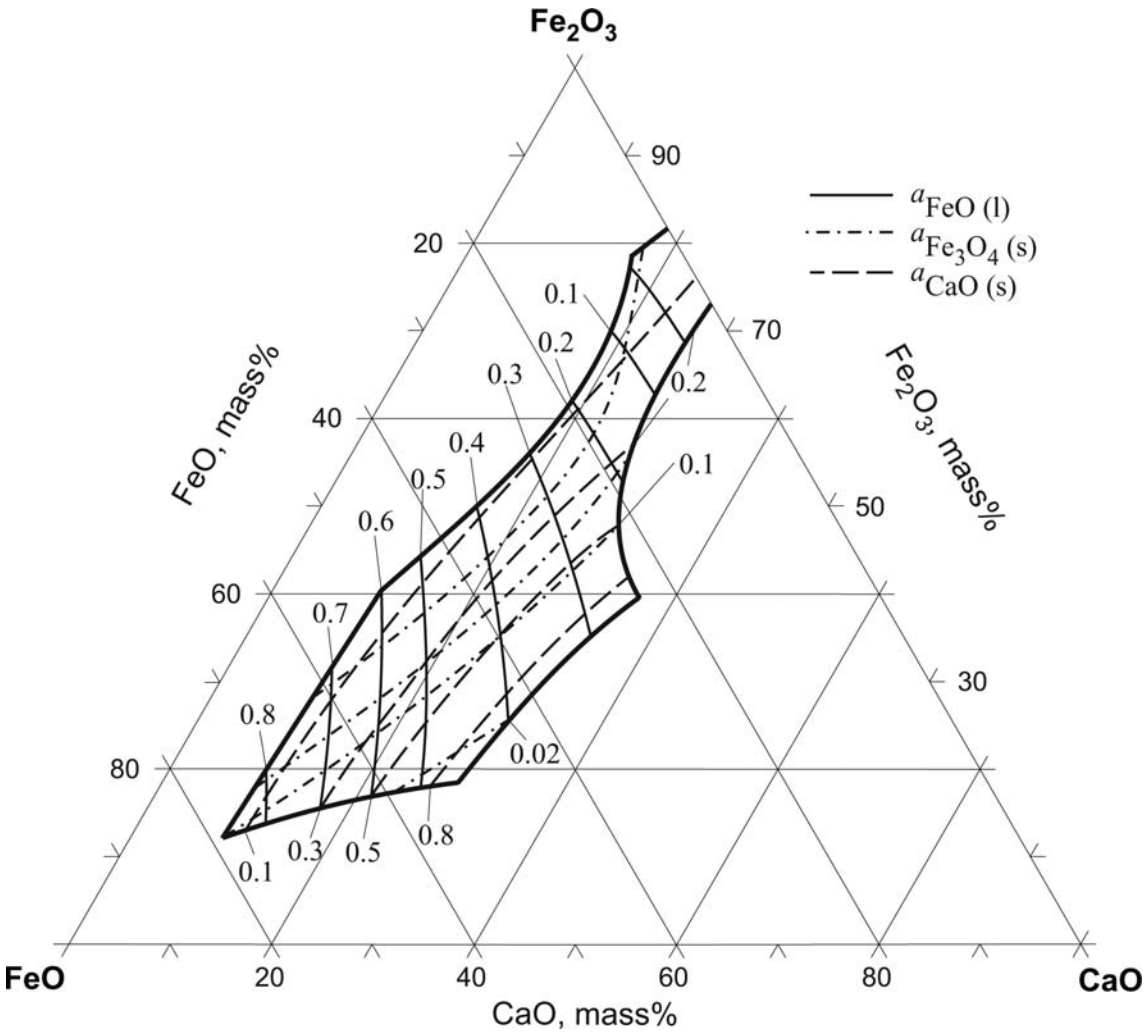

Fig. 10b. Ca-Fe-O. Isoactivity curves for CaO, FeO and Fe_3O_4 at 1300°C

DOI: 10.1007/978-3-540-74196-1_17

References

[1929Sch] Schenck, R., Franz, H., Willeke, H., "Investigations of Equilibrium of the Reduction, Oxydation and Carbonization Proceses of Iron" (in German), *Z. Anorg. Allg. Chem.*, **184**, 1–38 (1929) (Experimental, Interface Phenomena, Phase Relations, 7)

[1934Mar] Martin, E., Vogel, R., "The Iron-Iron Oxide-Calcium Orthoferrite System" (in German), *Arch. Eisenhuettenwes.*, **8**(6), 249–254 (1934) (Experimental, 3)

[1936Tav] Tavasci, B., "Investigation of the System CaO-Fe_2O_3" (in Italian), *Ann. Chim. (Rome)*, **26**, 291–300 (1936) (Experimental, Phase Relations, 7)

[1937Sch] Schenck, R., Laymann, A., Jenckel, E., "Equilibrium Relationships in Reduction, Oxidation and Carbonization of Iron" (in German), *Z. Anorg. Allg. Chem.*, **235**, 65–67 (1937) (Experimental, Phase Relations, 3)

[1939Cro] Crook, W.J., "The Series Iron Oxides-Lime", *J. Am. Ceram. Soc.*, **22**(10), 313–322 (1939) (Review, Experimental, 21)

[1940Koe] Koerber, F., Oelsen, W., "Forming Slags as a Basis of the Ferrous Metallurgy" (in German), *Stahl Eisen*, **60**(43), 948–955 (1940) (Experimental, Phase Diagram, Phase Relations, 38)

[1943Whi] White, J., "The Physical Chemistry of Open-Hearth Slags", *J. Iron Steel Inst., London*, **148**, 579–694 (1943) (Phase Diagram, Review, 195)

[1946Pet] Pettersson, H., "Investigations of the Solubility in the Solid State in the Binary Systems of the Oxides CaO, MnO, MgO and FeO" (in Sweedish), *Jernkontorets Ann.*, **130**(12), 653–663 (1946) (Crys. Structure, Experimental, Phase Diagram, Phase Relations, 19)

[1947Cir] Cirilli, V., "Reduction of Calcium Ferrites with Carbon Oxide at High Temperature" (in Italian), *Ricerca Sci.*, 17(6), 942–945 (1947) (Experimental, 5)

[1950Gur] Gurry, R.W., Darken, L.S., "The Composition of CaO-FeO-Fe_2O_3 and MnO-FeO-Fe_2O_3 Melts at Several Oxygen Pressures in the Vicinity of 1600°C", *J. Am. Chem. Soc.*, **72**, 3906–3910 (1950) (Experimental, Phase Relations, 10)

[1952Bur] Burdese, A., "Reduction Equilibria of the CaO-Fe_2O_3 System" (in Italian), *Metall. Ital.*, **44**, 343–346 (1952) (Phase Diagram, 6)

[1952Cir] Cirilli, V., Burdese, A., "Reduction on (Mono)calcium Ferrite at Different Temperature" (in Italian), *Atti Accad. Sci. Tor., C. Sci. Fis. Mat. Nat.*, **86**, 46–57 (1952) (Experimental, 11)

[1953Lar] Larson, H., Chipman, J., "Oxygen Activity in Iron Oxide Slags", *Trans. Am. Inst. Min. Metall. Pet. Eng., J. Metals*, **197**, 1089–1096 (1953) (Experimental, 16)

[1954Bon] Bonnickson, K.R., "High Temperature Heat Contents of Calcium and Magnesium Ferrites", *J. Am. Chem. Soc.*, **76**, 1480–1482 (1954) (Experimental, Thermodyn., *, 7)

[1954Kin] King, E.G., "Heat Capacities at Low Temperatures and Entropies at 298.16-Degrees-K of Calcium and Magnesium Ferrites", *J. Am. Chem. Soc.*, **76**, 5849–5850 (1954) (Experimental, Thermodyn.,*, 6)

[1954Bur] Burdese, A., "The System CaO-Fe-Fe_2O_3" (in Italian), *Ricerca Sci*., **24**, 782–791 (1954) (Experimental, Phase Diagram, 36)

[1955All] Allen, W.C., Snow, R.B., "The Orthosilicate-Iron Oxide Portion of the System CaFeO-SiO_2", *J. Am. Ceram. Soc.*, **38**(8), 264–280 (1955) (Experimental, 12)

[1955Tro] Troemel, G., Jaeger, W., Schuermann, E., "The Fe-FeO-CaO System" (in German), *Arch. Eisenhuettenwes.*, **26**(11), 687–700 (1955) (Experimental, 23)

[1956New] Newman, E.S., Hoffman, R., "Heats of Formation of Hexacalcium Dialumino Ferrite and Dicalcium Ferrite", *J. Res. Natl. Bur. Standards*, **56**(6), 313–318 (1956) (Experimental, Thermodyn., 14)

[1957Dec] Decker, B.F., Kasper, J.S., "The Structure of Calcium Ferrite", *Acta Crystallogr.*, **10**, 332–337 (1957) (Crys. Structure, Experimental, Morphology, 13)

[1958Eds] Edstroem, J.O., "Some Chemical Reactions Involved in Pelletizing and Iron Ore Reduction", (in Swedish), *Jernkontorets Ann.*, **142**, 401–466 (1958) (Crys. Structure, Experimental, Interface Phenomena, Kinetics, Morphology, Phase Diagram, Theory, 40)

DOI: 10.1007/978-3-540-74196-1_17

[1958Phi] Phillips, B., Muan, A., "Phase Equilibria in the System CaO - Iron Oxide in Air and at 1 Atm. O_2 Pressure", *J. Am. Ceram. Soc.*, **41**(11), 445–454 (1958) (Experimental, Phase Diagram, Phase Relations, 16)

[1960Bur] Burdese, A., Lucco Borlera, M., "Calcium Ferrite-Magnetite-Hematite System. Field of Stability, Composition and Most Probable Structure of the Phase Incorrectly Indicated with '$CaO{\cdot}2Fe_2O_3$' Formula" (in Italian), *Metall. Ital.*, **52**(11), 710–715 (1960) (Crys. Structure, Experimental, Phase Diagram, Phase Relations, 24)

[1960Phi] Phillips, B., Muan, A., "Stability Relations of Calcium Ferrites: Phase Equilibria in the System $2CaO{\cdot}Fe_2O_3$-$FeO{\cdot}Fe_2O_3$-Fe_2O_3 Above 1135°C", *Trans. Metall. Soc. AIME*, **218**, 1112–1118 (1960) (Experimental, Phase Diagram, 9)

[1960Ell] Elliott, J.F., Gleiser, M., "*Thermochemistry for Steelmaking*", Vol. 1, Addison-Wesley Publ. Co. Reading, Massachusetts, (1961) as quoted by [1961Tur]

[1960Hol] Holmquist, S.B., "Two New Complex Calcium Ferrite Phases", *Nature*, **185**, 604 (1960) (Crys. Structure, Experimental, 3)

[1960Sno] Snow, R.B., "Procedure for Distinguishing Calcium Ferrite Minerals by Etching Techniques Devised", *Blast Furnace, Coke Oven, and Raw Materials Conference, (1960)*, **18**, 447–453 (1960) (Experimental, 0)

[1961Koe] Koehler, M.F., Barany, R., Kelley, K.K., "Heats and Free Energies of Formation of Ferrites and Aluminates of Calcium, Magnesium, Sodium, and Lithium", *Report of Investigations, U.S. Bureau of Mines*, **5711**, 1–14 (1961) (Experimental, Thermodyn., *, 32)

[1961Tur] Turkdogan, E.T., "Activities of Oxides in CaO-FeO-Fe_2O_3 Melts", *Trans. Metall. Soc. AIME*, **221**, 1090–1095 (1961) (Experimental, Thermodyn., 22)

[1962Che] Chessin, H., Turkdogan, E.T., "A Crystallographic Investigation of Calcium Diferrite", *J. Am. Ceram. Soc.*, **45**(12), 597–599 (1962) (Crys. Structure, Experimental, Magn. Prop., Thermodyn., 13)

[1963Ell] Elliott, J.F., Gleiser, M., Ramakrishna V., "*Thermochemistry for Steelmaking*", Vol. 2, Addison-Wesley Publ. Co. Reading, Massachusetts, (1963) as quoted by [1986Sha]

[1963Leo] Leont'yev, L.I., Bogoslovskiy, V.N., Chufarov, G.I., "About Existence of the Solid Solutions Between Mono- and Two-calcium Ferrites" (in Russian), *Zh. Neorg. Khim*., **8**(1), 257–258 (1963) (Experimental, Phase Relations, 8)

[1965Mua] Muan, A., Osborn, E.F., "Ca-Fe-O", *Phase Equilibria Among Oxides in Steel Making*, Addison-Wesley, Reading, MA, 81–82 (1965) (Review, *, 10)

[1967Bra] Bratchikov, S.G., Toporishchev, G.A., "Heat Capacity and Formation Heat for Calcium Ferrites" (in Russian), *Izv. Vyssh. Uchebn. Zaved. Chern. Metallurg.*, (12), 8–11 (1967) (Experimental, Thermodyn., 7)

[1967Buz] Buzek, Z., Schindlerova, V., Macoszek, M., "The Influence of Cr, Mn, V, Si, Ti, Al, Zr, Ce and Ca on the Activity and Solubility of Oxygen in Liquid Iron" (in Czech), *Sb. Ved. Pr. Vys. Sk. Banske Ostrave, Rada Hutn.*, **13**(2–3), 175–193 (1967) (Calculation, Thermodyn., 26)

[1967Hug] Hughes, H., Roos, P., Goldring, D.C., "X-Ray Data on Some Calcium-Iron-Oxygen Compounds", *Mineral. Mag.*, **36**, 280–291 (1967) (Crys. Structure, Experimental, Morphology, Phase Diagram, 9)

[1967Per] Perrot, P., "Relations Between CaO and Fe_2O_3 and the Solid Solution Formation with MgO" (in French), *Rev. Chim. Miner.*, **4**, 465–493 (1967) (Experimental, Phase Diagram, 17)

[1967Ree1] Reeve, D.A., Gregory, A.G., "The System CaO-FeO-Fe_2O_3 at Liquidus Temperatures", *Trans. Inst. Min. Metall., Sect. C.*, **76C**, C268–C272 (1967) (Experimental, 15)

[1967Ree2] Reeve, D.A., Gregory, A.G., "Modification for the Oxygen Potential Diagram for the System Fe-Ca-O", *Trans. Inst. Min. Metall., Sect. C.*, **76C**, C273–C277 (1967) (Experimental, 10)

[1967Rez] Rezukhina, T.N., Bagin'ska, Ya., "Thermodynamic Properties of $CaFe_2O_4$ and $Ca_2Fe_2O_5$ from the Measurements of Galvanic Cells with Solid Electrolyte at the Temperatures Above 1000 K" (in Russian), *Elektrokhimiya*, **3**(6), 1146–1149 (1967) (Experiment, Thermodyn., 18)

DOI: 10.1007/978-3-540-74196-1_17

[1969Duf] Dufour, M.-C., Perrot, P., Tridot, G., "Thermodynamic Properties of Ternary Oxides: $CaO{\cdot}FeO{\cdot}Fe_2O_3$ and $CaO{\cdot}3FeO{\cdot}Fe_2O_3$" (in French), *Compt. Rend. Acad. Sci. Paris, Ser. C*, **268**(9), 831–833 (1969) (Experimental, Thermodyn., 6)

[1970Aub] Aubry, J., Berthet, A., Duchene, R., Etienne, H., Evrard, O., Jeannot, F., Gleitzer, C., Offroy, C., Perrot, P., "Stabilisation of Iron Monoxide by formation of Solid Solution" (in French), *Ann. Chim.*, **5**, 299–308 (1970) (Experimental, Phase Diagram, Phase Relations, 45)

[1970Kan] Kanamaru, F., Miyamoto, H., Mimura, Y., Koizumi, M., Shimada, M., Kume, S., Shin, S., "Synthesis of a New Perovskite $CaFeO_3$", *Mater. Res. Bull.*, **5**(4), 257–261 (1970) (Crys. Structure, Experimental, Mechan. Prop., Phys. Prop., 6)

[1970Nek] Nekrasov, Z.I., Gladkov, N.A., Gamazova, L.B., Drozdov, G.M., "Phase Reactions in the Fe-FeO-CaO System", *Russ. Metall. (Engl. Transl.)*, **4**, 5–9 (1970) (Phase Relations, 9)

[1970Tim] Timucin, M., Morris, A.E., "Phase Equilibria and Thermodynamic Studies in the System $CaO\text{-}FeO\text{-}Fe_2O_3\text{-}SiO_2$", *Metall. Trans.*, **1**, 3193–3201 (1970) (Calculation, Experimental, Phase Diagram, Phase Relations, Thermodyn., 22)

[1971Apo] Apostolov, A., Basi, Zh., "Refinement of the Calcium Ferrite Structure" (in Bulgarian), *Godishn. Sofiysk. in-ta. Fiz. Fak.*, **63**, 177–187 (1971) (Experimental, Crys. Structure, 13)

[1971Ber] Berggren, J., "Refinement of the Crystal Structure of Dicalcium Ferrite, $Ca_2Fe_2O_5$", *Acta Chem. Scand.*, **25**(10), 3616–3624 (1971) (Experimental, Crys. Structure, 18)

[1971Iml] Imlach, J.A., Glasser, F.P., "Sub-Solidus Phase Relations in the System $CaO\text{-}Al_2O_3\text{-}Fe\text{-}Fe_2O_3$", *Trans. J. Br. Ceram. Soc.*, **70**, 227–234 (1971) (Phase Diagram, Phase Relations, 7)

[1971Ino] Inoue, H., Sanbongi, K., "Dissociation Pressures of Binary and Ternary Compounds in the Iron-Calcium-Oxygen System", *Proc. Int. Conf. Sci. Technol. Iron Steel*, 1970 (Pub. 1971), Pt. 1,466–470. Edited: Iron Steel Inst. Jap., Tokyo, Japan., 1970 (1971) (Phase Relations, Experimental)

[1971Jas] Jasienska, S., "Investigation of Physico-Chemical Properties of Ferrite of Lime $CaO\text{-}FeO\text{-}Fe_2O_3$ Crystallising in Self-fluxing Agglomerates", (in French), *Mem. Sci. Rev. Metall.*, **68**(11), 809–814 (1971) (Experimental, 13)

[1971Miy] Miyashita, Y., Nishikawa, K., "The Deoxidation of Liquid Iron with Calcium" (in Japanese), *Tetsu to Hagane*, **57**(13), 1969–1975 (1971) (Experimental, Phase Relations, 11)

[1972Lyk] Lykasov, A.A., Kuznetsov, Yu.C., "For Thermodynamics of the Solid Solutions of Calcium Oxide in Wustite" (in Russian), *Sborn. Nauchn. Tr. Chelyabins. Politekhn. Inst.*, (107), 39–42 (1972) (Experimental, Thermodyn., Phase Relations, 5)

[1973Abb1] Abbattista, F., Maja, M., "High Temperature Equilibria between Wüstite, Iron, Lime and Dicalcium Ferrite" (in Italian), *Atti Accad. Sci. Tor., C. Sci. Fis. Mat. Nat.*, **107**, 151–163 (1973) (Experimental, 13)

[1973Abb2] Abbattista, F., Burdese, A., Maja, M., "High-Temperature Equilibria Involving Wustite, Iron, Calcium Oxide, and Dicalcium Ferrite Determination of Oxygen Pressure Using the Emf of Solid Electrolytic Cells" (in Italian), *Metall. Ital.*, **65**, 675–678 (1973) (Phase Relations, Thermodyn., 16)

[1973Reg] Regnard, J.R., "Moessbauer Study of ^{57}Fe in Doped CaO Crystals", *Solid State Commun.*, **12**(3), 207–209 (1973) (Electronic Structure, 10)

[1973Sch] Schuermann, E., Wurm, P., "Phase Diagrams and Reduction Equilibria of the Ternary System $Fe\text{-}Fe_2O_3\text{-}CaO$ Between 550 and 1070°C" (in German), *Arch. Eisenhuettenwes.*, **44**(9), 637–645 (1973) (Experimental, Phase Diagram, *, 23)

[1974Abb] Abbatista, F., Maja, M., "High Temperature Behaviour of the Calcium Oxide-Wustite and Iron Oxide-Bicalcium Ferrite Systems" (in Italian), *Atti Accad. Sci. Tor., C. Sci. Fis. Mat. Nat.*, **108**(2), 219–233 (1974) (Phase Relations, Experimental, 6)

[1974Sch] Scheel, R., "Investigations Into the System Lime-Iron-Oxygen" (in German), *Arch. Eisenhuettenwes.*, **45**(11), 751–756 (1974) (Experimental, Morphology, Phase Diagram, Phase Relations, 16)

DOI: 10.1007/978-3-540-74196-1_17

[1975Abb] Abbattista, F., Burdese, A., Maja, M., "Equilibrium Diagrams of CaO-FeO_x System" (in French), *Rev. Int. Hautes Temp. Refract.*, **12**(4), 337–342 (1975) (Phase Diagram, Phase Relations, 17)

[1985Kul] Kulikov, I.S., "The Deoxidation of Iron by the Alkaline Earth Metals" (in Russian), *Izv. AN SSSR. Met.,* (6), 9–15 (1985) (Calculation, Thermodyn., 8)

[1975Tar] Tare, V.B., Deo, B., "Thermodynamic Investigations on the Calcium Oxide-Iron(ii) Oxide System", *Conf. Int. Thermodyn. Chim.*, (C.R.), 4th Edited: Rouquerol Jean; Sabbah Raphael, Cent. Rech. Microcalorimetrie Thermoch Im. CNRS, Marseille., 104–113 (1975) (Experimental, Thermodyn., Phase Relations, 9)

[1976Lyk] Lykasov, A.A., Kozheurova, N.V., Baeva, T.L., Zabeyvorota, N.S., Sergeeva, L.N., "Phase Equilibrium in the System Fe-Ca-O at Temperatures 850–1050°C" (in Russian), *Sborn. Nauchn. Trudov Chelyab. Politekhn. Inst.*, **177**, 25–32 (1976) (Experimental, 9)

[1976Mus] Musiyenko, K.A., Rostovtsev, S.T., "Thermodynamic and Kinetics of Calcium-Ferrites Reduction", *Russ. Metall.*, **6**, 4–8 (1976), translated from *Izv. Akad. Nauk SSSR, Met.,* **6**, 3–9 (1976) (Thermodyn., Kinetics, Experimental, 17)

[1976Oto] Ototani, T., Kataura, Y., Degawa, T., "Deoxidation of Liquid Iron and Its Alloys by Calcium Contained in Lime Crucible", *Trans. Iron Steel Inst. Jpn.*, **16**, 275–282 (1976) (Experimental, Interface Phenomena, Morphology, Thermodyn., 14)

[1976Sch1] Schuermann, E., Kramme, G., "Phase Diagram CaO-Fe_2O_3 in Equilibrium with Air" (in German), *Arch. Eisenhuettenwes.*, **47**(5), 267–269 (1976) (Experimental, Phase Diagram, Phase Relations, *, 15)

[1976Sch2] Schuermann, E., Kraume, G., "Melting Equilibria in the System FeO-Fe_2O_3-CaO" (in German), *Arch. Eisenhuettenwes.*, **47**(7), 435–439 (1976) (Experimental, Phase Diagram, Phase Relations, Review, *, 12)

[1976Sch3] Schuermann, E., Kraume, G., "Phase Equilibria on the Section FeO(n)-CaO in the Ternary System FeO-Fe_2O_3-CaO at Saturation of Iron" (in German), *Arch. Eisenhuettenwes.*, **47**(6), 327–331 (1976) (Experimental, Phase Diagram, Phase Relations, Review, *, 30)

[1976Sch4] Schuermann, E., Kraume, G., "Reduction Equilibria in the System Fe-Fe_2O_3-CaO Above 1050°C" (in German), *Arch. Eisenhuettenwes.*, **47**(8), 471–476 (1976) (Phase Relations, Review, 41)

[1978Spe] Spencer, P.J., Chart, T.G., "Summary of Proceedings of the Seventh Calphad Meeting", *Calphad*, **2**(3), 197–205 (1978) (Abstract, Calculation, Crys. Structure, Phase Diagram, Thermodyn.)

[1979Kau] Kaufman, L., "Calculation of Quasibinary and Quasiternary Oxide Systems I", *Calphad*, **3**(1), 27–44 (1979) (Calculation, Phase Diagram, 5)

[1979Shi] Shin, S., Hatakeyama, Y., Ogawa, K., Shimomura, K., "Catalytic Decomposition of no Over Brownmillerite-Like Compounds, $Ca_2Fe_2O_5$ and $Sr_2Fe_2O_5$", *Mater. Res. Bull.*, **14**(1), 133–136 (1979) (Crys. Structure, Experimental, Kinetics, 7)

[1979Ute] Utesheva, V., Vagina, T., Ermolaeva, L., Maslov, Yu.P., Maslov, P.G., Rymkevich, P.P., Perevozchikov, E.N., Korshunov, V.S., "Formulas for the Temperature Dependence of Thermodynamic Properties of Certain Complex Crystalline Oxides", *J. Appl. Chem. USSR*, **12**, 2619–2623 (1979), translated from *Zh. Prikl. Khim.*, **52**(12), 2771–2776 (1979) (Calculation, Thermodyn., 9)

[1980Ban] Ban-ya, S., Chiba, A., Hikosaka, A., "Thermodynamics of Fe_tO-M_xO_y (M_xO_y = CaO, SiO_2, TiO_2, and Al_2O_3) Binary Melts in Equilibrium with Solid Iron" (in Japanese), *Tetsu to Hagane*, **66**(10), 1484–1493 (1980) (Experimental, 27)

[1980Ban] Ban-Ya, S., Chiba, A., Hikosaka, A., "Thermodynamics of Fe_tO-M_xO_y (M_xO_y = CaO, SiO_2, TiO_2 and Al_2O_3) Binary Melts Saturated With Solid Iron", *Austral.-Jap. Extractive Metall. Symp., Sydney, Australia,16–18 July 1980*, Australian Inst. Min. Metall., **23**, 457–467 (1980) (Experimental, Thermodyn., 22)

[1980Evr] Evrard, O., Malaman, B., Jeannot, F., Courtois, A., Alebouyeh, H., Geradin, R., "Evidence of Calcium Ferrite $CaFe_4O_6$ and Determination of the Crystal Structure of $CaFe_{2+n}O_{4+n}$ (n = 1,

DOI: 10.1007/978-3-540-74196-1_17

2, 3): A New Example of Intergrowth" (in French), *J. Solid State Chem.*, **35**(1), 112–119 (1980) (Experimental, Crys. Structure, 18)

[1980Gus1] Gustafsson, S., Mellberg, P.O., "On the Free Energy Interaction Between Some Strong Deoxidizers, Especially Calcium and Oxygen in Liquid Iron", *Scand. J. Metall.*, **9**(3), 111–116 (1980) (Thermodyn., Calculation, 7)

[1980Gus2] Gustafsson, S., Mellberg, P.O., "On the Free Energy Interaction Between some Strong Deoxidizers, Especially Calcium, Aluminum and Oxygen in Liquid Iron", *Scaninject Ii, Injection Metal. (Proc. Conf.), Lulea, Sweden*, **20**(23), 1–19 (1980) (Experimental, Calculation, 7)

[1980Har] Harder, M., Mueller-Buschbaum, H., "Preparation and Investigation of $Sr_2Fe_2O_5$ Single Crystals. A Contribution to Solid State Chemistry of $M_2Fe_2O_5$ Compounds" (in German), *Z. Anorg. Allg. Chem.*, **464**, 169–175 (1980) (Crys. Structure, Experimental, Theory, 11)

[1980Lyk] Lykasov, A.A., Kozheurova, N.V., "Solid Solutions of Calcium Oxide in Wustite" (in Russian), *Izv. Vyssh. Uchebn. Zaved. Chern. Metall.*, (4), 10–13 (1980) (Experimental, Phase Relations, 9)

[1980Tak1] Takeda, Y., Nakazawa, S., Yazawa, A., "Thermodynamics of Calcium Ferrite Slags at 1200 and 1300°C", *Can. Metall. Quart.*, **19**(3), 297–305 (1980) (Thermodyn., Experimental, 26)

[1980Tak2] Takeda, Y., Yazawa, A., "Thermodynamic Study of Liquid Fe-O-CaO System Saturated with Iron" (in Japanese), *Nippon Kogyo Kaishi*, 901–905 (1980) (Experimental, Thermodyn., 17)

[1981Bur] Burdese, A., Firrao, D., Dzhanolyo, Ch., "Investigation and Analysis of the Equilibria at the Reduction in the Ca-Fe-O System" in "*Fiz. Khimiya Okislov Metallov*" (in Russian), Moscow, Nauka, 82–88 (1981) (Review, Phase Relations, Crys. Structure, 29)

[1981Lyk] Lykasov, A.A., Kozheurova, N.V., "The Phase Diagram of the Fe- Fe_3O_4- CaO System", *Inorg. Mater. (Engl. Trans.)*, **16**(6), 751–754 (1981), translated from *Izv. Akad. Nauk. SSSR, Neorg. Mater.*, **16**(6), 1079–1082 (1980) (Experimental, Phase Diagram, Phase Relations, 10)

[1981Mal] Malaman, B., Alebouyeh, H., Jeannot, F., Courtois, A., Gerardin, R., Evrard, O., "Preparation and Characterization of Calcium Ferrites $CaFe_{2+n}O_{4+n}$ with Fractional Values of n (3/2,5/2) and their Incidence on Fe-Ca-O Diagram at 1120°C" (in French), *Mater. Res. Bull.*, **16**(9), 1139–1148 (1981) (Experimental, Crys. Structure, 14)

[1981Tak] Takeda, Y., Nakazawa, S., Yazawa, A., "Phase Equilibria in the System FeO-Fe_2O_3-CaO" (in Japanese), *Nippon Kogyo Kaishi*, **97**(1120), 473–478 (1981) (Experimental, Phase Relations, 25)

[1981Yaz] Yazawa, A., Takeda, Y., Waseda, Y., "Thermodynamic Properties and Structure of Ferrite Slags and their Process Implications", *Can. Metall. Quart.*, **20**(2), 129–134 (1981) (Thermodyn.,Crys. Structure, 22)

[1982Bau] Baur, W.H., "The Structures of $CaFe_2O_4$(FeO)n (n=1, 2, 3) and their Relationship to $CaTi_2O_4$", *J. Solid State Chem.*, **43**, 222–224 (1982) (Crys. Structure, 7)

[1982Mal1] Malaman, B., Alebouyeh, H., Courtois, A., Gerardin, R., Evrard, O., "The Crystal Structure of $Ca_4Fe_9O_{17}$" (in French), *Mater. Res. Bull.*, **17**(6), 795–800 (1982) (Experimental, Crys. Structure, 9)

[1982Mal2] Malysheva, T.Ya., Lyadova, V.Ya., Korovushkin, V.V., Ostrovskaya, I.V., "Mechanism and Kinetics of Formation of Ferrite in the Solid Phase in the CaO-Fe_2O_3 System", *Russ. Metall. (Engl. Transl.)*, **1**, 5–8 (1982) (Phase Relations, Kinetics, 10)

[1983Ara] Arakcheeva, A.V., Karpinskii, O.G., "Crystal Structure of the Hexagonal Ferrite $Ca_{2.95}Fe_{14.85}O_{25}$", *Sov. Phys.- Dokl.(Engl. Transl.)*, **28**(12), 979–980 (1983), translated from *Dokl. Akad. Nauk SSSR*, **273**, 1127–1129 (1983) (Experimental, Crys. Structure, 7)

[1983Lyk] Lykasov, A.A., Kozheurova, N.V., Sergeev, G.I., "Thermodynamic Analysis of Phase Transformations in the System Fe-Fe_3O_4-$Ca_2Fe_2O_5$-CaO" (in Russian), *Nauchn. Trudy Mosk. Inst. Stali i Splavov*, (148), 116–119 (1983) (Experimental, Phase Diagram, Phase Relations, 11)

[1983Mod] Model, M.S., Chugunova, N.V., Lyadova, V.Ya., Malysheva, T.Ya., Chumak, A.D., "Formation of Solid Solutions Based on Semicalcium Ferrite in the CaO-Fe_2O_3-FeO System" (in Russian), *Izv. Akad. Nauk SSSR, Met.*, (5), 6–16 (1983) (Crys. Structure, Experimental, Phase Diagram, Phase Relations, 17)

DOI: 10.1007/978-3-540-74196-1_17

[1983Tak] Takano, M., Takeda, Y., "Electronic State of Fe'$^{4+}$ Ions in Perovskite-Type Oxides", *Bull. Inst. Chem. Res. Kyoto Univ.*, **61**(5–6), 406–425 (1983) (Electr. Structure., Review, 29)

[1984Bjo] Bjoerkman, B., "A Solid State EMF Study of the System CaO-$Ca_2Fe_2O_5$-Fe_tO-Fe", *Scand. J. Metall.*, **13**(4), 193–200 (1984) (Experimental, 24)

[1984Har1] Hara, S., Araki, T., Ogino, K., "Phase Equilibrium Studies in the FeO-Fe_2O_3-CaO and FeO-Fe_2O_3-2CaO·SiO_2 Systems", *Second Int. Symp. Metal. Slags and Fluxes,* Lake Tahoe, Nevada, U.S.A., 1984, The Metal. Soc./AIME, 420 Commonwealth Street, Warrendale, Pennsylvania 15086, U.S.A., 441–451 (1984) (Experimental)

[1984Har2] Hara, S., Araki, T., Ogina, K., "Phase Equilibrium Studies in the FeO-Fe_2O_3-CaO and FeO-Fe_2O_3-2CaO·SiO_2 Systems", *J. Met.*, **36**(8), 89–89 (1984) (Phase Relations, Experimental)

[1984Iwa] Iwase, M., Yamada, N., Nishida, K., Ichise, E., "Rapid Determinations of the Activities in CaO-Fe(x)O Liquid Slags by Disposable Electrochemical Oxygen Probes", *Trans. AIME*, (4), 69–75 (1984) (Thermodyn., Exsperimental, 23)

[1984Vid] Vidyasagar, K., Gopalakrishnan, J., Rao, C.N.R., "A Convenient Route for the Synthesis of Complex Metal Oxides Employing Solid-Solution Precursors", *Inorg. Chem.*, **23**(9), 1206–1210 (1984) (Crys. Structure, Experimental, 19)

[1985Igu] Iguchi, Y., Kubokoya, R., Hirao, J., "Redox Equilibria in Wustite Doped with CaO, SrO, and BaO" (in Japanese), *Nippon Kinzoku Gakkai-shi*, **49**(4), 279–284 (1985) (Experimental, 27)

[1985Kar] Karpinskii, O.G., Arakcheeva, A.V., "Crystal Structure of Ternary Hexagonal Ferrite Phase of $Ca_{3.565}Fe_{0.06}Fe_{14.25}O_{25}$", *Sov. Phys.- Dokl. (Engl. Transl.)*, **30**(6), 439–440 (1985), translated from *Dokl. Akad. Nauk SSSR,* **282**, 1139–1141 (1985) (Experimental, Crys. Structure, 2)

[1985Wri] Wriedt, H.A., "The Ca-O System", *Bull. Alloy Phase Diagrams*, **6**(4), 337–342 (1985) (Review, Thermodyn., Phase Diagram, Crys. Structure, 54)

[1986Ber] Bergman, B., "Solid-State Reactions Between CaO Powder and Fe_2O_3", *J. Am. Ceram. Soc.*, **69**(8), 608–611 (1986) (Experimental, Phase Relations, 10)

[1986Mil] Millon, E., Evrard, O., Bonazebi, A., Brice, J.F., Gerardin, R., "The Diagram of Fe-Ca-O System at 1200°C: Section Fe_3O_4- Fe_2O_3- $CaFe_2O_4$-$CaFe_3O_5$" (in French), *Mem. Etud. Sci. Rev. Metall.*, **83**(11), 583–593 (1986) (Crys. Structure, Experimental, 18)

[1986Nad] Nadif, M., Gatellier, C., "Influence of Ca or Mg on the Solubility of O and S in Liquid Steel" (in French), *Rev. Metall. Cah. Inf. Tech.*, **83**(5), 377–394 (1986) (Experimental, 26)

[1986Sha] Sharma, K.C., Agrawal, R.D., Kapoor, M.I., "Activity Measurements in The Binary System FeO-CaO at 1000 K", *Indian J. Technol.*, **24**, 751–753 (1986) (Thermodyn., Exsperimental, 12)

[1987Ara] Arakcheevak, A.V., Karpinskii, O.G., "Crystal Structure of the Ternary Hexagonal Ca Ferrite $Ca_{3.0}Fe_{14.82}O_{25}$ (γ-CFF Phase)", *Sov. Phys.-Crystallogr.*, **32**(1), 31–32 (1987), translated from *Kristallografiya*, **32**(1), 59–61 (1987) (Experimental, Crys. Structure, 4)

[1987Ber] Bergman, B., Song, C., "Decomposition of Wustite in the System Ca-Fe-O", *TRITA-MAC-Rep. No. 0339, Royal Inst. Tech., Stockholm*, 1–6 (1987) (Experimental)

[1987Kar] Karpinskii, O.G., Arakcheeva, A.V., "Crystal Structure of Triple Hexagonal Ca-Ferrite $Ca_{3.0}Fe_{14.82}O_{25}$ (α-CFF-Phase)", *Sov. Phys.-Crystallogr.*, **32**(1), 28–30 (1987), translated from *Kristallografiya*, **32**(1), 55–58 (1987) (Experimental, Crys. Structure, 10)

[1987Raj] Rajagopalan, K.V., Kalyanaraman, R., Sundaresan, M., "Thermodynamic Properties of Dicalcium Ferrite by Calcium Fluoride Galvanic Cells", *J. Electrochem. Soc. India*, **36**(3), 157–159 (1987) (Thermodyn., Exsperimental, 7)

[1988Ara] Arakcheeva, A.V., Karpinskii, O.G., "Polytypic Relations in the Structures of the Group of Hexagonal Ferrites. I. Ca Ferrites of the Structural Type of $Ca_2Fe_{16}O_{25}$", *Sov. Phys. Crystallogr.*, **33**(3), 378–380 (1988) (Experimental, Crys. Structure, 5)

[1988Bag] Bagdavadze, D. I., Tsagareishvili, D. Sh., Tskhadaya, R. A., Gvelesiani, G. G., "Method of Computation of Enthalpy Increment of Crystalline Inorganic Compounds at0–298.15 K Temperature Range" (in Russian), *Izv. Akad. Nauk Gruz. SSR, Ser. Khim*, **14**(3), 199–206 (1988) (Calculation, Review, Thermodyn., 8)

DOI: 10.1007/978-3-540-74196-1_17

[1988Ber] Bergman, B., Song, C., "Decomposition of Wustite in the System Ca-Fe-O", *J. Am. Ceram. Soc.*, **71**(3), C121-C125 (1988) (Experimental, Phase Diagram, Phase Relations, 7)

[1988Chu] Chung, W.S., Murayama, T., Ono, Y., "Direct Measurement of Reduction Equilibria of Calcium Ferrite with CO-CO_2 Gas Mixtures by E.M.F Method Using Solid Oxide Electrolyte in the Temperature Range 1273 to 1373K", *Trans. Iron Steel Inst. Jpn.*, **28**, B4 (1988) (Experimental, 4)

[1988Dob] Dobrovsky, L., Linzer, E., Unzeitigova, H., "Analysis of the Fundamental Thermodynamic Data of Calcium Systems" (in Czech), *Sborn. Ved. Praci Vysok. Skoly Banske v Ostrava (Trans. Inst. Min. Metall. Ostrava Met. Series)*, **1**, 1–20 (1988) (Calculation, Thermodyn., 31)

[1988Han] Han, Q., Zhang, X., Chen, D., Wang, P., "The Calcium-Phosphorus and the Simultaneous Calcium-Oxygen and Calcium-Sulfur Equilibria in Liquid Iron", *Metall. Trans. B*, **19B**, 617–622 (1988) (Phase Relations, Experimental, 29)

[1988Ota] Ota, K., Mitsushima, S., Kamiya, N., "Solubility of Iron(III) Oxide in Molten Carbonates" (in Japanese), *Denki Kagaku Oyobi Kogyo Butsuri Kagaku*, **56**(9), 793–794 (1988) (Experimental, 9)

[1988Wan] Wang, P., Han, Q., "Ca-O Equilibria in Liquid Fe and Fe-C Alloys" (in Chinese), *Jinshu Xuebao*, **24**(1), B7–B11 (1988) (Experimental, Phase Relations, 10)

[1989Ber] Bergman, B., Song, C., "Microstructural Study of Phase Equilibria in The Fe-Ca-O System Involving $CaFe_5O_7$", *J. Amer. Ceram. Soc.*, **72**(8), 1364–1367 (1989) (Experimental, Morphology, Phase Diagram, Phase Relations, 13)

[1989Bog] Bogachenko, A.G., Pyatnitsa, N.V., Saenko, V.Ya., Shtanko, Yu.P., Yakovlev, N.V., Paton, E.O., "Thermodynamic Examination of Deoxidation of Iron with Calcium", *Adv. Spec. Electrometall.*, **5**(3), 160–162 (1989), translated from Probl. Spec. Elektrometall., 5(3), 11–15 (1989) (Thermodyn., Exsperimental, 7)

[1989Rag] Raghavan, V., "The Ca-Fe-O System", *Phase Diagrams of Ternary Iron Alloys*, Indian Inst. of Metals Calcutta, **5**, 48–72 (1989) (Phase Diagram, *, 49)

[1989Sel] Selleby, M., Hillert, M., Sundman, B., "An Assessment of the Ca-Fe-O System", *TRITA-MAC Report No. 0397, Materials Research Centre, Royal Institute of Technology, Stockholm*, 14 (1989) (Review, Thermodyn.)

[1989Suh] Suh, I.-K., Sugiyama, K., Waseda, Y., Toguri, J.M., "Structural Study of the Molten CaO-Fe_2O_3 System by X-ray Difraction", *Z. Naturforsch. A*, **A44**(6), 580–584 (1989) (Experimental, Phase Relations, 20)

[1989Zha] Zhak, A.R., Pyrikov, A.N., Boldina, N.S., "Solid-Phase Reactions in the Ferrous Oxide-Calcium Oxide System" (in Russian), *Izv. Vyss. Uchebn. Zaved., Chern. Metall.*, **3**, 12–14 (1989) (Phase Relations, Exsperimental, 6)

[1990Hil] Hillert, M., Selleby, M., Sundman, B., "An Assessment of the Ca-Fe-O System", *Metall. Trans. A*, **21A**, 2759–2776 (1990) (Calculation, Phase Diagram, Phase Relations, Thermodyn., 44)

[1990Raj] Rajagopalan, K.V., Kalyanaraman, R., Sunderesan, M., "Thermodynamic Properties of Monocalcium Ferrite from Calcium Fluoride Galvanic Cell", *J. Electrochem. Soc. India*, **39**(4), 224–226 (1990) (Thermodyn., Experimental, 9)

[1990Rez] Reznitskii, L.A., "Thermochemistry of Anion-Deficient Perovskites and Compounds with Brownmillerite Structure", *Russ. J. Phys. Chem.*, **64**(8), 1197–1199 (1990), translated from *Zh. Fiz. Khim.*, **64**, 2228–2231, (1990) (Thermodyn., Calculation, 14)

[1991Sun] Sundman, B., "An Assessment of the Fe-O System", *J. Phase Equilib.*, **12**(1), 127–140 (1991) (Thermodyn., Phase Relations, Assessment, 53)

[1991Har] Hara, S., Yamamoto, S., Tateishi, S., Gaskell, D.R., Ogino, K., "Surface Tension of Melts in the FeO-Fe_2O_3-CaO and FeO-Fe_2O_3-2CaO·SiO_2 Systems under Air and CO_2 Atmosphere", *Mater. Trans., JIM*, **32**(9), 829–836 (1991) (Experimental, Phys. Prop., 14)

DOI: 10.1007/978-3-540-74196-1_17

[1993Sch] Schuermann, E., Janhsen, U., "Reduction Equilibria of the Calcium Ferrites in the Fe-Fe_2O_3-CaO System as a Function of Oxygen Concentration and Temperature", *Steel Res.*, **64**(7), 331–339 (1993) (Phase Diagram, Phase Relations, Experimental, 33)

[1993Wu] Wu, P., Eriksson, G., Pelton, A.D., "Critical Evaluation and Optimization of the Thermodynamic Properties and Phase Diagrams of the CaO-FeO, CaO-MgO, CaO-MnO, FeO-MgO, FeO-MnO, and MgO-MnO Systems", *J. Am. Ceram. Soc.*, **76**(8), 2065–2075 (1993) (Calculation, Phase Diagram, Thermodyn., 73)

[1993Gla] Gladkiy, V.N., Shevelev, N.T., "New Data on the Fe-Ca Phase Diagram", *Russ. Metall.*, (6), 113–115, translated from *Izv. Akad. Nauk SSSR. Met.*, 207–209 (1993) (Experimental, Phase Diagram, Phase Relations, 6)

[1994Cho] Cho, S.-W., Suito, H., "Assessment of Calcium-Oxygen Equilibrium in Liquid lron", *ISIJ Int.*, **34**(3), 265–269 (1994) (Thermodyn., Calculation, 20)

[1994Gib] Gibb, T.C., Herod, A.J., Munro, D.C., Peng, N., "Synthesis under High Pressure and Characterisation by Mossbauer Spectroscopy of Non-Stoichiometric $Ca_2Fe_2O_{5.12}$", *J. Mater. Chem.*, **4**(9), 1451–1455 (1994) (Experimental, Phase Relations, 26)

[1994Kim] Kimura, T., Suito, H., "Calcium Deoxidation Equilibrium in Liquid Iron", *Metall. Mat. Trans. B*, **25B**, 33–42 (1994) (Experimental, 21)

[1994Oka] Okamoto, H., "Comment on Ca-Fe (Calcium-Iron)", *J. Phase Equilibr.*, **15**(5), 565–566 (1994) (Review, Phase Diagram, 4)

[1995Fuj] Fujiwara, H., Tano, M., Yamamoto, K., Ichise, E., "Solubility and Activity of Calcium in Molten Iron in Equilibrium with Lime and Thermodynamics of Calcium Containing Iron Melts", *ISIJ Int.*, **35**(9), 1063–1071 (1995) (Experimental, Phase Relations, Thermodyn., 23)

[1995Jow1] Jowsa, J., "Calcium and Oxygen in Liquid Iron-Discrepancies Between Thermodynamic Data and its Consequences" (in Polish), *Hutnik-Wiadomosci Hutnicze*, **7**, 246–250 (1995) (Calculation, 22)

[1995Jow2] Jowsa, J., "Phase Equilibrium of Fe-O-i Systems (i = Ca, Al) Used for Steelmaking", (in Polish), *Hutnik-Wiadomosci Hutnicze*, **8**, 301–304 (1995) (Calculation, Phase Relations, 13)

[1995Lyk] Lykasov, A.A., Popova, T.V., "Conditions for the Existence of Ternary Compounds in the FeO-Fe_2O_3-CaO System", *Inorg. Mater. (Engl. Trans.)*, **31**(1), 76–79 (1995), translated from *Neorg.Mater.*, **31**(1), 84–87 (1995) (Crys. Structure, Experimental, Phase Diagram, Phase Relations, 16)

[1996Sel] Selleby, M., Sundmann, B., "A Reassessment of the Ca-Fe-O System", *Calphad*, **20**(3), 381–392 (1996) (Assessment, Phase Relations, Thermodyn., *, 26)

[1997Elg] El-Geassy, A.A., "Stepwise Reduction of CaO and/or MgO Dopped-Fe_2O_3 Compacts to Magnetite Then Subsequently to Iron at1173–1473 K", *ISIJ Int.*, **37**(9), 844–853 (1997) (Phase Relations, Experimental, 32)

[1997Ito] Itoh, H., Hino, M., BanYa, S., "Deoxidation Equilibrium of Calcium in Liquid Iron" (in Japanese), *Tetsu to Hagane*, **83**(11), 695–700 (1997) (Phase Relations, Experimental, 34)

[1998Elg] El-Geassy, A.-H., "Stepwise Reduction of CaO and/or MgO Doped-Fe_2O_3 Compacts (Hematite-Wuestite-Iron Transformation Steps)", *Scand. J. Metall.*, **27**(5), 205–213 (1998) (Phase Relations, Experimental, 33)

[1999Bel] Belashenko, D.K., Ostrovskii, O.I., "Molecular Dynamics Simulation of CaO-FeO Melts and Calculation of thair Thermodynamic Properties" (in Russian), *Zh. Fiz. Khim.*, **73**(4), 704–709 (1999) (Calculation, Thermodyn., 9)

[1999Gom] Gomez, M.I., de Moran, J.A., Carbonio, R.E., Aymonino, P.J., "Synthesis of $AFeO_{2.5+x}$ ($0<x<0.5$; A=Sr, Ca) Mixed Oxides from the Oxidative Thermal Decomposition of $A(Fe(CN)_5NO) \cdot 4H_2O$", *J. Solid State Chem.*, **142**(1), 138–145 (1999) (Experimental, Crys. Structure, 43)

[1999Jac] Jacob, K.T., Dasgupta, N., Waseda, Y., "Thermodynamic Properties of the Calcium Ferrites $CaFe_2O_4$ and $Ca_2Fe_2O_5$", *Z. Metallkd.*, **90**(7), 486–490 (1999) (Experimental, Thermodyn., 20)

DOI: 10.1007/978-3-540-74196-1_17

[2000Min] Minyaylova, I.G., Presnyakov, I.A., Pokholok, K.V., Sobolev, A.V., Baranov, A.V., Demazeau, G., Govor, G.A., Vetcher, A.K., "Hyperfine Interactions and Dynamic Characteristics of ^{119}Sn Dopnat Atoms in $Ca_2Fe_2O_5$", *J. Solid State Chem.*, **151**, 313–316 (2000) (Crys. Structure, Experimental, Electronic Structure, 14)

[2000Woo] Woodward, P.M., Cox, D.E., Moshopoulou, E., Sleight, A.W., Morimoto, S., "Structural Studies of Charge Disproportionation and Magnetic Order in $CaFeO_3$", *Phys. Rev. B*, **62**(2), 844–855 (2000) (Crys. Structure, Electronic Structure, Experimental, Magn. Prop., 48)

[2000Zai] Zaitsev, A.L., Korolev, N.V., Lyakishev, N.P. Mogutnov, B.M., "Thermodynamic Properties and Phase Equilibria in the Ca-CaO System", *Russ. J. Inorg. Chem.*, **45**(7), 1211–1123 (2000) (Calculation, Experimental, Phase Diagram, Thermodyn., 17)

[2001Bel] Belashchenko, D.K., Ostrovski, O.I., Skvortsov, L.V., "Molecular Dynamic Simulation of Binary CaO-FeO, MgO-SiO_2, FeO-SiO_2 and Ternary CaO-FeO-SiO_2 Systems", *Thermochim. Acta*, **372**, 153–163 (2001) (Calculation, Thermodyn., 20)

[2001Ber] Berenov, A.V., MacManus-Driscoll, J.L., Kilner, J.A., "Observation of the Compensation Law During Oxygen Diffusion in Perovskite Materials", *Int. J. Inorg. Mater.*, **3**(8), 1109–1111 (2001) (Calculation, Electronic Structure, 25)

[2001Fri] Frisk, K., Selleby, M., "The Compound Energy Formalism: Applications", *J. Alloys Compd.*, **320**(2), 177–188 (2001) (Assessment, Phase Relations, Review, 41)

[2002For] Forsberg, S., Wikstroem, P., Rosen, E., "Determination of Gibbs Energies of Formation of $CaFe_2O_4$ and $Ca_2Fe_2O_5$ from Solid-State EMF Measurements Using CaF_2 as Solid Electrolyte", *Metall. Mater. Trans. B*, **33b**(3), 385–392 (2002) (Experimental, Thermodyn., 31)

[2002Fuk] Fukuyama, H., Hossain, M.K., Nagata, K., "Solid-State Reaction Kinetics of the System CaO-FeO", *Metall. Mater. Trans. B*, **33b**(2), 257–264 (2002) (Experimental, Phase Relations, 26)

[2002Ina] Inami, T., Suzuki, K., "Lattice Parameter and Redox Equilibria in CaO-Containing Wustite", *ISIJ Int.*, **42**(2), 150–154 (2002) (Crys. Structure, Experimental, Phase Diagram, Phase Relations, 12)

[2002Kaw] Kawakami, T., Nasu, S., Sasaki, T., Kuzushita, K., Morimoto, S., Endo, S., Kawasaki, S., Takano, M., "High-Pressure Moessbauer Study of Perovskite Iron Oxides", *J. Phys.: Condens. Matter*, **14**(44), 10713–10718 (2002) (Experimental, Phase Diagram, Phys. Prop., 9)

[2002Ros] Ross, N., Angel, R.J., Seifert, F., "Compressibility of Brownmillerite ($Ca_2Fe_2O_5$): Effect of Vacancies on the Elastic Properties of Perovskites", *Phys. Earth Planet. Interiors*, **129**, 145–151 (2002) (Experimental, Crys. Structure, 33)

[2003Kon] Kongoli, F., McBow, I., Yazawa, A., "Liquidus Surface of "Lime Ferrite" Slags at Intermediate Oxygen Potentials", *Mater. Trans.*, **44**(10), 2136–2140 (2003) (Phase Relations, Calculation, Phase Diagram, 22)

[2003Mue] Mueller-Buschbaum, H., "The Crystal Chemistry of AM_2O_4 Oxometallates", *J. Alloys Compd.*, **349**(1–2), 49–104 (2003) (Crys. Structure, Review, 476)

[2004Fre] Fredriksson. P., Seetharaman, S., "Thermodynamics Activities of FeO in some Binary FeO-Containing Slags", *Steel Res.*, **75**, 240–246 (2004) (Calculation, Experimental, Thermodyn., 23)

[2004Sal] Saleh, H.I., "Synthesis and Formation Mechanisms of Calcium Ferrite Compounds", *J. Mater. Sci. Technol.*, **20**(5), 530–534 (2004) (Crys. Structure, Experimental, Magn. Prop., 30)

[2004Red] Redhammer, G.J., Tippelt, G., Roth, G., Amthauer, G., "Structural Variations in the Brownmillerite Series $Ca_2(Fe_{2-x}Al_x)O_5$: Single-Crystal X-ray Diffraction at 25°C and High-Temperature X-ray Powder Diffraction (25°C < T < 1000°C)", *Am. Mineralog.*, **89**, 405–420 (2004) (Crys. Structure, Experimental, 28)

[Mas2] Massalski, T.B. (Ed.), *Binary Alloy Phase Diagrams*, 2nd edition, ASM International, Metals Park, Ohio (1990)

[V-C2] Villars, P. and Calvert, L.D., *Pearson's Handbook of Crystallographic Data for Intermetallic Phases*, 2nd edition, ASM, Metals Park, Ohio (1991)

DOI: 10.1007/978-3-540-74196-1_17

Cobalt – Chromium – Iron

Gautam Ghosh

Introduction

A summary of experimental studies on phase relations, structure and thermodynamics is given in Table 1. It may be noted that a large number of experimental studies have been carried out in this system. These studies may be conveniently grouped into following categories: (i) kinetics and mechanism of phase separation in Fe rich bcc alloys [1974Vin, 1975Mal, 1975Vin, 1976Ivc, 1977Ale1, 1977Ale2, 1977Bel, 1977Iva, 1977Vin, 1978Dom, 1978Vin, 1979Kok1, 1980Eib, 1980Jin1, 1980Mah, 1983Bel, 1983Chi, 1984Bre, 1984Ser, 1986Kol, 1986Zhu, 1987Ser, 1989Sim, 1992Vin, 1994Lyo, 2000All, 2002Ben, 2005Ben, 2005Gao, 2006Koy] in the search for optimum magnetic properties, (ii) order-disorder ($B2 \rightleftharpoons A2$) transition in FeCo based alloys [1952Jos, 1973Cle, 1975Buc, 1976Hag, 1977Dzh, 1979Buc, 1979Kok1, 1979Kok2, 1980Jin2], (iii) phase relations [1909Jae, 1929Wev, 1932Koe, 1949Bec, 1951Rid, 1952Bec, 1959Koe, 1959Sve, 1973Kra, 1975Kan, 1976Dem, 1976Kan, 1978Dom, 1979Dom, 1983Chi, 1984Bel], (iv) experimental measurements of thermodynamic data [1977Kub, 1982Arg, 1985Bla, 1990Zub], (v) thermodynamic modelling of phase equilibria within calculation of phase diagram (CALPHAD) formalism [1974Kau, 1975Kau, 1978Dom, 1979Nis, 1979Spe, 1981All, 1981Nis, 1987Vin, 1994Hil, 1995Nis]. The phase relations have been reviewed from time to time [1949Jae, 1975Cha, 1988Ray, 1994Rag], while the magnetic properties have been reviewed elsewhere [1999McH, 2005Sou].

[1932Koe] carried out thermal analysis of 40 ternary alloys, and reported nine vertical sections at constant Fe contents, and an isothermal section 20°C. [1952Bec] presented the fcc + hcp equilibria in the form of two vertical sections at 20 and 32 mass% Cr. [1951Rid] investigated an unspecified number of alloys that were heat treated at 1200°C for at least 97 h, and reported the corresponding isothermal section. They also found that at 800°C, the σ phase of Co-Cr and Cr-Fe systems forms a continuous solid solution. [1959Koe] investigated the phase relations in 28 ternary alloys using X-ray diffraction, and reported two isothermal sections at 700 and 600°C. [1959Sve] investigated 30 ternary alloys by means of metallography, and reported isothermal sections at 1000 and 600°C, and also three vertical sections at constant Fe contents. [1973Kra] determined the partitioning coefficients of Co and Cr between bcc and fcc phases at 1100°C.

[1979Dom] carried out a systematic study of phase equilibria, and reported six isothermal sections in the temperature range of 1300-800°C, at 100°C interval. They prepared a number of alloys, using 99.9% electrolytic Co, 99.9% electrolytic Cr and 99.95% Fe, in an induction furnace and under He atmosphere. The alloys were heat treated at 1300°C for 8 h, at 1200°C for 25 h, at 1100°C for 35 h, at 1000°C for 105 h, at 900°C for 150 h and at 800°C for 300 h. and then characterized by conventional metallography, hardness measurements, electron probe microanalysis of phases, DTA, and X-ray diffraction. [1984Bel] reported the phase relations of Fe corner only at 1300, 1100, 1000 and 900°C. Vertical sections at 12 mass% Co [1983Chi] and at 15 mass% Co [1975Kan, 1976Kan] have also been reported.

Thermodynamic properties of solid and liquid phases have been measured by adiabatic calorimetry [1977Kub, 1985Bla], Knudsen cell mass spectrometry [1982Arg], and solution calorimetry [1990Zub]. The measured properties include activity of components in the liquid phase [1982Arg], the heat of mixing of liquid [1982Arg], bcc [1982Arg], fcc [1982Arg], σ [1990Zub] phases, the heat of formation of bcc [1977Kub], fcc [1977Kub], σ [1990Zub] phases, and the heat of transformation of $\sigma \rightleftharpoons \alpha$ [1977Kub] and $\alpha \rightleftharpoons \gamma$ [1985Bla].

Binary Systems

The Co-Cr system is accepted from [1990Ish], the Co-Fe system is accepted from [2002Ohn], and the Cr-Fe binary phase diagram is accepted from [1982Kub].

DOI: 10.1007/978-3-540-74196-1_18

Solid Phases

A large number of studies have been devoted to the phase separation of Fe rich bcc solid solutions by spinodal mechanism in the temperature range of 400 to 700°C. Various experimental techniques, such as atom-probe field ion microscopy (AP-FIM) [1984Bre, 1986Zhu], Mössbauer spectroscopy and X-ray diffraction [1976Ivc, 1977Ale1, 1977Ale2, 1977Bel, 1977Iva, 1980Eib, 1986Kol, 1989Sim, 2000All, 2002Ben, 2005Ben, 2005Gao], nuclear magnetic resonance (NMR) [1984Ser, 1987Ser], neutron diffraction/scattering [1975Mal, 1975Vin, 1977Vin, 1978Vin, 1979Kok1, 1983Bel, 1994Lyo], transmission electron microscopy (TEM) [1977Ale2, 1978Dom, 1980Eib, 1980Jin1, 1980Mah, 1983Bel, 1983Chi, 2005Gao] have been used to understand the mechanism and kinetics of phase separation in metastable bcc alloys into Fe rich ferromagnetic and Cr rich paramagnetic domains. However, the atomic arrangements during early stages of phase separation, as shown in neutron diffraction patterns [1975Mal], Mössbauer spectra [1976Ivc, 1977Ale2] and NMR spectra [1984Ser, 1987Ser], are rather complex. Also, depending on the aging treatment, the ferromagnetic domains may have ordered ($B2$) structure [1974Vin, 1975Vin, 1976Ivc, 1977Vin, 1984Ser]. Nevertheless, these studies have played a key role in understanding the magnetic properties, such as coercive force (H_c), residual induction (B_r), and permeability ($(BH)_{max}$) arising from nanoscale ferromagnetic and paramagnetic domains in phase separated microstructures.

In addition to phase separation by a spinodal mechanism during thermal aging of bulk alloys, spinodal microstructures also develop during mechanical milling of elemental powders [2002Ben, 2005Ben, 2005Gao]. Mössbauer spectra of ball milled and conventional heat treated specimens are the same in terms of hyperfine field, isomer shift and quadruplar shift [2002Ben].

The coarsening kinetics of spinodal microstructures during thermal aging follow a t^n type power law, but widely differing values of n, ranging from $n = 0.14$ [1984Bre], $n = 0.2$-0.25 [1986Zhu], and $n = 0.27 \pm 0.03$ [1989Sim] have been reported.

[1984Bel] studied martensitic transformation in Fe-(14-24)Co-(18-35)Cr (mass%) alloys. Depending on the alloy composition, they observed $\gamma \rightleftharpoons \alpha$, $\gamma \rightleftharpoons \varepsilon \rightleftharpoons \alpha$, and $\gamma \rightleftharpoons \varepsilon$ transformations.

[2005Ben] reported the formation of a primitive cubic phase with lattice parameter $a = 441$-457 pm during mechanical alloying, but other crystallographic details were not reported.

[1985Mor] estimated the solid solubility of fcc alloys in the ternary regime based on the electronic structure calculations by discrete variational DV-X_α method. They introduced a parameter M_d, which is the average energy level of d orbitals of the alloying elements, and it carries both electronegativity and atomic size factor effects. At 1200°C, the predicted solubility underestimates the experimental data.

Using a linear muffin-tin orbital method, [2002Boz] calculated the formation energies of $(Co,Cr)_{0.5}Fe_{0.5}$ and $Co_{0.5}(Fe,Cr)_{0.5}$ alloys with $B2$ structure. They predicted that in both cases Cr atoms prefer to occupy the Fe sublattice. Also, the calculated formation energies are predicted to be more positive compared to binary $Co_{0.5}Fe_{0.5}$.

The details of the crystal structures and lattice parameters of the solid phases are listed in Table 2.

Order – Disorder Phase Transition

Addition of Cr in FeCo-based alloys lowers the order-disorder ($B2 \rightleftharpoons A2$) temperature [1952Jos, 1976Hag, 1977Dzh, 1980Jin2]. [1976Hag] carried out a systematic study of the composition dependence of order-disorder ($B2 \rightleftharpoons A2$) transition temperature in Co-Cr-Fe alloys. They investigated 21 ternary alloys that were solution treated at 1150°C for 5 h and subsequently water quenched. Differential thermal analysis was carried out at a constant heating rate of $10°C \cdot min^{-1}$ to determine the order-disorder temperature. Figure 1 shows the contour plots of order-disorder temperatures [1976Hag] as a function of alloy composition. In $(Fe_{0.5}Co_{0.5})_{1-x}Cr_x$ alloys, the order-disorder transition temperature decreases by about 5.1°C per at.% Cr [1976Hag].

However, the effect of Cr on the kinetics and mechanism of chemical ordering ($A2 \rightleftharpoons B2$) is somewhat controversial [1973Cle, 1975Buc, 1979Buc, 1979Kok1, 1979Kok2]. [1973Cle] measured the long-range order parameter and antiphase domain size in FeCo and FeCo-0.4%Cr at 435 and 550°C, and concluded that Cr has a significant effect on the kinetics of ordering. Based on the neutron diffraction study of $Fe_{0.5}(Co_{0.5-x}Cr_x)$ alloys, [1979Kok1] reported that slow cooling of alloys with $x = 0.021$ and $x = 0.088$ from 1100°C leads to a high degree of order that does not change after subsequent annealing at 560°C. Electrical

DOI: 10.1007/978-3-540-74196-1_18

resistivity data of $Fe_{0.5}(Co_{0.5-x}Cr_x)$ alloys show that the rate of ordering decreases with increasing Cr concentration [1979Kok2]. On the other hand, [1975Buc] showed that the ordering kinetics and mechanisms in FeCo-0.4%Cr are the same as in binary FeCo alloys. In the temperature range 500-600°C homogeneous ordering followed by domain coarsening takes place, while below 430°C nucleation and growth of grain boundary films of fully ordered structure take place. [1979Buc] reported the effect of cold work on ordering and recrystallization kinetics of FeCo and FeCo-0.4%Cr alloys. Cold deformation of about 50% can induce completely disordered state. During subsequent annealing in the temperature range of 475-600°C, homogeneous ordering precedes recrystallization, while in the temperature range of 250-475°C ordering takes place by nucleation and growth.

Isothermal Sections

Isothermal sections, including partial and complete, have been reported at following temperatures: at 20°C [1932Koe], at 1200 and 800°C [1951Rid], at 700 and 600°C [1959Koe], at 1000 and 600°C [1959Sve], from 1300 to 800°C at 100°C interval [1979Dom], and at 1300, 1100, 1000 and 900°C [1984Bel]. The isothermal sections shown here are adopted from [1959Koe] and [1979Dom].

Figures 2, 3, 4, 5, 6, and 7 shows the isothermal sections at 1300, 1200, 1100, 1000, 900 and 800°C, respectively, after [1979Dom], while Figs. 8 and 9 shows the isothermal sections at 700 and 600°C, respectively, after [1959Koe]. At a temperature just below the upper temperature limit of σ phase stability in the Co-Cr system, a three phase field α + γ + σ appears in the isothermal sections. With decreasing temperature, the three phase field gradually moves from Co-Cr side towards Cr-Fe side. Also, between 1200 and 800°C the (Cr)/(Cr) + σ boundary develops a significant curvature. At 800°C, the isothermal section of [1979Dom] shows a good agreement with the earlier results [1949Bec, 1951Rid]. Around 900°C, another three phase field γ + ε + σ appears due to (γCo) ⇌ (εCo) transformation in the Co rich Co-Cr alloys. This three phase field was not identified by [1979Dom] in 900 and 800°C isothermal sections. On the other hand, [1959Koe] firmly established the γ + ε + σ field at 700°C.

There is some uncertainty about the phase relations involving α, γ, and ε at 600°C. [1959Koe] proposed a solid state transition reaction γ + σ ⇌ α + ε around 600°C. In Fig. 9, the merger of two three phase fields, α + γ + σ and γ + ε + σ, has given rise to a reaction quadrilateral. This implies that even 1000 h of heat treatment at 600°C is insufficient to establish the phase equilibria. On the other hand, thermodynamic calculations show that α + γ + σ is a stable tie-triangle at 600°C [1978Dom]. However, it is not clear if [1978Dom] considered the ε phase in thermodynamic calculations as the calculated isothermal section at 400°C also shows the α + γ + σ tie-triangle.

In Figs. 2 to 9, adjustments have been made to comply with the accepted binary phase diagrams.

Temperature – Composition Sections

Temperature - composition sections have been determined at following constraints: at a constant ratio of Co and Cr (by mass) of 70/30, 60/40, 55/45, 50/50, 40/60, 30/70, 20/80 and 10/90 [1929Wev], at a constant Fe content of 30, 40, 45, 50, 60, 70, 80, 85 and 95 mass% [1932Koe], at a constant Cr content of 20 and 32 mass% [1952Bec], at a constant Fe content of 10, 30 and 50 mass% [1959Sve], at a constant Co content of 15 mass% [1975Kan, 1976Kan], at a constant Co content of 12 mass% [1983Chi]. This information is also embodied in the isothermal sections shown in Figs. 2 to 9.

Due to its practical importance in optimizing the magnetic properties of Fe rich alloys, the metastable miscibility gap boundaries in bcc phase have been investigated several times [1976Hag, 1977Kan, 1980Min, 1992Vin]. Figure 10 shows the metastable miscibility gap boundaries, determined by monitoring the change in magnetic property during isothermal annealing, at various ratios of Fe and Co in the alloy, after [1980Min]. As the value of ratio decreases, the miscibility gap develops a “ridge” or a “horn” protruding towards the FeCo side. The results of [1977Kan] are qualitatively similar to [1980Min], but they do not exhibit so pronounced ridges. Thermomagnetic treatment of homogeneous alloys in the “ridge” or “horn” region of the miscibility gap is the most efficient approach to obtain an optimal magnetic properties.

Figure 11 shows the calculated miscibility gaps based on analytical Gibbs energy functions, with and without the contribution of magnetic ordering [1995Nis]. It is obvious that the shape and the critical temperature of miscibility gap are strongly influenced by magnetic ordering, from a nearly parabolic shape with a low

DOI: 10.1007/978-3-540-74196-1_18

critical temperature in the absence magnetic ordering to a highly asymmetric with a much higher critical temperature in the presence magnetic ordering [1979Nis, 1995Nis]. The horn shaped miscibility gaps shown in Fig. 10 has also been called the "Nishizawa horn" [1994Hil].

Thermodynamics

Thermodynamic properties of ternary alloys have been investigated a number of times by measuring the heat of formation of bcc [1977Kub, 1982Arg], fcc [1977Kub, 1982Arg], σ [1990Zub] and liquid [1982Arg] phases, and the activity of Co, Cr and Fe in liquid alloys [1982Arg]. Available thermodynamic data is summarized in Tables 3, 4 and 5.

[1977Kub] used an adiabatic calorimeter to determine the heat of formation of bcc and fcc solid solutions at 1350°C. They also determined the heat of transformation, σ ⇌ α, of eight alloys. [1982Arg] employed Knudsen cell mass spectrometry to determine the activity of components in solid and liquid alloys at 1400 and 1600°C, respectively. Using the measured data, they derived the heat of mixing of solid and liquid alloys. [1985Bla] used an adiabatic calorimeter to determine the heat of transformation, α ⇌ γ, of six Fe rich alloys. In addition, they also calculated the heat of transformation of the same alloys at a constant temperature of 911°C using analytical thermodynamic functions.

[1990Zub] measured the enthalpy of formation of σ phase by solution calorimetry. Eighteen ternary alloys were prepared in an arc furnace under argon atmosphere, and they were remelted at least four times. Electrolytic grade Cr, K-O grade Co, and carbonyl grade Fe were used. Alloys were homogenized at 1150°C for 12 h followed by annealing at 800°C for 300-500 h. The heat of formation was determined from the difference in heats of dissolution of ternary alloys and of the pure components in liquid aluminium at 800°C.

Thermodynamic modeling of the ternary system has also been carried out by the CALPHAD method [1974Kau, 1975Kau, 1978Dom, 1979Nis, 1981All, 1987Vin, 1994Hil, 1995Nis], where the Gibbs energies of the relevant phases are described by simple analytical functions. The following isothermal sections have calculated by CALPHAD method: at 1427, 1227, 1200, 1027, 927, 902, and 827°C [1974Kau, 1975Kau], at 700, 600 and 400°C [1978Dom], and from 1500 to 700°C at 100°C interval [1981All]. Figure 12 shows the calculated miscibility gap isotherms at 800, 700 and 600°C [1995Nis]. Once again, due to increasingly importance of magnetic ordering energy with decreasing temperature, the miscibility gap expands and develops characteristic ridge along the Curie temperature line.

Notes on Materials Properties and Applications

A summary of experimental investigation of properties is given in Table 6.

Table 7 lists the Curie temperature and average magnetic moment of some Fe rich bcc alloys [1980Gal, 1980Jin2, 1985Bla], while Fig. 13 shows the Curie temperature plots of Cr rich bcc alloys [1977Kan].

The phase separation in Fe rich bcc alloys during thermal aging under a magnetic field has a dramatic influence on the magnetic properties (H_c, B_r, and $(BH)_{max}$) [1974Vin, 1975Kan, 1976Kan, 1978Vin, 1980Jin2, 1980Min, 1983Bel, 1983Chi]. For example, the increase in coercivity from several tens of $A \cdot m^{-1}$ in homogeneous alloys to several tens of $kA \cdot m^{-1}$ after magnetic annealing is attributed to the formation of coherent elongated ferromagnetic domains (Fe rich) embedded in a weakly magnetic (Cr rich) matrix. Also, during thermomagnetic annealing the ferromagnetic domains align only in the direction of applied magnetic field, and independent of crystallographic direction even when single crystals are used [1983Bel]. In such microstructures, the elastic strain energy contribution is estimated to be minimal due to small difference in lattice parameter between ferromagnetic and paramagnetic regions [1978Vin]. The anisotropic growth of fluctuations along the direction of applied magnetic field is due the tendency towards lower demagnetizing and magnetostatic energy [1978Vin]. This tendency is largest in a narrow temperature range defined by the Curie temperatures of α_1 and α_2 phases. Therefore, control of diffusion by the gradient of magnetic energy is crucial in optimizing the magnetic properties. Recent phase field modelling [2006Koy] of microstructure evolution in Fe-12Co-35Cr (at.%) has provided further insight into the mechanism and kinetics of phase separation. [2006Koy] showed that even in the absence of magnetic field, the lamellar morphology develops during phase separation.

[1983Chi] carried out a systematic study of magnetic annealing on the properties of phase separated alloys with composition Fe-12Co-(21-30)Cr (mass%). These alloys were magnetically annealed in the temperature

DOI: 10.1007/978-3-540-74196-1_18

range of 630-690°C. Despite the fact that these alloys have spinodal temperature higher than the Curie temperature of homogeneous alloy, magnetic annealing is found to be very effective in improving the magnetic properties. This is due to the fact that the effectiveness of magnetic annealing is determined the by the difference in Curie temperatures of α_1 and α_2 phases, and not by Curie temperature of homogeneous alloy. In addition, [1983Chi] reported that the efficacy of magnetic aging is highest when the difference between the spinodal temperature and Curie temperature is about 10°C. Furthermore, the best attainable magnetic properties of Fe-12Co-28Cr (mass%) after aging at 650°C under 3000 Oe field are H_c = 610 Oe, B_r = 13 kG, and $(BH)_{max}$ = 5 MGOe [1983Chi]. Plastic deformation accelerates the formation of γ and σ phases during thermal aging [1977Bel, 1977Iva], which in turn deteriorate the magnetic properties [1982Sei].
[1980Bel] determined the single crystal elastic constants of Fe-15Co-35Cr (mass%) and Fe-23Co-31Cr (mass%) alloys in the temperature range of 22 to –73°C.
The formability and high temperature tensile and torsion properties of ternary alloys have been discussed by [1984Mue] and [1987Klo], while the fracture behavior of phase separated alloys has been presented by [1980Jin2].

Table 1. Investigations of the Co-Cr-Fe Phase Relations, Structures and Thermodynamics

Reference	Method/Experimental Technique	Temperature/Composition/Phase Range Studied
[1909Jae]	Thermal analysis	Liquidus temperature
[1929Wev]	Metallography, thermal analysis, X-ray diffraction, hardness	Liquidus isotherms
[1932Koe]	Thermal analysis	Up to 60 mass% Co, up to 40 mass% Cr, Fe = bal.
[1951Rid]	Metallography, X-ray diffraction	1200°C, 800°C; bcc + fcc and bcc + fcc + σ phase regions
[1952Bec]	Metallography, X-ray diffraction	20-32 mass% Cr, < 6 mass% Fe, Co = bal.; 640-1040°C; fcc + hcp phase equilibria
[1952Jos]	Dilatometry, resistivity	35.44 mass% Co, 0.86 mass% Cr, Fe = bal.
[1959Koe]	X-ray diffraction	10-80 mass% Co, 5-30 mass% Cr, Fe = bal.; 600-700°C
[1959Sve]	Metallography, thermal analysis	Up to 1000°C
[1973Kra]	Electron probe microanalysis	19.19-25.59 mass% Co, 27.82-30.91 mass% Cr, Fe = bal.; 1100°C; bcc+fcc phase region
[1974Vin]	Metallography, X-ray diffraction, neutron diffraction	7.6-20 mass% Co, 31-37.8 mass% Cr, Fe = bal.
[1975Kan]	Metallography, X-ray diffraction, magnetometry	15 mass% Co, 15-40 mass% Cr, Fe = bal.; 600-1300°C; bcc + fcc and bcc+ fcc + σ phase regions
[1975Mal]	High-temperature neutron diffraction	$(FeCo)_{1-x}Cr_x$, $x < 0.05$; 400-850°C; spinodal decomposition in bcc phase
[1975Vin]	Metallography, neutron diffraction, X-ray diffraction	up to 20 mass% Co, Fe/Cr = 1.5; bcc and σ phases

(*continued*)

DOI: 10.1007/978-3-540-74196-1_18

Reference	Method/Experimental Technique	Temperature/Composition/Phase Range Studied
[1976Dem]	Magnetometry, X-ray diffraction	23 mass% Co, 31.5 mass% Cr, Fe = bal.; 600-1300°C
[1976Hag]	Differential thermal analysis	40-65 at.% Co, 10 at.% Cr, Fe = bal; bcc phase
[1976Ivc]	Calorimetry, Mössbauer spectroscopy	5.1-14.3 mass% Co, 4.95-12.92 mass% Cr, Fe = bal.; bcc phase; spinodal decomposition
[1976Kan]	Metallography, X-ray diffraction, magnetometry	15 mass% Co, 15-40 mass% Cr, Fe = bal.; 600-1300°C; bcc + fcc and bcc + fcc + σ phase regions
[1977Ale1]	Mössbauer spectroscopy, transmission electron microscopy, X-ray diffraction	25-35 mass% Co, 1.5-2 mass% Cr, Fe = bal.; 300-525°C; spinodal decomposition of bcc phase
[1977Ale2]	Transmission electron microscopy, Mössbauer spectroscopy	25-35 mass% Co, 0.5-2 mass% Cr, Fe = bal.; 300-525°C; spinodal decomposition of bcc phase
[1977Bel]	X-ray diffraction, Mössbauer spectroscopy	25 mass% Co, 15 mass% Cr, Fe = bal.; spinodal decomposition in bcc alloy
[1977Dzh]	Transmission electron microscopy, X-ray diffraction	25-35 mass% Co, 0.3-2 mass% Cr, Fe = bal.; bcc phase; 450-525°C
[1977Iva]	X-ray diffraction, magnetometry	23.3 mass% Co, 31 mass% Cr, Fe = bal.; 600-640°C; spinodal decomposition in bcc phase
[1977Kan]	Hardness, magnetometry	< 50 mass% Co, 20-80 mass% Cr, Fe = bal.; phase separation in bcc phase
[1977Kub]	Calorimetry	5-65 at.% Co, 10-85 at.% Cr, Fe = bal.; 900-1350°C; heat of formation of bcc phase and heat of transformation of $\sigma \rightleftharpoons \alpha$
[1977Vin]	X-ray diffraction and small-angle neutron scattering	15.5-22.5 mass% Co, 31-35.4 mass% Cr, Fe = bal; 580-650°C; spinodal decomposition in bcc phase
[1978Dom]	Differential thermal analysis, resistivity, magnetometry, neutron diffraction, transmission electron microscopy, X-ray diffraction	20.5 at.% Co, 33 at.% Cr, Fe = bal.; 400-700°C
[1978Vin]	Small-angle neutron scattering, magnetometry	23 mass% Co, 31 mass% Cr, Fe = bal.; 580-640°C
[1979Dom]	Metallography, electron probe microanalysis, differential thermal analysis, X-ray diffraction	800-1300°C isothermal sections

(*continued*)

DOI: 10.1007/978-3-540-74196-1_18

Reference	Method/Experimental Technique	Temperature/Composition/Phase Range Studied
[1979Kok1]	Neutron diffraction	$Fe_{0.5}(Co_{0.5-x}Cr_x)$, $0.021 \le x \le 0.133$; 560-1100°C; chemical ordering and spinodal decomposition in bcc phase
[1979Kok2]	Electrical resistivity	$Fe_{0.5}(Co_{0.5-x}Cr_x)$, $0.021 \le x \le 0.133$; chemical ordering in bcc phase
[1980Bel]	Resonance method	15-23 mass% Co, 31-35 mass% Cr, Fe = bal.; –73-22°C; single crystal elastic constants of bcc phase
[1980Eib]	Transmission electron microscopy, Mössbauer spectroscopy	11.5 mass% Co, 33 mass% Cr, Fe = bal., 500-680°C; spinodal decomposition in bcc phase
[1980Gal]	Thermomagnetometry	10.5 mass% Co, 28 mass% Cr, Fe = bal.; up to 1200°C; bcc phase
[1980Jin1]	Metallography, scanning electron microscopy, transmission electron microscopy, hardness	9.38-11.13 mass% Co, 26.75-27.5 mass% Cr, Fe = bal.; 500-930°C; spinodal microstructure of bcc phase
[1980Jin2]	Magnetometry, transmission electron microscopy	5-9 mass% Co, 27-28 mass% Cr, Fe = bal.; 500-640°C
[1980Mah]	Transmission electron microscopy	10.5 mass% Co, 28 mass% Cr, Fe = bal.; spinodal decomposition in bcc phase
[1980Min]	Transmission electron microscopy, magnetometry, magnetic aging	6-20 mass% Co, 20-35 mass% Cr, Fe = bal.; 400-685°C
[1982Arg]	Knudsen-cell mass spectrometry	1077-1727°C; activities in liquid phase, heat of mixing of liquid, bcc and fcc phases
[1982Sei]	Metallography, transmission electron microscopy, magnetometry	10 mass% Co, 28-30 mass% Cr, Fe = bal.; 540-650°C; spinodal decomposition in bcc phase
[1983Bel]	Transmission electron microscopy, small-angle neutron scattering	23 mass% Co, 30 mass% Cr, Fe = bal.; 500-645°C; spinodal decomposition in bcc phase
[1983Chi]	Transmission electron microscopy, magnetometry, magnetic aging	12 mass% Co, 21-30 mass% Cr, Fe = bal.; spinodal decomposition in bcc phase
[1984Bel]	Metallography, X-ray diffraction	14-24 mass% Co, 18-35 mass% Cr, Fe = bal.; martensitic transformations ($\gamma \rightleftharpoons \alpha$ and $\gamma \rightleftharpoons \varepsilon$)
[1984Bre]	Atom-probe field ion microscopy, transmission electron microscopy	10.6 mass% Co, 28.5 mass% Cr, Fe = bal.; 525-640°C; spinodal decomposition in bcc phase
[1984Ser]	Nuclear gamma and nuclear magnetic resonance	23 mass% Co, 29 mass% Cr, Fe = bal.; 540-630°C; spinodal decomposition in bcc phase

(*continued*)

DOI: 10.1007/978-3-540-74196-1_18

Reference	Method/Experimental Technique	Temperature/Composition/Phase Range Studied
[1985Bla]	Adiabatic calorimetry	5-15 at.% Co, 5-14 at.% Cr, Fe = bal.; bcc and fcc
[1986Kol]	X-ray diffraction	23 mass% Co, 31 mass% Cr, Fe = bal.; spinodal decomposition in bcc phase;
[1986Zhu]	Atom-probe field ion microscopy	11.5-24 mass% Co, 29-33 mass% Cr, Fe = bal.; 525-640°C; spinodal decomposition in bcc phase
[1987Ser]	Nuclear magnetic resonance, nuclear gamma resonance, magnetometry, magnetic annealing	5-20 mass% Co, 25-30 mass% Cr, Fe = bal.; 620-660; spinodal decomposition in bcc phase
[1989Sim]	Anomalous small angle X-ray scattering	12.5 at.% Co, 29.5 at.% Cr, Fe = bal.; 510-620°C; spinodal decomposition in bcc phase
[1990Zub]	Solution calorimetry	5-35 at.% Co, 45-65 at.% Cr, Fe = bal.; σ phase
[1992Vin]	Magnetometry	15 mass% Co, 21 mass% Cr, Fe = bal.; 500-670°C; spinodal decomposition in bcc phase
[1994Lyo]	Small angle neutron scattering	12 mass% Co, 29 mass% Cr, Fe = bal.; 566°C; spinodal decomposition in bcc phase
[2000All]	Mössbauer spectroscopy, X-ray diffraction	12.2 mass% Co, 30.8 mass% Cr, Fe = bal.; spinodal decomposition in bcc phase
[2002Ben]	Mössbauer spectroscopy, X-ray diffraction	12 at.% Co, 31 at.% Cr, Fe = bal.; spinodal decomposition in bcc phase
[2005Gao]	Mössbauer spectroscopy, transmission electron microscopy, magnetometry	12 mass% Co, 25 mass% Cr, Fe = bal.; 500-600°C; spinodal decomposition in bcc phase
[2005Ben]	Mössbauer spectroscopy, X-ray diffraction	12 at.% Co, 31 at.% Cr, Fe = bal.; spinodal decomposition in bcc phase

Table 2. Crystallographic Data of Solid Phases

Phase/ Temperature Range [°C]	Pearson Symbol/ Space Group/ Prototype	Lattice Parameters [pm]	Comments/References
γ, $Cr_{1-x-y}Fe_xCo_y$ (γCo) 1495 - 422	*cF*4 $Fm\bar{3}m$ Cu	a = 354.47	$0 \le x \le 1$, $0 \le y \le 1$ pure γCo at 25°C [Mas2]
(γFe) (h1) 1394 - 912		a = 364.67	pure γFe at 25°C [Mas2]

(*continued*)

DOI: 10.1007/978-3-540-74196-1_18

Phase/ Temperature Range [°C]	Pearson Symbol/ Space Group/ Prototype	Lattice Parameters [pm]	Comments/References
(εCo) < 422	*hP*2 $P6_3/mmc$ Mg	*a* = 250.71 *c* = 406.86	pure εCo at 25°C [Mas2]
		a = 253 *c* = 409	Fe-20Co-(20-22)Cr (mass%), ε-martensite [1984Bel]
α, $Cr_xFe_yCo_{1-x-y}$ (αFe) (r) ≤ 912	*cI*2 $Im\bar{3}m$ W	*a* = 286.65	0 ≤ *x* ≤ 1, 0 ≤ *y* ≤ 1 pure αFe at 25°C [Mas2]
(δFe) (h2) 1538 - 1394		*a* = 293.15	pure δFe at 1480°C [Mas2]
(Cr) ≤ 2623		*a* = 286.82 *a* = 286.82	pure Cr at 25°C [Mas2] Fe-23.3Co-3Cr (mass%) [1977Iva]
σ, $(Fe_xCo_{1-x})Cr$ σ, CrCo ≤ 1283	*tP*30 $P4_2/mnm$ CrFe	*a* = 881.1 *c* = 456.1	0 ≤ *x* ≤ 1 at *x* = 0 53.6 to 57.2 at.% Cr [V-C2]
CrFe 830 - 440		*a* = 879.66 *c* = 455.82	at *x* = 1 50 to 55.5 at.% Fe [1982Kub]
FeCo ≤ 730	*cP*2 $Pm\bar{3}m$ CsCl	*a* = 285.04	29 to 75 at.% Fe [V-C2]
X	*cP**	*a* = 441 to 457	Fe-12Co-31Cr (mass%), metastable [2005Ben]

Table 3. Thermodynamic Data of Reaction

Reaction	Temperature [°C]	Quantity, per mol of atoms [J·mol^{-1}]	Comments
$xCo(\gamma) + yCr(\alpha) + zFe(\gamma)$ $= Co_xCr_yFe_z$ (α)	1350	Δ_fH = 3102 Δ_fH = 2495 Δ_fH = 6245 Δ_fH = 6901 Δ_fH = 6166 Δ_fH = 4247	$Co_{0.047}Cr_{0.745}Fe_{0.208}$ $Co_{0.070}Cr_{0.847}Fe_{0.083}$ $Co_{0.172}Cr_{0.511}Fe_{0.317}$ $Co_{0.177}Cr_{0.612}Fe_{0.212}$ $Co_{0.188}Cr_{0.399}Fe_{0.413}$ $Co_{0.242}Cr_{0.665}Fe_{0.093}$ Adiabatic calorimetry [1977Kub]

(*continued*)

DOI: 10.1007/978-3-540-74196-1_18

Reaction	Temperature [°C]	Quantity, per mol of atoms [J·mol^{-1}]	Comments
xCo(γ) + yCr(α) + zFe(γ) = $Co_xCr_yFe_z$ (γ)	1350	$\Delta_f H$ = 1620	$Co_{0.37}Cr_{0.18}Fe_{0.45}$
		$\Delta_f H$ = 2529	$Co_{0.387}Cr_{0.333}Fe_{0.28}$
		$\Delta_f H$ = 1206	$Co_{0.42}Cr_{0.16}Fe_{0.42}$
		$\Delta_f H$ = 1073	$Co_{0.545}Cr_{0.195}Fe_{0.26}$
		$\Delta_f H$ = 2149	$Co_{0.648}Cr_{0.101}Fe_{0.251}$
			Adiabatic calorimetry [1977Kub]
xCo(γ) + yCr(γ) + zFe(γ) = $Co_xCr_yFe_z$ (γ)	1400	ΔH_{mix} = –820	$Co_{0.2}Cr_{0.2}Fe_{0.6}$
		ΔH_{mix} = –4400	$Co_{0.4}Cr_{0.2}Fe_{0.4}$
		ΔH_{mix} = –4150	$Co_{0.6}Cr_{0.2}Fe_{0.2}$
		ΔH_{mix} = –2670	$Co_{0.4}Cr_{0.4}Fe_{0.2}$
			Knudsen-cell mass spectrometry [1982Arg]
xCo(α) + yCr(α) + zFe(α) = $Co_xCr_yFe_z$ (α)	1400	ΔH_{mix} = 1040	$Co_{0.2}Cr_{0.4}Fe_{0.4}$
		ΔH_{mix} = 280	$Co_{0.2}Cr_{0.6}Fe_{0.2}$
			Knudsen-cell mass spectrometry [1982Arg]
xCo(L) + yCr(L) + zFe(L) = $Co_xCr_yFe_z$ (L)	1600	ΔH_{mix} = –380	$Co_{0.2}Cr_{0.2}Fe_{0.6}$
		ΔH_{mix} = –6380	$Co_{0.4}Cr_{0.2}Fe_{0.4}$
		ΔH_{mix} = –4640	$Co_{0.6}Cr_{0.2}Fe_{0.2}$
		ΔH_{mix} = –770	$Co_{0.2}Cr_{0.4}Fe_{0.4}$
		ΔH_{mix} = –1380	$Co_{0.4}Cr_{0.4}Fe_{0.2}$
		ΔH_{mix} = –1800	$Co_{0.2}Cr_{0.6}Fe_{0.2}$
			Knudsen-cell mass spectrometry [1982Arg]
xCo(ε) + yCr(α) + zFe(α) = $Co_xCr_yFe_z$ (σ)	31	$\Delta_f H$ = 3600 ± 1100	$Co_{0.05}Cr_{0.45}Fe_{0.50}$
		$\Delta_f H$ = 2500 ± 1300	$Co_{0.10}Cr_{0.45}Fe_{0.45}$
		$\Delta_f H$ = 3800 ± 1700	$Co_{0.15}Cr_{0.45}Fe_{0.40}$
		$\Delta_f H$ = 5800 ± 700	$Co_{0.20}Cr_{0.45}Fe_{0.35}$
		$\Delta_f H$ = 8300 ± 1200	$Co_{0.25}Cr_{0.45}Fe_{0.30}$
		$\Delta_f H$ = 9100 ± 2000	$Co_{0.05}Cr_{0.50}Fe_{0.45}$
		$\Delta_f H$ = 8300 ± 1100	$Co_{0.10}Cr_{0.50}Fe_{0.04}$
		$\Delta_f H$ = 5200 ± 1300	$Co_{0.15}Cr_{0.50}Fe_{0.35}$
		$\Delta_f H$ = 4300 ± 1700	$Co_{0.20}Cr_{0.50}Fe_{0.30}$
		$\Delta_f H$ = 6400 ± 1100	$Co_{0.25}Cr_{0.50}Fe_{0.25}$
		$\Delta_f H$ = 6400 ± 700	$Co_{0.05}Cr_{0.50}Fe_{0.20}$
		$\Delta_f H$ = 6300 ± 1500	$Co_{0.10}Cr_{0.55}Fe_{0.30}$
		$\Delta_f H$ = 6700 ± 1400	$Co_{0.15}Cr_{0.55}Fe_{0.25}$
		$\Delta_f H$ = 4900 ± 1300	$Co_{0.20}Cr_{0.55}Fe_{0.20}$
		$\Delta_f H$ = 1600 ± 1400	$Co_{0.25}Cr_{0.55}Fe_{0.15}$
		$\Delta_f H$ = 4800 ± 800	$Co_{0.30}Cr_{0.60}Fe_{0.05}$
		$\Delta_f H$ = 2900 ± 1300	$Co_{0.15}Cr_{0.60}Fe_{0.10}$
		$\Delta_f H$ = 4700 ± 1100	$Co_{0.20}Cr_{0.65}Fe_{0.05}$
			Solution calorimetry [1990Zub]

DOI: 10.1007/978-3-540-74196-1_18

Table 4. Thermodynamic Data of Transformation

Transformation	Temperature [°C]	Quantity, per mol of atoms [J·mol^{-1}]	Comments
σ ⇌ α	870-920	$\Delta_{tr}H = 1557$	$Co_{0.05}Cr_{0.46}Fe_{0.49}$
	960-988	$\Delta_{tr}H = 1637$	$Co_{0.083}Cr_{0.453}Fe_{0.464}$
	970-1000	$\Delta_{tr}H = 1795$	$Co_{0.11}Cr_{0.46}Fe_{0.43}$
	1025-1051	$\Delta_{tr}H = 2126$	$Co_{0.14}Cr_{0.51}Fe_{0.35}$
	1130-1145	$\Delta_{tr}H = 2110$	$Co_{0.195}Cr_{0.568}Fe_{0.237}$
	1105	$\Delta_{tr}H = 2093$	$Co_{0.20}Cr_{0.50}Fe_{0.30}$
	1228-1232	$\Delta_{tr}H = 2863$	$Co_{0.33}Cr_{0.57}Fe_{0.10}$
	1220-1230	$\Delta_{tr}H = 2922$	$Co_{0.365}Cr_{0.525}Fe_{0.11}$
			Adiabatic calorimetry [1977Kub]
α ⇌ γ	846-853	$\Delta_{tr}H = 1831 \pm 41$	$Co_{0.05}Cr_{0.059}Fe_{0.891}$
	786-800	$\Delta_{tr}H = 2522 \pm 30$	$Co_{0.051}Cr_{0.097}Fe_{0.852}$
	749-779	$\Delta_{tr}H = 2700 \pm 168$	$Co_{0.059}Cr_{0.138}Fe_{0.803}$
	837-870	$\Delta_{tr}H = 4391 \pm 58$	$Co_{0.101}Cr_{0.048}Fe_{0.851}$
	777-802	$\Delta_{tr}H = 2730 \pm 85$	$Co_{0.10}Cr_{0.099}Fe_{0.801}$
	830-895	$\Delta_{tr}H = 7352 \pm 106$	$Co_{0.151}Cr_{0.049}Fe_{0.80}$
			Adiabatic calorimetry [1985Bla]
α ⇌ γ	911	$\Delta_{tr}H = 962$	$Co_{0.05}Cr_{0.059}Fe_{0.891}$
		$\Delta_{tr}H = 249$	$Co_{0.051}Cr_{0.097}Fe_{0.852}$
		$\Delta_{tr}H = -165$	$Co_{0.059}Cr_{0.138}Fe_{0.803}$
		$\Delta_{tr}H = 1780$	$Co_{0.101}Cr_{0.048}Fe_{0.851}$
		$\Delta_{tr}H = -194$	$Co_{0.10}Cr_{0.099}Fe_{0.801}$
		$\Delta_{tr}H = 2824$	$Co_{0.151}Cr_{0.049}Fe_{0.80}$
			Thermodynamic calculation [1985Bla]

Table 5. Thermodynamic Properties of Single Phases

Phase	Temperature Range [°C]	Activity	Comments
Liquid	1600	$a_{Co} = 0.202$, $a_{Cr} = 0.198$, $a_{Fe} = 0.602$	$Co_{0.2}Cr_{0.2}Fe_{0.6}$
		$a_{Co} = 0.258$, $a_{Cr} = 0.154$, $a_{Fe} = 0.271$	$Co_{0.4}Cr_{0.2}Fe_{0.4}$
		$a_{Co} = 0.518$, $a_{Cr} = 0.124$, $a_{Fe} = 0.129$	$Co_{0.6}Cr_{0.2}Fe_{0.2}$
		$a_{Co} = 0.170$, $a_{Cr} = 0.443$, $a_{Fe} = 0.336$	$Co_{0.2}Cr_{0.4}Fe_{0.4}$
		$a_{Co} = 0.358$, $a_{Cr} = 0.384$, $a_{Fe} = 0.226$	$Co_{0.4}Cr_{0.4}Fe_{0.2}$
		$a_{Co} = 0.140$, $a_{Cr} = 0.644$, $a_{Fe} = 0.192$	$Co_{0.2}Cr_{0.6}Fe_{0.2}$
			Knudsen-cell mass spectrometry [1982Arg]

DOI: 10.1007/978-3-540-74196-1_18

Table 6. Investigations of the Co-Cr-Fe Materials Properties

Reference	Method / Experimental Technique	Type of Property
[1974Vin]	Magnetometry	B_r, H_c, $(BH)_{max}$
[1975Kan]	Magnetometry	B_r, H_c, $(BH)_{max}$
[1975Vin]	Magnetometry	B_r, H_c
[1976Dem]	Magnetometry	B_r, H_c, $(BH)_{max}$
[1976Kan]	Magnetometry	B_r, H_c, $(BH)_{max}$
[1977Vin]	Magnetometry	B_r, H_c
[1980Bel]	Resonance technique	Single crystal elastic constants of bcc alloys
[1980Gal]	Thermomagnetic method	Curie temperature of bcc alloys
[1980Jin1]	Mechanical tests	Hardness, tensile properties, fracture mode
[1980Jin2]	Magnetometry	B_r, H_c, $(BH)_{max}$, Curie temperature
[1980Min]	Magnetometry	B_r, H_c, $(BH)_{max}$, hysteresis loop
[1982Sei]	Magnetometry	B_r, H_c
[1983Bel]	Magnetometry	B_r, H_c, $(BH)_{max}$
[1983Chi]	Thermomagnetic method	B_r, H_c, $(BH)_{max}$, Curie temperature
[1984Bel]	Magnetometry	B_r, H_c, $(BH)_{max}$
[1984Mue]	Mechanical tests	Hardness and formability
[1984Ser]	Magnetometry	H_c
[1985Bla]	Magnetometry	Magnetic moment
[1987Klo]	Mechanical tests	Hardness, formability, tensile and torsion properties

Table 7. Curie Temperature and Magnetic Moment of Single Phase

Phase	Curie Temperature [°C]	Average Magnetic Moment in Bohr Magneton (μ_B) at 27°C	Comments
bcc	650		10.5Co28Cr61.5Fe (mass%) Magnetometry [1980Gal]
bcc	640 630		9Co27Cr64Fe (mass%) 9Co27Cr64Fe (mass%) Magnetometry [1980Jin2]
bcc	821 799 758 855 785 851	2.26 2.03 2.02 2.22 2.16 2.25	$Co_{0.05}Cr_{0.059}Fe_{0.891}$ $Co_{0.051}Cr_{0.097}Fe_{0.852}$ $Co_{0.059}Cr_{0.138}Fe_{0.803}$ $Co_{0.101}Cr_{0.048}Fe_{0.851}$ $Co_{0.10}Cr_{0.099}Fe_{0.801}$ $Co_{0.151}Cr_{0.049}Fe_{0.80}$ Magnetometry [1985Bla]

DOI: 10.1007/978-3-540-74196-1_18

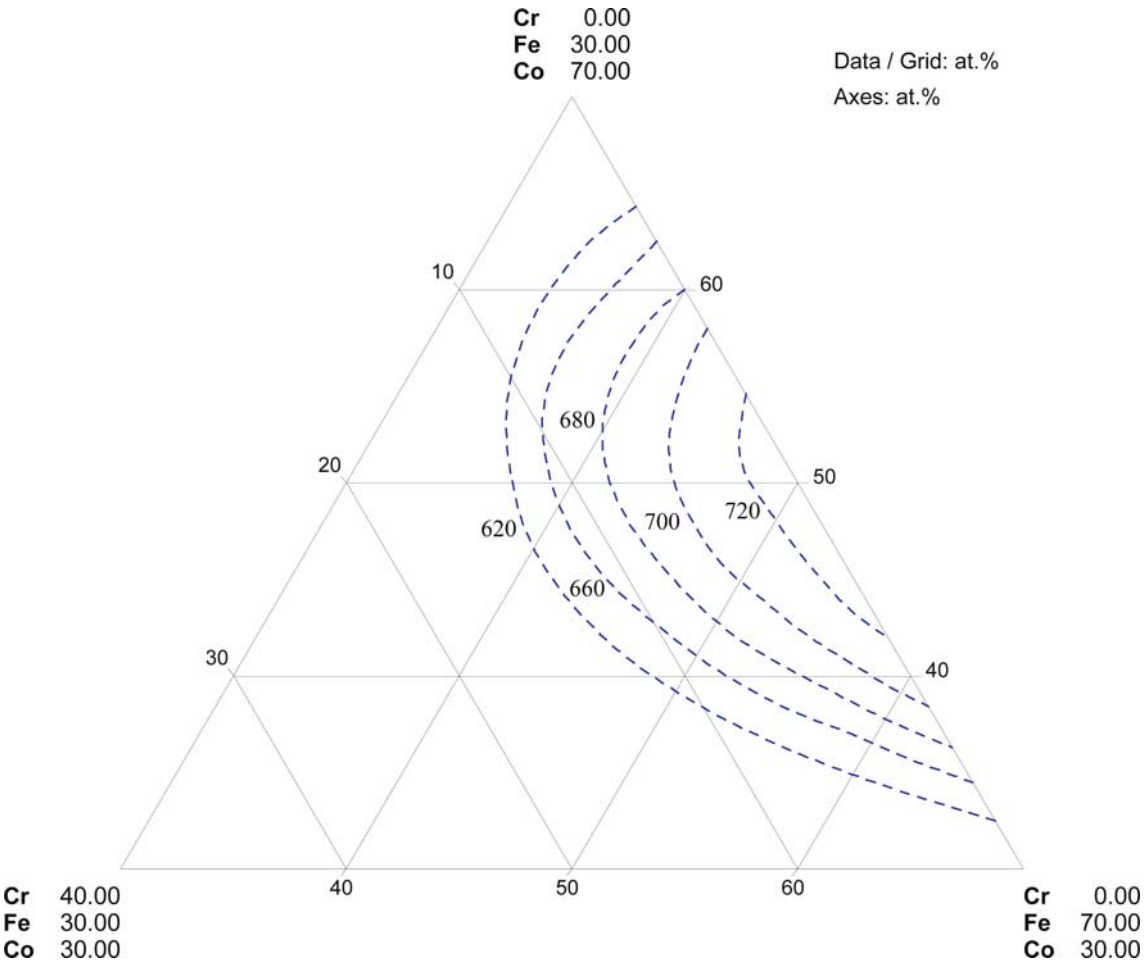

Fig. 1. Co-Cr-Fe. Iso-critical temperatures for order-disorder (*B2-A2*) transition

DOI: 10.1007/978-3-540-74196-1_18

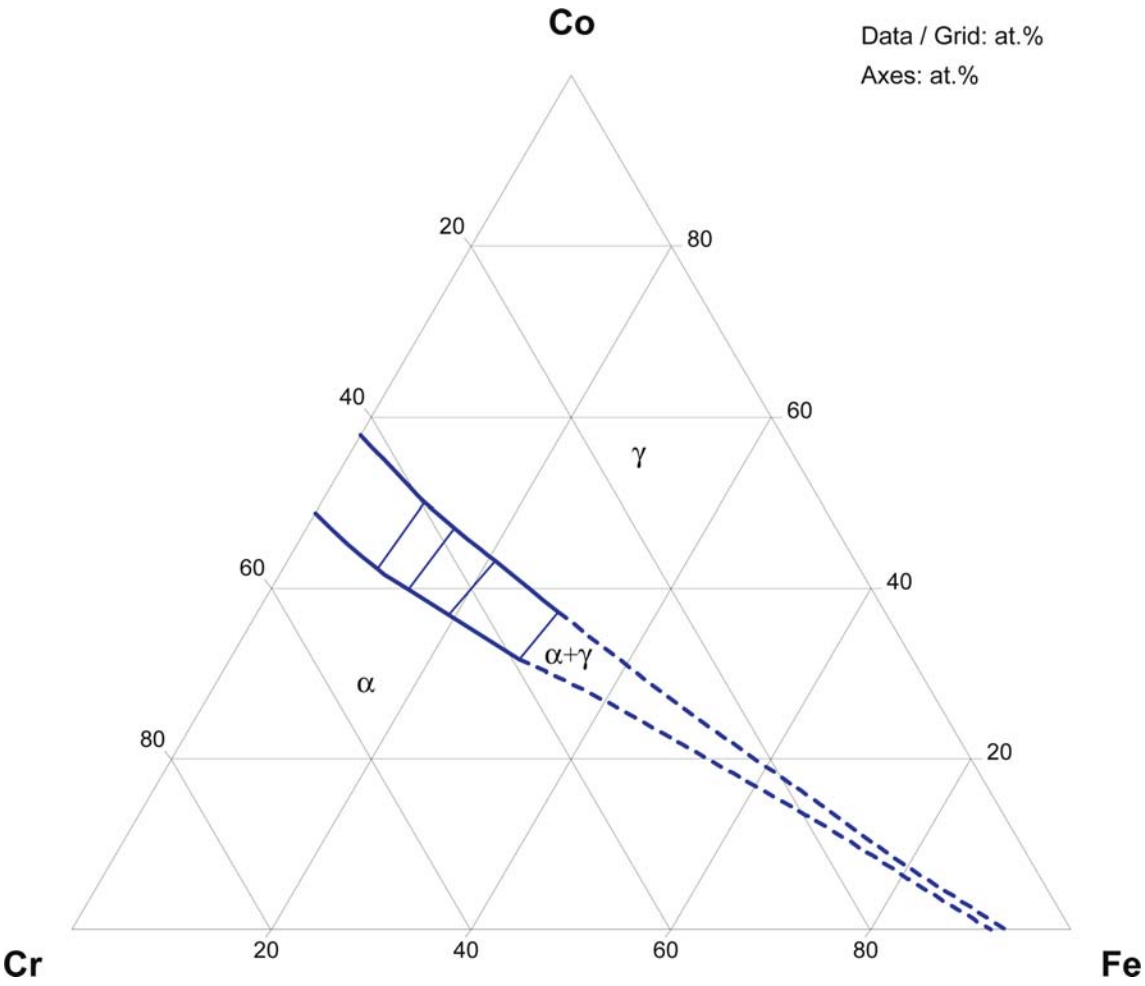

Fig. 2. Co-Cr-Fe. Isothermal section at 1300°C

DOI: 10.1007/978-3-540-74196-1_18

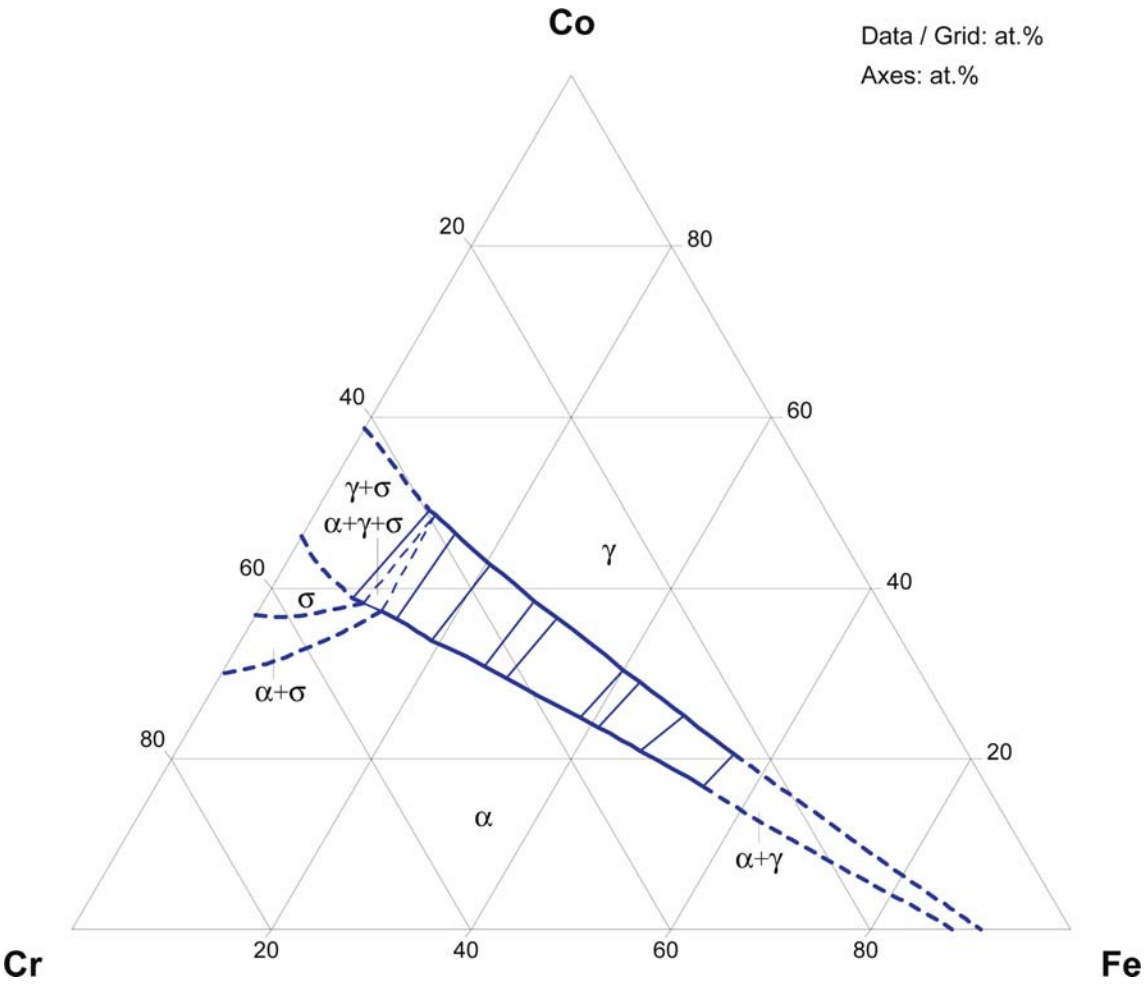

Fig. 3. Co-Cr-Fe. Isothermal section at 1200°C

DOI: 10.1007/978-3-540-74196-1_18

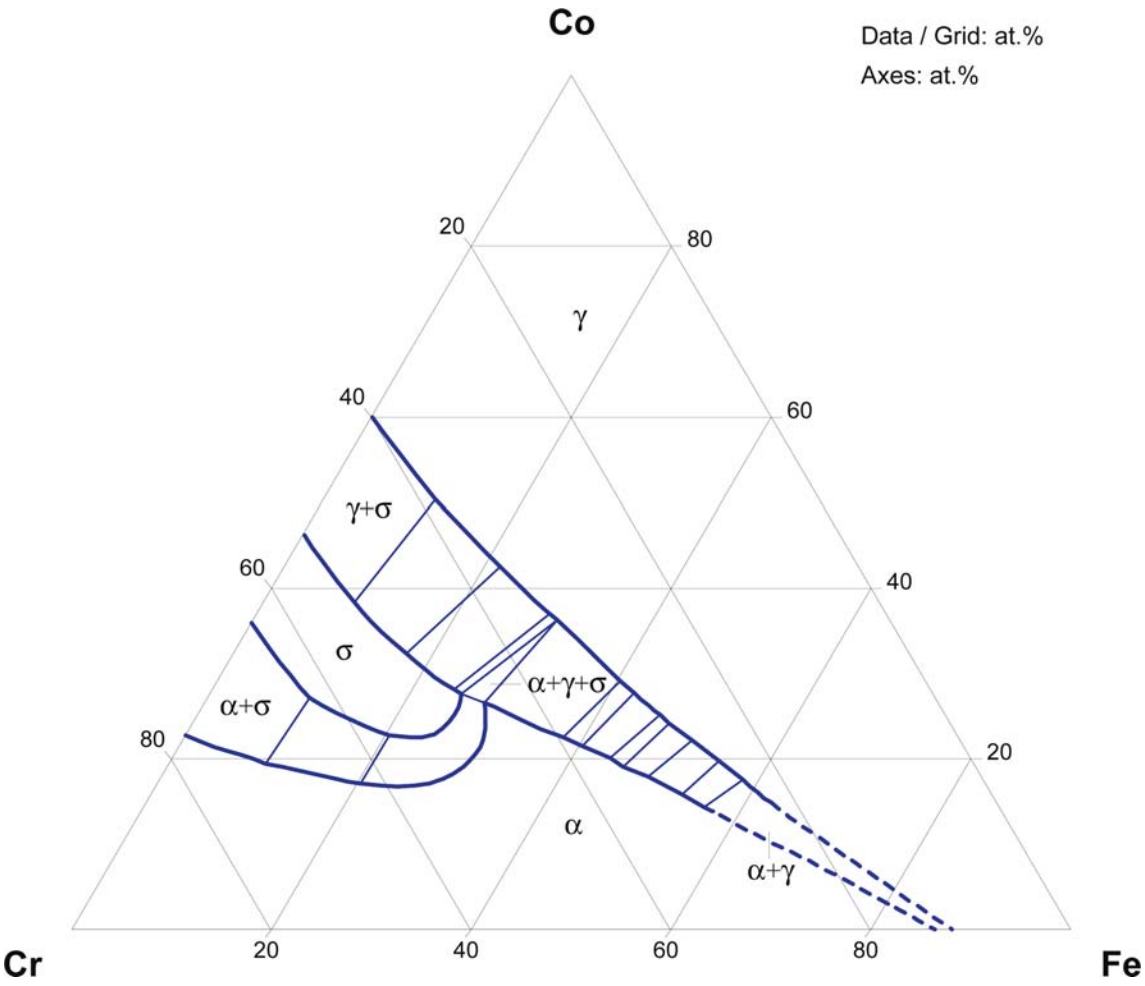

Fig. 4. Co-Cr-Fe. Isothermal section at 1100°C

DOI: 10.1007/978-3-540-74196-1_18

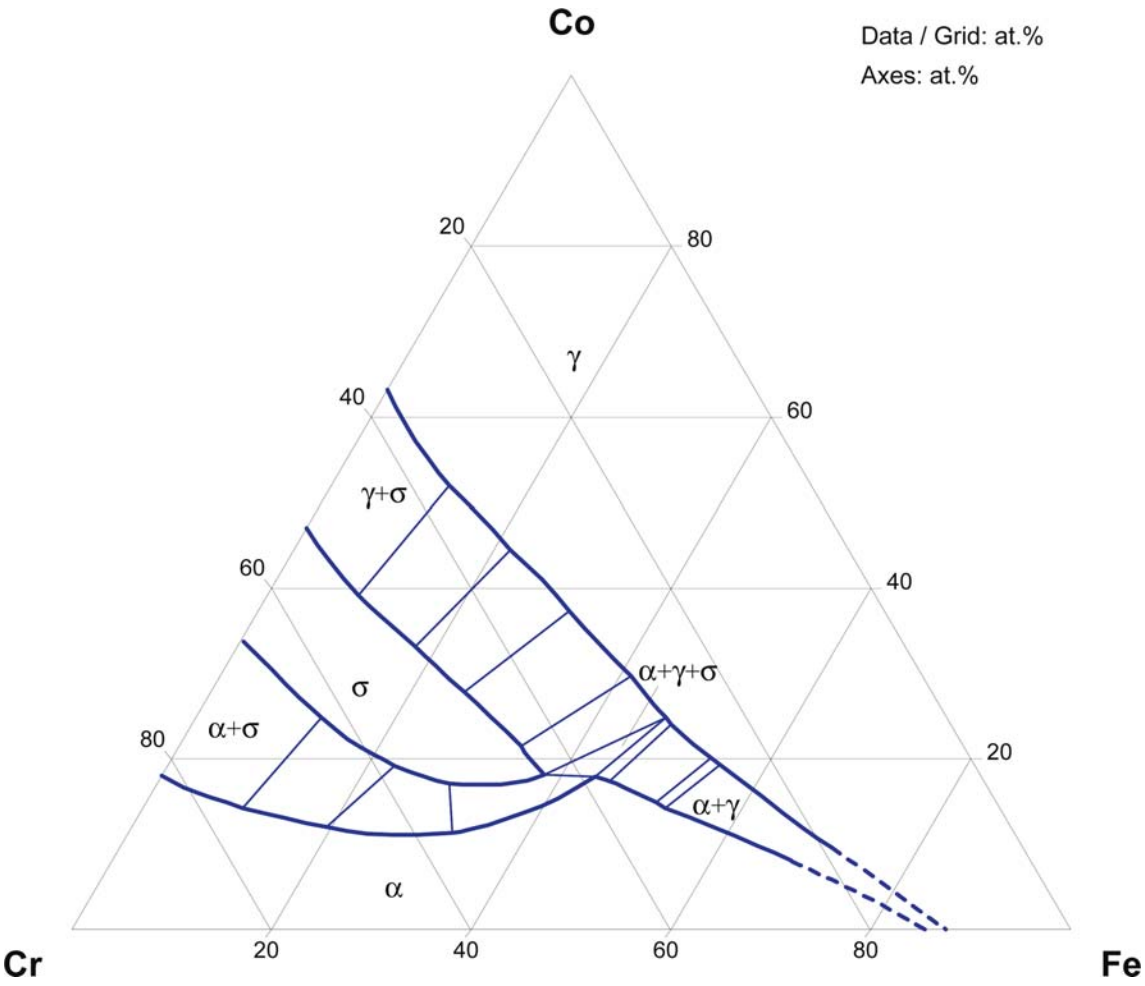

Fig. 5. Co-Cr-Fe. Isothermal section at 1000°C

DOI: 10.1007/978-3-540-74196-1_18

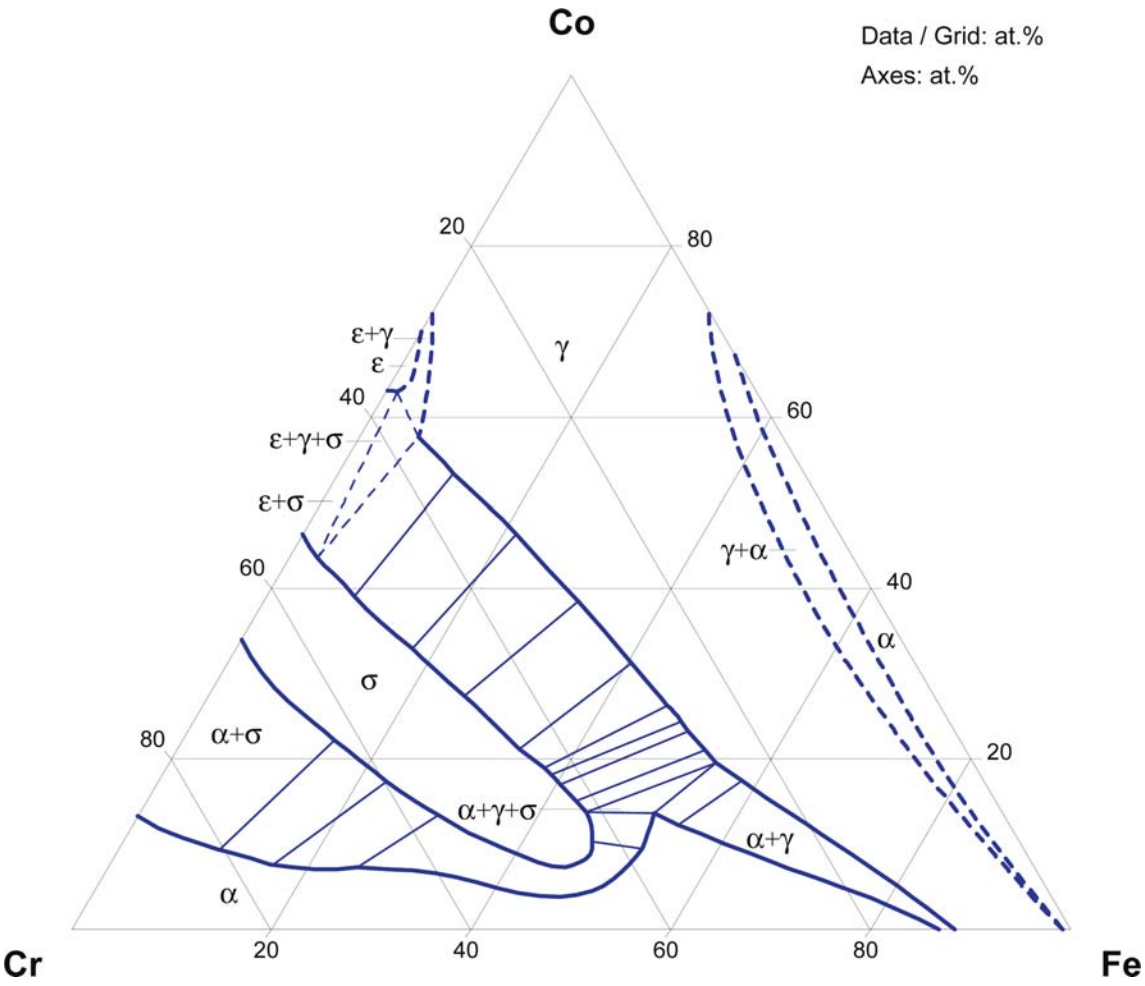

Fig. 6. Co-Cr-Fe. Isothermal section at 900°C

DOI: 10.1007/978-3-540-74196-1_18

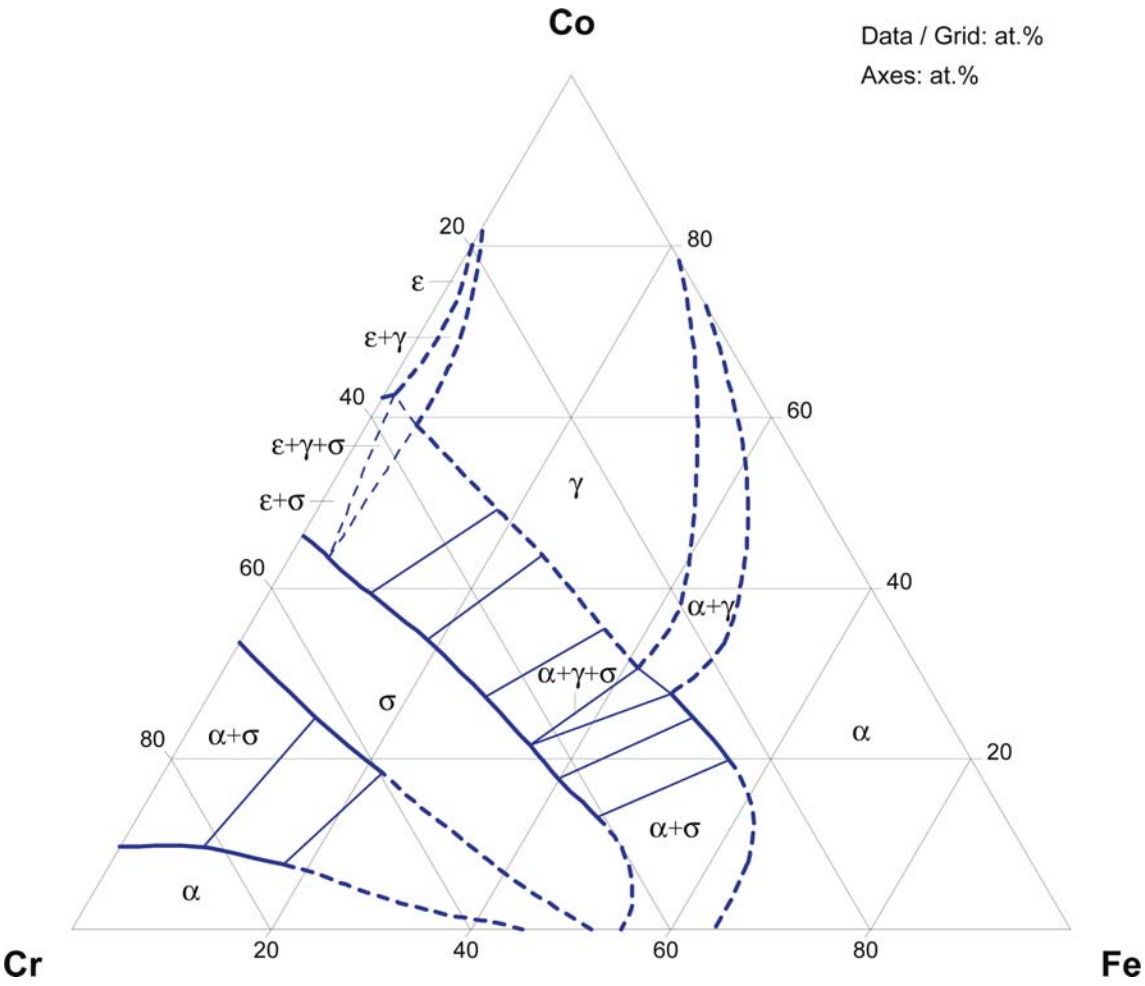

Fig. 7. Co-Cr-Fe. Isothermal section at 800°C

DOI: 10.1007/978-3-540-74196-1_18

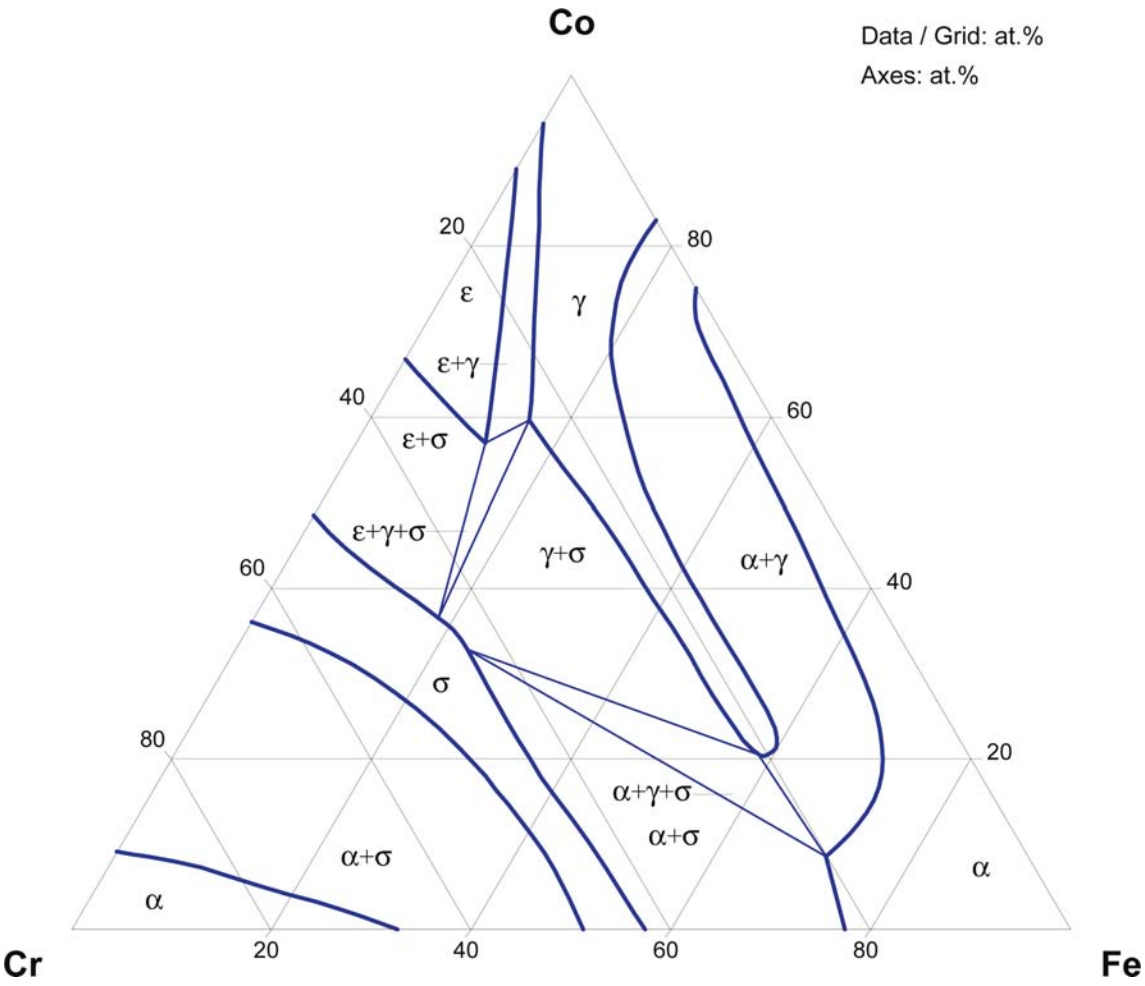

Fig. 8. Co-Cr-Fe. Isothermal section at 700°C

DOI: 10.1007/978-3-540-74196-1_18

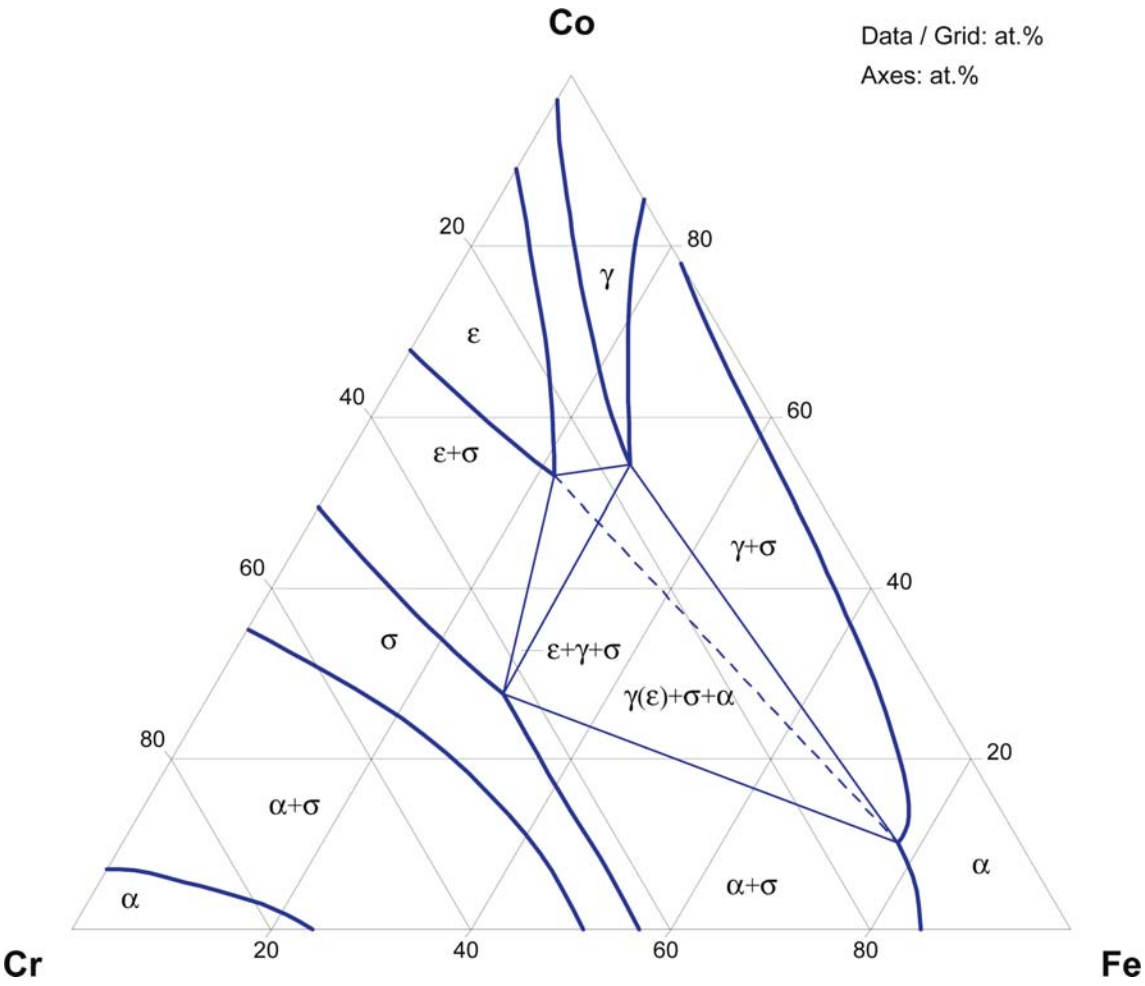

Fig. 9. Co-Cr-Fe. Isothermal section at 600°C

DOI: 10.1007/978-3-540-74196-1_18

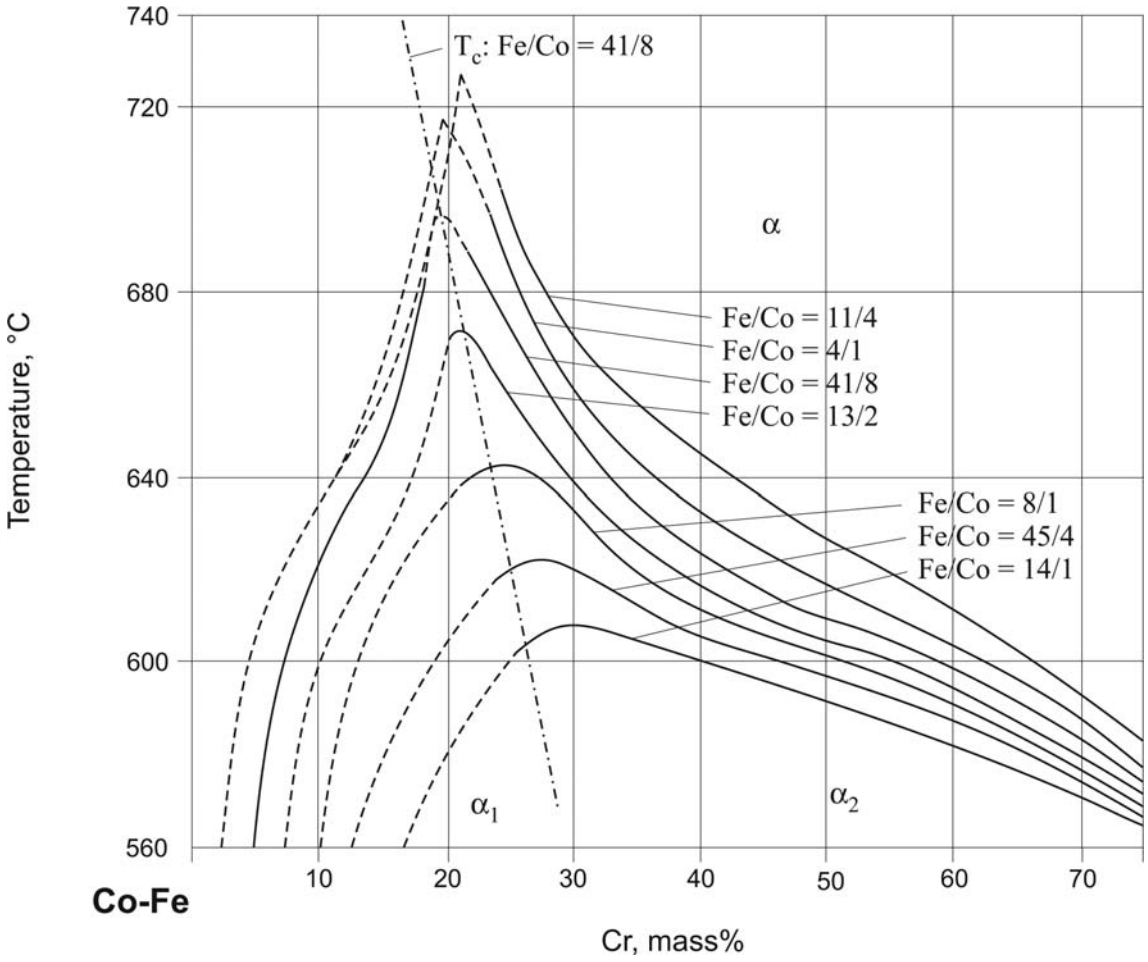

Fig. 10. Co-Cr-Fe. Experimental miscibility gap in bcc phase at constant Fe/Co ratios

DOI: 10.1007/978-3-540-74196-1_18

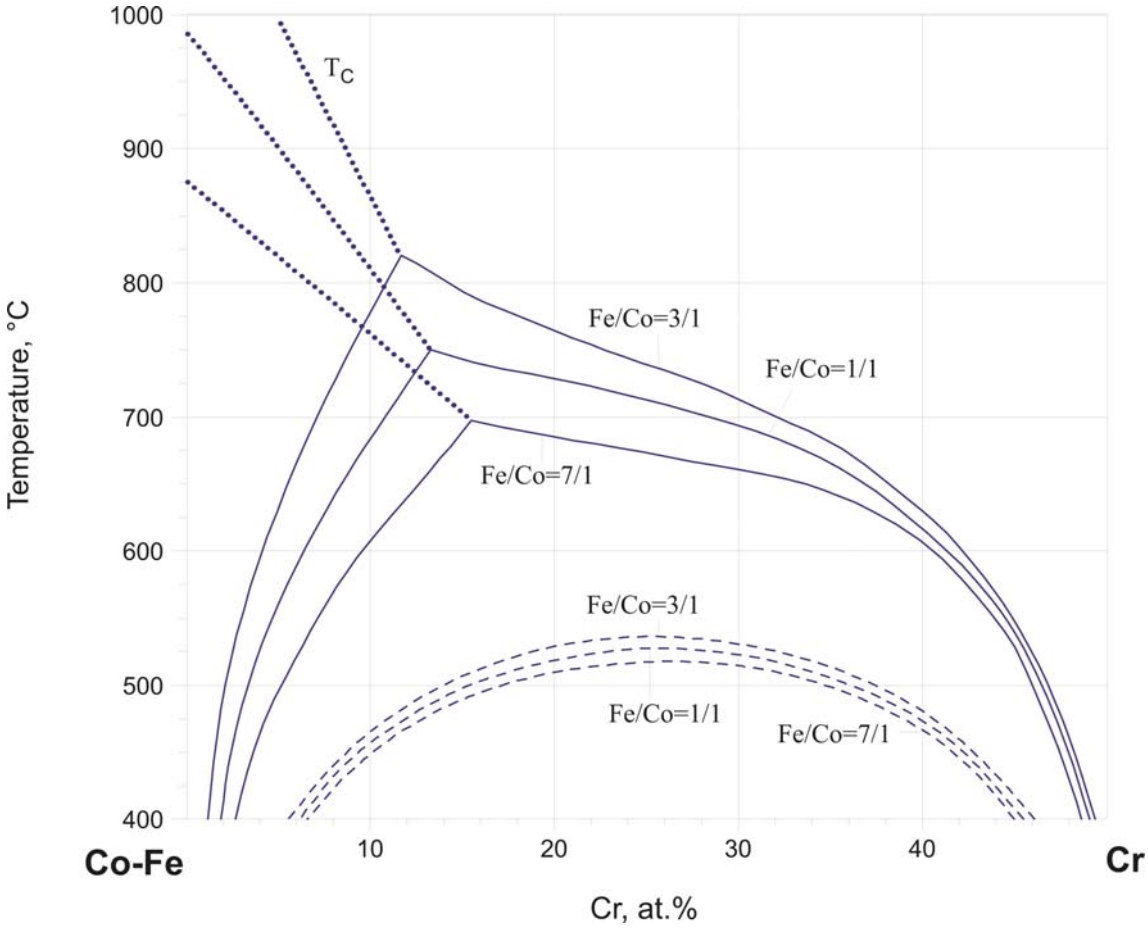

Fig. 11. Co-Cr-Fe. Calculated miscibility gaps in the phase with (solid lines) and without (dashed lines) magnetic ordering

DOI: 10.1007/978-3-540-74196-1_18

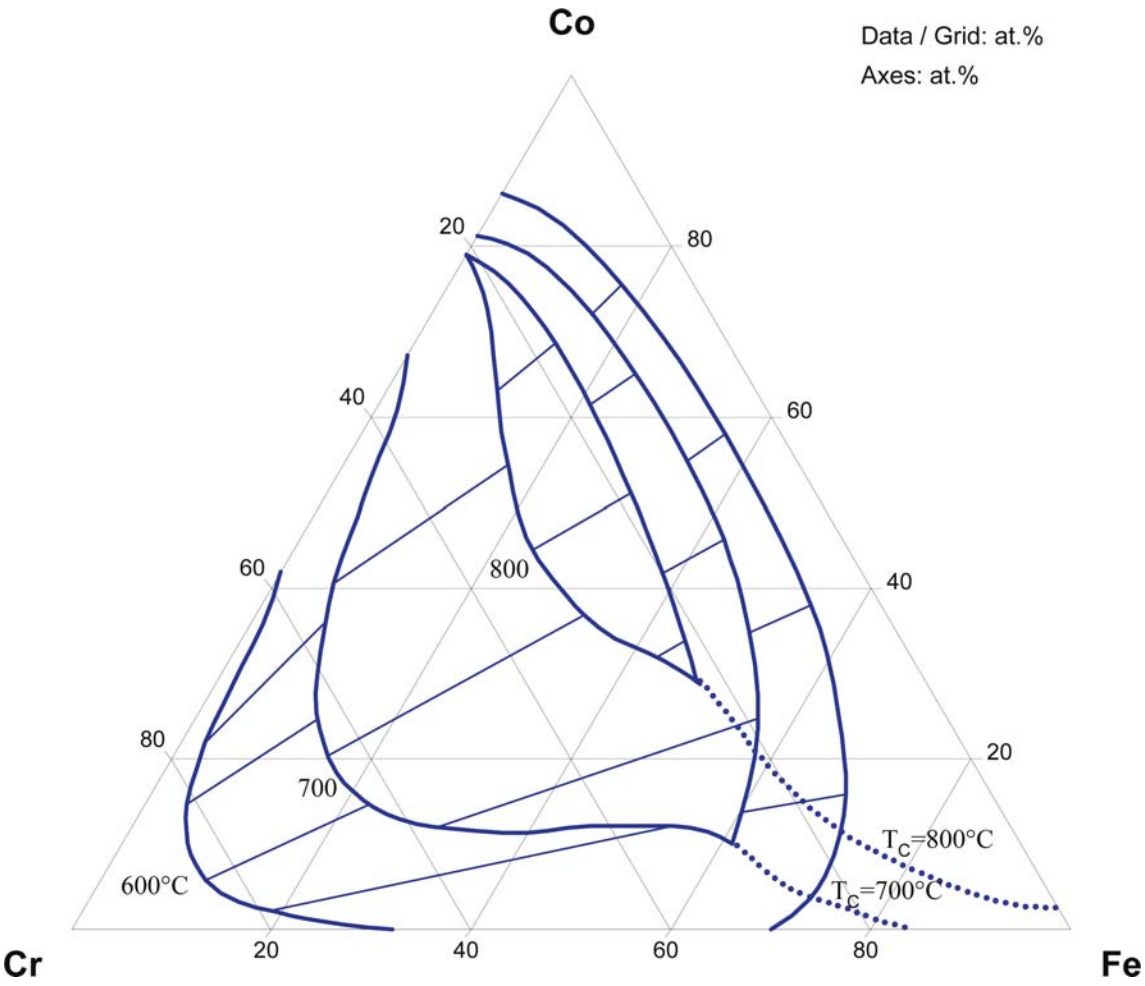

Fig. 12. Co-Cr-Fe. Calculated miscibility isotherms

DOI: 10.1007/978-3-540-74196-1_18

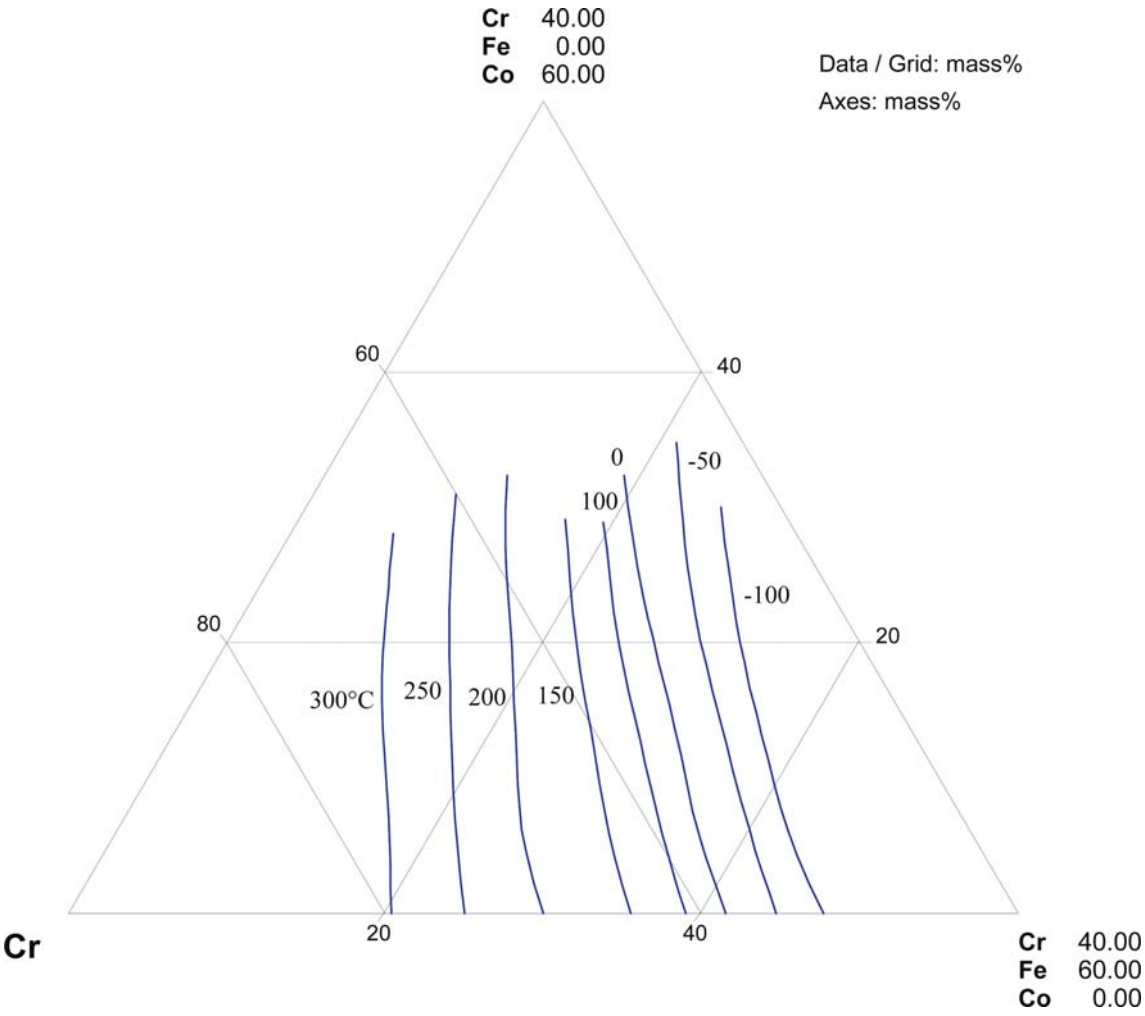

Fig. 13. Co-Cr-Fe. Curie temperatures of DCC alloys

DOI: 10.1007/978-3-540-74196-1_18

References

[1909Jae] Jaenecke, E., "Ternary Alloys of Cu, Ag, Au; Cr, Mn; Fe, Co, Ni; Pd, Pt Metals" (in German), *Z. Phys. Chem.*, **67**, 668–688 (1909) (Experimental, Phase Diagram, Phase Relations)

[1929Wev] Wever, F., Hashimoto, U., "About the Binary Cobalt-Chromium System, With a Contribution to the Knowledge of the Qualities of Cobalt-Chromium Alloys, and an Appendix About the Influence of Some Elements on the Qualities of the Cobalt-Chromium Alloys" (in German), *Mitt. K. W. Inst. Eisenforschung*, **11**, 293–330 (1929) (Experimental, Phase Diagram, Phase Relations, #, *, 50)

[1932Koe] Koester, W., "The Iron-Cobalt-Chromium System" (in German), *Arch. Eisenhuettenwes.*, **6**(3), 113–116 (1932) (Experimental, Phase Diagram, Phase Relations, #, *, 5)

[1949Bec] Beck, P.A., Manly, W.D., "The Sigma Phase in Ternary Cr-Co-Fe and Cr-Co-Ni Alloys", *Trans. Amer. Inst. Min. Met. Eng.*, **186**, 354 (1949) (Experimental, 1)

[1949Jae] Jaenecke, E., "Co-Cr-Fe" (in German), *Kurzgefasstes Handbuch aller Legierungen*, Winter Verlag Heidelberg, 630–632 (1949) (Phase Diagram, Phase Relations)

[1951Rid] Rideout, S., Manly, W.D., Kamen, E.L., Lement, B.S., Beck, P.A., "Intermediate Phases in Ternary Alloy Systems of Transition Elements", *Trans. Amer. Inst. Min. Met. Eng.*, **191**, 872–876 (1951) (Experimental, Phase Diagram, Phase Relations, #, *, 13)

[1952Bec] Beck, R.L., Fletcher, E.E., Elsea, A.R., Westerman, A.B., Manning, G.K., "Alloys for High-Temperature Service", *U. S. Atomic Energy Commission Publ. (AD-11576)*, **AD-11576**, 1–25 (1952) (Crys. Structure, Experimental, Phase Diagram, Phase Relations, #, *, 3)

[1952Jos] Josso, E., "Order-Disorder Transformation in Ternary Alloys" (in French), *Rev. Metall.*, **49**, 727–732 (1952) (Experimental, Crys. Structure, Phase Relations, *, 15)

[1959Koe] Koester, W., Hofmann, G., "About Equilibria in Ternary Iron-Cobalt-Chromium System" (in German), *Arch. Eisenhuettenwes.*, **30**(4), 249–251 (1959) (Experimental, Phase Diagram, Phase Relations, #, *, 3)

[1959Sve] Svechnikov, V.N., Spektor, A.T., Maystrenko, E.E., "Investigation of the Solid State Transformation of the Co-Cr-Fe Alloys" (in Russian), *Sb. Nauchn. Rab. Inst. Metallofiz., Akad. Nauk Ukr. SSR*, **10**(10), 168–181 (1959) (Experimental, Morphology, Phase Diagram, Phase Relations, *, 6)

[1973Cle] Clegg, D.W., Buckley, R.A., "The Disorder – Order Transformation in Iron-Cobalt-based Alloy", *Metal Sci. J.*, **7**, 48–54 (1973) (Experimental, Phase Relations, *, 28)

[1973Kra] Kralik, F., Kovacova K., "Determination of the $\alpha+\gamma/\gamma$ Phase Region Boundary in Fe-Cr-Ni, Fe-Cr-Co and Fe-Cr-Mn Systems", *Kovove Mat.*, **11**, 6–15 (1973) (Experimental, Phase Relations, *, 7)

[1974Kau] Kaufman, L., Nesor, H., "Calculation of Superalloy Phase Diagrams: Part I", *Metall. Trans.*, **5**(7), 1617–1621 (1974) (Calculation, Phase Diagram, Phase Relations, *, 19)

[1974Vin] Vintaykin, Ye.Z., Urushadze, G.G., Belyatskaya, I.S., Sukharova, Ye.A., "On the Structure of Magnetic Iron-Chromium-Cobalt Alloys", *Phys. Met. Metallogr.*, **38**(5), 102–105 (1974), translated from *Fiz. Metal. Metalloved.*, **38**(5), 1012–1015 (1974) (Experimental, Magn. Prop., 11)

[1975Buc] Buckley, R.A., "Microstructure and Kinetics of the Ordering Transformation in Iron-Cobalt Alloys, FeCo, FeCo-0.4%Cr, FeCo-2.5%V", *Metal Sci.*, **9**, 243–247 (1975) (Experimental, Kinetics, Morphology, *, 8)

[1975Cha] Chart, T.G., Counsell, J.F., Jones, G.P., Slough, W., Spencer, P.J., "Provision and Use of Thermodynamic Data for the Solution of High-Temperature Practical Problems", *Int. Met. Rev.*, **20**, 57–82 (1975) (Assessment, Phase Diagram, Phase Relations, 212)

[1975Kan] Kaneko, H., Homma, M., Fukunaga, T., Okada, M., "Fe-Cr-Co Permanent Magnet Alloys Containing Nb and Al", *IEEE Trans. Magn.*, **MAG-11**, 1440–1442 (1975) (Experimental, Magn. Prop., #, *, 3)

[1975Kau] Kaufman, L., Nesor, H., "Calculation of Superalloy Phase Diagrams. Part III.", *Metall. Trans. A*, **6**(11), 2115–2122 (1975) (Calculation, Phase Diagram, Phase Relations, Thermodyn., 35)

DOI: 10.1007/978-3-540-74196-1_18

[1975Mal] Mal'tsev, Ye.I., Goman'kov, V.I., Mokhov, B.H., Puzey, I.M., Nogin, N.I., "Influence of Alloying Elements on the Fe-Co Superlattice", *Phys. Met. Metallogr.*, **40**(2), 190–193 (1975), translated from *Fiz. Met. Metalloved*., **40**(2), 443–445 (1975) (Experimental, Crys. Structure, 11)

[1975Vin] Vintaikin, E.Z., Urushadze, G.G., Belyatskaya; I.S., Barkalaya, A.A., "Stratification in an Fe-Cr-Co Alloy" (in Russian), *Trudy Gruz. Politekhn. Inst.*, (5), 62–65 (1975) (Experimental, Magn. Prop., 11)

[1976Dem] Dementyeva, G.P., Eliokums, O.A., Kavalerova, L.A., Livshits, B.G., Milyaev, I.M., "Phase Transformation in an Fe-Cr-Co Alloy in the Temperature Range 600–1300°C" (in Russian), *Izv. Vyssh. Ucheb. Zaved., Chern. Met.*, **5**, 149–150 (1976) (Experimental, Magn. Prop., 3)

[1976Hag] Hagiwara, M., Suzuki, T., "The Effect of the Addition of a Third Element (Cr, Mn, or V) on the Order-Disorder Transition Temperature in FeCo" (in Japanese), *J. Jpn. Inst. Met.*, **40**, 738–743 (1976) (Experimental, Magn. Prop., #, *, 34)

[1976Ivc] Ivchinnikov, V.V., Zvigintsev, N.V., Litivinov, V.S., Osminkin, V.A., "Calorimetric and Nuclear γ Resonance Investigation of the Ageing of Fe-Cr-Co Alloys", *Phys. Met. Metallogr.*, **42**(2), 71–78 (1976), translated from *Fiz. Met. Metalloved*., **42**(2), 310–317 (1976) (Crys. Structure, Experimental, 23)

[1976Kan] Kaneko, H., Homma, M., Minowa, T., "Effects of V and V + Ti Additions on the Structure and Properties of Fe-Cr-Co", *IEEE Trans. Magn.*, **MAG-12**(6), 977–979 (1976) (Experimental, Magn. Prop., #, *, 6)

[1977Ale1] Alekseev, L.A., Dzhavadov, D.M., Tyapkin, Yu.D., Levi, R.B., "Nature of the Effect of Cr on the Structure of Ordering Iron-Cobalt Alloys", *Sov. Phys. Dokl*., **22**(6), 329–331 (1977), translated from *Dokl. Akad. Nauk SSSR.*, **234**, 818 (1977) (Crys. Structure, Experimental, 9)

[1977Ale2] Alekseyev, L.A., Dzhavadov, D.M., Tyapkin, Yu.D., Levi, R.B., "Influence of Chromium on the Structure of Ordered Iron-Cobalt Alloys", *Phys. Met. Metallogr.*, **44**(4), 180–182 (1977), translated from *Fiz. Metal. Metalloved*., **44**(4), 879–881 (1977) (Crys. Structure, Experimental, 4)

[1977Bel] Belozerskii, G.V., Dudoladov, V.V., Ukraintseva, S.B., Khazanov, S.A., Khimich, Yu.P., Chernyak, A.A., "Phase Transformations in Fe-Co-Cr Alloys", *Phys. Met. Metallogr.*, **43**(1), 76–82 (1977), translated from *Fiz. Metal. Metalloved*., **43**(1), 90–96 (1977) (Experimental, Phase Relations, 13)

[1977Dzh] Dzhavadov, D.M., Tyapkin, Yu.D., "The Structure of Iron-Cobalt with Chromium Additions", *Russ. Metall*., (6), 152–154 (1977), translated from *Izv. Akad. Nauk SSSR*, *Met*., (6), 188–191 (1977) (Experimental, Phase Relations, 7)

[1977Iva] Ivanova, G.V., Lapina, T.P., Magat, L.M., Belozerov, Ye.V., Maykov, V.G., Shur, Ya.S., "Structural Transformations and Magnetic Properties of Fe-Cr-Co-Mo Alloys", *Phys. Met. Metallogr.*, **43**(6), 68–78 (1977), translated from *Fiz. Metal. Metalloved*., **43**(6), 1201–1211 (1977) (Experimental, Crys. Structure, Magn. Prop., 12)

[1977Kan] Kaneko, H., Homma M., Nakamura, K., Okada M., Thomas, G., "Phase Diagram of Fe-Cr-Co Permanent Magnet System", *IEEE Trans. Magn.*, **MAG-13**(5), 1325–1327 (1977) (Experimental, Phase Relations, Magn. Prop., #, *, 4)

[1977Kub] Kubaschewski, O., Grundmann, J., "Application of an Adiabatic High-Temperature Calorimeter to the Determination of Heats of Formation in the System Iron-Cobalt-Chromium", *Ber. Bunsen-Ges. Phys. Chem.*, **81**(12), 1239–1242 (1977) (Experimental, Thermodyn., *, 9)

[1977Vin] Vintaykin, Ye.Z., Barkalaya, A.A., Belyatskaya, I.S., Sachno, V.M., "Fine Crystalline Structure of Hard Fe-Cr-Co Magnetic Alloys", *Phys. Met. Metallogr.*, **43**(4), 48–56 (1977), translated from *Fiz. Metal. Metalloved*., **43**(4), 734–742 (1977) (Crys. Structure, Experimental, Magn. Prop., 16)

[1978Dom] Dombre, M., Allibert, C., Bronner, C., Driole, J., "Transformation of Phases in Some Magnetic Alloys of Fe-Co-Cr" (in French), *Mem. Sci. Rev. Metall.*, **75**(10), 605–613 (1978) (Experimental, Phase Relations, *, 10)

DOI: 10.1007/978-3-540-74196-1_18

[1978Vin] Vintaykin, Ye.Z., Barkalaya, A.A., Belyatskaya, I.S., "Decomposition of Fe-Cr and Fe-Cr-Co Solid Solutions in a Magnetic Field", *Phys. Met. Metallogr.*, **45**(5), 77–82 (1978), translated from *Fiz. Metal. Metalloved*., **45**(5), 990–996 (1978) (Crys. Structure, Experimental, 8)

[1979Buc] Buckley, R.A., "Ordering and Recrystallization in Fe-50Co-0.4% Cr", *Metal Sci.*, **13**, 67–72 (1979) (Experimenta, Phase Relations, *, 16)

[1979Dom] Dombre, M., Silva Campos, O., Valignat, N., Allibert, C., Bernard, C., Driole, J., "Solid State Phase Equilibrium in the Ternary Fe-Co-Cr System: Experimental Determination of Isothermal Sections in the Temperature Range 800 - 1300°C", *J. Less-Common Met.*, **66**, 1–11 (1979) (Experimental, Phase Diagram, Phase Relations, #, *, 8)

[1979Kok1] Kokotov, S.I., Fadin, V.P., "Neutron Diffraction Analysis of $Fe_{0.5}(Co_{0.5-x}Cr_x)$ Alloys", *Sov. Phys. J. (Engl. Transl.)*, **22**(11), 1252 (1979), translated from *Izv. Vyss. Uchebn. Zaved., Chern. Metall*., **22**(11), 145, (1979) (Experimental, Abstract)

[1979Kok2] Kokotov, S.I., Fadin, V.P., "Study of the Effect of Temperature on the Character of Atomic Rearrangements in $Fe_{0.5}(Co_{0.5-x}Cr_x)$ Alloys", *Sov. Phys. J. (Engl. Transl.)*, **22**(12), 1354 (1979), translated from *Izv. Vyss. Uchebn. Zaved., Chern. Metall*., **22**(12), 108 (1979) (Experimental, Abstract)

[1979Nis] Nishizawa, T., Hasebe, M., Ko, K., "Thermodynamic Analysis of Solubility and Miscibility Gap in Ferromagnetic α Iron Alloys", *Acta Metall.*, **27**, 817–828 (1979) (Experimental, Phase Diagram, Thermodyn., *, 40)

[1979Spe] Spencer, P.J., "Calculation of Phase Diagrams for Alloy System During σ Phase Formation" in "*Calculation of Phase Diagram and Thermochemistry of Alloy Phases*", Chang, Y.A., Smith, J.F. (Eds.), TMS/AIME, Warraendale, PA, 14–25 (1979) (Review, Phase Diagram, Thermodyn., Phase Relations, 33)

[1980Bel] Belyatskaya, I.S., Serebryakov, V.G., "Anisotropy of Elastic Properties in Iron-Chromium-Cobalt Alloys", *Phys. Met. Metallogr.*, **49**(5), 189–190 (1980), translated from *Fiz. Met. Metallovd*., **49**(5), 1113–1114 (1980) (Experimental, Phys. Prop., 5)

[1980Eib] Eibschutz, M., Mahajan, S., Jin, S., Brasen, D., "Phase-Separation in a Low-Cobalt Cr-Co-Fe Alloy", *J. Magn. Magn. Mater.*, **15–18**, 1181–1182 (1980) (Experimental, Phase Relations, 11)

[1980Gal] Gallagher, P.K., Coleman, E., Jin, S., Sherwood, R.C., "Some Applications of Thermomagnetometry to the Study of Chromindur Alloys", *Thermochim. Acta*, **37**, 291–300 (1980) (Experimental, Magn. Prop., 8)

[1980Jin1] Jin, S., Mahajan, S., Brasen, D., "Mechanical-Properties of Fe-Cr-Co Ductile Permanent-Magnet Alloys", *Metall. Trans. A*, **11A**(1), 69–76 (1980) (Experimental, Mechan. Prop., 37)

[1980Jin2] Jin, S., Gayle, N.V., "Low-Cobalt Cr-Co-Fe Magnet Alloys Obtained by Slow Cooling Under Magnetic-Field", *IEEE Trans. Magn.* **Mag-16**(3), 526–529 (1980) (Experimental, Magn. Prop., 16)

[1980Mah] Mahajan, S., Jin, S., Brasen, D., "Micro-twinning in a Spinodally Decomposed Fe-Cr-Co Alloy", *Acta Metall.*, **28**, 971–977 (1980) (Experimental, Phase Relations, 24)

[1980Min] Minowa, T., Okada, M., Homma, M., "Further-studies of the Miscibility Gap in an Fe-Cr-Co Permanent-Magnet System", *IEEE Trans. Magn.*, **Mag-16**(3), 529–533 (1980) (Experimental, Magn. Prop., #, *, 13)

[1981All] Allibert C., Bernard C., Effenberg G., Nussler H.-D., Spencer P.J., "A Thermodynamic Evaluation of The Fe-Co-Cr System", *Calphad*, **5**(4), 227–237 (1981) (Calculation, Phase Diagram, Thermodyn., *, 25)

[1981Nis] Nishizawa, T., Hasebe, M., "Computer Calculation of Phase Diagrams of Iron Alloys" (in Japanese), *Tetsu to Hagane*, **67**(14), 2086–2097 (1981) (Review, Phase Relations, Thermodyn., 110)

[1982Arg] Argent, B.B., Ellis, M., Effenberg, G., "A Mass Spectrometric Investigation of the Non-Chromium-Cobalt System", *High Temp.-High Press.*, **14**(4), 409–416 (1982) (Experimental, Thermodyn., *, 8)

DOI: 10.1007/978-3-540-74196-1_18

[1982Kub] Kubaschewski, O., "Iron-Chromium" in "*Iron-Binary Phase Diagrams"*, Springer-Verlag, Berlin, 31–34 (1982) (Phase Relations, Phase Diagram, Review, 22)

[1982Sei] Sein, V.A., Andreyeva, A.V., Milyayev, I.M., "Structural Features of Fe-Cr-Co Alloys Containing 10% Co", *Phys. Met. Metallogr.*, **54**(6), 175–177 (1982), translated from *Fiz. Met. Metalloved*., **54**(6), 1221–1223 (1982) (Crys. Structure, Experimental, Magn. Prop., 5)

[1983Bel] Belyatskaya, I.S., Vintaykin, Ye.Z., Mezhennyy, Yu.O., "Concerning the Structural Features of Decomposition in Fe-Cr-Co Magnet Alloys", *Phys. Met. Metallogr.*, **55**(5), 115–121 (1983), translated from *Fiz. Met. Metallovd*., **55**(5), 960–966 (1983) (Crys. Structure, Experimental, Thermodyn., Magn. Prop., 13)

[1983Chi] Chin, T.-S., Wu, T.-S., Chang, C.Y., "Spinodal Decomposition and Magnetic Properties of Fe-Cr-12Co Permanent Magnet Alloy", *J. Appl. Phys.*, **54**(8), 4502–4511 (1983) (Experimental, Magn. Prop., Phase Diagram, #, *, 25)

[1984Bel] Belyatskaya, I.S., "Martensitic Transformation in Fe-Cr-Co Magnet Alloys", *Russ. Met.*, (2), 125–128 (1984), translated from *Izv. Akad. Nauk SSSR Metally*, (2), 130–133 (1984) (Crys. Structure, Experimental, Phase Diagram, Magn. Prop., *, 8)

[1984Bre] Brenner, S.S., Camus, P.P., Miller, M.K., Soffa, W.A., "Phase Separation and Coarsening in Fe-Cr-Co Alloys", *Acta Metall.*, **32**(8), 1217–1227 (1984) (Experimental, Phase Relations, Kinetics, 52)

[1984Mue] Mueller, P., "Transforming Report of Iron-Chromium-Cobalt Alloys" (in German), *Neue Huette*, **29**, 268–270 (1984) (Experimental, Phase Diagram, Mechan. Prop., 4)

[1984Ser] Serikov, V.V., Kleynerman, N.M., Yurchikov, Ye.Ye., Belozerov, Ye.V., Shur, Ya.S., "NMR and NGR Investigations of the Modulated Structure in Alloys of the Fe-Co-Cr System for Permanent Magnets", *Phys. Met. Metallogr.*, **58**(2), 62–68 (1984), translated from *Fiz. Metal. Metalloved*., **58**(2), 282–287 (1984) (Crys. Structure, Experimental, Phase Diagram, Magn. Prop., 14)

[1985Bla] Blacktop, J., Crangle, J., Argent, B.B., "Calorimetric and Magnetic Study of Solid Fe-Co-Cr Alloys", *Mater. Sci. Tech.*, **1**(6), 448–453 (1985) (Experimental, Thermodyn., Magn. Prop., #, *, 15)

[1985Mor] Morinaga, M., Yukawa, N., Ezaki, H., "Solid Solubilities in Transition-Metal-Based f.c.c. Alloys", *Philos. Mag. A*, **51**(2), 223–246 (1985) (Calculation, Theory, 45)

[1986Kol] Kolobova, K.M., Trofimova, V.A., Nemnonov, S.N., Maykov, V.G., "X-Ray Spectral Investigation of the Electronic Structure of Ternary Alloys Fe-Co-Cr", *Phys. Met. Metallogr.*, **62**(4), 80–84 (1986), translated from *Fiz. Metal. Metalloved*., **62**(4), 714–718 (1986) (Crys. Structure, Experimental, Thermodyn., 10)

[1986Zhu] Zhu, F., Haasen, P., Wagner, R., "An Atom Probe Study of the Decomposition of Fe-Cr-Co Permanent Magnet Alloys", *Acta Metall.*, **34**(3), 457–463 (1986) (Experimental, Phase Relations, Kinetics, 21)

[1987Klo] Kloss, H., Mueller, P., "Studies on the Deformation-Behavior of Iron Rich Fe-Cr-Co Alloys" (in German), *Neue Huette*, **32**, 252–256 (1987) (Experimental, Mechan. Prop., 10)

[1987Ser] Serikov, V.V., Kleynerman, N.M., Belozerov, Ye.V., Yurchikov, Ye.Ye., Lapina, T.P., Shur, Ya.S., "NMR and NGR Investigations of Alloys for Permanent Magnets of the Fe-Co-Cr System with Different Cobalt Contents", *Phys. Met. Metallogr.*, **64**(2), 114–118 (1987), translated from *Fiz. Metal. Metalloved*., **64**(2), 333–337 (1987) (Experimental, Thermodyn., 10)

[1987Vin] Vintaikin B.E., Kuzmin R.N., "A Thermodynamic Study of $\alpha \rightleftharpoons \alpha_1 + \alpha_2$ Stratification in High-Coercivity Alloys Fe-Cr-Co, Fe-Cr-Co-Mo, Fe-Cr-Co-W, and Fe-Cr-Co-Nb" (in Russian), *Metallofizika*, **9**(3), 16–21 (1987) (Calculations, Theory, 13)

[1988Ray] Raynor, G.V., Rivlin, V.G., "Co-Cr-Fe", *Phase Equilibria in Iron Ternary Alloys*, Institute of Metals, London, 213–230 (1988) (Phase Diagram, Phase Relations, Review, 29)

[1989Sim] Simon, J.P., Lyon, O., "Phase Separation in a Fe-Cr-Co Alloy Studied by Anomalous Small Angle X-ray Scattering", *Acta Metall.*, **37**(7), 1727–1733 (1989) (Experimental, Phase Separation, Kinetics, 20)

DOI: 10.1007/978-3-540-74196-1_18

[1990Ish] Ishida, K., Nishizawa, T., "The Co-Cr (Cobalt-Chromium) System", *Bull. Alloy Phase Diagrams*, **11**(4), 357–370 (1990) (Phase Diagram, Phase Relations, Review, 56)

[1990Zub] Zubkov, A.A., Mogutnov, B.M., Shaposhnikov, N.G., "Heats of Formation of σ-Phases in Iron-Chromium, Cobalt-Chromium, and Iron-Cobalt-Chromium Systems" (in Russian), *Dokl. Akad. Nauk SSSR*, **311**(2), 388–392 (1990) (Thermodyn., Experimental, 14)

[1992Vin] Vintaikin, B.E., Istratov, Yu.S., Libman, M.A., Potapov, N.N., "Principles of Formation of Magnetic Properties in Fe-Cr-Co Alloys", *Russ. Metall. (Engl. Transl.)*, **3**, 160–165 (1992), translated from *Izv. Akad. Nauk SSSR Met.*, 3, 172–177, (1992) (Experimental, 8)

[1994Lyo] Lyon, O., Simon, J.P., "Use of Anomalous Small-angle Scattering for Analysis of Phase-separation of Ternary Alloys" (in French), *J. Physique IV*, **4**, C3-25-34 (1994) (Experimental, Morphology, Phase Diagram, 22)

[1994Rag] Raghavan, V., "Co-Cr-Fe (Cobalt- Chromium-Iron)", *J. Phase Equilib.*, **15**(5), 524 (1994) (Phase Diagram, Review, 12)

[1994Hil] Hillert, M., "Historic Note on the Two-Peak Miscibility Gap", *J. Phase Equilib.*, **15**(1), 35–36 (1994) (Calculation, Phase Diagram, 8)

[1995Nis] Nishizawa, T., "Effect of Magnetic Transition on Phase Equilibria in Iron Alloys", *J. Phase Equilib.*, **16**(5), 379–389 (1995) (Magn. Prop., Phase Relations, Review, Thermodyn., #, *, 28)

[1999McH] McHenry, M.E., Willard, M.A., Laughlin, D.E., "Amorphous and Nanocrystalline Materials for Applications as Soft Magnets", *Prog. Mater. Sci.*, **44**(4), 291–433 (1999) (Crys. Structure, Electr. Prop., Experimental, Magn. Prop., Phase Relations, Review, 302)

[2000All] Alleg, S., Bouzabata, B., Greneche, J.M., "Study of the Local Environment during the Phase Decomposition of Fe-30.8Cr-12.2Co Alloy by Mössbauer Spectrometry", *J. Alloys Compd.*, **312**, 265–272 (2000) (Experimental, Magn. Prop., 41)

[2002Ben] Bentayeb, F.-Z., Alleg, S., Bouzabata, B., Greneche, J.M., "Mössbauer Study of Mechanically Alloyed $Fe_{57}Cr_{31}Co_{12}$", *Phys. Status Solidi A*, **189**(3), 841–844 (2002) (Crys. Structure, Experimental, 7)

[2002Boz] Bozzolo, G.H., Noebe, R.D., Amador, C., "Site Occupancy of Ternary Additions to *B*2 Alloys", *Intermetallics*, **10**, 149–159 (2002) (Crys. Structure, Review, 27)

[2002Ohn] Ohnuma, I., Enoki, H., Ikeda, O., Kainuma, R., Ohtani, H., Sundman, B., Ishida, K., "Phase Equilibrium in the Fe-Co Binary System", *Acta Mater.*, **50**, 379–393 (2002) (Phase Diagram, Thermodyn., Assessment, 50)

[2005Sou] Sourmail, T., "Near Equiatomic FeCo Alloys: Constitution, Mechanical and Magnetic Properties", *Prog. Mater. Sci.*, **50**(7), 816–880 (2005) (Crys. Structure, Electr. Prop., Kinetics, Magn. Prop., Mechan. Prop., Morphology, Phase Diagram, Phase Relations, Review, 122)

[2005Gao] Gao, R.S., Zhen, L., Shao, W.Z., Sun, X.Y., Zhu, D.Y., Xu, R.G., "Magnetic Stability of Fe-Cr-Co Permanent Magnet Materials at High Temperature", *Mat. Sci. Forum*, **475–479**, 2135–2138 (2005) (Crys. Structure, Electronic Structure, Experimental, Magn. Prop., Phase Relations, 10)

[2005Ben] Bentayeb, F.Z., Alleg, S., Bouzabata, B., Greneche, J.M., "Study of Alloying Mechanisms of Ball Milled Fe-Cr and Fe-Cr-Co Powders", *J. Magn. Magn. Mater.*, **288**, 282–296 (2005) (Crys. Structure, Electronic Structure, Experimental, Magn. Prop., Phase Relations, 57)

[2006Koy] Koyama, T., Onodera, H., "Modeling of Microstructure Changes in Fe-Cr-Co Magnetic Alloy Using the Phase-Field Method", *J. Phase Equilib. Diffus.*, **27**(1), 22–29 (2006) (Calculation, Kinetics, Morphology, 23)

[Mas2] Massalski, T.B. (Ed.), *Binary Alloy Phase Diagrams*, 2nd edition, ASM International, Metals Park, Ohio (1990)

[V-C2] Villars, P. and Calvert, L.D., *Pearson's Handbook of Crystallographic Data for Intermetallic Phases*, 2nd edition, ASM, Metals Park, Ohio (1991)

DOI: 10.1007/978-3-540-74196-1_18

Cobalt – Copper – Iron

Mikhail Turchanin, Tamara Velikanova

Introduction

The first extensive investigations of the Co-Cu-Fe system were undertaken by Jellinghaus [1936Jel1, 1936Jel2] and Maddocks and Claussen [1936Mad] to determine the shape of liquidus surface and the solid solubility of the elements. Five temperature-composition sections along lines of constant Co content were reported by [1936Jel1, 1936Jel2] and four temperature-composition sections were reported by [1936Mad]. It was shown that ternary liquid alloys are completely miscible and the solid solutions extend markedly into the ternary system. No ternary phases have been reported. These results were generally confirmed by later investigations [1974Bei, 1981Oik, 1991Nik, 1997Oht, 2000Kim1, 2000Kim2, 2002Bam, 2002Wan, 2005Cao, 2006Mun] where a great number of isothermal sections in the temperature range from 800 to 1310°C were studied. Most of the investigations of phase relationships and crystal structure of the phases are listed in Table 1. The experimental work on the phase relations has been critically reviewed by [1969Gue, 1979Cha, 1979Dri, 2002Rag, 2004Rag].

The nature of the metastable immiscibility of supercooled liquid alloys has been under extensive investigation [1998Mun, 2000Kim1, 2000Kim2, 2000Kim3, 2004Wan2, 2005Cao, 2006Mun, 2006Pal]. The results of these works will be discussed in the Miscellaneous section.

Thermodynamic modeling of the stable and metastable transformations in the Co-Cu-Fe system was performed by [1989Kum, 1997Oht, 2002Bam, 2002Wan, 2004Wan1, 2005Wan, 2006Pal]. The thermodynamic parameters of the ternary system were evaluated by [1997Oht] on the basis of their own experimental results on the solubility of the phases over the temperature interval 1100-1300°C. A thermodynamic assessment of the phase equilibria in the Co-Cu-Fe system was carried out by [2002Wan, 2004Wan2, 2005Wan] on the basis of their own experimental results and taking into account data of previous work. A thermodynamic description of the system [2002Bam] was derived using thermodynamic parameters from the SSOL thermodynamic database that were modified using experimentally determined melting temperatures of a number of ternary compositions. Experimental data that have appeared recently have been used by [2006Pal] to describe the stable and metastable phase transformations of the system. A significant improvement with respect to previous thermodynamic descriptions has been achieved. The liquidus points from [2002Bam] were neglected in the optimization. The cluster variation method was used by [2000Ant, 2001Ant, 2001Col] for empirical calculation of the Co-Cu-Fe γ/α phase diagram.

An optimized and self-consistent thermodynamic description of the Co-Cu-Fe system [2006Pal] was used for the generation of the majority of figures on phase relations and the reaction scheme presented in the current assessment.

Binary Systems

Assessments of the Co-Fe system by [2002Ohn], of the Co-Cu system by [2006Pal] and of the Cu-Fe system by [1986Jan] are accepted. These works are in good agreement with [Mas2, 2007Ans, 2007Tur]. The thermodynamic data sets for binary systems presented by [1986Jan, 2002Ohn, 2006Pal] were used by [2006Pal] for thermodynamic assessment of the ternary Co-Cu-Fe system.

Solid Phases

Table 2 summarizes the crystallographic data of the solid phases of the Co-Cu-Fe and their temperature and concentration ranges of stability. No ternary compounds have been found in the system. The α and γ phases show marked solubility in the ternary system.

Iron and cobalt are found to decrease the mutual solubility in copper. At Co:Fe = 1 it is of 2.25 at.% at 1096°C following the thermodynamic description of [2006Pal]. The Cu solubility in the γ phase in the ternary system has a retrograde character as in the Co-Cu and Cu-Fe binary systems. It increases slightly in the

DOI: 10.1007/978-3-540-74196-1_19

ternary system as compared to the Co-Cu and Cu-Fe binary systems, reaching 20 mass% Cu at 75 mass% Co and 1330°C. Both Fe and Cu decrease the temperature of the polymorphous transition of fcc (αCo) to hexagonal (εCo) down to 213°C at 2.35 at.% Fe and 0.01 at.% Cu, after calculation using the thermodynamic description of [2006Pal]. The experimental information confirms the existence of a narrow composition range for the (εCo) phase. After Masumoto [1926Mas], the data of which were cited by [1936Jel1], the hexagonal form of cobalt was observed experimentally in Co-Cu-Fe alloys only up to 5 mass% Fe. Cu decreases the temperature of the congruent γ ⇌ α + (Cu) transformation in the ternary system, from 985°C at 55 at.% Fe to 929°C at the e_1 (max) point. 213°C is the lowest temperature at which the γ phase is stable in the ternary system.

The influence of Cu on both the magnetic as well as chemical ordering of the γ and α phases has not been established experimentally. A rather strong contraction of the α' phase field with Cu addition is suggested by CVM calculation in [2001Ant]. The Bozzolo-Ferrante-Smith quantum approximate method has been used by [2002Boz] for the analysis of the site-substitution behavior of Cu in the ordered α' phase.

The indirect experimental data in [1936Jel1, 1936Mad] suggests that the ternary α' phase could be produced in annealed or slowly cooled alloys. For example, the alloy at 3Cu50Co (mass%) cooled very slowly from 1200°C down to RT or quenched from 800°C and subsequently annealed at 650°C had a slightly lower specific density and the coefficient of thermal expansion was relatively small. Its X-ray spectrum (in Co-radiation only) showed some lines not belonging to the (αFe) lattice [1936Jel1]. However, no direct identification of the ordered structure was obtained. Therefore, the ordered α' phase was not indicated in the vertical sections by [1936Jel1].

Invariant Equilibria

Two invariant three-phase equilibria involving the liquid phase were found by thermodynamic calculation by [2006Pal]. A maximum for the incongruent monovariant L + (δFe) ⇌ γ lies at 1502°C and a minimum for the incongruent monovariant L + γ ⇌ (Cu) at 1096°C. They are shown in Fig. 1 and the compositions of the phases are given in Table 3. A four-phase eutectoid type invariant equilibrium involving the (εCo), γ, α and (Cu) phases lies close to the Co-Cu side of the system according to the calculation. Experimental confirmation has not yet been obtained.

Liquidus, Solidus and Solvus Surfaces

Data for the liquidus surface of the system has been published in [1936Jel1, 1936Jel2, 1936Mad, 1997Oht, 2000Kim1, 2000Kim2, 2005Cao, 2006Mun] and are in general agreement with each other. The data were used for the development of the thermodynamic description of the system given by [2006Pal]. The calculated liquidus surface projection is given in Fig. 2. The results of [2002Bam] differ from other data and are not considered here.

Complete miscibility in the liquid state of the ternary system as in the corresponding binaries was suggested by [1936Jel1, 1936Jel2, 1936Mad] based on thermal analysis and microstructural investigation of ternary alloys over the whole composition range. The liquidus surface of the ternary system consists of three fields of primary crystallization belonging to the α, γ and (Cu) phases. The γ phase primary crystallization field is the most extended. The temperature of the peritectic monovariant L + δ ⇌ γ decreases from the Co-Fe to Cu-Fe binary systems as does that for the L + (αCo) ⇌ (Cu) monovariant, which extends from the Co-Cu to Cu-Fe binary [1936Jel1, 1936Jel2, 1936Mad, 1969Gue, 1979Dri, 1979Cha]. The more recent experimental data of [1997Oht, 2000Kim1, 2000Kim2, 2005Cao, 2006Mun] for the solid / liquid equilibria are in general agreement with earlier data. However, according to the thermodynamic calculation by [2006Pal] there exist weak extreme on the monovariant liquid lines, as shown in the reaction scheme and liquidus projection in Figs. 1 and 2, respectively. The minimum in the liquidus of the γ phase, found at about 33 at.% Fe in the Co-Fe binary system ends in the ternary diagram somewhere below 10 at.% Cu and 85 at.% Co in the calculation.

The liquidus surface of the γ phase is relatively flat over almost the whole of the composition triangle and decreases sharply in the Cu rich corner.

The solidus surface projection is given in Figs. 3a and 3b as calculated by [2006Pal]. Experimental data for the solidus surface have been reported by [1936Jel1, 1936Jel2, 1936Mad, 2000Kim1, 2000Kim2, 2006Mun].

DOI: 10.1007/978-3-540-74196-1_19

The solidus surface of the ternary system is composed of those three phases - a rather limited α and (Cu) and an extended γ solid solutions. According to [1936Jel1, 1936Jel2, 1936Mad], the maximum solubility of Cu in the γ phase indicated by the solubility at the peritectic δ + L ⇌ γ temperature independent of the Co to Fe ratio is approximately 8 mass%. Taking into account new data on the Cu-Fe and Co-Cu boundary binary phase diagrams by [2007Ans, 2007Tur], the solubility must be markedly higher, not only because of higher solubility in the peritectic reaction but because of the existence of retrograde solubility of Cu in the γ phase. The tie-lines with maximum and minimum temperatures of 1502 and 1096°C in δ + (γ) and (γ) + (Cu) linear surfaces, respectively, are revealed by the thermodynamic calculation.

Isothermal Sections

The equilibrium compositions of the solid and liquid phases of the Co-Cu-Fe system at 1100, 1200 and 1300°C were measured by [1997Oht] using solid-liquid diffusion couples. The samples were held at the reaction temperatures for 24-48 h and subsequently quenched in iced brine. The average composition of the frozen solid and liquid at the interface boundaries of the diffusion couples were obtained, up to a Co content of 23.93, 30.90 and 45.02 mass% in the solid and 1.34, 2.10, and 5.40 mass% in liquid at 1100, 1200 and 1300°C, respectively. It was shown that the addition of Co slightly increases the solubility of Cu in Fe based phases.

The composition of the equilibrium phases, (Cu)/α at 800°C and (Cu)/γ at 900 and 1000°C, were reported by [2002Wan] for the Fe rich alloys of the Co-Cu-Fe system. The alloys were prepared by melting and were subsequently hot-rolled at 900°C, solution-treated at 900°C for 24 h, heat-treated at 800 to 1000°C for 336-1680 h and then quenched into iced water. It was confirmed that the specimens had reached the equilibrium state. The equilibrium compositions were obtained up to Co contents of 9.97, 9.32, 9.26 mass% in Fe based phases and 0.68, 0.87, 0.84 mass% in the (Cu) phase at 800, 900 and 1000°C, respectively.

The experimental data of [1997Oht], being obtained using the diffusion couple technique, should be less reliable than those of [2002Wan] who used conventional metallurgical methods and good equilibrated alloys. However, both sets of data are in perfect agreement and the experimental data are consistent with the calculated phase boundaries.

These data were used as a basis for further thermodynamic modeling of the phase equilibria in more extended ranges of composition and temperature. Isothermal sections at 1100, 1200 and 1300°C have been published by [1997Oht], at 1250, 1310°C by [2000Kim1], at 1000, 1127, 1200 and 1300°C by [2002Wan, 2004Wan1] and at 800, 900, 1000, 1127, 1200 and 1300°C by [2006Pal]. The isothermal sections at 800, 900 and 1000°C have been derived by [1992Rag] from the vertical sections experimentally determined by [1936Jel1, 1936Mad]. The later experimental data on the phase equilibria in the ternary system concerning the temperature range from 800 to 1310°C, usually in limited composition regions, are reported by [1981Oik, 1990Jia, 1997Oht, 2000Bei, 2000Kim1, 2002Wan] (see Table 1). The above mentioned results are generally in a good agreement.

Calculated isothermal sections at 200, 300, 800, 900, 1000, 1127 and 1480°C given in Figs. 4 to 10, respectively, were given by [2006Pal] (at 200, 300 and 1480°C for the first time). The three-phase equilibria with extended α and rather restricted (εCo) and (Cu) solid solutions are presented only in the isothermal section at 200°C given in Fig. 4. However, the proposed phase equilibria for 0°C by [1936Jel1] and the corrected variant given by [1969Gue] are not in agreement with the calculation at 200°C. This is because [1936Jel1] supposed that the γ phase and the corresponding two- and three-phase fields, (α+(Cu), γ+(Cu)) and a very narrow α + γ + (Cu) close to 20 at.%, exist at RT. This proposition was based on the structure of specimens slowly cooled from high temperature down to RT, which cannot be considered as equilibrated at room temperature. The modified diagram of [1969Gue] includes only the additional (εCo)-containing phase ranges as a consequence of the later version of the binary Co-Fe phase diagram. The isothermal section at 25°C calculated by [2006Mun] is similar to that given by [1936Jel1], but a wide three-phase region is shown between 1 and 20 at.% Fe. The calculation was performed using the dataset given by [2002Bam] modified to give agreement with the experimental data for the liquidus. The experimental data presented by [2006Mun] show a narrow three-phase region α + γ + (Cu) close to 20 at.% Fe (similarly to [1936Jel1]). The alloys were obtained by induction melting, homogenized at 1600°C (in the liquid state), then cooled

DOI: 10.1007/978-3-540-74196-1_19

down to 1000°C at a rate of $3 \cdot 10^{-2}$ K·s^{-1}, then cooled to room temperature in the furnace. This unstable state was, without any justification, related to room temperature.
The alloys prepared by [1936Jel1] as well as [2006Mun], are in effect related to temperatures higher than 213°C. The isothermal section at 300°C is given in Fig. 5.
Three three-phase fields, α + (Cu) + γ, γ + (Cu) + ε and α + γ + ε are represented in accordance with the three monovariant equilibria preceding the eutectoid decomposition of the γ phase at 213°C. The third of the above equilibria is practically degenerate and coincides with the Co-Fe side of the composition triangle at the selected scale of the figure, (Fig. 5), because of the low solubility of Cu in the phases (10^{-2} to 10^{-3} %), at low temperatures. Such equilibria will exist up to 417.6°C, the lowest temperature of the γ eutectoid decomposition in the boundary systems. The phase equilibria shown in Fig. 6 for 800°C are characteristic for a wide temperature range, beginning at 420°C, which is the temperature of γ ⇌ ε transformation in the binary Co-Fe. Experimental isothermal sections for temperatures below 800°C are not available. Calculations for 650 and 750°C at 0 to 3 mass% Cu are reported by [1989Kum], using only binary interaction parameters in the thermodynamic modeling. The isothermal section at 900°C is given in Fig. 7.
Phase equilibria like those shown for 900°C in Fig. 7 exist over a narrow temperature range - from 912 to 978°C, the maximum temperature of the γ ⇌ α transition in the Co-Fe binary system. The equilibria involving the γ solid solution in both the (Cu) phase at 1000°C (given in Fig. 8) as well as with the liquid at 1300°C (given in Fig. 9), which extend along the whole of the Co-Fe edge, are in agreement with experimental data. One can see in Fig. 9 that the Cu solubility in the γ phase that is in equilibrium with the liquid decreases monotonously with increasing Fe content, beginning from a Co:Fe ratio of 9. However in equilibrium with (Cu), a slight maximum in the solubility of Cu in the γ phase exists in the vicinity of a Co:Fe ratio of about 4; Fig. 8. The shift in the minimum on the liquidus towards the Co rich corner on the addition of copper is shown in the isothermal section at 1480°C given in Fig. 10.

Temperature – Composition Sections

Six partial temperature-composition sections have been derived experimentally by [1936Jel1, 1936Jel2] and four sections by [1936Mad]. Calculated sections at Co:Fe = 1, at 10, 20, 30 mass% Co and at 10, 20 mass% Fe have been published by [2002Wan, 2004Wan1, 2004Wan2]. Earlier experimental data were combined with their own for the thermodynamic modeling. In Figs. 11 to 17, the temperature-composition sections at Co : Fe = 0.33 and 1 (at.%); 10, 50, 70 and 75 at.% Co; 10 at.% Cu across the whole composition range for temperatures from liquidus down to 200°C are given as calculated using the thermodynamic model published by [2006Pal]. The results of the calculation agree well with the experimental sections at 10, 25 and 50 mass% Cu after [1936Jel1, 1936Jel2].
The section at Co:Fe = 1 given in Fig. 11 differs only slightly in the temperature of the γ + α + (Cu) equilibrium and the extension of the γ phase in equilibrium with (Cu) and the liquid phase. According to the calculation, which is in perfect agreement with the experimental data of [1936Jel1, 1936Jel2], cobalt first increases the temperature of the γ ⇌ α + (Cu) equilibrium from 847°C in the Cu-Fe up to a maximum before decreasing. It can be seen from a comparison of the sections Co:Fe = 1 and Co:Fe = 3, given in Figs. 11 and 12, respectively. The maximum temperature is shown in the section at 10 mass% Cu given in Fig. 13. The agreement between the data of [1936Jel1, 1936Jel2] and the calculation becomes worse at Co contents of more than 50% and at the temperatures lower 800°C. This can be explained by the relatively short heat treatment, which was insufficient for complete decomposition of the γ phase in the experiments of [1936Jel1, 1936Jel2]. The tendency of this increase in Cu solubility in the γ phase with increasing Co contents (up to a maximum at about Co:Fe = 1:9, as shown above) is clear on comparing the vertical sections at Co:Fe = 3 (at.%) given in Fig. 12 and at 10, 50, 70, 75 mass% Co (Figs. 13 - 16, respectively). The γ + (Cu) + L three phase field is very narrow across the whole composition range. The sharp reduction in the temperature of the γ ⇌ α + (Cu) reaction from about 950°C, the temperature maximum in the ternary system, down to 213°C, the eutectoid decomposition of the γ phase in the ternary system, was shown by calculation.
The retrograde solubility of the γ phase as shown in the radial vertical sections in Figs. 11 - 13 and in the isopleths at constant Co content (Figs. 14 - 16) in the ternary system is somewhat higher than in both the Cu-Fe and Co-Cu boundaries: it is close to 20 at.% Cu at 1300°C.

DOI: 10.1007/978-3-540-74196-1_19

Both the magnetic ordering in the γ- and α-phases as well as chemical ordering of the α phase (α ⇌ α' transition) are not indicated in the vertical sections because the required data are not available for the ternary alloys.

Thermodynamics

Experimental information on the thermodynamic properties of the ternary phases is not available.
The first attempts at modeling the thermodynamic properties of ternary phases from information on the properties of binary systems are given by [1985Bur, 1989Kum]. In [1985Bur], the thermodynamic properties of liquid Co-Cu-Fe alloys (excess Gibbs free energy of mixing and thermodynamic activities of components) were estimated on the basis of experimental data on the properties of boundary binary systems. In [1989Kum], the binary interaction parameters were used for computation of the α/γ equilibrium in ternary alloys.
As shown in [1997Oht, 2002Bam, 2002Wan, 2006Pal], ternary interaction parameters must by taken into account in order to eliminate phase separation in the ternary liquid. Also, ternary interaction parameters were used for thermodynamic modeling of the α phase [2002Wan, 2006Pal] and the fcc solid solution (γ- and (Cu) phase) [1997Oht, 2002Bam, 2002Wan, 2006Pal].
A thermodynamic assessment of the Co-Cu-Fe system was carried out by [2006Pal] using the Calphad approach. Binary interaction parameters for the Co-Fe and Cu-Fe systems were taken from previous work [2002Ohn, 1986Jan]. The Co-Cu system was reassessed in [2006Pal] taking into account newly available experimental data. The assessment of the ternary Co-Cu-Fe system [2006Pal] shows good agreement with experimental data in both the binary and ternary phase diagrams. A significant improvement in the description of the miscibility gap in the liquid phase has been achieved. To reproduce the figures shown in [2006Pal] the published set of thermodynamic parameters must be supplemented with a binary interaction parameter of 35000 $J \cdot mol^{-1}$ for the hypothetical bcc phase of the Co-Cu system.
Experimental investigations of the thermodynamic properties of ternary phases are required.

Notes on Materials Properties and Applications

The experimental work devoted to the study of materials properties in the Co-Cu-Fe system are listed in Table 4.
The magnetic structure of non-coherent γ phase precipitates in the (Cu) matrix and the influence of particle size on the spin density wave in γ precipitates has been studied by neutron diffraction by [1989Tsu, 1990Tsu]. It was shown that the smaller the particle size, the longer is the wavelength and the higher is the Neel temperature.
The Co-Cu-Fe system is well known as a basic system for the preparation of ternary and multicomponent supersaturated γ-solid solutions by rapid quenching from the liquid and by mechanical alloying.
The evaluation of the structure of a $Co_{10}Cu_{80}Fe_{10}$ granular metallic ribbon prepared by rapid quenching from the melt was investigated with as-quenched and annealed samples by [1999Cri]. Upon annealing, the magnetic Fe rich α phase particles dissociate from the as-quenched (Cu)-matrix. The study shows evidence of local mechanisms concerning the superparamagnetic behavior of iron phases. Magnetoresistance of $Co_5Cu_{90}Fe_5$ as-quenched melt-spun ribbons as a function of annealing temperature has been measured by [2006Sin]. An annealing at 400°C leads to a maximum segregation of magnetic impurities in the copper matrix.
The temperature dependence of magnetization in nanocrystalline $Co_xCu_{0.5}Fe_{0.5-x}$, at x = 0, 0.1, 0.2, 0.4 powders, manufactured by mechanical alloying in a high-energy ball mill, has been studied by [1996Yoo1]. The effect of Co additions on structural and magnetic properties during mechanical alloying has been studied by [1995Yoo], and an increase in the Curie temperatures of the solid solutions with increasing Co content was shown. The microstructure and magnetic properties of a $Co_xCu_{0.8}Fe_{0.2-x}$ alloy manufactured by mechanical alloying were studied by [1996Yoo2].
The giant magnetoresistance and the magnetization of raw and annealed mechanically alloyed $Co_{14}Cu_{80}Fe_6$ samples were measured by [1997Nag]. The fraction of the ferromagnetic component increases monotonically with annealing temperature. The largest amplitude of magnetoresistance is observed for the sample annealed at 500°C.

DOI: 10.1007/978-3-540-74196-1_19

The local order around Fe, Co and Cu atoms has been investigated at room temperature, and long range order has been studied in nanocrystalline $Co_{50-x}Cu_{50}Fe_x$ (x = 10, 20, 30, 40, 50) alloys prepared by mechanical alloying [1999Gay, 1999Pri, 1999Yan]. In order to determine the evolution of the alloying process, samples were studied after several processing times. It can be concluded that within the first 20 h of milling, the majority of the Co atoms are alloyed in an γ solid solution, while Fe atoms are mainly separate from this phase and remain in the α structure. In a second step, after more than 40 h of milling, the Fe atoms enter the alloy which still has an fcc structure.

Structural and magnetic properties of nanocrystalline an γ $Co_{0.1}Cu_{0.70}Fe_{0.2}$ alloy prepared by high energy ball milling have been studied by [2001Nas]. The alloy shows the typical behavior of a magnetic material with a T_c of about (420 ± 1) K. The precipitation of the α phase on heat treatment of the final milled samples is strongly dependent on the method of preparation.

The influence of the ball-milling temperature and intensity on the nanostructure of the $Co_{14}Cu_{80}Fe_6$ powder alloy has been studied by [2002Gal]. The ball milling of mixed powders of Cu-Fe and Co-Cu supersaturated solid solutions allows the formation of very fine $Fe_{30}Co_{70}$ precipitates in a (Cu) matrix, interesting for its magnetoresistive properties. The ball-milling conditions were correlated to the nanostructure and the magnetic properties of the ternary alloys.

High-energy ball milling was used by [2005Lar] to prepare a magnetoresistive granular $Co_6Cu_{80}Fe_{14}$ alloy composed of $Co_{30}Fe_{70}$ magnetic clusters dispersed in a (Cu) matrix. Two milling processes were tested. The first process consists of milling a mixture of pure Cu, Fe and Co powders. The second process consists of milling a mixture of Cu and $Co_{30}Fe_{70}$ powders. The microstructure and the magnetoresistive properties of a granular $Co_6Cu_{80}Fe_{14}$ alloy depend on the milling process. Milling Cu, Fe and Co powders leads to an inhomogeneous Co-Cu-Fe solid solution after 20 h. The optimum magnetoresistive amplitude (16%) was obtained after annealing at 415°C for 1 h. In powders obtained by milling Cu and $Co_{30}Fe_{70}$, no magnetoresistive optimum is observed with the milling time, the magnetoresistive amplitude gradually increases up to 10% after 47 h of milling. Milling Cu and $Co_{30}Fe_{70}$ does not give rise to a better magnetoresistivity value. Heat treatments are thus needed to optimize the magnetoresistive properties, but milling Cu, Fe and Co powders is preferable to milling Cu and $Co_{30}Fe_{70}$.

A new cobalt based ternary alloy with high magnetic properties and near-zero magnetostriction was produced by electrodeposition [1992Cha]. This alloy is a promising alternative to the electroplated permalloy - the material most commonly used in the production of thin-film recording heads. A detailed ternary phase diagram was reported for the low-coercivity, low-magnetostriction composition range of approximately 4 to 15 mass% Cu and 9 to 13 mass% Fe. X-ray diffraction reveals the coexistence of both γ and α phases which yield the optimum soft magnetic properties. The relative stability of the mixed phases was demonstrated by detecting only minimal changes in the magnetic properties of film samples annealed at 230°C for 2 h.

The strength and conductivity of drawn $Co_{1.2}Cu_{89.8}Fe_9$ microcomposite wires and their thermomechanical treatments were investigated by [2000Son, 2001Hon]. During cold working, the primary and secondary dendrite arms were aligned along the drawing direction and elongated into filaments. The strengthening in the microcomposites results from the presence of the aligned Co-Fe filaments and correlates with the fineness of the microstructural scale. The observed strength was 855 MPa. The increase in the conductivity in $Co_{1.2}Cu_{89.8}Fe_9$ microcomposite wires after intermediate heat treatments at 450°C was attributed to the precipitation of Fe and Co atoms which were dissolved during heavy deformation processing in the (Cu) matrix. The tensile strength / electrical combination of 855 MPa/53.3% IACS was achieved in the $Co_{1.2}Cu_{89.8}Fe_9$ microcomposite at a cold drawing strain of $\eta = 6.2$.

[2001Vil] investigated two ternary $Co_{24.1}Cu_{49.5}Fe_{25.2}$ and $Co_{22.6}Cu_{61.7}Fe_{14.7}$ alloys (the rest of the composition can be attributed to oxygen) as novel metallic binders with reduced cobalt contents for use in the fabrication of diamond cutting tools. As a metallic binder, the investigated alloys show attractive sintering, hardness, density, water resistance properties and good diamond integrity.

The temperature curves of the thermal emf of binary and ternary alloys of copper with iron and cobalt were measured in the range of 2 to 300 K [1974Bei]. It was shown that the iron and cobalt contributions to the thermal emf are practically independent, which means that for the ternary alloys, it is essentially the superposition of the contributions from the binary alloys. This gives the possibility of determining the compositions of alloys for low temperature thermocouples with a given temperature dependence of the thermal emf.

DOI: 10.1007/978-3-540-74196-1_19

Miscellaneous

The metastable liquid phase separation in supercooled Co-Cu-Fe ternary melts was investigated by [1998Mun, 2000Kim1, 2000Kim2, 2000Kim3, 2004Wan2, 2005Cao, 2006Mun]. Electron beam surface melting of the Co-Cu-Fe alloys was used for a bulk supercooling of at least 150 K, which causes melt separation into two liquids. No evidence of metastable liquid separation was found for alloys with a Cu content of less than 50 mass% Cu.

In [2000Kim1, 2000Kim2, 2000Kim3], the liquid phase separation of Co-Cu-Fe alloys was studied by direct determination upon continuous cooling of electromagnetically levitated samples. It was found that in Cu rich alloys, phase separation generally appeared as dispersed (Fe,Co) rich droplets in a Cu rich matrix, for alloys containing more Cu than the line connecting $Cu_{54}Fe_{46}$ and $Cu_{49}Co_{51}$ (at.%) in the composition triangle. For alloys containing less copper than the line, Cu rich droplets formed in a (Fe,Co) rich matrix. The metastable miscibility gap in the ternary liquid was confirmed by [2004Wan2] by studying alloys cast in a cylindrical cast-iron mold.

The glass fluxing technique was used in [2005Cao] to achieve deep supercooling of bulk liquid ternary Co-Cu-Fe alloys. The liquid phase separation temperature decreases monotonically with increasing Co content. It is clearly shown in Fig. 18, which represents the projection of the miscibility gap surface calculated by [2006Pal]. The boundary lines of the miscibility gap, which were determined in [2005Cao] for the three cross-sections of the system and calculated in [2006Pal], show remarkably flat domes. In addition, it was found by [2005Cao] that the occurrence of phase separation in the undercooled melt shows an obvious influence on the subsequent solid phase transformation of γ to α.

Electromagnetic levitation was used in [2006Mun] to supercool liquid alloys by 180°C. Bulk supercooling of liquids containing 44-80 at.% Cu below a certain temperature resulted in metastable melt separation into two liquids, a Co rich L_1, and a Cu rich L_2. The microstructures of the phase separated specimens consisted of spherulites of one liquid embedded in the other. For alloys containing less than 40 at.% Co + Fe, the spherulites solidified from the L_1; those containing more than 50 at.% Co + Fe, the spherulites solidified from the L_2. The microstructure of the Co-Cu-Fe alloy exhibited a peritectic microstructure, in good agreement with theoretical calculations. Alloys containing 11 at.% Cu and more than 72 at.% Co exhibited γ(Fe,Co) and γ (Cu) phases. For less than 65 at.% Co, two phase mixture of α(Fe,Co) and γ(Cu) coexisted. Between these two regions, a three phase mixture of α(Fe,Co), γ(Fe,Co) and γ (Cu) was observed.

The γ to α martensitic transformation activated by different factors in the (Fe,Co) rich particles precipitated in a (Cu)-matrix was investigated by [1993Lin, 1992Mon, 1993Mon1, 2003Fuj]. The martensitic transformation on subambient cooling has been monitored in defect-free nanocrystalline γ particles that have been coherently precipitated in a (Cu) matrix [1993Lin]. The observed transformation characteristics are entirely consistent with classical homogeneous coherent nucleation, whereas heterogeneous nucleation and homogeneous semicoherent nucleation can be ruled out in this case. An observed variation in transformation temperature was explained by the experimentally determined differences in Co content (and hence, in transformational driving force) among the γ precipitates in relation to the distribution of particle size. The role of thermal activation in the homogeneous nucleation process was demonstrated by applying a high magnetic field to impose an increment of driving force at low temperatures. The γ to α martensitic transformation in small coherent Co-Fe particles has been induced by applying external stress to single crystals of a Co-Cu-Fe alloy without activating crystal dislocations [1992Mon, 1993Mon1]. The orientation of the stress-induced martensite variants is sensitively dependent on the direction and sense (tension or compression) of the applied stress. The experimental results were explained by postulating that the applied stress helps the lattice shear deformation involved in the γ to α lattice change. The γ to α martensitic transformation in precipitate particles was induced by applying a magnetic field to Co-Cu-Fe alloy single crystals at a range of temperature between 4 and 300 K [2003Fuj]. The volume fractions of martensite were estimated from the values of the saturation magnetization of the bulk specimens. The amount of transformation was strongly dependent on the cooling temperature, and reaches its peak at around 77 K.

The wide spectrum of phenomena accompanying the growth of α precipitate particles on {011} twist boundaries with different misorientation angles has been investigated in bicrystals of a Cu-1.4Fe- 0.6Co (mass%) alloy grown by the Bridgman method using two seed crystals [1988Mon, 1990Mon, 1993Fuj, 1993Mon1, 1993Mon2, 1993Mon3, 1994Mon2, 1994Mon3, 1996Mon1, 1997Mon1, 1997Mon2,

DOI: 10.1007/978-3-540-74196-1_19

1997Mon3, 1997Mon4, 1997Mon5, 1999Mon1, 1999Mon2]. The grain boundary properties of α(Fe,Co) rich precipitates in a (Cu) matrix was studied in [1994Mon1, 1996Mon2].
The magnetic properties of different Co, Cu and Fe multilayers were investigated by [1994Idz, 1996Lan, 2000Kuc]. A material asymmetry in the Co/Cu/Fe junction structure has been prepared for the study of spin-polarized electron injection at 77 K [2000Wan]. The sample performance was demonstrated to be analogous to that of a bipolar transistor.
The structures of $Co_{90}Fe_{10}$/Cu multilayers were investigated by X-ray anomalous scattering techniques by [2006An]. It was found that the Cu/$Co_{90}Fe_{10}$ and $Co_{90}Fe_{10}$/Cu interfaces have different thermal behavior upon annealing. For the as-deposited sample, a $Cu_{66}C_{34}$ intermixing region exists at the Cu/$Co_{90}Fe_{10}$ interface, while the $Co_{90}Fe_{10}$/Cu interface is sharp. There exists only a $Co_{70}Fe_{30}$ sublayer close to the interface in the $Co_{90}Fe_{10}$ layer. After annealing at 285°C for 2 h, more Cu reacts with Co to create a $Cu_{75}Co_{25}$ intermixing region at the Cu/$Co_{90}Fe_{10}$ interface, while no obvious change is observed at the $Co_{90}Fe_{10}$/Cu interface. X-ray diffuse scattering measurements revealed an island growth mechanism of the multilayers [2006Bou]. Correlation between microstructure and electric behavior of rapidly quenched Fe substituted granular Co-Cu alloys was investigated by [2006Ray].

Table 1. Investigations of the Co-Cu-Fe Phase Relations, Structures and Thermodynamics

Reference	Method/Experimental Technique	Temperature/Composition/Phase Range Studied
[1936Jel1] [1936Jel2]	Thermal analysis, optical microscopy, hardness measurements, specific density measurements	Temperature-composition sections at 10, 25, 50, 70, 75 mass% and 3 to 12 mass% Cu; Liquidus and solidus temperatures at 20 mass% Cu

[1936Mad]	Thermal analysis, optical microscopy	Temperature-composition sections:
		at Cu/Co = 1 and 80 to 100 mass% Fe;
		at Fe/Co = 3 and 4 to 8 mass% Cu;
		at Fe/Co = 1 and 0 to 100 mass% Cu;
		at Fe/Co = 0.33 and 5 to 7 mass% Cu;
		at 50 mass% Cu and 0 to 50 mass% Co.
		Melting temperatures, α/γ and γ/ε phase boundaries

[1991Nik]	XRD	Co - 2 mass% Fe - 3.5 mass% Cu, martensitic transformation in a single crystal quenched and thermocycled alloys
[1997Oht]	SEM - electron dispersive X-ray analysis of quenched samples	1100–1300°C, γ/L phase boundaries
[1998Mun]	optical microscopy, SEM - energy dispersive spectroscopy	5 to 40 mass% Co, 15 to 90 mass% Cu, 5 to 60 mass% Fe, melt separation
[2000Kim1, 2000Kim2]	Pyrometry, optical microscopy, SEM - electron dispersive X-ray analysis	40 to 80 mass% Cu, 10 to 50 mass% Co, 10 to 50 mass% Fe, liquidus and solidus temperatures, melt separation temperatures
[2002Bam]	Thermal analysis of levitated specimens by two-color optical pyrometer	38 to 96 mass% Cu, 2 to 37 mass% Co, 2 to 36 mass% Fe, melting temperatures
[2002Wan]	SEM - electron dispersive X-ray analysis of quenched samples	800 to 1000°C, α/(Cu) and γ/(Cu) phase boundaries

(*continued*)

DOI: 10.1007/978-3-540-74196-1_19

Reference	Method/Experimental Technique	Temperature/Composition/Phase Range Studied
[2004Wan2]	Optical microscopy	47 to 70 mass% Cu, 8 to 49.5 mass% Fe, 1 to 22 mass% Co, miscibility gap in liquid phase
[2005Cao]	DTA in combination with glass fluxing technique	10 to 84 at.% at Co/Fe = 0.33, 1 and 3, liquidus temperatures, melt separation temperatures
[2006Mun]	Thermal analysis of levitated specimens by two-color optical pyrometer, XRD, energy dispersive spectroscopy, wavelength dispersive spectroscopy, optical microscopy	5 to 96 at.% Cu, 2 to 80 at.% Co, 2 to 85 at.% Fe, melting temperatures, melt separation temperatures

Table 2. Crystallographic Data of Solid Phases

Phase/ Temperature Range [°C]	Pearson Symbol/ Space Group/ Prototype	Lattice Parameters [pm]	Comments/References
(Cu), $Co_xCu_yFe_{1-x-y}$ < 1084.87	*cF*4 $Fm\bar{3}m$ Cu		$0.953 \le y \le 1$ at $x = 0$ and 1098°C [1986Jan]; $0.909 \le y \le 1$ at $x + y = 1$ and 1105°C [2006Pal];
		$a = 361.46$	at $x = 0$, $y = 1$ and 25°C [V-C2, Mas2]
γ, $Co_xCu_yFe_{1-x-y}$ 1494.85 - 213	*cF*4 $Fm\bar{3}m$ Cu		$0 \le y \le 0.104$ at $x = 0$ [1986Jan]; $0 \le x \le 1$ at $y = 0$ [2002Ohn]; $0 \le y \le 0.181$ at $x + y = 1$ and 1329°C [2006Pal];
(γFe) 1394.85 - 912		$a = 364.68$	at $x = 0$, $y = 0$ and 912°C [V-C2, Mas2];
(αCo) 1495 - 421.8		$a = 356.88$ $a = 354.47$	at $x = 1$, $y = 0$ and 520°C [V-C2]; at $x = 1$, $y = 0$ and 25°C [Mas2]
α, $Co_xCu_yFe_{1-x-y}$ < 1538	*CI*2 $Im\bar{3}m$ W		$0 \le y \le 0.067$ at $x = 0$ and 1490°C, $0 \le y \le 0.016$ at $x = 0$ and 842°C [1986Jan]; $0 \le x \le 0.167$ and 1499°C at $y = 0$ [2002Ohn];
(δFe) 1538 - 1394		$a = 293.15$	at $x = 0$, $y = 0$ and 1394°C [V-C2, Mas2]
(αFe) < 912		$a = 293.22$	at $x = 0$, $y = 0$ and 25°C [V-C2, Mas2]

(*continued*)

DOI: 10.1007/978-3-540-74196-1_19

Phase/ Temperature Range [°C]	Pearson Symbol/ Space Group/ Prototype	Lattice Parameters [pm]	Comments/References
(εCo), $Co_xCu_yFe_{1-x-y}$ < 421.8	*hP*2 $P6_3/mmc$ Mg		$0 \le y \le 0.0013$ at $x + y = 1$ and 412.4°C [2006Pal]; $0.98 \le x \le 1$ at $y = 0$ and 239°C, [2002Ohn]
		$a = 250.71$ $c = 406.86$	at $x = 1$, $y = 0$ and 25°C [Mas2]
α', Co_xFe_{1-x} < 735	*cP*2 $Pm\bar{3}m$ CsCl	$a = 285.27$ to 284.34	$x = 0.45$ - 0.60 [V-C2]

Table 3. Invariant Equilibria

Reaction	*T* [°C]	Type	Phase	Composition (at.%)		
				Co	Cu	Fe
L + α ⇌ γ	1502	p_1 (max)	L	12.91	3.61	83.48
			α	12.03	3.01	84.96
			γ	12.48	3.27	84.25
L + γ ⇌ (Cu)	1096	p_6 (min)	L	1.64	96.77	1.58
			γ	40.26	11.14	48.60
			(Cu)	2.21	95.54	2.25
γ ⇌ α + (Cu)	929	e_1, (max)	γ	36.40	6.50	57.10
			α	1.20	40.30	58.50
			(Cu)	0.90	98.00	1.10
γ ⇌ α + ε (Cu)	213	E_1	γ	94.73	0.02	5.25
			α	75.43	0.02	24.55
			ε	97.64	0.01	2.35
			(Cu)	0	100.00	0

Table 4. Investigations of the C-Fe-Mo Materials Properties

Reference	Method / Experimental Technique	Type of Property
[1974Bei]	emf measurements	Cu based alloys at 2 to 300 K, 0.04 to 1.0 at. % Co and 0.024 to 0.2 at.% Fe
[1989Tsu] [1990Tsu]	Neutron diffraction, magnetization measurements	γ phase precipitates in (Cu) matrix

(*continued*)

DOI: 10.1007/978-3-540-74196-1_19

Reference	Method / Experimental Technique	Type of Property
[1992Cha]	Magnetic properties measurements, magnetostriction measurements, XRD	Co based alloys with 4 to 15 mass% Cu and 9 to 13 mass% Fe, structural and magnetic properties of electrodeposited alloys
[1995Yoo]	XRD, magnetometry	$Co_xCu_{0.5}Fe_{0.5-x}$, at $x = 0$, 0.1, 0.2, 0.4, effect of Co additions on structural and magnetic properties of nanocrystalline powders produced by mechanical alloying
[1996Yoo2]	XRD, magnetometry	$Co_xCu_{0.8}Fe_{0.2-x}$, structural and magnetic properties of nanocrystalline powder alloy produced by mechanical alloying
[1996Yoo1]	Magnetometry and ferromagnetic resonance measurements, XRD	$Co_xCu_{0.5}Fe_{0.5-x}$, at $x = 0$, 0.1, 0.2, 0.4, temperature dependence of magnetization of nanocrystalline powders produced by mechanical alloying
[1997Nag]	Magnetization measurements, four-probe method measurement if magnetoresistivity	$Co_{14}Cu_{80}Fe_6$, giant magnetoresistance and magnetization properties of raw and annealed mechanically alloyed samples
[1999Cri]	XRD, Mössbauer spectrometry, zero-field-cooled and field-cooled magnetization measurements	$Co_{10}Cu_{80}Fe_{10}$, structure and magnetic properties of as-quenched and annealed melt-spun ribbon
[1999Gay]	Extended X-ray absorption fine structure spectroscopy	$Co_{20}Cu_{50}Fe_{30}$, structure of mechanically alloyed nanocrystalline alloys
[1999Pri]	XRD, X-ray absorption spectroscopy	$Co_{50-x}Cu_{50}Fe_x$ at $x = 10$, 20, 30, 40, 50 structure of mechanically alloyed nanocrystalline alloys
[1999Yan]	Extended X-ray absorption fine structure spectroscopy, XRD	$Co_{10}Cu_{50}Fe_{40}$, structure of mechanically alloyed nanocrystalline alloys
[2000Son] [2001Hon]	Tensile tests, electrical resistivity measurements, TEM, image analysis	$Co_{1.2}Cu_{89.8}Fe_9$, mechanical and electrical properties of drawn microcomposite wires
[2001Nas]	XRD, Mössbauer spectrometry, magnetization measurements, SEM energy dispersion X-ray spectrometry	$Co_{10}Cu_{70}Fe_{20}$, structural and magnetic properties of mechanically alloyed samples, prepared in different ways
[2001Vil]	DTA, dilatometry, optical microscopy, density measurements, hardness tests, XRD, SEM, energy dispersion X-ray spectrometry	$Co_{24.1}Cu_{49.5}Fe_{25.2}$ and $Co_{22.6}Cu_{61.7}Fe_{14.7}$ sintered alloys, sintering properties, hardness, density, water resistance, diamond integrity
[2002Gal]	Neutron diffraction, SANS, magnetic measurements, extended X-ray absorption fine structure spectroscopy	$Co_{14}Cu_{80}Fe_6$, structural and magnetic properties of ball milled nanocrystalline powders

(*continued*)

DOI: 10.1007/978-3-540-74196-1_19

Reference	Method / Experimental Technique	Type of Property
[2005Lar]	Magnetic and magnetoresistive measurements, XRD, Mössbauer spectrometry	$Co_6Cu_{80}Fe_{14}$, microstructure and magnetoresistive properties of the granular ball milled alloy
[2006Sin]	XRD, magnetic force microscopy, atomic force microscopy, magnetic susceptibility measurements, electrical resistivity measurements	$Co_5Cu_{90}Fe_5$, microstructural, magnetic and electrical transport properties of melt-spun as-quenched and annealed ribbons

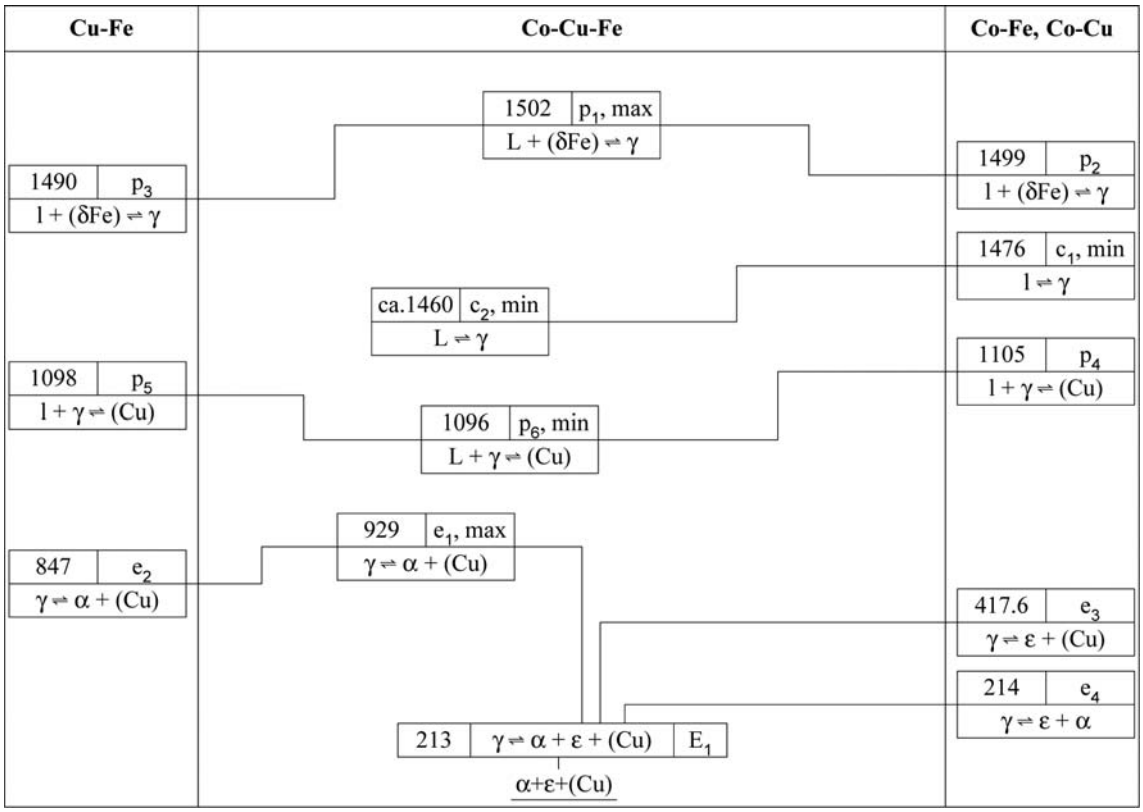

Fig. 1. Co-Cu-Fe. Reaction scheme

DOI: 10.1007/978-3-540-74196-1_19

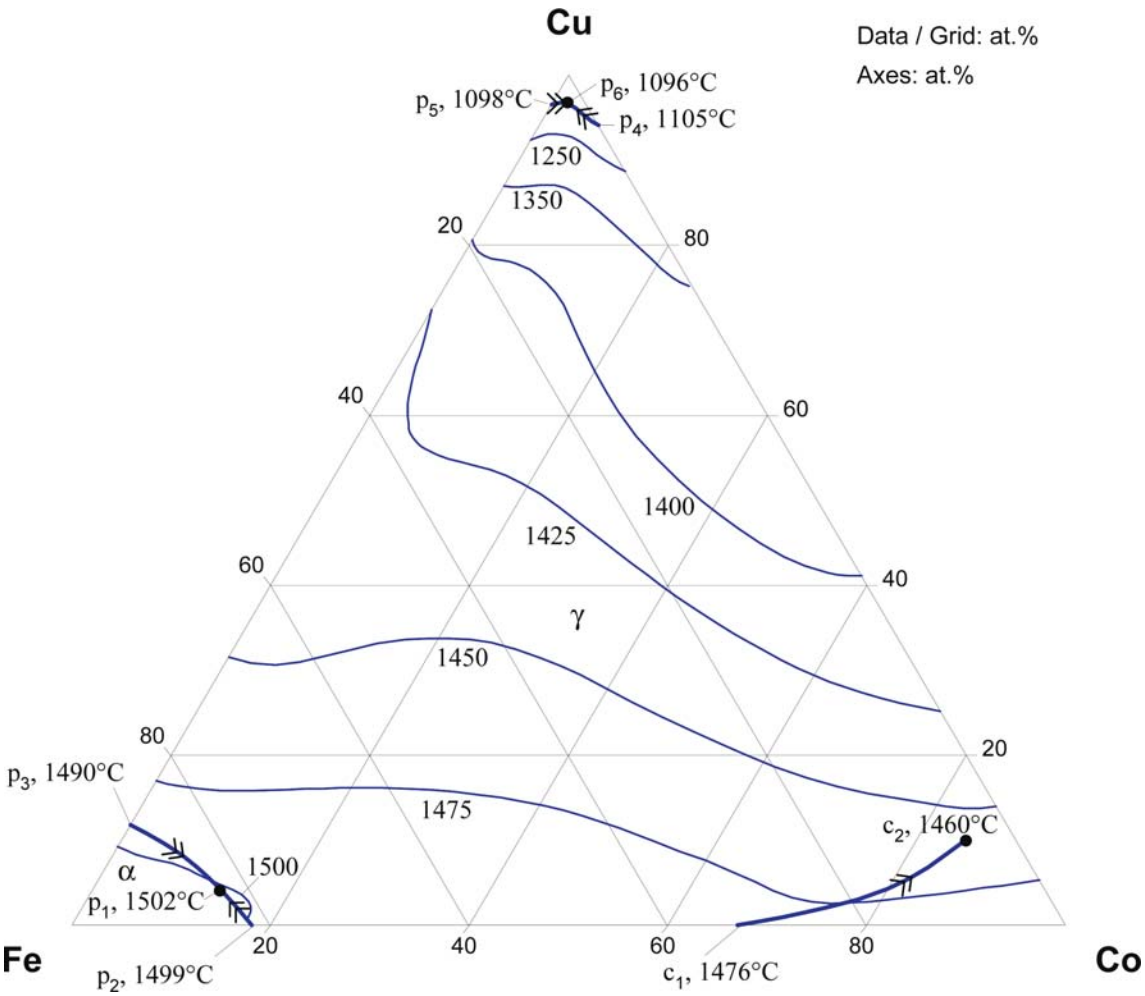

Fig. 2. Co-Cu-Fe. Liquidus surface projection

DOI: 10.1007/978-3-540-74196-1_19

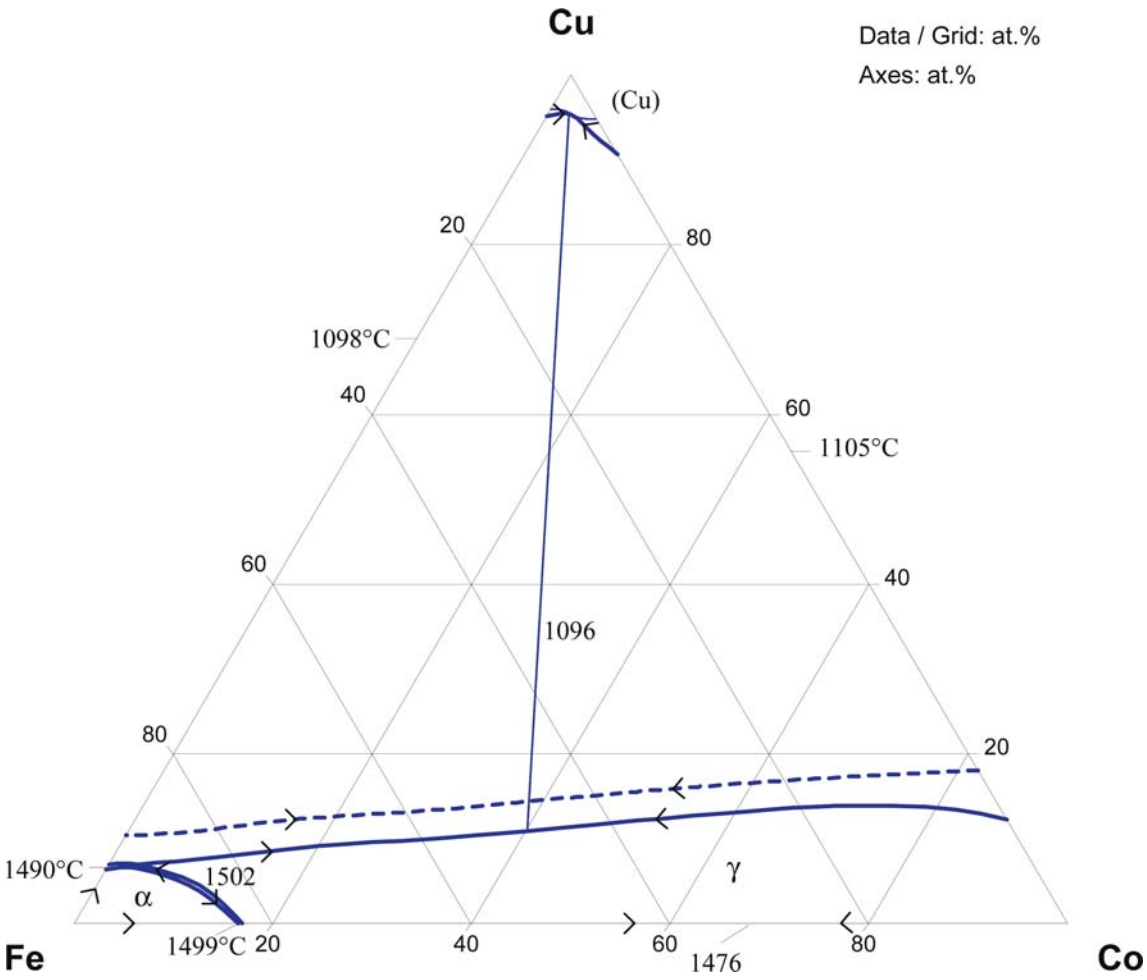

Fig. 3a. Co-Cu-Fe. Solidus surface projection

DOI: 10.1007/978-3-540-74196-1_19

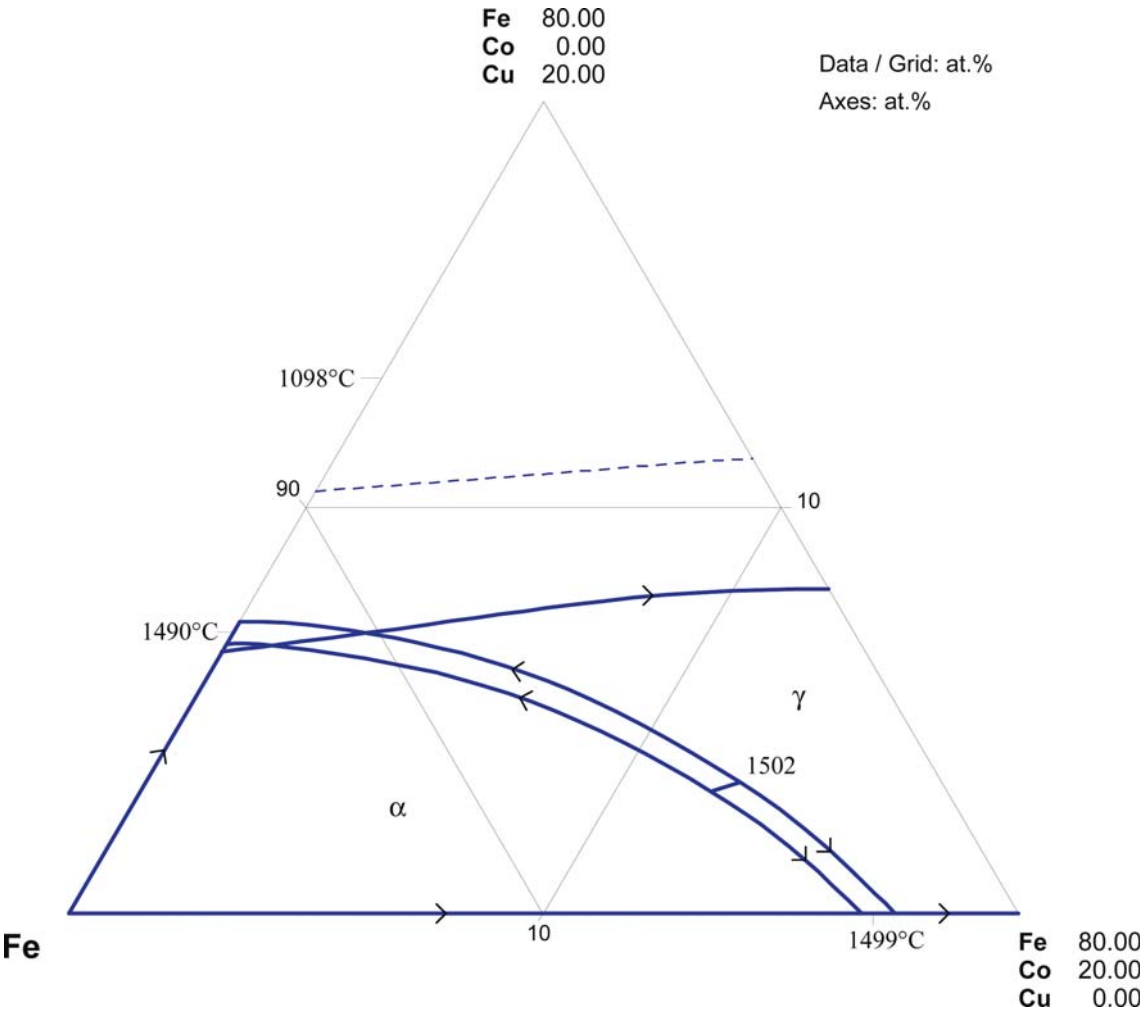

Fig. 3b. Co-Cu-Fe. Enlarged portion of the solidus surface projection in the iron rich corner

DOI: 10.1007/978-3-540-74196-1_19

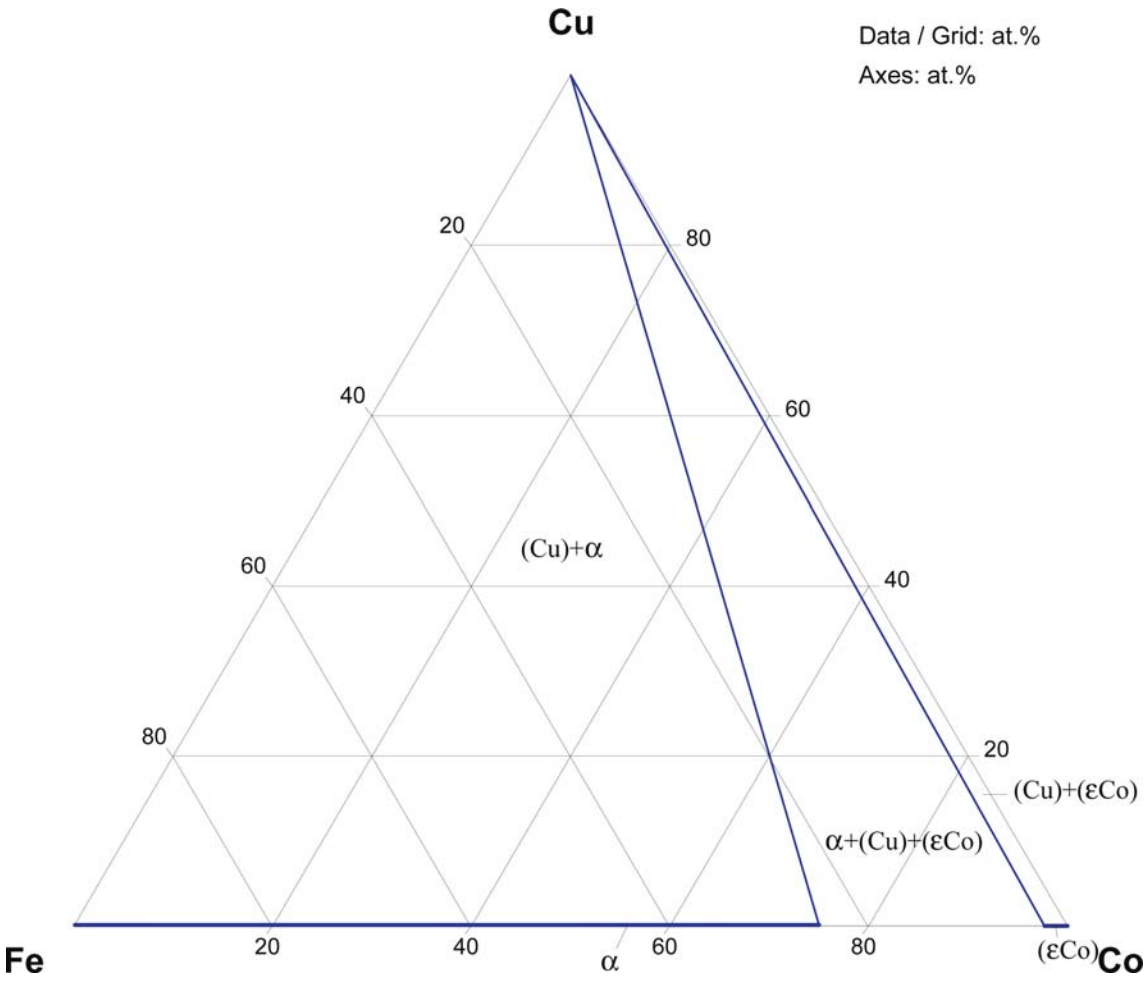

Fig. 4. Co-Cu-Fe. Isothermal section at 200°C

DOI: 10.1007/978-3-540-74196-1_19

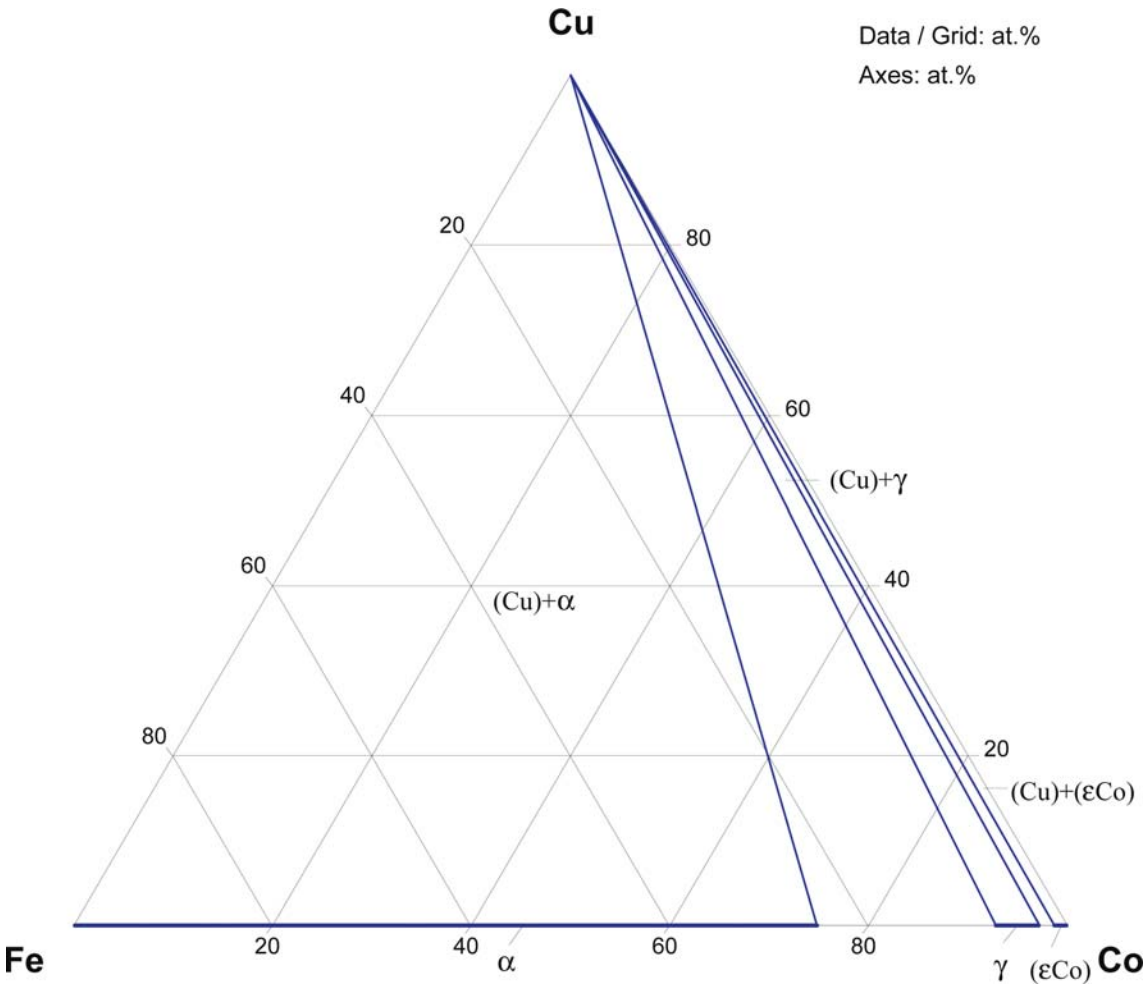

Fig. 5. Co-Cu-Fe. Isothermal section at 300°C

DOI: 10.1007/978-3-540-74196-1_19

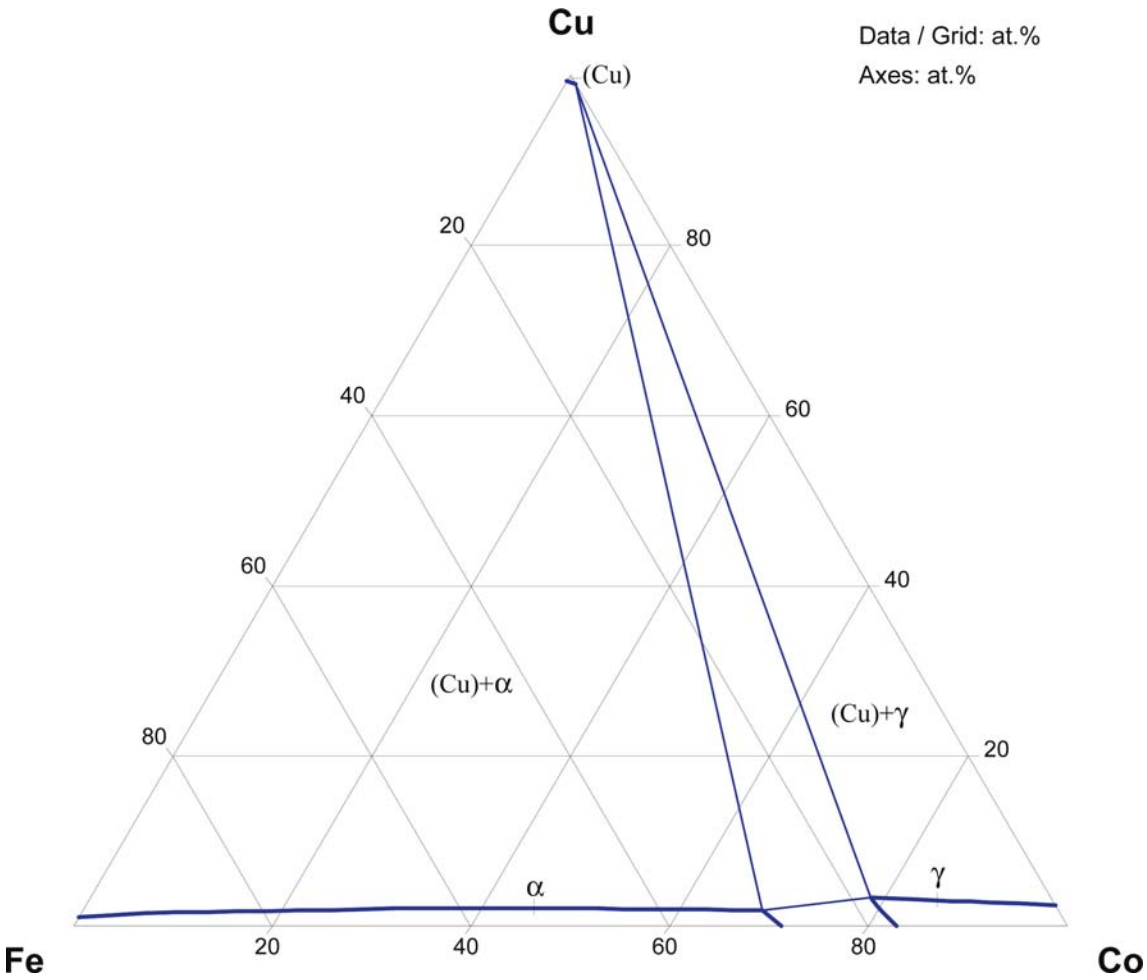

Fig. 6. Co-Cu-Fe. Isothermal section at 800°C

DOI: 10.1007/978-3-540-74196-1_19

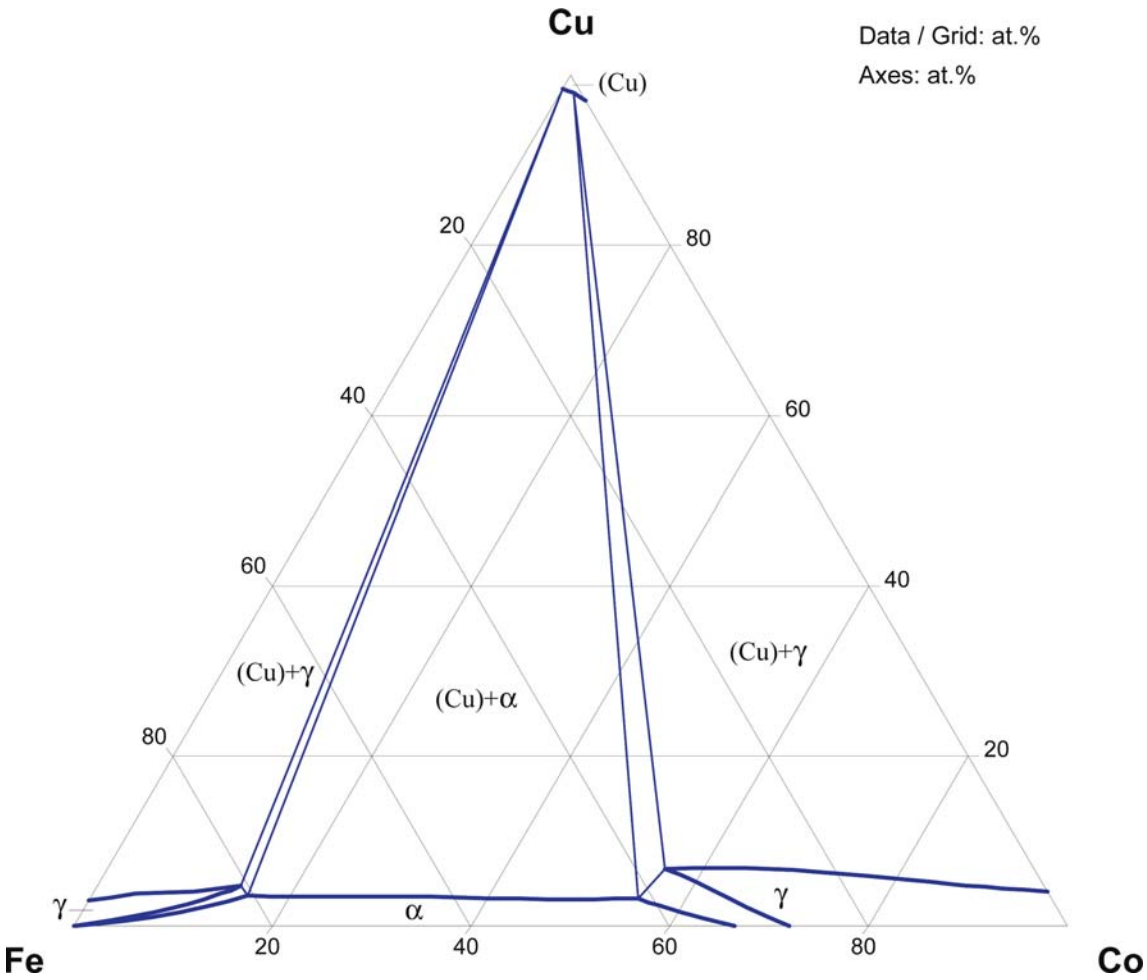

Fig. 7. Co-Cu-Fe. Isothermal section at 900°C

DOI: 10.1007/978-3-540-74196-1_19

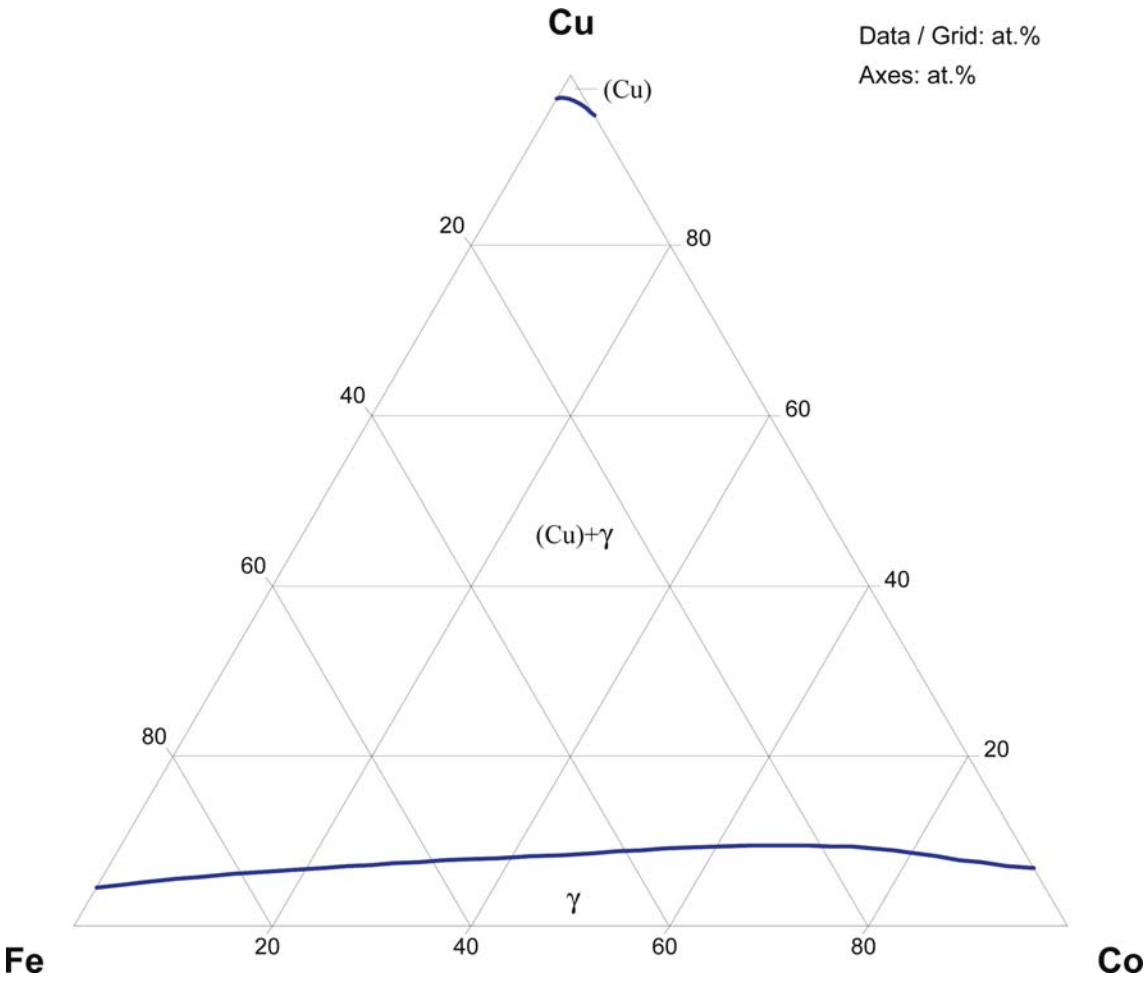

Fig. 8. Co-Cu-Fe. Isothermal section at 1000°C

DOI: 10.1007/978-3-540-74196-1_19

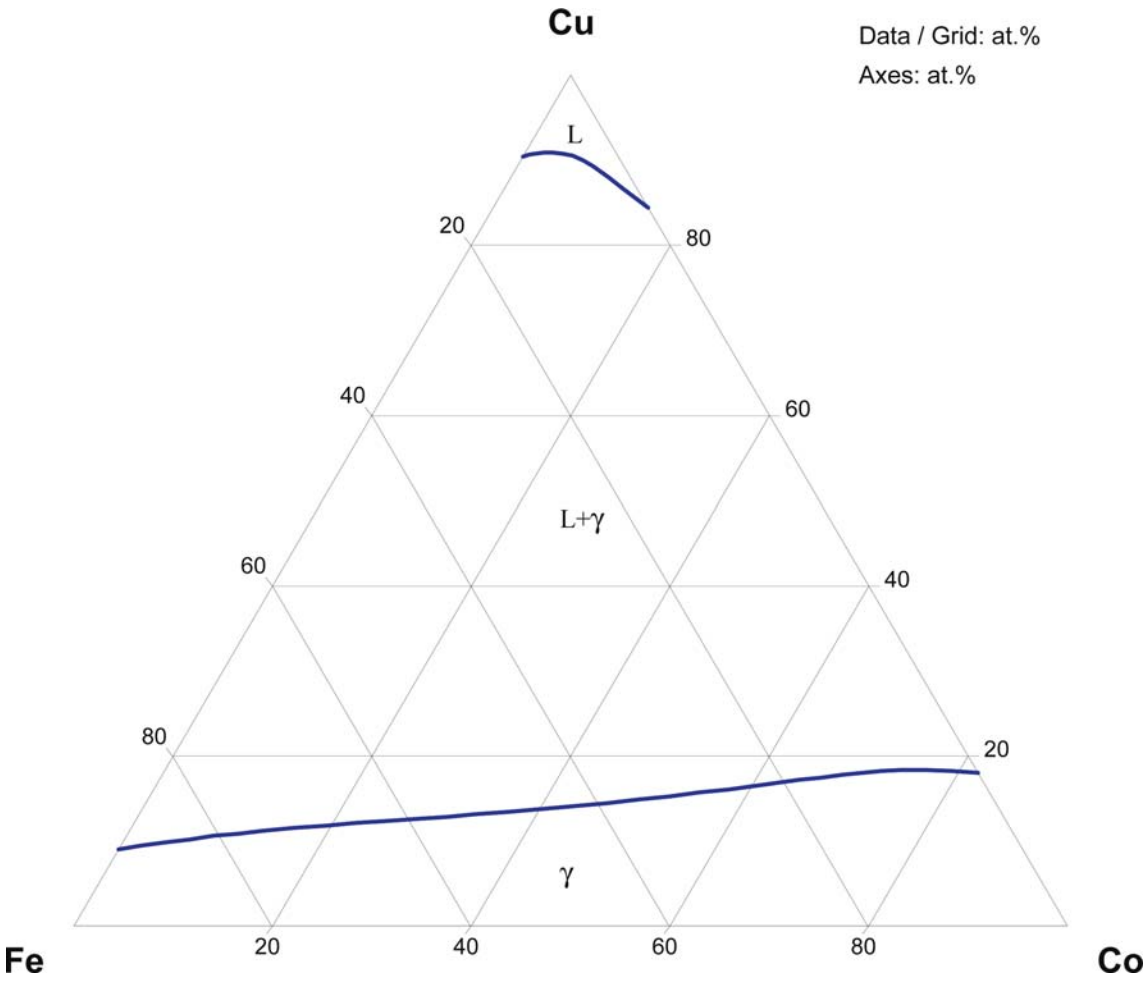

Fig. 9. Co-Cu-Fe. Isothermal section at 1300°C

DOI: 10.1007/978-3-540-74196-1_19

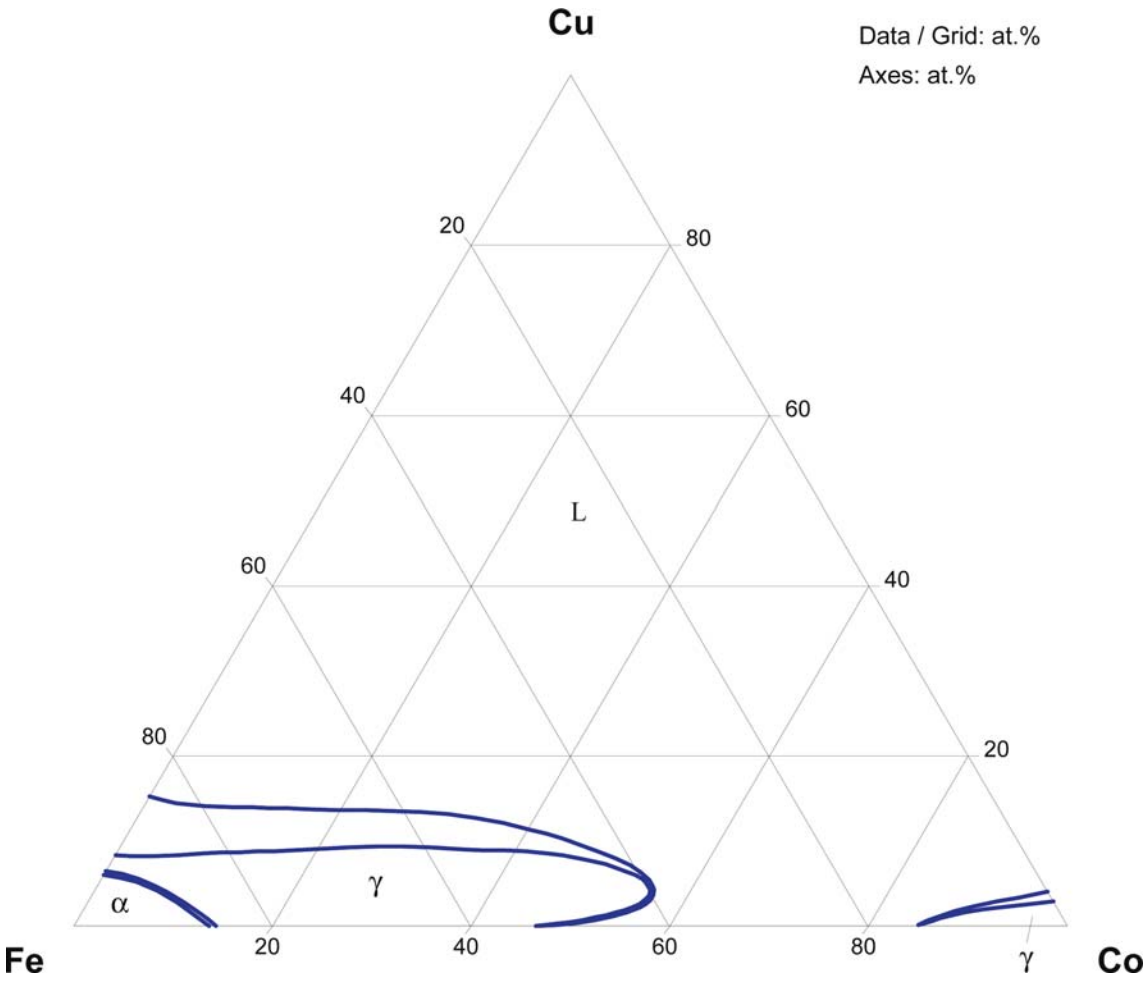

Fig. 10. Co-Cu-Fe. Isothermal section at 1480°C

DOI: 10.1007/978-3-540-74196-1_19

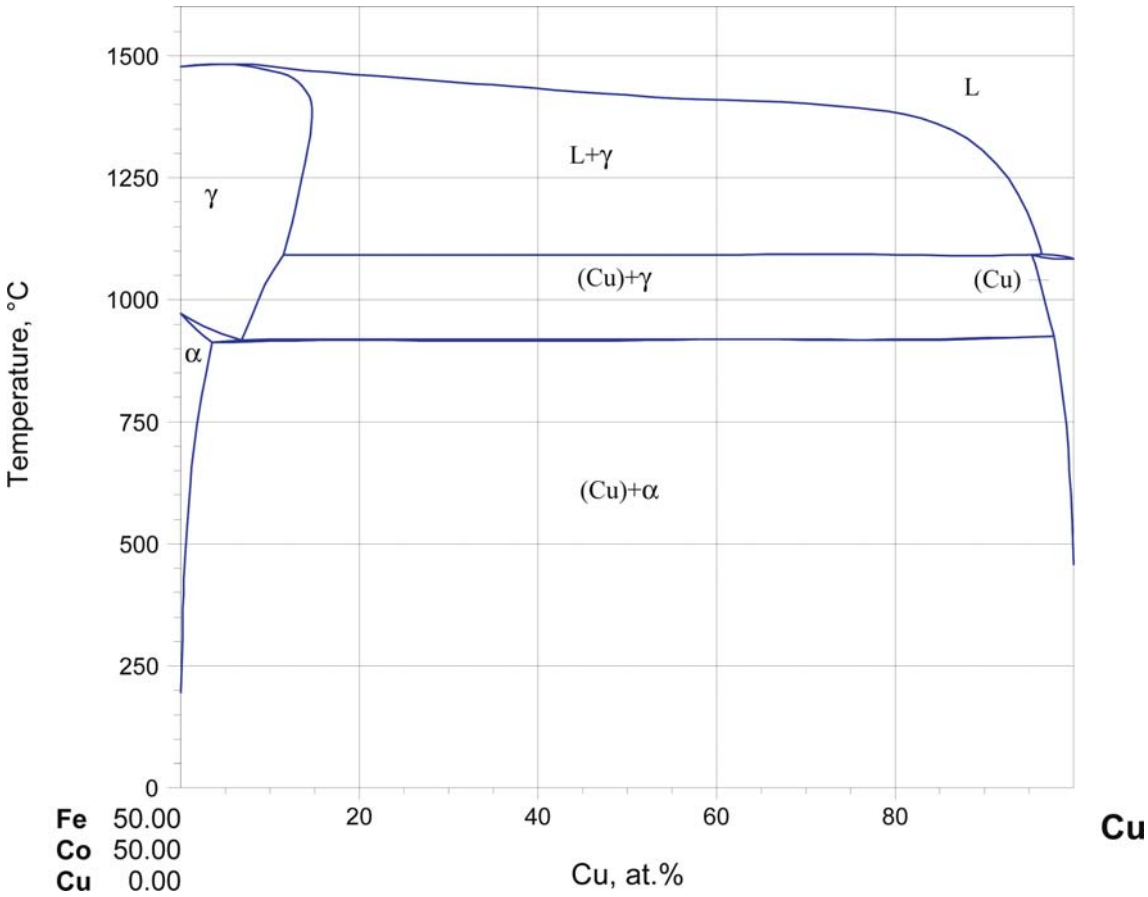

Fig. 11. Co-Cu-Fe. Vertical section at Co : Fe = 1 : 1 (at.%)

DOI: 10.1007/978-3-540-74196-1_19

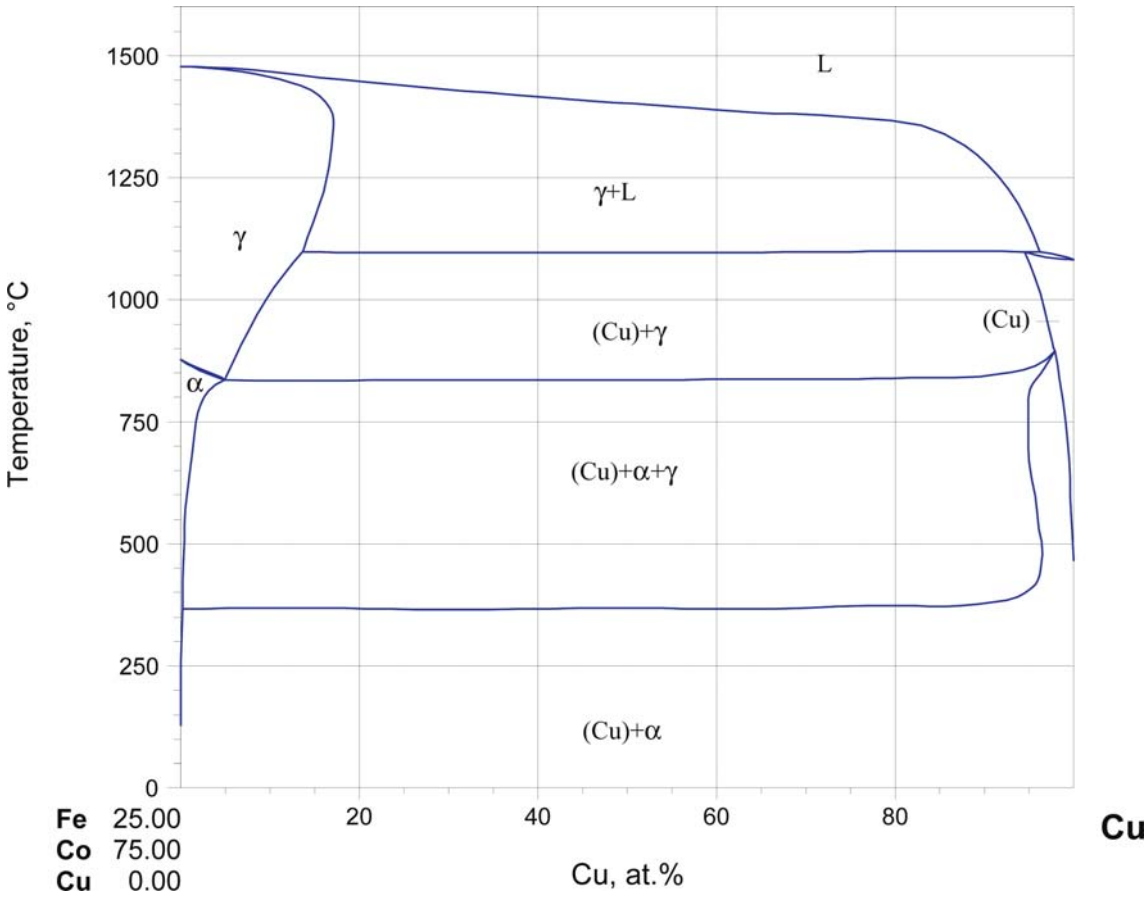

Fig. 12. Co-Cu-Fe. Vertical section at Co : Fe = 3 : 1 (at.%)

DOI: 10.1007/978-3-540-74196-1_19

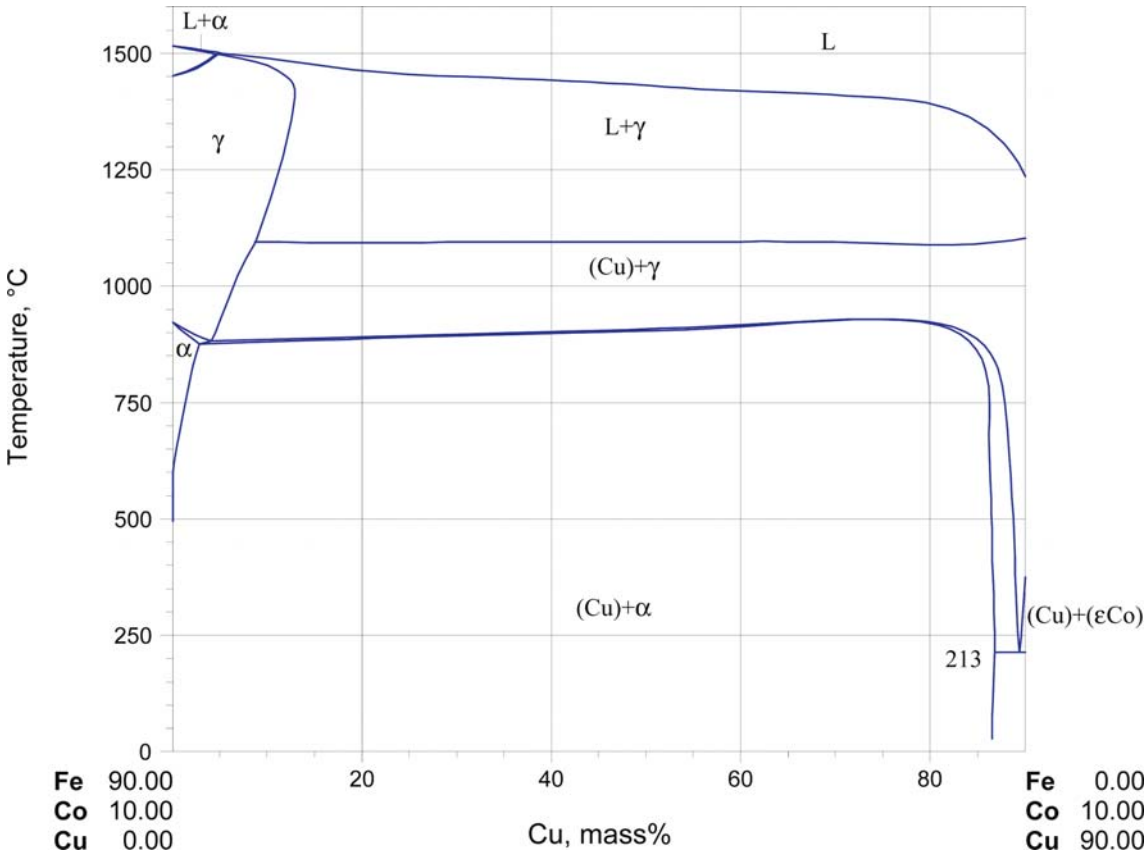

Fig. 13. Co-Cu-Fe. Vertical section at 10 mass% Co

DOI: 10.1007/978-3-540-74196-1_19

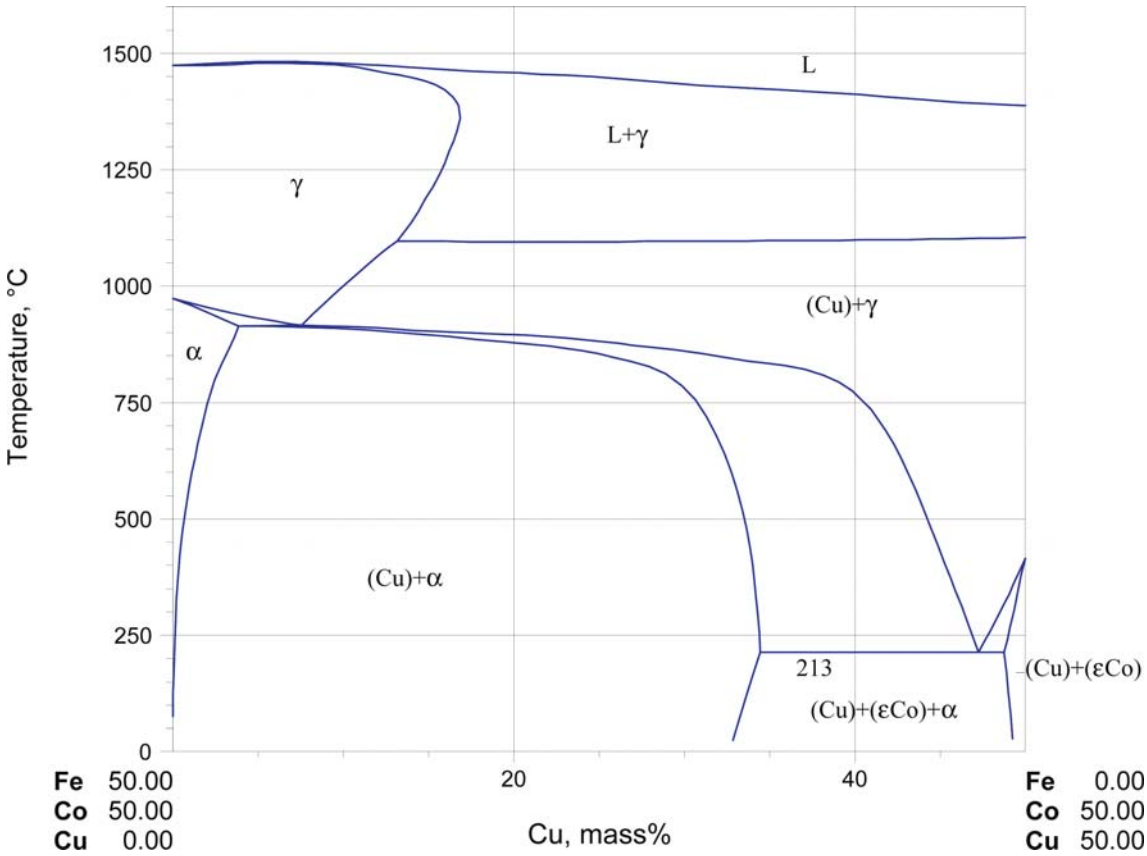

Fig. 14. Co-Cu-Fe. Vertical section at 50 mass% Co

DOI: 10.1007/978-3-540-74196-1_19

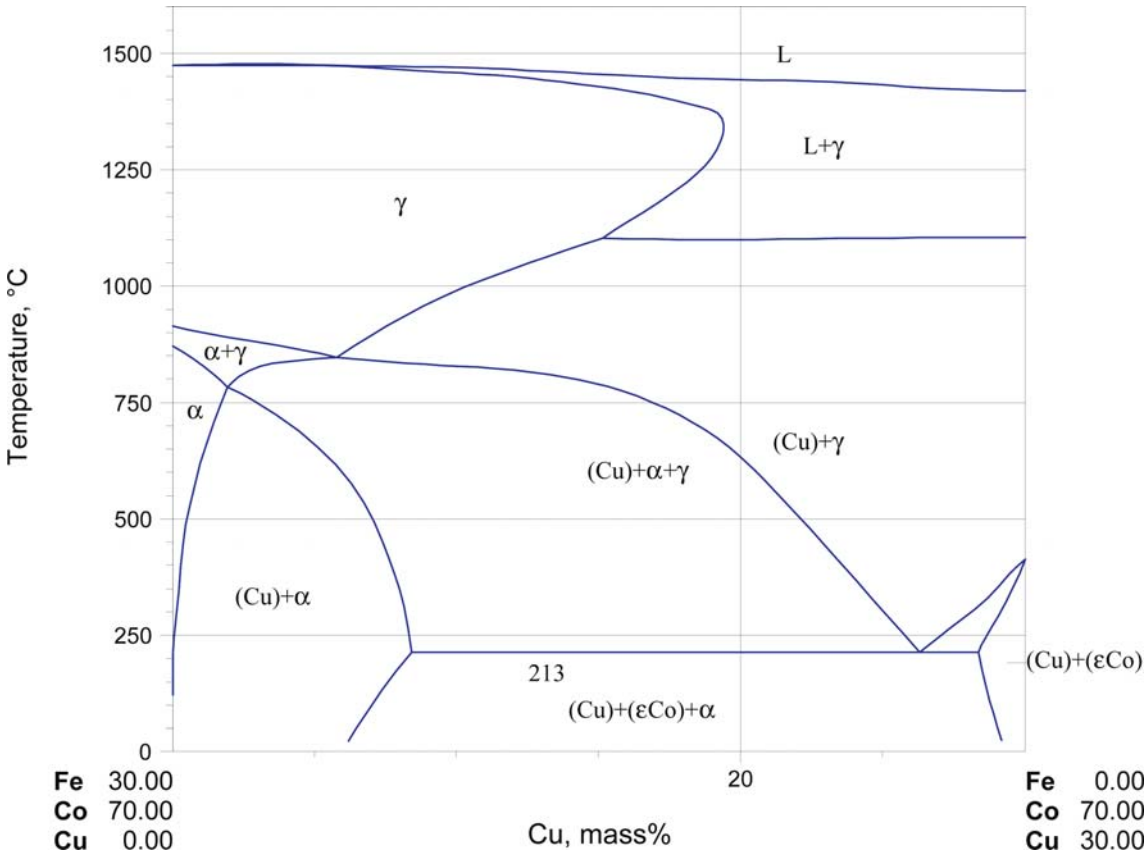

Fig. 15. Co-Cu-Fe. Vertical section at 70 mass% Co

DOI: 10.1007/978-3-540-74196-1_19

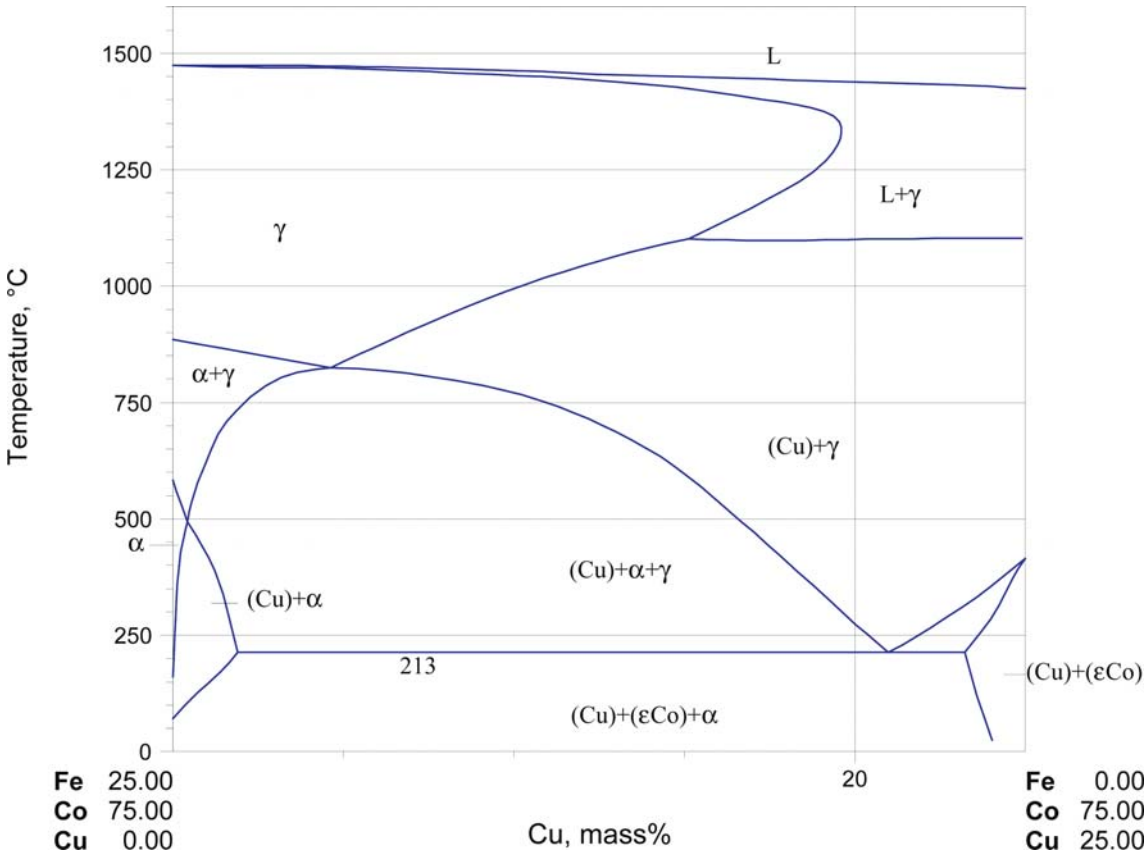

Fig. 16. Co-Cu-Fe. Vertical section at 75 mass% Co

DOI: 10.1007/978-3-540-74196-1_19

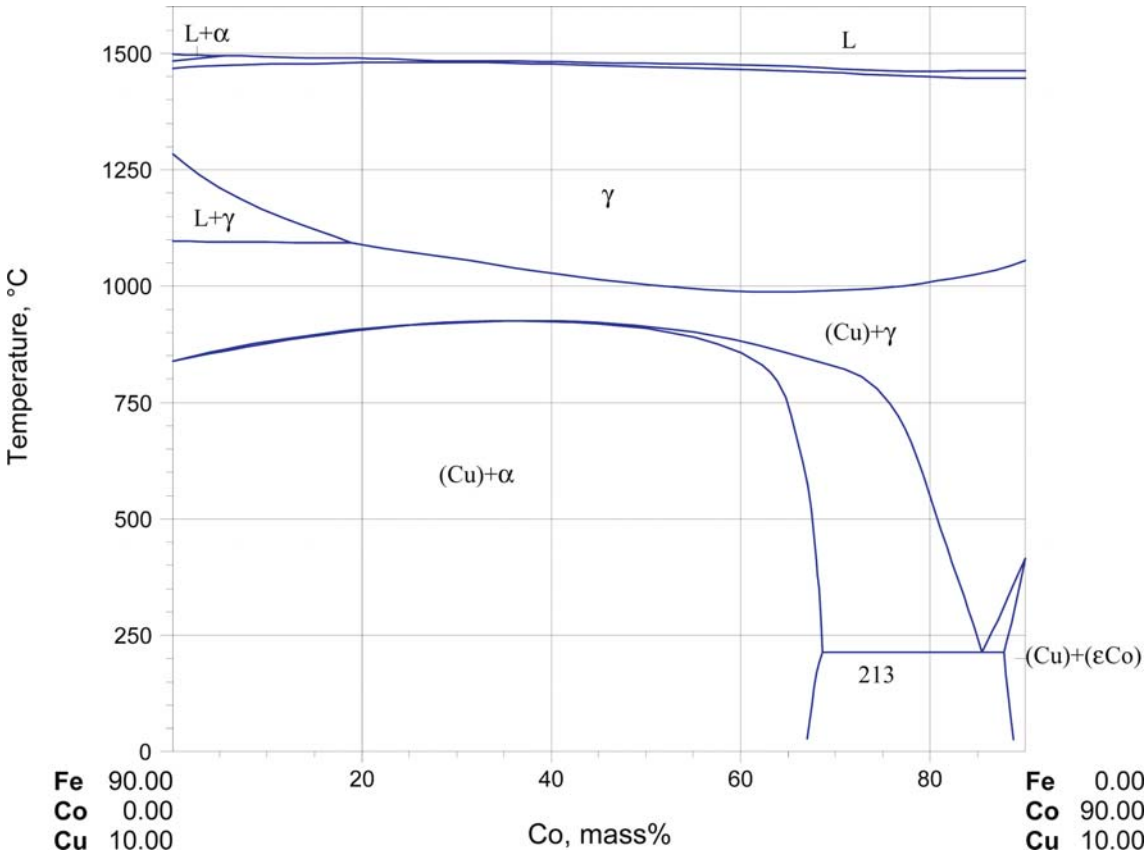

Fig. 17. Co-Cu-Fe. Vertical section at 10 mass% Cu

DOI: 10.1007/978-3-540-74196-1_19

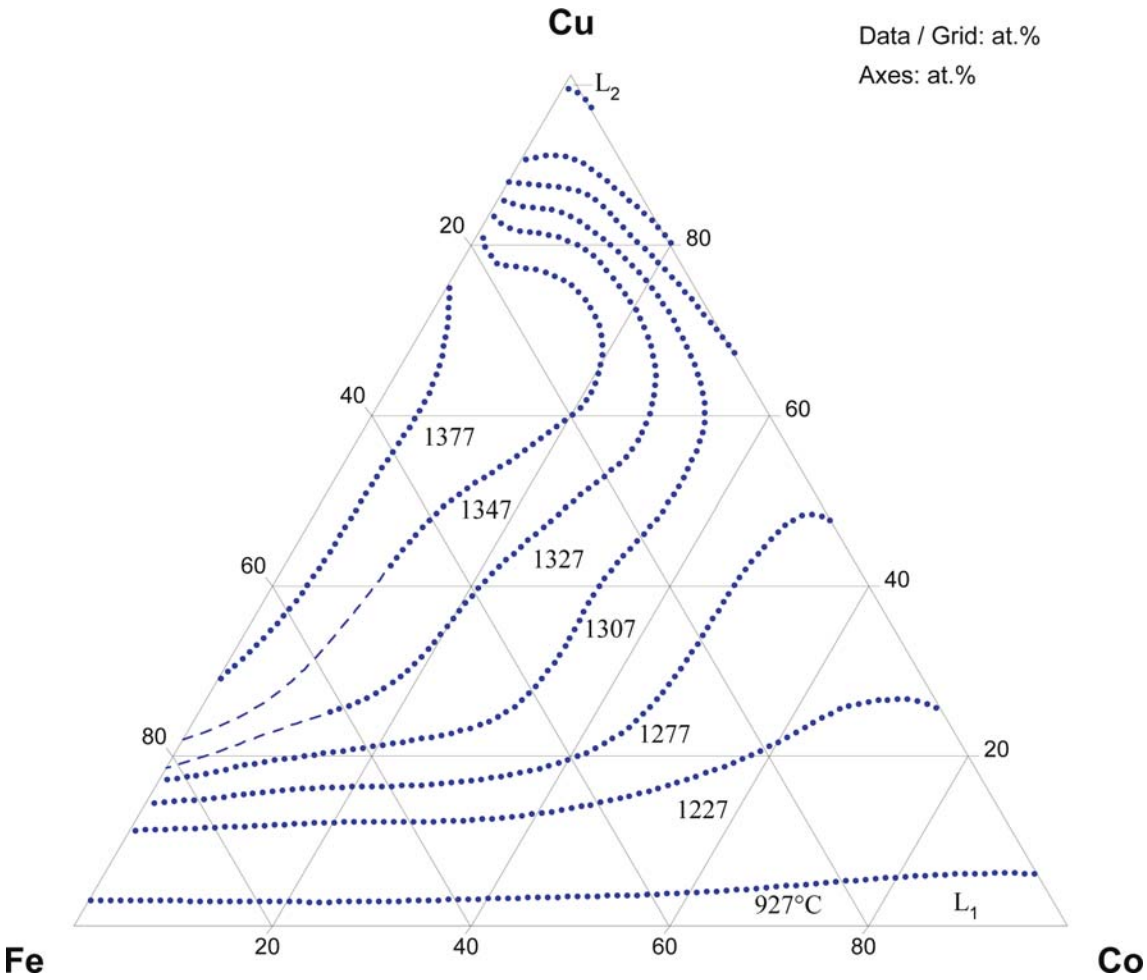

Fig. 18. Co-Cu-Fe. Calculated metastable miscibility gap in the liquid phase at several temperatures

DOI: 10.1007/978-3-540-74196-1_19

References

[1926Mas] Masumoto, *Sci. Rep. Tohoku Univ.*, **15**, 449–477 (1926) as quoted by Jellinghaus, W., "The Iron-Cobalt-Copper System" (in German), *Arch. Eisenhuettenwes.*, **10**, 115–118 (1936)

[1933Rol] Roll, F., "The Influence of Aluminium and Cobalt on the Miscibility Gap of the Iron-Copper System in the Solid State" (in German), *Z. Anorg. Allg. Chem.*, **216**, 133–137 (1933) (Experimental, 16)

[1936Jel1] Jellinghaus, W., "The Iron-Cobalt-Copper System" (in German), *Arch. Eisenhuettenwes.*, **10**, 115–118 (1936) (Experimental, Morphology, Phase Diagram, 16)

[1936Jel2] Jellinghaus, W., "Iron-Cobalt-Copper Alloys", *Metallurgist*, **10**, 180–182 (1936) (Phase Diagram, Phase Relations, 3)

[1936Mad] Maddocks, W.R., Claussen G.E., "Alloys of Iron-Copper-Carbon-Cobalt", *Iron Steel Inst., Special Rep.*, **14**, 97–124 (1936) (Morphology, Phase Diagram, Phase Relations, Experimental, Magn. Prop., 3)

[1949Jae] Jaenecke, E., "Co-Fe-Cu" (in German), *Kurzgefasstes Handbuch aller Legierungen*, Winter, Heidelberg, 606 (1949) (Phase Diagram)

[1956Gue] Guertler, W., *Konstitution der Ternären Metallischen Systeme* (Handbuch), Dahlem, Berlin, (1956)

[1969Gue] Guertler, W., Guertler, M., Anastasiadias, E., "Ternary System Iron-Cobalt-Copper", *A Comp. of Const. Ternary Diagr. Met. Systems, Isr. Pro. Sci. Tr., Jerus*, 151–153 (1969) (Magn. Prop., Phase Diagram, Phase Relations, Review, 2)

[1974Bei] Beilin, V.M., Medvedeva, L.A., Rogelberg, I.L., "Low-Temperature Thermal EMF of Diluted Binary and Ternary Alloy of Cu with Fe and Co", *Phys. Met. Metallogr.*, **37**(4), 112–116 (1974) (Experimental, Electr. Prop., 10)

[1979Cha] Chang, Y.A., Neumann, J.P., Mikula, A., Goldberg, D., "Co-Cu-Fe", *INCRA Monograph Series 6. Phase Diagrams and Thermodynamic Properties of Ternary Copper-Metall Systems*, NSRD, Washington, 418–421 (1979) (Phase Diagram, Phase Relations, Review, 3)

[1979Dri] Drits, M.E., Bochvar, N.R., Guzei, L.S., Lysova, E.V., Padezhnova , Rokhlin, L.L., Turkina, N.I., "Co-Cu-Fe" in "*Binary and Multicomponent Copper-Base Systems*" (in Russian), Nauka, Moscow, 111–112 (1979) (Phase Diagram, Phase Relations, Review, 2)

[1981Oik] Oikawa, K., "Thermodynamic Assessment of the Co-Cu-X (Cr, Mn, Fe, Ni) Systems", Thesis of Master of Engineering, Tohoku University, Japan, (1981) (Thermodyn.) cited from abstract

[1985Bur] Burylev, B.P., Tsemekhan, L.Sh., "Thermodyn. of Melts of the Iron-Cobalt-Copper System" (in Russian), *FIZ.-Khim. Issed. Metall. Protsessov*, (13), 76–80 (1985) (Thermodyn., Calculation, Review, 9) cited from abstract

[1986Jan] Janson, A., *Report D73 Metallografi KTH*, (1986) also in *SSOL Database, Termo-Calc AB*

[1988Mon] Monzen, R., Kitagawa, K., "Grain Boundary Precipitation of BCC Precipitates in Co-Cu-Fe Alloy Bicrystals", *Scr. Metall.*, **22**(2), 173–177 (1988) (Abstract, Experimental, Morphology, Crys. Structure, 12) cited from abstract

[1989Kum] Kumar, Hari, K.C., Raghavan, V., "The bcc-fcc Equilibrium in Ternary Iron Alloys - III", *J. Alloy Phase Diagrams*, **5**(3), 201–220 (1989) (Experimental, Phase Relations, Phase Diagram, 28)

[1989Tsu] Tsunoda, Y., "Magnetic Structure of Non-Coherent γ-FeCo Precipitates in Cu", *Sol. State Commun.*, **72**(9), 863–866 (1989) (Abstract, Experimental, Morphology, Crys. Structure, Magn. Prop., 15) cited from abstract

[1990Jia] Jiang, M., Hao, S., "The Determination and Illustration of a 1000°C Isothermal Phase Diagram of Fe-Ni-Co-Cu System", *Proc.: 6th National Symp. Phase Diagrams, Shenyang,* China, 20.-24.11.90, 150–152 (1990) (Phase Diagram, Phase Relations, Experimental, Abstract, 0) cited from abstract

[1990Mon] Monzen, R., Kitagawa, K., Kato, M., Mori, T., "Grain Boundary Precipitation in Co-Cu-Fe Bicrystals", *J. Jpn. Inst. Met.*, **54**(12), 1308–1313 (1990) (Abstract, Experimental, Morphology, Crys. Structure, 22)

DOI: 10.1007/978-3-540-74196-1_19

[1990Tsu] Tsunoda, Y., "Influence of Particle Size on SDW-γ-FeCo Precipitates in Cu", *Progr. Theor. Phys. Suppl.*, **101**, 133–138 (1990) (Abstract, Experimental, Morphology, Crys., 8)

[1991Nik] Nikolin, B.I., Sizova, T.L., "Influence of Carbon, Copper, and Niobium on the Crystal Structure of Martensite in Co-Fe, Co-Ni Alloys" (in Russian), *Fiz. Met. Metalloved.*, (11), 117–121 (1991) (Abstract, Experimental, Crys. Structure, 9)

[1992Cha] Chang, J.W., Andricacos, P.C., Petek, B., Romankiw, L.T., "Electrodeposition of High M a CoFeCu Alloys for Recording Heads", *The Electrochem. Soc. Inc.*, **9**(10/7), 275–287 (1992) (Abstract, Magn. Prop., 11)

[1992Mon] Monzen, R., Kato, M., "Face-Centred Cubic to Body-Centred Cubic Martensitic Transformation of Co-Fe Particles in a Copper Matrix",*J. Mater. Sci. Lett.*, **11**(1), 56–58 (1992) (Experimental, Phase Relations, 14)

[1992Rag] Raghavan, V., "The Co-Cu-Fe (Cobalt-Copper-Iron) System", *Phase Diagrams of Ternary Iron Alloys*, Indian Institut of Metals, Calcutta, **6A**, 597–599 (1992) (Crystal Structure, Phase Diagram, Phase Relations, Review, 3)

[1993Lin] Lin, M., Olson, GB., Cohen, M., "Homogeneous Martensitic Nucleation in Co-Fe Precipitates Formed in a Cu Matrix", *Acta Metall. Mater.*, **41**(1), 253–263 (1993) (Abstract, Experimental, Morphology, 22)

[1993Mon1] Monzen, R., Kato, M., "Stress-Induced Martensitic Transformation of Small Co-Fe Particles in a Cu Matrix", *ISIJ International*, **33**(8), 898–902 (1993) (Abstract, Experimental, Morphology, 23) cited from abstract

[1993Mon2] Monzen, R., Futakachi, M., Kitagawa, K., Mori, T., "Measurement of Grain Boundary Sliding of {011} Twist Boundaries in Copper by Electron Microscopy", *Act. Metall. Mater.*, **41**(6), 1643–1646 (1993) (Abstract, Experimental, Morphology, 16) cited from abstract

[1993Mon3] Monzen, R., Mori, T., "Detection of Stress Relaxation Owing to Diffusion Around a Second Phase Particle by Electron Microscopy", *Mat. Sci. Eng. A*, **161A**(2), 209–212 (1993) (Abstract, Experimental, Morphology, Mechan. Prop. 11)

[1993Fuj] Fujii, T., Moriyama, M., Kato, M., Mori, T., "Growth of Grain-Boundary Precipitates in Co-Cu-Fe Bicrystals", *Phil. Mag. A-Phys. Cond. Mat. Def. Mech. Prop.*, **68**(1), 137–149 (1993) (Abstract, Experimental, Morphology, 29) cited from abstract

[1994Idz] Idzerda, Y.U., Lin, H.-J., Ho, G., Meigs, G., Chaiken, A., Prinz, G.A., Chen, C.T., "Element Specific Magnetic Hysteresis Curves of Fe/Cu/Co Multilayers", *J. Appl. Phys.*, **75**(10), pt. 2A, 5808 (1994) (Abstract, Experimental, Morphology, Magn. Prop., 1)

[1994Mon1] Monzen, R., Mori, T., "An Internal Stress Induced by Node-Blocked Grain Boundary Sliding and Associated Backward Sliding", *Scr. Metall. Mater.*, **30**(9), 1099–1104 (1994) (Abstract, Experimental, Morphology, Mechan. Prop., 7) cited from abstract

[1994Mon2] Monzen, R., Sumi, Y., "Determination of Activation Energy for Nanometre-Scale Grain-Boundary Sliding in Copper", *Phil. Mag. A-Phys. Cond. Mat. Def. Mech. Prop.*, **70**(5), 805–817 (1994) (Abstract, Experimental, Morphology, 30) cited from abstract

[1994Mon3] Monzen, R., Mori, T., "Measurement of Nanometer Grain Boundary Sliding in Copper by Electron Microscopy", *Fundamental Physical Aspects of the Strength of Crystalline Materials.,* Proc. 10th International Conf. Strength Mater., ICSMA 10, Japan Inst. Metals, Sendai., Japan*,* 903–906 (1994) (Abstract, Experimental, Morphology, 16) cited from abstract

[1995Yoo] Yoo, Y.G., Kim, W.T., Yu, S.C., Kim, Y.D., "Magnetic Properties of Nanocrystalline Co-Cu-Fe Alloys Processed by Mechanical Alloying", *IEEE Trans. Magn.*, **31**(6), 3769–3771 (1995) (Abstract, Experimental, Morphology, Magn. Prop., 6) cited from abstract

[1996Lan] Langer, J., Mattheis, R., Schmidt, S., Senz, St., Zimmermann, T., "Unexpected Growth of GMR Multilayers: {111} in-plane Texture and Grain Bundling in 5 nm Fe/(Co/Cu)24", *J. Magn. Magn. Mater.*, **156**(1–3), 19–20 (1996) (Abstract, Experimental, Morphology, Phys. Prop., 7) cited from abstract

[1996Mon1] Monzen, R., Suzuki, T., "Nanometre-scale Grain-boundary Sliding in Copper Bicrystals with {001} Twist Boundaries", *Philos. Mag. Lett.*, **74**(1), 9–15 (1996) (Abstract, Experimental, Morphology, 14) cited from abstract

DOI: 10.1007/978-3-540-74196-1_19

[1996Mon2] Monzen, R., Hida, M., Kitagawa, K., Kato, M., "Effects of Element Segregation on Nanometer Grain Boundary Sliding in Copper", *Trans. Tech. Publ. Mater. Sci. For., Switzerland*, **207–2091**, 165–168 (1996) (Abstract, Experimental, Morphology, 15) cited from abstract

[1996Yoo1] Yoo, Y.G., Kim, W.T., Yu, S.C., Kim, Y.D., "Temperature Dependence of Magnetization in Nanocrystalline Co-Cu-Fe Alloys", *J. Magn. Magn. Mater.*, **158**, 233–234 (1996) (Experimental, Magn. Prop., 6)

[1996Yoo2] Yoo, Y.G., Yu, S.C., Kim, W.T., "Microstructure and Magnetic Properties of $Cu_{0.8}(Fe_{1-x}Co_x)_{0.2}$ Alloy Powders Manufactured by a Mechanical Alloying Process", *J. Appl. Phys.*, **79**(8), 5476–5478 (1996) (Experimental, Phase Relations, 9)

[1997Mon1] Monzen, R., Takada, N., "Nanometer Sliding of (001) Symmetric Tilt Boundaries in Copper With Boundary Precipitates", *Mater. Sci. Eng. A*, **A234–236**, 202–204 (1997) (Experimental, Mechan. Prop., 13)

[1997Mon2] Monzen, R., Hasegawa, T., "Growth of bcc Co-Fe Particles on (011) Twist Boundaries of Cu", *Philos. Mag. Lett.*, **76**(2), 69–75 (1997) (Experimental, Abstract, 15) cited from abstract

[1997Mon3] Monzen, R., Takada, N., "Nanometer-Scale Sliding and Inherent Viscosity of {001} Symmetric Tilt Boundaries in Cu with Boundary Particles", *Mater. Trans. JIM*, **38**(11), 978–982 (1997) (Abstract, Experimental, Morphology, 22) cited from abstract

[1997Mon4] Echigo, T., Monzen, R., "Growth of α-Co-Fe Particles on {001} Symmetric Tilt Boundaries in Cu Bicrystals", *Scri. Mater.*, **37**(10), 1505–1510 (1997) (Abstract, Experimental, Morphology, 17) cited from abstract

[1997Mon5] Monzen, R., Echigo, T., "Growth of Bcc Co-Fe Particles Precipitated at Boundaries in Co-Cu-Fe Bicrystals", JIM, **61**(11), 1206–1210 (1997) (Abstract, Experimental, Morphology, 19) cited from abstract

[1997Nag] Nagamine, L.C.C.M., Chamberod, A., Auric, P., Auffret, S., Chaffron, L., "Giant Magnetoresistance and Magnetic Properties of $(Co_{0.7}Fe_{0.3})Cu_{80}$ Prepared by Mechanical Alloying", *J. Magn. Magn. Mater.*, **174**, 309–315 (1997) (Crys. Structure, Experimental, 14)

[1997Oht] Ohtani, H., Suda, H., Ishida, K., "Solid/Liquid Equilibria in Fe-Cu Based Ternary Systems", *ISIJ Int.*, **37**(3), 207–216 (1997) (Calculation, Experimental, Phase Relations, Review, Thermodyn., 47)

[1998Mun] Munitz, A., Abbaschian, R., "Liquid Separation in Cu-Co and Cu-Co-Fe Alloys Solidified at High Cooling Rates", *J. Mater. Sci.*, **33**(14), 3639–3649 (1998) (Experimental, Morphology, Phase Relations, 23)

[1999Cri] Crisan, O., Le Breton, J.M., Jianu, A., Maignan, A., Nogues, M., Teillet, J., Filoti, G., "Structural and Magnetic Properties of Magnetoresistive Cu-Co-Fe Ribbons", *J. Magn. Magn. Mater.*, **197**, 467–469 (1999) (Experimental, Magn. Prop., 7)

[1999Gay] Gay-Sanz, N., Prieto, C., Munoz-Martin, A., de Andres, A., Vazquez, M., Yu, S.C., "Time Evolution of the Structural Short-Range Order During the Mechanical Milling of Co-Fe-Cu Nanocrystalline Alloys", *J. Mater. Res.*, **14**(10), 3882–3888 (1999) (Abstract, Experimental, Morphology, Crys. Structure, 13) cited from abstract

[1999Mon1] Monzen, R., Echigo, T., "Coarsening of bcc Co-Fe Precipitate Particles on (001) Twist Boundaries of Cu", *Scr. Mater.*, **40**(8), 963–967 (1999) (Experimental, 11) cited from abstract

[1999Mon2] Monzen, R., Echigo, T., "Growth of Bcc Co-Fe Precipitate Particles at Boundaries in Cu Bicrystals", *Trans. Tech. Publ. Mater. Sci. For., Switzerland*, **294–296**, 609–612 (1999) (Abstract, Experimental, Morphology, 14) cited from abstract

[1999Pri] Prieto, C., de Bernabe, A., Gay-Sanz, N., Vazquez, M., Seong-Cho, Y., "Structural Study of the Mechanically Alloyed Co-Fe-Cu Nanocrystalline System", *J. Non-Cryst. Solids*, **246**, 169–176 (1999) (Crys. Structure, Experimental, 17)

[1999Yan] Yang, D.S., Yoo, Y.G., Yu, S.C., "Exafs Study on Nanocrystalline $Fe_{40}Co_{10}Cu_{50}$ Alloy Processed by Mechanical Alloying", *Nanostruct. Mater.*, **12**(5–8), 665–668 (1999) (Crys. Structure, Experimental, 5)

DOI: 10.1007/978-3-540-74196-1_19

[2000Ant] Antoni-Zdziobek, A., Colinet, C., "CVM Calculations of Phase Equilibria in the Fe-Cu-Co System Including Both Chemical and Magnetic Interactions", *Proc. Disc. Meet. Thermodyn. Alloys*, 35 (2000) (Phase Relations, Thermodyn., 0)

[2000Bei] Bein, S., Colinet, C., Durand-Charre, M., "CVM Calculation of the Ternary System Co-Cu-Fe", *J. Alloys Comp.*, **313**, 133–143 (2000) (Phase Relations, Calculation, 18)

[2000Kim1] Kim, D.I., Abbaschian, R., "The Metastable Liquid Miscibility Gap in Cu-Co-Fe Alloys", *J. Phase Equilib.*, **21**(1), 25–31 (2000) (Experimental, Phase Relations, 18)

[2000Kim2] Kim, D.I., Abbaschian, R., "Metastable Liquid Phase Separation and Solidification Structure in Cu-Co-Fe Alloys", *J. Korean Inst. Met. Mater.*, **38**(2), 227–233 (2000) (Abstract, Experimental, Morphology, 18) cited from abstract

[2000Kim3] Kim, D.I., Abbaschian, R., "The Effect of Cooling Rate on Metastable Liquid Phase Separation", *J. Korean Inst. Met. Mater.*, **38**(9), 1153–1159 (2000) (Abstract, Experimental, Morphology, 18) cited from abstract

[2000Kuc] Kuch, W.A., Gilles, J., Kang, S.S., Offi, F., Kirschner J., Imada, S., Suga, S., "Quantitative X-ray Magnetic Circular Dichroism Microspectroscopy of Fe/Co/Cu(001) Using a Photoemission Microscope", *AIP. Journal of Applied Physics*, **87**(9), 5747–5749 (2000) (Abstract, Experimental, Morphology, Phys. Prop., 23) cited from abstract

[2000Son] Song, J.S., Hong, S.I., "Strength and Electrical Conductivity of Cu-9Fe-1.2Co Filamentary Microcomposite Wires", *J. Alloys Compd.*, **311**(2), 265–269 (2000) (Electr. Prop., Experimental, Mechan. Prop., Morphology, Phase Relations, 18)

[2000Wan] Wang, S.-G., Chen, Y.-X., Wang, Z.-H., Chen, Q., Chen, J.-L., Shen, H.-L., Liu, Y.-H., Xie, S.-J., Mei, L.-M., "Spin-polarized Electron Injection in Co/Cu/Fe Sandwich Structure", *Chinese Physics Letters*, **17**(8), 603–605 (2000) (Abstract, Experimental, Morphology, Phys. Prop., 11) cited from abstract

[2001Ant] Antoni-Zdziobek, A., Colinet, C., "CVM Calculations of Phase Equilibria in the Fe-Cu-Co System Including Both Chemical and Magnetic Interactions", *Scand. J. Metall.*, **30**(4), 265–272 (2001) (Assessment, Phase Diagram, Thermodyn., 33)

[2001Col] Colinet, C., "Applications of the Cluster Variation Method to Empirical Phase Diagram Calculations", *Calphad*, **25**(4), 607–623 (2001) (Assessment, Phase Relations, Review, 96)

[2001Nas] Nascimento, V.P., Passamani, E.C., Takeuchi, A.Y., Larica, C., Nunes, E., "Single Magnetic Domain Precipitates of Fe/Co and Fe and Co in Cu Matrix Produced from (Co-Fe)/Cu Metastable Alloys", *J. Phys.: Condens. Matter*, **13**(4), 665–682 (2001) (Crys. Structure, Experimental, Magn. Prop., Phase Relations, 17)

[2001Vil] del Villar, M., Muro, P., Sanchez, J. M., Iturriza, I., Castro, F., "Consolidation of Diamond Tools Using Cu-Co-Fe Based Alloys as Metallic Binders", *Powder Met.*, **44**(1), 82–90 (2001) (Crys. Structure, Experimental, Mechan. Prop., Phase Relations, 10)

[2001Hon] Hong, S.I., Song, J.S., Kim, H.S., "Thermo-Mechanical Processing and Properties of Cu-9Fe-1.2Co Microcomposite Wires", *Scr. Mater.*, **45**(11), 1295–1300 (2001) (Experimental, Mechan. Prop., 18)

[2002Bam] Bamberger, M., Munitz, A., Kaufman, L., Abbaschian, R., "Evaluation of the Stable and Metastable Cu-Co-Fe Phase Diagrams", *Calphad*, **26**(3), 575–384 (2002) (Calculation, Experimental, Phase Relations, Thermodyn., 21)

[2002Boz] Bozzolo, G.H., Noebe, R.D., Amador, C., "Site Occupancy of Ternary Additions to *B*2 Alloys", *Intermetallics*, **10**, 149–159 (2002) (Crys. Structure, Review, 27)

[2002Gal] Galdeano, S., Mathon, M.H., Chaffron, L., Andre, G., Vincent, E., Traverse, A., de Novion, C.H., "Study of the Nanocrystalline Ball-Milled Cu-80(Fe0.3Co0.7)(20) Compound", *Appl. Phy. A. Mater. Scien. Proces.*, **74**(2), 1046–1048 (2002) (Abstract, Experimental, Morphology, Magn. Prop., 18) cited from abstract

[2002Ohn] Ohnuma, I., Enoki, H., Ikeda, O., Kainuma, R., Ohtani, H., Sundman, B., Ishida, K., "Phase Equilibria in the Co-Fe Binary System", *Acta Mater.*, **50**, 379–393 (2002) (Assessment, Calculation, Experimental, Phase Relations, Thermodyn., 50)

DOI: 10.1007/978-3-540-74196-1_19

[2002Rag] Raghavan, V., "Co-Cu-Fe (Cobalt-Copper-Iron)", *J. Phase Equilib.*, **23**(3), 253–256 (2002) (Phase Relations, Review, 12)

[2002Wan] Wang, C.P., Liu, X.J., Ohnuma, I., Kainuma, R., Ishida, K., "Phase Equilibria in Fe-Cu-X (X: Co, Cr, Si, V) Ternary Systems", *J. Phase Equilib.*, **23**(3), 236–245 (2002) (Calculation, Phase Relations, 38)

[2003Fuj] Fujii, T., Kato, T., Yamada, T., Kato, M., Nimori, S., Ohtsuka, H., "Magnetic Field-Induced Martensitic Transformation of Co-Fe Particles in a Cu Matrix", *Mater. Trans.*, **44**(12), 2545-2549 (2003) (Abstract, Experimental, Morphology, 10) cited from abstract

[2004Rag] Raghavan, V., "Co-Cu-Fe (Cobalt-Copper-Iron)", *J. Phase Equilib. Diffus.*, **25**(6), 543 (2004) (Phase Diagram, Phase Relations, Review, 3)

[2004Wan1] Wang, C.P., Liu, X.J., Ohnuma, I., Kainuma, R., Ishida, K., "Thermodynamic Database of the Phase Diagrams in Cu-Fe Base Ternary Systems", *J. Phase Equilib. Diffus.*, **25**(4), 320–328 (2004) (Calculation, Phase Diagram, Phase Relations, Review, Thermodyn., 40)

[2004Wan2] Wang, C.P., Liu, X.J., Takaku, Y., Ohnuma, I., Kainuma, R., Ishida, K., "Formation of Core-Type Macroscopic Morphologies in Cu-Fe Base Alloys With Liquid Miscibility Gap", *Metall. Mater. Trans. A*, **35a**(4), 1243–1253 (2004) (Calculation, Experimental, Morphology, Phase Relations, Thermodyn., 31)

[2005Cao] Cao, C.D., Gorler, G.R., "Direct Measurement of the Metastable Liquid Miscibility Gap in Co-Fe-Cu Ternary Alloy System", *Chinese Physics Letters*, **22**, 482–484 (2005) (Experimental, Phase Diagram, Phase Relations, 19)

[2005Lar] Larde, R., Breton, J.M., "Influence of the Milling Conditions on the Magnetoresistive Properties of a Cu80(Fe0.7Co0.3)20 Granular Alloy Elaborated by Mechanical Alloying", *J. Magn. Magn. Mater.*, **290–291**(2), 1120–1122 (2005) (Crys. Structure, Electr. Prop., Electronic Structure, Experimental, Magn. Prop., Phase Relations, 2)

[2005Wan] Wang, C.P., Liu, X.J., Jiang, M., Ohnuma, I., Kainuma, R., Ishida, K., "Thermodynamic Database of the Phase Diagrams in Copper Base Alloy Systems", *J. Phys. Chem. Solids*, **66**(2–4), 256–260 (2005) (Calculation, Phase Diagram, Thermodyn., 14)

[2006An] An, Y.K., Dai, B., Mai, Z.H., Cai, J.W., Wu, Z.H. "Structures of Co90Fe10/Cu multilayers determined by X-ray anomalous scattering measurements", *Thin Solid Films*, **496**(2), 571-575 (2006) (Morphology, Experimental, 16)

[2006Bou] Bouziane, K., Al Rawas, A.D., Maaza, M., Mamor, M., "Buffer Effect on GMR in Thin Co/Cu Multilayers", *J. Alloys Compd.*, **414**(1–2), 42–47 (2006) (Crys. Structure, Experimental, Magn. Prop., Phase Relations, Transport Phenomena, 17)

[2006Mun] Munitz, A., Bamberger, A.M., Wannaparhun, S., Abbaschian, R., "Effects of Supercooling and Cooling Rate on the Microstructure of Cu-Co-Fe Alloys (Review)", *J. Mater. Sci.*, **41**(10), 2749–2759 (2006) (Experimental, Morphology, Phase Diagram, Phase Relations, Review, 23)

[2006Pal] Palumbo, M., Curiotto, S., Battezzati, L., "Thermodynamic Analysis of the Stable and Metastable Co-Cu and Co-Cu-Fe Phase Diagrams", *Calphad*, **30**(2), 171–178 (2006) (Calculation, Phase Diagram, Phase Relations, Thermodyn., 49)

[2006Ray] Ray, S.K., Singha, R., Dhar, A., Bhattacharya, D., Chakraborty, M., Srinivas, V., "Correlation Between Microstructure and Electric Behaviour in Rapidly Quenched Fe-Substituted Granular Cu-Co Alloys", *Thin Solid Films*, **505**(1–2), 157–160 (2006) (Abstract, Experimental, Morphology, Phys. Prop., 13) cited from abstract

[2006Sin] Singha, R., Dhar, A., Bhattacharya, D., Chakraborty, M., Srinivas, V., Ray, S.K., "Correlation Between Microstructure and Electronic Behaviour in Rapidly Quenched Fe-substituted Granular Cu-Co Alloys", *Thin Solid Films*, **505**(1–2), 157–160 (2006) (Crys. Structure, Experimental, Magn. Prop., Phase Relations, 13)

[2007Ans] Ansara, I., Ivanchenko, V., Turchanin, M., Agraval P., "Co - Cu (Cobalt - Copper)", MSIT Binary Evaluation Program, in *MSIT Workplace*, Effenberg, G. (Ed.), MSI, Materials Science International Services, GmbH, Stuttgart; to be published, (2007) (Crys. Structure, Phase Diagram, Assessment, 19)

DOI: 10.1007/978-3-540-74196-1_19

[2007Tur] Turchanin, M., Agraval, P., "Cu-Fe (Copper-Iron)", MSIT Binary Evaluation Program, in *MSIT Workplace*, Effenberg, G. (Ed.), MSI, Materials Science International Services GmbH, Stuttgart; to be published, (2007) (Phase Diagram, Crys. Structure, Thermodyn., Assessment, 31)

[Mas2] Massalski, T.B. (Ed.), *Binary Alloy Phase Diagrams*, 2nd edition, ASM International, Metals Park, Ohio (1990)

[V-C2] Villars, P. and Calvert, L.D., *Pearson's Handbook of Crystallographic Data for Intermetallic Phases*, 2nd edition, ASM, Metals Park, Ohio (1991)

DOI: 10.1007/978-3-540-74196-1_19

Cobalt – Iron – Manganese

Viktor Kuznetsov

Introduction

The system combines three magnetic components, and the main interest of investigators is focussed on magnetic properties of the alloys.

Phase relations are studied moderately well. The liquidus surface which extends in composition ranges from Co-Fe side up to 50 mass% Mn is presented by [1933Koe]. Unfortunately, that is presented as the small-scale graph and without any details of experiment. [1962Koe] studied three partial isothermal sections at 800, 700 and 600°C using about 50 alloys with Mn content up to 40 mass% and Co content up to 100%. They also studied equilibria between γ phase, disordered (αFe) and ordered α′ phases on partial vertical section at 45 mass% Co and 0 to 30 mass% Mn. In addition, both [1933Koe] and [1962Koe] present seemingly the same diagram of "metastable state at 20°C" corresponding to "cooling at usual conditions". These results are presented also in reviews [1983Riv, 1988Ray]; update performed by [1994Rag] added to those only calculated results of [1990Hua].

The influence of Mn addition on the temperature of the order-disorder transformation of α' was studied by [1962Koe] and [1976Hag]. [1976Hag] performed DTA to study the influence of Mn addition on the temperature of disordering of alloyed α′ (partly metastable with respect to precipitation of the γ phase) and its dependence on the heating rate. He also treated his measurements of ordering temperatures of alloyed α′ phase in terms of simple GBW (Gorsky-Bragg-Williams) like model; good description was achieved. The degree of atomic order in this phase with Mn addition was studied by neutron diffraction by [1975Mal] on samples annealed at 400°C at the time sufficient to achieve full ordering of pure α′.

The only thermodynamic study of the system was performed by [1989Hay] who used torsion effusion method for measuring Mn vapor pressure in alloys with iron to cobalt ratio 1.05 and Mn content 10.8 to 93.7 at.% at 977 to 1177°C. The alloys of the Fe-Mn and Co-Mn edges with the same Mn content range were also studied.

The system proved to be favorable for CALPHAD calculations. [1989Kum] calculated the equilibria between (αFe) and γ phases at 650 to 950°C; no detailed comparison with experiment was performed. [1990Hua] found that "summation of the binary expressions, which are expressed as Redlikh-Kister polynomials" (procedure identical to Muggianu extrapolation of description of the three binary systems) can be used to calculate thermodynamic properties of phases and the phase diagram. Both are in nearly perfect agreement with available experiment except the liquidus surface.

Investigations of phase equilibria, structures and thermodynamic properties are reviewed in Table 1.

Binary Systems

All three binary systems are taken from [Mas2].

Solid Phases

As chemical analogues, Co, Fe and Mn do not form ternary phases. The modifications αCo, γFe and γMn with fcc structure form continuous solid solution across the system. The solubilities of the third component in the binary bcc solutions based on (αFe), (δFe) and (δMn) are close to those of the corresponding binaries. Received by [1962Koe] and [1976Hag] data of influence of Mn on the temperature of order-disorder reaction in α′ are contradicting. [1962Koe] found that addition of 3% Mn decreases this temperature by 50°, whereas [1976Hag] found stabilization of ordered state of α′ by Mn additions (maximal value of 775°C was found at the composition ~$Co_{50}Fe_{36}Mn_{14}$, where this phase is metastable with respect to precipitation

DOI: 10.1007/978-3-540-74196-1_20

of the γ phase). On the other hand, the data of both authors for the positions of (αFe) or α′ / ((αFe) or α′ + γ) / γ boundaries are in good mutual agreement. The reasons of discrepancy are unclear. The results of [1976Hag] are corroborated by the observation of [1975Mal] that a long-range order parameter of α′ phase, annealed at 400°C, is essentially independent on Mn content until γ phase appears. So they are accepted here, though further investigations are desirable.
On cooling at usual rate γ phase undergoes martensitic transformation to bcc (αFe)[1] at the Mn content up to 12 to 14 mass%, Co up to ~18 mass% or ε phase at greater Mn content [1999Mar, 2002Mar]. The latter is metastable and is considered as extension of a hexagonal phase based on the hcp modification of Co and a high-pressure form of iron [1980Ben]. Critical cooling rate for γ → (αFe) transformation is found to be between 5 and 0.1 $K \cdot s^{-1}$ [1999Mar].
Crystallographic data of solid phases are presented in Table 2.

Liquidus, Solidus and Solvus Surfaces

The liquidus projection presented by [1933Koe] is in strong disagreement with the accepted versions of both Co-Fe and Fe-Mn edges (up to 30 K at fixed composition or to 10 at.% at constant temperature) and can not be recommended. This conclusion is identical to that in the assessments [1983Riv, 1988Ray].
Figure 1 presents a calculated liquidus surface obtained by [1990Hua] by extrapolation of CALPHAD assessments of the boundary systems. This calculation proved to be in nearly perfect agreement with the solid state equilibria as well as with experimental thermodynamic data so is tentatively accepted for liquidus-solidus lines as well.
In the Mn rich region (where no experimental data exist) calculation [1990Hua] predicts the existence of the only invariant reaction (U type) L + (δMn) ⇌ (βMn) + γ and of a maximum on the eutectic line L ⇌ (βMn) + γ. Unfortunately, neither a temperature nor exact compositions of the participating phases are provided.
Of course, experimental re-investigation of melting equilibria remains highly desirable.

Isothermal Sections

Figures 2, 3 and 4 present partial isothermal sections correspondingly at 600, 700 and 800°C. The boundaries between the bcc based phases (αFe) and α′ and γ are taken from the assessment [1983Riv, 1988Ray]. Those are based solely on data of [1962Koe].
The lines subdividing phase fields (αFe) and α′ in Figs. 2 and 3 are taken from [1976Hag]. As a transition between those is of a second order, no two-phase region should exist. Position of the tie lines between the fields ((αFe)+γ) and (α′+γ) (which indeed are degenerated three-phase tie triangles ((αFe)+α′+γ)) are drawn rather arbitrarily, which is indicated by question marks.
The results of the calculation by [1990Hua] for the same temperatures are in very good agreement with the experimental data of [1962Koe]. As the calculations did not use ternary experimental data, this agreement mutually corroborates both datasets. So, to build more complete picture of phase equilibria, calculated isothermal sections at 1000 and 1200°C are also presented in Figs. 5 and 6.

Temperature – Composition Sections

Figure 7 presents partial vertical section at 45 mass% Co after [1962Koe]. In addition to phase equilibria (solid lines) the temperatures of martensitic transformations Ac_3 (beginning of transformation of (αFe) to γ at heating) and Ar_3 (beginning of transition of γ → (αFe) at cooling) are shown by dashed lines. The former are very close to the true phase boundary γ / (γ + (αFe)). As the data of [1962Koe] for (αFe) / α′ transformation are not accepted here, they are removed from Fig. 7 and replaced by the results of [1976Hag] given as dotted lines. The partial section at 50 at.% Co, presented by [1976Hag], contains only lines of non-equilibrium transformations (except for the transition α′ → (αFe) at the slowest heating) and therefore is not presented here.

[1] In the original work metastable martensitic extension of (αFe) phase is called α′.

DOI: 10.1007/978-3-540-74196-1_20

Thermodynamics

Figure 8 presents calculated by [1990Hua] values of Mn activity along a section with x(Fe) / x(Co) = 1.05 at 1135 and 1043°C. Experimental points are from [1989Hay].

Notes on Materials Properties and Applications

[1973Mat] studied magnetic properties of the γ phase including a possibility of Invar effect. The influence of various mechanical treatments on magnetic properties of alloys was studied by [1973Yam, 1981Mog, 1993Ste]. A number of physical properties including hardness, resistivity, and elastic moduli were measured by [1962Koe] and [1974Mas]. Magnetic moments of the γ phase were treated theoretically by [1963Che1, 1963Che2] and experimentally by [1973Mat].
[1973Yam] investigated the influence of regimes of ageing and composition of cold-rolled Co-Fe-Mn alloys to search for workable materials with square hysteresis loop. [1992Ste, 1993Ste] studied several aspects of influence of mechanical treatment on structure and magnetic properties of α′ based magnets. [1991Ham] studied shape memory properties.

Miscellaneous

Magnetic structure of the γ phase was studied by [1972Ada, 1973Ada, 1973Mat]. [1972Ada, 1973Mat] delineated the regions of ferro- and antiferromagnetic states.
[1973Ada] using neutronography did not found any atomic ordering in the γ phase.
Contours of lattice parameters of the γ phase for the quenched samples are presented in Fig. 9, taken from [1973Mat]. Figure 10 displays the values of Curie/Neel temperature, taken from the same source.
The temperatures of α′ → (αFe) transition obtained by [1976Hag] (partly metastable with respect to γ phase formation) are presented in Fig. 11.
The martensitic transformation in Co-Fe-Mn system were investigated by [1980Ben, 1997Bar, 1999Mar, 2002Mar, 2004Mar]. [1980Ben] studied martensitic transformation including microstructure and orientation relations. [2002Mar] determined the lattice parameters of the metastable γ and ε phases and discussed the structural changes accompanying the martensitic transformation. [2004Mar] estimated the heat of martensitic transformation γ → ε in several ternary alloys and its change at thermal cycling using DSC and dilatometric data for a fraction of the transformed material.
The reviews [2004Sun, 2005Sou, 2005Sun] mention Mn amongst various additions to magnetic alloys based on α′. A series of works [1997Bar, 1999Mar, 2004Mar] is devoted to thermodynamic assessment of the data on martensitic transformations between (αFe), γ and ε phases.
[1980Sri] reviewed conditions for electrodeposition of various alloys including Co-Fe-Mn from aqueous solutions.
[1995Tan] calculated the equilibria between (αFe) and γ phases just as a test of models used thereafter for calculation of C containing quaternaries.

DOI: 10.1007/978-3-540-74196-1_20

Table 1. Investigations of the Co-Fe-Mn Phase Relations, Structures and Thermodynamics

Reference	Method / Experimental Technique	Temperature / Composition / Phase Range Studied
[1933Koe]	Metallography, XRD, DTA	Melting equilibria and room temperature data 0 to 100% Co, 0 to ~45 mass% Mn
[1962Koe]	Metallography, XRD, DTA	600, 700, 800°C, 0 to 100% Co, 0 to 40 mass% Mn
[1975Mal]	Long-range order parameter of FeCo by neutron diffraction	400°C, $(FeCo)_{1-x}Mn_x$ (x = 0.015 to 0.05)
[1976Hag]	DTA	~700 to 1000°C, 50 at.% Co, Mn to ~15 at.%
[1980Ben]	Metallography, XRD	Approx. section with 20 to 25 mass% Mn, alloys cooled by liquid nitrogen
[1989Hay]	Torsion-effusion technique, Mn vapor pressure	977 to 1177°C, Fe/Co = 1.05, 10.8 to 93.7 at.% Mn
[1989Kum]	CALPHAD assessment	650 to 950°C, all stable solid phases excepting α′
[1990Hua]	CALPHAD extrapolation of description of binary edges	300°C up to melting, all stable phases excepting α′

Table 2. Crystallographic Data of Solid Phases

Phase/ Temperature Range [°C]	Pearson Symbol/ Space Group/ Prototype	Lattice Parameters [pm]	Comments/References
γ, $(Co_{1-x-y}Fe_xMn_y)$	*cF*4 $Fm\bar{3}m$ Cu		
(αCo) 1495 - 422		a = 356.88 a = 354.47	at 520°C [V-C2] [Mas2]
(γFe) 1394 - 912		a = 364.67	pure Fe at 915°C [V-C2, Mas2]
(γMn) 1138 - 1100		a = 386.0	pure Mn [Mas2]
(δFe) 1538 - 1394	*cI*2 $Im\bar{3}m$ W	a = 293.15	dissolves up to 10 at.% Mn, 17 at.% Co [Mas2]
(αFe) < 912	*cI*2 $Im\bar{3}m$ W	a = 286.65	at 25°C [Mas2] dissolves up to 3 at.% Mn, 75 at.% Co [Mas2]
(δMn) 1246 - 1138	*cI*2 $Im\bar{3}m$ W	a = 308.0	[Mas2] dissolves up to 9 at.% of both Fe and Co
(βMn) 1100 - 727	*cP*20 $P4_132$ βMn	a = 631.52	[Mas2] dissolves up to 35 at.% Fe, 49 at.% Co

(*continued*)

DOI: 10.1007/978-3-540-74196-1_20

Phase/ Temperature Range [°C]	Pearson Symbol/ Space Group/ Prototype	Lattice Parameters [pm]	Comments/References
(αMn) < 727	*cI*58 $I\bar{4}m$ αMn	a = 891.26	at 25°C [Mas2] dissolves up to 35 at.% Fe, 49 at.% Co
α′, FeCo < 730	*cP*2 $Pm\bar{3}m$ CsCl	a = 285.04	[Mas2, V-C2] dissolves up to ~5 at.% Mn [1976Hag]
ε, ($Co_{1-x-y}Fe_xMn_y$)	*hP*2 $P6_3/mmc$ Mg		metastable martensitic phase excepting Co rich low-temperature region
(εCo) < 422		a = 250.71 c = 406.86	at 25°C [Mas2]
(εFe)(HP)		a = 246.8 c = 396.0	at 25°C, 13 GPa [Mas2]
			[2002Mar], data for martensitic phase:
		a = 253.26 ± 0.5 c = 408.5 ± 0.5	at x = 0.818, y = 0.153
		a = 253.42 ± 0.5 c = 408.7 ± 0.5	at x = 0.792, y = 0.183
		a = 253.52 ± 0.5 c = 409.2 ± 0.5	at x = 0.773, y = 0.195
		a = 253.69 ± 0.5 c = 409.3 ± 0.5	at x = 0.741, y = 0.231
		a = 254.07 ± 0.5 c = 410.1 ± 0.5	at x = 0.718, y = 0.252
		a = 254.16 ± 0.5 c = 410.1 ± 0.5	at x = 0.683, y = 0.282
		a = 254.26 ± 0.5 c = 409.9 ± 0.5	at x = 0.681, y = 0.290
		a = 253.18 ± 0.5 c = 408.5 ± 0.5	at x = 0.735, y = 0.178
		a = 253.49 ± 0.5 c = 409.2 ± 0.5	at x = 0.706, y = 0.205
		a = 253.65 ± 0.5 c = 409.1 ± 0.5	at x = 0.684, y = 0.228
		a = 254.10 ± 0.5 c = 409.3 ± 0.5	at x = 0.637, y = 0.273
		a = 254.19 ± 0.5 c = 409.7 ± 0.5	at x = 0.637, y = 0.273
		a = 253.11 ± 0.5 c = 408.4 ± 0.5	at x = 0.668, y = 0.177
		a = 253.56 ± 0.5 c = 409.0 ± 0.5	at x = 0.615, y = 0.233
		a = 253.65 ± 0.5 c = 409.1 ± 0.5	at x = 0.597, y = 0.247

DOI: 10.1007/978-3-540-74196-1_20

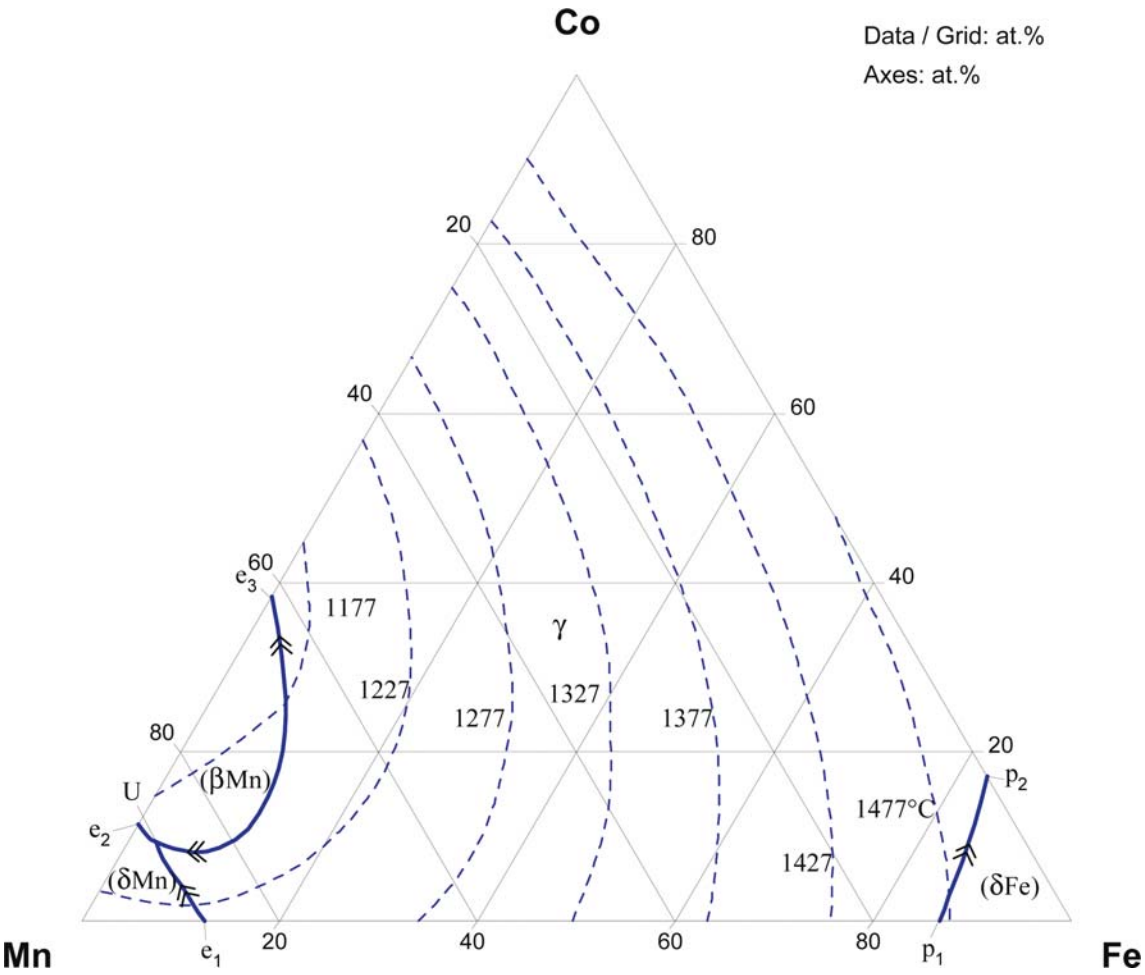

Fig. 1. Co-Fe-Mn. Calculated liquidus surface projection

DOI: 10.1007/978-3-540-74196-1_20

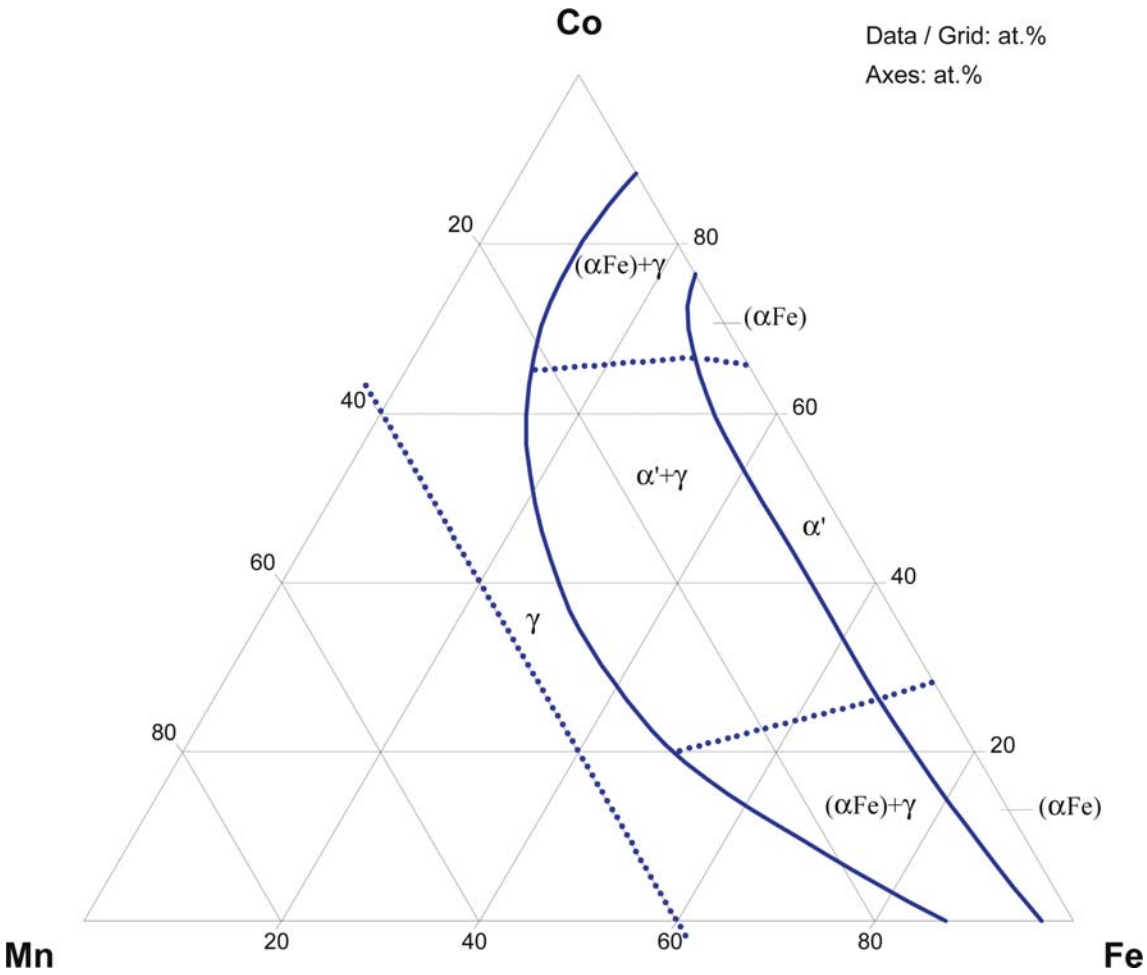

Fig. 2. Co-Fe-Mn. Partial isothermal section at 600°C

DOI: 10.1007/978-3-540-74196-1_20

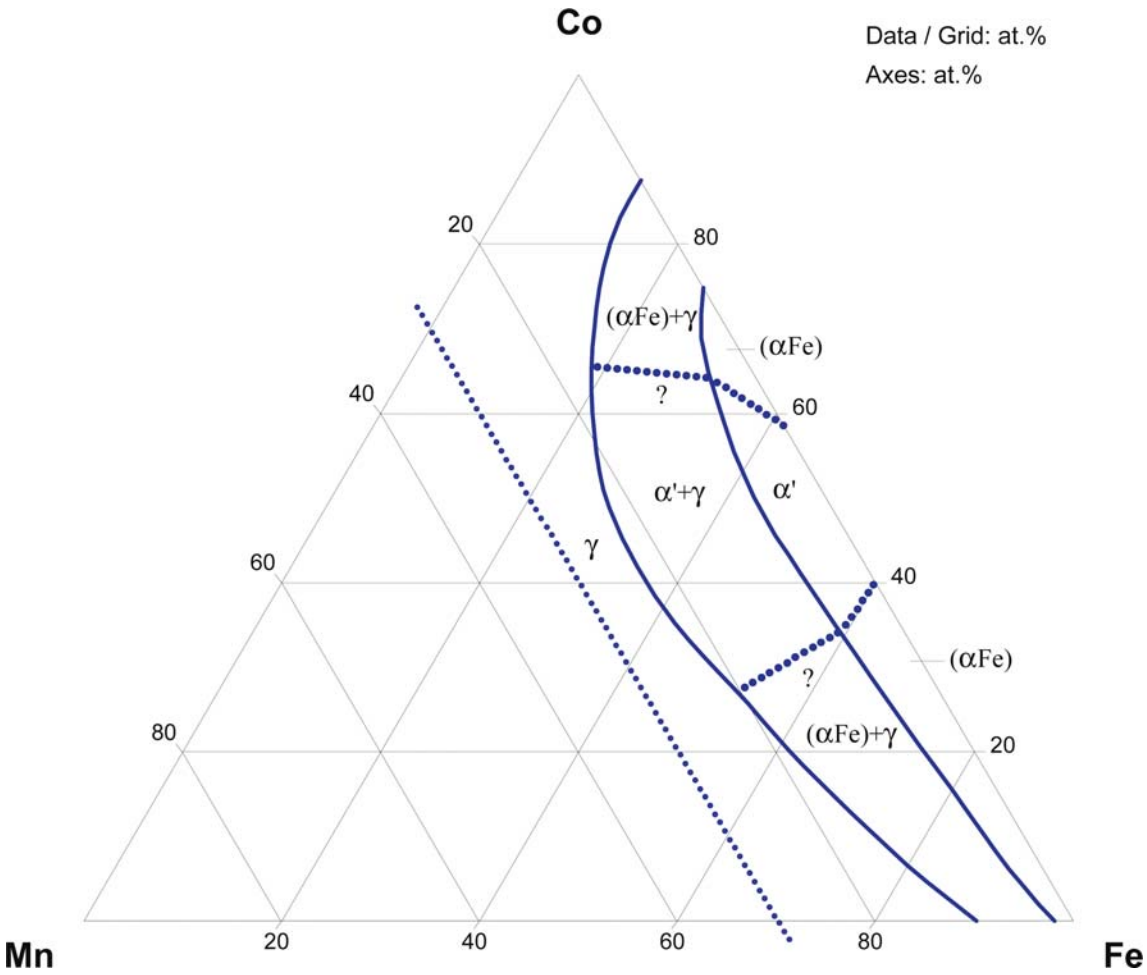

Fig. 3. Co-Fe-Mn. Partial isothermal section at 700°C

DOI: 10.1007/978-3-540-74196-1_20

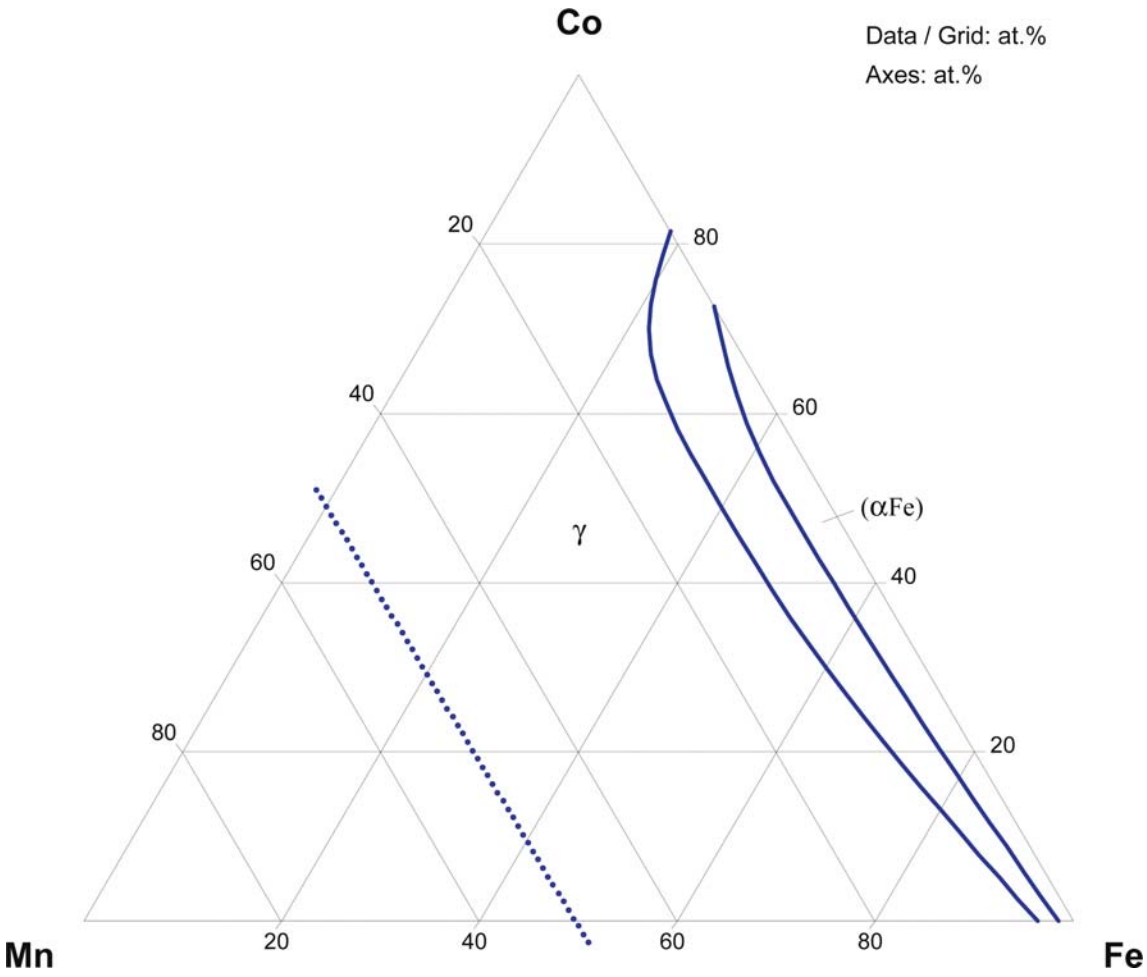

Fig. 4. Co-Fe-Mn. Partial isothermal section at 800°C

DOI: 10.1007/978-3-540-74196-1_20

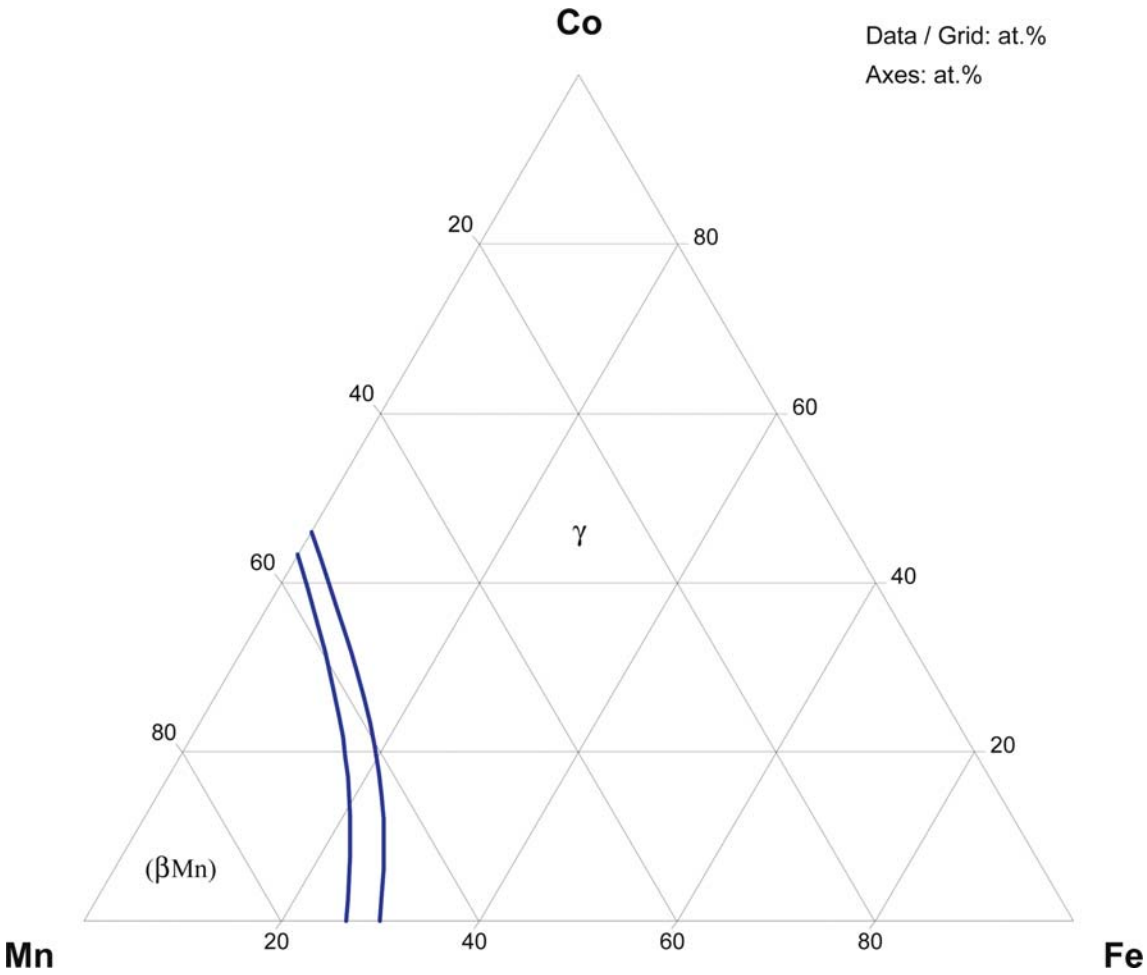

Fig. 5. Co-Fe-Mn. Calculated isothermal section at 1000°C

DOI: 10.1007/978-3-540-74196-1_20

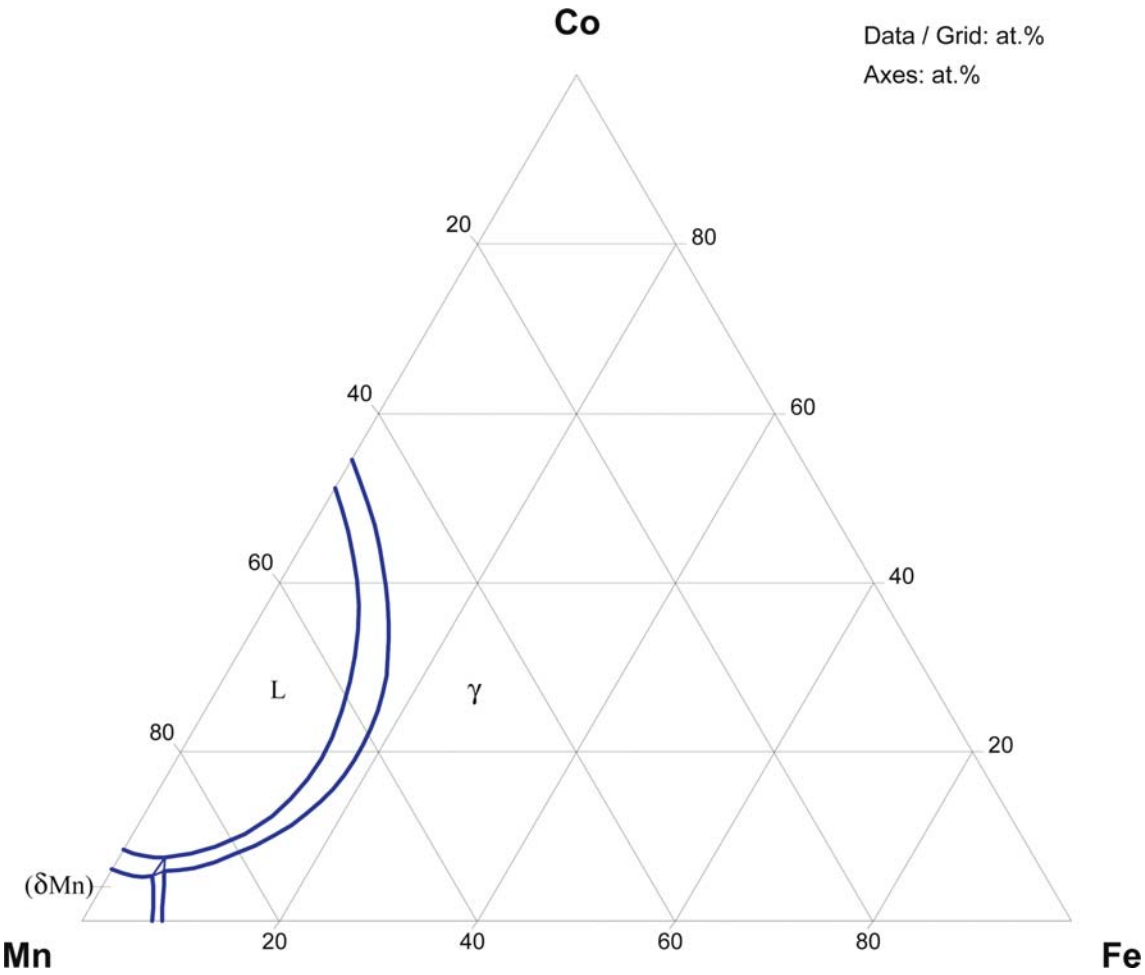

Fig. 6. Co-Fe-Mn. Calculated isothermal section at 1200°C

DOI: 10.1007/978-3-540-74196-1_20

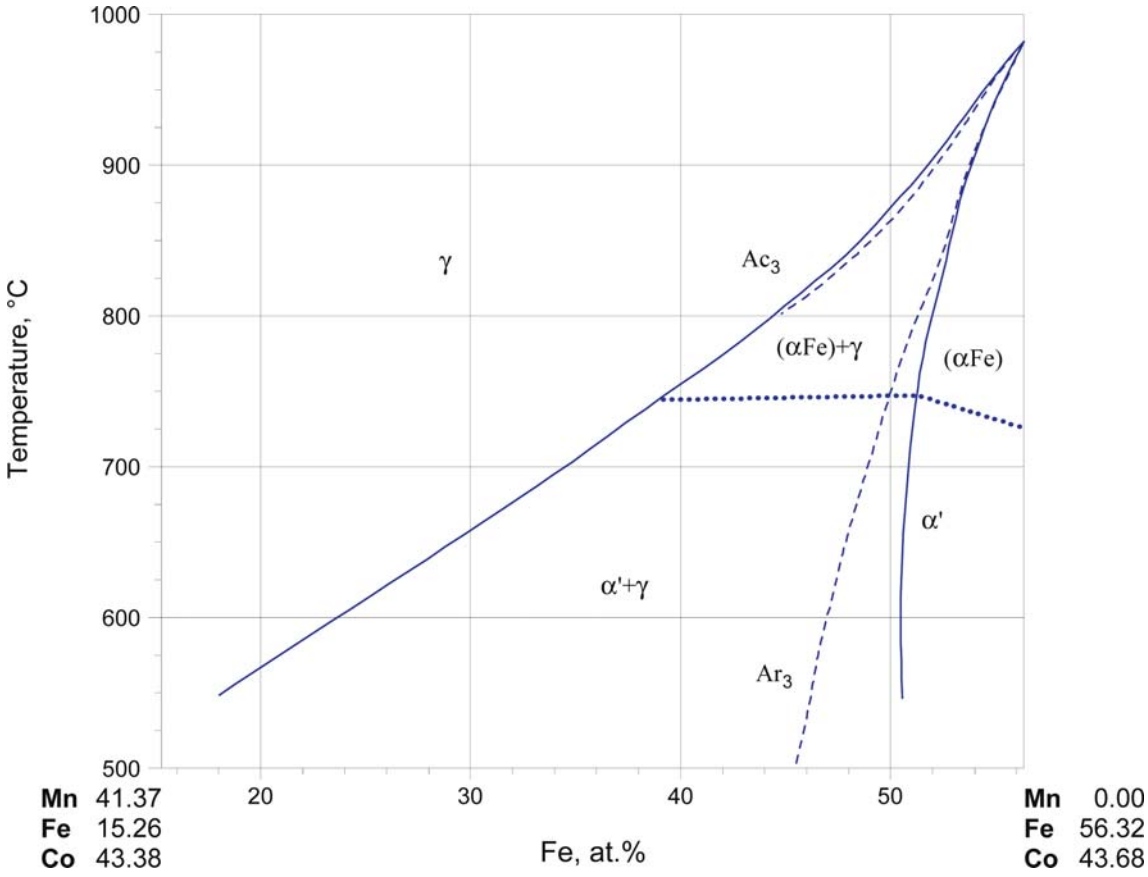

Fig. 7. Co-Fe-Mn. Partial vertical section at 45 mass% Co (plotted in at.%). Solid lines are equilibrium boundaries, dashed are lines *Ac3* and *Ar3* of the martensitic transformations, dotted - order-disorder second order transformation $\alpha' \rightarrow (\alpha Fe)$

DOI: 10.1007/978-3-540-74196-1_20

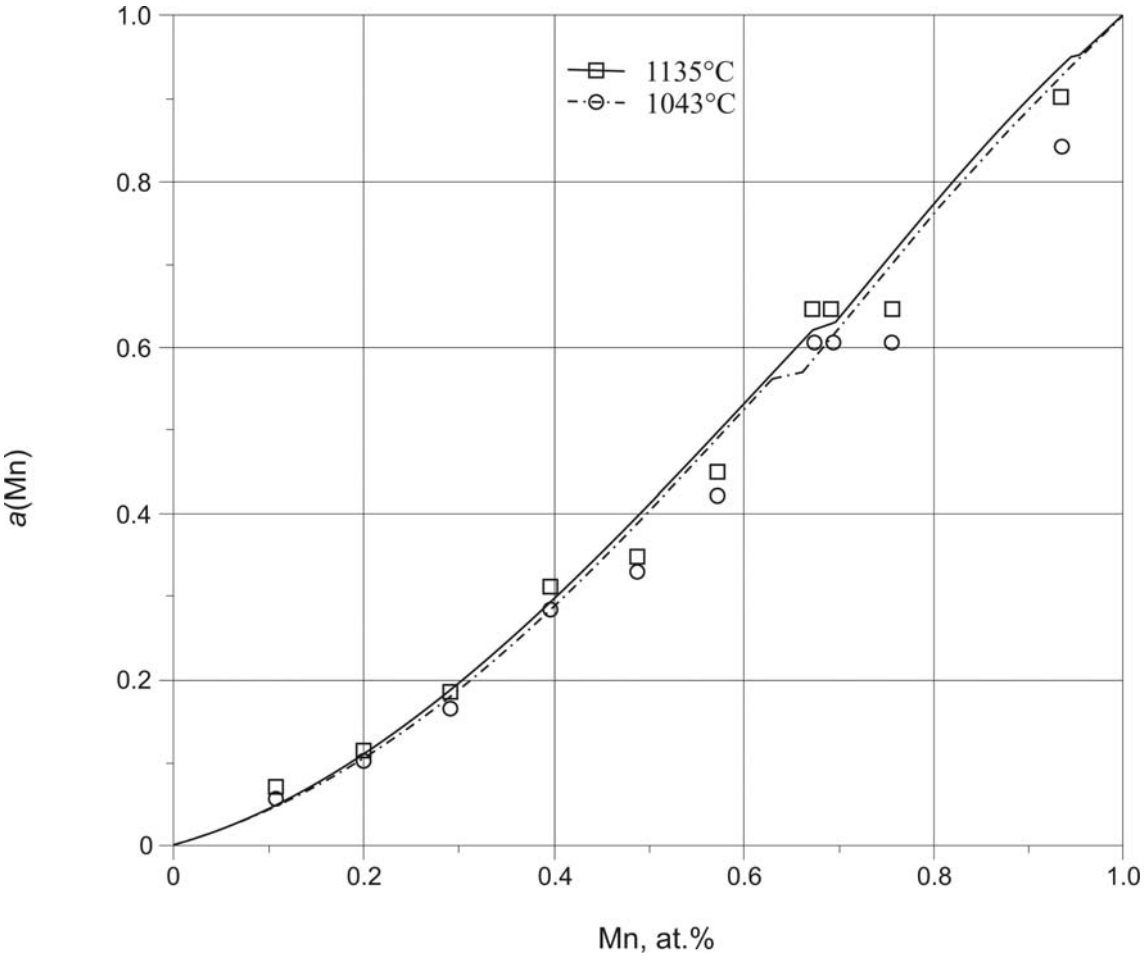

Fig. 8. Co-Fe-Mn. Activity of Mn along the section x(Fe)/x(Co) = 1.05 at 1135 and 1043°C

DOI: 10.1007/978-3-540-74196-1_20

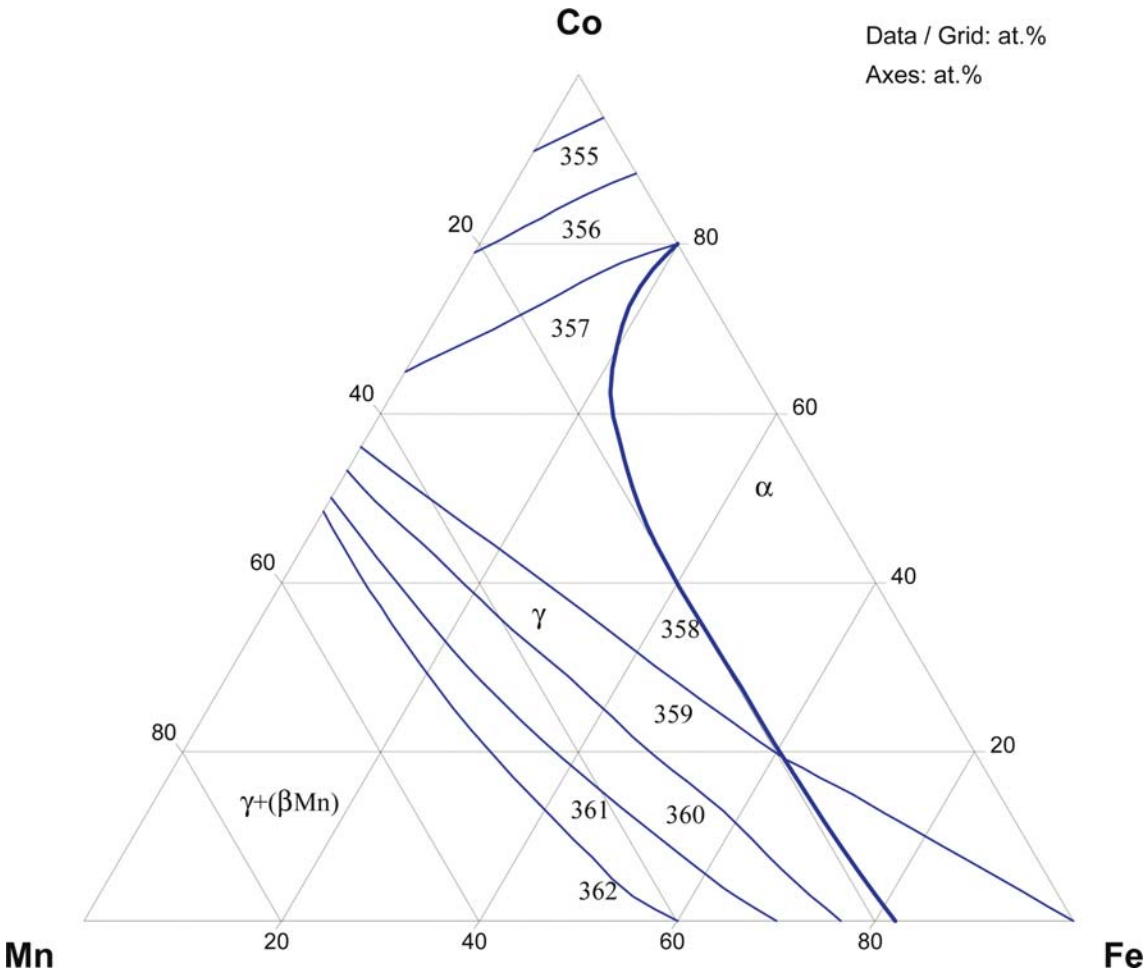

Fig. 9. Co-Fe-Mn. Lattice parameters (in pm) of γ phase

DOI: 10.1007/978-3-540-74196-1_20

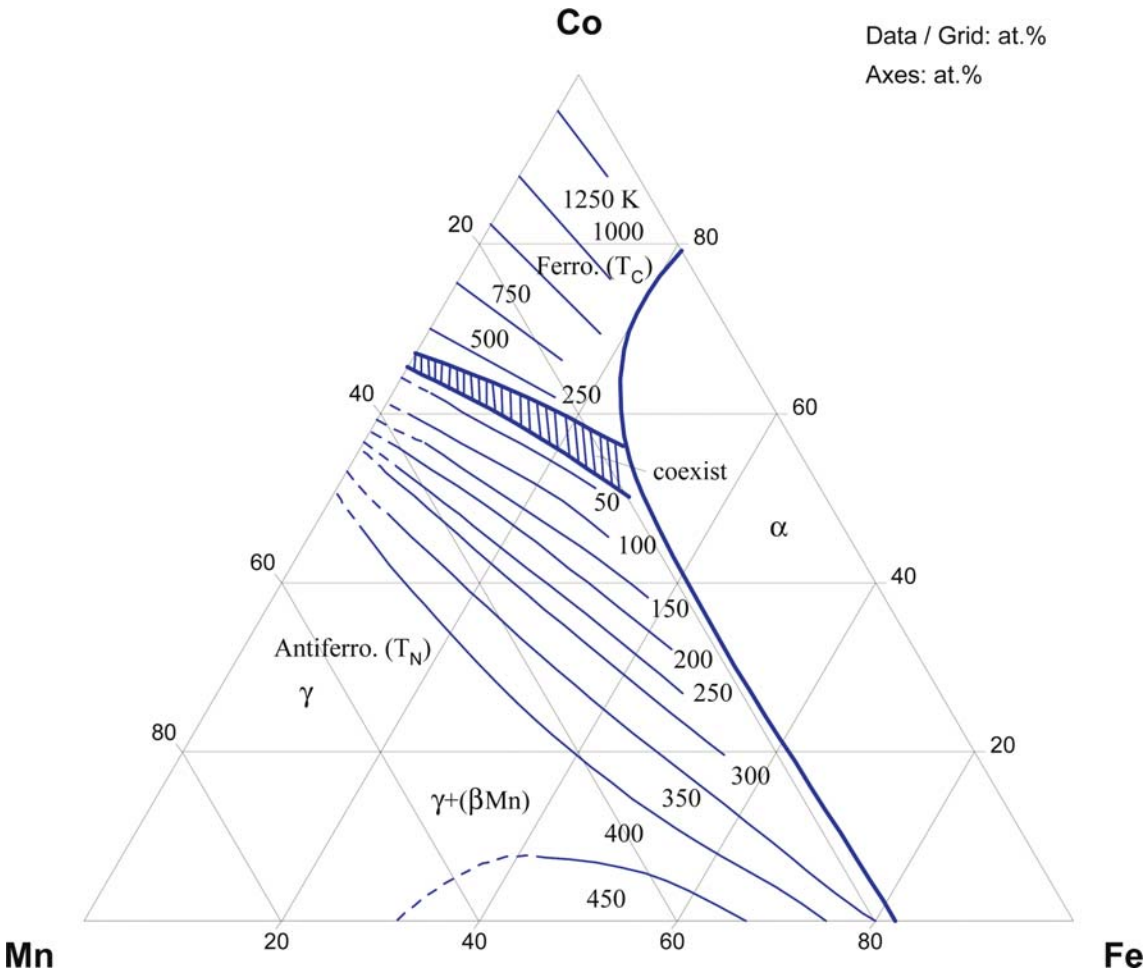

Fig. 10. Co-Fe-Mn. The values of Curie and Neel temperatures (in K) of the γ phase and the character of magnetic ordering. In the dashed region ferro- and antiferromagnetic states coexist

DOI: 10.1007/978-3-540-74196-1_20

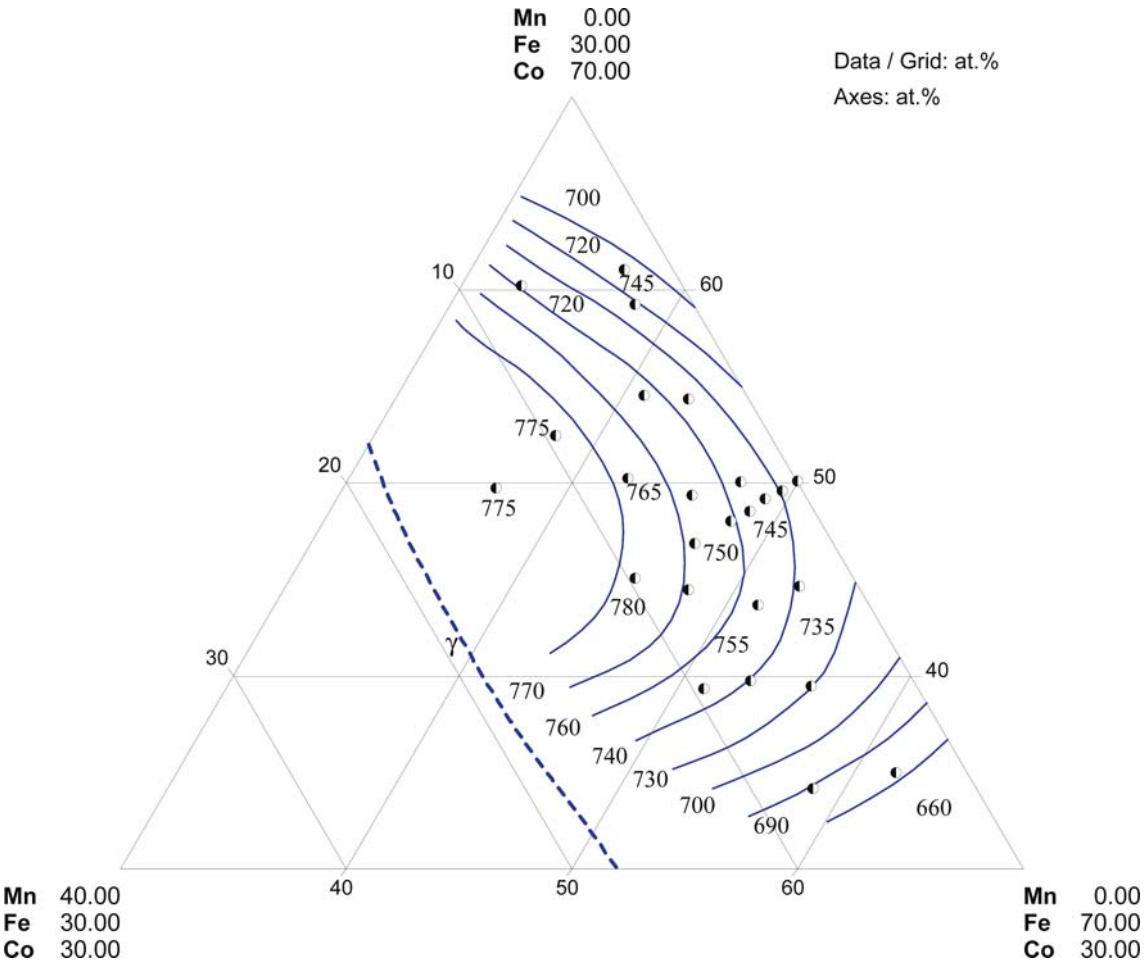

Fig. 11. Co-Fe-Mn. Temperatures (°C) of the $\alpha' \rightarrow (\alpha Fe)$ transition. Points are experimental data, lines are calculated. At Mn content > app. 7 to 8 at.% equilibria between (αFe) and α' are metastable with respect to the precipitation of the γ phase

DOI: 10.1007/978-3-540-74196-1_20

References

[1933Koe] Köster, W., Schmidt, W., "The System Iron-Cobalt-Manganese" (in German), *Arch. Eisenhuettenwes.*, **7**, 121–126 (1933) (Phase Diagram, Experimental, *, 12)

[1962Koe] Köster, W., Speidel, M., "About the Establishing of Equilibrium in the Iron-Cobalt-Manganese Ternary System" (in German), *Arch. Eisenhuettenwes.*, **33**, 873–876 (1962) (Phase Diagram, Magn. Prop., Phys. Prop., *, #, 6)

[1963Che1] Chen, C.W., "Magnetic Moments and Electronic Properties of Manganese-Substituted Iiron-Cobalt Alloys", *J. Appl. Phys.*, **34**, 1374–1375 (1963) (Magn. Prop., Electr. Prop., Electronic Structure, Theory, 6)

[1963Che2] Chen, C.W., "Electronic Structures of Manganese-Substituted Iron-Cobalt Alloys", *Phys. Rev.*, **129**, 121–124 (1963) (Magn. Prop., Electr. Prop., Electronic Structure, Theory, 11)

[1972Ada] Adachi, K., Sato, K., Matsui, M., Mitani, S., "Magnetic Properties of fcc Co-Mn-Fe System", *IEEE Trans. Magn.*, **8**, 693–695 (1972) (Crys. Structure, Magn. Prop., Experimental, 7)

[1973Ada] Adachi, K., Sato, K., Matsui, M., Mitani, S., "Neutron Diffraction Investigations of $(CoMn)_{1-x}Fe_x$", *J. Phys. Soc. Jpn.*, **35**, 426–433 (1973) (Crys. Structure, Magn. Prop., Experimental, 15)

[1973Mat] Matsui, M., Sato, K., Adachi, K., "Magnetic Properties of fcc γ-phase in the Ternary Co-Mn-Fe System", *J. Phys. Soc. Jpn.*, **35**, 419–425 (1973) (Crys. Structure, Magn. Prop., Experimental, *, #, 19)

[1973Yam] Yamada, Y., Uemura, C., Sugihara, M., "The Effect of Heat Treatment on the Magnetic Properties of Cold Rolled Fe-Mn-Co Alloys" (in Japanese), *J. Jpn. Inst. Met.*, **37**, 235–241 (1973) (Magn. Prop., Experimental, 8)

[1974Mas] Masumoto, H., Saito, H., Nakamura, N., "Strain Gauge Factor and Electrical Properties of Co-Fe -Mn Alloys", *Trans. Japan Inst. Metals*, **15**, 139–142 (1974) (Mech. Prop., Electr. Prop., Experimental, 10)

[1975Mal] Mal'tsev, Ye.I., Goman'kov, V.I., Mokhov, B.H., Puzey, I.M., Nogin, N.I., "Influence of Alloying Elements on the Co-Fe Superlattice", *Phys. Met. Metallogr.*, **40**, 190–193 (1975), translated from *Fiz. Met. Metalloved.*, **40**, 443–445 (1975) (Crys., Structure, Experimental, 11)

[1976Hag] Hagiwara, M., Suzuki, T., "The Effect of the Addition of a Third Element (Cr, Mn, V) on the Order-Disorder Transition Temperature in FeCo" (in Japanese), *J. Jpn. Inst. Met.*, **40**, 738–743 (1976) (Phase Relations, Experimental, Calculation, 34)

[1980Ben] Benkisser, G., Lyssak, L.I., Nikolin, B.I., Schumann, H., "The Hexagonal ε-Phase in the Iron-Manganese-Cobalt Alloys" (in German), *Neue Huette*, **25**, 326–329 (1980) (Crys. Structure, Experimental, Phase Diagram, 22)

[1980Sri] Srivastava, S.C., "Electrodeposition of Ternary Alloys: Developments in 1972–1978", *Surf. Technol.*, **10**, 237–257 (1980) (Electrochem., Magn. Prop., Review, 121)

[1981Mog] Mogutnov, B.M., Motrenko, V.F., Perkas, M.D., Pryakhin, V.A., Rodionov, Yu.L., Shaposhnikov, N.G., "Investigation into Hardening of Martensite of Fe-Mn-Co Alloys" (in Russian), *Metallofizika*, **3**, 110–117 (1981) (Kinetics, Experimental, 9)

[1983Riv] Rivlin, V.G., Raynor, G.V., "Phase Equilibriums in Iron Ternary Alloys. 9: Critical Review of Constitution of Ternary Systems Fe-Mn-X (X = Ti, V, Cr, Co, Ni, Cu)", *Int. Met. Rev.*, **28**, 23–64 (1983) (Phase Diagram, Review, 68)

[1988Ray] Raynor, G.V., Rivlin, V.G., "Co-Fe-Mn", in "*Phase Equilibria in Iron Ternary Alloys*", Institute of Metals, London, **4**, 230–232 (1988) (Phase Diagram, Review, *, #, 4)

[1989Hay] Hayes, F.H., McHugh, G., "Torsion Effusion Measurements on Fe-Mn, Co-Mn and Fe-Co-Mn Alloys", *NATO ASI Ser., Ser. C (Thermochem. Alloys)*, 227–292 (1989) (Experimental, Thermodyn., *, 28)

[1989Kum] Kumar, Hari, K.C., Raghavan, V., "The bcc-fcc Equilibrium in Ternary Iron Alloys - III", *J. Alloy Phase Diagrams*, **5**, 201–220 (1989) (Calculation, Phase Diagram, Phase Relations, 28)

[1990Hua] Huang, W., "Thermodynamics of the Co-Fe-Mn System", *Calphad*, **14**(1), 11–22 (1990) (Phase Diagram, Thermodyn., Calculation, *, #, 19)

DOI: 10.1007/978-3-540-74196-1_20

[1991Ham] Hamers, A.A.H., Wayman, C.M., "Shape Memory Behavior in Fe-Mn-Co Alloys", *Scr. Metall. Mater.*, **25**, 2723–2728 (1991) (Mechan. Prop., Experimental, 13)

[1992Ste] Stetsenko, F.I., Potapov, N.N., Zanegina, G.A., "Magnetic Properties, Temperature and Dynamic Characteristics of Deformable Magnetically Hard Fe-Co-Mn Alloys" (in Russian), *Fiz. Met. Metalloved.*, **74**, 133–137 (1992) (Magn. Prop., Experimental, 10)

[1993Ste] Stetsenko, F.I., "Dynamical Characteristics and Micromagnetic Structure Parameters of Ductile Hard Magnetic Fe-Co-Mn Alloys" (in Russian), *Fiz. Met. Metalloved.*, **75**, 60–64 (1993) (Magn. Prop., Experimental, 8)

[1994Rag] Raghavan, V., "Co-Fe-Mn (Cobalt-Iron-Manganese)", *J. Phase Equilib.*, **15**, 525–526 (1994) (Phase Diagram, Review, 4)

[1995Tan] Tanaka, T., Aaronson, H.I., Enomoto, M., "Calculations of α/γ Phase Boundaries in Fe-C-X1-X2 Systems from the Central Atoms Model", *Metall. Mater. Trans. A*, **26A**, 535–545 (1995) (Calculation, Phase Relations, Thermodyn., 27)

[1997Bar] Baruj, A., Guillermet, A.F., Sade, M., "The FCC/HCP Relative Phase Stability in the Fe-Mn-Co System - Martensitic Transformation Temperatures, Assessment of Gibbs Energies and Thermodynamic Calculation of T0 Lines", *J. Physique IV*, **7**(C5), 405–410 (1997) (Phase Relations, Thermodyn., Calculation, 18)

[1999Mar] Marinelli, P., Baruj, A., Cotes, S., Guillermet, A.F., Sade, M., "The $\gamma \rightarrow \alpha$ Martensitic Transformation in Fe-Mn and Fe-Mn-Co Alloys: Experiments, Thermodynamic Analysis and Systematics of Driving Forces", *Mater. Sci. Eng. A*, **275**, 498–502 (1999) (Calculation, Experimental, Phase Relations, Thermodyn., 19)

[2002Mar] Marinelli, P., Sade, M., Guillermet A.F., "On the Structural Changes Accompanying the fcc/hcp Martensitic Transformation in Fe-Mn-Co Alloys", *Scr. Mater.*, **46**(11), 805–811 (2002) (Crys. Structure, Experimental, Phase Relations, 23)

[2004Mar] Marinelli, P., Guillermet, A.F., Sade, M., "The Enthalpy Change of the hcp $\rightarrow$ fcc Martensitic Transformation in Fe-Mn-Co Alloys: Composition Dependence and Thermal Cycling Effects", *Mater. Sci. Eng. A*, **373**(1–2), 1–9 (2004) (Experimental, Phase Relations, Phys. Prop., Thermodyn., 30)

[2004Sun] Sundar, R.S., Deevi, S.C., "Influence of Alloying Elements on the Mechanical Properties of FeCo-V Alloys", *Intermetallics*, **12**, 921–927 (2004) (Magn. Prop., Mechan. Prop., Morphology, Review, 32)

[2005Sou] Sourmail, T., "Near Equiatomic FeCo Alloys: Constitution, Mechanical and Magnetic Properties", *Progr. Mater. Sci.*, **50**, 816–880 (2005) (Crys. Structure, Electr. Prop., Kinetics, Magn. Prop., Mechan. Prop., Morphology, Phase Diagram, Phase Relations, Review, 122)

[2005Sun] Sundar, R.S., Deevi, S.C., "Soft Magnetic Fe-Co Alloys: Alloy Development, Processing, and Properties", *Int. Mater. Rev.*, **50**, 157–192 (2005) (Crys. Structure, Electr. Prop., Magn. Prop., Mechan. Prop., Phase Diagram, Phase Relations, Review, 258)

[Mas2] Massalski, T.B. (Ed.), *Binary Alloy Phase Diagrams*, 2nd edition, ASM International, Metals Park, Ohio (1990)

[V-C2] Villars, P. and Calvert, L.D., *Pearson's Handbook of Crystallographic Data for Intermetallic Phases*, 2nd edition, ASM, Metals Park, Ohio (1991)

DOI: 10.1007/978-3-540-74196-1_20

Cobalt – Iron – Molybdenum

Andy Watson, Lesley Cornish

Introduction

Most of the phase diagram work carried out on this system was conducted before the nature of the Co-Mo and Fe-Mo binary systems was complete. Consequently, any appraisal of the work has to be made with this in mind.

The first comprehensive study of the ternary system was conducted by [1932Koe1] and later reviewed by [1949Jae]. Thermal analysis and metallographic techniques were employed to determine the liquidus surface, isothermal sections at 1300 and 20°C and 2 vertical sections. However, the versions of the Co-Mo and Fe-Mo binary phase diagrams they used in their analysis were somewhat different from those accepted in later work. This will be dealt with later.

[1952Das, 1953Das] determined an isothermal section of the system for 1200°C. 65 alloys were prepared by vacuum induction melting in zirconia or alumina crucibles followed by a double forging before annealing under a mixture of 92% He / 8% H_2. Alloys were annealed for 90 h (compositions giving fcc or bcc alloys) or 150 h before water quenching. The resulting section showed complete solubility between the Mo_6Co_7 and Mo_6Fe_7 phases. They also concluded that the resulting phase field followed the line of constant electron vacancy.

Phase diagram studies up to 1971 were reviewed by [1971Wes] who was the first to be alerted to problems in the work of [1932Koe1] resulting from the binary systems available to them at the time. Subsequent to this review, few studies have been made. [1971Dom, 1972Dom] made a study of the Fe rich corner of the system at 1205, 1093 and 982°C. Samples were prepared by arc-melting using a non-consumable tungsten electrode and water cooled copper hearth. The cast alloys were then homogenized under high vacuum for 40 h at 1200°C. They were then annealed in either argon filled quartz ampoules (high temperatures) or vycor (low temperatures) for 100 h. Optical microscopy, XRD and microprobe analysis were used to determine phase assemblages in the samples. [1979Pro] studied phase equilibria in the system at temperatures of 800 and 1200°C. Alloys were prepared by arc-melting high purity materials and quenching after heat treatment. Microstructural, XRD, SEM, hardness and microhardness analyses were used. [1980Loo] used a diffusion couple technique at 1100°C. Argon-arc melted samples were homogenized for between 3 and 10 d at 1100°C in sealed silica ampoules. The couples were made by resistance welding samples clamped between Mo electrodes. The presence of a large μ phase field was confirmed. All of the experimental studies have been reviewed in [1984Ray, 1988Ray].

An isothermal section for 1200°C was calculated by [1984Eri]. Unfortunately, the σ phase was not considered.

There has only been one thermodynamic study of this system. [1983Kub] measured the heats of formation of alloys lying in the μ phase field at 1323 and 1500K by direct reaction calorimetry. Only three ternary compositions were studied.

Details of the experimental studies of the system are given in Table 1.

Binary Systems

The Co-Fe system is accepted from a *Calphad* assessment given by [2002Ohn]. The phase diagram is essentially the same as given in [Mas2], but it extends to lower temperatures following phase equilibrium studies using thin films. A number of *Calphad* assessments for the Co-Mo system are available in the literature. [1999Dav] modeled the system using experimental phase diagram and thermochemical data. The fit of the calculated phase diagram to the diagram given in [Mas2] is very good, but it was later pointed out by [2001Che] that there were some problems in the modeling of the liquid, σ, and μ phases. This led to a re-assessment of the system by [2003Dav], but the fit of the calculated phase diagram to that in [Mas2] now suffered. More recently, [2005Hou] used *ab initio* techniques to model the σ phase in the binary

DOI: 10.1007/978-3-540-74196-1_21

system, leaving the rest of the modeling essentially the same as in [2003Dav]. For these reasons, the Co-Mo phase diagram has been taken from [Mas2]. The Fe-Mo system has also been assessed a number of times. The version of the phase diagram given in [Mas2] is based on the assessment by [1982Gui1]. However, there are discrepancies between the phase diagrams appearing in both articles. An alternative version is given in [1982Gui2], although the parameters listed are the same as used in [1982Gui1]. Interestingly, the phase diagrams from both [1982Gui1] and [1982Gui2] show a very shallow minimum in the Fe rich liquidus and solidus, but this feature cannot be discerned in the diagram in [Mas2]. This suggests that the equilibrium between the (αδFe), L and R phase is probably degenerate. The phase diagram accepted here is taken from [1982Gui2].

Solid Phases

The system is characterized by a continuous solid solution of the μ phase which stretches from the Co-Mo to the Fe-Mo system. It is highly likely that the σ phase exists as a continuous solid solution across the system as well [1988Ray], although this feature wasn't seen in any of the early phase diagram studies. This was because no study has been made of Mo rich alloys. Considerable dissolution of Co into the Fe-Mo αδ phase is also evident. This can be of the order of ~25 mass% at 1300°C according to [1932Koe1]. As a consequence of the complete mutual solubility of Fe and Co in the γ phase, this phase field stretches from the Co-Fe binary edge to Mo contents of up to ~25 mass% at 1300°C according to [1932Koe1].
There is evidence of *B*2 ordering in the Co-Fe system, where with decreasing temperature, ferrite transforms from the disordered bcc phase to the ordered structure. There is no indication how this phase extends into the ternary system, although the kinetic evolution of *B*2 ordering in FeCo-Mo alloys was studied by [2001Sar] using Mössbauer spectroscopy, and site occupancy of this phase was studied by [2002Boz].
There is some evidence of dissolution of Co in the $MoFe_2$ laves phase. [1979Sha] investigated the precipitation due to aging of the compound $MoFe_2$ in alloys of composition Fe+10% Mo+(0-20%) Co by hardness measurement. An increase in hardness with Co addition was observed and a thermodynamic analysis of this process established that an increase in the volume proportion of the precipitates of the hardening Laves phase occurred owing to the dissolution of cobalt in the compound, increasing its thermodynamic stability. No ternary phases have been reported in this system. Crystallographic information of the solid phases is given in Table 2.

Invariant Equilibria

Invariant equilibria were determined by [1932Koe1], but as indicated by [1971Wes, 1984Ray, 1988Ray] and previously stated, owing to deficiencies in the Fe-Mo and Co-Mo binaries they used, their results require reinterpretation. [1932Koe1] suggested the existence of two transition reactions. The first is at ~1300°C and is defined by the reaction L + (αδFe) ⇌ γ + μ. The second is at a temperature of 1485°C and is defined by the reaction L + (Mo) ⇌ σ+ μ. However, as the σ phase forms in both the Fe-Mo and Co-Mo systems by peritectic reaction the latter ternary invariant reaction is unlikely and so is not considered further here. A further problem occurs in that the primary solidification of R-phase, which occurs in the Fe-Mo binary phase diagram, is missing from the liquidus projection presented by [1932Koe1], and with it associated invariant reactions in the ternary system. In their analysis of the data of [1932Koe1], [1984Ray, 1988Ray] assumed two extra invariants associated with the R-phase. The invariant equilibria are listed in Table 3 and a tentative reaction scheme taken from [1988Ray] is presented in Fig. 1.

Liquidus, Solidus and Solvus Surfaces

The liquidus surface taken from [1988Ray] which is based on the work of [1932Koe1] is presented in Fig. 2. As mentioned above, the invariant L + (Mo) ⇌ σ + μ is unlikely to exist in the system. This is removed from the original liquidus surface as presented by [1932Koe1]. Instead, there is now a monovariant connecting the binary peritectic reactions related to the formation of the σ phase in the Fe-Mo and Co-Mo systems. It is also necessary to add a monovariant related to the peritectic formation of the R phase in the Fe-Mo system. This line is shown to meet the monovariant line from the peritectic point in the Co-Mo binary associated with the formation of the μ phase. At this intersection, a new monovariant joins the monovariant

DOI: 10.1007/978-3-540-74196-1_21

from the degenerate reaction involving L, (Fe) and the R phase in the Fe-Mo system at a new invariant point. The location of this monovariant line is uncertain and is therefore shown dashed in Fig. 2.

Isothermal Sections

Figure 3 shows the partial isothermal section for 1200°C taken from [1988Ray] based on the work of [1952Das]. This section is in good agreement with the work of [1972Dom] who studied phase equilibria of alloys in the Fe rich corner of the diagram. According to the accepted binary phase diagrams, the R phase in the Fe-Mo and the θ phase in the Co-Mo systems should just be stable at this temperature. However, it's worth noting that neither of these phases was seen in the experimental work to determine this section. Figure 4 shows the partial isothermal section for 1100°C taken from [1988Ray] based on [1980Loo]. This section is in good agreement with that for 1200°C, particularly in that the length of the thin (Fe) + γ + μ three phase region lies roughly parallel to the Fe-Mo binary edge. This is somewhat contrary to how it appears in the section for 1300°C produced by [1932Koe1] where it appears to be more in line with the Co-Mo binary edge. As pointed out by [1988Ray], it is unlikely that such a substantial change in the location of this phase field would occur by falling temperature, and hence, the section for 1300°C has not been reproduced here. Figure 5 shows a partial isothermal section for 982°C taken from [1988Ray] based on [1972Dom]. Many of the phase boundaries are tentative in that they were not directly determined in the original work. It is necessary to add the κ phase to this section since it appears in the Co-Mo binary phase diagram. The partial isothermal section for 800°C is presented in Fig. 6; taken from [1988Ray] based on [1979Pro]. The location of many of the phase boundaries is tentative, resulting from the phase analysis of a series of alloys lying the section of approximately 10 mass% Mo. Equilibria relating to the λ phase in the Fe-Mo system have been added. Adjustments have been made to the diagrams where necessary to ensure compatibility with the phase boundaries of the accepted binary systems.

Temperature – Composition Sections

Isoplethal sections for 10, 20, 30 and 45 mass% Mo were constructed by [1932Koe1] using thermal analysis. However, as no indication of the experimental conditions used was given, and also because of the problems associated with the binary phase diagrams used in their analyses, these sections are deemed to be unreliable and are not reproduced here.

Thermodynamics

Enthalpies of formation of alloys in the μ phase field as determined by [1983Kub] using direct reaction calorimetry are given in Table 4.

Notes on Materials Properties and Applications

Magnetic and mechanical properties were measured by [1932Koe2]. Brinell hardness, coercivity and magnetic remanence were measured. [1985Koz] measured the microhardness of modulated structures in the metastable spinodal alloys. Physical property investigations are listed in Table 5.

Miscellaneous

[1979Nis] conducted a thermodynamic analysis of (αFe)-X alloys. An expression for the free energy of the solution was resolved into magnetic and non-magnetic parts and it was found that the chemical potential is very high in the ferromagnetic state. However, this decreases markedly as the Curie temperature is approached, affecting solubility. The addition of Co increases the chemical potential further and enlarges the magnetic anomalies.
[1985Mor] estimated the location of the γ/γ+μ phase boundary using ab initio techniques. Using cluster calculations of electronic structure, a parameter, M_d was used to estimate the location of the phase boundary. This parameter is related to both electronegativity and atomic size, which are also used in classical approaches. The estimated phase boundary is in good agreement with that given by [1953Das].

DOI: 10.1007/978-3-540-74196-1_21

[1991Nik, 1993Nik] studied the crystal structure of martensites in Co-Fe-Mo alloys. XRD was used to study the martensite single crystals following quenching and preliminary aging. Continuous decomposition of the structures at aging temperatures between 500 and 700°C was observed. The aging of martensite was also studied by [1974Edn]. It was found that cobalt addition to Fe-Mo alloys broadens the γ region at high temperatures, which permits the γ→α transformation by a martensitic mechanism during subsequent cooling. A high dislocation density and other defects that result from the displacement mechanism of the γ→α transformation leads not only to hardening of the matrix but also creates conditions favorable for the formation of large numbers of centers for precipitation of phases during aging. Cobalt substantially accelerates the aging process.
Strain aging of Co-Fe-Mo alloys was studied by [1979Tok] using electrical resistivity measurements. These revealed a strain aging stage and reversion process caused by substitutional solute atoms corresponding to the low-temperature aging in maraging steels.
The solubility of hydrogen in liquid ternary Co-Fe-Mo alloys has been investigated by [1986Mit] using Sieverts' method. It was found that the addition of molybdenum lowers the hydrogen solubility. At constant alloy concentration, the hydrogen solubility increases with increasing temperature. Calculations using the "central atoms" model allowed an estimation of the concentration dependence of the hydrogen solubility in liquid ternary alloys using the experimentally determined hydrogen solubilities of only two binaries, *e.g.* Co-Fe and Fe-Mo or Co-Fe and Co-Mo.

Table 1. Investigations of the Co-Fe-Mo Phase Relations, Structures and Thermodynamics

Reference	Method/Experimental Technique	Temperature/Composition/Phase Range Studied
[1932Koe1]	Thermal analysis, metallography	Liquidus projection (Fe and Co rich regions), vertical sections at 10, 20, 30, 45 mass% Mo. Isothermal section at 1300°C.
[1952Das, 1953Das]	Microstructural and powder XRD analysis of annealed specimens	Isothermal section at 1200°C
[1971Dom, 1972Dom]	Microstructural, XRD and microprobe analyses	Fe rich corner of isothermal sections at 1205, 1093 and 982°C
[1979Pro]	Microstructural, XRD hardness and microhardness analyses	Isothermal sections at 800 and 1200°C
[1980Loo]	Diffusion couples, optical microscopy, microprobe analysis, XRD	Isothermal section at 1100°C.
[1983Kub]	High-temperature adiabatic calorimetry	Enthalpy of formation of the μ phase at 1200 and 1277°C
[1985Koz]	TEM of aged alloys, CVM calculations	Metastable spinodal region at 500-650°C

DOI: 10.1007/978-3-540-74196-1_21

Table 2. Crystallographic Data of Solid Phases

Phase/ Temperature Range [°C]	Pearson Symbol/ Space Group/ Prototype	Lattice Parameters [pm]	Comments/References
γ, $Mo_{1-x-y}Fe_xCo_y$	*cF*4 $Fm\bar{3}m$		$0 \le x \le 1$, $0 \le y \le 1$
(γFe) (h1) 1394 - 912	Cu	a = 364.67	$x = 1$, $y = 0$ at 915°C [V-C2, Mas2]
(αCo) 1495 - 422		a = 356.88 a = 354.47	$x = 0$, $y = 1$ at 520°C [V-C2] [Mas2] Austenite
(εCo) < 700	*hP*2 $P6_3/mmc$ Mg	a = 250.71 c = 406.86	at 25°C [Mas2]
(αδFe)	*cI*2 $Im\bar{3}m$		
(αFe) (r) ≤ 912	W	a = 286.65	pure αFe at 25°C [Mas2]
(δFe) (h2) 1538 - 1394		a = 293.15	pure δFe at 1480°C [Mas2]
(Mo) < 2623	*cI*2 $Im\bar{3}m$ W	a = 314.70	at 25°C [Mas2]. Dissolves ~10 at.% Co at 1620°C, 31.3 at.% Fe at 1611°C [Mas2]
α', $Fe_{1-x}Co_x$ < 730	*cP*2 $Pm\bar{3}m$ CsCl		$0.25 < x < 0.75$. Maximum temperature at ~50 at.% Fe
σ, $Mo_x(Fe_{1-y}Co_y)_{1-x}$	*tP*30 $P4_2/mnm$ σCrFe		
Mo_3Co_2 1620 - 1000		a = 927.9 c = 487.1	at $y = 1$, $\sim 0.61 < x < 0.615$ [Mas2, 1984Ray]
MoFe 1611 - 1235		a = 918.8 c = 481.2	at $y = 0$, $\sim 0.429 < x < 0.567$ [Mas2, 1984Ray]
μ, $Mo_x(Fe_{1-y}Co_y)_{1-x}$	*hR*39 $R\bar{3}m$ W_6Fe_7		$0 \le y \le 1$
Mo_6Co_7 < 1510		a = 476.7 c = 2565	at $y = 1$, $\sim 0.412 < x \lesssim 0.492$ [Mas2, 1984Ray]
Mo_6Fe_7 < 1370		a = 475.4 ± 0.6 c = 2571 ± 0.6	at $y = 0$, $\sim 0.39 < x \lesssim 0.44$ [Mas2, 1984Ray]

(*continued*)

DOI: 10.1007/978-3-540-74196-1_21

Phase/ Temperature Range [°C]	Pearson Symbol/ Space Group/ Prototype	Lattice Parameters [pm]	Comments/References
κ, $Mo_{1-x}Co_x$ < 1025	*hP*8 $P6_3/mmc$ Ni_3Sn	a = 512.45 c = 411.25	~0.745 < x ≲ 0.755 [Mas2, 1984Ray]
θ, Mo_9Co_2 1200 - 1018	*hP*2 $P6_3/mmc$ Mg	a = 259.73 c = 421.33	[Mas2, 1984Ray]
λ, $MoFe_2$ < 927	*hP*12 $P6_3/mmc$ $MgZn_2$	a = 474.5 c = 734.0	[Mas2, 1984Ray] Laves phase
R, $Mo_{1-x}Fe_x$	*hR*159 $R\bar{3}$ R-(Co,Cr,Mo)	a = 1091.0 c = 1935.4	0.339 < x < 0.385 [Mas2, 1984Ray]

Table 3. Invariant Equilibria

Reaction	T [°C]	Type	Phase	Composition (at.%)		
				Co	Fe	Mo
L + σ ⇌ μ + R	?	U_1	-	-	-	-
L + R ⇌ (αδFe) + μ	?	U_2	-	-	-	-
L + (αFe) ⇌ μ + γ	1300	U_3	L	29.4	51.8	18.8

Table 4. Thermodynamic Data of Reaction or Transformation

Reaction or Transformation	Temperature [°C]	Quantity, per mol of atoms [kJ, mol, K]	Comments
0.13 Co(γ) + 0.4556 Fe(γ) + 0.4144 Mo(α) → $Co_{0.13}Fe_{0.4556}Mo_{0.4114}$(μ)	1277	ΔH = 1.522	[1983Kub] Adiabatic calorimetry
0.26 Co(γ) + 0.3037 Fe(γ) + 0.4362 Mo(α) → $Co_{0.26}Fe_{0.3037}Mo_{0.4362}$(μ)	1100	ΔH = 1.795	[1983Kub] Adiabatic calorimetry
0.39 Co(γ) + 0.153 Fe(γ) + 0.458 Mo(α) → $Co_{0.13}Fe_{0.4556}Mo_{0.4114}$(μ)	1277	ΔH = 0.9	[1983Kub] Adiabatic calorimetry
0.5 Co(γ) + 0.4 Fe(γ) + 0.1 Mo(α) → $Co_{0.5}Fe_{0.4}Mo_{0.1}$(γ)	1050	ΔH = 2.41	[1983Kub] Adiabatic calorimetry
0.8 Co(γ) + 0.1 Fe(γ) + 0.1 Mo(α) → $Co_{0.8}Fe_{0.1}Mo_{0.1}$(γ)	1050	ΔH = 1.64	[1983Kub] Adiabatic calorimetry

DOI: 10.1007/978-3-540-74196-1_21

Table 5. Investigations of the Co-Fe-Mo Materials Properties

Reference	Method / Experimental Technique	Type of Property
[1932Koe2]	Brinell hardness, electrical resistivity, magnetic saturation, dispersive solidification	Coercivity and magnetic remanence of Fe-12Co-18Mo (mass%) alloy
[1985Koz]	Microhardness measurement	Microhardness of metastable alloys with modulated structure

DOI: 10.1007/978-3-540-74196-1_21

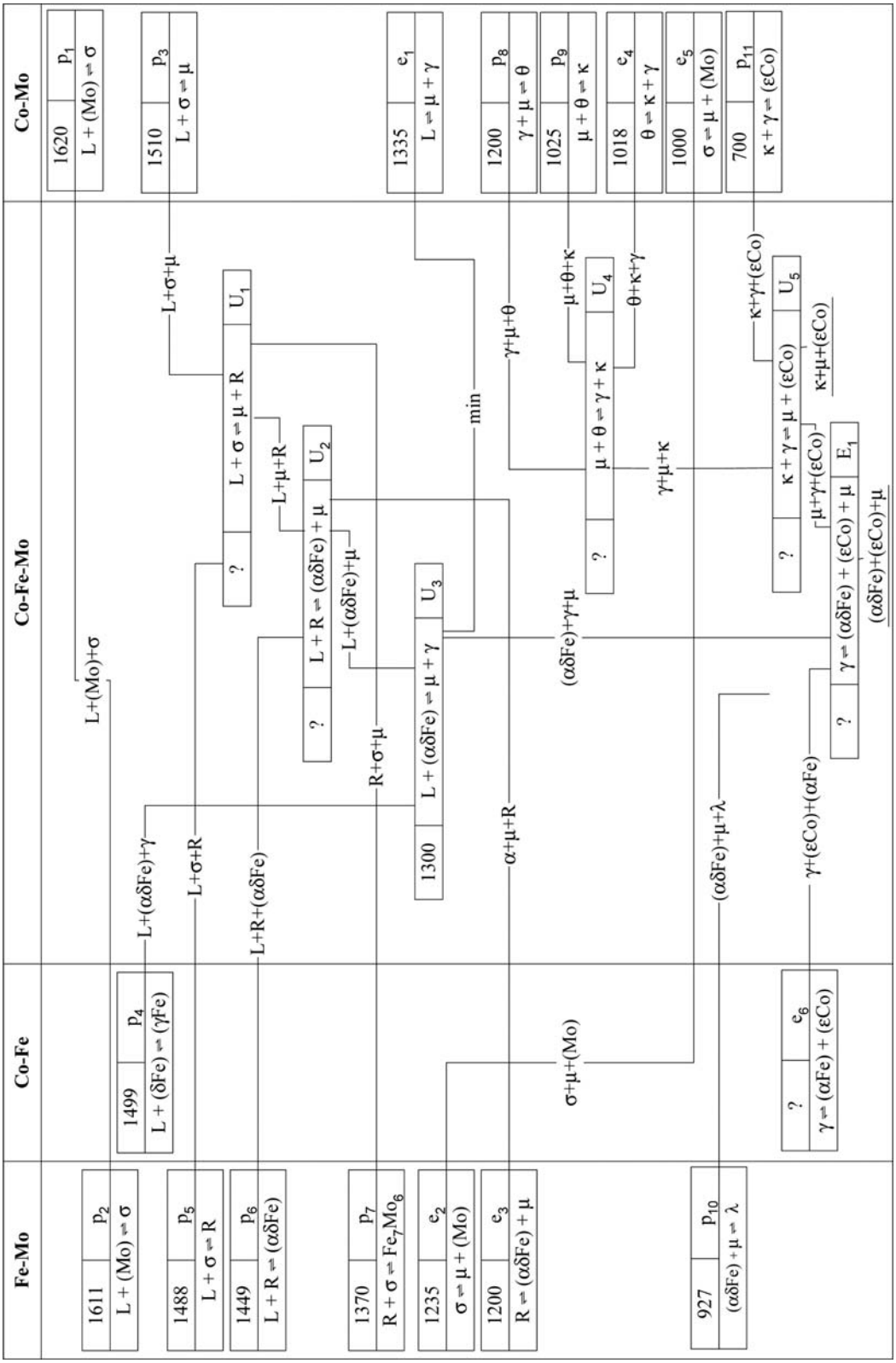

Fig. 1. Co-Fe-Mo. Reaction scheme

DOI: 10.1007/978-3-540-74196-1_21

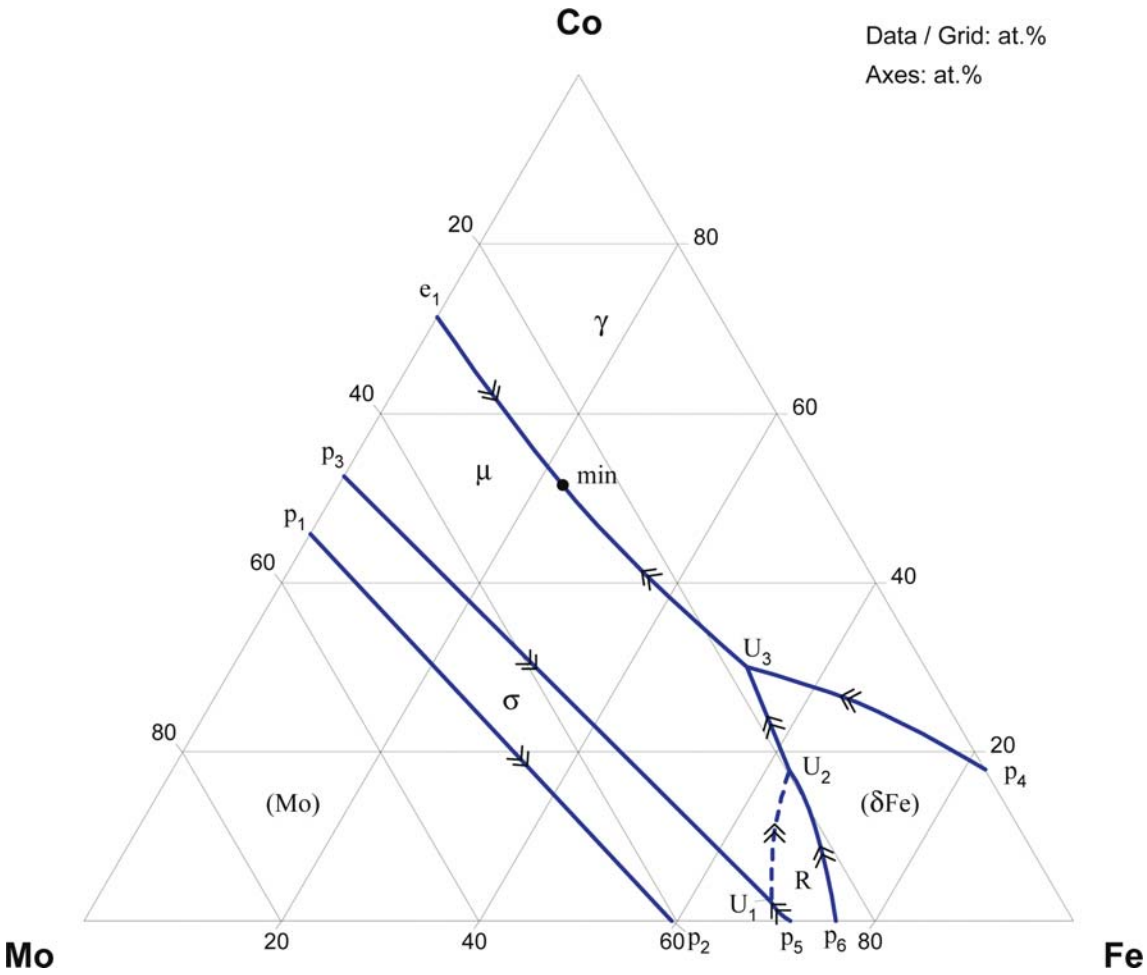

Fig. 2. Co-Fe-Mo. Partial liquidus surface

DOI: 10.1007/978-3-540-74196-1_21

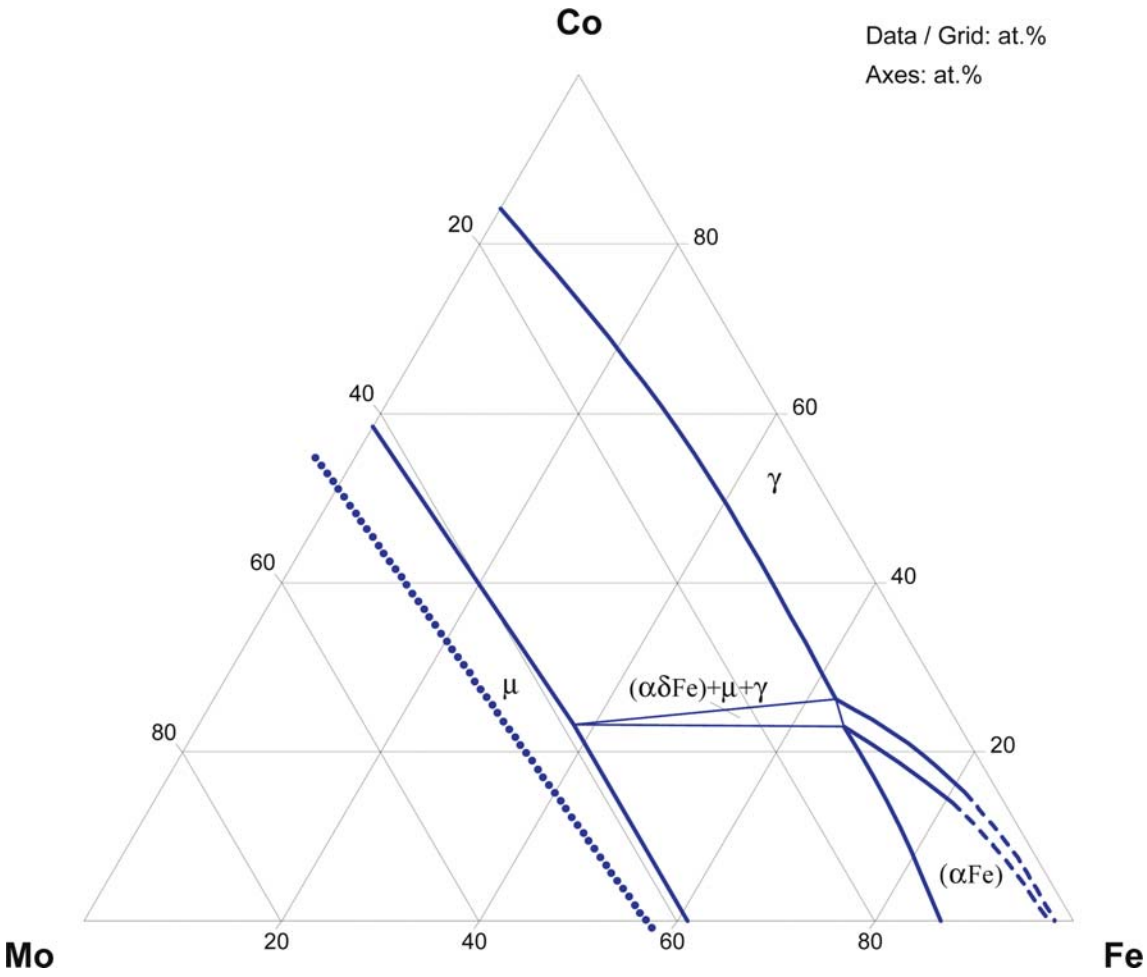

Fig. 3. Co-Fe-Mo. Partial isothermal section at 1200°C

DOI: 10.1007/978-3-540-74196-1_21

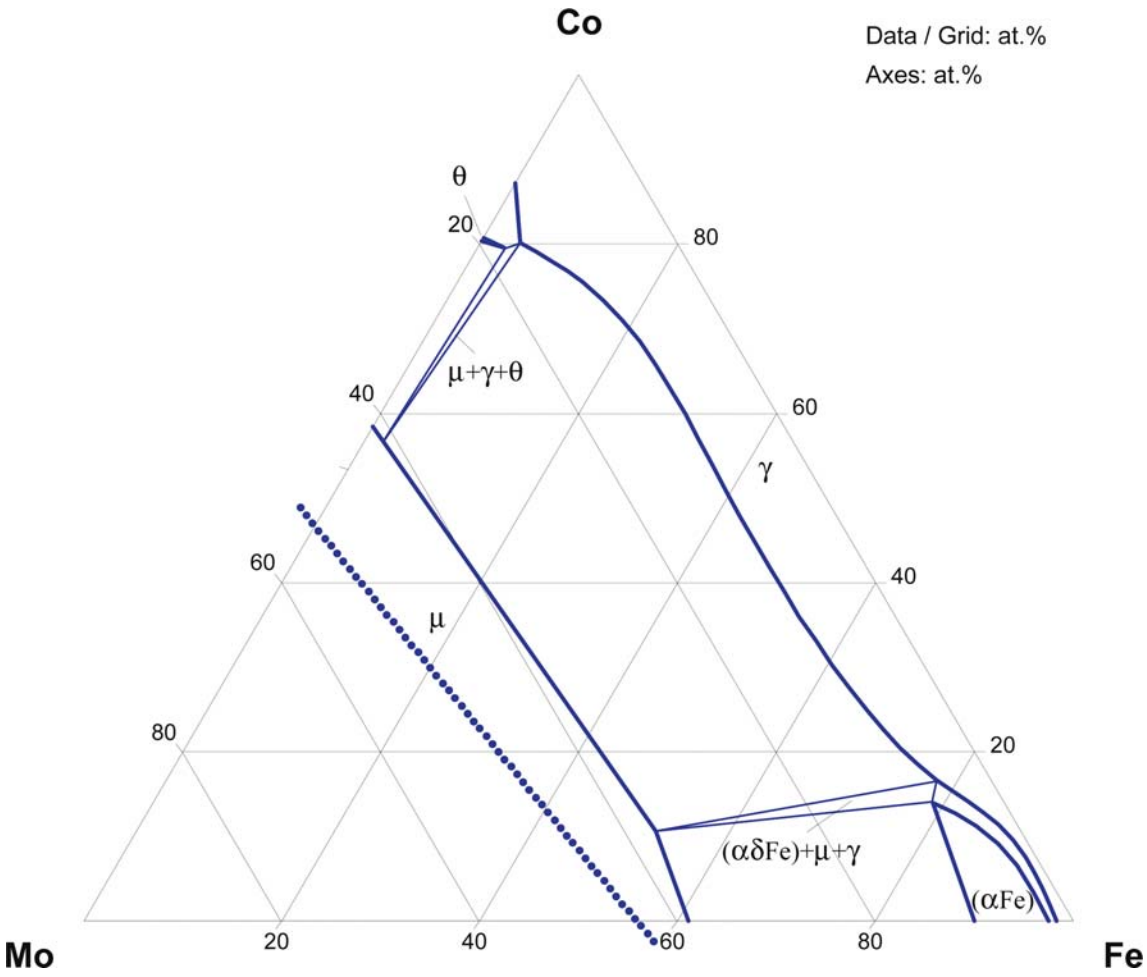

Fig. 4. Co-Fe-Mo. Partial isothermal section at 1100°C

DOI: 10.1007/978-3-540-74196-1_21

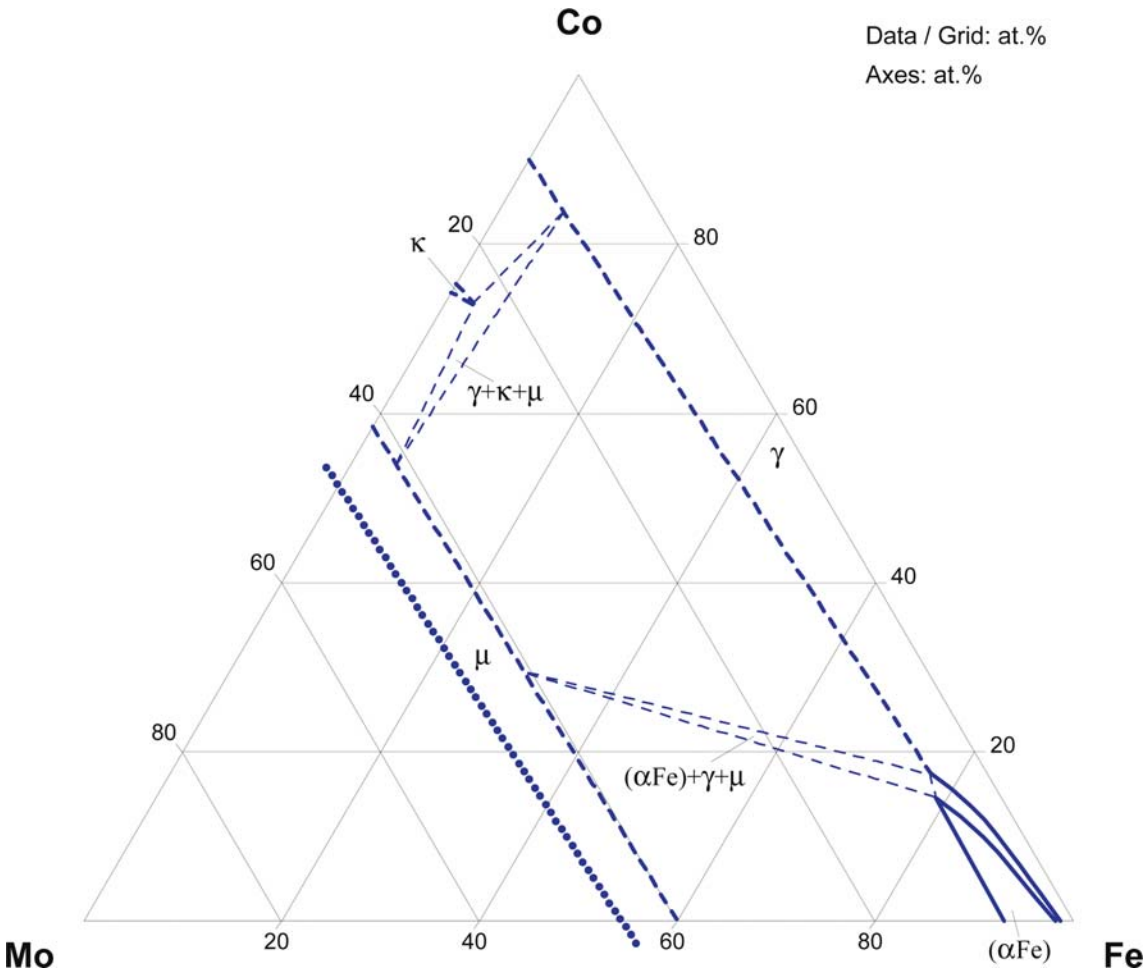

Fig. 5. Co-Fe-Mo. Partial isothermal section at 982°C

DOI: 10.1007/978-3-540-74196-1_21

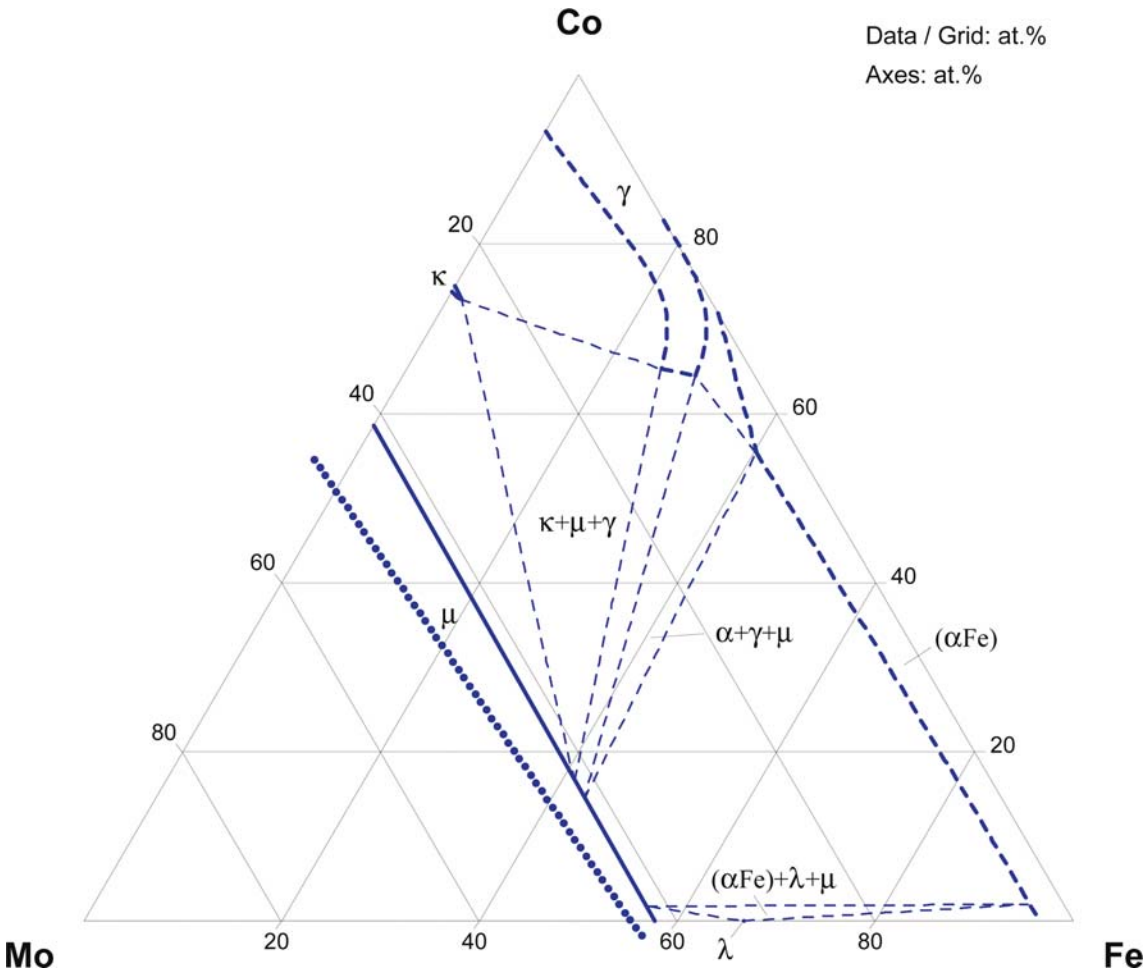

Fig. 6. Co-Fe-Mo. Partial isothermal section at 800°C

DOI: 10.1007/978-3-540-74196-1_21

References

[1932Koe1] Koester, W., Tonn, W., "The System Iron-Cobalt-Molybdenum" (in German), *Arch. Eisenhuettenwes*., **5**(12), 627–630 (1932) (Experimental, Morphology, Phase Diagram, Phase Relations, 5)

[1932Koe2] Koester, W., "Mechanical and Magnetic Properties of Iron-Cobalt-Tungsten and Iron-Cobalt-Molybdenum Alloys" (in German), *Arch. Eisenhuettenwes*., **6**(1), 17–23 (1932) (Magn. Prop., Mechan. Prop., Experimental, 10)

[1949Jae] Jaenecke, E., "Co-Fe-Mo" (in German), *Kurzgefasstes Handbuch aller Legierungen*, Winter, Heidelberg, 638–639 (1949) (Phase Diagram, Phase Relations, Review)

[1952Das] Das, D.K., Rideout, S.P., Beck, P.A., "Intermediate Phases in the Mo-Fe-Co, Mo-Fe-Ni and Mo-Ni-Co Ternary Systems", *Trans. Amer. Inst Min. Met. Eng*., **194**(10), 1071–1075 (1952) (Crys. Structure, Experimental, Morphology, Phase Diagram, Phase Relations, 23)

[1953Das] Das, D.K., Beck, P.A., "Survey of Portions of the Iron-Nickel-Molybdenum and Cobalt-Iron-Molybdenum Ternary Systems at 1200°C", *Nat. Adv. Com. Aeronautic*, Techn. Note 2896, 2896, 1–56 (1953) (Crys. Structure, Experimental, Morphology, Phase Diagram, Phase Relations, 15)

[1971Dom] Domagala, R.F., Simcoe, C.R., "Unusual Microstructure in Quenched Iron-Molybdenum-Cobalt Alloys", *Metallography*, **4**(6), 569–571 (1971) (Experimental, Morphology, Phase Diagram, 3)

[1971Wes] West, D.R.F., "The Constitution of Fe-Rich Alloys of the Fe-Cr-Co-Mo System - a Review" (in German), *Kobalt*, (51), 68–80 (1971) (Crys. Structure, Phase Diagram, Phase Relations, Review, 104)

[1972Dom] Domagala, R.F., Simcoe, C.R., "The Iron-Molybdenum-Cobalt System" (in German), *Kobalt*, **54**, 11–14 (1972) (Experimental, Morphology, Phase Diagram, Phase Relations, 9)

[1974Edn] Edneral, A.F., Zhukov, O.P., Perkas, M.D., "Effect of Cobalt on Ageing of Martensite and Ferrite in Fe-Co-W and Fe-Co-Mo Alloys", *Met. Sci. Heat Treat*., **16**(9–10), 840–843 (1974) (Morphology, Experimental, Mechan. Prop., 6)

[1979Nis] Nishizawa, T., Hasebe, M., Ko, K., "Thermodynamic Analysis of Solubility and Miscibility Gap in Ferromagnetic α Iron Alloys", *Acta Met*., **27**, 817–828 (1979) (Calculation, Theory, Phase Diagram, Thermodyn., 40)

[1979Pro] Prokof'yev, D.I., Kurbatkina, O.L., "Phase Diagram of the Fe-Co-Mo Ternary System", *Russ. Metall.*, (2), 164–166 (1979), translated from *Izv. Akad. Nauk SSSR, Met.*, (2), 204–208 (1979) (Experimental, Phase Diagram, Phase Relations, 9)

[1979Tok] Tokunaga, Y., Kusaba, T., "Strain Aging of Fe-Co-Mo Alloys" (in Japanese), *J. Jpn. Inst. Met.*, **39**(1), 13–19 (1975) (Phase Relations, Experimental, Thermodyn., Electr. Prop., Mechan. Prop., 22)

[1979Sha] Shaposhnikov, N.G., Mogutnov, B.M., Edneral, A.F., "Influence of Cobalt on the Solubility of the Laves Phase Fe_2Mo in Maraging Steels", (in Russian), *Fiz. Met. Metalloved.*, **48**(2), 285–291 (1979) (Phase Relations, Morphology, Thermodyn., Calculation, Experimental, Mechan. Prop., 14).

[1980Loo] van Loo, F.J.J., Bastin, G.F., Vrolijk, J.W.G.A., Hendricks, J.J.M., "Phase Relations in the Systems Fe-Ni-Mo, Fe-Co-Mo and Ni-Co-Mo at 1100°C", *J. Less-Common Met*., **72**(2), 225–230 (1980) (Experimental, Phase Diagram, Phase Relations, Crys. Structure, Morphology, 11)

[1982Gui1] Guillermet, A.F., "The Fe-Mo (Iron-Molybdenum) System", *Bull. Alloy Phase Diagrams*, **3**(3), 359–367 (1982) (Phase Diagram, Phase Relations, Thermodyn., Crys. Structure, Assessment, Calculation, 40)

[1982Gui2] Guillermet, A.F., "An Assessment of the Fe-Mo System", *Calphad*, **6**(2), 127–140 (1982) (Phase Diagram, Phase Relations, Thermodyn., Assessment, Calculation, 40)

[1983Kub] Kubaschewski, O., Hoster, T., "Enthalpy of Formation and Transformation in Binary and Ternary Systems of the Metals Iron, Cobalt, Nickel and Molybdenum" (in German), *Z. Metallkd*., **74**(9), 607–609 (1983) (Experimental, Thermodyn., 8)

DOI: 10.1007/978-3-540-74196-1_21

[1984Eri] Eriksson, G., Hack, K., "Calculation of Phase Equilibria in Multicomponent Alloy Systems Using a Specially Adapted Version of the Program SOLAGASMIX", *Calphad*, **8**(1), 15–24 (1984) (Calculation, Phase Diagram, Phase Relations, 24)

[1984Ray] Raynor, G.V., Rivlin, V.G., "Phase Equilibria in Iron Ternary Alloys. XV. Critical Evaluation of Ternary Alloys of Iron and Molybdenum with Cobalt, Chromium, Manganese, and Nickel", *Int. Metall. Rev.*, **29**(5), 329–375 (1984) (Phase Diagram, Phase Relations, Review, 70)

[1985Koz] Kozakai, T., Aihara, H., Doi, M., Miyazaki, T., "Spinodal Decomposition in Fe-Mo-Co and Fe-Mo-V Ternary Systems", *Trans. Iron Steel Inst. Jpn*., **25**(1), 159–164 (1985) (Calculation, Crys. Structure, Experimental, Morphology, Phase Diagram, Theory, Thermodyn., Mechan. Prop., 8)

[1985Mor] Morinaga, M., Yukawa, N., Ezaki, H., "Solid Solubilities in Transition-Metal-Based f.c.c. Alloys", *Philos. Mag. A*, **51**(2), 223–246 (1985) (Phase Diagram, Phase Relations, Calculation, 45)

[1986Mit] Mitra, M., Lange, K.W., "Measurements and Estimates of Hydrogen Solubilities in Liquid Iron-Cobalt-Molybdenum Alloys", *Steel Research*, **57**(11), 552–556 (1986) (Phase Relations, Thermodyn., Calculation, Experimental, 22)

[1988Ray] Raynor, G.V., Rivlin, V.G., "Co-Fe-Mo", *Phase Equilibria in Iron Ternary Alloys*, Institute of Metals, London, 233–247 (1988) (Phase Diagram, Review, #, 6)

[1991Nik] Nikolin, B.I., Babkebich, A.Yu., Izdkovskaya, T.V., Petrova, S.N., "Change of Crystalline Structure of Martensite on the Alloying of Co-W and Co-Mo Alloys with a Third Element" (in Russian), *Fiz. Met. Metalloved.*, 5, 99–105 (1991) (Morphology, Experimental 7)

[1993Nik] Nikolin, B.I., Babkevich, A.Yu., Izdkovskaya, V., Petrova, S.N., "Effect of Heat Treatment on the Crystalline Structure of Martensite in Iron-, Nickel-, Manganese- and Silicon-Doped Co-W and Co-Mo Alloys.", *Acta Metall. Mater.*, **41**(2), 513–515 (1993) (Morphology, Experimental, 9)

[1999Dav] Davydov, A., Kattner, U.R., "Thermodynamic Assessment of the Co-Mo System", *J. Phase Equilib.*, **20**(1), 5–16 (1999) (Phase Diagram, Phase Relations, Thermodyn., Assessment, Calculation, 45)

[2001Che] Chen, S-L., Daniel, S., Zhang, F., Chang, Y.A., Oates, W.A., Schmid-Fetzer, R., "On the Calculation of Multicomponent Stable Phase Diagrams", *J. Phase Equilib.*, **22**(4), 373–378 (2001) (Phase Relations, Calculation, Theory, 26)

[2001Sar] Sarkar, S., Bansal, C., "Kinetic Paths for *B*2 Order in Nanocrystalline FeCo-Mo: A Mössbauer Spectroscopic Study", *Acta Mater*, **49**(10), 1789–1792 (2001) (Crys. Structure, Experimental, 16)

[2002Boz] Bozzolo, G.H., Noebe, R.D., Amador, C., "Site Occupancy of Ternary Additions to *B*2 Alloys", *Intermetallics*, **10**, 149–159 (2002) (Crys. Structure, Review, 27)

[2002Ohn] Ohnuma, I., Enoki, H., Ikeda, O., Kainuma, R., Ohtani, H., Sundman, B., Ishida, K., "Phase Equilibria in the Fe-Co Binary System", *Acta Mater.*, **50**, 379–393 (2002) (Assessment, Calculation, Experimental, Phase Relations, Thermodyn., 50)

[2003Dav] Davydov, A., Kattner, U.R., "Revised Thermodynamic Description of the Co-Mo System", *J. Phase Equilib.*, **20**(1), 5–16 (1999) (Phase Diagram, Thermodyn., Assessment, Calculation, 14)

[2005Hou] Houserova, J., Vešt'ál, J., Sob, M. "Phase Diagram Calculations in the Co-Mo and Fe-Mo Systems using First-Principles Results for the σ Phase", *Calphad*, **29**(2), 133–139 (2005) (Phase Diagram, Phase Relations, Thermodyn., Assessment, Calculation, 34)

[Mas2] Massalski, T.B. (Ed.), *Binary Alloy Phase Diagrams*, 2nd edition, ASM International, Metals Park, Ohio (1990)

[V-C2] Villars, P. and Calvert, L.D., *Pearson's Handbook of Crystallographic Data for Intermetallic Phases*, 2nd edition, ASM, Metals Park, Ohio (1991)

DOI: 10.1007/978-3-540-74196-1_21

Cobalt – Iron – Nickel

Jean-Claude Tedenac

Introduction

The Co-Fe-Ni system is of great industrial and technological importance as a basis for a number of commercial alloyed steels (Invar alloys, for instance), Ni-superalloys, bulk and layered magnetic materials. Since the first experimental work of [1909Jae], the liquid-solid and solid-solid phase equilibria were experimentally studied by [1927Kas, 1939Wym1, 1939Wym2, 1957Vit1, 1957Vit2, 1969Koe, 1977Wid, 1973Ser, 1995She]. [1927Kas] reported the liquidus surface. Isothermal sections at 400 to 800°C were constructed by [1957Vit1, 1957Vit2, 1969Koe, 1973Ser, 1977Wid], the temperature-composition sections - by [1927Kas, 1957Vit1, 1957Vit2, 1969Koe, 1977Wid]. Thermodynamic calculations of the Co-Fe-Ni phase diagram were performed by [1973Kau, 1974Kau, 1987Gui, 1989Gui, 1989Kum, 1995Hai]. The system was critically evaluated several times by [1930Kue, 1940Bra1, 1940Bra2, 1949Jae, 1981Riv, 1988Ray, 2005Sou] and updated by [1994Rag].
[1970Gom1, 1970Gom2, 1975Mal1, 1975Mal2, 2002Boz] reported the influence of Co and Ni on the superstructure of Ni_3Fe and CoFe, respectively.
Large amount of works concerns magnetic, electrical, mechanical properties, thin films of the Co-Fe-Ni compositions. The experimental researches of the ternary Co-Fe-Ni system are summarized in Table 1.

Binary Systems

The Co-Fe, Fe-Ni and Co-Ni binary systems are accepted from [2002Ohn], [2007Kuz] and [Mas2], respectively.

Solid Phases

The Co-Fe-Ni solid phases are reported in Table 2. No ternary compounds form in the system. The system is characterized by the component based solid solutions and by the binary phases Fe_3Ni and CoFe. According to [1970Gom1, 1970Gom2], Fe_3Ni dissolves up to 10-12 at.% Co, and according to [1975Mal1, 1975Mal2], at 400°C CoFe dissolves 5-10 at.% Ni. These results correspond well to data of [1957Vit1, 1957Vit2]. [1970Gom1, 1970Gom2, 2002Boz] state that in these compounds Ni and Co substitute for each other.

Liquidus, Solidus and Solvus Surfaces

By the method of thermal analysis [1927Kas] first constructed the liquidus surface of the system. It involves two fields of primary crystallization of the phases (δFe) and (αCo,γFe,Ni), divided by the monovariant peritectic type curve p_1p_2 of the joint crystallization. The temperature decreases from the Fe-Ni towards the Co-Fe binary.
Based on data by [1927Kas], [1988Ray] calculated the liquidus and solidus surfaces. The later is characterized by the wide single phase fields (δFe) and (αCo,γFe,Ni) and by a respective narrow two-phase region. Tentative liquidus surface shown in Fig. 1 is drawn after [1988Ray] but adjusted to the accepted binary systems.

Isothermal Sections

The phase boundaries between (αFe) (bcc) and (αCo,γFe,Ni) (fcc) were experimentally determined by [1969Koe] and [1977Wid] and given as the fragments of isothermal sections at 800, 700, 600, 500°C [1969Koe], and at 800, 750, 700, 650°C [1977Wid]. The sections of [1969Koe] involve the concentration interval up to 40 mass% Ni and up to 80 mass% Co, [1977Wid] considers the Fe-portion of the system. Calculated sections are reported for 950, 850 [1989Kum], 800, 750, 650 [1974Kau, 1987Gui, 1989Gui],

DOI: 10.1007/978-3-540-74196-1_22

700, 500 [1987Gui, 1989Gui], 600 [1974Kau, 1987Gui, 1989Gui, 1995Hai], 510°C [1995Hai]. The Fe-portions of the sections at 950 to 650°C calculated by [1989Kum] do not correspond to the accepted here binaries, and are not assumed in the present evaluation. [1974Kau] calculated the sections at 377 to 1527°C, however, the details are given only for the sections at 800 and 600°C. The iron rich regions of the experimental and the calculated isothermal sections at 800, 750, 700 and 650°C presented in Figs. 2a, 2b, 2c, 2d are adjusted to the accepted binary systems. In the critical assessment [1988Ray] has underlined a satisfactory agreement of the two sets of experimental data at 700°C, while at 800°C significant discrepancy exists regarding the location of the (αFe)+(αCo,γFe,Ni) / (αCo,γFe,Ni) phase boundary. Data of [1977Wid] correspond to the thermodynamic descriptions of [1973Kau, 1974Kau, 1987Gui, 1989Gui] better than those of [1969Koe].
[1994Rag] summarized the available results on phase equilibria and presented isothermal sections in the whole concentration intervals at 800 and 500°C, based on data of [1969Koe, 1989Gui]. Figure 3 shows the section at 500°C, adjusted to the accepted binary systems.
[1957Vit1] and [1957Vit2] reported portions of the isothermal sections at 400°C in the vicinity of $FeNi_3$ and at 500 and 600°C in the vicinity of FeCo. These, however, show only the solubility of the third component in the binary phases.
[1988Ray] presented schematic isothermal sections at 911 to 985°C, showing narrowing of the (αFe) region when the temperature increases.

Temperature – Composition Sections

[1927Kas] constructed the temperature-composition sections for the temperatures below the solidus along the isoconcentrates 10, 20, 30, 40, 50, 60, 70, 80 and 90 mass% Ni, and 10, 20, 30, 60 and 80 mass% Co. The temperatures of polymorphous and magnetic transformations were determined by dilatometric and magnetic analyses. As being based on the previous versions of the binaries, these are not accepted here. [1957Vit1] proposed fragments of the vertical section $FeNi_3$-Co. [1957Vit2] gave vertical sections along the FeCo-Ni line and along the isoconcentrates of 2, 5 and 8 at.% Ni, which can be accepted as tentative in the temperature interval ~800-1000°C. Fragments of the sections at 10, 20, 40 mass% Co, and 50Fe50Co-Ni are given by [1969Koe]. [1977Wid] constructed parts of the sections involving the (αFe)+(αCo,γFe,Ni) equilibrium at 2.5, 5 and 7.5 mass% Co. [2005Sou] reports the FeCo-Ni (mass%) vertical section based on isothermal sections [1981Riv, 1969Koe, 1977Wid]. It is shown in Fig. 4.

Thermodynamics

By studying vapor-liquid equilibrium, [1978Sir] gave isopressure curves of the vapor over liquid alloys and isolines of the free energy at 2222°C. By the same method [1988Ale] determined activities of the components in the liquid at 1600°C. After [1980Fra], [2000Tse] and [2005Mor] also measured activity of the components in the ternary melts at 1600°C. The results agree well. [2003Mor] reported the integral Gibbs energy and the enthalpy of mixing of liquid alloys at this temperature. These results are in satisfactory agreement with data of [2004Tom1] obtained by the Knudsen cell mass spectrometry at 1578°C. [1983Bar, 1985Gok] used the Margules equations to calculate the activity coefficients of the components at 1552°C, based on the binary data. The system in the liquid state is characterized by negative deviations from the ideal behavior with significant and insignificant asymmetry near the Fe-Ni and Co-Fe binaries, respectively, and by ideal behavior near to the Co-Ni binary system. [2005Ziv] calculated the viscosity of liquid ternary alloys at 1600°C from the binary data by Redlich-Kister formalism. The isoviscosity curves were constructed.
By the Knudsen cell mass spectrometry [2004Tom2] measured the molar excess properties (Gibbs energy, enthalpy of mixing, entropy) and activities of the components in (αCo,γFe,Ni) ternary solid solution at 1327°C. By the Knudsen method [1976Vel] measured the activities of the components at 1227°C. Their behavior is close to ideal. Excess free enthalpy and mixing enthalpy were also calculated. Previously the excess integral Gibbs free energy and the chemical potentials were derived from mass spectrometry data by [1969Nec].
Calculated by the Calphad method thermodynamic properties of (αCo,γFe,Ni) [1987Gui, 1989Gui] show rather good agreement of activities (a_{Ni}) with those reported by [1976Vel] along the section Ni_3Co-Fe, while

DOI: 10.1007/978-3-540-74196-1_22

the experimental a_{Co} and a_{Fe} are essentially lower than the calculated values. Along the section FeCo-Ni a_{Ni} and a_{Fe} well agree, and the experimental a_{Co} are essentially higher than the calculated ones. Along the section Ni_3Co-Fe a_{Fe} and a_{Co} agree well, experimental a_{Ni} are somewhat higher than calculated. [1985Col] has carried out *ab-initio* calculations of the heat of formation of solid alloys along three sections Ni/Co–Fe (Ni/Co=1/4, 1/1, 4/1). The results are in reasonable agreement with experimental data [1972Spe] for these sections. Enthalpy of formation of Co-Fe-Ni alloys at 1200°C, as measured [1973Spe] and calculated by Calphad technique [1987Gui, 1989Gui] is given in Table 3. The fit between calculated and experimental results is satisfactory.

By a low temperature differential thermal analysis technique [1965Gol] has measured the heat of martensitic transformation (fcc→bcc) in the alloy Fe-31.3Ni-5.7Co mass%). [2001Gho] have calculated this value by using the developed database kMART (kinetics of MARtensitic Transformation) and SSOL database of the Thermocalc software. Experimental and calculated ΔH shows, all in $J \cdot mol^{-1}$: –900±90 (experimental), –918 (SSOL) and –783 (kMART). Kinetics of the martensitic transformation in Fe-Ni alloys with low additions of Co was studied also by [2000Rag]. The mechanism of the transformation, depending on Co content and on the heating rate was investigated by [1977Ser]. Using a Thermocalc software, [1995Hai] calculated free-energy isolines of the fcc and bcc phases at 27°C, and the free-energy change for the martensitic transformation at this temperature.

[1939Kay] reported the specific heat capacity of the ternary alloys at heating.

Notes on Materials Properties and Applications

[1931Mas, 1939Wym1, 1939Wym2] measured thermal expansion of the ternary alloys, and [1931Mas] gives the diagram of iso-coefficients of thermal expansion. Composition dependences of elastic modulus are given by [1969Koe].

[1957Vit1, 1957Vit2] studied the temperature dependencies of electrical resistance of annealed and quenched ternary alloys in a wide composition range. [1932Kue, 1969Koe] measured magnetic properties of the alloys. [1929Mas] reported on the intensity of magnetization for 5 alloys of the following compositions (in mass%): 9.90%Co-5%Ni-85.1%Fe, 10%Ni-80.1%Fe, 20%Ni-70.1%Fe, 25%Ni-65.04%Fe, 28% Ni-62.04%Fe.

[1970Col, 1991Ach1, 1991Ach2] studied the influence of thermal and mechanical history, microstructure, composition on electrical and magnetic properties (coercive force, magnetization) of alloys at the austenite → martensite transformation.

[1991Ach2] measured the composition dependence of the resistivity for seven alloys varying the Co content from 11 to 7 at.%.

[1994Miy] determined the isocurves of zero saturation magnetostriction at room temperature, necessary for soft magnetic materials.

[1963Art, 1964Pil] developed the model of Zener and Carr to predict the Curie temperatures in the ternary alloys, based on the binary data. For the Co-Fe-Ni system the predicted values correspond to the experimental ones within 30°C.

[1972Sch] reported the magnetic moment of Fe μ_{Fe} in the Co-Fe-Ni fcc solid solution to decrease when Fe and Co concentrations increase from 10 to 30 at.% Fe and from 0 to 80 at.% Co, respectively. According to [1979Sch], μ_{Co} increases against Co concentration and decreases when Fe concentration increases from 0 to 40 at.%.

Fast development of electronics, tape recording, computer technologies has caused extensive study of magnetic thin films with high saturation magnetization, *e.g.* [2001Koh, 2001Liu, 2001Ohs, 2001Osa], magnetic multilayers with Giant magnetoresistance (NiFeCo/Cu) [2001Mta].

[1927Kas] measured hardness of as-cast Co-Fe-Ni alloys and determined iso-hardness curves in the whole concentration range. Maximum values were observed at 25-50 mass% Co and 10-20 mass% Ni, corresponding to a sharp decrease of the temperature of the (γFe) → (αFe) transformation. Vickers hardness of annealed (400-490°C for 1500 h) and quenched (from 500-1000°C) alloys was measured by [1957Vit1, 1957Vit2]. Hardness and elasticity modulus are given by [1969Koe], as well.

[2005Zar] have shown non-monotonous temperature dependencies of dynamic yield and fracture stress of two refractory Ni based Co-Fe-Ni alloys (IN738LC and PWA 1483) for gas turbines measured under

DOI: 10.1007/978-3-540-74196-1_22

shock-wave loading at up to 680°C. This is accounted for by structural rearrangement in γ-matrix. Local atomic configurations in Elinvar alloys based on Co-Fe-Ni is presented in [1986Vla].
In their reviews [2004Sun] and [2005Sou] mentioned Ni among the prospective ternary additions to CoFe structural intermetallic, providing the balance of mechanical and magnetic properties. When added to the conventional CoFe-2V alloy, Ni results in a significant increase of ductility and in a stability of elongation and yield stress against the heat treatment temperature.
[2005Kai] studied oxidation of the single-phase equi-molar alloy CoFeNi in dry air at 800-1000°C. The oxidation kinetics follows the two-stage parabolic law with the constants increasing with the temperature. The scales formed consisted of three oxide layers: FeCoNi/$CoNiO_2$+Fe_3O_4/Fe_3O_4/CoO.
[1966Blo, 1971Blo] have shown that solubility of nitrogen (1550-1700°C) and hydrogen (1500-1700°C), respectively, in liquid Co-Fe-Ni alloys follows the Sievert's law for all the concentrations.
[1980Sri] summarized the works on the preparation of thin films by electrodeposition in aqueous solutions.
[1986Lee] studied the production and properties of Co-Fe-Ni diffusion coatings on carbon steels, which are shown to be more effective than electrodeposites.
By using the tight-binding linearized muffin-tin orbital method combined with the coherent-potential approximation (TB-LMTO-CPA) the total energies, bulk moduli, equilibrium lattice parameters, magnetic moments, and hyperfine fields of bcc solid solution were calculated by [2000San], and are in qualitative agreement with experimental trends.
In the reviews of [2005Sou, 2005Sun] the influence of the alloying elements (including Ni) on mechanical and magnetic properties of the FeCo intermetallic are considered.

Miscellaneous

In the review [1978Tho] the TEM micrograph and electron diffraction picture of a Co-Fe-Ni alloy (composition not specified) are given to discuss appearance of double reflections.
[2000Mue] presented magnetic properties of amorphous and partly crystallized multicomponent alloys $(Co,Fe,Ni)_{86}Zr_7B_6Cu$.
[2006Yoo] proposed the Co-Fe-Ni "continuous phase diagram" (CPD) representing phase composition at different concentration of the elements in thin films. Two very narrow amorphous regions were detected.

DOI: 10.1007/978-3-540-74196-1_22

Table 1. Experimental Investigations of the Co-Fe-Ni System

Reference	Method / Experimental Technique	Temperature / Composition / Phase Range Studied
[1939Wym1] [1939Wym2]	Sintering of the pressed bars at 1350°C for 32 h in hydrogen; hot working; annealing at 1100°C for 1 h in hydrogen; thermal expansion; metallography.	–200-1000°C / temperature of solid-state transformations
[1927Kas]	DTA, microstructure analysis, hardness, magnetic properties, thermal expansion measurements	Liquidus surface, vertical sections below solidus at 10, 20, 30, 40, 50, 60, 70, 80, 90 mass% Ni and 10, 20, 30, 60, 80 mass% Co / full concentration interval.
[1931Mas]	Thermal expansion, magnetization measurements	Liquid air temperature – 700°C / full concentration interval.
[1932Kue]	α-γ phase transformations, magnetic properties measurements at 450-552°C	0-800°C / $Co_{0.25}Ni_{0.45}Fe._3$
[1939Kay]	Heat capacity; magnetization measurements	C_p temperature dependence (at 100-800°C) of (10-20)Co-25Fe-(65-55)Ni, 58Co-22Fe-22Ni, 75Co-(5;20)Fe-(20;5)Ni; magnetic field 0-1.5 Oe for μ; 0-30 Oe for permeability of Invar alloys
[1957Vit1]	Preparation from powders; annealing at 400-490°C for 1500 h; microstructure analysis; Vickers hardness; electrical resistance.	Concentration dependence of H and ρ; temperature dependence of ρ partial isothermal section at 400°C in the vicinity of $FeNi_3$; partial vertical section Fe_3Ni-Co below 500°C.
[1957Vit2]	Hardness measurements	Annealed 500°C/ < 21 at.% Co
[1966Blo]	Solubility of N in liquid alloys/nitrogen pressure measurements	1600°C/the ternary/ concentration dependence of the N content
[1969Koe]	Metallography/DTA	Annealed at 500-800°C/ 0 < at.%Ni < 40
[1970Col]	Dilatometry	525°C < T < 725°C/ 11.8Co-57.3Fe-30.1Ni, mass%
[1970Gom1]	Neutron diffraction	Around the compound Ni_3Fe / <12 at.% Co
[1970Gom2]	Neutron diffraction	Around the compound Ni_3Fe / <12 at.% Co
[1971Blo]	Solubility of hydrogen in liquid Fe-Co-Ni alloys	1600°C/concentration dependence of H content (in mass%)
[1972Sch]	Mössbauer effect / magnetic moment on Fe in ternary alloys Co-Fe-Ni	Co concentration dependence of the magnetic moment of iron
[1972Spe]	Adiabatic calorimeter / calorimetric measurement from 200°C to the alloying temperature of 1200°C	Concentration dependence of the enthalpy of Co-Fe-Ni alloys

(*continued*)

DOI: 10.1007/978-3-540-74196-1_22

Reference	Method / Experimental Technique	Temperature / Composition / Phase Range Studied
[1973Ser]	Metallography, DTA, dilatometry, thermagnetic measurements	25 - 820°C/ 39 alloys with Ni/Fe ratio = 0.064 - 0.43 (mass%)
[1973Spe]	Adiabatic calorimeter/ calorimetric measurement from 200°C to the alloying temptress of 1200°C	Concentration dependence of the enthalpy of Co-Fe-Ni alloys
[1975Mal1] [1975Mal2]	Neutron diffraction, Mössbauer spectroscopy	$507 < T < 1070$/ 0.25-0.75 at.% Co /$L2_0$
[1976Vel	Activities, effusion cells	1227°C / Co-Fe-Ni alloys
[1977Ser]	Metallography, DTA	Co-Fe-Ni /maraging alloys
[1977Wid]	DTA, Microscopy	650-800°C (four sections) / all compositions in the ternary/(α+β)
[1978Sir]	Vapor pressure measurements, activities	2227°C, all compositions in the ternary
[1979Sch]	Neutron diffraction, Mössbauer spectroscopy, phase transitions	Room temperature, Nickel rich corner
[1980Fra]	Activity measurements by Knudsen cell mass spectrometry	Condensation processes in the solar nebula
[1983Bar] [1985Gok]	Activities, /pressure measurements	Co-Fe-Ni and Co-Fe-Ni-S/ 1552°C
[1986Lee]	Diffusion coating/plating deposition in sulphamate bath	$900°C < T < 1100°C$ / 94 at.% Ni, 4 at.% Co / coatings on AISI1022
[1986Vla]	Electrodeposition from aqueous solution	60°C / 0.2Co-0.4Fe-0.4Ni, at.%
[1988Ale]	Activities / liquid-vapor equilibrium	1623°C, the entire composition range
[1991Ach1]	Magnetic measurements/ α-γ phase transitions	$800°C < T < 1000°C$ / $(Fe_xNi_{1-x})_yCo_{100-y}$
[1991Ach2]	Magnetic properties / magnetization saturation	$(Fe_xNi_{1-x})_yCo_{100-y}$/ α-γ transformation
[1993Tom1]	Knudsen effusion cells method/Activities measurements / Computer-aided Knudsen cell mass spectrometry	1577°C / $Fe_xNi_xCo_{1-2x}$ liquid ternary alloys
[1993Tom2]	Knudsen effusion cells method / Activities measurements / Computer-aided Knudsen cell mass spectrometry	1227-1417°C / $Fe_xNi_xCo_{1-2x}$ solid ternary alloys
[1994Miy]	fcc crystal structure, magnetostriction	Room temperature/compositions over at.% Ni and at.% Co = 25
[2000Mue]	Magetostriction/coercive field	(FeCoNi)-ZrBCu amorphous
[2000Rag]	Martensitic transformation / C-curves	T = 200-280 K / $Co_{28.4}Ni_{0.2}$Mn-Fe

(*continued*)

DOI: 10.1007/978-3-540-74196-1_22

Reference	Method / Experimental Technique	Temperature / Composition / Phase Range Studied
[2000Tse]	Activities measurements / isopiestic method	1600°C / all compositions in the ternary
[2001Koh]	Mössbauer spectroscopy	2 at.% Co, 1.8 at.% Ni, bcc Fe
[2001Liu]	Pulsed-current electrodeposition/ thin films	Room temperature / γ-α mixture
[2001Mta]	Magnetoresistance/ giant magnetoresistance	(NiFeCo/Cu)
[2001Ohs]	Electrodeposition / electroplated films	$Co_{90-x}Ni_{10}Fe_x$, $8 < x < 40$
[2001Osa]	Resistivity measurements / electrodeposited CoNiFe thin films	$Co_{73}Ni_{12}Fe$
[2004Tom1] [2004Tom2]	Activities measurements / Knudsen effusion cells	1327°C/ all compositions in the ternary / fcc
[2005Kai]	Air oxidation, X-ray, TGA, EDS, EPMA measurements	800°C < T < 1000°C, 0.337 at.% Co, 0.31 at.% Fe, 0.353 at.% Ni / γ phase
[2005Zar]	Dynamic yield, fracture stress, shock wave method	< 680°C / single crystal / 35Co-28Ni-25Fe, mass%
[2006Yoo]	X-ray diffraction, FWHM measurements	Full width half maximum used for identification of amorphous phases

Table 2. Crystallographic Data of Solid Phases

Phase/ Temperature [°C]	Range	Pearson Symbol/ Space Group/ Prototype	Lattice Parameters [pm]	Comments/References
(εCo) < 422		*hP*2 $P6_3/mmc$ Mg	a = 250.71 c = 406.86	at 25°C [Mas2]
(εFe)		*hP*2 $P6_3/mmc$ Mg	a = 246.8 c = 396.0	at 25°C, 13 GPa [Mas2]
(δFe) 1538 - 1394		*cI*2 $Im\bar{3}m$ W	a = 293.15	[Mas2]
(αFe) < 912 $Co_xFe_{(1-x)}$		*cI*2 $Im\bar{3}m$ W	a = 286.65 a = 286.07 to 283.68 a = 286.60 to 284.25	pure Fe at 25°C [Mas2] dissolves up to 77 at.% Co [2002Ohn] $0 < x < 0.7$, 750°C [V-C2] $0 < x < 0.7$, 750°C [V-C2]

(*continued*)

DOI: 10.1007/978-3-540-74196-1_22

Phase/ Temperature Range [°C]	Pearson Symbol/ Space Group/ Prototype	Lattice Parameters [pm]	Comments/References
γ, (αCo,γFe,Ni)	*cF*4		
(αCo)	$Fm\bar{3}m$	a = 356.88	at 520°C [V-C2]
1495 - 422	Cu	a = 354.47	[Mas2]
(γFe)		a = 364.67	at 915°C [V-C2, Mas2]
< 1394 - 912			
(Ni)		a = 352.40	at 25°C [Mas2]
< 1455			
α', Co_xFe_{1-x}	*cP*2	a = 285.27 to 284.34	x = 0.45 - 0.60 at 575°C [V-C2]
< 735	$Pm\bar{3}m$		
	CsCl		
$FeNi_3$	*cP*4	a = 355.23	63 to 85 at.% Ni [2007Kuz]
< 517	$Pm\bar{3}m$		
	$AuCu_3$		

Table 3. Experimental [1973Spe] and Calculated [1987Gui, 1989Gui] Enthalpy of Formation of Co-Fe-Ni Alloys at 1200°C [J·mol^{-1}]

Composition			$\Delta_f H°$(exp.)	$\Delta_f H°$(calc.)
x_{Fe}	x_{Co}	x_{Ni}		
0.9	0.08	0.02	–402±71	–545
0.9	0.02	0.08	–544±138	–382
0.8	0.16	0.04	–778±38	–1023
0.7	0.15	0.15	–1389±159	–1349
0.445	0.11	0.445	–3238±335	–2775
0.445	0.445	0.11	–1171±230	–1438
0.4	0.2	0.4	–2841±178	–2941
0.333	0.333	0.333	–2176±280	–2049
0.25	0.5	0.25	–1443±259	–1510
0.19	0.76	0.05	–648±159	–886
0.167	0.167	0.667	–2653±427	–2232
0.167	0.667	0.167	–1088±50	–1021
0.11	0.445	0.445	–1079±485	–1109
0.05	0.76	0.19	–385±234	–375

DOI: 10.1007/978-3-540-74196-1_22

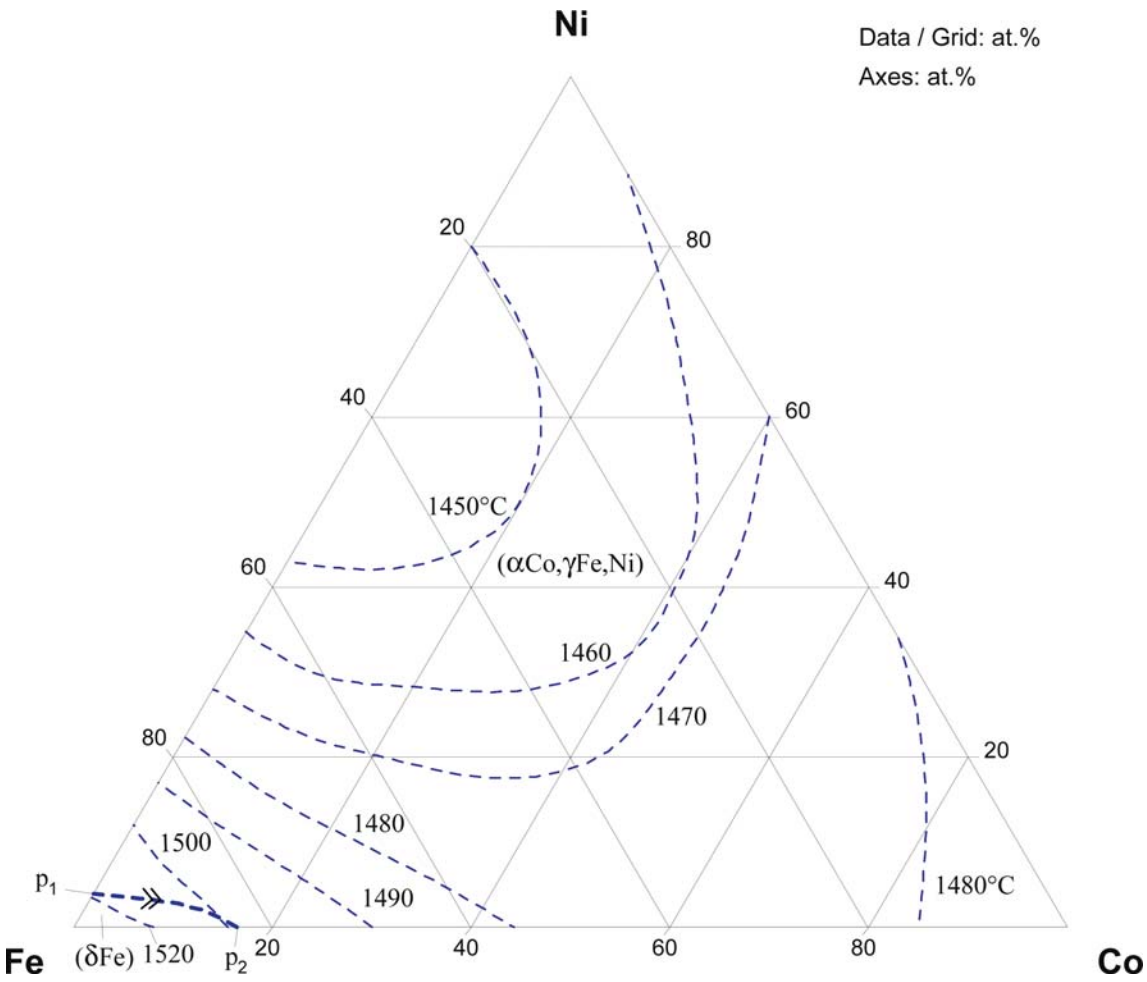

Fig. 1. Co-Fe-Ni. Liquidus surface projection

DOI: 10.1007/978-3-540-74196-1_22

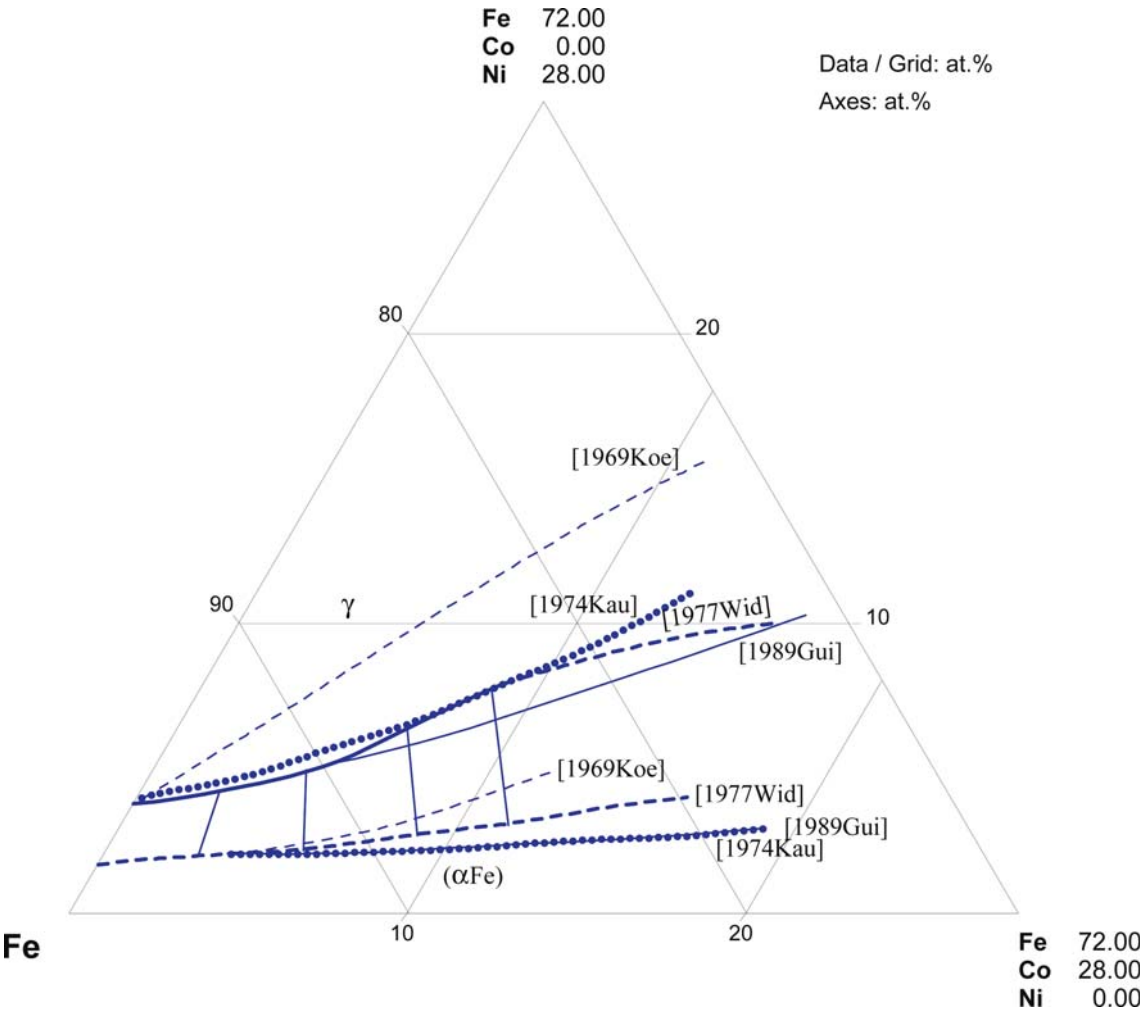

Fig. 2a. Co-Fe-Ni. Isothermal sections in the Fe rich corner at 800°C. Thick lines - experimental data [1977Wid]; thin curves - calculation [1987Gui, 1989Gui]; dashed thin lines– experimental data [1969Koe]; dotted lines- calculation [1974Kau]

DOI: 10.1007/978-3-540-74196-1_22

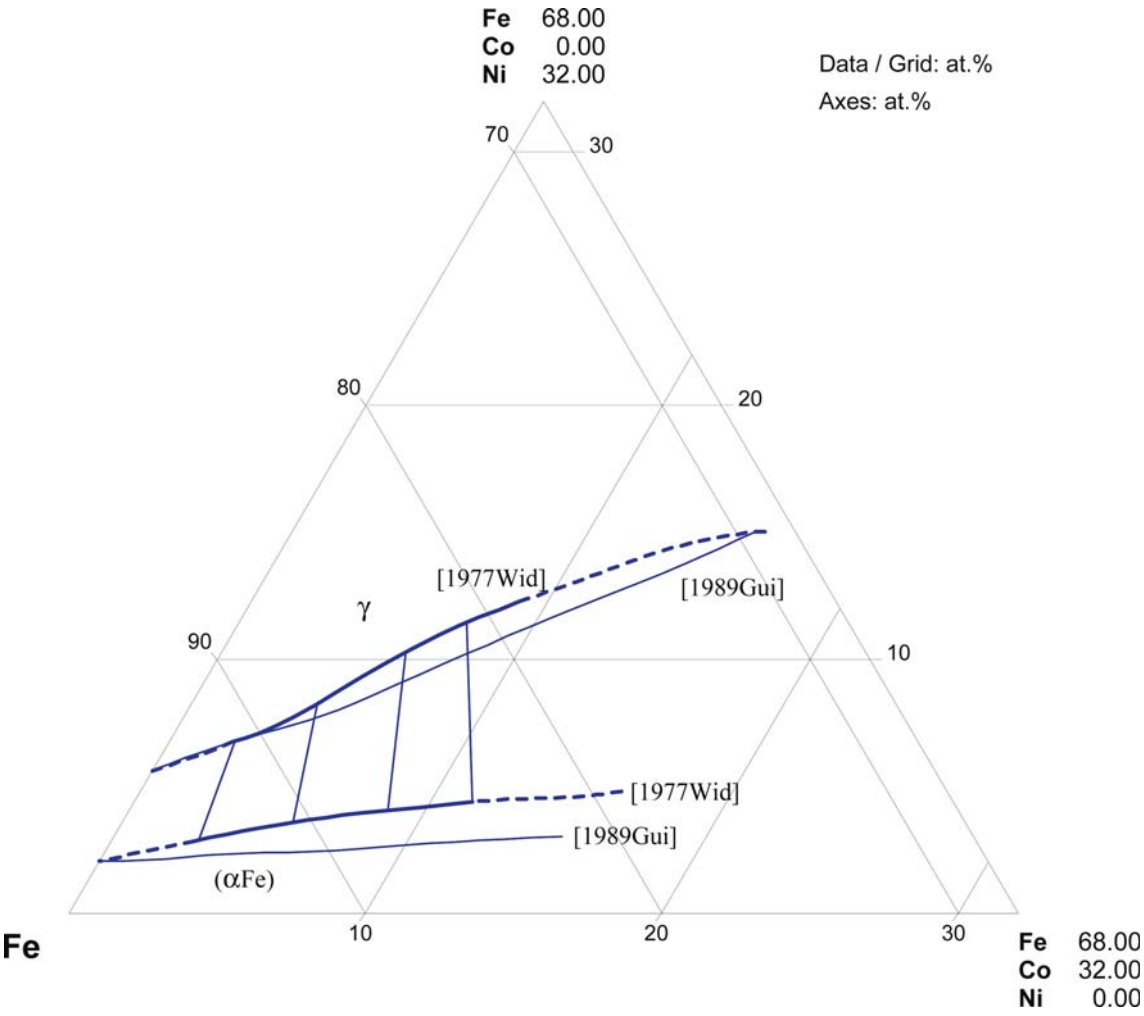

Fig. 2b. Co-Fe-Ni. Isothermal sections in the Fe rich corner at 750°C. Thick lines - experimental data [1977Wid]; thin curves - calculation [1987Gui, 1989Gui]

DOI: 10.1007/978-3-540-74196-1_22

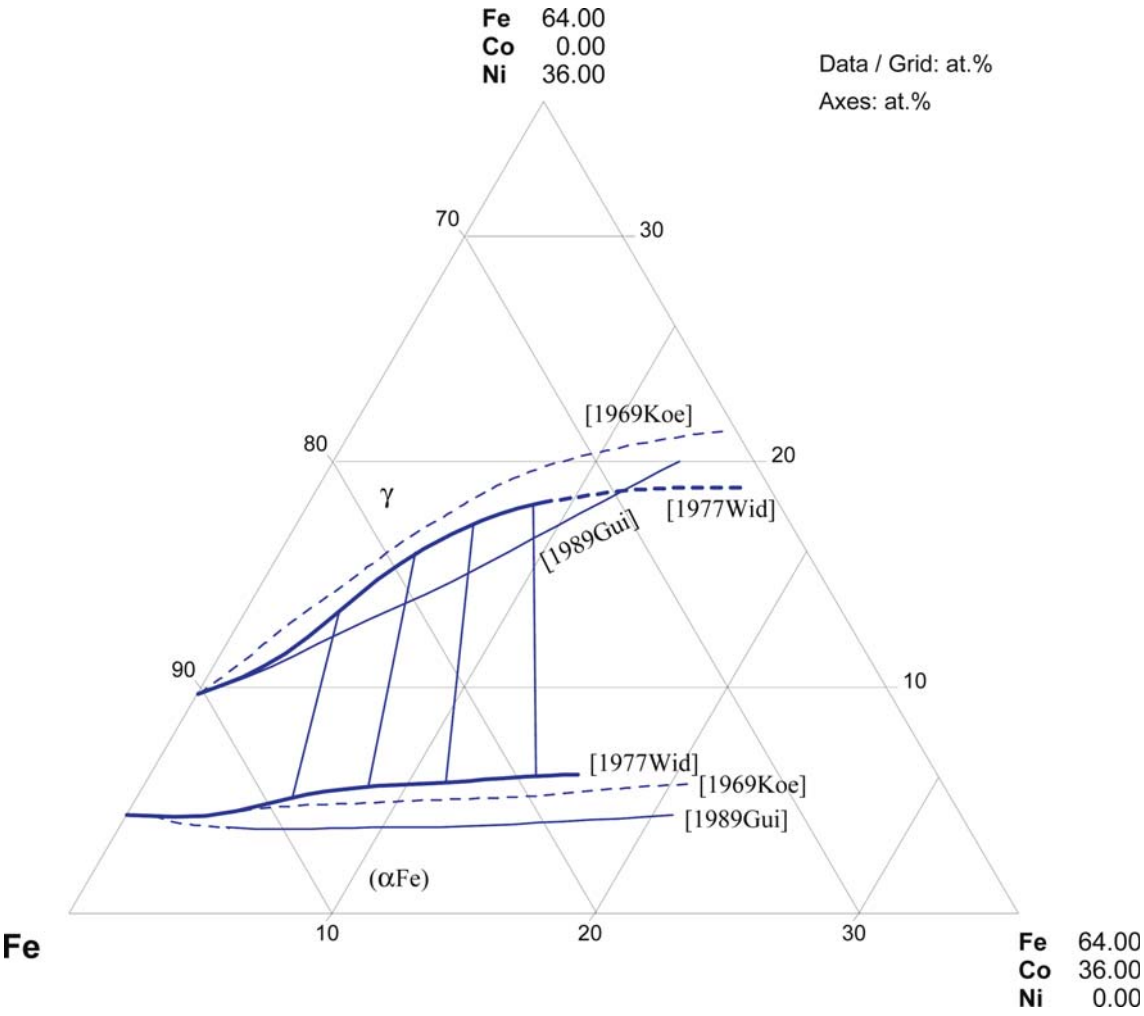

Fig. 2c. Co-Fe-Ni. Isothermal sections in the Fe rich corner at 700°C. Thick lines - experimental data [1977Wid]; thin curves - calculation [1987Gui, 1989Gui]; dashed lines– experimental data [1969Koe]

DOI: 10.1007/978-3-540-74196-1_22

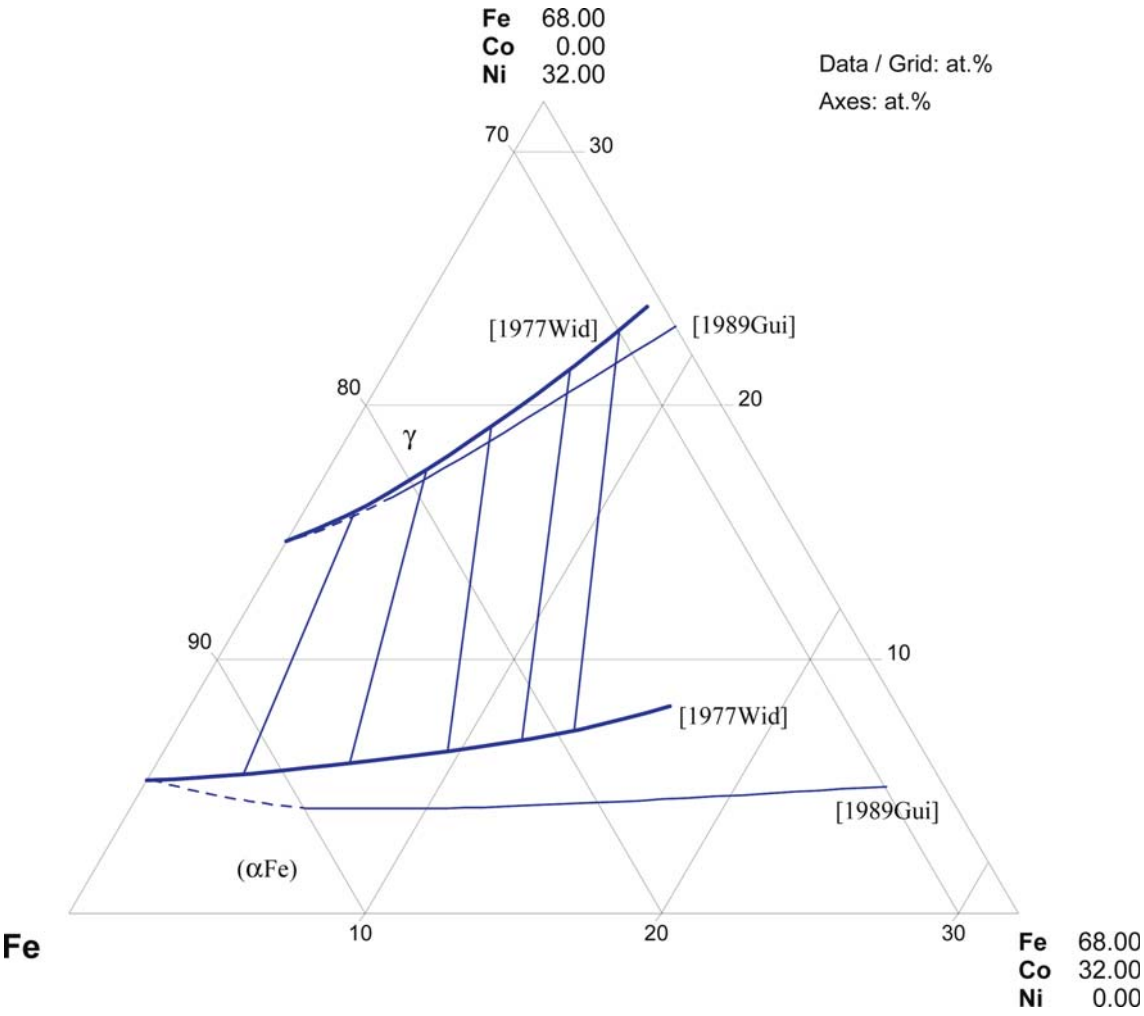

Fig. 2d. Co-Fe-Ni. Isothermal sections in the Fe rich corner at 650°C. Thick lines - experimental data [1977Wid]; thin curves - calculation [1987Gui, 1989Gui]

DOI: 10.1007/978-3-540-74196-1_22

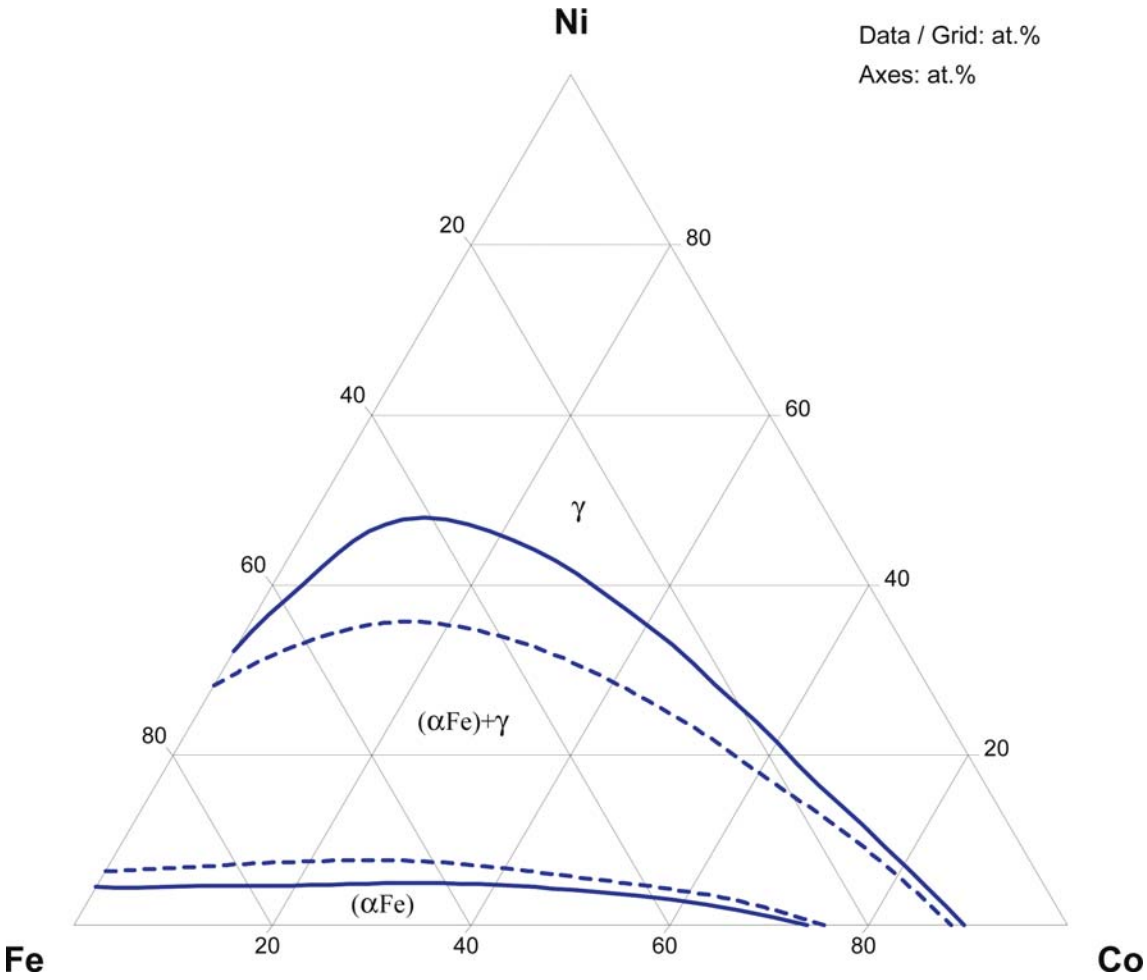

Fig. 3. Co-Fe-Ni. Experimental (solid lines) and computed (dashed lines) isothermal section at 500°C adjusted to the accepted binaries

DOI: 10.1007/978-3-540-74196-1_22

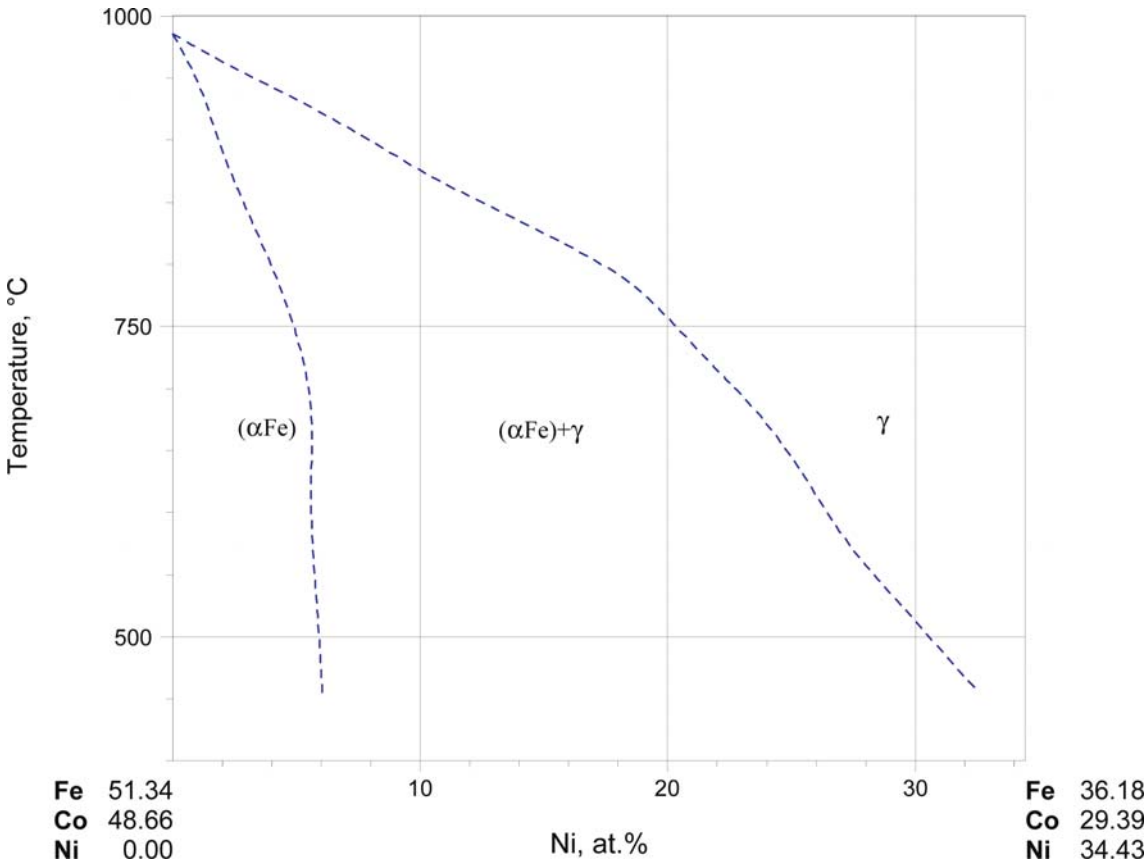

Fig. 4. Co-Fe-Ni. Partial vertical section FeCo-Ni

DOI: 10.1007/978-3-540-74196-1_22

References

[1909Jae] Jänecke, E., "Ternary Alloys of Cu, Ag, Au; Cr, Mn; Fe, Co, Ni; Pd, Pt Metals" (in German), *Z. Phys. Chem.*, **67**, 668–688 (1909) (Experimental, Phase Diagram, Phase Relations, 1)

[1927Kas] Kase, T., "On the Equilibrium Diagram of the Iron-Cobalt-Nickel System", *164th Rep. Res. Inst. Iron, Steel, Other Metals*, **16**, 491–513 (1927) (Phase Diagram, Phase Relations, Phys. Prop., 17)

[1929Mas] Masumoto, H., "On the Intensity of Magnetization in Iron-Nickel-Cobalt Alloys", *221st Rep. Res. Inst. Iron, Steel, Other Metals*, **18**, 195–229 (1929) (Phase Diagram, Phase Relations, Experimental, Magn. Prop., 23)

[1930Kue] Kuehlewein, H., "The Iron-Nickel-Cobalt Alloys" (in German), *Physikal. Z.*, **31**, 626–640 (1930) (Experimental, Magn. Prop., Mechan. Prop., Phase Diagram, Phase Relations, 59)

[1931Mas] Masumoto, H., "On the Thermal Expansion of the Alloys of Iron, Nickel and Cobalt, and the Cause of the Small Expansibility of Alloys of the Invar Type", *Sci. Rep. Tohoku Imp. Univ.*, **20**, 101–123 (1931) (Experimental, Thermodyn., 27)

[1932Kue] Kuehlewein, H., "About Magnetic Properties of Iron, Nickel, Cobalt and a Alloys at High Temperature" (in German), *Wiss. Veroeff. Siemens-Konzern*, **11**, 124–140 (1932) (Experimental, Magn. Prop., Phase Diagram, Phase Relations, 10)

[1939Kay] Kaya, S., Nakayama, M., "About Structure Formation in Iron-Nickel-Cobalt Alloys and Problem in the Perminvar" (in German), *Z. Phys.*, **112**, 420–429 (1939) (Crys. Structure, Experimental, Magn. Prop., Phase Relations, 5)

[1939Wym1] Wyman, L.L., "Low-Temperature Transformation in Iron-Nickel-Cobalt Alloys", *Am. Inst. Min. Metall. Pet. Eng. Techn. Publ.* No.1013, **6**, 1–14 (1939) (Crys. Structure, Experimental, Mechan. Prop., Morphology, Phase Relations, 10)

[1939Wym2] Wyman, L.L., "Low-Temperature Transformation in Iron-Nickel-Cobalt Alloys", *Trans. Am. Inst. Min. Metall. Eng.*, **135**, 542–553 (1939) (Experimental, Mechan. Prop., Phase Relations, 9)

[1940Bra1] Bradley, A.J., Bragg, W.L., Sykes, C., "Researches into the Structure of Alloys", *J. Iron Steel Inst.(London)*, **80**, 63–156 (1940) (Crys. Structure, Phase Diagram, 22)

[1940Bra2] Bradley, A.J., Bragg, W.L., Sykes, C., "The Iron-Nickel-Cobalt System", *J. Iron Steel Inst., London*, **141**, 109–111 (1940) (Crys. Structure, Phase Diagram, Review, 0)

[1949Jae] Jänecke, E., "Co-Fe-Ni" (in German), in "*Kurzgefasstes Handbuch aller Legierungen*", Winter, Heidelberg, 598–601 (1949) (Phase Diagram, Review, 0)

[1957Vit1] Viting, L.M., "Investigation of the Iron-Nickel-Cobalt System in the Region of Metallic Compounds Ni_3Fe and FeCo", *J. Inorg. Chem.*, **2**(2), 229–240 (1957), translated from *Zh. Neorg. Khim.*, **2**(2), 375–382 (1957) (Experimental, Mechan. Prop., Morphology, Phase Relations, 8)

[1957Vit2] Viting, L.M., "Investigation of the Fe-Ni-Co System in the Region of the Metallic Compounds Ni_3Fe and FeCo", *J. Inorg. Chem.*, **11**(4), 220–232 (1957), translated from *Zh. Neorg. Khim.*, **2**(4), 852–859 (1957) (Electr. Prop., Experimental, Mechan. Prop., Morphology, Phase Diagram, 6)

[1963Art] Artley, J.L., Pilkington, T.C., Wooten, F.T., "Prediction of Curie Temperatures in Ternary Fe-Co-Ni Alloys", *J. Appl. Phys.*, **34**(4), 972–974 (1963) (Phase Diagram, Phase Relations, 10)

[1964Pil] Pilkington, T.C., Artley, J.L., Wooten, F.T., "Prediction of Curie Temperatures in Ternary Fe-Co-Ni Alloys. II.", *J. Appl. Phys.*, **35**(12), 3493–3497 (1964) (Phase Diagram, Phase Relations, 17)

[1966Blo] Blossey, R.G., Pehlke, R.D., "The Solubility of n in Liquid Fe-Ni-Co Alloys.", *Trans. Met. Soc. AIME*, **236**, 566–569 (1966) (Experimental, Phase Relations, 12)

[1965Gol] Goldman, A.J., Robertson, W.D., "A Correlation of Elastic Moduli, Supercooling and Heat Evolved in the Martensitic Transformation in Iron Alloys", *Acta Metall.*, **13**(4), 379–447, 391–401 (1965) (Thermodyn., Phase Relations, Phys. Prop.) cited from abstract

DOI: 10.1007/978-3-540-74196-1_22

[1969Koe] Köster, W., Haehl, W.-D., "The Real Constitution Diagram and the Obtention of Equilibrium in the Ternary System Iron-Cobalt-Nickel" (in German), *Arch. Eisenhuettenwes*., **40**(7), 569–574 (1969) (Phase Diagram, Phase Relations, Experimantal, 13)

[1969Nec] Neckel, A., Wagner, S., "Mass-Spectrometric Determination of Thermodynamic Activities in Ternary Systems" (in German), *Monatsch. Chem.*, **100**, 664–670 (1969) (Experimental, Thermodyn., 24)

[1970Col] Colling, D.A., "Influence of Martensite-to-Austenite Reverse Transformation on the Temperature Dependence of Coercive Force of an Fe-Ni-Co Alloy", *J. Appl. Phys.*, **41**(3), 1038–1039 (1970) (Experimental, Phase Relations, Magn. Prop., 7)

[1970Gom1] Goman'kov, V.I., Puzey, I.M., Mal'tsev, E.I., "Effect of Alloying Elements on the Superstructure of Ni_3Fe" (in Russian), *Dokl. Akad. Nauk SSSR*, **194**(2), 309–311 (1970) (Crys. Structure, Experimental, Magn. Prop., 6)

[1970Gom2] Goman'kov, V.I., Puzey, I.M., Mal'tsev, Ye. I., Petrenko, E.D., "Ordering in the γ Range of the System Nickel-Iron-Cobalt", *Phys. Met. Metallogr.*, **29**(2), 212–215(1970), translated from *Fiz. Met. Metalloved*., **29**(2), 429–431, (1970) (Crys. Structure, Experimental, Phase Diagram, 7)

[1971Blo] Blossey, R.G., Pehlke, R.D., "Solubility of Hydrogen in Liquid Fe-Co-Ni Alloys", *Metall. Trans*., **2**, 3157–3161 (1971) (Experimental, Phase Relations, 26)

[1972Sch] Schibuya, N., Kunitomi, N., "Magnetic Moment on Fe in Ternary Alloy Fe-Ni-Co", *J. Phys. Soc. Jpn.*, **33**, 853 (1972) (Magn. Prop., Experimental, 6)

[1972Spe] Spencer, P.J., Hayes, F.H., Elfort, L., *Metallurgical Chemistry*, Proc. Symp. 1971, Kubaschewski, O. (Ed.), HMSO, London, 322 (1972) as quoted in [1988Ray]

[1973Kau] Kaufman, L., Nesor, H., "Calculation of Superalloy Phase Diagrams: Part I", *Z. Metallkd.*, **64**(4), 249–257 (1973) (Calculation, Crys. Structure, Phase Diagram, 19), as quoted in [1976Vel]

[1973Ser] Servant, C., Gizeron, G., Lacombe, P., "Study of the Fe-Ni-Co System", *J. Iron and Steel Inst.*, 75–82 (1973) (Phase Relations, 22)

[1973Spe] Spencer, P.J., Hayes, F.H., Elfort, L., "Chemical Metallurgy of Iron and Steel", *The Iron and Steel Institute, London,* 322–326 (1973) (Thermodyn., 16) as quoted in [1987Gui]

[1974Kau] Kaufman, L., Nesor, H., "Calculation of Superalloy Phase Diagrams: Part I", *Metall. Trans*., **5**(7), 1617–1621 (1974) (Calculation, Crys. Structure, Phase Diagram, 19)

[1975Mal1] Mal'tsev, Ye.I., Goman'kov, V.I., Puzey, I.M., Makarov, V.A., Kozis, Ye.V., "Neutron Diffraction and Mössbauer Investigations of the Processes of Ordering and Decomposition in Iron-Cobalt-Nickel Alloys", *Phys. Met. Metallogr.*, **39**(3), 84–93 (1975), translated from *Fiz. Met. Metalloved*., **39**(3), 543–552, (1975) (Experimental, Crys. Structure, 18)

[1975Mal2] Mal'tsev, Ye.I., Goman'kov, V.I., Mokhov, B.H., Puzey, I.M., Nogin, N.I., "Influence of Alloying Elements on the Co-Fe Superlattice", *Phys. Met. Metallogr.*, **40**(2), 190-193 (1975), translated from *Fiz. Met. Metalloved*., **40**(2), 443–445, (1975) (Experimental, Crys. Structure, 11)

[1976Vel] Velisek, J., Vrestal, J., Stransky, K., "Thermodynamic Activities in the Ternary System Fe-Ni-Co at 1500 K", *Kovove Mater.*, **14**(2), 121–136 (1976) (Experimental, Theory, Thermodyn., 19)

[1977Ser] Servant, C., Lacombe, P., "Structural Transformations Produced During Tempering of Fe-Ni-Co-Mo Alloys", *J. Mater. Sci*., **12**, 1807–1826 (1977) (Experimental, Morphology, 42)

[1977Wid] Widge, S., Goldstein, J.I., "Redetermination of the Fe-Rich Portion of the Fe-Ni-Co Phase Diagram", *Metall. Trans*., **8A**, 309–315 (1977) (Calculation, Morphology, Phase Diagram, 18)

[1978Sir] Sirota, N.N., Breslav-Maslennikov, M.B., "Vapor Pressures of Fe-Ni-Co Liquid Alloys at 2500K", *Dokl. Akad. Nauk Beloruss. SSR*, **22**(5), 412–414 (1978) (Experimental, Phase Diagram, Phys. Prop., Thermodyn., 6)

DOI: 10.1007/978-3-540-74196-1_22

[1978Tho] Thomas, G., "Some Applications of Transmission Electron Microscopy to Phase Transitions", in "*Diffraction and Imaging Techniques in Material Science*", Amelinckx, S., Gevers, R., Van Landuyt, J. (Eds.), Vol. **1**, North-Holland Publ. Comp., Amsterdam, New York-Oxford, **1**, 217–249 (1978) (Crys. Structure, Morphology, Review, 46)

[1979Sch] Schibuya, N., Nakai, Y., Yamasaki, K., Kunitomi, N., "Neutron and Mössbauer Studies of Atomic Magnetic Moments in a Ternary Alloy Fe-Co-Ni", *J. Phys. Soc. Jpn.*, **46**(2), 475–480 (1979) (Phase Diagram, Phase Relations, 10)

[1980Fra] Fraser, D.G., Rammensee, W., "Activity Measurements by Knudsen cell Mass Spectrometry the System Fe-Co-Ni and Implications for Condensation Processes in the Solar Nebula", *Geochim. Cosmochim. Acta*, **46**, 549–556 (1980) as quoted in [2000Tse] by [2005Mor]

[1980Sri] Srivastava, S.C., "Electrodeposition of Ternary Alloys: Developments in 1972 - 1978", *Surf. Technol*., **10**, 237–257 (1980) (Electrochem., Magn. Prop., Review, 121)

[1981Riv] Rivlin, V.G., "Critical Evaluation of Constitution of Cobalt-Chromium-Iron and Cobalt - Iron - Nickel Systems", *Intern. Met. Rev.*, **5**, 269–300 (1981) (Phase Relations, Phase Diagram, Review, Assessment, 56)

[1983Bar] Baren, M.R., Gokcen, N.A., "Thermodynamic Properties of Fe-Co-Ni-S and Fe-Co-Ni Systems", *JOM*, **35**(12), 43 (1983) (Thermodyn., Experimental) cited from abstract

[1985Col] Colinet, C., Pasturel, A., Hicter, P., "A d Band Bonding Model of the Enthalpy of Formation of Ternary Transition Metal Alloys", *Z. Metallkd*., **76**(8), 542–545 (1985) (Calculation, Phase Diagram, Thermodyn., 33)

[1985Gok] Gokcen, N.A., Baren, M.R., "Thermodynamic Properties of S-Fe-Co-Ni And Fe-Co-Ni Systems", *Metall. Trans. A*, **16A**, 907–911 (1985) (Calculation, Experimental, Thermodyn., 18)

[1986Lee] Lee, G.M.C., "The Metallurgy of Iron-Nickel and Iron-Nickel-Cobalt Diffusion Coatings", *Canad. Metall. Quart*., **25**(4), 327–335 (1986) (Experimental, Phase Diagram, Phase Relations, Interface Phenomena, Transport Phenomena, 15)

[1986Vla] Vlasova, Ye.N., Matorin, V.I., Zasimov, V.S., Gavrilova, A.V., "Change of the Fine Structure and Local Atomic Configurations in Elinvar Alloys Based on Ni-Fe-Co", *Phys. Met. Metallogr*., **61**(1), 63–67 (1986), translated from *Fiz. Met. Metalloved*., **61**(1), 69–73, (1986) (Crys. Structure, Experimental, Morphology, Thermodyn., 4)

[1987Gui] Fernández Guillermet, A., "Thermodynamics of The Fe-Co-Ni System Above 773 K: Experiments Versus Predictions from Binary Information", *Trita-Mac 0337 Oct. 1987* (Revised Version of *Sept 1987 Trita-Mac 0337*) Materials Res. Center, Royal Institute Techn., Stockholm, Sweden, 1–18 (1987) (Calculation, Phase Diagram, Thermodyn., 38)

[1988Ale] Alekseeva, N.N., Tsemekhman, L.Sh., Grodinskii, G.I., Burylev, B.P., "Determination of the Activity of the Components in the Fe-Ni-Co System" (in Russian), *Tsvetn. Metall*., **1**, 26–27 (1988) (Experimental, Thermodyn., 18)

[1988Ray] Raynor, G.V., Rivlin, V.G., "Co-Fe-Ni" in "*Phase Equilibria in Iron Ternary Alloys*", Inst. Metals, London, 247–255 (1988) (Phase Diagram, 12)

[1989Gui] Guillermet, F.A., "Assessing the Thermodynamics of The Fe-Co-Ni System Using a CALPHAD Predictive Technique", *Calphad*, **13**(1), 1–22 (1989) (Calculation, Phase Diagram, Thermodyn., 42)

[1989Kum] Kumar, Hari, K.C., Raghavan, V., "The bcc-fcc Equilibrium in Ternary Iron Alloys - III", *J. Alloy Phase Diagrams*, **5**(3), 201–220 (1989) (Experimental, Phase Diagram, 28)

[1991Ach1] Achilleos, C.A., Kyprianidis, I.M., Tsoukalas, I.A., "On the Magnetic Properties and $\alpha \rightarrow \gamma$ Transformation of Some Fe-Co-Ni Ternary Alloys", *Solid State Commun*., **79**(3), 209–216 (1991) (Experimental, Magn. Prop., Phase Relations, 33)

[1991Ach2] Achilleos, C.A., Chadjivasiliou, S.C., Tsoukalas, I.A., "On the Electrical Properties and $\alpha \rightarrow \gamma$ Transformation of Some Fe-Co-Ni Ternary Alloys", *Mater. Res. Bull*., **26**(8), 821–834 (1991) (Experimental) (Experimental, Electr. Prop., Phase Relations, 25)

DOI: 10.1007/978-3-540-74196-1_22

[1993Tom1] Tomiska, J., Belegratis, M.S., Kopecky, K., Neckel, A., "Thermodynamics of Liquid Ternary $Fe_xNi_xCo_{1-2x}$ Alloys by Computer-Aided Knudsen Cell Mass Spectrometry", *J. Non-Cryst. Sol.*, **156–158**, 425–428 (1993) (Thermodyn., 11)

[1993Tom2] Tomiska, J., Kopecky, K., Belegratis, M.S., Neckel, A., "Thermodynamic Excess Quantities of Solid Ternary $Fe_xNi_xCo_{1-2x}$ Alloys by Computer-aided Knudsen Cell Mass Spectrometry", *Z. Metallkd.*, **884**(9), 619–621 (1993) (Experimental, Thermodyn., 9)

[1994Miy] Miyazaki, T., Oomori, T., Sato, F., Ishio, S., "Zero Magnetostriction Composition in Fe-Ni-Co Ternary Alloy System", *J. Magn. Magn. Mater.*, **129**, L135–L136 (1994) (Phase Diagram, Phase Relations, Magn. Prop., 3)

[1994Rag] Raghavan, V., "Co-Fe-Ni (Cobalt-Iron-Nickel)", *J. Phase Equilib.*, **15**(5), 526–527 (1994) (Phase Diagram, Review, 8)

[1995Hai] Haidemenopoulos, G.N., Grujicic, M., Olson, G.B., Cohen, M., "Thermodynamics Based Alloy Design Criteria for Austenite Stabilization and Transformation Toughening in the Fe-Ni-Co System", *J. Alloys Compd.*, **220**, 142–147 (1995) (Calculation, Experimental, Phase Relations, 15)

[1995She] Shen, H., Zhang, W., Wang, R., Du, Z., Liu, G., "Experimental Measurement of the Phase Equilibria of the Fe-Co-Ni Ternary System", Proceedings of the 8th Nat. Symp. Phase Diagrams, 60–61 (1995) (Experimental, Phase Relations) cited from abstract

[2000Mue] Mueller, M., Grahl, H., Mattern, N., Schnell, B., "(FeCoNi)-ZrBCu Base Alloys, the Influence of Transition Metal Composition and Treatment on Structure and Magnetic Properties", *J. Magn. Magn. Mater.*, **215–216**, 437–439 (2000) (Magn. Prop., Phase Relations, 4)

[2000Rag] Raghavan, V., "The Martensitic Fransformation in Fe-Ni and Fe-Ni-X Alloys at Subzero Temperatures", *Trans. Indian Inst. Met.*, **53**(6), 597–603 (2000) (Experimental, Kinetics, 44)

[2000San] Sanyal, B., Bose, S.K., "Electronic Structure and Related Thermal and Magnetic Properties of Some Ternary Invar Alloys", *Phys. Rev. B*, **62**(19), 12730–12742 (2000) (Calculation, Magn. Prop., Phys. Prop., 38)

[2000Tse] Tsemekhman, L.S., Alekseeva, N.N., Parshukova, L.N., "The Activities of Components in Fe-Ni-Co System" (in Russian), *Metally*, (1), 25–29 (2000) (Experimental, Phase Diagram, 16)

[2001Gho] Ghosh, G., Olson, G.B., "Computational Thermodynamics and the Kinetics of Martensitic Transformation", *J. Phase Equilib.*, **22**, 199–207 (2001) (Calculation, Phase Relations, Thermodyn., 65)

[2001Koh] Kohmoto, O., Hanafusa, T., Yokoyama, M., Haneda, K., "Mössbauer Effect of Fe Particles in Metal Audio Tape", *Jpn. J. Appl. Phys. 1*, **40**(7), 4533–4534 (2001) (Crys. Structure, Experimental, Phys. Prop., 6)

[2001Liu] Liu, X., Zangari, G., "High Moment FeCoNi Alloy Thin Films Fabricated by Pulsed-Current Electrodeposition", *IEEE Trans. Magn.*, **37**(4), 1764–1766 (2001) (Experimental, Magn. Prop., Phys. Prop., 9)

[2001Mta] Mtalsi, D.M., Harfaoui, M.E., Qachaou, A., Faris, M., Youssef, J.B., Gall, H.L., "Magnetic Layer Composition Effect on Giant Magnetoresistance in (NiFeCo/Cu) Multilayers", *Phys. Status Solidi*, **187**(2), 633–640 (2001) (Experimental, Magn. Prop., 13)

[2001Ohs] Ohshima, N., Saito, M., Ohashi, K., Yamamoto, H., Mibu, K., "Structural and Magnetic Properties of High Saturation Induction CoNiFe Electroplated Films", *IEEE Trans. Magn.*, **37**(4), 1767–1769 (2001) (Crys. Structure, Experimental, Magn. Prop., 6)

[2001Osa] Osaka, T., Yokoshima, T., Nakanishi, T., "Effects of Impurities on Resistivity of Electrodeposited High-Bs CoNiFe based Soft Magnetic Thin Films", *IEEE Trans. Magn.*, **37**(4), 1761–1763 (2001) (Electr. Prop., Experimental, Magn. Prop., 14)

[2002Boz] Bozzolo, G.H., Noebe, R.D., Amador, C., "Site Occupancy of Ternary Additions to B2 Alloys", *Intermetallics*, **10**, 149–159 (2002) (Crys. Structure, Review, 27)

[2002Ohn] Ohnuma, I., Enoki, H., Ikeda, O., Kainuma, R., Ohtani, H., Sundman, B., Ishida, K., "Phase Equilibria in the Co-Fe Binary System", *Acta Mater.*, **50**, 379–393 (2002) (Assessment, Calculation, Experimental, Phase Relations, Thermodyn., 50)

DOI: 10.1007/978-3-540-74196-1_22

[2003Mor] Morachevskii, A.G., Tsemekhman, L.Sh., Tsymbulov, L.B., Fedorova, N.A., "Thermodynamic Properties of Liquid Alloys of the System Iron-Nickel-Cobalt", *Russ. J. Appl. Chem.*, **76**(11), 1728–1733 (2003), translated from *Zh. Priklad. Khim.*, **76**(11) 1779–1784, (2003) (Phase Diagram, Phase Relations, Thermodyn., 27)

[2004Sun] Sundar, R.S., Deevi, S.C., "Influence of Alloying Elements on the Mechanical Properties of FeCo-V Alloys", *Intermetallics*, **12**(7–9), 921–927 (2004) (Magn. Prop., Mechan. Prop., Morphology, Review, 32)

[2004Tom1] Tomiska, J., "Computer-Aided Thermodynamics of Liquid Ternary Fe-Ni-Co Alloys by Knudsen Cell Mass Spectrometry", *J. Alloys Compd.*, **373**(1–2), 142–150 (2004) (Experimental, Thermodyn., 11)

[2004Tom2] Tomiska, J., "Ternary Thermodynamics by Computer-Aided Knudsen Cell Mass Spectrometry: fcc Solid Fe-Ni-Co Alloys", *Z. Metallkd.*, **95**(3), 136–141 (2004) (Experimental, Phase Diagram, Thermodyn., 5)

[2005Kai] Kai, W., Jang, W.L., Huang, R.T., Lee, C.C., Hsieh, H.H., Du, C.F., "Air Oxidation of FeCoNi-Base Equi-Molar Alloys at 800°C-1000°C", *Oxid. Met.*, **63**(3–4), 169–192 (2005) (Crys. Structure, Experimental, Interface Phenomena, Kinetics, Morphology, Phase Relations, 21)

[2005Mor] Morachevskii, A.G., Kolosova, E.Yu., Tsymbulov, L.B., Tsemekhman, L.Sh., "Activity of Components in Liquid Alloys of the Iron-Cobalt-Nickel System", *Russ. J. Appl. Chem.*, **78**(12), 1930–1933 (2005), translated from *Zh. Prikl. Khim.*, **78**(12), 1963–1966, (2005) (Phase Diagram, Phase Relations, Thermodyn., 19)

[2005Sou] Sourmail, T., "Near Equiatomic FeCo Alloys: Constitution, Mechanical and Magnetic Properties", *Prog. Mater. Sci.*, **50**(7), 816–880 (2005) (Crys. Structure, Electr. Prop., Kinetics, Magn. Prop., Mechan. Prop., Morphology, Phase Diagram, Phase Relations, Review, 122)

[2005Sun] Sundar, R.S., Deevi, S.C., "Soft Magnetic Co-Fe Alloys: Alloy Developmet, Processing, and Properties", *Int. Mater. Rev.*, **50**(3), 157–192 (2005) (Crys. Structure, Electr. Prop., Magn. Prop., Mechan. Prop., Phase Diagram, Phase Relations, Review, 258)

[2005Zar] Zaretsky, E.B., Kanel, G.I., Razorenov, S.V., Baumung, K., "Impact Strength Properties of Nickel based Refractory Superalloys at Normal and Elevated Temperatures", *Int. J. Impact. Eng.*, **31**, 41–54 (2005) (Experimental, Mechan. Prop., Review, 19)

[2005Ziv] Zivkovic, D., Manasijevic, D., "An Optimal Method to Calculate the Viscosity of Simple Liquid Ternary Alloys from the Measured Binary Data", *Calphad*, **29**, 312–316 (2005) (Phase Diagram, Phase Relations, 21)

[2006Yoo] Yoo, Y.K., Xue, Q., Chu, Y.S., Xu, S., Hangen, U., Lee, H.-C., Stein, W., Xiang, X.-D., "Identification of Amorphous Phases in the Fe-Ni-Co Ternary Alloy System Using Continuous Phase Diagram Material Chips", *Intermetallics*, **14**(3), 241–247 (2006) (Crys. Structure, Experimental, Mechan. Prop., Phase Relations, 18)

[2007Kuz] Kuznetsov, V., "Fe-Ni (Iron-Nickel)", MSIT Binary Evaluation Program, in *MSIT Workplace*, Effenberg, G. (Ed.), MSI, Materials Science International Services GmbH, Stuttgart; to be published (2007) (Crys. Structure, Phase Diagram, Assessment, 41)

[Mas2] Massalski, T.B. (Ed.), *Binary Alloy Phase Diagrams*, 2nd edition, ASM International, Metals Park, Ohio (1990)

[V-C2] Villars, P. and Calvert, L.D., *Pearson's Handbook of Crystallographic Data for Intermetallic Phases*, 2nd edition, ASM, Metals Park, Ohio (1991)

DOI: 10.1007/978-3-540-74196-1_22

Cobalt – Iron – Sulphur

Vasiliy Tomashik

Introduction

A critical assessment of the Co-Fe-S system has been published by [1988Rag], which included data published up to 1987. The literature up to 1997 and up to 2002 was discussed in [1998Rag] and [2004Rag], respectively. The present assessment takes into account all available data.

$Co_{1-x}S$ and $Fe_{1-x}S$ form a continuos series of solid solutions from the solidification range down to at least 500°C with lattice parameters varying nonlinearly with the composition [1951Asa, 1953Vog, 1960Per, 1963Kan, 1982Kra, 1982McC, 1987Bar, 1987Col, 2001Far, 2002Far].

CoS_2 and FeS_2 also dissolve in each other [1962Kle, 1965Ril, 1968Bou, 1968Ril, 2003Che]. The solubility of CoS_2 in FeS_2 is equal to 17, 17 and 25 mol% at 400, 500 and 600°C, respectively and the solubility of FeS_2 in CoS_2 at the same temperatures reaches up to 7, 33 and 55 mol%. The complete solubility exists at 700°C [1962Kle]. The data of [1962Kle] were included in the review of [1964Kul]. Within the range of solid solubility the lattice parameter of the $Fe_xCo_{1-x}S_2$ solid solution varies linearly between the values of CoS_2 and FeS_2 [1965Ril]. [1976Wys] investigated mutual solubility of CoS_2 and FeS_2. According to [1976Wys], the solubility of CoS_2 in FeS_2 is very limited, amounting below 2 mass%. On the other hand, the solubility of FeS_2 in CoS_2 is rather high and increases with increasing temperature. Thus, solubility of FeS_2 in CoS_2 is 37, 60 and 75 mass% at 500, 600 and 700°C, respectively [1976Wys]. According to [1976Wys] solubility of FeS_2 in CoS_2 reaches a maximum value of 80 mass% at an invariant reaction at 735°C with the participation of FeS_2, CoS_2, λ and the liquid phase.

The solidification characteristics of vertical sections along the FeS-Co_4S_3 and FeS-"Co_6S_5" sections were investigated by [1949Vog, 1957Mol, 1958Mol]. Some polythermal sections of this ternary system were constructed by [1953Vog] and [1958Mol]. The first experimental data were falsely interpreted that the FeS-Co_4S_3 system could be described by a eutectic type phase diagram.

Interaction of Co_4S_3 and Fe at 700°C leads to the formation of FeS and $(Fe_{1-x}Co_x)_4S_3$ solid solution [1979Sha].

The liquidus surface of the Fe-FeS-CoS-Co part has been determined by [1953Vog, 1958Mol]. Isothermal sections of the Co-Fe-S ternary system at 1350, 1300, 1250, 1200, 800, 700, 600, 500 and 325°C were constructed by [1976Moh, 1976Wys, 1977Wys, 1985Sch, 1997Sol, 2002Far].

Co_8FeS_8 and $Co_7Fe_2S_8$ (π phases), which are the solid solutions of Fe in Co_9S_8, were prepared by dry synthesis by [1962Kno, 1976Kno].

It was established by [1965Buz] that the ratio Co/S in the cobalt sulfide of the Co-Fe-S system equals 0.97, which corresponds to the $Co_{1-x}S$ binary compound.

Thermodynamic properties of the solid and liquid alloys in the Co-Fe-S ternary system were investigated by [1960Alc, 1966Ada, 1968Chm, 1969Ban, 1970Vay, 1971Vay, 1972Vay, 1999Sol, 1973Buz, 1974Khe, 1974Sig, 1981Fit, 1994Sor, 1999Kon].

Table 1 lists the numerous experimental works on phase equilibria, crystal structure and thermodynamics of the Co-Fe-S system.

Binary Systems

The Co-Fe and Fe-S binary systems are accepted from [Mas2]. The accepted version of the Co-S phase diagram [2006MSIT] (Fig. 1) is basically taken from the calculation of [1979Cha], but it incorporates new experimental findings of [1997Bry] regarding the congruent transformation of $Co_{1-x}S$ into an ordered form (λ').

Solid Phases

The solid phases and their crystallographic data are listed in Table 2.

DOI: 10.1007/978-3-540-74196-1_23

Complete series of solid solutions exist in the systems CoS-FeS [1951Asa, 1953Vog, 1960Per, 1963Kan, 1982Kra, 1982McC, 1987Bar, 1987Col, 2001Far, 2002Far] and CoS_2-FeS_2 [1962Kle, 1965Ril, 1968Bou, 1968Ril, 2003Che] at high temperatures. The low temperature transitions in the $Fe_{1-x}Co_xS$ alloys have been studied by [1987Bar], who observed after quenching from 700°C superstructure $a\sqrt{3}$, 2c of the NiAs type (2C phase) for $0 \leq x < 0.17$ and the pure NiAs type (1C phase) for $0.17 < x \leq 1$. Transition temperature from the pure NiAs type phase to a superstructural one decreased with increasing Co content in $Fe_{1-x}Co_xS$. Co substitution effectively stabilizes the high-temperature modification of FeS [1982Kra, 1987Col]. For the section CoS-FeS the ordered NiAs type phase 3C with parameters $a = 2a_0$ and $c = 3c_0$ are also reported [2002Far, 2004Rag], where a_0 and c_0 are parameters of the NiAs type lattice without ordering.
The continuous solid solution $Fe_{1-x}Co_xS_2$ between CoS_2 and FeS_2 exists at high temperatures and decomposes into CoS_2 and FeS_2 at low temperatures. Extrapolation of the data of [1962Kle] on the mutual solubility of CoS_2 and FeS_2 at different temperatures gives the upper point of miscibility gap between CoS_2 and FeS_2 solid solution at about 65 mol% FeS_2 and 630°C. The mutual solubility of Co_4S_3 and FeS at room temperature is equal to 24.5 mass% Co_4S_3 and 20 mass% FeS [1957Mol, 1958Mol]. The solubility of Co_4S_3 into FeS increases to 42.7 mass% at 900°C and the solubility of FeS into Co_4S_3 practically does not change with the temperature increasing.
The Co_8FeS_8 and $Co_7Fe_2S_8$ phases (solid solutions of Fe in Co_9S_8) exist in this system [1962Kno, 1976Kno].
The solubility of S in the metallic phases as well as that of the metals or their sulfides respectively in liquid S are too small to be detected by the methods used by [1976Moh, 1977Wys].

Invariant Equilibria

A reaction scheme for the Co-Fe-S system is given in Fig. 2 mainly after [1988Rag]. It is based on the results of [1953Vog]. However, some corrections were made taking into account the accepted binary phase diagrams and the existence of a complete solid solution between CoS_2 and FeS_2 at above ~630°C. The temperature of the U_3 reaction is placed by [1988Rag] above 800°C instead of 785°C [1953Vog] in order to be consistent with the isothermal section at 800°C. Two other solid state invariant reactions U_5 and U_6 are required above 700°C to account for the 700°C isothermal section of [1976Wys]. The data on invariant reactions are presented in Table 3. The peritectic type of the three-phase reaction p_7, $L + \gamma = (\alpha Fe)$ is assumed taking into account its temperature (~950°C) to be higher than the temperature of the transformation $(\gamma Fe) \rightleftharpoons (\alpha Fe)$ in pure Fe (912°C).

Liquidus, Solidus and Solvus Surfaces

The liquidus surface is shown in Fig. 3a mainly after [1988Rag] with some corrections to make it consistent with the accepted binary diagrams. The part of the liquidus surface in the Fe-FeS-CoS-Co region is based on the data of [1953Vog]. The data of [1958Mol] practically coincide with the experimental results of [1953Vog]. The liquidus temperatures obtained by [1997Sol] are slightly higher than the data of [1953Vog]. The probable nature of the liquidus surface in the S rich part of the composition triangle is shown schematically in Fig. 3b after [1988Rag].

Isothermal Sections

[1997Sol] determined isothermal sections at 1350, 1300, 1250 and 1200°C by equilibrating the liquid sulfide phase with the solid metallic phase. These sections show the liquidus lines and the tie-lines at the above mentioned temperatures.
Figures 4 and 5 show partial isothermal sections at 1350 and 1200°C from [1997Sol].
The isothermal section at 800°C was determined by [1977Wys, 1985Sch]. The main difference between the results of these works is in the solubility of Fe in the Co_4S_3 phase. [1977Wys] shows a ternary phase $(Fe_{1-x}Co_x)_4S_3$ at this temperature, which is more likely to be a ternary solid solution based on Co_4S_3 [1985Sch]. Figure 6 gives the isothermal section determined by [1985Sch] and included in the review of [1988Rag]. The results of the investigations of the Co-Fe-S ternary system at 700, 600 and 500°C are shown in Figs. 7 to 9. The diagrams are based on the works of [1976Moh, 1976Wys] (the isothermal sections at

DOI: 10.1007/978-3-540-74196-1_23

700 and 500°C were also included in the review of [1988Rag]). [1976Wys] showed the (αFe) ⇌ α' transition as a first order transition, however it is well established in the Co-Fe binary system, that this is a second order transition. Therefore in Figs. 7 to 9 the two-phase field (αFe) + α' assumed by [1976Wys] is disregarded; and instead dotted lines denote an approximate position of the (αFe) / α' border.
A partial isothermal section at 325°C determined in the monosulfide region is presented in Fig. 10 from [2002Far] as quoted by [2004Rag]. It shows the λ phase of the NiAs type (1C) and its superstructure (3C), see section "Solid Phases".
Slight modifications have been applied to Figs. 6-9 to make them consistent with the phase diagrams of the binary systems accepted in the present evaluation.

Temperature – Composition Sections

The polythermal sections FeS-Co_4S_3 and FeS-"Co_6S_5" were constructed by [1949Vog] and the vertical sections Co_xFe_{1-x}-S at $x = 0.125$, 0.25, 0.70, 0.80, 0.85 and 0.90 were determined by [1953Vog]. Eight vertical sections of the Co-Fe-S ternary system at the 20, 25 and 27.5 mass% S, 15.8, 24 and 56 mass% Fe and at the Fe/Co ratios of 1:1 and 2:3 were constructed by [1958Mol].
The CoS-FeS vertical section at an overall composition of S equal to 52 at.% is shown in Fig. 11 [2002Far, 2004Rag]. It should be mentioned that a small amount of Co_9S_8 was present in the studied samples. According to the section, between 425 and 400°C the single monosulfide phase decomposes into two phases by a eutectoid reaction at 425°C. The Fe rich phase has the structure of NiAs (1C) and the Co rich phase has the superstructure 3C. At higher temperatures this section is not constructed, but it can be supposed to be quasibinary considering congruent melting of both compounds and the formation of a continues solid solution between them at 500 to 800°C.

Thermodynamics

The thermodynamic properties of the Co-Fe-S system were determined by equilibrating the alloys with a known S pressure established by using a gas mixture of H_2S/H_2 [1999Sol]. Sulphur isopartial pressures in the Co-Fe-S system at 1200, 1275 and 1350°C are given in Fig. 12. In Fig. 13 the change in S partial pressure *vs* the sulphure mole fraction for different ratios of Co/Fe at 1200, 1275 and 1350°C are shown. The metal saturation line is also given in this figure.
Isoactivities of Co and Fe in the Co-Fe-S system at 1200, 1275 and 1350°C are shown in Figs. 14-16 [1999Sol]. The data of [1999Sol] practically coincide with the experimental results of [1970Vay, 1971Vay, 1972Vay, 1974Khe] obtained at 1300°C, and with the calculation of [1994Sor]. The activity coefficients of Co in the dilute solutions of Co in Co-Fe-S were calculated by [1999Sol]. It was found that in the dilute solutions the system shows a negative deviation from the Raoult's law. The activity coefficient of Co was constant up to approximately 2 at.% Co. The partial heats of solution of Fe, Co and S were calculated and it was found to be positive for Fe and Co, while that for S was negative [1999Sol].
The thermodynamic properties of the liquid Co-Fe-S solutions were predicted using the modified quasi-chemical model for short-range ordering by [1999Kon] and very good agreement with experimental data was obtained.
Co increases slightly the activity coefficient of S in liquid Fe [1960Alc, 1968Chm, 1969Ban, 1973Buz]. The first order interaction parameters up to 20 mass% Co are equal $e^{Co}_S = + 0.006$ and $\varepsilon^{Co}_S = + 1.52$ [1968Chm] ($e^{Co}_S = + 0.0026$ at < 50 at.% Co [1969Ban, 1974Sig], $e^{Co}_S = + 0.003$ and $\varepsilon^{Co}_S = + 0.67$ at 9-20 mass% S, $\varepsilon^{Co}_S = + 0.85$ [1981Fit]). Interaction parameter Θ^{Co}_S is equal 0.576 at < 50 at.% Co [1969Ban]. However, [1966Ada] have determined that Co would decrease the activity coefficient of S in liquid Fe up to 10 mass% Co but indicated the opposite tendency above this concentration. According the data of [1966Ada] the first order interaction parameters are the following: $e^{Co}_S = - 0.010$, $\varepsilon^{Co}_S = - 2.49$ and $e^{S}_{Co} = - 0.022$. The second order interaction coefficient r^{Co}_S is equal zero [1974Sig].

Notes on Materials Properties and Applications

The resistance of Co-Fe alloys to sulfidation at high temperatures and the extraction of Co from sulfide ores are of considerable technological significance [1985Sch].

DOI: 10.1007/978-3-540-74196-1_23

The effective magnetic moment, μ, per atom in μ_B of Co-Fe-S deposits at room temperature was observed to decrease linearly with increasing S content, and the decrease of μ per at.% S is obtained to be about $-2.5 \cdot 10^{-2}$ [1969Kur].

There are three phase transitions in the alloys $Fe_{1-x}Co_xS$ ($0 \le x \le 0.13$) within the temperature range from 27 to 800°C [1981Ter]: 1) a metal - semiconductor transition; 2) a spin-rotation transition and 3) a transition from an antiferromagnetic to a paramagnetic state. The spin-rotation transition (Morin transition at about 130°C) proceed in a certain temperature interval. Increasing of Co content leads to an increase of the Neel temperature (347°C at $x = 0.09$ and 407°C at $x = 0.13$).

Co-doped FeS_2 is an *n* type semiconductor [2006Leh]. Resistivity ranges from 0.009 to 0.02 Ω cm, carrier concentration is within the interval from $10^{18.7}$ to $10^{19.3}$ cm^{-3} and Hall mobility is ranging from 60 to 270 $cm^2 \cdot V^{-1} \cdot s^{-1}$. The carrier concentration increases with increased Co concentratrion.

The room temperature Mössbauer spectra of the $Fe_{1-x}Co_xS$ ($x < 0.15$) can be explained by the simultaneous occurrence of the high-temperature 1C-state besides the semiconducting low-temperature 2C-state [1982Wie, 1982Kra]. The transition 1C → 2C is associated with a drastic volume expansion [1987Bar].

Miscellaneous

The Curie temperature of the $Co_{0.4}Fe_{0.6}S_{1.15}$ alloy is equal approximately 250 K [1960Per]. A half-metallic magnetization of 1 ± 0.3 μ_B per Co atom was found for the $Fe_{1-x}Co_xS_2$ solid solutions at $x = 0.35$-0.9 and T_C was determined to be 107, 120, 153 and 145 K for $x = 0.35$, 0.5, 0.75 and 0.9 respectively [2003Che].

The use of mixed sulfates ($FeSO_4$ + $CoSO_4$ water solutions) is a definite advantage in the preparation of mixed pyrites $Fe_{1-x}Co_xS_2$ [1968Bou]. The critical step can be probably the low-temperature treatment with H_2S, which results in a very divided intermediate product that is fairly reactive and very close to MX_2 stoichiometry. As a consequence of the homogeneity obtained by the mixed sulfates, formation of a single-phase, well-crystallized $Fe_{1-x}Co_xS_2$ solid solution is facilitated at higher temperatures (650-700°C during 2-3 days).

Theory and experiments show that using GeI_2 as transport agent the phase $Fe_{1-y}Co_yS_x$ with low S and Co concentrations ($x \approx 1$, $y < 0.4$) will be transported under diminishing the content of Co and under enrichment of Fe and S, whereas by use HI (NH_4I) as transport agent the transport occurs under enrichment of Co and diminishing the Fe and S contents, respectively [1979Kra]. The crystals of the $Fe_{1-x}Co_xS_2$ solid solutions could be grown from the solution in Te melts [2003Che]. Inductively coupled plasma and energy X-ray dispersive spectroscopy results confirm a sulfur deficiency of ~ 1.5-10% {($Fe_{1-x}Co_xS_{2-y}$, $0.03 \le y \le 0.2$} and small amounts of Te. Single crystals of $Fe_{1-x}Co_xS_2$ solid solutions can be also prepared be chemical transport with Br_2 [1971But]. The composition of the obtained single crystals is slightly dependent on Br_2 pressure. High bromine pressures seem to favor higher Co content.

$Fe_{1-x}Co_xS_2$ solid solutions with various morphologies could be synthesized at low temperature via solvothermal process with ethanol as the solvent [2006Han]. Co and Fe nitrates were used as starting chemicals and thiourea as a source of S. With the same synthetic condition, the morphology is strongly dependent of Fe content. The grain shape varies from nanoscaled sphericity to round nanorods and finally to rectangle rods with decreasing *x*. Magnetic measurements show a clear ferromagnetic-paramagnetic transition for the samples with $x \le 0.5$.

FeS_2 crystals doped with Co were synthesized using a chemical vapor transport with $FeBr_3$ as a transport agent [2006Leh]. Co concentration was ~450-3700 ppm.

DOI: 10.1007/978-3-540-74196-1_23

Table 1. Investigations of the Co-Fe-S Phase Relations, Structures and Thermodynamics

Reference	Method / Experimental Technique	Temperature / Composition / Phase Range Studied
[1949Vog]	DTA, XRD, metallography	Up to 1200°C / FeS-Co_4S_3 and FeS-"Co_6S_5" sections
[1951Asa]	DTA	Up to 1200°C / $Co_{1-x}S$-$Fe_{1-x}S$ section
[1953Vog]	DTA, XRD, metallography	Up to 1500°C / Co-Fe-S
[1957Mol]	DTA, metallography, dilatometry	Up to 1200°C / FeS-Co_4S_3 section
[1957Mol]	DTA, DTG, metallography, dilatometry	Up to 1200°C / Fe-FeS-Co_4S_3-Co
[1960Alc]	Activity coefficient measurement	1540°C // (Co-Fe) + S
[1960Per]	XRD	Up to 1200°C / $Co_xFe_{1-x}S_{1.15}$
[1962Kle]	XRD	400-700°C / CoS_2-FeS_2
[1962Kno]	XRD	Room temperature / Co_8FeS_8
[1963Kan]	XRD, chemical analysis	950°C / CoS-FeS
[1965Ril]	XRD, chemical analysis	CoS_2-FeS_2
[1966Ada]	Gas bubbling technique	1600-1650°C / (Co-Fe-S) + H_2S/H_2 (up to 2.5 mass% S and 18 mass% Co)
[1968Bou]	XRD	Up to 700°C / CoS_2-FeS_2
[1968Chm]	Chemical analysis	Co-Fe-S
[1968Ril]	XRD, EPMA	CoS_2-FeS_2
[1969Ban]	Chemical analysis	1550°C / Co-Fe-S
[1969Kur]	EPMA, saturation magnetization measurement	Room temperature / Co-Fe-S
[1970Vay, 1971Vay, 1972Vay]	EMF measurements	1300°C / Co-Fe-S
[1971But]	XRD, electric resistivity and magnetic measurement	Room temperature / $Co_xFe_{1-x}S_2$
[1973Buz]	XRD, EPMA	1600°C / Co-Fe-S
[1974Khe]	EMF measurements	1300°C / Co-Fe-S
[1976Kno]	XRD, Mössbauer spectroscopy, neutron diffraction powder, magnetic susceptibility	4.2 K - room temperature / Co_8FeS_8 and $Co_7Fe_2S_8$ solid solutions
[1976Moh]	XRD, DTA, metallography	800°C / Co-Fe-S
[1976Wys]	XRD, DTA, metallography	500, 600, 700°C / Co-Fe-S
[1977Wys]	XRD, DTA, metallography	800°C / Co-Fe-S
[1979Sha]	SEM, metallography	700°C / Co_4S_3 + Fe

(*continued*)

DOI: 10.1007/978-3-540-74196-1_23

Reference	Method / Experimental Technique	Temperature / Composition / Phase Range Studied
[1981Ter]	Faraday method	Up to 800°C / $Co_xFe_{1-x}S$ ($x < 0.13$)
[1982Kra]	DTA, electrical properties measurements	Up to 800°C / $Co_xFe_{1-x}S$ ($x < 0.15$)
[1982McC]	XRD, EPMA, Mössbauer spectroscopy	4.2 and 298 K / $(Fe,Co)S_{1+x}$
[1982Wie]	Mössbauer spectroscopy	Room temperature / $Co_xFe_{1-x}S$ ($x < 0.15$)
[1985Sch]	EPMA, metallography	800°C / Co-Fe-S
[1987Bar]	XRD, DTA, Faraday method	Up to 700°C / $Co_xFe_{1-x}S$
[1987Col]	XRD, electric resistivity and magnetic susceptibility measurements	100-500 K / $Co_xFe_{1-x}S$ ($x < 0.25$)
[1997Sol]	EPMA, metallography, chemical analysis	1200-1350°C / Co-Fe-S
[1999Sol]	Vapor pressure measurements	1200, 1275 and 1350°C / Co-Fe-S
[2000Kim]	XRD, Mössbauer spectroscopy	77-600 K / $Co_{0.025}Fe_{0.975}S$
[2001Far]	XRD, sulfur K-edge spectra	Room temperature / $Co_{0.923}S$- $Fe_{0.923}S$
[2002Far]	XRD, STEM, EPMA	Up to 450 °C / $Co_xFe_{1-x}S$
[2003Che]	XRD, SEM, optical microscopy, magnetic measurements	77-300 K / $Co_xFe_{1-x}S_2$
[2005Nam]	XRD, Mössbauer spectroscopy	77-600 K / $Co_{0.025}Fe_{0.975}S$
[2006Han]	XRD, SEM, SQUID magnetization measurements	Up to 180°C / $Co_xFe_{1-x}S_2$
[2006Leh]	XRD, EPMA synchrotron XRD, mass spectrometry	Room temperature / FeS_2 + Co

Table 2. Crystallographic Data of Solid Phases

Phase/ Temperature Range [°C]	Pearson Symbol/ Space Group/ Prototype	Lattice Parameters [pm]	Comments/References
γ, (γFe,αCo)	*cF*4 $Fm\bar{3}m$ Cu		continuous solid solution
(αCo) 1495 - 422		a = 356.88 a = 354.47	at 520°C [V-C2] [Mas2]
(γFe) 1394 - 912		a = 286.65	at 25°C [Mas2]

(*continued*)

DOI: 10.1007/978-3-540-74196-1_23

Phase/ Temperature Range [°C]	Pearson Symbol/ Space Group/ Prototype	Lattice Parameters [pm]	Comments/References
(εCo) < 422	*hP*2 $P6_3/mmc$ Mg	*a* = 250.71 *c* = 406.86	pure Co at 25°C [Mas2]
(δFe) 1538 - 1394	*cI*2 $Im\bar{3}m$ W	*a* = 293.15	pure Fe [Mas2] dissolves up to 17 at.% Co.
(αFe) < 912	*cI*2 $Im\bar{3}m$ W	 *a* = 286.65	dissolves up to 75 at.% Co, up to 0.033 at.% S pure Fe at 25°C [Mas2].
(βS) 115.22 - 95.5	*mP*64 $P2_1/c$ βS	*a* = 1102 *b* = 1096 *c* = 1090 β = 96.7°	[Mas2]
(αS) < 95.5	*oF*128 *Fddd* αS	*a* = 1046.4 *b* = 1286.60 *c* = 2448.60	pure S at 25°C [Mas2]
α, $Fe_{1-x}Co_x$ < 730	*cP*2 $Pm\bar{3}m$ CsCl	 *a* = 285.25 to 285.53	0.25 ≤ *x* ≤ 0.75 [Mas2] *x* = 0.5 [1984Nis]
Co_4S_3 930 - 785	-	-	[Mas2]
Co_9S_8 < 834	*cF*68 $Fm\bar{3}m$ Co_9C_8	*a* = 992.73 ± 0.04	[V-C2, Mas2]
$Co_{9-x}Fe_xS_8$ (π phase)		*a* = 994.5 ± 0.3 *a* = 995.1 ± 0.1	*x* = 1 [1962Kno, 1976Kno] *x* = 2 [1962Kno, 1976Kno]
λ, $Fe_{1-x}Co_xS_{1+y}$ < 1182	*hP*4 $P6_3/mmc$ NiAs		0 ≤ *x* ≤ 1 0 ≤ *y* ≤ 0.22 also designated as 1C
$Fe_{0.009}Co_{0.991}S_{1.148}$		*a* = 338.8 ± 0.1 *c* = 520.6 ± 0.2	at *x* = 0.991, *y* = 0.148 [1982McC]
$Fe_{0.156}Co_{0.844}S_{1.088}$		*a* = 339.2 ± 0.1 *c* = 525.0 ± 0.2	at *x* = 0.844, *y* = 0.088 [1982McC]
$Fe_{0.25}Co_{0.75}S_{1.083}$		*a* = 339.4 ± 0.1 *c* = 530.3 ± 0.2	at *x* = 0.75, *y* = 0.083 [2001Far]
$Fe_{0.503}Co_{0.497}S_{1.068}$		*a* = 340.7 ± 0.1 *c* = 542.1 ± 0.3	at *x* = 0.497, *y* = 0.068 [1982McC]
$Fe_{0.5}Co_{0.5}S_{1.083}$		*a* = 340.4 ± 0.1 *c* = 541.2 ± 0.2	at *x* = 0.5, *y* = 0.083 [2001Far]
$Fe_{0.692}Co_{0.308}S_{1.044}$		*a* = 342.2 ± 0.1 *c* = 557.5 ± 1.2	at *x* = 308, *y* = 0.044 [1982McC]
$Fe_{0.75}Co_{0.25}S_{1.083}$		*a* = 342.7 ± 0.3	at *x* = 0.25, *y* = 0.083 [2001Far]

(*continued*)

DOI: 10.1007/978-3-540-74196-1_23

Phase/ Temperature Range [°C]	Pearson Symbol/ Space Group/ Prototype	Lattice Parameters [pm]	Comments/References
$Fe_{0.834}Co_{0.166}S_{1.053}$		$c = 561.2 \pm 0.4$ $a = 343.5 \pm 0.1$ $c = 567.6 \pm 0.2$	at $x = 0.166$, $y = 0.053$ [1982McC]
γFeS < 1188		$a = 344.36 \pm 0.05$ $c = 587.59 \pm 0.05$	at $x = 0$, $y = 0$ [V-C2, Mas2]
CoS 1180 - 425		$a = 338.4$ $c = 519.6$	at $x = 1$, $y = 0$ [V-C2, Mas2]
λ' ≲ 545	-	-	presumably an ordered form of CoS [1997Bry]
3C	*cI** superstructure of the NiAs type	$a = 2a_0$ $c = 3c_0$	[2002Far]
Co_3S_4 ≲ 657	*cF*56 $Fd\bar{3}m$ Al_2MgO_4	$a = 940.4 \pm 0.1$	[V-C2, Mas2]
$Fe_{1-x}Co_xS_2$	*cP*12 $Pa\bar{3}$ FeS_2 (pyrite)		$0 \le x \le 1$ [V-C2, Mas2, 1962Kle, 1988Rag]
		$a = 552.33 \pm 0.05$	at $x = 0.90$ [1968Bou]
		$a = 551.6$	at $x = 0.90$ [2003Che]
		$a = 551.30 \pm 0.05$	at $x = 0.80$ [1968Bou]
		$a = 550.3$	at $x = 0.75$ [2003Che]
		$a = 548.96 \pm 0.05$	at $x = 0.60$ [1968Bou]
		$a = 547.80 \pm 0.05$	at $x = 0.50$ [1968Bou]
		$a = 547.1$	at $x = 0.50$ [2003Che]
		$a = 546.53 \pm 0.05$	at $x = 0.40$ [1968Bou]
		$a = 545.3$	at $x = 0.35$ [2003Che]
		$a = 545.29 \pm 0.05$	at $x = 0.30$ [1968Bou]
		$a = 544.76 \pm 0.05$	at $x = 0.25$ [1968Bou]
		$a = 543.98 \pm 0.05$	at $x = 0.20$ [1968Bou]
		$a = 543.33 \pm 0.05$	at $x = 0.15$ [1968Bou]
		$a = 542.71 \pm 0.05$	at $x = 0.10$ [1968Bou]
		$a = 542.30 \pm 0.05$	at $x = 0.05$ [1968Bou]
CoS_2 < 1027		$a = 553.85 \pm 0.02$	at $x = 1$ [V-C2, Mas2, 1988Rag]
βFeS_2 743 - 444.5		$a = 541.79 \pm 0.11$	at $x = 0$, mineral pyrite [Mas2, 1982Kub] [V-C2, Mas2]
		$a = 534.8 \pm 0.2$	at 1.57 GPa [V-C2]
		$a = 529.3 \pm 0.2$	at 2.87 GPa [V-C2]
		$a = 525.5 \pm 0.2$	at 3.85 GPa [V-C2]

(*continued*)

DOI: 10.1007/978-3-540-74196-1_23

Phase/ Temperature Range [°C]	Pearson Symbol/ Space Group/ Prototype	Lattice Parameters [pm]	Comments/References
βFeS	*hP*24	a = 596.3 ± 0.1	at 21°C [V-C2, Mas2]
≲ 315	$P\bar{6}2c$	c = 1175.4 ± 0.1	
	?	a = 586.1	at 21°C and 3.33 GPa [V-C2, Mas2]
		c = 1157.7 ± 0.1	
		a = 599.8 ± 1.1	at 120°C [V-C2, Mas2]
		c = 1171 ± 1	
$Co_{0.025}Fe_{0.975}S$		a = 599.1 ± 0.2	[2000Kim, 2005Nam]
		c = 1154 ± 5	
$Co_{0.08}Fe_{0.92}S$		a = 595.9 ± 0.3	at 25°C [1987Col]
		c = 1166.4 ± 0.4	
		a = 692.6 ± 0.3	at 92°C [1987Col]
		c = 578.0 ± 0.3	
$Co_{0.2}Fe_{0.8}S$		a = 688.2 ± 0.3	at 25°C [1987Col]
		c = 572.3 ± 0.3	
αFeS	*hP*6	a = 345.59 ± 0.05	[V-C2, Mas2]
≲ 138	$P6_3/mmc$	c = 577.89 ± 0.05	
	FeS		
FeS	*oP*8	a = 582.5 ± 0.2	at 190°C [V-C2]
(HP)	*Pnma*	b = 346.8 ± 0.1	
	MnP	c = 693.5 ± 0.6	
		a = 571.6 ± 0.9	at 21°C and 4.15 GPa [V-C2]
		b = 334.7 ± 0.3	
		c = 669.4 ± 0.9	
		a = 565 ± 1	at 21°C and 6.35 GPa [V-C2]
		b = 331.6 ± 0.3	
		c = 663.1 ± 0.8	
FeS	*tP*4	a = 376.8	[V-C2]
	*P*4/*nmm*	c = 503.9	mineral mackinawite
	PbO		
αFeS_2	*oP*6	a = 444.1	mineral marcasite [V-C2, Mas2,
≲ 444.5	*Pnnm*	b = 542.5	1982Kub]
	FeS_2 (marcasite)	c = 338.7	
		a = 446.4	at 327°C [V-C2]
		b = 544	
		c = 339	
Fe_2S_3	*tP*80	a = 1053	[V-C2]
	$P4_32_12$	c = 1001	
	?		

(*continued*)

DOI: 10.1007/978-3-540-74196-1_23

Phase/ Temperature Range [°C]	Pearson Symbol/ Space Group/ Prototype	Lattice Parameters [pm]	Comments/References
Fe_3S_4	*hR*21 $R\bar{3}m$ Fe_3S_4	*a* = 347 ± 2 *c* = 345 ± 20	mineral smythite [V-C2]
Fe_7S_8	*hP*45 $P3_121$ Fe_7S_8	*a* = 686.52 ± 0.06 *c* = 1704.6 ± 0.2	metastable phase, mineral pyrrhotite-3C [V-C2]

Table 3. Invariant Equilibria

Reaction	*T* [°C]	Type	Phase	Composition (at.%)		
				Co	Fe	S
L + γ ⇌(αFe)	~950	p_3	-	-	-	-
L + γ ⇌(αFe) + λ	947	U_1	-	-	-	-
L + γ ⇌(αFe) + Co_4S_3	860	U_2	Co_4S_3	57.14	0	42.86
L ⇌ (αFe) + λ + Co_4S_3	847	E_1	Co_4S_3	57.14	0	42.86
Co_4S_3 + (αFe) ⇌ γ + λ	~820	U_3	Co_4S_3	57.14	0	42.86
Co_4S_3 ⇌ γ + λ + Co_9S_8	747	E_2	Co_4S_3 Co_9S_8	57.14 52.94	0 0	42.86 47.06
L + λ ⇌CoS_2 + βFeS_2	735	U_4	CoS_2 βFeS_2	33.33 0	0 33.33	66.67 66.67
γ + λ ⇌ (αFe) + Co_9S_8	730	U_5	Co_9S_8	52.94	0	47.06
L ⇌ (S) + CoS_2 + αFeS_2	~113	E_3	(S) CoS_2 αFeS_2	0 33.33 0	0 0 33.33	~100 66.67 66.67

DOI: 10.1007/978-3-540-74196-1_23

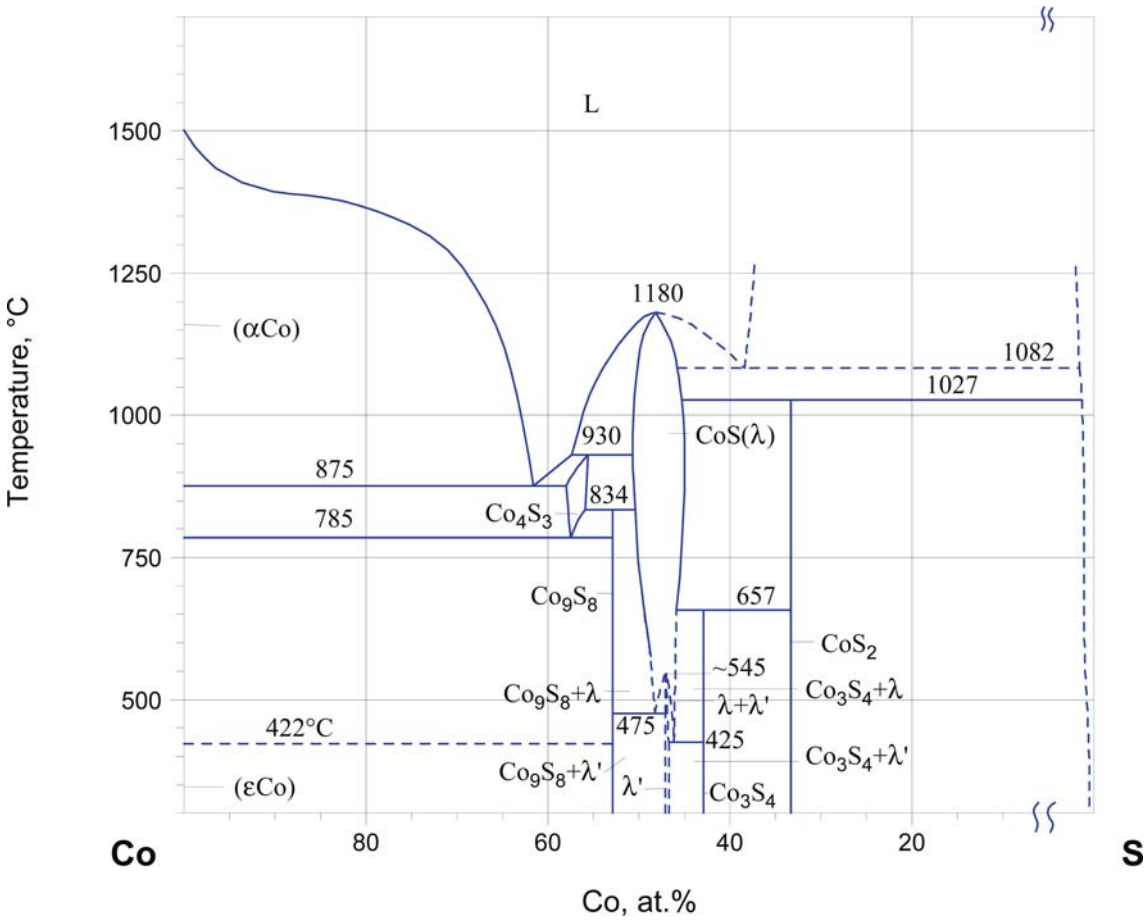

Fig. 1. Co-Fe-S. Phase diagram of the Co-S binary system

DOI: 10.1007/978-3-540-74196-1_23

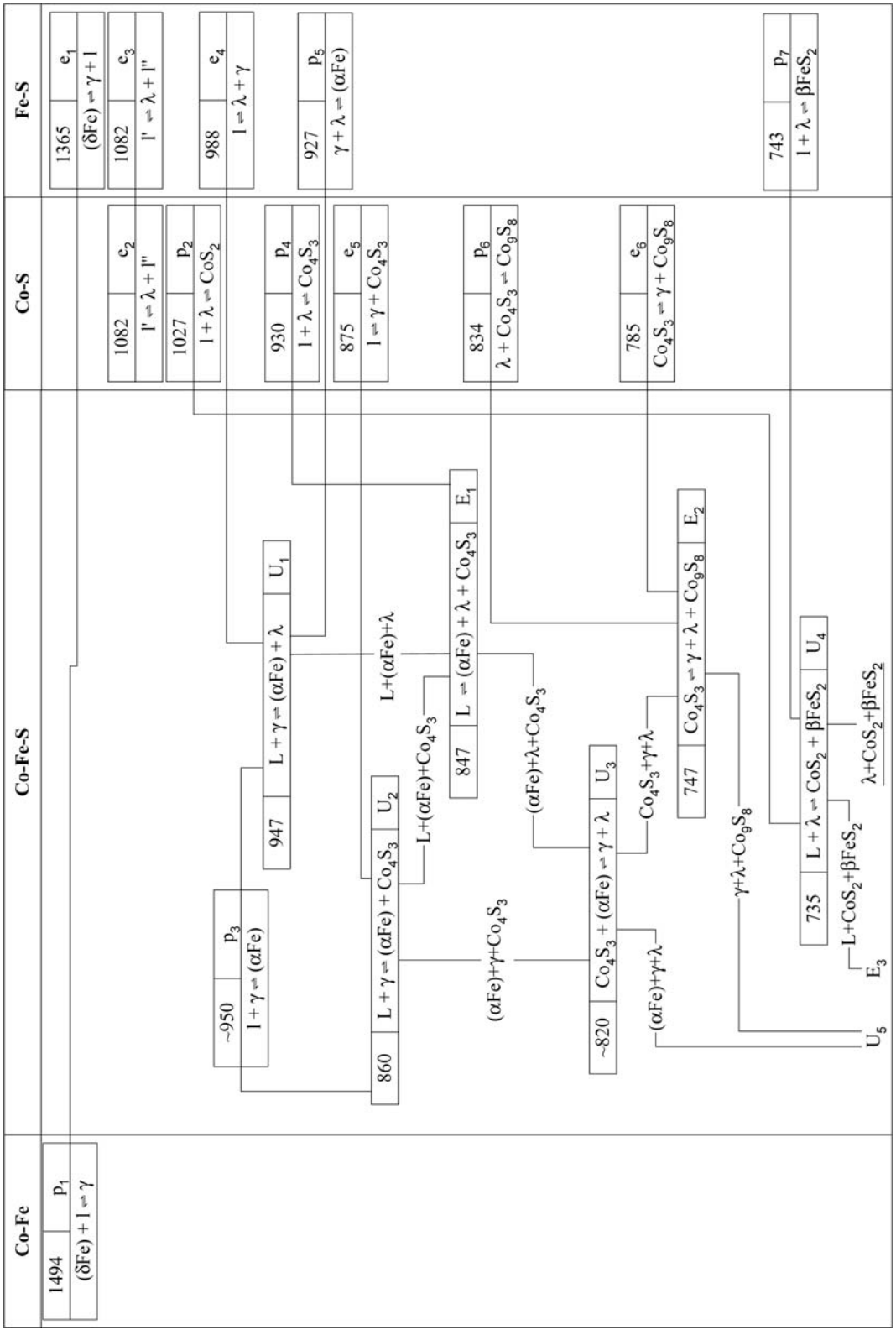

Fig. 2a. Co-Fe-S. Reaction scheme, part 1

DOI: 10.1007/978-3-540-74196-1_23

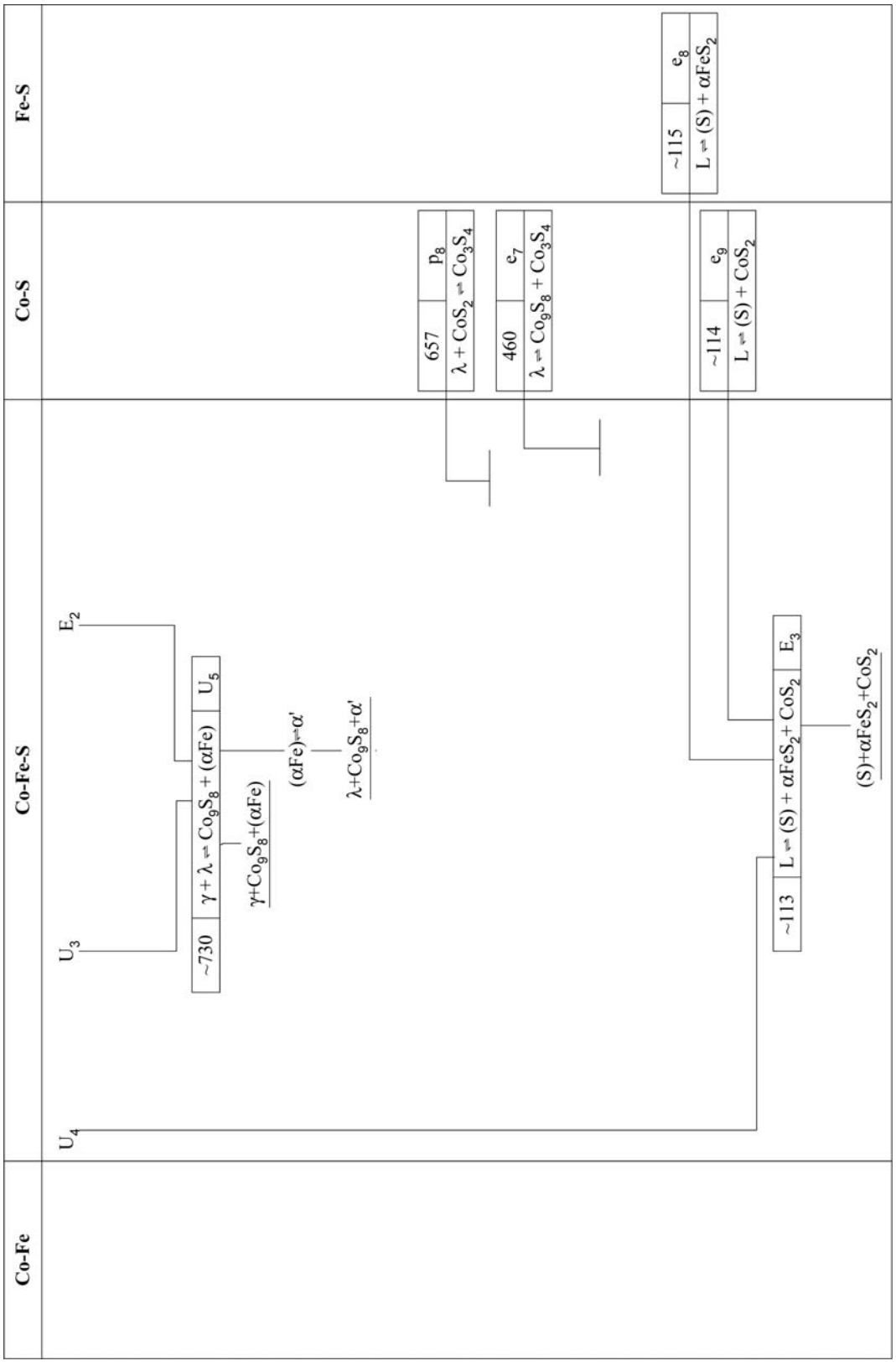

Fig. 2b. Co-Fe-S. Reaction scheme, part 2

DOI: 10.1007/978-3-540-74196-1_23

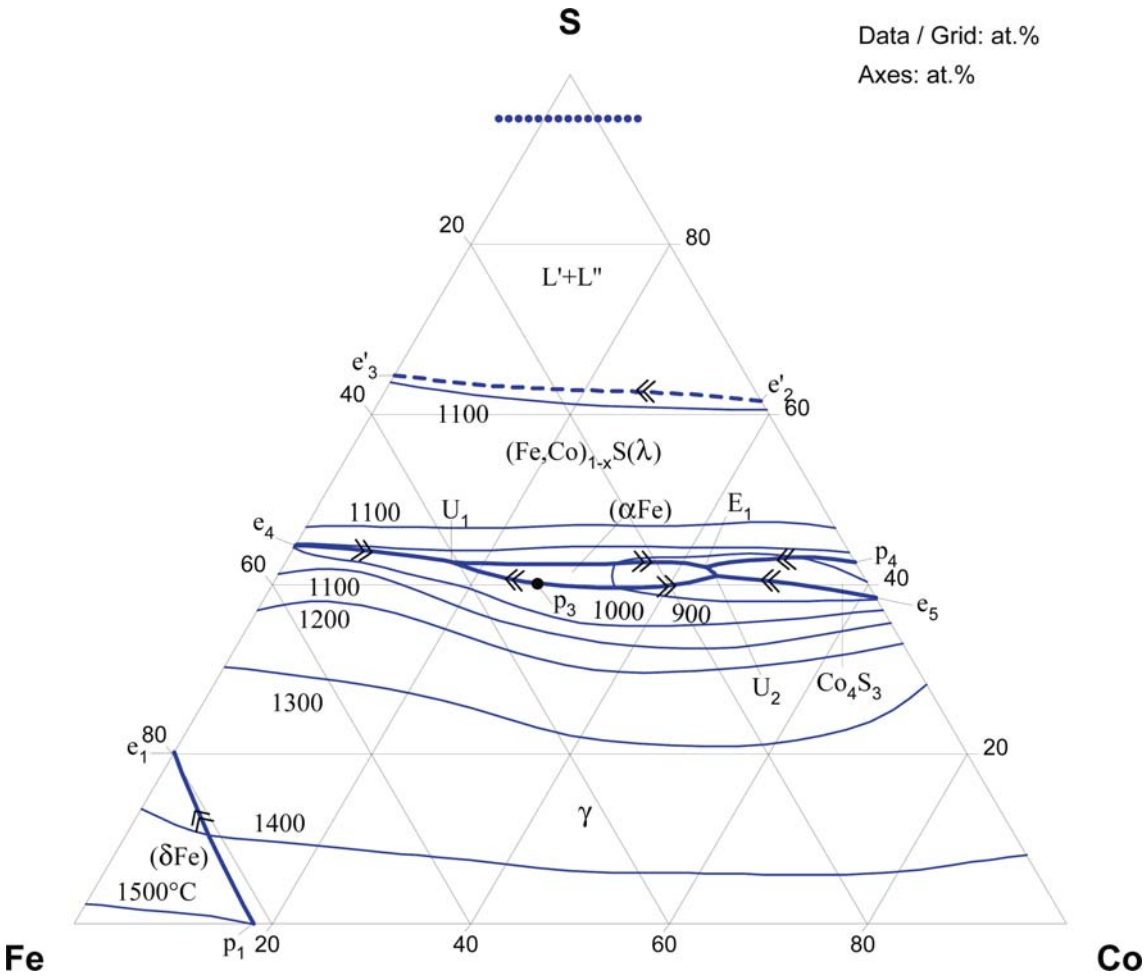

Fig. 3a. Co-Fe-S. Liquidus surface projection

DOI: 10.1007/978-3-540-74196-1_23

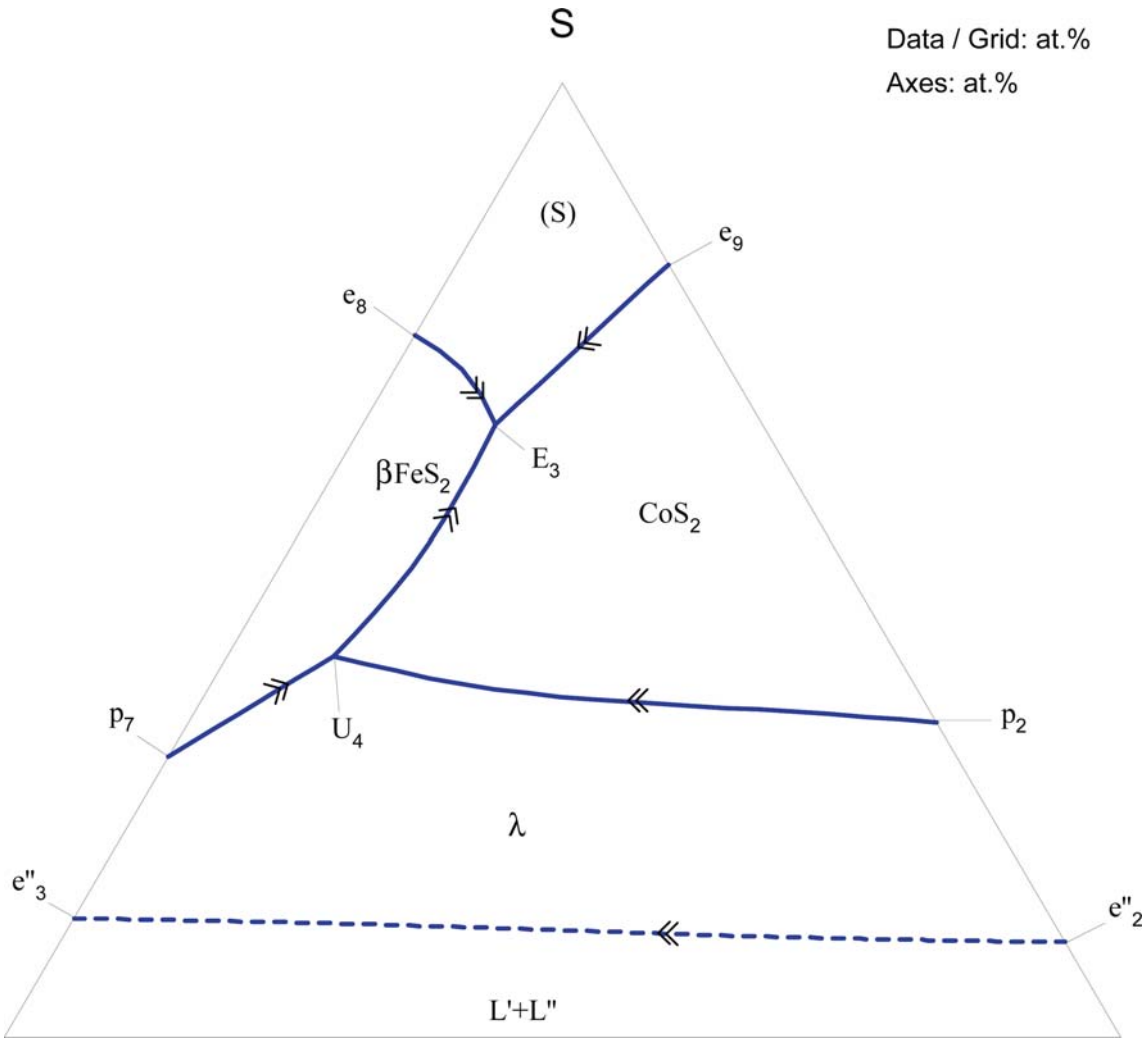

Fig. 3b. Co-Fe-S. Probable liquidus surface projection in the S corner (schematic)

DOI: 10.1007/978-3-540-74196-1_23

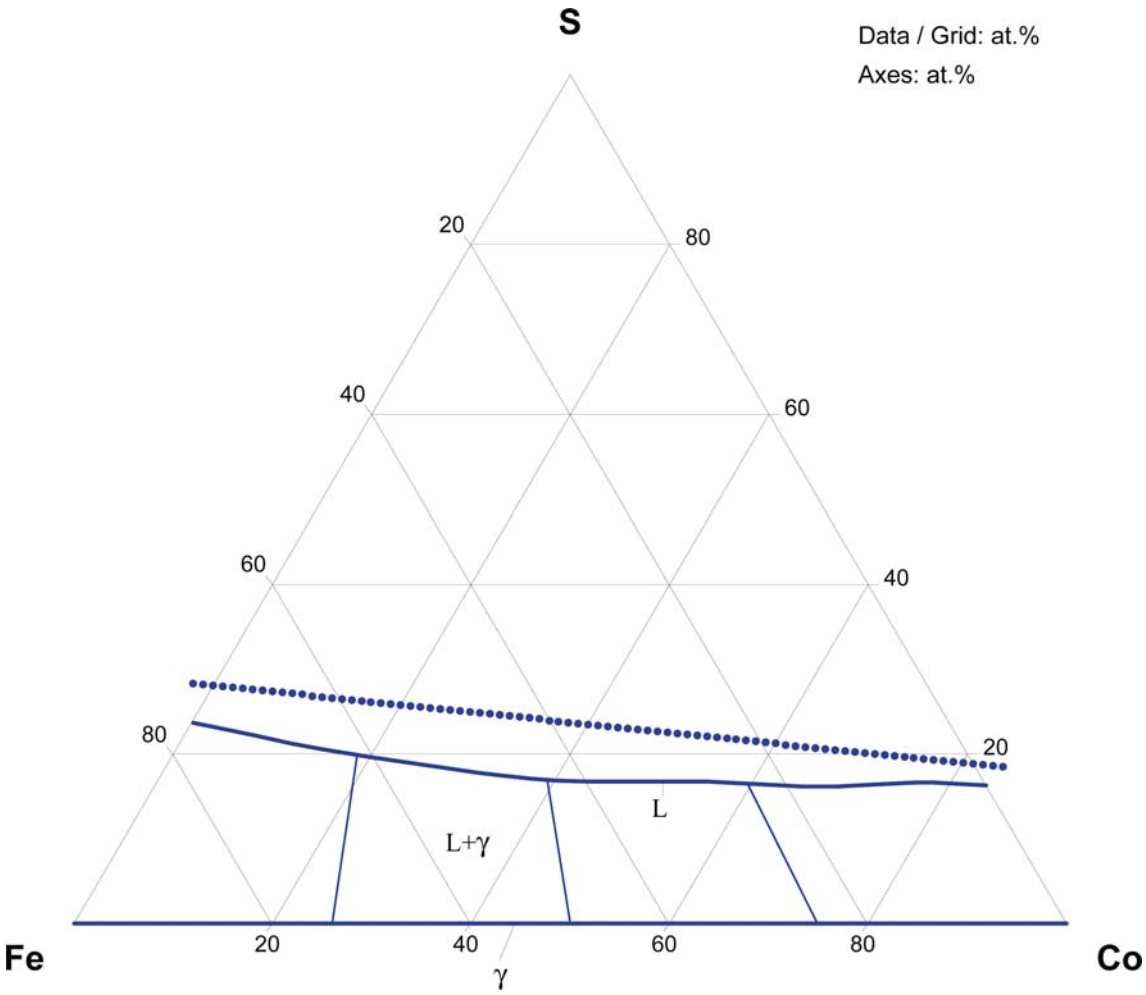

Fig. 4. Co-Fe-S. Isothermal section at 1350°C

DOI: 10.1007/978-3-540-74196-1_23

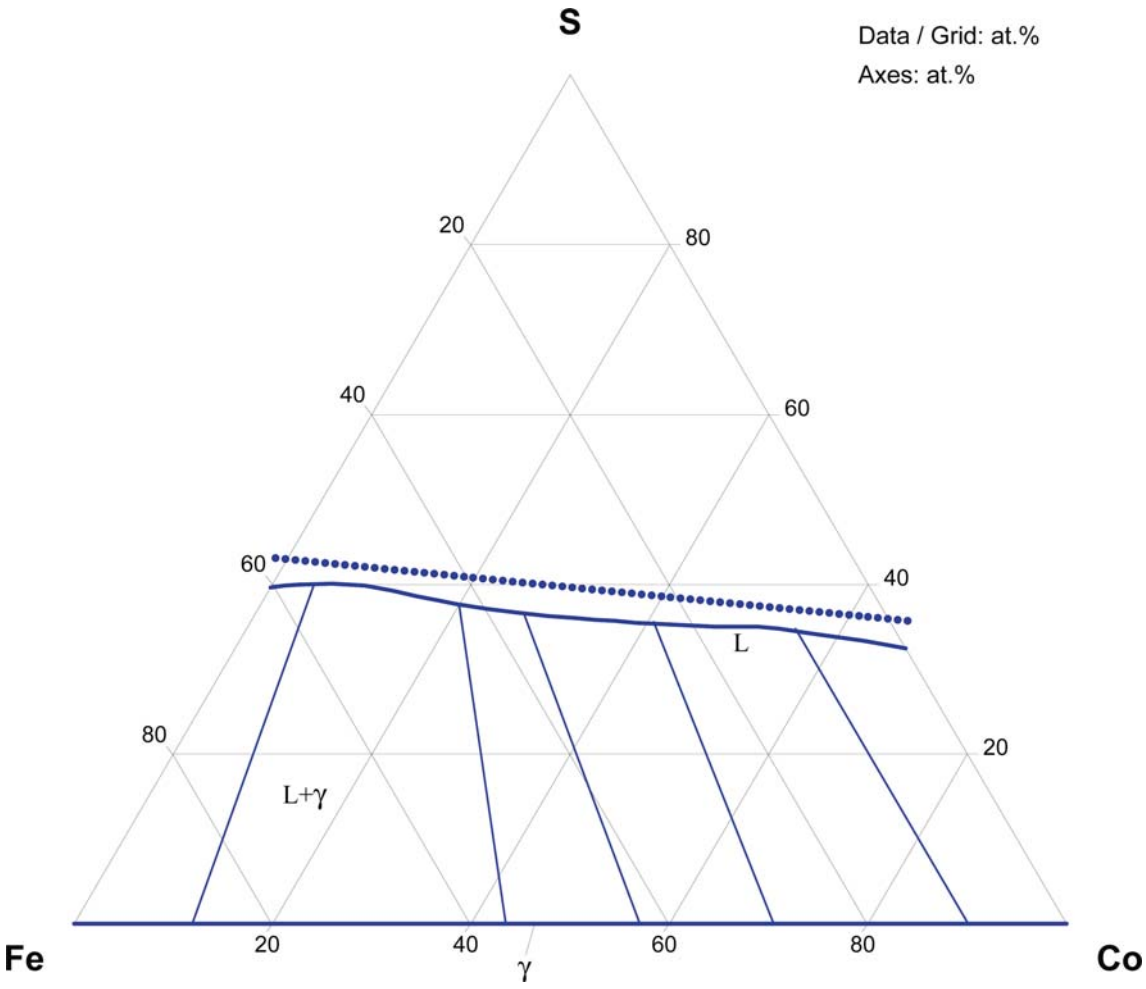

Fig. 5. Co-Fe-S. Isothermal section at 1200°C

DOI: 10.1007/978-3-540-74196-1_23

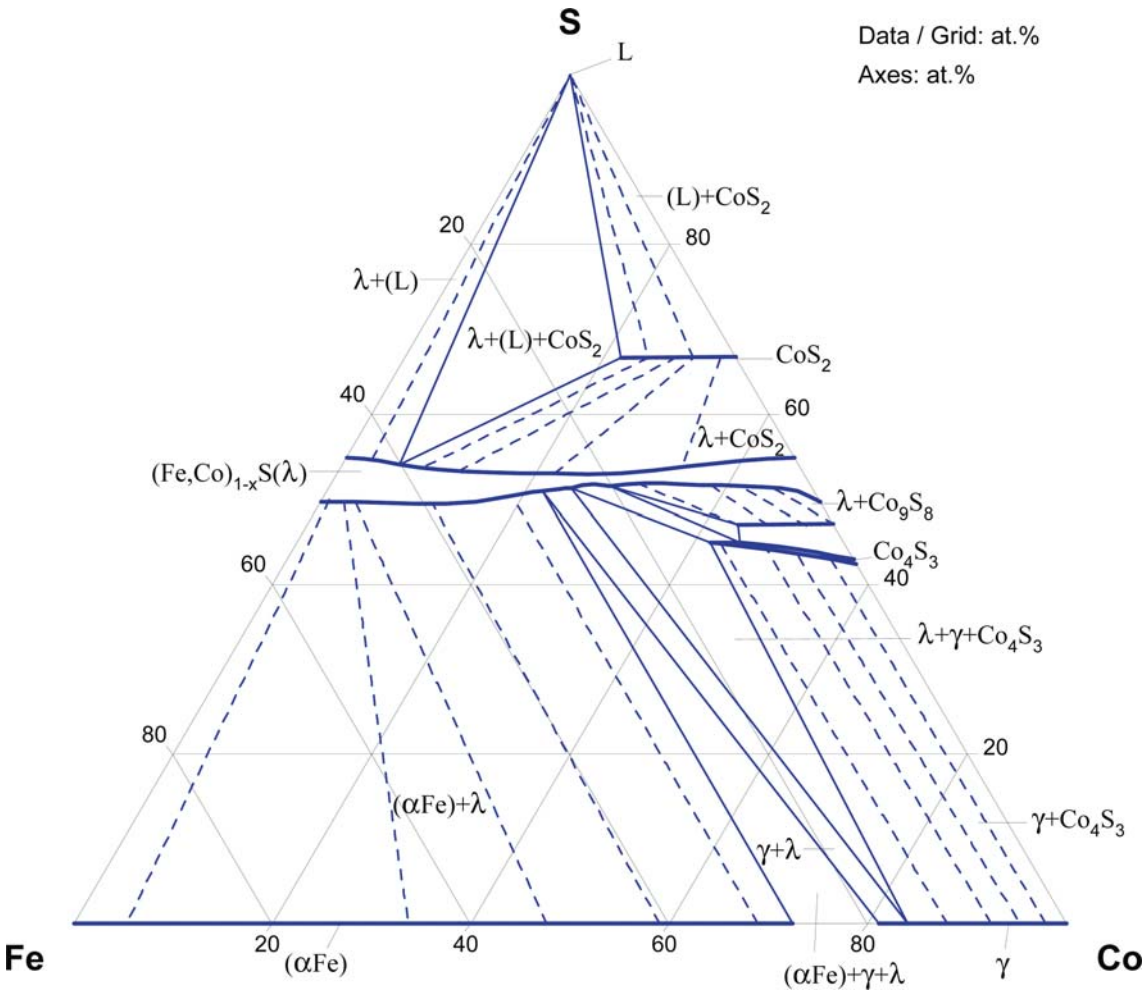

Fig. 6. Co-Fe-S. Isothermal section at 800°C

DOI: 10.1007/978-3-540-74196-1_23

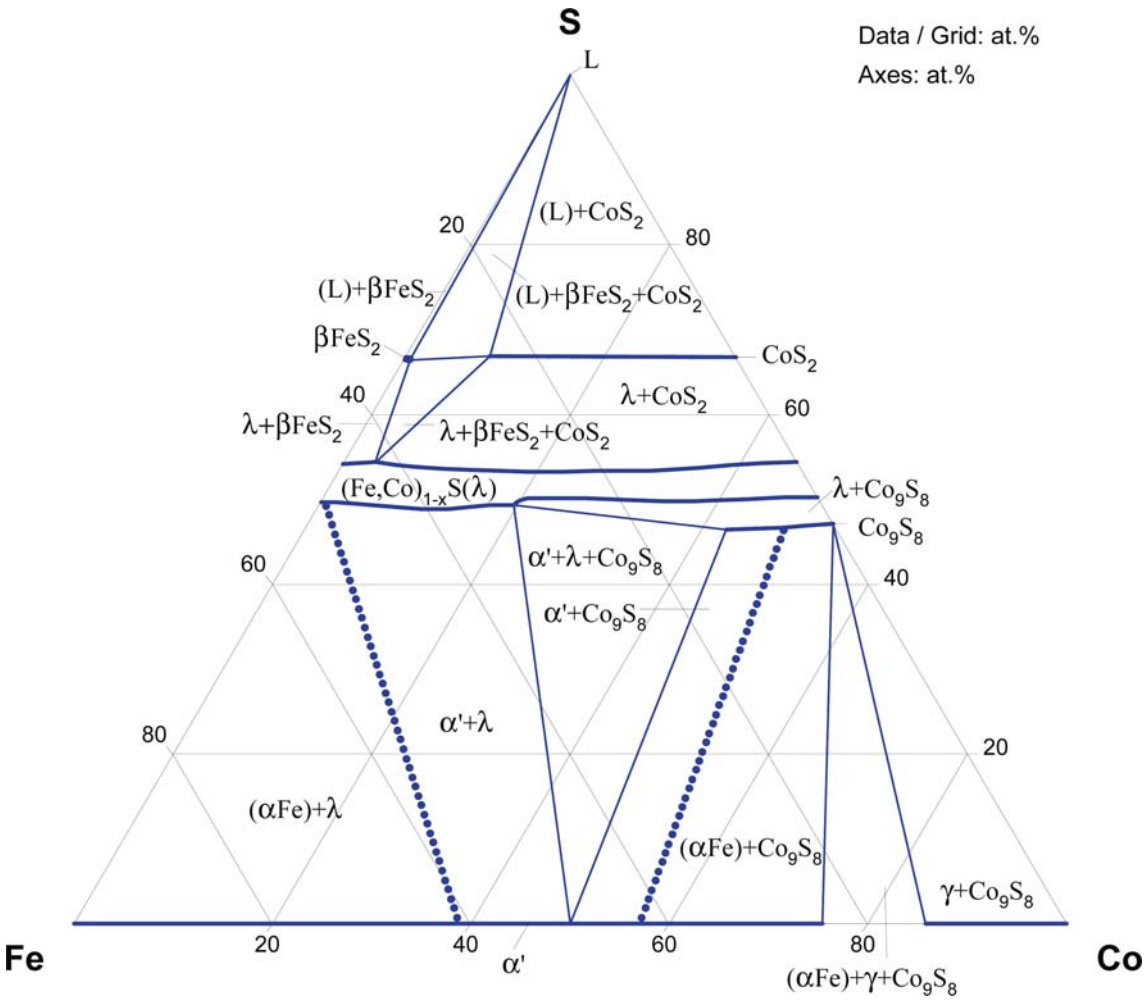

Fig. 7. Co-Fe-S. Isothermal section at 700°C

DOI: 10.1007/978-3-540-74196-1_23

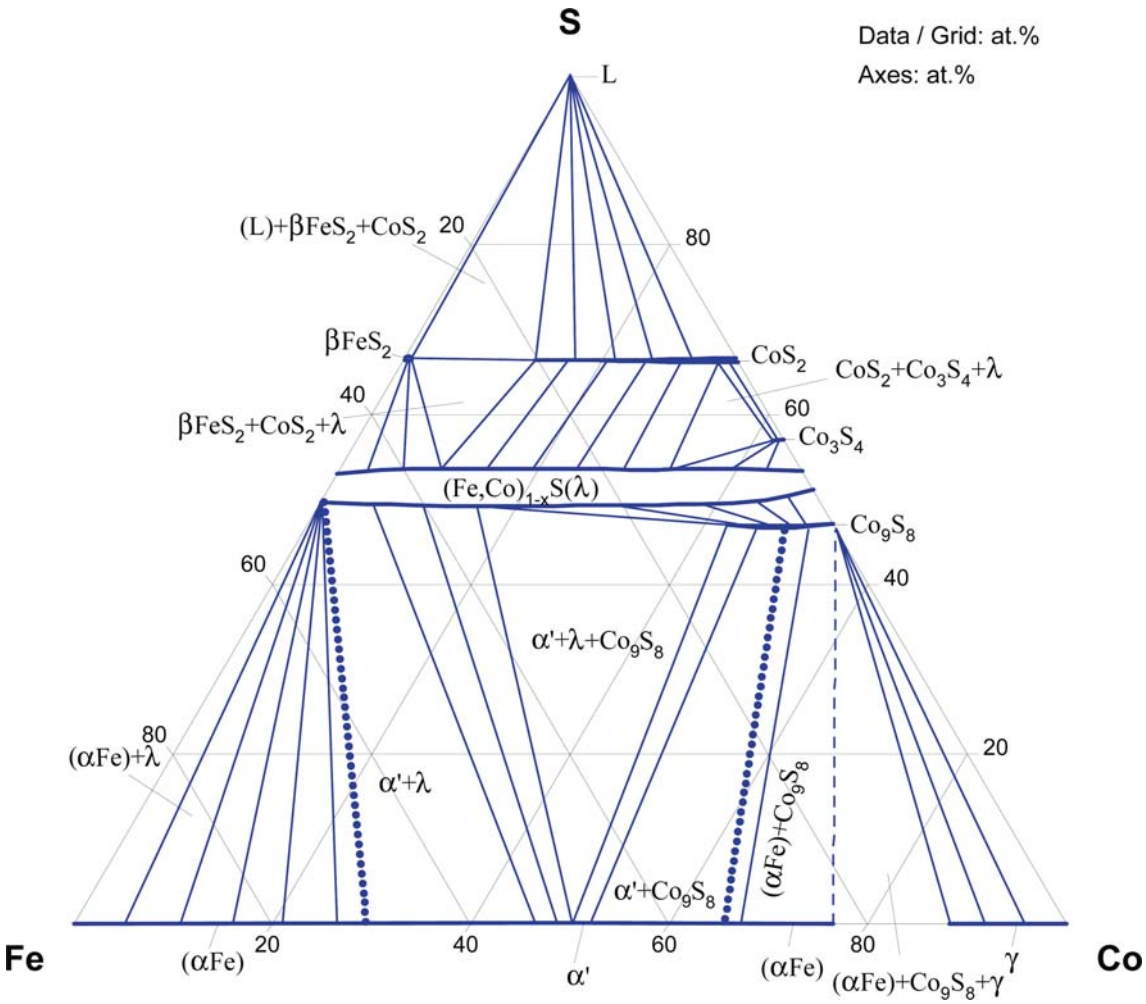

Fig. 8. Co-Fe-S. Isothermal section at 600°C

DOI: 10.1007/978-3-540-74196-1_23

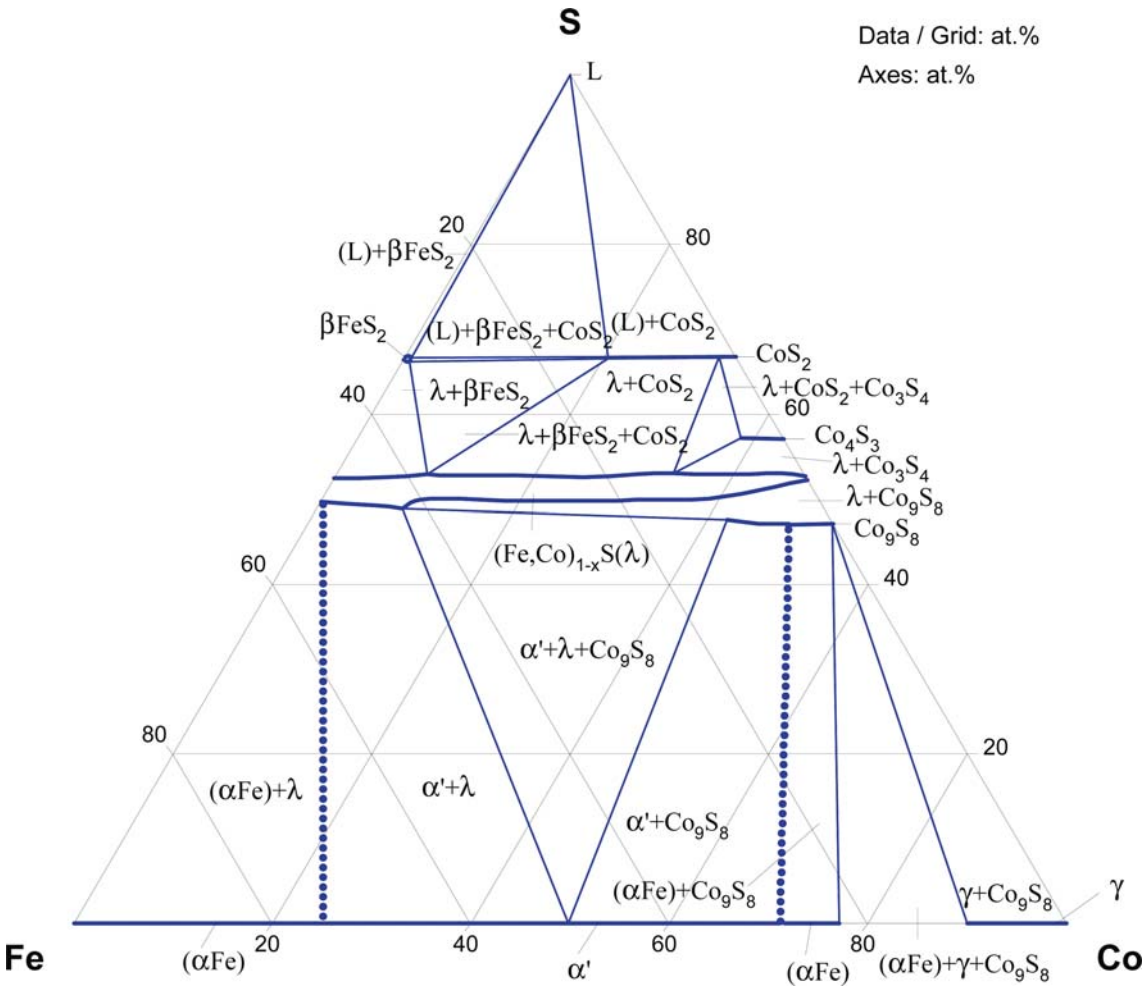

Fig. 9. Co-Fe-S. Isothermal section at 500°C

DOI: 10.1007/978-3-540-74196-1_23

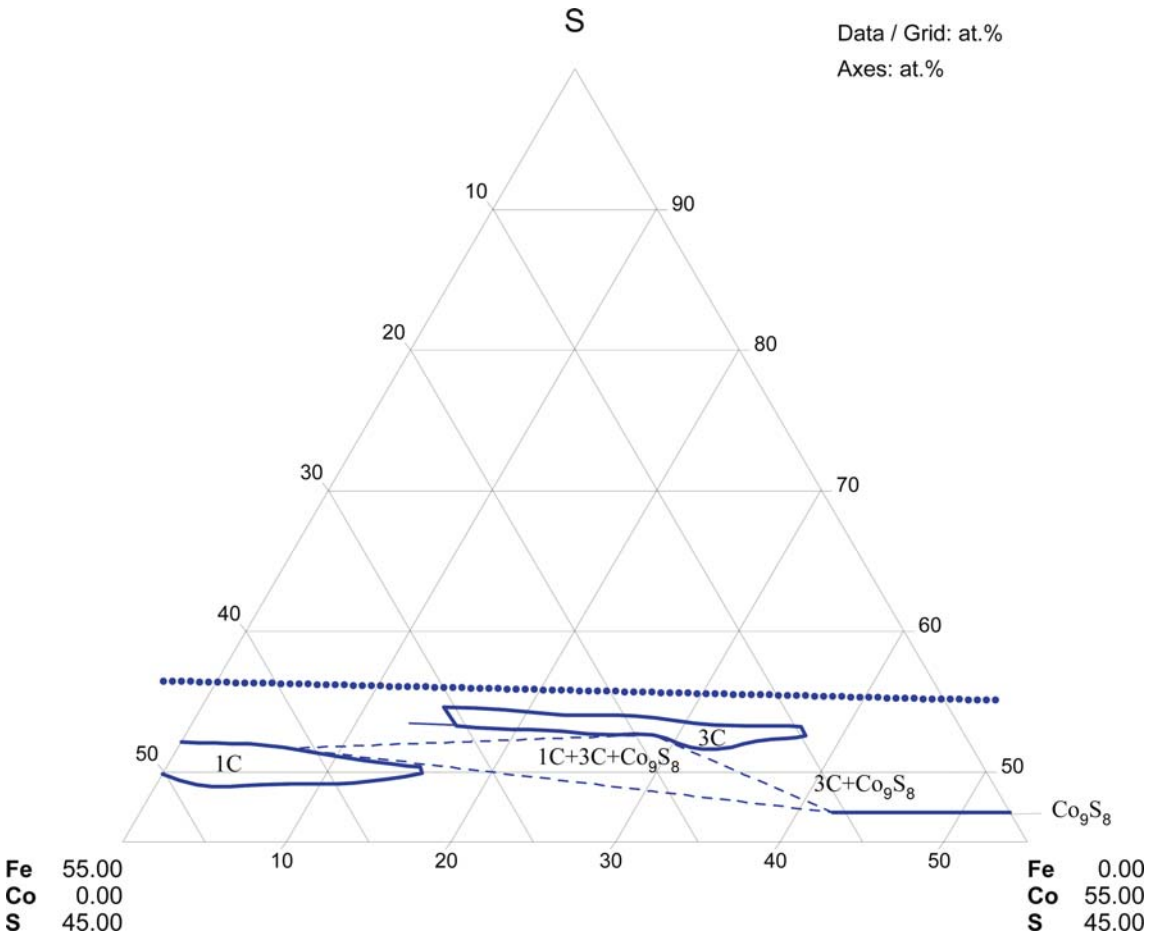

Fig. 10. Co-Fe-S. Isothermal section at 325°C

DOI: 10.1007/978-3-540-74196-1_23

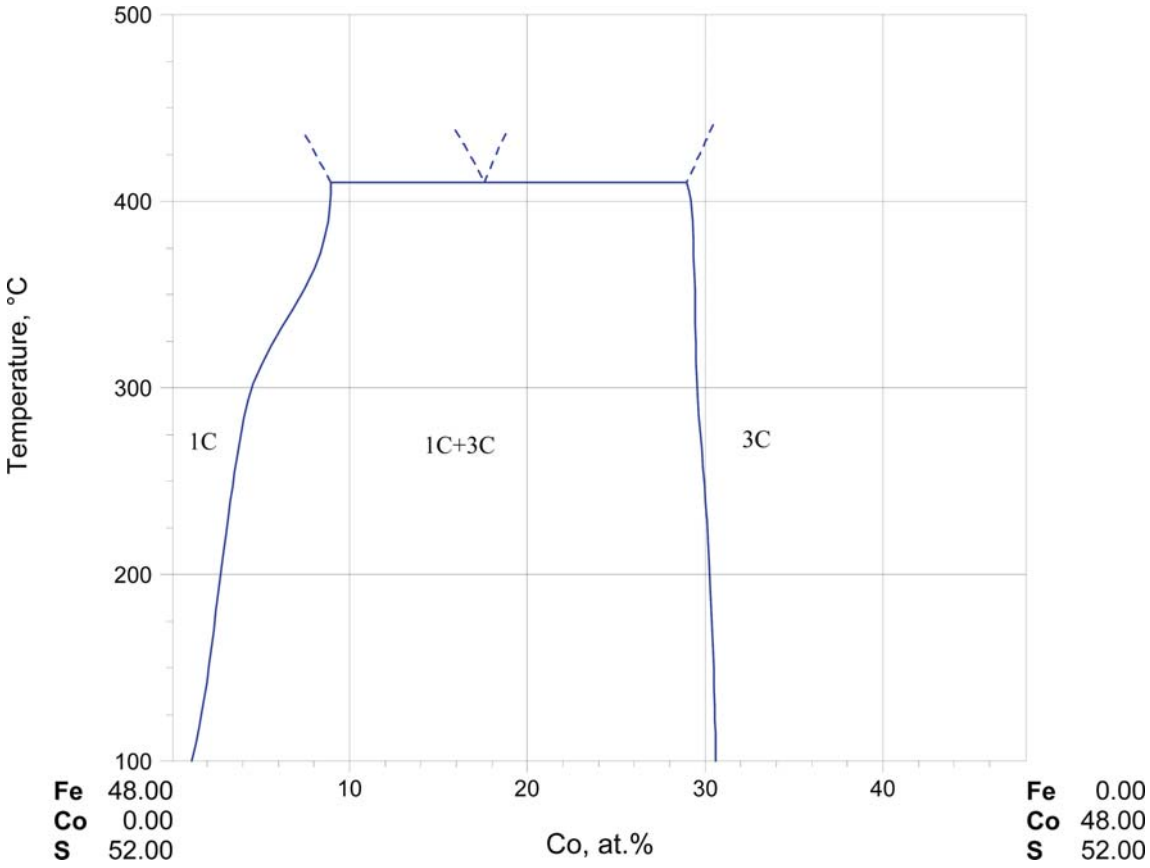

Fig. 11. Co-Fe-S. Vertical section $Co_{1-x}S$-$Fe_{1-x}S$ for 52 at.% S in the presence of Co_9S_8

DOI: 10.1007/978-3-540-74196-1_23

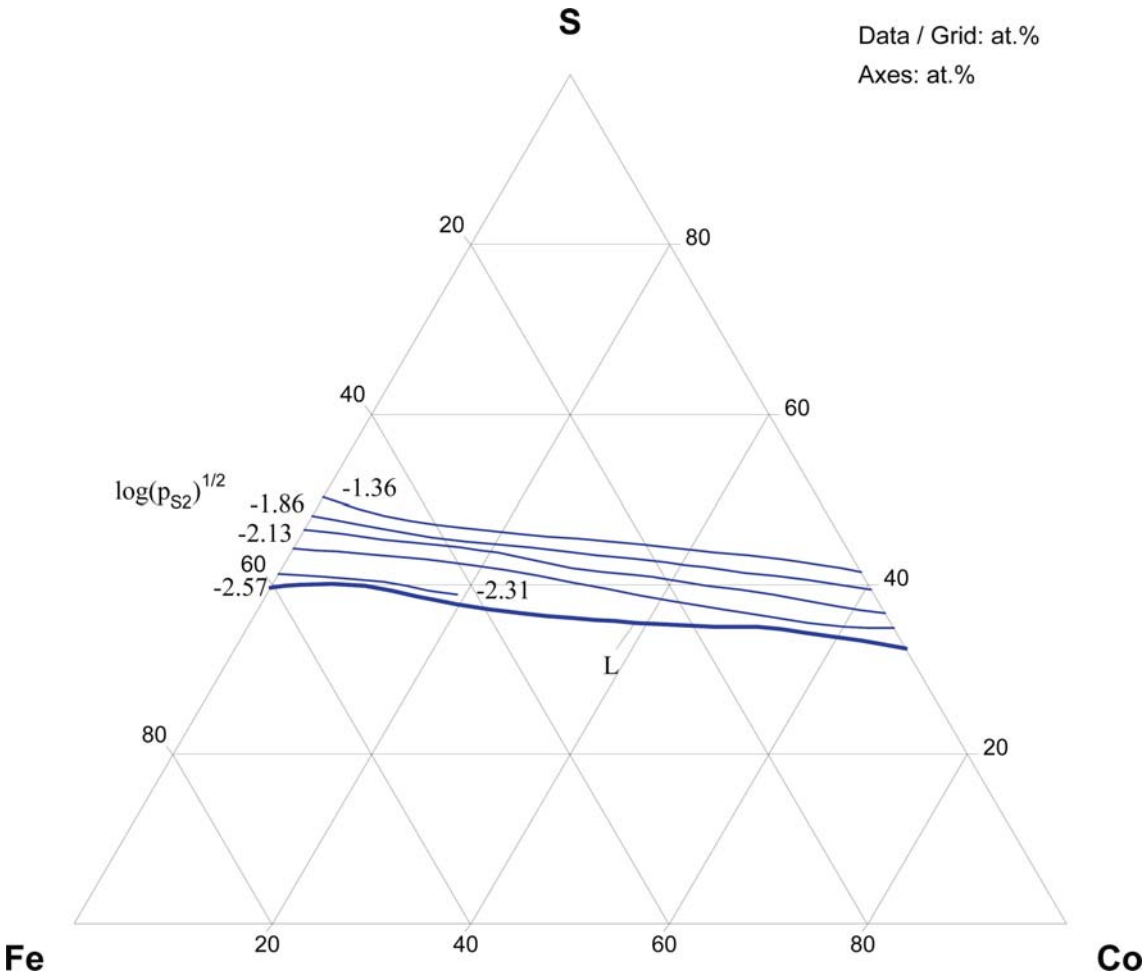

Fig. 12a. Co-Fe-S. Sulphur isopartial pressure at 1200°C

DOI: 10.1007/978-3-540-74196-1_23

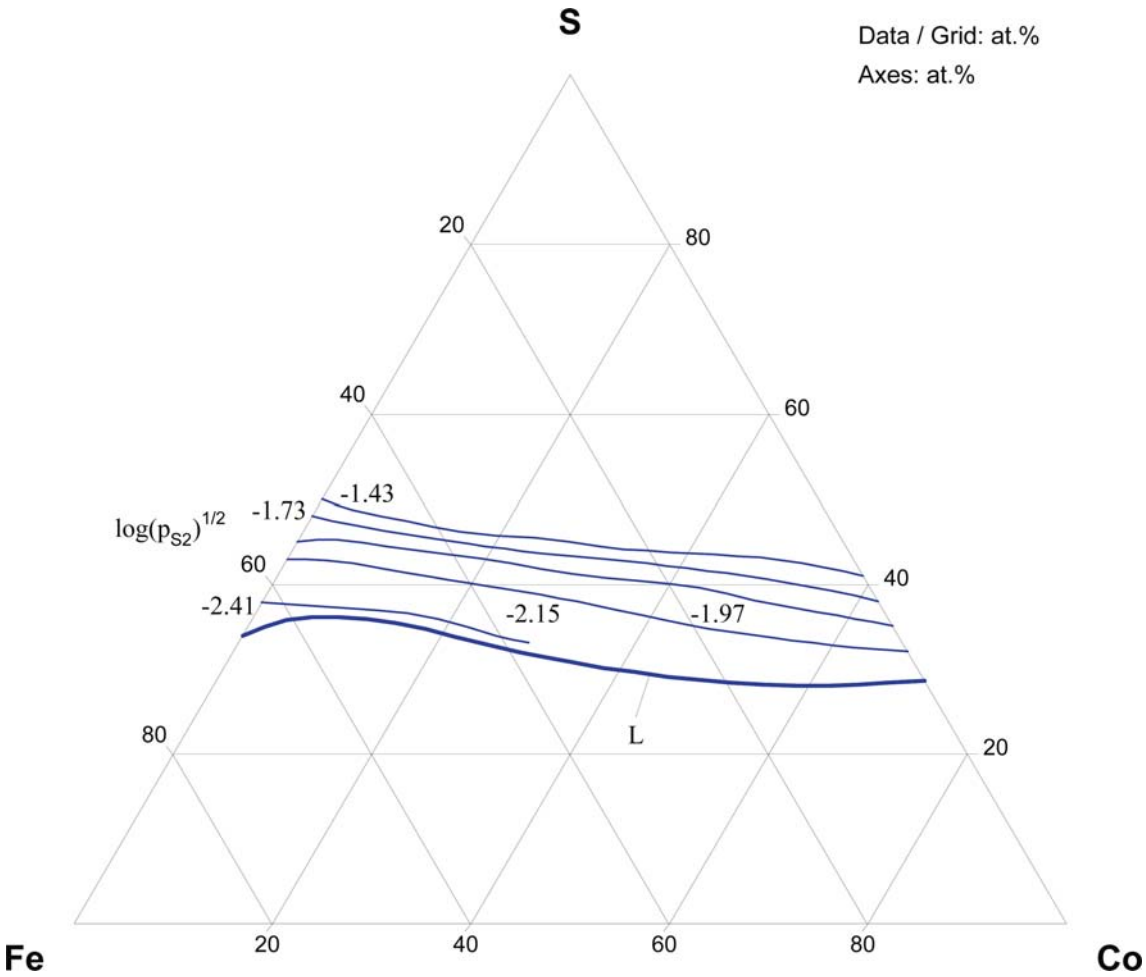

Fig. 12b. Co-Fe-S. Sulphur isopartial pressure at 1275°C

DOI: 10.1007/978-3-540-74196-1_23

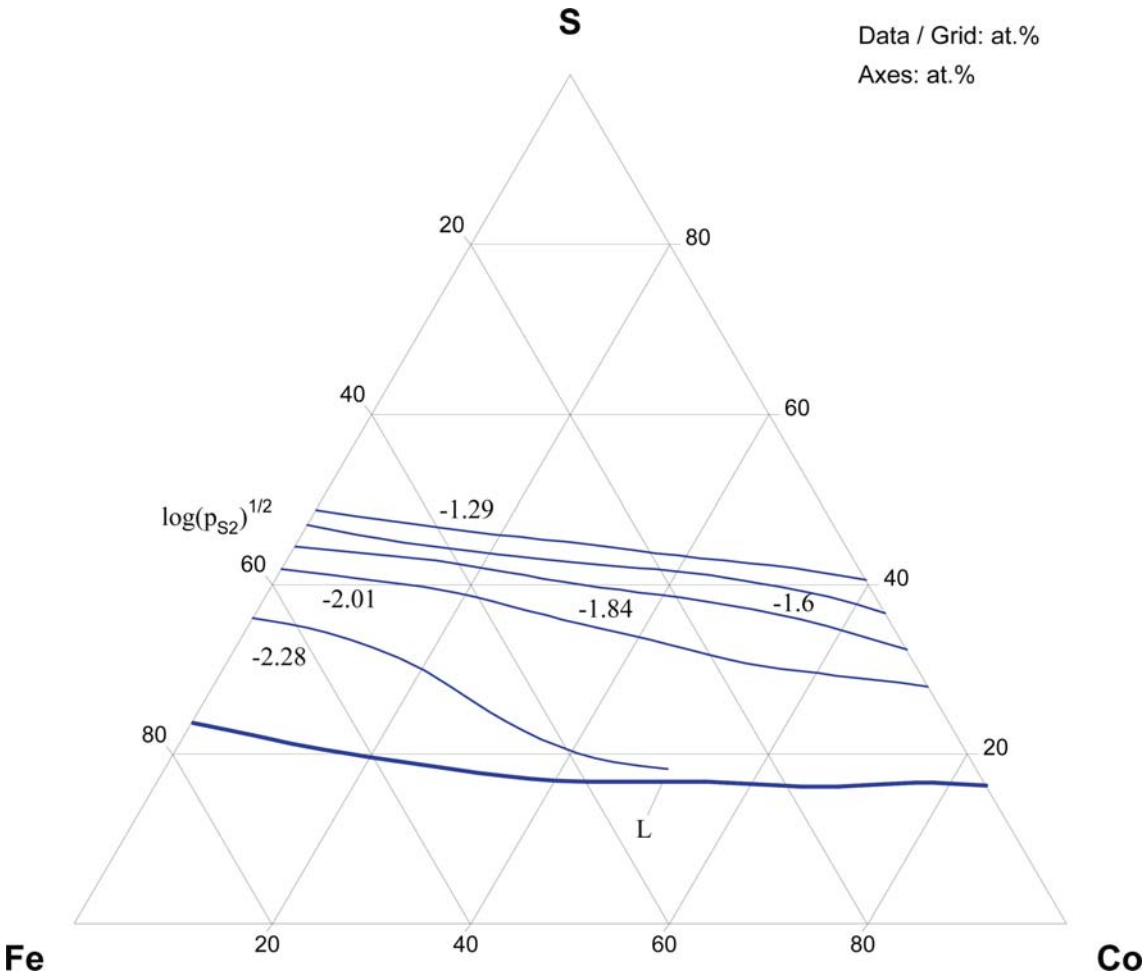

Fig. 12c. Co-Fe-S. Sulphur isopartial pressure at 1350°C

DOI: 10.1007/978-3-540-74196-1_23

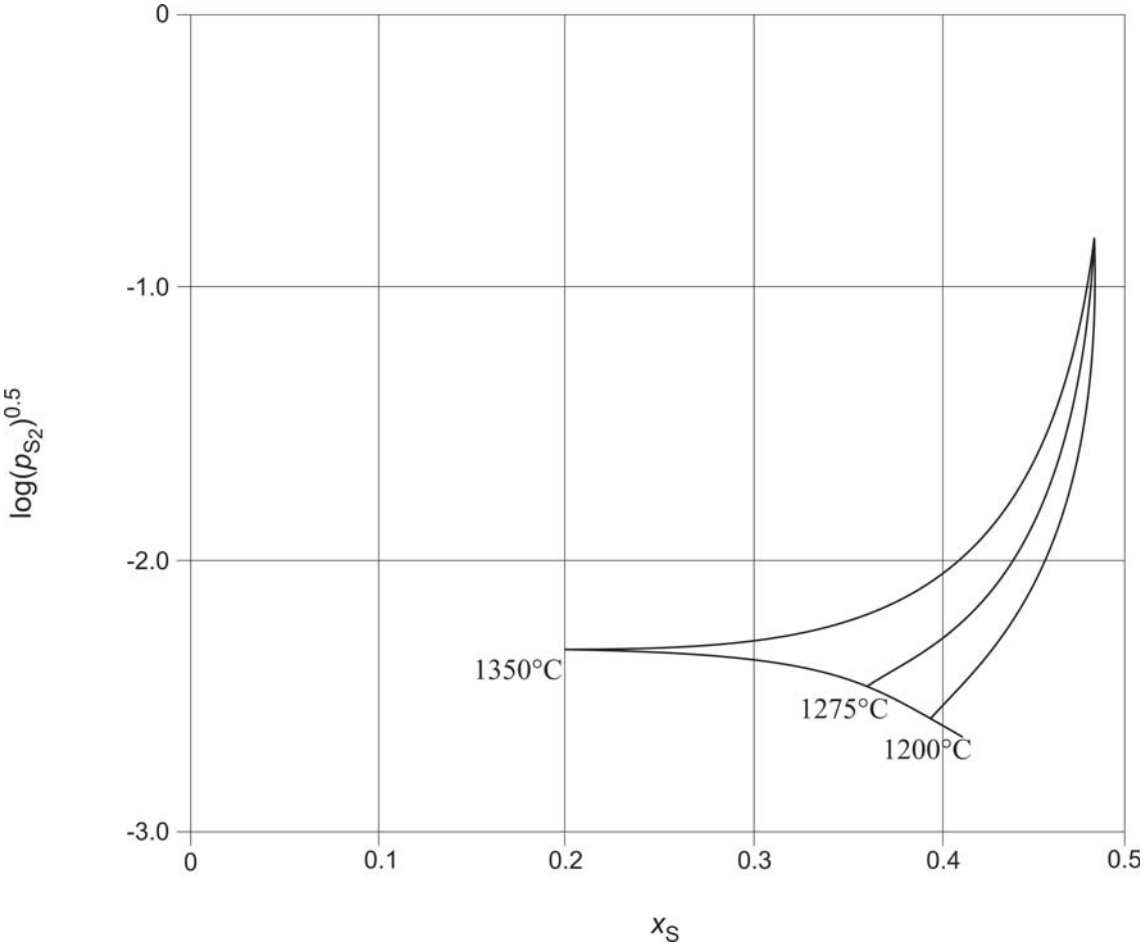

Fig. 13a. Co-Fe-S. Partial pressure of S_2 (gas) in equilibrium with Co-Fe-S mattes at Co/Fe = 0.25 at different temperatures

DOI: 10.1007/978-3-540-74196-1_23

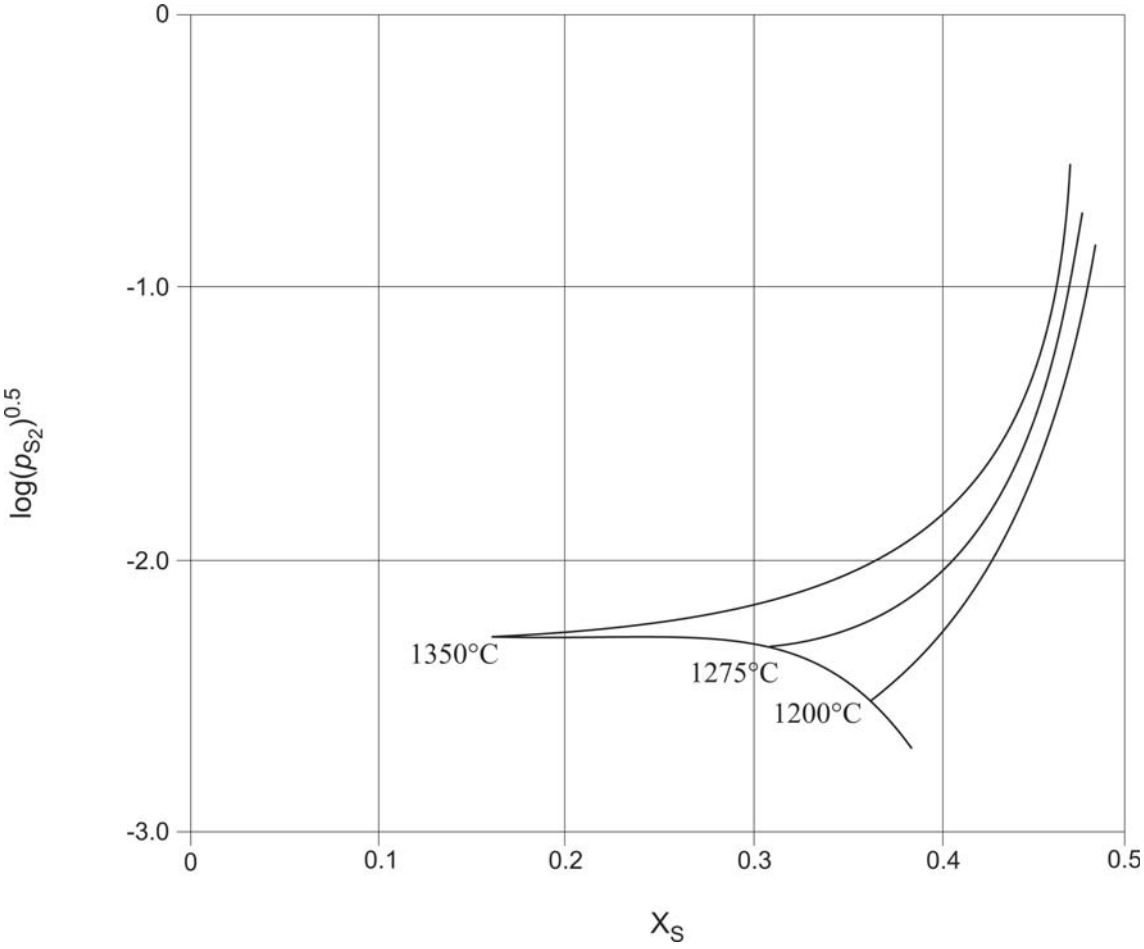

Fig. 13b. Co-Fe-S. Partial pressure of S_2 (gas) in equilibrium with Co-Fe-S mattes at Co/Fe = 1 at different temperatures

DOI: 10.1007/978-3-540-74196-1_23

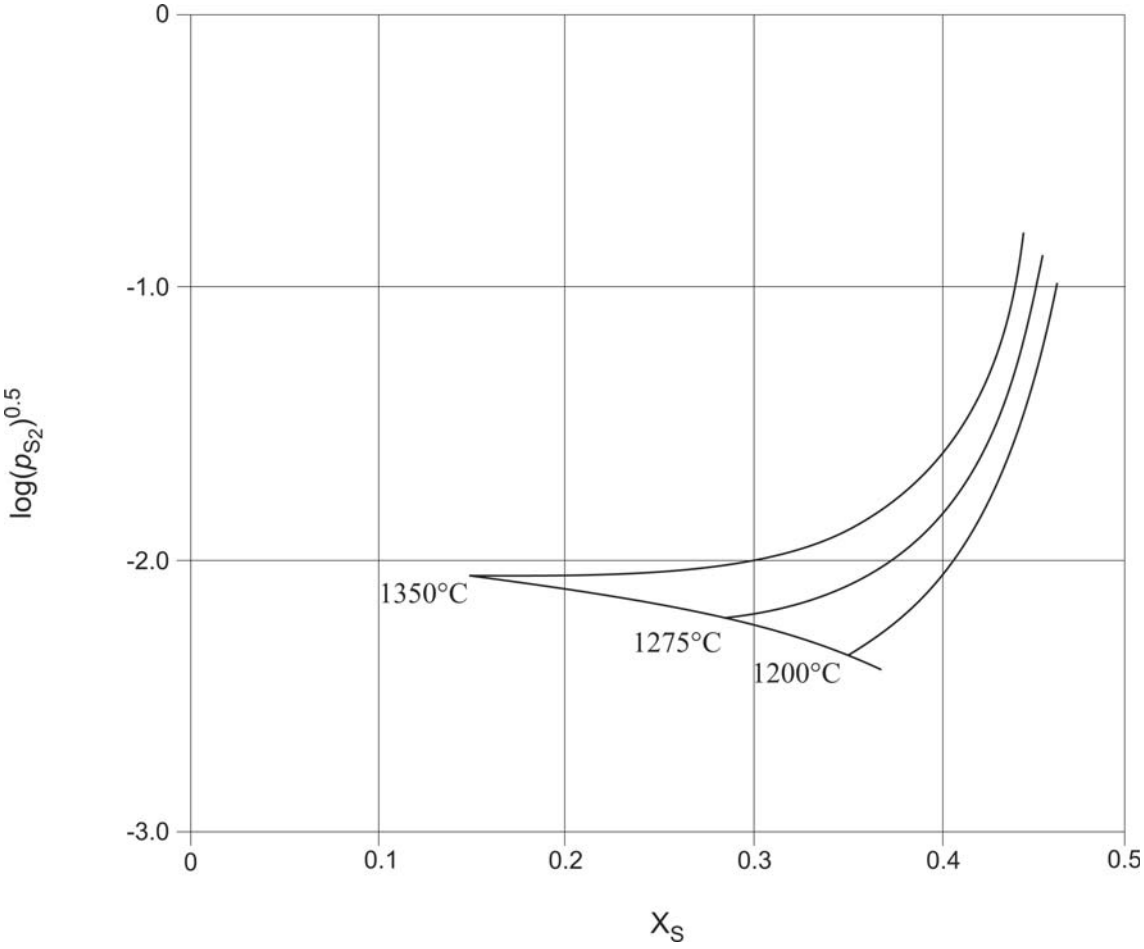

Fig. 13c. Co-Fe-S. Partial pressure of S_2 (gas) in equilibrium with Co-Fe-S mattes at Co/Fe = 1 at different temperatures

DOI: 10.1007/978-3-540-74196-1_23

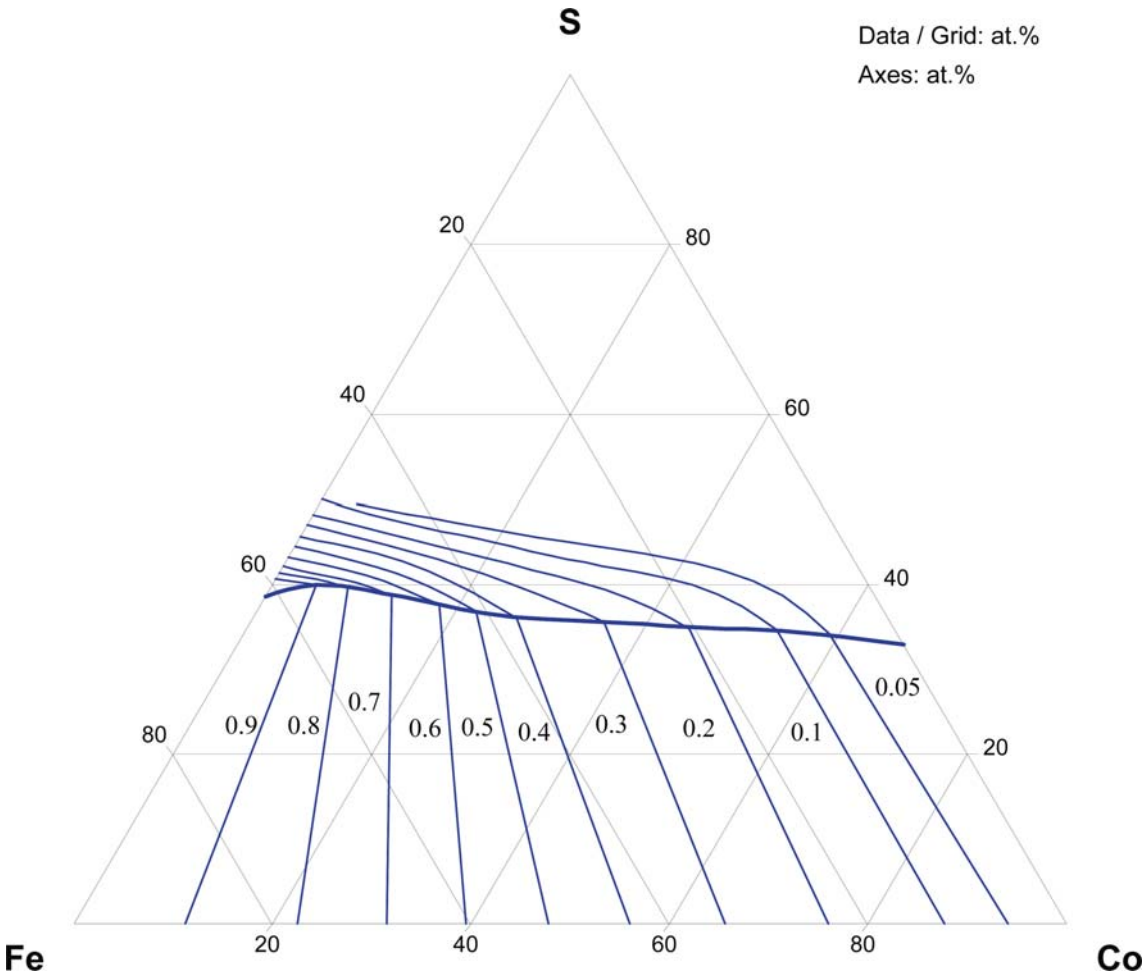

Fig. 14a. Co-Fe-S. Isoactivities of Fe at 1200°C (pure solid standard state)

DOI: 10.1007/978-3-540-74196-1_23

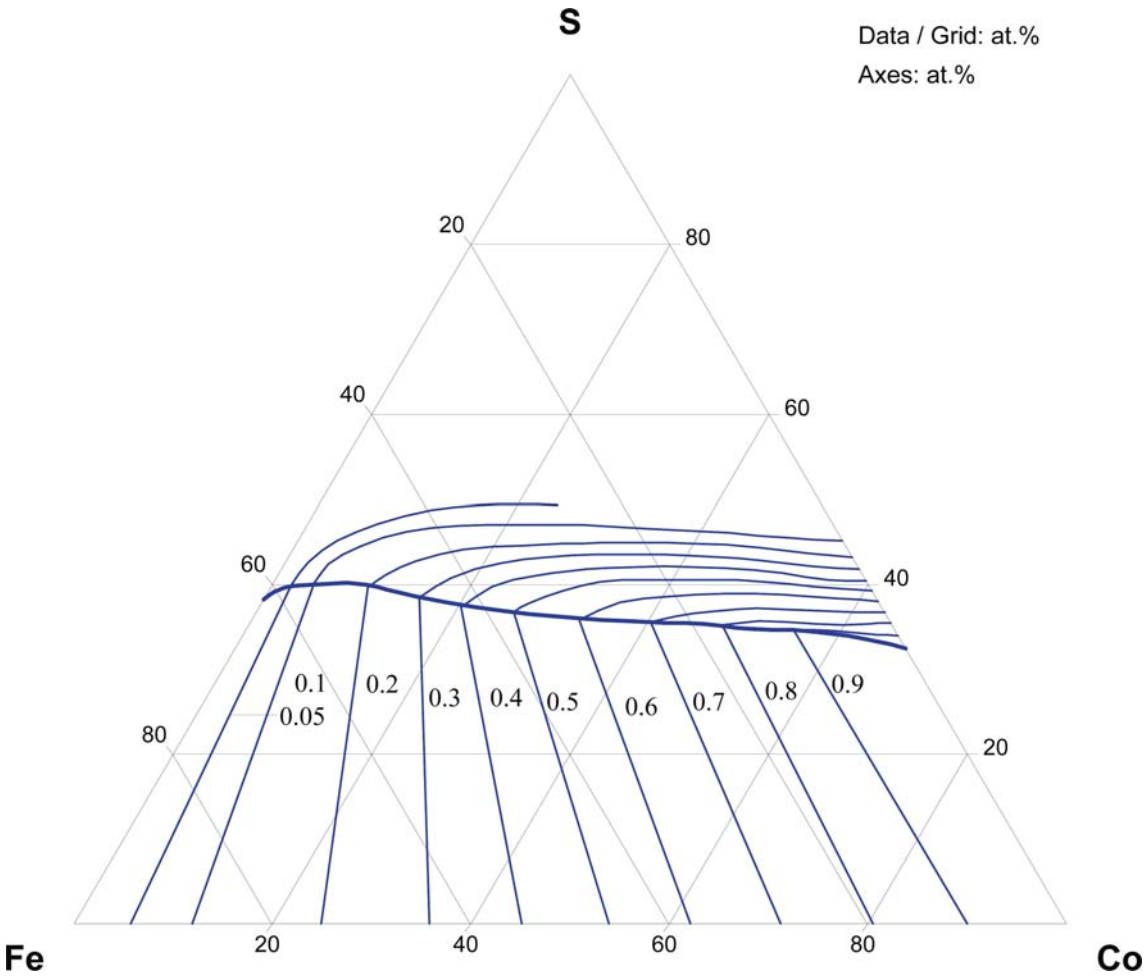

Fig. 14b. Co-Fe-S. Isoactivities of Co at 1200°C (pure solid standard state)

DOI: 10.1007/978-3-540-74196-1_23

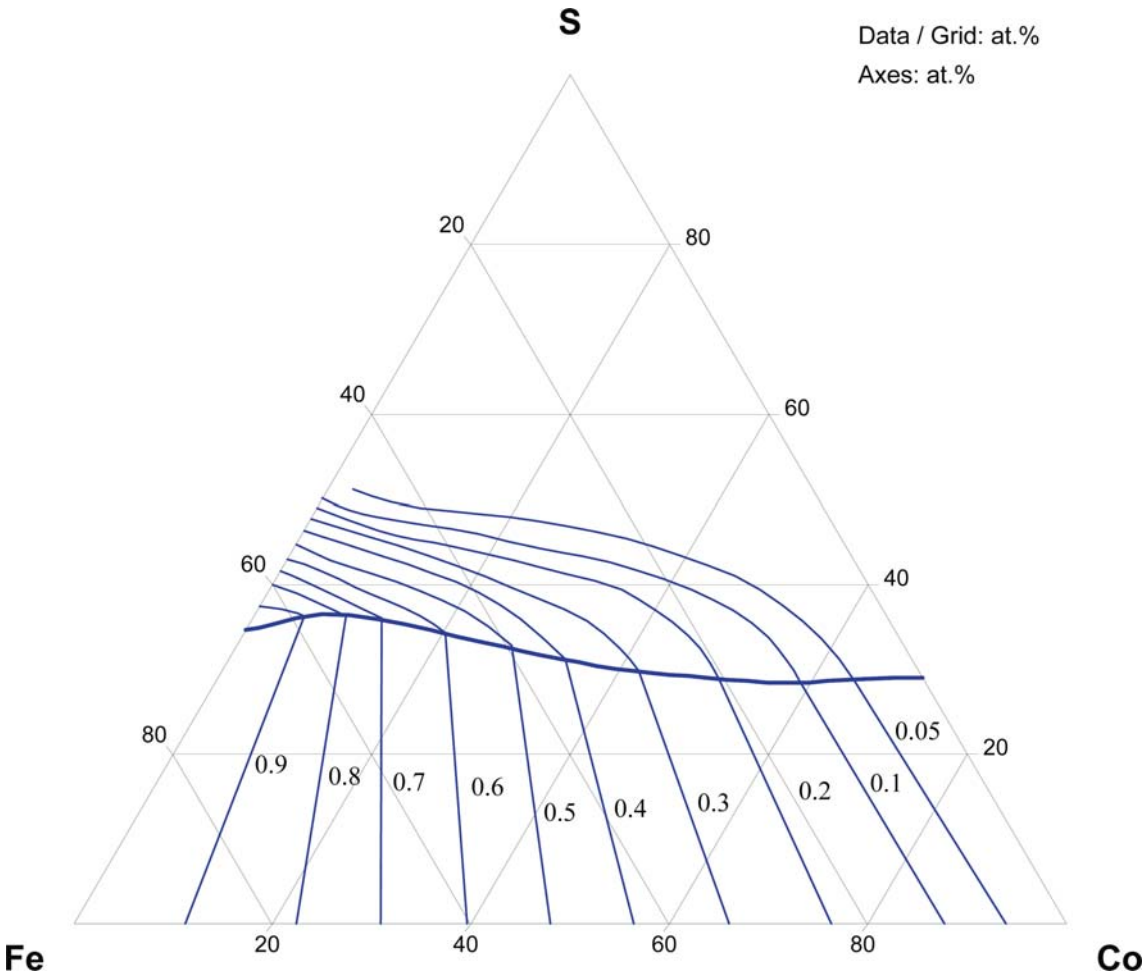

Fig. 15a. Co-Fe-S. Isoactivities of Fe at 1275°C (pure solid standard state)

DOI: 10.1007/978-3-540-74196-1_23

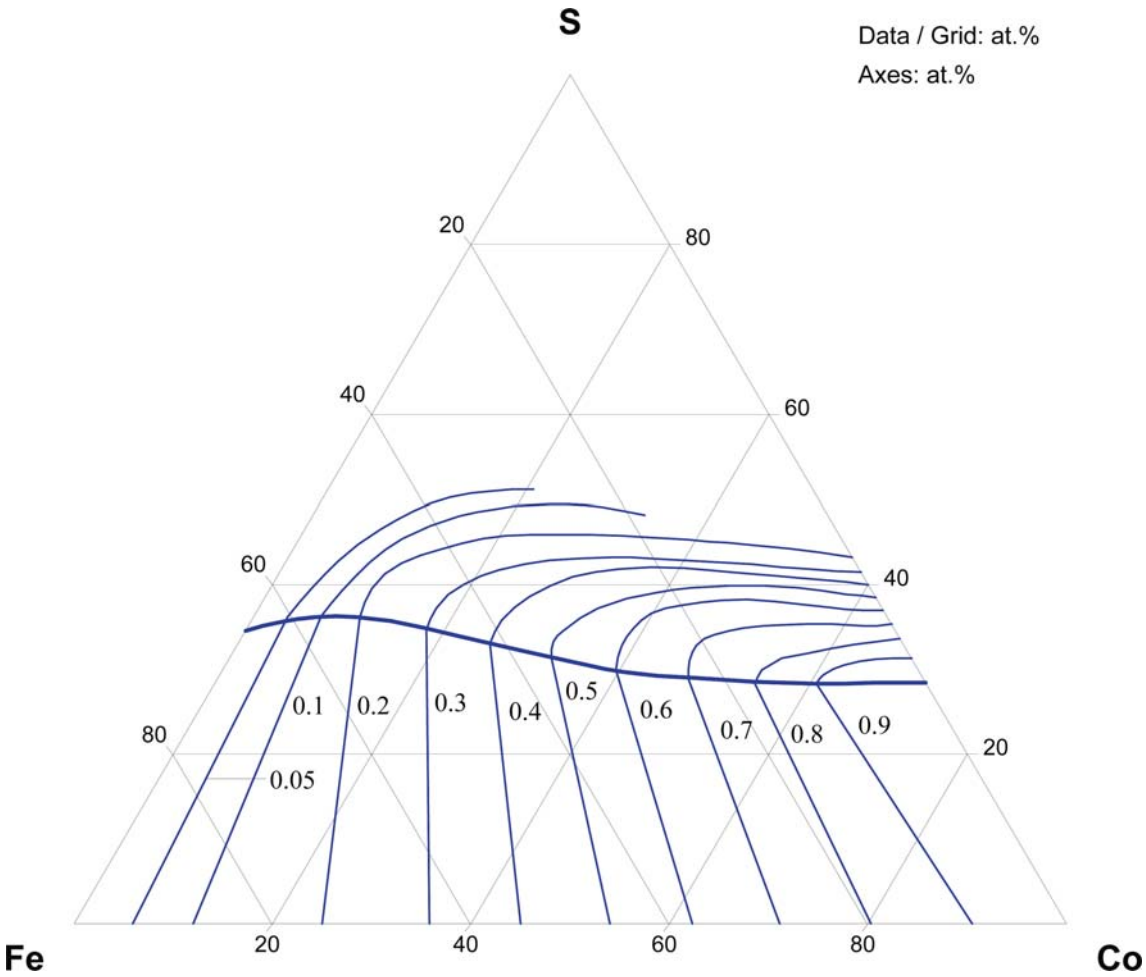

Fig. 15b. Co-Fe-S. Isoactivities of Co at 1275°C (pure solid standard state)

DOI: 10.1007/978-3-540-74196-1_23

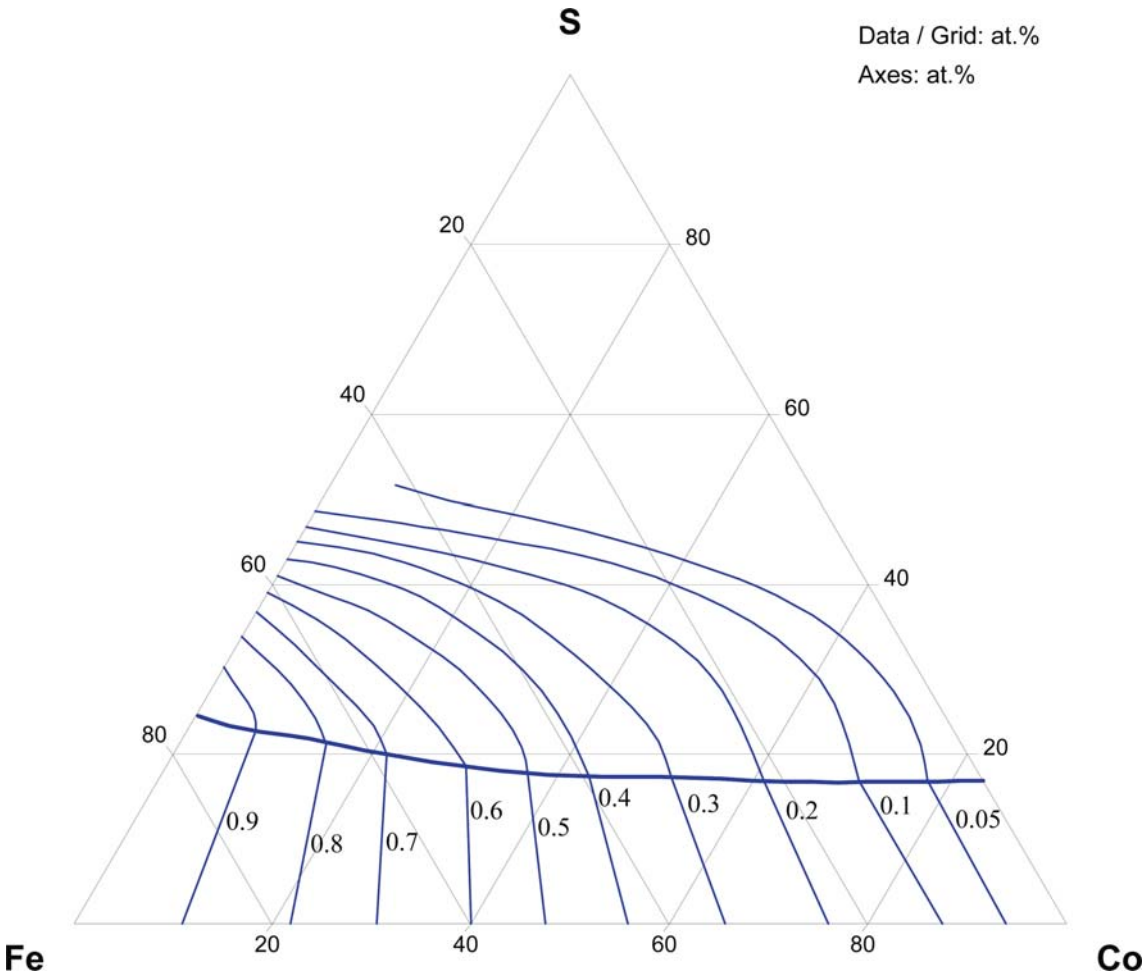

Fig. 16a. Co-Fe-S. Isoactivities of Fe at 1325°C (pure solid standard state)

DOI: 10.1007/978-3-540-74196-1_23

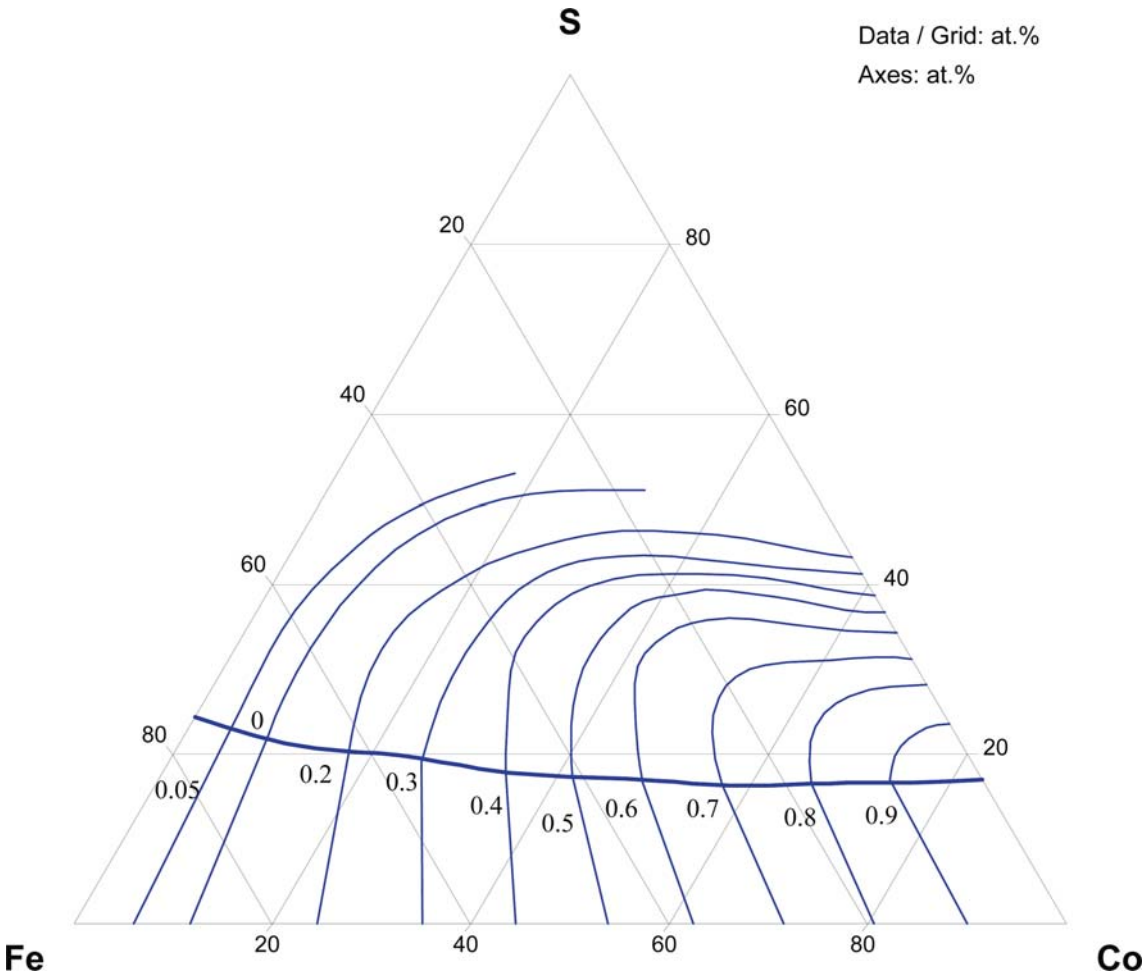

Fig. 16b. Co-Fe-S. Isoactivities of Co at 1325°C (pure solid standard state)

DOI: 10.1007/978-3-540-74196-1_23

References

[1949Vog] Vogel, R., Au, R., "On the Solubility of FeS in the Cobalt Sulphides Co_6S_5 and Co_4S_3" (in German), *Z. Metallkd.*, **40**(8), 290–295 (1949) (Experimental, Phase Diagram, Phase Relations, 5)

[1951Asa] Asanti, P., Kohlmeyer, E.J., "On the Thermal Analysis of Compounds of Iron and Cobalt with Oxygen and Sulphur" (in German), *Z. Anorg. Chem.*, **265**, 90–98 (1951) (Experimental, Phase Diagram, 24)

[1953Vog] Vogel, R., Hillner, G.F., "Phase Diagram of Iron-Iron Sulphide-Cobalt Sulphide-Cobalt" (in German), *Arch. Eisenhuettenwes.*, **24**(3–4), 133–141 (1953) (Experimental, Phase Diagram, Phase Relations, #, *, 13)

[1957Mol] Moleva, N.G., Kusakin, P.S., Vetrenko, E.A., Diev, N.P., "About Crystallization of Alloys in the FeS-Co_4S_3 System" (in Russian), *Zh. Prikl. Khim.*, **30**(9), 1402–1405 (1957) (Experimental, Phase Diagram, 7)

[1958Mol] Moleva, N.G., Kusakin, P.S., Vetrenko, E.A., Diev, N.P., "Phase Diagram of the Fe-Co-S System" (in Russian), *Zh. Neorg. Khim.*, **3**(4), 904–910 (1958) (Experimental, Phase Diagram, * 15)

[1960Alc] Alcock, C.B., Cheng, L.L., "A Thermodynamic Study of Dilute Solutions of Sulphur in Liquid Iron, Cobalt and Nickel and Binary Alloys Between these Metals", *J. Iron Steel Inst.*, **195**(2), 169–173 (1960) (Experimental, Thermodyn., 18)

[1960Per] Perthel, R., "About a Ferromagnetism of Nonstoichiometric Iron Sulphide" (in German), *Ann. Phys*., **5**(5–6), 273–295 (1960) (Experimental, Crys. Structure, Magn. Prop., 18)

[1962Kle] Klemm, D.D., "Investigations on Solid Solution Formation in the Ternary FeS_2-CoS_2-NiS_2 and its Relation to the Constitution of Natural Bravoite" (in German), *Neues Jahrb. Mineral. Monatsh.*, (3–4), 76–91 (1962) (Experimental, Phase Relations, 61)

[1962Kno] Knop, O., "Occurence of the π-Phase Among Chalcogenides", *Chem. Ind. (London)*, 739–740 (1962) (Experimental, Crys. Structure, 3)

[1963Kan] Kaneko, H., Nishizawa, T., Tamaki, K., "Study on Phase Diagrams of Sulphides in Steels" (in Japanese), *Nippon Kinzoku Gakkai Shi*, **27**(7), 312–319 (1963) (Experimental, Phase Relations, 23)

[1964Kul] Kullerud, G., "Review and Evaluation of Recent Research on Geologically Significant Sulfide-Type Systems", *Fortschritte Mineral.*, **41**(2), 221–270 (1964) (Review, Phase Diagram, 109)

[1965Buz] Buzek, Z., Prabhala, K.S., "The Character and Type of Sulphur Solutions in the Fe-S-Ni and Fe-S-Cr Systems" (in Czech), *Sborn. Ved. Praci Vysoke Skoly Banske Ostrave*, **11**(3), 563–568 (1965) (Theory, Thermodyn., Phase Relations, 8)

[1965Ril] Riley, J.F., "An Intermediate Member of the Binary System FeS_2(Pyrite)-CoS_2 (Cattierite)", *Am. Mineral.*, **50**(7–8), 1083–1086 (1965) (Experimental, Crys. Structure, 2)

[1966Ada] Adachi, A., Morita, Z., "Effect of Cobalt on the Activity of Sulfur in Liquid Iron", *Technol. Repts. Osaka Univ.*, (744), 719–723 (1966) (Experimental, Thermodyn., 12)

[1968Bou] Bouchard, R.J., "The Preparation of Pyrite Solid Solutions of the Type $Fe_xCo_{1-x}S_2$, $Co_xNi_{1-x}S_2$ and $Cu_xNi_{1-x}S_2$", *Mater. Res. Bull.*, **3**, 563–570 (1968) (Experimental, Crys. Structure, 6)

[1968Chm] Chmelar, I., Buzek, Z., Hlineny, J., "Determination of the Sulfur Activity in the Fe-X-S Systems using a Laboratory Electroslag Furnace" (in Czech), *Sborn. Ved. Praci Vysoke Skoly Banske Ostrave*, **14**(3), 175–181 (1965) (Experimental, Thermodyn., 8)

[1968Ril] Riley, J.F., "The Cobalttiferous Pyrite Series", *Am. Mineral.*, **53**(1–2), 293–295 (1968) (Experimental, Phase Relations, 3)

[1969Ban] Ban-ya, S., Chipman, J., "Sulfur in Liquid Iron Alloys: II - Effects of Alloying Elements", *Trans. Met. Soc. AIME*, **245**(1), 133–143 (1969) (Experimental, Thermodyn., 18)

[1969Kur] Kuriki, S., Sato, M., Maeda, M., "Magnetic and Structural Properties of Electrodeposited Co-Fe-S Alloys", *Japan. J. Appl. Phys.*, **8**, 1570 (1969) (Experimental, Magn. Prop., 4)

DOI: 10.1007/978-3-540-74196-1_23

[1970Vay] Vaysbrud, S.E., Remen', T.F., Novikova, N.N., "Thermodynamic Properties of Liquid Slags and Mattes and Component Distribution Between them" (in Russian), *Tr. Proekt. Nauchno-Issled. Inst.* "*Gipronikel*", (46), 5–31 (1970) (Experimental, Thermodyn., 41)

[1971But] Butler, S.R., Bouchard, R.J., "Saingle Crystal Growth of Pyrite Solid Solutions", *J. Cryst. Growth.*, **10**(2), 163–169 (1971) (Experimental, Crys. Structure, Electr. Prop., Magn. Prop., 4)

[1971Vay] Vaysbrud, S.E., Burylev, B.P., Remen', T.F., "Component Activities in the Melts of the Fe-Co-S Ternary System" (in Russian), *Zh. Fiz. Khim.*, **45**(8), 2041–2043 (1971) (Experimental, Calculation, Thermodyn., 11)

[1972Vay] Vaysbrud, S.E., Burylev, B.P., Zedina, I.N., Remen', T.F., "Thermodynamic Properties of Sulfire Melts and their Quantitative Description" (in Russian), *Zh. Fiz. Khim.*, **46**(6), 1528–1531 (1972) (Experimental, Thermodyn., 9)

[1973Buz] Buzek, Z., "Effect of Alloying Elements on the Solubility and Activity of Oxygen and Sulphur in Liquid Iron at 1600°C", *Int. Symp. Metall. Chem. - Appl. Ferrous Metall.*, Iron and Steel Inst, London, 173–177 (1973) Sheffield, July 1971 (Experimental, Review, Crys. Structure, 8)

[1974Khe] Kheifets, V.L., Vaysburd, S.E., "About some Properties of Sulfide Melts of Iron Group Metals", in "*Elektrochim. Rasplavy*", Moscow, Nauka, 118–122 (1974) (Review, Thermodyn., 21)

[1974Sig] Sigworth, G.K., Elliott, J.F., "The Thermodynamics of Liquid Dilute Iron Alloys", *Met. Sci.*, **8**, 298–310 (1974) (Review, Thermodyn., 249)

[1976Kno] Knop, O., Huang, C.-H., Reid, K.I.G., Carlow, J.S., Woodhams, F.W.D., "Chalcogenides of the Transition Elements. X. X-ray, Neutron, Mössbauer and Magnetic Studies of Pentlandite and the π Phases π (Fe, Co, Ni, S), Co_8MS_8 and $Fe_4Ni_4MS_8$ (M = Ru, Rh, Pd)", *J. Solid State Chem.*, **16**(1–2), 97–116 (1976) (Experimental, Crys. Structure, Phase Relations, 38)

[1976Moh] Moh, G.H., "Experimental and Descriptive Ore Mineralogy", *Neues Jahrb. Mineral., Abh.*, **128**(2), 115–188 (1976) (Experimental, Phase Diagram, Phase Relations, 101)

[1976Wys] Wyszomirski, P., "Experimental Studies of the Ternary Fe-Co-S System in the Temperature Range of 500–700°C", *Miner. Pol.*, **7**(1), 39–49 (1976) (Experimental, Phase Diagram, Phase Relations, *, #, 35)

[1977Wys] Wyszomirski, P., "Phase Relation in the Fe-Co-S System at 800°C", *Miner. Pol.*, **8**(1), 75–78 (1978) (Experimental, Phase Diagram, #, *, 9)

[1979Cha] Chang, Y.A., Sharma, R.C., "Application of an Associated Solution Model to the Metal-Sulfur Phase Diagrams", *Calculation of Phase Diagrams and Thermochemisty of Alloy Phase*, Chang, Y.A. (Ed.), Met. Soc. AIME, Warrendale, 145–174 (1979) (Review, Thermodyn., 51)

[1979Kra] Krabbes, G., Oppermann, H., "Chemical Transport and some Physical Properties of Cobalt Iron Sulfide $Co_yFe_{1-y}S_x$" (in German), *Z. Anorg. Allg. Chem.*, **450**(3), 27–35 (1979) (Experimental, Phys. Prop., Transport Phenomena, 17)

[1979Sha] Shatynski, S.R., Hirth, J.P., Rapp, R.A., "Solid-State Displacement Reactions Between Selected Metals and Sulfides", *Metall. Trans. A*, **10A**(5), 591–598 (1979) (Experimental, Phase Relations, Morphology, 16)

[1981Fit] Fitzner, K., Chang, Y.A., "The Activity Coefficient of Sulfur in Dilute Binary Liquid Metal Alloys", *Chem. Metal. - Tribute Carl Wagner,* Proc. Symp., 119–135 (1981) (Review, Thermodyn., 45)

[1981Ter] Terukov, E.I., Roth, S., Krabbes, G., Oppermann, H., "The Magnetic Properties of Cobalt-Doped Iron Sulphide $Fe_{1-y}Co_yS$ ($y \leq 0.13$)", *Phys. Status Solidi, A*, **68**(1), 233–238 (1981) (Experimental, Magn. Prop., Crys. Structure, 16)

[1982Kra] Krabbes, G., Terukov, E.I., Oppermann, H., "Time-Dependent Behavior of the Electrical-Resistance in an α-Phase Transition in a Strongly Doped Cobalt-Iron-Sulfide $Co_yFe_{1-y}S$" (in German), *Phys. Status Solidi A*, **71**(2), K143-K146 (1982) (Experimental, Phase Relations, Electr. Prop., 9)

DOI: 10.1007/978-3-540-74196-1_23

[1982Kub] Kubaschewski, O., "Iron-Sulfur", in "*Iron - Binary Phase Diagrams*", Springer-Verlag, New York, 125–128 (1982) (Phase Diagram, Review, #, 20)

[1982McC] McCammon, C.A., Price, D.C., "Mössbauer Effect Investigation of the Magnetic Behaviour of (Fe,Co)S_{1+x} Solid Solution", *J. Phys. Chem. Solids*, **43**(5), 431–437 (1982) (Experimental, Magn. Prop., Crys. Structure, 26)

[1982Wie] Wieser, E., Krabbes, G., Terukov, E.I., "Detection of the Metastable Simultaneous Occurence of High- and Low-Temperature States in $Co_yFe_{1-y}S$ by Mössbauer Spectriscopy", *Phys. Status Solidi, A*, **72**(2), 695–699 (1982) (Experimental, Phase Relations, Magn. Prop., Electr. Prop., 12)

[1984Nis] Nishizawa, T., Ishida, K., "The Co-Fe (Cobalt-Iron) System", *Bull. Alloy Phase Diagrams*, **5**(3), 250–259 (1984) (Crys. Structure, Phase Diagram, Review, Thermodyn., 129)

[1985Sch] Schmid, R., Musbah, O., Chang, Y.A., "Phase Relations and Thermodynamics of the Fe-Co-S System at 1073 K", *Z. Metallkd.*, **76**(1), 1–6 (1985) (Experimental, Phase Diagram, Thermodyn., *, #, 17)

[1987Bar] Barthelemy, E., Carcaly, C., "Phase Relations and Ageing Effects in $Fe_{1-x}Co_xS$ System", *J. Solid State Chem.*, **66**, 191–203 (1987) (Experimental, Phase Relations, Magn. Prop., 15)

[1987Col] Collin, G., Gardette, M.F., Comes, R., "The $Fe_{1-x}Co_xS$ System ($x < 0.25$); Transition and the High Temperature Phase", *J. Phys. Chem. Solids*, **48**(9), 791–802 (1987) (Experimental, Magn. Prop., Crys. Structure, Electr. Prop., Thermodyn., 26)

[1988Rag] Raghavan, V., "The Co-Fe-S (Cobalt-Iron-Sulphur) System", *Phase Diagrams of Ternary Iron Alloys*, Indian Institute of Metals, Calcutta, **2**, 93–106 (1988) (Review, Phase Relations, Phase Diagram, *, #, 20)

[1994Sor] Sorokin, M.L., Nikolaev, A.G., Bystrov, V.P., "Thermodynamics of the Co-Fe-S System", *Tsvetn. Met.,* (12), 17–217 (1994) (Calculation, Thermodyn., Phase Diagram, Phase Relations, 16)

[1997Bry] Bryukvin, V.A., Blokhina, L.I., "Phase Equilibria in the System Iron-Cobalt-Sulfur", in *Pyrometall. Fundament. Process Dev. Proc. Nickel-Cobalt 97 Int. Symp.*, Levac, C.A., Berryman, R.A. (Eds.), Canad. Inst. Min., Metall. Petroleum, Montreal, Quebec, 337–341 (1997) as quoted by [2004Rag]

[1997Sol] Soltanieh, M., Toguri, J.M., Sridhar, R., "The Liquidus Surface and Tie-Lines in the Iron-Cobalt-Sulfur System Between 1473 and 1623 K", *Metall. Mater. Trans. B*, **28B**(4), 647-650 (1997) (Experimental, Phase Diagram, 16)

[1998Rag] Raghavan, V., "Co-Fe-S (Cobalt-Iron-Sulfur)", *J. Phase Equilib.*, **19**(3), 264 (1998) (Review, Phase Relations, *, 5)

[1999Kon] Kongoli, F., Pelton, A.D., "Model Prediction of Thermodynamic Properties of Co-Fe-Ni-S Mattes", *Metall. Mater. Trans. B*, **30B**, 443–450 (1999) (Calculation, Phase Relations, Thermodyn., 51)

[1999Sol] Soltanieh, M., Toguri, J.M., Sridhar, R., "The Thermodynamics of the Fe-Co-S Ternary System", *Can. Metall. Quart.*, **38**(4), 227–236 (1999) (Experimental, Thermodyn., #, *, 24)

[2000Kim] Kim, E.C., "Crystallographic and Magnetic Properties of Iron Sulfides Doped with 3d Transition Metals", *J. Mater. Sci. Letter.*, **19**, 693–694 (2000) (Experimental, Crys. Structure, Magn. Prop., 8)

[2001Far] Farrell, S.P., Fleet, M.E., "Sulfur K-Edge XANES Study of Lokal Electronic Structure in Thernary Monosulfide Solid Solution {(Fe, Co, Ni)$_{0.923}$S}", *Phys. Chem. Miner.*, **28**, 17-27 (2001) (Experimental, Crys. Structure, Electronic Structure, 56)

[2002Far] Farrell, S.P., Fleet, M.E., "Phase Separation in $(Fe,Co)_{1-x}S$ Monosulfide Solid-Solution below 450°C, with Consequences for Coexisting Pyrrotite and Pentlandite in Magmatic Sulfide Deposits", *Can. Mineral.*, **40**, 33–46 (2002) as quoted in [2004Rag]

[2003Che] Cheng, S.F., Woods, G.T., Bussmann, K., Mazin, I.I., Soulen, R.J., Jr., Carpenter, E.E., Das, B.N., Lubitz, P., "Growth and Magnetic Properties of Single Crystal $Fe_{1-x}Co_xS_2$ (x = 0.35-1)", *J. Appl. Phys.*, **93**(10), 6847–6849 (2003) (Experimental, Crys. Structure, Magn. Prop., Electr. Prop., 17)

DOI: 10.1007/978-3-540-74196-1_23

[2004Rag] Raghavan, V., "Co-Fe-S (Cobalt-Iron-Sulfur)", *J. Phase Equilib. Diffus.*, **25**(4), 365–367 (2004) (Review, Phase Diagram, Phase Relations, *, #, 13)

[2005Nam] Nam, H.D., Kim, E.C., Han, J.S., "Mössbauer Study of Iron Sulfides Doped with 3d-transition Metals", *Solid State Commun.*, **135**(5), 327–329 (2005) (Experimental, Crys. Structure, Electronic Structure, Phase Relations, 8)

[2006Han] Han, J.-T., Huang, Y.-H., Huang, W., "Solvothermal Synthesis and Magnetic Properties of Pyrite $Co_{1-x}Fe_xS_2$ with Various Morphologies", *Mater. Lett.*, **60**(15), 1805–1808 (2006) (Experimental, Morphology, Magn. Prop., 17)

[2006Leh] Lehner, S.W., Savage, K.S., Ayers, J.C., "Vapor Growth and Characterization of Pyrite (FeS_2) Doped with Co, Ni, and As: Variations in Semiconducting Properties", *J. Cryst. Growth*, **286**(2), 306–317 (2006) (Experimental, Electr. Prop., Semicond., 38)

[2006MSIT] "Co-S (Cobalt-Sulpher)", Diagrams as Published in MSIT Workplace, Effenberg, G. (Ed.), MSI; Materials Science International Services GmbH, Stuttgart; to be published, (2007) (Crys. Structure, Phase Diagram, Phase Relations, #, 2)

[Mas2] Massalski, T.B. (Ed.), *Binary Alloy Phase Diagrams*, 2nd edition, ASM International, Metals Park, Ohio (1990)

[V-C2] Villars, P. and Calvert, L.D., *Pearson's Handbook of Crystallographic Data for Intermetallic Phases*, 2nd edition, ASM, Metals Park, Ohio (1991)

DOI: 10.1007/978-3-540-74196-1_23